BIOASTRONAUTICS DATA BOOK

Final Report

Funded Through
Office of Naval Research
Physiology Programs

Under

Contract No. N00014-67-C-0526
Work Unit No. NR 309-022

September 1972

Reproduction in whole or in part is permitted for any purpose of the United States Government.

This document has been approved for public release and sale; its distribution in unlimited

REPRODUCED BY
NATIONAL TECHNICAL
INFORMATION SERVICE
U. S. DEPARTMENT OF COMMERCE
SPRINGFIELD, VA. 22161

AD 749887

UNCLASSIFIED
Security Classification

DOCUMENT CONTROL DATA - R&D

(Security classification of title, body of abstract and indexing annotation must be entered when the overall report is classified)

1 ORIGINATING ACTIVITY (Corporate author) BioTechnology, Inc. 3027 Rosemary Lane Falls Church, Virginia 22042	2a REPORT SECURITY CLASSIFICATION U 2b GROUP N/A

3 REPORT TITLE

BIOASTRONAUTICS DATA BOOK

4 DESCRIPTIVE NOTES (Type of report and inclusive dates)

Final Report

5 AUTHOR(S) (Last name, first name, initial)

Managing Editors: Parker, James F., Jr.
West, Vita R.

6 REPORT DATE September 1972	7b NO. OF REFS
8a CONTRACT OR GRANT NO N00014 67-C-0526 b PROJECT NO Work Unit No. NR 309-022 c	9a ORIGINATOR'S REPORT NUMBER(S) 9b OTHER REPORT NO(S) (Any other numbers that may be assigned this report)

10 AVAILABILITY/LIMITATION NOTICES

This document has been approved for public release and sale; its distribution is unlimited.

11 SUPPLEMENTARY NOTES	12 SPONSORING MILITARY ACTIVITY Physiology Programs Office of Naval Research Arlington, Virginia 22217

13 ABSTRACT

This revision of the Bioastronautics Data Book was prepared in order to bring together the essentials of the large body of human research information generated in recent years and to present it in a form suitable for engineers and others concerned with the development and evaluation of modern systems. This effort represents an updating and expansion of an earlier document prepared for the National Aeronautics and Space Administration in 1964 by Webb Associates. The revision was prepared under the guidance of Working Group 5 of the Committee on Hearing, Bioacoustics and Biomechanics of the National Academy of Sciences.

The revised Bioastronautics Data Book was prepared by BioTechnology, Inc. under contract to the Office of Naval Research with support from the National Aeronautics and Space Administration. It deals with a substantial array of content areas within the broad domain of life sciences and presents primarily that information deemed of value for system design and evaluation.

DD FORM 1 JAN 68 1473

UNCLASSIFIED
Security Classification

NOTICE

THIS DOCUMENT HAS BEEN REPRODUCED FROM THE BEST COPY FURNISHED US BY THE SPONSORING AGENCY. ALTHOUGH IT IS RECOGNIZED THAT CERTAIN PORTIONS ARE ILLEGIBLE, IT IS BEING RELEASED IN THE INTEREST OF MAKING AVAILABLE AS MUCH INFORMATION AS POSSIBLE.

PREFACE

The rapid technological progress of the 1960s is characterized by the advanced systems produced during this period. The Apollo spacecraft, the metroliner, jet aircraft capable of carrying several hundred passengers, commercial nuclear power plants, and high-speed data processing facilities stand out as examples. These systems are highly visible and have had a marked effect on the American public. They represent what we accept as milestones of "progress."

Advances made in the life sciences during the 1960s are not as visible and only now are being accepted by the public as comparable in importance to progress in the physical and engineering sciences. It now is becoming very clear that a body of life sciences information is needed not only to determine the best way in which to utilize man in complex systems, but also to assess the impact of system operation on man. In this latter sense, we refer to impact on all mankind and not just to effects on humans working within a system.

As the problems of living in a technological age become more obvious, work must be accelerated towards solutions for human-oriented issues. Fortunately, there is a substantial body of life sciences data upon which one may draw. Although not generally recognized, basic research in the life sciences has kept pace with that in the physical sciences during recent years. In 1970, Federal expenditures in this field approached 700 million dollars, a fourfold increase over those of 1960. Data collected by the National Science Foundation indicate that, in 1969, basic research in the life sciences, social sciences, and psychology received 52 percent of the total Federal basic research funds, as opposed to 47 percent for the physical sciences, engineering sciences and mathematics.

This revision of the *Bioastronautics Data Book* was prepared in order to bring together the essentials of the large body of human research information generated in recent years and to present it in a form suitable for engineers and others concerned with the development and evaluation of modern systems. This effort represents an updating and expansion of an earlier document prepared for the National Aeronautics and Space Administration in 1964 by Webb Associates. The revision was prepared under the guidance of Working Group 5 of the Committee on Hearing,

Bioacoustics and Biomechanics of the National Academy of Sciences. Members of this group include:

A. Pharo Gagge, Ph.D, Chairman
Walton L. Jones, M.D.
Milton A. Whitcomb, Ph.D
Gilbert C. Tolhurst, Ph.D
Donald P. Woodward, Ph.D
Randall M. Chambers, Ph.D
Henning E. von Gierke, Ph.D
Edward J. Baldes, Ph.D

The revised *Bioastronautics Data Book* was prepared by BioTechnology, Inc. under contract to the Office of Naval Research with support from the National Aeronautics and Space Administration. It deals with a substantial array of content areas within the broad domain of life sciences and presents primarily that information deemed of value for system design and evaluation. We in NASA trust that it will prove as useful as the earlier *Data Book* and that it will contribute to solutions for some of the pressing problems in human ecology now faced by man.

Charles A. Berry, M.D.
NASA Director for Life Sciences
National Aeronautics and Space Administration

Walton L. Jones, M.D.
Deputy NASA Director for Life Sciences
National Aeronautics and Space Administration

TABLE OF CONTENTS

Chapter		Page
1.	Barometric Pressure	1
	Survival Under Near-Vacuum Conditions	2
	Human Tolerance for Low Barometric Pressures	6
	Human Tolerance for Gaseous Environments Composed of Air	7
	Human Tolerance for High Barometric Pressures	8
	Changes in Barometric Pressure	12
2.	Atmosphere	35
	General Considerations	35
	Oxygen	37
	Carbon Dioxide	47
	The Inert Gases	52
	Other Gaseous Compounds	59
3.	Temperature	65
	Physiological Parameters	66
	Energy Balance Equation	71
	Heat Transfer Equations	72
	Thermal Comfort	86
	Heat Stress	91
	Cold Stress	115
	Clothing	127
	Appendix	142
4.	Sustained Linear Acceleration	149
	Subjective Effects of Sustained Acceleration	150
	Physiological Effects of Sustained Acceleration	153
	Tolerance to Sustained Acceleration	171
	Performance Under Sustained Acceleration	179
5.	Rotary Acceleration	191
	Subjective Reactions and Tolerance	191
	Performance During Rotary Acceleration	202
	Physiological Effects of Rotary Acceleration	205
	Pathological Effects of Rotary Acceleration	217

Chapter		Page
6.	Impact	221
	Terms and Definitions	222
	Acceleration	225
	The "G" System of Units	225
	Interpreting the Data	227
	Human Tolerance Limits	227
	Physiological and Biochemical Response to Impact	239
	Biomechanical Factors of Impact	242
	Impact Other Than Along Primary Axis ("Off Axis")	278
7.	Vibration	297
	The Vibration Environment	298
	Performance Effects	304
	Physiological Effects	317
	Biodynamic Effects	323
	Subjective Tolerance Levels	332
	Interaction of Vibration with Other Environmental Parameters	342
8.	Weightlessness	349
	Effects of Weightlessness on Physiological Systems	351
	The Effects of Zero Gravity Upon Performance	400
	Counteracting the Physiological Effects of Weightlessness	405
	Appendix	412
9.	Ionizing Radiation	417
	Radiation Terms and Measures	420
	Classes and Sources of Ionizing Radiation	424
	Whole Body Radiation Effects	433
	Radiation Effects on Specific Body Systems	438
	Late Effects of Radiation	448
10.	Toxicology	455
	Oxygen Toxicity and The Effects of Variations In Oxygen Partial Pressure on Toxicity	456
	Effects of Oxygen on the Toxicity of Ozone and Nitrogen Dioxide	458
	Toxicity of Fuels and Oxidizers	459
	Carbon Monoxide	467
	Spacecraft Threshold Limit Values	470
	Emergency Exposure Limits (EEL)	471
	Spacecraft Contaminants	472
	Water Quality Standards for Space Missions	478

Chapter		Page
11.	Respiratory System	489
	General Anatomy of Chest and Lungs	490
	General Function of Respiration	491
	Respiration	493
	Breathing Movements	494
	Control of Breathing	495
	Lung Volumes and Capacities	498
	Mechanical Relations	503
	Factors Relevant to Respiratory Support Equipment Design	523
12.	The Vestibular System	533
	The End Organs	535
	Central Nervous System Connections	544
	Static and Dynamic Characteristics	547
	Vestibular Servation In Man	555
	Early Guidelines in the Prevention of Vestibular Side Effects on Space Missions Involving The Generation of Artificial Gravity	584
	Appendix A	591
	Appendix B	601
	Symbols	609
13.	Vision	611
	The Visual Environment	617
	Structure of the Visual System	621
	Visual Performance	637
	Vision Under Stress	655
	Visual Tasks in Space Operations	659
14.	Auditory System	667
	Physical Correlates of Hearing	668
	The Auditory System	669
	Hearing Loss	679
15.	Noise and Blast	693
	Description of the Noise and Blast Environment	694
	Effects of Noise and Blast on Hearing	705
	Effects of Hearing Loss on Performance	719
	Subjective and Behavioral Responses to Noise Exposure	721
	Physiological (Nonauditory) Responses to Noise Exposure	730
	Design Criteria	735

Chapter		Page
16.	Human Control Capabilities	751
	Controller Characteristics	751
	Controls and Manipulators	784
	Displays	787
17.	Atmosphere Control	807
	Carbon Dioxide	809
	Oxygen Regeneration	821
	Trace Contaminants Removal	836
	Humidity Control	839
	Storage Systems for Atmospheric Constituents	841
18.	Work, Heat, and Oxygen Cost	847
	Daily Energy Exchange	851
	Work and Heat Dissipation	854
	Oxygen Costs of Specific Activities	858
	Work Capacity	866
	Anaerobic Work	871
	Working in Space Suits	873
19.	Combined Environmental Stresses	881
	Combined Stress Interactions	882
	Approach to the Study of Combined Environmental Stress	888
	Combined Stress Data	889
	Facilities for Study of Combined Stress	889
20.	Aerospace Vehicle Water-Waste Management	915
	Requirements	916
	Collection and Transport	917
	Waste Processing	922

CHAPTER 1

BAROMETRIC PRESSURE

by

Charles E. Billings, M.D.
The Chio State University

Physiological studies of pressure effects have been conducted for over a century. Still, many facets of the problem have been incompletely explored. It is known that if man is supplied with an appropriate gas mixture, he can survive considerable periods of exposure to a wide range of barometric pressures (figure 1-1). Man's ultimate tolerance limits for high and low barometric pressures are not known, however. Likewise, it is not known whether the gas mixtures required for such exposures are in themselves toxic.

This chapter describes the effects of alterations in barometric pressure on human beings. The subject is of considerable importance in both aerospace and underwater exploration, although the former area is given primary emphasis here. The effects of barometric pressure as such must be differentiated from the effects of changes in pressure. In the latter case, our knowledge is more complete. Abrupt and controlled changes in pressure can be produced in compression and decompression chambers, shock tubes, wind tunnels, and the like.

Increases in barometric pressure are experienced most commonly during descents through the atmosphere and underwater diving. High dynamic (unbalanced) pressures are encountered during escape from aircraft. Still higher pressures occur in the vicinity of explosions. Decreases in pressure are encountered during ascents through water or the atmosphere or during depressurization of an aircraft or space vehicle. The physical effects of these changes are considered in this chapter. Exposure throughout the tolerable range of pressures is discussed first, followed by descriptions of the effects of increases, and then decreases, in barometric pressure.

In view of the multiplicity of systems for describing pressure, the following tables have been included as an aid to the reader wishing to convert pressure

Reviewed by the late Wing Commander D. I. Fryer, O.B.E., RAF, MC, Institute of Aviation Medicine, Farnborough, England.

terms from one notational system to another. Tables 1-1 and 1-2 shown here contain many, though not all, the units of pressure measurement in common use. The preferred units for scientific use are those of the new International System (Systeme Internationale), which recommends Newtons per square meter but accepts the bar and millibar for common usage. The inch of mercury and millibar are widely used in aviation. Millimeters of mercury are in common biomedical use in the United States and elsewhere. In diving medicine, the atmosphere is commonly used. Note in table 1-1 that zero feet of water equals 1 atmosphere. The increase of pressure with increasing depth in sea water is roughly 1 atm for each 33 feet. Since air is compressible, the altitude scale is logarithmic. The data for altitude are from the U.S. Standard Atmosphere (1954).

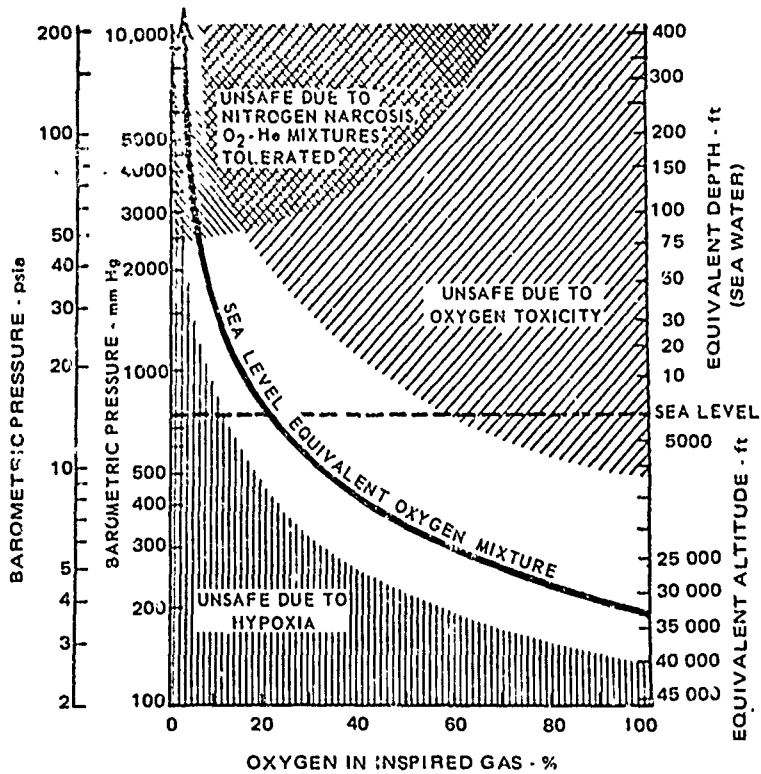


Figure 1–1. Approximate range of barometric pressure (above and below sea level) tolerated by humans breathing gas mixtures containing the indicated concentrations of O_2. Heavy curve indicates gas mixture which will maintain sea level equivalent PO_2 in the lungs at the indicated barometric pressures. (U.S. House of Representatives Select Committee on Astronautics and Space Exploration, 1959)

Survival Under Near-Vacuum Conditions

The vapor pressure of water at a body temperature of 37°C is 47 mm Hg (0.9 psia). Since the human body is largely composed of water, exposure to barometric pressures much below 47 mm Hg absolute leads rapidly to

vaporization of body fluids, a process known as ebullism. That this phenomenon does not occur precisely at 47 mm Hg is due to some degree of counterpressure exerted by the skin and connective tissues and blood vessels.

Table 1–1

Equivalent Pressures, Altitudes and Depths

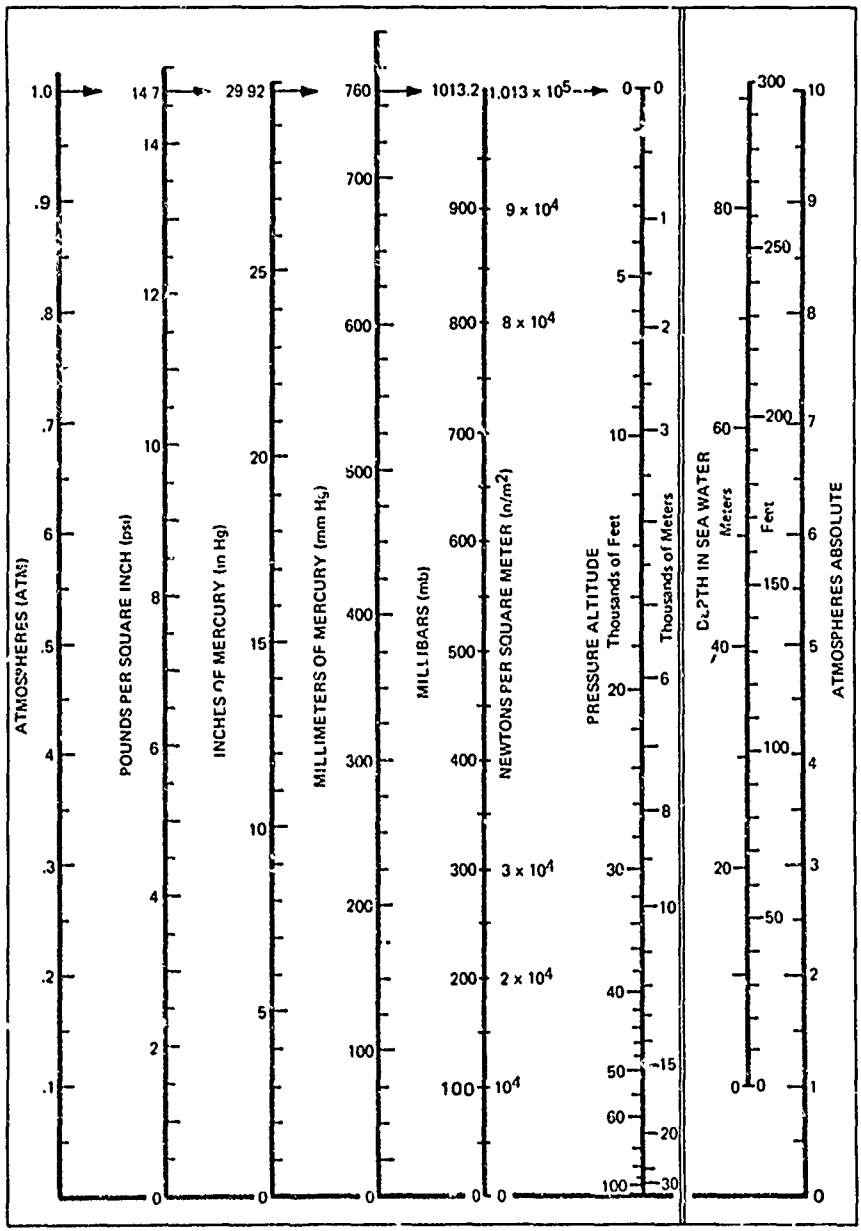


Table I–2

Conversion Table for Barometric Pressure Units

	Atm	N/M^2	bars	mb	kg/cm^2	gm/cm^2 (cm H_2O)	mm Hg	in. Hg (" Hg)	lb/in^2 (psi)
1 Atmosphere =	1	1.013×10^5	1.013	1013	1.033	1033	760	29.92	14.70
1 Newton/M^2 (N/M^2) =	$.9869 \times 10^{-5}$	1	10^{-5}	.01	1.02×10^{-5}	.0102	.0075	$.2953 \times 10^{-3}$	$.1451 \times 10^{-3}$
1 bar =	.9869	10^5	1	1000	1.02	1020	750.1	29.53	14.51
1 millibar (mb) =	$.9869 \times 10^{-3}$	100	.001	1	.00102	1.02	.7501	.02953	.01451
1 kg/cm^2 =	.9681	$.9807 \times 10^5$	.9807	980.7	1	1000	735	28.94	14.22
1 gm/cm^2 (1 cm H_2O) =	968.1	98.07	$.9807 \times 10^{-3}$	.9807	.001	1	.735	.02894	.01422
1 mm Hg =	.001316	133.3	.001333	1.333	.00136	1.36	1	.03937	.01934
1 in. Hg (" Hg) =	.0334	3386	.03386	33.86	.03453	34.53	25.4	1	.4910
1 lb/in^2 (psi) =	.06804	6895	.06895	68.95	.0703	70.3	51.70	2.035	1

Recent studies of dogs, squirrel monkeys, and baboons decompressed in 2 seconds from 250 to 1 to 2 mm Hg absolute (Bancroft & Dunn, 1965; Cooke et al., 1967; Cooke et al., 1968) have demonstrated remarkable similarity among these species in responses to exposure to a near vacuum. Chimpanzees respond in the same way, though at a slower rate, to this stress. It is reasonable to assume that similar responses would occur in humans exposed to very low pressures by puncture of a space vehicle or suit or failure of a pressure seal under space-equivalent conditions.

Some degree of consciousness will probably be retained for 9 to 11 seconds (see chapter 2 under the heading *Hypoxia*). In rapid sequence thereafter, paralysis will be followed by generalized convulsions and paralysis once again. During this time, water vapor will form rapidly in the soft tissues and somewhat less rapidly in the venous blood. This evolution of vapor will cause marked swelling of the body to perhaps as much as twice its normal volume unless it is restrained by a pressure suit. (It has been demonstrated that a properly fitted elastic garment can entirely prevent ebullism at pressures as low as 15 mm Hg absolute [Webb, 1969, 1970].) Heart rate may rise initially but will fall rapidly thereafter. Arterial blood pressure will also fall over a period of 30 to 60 seconds, while venous pressure rises due to distension of the venous system by gas and vapor. Venous pressure will meet or exceed arterial pressure within 1 minute. There will be virtually no effective circulation of blood. After an initial rush of gas from the lungs during decompression, gas and water vapor will continue to flow outward through the airways. This continual evaporation of water will cool the mouth and nose to near-freezing temperatures; the remainder of the body will also become cooled, but more slowly.

Cooke and Bancroft (1966) reported occasional deaths in animals due to fibrillation of the heart during the first minute of exposure to near-vacuum conditions. Ordinarily, however, survival was the rule if recompression occurred within about 90 seconds. The hearts in these studies tolerated even repeated decompression well (Cooke & Bancroft, 1966), although it is by no means certain that the human heart will be as tolerant. Once heart action ceased, death was inevitable, despite attempts at resuscitation. During recompression, as the absolute pressure exceeded about 50 mm Hg (1 psia), a dramatic reduction in swelling was demonstrated. Breathing usually began spontaneously, the time being dependent on the duration of exposure at minimum pressure. Heart rate and blood pressure rose to fairly high levels, then gradually returned toward normal. There was suggestive evidence in the Cooke and Bancroft studies that denitrogenation prior to exposure, and recompression with 100 percent oxygen, both improved recovery time and decreased mortality. Neurological problems, including blindness and other defects in vision, were common after exposures (see problems due to evolved gas), but usually disappeared fairly rapidly.

It is very unlikely that a human suddenly exposed to a vacuum will have more than 5 to 10 seconds to help himself. If immediate help is at hand, although one's appearance and condition will be grave, it is reasonable to assume that recompression to a tolerable pressure (200 mm Hg, 3.8 psia) within 60 to 90 seconds could result in survival, and possibly in rather rapid

recovery. There is, of course, no guarantee of a successful outcome; some animals have died within seconds of decompression and a few others have had severe, lasting central nervous system damage (Casey, Bancroft, & Cooke, 1966).

Barometric pressures below those at which adequate blood and tissue oxygenation can be maintained (about 190 mm Hg, 3.7 psia) must be considered hostile for more than brief exposures without proper protective equipment (see chapter 2); those below about 100 mm Hg (1.9 psia) must be considered hostile for any exposure. Pressures much below 50 mm Hg cause almost immediate failure of the circulation and total anoxia and must be considered lethal if sustained for more than 60 to 90 seconds.

Human Tolerance for Low Barometric Pressures

As indicated previously, the partial pressure of water vapor in the lungs is about 47 mm Hg (0.9 psia). The normal partial pressure of carbon dioxide in the lungs ranges from 35 to 45 mm Hg (0.7 to 0.9 psia). A partial pressure of oxygen in the lungs of about 100 mm Hg (1.94 psia) will maintain essentially complete oxygen saturation of arterial blood. A total barometric pressure of 190 mm Hg (3.66 psia), then, will support a human being if his environment consists of pure oxygen. It should be noted, however, that this figure leaves little room for further reductions such as would occur in the face of space cabin or pressure suit leaks, temporary failures of gas supply, dilution of the atmosphere by nitrogen or other inert gases, or carbon dioxide buildup due to inefficient absorption or scrubbing.

Although this pressure environment will support life for long periods of time, it has certain inherent disadvantages. Even after virtually complete removal of inert gases from the body, there is a finite, though minimal, risk of decompression sickness due to evolved gas. Because oxygen and carbon dioxide are physiologically active gases, they are absorbed rather rapidly from gas-containing cavities in the body. This can result in symptoms, especially in the ears, sinuses, and lungs (Hyde, Pines, & Saito, 1963).

The low density of a pure oxygen environment at 190 mm Hg (0.357 gm/liter, 28 percent of air at sea level) attenuates sound transmission and also alters, to some extent, the mechanics of the lung-chest system. The maximum pressure which can be developed by the system is lowered substantially. This inhibits the effectiveness of coughing and may make it difficult to rid the lungs of secretions or foreign matter. Breath holding time is also markedly reduced. On the other hand, the work of breathing at high flow rates is decreased due to reduction in the proportion of turbulent flow at low gas density. Thus, it is easier to sustain high ventilation volumes during the performance of muscular work (Boothby, 1964). Also, respiratory water loss may be decreased somewhat at low total pressures (Wortz et al., 1966).

It is not known whether man can tolerate an environment free of "inert" gases indefinitely. The 14-day Gemini flight and a few altitude chamber tests for

up to 30 days represent the only available data, and it is noteworthy that these exposures have been at 258 to 282 mm Hg (5 to 5.5 psia), in the main, rather than at the minimum tolerable pressures. When much longer exposures are contemplated, a number of more subtle factors must be considered. These include the possible dependence of man himself, or of his normal and essential saprophytic bacteria, on trace amounts of nitrogen or other "inert" gases. One study has also indicated that cell wall fragility may be increased at low total pressures (Bonadini, 1966). Such questions as these can only be answered by much longer experiments than those which have been conducted to date.

Man has successfully tolerated exposures of 56 days to environments containing physiological pressures of oxygen, with helium as the diluent, at a total pressure of 258 mm Hg (5.0 psia). Very careful medical, biochemical, physiological, and psychological studies disclosed no adverse effects during this period of exposure other than those which are inevitable under reduced pressure and which have been mentioned (Welch et al., 1966).

In summary, low barometric pressures, in and of themselves, do not appear to be harmful to man, insofar as they have been studied critically. There are disadvantages at pressures so low that pure oxygen must be used as the sole atmospheric constituent; many of these are minimized or alleviated by the addition of a small proportion of a diluent gas. Pressures as low as 5 psia appear to be innocuous for fairly long exposures.

Human Tolerance for Gaseous Environments Composed of Air

Man has been successfully adapting to a wide range of barometric pressures for many centuries. A skeleton roughly 9000 years old was recently found in Peru at an elevation of 13 800 feet, equivalent to a pressure of 450 mm Hg (8.65 psia). Extensive studies have been carried out on acclimatized natives at elevations of 15 000 feet in the Andes and on partially acclimatized mountaineers at 19 000 feet and above in the Himalayas. These environments are not optimal, and they exert a considerable physiological toll (see chapter 2 under the heading *Hypoxia*), but they are survivable for substantial periods of time. There is little evidence that long-term inhabitants at elevations above 10 000 feet differ substantially from their sea level counterparts except for decreased work tolerance and the presence of certain body adjustments to the lower partial pressure of oxygen at that altitude.

The usual range of barometric pressure at sea level in the United States is from about 29 to 31 inches of mercury (14.25 to 15.25 psia). Changes occur relatively slowly except under very unusual meterological conditions. While certain psychological and physiological disorders have been attributed to such changes in pressure, there is no proof of a causal relationship.

There are mines on earth in which maximum depths exceed 10 000 feet below sea level, equivalent to a barometric pressure of at least 20 psia. There is no evidence that men working at these depths have been harmed by the pressure

Increasing interest in undersea exploration during recent years has led to a number of long-term human studies at pressures substantially higher than those normally encountered by man. While excessive pressures of both nitrogen and oxygen are toxic to man and animals (see chapter 2), some of the earlier studies in which air was used as the gaseous medium (Conshelf I, two men, 7 days, 2.05 atm absolute; Conshelf II, six men, 30 days, 1.95 atm absolute; Tektite, four men, 60 days, 2.27 atm absolute) have shown that man can tolerate at least 2 months of exposure to these environments without apparent harm (Aquadro & Chouteau, 1967).

Human Tolerance for High Barometric Pressures

Bert, in 1876 (translated by Hitchcock & Hitchcock, 1943), described oxygen toxicity. While this problem is discussed in chapter 2, it should be noted here that as man has extended his technological capability under the seas, he has found that if oxygen poisoning and nitrogen narcosis can be avoided, his tolerance for high barometric pressures is considerable.

If the partial pressure of oxygen in the lungs is maintained at physiological levels, and if the partial pressure of nitrogen is kept below toxic limits, other inert gases may be added to man's environment in large amounts. The majority of work in this area has used helium as the inert pressurizing gas, though some research has been conducted with other noble gases, notably argon and neon. Hydrogen has not been popular because of its flammability when mixed with oxygen, though it also is physiologically inert and has some theoretical advantages for work at extremely high pressure (see chapter 2).

Leaving aside problems due to changing pressures, the physiological problems encountered in a high pressure environment are due almost entirely to the physical characteristics of the gas mixture used to create that environment.

At rest, man's instantaneous respiratory flow rate rarely exceeds 1 liter per second. Under these circumstances, most flow in the airway system is laminar; turbulent flow occurs only at branchings and in the smallest terminal bronchial tubes. When physical work is performed, however, ventilation volume and flow rates increase in proportion to the power output. Under these circumstances, volumes of 60 to 120 liters per minute and peak flow rates of 5 liters per second are not uncommon. The proportion of turbulent flow increases substantially and with it, the metabolic work required to move the air.

Otis, Fenn, and Rahn (1950) derived equations which describe the work of breathing at various barometric pressures. They showed that the work required to produce laminar flow is linearly related to the instantaneous velocity of air movement and is essentially independent of barometric pressure, whereas the work required for turbulent flow is a function of the second power of velocity and is directly related to density or pressure. (In calculating the work of breathing at altitude, the compressibility of alveolar air must be taken into account [Jaeger & Otis, 1964]; this factor is relatively unimportant at high barometric pressures.) Figures 1-2 and 1-3 illustrate some effects of high

pressures on ventilation. Wood, Bryan, and Koch (1969) have recently demonstrated some of the limiting factors in respiratory mechanics at very high pressures. The theoretical limit for steady-state breathing at depth is the point at which the work to move a given quantity of gas requires all the oxygen which can be extracted by the blood from that increment of gas while it is in the lungs.

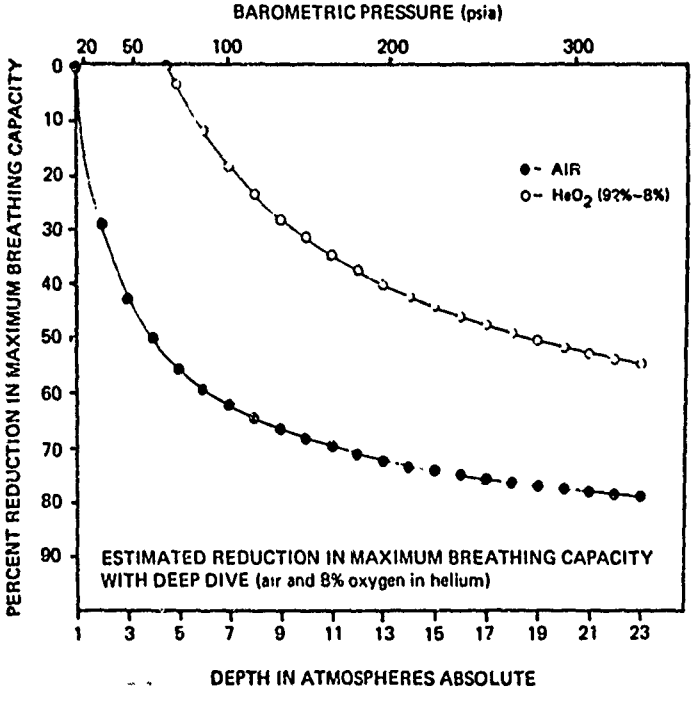


Figure 1–2. Calculated reductions in maximum ventilatory capacity with increasing depth breathing air or He–O_2. (Data of Workman, cited by Wood, 1963)

It is possible, by using combinations of oxygen, nitrogen, and helium, to maintain a gaseous environment whose partial pressure of oxygen and density remain at sea level values up to a total pressure of 5.74 atm absolute (84.4 psia), at which pressure the mixture contains 3.7 percent oxygen and 96.3 percent helium (figure 1-4). At greater pressures, the density of an appropriate oxygen-helium mixture increases almost in proportion to the total pressure (figure 1-5). Using oxygen-helium mixtures, brief habitability studies have been carried out at pressures as great as 684 psia (equivalent to 1500 feet of water) and much longer experiments have been conducted to lesser depths (Aquadro & Chouteau, 1967). These are discussed in more detail in chapter 2, since it appears that most of the physiological changes observed are due to the gases in the breathing mixtures, rather than to the pressure *per se*.

Other problems must be considered when man lives in a gaseous environment composed mostly of helium. The thermal conductivity of this gas is high; as a result, higher environmental temperatures are required to maintain man in the

zone of thermal neutrality (see chapter 3, *Temperature*). Very recent studies indicate that during work at depths greater than 600 feet, respiratory heat losses are considerable and can threaten man's ability to maintain thermal equilibrium even in the face of increased heat production (Rawlins, 1970). Speech is also a problem; the low density of helium produces a rise in the fundamental pitch of the human voice (Cooke, 1964; Cooke & Beard, 1965; Wather-Dunn, 1967). While this is partially compensated for over a period of time, intelligibility is appreciably decreased.

Man's ultimate tolerance limits for high barometric pressure are not known. It is possible that the work of breathing at rest will set a practical limit, although there may well be other factors yet-undetected, which will limit longer stays at lesser pressures (see chapter 2). In an effort to extend very considerably the tolerance limits, Kylstra (1967) has conducted experiments in which water instead of air is used as the carrier of oxygen and carbon dioxide. This technique, radical though it seems, may well be feasible at a later point in time. Extremely high static pressures may curtail or interfere with biochemical reactions which involve changes in tissue or molecular volume (Fenn, 1967).

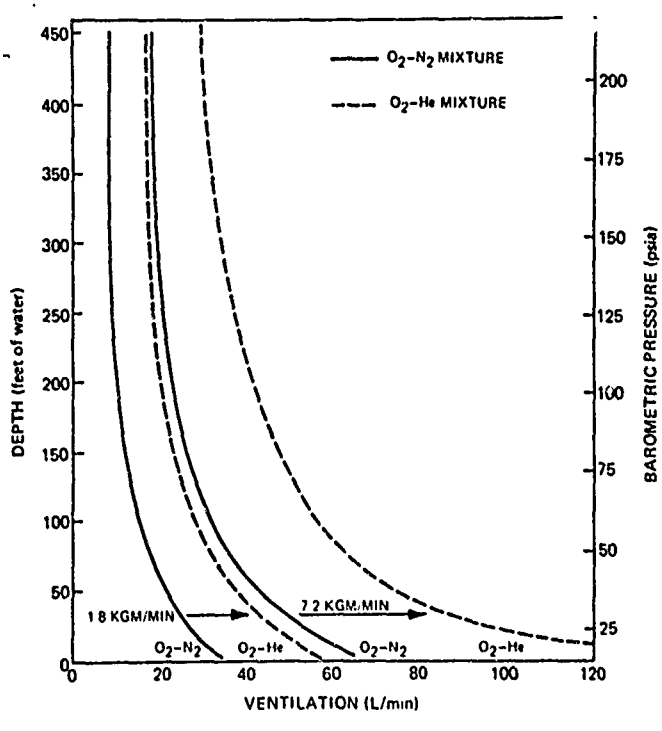


Figure 1–3. Measured (to 200 ft) and computed data for decreases in ventilation with increasing depth at constant values of respiratory work. 1.8 kgM/min, "a level which can be sustained for many hours," and 7.2 kgM/min, "respiratory work which can only be performed for a few minutes." (Redrawn from the data of Buhlmann, 1963)

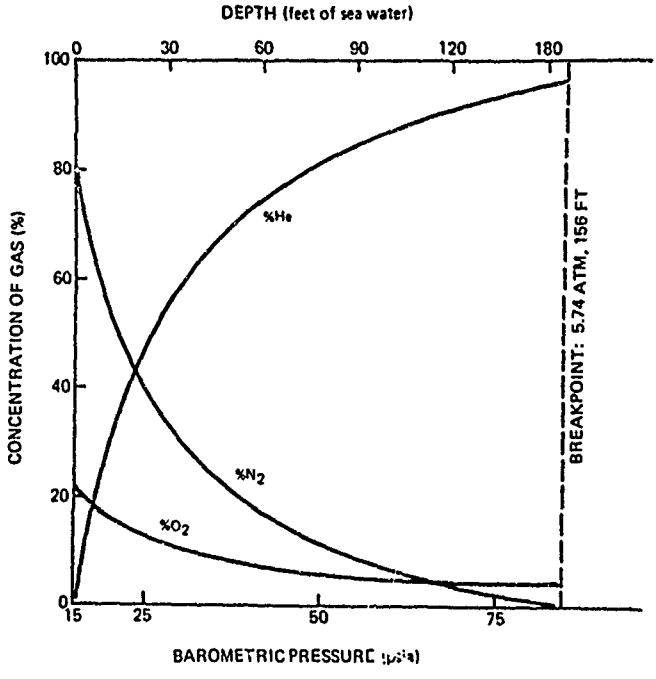


Figure 1–4. Mixtures of O_2, N_2, and He which will maintain sea level equivalent density and normal PO_2 in the lungs at various total pressures. Above 5.74 atm absolute, sea level gas density cannot be maintained without resorting to H_2-O_2 mixtures. (Billings, 1964)

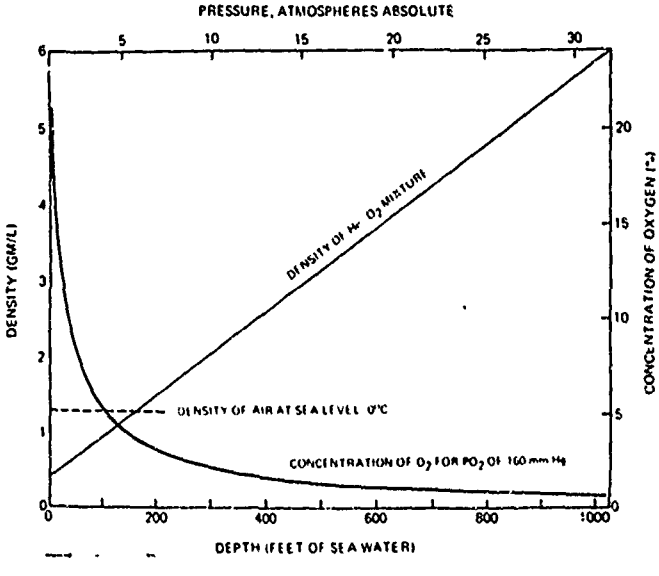


Figure 1–5. Density of mixtures of He and O_2 which will maintain a sea level equivalent PO_2 in the lungs, as a function of barometric pressure and depth in the sea water. (Billings, 1964)

Changes in Barometric Pressure

It has been indicated that human tolerance for barometric pressure extends from less than four to at least several hundred psia. Changes in barometric pressure in themselves, however, also exert profound physical and physiological effects on man. This section deals with increases and decreases in pressure.

Effects of Increases in Barometric Pressure

Increases in barometric pressure are encountered during descents through the atmosphere (whether in space vehicles, aircraft, or elevators), during repressurization of a space vehicle following extravehicular activity, and during dives in water. Local increases in pressure within the body, sometimes of considerable magnitude, occur with coughing, sneezing, blowing the nose, and with mechanical straining in the act of defecation. Exposure to high dynamic pressures, as well as high rates of change of pressure, occur when the body is suddenly subjected to windblast during ejection from aircraft. Still higher pressures are encountered in the vicinity of an explosion.

Problems Due to Trapped Gas Within the Body. If the human body were composed entirely of fluids, it would tolerate quite sudden changes in pressure well. The body has several cavities, however, which normally contain gas. The most important during increases in pressure are the ears, the paranasal sinuses, and the lungs. When rates of compression are relatively slow (no more than 1 to 2 psi/second), the primary concern is the ear. Such rates of change can occur during the dive of a fighter aircraft, during emergency recompression of an altitude chamber, or during a diver's descent through water.

The Ear. The eardrum is a slightly flexible partition between the external ear canal and the middle ear, a small air filled cavity which communicates with the environment only through the Eustachian tube, which opens into the back of the nose (figure 1-6). Air leaves the middle ear passively during decompression or ascent, but the mucous membrane lining the tube tends to prevent air from reentering the Eustachian tube without voluntary muscular effort during recompression.

Rapid recompressions from 28 000 feet to sea level, an increase of 10 psia, were performed by Racke and Freedman (1961). The rates of change are shown in figure 1-7. None of the subjects sustained serious ear damage during the tests. In three of 28 tests, however, it was necessary to initiate reascent of the chamber to aid the subjects in equalizing pressure across the eardrum.

Table 1-3 summarizes the symptoms which result from a differential pressure across the eardrum. Once high differentials exist, it is difficult or impossible to force air into the middle ear voluntarily; avoidance of such differentials requires frequent attention during rapid descents. Descents of less than 500 feet per minute in the lower atmosphere (0.25 psia/minute) are usually tolerated by inexperienced air passengers without difficulty, though modern pressurization controllers are usually operated at perhaps half this rate.

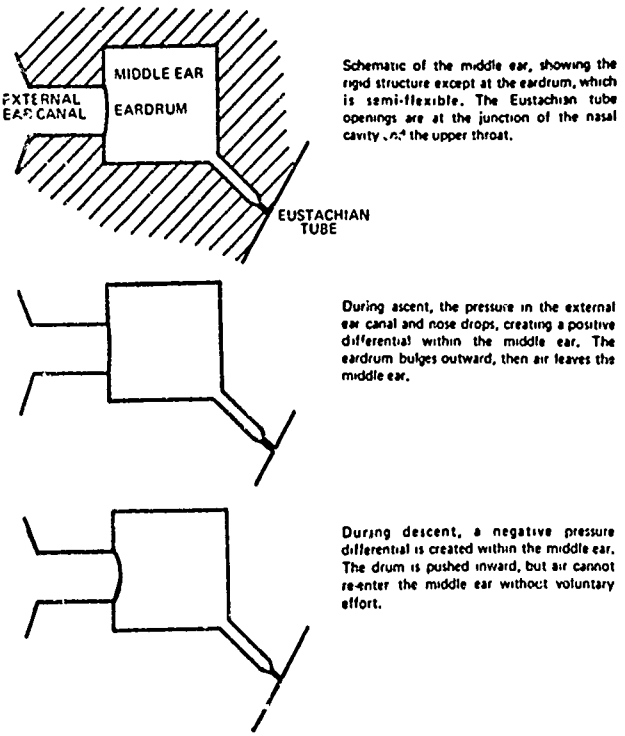


Figure 1–6. Effect of pressure change on middle ear.

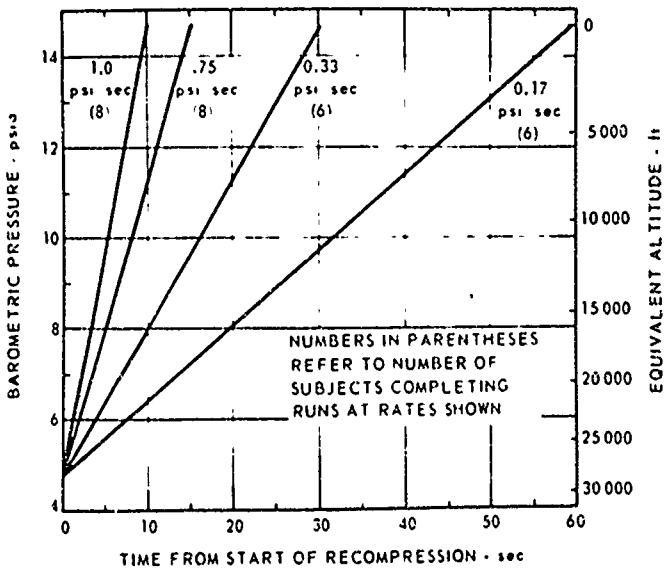


Figure 1–7. Rapid compressions from 4.7 to 14.7 psi (28 000 ft to sea level). (Raeke & Freedman, 1961)

Table 1–3

Type of Ear Complaints Encountered During Change in Barometric Pressure

Ascent (mm Hg)	Complaint	Descent (mm Hg)
0	No sensation; hearing is normal (level flight)	0
+ 3 – 5	Feeling of fullness in ears	– 3 – 5
+10 – 15	More fullness, lessened sound intensity	– 10 – 15
+15 – 30	Fullness, discomfort, tinnitus in ears: Ears usually "pop" as air leaves middle ear Desire to clear ears; if this is done, symptoms stop	– 15 – 20
+30 plus	Increasing pain, tinnitus, and dizziness	– 30 – 60
	Severe and radiating pain, dizziness, and nausea	– 60 – 80
	Voluntary clearing becomes difficult or impossible	–100
	Eardrum ruptures	200+

(Modified from Adler, 1964)

NOTE. During ascent pressure in middle ear is higher than ambient pressure; during descent, middle ear pressure is lower than ambient.

The likelihood of difficulty in "clearing the ears," and thus the likelihood of barotitis, as ear trouble due to pressure change is called, is much greater in an individual in whom the nasal mucous membranes are swollen, with resultant constriction of the Eustachian tube orifice. This occurs with upper respiratory infections such as the common cold, nasal allergies (hay fever), and the like. Barotitis is the most common medical problem in the flying population, largely because the conditions which cause it are so common in temperate climates.

The Sinuses. The paranasal sinuses are small, rigid air filled cavities in the skull. They communicate with the nose through small ducts. Unlike the Eustachian tube, these ducts show no particular predisposition to blockage during descent. Inflammation or swelling of the mucous membranes of the sinuses or nose, however, can cause partial or complete obstruction of these ducts, and thus a differential pressure between the sinus and the environment during changes of environmental pressure. Severe or incapacitating pain may result, a condition known as barosinusitis.

The Teeth. Occasionally, toothaches are reported during changes in barometric pressure, this is called barodontalgia. The condition usually occurs in teeth which have been filled, or in which cavities are present. The explanation usually given is that a small air bubble is trapped below a

restoration or in the decayed tooth substance. There is, however, evidence that loose fillings may allow saliva to penetrate into the interior of these teeth during changes of pressure (Restarski, quoted by Adler, 1964).

In summary, symptoms due to trapped gas are relatively common in altitude chamber flights, where the changes in pressure are fairly large. It should be noted, however, that the rate of pressure change with changes in altitude is greatest near sea level. The three problems cited, therefore, commonly occur at comparatively low altitudes and in diving. Barotitis, in particular, often occurs below 5000 feet altitude. The incidence of such problems in a large number of routine altitude indoctrination "flights" is shown in table 1-4.

Table 1–4

Incidence of Symptoms Due to Trapped Gas in 51 580 Altitude Indoctrination Flights*

Symptoms	Severity (Grade)				Total
	I	II	III	IV	
E .. pain	6650	2437	514	–	9601
Abdominal pain	2738	1187	322	12	4259
Sinus pain	1516	723	176	–	2415
Toothache	285	142	118	–	545
TOTAL	11 189	4489	1130	12	16 820

*Numbers shown are rates per 100 000 man-flights.
(From data of Berry, 1958)

The Lungs. Unlike the middle ear, sinuses, and teeth, the lung-chest system is capable of wide variations in volume. Its minimum, or residual, volume in an adult male is commonly less than 1.5 liters; its maximum volume during full inspiration may exceed 8 liters. When barometric pressure increases, therefore, the volume of gas in the lungs is free to contract. If the lungs are in communication with the environment, air flows into them. During breath-holding diving, however, the volume of air in the lungs contracts in accordance with Boyle's law (allowing for the constant pressure of water vapor).

If the pressure ratio (ratio of final to initial pressure) is such as to compress the air in the lungs to less than the residual volume of the system, a phenomenon known commonly as "squeeze" occurs. The relative vacuum in the lungs causes an increase in the blood volume in the chest. The lungs are pulled toward a position of greater collapse than they can attain within the closed chest: the result is pain and hemorrhage into the lung tissue and airways. This condition is of practical importance only in underwater work, where large changes in

pressure can occur rapidly. It is the limiting factor in breath-holding diving (Schaefer et al., 1968). Squeeze can also occur in face masks used in diving if air is not introduced into the mask during descent.

Problems Due to High Dynamic Pressures on the Body. During ejection or manual escape from aircraft, a pilot is suddenly thrust from a cockpit in which the air around him is moving at the same velocity he is into an environment in which he is a projectile. The dynamic pressure Q exerted on the frontal surface of his body (if he is facing forward) is a function of the air density and his airspeed.

$$Q = \frac{Pv^2}{2}$$

Pressures of 1000 psf (7 psig) are not uncommon during high speed, low altitude ejections. Figure 1-8 shows data collected during human exposures to high dynamic pressure produced on an underwater centrifuge. The figure shows injuries produced by the more severe exposures. Figure 1-9 shows the separation forces developed on the arms and legs plotted against overall dynamic pressures (Fryer, 1962). It should be noted that ejection in the rearward facing position offers a substantial degree of protection against Q forces, by interposing the seat between the subject and the source of pressure (see chapter 4, *Sustained Linear Acceleration*).

Problems Due to Blast. A pressure wave, moving outward from the source of an explosion, may act as do high dynamic pressures on people and objects in its path. Many injuries caused by explosives are due to bodies being thrown about. If a body is restrained, however, the overpressure will cause different displacements of the compressible and incompressible portions of the body. These overpressures, and the following underpressures, involve very rapid changes of pressure and thus of local force fields within the body. The chest, and other air filled cavities, not being entirely elastic, cannot respond instantaneously. As a result, substantial shear forces are produced, with tearing of tissues.

No data are available on fatal shock pressures in man. Figure 1-10 shows 50 percent lethal shock pressures for animals restrained in a shock tube, with an estimate of the median lethal overpressure for man. Figure 1-11 shows calculated curves of equal maximum strain in the human lung.

The pulse signature of sonic booms involves an almost instantaneous rise in pressure, a ramp decay, and a very rapid return to atmospheric pressure following the passage of the wave (N wave). Sonic booms, however, rarely involve peak pressures of more than 10 psf; pressure changes of this magnitude are annoying, but not physically harmful, to humans. Most booms encountered on the ground have peak pressures no higher than 1 to 2 psf.

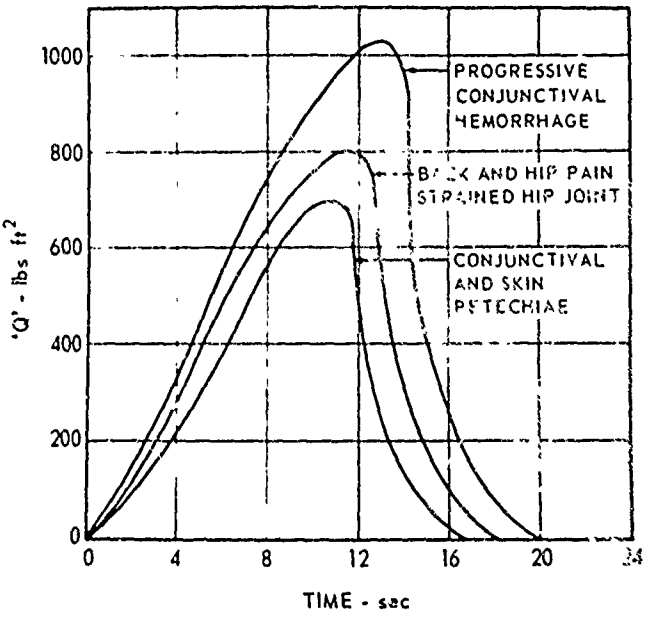


Figure 1–8. Data obtained on two subjects in ejection seat attached to arm of underwater centrifuge. Subjects wore rubber suits, full face helmets, and mouthpieces for underwater breathing. They held their breath during accelerations. Maximum forces shown (1030 psf were obtained at 32.6 fps equivalent to 515 kts in air. Time course of runs is shown. (Drawn from data of Fryer, 1962)

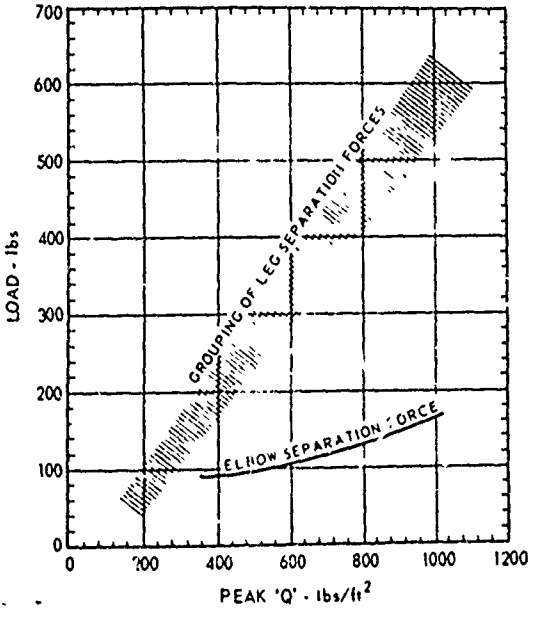


Figure 1–9. Leg and elbow separation forces, determined by strain gauges attached to a and leg restraints during underwater centrifuge runs shown in figure 1–8. (Drawn from d of Fryer, 1962)

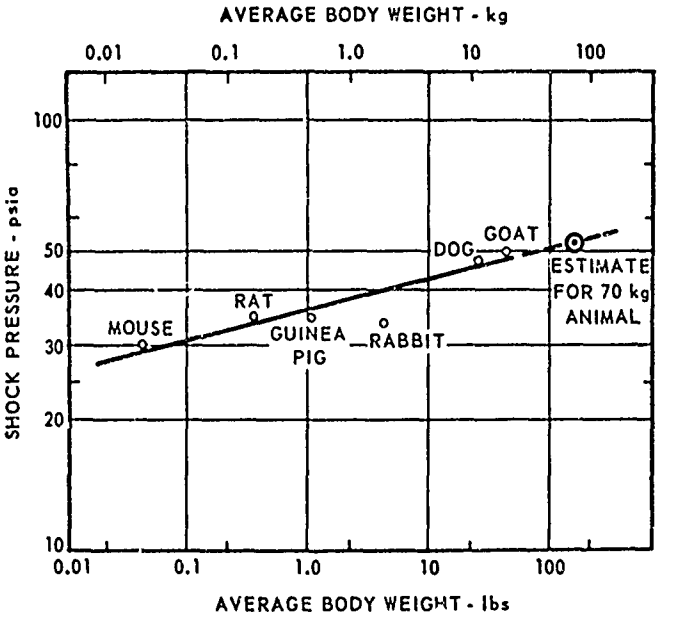


Figure 1–10. Overpressures necessary to kill 50% of animals of various species exposed in a shock tube to overpressure lasting 350 to 412 msec, extrapolated to estimate median lethal overpressure for 70 kg (man-sized) animal. (Sources: Richmond & White, 1962)

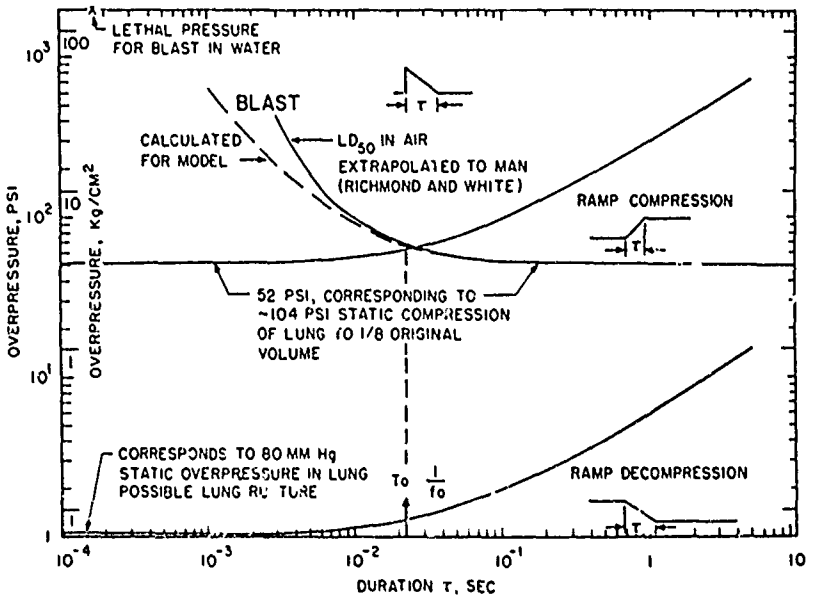


Figure 1–11. Calculated curves of equal strain in human lung in response to blast, ramp compression, and ramp decompression, as a function of overpressure and duration of event (Source: von Gierke, 1964)

Effects of Decreases in Barometric Pressure

Decreases in barometric pressure occur when a diver ascends through water, or when an aircraft or space vehicle ascends through the atmosphere. More sudden decreases in pressure are encountered during depressurization of an aircraft, space cabin or pressure suit, whether accidental or intentional.

Effect of Decompression on Trapped Gases.

The Ears, Sinuses, and Teeth. It was mentioned previously that the ear rarely poses a problem during ascent because the structure of the Eustachian tube allows air to escape from the middle ear passively. Pain in the sinuses is more likely to occur if an obstruction to airflow exists. Tooth pain is probably more common during ascent than descent.

The Stomach and Intestines. The human gut contains a variable amount of gas, some of it swallowed with food and saliva, the rest arising from the metabolic activity of gas-forming bacteria in the intestinal tract. The volume of intestinal gas at sea level usually varies from about 0.05 to 0.10 liters. Ingestion of gas-forming foods, such as baked beans, can, however, elevate this value by an order of magnitude (Allen & Chinn, cited by Greenwald, Allen, & Bancroft, 1967). In one series of experiments, Greenwald and coworkers (1967) observed increases in intestinal gas volume in subjects decompressed to high altitude (figure 1-12), together with a roughly predictable increase in the incidence of abdominal symptoms (figure 1-13). In these studies, however, subjects attempted to retain intestinal gas throughout the exposures.

Normally, an increase in the volume of a gas bubble in the gut causes stretching of the walls of the tube, which reflexly causes propulsive muscular contraction of the walls, together with the feeling known as "cramps." These propulsive contractions usually move the gas to the lower bowel, from which it is expelled. If the gas is in the stomach, it is expelled by belching. Such gas bubbles have, however, been known to cause vomiting in divers during ascent. Adler (1964) reported a lower incidence of symptoms due to intestinal gas during routine altitude chamber flights.

Bryan (1961) has hypothesized that whereas relatively slow expansions of intestinal gas leads to muscular contractions, cramps, and, usually, to expulsion of gas, very rapid expansion during a rapid decompression may simply result in extreme stretching of a relaxed gut wall, which, by reflex action, can cause marked slowing of the heart and unconsciousness without warning. It may be difficult to differentiate fainting due to this from that due to lack of oxygen or to decompression sickness.

The Lungs. Although the air in the lungs and airways is normally in free communication with the environment, the outward flow of air during a very rapid decrease in barometric pressure is limited by aerodynamic considerations. The physical damage that may occur in the lungs is generally considered to be the critical limiting factor in human tolerance for very rapid

decompressions. Haber and Clamann (1953) have defined pressure transients during rapid decompression in terms of the two principal parameters. The *time characteristic*, t_c, has the general form:

$$t_c = \frac{V}{A \cdot C}$$

Where V is the volume of the container being compressed, A is the effective area of the orifice (A is always somewhat smaller than the geometric orifice, for aerodynamic reasons), and C is the velocity of sound.

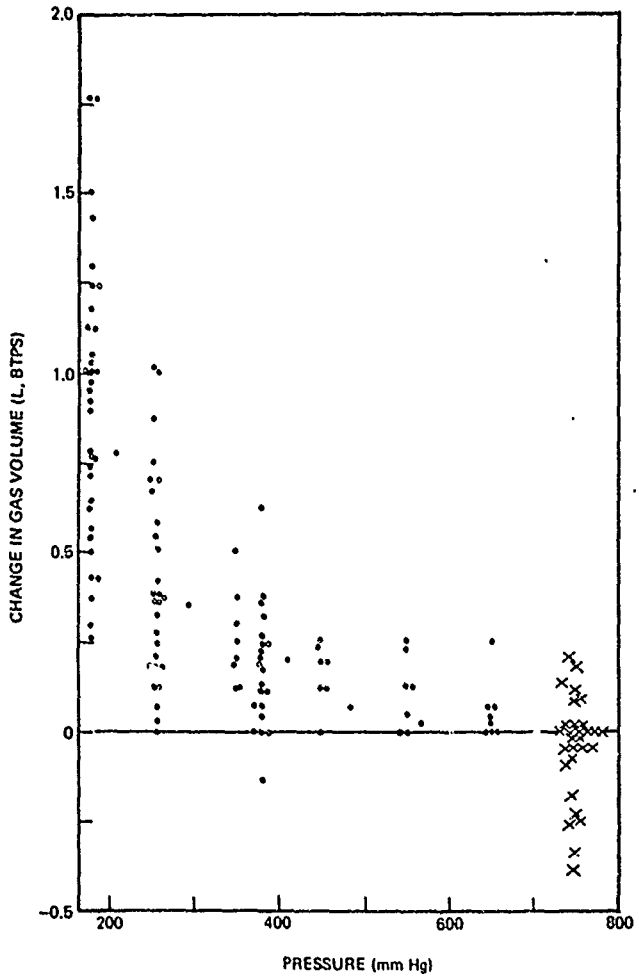


Figure 1–12. Expansion of lower trunk during slow decompressions from near sea level to indicated barometric pressures. Filled circles denote studies in which water-filled stomach tube was connected to pressure transducer; open circles represent experiments without tube. X's show lower trunk volumes after decompression and return to original pressure. (Adapted from Greenwald, Allen, & Bancroft, 1967)

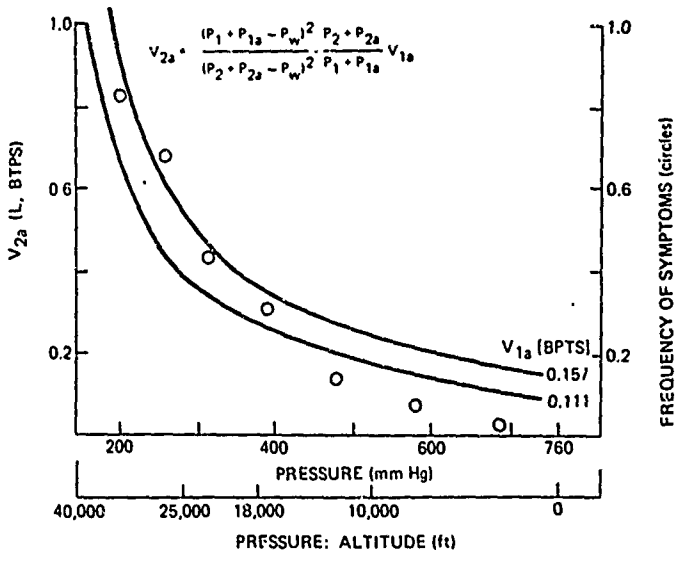


Figure 1–13. Incidence of symptoms of abdominal fullness or pain (circles) during slow decompressions, versus average increase in intestinal gas volume at indicated pressures. Curves for initial gas volumes were derived from equation shown, in which P_1 = ambient ground level pressure, P_2 = pressure at any point during ascent, P_{1a} = intraabdominal pressure (gauge), and P_w = water vapor pressure at body temperature. (Adapted from Greenwald, Allen, & Bancroft, 1967)

The *pressure factor P'* is a function of the initial pressure P_i and the final pressure P_f in the container (figure 1-14).

$$P' = f\left[\frac{P_i - P_f}{P_i}\right]$$

The total decompression time, or duration of the transient t_d is the product of the time characteristic of the system t_c and the pressure factor P':

$$t_d = t_c \cdot P'$$

If the time characteristic of the human lungs and airways is greater than the time characteristic of the pressure suit or cabin in which a subject is confined during a decompression, a transient differential pressure buildup must occur within the lungs. This is illustrated diagrammatically in figure 1-15.

Figure 1-16 shows experimental data demonstrating the differential pressures observed during various decompressions. Points have been derived

from the data of Luft and Bancroft (1956) and Luft, Bancroft, and Carter (1953). Though Adams and Polak (1933) have shown that the mammalian lung may rupture when distended by a differential pressure above about 80 mm Hg, the subjects for whom data are shown in the figure were apparently uninjured. Figure 1-17 shows the time characteristic as a function of container volume V and effective orifice area A. The time characteristic for one of the subjects whose data are plotted in figure 1-16 is shown. Since the volume of the lungs varies with respiration, it is obvious that the time characteristic of the lungs may vary considerably, depending on the phase of respiration during which a rapid decompression occurs. The time characteristic increases to infinity during swallowing or straining, when the airway is closed by the glottis. Severe lung injury or death can result from a rapid decompression while the glottis is closed.

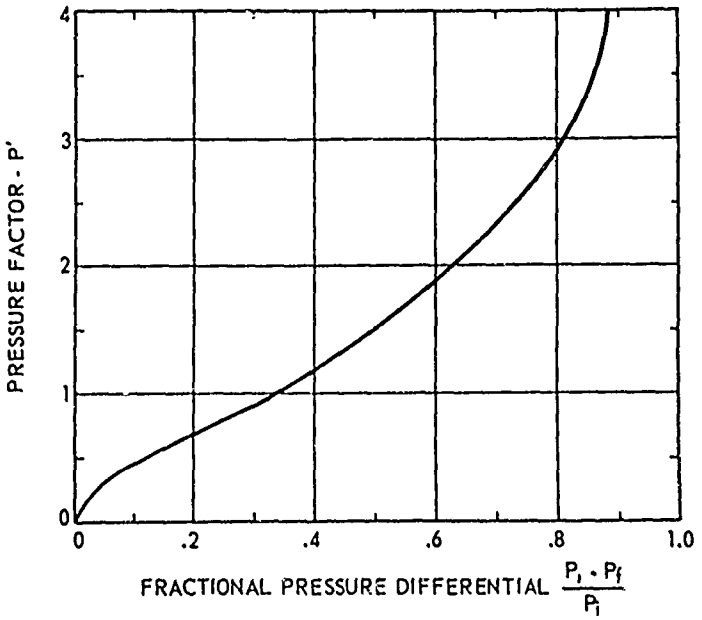


Figure 1–14. Pressure factor P' related to fractional pressure differential. (Drawn from data of Haber & Clamann, 1953)

Experiments on dogs rapidly decompressed from 180 to less than 2 mm Hg (a fractional pressure differential of 0.99) in 1.0 or 0.2 seconds demonstrated lung damage in all cases. Changes in the lungs after a 1 second decompression, however, were reversible in animals who stayed at the low pressure for short periods of time; they became more severe and lasting as exposure time at 2 mm Hg increased (figure 1-18). If total exposure time was less than 90 seconds only mild residual findings were observed. Faster decompressions produced more severe and lasting damage (Dunn, 1965). Estimates of the probable danger zone for explosive decompressions are shown in figure 1-19.

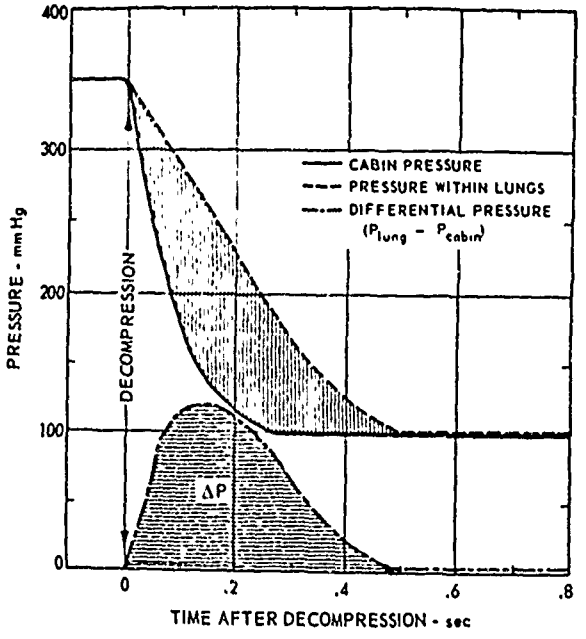


Figure 1–15. Schematic diagram of origin of pressure differentials in the lungs during rapid decompression. (Redrawn from Luft, 1954)

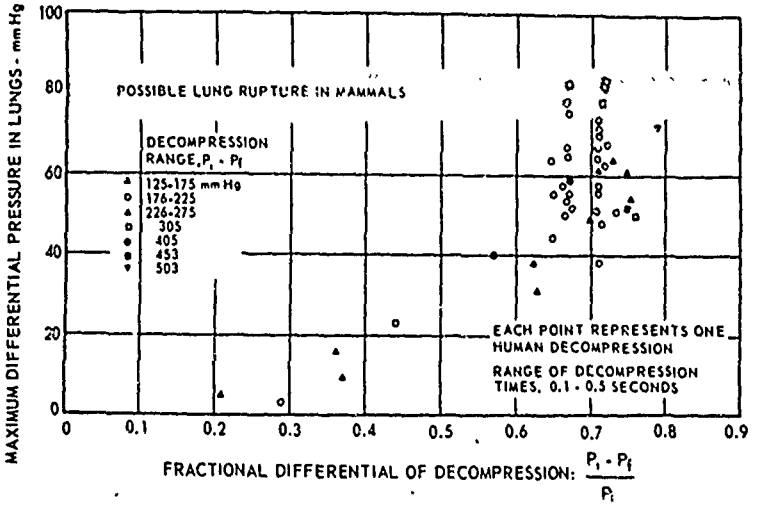


Figure 1–16. Human exposure to rapid decompressions involving significant pressure differentials in lungs. (Drawn from data of Luft & Bancroft, 1956; and Luft, Bancroft, & Carter, 1953)

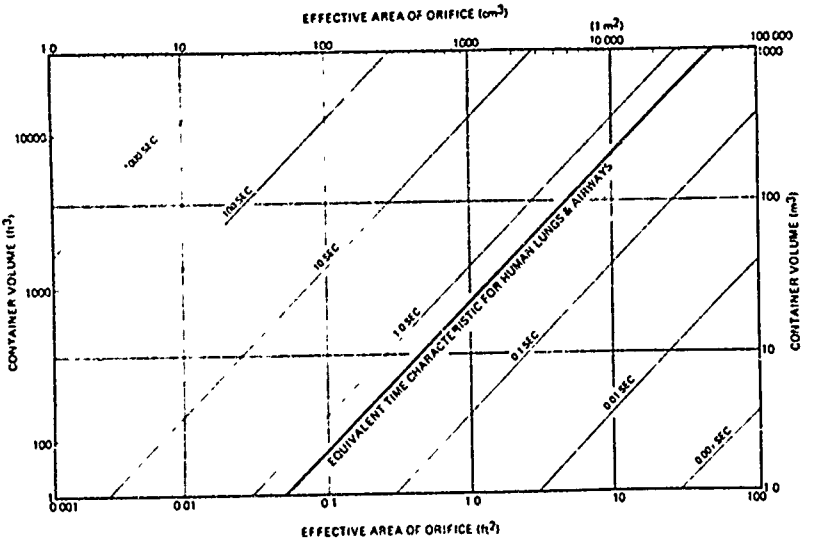


Figure 1–17. Time characteristic, t_c, as a function of container volume and effective area of orifice. (After Luft & Bancroft, 1956)

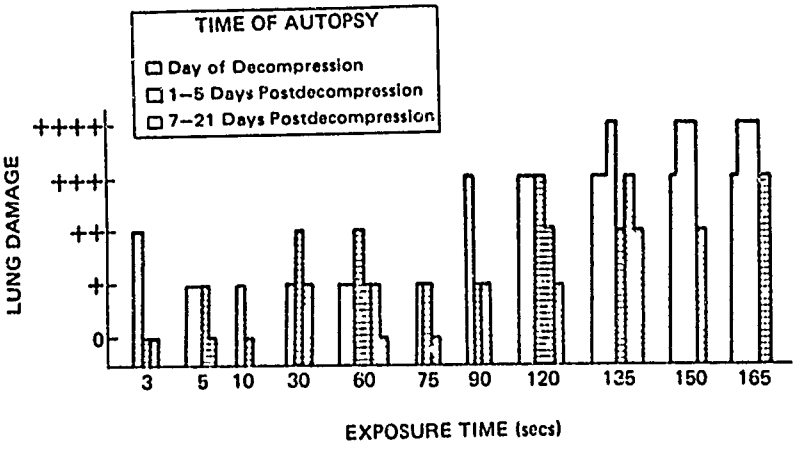


Figure 1–18. Damage produced in lungs of dogs decompressed from 180 to less than 2 mm Hg in 1 sec with 5-sec recompressions after various times at peak altitude. Each column represents one dog, autopsied at time indicated by shading. Scale of damage:

+: Mild reversible changes
++: Several reversible changes together, or moderate damage
+++: Severe changes, including hemorrhage involving 30% of the lungs
++++: Hemorrhage involving 30% of the lung substance.

(Taken from Dunn, 1965)

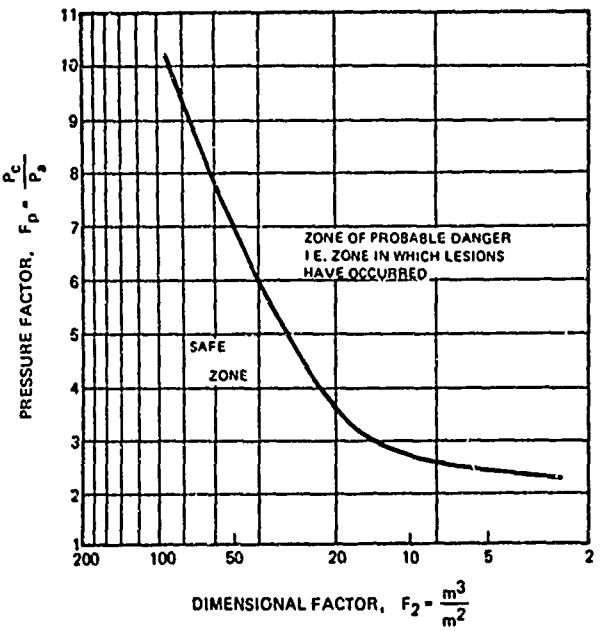


Figure 1–19. Curve derived from data of Violette, defining zones of safety and probable danger in explosive decompression. (Source: Fryer, 1965; reprinted by permission of the Controller of Her Britannic Majesty's Stationery Office)

Problems Due to Evolved Gas Within the Body. During prolonged exposure to atmospheres that contain physiologically inert gases (nitrogen, hydrogen, helium, argon, xenon, and krypton), the body fluids (water and fat) contain amounts of these gases in solution proportional to the partial pressure of the gas in inspired air and the solubility of the gas in water and fat at body temperature. If the body is subsequently exposed to a much lower barometric pressure, inert gases tend to come out of solution (the phenomenon of effervescence). Oxygen, carbon dioxide, and water vapor diffuse rapidly into evolved bubbles of inert gas. Such bubbles, if they form in tissues, may produce pain, especially around the joints. Bubbles within fat cells may cause rupture of the cell walls, allowing fat to enter the circulation. If bubbles form within blood vessels, they are carried to the small terminal vessels of the body (especially the lungs) where they lodge, cutting off the blood supply of the tissues behind them. The symptoms caused by evolved gas are known collectively as decompression sickness.

This disorder is a potential problem in divers who ascend to the surface of the water after minutes or hours at depth, in caisson workers who are decompressed at the end of each working day, and in aviators or astronauts who are exposed to low barometric pressures after reaching equilibrium at higher pressures.

Decompression Sickness. Decompression sickness in its various forms is much more common in divers and caisson workers than in aviation personnel. In

the latter context, it has been reported at altitudes as low as 8000 feet (10.9 psia) in pilots who took off shortly after a period of scuba diving at modest depths. This problem and its prevention are discussed by Edel and coworkers (1969). Decompression sickness has been reported at altitudes of 17 000 feet (7.64 psia) without previous underwater exposure; one fatality has occurred after exposure to 18 000 feet (7.3 psia). Despite these isolated cases the disorder is uncommon below about 30 000 feet (4.4 psia).

The symptoms of decompression sickness are rarely observed during the first few minutes of exposure to low pressure. Thereafter, the rate of appearance of symptoms is a function of exposure time (figure 1-20). Several factors influence the incidence of decompression sickness at high altitude. Among the most important is exercise (figure 1-21). Other factors which are strongly positively correlated are age and body weight (especially body fat mass) (figure 1-22). There is evidence that cold also increases the incidence of decompression sickness.

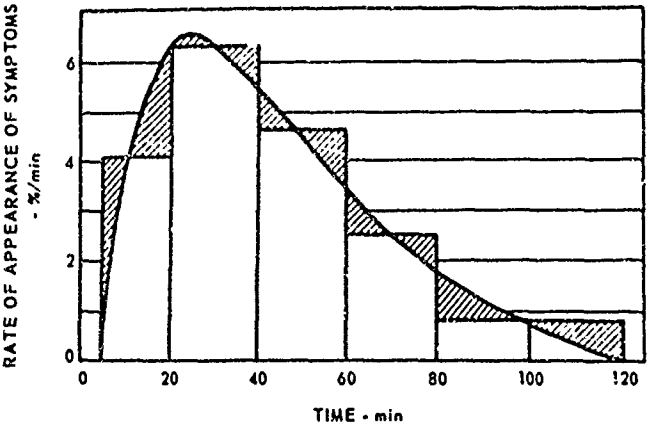


Figure 1-20. Rate of appearance of symptoms of decompression sickness as a function of exposure time under standard conditions. Histogram represents observed data; curve overlying it is derived from a formula for bubble formation. (Redrawn from Nims, 1951, cited by Fulton, 1951)

While joint pains (bends) are by far the most common manifestation of the disorder, other more serious symptoms are also observed. The relative incidence of these manifestations in two large series of observations is shown in table 1-5.

There is little doubt that the cause of decompression sickness is bubbles of gas evolved from solution in the body fluids. There are probably other related factors, however, having to do with the circulation of blood to various regions of the body. Useful general references which treat the subject in detail are Nims (1951), Anderson (1965), and Fryer (1969).

Protection Against Decompression Sickness. Since the appearance of decompression sickness is highly correlated with the quantities of inert gases in the body in relation to their solubility in body fluids, one effective means of decreasing the incidence of this disorder is to affect partial elimination of these

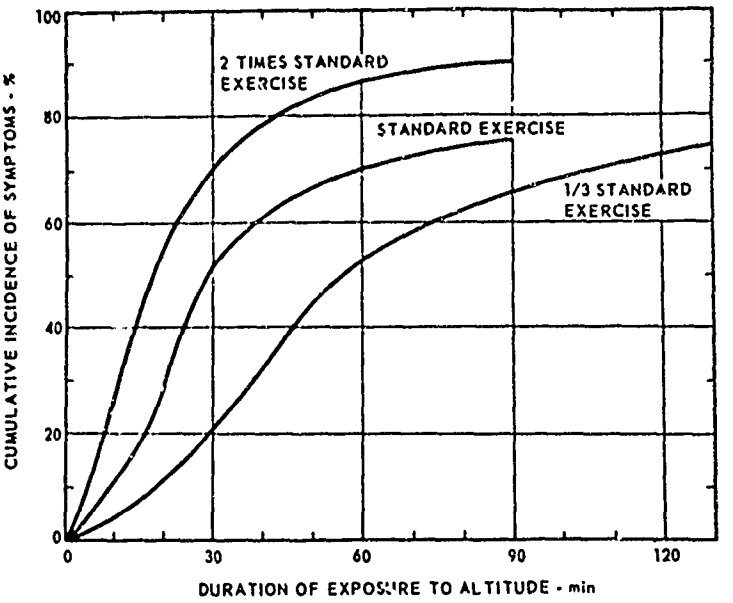


Figure 1–21. Effect of muscular exercise on appearance of symptoms of decompression sickness at 38 000 ft (3 psia). Number of subjects varied from 53 to 139. Standard exercise was 10 step-ups onto a 9 in stool in 30 sec, repeated every 5 min. (Drawn from Henry, 1956)

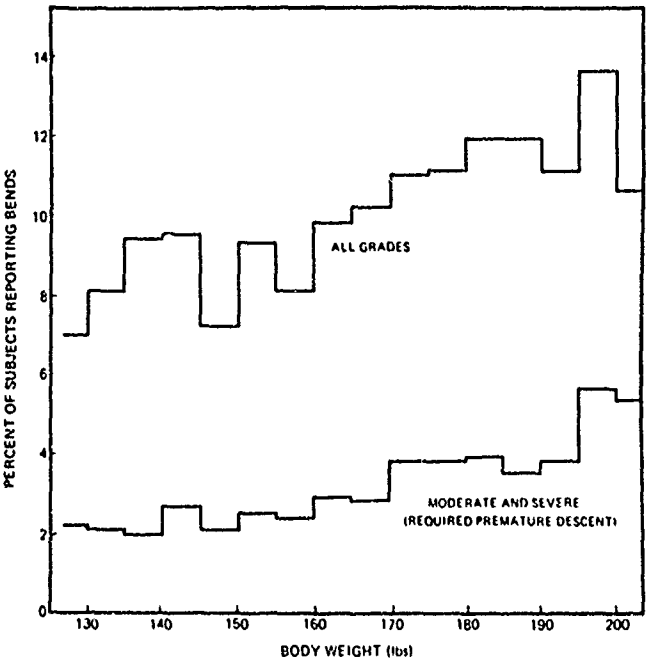


Figure 1–22. Proportional incidence of bends as a function of body weight in 44 181 trainees undergoing altitude chamber training during World War II. (Data of Motley et al., summarized by Adler, 1964)

inert gases prior to or during ascent. The quantity of inert gas in solution in the human body at equilibrium is a function of the partial pressure of that gas in the inspired air and the solubility of the gas in water and in fat. When the inert gas is removed from the inspired gas mixture, the gas will be cleared from the body (washed out) at a rate which depends on a number of factors. Among these are the ventilation volume and the cardiac output, both of which are elevated during exercise. Inert gas in the lungs is diluted and washed out very quickly. Blood coming to the lungs is also cleared relatively rapidly. The clearance of gas from the various tissues of the body proceeds at a rate proportional to the blood flow through the tissues, the solubility of the gas in water versus that in oil, and tissue-blood vessel geometry.

Table 1–5

Incidence of Decompression Sickness in High Pressure Environments and at High Altitude

Type	Incidence (%)	
	Caisson Workers*	Altitude Workers**
Bends (alone or with other symptoms)	33.34	2.4
CNS symptoms	2.98	0.03
Chokes	0.60	0.07

*Data of Keays, in Adler (1964) for 557 000 work shifts in 10 000 caisson workers.

**Data of Berry (1958) for 51 580 man-exposures in altitude chamber training flights. Number of subjects is not specified, but the number of exposures per man was probably one in nearly all cases.

Nitrogen is very soluble in fat and less soluble in water. In contrast, helium is only slightly soluble in body fluids. Nitrogen is cleared from the body rather slowly, helium much more rapidly. Elimination of either gas is facilitated by exercise. This is illustrated in figure 1-23.

As noted above, inert gas may be eliminated from the body by breathing air free of that gas. Most studies of decompression sickness have utilized 100 percent oxygen as the inspired gas during the nitrogen washout period. The effect of such preoxygenation (actually preexposure denitrogenation) is illustrated in figure 1-24. In all cases, after a control period at ground level, subjects were taken to 38 000 feet breathing oxygen, at which altitude they performed five knee bends every 3 minutes until the appearance of joint pains, presumably caused by extravascular bubble formation. The protective effect of nitrogen washout is in part a function of the duration of preoxygenation prior to exposure to altitude, but protection is not entirely proportional to the extent to which body nitrogen stores are depleted. Occasional cases of decompression sickness are seen even after many hours of preexposure denitrogenation.

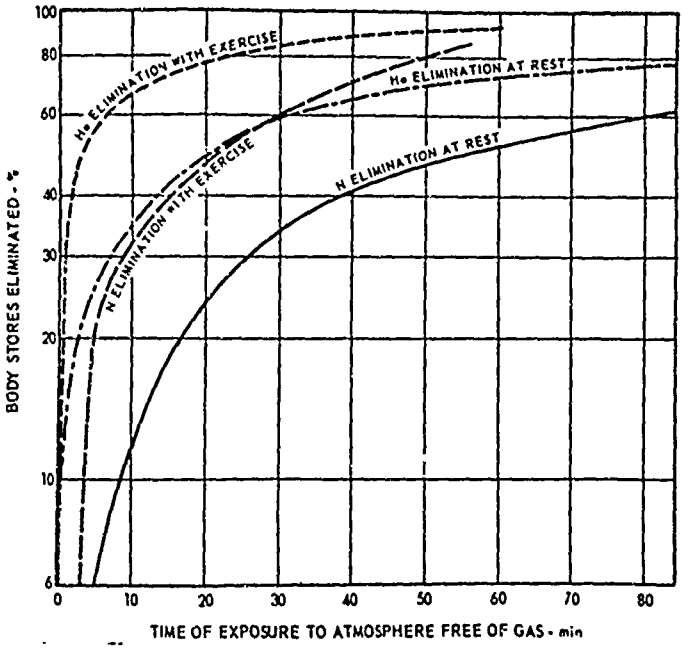


Figure 1–23. N_2 and He washout by O_2 breathing at sea level, with and without exercise. (Drawn from data of Behnke, 1945; Balke, 1954; and Roth, 1959; reprinted by permission of Williams & Wilkins Co., Baltimore, Maryland)

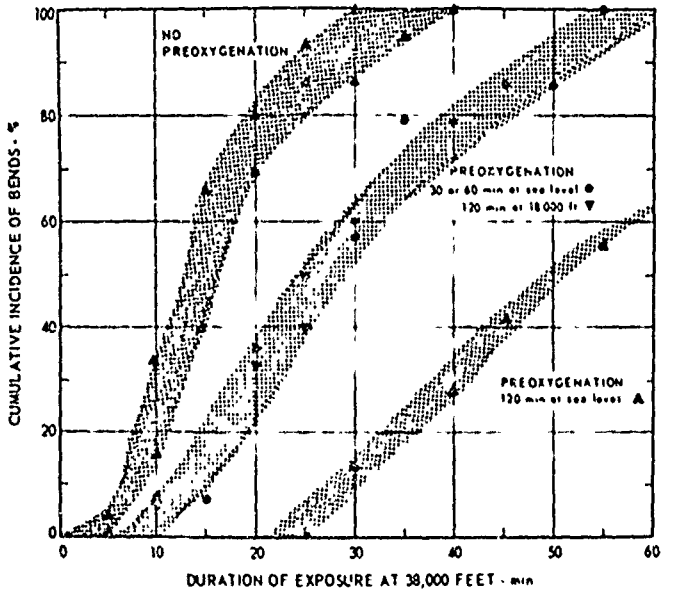


Figure 1–24. Effect of N_2 washout (effected by breathing O_2 for 30 to 120 min at sea level or 18 000 ft) on appearance of bends during subsequent exposure at 38 000 ft with exercise. (Drawn from data of Balke, 1954, and Marbarger, 1957)

The washout rates of nitrogen and helium were illustrated in figure 1-23. Since both of these gases (as well as neon) have been suggested as atmospheric constituents for long-term space missions, it is well to mention that there are appreciable differences between the two as regards the decompression sickness which can occur when they are used. Figures 1-25 and 1-26 indicate that following decompression from 7.0 to 3.5 psia, bends symptoms appeared earlier with helium than with nitrogen, and required greater increases in pressure before relief of symptoms occurred (Beard et al., 1967). This is similar to the experience in diving, in which both gases have been used extensively. Even though the blood and tissue fluids contain less helium than nitrogen after saturation at any pressure, exposure to a lower pressure where bends can occur is more likely to lead to symptoms, and the symptoms are likely to be more severe, with helium. This is presumably because of helium's relative insolubility in body fluids as compared with nitrogen.

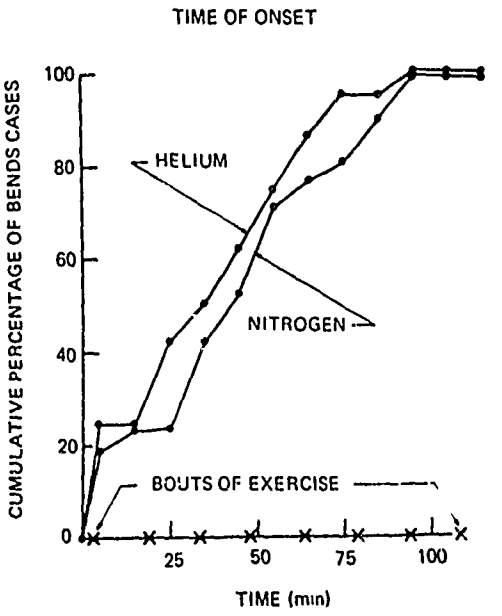


Figure 1-25. Time of onset of bends during standard work at 3.5 psia following prolonged exposure to He-O_2 at 7 psia (24 cases of bends in 106 flights) or N_2-O_2 at 7 psia (21 cases of bends in 119 flights). Subjects breathed 100% O_2 while at 3.5 psia. (Taken from Beard et al., 1967)

Treatment of Decompression Sickness. The treatment of decompression sickness consists primarily of measures designed to decrease the size of bubbles as much as possible and to hasten their dissolution. The first is accomplished by recompression or overcompression (a bubble, once formed, will behave according to Boyle's law as the pressure on it is increased; it will not disappear upon return to the pressure from which the experiment began). Dissolution of the bubbles is thought to be enhanced by treatment with 100 percent oxygen, if the treatment is carried out at 3 atm absolute, or less, or with the highest safe oxygen tension when higher total pressures are used (Melver, 1966)

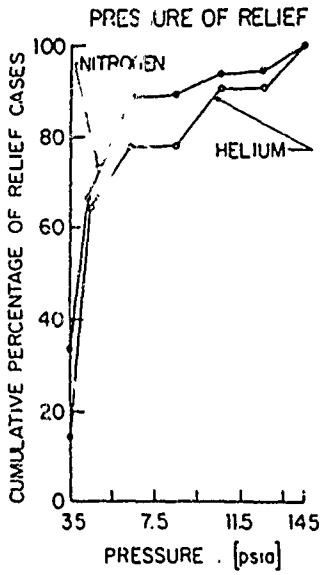


Figure 1–26. Increase in pressure required to relieve bends symptoms shown in figure 1–25. (Taken from Beard et al., 1967)

McIver and coworkers (1967) have pointed out in this regard that by using both maximum space cabin pressure and maximum differential suit pressure, it is possible to provide a limited degree of overcompression in 100 percent oxygen for treatment of decompression sickness occurring during space flight. Their studies indicate the shortcomings of this approach, but they also indicate that it would be at least partially effective.

References

Adams, B. H., & Peiak, I. B. Traumatic lung lesions produced in dogs by simulating submarine escape. *U.S. Naval Medical Bulletin*, 1933, *31*(18).

Adler, H. F. Dysbarism. USAF SAM Review 1-64, School of Aviation Medicine, Brooks Air Force Base, Texas, 1964.

Anderson, H. R. Historical review of the bubble theory of the etiology of decompression sickness as related to high altitude exposure. USAF SAM Review 10-65, School of Aviation Medicine, Brooks Air Force Base, Texas, 1965.

Aquadro, C. F., & Chouteau, J. Problems of extreme duration in open sea saturation exposure. In C. J. Lambertsen (Ed.), *Proceedings of the third symposium on underwater physiology*. Baltimore: Williams and Wilkins Co., 1967, Pp. 98-108.

Armstrong, H. G. (Ed.) *Aerospace Medicine*. Baltimore: Williams and Wilkins Co., 1961.

Balke, B. Rate of gaseous nitrogen elimination during rest and work in relation to the occurrence of decompression sickness at high altitude. USAF SAM Project No. 21-1201-0014, Report No. 6, School of Aviation Medicine, Brooks Air Force Base, Texas, 1951.

Bancroft, R. W., & Dunn, J. E. Experimental animal decompressions to a near vacuum environment. USAF SAM TR-65-48A, School of Aviation Medicine, Brooks Air Force Base, Texas, 1965.

Beard, S. E., et al. Comparison of helium and nitrogen in production of bends during simulated orbital flights. USAF SAM TR-67-201, School of Aviation Medicine, Brooks Air Force Base, Texas, 1967.

Behnke, A. R. The absorption and elimination of gases of the body in relation to its fat and water content. *Medicine*, 1945, *24*, 359-379.

Berry, C. A. Severe dysbarism in Air Force operations and training. *U.S. Armed Forces Medical Journal*, 1958, *9*, 936.

Bert, P. *Barometric Pressure*. Columbus, Ohio: College Book Co., (translated by Hitchcock, M. A., & Hitchcock, F. A.), 1943.

Billings, C. A. Pressure. In P. Webb (Ed.), Bioastronautics Data Book. NASA SP-3006, National Aeronautics and Space Administration, Washington, D.C., 1964.

Bomadmi, A. T., & Pryor, W. H., Jr. Effect of hypobaric and hyperbaric pressure on cell permeability. USAF SAM TR-66-108, School of Aviation Medicine, Brooks Air Force Base, Texas, 1966.

Boothby, W. (Ed.) Handbook of respiratory physiology. USAF School of Aviation Medicine, Randolph Air Force Base, Texas, 1954.

Bryan, A. C. Personal communication, 1961.

Buhlmann, A. A. Respiratory resistance with hyperbaric gas mixtures. In C. J. Lambertsen & L. J. Greenbaum, Jr. (Eds.), *Proceedings of the second symposium on underwater physiology*. Research Council Publication 1181, Washington, D.C.: National Academy of Sciences-National Research Council, 1963, Pp. 98-107.

Casey, H. W., Bancroft, R. W., & Cooke, J. P. Residual pathologic changes in the central nervous system of a dog following rapid decompression to 1 mm Hg. USAF SAM TR-66-203, School of Aviation Medicine, Brooks Air Force Base, Texas, 1966.

Cooke, J. P. Sound transmission in helium and various gases at low pressure. USAF SAM TDR-64-43, School of Aviation Medicine, Brooks Air Force Base, Texas. 1964.

Cocke, J. P., & Bancroft, R. W. Some cardiovascular responses in anesthetized dogs during repeated decompressions to a near vacuum. USAF SAM TR-66-88, School of Aviation Medicine, Brooks Air Force Base, Texas, 1966.

Cooke, J. P., & Beard, S. E. Verbal communication intelligibility in oxygen-helium and other breathing mixtures, at low atmospheric pressures. USAF SAM TR-65-269, School of Aviation Medicine, Brooks Air Force Base, Texas, 1965.

Cooke, J. P., Cam, S. M., & Bancroft, R. W. High venous pressures during exposure of dogs to near vacuum conditions. USAF SAM TR-67-257, School of Aviation Medicine, Brooks Air Force Base, Texas, 1967.

Cooke, J. P., Fife, W. P., & Bancroft, R. W. Comparative cardiovascular responses of baboons and dogs to near vacuum pressures. USAF SAM TR-68-44, School of Aviation Medicine, Brooks Air Force Base, Texas, 1968.

Dunn, J. E. Experimental animal decompressions to less than 2 mm Hg absolute: Pathologic effects. USAF SAM TR-65-48 B, School of Aviation Medicine, Brooks Air Force Base, Texas, 1965.

Edel, P. O., et al. Interval at sea-level pressure required to prevent decompression sickness in humans who fly in commercial aircraft after diving. *Aerospace Medicine*, 1969 *40*, 1105-1110.

Fenn, W. O. Possible role of hydrostatic pressure in diving. In C. J. Lambertsen (Ed.), *Proceedings of the third symposium on underwater physiology*. Baltimore: Williams and Wilkins Co., 1967.

Fryer, D. I. Failure of pressure cabins. In J. A. Gillies (Ed.), *Textbook of aviation physiology*. Oxford: Pergamon Press, 1965, Pp. 187-206.

Fryer, D. I. Physiologic effects of exposure to ram pressure. *Aerospace Medicine*, 1962, *33* 34-41.

Fryer, D. I. Subatmospheric decompression sickness in man. AGARDograph No. 125, Technivision Services, Slough, England, 1969.

Greenwald, A. J., Allen, T. H., & Bancroft, R. W. Abdominal gas volume at altitude and at ground level. USAF SAM TR-67-102, School of Aviation Medicine, Brooks Air Force Base, Texas, 1967.

Haber, F., & Clamann, H. G. A general theory of rapid decompression. Project No. 21-1201-0008, Report No. 3, School of Aviation Medicine, Randolph Air Force Base, Texas, 1953.

Henry, F. M. Effects of exercise and altitude on the growth and decay of aviator's bends. *Journal of Aviation Medicine*, 1956, *27*, 250-259.

Hyde, A. S., Pines, J., & Saito, I. Atelectasis following acceleration: A study of causality. *Aerospace Medicine*, 1963, *34*, 150-157.

Jaeger, M. J., & Otis, A. B. Effects of the compressibility of alveolar gas on the dynamics and work of breathing. USAF SAM TDR-63-71, School of Aviation Medicine, Brooks Air Force Base, Texas, 1964.

Kylstra, J. A. Advantages and limitations of liquid breathing. In C. J. Lambertsen (Ed.), *Proceedings of the third symposium on underwater physiology*. Baltimore: Williams and Wilkins Co., 1967.

Luft, U. C. Physiological aspects of pressure cabins and rapid decompression. In W. Boothby (Ed.), *Handbook of respiratory physiology*. Randolph Air Force Base, Texas: School of Aviation Medicine, 1954.

Luft, U. C., & Bancroft, R. W. Transthoracic pressure in man during rapid decompression. USAF SAM Report No. 56-61, School of Aviation Medicine, Brooks Air Force Base, Texas, 1956.

Luft, U. C., Bancroft, R. W., & Carter, E. T. Rapid decompression with pressure-demand oxygen equipment. USAF SAM Project No. 21-1001-0008, Report No. 2, School of Aviation Medicine, Brooks Air Force Base, Texas, 1953.

Marbarger, J. P., et al. Studies in aeroembolism. USAF SAM Report No. 57-44, School of Aviation Medicine, Brooks Air Force Base, Texas, 1957.

Melver, R. G. Treatment of altitude dysbarism with oxygen under high pressure-report of three cases. USAF SAM TR-66-318, School of Aviation Medicine, Brooks Air Force Base, Texas, 1966.

Melver, R. G., et al. Treatment of decompression sickness in simulated space flight. USAF SAM TR-67-249, School of Aviation Medicine, Brooks Air Force Base, Texas 1967.

Nims, L. F. Environmental factors affecting decompression sickness. In J. F. Fulton (Ed.), *Decompression sickness*. Philadelphia: W. B. Saunders Co., 1951.

Otis, A. B., Fenn, W. O., & Rahn, H. Mechanics of breathing in man. *Journal of Applied Physiology*, 1950, *2*, 592-607.

Raeke, J. W., & Freedman, T. Human response to rapid recompression. Presented to Aerospace Medical Association Meeting, Chicago, 1961.

Rawlins, J. Personal communication, 1970.

Richmond, D. R., Clare, V. R., Goldizen, V. C., Pratt, D. E., Sanches R. T., & White, C. S. Biological effects of overpressure. *Aerospace Medicine*, 1961, *32*, 997-1008.

Richmond, D. R., & White, C. S. A tentative estimate of man's tolerance to overpressures from air blast. Technical progress report on Contract DA-49-146-XZ-055, Lovelace Foundation, Albuquerque, New Mexico, 1962.

Roth, E. Some theoretic aspects of the use of inert gases in sealed cabin environments. USAF SAM Report No. 58-152, School of Aviation Medicine, Brooks Air Force Base, Texas, 1959.

Schaefer, K. E., et al. Pulmonary and circulatory adjustments determining the limits of depth in breathhold diving. *Science*, 1968, *162*, 1020-1023.

United States House of Representatives Select Committee on Astronautics and Space Exploration. *Space handbook: Astronautics and its applications.* House Document No. 86, First Session, 86th Congress. Washington, D.C.: U.S. Government Printing Office, 1959.

von Gierke, H. W. Biodynamic response of the human body. *Applied Mechanics Review*, 1964, *17*, 951-958.

Wather-Dunn, W. Limitations of speech at high pressures in a helium environment. In C. J. Lambertsen (Ed.), *Proceedings of the third symposium on underwater physiology.* Baltimore: Williams and Wilkins Co., Pp. 128-137.

Webb, P. Personal communications, 1969, 1970.

Welch, B. E., et al. The study of man during a 56-day exposure to an oxygen-helium atmosphere at 258 mm Hg total pressure: Thirteen reports by various participating investigators. *Aerospace Medicine*, 1966, *37*, 449-462, 552-608.

Wood, L. H., Bryan, A. C., & Koch, G. H. Limitations of ventilation in a hyperbaric environment. Preprints of Scientific Program, Aerospace Medical Association Meeting, Washington, D.C., May 1969, Pp. 196-197.

Workman, R. O., cited by Wood, W. B. Ventilatory dynamics under hyperbaric states. In C. J. Lambertsen & L. J. Greenbaum, Jr. (Eds.), *Proceedings of the second symposium on underwater physiology.* Publication 1181, Washington, D.C.: National Academy of Sciences-National Research Council, 1963, Pp. 108-123.

Wortz, E. C., et al. Reduced barometric pressure and respiratory water loss. USAF SAM TR-66-4, School of Aviation Medicine, Brooks Air Force Base, Texas, 1966.

CHAPTER 2
ATMOSPHERE

by

Charles E. Billings, M.D.
The Ohio State University

The composition and pressure of the gaseous environment in which man lives are critical in life processes. Chapter 1 described the effects of barometric pressure *per se*. In this companion chapter, consideration is given to the properties of elements and compounds which make up or may be added to a gaseous environment suitable for the human. Both abundant and rare gases are discussed, since virtually all the inorganic gases found in earth's atmospheric envelope have been used or considered for use in life support systems. Oxygen is considered first since it is the one atmospheric constituent whose presence is absolutely necessary for survival. Carbon dioxide is considered next. Although its presence in the environment is not necessary for human life, it, too, is involved in human metabolism and is produced in considerable quantities by man. The remainder of the chapter is devoted to nitrogen, the noble gases, and a brief consideration of other gaseous compounds.

General Considerations

Nearly all the oxygen and carbon dioxide in the human body are present as loosely-bound chemical compounds. These gases enter and leave the body (mostly through the lungs) by diffusion in response to gradients between their partial pressures in the body fluids and in alveolar gas. In the absence of a pressure gradient either in the lungs or in the body tissues, no net flow of either gas can occur. Carbon dioxide is an extremely diffusible gas in tissues made up largely of water; oxygen is less easily diffused.

Figure 2-1 shows the partial pressures (tensions) of oxygen in the environment, in the airways during inspiration, in alveolar gas, in the arterial blood as it leaves the lungs, and in the tissues, where the gas is transferred to its ultimate utilization sites. Similarly, carbon dioxide tensions are shown in the tissues, where carbon dioxide is produced by the combustion of foodstuffs, in the

Reviewed by Christian J. Lambertsen, M.D., University of Pennsylvania Medical Center.

venous blood which carries it to the lungs, and in the alveolar air and arterial blood.

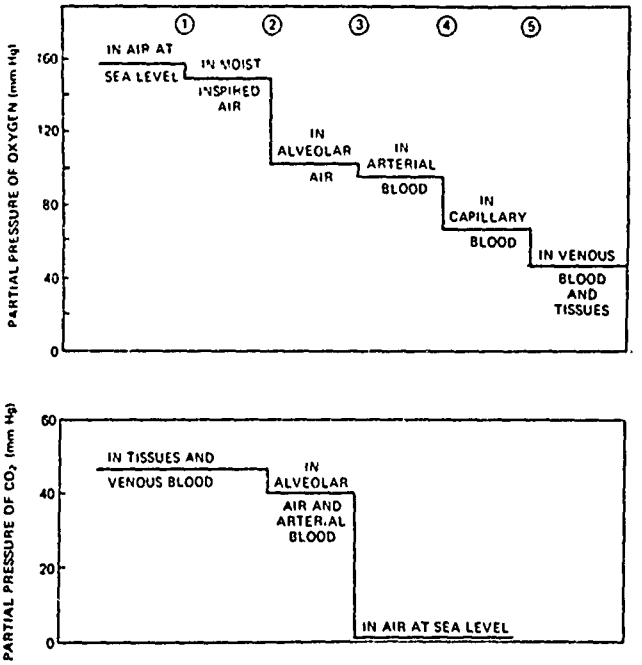


Figure 2–1. Partial pressures of O_2 (above) and CO_2 (below) in air at sea level and at various points within the body. Drop in PO_2 at (1) is due to saturation of incoming air with water vapor; at (2) to presence of CO_2 in alveolar gas; at (3) to limitations in diffusing capacity of O_2; at (4) to extraction of O_2 from arterial blood. The value shown for capillary blood is a mean. Venous blood in man at rest has a PO_2 about half that of arterial blood. All values are approximate. CO_2 is 20 times as diffusible as O_2. Venous blood is in virtual equilibrium with tissue; arterial blood is in equilibrium with alveolar air.

Since all gases in the body are saturated with water vapor, the sum of partial pressures of components of the gas mixture must always be less than the ambient environmental pressure by roughly 47 mm Hg (the partial pressure of water vapor at 37°C mean body temperature). To re-express Dalton's law in these terms,

$$P_B - P_{H_2} = P_{O_2} + P_{CO_2} + P_{N_2} + P_A + \ldots$$

where P_B is barometric pressure and P_A, etc., the partial pressures of the various gases.

The effect of saturation can be seen in figure 2-1: as air enters the upper airways, the partial pressures of oxygen and nitrogen drop slightly due to the addition of water vapor to the gas mixture.

It is important to keep in mind that it is the *partial pressures*, rather than the *concentrations*, of these substances which govern their movement in the body. As an example, the concentration of carbon dioxide in alveolar air at sea level is roughly 5.3 percent (40 mm Hg partial pressure at a barometric pressure of 760 mm Hg). At a pressure altitude of 39 000 feet (P_B 147.5 mm Hg), its concentration at the same partial pressure is 27.1 percent.

All gases present in the atmosphere are also found in solution in the body fluids. The quantity of any gas in the body at equilibrium with its environment is a function of the partial pressure of that gas in the lungs and its solubility in water and fat. Roth (1967) provides a detailed discussion of this topic.

The human body utilizes oxygen in the combustion of fats, sugars, and proteins in the process known as metabolism. The end products of its metabolic processes are carbon dioxide, water, and nitrogenous compounds, principally ammonia and urea. The molar ratio of carbon dioxide produced to oxygen consumed varies from 0.7, when fat is burned, to 1.0 for sugar. Since other gases in the environment are not known to participate in metabolic reactions, they are often called *inert*. There is some doubt whether this appellation is appropriate, but it is commonly encountered in medical and biological literature. It should be noted that this use of the term refers only to the role of these gases within the body. Hydrogen, for instance, is said to be a physiologically inert gas, despite its chemical reactivity.

Oxygen

The presence of molecular oxygen in the environment is absolutely essential for survival. The stores of molecular oxygen in the human body are extremely limited, amounting to little more than a liter of gas at sea level. The brain and associated sensory apparatus (especially the retina of the eye) have the highest oxygen uptake per unit mass of any system of the body; this system amounts to only 2 percent of the body's mass, yet uses 20 percent of the oxygen consumed at rest. Since there is no means whereby the brain can store oxygen or glucose, its only energy source, it is totally dependent on the continuous delivery of adequately oxygenated arterial blood. Deprivation of blood, oxygen, or glucose for more than a few seconds leads to unconsciousness, convulsions, and, thereafter, death of nervous tissue. This is dramatically demonstrated in rapid decompression to a virtual vacuum, described in chapter 1.

Since the partial pressure of oxygen in alveolar air determines its partial pressure in the blood, and, therefore, the quantity of the element carried by hemoglobin, this variable has been studied in some detail. Blockley and Hanifan (1961), in an extensive review of hypoxia following rapid decompressions, have estimated that acute impairment of brain function occurs within about 13 seconds whenever the alveolar oxygen tension drops below a critical level. The severity of impairment and the extent of change in brain electrical activity are proportional to the integral of oxygen tension depression below 30 mm Hg with respect to time (Ernsting, 1961b, 1969). This is illustrated in figure 2-2.

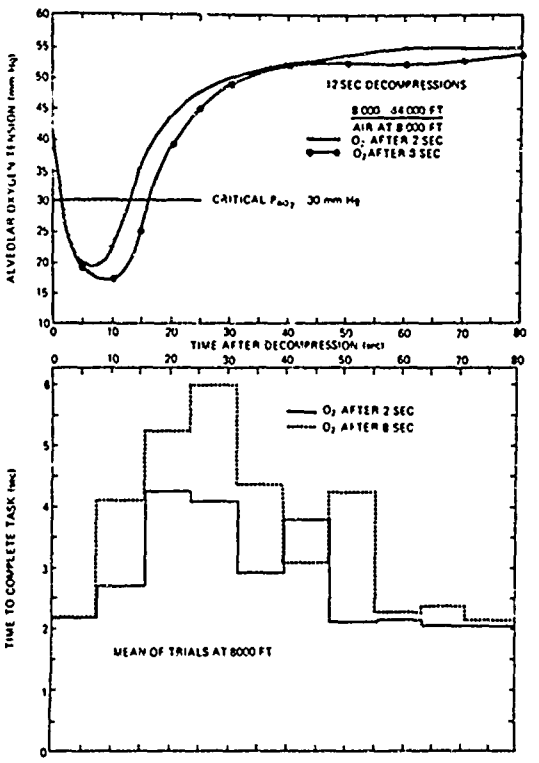


Figure 2–2. *Top.* time course of alveolar O_2 tension when subject breathing air at 8000 ft is rapidly decompressed to 44 000 ft. O_2 was provided either 2 sec or 8 sec after the onset of decompression. O_2 desaturation integrals for the two conditions are crosshatched. *Bottom:* performance decrements resulting from decompression. (Redrawn from data of Ernsting, 1969)

When no oxygen is available for metabolism, as following decompression to a vacuum, the term *anoxia* is used. Anoxia always results in near-immediate unconsciousness, convulsions, and paralysis. If prolonged for more than 90 to 180 seconds, anoxia is almost invariably fatal. The condition caused by a relative lack of oxygen in the body is called *hypoxia.* Depending on its severity, the effects of hypoxia can range from symptoms as severe as those of anoxia to very subtle effects, detectable only by searching examination of the highest functions of the central nervous system. This is illustrated in figure 2-3. As arterial oxygen tension falls, progressive central nervous system impairment occurs. This is indicated on the chart by zones of increasing density. These changes occur in resting subjects who are not fatigued or otherwise stressed. The oxygen saturation of the arterial blood is shown as a function of oxygen tension (the oxyhemoglobin dissociation curve). A range of saturations is shown because temperature and acidity also influence the saturation values.

The lowest barometric pressure at which any sort of purposeful activity can be carried on was discussed in chapter 1. It was defined as a pressure sufficient to permit a reasonable partial pressure of oxygen in the alveolar air, with regard

to the obligatory water vapor pressure at that site of about 47 mm Hg, and the inevitability of a certain partial pressure of carbon dioxide, which is discussed below. The optimal carbon dioxide tension is about 40 mm Hg. At barometric pressures greater than about 87 mm Hg (an altitude equivalent of 30 000 feet), then, at least some oxygen can be made available. Extensive studies of hypoxia at altitudes between 18 000 feet (P_B 380 mm Hg) and 30 000 feet have been related primarily to maintenance of consciousness in acutely exposed subjects. It has been found that healthy individuals at rest rarely lose consciousness below about 18 000 feet. Above that altitude, as indicated in figure 2-3, the duration of exposure before consciousness is lost is related to altitude and thus to the severity of the hypoxia produced.

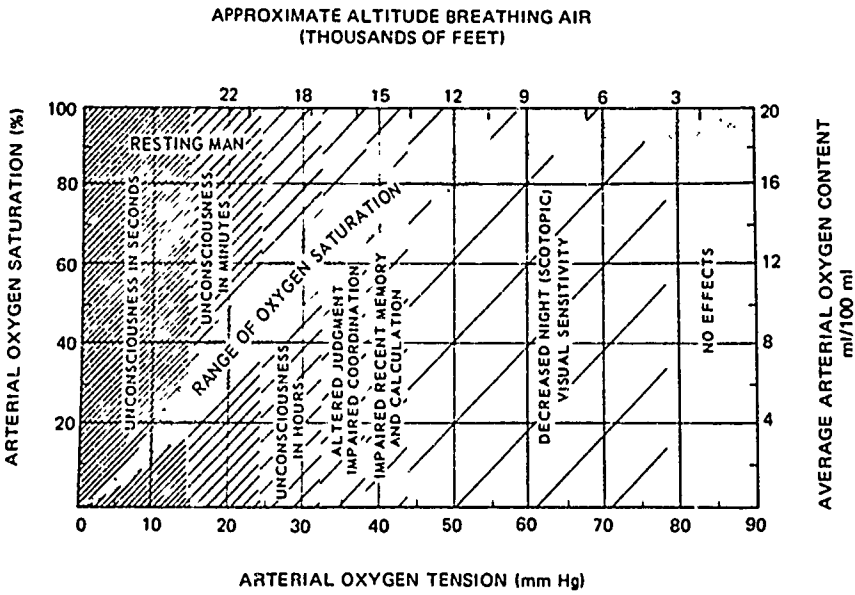


Figure 2–3. O_2 saturation in arterial blood as a function of alveolar O_2 tension in relation to altitude and to some reported symptoms of hypoxia. (Sources. USAF Flight Surgeon's Manual, 1968, Boothby, 1951, from *Human factors in air transportation*, McFarland. Copyright 1953 by McGraw-Hill Book Company. Used by permission of McGraw-Hill Book Company)

Since it is often difficult to assess exactly when total consciousness is lost, the concept of "time of useful consciousness" has evolved. Useful consciousness, as it is usually evaluated, represents the ability of a test subject to continue performing some purposeful act. The time of useful consciousness during an acute exposure to an hypoxic environment represents, therefore, an approximation of the time during which a subject may be expected to be sufficiently alert to ascertain the cause of the hypoxia and take effective action to protect himself or remove himself from the environment.

The time of useful consciousness varies according to the way in which the hypoxic environment is produced and according to the circumstances prevailing before the hypoxic exposure. If a subject breathing oxygen at altitude removes

his oxygen mask or becomes disconnected from his oxygen supply, the partial pressure of oxygen in the lungs drops with each succeeding breath of air, the decrease being dependent on the lung volume, the dilution of that volume by each breath's volume, and the altitude. In contrast, if a subject breathing air at low altitude is suddenly decompressed, the partial pressure of oxygen in his lungs drops immediately to a level which is dependent only on the final altitude. Venous blood is immediately exposed to low oxygen tension in the alveoli; the effects of hypoxia become evident as soon as inadequately oxygenated blood reaches the brain. Times of useful consciousness are much shorter than following oxygen mask removal at altitude. These times are shown in figure 2-4 for rapid decompressions to various altitudes of subjects breathing either air or oxygen prior to decompression.

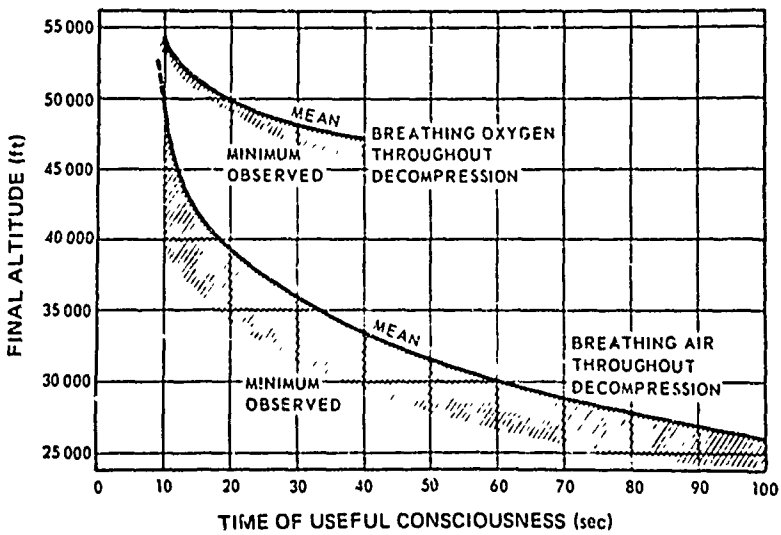


Figure 2–4. Minimum and average duration of effective consciousness in subjects following rapid decompression breathing air (lower curve) and O_2 (upper curve). At altitudes above 20 000 to 23 000 ft, unacclimatized subjects breathing air lose consciousness after a variable period of time. (Source: Blockley & Hanifan, 1961)

The appropriate protective action following a decompression in an aircraft is to don an oxygen mask. The ranges of times required to perform this action are shown in figure 2-5 for airline pilots studied in flight and for naive subjects studied in an altitude chamber. The rate of decompression for the airline pilots was 500 feet per second (fps) to a final altitude of 30 000 feet. The pilots had had training in decompression emergency procedures within a year prior to the exposures (Bennett, 1961). In the naive subject group, 60 young males were exposed to 10-second decompressions from 8000 to 30 000 feet (Hoffler & coworkers, 1968), and 40 male and female subjects were exposed to 5000- to 20 000-foot decompressions (Chisolm & coworkers, 1969). None of the naive subjects had been previously exposed to rapid decompression; their only indoctrination was a standard airline passenger briefing.

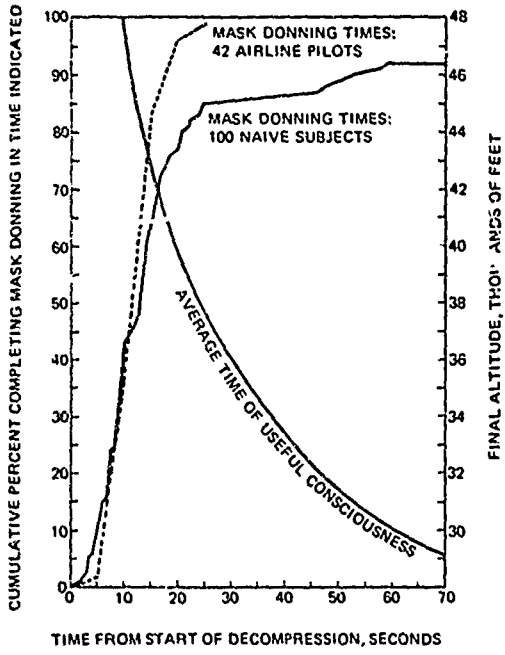


Figure 2–5. Mask-donning behavior related to time of useful consciousness. Subjects comprised 42 airline pilots (—·—) and 100 naive subjects (——). Exponential curve (see figure 2-4) represents average times of useful consciousness for subjects breathing air prior to decompression. (Data of Bennett, 1961; Hoffler & coworkers, 1968; Chisolm & coworkers, 1969; calculated by Blockley & Hanifan, 1961)

Any diluent gas which is present in a breathing system will influence the immediate usefulness of that system following a rapid decompression. This is shown in figure 2-6, which demonstrates the effect of oxygen hose volume on tracheal (upper airway) oxygen tension following rapid (1 second and 9 second) decompressions from 8000 to 40 000 feet. In the case illustrated, a diluter-demand regulator delivered 38 percent oxygen at 8000 feet and 100 percent oxygen at 40 000 feet. Pure oxygen is delayed in reaching the subject's lungs because of the volume of air-oxygen mixture in the hose at the time of decompression.

Even the very severe decompressions discussed in chapter 1 may not produce irreversible brain damage. However, the degree of brain dysfunction acceptable for pilots is considerably less than for passengers. Also, variations in individual tolerance for hypoxia make it risky to allow more than an unavoidable minimum of severe hypoxia to occur. Recent studies related to the development of a supersonic transport aircraft have resulted in the elucidation of criteria for "safe periods of unconsciousness" for passengers in such aircraft. It must be recognized, however, that persons with impaired brain circulation, the elderly, and certain others are far less tolerant of hypoxia than the healthy subjects who form the basis of the curves shown in figures 2-3 and 2-4. Taking into account

the behavioral variation shown in figure 2-5, it would appear essential to attempt to prevent the untoward hypoxic effects of decompression.

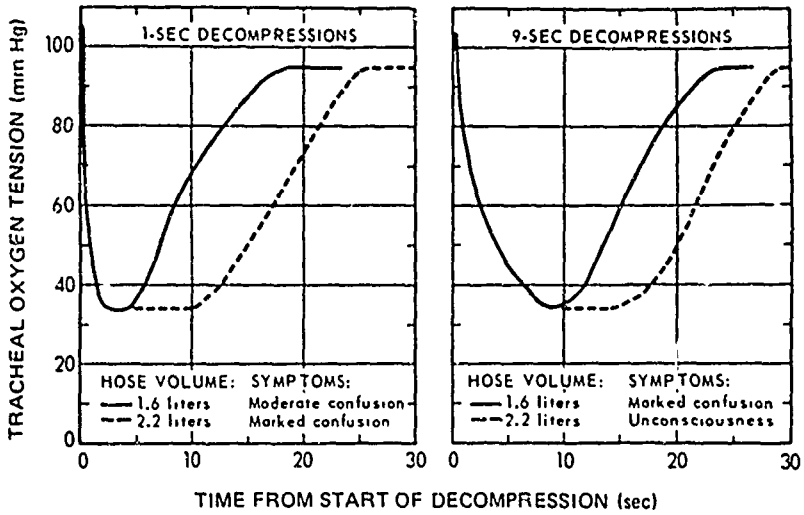


Figure 2–6. Effect of O_2 hose volume on tracheal O_2 tension following rapid decompression (Drawn from data of Ernsting, 1961 a; reprinted by permission of Her Britannic Majesty's Stationery Office)

At very high altitudes, even immediate mask donning will not prevent mental impairment following decompression of a subject who breathed air before the event. Ernsting, McHardy, and Roxburgh (1960) and Blockley and Hanifan (1961) have estimated the concentrations of oxygen which must be breathed prior to decompression if such impairment is to be avoided. These are shown in figure 2-7. In a cabin pressurized to 8000 feet (565 mm Hg), it is estimated that the critical alveolar oxygen partial pressure is 33 mm Hg. This calculation assumes that 100 percent oxygen is immediately supplied (under positive pressure at final altitudes above 45 000 feet). It should be noted in this context that studies by Barron (1965) of decompressions to 45 000 feet suggest that no combination of maneuvers aside from prebreathing oxygen-enriched air will prevent at least some transient hypoxic effects at that altitude. This is also suggested in figure 2-4.

Examination of the oxygen saturation curves in figure 2-3 indicates that near-normal blood oxygen levels, and thus essentially normal function, can be maintained with alveolar oxygen tensions as low as 50 to 60 mm Hg. It follows from this that a barometric pressure of 140 to 150 mm Hg will be sufficient to allow proper alveolar oxygen and carbon dioxide tensions to be maintained if no other gases are present in the respiratory tract. These barometric pressures are encountered at 39 000 to 40 000 feet. Human subjects, however, are capable of breathing against a limited degree of continuous positive pressure, although this is not accomplished without a physiological penalty (Ernsting, 1965, 1966). The elevation of total pressure within the chest causes a diminution in the volume of blood returning to the heart and thus a decrease in the heart's output.

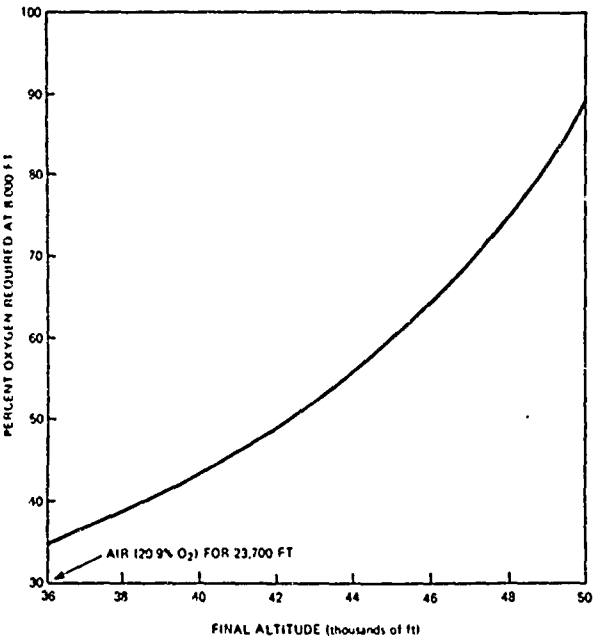


Figure 2–7. O_2 enrichment of air in pressurized cabin estimated to be required to prevent critical fall in alveolar O_2 tension during rapid decompression to various final altitudes. (Source: Blockley & Hanifan, 1961)

Despite the limitations of the technique, it is possible to maintain total lung pressure, and therefore alveolar oxygen tension, at minimal adequate levels up to altitudes of roughly 50 000 feet by provision of continuous positive pressure oxygen. At this altitude (P_B 87 mm Hg), a pressure of 60 mm Hg is required to maintain a P_{O_2} in the lungs of 60 mm Hg. It has been found, however, that a continuous positive pressure of 30 mm Hg is about the maximum which can be tolerated by trained subjects for even a short period of time without the application of counterpressure on the chest (which increases stagnation of blood in the abdomen and the extremities). The use of positive pressure at these altitudes, therefore, is clearly a short-term emergency measure. It is for this reason that overall pressure garments become mandatory at altitudes much above 50 000 feet.

At altitudes below about 20 000 feet (P_B 350 mm Hg), human survival and function at some meaningful level is possible without added oxygen. This is possible because higher life forms have a considerable ability to adapt themselves, or become acclimatized, to hypoxia. Consideration of this topic is beyond the scope of this chapter. It should be said, however, that people vary considerably in their tolerance for chronic, or long-term, hypoxia, as they do for acute exposures. Some persons will become acutely ill after several hours at altitudes as low as 12 000 feet (P_B 480 mm Hg), whereas others encounter less difficulty at altitudes as high as 18 000 feet (P_B 380 mm Hg).

Virtually everyone will develop some symptoms of acute altitude sickness (shortness of breath, headaches, insomnia, impaired ability to concentrate or perform complex tasks, and sometimes nausea and vomiting) after exposure to air at altitudes of 11 000 to 12 000 feet for periods longer than 8 to 24 hours. In most people, these symptoms decline in frequency and severity over a period of 2 to 5 days (figure 2-8). Ability to perform muscular work is moderately or severely impaired, and this impairment persists for long periods of time (figure 2-9).

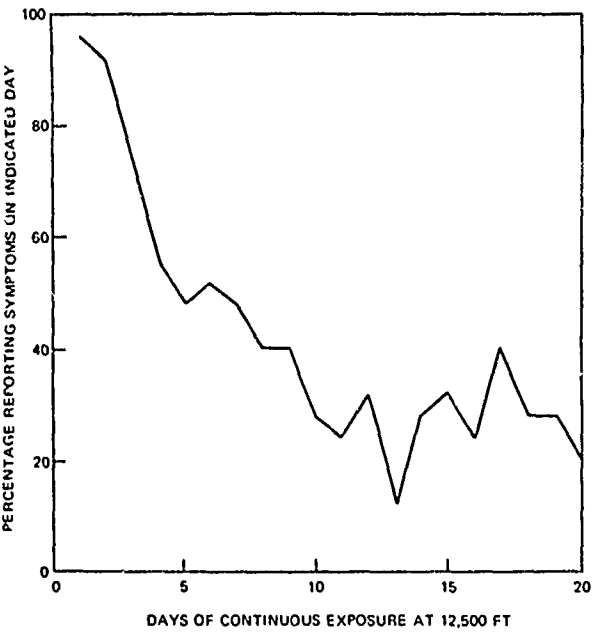


Figure 2–8. Proportion of subjects reporting symptoms of acute altitude sickness (headache, nausea, lightheadedness, fatigue, shortness of breath, or insomnia) during each of 20 days of continuous exposure at an elevation of 12 500 ft (3800 m, 175 mm Hg). (After Billings & coworkers, 1969, reprinted by permission of the Archives of Environmental Health, 1969, *18*, 987-995)

Hypoxic symptoms are less pronounced at lower altitudes or for shorter periods of exposure. They exist, nonetheless, and may be important under certain circumstances (figure 2-3). Visual thresholds have been shown to increase at altitudes above 4000 feet, probably because of the very high oxygen requirements of the light-sensing cells in the eye. Impairment of ability to learn new complex tasks has been demonstrated at 8000 feet (P_B 565 mm Hg) (Ledwith & Denison, 1964), impairment of recent memory, judgment and ability to perform complex calculations are seen at altitudes in the neighborhood of 10 000 feet (P_B 520 mm Hg) (McFarland, 1953).

Man at sea level is rarely exposed to partial pressures of oxygen greater than 170 mm Hg. Oxygen has been used as a therapeutic agent almost since its

discovery, however, and it was thought for a considerable time that gas mixtures containing several times the usual sea level concentration of 20.9 percent were entirely without harmful effects. It is now known that this is not the case, although it is not certain that 160 mm Hg is the optimal partial pressure under all circumstances.

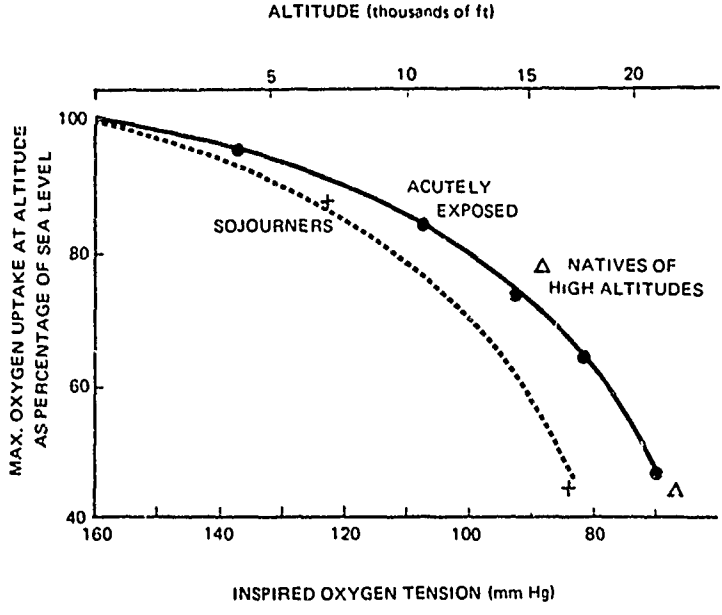


Figure 2–9. Impairment of capacity for muscular work by acute and chronic hypoxia. (Data from various sources, collated by Cerretelli, 1967, whose graph has been adapted for use here)

Too high a partial pressure of oxygen is not well tolerated by man, though our species is more tolerant than many species of experimental animals. The toxicity of oxygen at above-normal partial pressures is a time-dependent function whose characteristics are shown in figure 2-10. At pressures above 1 atm, central nervous system signs predominate (nausea, dizziness, faintness, and convulsions). At around 1 atm, respiratory symptoms are common. These symptoms are seen with longer periods of exposure at pressures as low as 200 mm Hg, although they are uncommon below about 250 mm Hg. At pressures of oxygen only slightly higher (253 mm Hg or 5 psia) than normal sea level P_{O_2} changes in red blood cell fragility and cell wall permeability have been reported (Berry, 1967). Whether oxygen *per se* is toxic at pressures in the range of 180 to 250 mm Hg, or whether the absence of a diluent gas is responsible for toxic manifestations, is not certain.

At higher oxygen tensions (250 to 750 mm Hg), signs of lung irritation are noticed after 12 to 72 hours of exposure. It is also known that oxygen tensions in this range can cause blindness in newborn and premature infants (the

condition called retrolental fibroplasia). On the other hand, many thousands of adult patients have been given oxygen in this pressure range for relatively long periods of time without apparent harm. While some patients have had diffusion defects such that elevated alveolar oxygen tensions merely maintained normal blood gas tensions, others have not. Ernsting (1961a) has demonstrated significant defects in diffusing capacity in man after 3 hours of exposure to 99 percent oxygen at sea level.

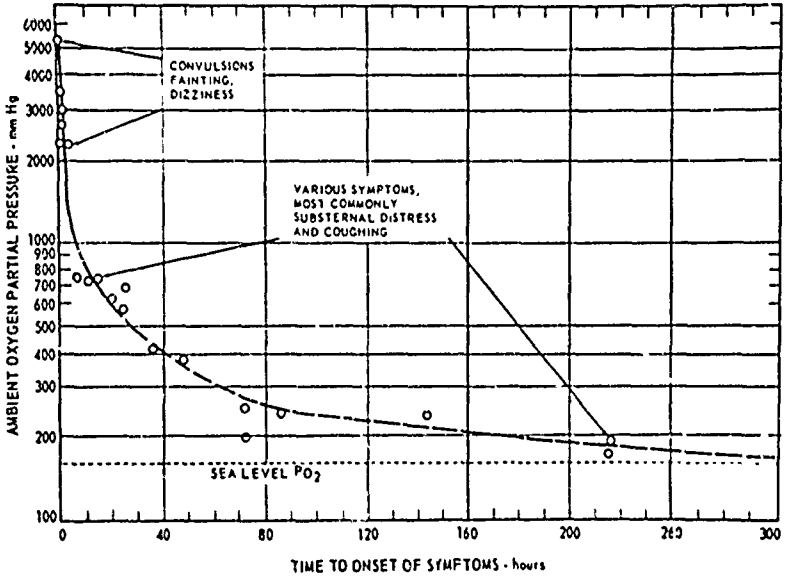


Figure 2–10. Approximate time of appearance of signs and symptoms of O_2 toxicity as a function of P_{O_2}. (Adapted from Welch & coworkers, 1963; Bean, 1945; Roth, 1964)

During exercise, supplemental oxygen causes a perceptible decrease in ventilation volume (Nielsen & Hansen, 1937); this may be considered a beneficial effect. Many pilots have described alleviation of fatigue when they placed themselves on supplemental oxygen for a short time before landing, especially at night. This is difficult to quantitate or even to verify, but the effect may be a real one (Roth, 1961).

Oxygen at partial pressures greater than 760 mm Hg (14.7 psia, 1.0 atm) has been used sporadically as a therapeutic agent. Only in recent years, however, have controlled studies been performed to evaluate its effects. The usefulness of oxygen in the treatment of carbon monoxide poisoning is beyond question; it is helpful in the treatment of gas gangrene, caused by a bacterium which cannot survive in the presence of high oxygen tensions. Its usefulness in treating tetanus (lockjaw), caused by a similar organism, is less certain. High oxygen tensions potentiate the effects of ionizing radiation, hyperbaric oxygen in combination with radiation therapy is used in treating certain advanced cancers. Its beneficial

effects in most of the other conditions in which it has been tried are questionable (Boerema, 1964).

Pure oxygen is used by Navy divers breathing from closed-circuit oxygen equipment when they wish to avoid leaving a trail of expired gas bubbles on the surface. Since oxygen at pressures greater than about 2 atm absolute can cause convulsions, however, the depths and times at which divers can use such equipment are very limited. As with hypoxia, individual susceptibility to hyperoxia varies widely. Performing physical work while breathing oxygen at high pressures decreases tolerance markedly. The risk of oxygen convulsions appears to be minimal in resting men exposed in a dry chamber to as much as 3.0 atm oxygen for 1 hour; oxygen pressures higher than this increase the risk considerably (Bennett, 1969). The risk is substantially greater under water in working subjects, especially if the water is cold. Figure 2-11 shows the limits currently imposed by the U.S. Navy (1970).

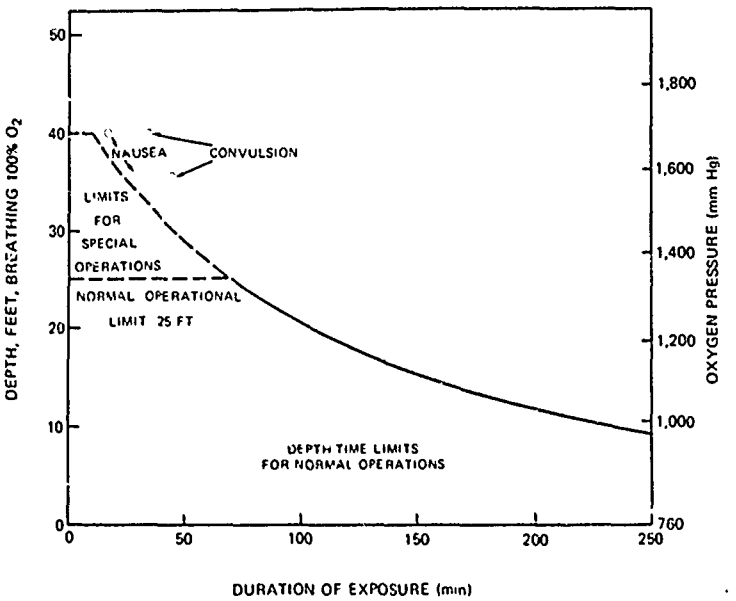


Figure 2–11. Navy published limits for divers using O_2 under water. Symptoms resulting from excessive exposure are shown. Limits assume moderate activity and minimal CO_2 tensions in the diver's breathing apparatus. (Redrawn from *U.S. Navy Diving Manual*, 1970)

Carbon Dioxide

Carbon dioxide is neither a necessary nor a desirable constituent of man's gaseous environment. Though man is normally exposed to low concentrations of this gas at sea level (on the order of 0.03 percent), it is quite certain that he can live indefinitely in an atmosphere entirely free of the gas, for he produces and excretes more than enough to meet his physiological needs.

Most of the 400 to 800 liters (15 to 30 ft^3) of carbon dioxide produced by an active man each day is excreted through the lungs as gaseous carbon dioxide; the remainder appears in the urine as bicarbonate ion, combined with basic elements, primarily sodium. Carbon dioxide is very soluble in water, with which it combines to form a weakly dissociated acid. The carbonic acid–bicarbonate buffer system is a major factor in the maintenance of the body's acid-base balance.

At and near sea level, man's breathing is controlled primarily by the amount of carbon dioxide he produces. Respiratory centers in the brain are exquisitely sensitive to very small changes in carbon dioxide tension and hydrogen ion concentration in the arterial blood. Carbon dioxide added to inspired air is a powerful respiratory stimulant: in higher doses, it stimulates heart rate as well (figure 2-12). Increases in arterial blood carbon dioxide tension also cause marked relaxation of the blood vessels in the brain; brain blood flow increases considerably. Figure 2-13 indicates the effects of both acute and prolonged exposures to carbon dioxide–air mixtures at 1 atm. In acute exposures, the boundary between "no effect" and "distracting discomfort" is narrow. In the area marked Zone II in the graph at the left side of figure 2-13, symptoms include small threshold hearing losses and a perceptible doubling in depth of respiration. In Zone III, mental depression, headache, dizziness, nausea, "air hunger," and decreased visual discrimination are experienced. Zone IV represents marked deterioration leading to dizziness and stupor, with inability to take steps for self-preservation. The final state is unconsciousness. The bar graph at the right of the figure shows that for prolonged exposures of 40 days, concentrations of carbon dioxide in air less than 0.5 percent (Zone A) cause no known biochemical or other effect; concentrations between 0.5 and 3.0 percent (Zone D) cause adaptive biochemical changes which may be considered a mild physiological strain; and concentrations above 3.0 percent (Zone C) cause pathological changes in basic physiological functions.

At partial pressures above about 60 mm Hg, the gas is a potent narcotic; it depresses brain function, elevates convulsion thresholds and causes respiratory depression. Very high partial pressures of this metabolite are fatal, probably because of the profoundly acidic blood and body fluids which are produced (Marshall, 1961).

Since man produces carbon continually at rates which vary from 0.2 to as high as 3 liters per minute (0.007 to 0.18 cubic feet per minute), this gas must be removed promptly from a closed environment, either by venting and replacement (as is done in pressurized aircraft) or by chemical or physical scrubbing (the methods used in spacecraft and certain submarines). The changes in gas composition in a sealed space containing a man are illustrated in figure 2-14. In the top part of this figure, the long straight line indicates oxygen depletion and carbon dioxide accumulation when no corrective measures are used. At 3.1 hours, when P_{O_2} has decreased to 108 mm Hg and P_{CO_2} has increased to 30 mm Hg (4 percent), respiratory volume has doubled. Curves emanating from this point indicate effects of adding pure oxygen, absorbing carbon dioxide, and ventilating with air and clearing carbon dioxide with absorber handling (12 liters of air/min/man). The dotted curve shows effects of using the same carbon dioxide absorber from the outset.

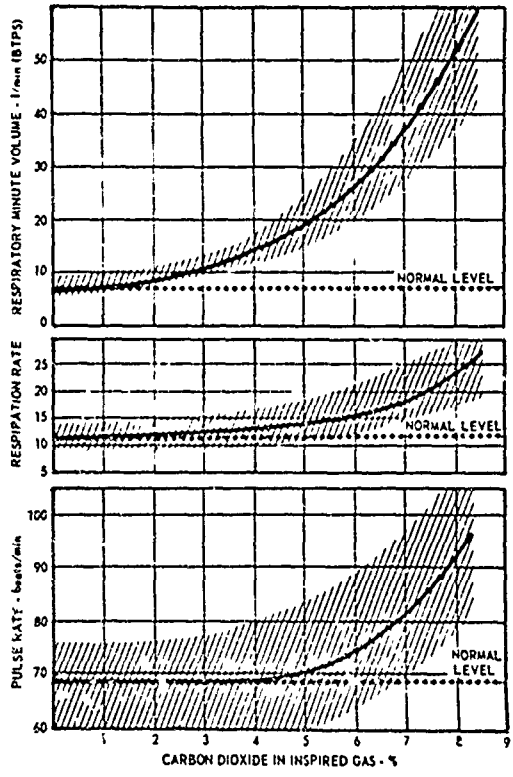


Figure 2–12. Immediate effects of increased CO_2 on pulse rate, respiration rate, and respiratory minute volume for subjects at rest. Hatched areas represent one S.D. on each side of the mean. To convert percentage of CO_2 to partial pressure, multiply percent by 760 mm Hg. (Adapted from Schaefer et al., 1952; & Dryden et al., 1956)

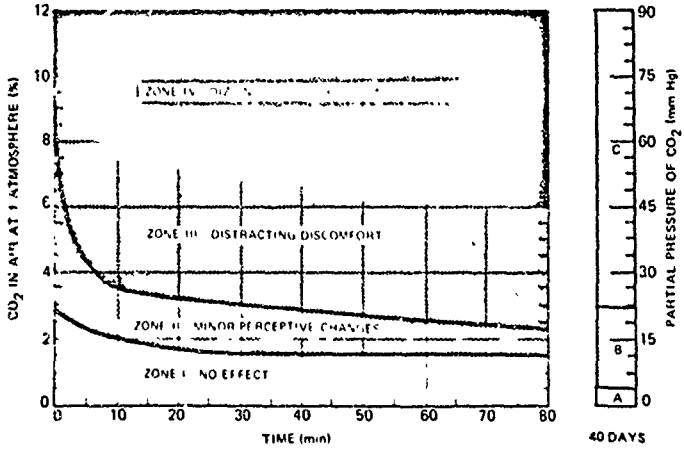


Figure 2–13 Symptoms common to most subjects exposed for various times to CO_2-air mixtures at 1 atm. At the right, effects of prolonged exposures are indicated. A = 0.5% CO_2, no effects; B = 0.5 to 3.0% CO_2, adaptive biochemical changes noted. C = >3.0% CO_2, pathological changes noted. (Drawn from data of King, 1949, Nevison, 1962; reprinted by permission of the *Journal of Industrial Hygienic Toxicology*, 1949, *31*, 365-375)

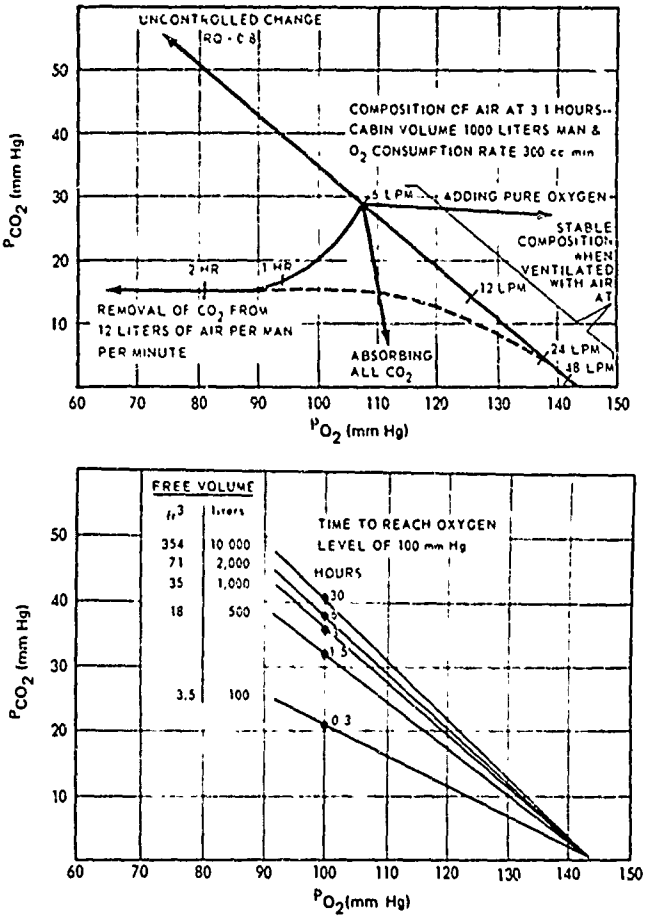


Figure 2–14. Change in P_{O_2} and P_{CO_2} within a sealed space. (Source: Rahn & Fenn, 1953)

The bottom part of figure 2-14 presents a series of lines indicating uncontrolled change for several cabin volumes. (Here too, RQ = 0.8 and oxygen consumption rate equals 300 cm^2/min.) The dots on the lines indicate the time in hours to reach a critical oxygen level of 100 mm Hg. Lower values for carbon dioxide for smaller free volumes, when oxygen is 100 mm Hg, result from relatively greater tissue storage of carbon dioxide. This effect is lessened in longer exposures in larger free volumes.

A number of studies have shown that psychomotor performance is impaired by moderate increases in arterial carbon dioxide tension. This is indicated in figure 2-15. In this figure, the zones above the line marked "normal alveolar CO_2" indicate increasing hypercapnea, limited by a zone of carbon dioxide narcosis. Below this dashed line, marked as zones of increasing hypocapnea, are lower levels of alveolar carbon dioxide, which commonly result from excessive respiratory ventilation. Low levels of alveolar P_{O_2} (severe hypoxia and hypoxic collapse) combine with hyper- and hypocapnea to affect performance as indicated.

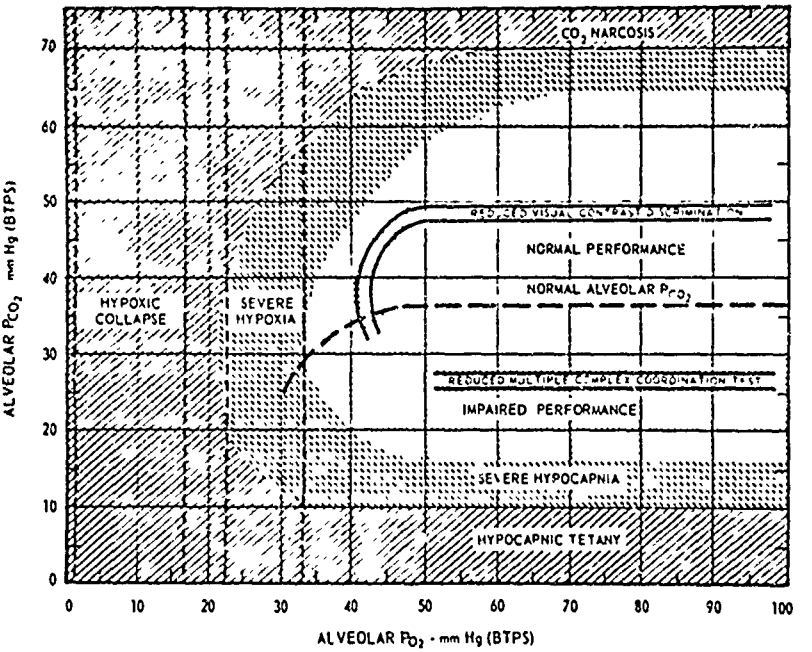


Figure 2–15. Relationship of alveolar O_2 and CO_2 composition to performance. (Adapted from Otis & coworkers, 1946, with additional data from Balke, 1956)

While a carbon dioxide tension of 22 mm Hg in the inspired air has been considered to be the maximum safe (though not innocuous) level for exposures lasting up to a month, comparatively few such tests have been conducted. It is not certain that such levels will be safe for the much longer sealed cabin exposures now being contemplated: this is an area which needs further research. Recent data suggest that tensions of 11 mm Hg (1.5 percent carbon dioxide at 750 mm Hg barometric pressure) for 42 days induce physiological changes which may be harmful under conditions of prolonged weightlessness (Ellingson, 1970).

It is also possible for blood carbon dioxide tensions to reach dangerously low values, usually as the result of ventilation in excess of need. Hyperventilation, as it is called, results in a decrease in alveolar carbon dioxide tension. The increased pressure gradient between alveolar air and the incoming venous blood leads to the removal from the blood of more carbon dioxide than is being produced in the tissues.

Otis (1946), Balke (1956), and others have shown that moderate, induced hyperventilation is associated with impaired performance of psychomotor tasks (figure 2-15). Balke (1957) has also demonstrated moderate to severe hyperventilation in pilots during transition to complex jet fighter aircraft. Aircraft accidents are thought to have resulted from severe hyperventilation, which not infrequently accompanies fear or panic.

Severe hyperventilation results in lightheadedness, feelings of numbness, tingling, markedly impaired performance, involuntary tetanic contractions of the skeletal muscles and, ultimately, in impaired consciousness. Unfortunately, the person who begins to hyperventilate as the result of fear tends to become more and more frightened by these bizarre symptoms; his fear, in turn, may increase his hyperventilation. It may also be difficult for even an experienced person to differentiate the symptoms of hyperventilation from those of hypoxia (Wayne, 1958), and it should be noted that moderate degrees of hypoxia in themselves provoke a degree of hyperventilation.

The Inert Gases

In this section are discussed the various gases generally considered to be physiologically inert: nitrogen, helium, neon, argon, krypton, and xenon. An introduction which describes their common attributes is followed by brief discussions of their individual characteristics. Table 2-1 summarizes certain important physical and biochemical properties of these elements.

Metabolic Role of Inert Gases

Perhaps the first serious doubts as to whether this group of elements was truly inert were cast by Cook, who performed studies on a variety of species to evaluate possible effects of helium. These are summarized in reviews by Cook and Leon (1959) and by Cook (1961). While many of the results reported in early studies could be accounted for by the high thermal conductivity of helium, producing high rates of heat loss in the organisms under study, others could not. It has been found that both oxidative and nonoxidative metabolic reactions are affected, though the exact biochemical sites of the effects have not been determined.

Schreiner and coworkers (1962) have also presented data suggesting that growth rates of certain molds are affected predictably by the "inert" gases in which they are cultured. Figure 2-16 summarizes their findings.

Allen (1963) attempted to grow chicken embryos in the absence of nitrogen, to determine whether nitrogen gas was required for the development of mammals. He found profound retardation of embryonic development in fertile eggs incubated in a number of environments deficient in nitrogen (figure 2-17). These results have been confirmed in part by others, though some workers feel they can be explained by factors other than an absence of nitrogen. The question remains an open one at this time. The few human studies which have been performed thus far have shown no effects which can be attributed to a metabolic effect of these gases, though the experiments have been of short duration.

Table 2–1

Physical and Biochemical Properties of Inert Gases

ELEMENT	Helium	Nitrogen	Neon	Argon	Krypton	Xenon
Symbol	He	N_2	Ne	A	Kr	Xe
Atomic number	2	7	10	18	36	54
Molecular weight	4.00	28.00	20.18	39.94	83.80	131.3
Density at 0°C, 1 atm, gm/l	0.1784	1.251	0.9004	1.784	3.708	5.851
Viscosity at 0°C, 1 atm, micropoise	194.1	175.0	311.1	221.7	249.6	226.4
Thermal conductivity at 0°C, 1 atm, cal/°C-cm-sec	34.0×10^{-5}	5.66×10^{-5}	11.04×10^{-5}	3.92×10^{-5}	2.09×10^{-5}	1.21×10^{-5}
Bunsen solubility coefficients:						
in water at 38°C	0.0086	0.013	0.0097	0.026	0.045	0.085
in olive oil at 38°C	0.015	0.061	0.019	0.14	0.43	1.7
in human fat at 37°C	?	0.062	0.020	?	0.41	1.6
oil:water solubility ratio	1.74	4.69	1.96	5.38	9.56	20.0

(Roth, 1967)

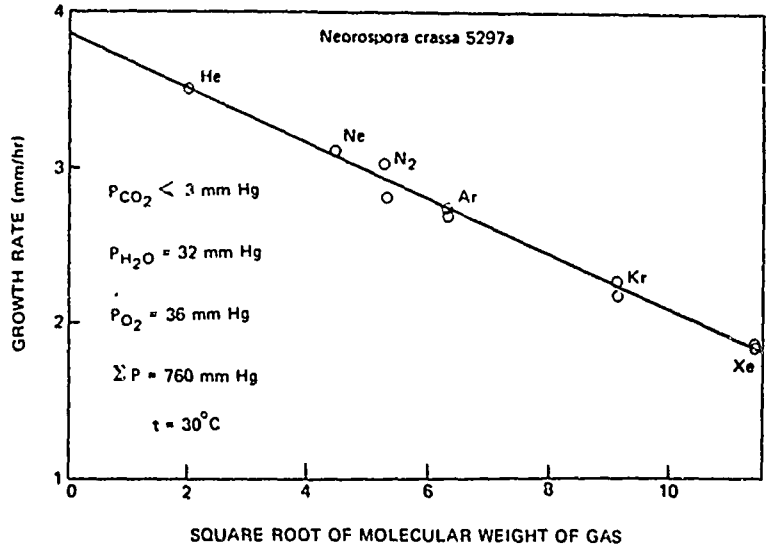
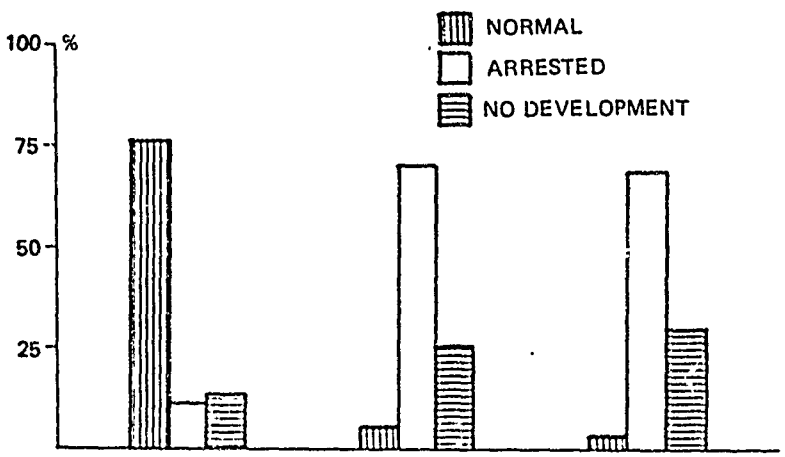


Figure 2–16. Relation of growth rates of *Neurospora crassa* molds to molecular weights of gases of the helium group in the environment. Significant effects ($P<0.01$) were associated with different inert gases. (Schreiner, 1962; copyright 1962 by the American Association for the Advancement of Science)



P_{N_2}	410-560	0-80	0	mm Hg
P_{O_2}	150-300	150-300	710	mm Hg
EMBRYOS	439	707	296	

Figure 2–17. Proportion of chick embryos showing arrested vascular development, or no signs of development, after 96 hr of incubation in various gas mixtures. (Redrawn from data of Allen, 1963)

Toxic Effects of Inert Gases

It has been known for many years that divers breathing air at considerable depths were prone to a disorder commonly called "raptures of the deep." The symptoms (elation, euphoria, deficient judgment, impaired motor coordination, diminished perception of pain and discomfort) are rather similar to those caused by alcohol. They have been variously attributed to high oxygen tensions, to carbon dioxide retention caused by inadequate ventilation of the lungs, and to nitrogen. It seems very probable that nitrogen is in fact the causative agent, though carbon dioxide retention may occur during work at depth and this gas is a potent narcotic, as noted earlier (Roth, 1967).

Later studies have indicated that xenon, krypton, argon, and, probably, helium all have narcotic potential in man and other mammals. Xenon at partial pressures of 0.8 atm (600 mm Hg, 11.75 psia) has been used as an anesthetic agent in human surgery (Cullen, 1951). Argon has been shown to be a potent narcotic at a tension of 3.2 atm (1950 mm Hg, 47 psia) (Behnke, 1939). Though the nitrogen in air exerts minor effects on human performance at barometric pressures as low as 2.5 atm absolute, the usual threshold is considered to be 4 atm, and serious symptoms are not ordinarily seen at pressures less than 7 atm (200-foot depth in sea water).

Recent studies by Bennett and Elliott (1969) have suggested that although the narcotic potential of helium is much less than that of any other inert gas, it does have some degree of potency at pressures in the range of 25 atm absolute. It thus appears that all of the inert gases are capable of exerting narcotic effects, though the mechanisms are not well understood. These narcotic effects, together with possible metabolic effects, may well be limiting factors in man's ability to tolerate long exposures at very high barometric pressures.

Role of the Inert Gases in Decompression Sickness

It was indicated in chapter 1 that the incidence of decompression sickness was materially reduced if inert gases, whether nitrogen, helium, or others, were washed out of the body prior to ascent. While this is often possible prior to ascent in aviation and space operations, the toxicity of oxygen prevents its use prior to ascent from depths greater than about 66 feet of water (3 atm absolute). Detailed discussion of the role of inert gases in decompression sickness is beyond the scope of this chapter; several excellent reviews are available (Roth, 1967; Bennett & Elliott, 1969).

Considerable research is in progress to define more clearly the limits of decompression tolerance in man after saturation exposures to various environments. This work will find applications both in space operations in which multiple-gas environments are used and in the long-term underwater habitability studies being carried out by several nations. The three gases which have been seriously considered as diluents for oxygen in such applications are helium, nitrogen, and neon. With respect to decompression

sickness, helium has certain theoretical advantages over nitrogen. Empirical data, however, are far from clear as to its practical advantages, particularly for space operations. In diving, the problem of nitrogen narcosis forces its replacement at depths below 200 to 250 feet. Preliminary studies suggest that neon may have advantages over either nitrogen or helium; confirmation of this awaits further research.

Hydrogen has been used in one series of dives at considerable depths; while it is not explosive when oxygen concentrations are less than 4 percent, theoretical considerations suggest that it may be no better than helium or perhaps even nitrogen with respect to decompression sickness.

Space-Occupying Role of Inert Gases

If a closed pocket of gas occurs or is created in the human body, the oxygen and carbon dioxide in the pocket are absorbed relatively rapidly; inert gases are also absorbed, but much more slowly because they are less soluble in blood (Makley & Billings, 1962). This has important implications when pure oxygen is breathed. During descent in an aircraft, it is necessary to ventilate the middle ear to relieve pressure differentials across the eardrum (see chapter 1). If the breathing gas is oxygen, the middle ear contains a high concentration of that gas after descent. The rapid absorption of oxygen over the next several hours can lead to symptoms identical to those which occur when a pressure differential arises during descent. This condition, called "delayed" or oxygen barotitis, is a common problem in military pilots.

It has also been found that during high-G maneuvers in fighter aircraft, small segments of the lungs can act like closed pockets of trapped gas. If oxygen and carbon dioxide are the only gases present in these segments, they are absorbed rapidly, causing collapse of small portions of the lung, and often chest pain and coughing. This condition, oxygen atelectasis, was described by Ernsting (1960) and has been studied in detail by Green and Burgess (1962).

Prevention of both these conditions is simple under conditions which permit the addition of an inert gas to the breathing mixture. The inert gas occupies space, and, since it is absorbed slowly, collapse is less likely to occur.

Other Considerations

If man must perform hard physical work, with attendant high ventilation rates, the density of the gas mixture will be important, particularly at high barometric pressures. The usefulness of helium in this regard has already been discussed. Another factor related to the physical characteristics of the breathing gas, however, is speech intelligibility. This is not an important problem at subatmospheric pressures, though it has been demonstrated that sound pressure levels are attenuated differentially by different gases at pressures below 1 atm (Cooke, 1964; Cooke & Beard, 1965).

At pressures encountered in diving operations, speech in helium-oxygen gas mixtures may become quite unintelligible. In some circumstances, it has been found necessary to add small amounts of nitrogen or neon to the breathing (Wathen-Dunn, 1967). Electronic processing has also been attempted in an effort to improve communications.

Thermal control is another area in which the inert gas plays a role. Since this appears to be a problem only when helium is used, it is discussed under that heading.

Finally, mention should be made of the last member of the family of noble gases, radon. Since it is intensely radioactive, it has been excluded from discussion here and from consideration for any role in life support systems.

Nitrogen

The work of Allen (1963) has raised the possibility that nitrogen in its elemental form may be necessary for mammalian growth and development. If this is true (and there are no other data which unequivocally support his contention), it is certainly true also that only small amounts of gaseous nitrogen are necessary for unimpaired functioning of adult human subjects. The helium-oxygen studies of Adams and coworkers, cited in chapter 1, involved nitrogen partial pressures as low as practicable, averaging 2 mm Hg for 56 days of exposure, other studies have been conducted for shorter periods at even lower nitrogen tensions without symptoms referable to the absence of the gas.

It also seems clear that partial pressures of nitrogen of at least 1200 mm Hg (found in air at 2 atm absolute) are not harmful for prolonged exposure. As noted previously, substantially higher pressures are required before frank symptoms of nitrogen intoxication appear, and there is evidence that some degree of adaptation to nitrogen narcosis is possible. Nonetheless, the partial pressures of nitrogen encountered at 200 feet depth, 4200 mm Hg, are clearly toxic to human subjects.

Helium

Studies of molds grown in helium-oxygen at a total pressure of 120 atm absolute (1764 psia) have shown that growth and metabolic activity are impeded. Interestingly, it appears that at this high pressure, helium depresses growth more than nitrogen, a reversal of the situation encountered at sea level (figure 2-16). Mice demonstrate narcotic effects of helium at 54 atm (794 psia), and the work of Bennett (1969) suggests that the threshold for narcotic effects in man may approximate 34 atm (500 psia). Nonetheless, with the possible exception of hydrogen, helium is the diluent gas best tolerated by man at very great depths.

The thermal conductivity of helium, six times that of nitrogen, does pose substantial problems. Figure 2-18 shows this parameter for various proportions of several inert gases with oxygen. Soviet and U.S. studies, among others,

have demonstrated that air temperatures must be 4 to 5°F higher for comfort of resting subjects in helium-oxygen environments; zones of thermal comfort are somewhat narrower (table 2-2). This may be a particular problem in undersea work; work temperatures are usually well below comfort levels and the gas mixture in underwater habitats is almost invariably saturated with water vapor. Substantial increases in environmental temperatures may be required for comfort (Raymond, 1967).

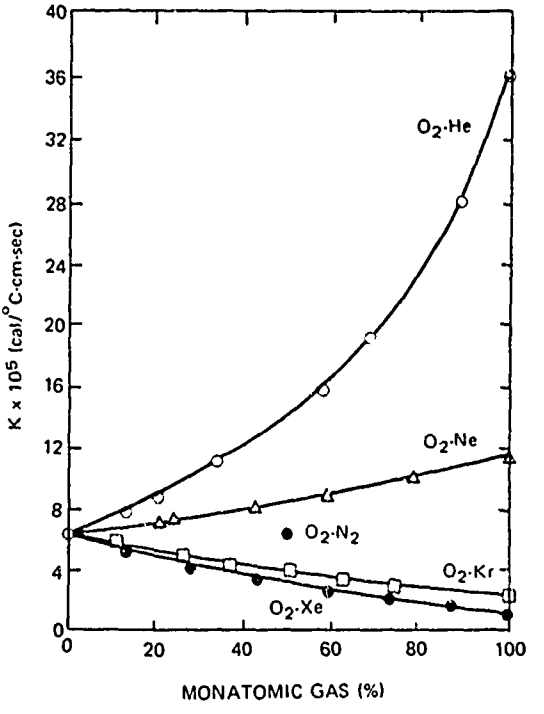


Figure 2–18. Thermal conductivity of binary gas mixtures containing O_2 at 30°C. (After Srivastava & Barua, 1960)

Table 2–2

Temperature Indicated to be Comfortable by Subjects in Space Cabin Simulator Experiments

Barometric Pressure		Gas Tension (mm Hg)			Selected Temperature
psia	mm Hg	O_2	He	N_2	°F
3.7	191	191	–	–	69.3
5.0	258	258	–	–	70.9
5.0	258	175	74	–	74.7
7.3	380	150	230	–	75.4
7.3	380	165	–	206	72.7

(From data of Welch, cited by Roth, 1968)

The problem of speech intelligibility has been studied intensively. Soviet workers have found an increase of about 0.7 octave in the fundamental frequency of the human voice at 1 atm in 80 percent helium-20 percent oxygen (Dianov, 1964). Similar findings are reported by U.S. groups (Sergeant, 1963).

Neon

Roth (1967), in his extensive review of inert gases for use in space vehicle atmospheres, concluded that "neon appears to offer some advantages over helium and nitrogen as an inert gas diluent..." This conclusion was reached on theoretical grounds, primarily because of the potential problem of decompression sickness, though it was pointed out that in all other areas as well, neon appears to be as good as or slightly better than nitrogen or helium.

There is, unfortunately, a shortage of data on human exposures to neon-oxygen mixtures. Bennett (1967) and Bennett and Elliott (1969) report the conduct of many short studies with the gas, some on humans; Weiss and coworkers (1968) have conducted longer studies on other mammals. On the basis of very incomplete data, it does not appear that the gas has toxic effects which would preclude its use in either space operations or in underwater work at moderate depths, where it can lessen problems in communications and heat loss without appreciably increasing the risk of inert gas narcosis or decompression sickness during reascent.

Argon, Krypton, and Xenon

It has been pointed out that argon is appreciably more narcotic than nitrogen, which severely limits its usefulness in underwater work. In addition, however, its use is associated with a substantially higher incidence of decompression sickness than either helium or nitrogen in animals (Behnke, 1939). These two considerations make it unlikely that the element would be seriously considered for use as the diluent gas in closed life support systems. It should be mentioned, however, that it has been proposed, and used, in ascents after very deep dives in an attempt to promote release of other inert gases from the tissues. Such specialized uses are beyond the scope of this discussion; a description of the technique has been published by Keller (1965).

The narcotic potency of krypton and xenon, together with much more severe potential for decompression sickness, precludes them from consideration for life support systems. It has been mentioned that xenon has been used as an anesthetic agent, and in this area it may have certain advantages if the problem of its cost can be overcome. Radioactive isotopes of both gases are used in studies of lung and circulatory physiology in animals and humans.

Other Gaseous Compounds

Carbon monoxide is generated in small amounts by most organisms. It results from the incomplete oxidation of foodstuffs. This compound is

discussed more fully in chapter 10, *Toxicology;* it is mentioned here only because of its physiological occurrence in closed ecological systems containing man or animals.

Methane and other gaseous products evolved in the course of digestion and bacterial action in the gut have varying toxicities. However, few studies involving long-term continuous exposure of man have been conducted.

Finally, sulfur hexafluoride, a physiologically inert gas with a molecular weight of 146.1, has been used in combination with oxygen in studies of the effects of high gas density on respiration. The density of a 79 percent sulfur hexafluoride-21 percent oxygen mixture is 4.2 times that of air at the same pressure. The toxicity of its breakdown products militates against the use of sulfur hexafluoride in other than experimental situations, where it can be quite useful.

References

Allen, S. C. A comparison of the effects of nitrogen lack and hypoxia on the vascular development of the chick embryo. *Aerospace Medicine,* 1963, *34,* 897-899.

Balke, B., & Lilleher, J. P. Effect of hyperventilation on performance. *Journal of Applied Physiology,* 1956, *9,* 371-376.

Balke, B., Wells, J. G., & Clark, R. T. In-flight hyperventilation during jet pilot training. *Journal of Aviation Medicine,* 1957, *28,* 241.

Barron, C. I., & Cook, T. J. Effects of variable decompressions to 45 000 feet. *Aerospace Medicine,* 1965, *36,* 425-430.

Bean, J. W. Effects of oxygen at increased pressure. *Physiological Review,* 1945, *25,* 1-147.

Behnke, A. R., & Yarbrough, O. D. Respiratory resistance, oil-water solubility, and mental effects of argon, compared with helium and nitrogen. *American Journal of Physiology,* 1939, *126,* 409-415.

Bennett, G. Reactions and performance of airline pilots following decompression. *Aerospace Medicine,* 1961, *32,* 134-136.

Bennett, P. B. Performance impairment in deep diving due to nitrogen, helium, neon, and oxygen. In C. J. Lambertsen (Ed.), *Underwater physiology.* Baltimore: Williams and Wilkins Co., 1967, Pp. 327-340.

Bennett, P. B., & Elliott, D. H. *The physiology and medicine of diving and compressed air work.* Baltimore: Williams and Wilkins Co., 1969.

Berry, C. A., & Catterson, A. D. Pre-Gemini medical predictions versus Gemini flight results. Gemini summary conference proceedings. SP-138, National Aeronautics and Space Administration, Washington, D. C., 1967.

Billings, C. E., Brashear, R. E., Bason, R., & Mathews, D. K. Medical observations during 20 days at 3800 meters. *Archives of Environmental Health,* 1969, *18,* 987-995.

Blockley, W. V., & Hamlan, D. T. An analysis of the oxygen protection problem at flight altitudes between 40 000 and 50 000 feet. Webb Associates, Santa Monica, California, 1961.

Boerema, I., et al. (Eds.) *Clinical application of hyperbaric oxygen.* Amsterdam. Elsevier Publishing Co., 1954.

Boothby, W. (Ed.) Handbook of respiratory physiology. School of Aviation Medicine, Randolph Air Force Base, Texas, 1954.

Cerretelli, P. Lactacid oxygen debt in acute and chronic hypoxia. In R. Margaria (Ed.), *Exercise at altitude*. Amsterdam: Excerpta Medica Foundation, 1967.

Chisolm, D. M., Billings, C. E., & Rason, R. Studies on the behavior of naive subjects during decompression. An evaluation of passenger oxygen equipment. Preprints of the 40th Aerospace Medical Association Meeting, San Francisco, 1969.

Cook, G. A. (Ed.) *Argon, helium and the rare gases: The elements of the helium group.* (2 Vols.) New York: Interscience Publishers, 1961.

Cook, S. F., & Leon, H. A. Physiological effects of inert gases. Report No. AFMDC-TR-59-26, University of California, Berkeley, 1959.

Cooke, J. P. Sound transmission in helium and various gases at low pressures. USAF SAM TDR-64-43, School of Aviation Medicine, Randolph Air Force Base, Texas, 1964.

Cooke, J. P., & Beard, S. E. Verbal communication intelligibility in oxygen-helium and other breathing mixtures, at low atmospheric pressures. USAF SAM TR-65-269, School of Aviation Medicine, Randolph Air Force Base, Texas, 1965.

Cullen, S. C., & Gross, E. G. The anesthetic properties of xenon in animals and human beings, with additional observations on krypton. *Science*, 1951, *113*, 580-582.

Dianov, A. G. The possibilities of replacing the nitrogen in the air with helium in spacecraft cabins and the effectiveness of using a helium-oxygen mixture for ventilation in space suits. NASA-TT-F-9012, National Aeronautics and Space Administration, Washington, D. C., translated from *Kosmicheskiye Issledovaniya*, 1964, 2, 498-503.

Dryden, C. E., et al. Artificial cabin atmosphere systems for high altitude aircraft. WADC-TR-55-353, Wright-Patterson Air Force Base, Ohio, 1964.

Ellingson, H. V., et al. Conference on carbon dioxide levels in the atmosphere of Skylab A: Preliminary report. Data of K. E. Schaefer, NASA Manned Spacecraft Center, Houston, Texas, unpublished, 1970.

Ernsting, J. Effects of breathing high concentrations of oxygen upon the diffusing capacity of the lungs in man. Report No. . . RC 1163, Flying Personnel Research Committee, Farnborough, England, 1961. (a)

Ernsting, J. The physiology of pressure breathing. In J. A. Gillies (Ed.), *Textbook of aviation physiology*. Oxford: Pergamon Press, 1965.

Ernsting, J. Prevention of hypoxia on rapid decompression to altitudes between 40 000 and 50 000 feet in transport aircraft. Royal Air Force Institute of Aviation Medicine, Farnborough, England, unpublished, 1969.

Ernsting, J. Some effects of oxygen breathing on man. *Proceedings of the Royal Society of Medicine*, 1960, *53*, 96-98.

Ernsting, J. Some effects of raised intrapulmonary pressures in man. Technivision, Ltd., Maidenhead, England, 1966.

Ernsting, J. Unpublished data. Royal Air Force Institute of Aviation Medicine, Farnborough, England, 1961. (b)

Ernsting, J., McHardy, G. J. R., & Roxburgh, H. L. The choice of gas mixture for breathing in high-performance aircraft. IAM Report No. 157, Royal Air Force Institute of Aviation Medicine, Farnborough, England, 1960.

Green, I. D., & Burgess, B. F. An investigation into the major factor contributing to postflight chest pain in fighter pilots. Report No. FPRC 1182, Flying Personnel Research Committee, Farnborough, England, 1962.

Hoffler, G. W., Turner, H. S., Wick, R. L., & Billings, C. E. Behavior of naive subjects during rapid decompressions from 8000 to 30 000 feet. Preprints of the 39th Aerospace Medical Association Meeting, Miami, 1968.

Keller, H., & Buhlmann, A. A. Deep diving and short decompression by breathing mixed gases. *Journal of Applied Physiology*, 1965, *20*, 1267-1270.

King, B. G. High concentration, short-time exposures and toxicity. *Journal of Industrial Hygienic Toxicology*, 1949, *31*, 365-375.

Ledwith, F., & Denson, D. M. Complex reaction times at a simulated cabin altitude of 8000 feet. IAM Report No. 284, Royal Air Force Institute of Aviation Medicine, Farnborough, England, 1964.

Makley, T. A., & Billings, C. E. Absorption of gases from the anterior chamber of the eye: Aeromedical considerations. *Aerospace Medicine*, 1968, *39*, 425-426.

Marshall, J. R., & Lambertsen, C. J. Interactions of increased oxygen tension and carbon dioxide tension effects in producing convulsions and death in mice. *Journal of Applied Physiology*, 1961, *16*, 1-7.

McFarland, R. A. *Human factors in air transportation.* New York: McGraw-Hill Book Co., 1953.

Nevison, T. O., Jr. Unpublished data. Lovelace Foundation, Albuquerque, New Mexico, 1962.

Nielsen, M., & Hansen, O. Maximale körperliche Arbeit bei Atmung Oxygen-reicher Luft. *Skandinav. Arch. für Physiol.*, 1937, *76*, 37-59.

Otis, A. B., et al. Performance as related to composition of alveolar air. *American Journal of Physiology*, 1946, *146*, 207-221.

Rahn, H., & Fenn, W. O. The oxygen-carbon dioxide diagram. WADC-TR-53-255, Wright-Patterson Air Force Base, Ohio, 1953.

Raymond, L. W. Temperature problems in multiday exposures to high pressures in the sea. Thermal balance in hyperbaric atmospheres. In C. J. Lambertsen (Ed.), *Underwater physiology*. Baltimore: Williams and Wilkins Co., 1967. Pp. 138-147.

Roth, E. M. (Ed.) Compendium of human responses to the aerospace environment. (4 Vols.) NASA CR-1205, National Aeronautics and Space Administration, Washington, D. C., 1968.

Roth, E. M. Space cabin atmospheres, Part I. Oxygen toxicity. NASA SP-47, National Aeronautics and Space Administration, Washington, D. C., 1964.

Roth, E. M. Space cabin atmospheres, Part III. Physiological factors of inert gases. NASA SP-117, National Aeronautics and Space Administration, Washington, D. C., 1967.

Schaefer, K. E. A concept of triple tolerance limits based on chronic carbon dioxide toxicity studies. *Aerospace Medicine*, 1961, *32*, 197-204.

Schaefer, K. E., et al. Respiration and circulation during and after inhalation of various concentrations of carbon dioxide. Report No. 189, Volume XI, No. 6, Naval Medical Research Laboratory, New London, Connecticut, 1952.

Schreiner, H. R., Gregoire, R. C., & Lawrie, J. A. New biological effect of the gases of the helium group. *Science*, 1962, *136*, 653-654.

Sergeant, R. L. Speech during respiration of a mixture of helium and oxygen. *Aerospace Medicine*, 1963, *34*, 826-829.

Srivastava, B. N., & Barua, A. K. Thermal conductivity of binary mixtures of diatomic and monatomic gases. *Journal of Chemical Physics*, 1960, *32*, 427-435.

United States Air Force. Flight Surgeon's Guide. No. AFP 161-18, Department of the Air Force, Washington, D. C., 1968.

United States Navy. *U.S. Navy diving manual.* NAVSHIPS 0994-001-9010, Washington, D C.: Government Printing Office, 1970.

Wathen-Dunn, W. Limitations of speech at high pressures in a helium environment. In C. J. Lambertsen (Ed.), *Underwater physiology*. Baltimore: Williams and Wilkins Co., 1967.

Wayne, H. H. Clinical differentiation between hypoxia and hyperventilation. *Journal of Aviation Medicine*, 1958, *29*, 307-315.

Weiss, H. J., et al. Three-week exposure of rodents to a neon enriched atmosphere. *Aerospace Medicine*, 1968, *39*, 1215-1217.

Welch, B. E., Morgan, T. E., Jr., & Clamann, H. G. Time concentration effects in relation to oxygen toxicity in man. *Federation Proceedings*, 1963, *22*, 1053-1056.

CHAPTER 3
TEMPERATURE

by

P.J. Berenson, Ph.D.

and

W.G. Robertson, Ph.D.
AiResearch Manufacturing Company

Human life can be maintained in environments ranging from Arctic cold, where the problem is to minimize heat loss and maximize heat production, to furnace-like heat, where the problem is to maximize heat loss. The spectrum of human response to temperature is broad, ranging from complete thermal comfort to the extremes of pain-limited exposures. The critical variable is exposure time, which may range from seconds in pain-limited situations to a lifetime. Thermal tolerance times can be increased by properly chosen clothing.

Within a period ranging from minutes (emergency situations) to days and weeks, differences between individuals and groups in response to thermal extremes are enormous, largely because of varying preceding experiences, or "acclimitization." Synthesis of available experimental data is extremely difficult in the absence of a reliable quantitative scale upon which to identify individual differences. Consequently, variations are emphasized in this chapter to illustrate how selection and training can influence response to any particular environment-activity-clothing combination. The conservative solution to the use of these data is the choice of the least resistant and least trained individuals.

The problems of comfort in heat stress are emphasized here, with less emphasis placed upon those problems associated with cold exposures. The chapter begins with a discussion of the physiological parameters related to human thermal interactions and closes with some data concerning thermal protective clothing. The terms and symbols used throughout this chapter are defined in the Glossary which precedes the References section at the end of the chapter.

Reviewed by A. Pharo Gagge, Ph.D., John B. Pierce Foundation. Appendix authored by the reviewer.

Preceding page blank

Physiological Parameters

The primary physiological parameters related to human thermal interactions are sweat rate, skin surface temperature, and body internal temperature; only small changes in the latter two can be tolerated without discomfort. Some latent heat rejection by evaporation occurs due to respiratory water loss, but most occurs at the skin surface, where water is deposited by the sweat glands and by diffusion through the skin. The remaining energy, termed sensible heat, is transferred to the atmosphere by a combination of convection and radiation heat transfer. All heat rejected at the skin's surface is transported from the deep body tissues by the flow of the blood.

Thermoregulatory Mechanisms

One of the heat-regulating mechanisms of the body involves control of the flow of blood to the skin by the constriction and dilation of the peripheral blood vessels. This vasoregulatory mechanism attempts to control sensible heat rejection from the body to maintain internal body temperature at a nominal value of 98.6°F (27°C). This mechanism, which is controlled by a combination of internal and skin temperatures, is capable of providing a factor-of-ten variation in sensible energy transfer between the body core and the surface (Robinson, 1963). Thus, under cold conditions, the body attempts to reduce the heat dissipation rate by reducing the flow of blood to the cold skin by constriction of the peripheral blood vessels. Under hot conditions, vasodilation, which occurs with the onset of active sweating, takes place and the blood flow to the hot skin is increased. Although the vasoregulatory mechanism is an important safeguard, it has little effect on thermal comfort analysis. Experiments indicate that at the limits of vasoregulation, the vasomotor system is capable of exerting a stabilizing effect on rectal and skin temperatures for a finite period (Winslow, Herrington, & Gagge, 1937). The period of stabilization is reduced as the severity of thermal stress is increased.

For each individual, there is an internal set-point temperature at which he is comfortable; the variation in the set point between individuals is approximately ±0.5°F (±0.3°C). At internal temperatures above the set point, vasodilation and active sweating occur; at internal temperatures below the set point, vasoconstriction and increased metabolism due to shivering occur. Because shivering and sweating are a function of both internal and skin temperatures, it is desirable to maintain the internal temperature below the set point to avoid sweating; at the same time, it is necessary to avoid excessively low skin temperatures that will produce shivering and a cold sensation. According to Kerslake (1962), a mean skin temperature of approximately 91.4°F (33°C) is near optimum; mean skin temperatures higher than 94°F (34.5°C) cause active sweating, and mean skin temperatures lower than 86°F (30°C) are associated with metabolic heat generation by shivering.

The eccrine sweat rate is dependent on the cranial internal temperature only for skin temperatures above 91.4°F (33°C); it is suppressed by reduced skin temperature at skin temperatures lower than 91.4°F (33°C) (Benzinger, 1961).

Because the relationship between the body skin temperature and internal temperature is determined by the external heat transfer characteristics, for particular environmental conditions, the eccrine sweat rate can be given as a function of skin temperature alone.

Skin Properties

Relevant properties of the skin are listed in table 3-1. Skin temperature is an important factor in body thermal control, although the heat rejection rate over which it is effective is small relative to that exercised by the sweat mechanism. The latter can generate water at a maximum rate corresponding approximately to 3000 BTU/hr (880 W or approximately 22gm/min for the average sized man). It can be determined that the sensible (radiation plus convection) energy rejection rate from the body will normally vary by approximately 20 BTU/hr (10 W) for each °F (°C) change in skin temperature. Therefore, in going from a comfortably cool skin temperature of 90°F to a comfortably warm skin temperature of 93°F, the heat rejection rate is increased by only 60 BTU/hr (17.5 W).

Regional Requirements

As shown in figure 3-1, different areas of the body have varying thermal characteristics and requirements. To be comfortable, the body must be maintained under conditions producing no eccrine sweating. A certain amount of moisture, however, will be removed from the body by insensible water loss, by diffusion through the skin and by respiration. The data in figure 3-1 show that the insensible water loss by diffusion varies greatly over the surface of the body and with the individual; most of the loss is from portions of the body that are generally unclothed.

Insensible water loss is a continuing nonadaptive process and results in loss of body heat under virtually all environmental conditions. The irreducible insensible water loss from skin and lungs is 0.06 of 1 percent of body weight per hour. The lower limit for insensible water loss from the skin alone at one atmosphere and T_a=68°F (20°C) is approximately 10 gm/sq m-hr. At air temperatures above 68°F (20°C) the rate of insensible water loss increases linearly to a value of about 25 gm/sq m-hr at T_a = 79°F (26°C). Below the sweating threshold, about 40 percent of the mositure loss is from the palm, sole of the foot, and head (about 13 percent of the total body surface.)

At air temperature between 79° (26°C) and 93° (34°C) on Earth, there is an increase in water loss as additional regional areas of the body begin to sweat. The progression of recruitment is generally from the extremities toward the central regions of the body and headward, and is subject to effects of training. In this temperature range and at rest, the onset of sweating produces water loss at rates of 40 to 60 gm/sq m-hr for all regions of the body. At ambient temperatures higher than 93°F (34°C), the increment in sweat rate increases linearly at the rate of 12 to 15 gm/sq m-hr-°C in well-trained subjects at rest. With full sweating, the trunk and lower limbs provide 70 to 80 percent of the total moisture perspired (Hertzman, Randall, Peiss et al., 1951, 1952). Tables 3-2, 3-3 and 3-4 summarize the order of recruitment, mean regional evaporative rates, and regional fractions of total evaporation, respectively.

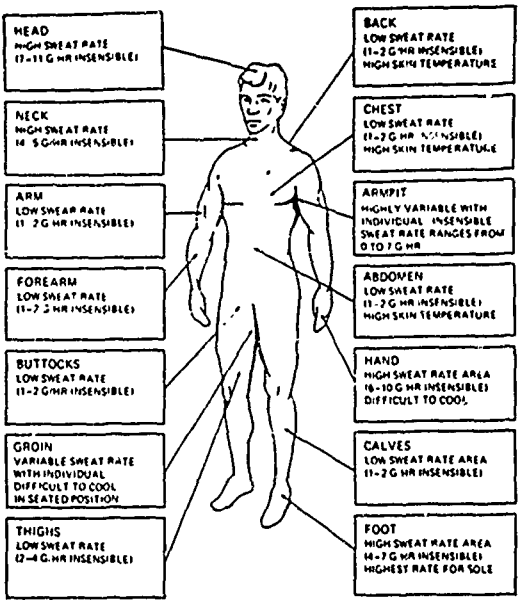
Table 3–1
Properties of the Skin

Approximate values of the physical dimensions of whole skin for the "average man" 154 lb, 5 ft 9 in		
Weight	8.8 lb	4 kg
Surface area	20 sq ft	1.8 sq m
Volume	3.7 qt	3.6 liters
Water content	70 to 75 percent	
Specific gravity	1.1	
Thickness	0.02 to 0.2 in.	0.5 to 5.0 mm
Approximate values for thermal properties of skin		
Heat production	240 kcal/day	
Conductance	9 to 30 kcal/sq m-hr-°C	
Thermal conductivity (k)	$(1.5 \cdot 0.3) \times 10^{-3}$ cal/cm sec-°C, at 23° to 25°C ambient	
Diffusivity (k/cc)	7×10^{-4} sq cm/sec (surface layer 0.26 mm thick)	
Thermal inertia (kcc)	90 to 400×10^{-5} cal^2/cm^4 sec $(°C)^2$	
Heat capacity	~ 0.8 cal/gm	

Skin temperature and thermal sensation

Pain threshold for any area of skin	113°F (45°C)	
When mean weighted skin temperature is		The typical sensation is
	above 95°F (35°C)	unpleasantly warm
	93°F (34°C)	comfortably warm
	below 88°F (31°C)	uncomfortably cold
	86°F (30°C)	shivering cold
	84°F (29°C)	extremely cold
When the hands reach	When the feet reach	They feel
68°F (20°C)	73.5°F (23°C)	uncomfortably cold
59°F (15°C)	64.5°F (18°C)	extremely cold
50°F (10°C)	55.5°F (13°C)	painful and numb

Approximate optical properties of skin	
Emissivity (infrared)	~ 0.99
Reflectance (wavelength dependent)	Maximum 0.6 to 1.1μ
	Minima < 0.3 and > 1.2μ
Transmittance (wavelength dependent)	Maxima 1.2, 1.7, 2.2, 6, 11μ
	Minima 0.5, 1.4, 1.9, 3, 7, 12μ
Solar reflectivity of surface	
Very white skin	42 percent
5 "white" subjects	28 to 40 percent, average 34 percent
6 "colored" subjects	19 to 24 percent, average 21 percent
Very black skin	10 percent
Solar penetration--very white skin	45.5 percent passes 0.1 mm depth
	39.6 percent passes 0.2 mm depth
	32.0 percent passes 0.4 mm depth
	19.0 percent passes 1.0 mm depth
	10.2 percent passes 2.0 mm depth
Solar penetration--very dark skin	75 percent passes 0.1 mm depth
	40 percent absorbed in the melanin layer
	35 percent passes 0.2 mm depth



REGION	PREFERRED TEMPERATURE (°F)	HEAT LOSS BTU/HR	AREA FT²	SKIN CONDUCTANCE BTU/FT²/HR/°F
HEAD	94.6	15.9	2.15	1.61
CHEST	94.6	37.8	1.83	3.87
ABDOMEN	94.6	17.9	1.29	3.02
BACK	94.6	49.3	2.48	4.31
BUTTOCKS	94.6	33.0	1.84	3.70
THIGHS	91.4	47.7	3.55	1.76
CALVES	87.9	58.0	2.15	7.26
FEET	83.5	38.7	1.29	1.98
ARMS	91.4	33.4	1.07	4.10
FOREARMS	87.9	34.2	0.86	3.45
HANDS	83.5	63.6	0.75	5.45

Figure 3–1. Regional cooling requirements of the human body in air at sea level at rest. (After Berenson, 1965, from data of Kerslake, 1964)

Table 3–2
Recruitment of Sweating

Area	Usual (But Not Invariable) Order of Recruitment
Dorsum foot	1
Lateral calf	2
Medial calf	3
Lateral thigh	4
Medial thigh	5
Abdomen	6
Dorsum hand	7 or 8
Chest	8 or 7
Ulnar forearm	9
Radial forearm	10
Medial arm	11
Lateral arm	12

(After Randall and Hertzman, 1953)

Table 3–3

Increments in Mean Regional Evaporative Rates With Rise in Environmental Temperature

Region	Evaporative Rate, °C			Increment in Evaporative Rate	
	T_a29	34	38	29 to 34	34 to 38
	gm/sq m/hr			gm/sq m/hr/°C	
Calf	18 0	86 5	169.0	13.7	20.4
Thigh	14 4	58.7	144.0	8.0	21.3
Abdomen	12.0	60.0	156.0	9.6	24.0
Chest	9.6	37.2	120.0	5.5	20.7
Forearm	12.0	21.6	96.0	1.9	18.6
Arm	10.8	14.4	65.0	0.7	13.0
Cheek	24.0	36.0	108.0	2.4	18.0
Forehead	24 0	60.0	240.0	7.2	45.0

(After Hertzman et al., 1952)

Table 3–4

Regional Fractions of Total Cutaneous Evaporation Expressed as Percentage of Total

Region	Air Temperature, °C							
	24	26	28	30	32	34	36	37
Head	11 8	12.1	11.9	9.7	8.0	7 0	8.5	8.4
Arm	4.6	4 4	4.2	3 4	2.6	2.2	3.1	3.3
Forearm	8.2	7.2	6.0	4.3	3.2	3 1	4 4	4.3
Trunk	22.8	2. 0	22.2	22.2	30.0	33.0	43 0	38.2
Thigh	13 6	13 1	17 1	20.2	22 6	23.8	25.5	22.3
Calf	8.5	9.0	11 9	16.0	20.3	22.8	24.1	19 8
Palm	15 6	15 3	13.1	9.6	6.8	4.6	3.5	2.5
Sole	14.7	15 1	13 5	9 9	6 4	3.7	2.3	1.5

(After Hertzman et al., 1952)

The maximum attainable perspiration rate of the human body is approximately 30 gm/min for an average sized man, which could provide maximum evaporative cooling rate of 1200 watts. At these rates, however, even with adequate consumption of water and electrolytes, the sweating mechanism fatigues in 3 to 4 hours and perspiration rates decrease significantly. This fatigue is a function of skin wetness. The maximum effective perspiration rate that can be sustained is extremely variable depending on the individual and his degree of acclimatization.

Energy Balance Equation

Heat is transfered between man and the environment through four avenues: radiation, convection, conduction, and vaporization. The body also stores energy in the tissues and body fluids. Thermal interactions between the human body and the environment can be examined in terms of the energy balance equation. This equation balances the normal energy gains and losses and can be expressed as follows (Blockley, McCutchan, & Taylor, 1954):

$$\dot{Q}_{sr} + \dot{Q}_m - W = \pm\dot{Q}_s \pm\dot{Q}_r + \dot{Q}_c \pm\dot{Q}_v + \dot{Q}_k + \dot{Q}_e \qquad (1)$$

For a steady-state thermal condition, the rate of heat storage rate is zero ($\dot{Q}_s = 0$). The conductive heat transfer mode is usually quite small and can be neglected in most instances ($\dot{Q}_k = 0$). Finally, if the body is shielded from direct solar radiation, the term ($\dot{Q}_{sr}$) can be omitted from the expression.

With these simplifications, the energy equation can be expressed as:

$$E_m - W = \pm Q_r \pm Q_c + Q_e + Q_v \qquad (2)$$

and the system can be analyzed quantitatively after these terms have been adequately defined.

Metabolism ($\dot{Q}_m$) is the sum of the basal metabolic rate plus an incremental increase in heat energy due to gravity and/or stress. Values of metabolism for various activities are presented in chapter 18, *Work, Heat and Oxygen Cost*. The most common activities require a metabolism between 300 and 1000 BTU/hr or 90 and 300 watts.

In the steady-state condition required for long-duration comfort, the metabolic energy is dissipated by the work accomplished and by heat rejection to the atmosphere. Because man is relatively inefficient in converting metabolic energy into useful work (the maximum work output being approximately 20 percent of the metabolism) (Fahnestock et al., 1963), most of the metabolic energy must be lost to the environment by heat rejection.

Radiation heat transfer (Q_r) occurs as a result of the temperature difference between the human body and the walls of the surroundings. Convection heat transfer (Q_c) occurs as a result of the temperature difference between the body and the gas atmosphere. Evaporation heat transfer (Q_e) results from the vaporization of moisture at the surface of the skin. Respiratory heat transfer (Q_v) is the heat loss (including vaporization of water) from the lungs because of respiration.

Determination of the thermal status of the human body in space operations requires analysis of a large number of variables. The effect of many of these

variables has no simple mathematical solution and must be derived from experimental data. Even then, the results must be treated with caution when applied to the small population represented by a flightcrew. Individual metabolic rates, health variations, tolerances, and motivation can cause wide deviations from predicted states and performance.

In general, all the variables can be collected under three major classifications: environment, body state, and clothing, as shown in table 3-5.

Since many of the variables are interdependent, solution of the complete energy balance equation becomes largely an iterative process modified by heavy reliance on reasonable assumptions and experimental results. Maintaining a thermal balance requires the regulation of environmental parameters to maintain man in a state of thermal equilibrium (or compensable quasi-equilibrium) at all anticipated levels of activity to ensure adequate performance and preclude irreversible physiological effects.

Heat Transfer Equations

Heat Conduction Through Clothing

The dry heat transfer from the skin to the outer surface of the clothed body is a complicated phenomenon involving internal convection and radiation processes in intervening air spaces, and conduction through the cloth itself. To simplify calculations, the following relationship between clothing surface temperature, T_c, and skin temperature, T_s, considers a simple conduction process through clothing of thickness, L:

$$T_c = T_s - \frac{L \quad Q}{k \; A_c} \tag{3}$$

The value L/k is known as the clothing or Clo value. The reference point for the Clo value is taken as a man in a suit with no gloves, or light gloves, and leather footgear with light socks. This is known as 1 Clo and corresponds to a value for L/k of 0.88°F-sq ft-hr/BTU or 0.155°C·m^2/W. The Clo value ranges from four for artic equipment to zero for the unclothed subject, as shown in table 3-6 (Fanger, Nevins, & McNall, 1968). A value of 0.6 Clo is often used because it is typical of light indoor clothing.

The effective Clo value for a person seated in a padded chair (or lying down) might be substantially larger than the Clo value for a standing person in the same clothing ensemble. The 1 Clo value is as high as can be expected in a shirt-sleeve environment. More typical values would be 0.25 Clo for the underwear worn by project Gemini astronauts. The heat loss from the skin surface is inversely proportional to $(I_a + I_{cl})$ where I_a is the insulation of the ambient air and I_{cl} - il is the intrinsic insulation of the clothing itself. The effect of helium in reducing the Clo values of different garments has not been studied. Preliminary studies confirm that Clo values tend to vary inversely with the thermal conductivity of the atmosphere.

Table 3–5
Variables Required for Prediction of Body Thermal Status (Roth, 1968)

Environment			
External (Natural)	Internal (Induced)	Body State	Clothing
Solar radiation (Q_{sr})	Wall temperature (T_w)	Metabolic rate (E_m)	Thermal resistance
Earth radiation (Q_{er})	Atmospheric temperature (T_a)	Weight	Vapor permeance
Lunar radiation (Q_{lr})	Atmospheric pressure (P)	Posture	Wind penetrability
Shadow cones (day/night)	Atmospheric velocity (V)	Area of body (A_b)	Weight
Atmospheric composition	Absolute humidity (p_a)	Skin temperature (T_s)	Color emissivity absorptivity
Vehicle velocity (if > C/7) (C velocity of light)	Atmospheric composition	Rectal temperature (T_r)	Wicking efficiency
Vehicle attitude or orientation	Diffusivity (D_v)	Mean body temperature (T_b)	
Vehicle altitude	Specific heat (C_p)	Respiration rate ($\dot{V}$)	
	Surface area (surroundings)	Insensible water loss	
	Shape emissivity factor (F_{cw})	Sweat rate	
	Crew operating mode	Wetted area (C)	
		Activity/work efficiency	

Table 3–5 (Continued)

Variables Required for Prediction of Body Thermal Status (Roth, 1968)

Environment			
External (Natural)	Internal (Induced)	Body State	Clothing
	Stress Factors		
	System failure	Physical condition	
	G-loads (weightlessness)	Degree of heat stress resistance (acclimatization)	
	Toxicity (CO_2, etc.) effects	Water/electrolyte balance	
	Radiation effects		
	Decompression (emergency)	Radiating area of body (A_r)	
	Hypoxia	Area of body irradicated	
	Psychological (morale, anxiety)	Effective skin absorbtance	
	Vibration		

Table 3–6
Data for Different Clothing Ensembles

Clothing Ensemble	Intrinsic Clo	A_c/A_b^*
Nude	0	1.0
Light working ensemble: jockey shorts, wool socks, cotton work shirt and work trousers; shirt tail out, neck open	0.6	1.1
U.S. Army "fatigues," man's lightweight underwear, cotton shirt and trousers, cushion sole socks, and combat boots	0.7	1.1
Typical American business suit	0.7 to 1.0	1.1 to 1.15
Light outdoor sportswear: cotton shirt, trousers, T-shirt, shorts, socks, shoes, and single-ply poplin (cotton and dacron) jacket	0.9	1.15
Heavy traditional European business suit: light cotton underwear with long legs and sleeves, shirt, woolen socks, leather shoes, tweed suit with trousers and fully lined jacket and vest	1.2	1.15 to 1.2
U.S. Army standard cold-wet uniform: cotton-wool undershirt and drawers, wool and nylon flannel shirt, wind resistant, water repellent trousers and field coat, cloth mohair and wool coat liner, and wool socks	1.5 to 2.0	1.3 to 1.4
Heavy wool pile ensemble (polar weather suit)	3 to 4	1.3 to 1.5

*Each clo of clothing insulation increases the ratio A_c/A_b by factor $(1 + 0.15\ I_{cl})$. Recent studies at Kansas State University (1972) may raise the factor 0.15 to 0.25. (Fanger, 1968).

The effective Clo values (i.e., I_a+I_{cl}) in a 7 psia 50 percent oxygen: 50 percent helium environment, therefore, would probably be 0.015: 0.017, or about 0.56 that of sea level air (Roth, 1967). The clothing surface area may be 50 percent greater than that of man (Nelson et al., 1947), although probably not all of the increased area is available for heat transfer. Table 3-6 presents typical ratios of the clothing surface area to the skin area.

Radiation Heat Transfer

The analysis of radiation heat transfer between an astronaut and his surroundings is complicated by a number of factors. These include:

1. Ability of the crew to move around and change position
2. Arrangement and surface temperatures of the various equipment enclosures
3. Localized differences in temperature of the cabin walls and size and location of windows.

The problem can be greatly simplified by theoretically collecting all equipment and structures into an equivalent enclosure at a mean radiation temperature. The following equation applies to a man in an enclosure at a single effective radiation temperature (McAdams, 1954). The man was assumed to be radiating heat at a single mean temperature equal to the temperature of the outer surface of the clothing.

$$\dot{Q}_r = \sigma F_{cw}\left(T_c^4 - T_w^4\right)A_r \tag{4}$$

Assuming that source and sink are gray bodies, the following equation, which includes the effect of geometric configuration, can be used for the radiation shape factor of a completely enclosed body (McAdams, 1954):

$$F_{cw} = \frac{1}{\frac{1}{\epsilon_c} + \frac{A_r}{A_w}\left(\frac{1}{\epsilon_w} - 1\right)} \tag{5}$$

The emissivity of human skin in the infrared range is approximately 0.99. The emissivity of clothing and skin at body temperature generally is assumed to be 0.95. The emissivity of surroundings (ϵ_w) will depend on the proportion of high and low emission surfaces subtended by the body. The range of emissivities will vary from 0.2 (for oxidized aluminum) through 0.9 (for transparent plastics and oil painted surfaces) to 0.95 for an adjacent crew member, also in shirtsleeves.

The effective radiation area of the body, A_r, will be less than the total exposed surface area of skin and clothing because some portions of the body are partially shielded from the surroundings. The measured ration between the effective radiation area and the total surface area are given in figure 3-2 for different positions (Guibert and Taylor, 1952).

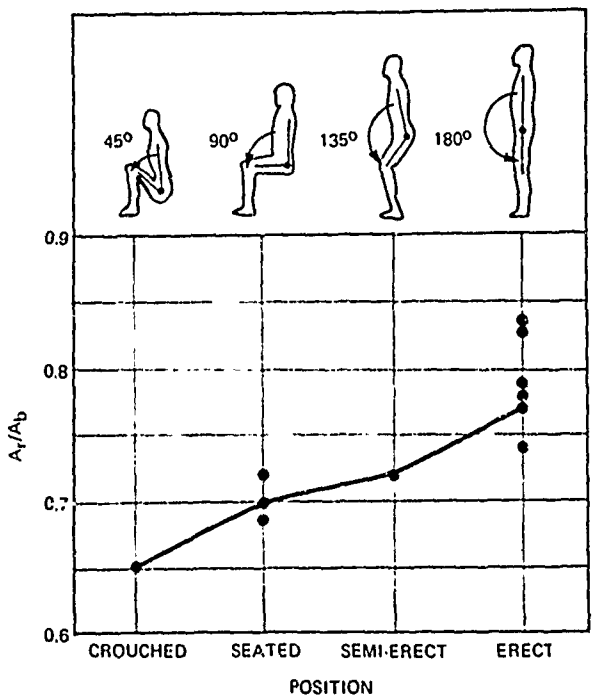


Figure 3–2. Body radiation area for various body positions. (From data of Guibert, 1952)

If man is in an enclosure much larger than himself, the ratio A_r/A_w in equation 5 is small, and $F_{cw} = \epsilon_c$. Therefore, equation 4 becomes

$$\dot{Q}_r = \sigma \epsilon_c A_r \left(T_c^4 - T_w^4 \right) \tag{6}$$

The radiation heat transfer coefficient is defined by the following equation:

$$\dot{Q}_r = h_r A_r (T_c - T_w) \tag{7}$$

Therefore, from Equation 4

$$h_r = \frac{\sigma F_{cw}(T_c^4 - T_w^4)}{T_c - T_w} \tag{8}$$

Values of the radiation heat transfer coefficient are presented in figure 3-3 for $F_{cw} = 0.9$.

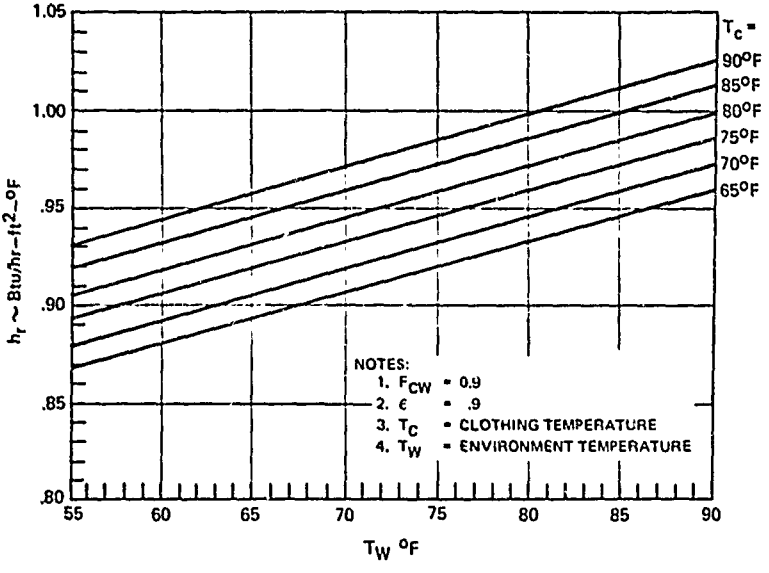


Figure 3–3. Values of the radiation heat transfer coefficient.

In addition to determining the mean radiant temperature of the surroundings, it is important to consider local effects. A man located between warm and cold surfaces at a neutral atmospheric temperature and apparently comfortable may experience pain and stiffness in the muscles exposed to the cold surface after a prolonged period of time, especially after sleep.

Forced Convection Heat Transfer

The rate of heat transfer by convection can be written:

$$\dot{Q}_c = h_c A(T_c - T_a) \tag{9}$$

The convective heat transfer coefficient, h_c, is a complicated function of fluid flow, thermal properties of the fluid, and the geometry of the body. Because there has been some variance between the values used by different groups in relating the h_c of man to the atmospheric gas velocity, selecting the appropriate heat transfer coefficient is a difficult problem. A discussion of the implications of different coefficients used in the analysis of forced convection about the human body was published by Kerslake, (1963).

Figure 3-4 represents a summary of several approaches to forced convective heat transfer coefficients (convective film coefficients) for man in an environment containing air at ½ atm. The first three curves represent the h_c values obtained from empirical studies of humans. These are compared with four theoretical curves: (1) a cylinder in longitudinal flow, (2) a cylinder 10 inches in diameter in crossflow, (3) a flat plate with flow perpendicular to it, (4) a cylindrical model of man in crossflow (figure 3-5). The value of h_c for the cylindrical model of man corresponds closely with those obtained by Nelson (1947) and are equivalent to h_c for crossflow about cylinders 5 inches in diameter.

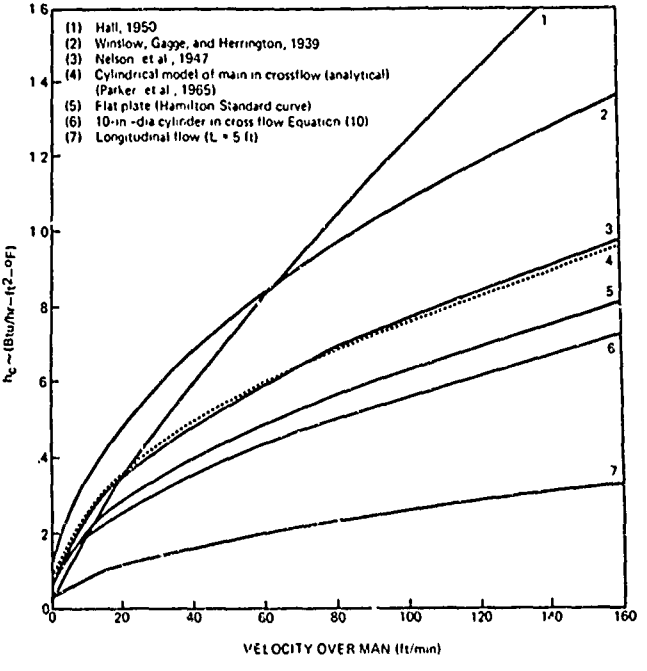


Figure 3–4. Comparison of forced convection film coefficients for man at 1/2 atm of air. (After Parker et al., 1965)

The following equation, derived from the heat transfer correlation for fluids flowing perpendicular to cylinders, estimates the forced convection heat transfer coefficient for all gas mixtures (Berenson, 1965):

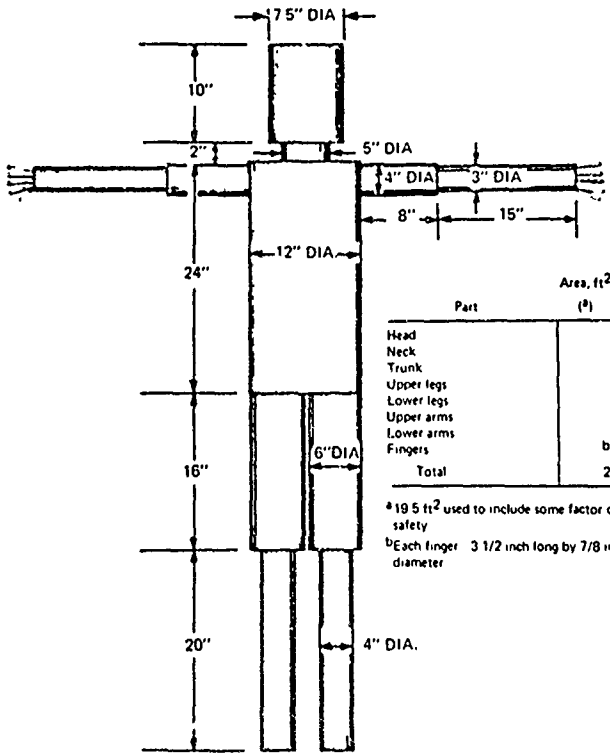
$$h_c = 0.021\, k_c \sqrt{PV} \qquad (10)$$

where P = psia, V = ft/min, and

k_c = a factor that depends on the transport properties of the gas mixture. For $0_2 - N_2$ mixtures, $k_c = 1$; for other gases,

$$k_c = \frac{k_{mix}}{k_{air}} \left(\frac{M_{mix}}{M_{air}} \times \frac{\mu_{air}}{\mu_{mix}} \right)^{0.5} \left(\frac{Pr_{mix}}{Pr_{air}} \right)^{0.33} \qquad (11)$$

For example, a 50-percent oxygen-helium atmosphere at 7 psia, $k_c = 1.6$.



Part	Area, ft² ([a])
Head	1.95
Neck	.22
Trunk	6.18
Upper legs	4.19
Lower legs	3.49
Upper arms	1.40
Lower arms	1.96
Fingers	[b] .67
Total	20.06

[a] 19.5 ft² used to include some factor of safety

[b] Each finger 3 1/2 inch long by 7/8 inch diameter

Figure 3–5. Cylindrical model of man. (After Parker et al., 1965)

Figure 3-6 shows the effect of gas velocity on the convection heat transfer coefficient based on the cylindrical model of man for various helium- oxygen and nitrogen-oxygen atmospheres. The partial pressure of oxygen at 170 mm Hg is near the sea level equivalent and is held constant with the diluent gas ranging from 0 to 400 mm Hg.

The values for neon mixtures will lie between those for helium and nitrogen. It is clear from comparing the physical properties of the gases that

for different mixtures of oxygen-nitrogen there is little sensitivity of h_c to percent composition of gas.

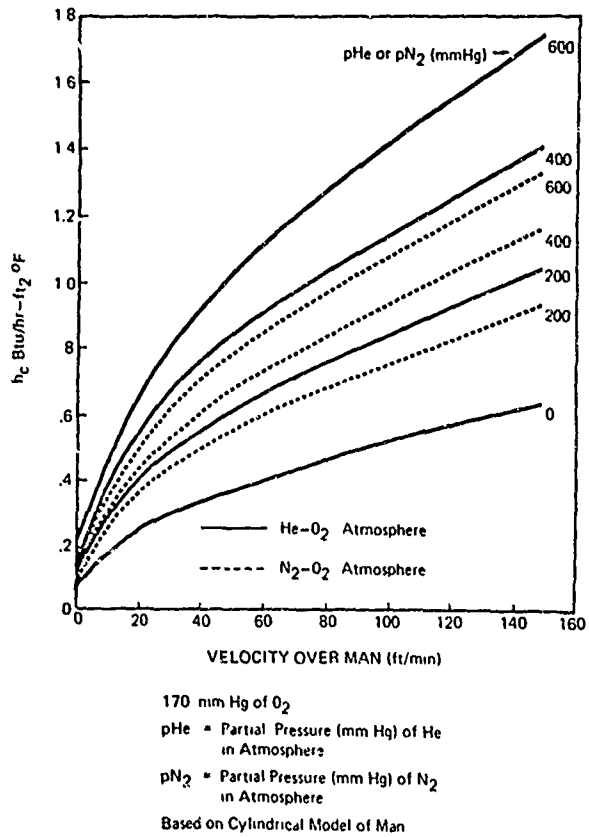


Figure 3–6 Heat transfer coefficients of man in $O_2 - He$ and $O_2 - N_2$ at different gas velocities. (After Parker et al., 1965)

All of the correlations for the forced-convection heat transfer coefficient are consistent with the following general theoretical correlation:

$$\frac{h_c D}{k} = \text{const.} \left(\frac{\rho V D}{\mu}\right)^{0.5} \left(\frac{C_p \mu}{k}\right)^{0.33} \tag{12}$$

The only difference between the equations is the value of the empirical correlating constant. As shown in figure 3-4, there is a variation of ±50 percent between the various correlations.

Free Convective Heat Transfer

In the presence of a gravitational field such as on the Earth, planetary surfaces, or rotating space stations, free convection is possible and is the preferred mode of cooling because no additional fan energy need be expended. General free-convection heat transfer equations yield the following simplified equation for free-convection cooling in nitrogen-oxygen mixtures (Berenson, 1965).

$$h_c = 0.06 \left[P^2 g (T_c - T_a)\right]^{0.5} \tag{13}$$

Mixed free and forced convection environments can be handled by McAdams' rule, which states that both the free and forced convective heat transfer coefficients are calculated and the higher of the two values used (McAdams, 1954). The critical forced convection velocity (v_{crit}), where the forced convection heat transfer coefficient is equal to the free convection coefficient, can be calculated for oxygen-nitrogen mixtures by equating equations 10 and 13.

$$V_{crit} = 8.3 \left[g (T_c - T_a)\right]^{0.5} \text{ ft/min} \tag{14}$$

If the forced convection velocity is less than the critical value, free convection is the dominant heat transfer process.

Forced Convection Evaporation

The rate of heat transfer by evaporation can be written (Berenson, 1965):

$$Q_e = h_D h_{fg} AC \left(\frac{P_s - P_a}{RT_s}\right)_{H_2O} \tag{15}$$

The mass transfer coefficient, h_D, is a complicated function of fluid flow, fluid properties, and body geometry. The mass transfer coefficient can be calculated from the heat transfer coefficient, h_c, by using the heat-mass transfer analogy with the following result (Eckert & Drake, 1959):

$$h_D = \frac{h_c \quad Pr^{2/3}}{\rho C_p \quad Sc^{2/3}} \tag{16}$$

The following equation for the evaporation heat loss results from combining equations 10, 15, and 16 (Berenson, 1965).

$$Q_e = 0.126\,CAT_a\,k_e\left(\frac{V}{P}\right)^{0.5}\left((P_s - P_a)\right) \tag{17}$$

where V = ft/min

P = psia

k_e = a fluid property parameter that depends on the diffusivity of water vapor in the gas mixture and on the transport properties of the gas mixture itself. For air, $k_e = 1$. For other gases,

$$k_e = (k_D)^{0.67}\left(\frac{M_{mix}}{M_{air}} \times \frac{\mu_{air}}{\mu_{mix}}\right)^{0.17} \tag{18}$$

The diffusion coefficient for water in helium is 3.5 times that for water in air. For the case where the water is diffusing into a mixture of helium and oxygen, diffusivity relative to air, k_D, is found from

$$k_D = \frac{1}{\dfrac{\text{MOL FRACT. He}}{3.5} + \dfrac{\text{MOL FRACT. } O_2}{1}} \tag{19}$$

For example, for the 50 percent oxygen atmosphere in helium at 7 pisa, $k_D = 1.554$. Therefore, for the k_e values calculated for the oxygen-helium atmosphere containing 50 percent oxygen,

$$k_e = (1.554)^{0.67}\left(\frac{18}{29} \times \frac{12.10}{13.47}\right)^{0.17} = 1.219$$

The exponent of V in equation 17 is 0.5. Some empirical data yielded an exponent of 0.63 (Clifford et al., 1959). In view of the other assumptions that must be made regarding clothing and body positions, the uncertainty introduced by this difference is not serious. In fact, the calculated values of maximum evaporative loss (C = 1) give predicted results only 10 percent higher than actually measured (Clifford et al., 1959; Webb, 1967). Since the rate of evaporation and the diffusion coefficient for water vapor are inversely

proportional to pressure, latent cooling capacity increases with decreasing (total) pressure (Taylor & Buettner, 1953).

Curves illustrating the general magnitude of the pressure, dew point, and gas stream velocity effects predicted by equation 17 are presented in figure 3-7. In the temperature range under consideration for space cabins, the temperature and the dew point have relatively little effect as compared to gas stream velocity and ambient pressure.

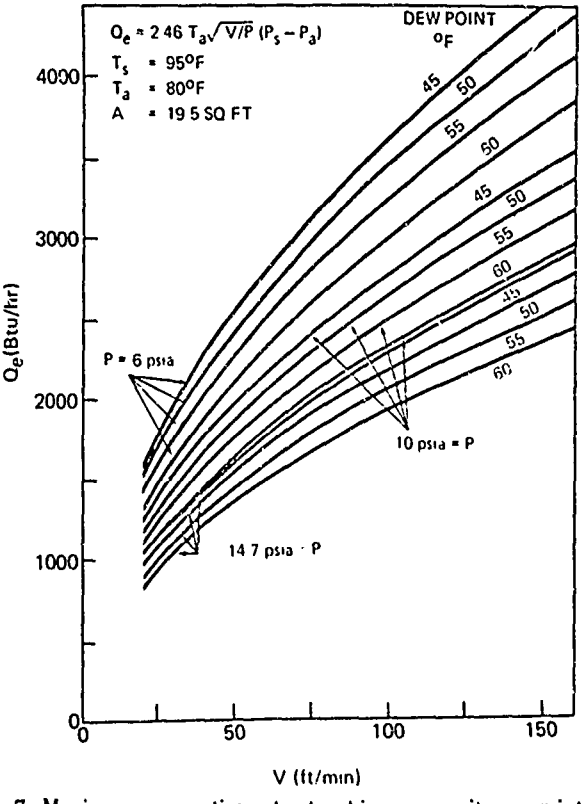


Figure 3–7. Maximum evaporation rate at rest in oxygen-nitrogen mixtures. (Berenson, 1965)

It is likely that the body does not become fully wetted with sweat until the sweat rate is about twice the maximum evaporative capacity. Loss of sweat by dripping probably begins when the sweat rate is about 1/3 of the maximum evaporative capacity (Kerslake, 1963). The effect of body position and geometry on the constants of these equations cannot be overemphasized. The effect of clothing also is an important factor in determining evaporation rates (Blockley et al., 1954).

Free Convection Evaporation

A free convection evaporation cooling equation also can be developed using the heat-mass transfer analogy. For example, combining equations 13,

15, and 16 yields the following equation for the free convection evaporation rate in oxygen-nitrogen mixtures (Berenson, 1965):

$$Q_e = 1.3A \frac{CT_a}{P} (P_s - P_a)\left\{Pg\left(0.005\,P(T_c - T_a) + 1.02\,(P_s - P_a)\right)\right\}^{0.25} \quad (20)$$

Respiratory Heat Loss

Heat loss due to respiration varies directly with metabolic rate and is influenced by atmospheric composition (including carbon dioxide and water vapor content) and pressure. Because the respiratory tract is a very efficient saturator of inspired air, heat gain to the body through respiration will not occur until atmospheric temperature approximates 185°F (McCutchan & Taylor, 1951).

Heat loss from the lungs approximates 10 percent of the metabolic rate (7 to 8 kcal/hr) in the neutral zone (Hardy, 1964). Definitive data are available for determining respiratory heat loss for the atmospheric compositions and pressures of interest in space flight environments, especially those of the space suit (Bryan, 1964; Webb, 1955; Wortz et al., 1966).

After determining the pulmonary ventilation rates corresponding to a specific activity level and stress factors such as hypoxia, hypercapnia, or anxiety, the heat loss due to respiration can be caluclated by determining the sensible heat required to raise the inspired atmosphere to expiration temperature and adding the heat of vaporization increment for the moisture lost to the inspired air from the respiratory tract.

One expression for calculating respiratory heat loss is (Wortz et al., 1966):

$$Q_v = \dot{V}\rho C_p (T_e - T_i) \div 0.58\,(W_e - W_i)\ (\text{cal/hr}) \quad (21)$$

where $\dot{V}$ = volume of atmosphere breathed per hour (liters/hr)
ρ = density of the atmosphere (gm/liter)
C_P = specific heat of atmosphere (kcal/Kg–°C)
T_e = temperature-expired atmosphere (°C)
T_i = temperature-inspired atmosphere (°C)
0.58 = heat of vaporization H_2O (kcal/gm)

W_e = weight of water in expired atmosphere (gm)

W_i = weight of water in inspired atmosphere (gm)

A more simplified approach is also available (McCutchan & Taylor, 1951).

Thermal Comfort

Comfort Criteria

Comfort zones have been defined in the literature in terms of skin temperature, sweat rates, and various indexes that relate environmental parameters to subjective impressions of comfort or measured values of selected physiological variables. For the same conditions and individuals, the established boundaries for thermal comfort, performance, and tolerance as described by the various design indexes may be completely consistent. Variations in activity, wearing apparel, individual health and acclimatization, and thermal exposure immediately prior to making a determination of comfort, however, will operate to shift the zones and introduce inconsistencies in results (Gagge, 1966).

A large amount of literature is available concerning human comfort and physiology under a wide range of conditions in the Earth environment. Examples of comfort indexes established in the past are the British Comfort Index (Dunham et al., 1946), ASHRAE (American Society of Heating and Air Conditioning Engineers) Effective Temperature, and Operative Temperature (cited in Webb, 1964). Unfortunately, because of important differences in gravity and pressure found in space environments, most of these data are not directly applicable to the design of spacecraft thermal control systems. The following comfort criterion is generally applicable.

Krantz (1964) describes a comfort design criterion developed by Winslow et al. (1937), based on p centage utilization of the maximum evaporative cooling capacity. It was found that on the hot side of comfortable conditions, sweat production was definitely related to the sensation of discomfort; on the cold side, skin temperature below 90°F produced a cool feeling. As shown in table 3-7 the sensation of comfort was related by Winslow et al. (1937) to the percent of the body covered by moisture.

The comfort design method described by Krantz (1964) involves analysis of the environmental conditions to estimate the radiation and convection heat transfer from the body. The metabolic rate necessary to sustain the activity level is estimated. The difference between the metabolic rate and the radiation and convection heat loss, therefore, is the required evaporative cooling. The environmental design conditions are then evaluated with respect to the maximum evaporative cooling capacity; if the required evaporative cooling represents from 10 to 25 percent of the maximum, the environment is in the comfortable range. If it is outside this range, some of the

environmental design factors (gas temperature, ventilating gas velocity, or wall temperature) should be changed to provide a comfortable environment. Although this concept is simplified and has not been proven for all values of total sweat output and atmospheric conditions, it is plausible and can be generally applied.

Table 3–7

Evaporative Capacity Comfort Criterion

Percent of Maximum Evaporative Capacity	Comfort Level	Skin Temperature	
		°F	°C
0 to 10	Cold	<89	31.7
10 to 25	Comfortable	90 to 92	32.2 – 33.3
25 to 70	Tolerable	93 to 94	33.9 – 34.4
70 to 100	Hot	>95	35
Over 100	Dangerous		

With resting, unclothed subjects, approximately 10 percent of the maximum evaporative capacity is provided by insensible moisture loss from the body by respiration and by diffusion through the skin. This moisture loss is not subject to thermoregulatory control, and an indicated evaporative cooling requirement less than this amount represents overcooling of the body. With normally clothed subjects the insensible moisture loss is 5 percent of the maximum evaporative capacity. These losses are, of course, a function of the metabolic output and respiratory rate. Recent unpublished data from the NASA Manned Spacecraft Center, Houston, suggest that the minimum latent heat loss by evaporation, $Q_{e\ min}$, is given by the following equation:

$$Q_{e\ min} = 0.125\, E_m + 50\ (\text{Btu/hr}) \qquad (22)$$

This fact alters previous approaches to setting the cold-comfort boundary using C = 0.1 as a criterion.

In summary, the thermal comfort design objectives are that body storage be zero, evaporative heat losses be limited to insensible evaporation of moisture produced only by respiration and diffusion through the skin without the activity of sweat glands, and that body and skin temperatures be maintained near normal values of 37°C (98.6°F) and 33° to 34°C (91.5° to 93.5°F) for a resting subject. During exercise each multiple increase in resting metabolism decrease the skin temperature for comfort by approximately 1°C and the rectal temperature rises by 0.2°C but the mean body temperature for comfort remains essentially the same during rest and exercise.

Comfort Zones

Because of the dearth of empirical data on comfort zones in uncommon gas environments, several attempts have been made to predict these values. Figures 3-8 and 3-9 represent typical results of one approach using equations 6, 10, 13, 17, and 20 to estimate the comfort zone in oxygen-nitrogen mixtures for various combinations of forced vs free convection, Clo values, etc. (Berenson, 1965). Comfort was established from the ratio of required evaporative cooling to predicted maximum evaporative capacity, C, using the criterion of table 3-7 with the exception that equation 22 was used to calculate the lower boundary of the comfort zone. In addition, the skin temperature was constant at 91.4°F instead of varying with C in the manner shown in table 3-7.

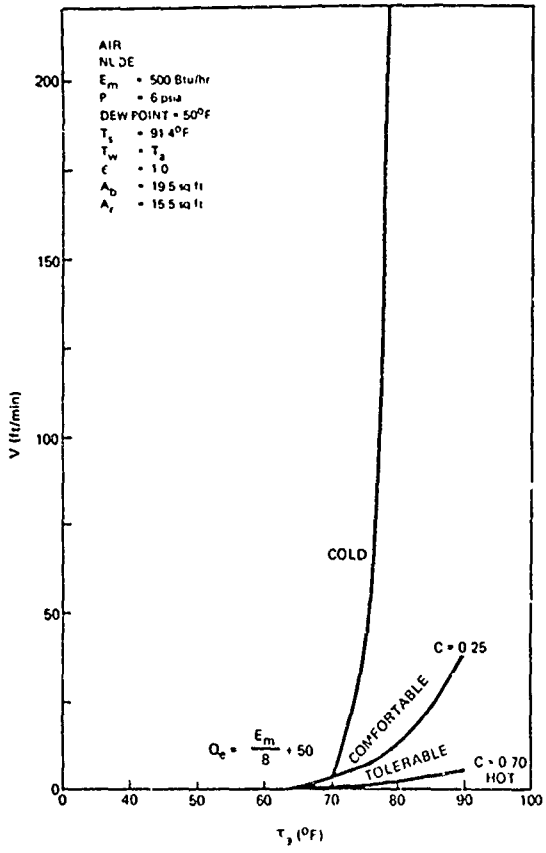


Figure 3–8. Forced-convection comfort zones during mild exercise. (Modified from Berenson, 1965)

Unfortunately, there are few empirical data to substantiate these curves. Preliminary studies tend to corroborate some of these predictions for different oxygen-nitrogen environments (Bonura & Nelson, 1967; Secord & Bonura, 1965; Roth, 1968). In addition, the predictions of this approach agree with the ASHRAE data (Berenson, 1965).

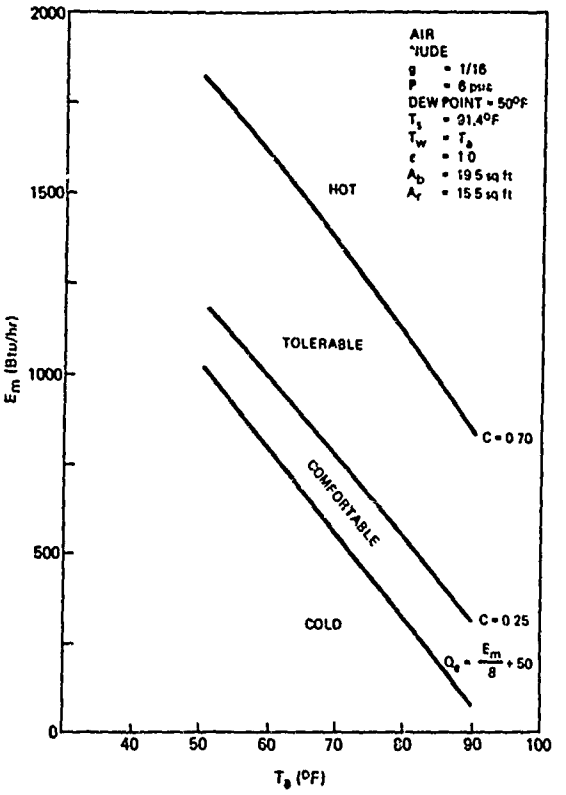


Figure 3–9. Lunar free-convection comfort zones as related to exercise rate in the nude. (Modified from Berenson, 1965)

For cabins with oxygen-helium mixtures, other heat flow constants must be used to determine comfort zones (see equations 10 and 17). Empirical comfort temperatures in different gas mixtures have not been systematically obtained. Comfort temperatures have been recorded only as the average cabin temperature set over periods of several weeks by subjects who had control over the thermostat within the cabins (Roth, 1968). These temperature settings for subjects in surgical clothes, which have about 0.5 Clo in air, are presented in table 3-8. These data include varied numbers of different subjects being studied under each gas mixture. No windspeed measurements were taken during these studies, however, the velocity was probably negligible.

Other studies found comfort temperatures in He-O_2 at higher levels (Bonura & Nelson 1967; Secord & Bonura, 1965). In these studies, the average temperature settings during a varied work-rest cycle with 0.7 Clo were 78° F for nitrogen-oxygen at 7 psia and 85° F for helium-oxygen at 5 psia.

Table 3-9 presents additional data on Earth comfort zone boundaries for men at rest in reduced pressure N_2-O_2 and He-O_2 atmosphere (Fanger et al., 1968). Gas velocity was varied from 20 to 80 ft/min with little effect on the comfort zone boundaries.

Table 3–8

Temperatures Selected by Subjects in Space Cabin Simulators

	3.7 psia O_2, 100 Percent	5 psia O_2, 100 Percent	5 psia P_{O_2}, 175 mm Hg pHe, 74 mm Hg	7.3 psia P_{O_2}, 150 mm Hg pHe, 230 mm Hg	7.3 psia P_{O_2}, 165 mm Hg P_{N_2}, 206 mm Hg
Selected Temperature, °F	69.3	70.9	74.7	75.4	72.7

(After Welch, 1966)

Table 3–9

Comfort Zones as a Function of Atmospheric Pressure and Composition

Gas mixture	Atmosphere								
	He - O_2					N_2 - O_2			
Pressure	5 psia		7 psia		10 psia	5 psia		7 psia	
Clo valve	0	0.7	0	0.7	0	0	0.7	0	0.7
Upper limit	93	92	94	94	95	95	83	94	84
Mean	84	82	86	85	86	86	77	86	78
Lower limit	76	73	77	76	78	76	71	78	73

(Data of Fanger et al., 1969)

Heat Stress

Space operations require an understanding of man's responses to thermal stress and his capacity to tolerate heat. Extensive data are required in addition to those presented previously on comfort zones to reach even an index of man's response to thermal loads. The dependent variables that must be considered include body temperatures, sweat response, pain and discomfort thresholds, body stress, and psychomotor performance.

Body Temperatures

The body temperatures used in thermal analyses are body core temperature (T_r), skin temperature (T_s), and mean body temperature (T_b).

Body Core Temperature (T_r). Internal body or deep body core temperature is an important factor in the thermoregulation of the body. Rectal temperature (T_r) is considered a reasonable measure of deep core temperature and is easily obtained. Core temperature remains remarkably constant at a mean of 37°C or 98.6°F as long as the body is in thermal equilibrium. Internal body temperature is to some extent a function of the external environment, but is less so than skin temperature. Even under conditions where thermal adequacy is provided, there is a tendency for increased core temperature at higher metabolic rates.

Changes in core temperature can affect the rate of reaction of the various biochemical reactions that make up the metabolic processes of the body. This effect is called the Q_{10} effect and results from the temperature dependence of the chemical reaction rates which provide metabolic energy. That is, at temperatures above approximately 98°F, there will be approximately a 7 percent increase in metabolic rate per °F increase in internal body temperature. Similarly, at temperatures less than 98°F, there will be a corresponding decrease in metabolic rate due to a decrease in the chemical reaction rate. The Q_{10} effect is important in considering the thermal tolerance limits for human endurance. If the body is unable to adjust suitably to the environment and the internal temperature falls outside the control range, the Q_{10} effect results in a more severe condition, by decreasing metabolic heat output under cold conditions, and by increasing metabolic heat output during hot conditions.

Skin Temperature (T_s). Skin temperature is primarily a function of the thermal environment of the body and the resulting heat exchange with the ambient. Decreasing environmental temperatures result in reduced skin temperatures; decreasing ambient pressure leads to increased skin temperatures. The following expression (equation 23) is used to derive a mean skin temperature, which can then be used in computing mean body temperature (equation 24) and energy balance (equation 1).

$$\begin{aligned} T_s = {} & 0.12\,T_{back} + 0.12\,T_{chest} + 0.12\,T_{abdomen} \\ & + 0.14\,T_{arm} + 0.19\,T_{thigh} + 0.13\,T_{leg} \\ & + 0.05\,T_{hand} + 0.07\,T_{head} + 0.06\,T_{foot} \end{aligned} \qquad (23)$$

Mean Body Temperature (T_b). Mean body temperature is derived from the weighted sum of the rectal and mean skin temperatures. The weighting varies as a function of ambient temperature (Stolwijk & Hardy, 1966). For ambient temperatures of less than 30°C (Burton, 1946):

$$T_b = 0.67\,T_r + 0.33\,T_s \qquad (24)$$

For zone of evaporative regulation temperatures (T_a>28°C, 85°F), the weighting is 1:4 for T_s: T_r or 1:9 for T_s: T_{es} (esophageal). Mean body temperature is used primarily as a determinant of heat storage or vice versa.

Heat Stress and Water Loss from the Body

The response of body core (rectal) temperature to heat stress induced by ambient conditions and metabolic loads is shown in figures 3-10 and 3-11. Note in figure 3-10 that for each level of work, there appears to be a characteristic internal or core temperature at equilibrium which is unaffected by the environment so long as the neutral boundary condition, is not exceeded. As the figure shows, the characteristic internal (rectal) temperature for a particular work load varies between groups; both physical training and training for work in the heat (acclimatization) produce lower values. Superficial differences between ethnic groups appear to be due to habit patterns and experience relative to working under hot conditions. Figure 3-11 clearly illustrates the effect of heat training (acclimatization) on the equilibrium rectal temperature, and the small, probably insignificant, effect of training on the location of the neutral boundary. Note that in the neutral zone, heat-trained men working at 1600 BTU/hr maintain body temperatures as low as or lower than novice workers working at 700 BTU/hr. However, when both groups are in the stress zones for their respective work levels, the difference between their mean body temperatures is 1.5°F. For comparison, new men working at 1600 BTU/hr have temperatures 1.5°F higher than similar men working at 700 BTU/hr, when both are in their neutral zone of environments. The figure plots mean thermal rectal temperature against effective temperature, which has been defined by the American Society of Heating, Refrigerating and Air Conditioning Engineers, Inc. (ASHRAE) as "an arbitrary index which combines into a single value the effect of temperature, humidity, and air movement on the sensation of warmth or cold felt by the human body. The numerical value is that of the temperature of still, saturated air which would induce an identical sensation."

Man's responses in atmospheres other than air at sea level are under evaluation (Epperson et al., 1966).

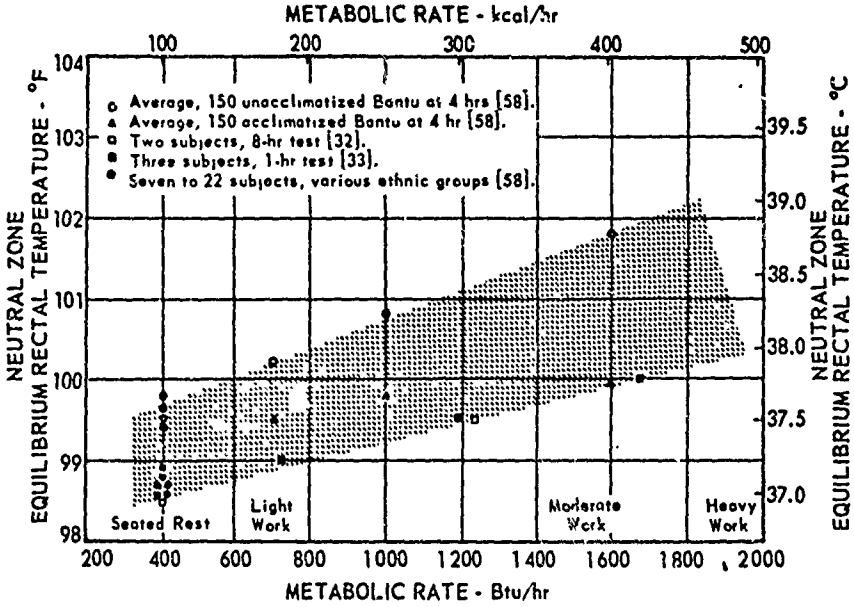


Figure 3–10. Variations in rectal temperature at sea level as a function of activity. (After Blockley, 1964: adapted from Hanifan et al., 1963, based on data from Lind, 1963; Strydom & Wyndham, 1963; & Wyndham et al., 1954)

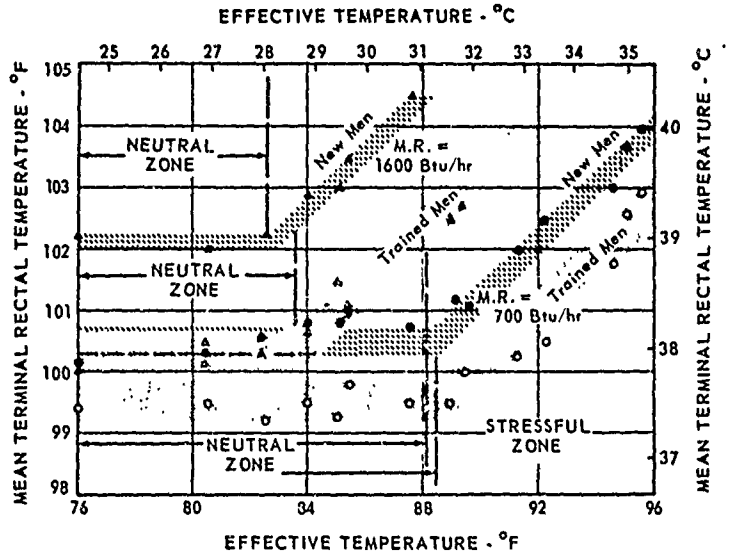


Figure 3–11. Rectal temperature and stress zones for work in heat at sea level. Data from 460 individuals, 2 work rates, and 15 different humid environments. Vertical lines separate "neutral" (environment-independent) and "stressful" (environment-driven) zones before and after training. (After Blockley, 1964, drawn from data of Wyndham et al., 1954)

Sweating and Respiratory Water Loss. In normal man, heat stress can be evaluated by the rate of water loss from the body. Analyses of evaporative heat exchange under various conditions were presented above. In addition to these data, which are applicable to space operations, figures 3-12 to 3-14 represent the sweat production rates to be expected under survival conditions on Earth. Figure 3-12 shows how loss of water through the skin by diffusion is influenced by the vapor pressure gradient, the skin temperature, and the barometric pressure. A high skin temperature is shown to be related to a high diffusion loss. Warm skin free of sweat was produced in the experiment illustrated by a high dosage of atropine. The graph also shows that diffusion is increased as barometric pressure is lowered. Figure 3-13 shows the effects of various environmental conditions on sweat production. Note in figure 3-13(a) that the relationship of skin temperature to sweat production is highly variable under various environmental conditions. In figure 3-14 data are plotted for six experiments on one subject, who was "fully acclimatized," of "better than average stamina," who marched at 3.5 mph up a 2.5 percent grade, at 100°F and 20 mm Hg, with a 10-minute rest every hour. The more water he drank, the lower was his rectal temperature. Other experiments with nude subjects resting at 110°F and vapor pressure of 25 mm Hg have shown that they were able to maintain equilibrium only if they replaced water continuously. It may be concluded that failure to replace completely the water lost in sweat, hour by hour, leads to elevation of body temperature and excessive physiological strain. Thirst or the desire to drink is unreliable as an indication of the requirement for water intake to make up for heavy sweating. Other work has shown that replacement of salt at regular mealtimes is adequate in contrast to the situation illustrated in figure 3-14 for water.

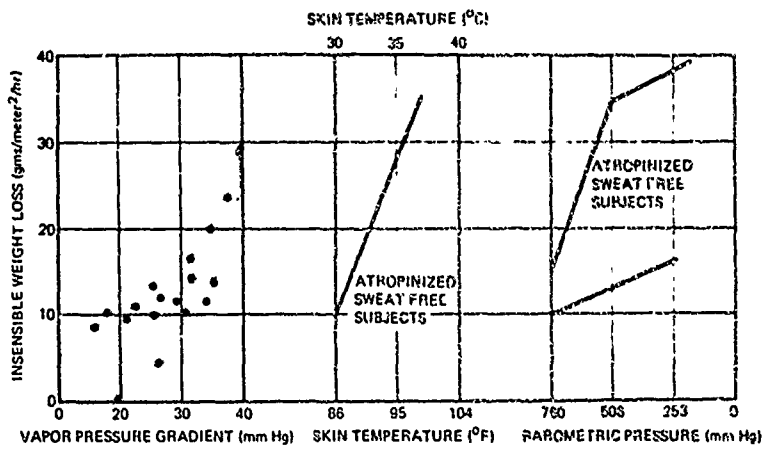
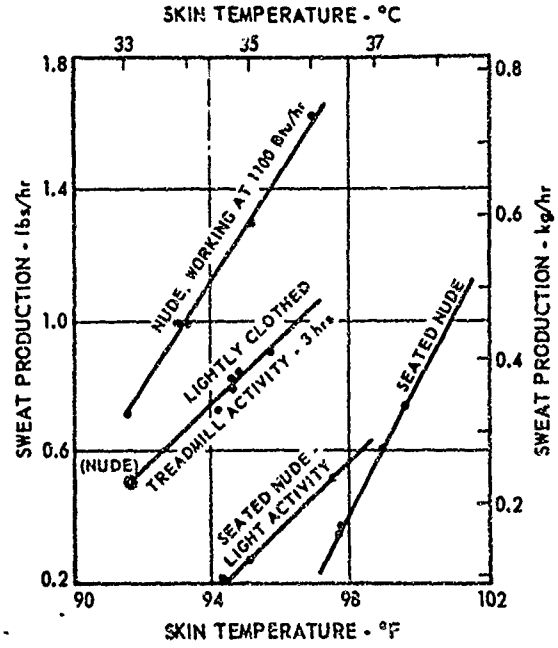
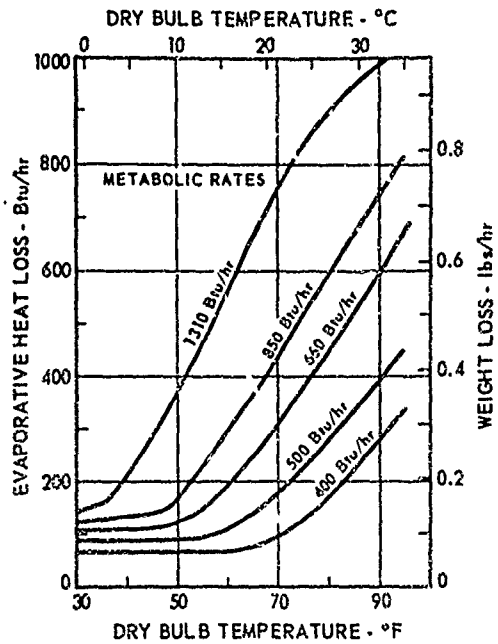


Figure 3–12. Insensible water loss from the skin as a function of absolute humidity, skin temperature, and barometric pressure. (After Blockley, 1964, drawn from data of Brebner et al., 1956; Hale et al., 1958; Webb et al., 1957; Zollner et al., 1955)

Figure 3-15 represents the sensitivity of water loss through respiration to a metabolic rate and ambient pressure and dew point (Wortz, 1966). Rates of nonthermal sweating are about 80 to 220 gm/hr from covered areas and 20 to 40 gm/hr from the rest of the skin (Webb, 1967). This can be increased by psychogenic stimuli of many types (Webb, 1967).



(a)



(b)

Figure 3–13. Water loss by sweating under different environmental conditions. A: sweat rates during various laboratory procedures; B: sweating and evaporative heat loss varying with air temperature and activity level. (After Blockley, 1964; adapted from a. MacPherson, 1960; reprinted by permission of the Controller of Her Britannic Majesty's Stationery Office; Robinson et al., Taylor & Buettner, 1953; and Webb et al., 1957; b. Thompson Ramo Wooldridge, Inc, 1961)

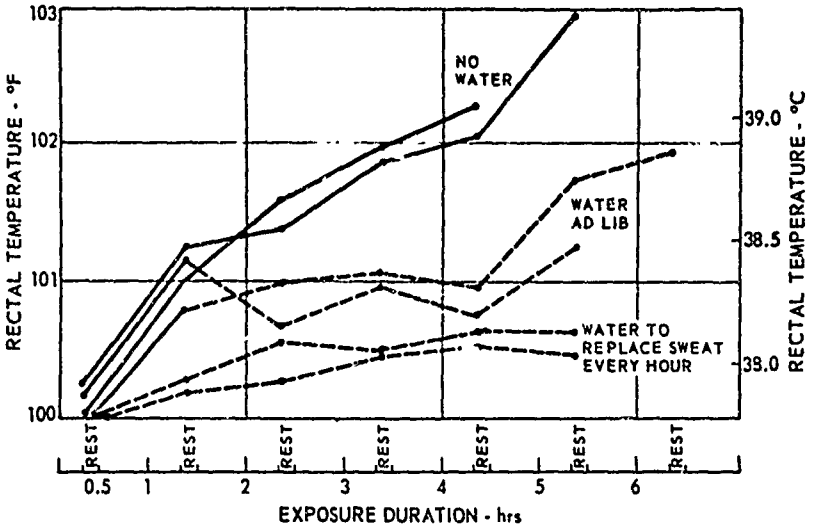


Figure 3–14. Sweating rates; water replacement. (After Blockley, 1964, adapted from Pitts et al., 1944)

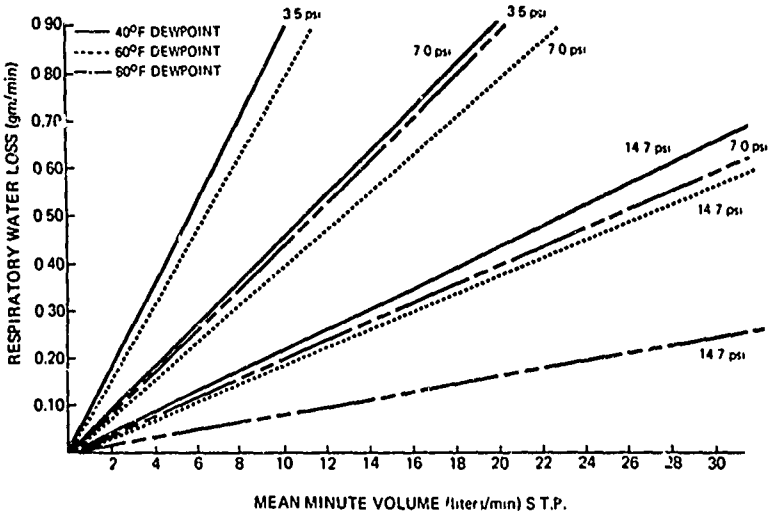


Figure 3–15. Respiratory water loss as a function of minute volume for all work rates and dry-bulb temperatures. (After Wortz et al., 1966)

Heat Stress Indexes. In the noncompensable zones of thermal control, performance and tolerance have an inverse exponential relationship with exposure time. Figure 3-16 reflects the general time-tolerance relationship for extremes of ambient air temperature under sea level conditions.

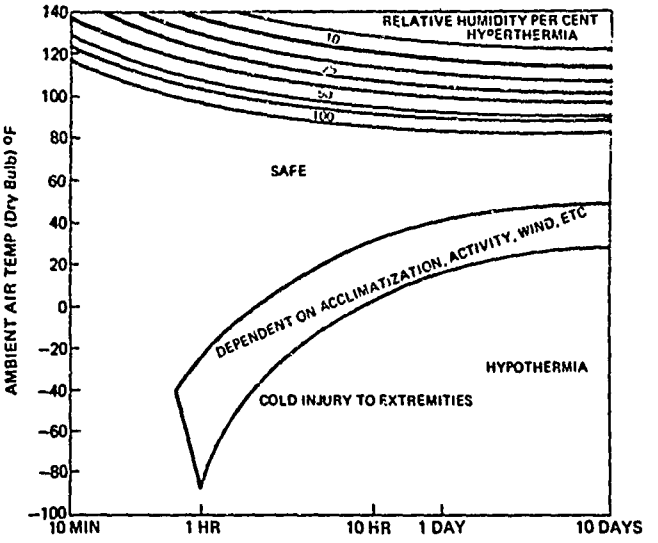


Figure 3–16. Approximate human time-tolerance temperature with optimum clothing. (After Breeze, 1961)

Figure 3-17 shows the physiological impairment that may be anticipated due to extremes of body temperature. The tolerance limits reflect the borders of physiological collapse to be used for rough evaluation of situations.

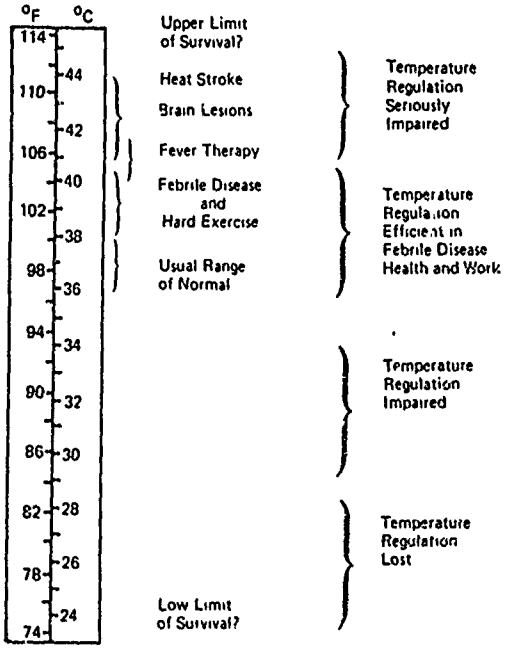


Figure 3–17. Human body temperature extremes defining zones of temperature regulations. (After Breeze, 1961)

Under conditions of heat stress, the mode of evaporative heat loss cannot completely compensate for the difference between total heat load and heat lost through other modes. This lack may be attributable to failure to achieve a sufficiently high perspiration rate or by failure to achieve a sufficiently high evaporation rate. Even though the perspiration rate is adequate to maintain thermal balance, conditions of high humidity and/or low ventilation may limit evaporation rates to values below that required for adequate cooling.

Some environmental correlates of comfort and stress were discussed previously. The more physiologically determined indexes will now be reviewed. A more detailed critique of the physically and physiologically determined heat stress indexes is available (MacPherson, 1962).

The Belding-Hatch Heat Stress Index (HSI). The Belding-Hatch (1955) heat stress index is defined as the ratio of evaporation rate required for energy balance to maximum perspiration rate safely attainable for prolonged periods—both expressed in liters (of sweat) per hours, or:

$$HSI = \frac{E}{E_{max}} \times 100 \qquad (25)$$

The criteria on which the heat stress index is based are:

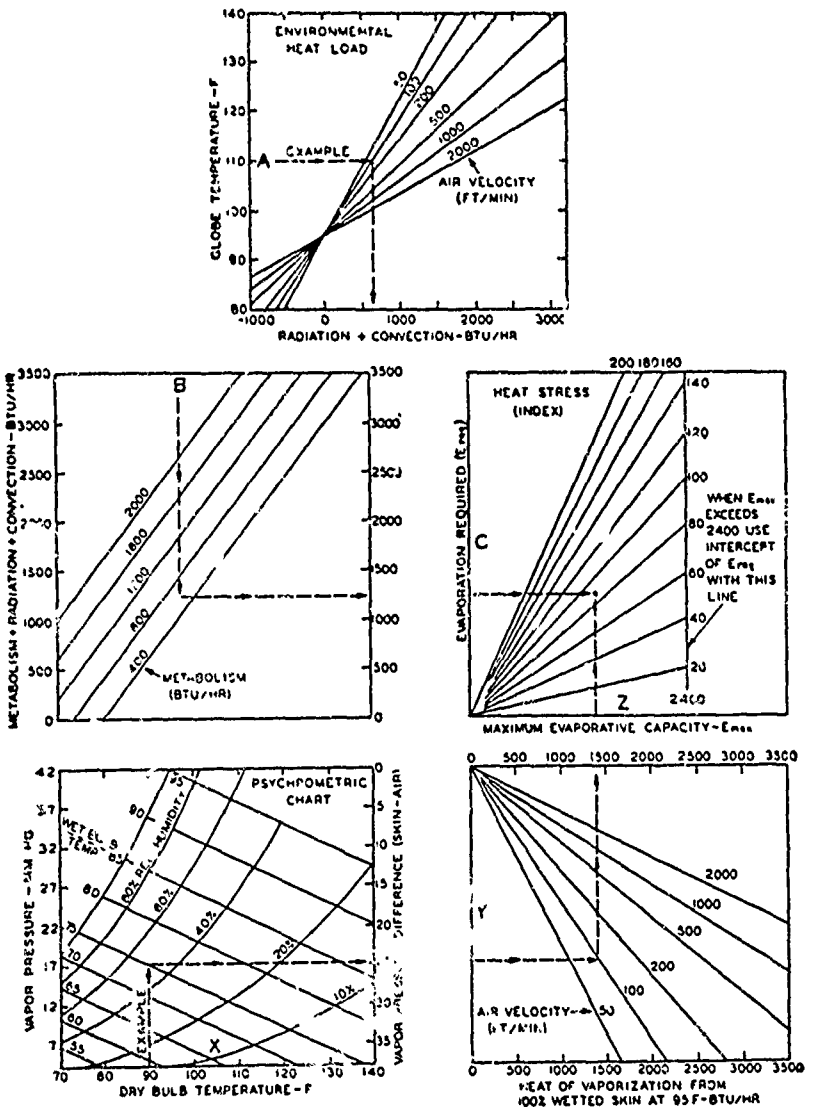
a. Body heat storage will not exceed the limit represented by a mean skin temperature of 95°F, and

b. E_{max} will not exceed 1 liter/hr; equivalent to 2400 Btu/hr (400 kcal/hr).

Figure 3-18 and table 3-10 can be used as indicated to estimate the physiological and general function impairment of an 8-hour exposure at sea level to several stressful thermodynamic parameters.

The P4SR Index. The sweat rate can be used as a predictor of thermal stress in another way. The predicted 4 hour sweat rate (P4SR) uses only the rate of sweating as a criterion of heat stress in environments that are hot enough to cause sweating (Wyndham, 1952). On the basis of British experimental work, empirical nomograms have been developed for predicting the probable amount of sweat in liters that would be secreted over a 4-hour period by fit, acclimatized men under different environmental conditions (Smith, 1955). A P4SR nomogram is shown in figure 3-19.

The group of curves marked S1 and S2 in the center of the nomogram, running downwards from right to left, constitute the scale from which the basic 4-hour sweat rate (B4SR) is read. If the predicted 4-hour sweat rate (P4SR) is required for men sitting in shorts, the calculation is very easy as the P4SR is the same as the B4SR. All that is necessary is to join the appropriate point on the dry-bulb scale to the wet-bulb temperature on the wet-bulb scale corresponding to the air movement. The P4SR is given by the point where this line intersects the curve on scales S1 and S2 corresponding with the air movement.



EXAMPLE: DETERMINE HEAT STRESS INDEX FOR WORKER DOING LIGHT ARM WORK WHILE STANDING AT A BENCH.

METABOLISM 600 Btu/hr

ENVIRONMENTAL CONDITION.

GLOBE THERMOMETER TEMPERATURE	110 deg
DRY-BULB TEMPERATURE	90°F
WET BULB TEMPERATURE	75°F
AIR VELOCITY	100 fpm

SOLUTION. FOLLOW THE BROKEN LINES FROM THE GLOBE THERMOMETER AND FROM DRY-BULB TEMPERATURE TO THEIR INTERACTION ON ABOVE DIAGRAM C TO READ A STRESS INDEX OF 90

Figure 3–18. Flow charts for determining heat stress index values at sea level conditions. (After ASHRAE, 1965)

Table 3–10
Evaluation of Index of Heat Stress

Index of Heat Stress at °F	Physiological and Hygienic Implications of 8-hr Exposures to Various Heat Stresses
-20 -10	Mild cold strain. This condition frequently exists in areas where men recover from exposure to heat.
0	No thermal strain.
+10 20 30	Mild to moderate heat strain. Where a job involves higher intellectual functions, dexterity or alertness, subtle to substantial decrements in performance may be expected. In performance of heavy physical work, little decrement expected unless ability of individuals to perform such work under no thermal stress is marginal.
40 50 60	Severe heat strain, involving a threat to health, unless men are physically fit. Break-in period required for man not previously acclimatized. Some decrement in performance of physical work is to be expected. Medical selection of personnel desirable because these conditions are unsuitable for those with cardiovascular or respiratory impairment or with chronic dermatis. These working conditions are also unsuitable for activities requiring sustained mental effort.

70 80 90	Very severe heat strain. Only a small percentage of the population may be expected to qual'i for this work. Personnel should be selected (a) by medical examination and (b) by trial on the job (after acclimatization). Special measures are needed to assure adequate water and salt intake. Amelioration of working conditions by any feasible means is highly desirable and may be expected to decrease the health hazard while increasing efficiency on the job. Slight "indisposition" which in most jobs would be insufficient to affect performance may render workers unfit for this exposure.
100	The maximum strain tolerated daily by fit, acclimatized young men.

(After Ashrae, 1965)

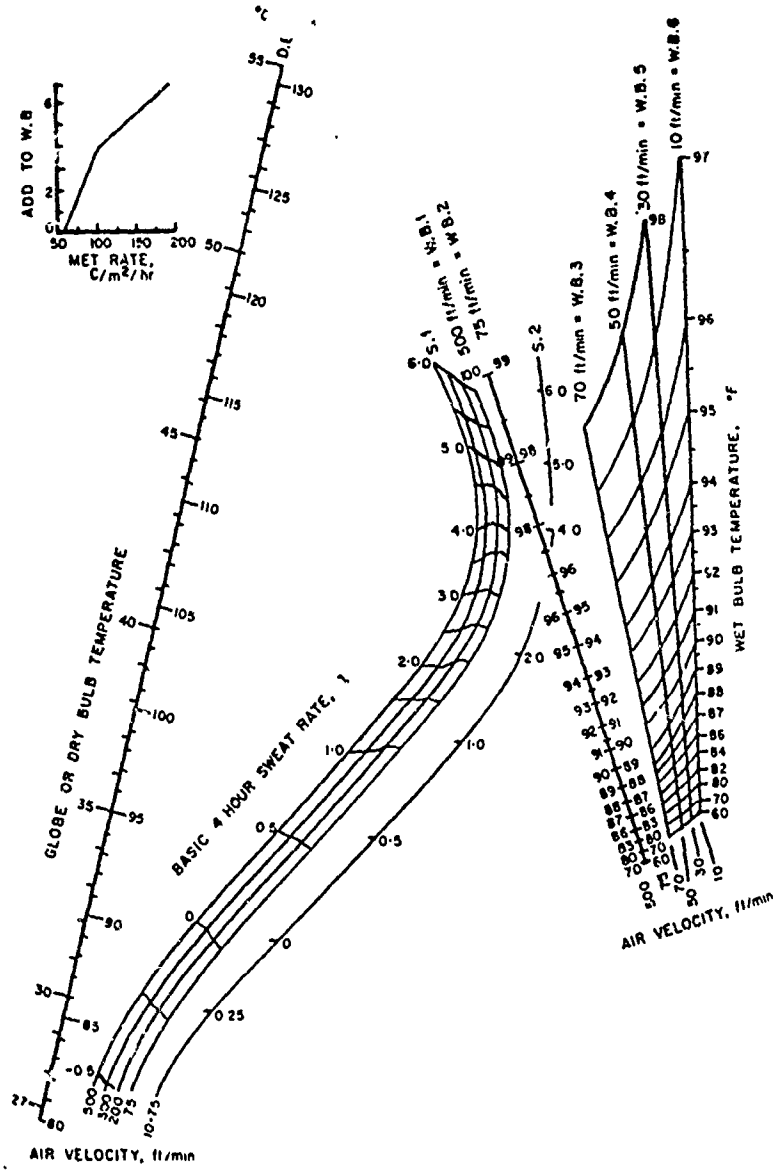


Figure 3–19. Nomogram for the prediction of 4-hour sweat rate (P4SR) at sea level. (After MacPherson, 1960; reprinted by permission of the Controller of Her Brittanic Majesty's Stationery Office)

The P4SR also may be calculated by the following three stages: In the first stage, the wet-bulb temperature may require modification depending on the amount of radiation, the metabolic rate, or the character of clothing. In the second stage, the nomogram is used to obtain the B4SR and in the third stage, the P4SR is obtained by adding certain constants to the B4SR depending

on the metabolic rate (see wet-bulb equivalent of metabolic rate in inset) and clothing. A P4SR of 4.5 liters was provisionally adapted as the upper limit of tolerance for physically fit men. Details regarding the three-stage modification are available (MacPherson 1960).

The P4SR, although derived under rather different conditions than expected in space flight, offers some possibilities if suitably extended (Webb, 1964). It was originally based on several types of experimental data taken on heat-acclimatized young men in Singapore and in environmental chambers. It is unsafe to use it as a means of predicting sweat rate, however, unless all the conditions are similar to those originally used. When used with care, the P4SR does allow prediction of thermal effect in a number of different situations (Blockley, 1965). The limitations are chiefly those of a narrow range of activity (up to 250 kcal/sq m-hr or five times the sitting subject rate) limited clothing combinations, and the fact that all the subjects were heat acclimatized. The P4SR is not recommended for predicting sweat. It can be used, however, for comparing environments in terms of thermal stress, to be followed by experimental evaluation of the environments, with sweat production being taken as one dependent variable (Gillies, 1965).

Human Performance During Heat Stress

Tolerance Time in Heat. The maximum tolerance time (θ_t) for heat gain that represents an emergency maximum for thermal stress is inversely proportional to the heat storage.

$$\theta_t = 3300/Q_s \text{ min or } 55/Q_s \text{ hr} \qquad (26)$$

where Q_s is calculated using equation 1.

The tolerance and general performance limits as a function of time and body heat storage are shown in figure 3-20. The heat storage at tolerance is inversely related to the rate of heat storage (Goldman et al., 1965). Recent evidence indicates that men actively exercising in space suits can store up to 1000 BTU in actively working muscle (Wortz, 1967). This storage must be considered during any analysis of tolerance times in exercising subjects..

Figure 3-21 indicates the conservative nature of earlier tolerance limits. The dashed lines in the figure and points 1, 2, 3, and 4 represent more recently established tolerance time levels. The tolerance limit at high temperature is based on faintness, dyspnea, nausea, and restlessness as an endpoint. Because these levels are nearly double the limits established by earlier workers, engineers designing in terms of earlier tables probably were more restricted than necessary or enjoyed a wide margin of safety even in the response of the most sensitive occupants. The ranges represented by these tables also reflect individual differences between subjects as well as differences in motivation. The dashed lines probably represent the capabilities of highly motivated spacecrews in top physical condition.

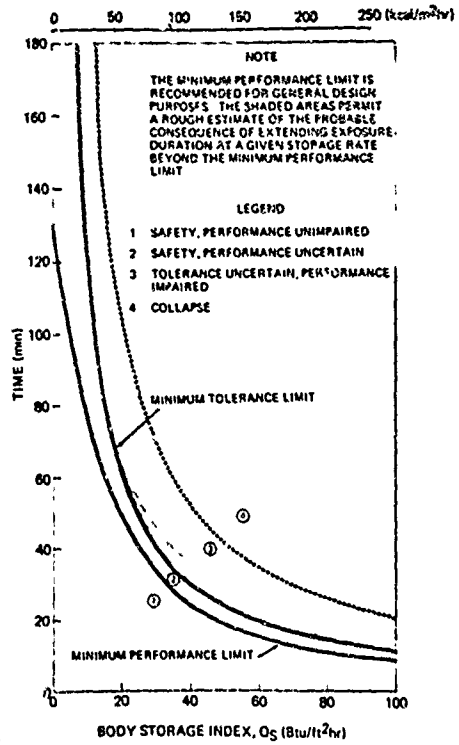


Figure 3–20. Performance and tolerance limits; transient zone. (After Blockley et al., 1954)

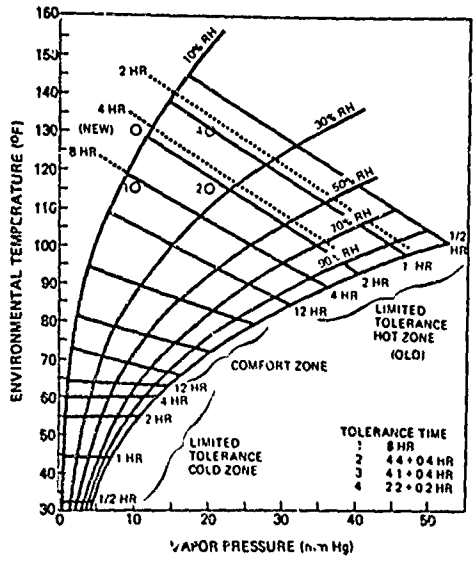
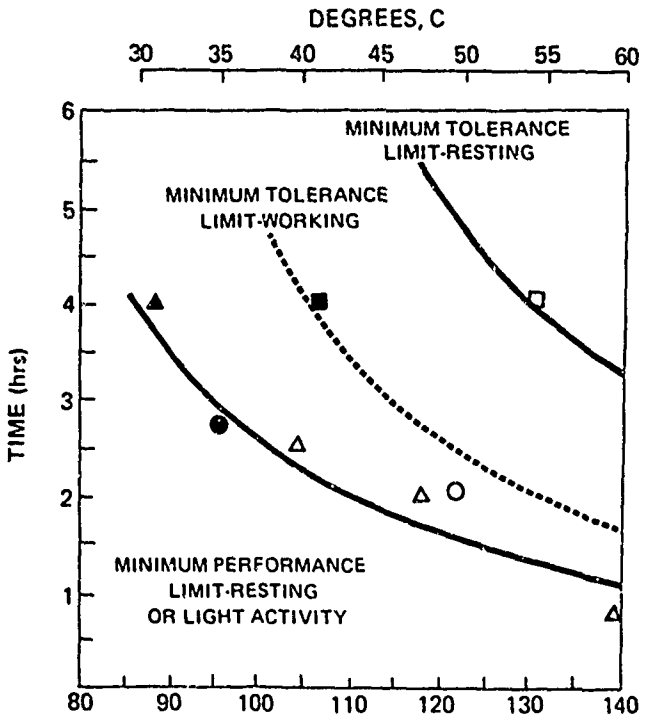


Figure 3–21. Maximum tolerance environments according to duration of exposure for sitting, clothed subjects under sea level conditions in aircraft design. (After Trumbull, 1956)

Figure 3-22 uses the reference operative temperature to determine performance and tolerance limits. There are high correlations between the final skin temperature, rate of rectal temperature rise, and rate of heart rate increase as linear functions of the Oxford index (Goldman, 1965).



T_{OR} = Operative temperature at 0.79 in. Hg vapor pressure

- ● Heavy pursuitmeter test
- ▲ Mixed test battery
- ■ Working men
- △ Wireless telegraphy test
- ○ Visual vigilance test
- □ Resting men

Figure 3–22. Performance and tolerance limits in the quasi-compensable zone for lightly dressed men. (After Blockley et al., 1954)

Performance Under Heat Stress. Performance begins to deteriorate in any given condition at about 75 percent of the physiological tolerance limit. Although highly motivated individuals may be capable of exceeding normally established performance and tolerance limits (Teichner, 1961), excessive penalties in recovery time may be required if normal limits are exceeded. Even though no other stresses are anticipated or evident, it is suggested that 75 percent of the average tolerance limit level not be exceeded until the significance of deconditioning that occurs during space flight is better understood. Figures 3-23 and 3-24 reflect performance decrements as a function of ambient and effective temperature.

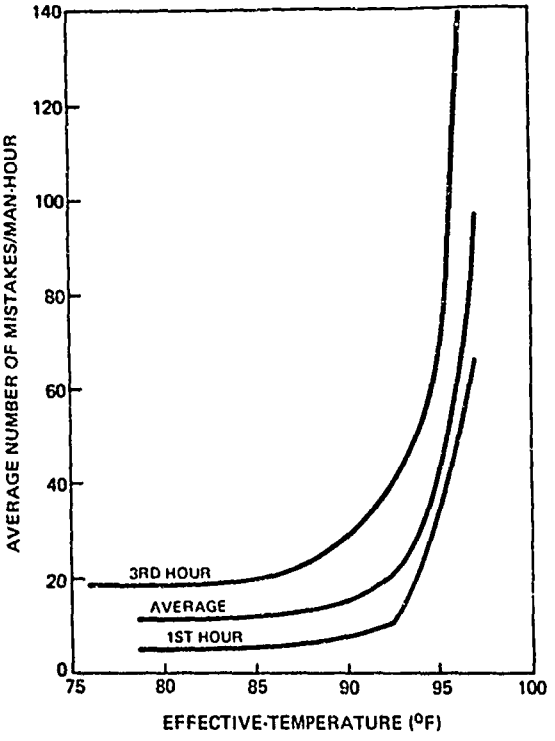


Figure 3–23. Combined performance averages for 11 wireless telegraph operators under conditions of extreme heat. (Roth, 1968)

Table 3-11 summarizes the physiological response increases and decreases in environmental temperature (Spector, 1956). The debilitating effects of heat have received much attention (Lind, 1963).

Table 3-12 classifies the symptoms to be expected from the debilitating effects of heat.

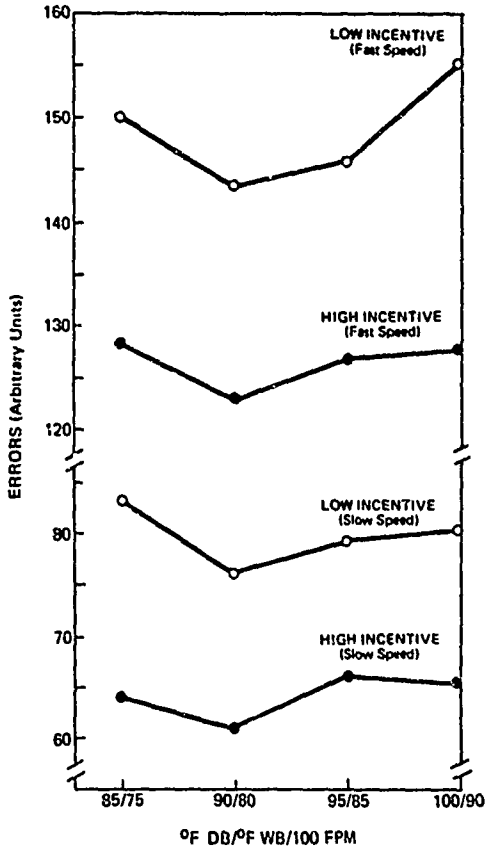


Figure 3–24. Effects of incentives, target speed, and environmental warmth on accuracy of manual tracking. (After Teichner, 1961; adapted from Pepler, 1959)

Acclimatization to Heat. Acclimatization can alter the response of humans to heat loads. Figures 3-25 and 3-26 represent the improvement in function that is possible through heat acclimatization. Figure 3-25(a) shows results obtained with the standard acclimatization procedure used in South African gold mines to prepare laborers recruited from remote villages for work in saturated environments underground. The duration of the daily work period was 5 hours, and the work, shoveling rock. For the first 6 days, the effective temperature was 84°F; for the next 6 days, the E.T. was 89.5°F and the amount of rock shoveled was increased. Note in the graph the fall in rectal temperature. The curves are means for over 100 men, and the bar shows ±1 S.D. during each of the 6-day work periods. In figure 3-25(b) results are shown for a heat acclimatization technique used at the U.S. Army Laboratories at Natick. In this experiment, men marched at 3.5 mph for 100 minutes each day in an environment of 120°F dry-bulb, 80°F wet-bulb, 200 ft/min air velocity (E.T. 89°F, vapor pressure 15 mm Hg).

Table 3–11

Effects of Environmental Temperature Change: Values are for Resting State

		Increase of Environmental Temperature			Decrease of Environmental Temperature		
		Single Exposure Response			Single Exposure Response		
Animal	Variable	General	15° to 20°C Increase	Repeated or Continued Exposure	General	15° to 20°C Decrease	Repeated or Continued Exposure
Man	Blood volume	Increase		Increase			Decrease
	Cardiac output	Increase		Return toward normal	Decrease		Return toward normal
	Food intake	Decrease	Variable	Decrease	Increase	Variable	Increase
	Heart rate	Increase	5/min	Return toward normal	Decrease	-5/min	Return toward normal
	Heat production	0 or slight[1]		Some decrease	Increase	50 to 100 cal[2]	Increase
	Manual skill	Deteriorates		Return toward normal	Deteriorates		Return toward normal
	Packed cell volume	Slight decrease	-2 to 3 percent	Decrease	Slight increase	2 to 3 percent	Increase
	Rectal temperature	Increase	0.5° to 1°C	Return toward normal	Decrease	-1° to 2 C	Return toward normal
	Skin temperature	Increase	10° to 15°C	Return toward normal	Decrease	-10° to 15°C	Return toward normal
	Output of urine	Decrease	-200 to 500[3]	Sustain low level	Increase	200 to 500[3]	Sustain high level
	Blood flow[4]	Decrease		Return toward normal	Increase		Return toward normal
	Water intake	Increase	400[3]	Sustain high level	Decrease	-400[3]	Sustain low level

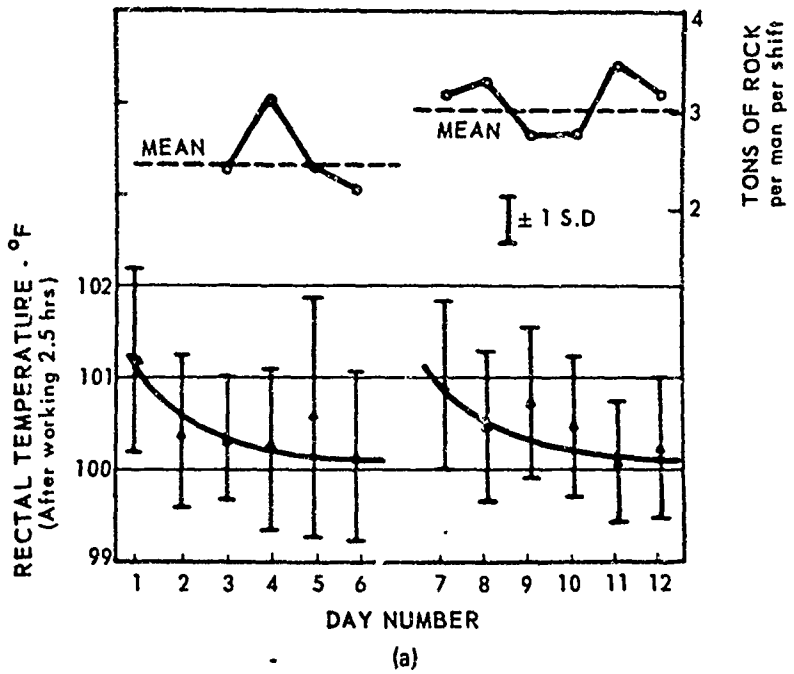
1. No change or slight increase.
2. Per sq m/hr.
3. ml/day.
4. Visceral

(After Spector, 1956)

Table 3–12
Classification of Debilitating Effects of Heat

Disorder	Cause	Symptoms	Prevention	First Aid
Heat cramps	Excessive loss of salt in sweating with inadequate replacement	Pain and muscle spasm; pupillary constriction with each spasm. Body temperature normal or below normal.	Normal diet and fluid intake	Rest, administer salt and water
Heat exhaustion	Cardiovascular inadequacy; dehydration	Giddiness, headache; fainting; rapid and weak pulse, vomiting; cold, pale, clammy skin; small rise in body temperature.	Frequent and early replacement of water, frequent pauses.	Rest in shade in recumbent position. Administer fluids.
Heat stroke	Failure of temperature regulatory center, due to excessively high body temperature.	High body temperature; irritability, prostration, delirium; hot, dry, flushed skin. Sweating diminished or absent.	Adequate pacing of activity, avoidance of severe effort by unacclimatized men in hot environment.	Alcohol spray bath or immersion in cold water. Medical emergency requiring a physician.

(After Buskirk & Bass, 1957)



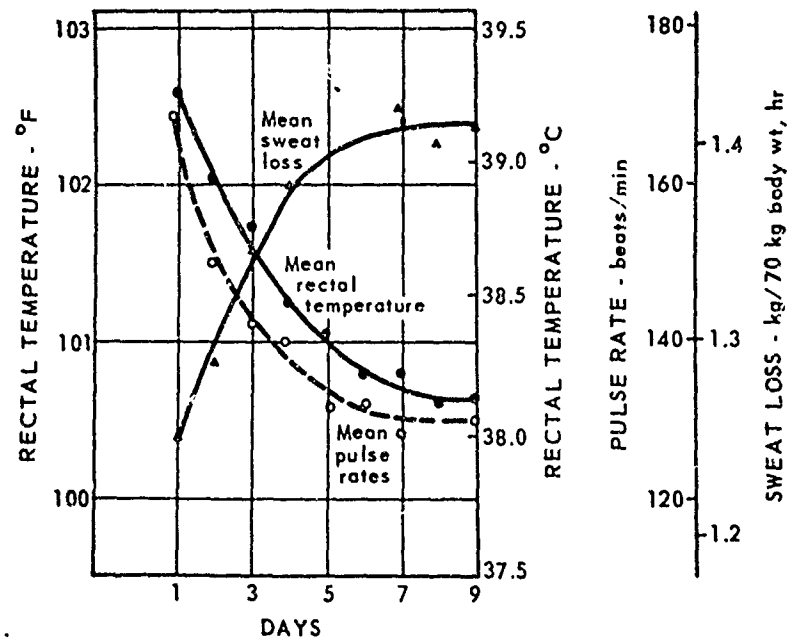
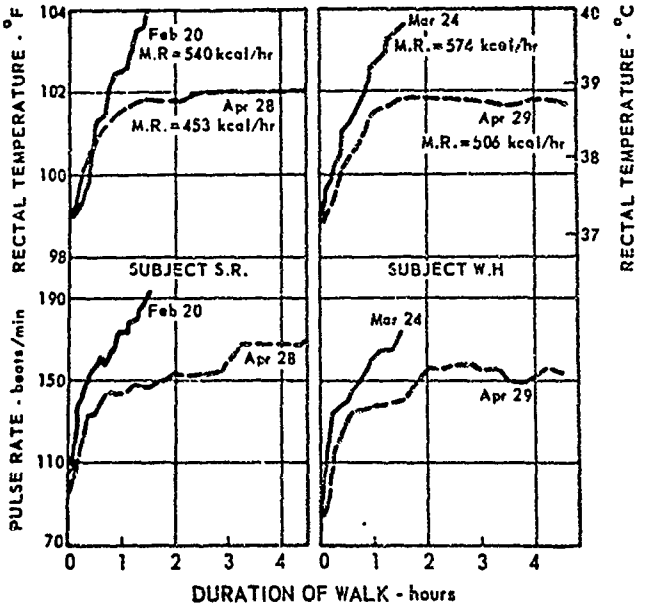
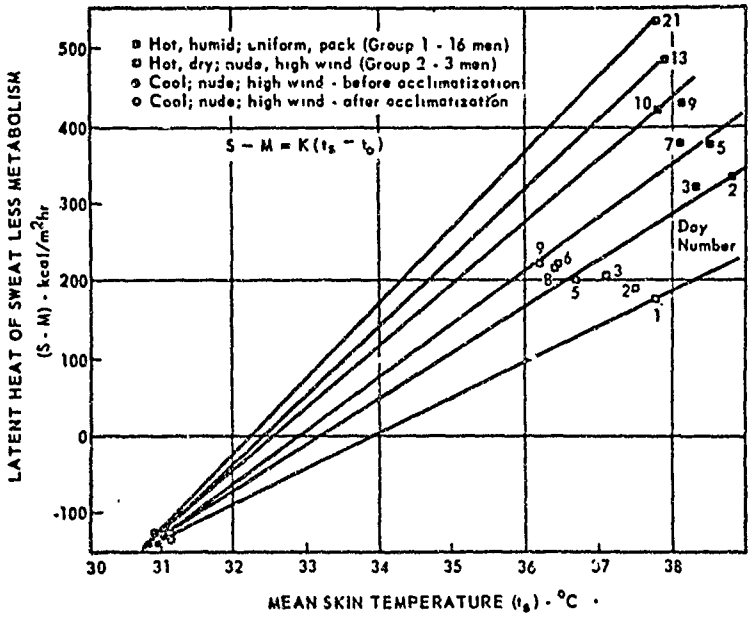


Figure 3–25. Acclimatization to heat. A: results of standard procedure used to acclimatize laborers for work in saturated environments underground; B: results of a U.S. Army Natick Laboratories technique. (After Blockley, 1964, adapted from a. Wyndham et al., 1954; b. Lind & Bass,1963)



(a)



(b)

Figure 3–26. Improvement in function from heat acclimatization demonstrated by two studies. (A: after Blockley, 1964, adapted from Robinson et al., 1943; B: after Blockley, 1964, adapted from Haufan et al., 1963; Eichna et al., 1950; Horvath & Shelly, 1946)

In figure 3-26(a), the results of a heat acclimatization experiment involving two subjects are shown. Subjects walked at 3.5 mph on a 5.6 percent grade in a room at a temperature of 104°F and a vapor pressure of 13 mm Hg (E.T. 84°F). Subject S.R. was acclimatized by 23 exposures between February 20 and March 20. After March 20 his only exposures were on April 16 and 28. Subject W.H. was acclimatized by 11 exposures between March 24 and April 8. After April 8, his only exposures were on April 22 and 29. On the first exposure, the experiment was terminated by the collapse of the subjects at 90 min. After acclimatization, the men were still maintaining equilibrium with ease after 4.5 hr. Acclimatization to heat is shown by the lowering of body temperatures and heart rates. Figure 3-26(b) is a diagrammatic presentation of mean results from two studies of the heat acclimatization phenomenon. Subjects in both groups were drawn from the same Army population at Fort Knox, Kentucky. The two studies are related by means of a parameter combining the sweat rate (expressed as its caloric value if evaporated) and metabolic rate. The slope of the straight lines in the diagram represents an estimate of the sensitivity of the sweat response to increases in temperature of the peripheral tissues or blood (expressed as a function of surface temperature and metabolic heat output). It can be seen that when men are unclothed and the air is dry, sweat rate changes but little, but the skin temperature needed to produce that amount of sweat becomes steadily lower in successive exposures when the climate is humid, and evaporation is impeded by clothing; the skin temperatures does not change much on successive days, but the quantity of sweat produced at that temperature is enormously increased as acclimatization progresses.

The value of the shorter exposure period technique in preparing men to work for long periods such as 5 hours or more in the heat is the subject of considerable controversy. Newer techniques pioneered by Fox (1964) in England concentrate on raising core temperature to the same fixed level each day, so that thermal strain, rather than the stress, remains constant throughout the acclimatization process. Under these conditions, improvement continues for longer periods and to greater levels than the standard exposure techniques. Heat acclimatization may not be as important in hot, wet environments where increased evaporative cooling cannot be produced even if there is an increased sweat secretion, since no increase in the internal thermal gradient between core and skin temperature can be achieved (Goldman, 1965).

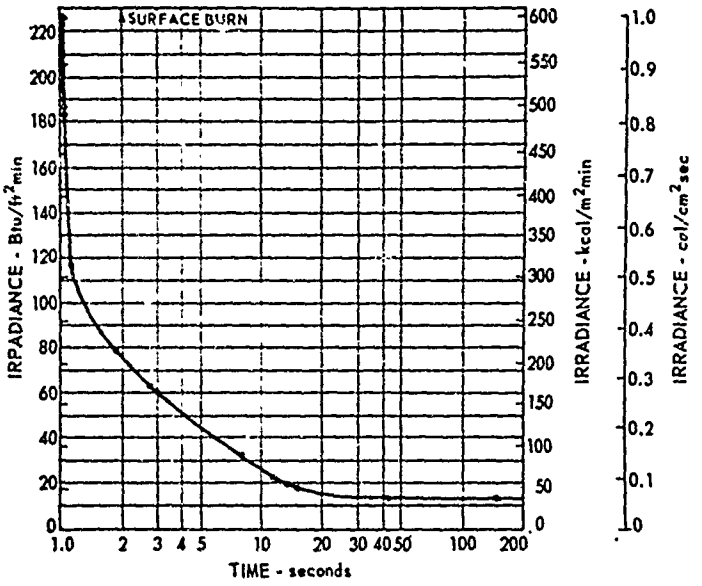
Skin Pain and Heat Pulses. Tables 3-1 and 3-13 and figure 3-27 show the pain thresholds for the skin from conductive, radiant, and convective heating. In general, the pain threshold is reached when the skin reaches a temperature of 45°C. A skin temperature of 46°C is intolerably painful. For small skin areas the curve shown in figure 3-27 becomes asymptotic at about 18 BTU sq ft/min. At this level and below, the blood supply to the skin is carrying off the heat as fast as it arrives, and heat is stored in the body. How long this can go on with the total body exposed is not established. A rise in skin temperature of 0.008°C will evoke a sensation of warmth in 3 seconds and a decrease in skin temperature of 0.0070°F will produce a cold sensation. The face and the neck are the most sensitive to thermal stimuli and the backs of the hands are next (Hardy 1954).

Table 3–13
Pain from Conductive Heating

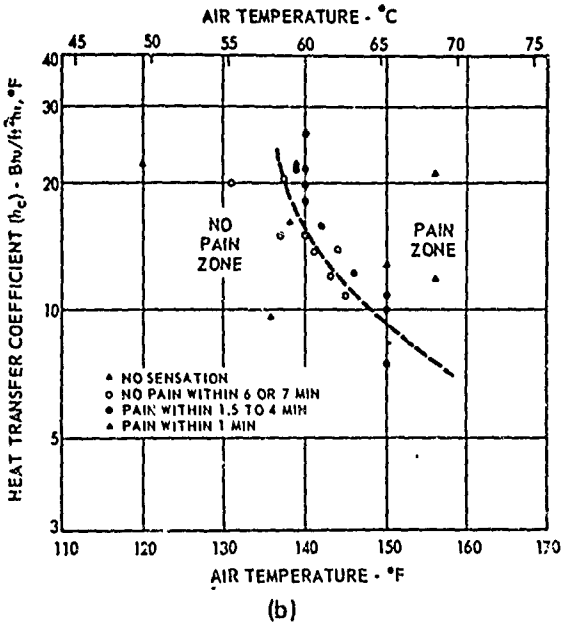
Body Area	Clothing Worn	Metal Surface Temperature, °F	Average Tolerance Time, sec
Hand	Bare skin	120	10 to 15
Kneecap	Bare skin	117	36
	Bare skin	120	5
Fingertip	AF/B-3A leather gloves	150	12.6
	AF/B-3A leather gloves	160	7.3
Hand - palm	AF/B-3A leather gloves	150	25.2
	AF/B-3A leather gloves	175	9.7
	AF/B-3A leather gloves	185	8.0
Forearm	SAC alert suit	150	20.0
	SAC alert suit	175	8.0
Upper arm	K-2B light AF flight coverall	150	7.5
	SAC alert suit	150	31.3
	Alert suit plus Brynje net string underwear	300	7.2
	K-2B suit	150	18.1
	K-2B suit plus Brynje underwear	150	61.9
Buttocks	SAC alert suit	150	70.3
	Alert suit plus Brynje underwear	300	21.7
	K-2B suit	150	32.5
	K-2B suit plus Brynje underwear	150	+90
Mid-thigh	SAC alert suit	150	35.6
	Alert suit plus Brynje underwear	300	13.1
	K-2B suit	150	13.6
	K-2B suit plus Brynje underwear	150	+90
Kneecap flexed	SAC alert suit	150	14.4
	Alert suit plus Brynje underwear	175	9.5
	K-2B suit	150	7.3
Calf muscle	SAC alert suit	150	14.4
	Alert suit plus Brynje underwear	300	11.4
	K-2B suit	150	13.2
	K-2B suit plus Brynje underwear	150	66.1
Upper arm	MD-3A wool-nylon antiexposure suit	300	12.0
	MD-3A wool-nylon antiexposure suit	400	10.2
Forearm	MD-3A suit	250	15.9
Palm of hand	Aluminized asbestos glove	250	13.5
Back of hand	Aluminized asbestos gloves	250	5.2
Palm of hand	Arctic mitten	300	18.7
	Arctic mitten plus B-3A glove	300	37.0
	Arctic mitten plus B-3A glove	400	27.6
	Pigskin 800°F heat glove	300	30.7
	Pigskin 800°F heat glove	400	21.0
	Pigskin 800°F heat glove	500	18.5

Notes: Light touch pressure (less than 1 psi) applied to heated metal surface. The elbow and knee sometimes received second-degree burns without pain.

(After Blockley, 1964)



(a)



(b)

Figure 3–27. Pain from radiant and convective heating. A: strong skin pain produced by sources ranging from intensity of nuclear weapon flash (approximately 100 BTU/sq ft/min) to slow heat pulse associated with reentry heating, where the heating is partly convective. (After Blockley, 1964, adapted from Buettner, 1952; Hardy, 1954; Kaufman et al., 1961; Stoll & Greene, 1959; Webb, 1953). B: dividing line between painful and nonpainful heating for air at various temperatures vs the heat transfer coefficient, which depends on air density, air velocity, and surface areas and shapes. (After Blockley, 1964)

The ability of the body to withstand high heat pulses is shown in figure 3-28. Figure 3-28(a) and (b) show the pulse responses and average skin temperatures of subjects exposed to three different severe heat exposure transients which come close to both the pain limit and the heat storage limit. Each curve represents the average data from five or six subjects. Clothing consisted of a standard flying coverall worn over long underwear with an insulation value of 1 Clo. Figure 3-28(c) shows the increase in tolerance times for subjects exposed to a heat pulse where wall temperature was increased at 100°F/min, and the subjects wore clothing affording various degrees of protection. With subjects wearing heavy aluminized coveralls, wall temperature increase was stopped at 500°F and that temperature held until tolerance was reached. Adding ventilation with air at about 85°F allowed these exposures to last beyond 20 min. Figure 3-28(d) graphs tolerance time for man in a hot environment. The time scale indicates prepain time for exposure of the skin to radiant heat, and escape time for the curve marked "body." The latter refers to a lightly clad man with his face exposed. The temperature scale denotes room temperature for the body curve and radiation temperatures for curves referable to the skin. The curve marked warm dry refers to experiments with an initially dry skin, and a skin temperature initially of about 30°C. A tourniquet was applied to obtain the data marked without circulation. The cold wet curve utilized skin exposed wet at an initial skin temperature of about 15°C. The clothed skin curve was obtained using skin covered with 1 cm insulating cloth with an initial skin temperature near 30°C.

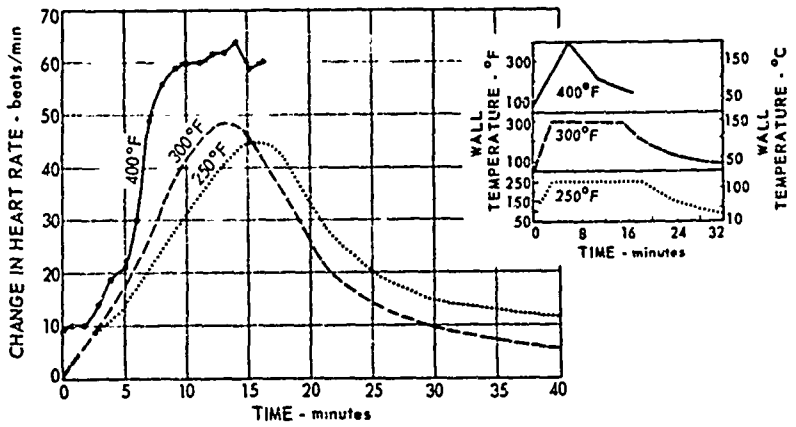
A computer program is available for evaluation of time-temperature histories of the skin at different depths following heat pulses (Weaver, 1967).

Cold Stress

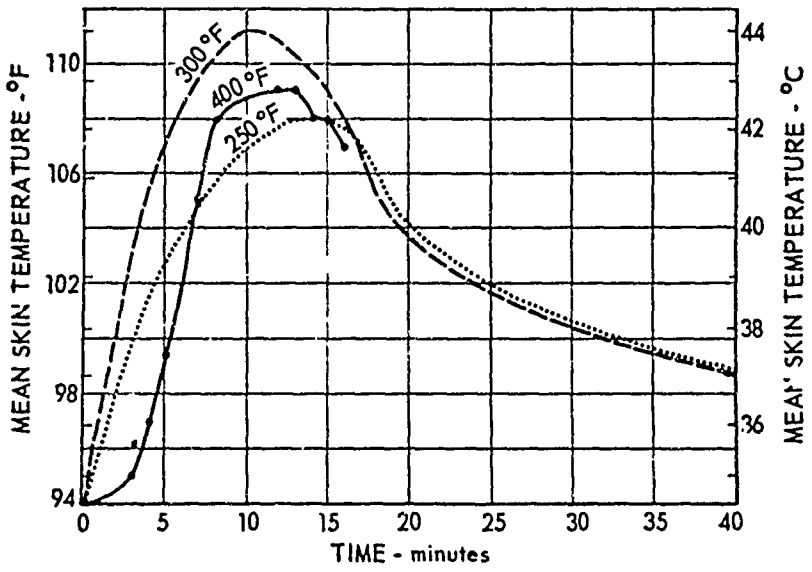
Shivering ensues when heat losses to the environment exceed the metabolic energy being produced by the body and body and skin temperatures reach critical values. The shivering reaction increases skeletal muscle activity (without doing measurable work) and results in an increase in metabolic heat production. A twofold increase in metabolism due to shivering has been observed after exposure to an ambient temperature of 41°F (5°C) for more than one hour. A fivefold increase in metabolism due to shivering is considered to be the maximum attainable (Bullard, 1963). Although shivering may add enough to metabolic heat production to prevent further heat loss, it is never sufficient to replace heat already lost. The shivering response may be triggered by the rate of decrease in temperature and not the temperature of the body *per se* (Burton, 1946).

Cold Stress Tolerance

The effective loss of about 80 kcal/sq m or 31 BTU/sq ft has been taken as the maximum heat loss a person can tolerate with severe discomfort (Spector, 1956). The heat available for loss can be taken as $0.75\ E_m + 80$ kcal/sq m, where E_m is the metabolic rate in kcal/sq m-hr. Sleep of unacclimatized Caucasians will be disturbed at 50 percent of this loss rate. The lowest ambient temperature at sea level that can be tolerated for prolonged thermal equilibrium is a function of the exercise rate, insulation, wind speed, and several other variables.

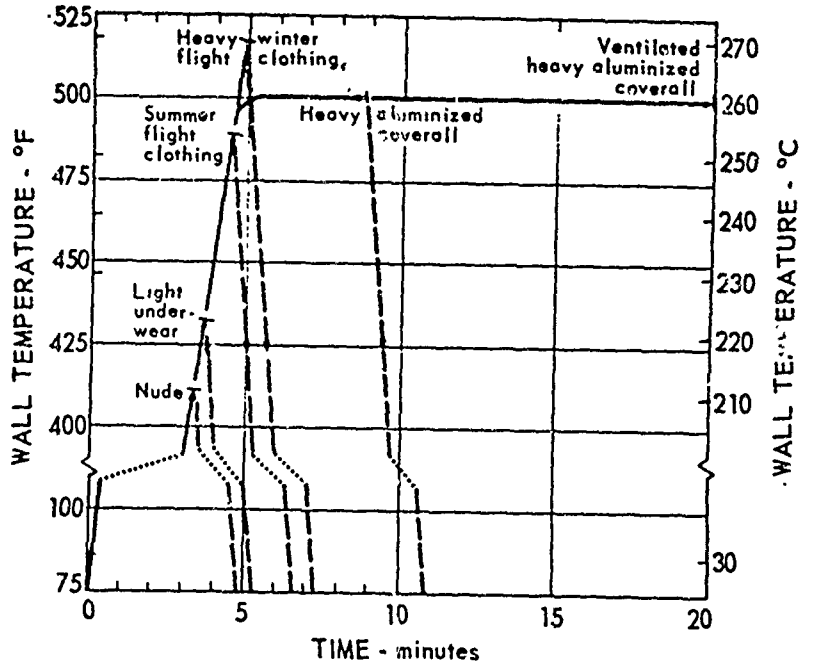


(a)

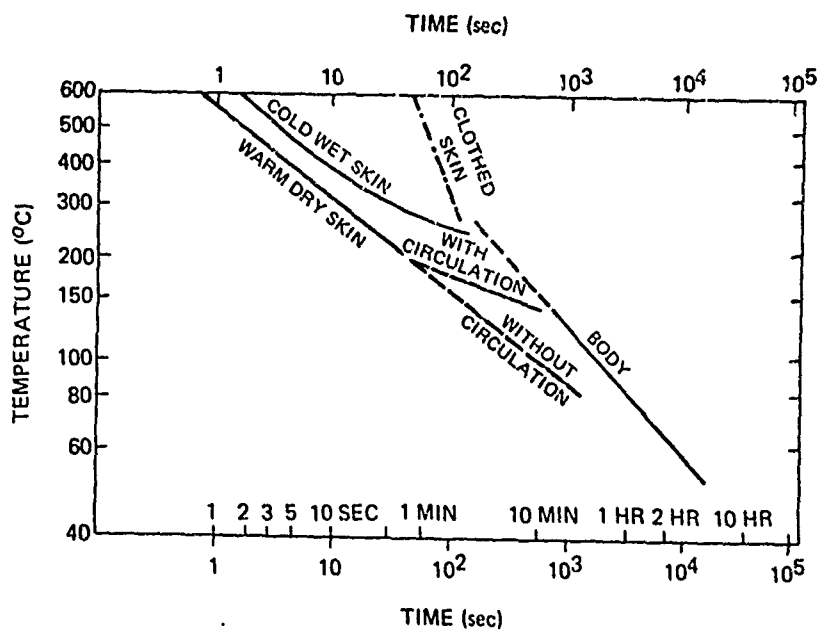


(b)

Figure 3–28. Tolerable heat pulses. (Part c is adapted by Blockley, 1964, from data of Kissen & Hall, 1963; Kaufman, 1963; Webb, 1963; Part d is after Buettner, 1952, based on data of Blockley & Taylor, 1948, and Pflenderer & Buettner, 1940)



(c)



(d)

Figure 3–28. Tolerable heat pulses. (Part c is adapted by Blockley, 1964, from data of Kissen & Hall, 1963; Kaufman, 1963; Webb, 1963; Part d is after Buettner, 1952, based on data of Blockley & Taylor, 1948, and Pflenderer & Buettner, 1940) – *Continued*

An empirical expression for the total cooling power of the environment, disregarding evaporation, is called windchill (Iampietro et al., 1958):

$$K_c = (V \times 100 + 10.45 - V)(33 - T_a) \qquad (27)$$

where K_c = windchill, that is, total cooling in kg-cal/sq m/hr

V = wind velocity in m/sec

T_a = air temperature in °C

Although K_c is not representative of human cooling and is probably not very closely representative of physical cooling either, windchill has come into common use as a single-valued index of the severity of the temperature-wind combinations. As such, it provides a descriptive quantity against which human cooling phenomena can be evaluated. A nomogram, giving rapid approximations of windchill, is provided as figure 3-29. In outdoor cold weather, the wind velocity has a profound, sometimes decisive, effect on the hazard to men who are exposed. The windchill concept provides a means for quantitative comparison of various combinations of temperature and windspeed. For example, note in the nomogram -50°F with an air movement of 0.1 mph has the same windchill value, and therefore is predicted to produce the same sensation on exposed skin, as -15°F with a wind of only 1 mph or +14°F with a wind of 5 mph. The windchill index does not account for physiological adaptations or adjustments and should not be used in a rigorous manner. It is based on field measurements by Paul Siple during World War II of the rate of cooling of a container of water.

When the rate of body heat production is greater than the windchill, excess heat is removed by evaporation; under bright, sunny conditions, the nomogram values should be reduced approximately 200 kg-cal.

For ocean recovery in winter months, the rate of cooling in water is important. Figure 3-30 is a nomogram for estimating tolerance time to cold water immersion (Smith et al., 1962). The nomogram was devised to relate the many factors involved in estimating tolerance in cold water, where one knows or can assume: water temperature (T_w); insulation of clothing and tissue (I_t); metabolic heat production per unit surface area (M/A); the immersed surface area (A); body mass (m); and exposure time (t). As shown by the dotted example line (for a nude man in water at 4°C, a metabolic rate of 400 kcal/sq m-hr, an immersed surface area of 1.75 sq m, a body mass of 75 kg, and an exposure time of one hour) the nomogram predicts: heat loss to the environment H_c/A; heat debt per unit surface area (D/A); heat debt (D); changes in mean body temperature ($d\theta$); and mean body temperature (θ).

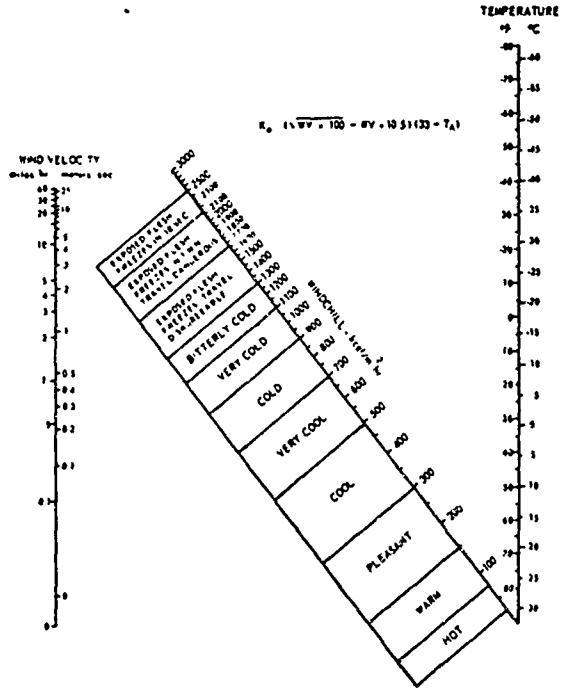


Figure 3–29. Windchill nomogram.
(After Blockley, 1964; adapted from Siple & Passell, 1945)

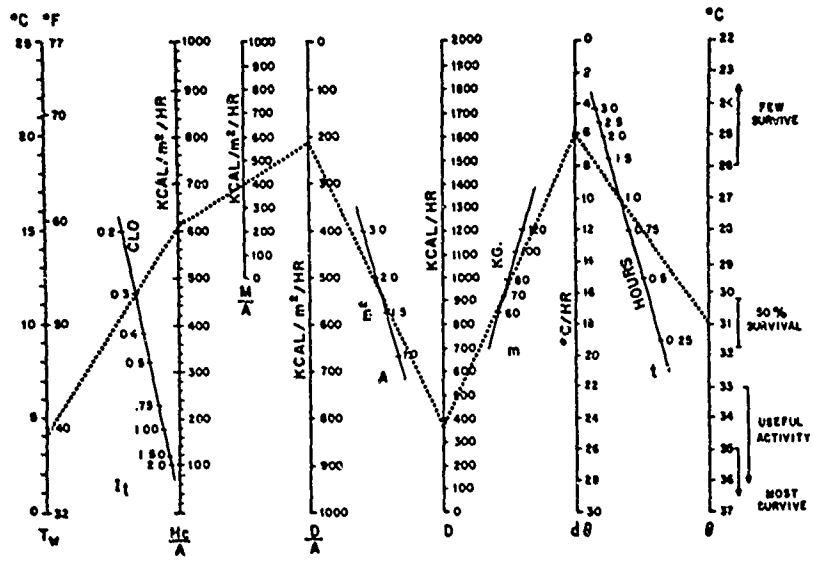


Figure 3–30. Nomogram for estimating tolerance times to cold water immersion.
(Adapted from Smith & Hames, 1962, by Gillies, 1965 and Blockley, 1964)

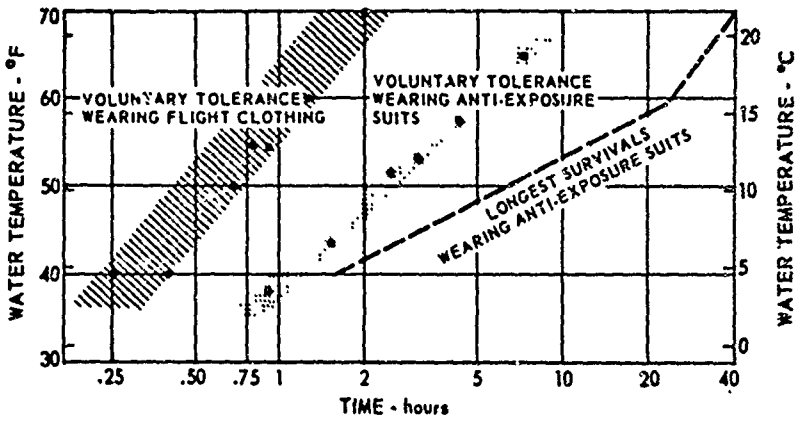
Figure 3-31 is a graphic presentation of practical experience in cold water tolerance with routine flight clothing and antiexposure suits. The "voluntary tolerance, flight clothing" zone in figure 3-31(a) shows the average results from numerous experimental studies, including a recent one using a diver's "wet suit" in conjunction with a flight suit and long underwear. Such experiments are typically terminated when the subject declines to accept the discomfort any longer, or reaches a skin temperature below 50°F. The second limit shown, pertaining to men protected by potentially waterproof garments, reflects the fact that hands and feet cannot be adequately insulated and remain functional. Nude men in 75°F water reach, within 12 hours, one or another tolerance limit (rectal temperature below 95°F, blood sugar below 60 mg/100 ml, or muscle cramps). The extent to which real survival time would exceed this limit is difficult to predict, due to the importance of injury, equipment available, and such psychological factors as belief in the possibility of rescue. An analysis of over 25,000 personnel on ships lost at sea during 1940-44 showed that of those who reached liferafts, half died by the sixth day if the air temperature was below 41°F (5°C); survival time increased with increasing air temperature. Figure 3-31(b) indicates life expectancy for individuals immersed in cold water wearing no protective clothing.

Figure 3-32 shows the time to reach critical core and skin temperatures after exposure to cold water in several types of exposure suits. A criterion of 76°F is based on the general observation of extreme discomfort when this point is passed. In most of the experiments summarized here, some subjects requested termination of the exposure at or near the time when the group average reached this point. Note for comparison the data point for nude exposure to water at 48°F. The value of exercising in cold air and the lack of an advantage in cold water is evident.

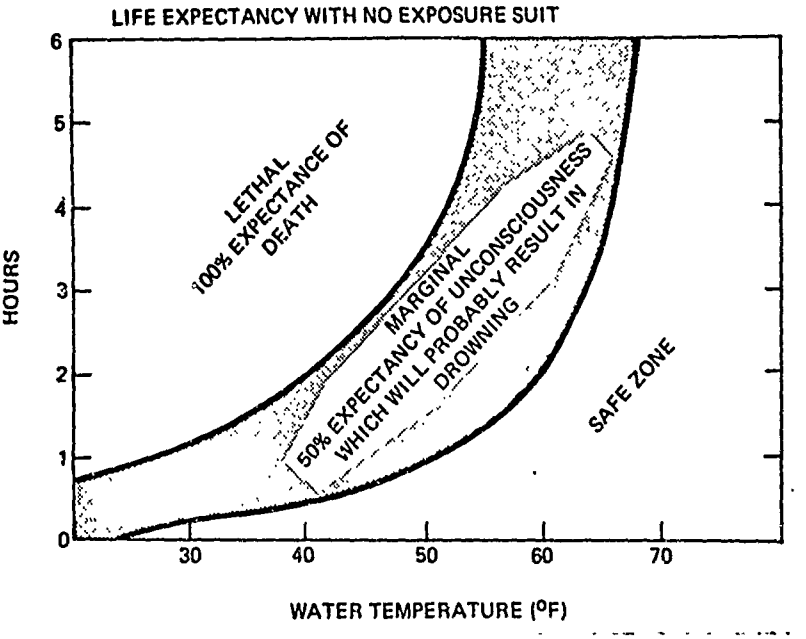
Recent developments in isotopic heating devices make practical the use of exposure garments heated for long periods of time (Sanders, 1966).

In cold air, injury to the extremities is often a limiting factor in human performance (Bullard, 1963). Figure 3-33 indicates the power required to attain given skin temperatures of hand and foot in electrically heated gloves and seals with subjects in an air temperature of -40°F in a 10 mph wind. The body core in these experiments was wound in a U.S. Army Quartermaster 4.3 Clo cold-dry standard clothing ensemble. Performance is severely hindered if the temperature of the fifth finger falls below 55°F (Clark, 1961).

Figure 3-34 presents a typical physiological response of a body immersed in cold water and rewarmed. The pathophysiology and treatment of hypothermia and cold injury in space operations were recently reviewed by Busby (1967).

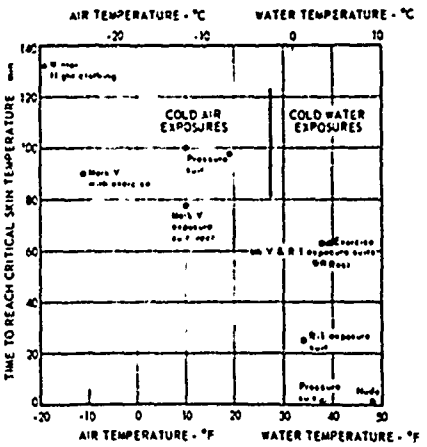


(a)



(b)

Figure 3–31. Survival in cold water. A: voluntary tolerance to cold water; B: life expectancy with no exposure suit. (After Blockley, 1964; adapted from Beckman & Revees. 1966; Damato & Radliff, 1964; Hall et al., 1953; McCance et al., 1956; Molnar, 1964; U.S. Navy, 1948; Barnett, 1962)



Suit	Water Temperature, °C	Air Temperature, °C	Time, hr*
RI-A	1.9	-18	5
RI-A	0	1	18
CWU-12/P	12	15	15
CWU-3/P	7	12	10

*Estimated time (in hours) required for subjects' rectal temperature to reach 31°C. Rapid rewarming of hypothermic subject in 42°C water required for resuscitation.

(After Milan, 1965)

b. Estimated Survival Times in Cold Water with Latest Survival Clothing

Figure 3–32. Clothing tests in cold air and water. A: time to reach critical skin temperature in cold air and water. (After Blockley, 1964; adapted from Barnett, 1962) B: estimated survival times in cold water with latest survival clothing. (After Milan, 1965)

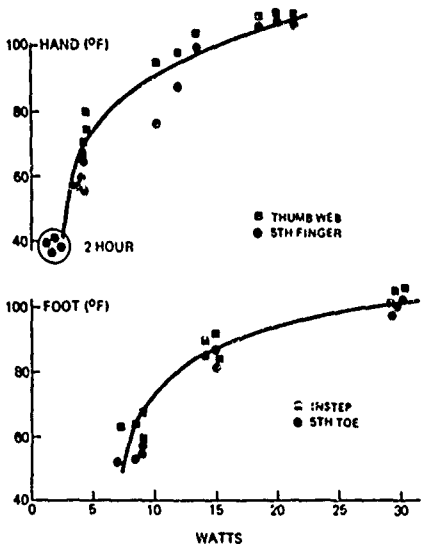


Figure 3–33. Hand and foot temperatures maintained as a function of power used for auxiliary heated gloves and socks. (After Goldman, 1965)

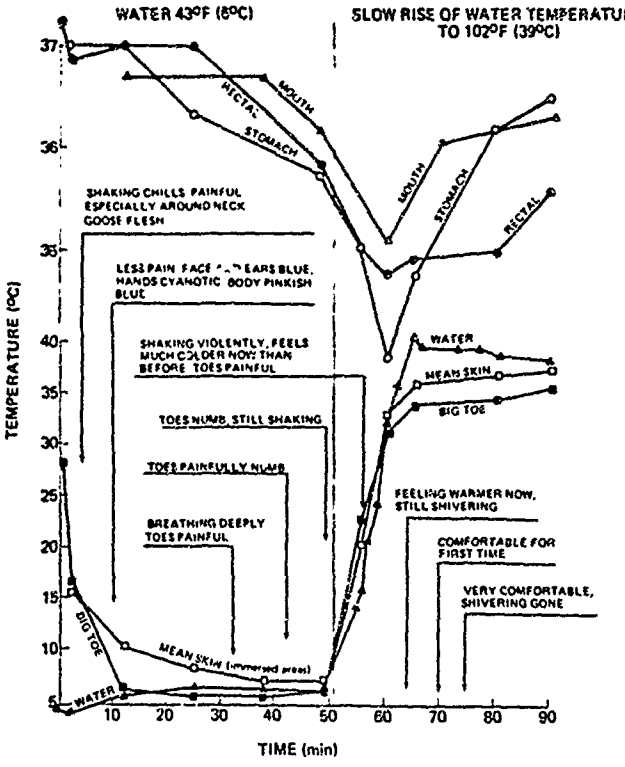


Figure 3–34. Changes in body and skin temperature of subject immersed in water at 6°C (43°F) for 52 min; water was then warmed to 39°C. (Note sharp fall of gastric, oral, and rectal temperatures initially on warming.) (After Behnke & Yaglou, 1951)

Performance in the Cold

Skilled motor performance shows a progressive loss with continued cold exposure (Trumbull, 1956). Tactual sensitivity is markedly affected by lowered skin temperature. A numbness index has been developed based on the ability of the individual to discriminate the separateness in space of two straight edges on which the finger is placed (V-test or two-edge limen) (Mackworth, 1946). Figure 3-35 shows the great difference in the size of gap required to detect the presence of the gap under varying conditions of air temperature and windspeed.

General performance also is altered by cold in a complex way. Figure 3-36 shows the effects of various combinations of air temperature and velocity (and thus windchill) on the manual dexterity of soldiers. Except as indicated, complete Arctic uniforms were worn. During the test trials, the subjects removed the heavy arctic gauntlet and performed with only the wool trigger-finger insert. The results are based on a total of 530 soldiers sorted into the various subgroups of the experiment. It may be seen that performance time increased in direct proportion to the windchill and that mean skin temperature and digital temperature were roughly inversely proportional to windchill. The rate of cooling is an important factor (Clark et al., 1960). There is clearly a relationship

between performance and the skin temperatures; however, analyses of these data and those of figure 3-37 indicate that the direct dependence of performance on finger and skin temperatures may be relatively small and that other factors of a psychological or physiological nature may be of equal or possibly greater importance.

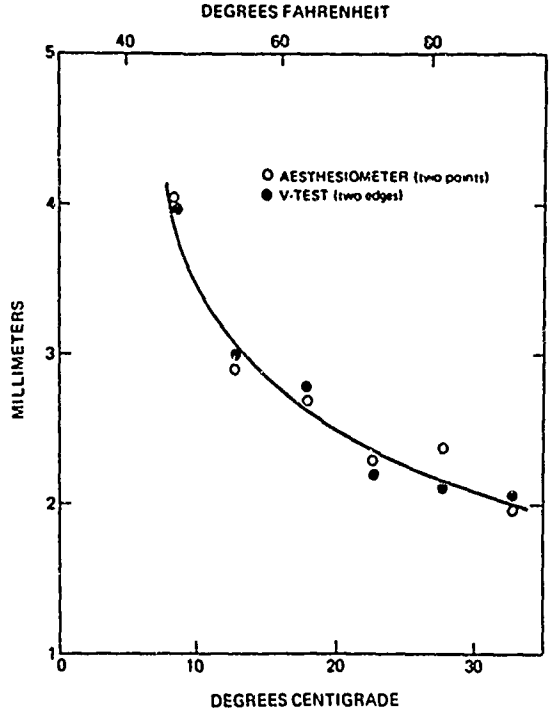


Figure 3–35. Comparison of two-edge and two-point thresholds as a function of skin temperature in air at sea level. (After Mills, 1957)

Total body cooling is not as significant a factor as finger temperature in dexterity tests (Gaydos, 1958); cooling of the hand decreases finger flexibility (LeBlanc, 1956).

The reaction speed of men to simple visual signals also is affected by the cold (Teichner, 1958). The relative loss is not as great as that of tactual sensitivity, but it is greater than that of manual dexterity. Figure 3-38 shows a comparison of these three phenomena for appropriately dressed, but unacclimatized men in terms of the percentage loss relative to optimum thermal conditions. It is reasonable to expect losses in a cold environment for all types of performance that depend on any of these functions, as well as tasks of eye-hand coordination (Teichner, 1954) and intellectual tasks requiring fast reactions such as the cold test (Horvath, 1947). Nothing has been reported to indicate that intellectual tasks not requiring fast reaction times, motor skills, or tactual sensitivity are affected by cold exposure, at least short of the accumulation of a serious heat debt.

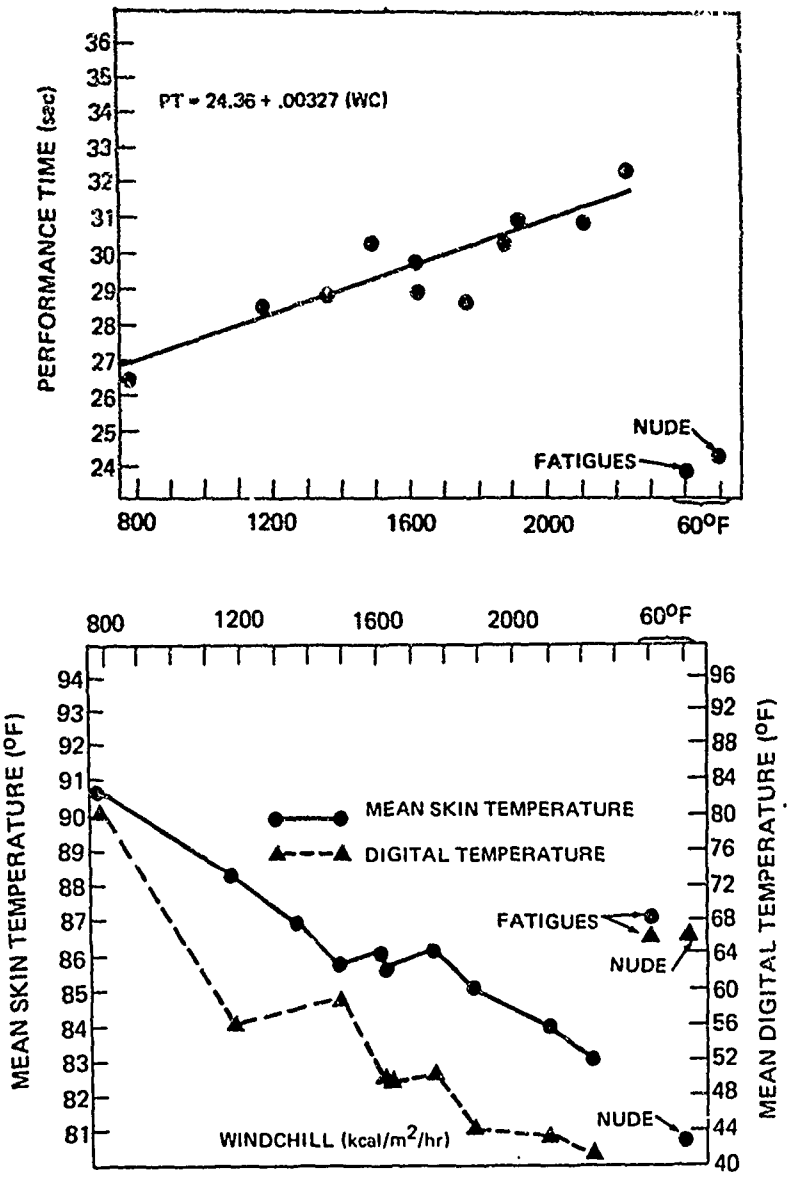


Figure 3–36. Performance time, skin, and digit temperature as a function of windchill; arctic clothing worn except where indicated. Hand exposed during performance only; follows approximately 35 min of exposure. (After Teichner, 1957; copyright 1957 by the American Psychological Association and reprinted with their permission)

Acclimatization to Cold

Recent evidence indicates that under cold conditions, increased voluntary caloric intake and other compensatory processes result from the increased energy expenditures associated with field activities (Davis, 1963) instead of from the low temperature as such.

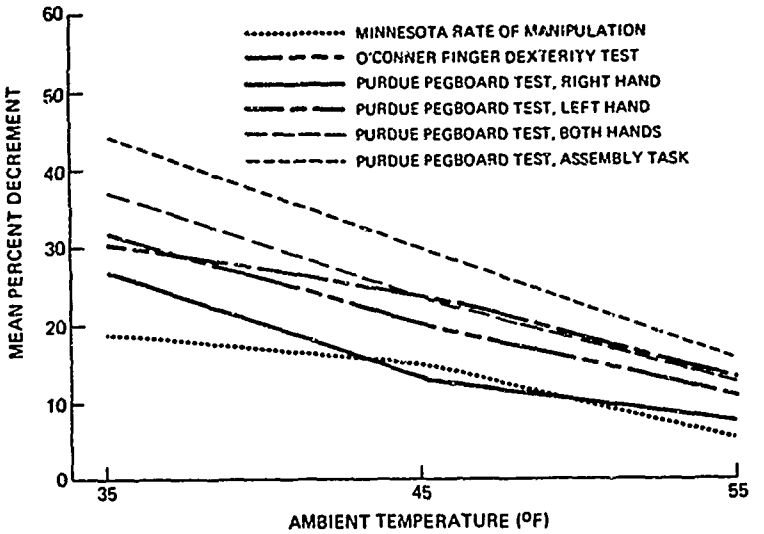


Figure 3–37. Percent decrement in performance as a function of ambient temperature at sea level. (After Dusek, 1957)

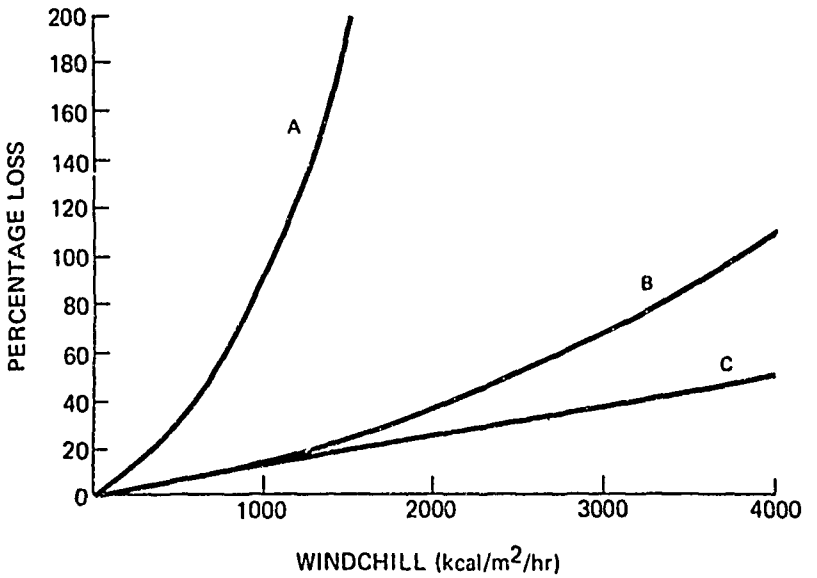


Figure 3–38. Minimum effects of the cold on selected functions. Each curve is an estimated percentage loss of the indicated type of performance for appropriately dressed but unacclimatized men. A: tactual sensitivity of the bare hand; B: simple visual reaction time; C: manual skill. (After Teichner,1958; copyright 1957 by the American Psychological Association and reprinted with their permission)

Whatever the direct cause, the result contributes to a beneficial increase in heat production, vasomotor and renal control. The major known physiological changes produced in the cold were shown in table 3-11. This table indicates that acclimatization takes the form of increased levels of some functions and the return to normal of others. The value of using cold acclimatization to increase the performance and survival capabilities of astronauts during emergencies, in such missions as lunar night operations, has not been established.

Clothing

The effects of clothing on thermal transfer from the body must be considered for all conditions of space flight. The basic principles of thermal physiology involved with the effects of wearing clothing have been discussed in this chapter. Other factors, however, need to be considered (Blockley, 1954, 1964; Burton, 1955; Newburgh, 1949; and Roth, 1966).

Insulation Values

The addition of clothing to the body surface reduces the quantity of heat that can be lost by evaporation because of the increased resistance to diffusion of water vapor. At the same time it reduces the quantity of heat gained or lost by the body by radiation and convection.

Two properties of clothing must be evaluated to determine the effect of clothing on thermal balance: these are thermal resistance (R_g) and vapor resistance (R'_g). Thermal resistance is the resistance of a particular clothing assembly to flow of heat. It is generally expressed in Clo units (see discussion after equation 3).

The total insulation value of a clothing assembly to the man must include the insulation of any gas layer trapped between clothing layers. Calculation of the total insulation value of newly designed garments and fabrics requires the knowledge of the equivalent thickness of the still-air layer (R'), which is equal to the sum of the clothing thickness (R'_g) as a still-air equivalent and the film thickness of the still-air layer (R'_e):

$$R' = R'_g + R'_e \tag{28}$$

Values for R'_g for standard fabrics are shown in table 3-14. If fabric thickness is known, the following relationship can be used:

$$\frac{R'_g}{L} = \frac{\text{equivalent air thickness}}{\text{fabric thickness}} \tag{29}$$

If thermal resistance in Clo units is known, the relationship shown in equation 30 can be used.

$$\frac{R'_g}{R_g} = \frac{\text{vapor resistance (in. of air)}}{\text{thermal resistance (Clo units)}} = \frac{0.5 \text{ in.}}{\text{Clo}} \text{ of air or } \frac{1.2 \text{ cm of air}}{\text{Clo}} \quad (30)$$

Vapor resistance (R'_g) depends on the vapor diffusion of evaporated water, weave and thickness of the fabric material, thickness of the air layers between the garments, and nature of the gaseous environment. While the rate of vapor transfer across near isothermal air layers is directly proportional to thickness, bellows action and resulting convection suggest use of the same maximum effective thickness for vapor transfer as for heat transfer, that is $R'_e = 0.3$ in. (0.75 cm). The values of R'/L in table 3-14 are a convenient estimate of the vapor resistance of similar fabrics.

After thermal resistance and vapor resistance of the garment assembly are determined, the boundary for heat transfer with the environment may be shifted from the skin of the body to the surface of the clothing. With clothing as the boundary, T_c is substituted for T_s in all expressions for heat transfer.

Ventilated Suits

Suit convective heat removal is computed from the mass flow of ventilating air and the difference between inlet air temperature and the desired surface temperature (Blockley, 1964).

$$Q = 0.24 (90 - T_{in}) w \quad \text{Btu/hr} \quad (31)$$

The cooling capacity of Apollo prototype ventilated suits as a function of gas flow at several internal suit pressures is shown in figure 3-39. The partition of cooling into sensible and latent loads is indicated. The capacity of Apollo prototype ventilated suits to handle different metabolic loads is shown in figure 3-40.

Liquid-Cooled Suits

For work loads greater than 600 BTU/hr, liquid cooling must be added. The broken line in figure 3-39 represents projected capacity for liquid cooling cascade addition to ventilated suits. Total liquid loop suits have been used to extract heat in a warm environment and heat the body in a cool environment (Burton, 1966; Lang, 1965).

Table 3–14
Vapor Resistance of Fabrics (R'_g)

Fabric	Weight (oz/sq yd)	Thickness (L) (cm)	Resistance (R') (cm air)	R'/L
Cottons				
Cotton net	4.4	0.100	0.12	1.2
Cotton twill (3 by 1 in.)	8.2	0.097	0.19	1.9
Cotton twill (5 by 1 in.)	8.8	0.112	0.24	2.1
Cotton twill (2 by 1 in.)	4.4	0.069	0.15	2.2
Cotton poplin	5.8	0.039	0.09	2.3
Cotton oxford	6 7	0.081	0.19	2.4
Cotton balloon cloth	2.2	0.015	0.04	2.6
Cotton "jungle cloth" (Bedford cord)	13.6	0.107	0.30	2.9
Heavy cotton	13.5	0.076	0.28	3.7
Close-weave cotton (Shirley L-30)	9.8	0.051	0.23	4.5
Wools				
Double-face wool pile	22	1.1	1.1	1
Wool twill (2 by 2 in.)	10	0.173	0.26	1.5
Worsted serge	6.1	0.056	0.12	2.1
Wool serge	10 7	0.130	0.31	2.4
Nylons				
Spun-nylon fabric	4.9	0.046	0.18	3.9
Nylon poncho cloth	1.5	0.018	0.07	3.9
Five-end nylon sateen	2.3	0.016	0.03	5.0
Filament nylon fabric	2.0	0.013	0.09	6.9
Plain weave nylon	2.6	0.020	0.19	9.5
Rayons				
Viscose rayon (2 by 2 in. twill (filament)	3.6	0.025	0.13	5.2
Acetate rayon satin (filament)	2.7	0.018	0.14	7.8
Glass				
Glass fabric	3.3	0.013	0.12	9.2
Plain weave glass fabric	6.6	0.030	0.32	10.5

(After Stockley et al., 1954)

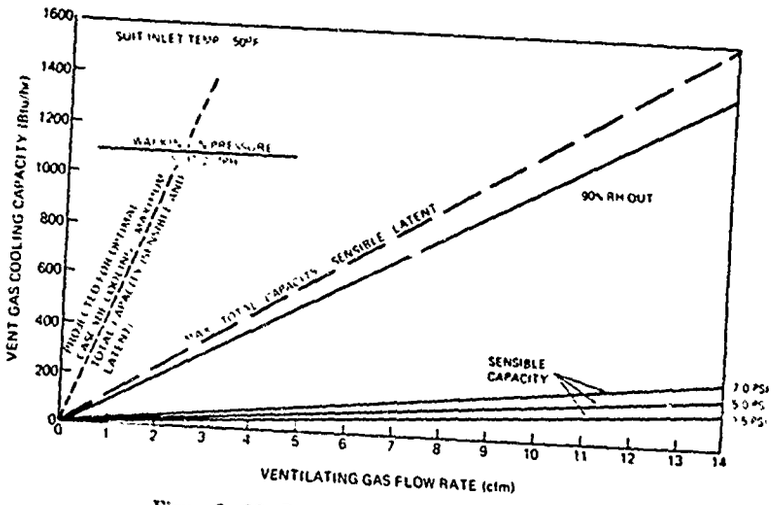


Figure 3–39. Pressure suit ventilating gas cooling. (After Burriss et al., 1963)

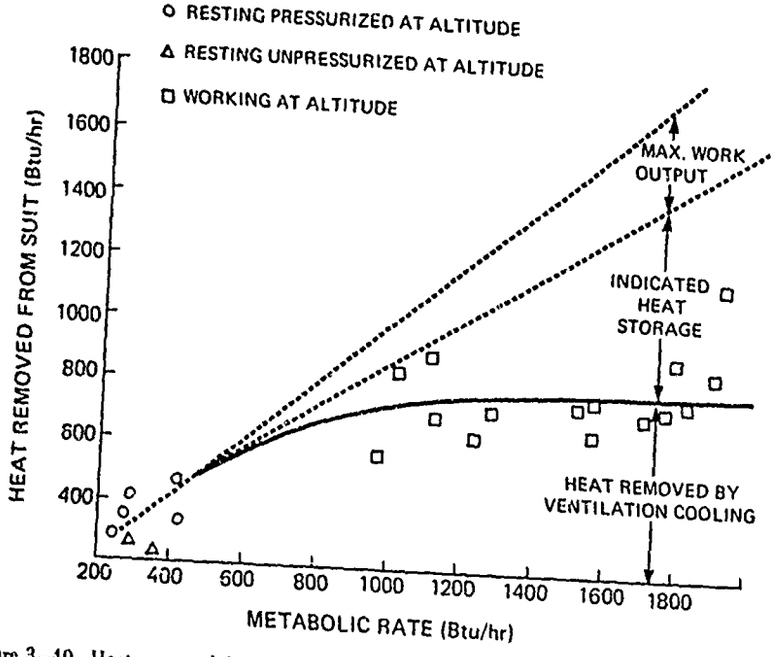


Figure 3–40. Heat removed from an International Latex prototype Apollo suit pressurized at 3.5 psi above ambient with airflow at 15 ft ^{3}/mm (AiResearch Manufacturing Company, Garrett Corporation, 1964)

If the cooling requirement for a given thermal situation is accurately known, the appropriate line in figure 3-41 gives a family of suitable inlet temperature and flow combinations to meet the requirement. The inlet temperature coordinate has a lower limit of 32°F because, for all practical purposes, pure water can exist only in liquid form above this temperature and because of the possibility of causing local frostbite. The upper limit of inlet temperature has been set at 113°F because temperatures above this are liable to burn the skin. Mass flow coordinates extend up to 150 lb/hr because this is about the maximum flow capacity of the present suit. The suit should be capable of absolute maximum cooling rates of 1930 BTU/hr and heating rates up to 700 BTU/hr at a flow of 150 lb/hr. If the cooling requirement is accurately known, the unit performance indicated in figure 3-41 should specify inlet temperatures to about 2°C or 3.2°F.

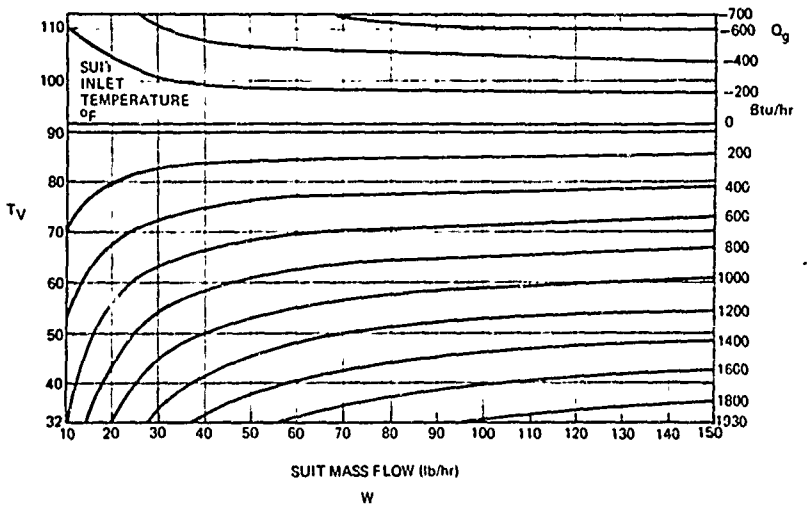


Figure 3–41. Suit performance for liquid-cooled suit. (After Burton, 1966)

The recommended distribution of tubing in a typical water-conditioned suit for use at rest required to give no local overcooling is shown in table 3-15 (Burton, 1965). Unfortunately, severe exercise may alter this distribution.

Data on the latency of cooling after exercise loads recently have been gathered and are most useful for design of thermal regulators for liquid suits (Webb, 1967). Figure 3-42 compares the equilibrium rectal temperatures attainable at different metabolic rates.

Figure 3-43 presents the shivering and sweating thresholds for subjects in Apollo prototype liquid-cooled suits. Extravehicular suits must be designed to remove at least 2000 BTU/hr 500 kcal/hr) of heat and remain within these thresholds (Lang, 1965).

Table 3–1.

Recommended Distribution of Tubing in Water-Conditioned Suit at Rest

Region	Percentage of Tubing
1/2 head	0
Hand	0
Foot	0
Forearm	9.3
Arm	16.9
1/2 back	10.0
1/2 chest	8.8
Calf	18.1
Thigh	25.6
Buttock	4.5
1/2 abdomen	6.8

(After Burton & Collier, 1965)

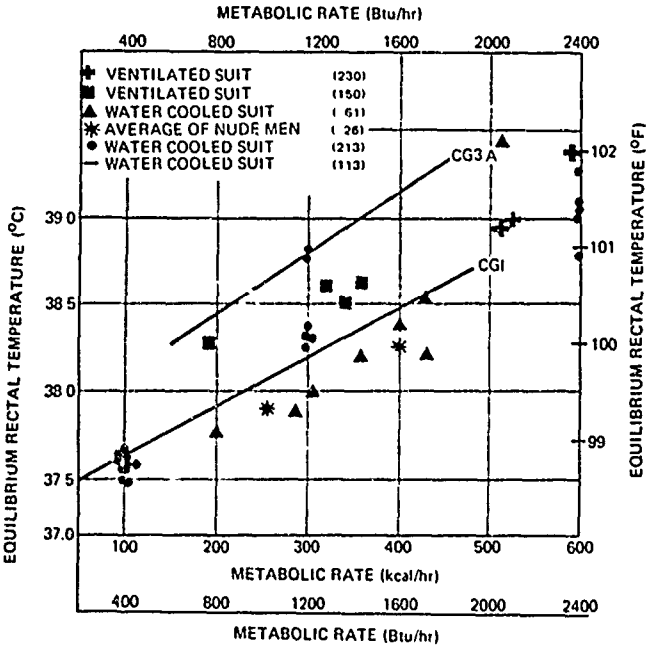


Figure 3–42. Plot of rectal temperatures at equilibrium (energy balance) vs work level, incorporating data from many sources. (Shaded area is an envelope of data from five sources.) (Webb, 1964; after Webb & Annis, 1965)

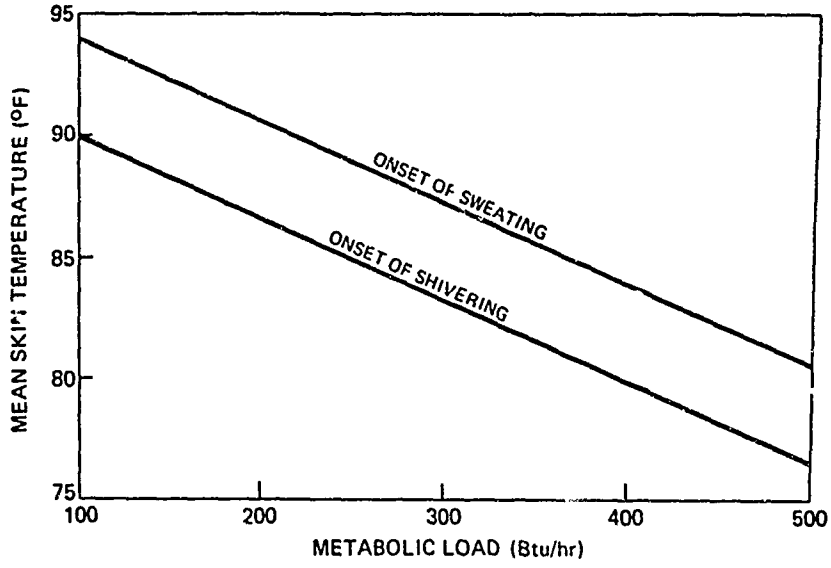


Figure 3–43. Comfort thresholds of sweating and shivering in prototype liquid-cooled Apollo suit. (After Lang & Syversen, 1965)

Conductive Heat Transfer

Liquid cooling garments require that physiological constraints to conductive cooling modes be quantifiably identified. These constraints include sensitivity to thermal and pressure gradients on the skin surface, tube to skin contact resistance, skin resistance, temperature ranges (for comfort) of body parts, and the effects of hair and perspiration on conductive exchange.

Unfortunately, the liquid-cooled space suit is worn under exercise conditions where skin comfort temperatures, thermal conductances to deeper subcutaneous structures, and similar factors are quite different from the resting conditions (Webb, 1966). The characteristics of the skin in thermal comfort cannot be used under the unusual environmental condition of exercise in a liquid-cooled suit. Specific data are needed on the determinants of skin comfort under such conditions. Figure 3-43 is a good example of the type of data needed.

To determine heat conduction in the steady state, the following equation may be used:

$$Q_k/A = \frac{k}{L}(T_1 - T_2) \qquad (32)$$

In the resting condition, the thermal constant for conducting heat from the interior of the body to the skin (tissue conductance only) is:

$$k = 1.5 \pm 0.3 \times 10^{-3} \text{ kcal/cm-sec-°C (at 23° to 25°C ambient)}$$

At full vasoconstriction, when tissue conductance is 9 to 10 kcal/sq m-hr-°C, the value for conductance corresponds to a tissue layer 1.8 to 2.2 cm thick. At the limit of vasodilation, thermal conductance is increased to values of 28 to 30 kcal/sq m-hr-°C. Although values above and below these limits have been reported in the literature, many of the subjects may have become acclimated by the tests and, accordingly, their values of conductance would exceed the norm. A change from full vasoconstriction to full vasodilation lowers thermal resistance of the body approximately the equivalent of 1 Clo unit.

Equivalent thermal conductance between adjacent radial layers of head, trunk, and extremities has recently been suggested. Assuming the thermal conductivity of tissue of 36 kcal-cm/sq m-hr-°C, physiologically effective masses and heat capacitance of different body compartments also have been calculated. The effectiveness of vascular convective heat transport can be measured quantitatively by deriving values of thermal conductance for the peripheral tissues of the body (Stolwijk, 1966). Cardiovascular changes, such as shunting during exercise, considerably complicate such calculations and, unfortunately, are key factors in operational situations.

In general, it can be concluded that as a physical thermal transfer system, conductive cooling can be adequate to maintain essential thermal equilibrium. It is essential, however, that the heat exchanger in contact with the skin operate at high enough temperatures to preclude vasoconstriction and guarantee adequate transfer of heat from the deep core to the skin to the heat exchanger. Current designs are not adequate to maintain man in the comfort zone during exercise at high metabolic rates.

GLOSSARY

Nomenclature

Symbol	Definition	BE Units
A	area	sq ft
A_b	surface area of body	sq ft
A_c	surface area of clothed body	sq ft
A_r	radiating area of body	sq ft
A_w	area of wall	sq ft
C	wetted area/A_b	
C_p	specific heat at constant pressure	Btu/lb°F
D	diameter or significant dimension	ft
D_v	vapor diffusivity	sq ft/hr
E_r	evaporative water loss	lb/sq ft
E_m	metabolism	Btu/hr

Symbol	Definition	BE Units
F_{cw}	shape-emissivity factor	dimensionless
g	fraction of earth gravity	
G	mass velocity (ρV)	lb/sq ft-hr
h_c	convection heat transfer coefficient	Btu/sq ft-hr-^{o}F
h_D	mass transfer coefficient	ft/hr
h_r	radiation heat transfer coefficient	Btu/sq ft-hr-^{o}F
h_{rb}	radiant conductance (blackbody)	Btu/sq ft-hr-^{o}F
h_{fg}	heat of vaporization	Btu/lb
k	thermal conductivity	Btu/ft-hr-^{o}F
L	thickness	ft
M	molecular weight	Btu/hr
P	atmospheric pressure	psia
P_o	standard barometric pressure	psia
p	water vapor pressure	psia
P_a	atmospheric water vapor pressure	psia
P_s	water vapor pressure at the skin	psia
$\dot{Q}_c$	convection heat transfer	Btu/hr
$\dot{Q}_e$	evaporation heat transfer	Btu/hr
$\dot{Q}_g$	garment cooling	Btu/hr
$\dot{Q}_m$	metabolic heat	
$\dot{Q}_r$	radiation heat transfer	Btu/hr
Q_s	storage rate	Btu/hr
$\dot{Q}_{sr}$	solar heat transfer to man	Btu/hr
$\dot{Q}_k$	conductive heat transfer	Btu/hr
$\dot{Q}_v$	respiratory heat transfer	Btu/hr
Q	total heat transfer	Btu/hr
R	Gas constant	ft-lb/lb-^{o}R
$R_g = 1/h_g$	thermal resistance of clothing	$\frac{\text{sq ft-}^{o}\text{F}}{\text{Btu}}$
R'	vapor resistance in terms of the equivalent thickness of still air	ft still air
R'_g	clothing vapor resistance	ft still air
T	temperature	^{o}R
T_a	atmospheric temperature	^{o}R
T_b	weighted mean body temperature	^{o}R
T_E	effective temperature	^{o}F

Symbol	Definition	BE Units
T_c	clothing surface temperature	$^\circ R$
T_o	operative temperature	$^\circ F$
T_{or}	reference operative temperature	$^\circ F$
T_r	rectal temperature	$^\circ F$
T_s	weighted body skin temperature	$^\circ R$
T_v	garment ventilating temperature	$^\circ F$
T_w	average wall temperature	$^\circ R$
T_f	film temperature	$^\circ R$
u	internal energy per unit mass	Btu/lb
U	overall heat transfer coefficient	Btu/hr-sq-ft-$^\circ F$
V	velocity	ft/hr or ft/min
$\dot{V}$	respiration rate	liters/hr
w	mass flow rate	lb/hr
W	work rate	Btu/hr

GREEK SYMBOLS

α	solar absorptivity of skin or garments	dimensionless
ϵ	emissivity	dimensionless
ϵ_c	emissivity of clothing	dimensionless
ϵ_w	emissivity of wall	dimensionless
θ	time of exposure	min or hr
θ_t	tolerance time	min or hr
μ	viscosity	lb/ft-hr
ρ	density	lb/cu ft
σ	Stefan-Boltzman constant	0.1714×10^{-8}

DIMENSIONLESS GROUPS OR NUMBERS

$Nu = \frac{h_c D}{k}$ Nusselt number

$Pr = \frac{C_p \mu}{k}$ Prandtl number

$Re = \frac{\rho V D}{\mu}$ Reynold number

$S_c = \frac{\mu}{\rho D_v}$ Schmidt number

References

AiResearch Manufacturing Co. Extravehicular suit thermal and atmospheric control, SS-3056, Los Angeles, 1964.

American Society of Heating, Refrigerating and Air-Conditioning Engineers, *ASHRAE guide and data book for 1965-66*. New York, 1965.

Barnett, P. Field tests of two anti-exposure assemblies. AAL-TDR-61-56, Arctic Aeromedical Lab., Fort Wainwright, Alaska, 1962.

Beckman, E. L., & Reeves, E. Physiological implications as to survival from immersion in 75° water. *Aerospace Medicine*, 1966, 37, 1136-1142.

Behnke, A. R., Yaglou, C. P. Physiological responses of men to chilling in ice water and to slow and fast rewarming. *Journal of Applied Physiology*, 1951, 3, 591-602.

Belding, H. S., & Hatch, T. F. Index for evaluating heat stress in terms of resulting physiologic strains. *Heating, Piping and Air Conditioning*, 1955, 27, 129-136.

Benzinger, T. H. The diminution of thermoregulatory sweating during cold-reception at the skin. *Proceedings of the National Academy of Sciences*, 1961, 47, 1683-1688.

Benzinger, T. H., Kitzinger, C., & Pratt, A. W. The human thermostat. In J. D. Hardy (Ed.), *Temperature, its measurement and control in science and industry*. Vol. 3. *Biology and Medicine*, New York: Reinhold, 1963.

Berenson, P. J. General analysis of human thermal comfort. Rep. SS-3245, AiResearch Mfg. Co., Division of Garrett Corporation, Los Angeles, Calif., January 1965.

Berenson, P. J. Prediction of human thermal comfort in oxygen-nitrogen atmospheres. In P. Horowitz (Ed.), *Physiological and performance determinants in manned space systems*. Vol. 5. *American Astronautical Society*. Baltimore, 1965.

Berenson, P. J., & Green, F. H. Human thermal comfort in helium-oxygen atmosphere. Rep. LS-149, AiResearch Mfg. Co., Division of Garrett Corporation, Los Angeles, Calif., May 1965.

Blockley, W. V. Changes in the boundary between neutral and stressful thermal conditions caused by respiratory protective equipment. Final report, Webb Associates, Yellow Springs, Ohio, 1964.

Blockley, W. V. Human sweat response to activity and environment in the compensable zone of thermal stress: A systematic study. NASA-CR-65260, 1965.

Blockley, W. V. Temperature. In P. Webb (Ed.), *Bioastronautics data book*. NASA-SP-3006, 1964.

Blockley, W. V., McCutchan, J. W., & Taylor, C. L. Prediction of human tolerance for heat in aircraft: A design guide. WADC-TR-53-346, May 1954.

Blockley, W. V., & Taylor, C. L. Studies of human tolerance for extreme heat. First summary report, Memo Rep. No. 696-113A, Air Materiel Command, Wright-Patterson AFB, Ohio, 1948.

Bonura, M. S., & Nelson, W. G. Engineering criteria for spacecraft cabin atmosphere selection. NASA-CR-891, September 1967.

Brebner, D. F., Kerslake, D. McK., Waddell, J. L. Diffusion of water vapor through human skin. *Journal of Physiology*, 1956, 132, 225-231.

Breeze, R. K. Space vehicle environmental control requirements based on equipment and physiological criteria. ASD-TR-61-161(Pt. 1), Aeronautical Systems Division, Wright-Patterson AFB, Ohio, 1961.

Bryan, A. C. Breathing. In P. Webb (Ed.), *Bioastronautics data book*. NASA-SP-3006, 1964.

Buettner, K. Effects of extreme heat and cold on human skin. III. Penetrating flash. *Journal of Applied Physiology*, 1952, 5, 207-220.

Buettner, K. Thermal aspects of travel in the aeropause problems of thermal radiation. In C. S. White & O. O. Benson, Jr. (Eds.), *Physics and medicine of the upper atmosphere*. Albuquerque: University of New Mexico Press, 1952.

Bullard, R. W. Sweating: Its rapid response to muscular work. *Science*, 1963, *141*, 643-646.

Bullard, R. W. Temperature regulation. In E. E. Selkurt (Ed.), *Physiology*. Boston: Little, Brown & Co., 1963.

Burriss, W. L., Wortz, E. C., Belton, J. J., et al. Internal thermal environment management program. SS-847, Rev. 2, AiResearch Mfg. Co., Los Angeles, September 1963.

Burton, A. C. Clothing and heat exchanges. *Federal Proceedings*, 1946, 5, 344-351.

Burton, D. R. Performance of water conditioned suits. *Aerospace Medicine*, 1966, *37*, 500-504.

Burton, D. R., & Collier, L. Performance of water conditioned suits. RAE-TR-65004, Royal Aircraft Establishment, Farnborough, England, 1965.

Busby, D. E. Clinical space medicine. NASA-CR-856, July 1967.

Buskirk, E. R., & Bass, D. E. Climate and exercise. QREC-EP-61, Quartermaster Research and Engineering Center, Natick, Mass., 1957.

Clark, R. E. The limiting hand skin temperature for unaffected manual performance in the cold. *Journal of Applied Psychology*, 1961, *45*, 193-194.

Clark, R. E., Cohen, A. Manual performance as a function of rate of change in hand skin temperature. *Journal of Applied Physiology*, 1960, *15*, 496-498.

Clifford, J., Kerslake, D. McK., & Waddell, J. L. The effect of wind speed on maximum evaporative capacity in man. *Journal of Physiology*, 1959, *147*, 253-259.

Damato, M. J., Radliff, M. H. Evaluation of divers' wet suit as considered for use by pilots of helicopters and fixed-wing aircraft. Naval Air Engineering Center, Air Crew Equipment Lab., Philadelphia, Pa. Paper presented at the 35th Annual Meeting, Aerospace Medical Association, Miami Beach, Fla., May 11-14, 1964.

Davis, T. R. A. Acclimatization to cold in man. In J.D. Hardy (Ed.) *Temperature: its measurement and control in science and industry*. Vol.3. *Biology and Medicine*. New York: Reinhold, 1963.

Dunham, W., Holling, H.E., Ladell, W.S., et al. The effects of air movements in severe heat. RNP-16/316, Royal Naval Personnel Research Committee, Medical Research Council, London, 1946.

Dusek, E. R. Effect of temperature on manual performance. In F.R. Fisher (Ed.), *Protection and functioning of the hands in cold climates*. Washington, D.C.: National Academy of Sciences, National Research Council, 1957.

Eckert, E. R. G., & Drake, R. M., Jr. *Heat and mass transfer*. New York: McGraw-Hill, 1959.

Eichna, L. W., Park, C. R., Nelson, N., et al. Thermal regulation during acclimatization in a hot, dry (desert type) environment. *American Journal of Physiology*, 1950, *163*, 585-597.

Epperson, W. L., Quigley, D. G., Robertson, W. G. Observations on man in an oxygen-helium environment at 380 mm Hg total pressure. III. Heat exchange. *Aerospace Medicine*, 1966, *37*, 457-462.

Fahnestock, M. K., Boys, F. E., Sargent II, F., Spring, W. E., & Siler, L. D. Comfort and physiological responses to work in an environment of 75°F and 45% relative humidity. *Journal of American Society of Heating, Refrigerating and Air Conditioning Engineers, Inc.*, 1963, *5*(3), 25-35.

Fanger, P. O., Nevins, R. G., & McNall, P. E. Predicted and measured heat losses and thermal comfort conditions for human beings. In *Thermal problems in biotechnology*. New York: American Society of Mechanical Engineers, 1968.

Fox, R. H., Goldsmith, R., Hampton, I. F. G., et al. The nature of the increase in sweating capacity produced by heat acclimatization. *Journal of Physiology*, 1964, *171*, 368-376.

Gagge, A.P. Comfort: New concepts and applications. *Building Research*, 1966, 3.

Gaydos, H. F., Dusek, E. R. Effects of localized hand cooling versus total body cooling on manual performance. *Journal of Applied Physiology*, 1958, *12*, 377-380.

Gillies, J. A. (Ed.) *A textbook of aviation physiology*. Edinburgh, Scotland: Pergamon Press, 1965.

Goldman, R. F., Green, E. B., Iampietro, P. F. Tolerance of hot, wet environments by resting men. *Journal of Applied Physiology*, 1965, *20*, 271-277.

Guibert, A., & Taylor, C. L. The radiation area of the human body. AF-TR-6706, Wright Air Development Center, Wright-Patterson AFB, Ohio, 1951. (Also in *Journal of Applied Physiology*, 1952, *5*(1), 24-37.)

Hale, F. C., Westland, R. A., Taylor, C. L. Barometric and vapor pressure influences on insensible weight loss. *Journal of Applied Physiology*, 1958, *12*(1), 20-28.

Hall, J. F., Jr., Polte, J. W., Kelley, R. L., et al. Cooling of clothed subjects immersed in cold water. WADC-TR-53-323, Wright Air Development Center, Wright-Patterson AFB, Ohio, April 1953.

Hanifan, D. T., Blockley, W. V., Mitchell, M. B., et al. Physiological and psychological effects of overloading fallout shelters. Dunlap Associates, Inc., Santa Monica, Calif., April 1963.

Hardy, J. D. (Ed.) *The physiological problems in space exploration*. Springfield, Ill.: Charles C. Thomas, 1954.

Hertzman, A. B., Randall, W. C., Peis, C. N., et al. The regional rates of evaporation from the skin. AF-TR-6680, Part 2. Aero-Medical Lab., Wright-Patterson AFB, Ohio, 1951.

Hertzman, A. B., Randall, W. C., Peis, C. N., et al. The regional rates of evaporation from skin at various environmental temperatures. *Journal of Applied Physiology*, 1952, 5(4), 153-161.

Horvath, S. M., & Freedman, A. The influence of cold upon the efficiency of man. *Journal of Aviation Medicine*, 1947, *18*, 158-164.

Horvath, S. M., Shelley, W. B. Acclimatization to extreme heat and its effect on ability to work in less severe environments. *American Journal of Physiology*, 1946, *146*, 336-343.

Iampietro, P. F., Bass, D. E., & Bushkirk, E. R. Heat exchanges of nude men in the cold. *Journal of Applied Physiology*, 1958, *12*, 351-356.

Kaufman, W. C., Swan, A. G., & Davis, H. T. Skin temperature responses to simulated thermonuclear flash. ASD-TR-61-510, Aeronautical Systems Division, Wright-Patterson AFB, Ohio, 1961.

Kerslake, D. McK. Errors arising from the use of mean heat exchange coefficients in the calculation of the heat exchanges of a cylindrical body in a transverse wind. In J. D. Hardy (Ed.), *Temperature*. Vol. 3. *Biology and Medicine*. New York: Reinhold, 1963.

Kerslake, D. McK. The physiological requirements for environmental comfort in terms of the microclimate. Presented at the Full Pressure Suit Symposium, 1962.

Kerslake, D. McK. An estimate of the preferred skin temperature distribution in man. FPRC-Memo-213, RAF Flying Personnel Res. Comm., Farnborough, England, 1964.

Kissen, A. T., Hall, J. F. Physiologic response to transient heat stress in reflective versus non-reflective clothing. AMRL-TDR-63-79, Aerospace Medical Research Labs., Wright-Patterson AFB, Ohio, August 1963.

Krantz, P. Calculating human comfort. *Journal of American Society of Heating, Refrigerating and Air Conditioning Engineers, Inc.*, 1964, *6*, 68-77.

Lang, R., & Syversen, R. G. Factors affecting the thermal equilibrium of a EMU subject in the Apollo. In *Proceedings of the Second Space Congress*, Cocoa Beach, Fla., April 5-7, 1965.

LeBlanc, J. S. Impairment of manual dexterity in the cold. *Journal of Applied Physiology*, 1956, *9*, 62-64.

Lind, A. R., & Bass, D. E. Optimal exposure time for development of acclimatization to heat. *Federal Proceedings*, 1963, 22(3), 704-708.

Mackworth, N. H. Effects of heat on wireless telegraphy operators hearing and recording Morse messages. *British Journal of Industrial Medicine*, 1946, *3*, 143-158.

MacPherson, R. K. The assessment of the thermal environment. *British Journal of Industrial Medicine*, 1962, *19*, 151-164.

MacPherson, R. K. Physiological responses to hot environments. MRC-SRS-298, Medical Research Council, Her Majesty's Stationery Office, London, 1960.

McAdams, W. H. *Heat transmission*. New York: McGraw-Hill, 1954.

McCance, R. A., Ungley, C. C., Crossfill, J. W. L., et al. The hazards to men in ships lost at sea, 1940-1944. MRC-SR-291, Medical Research Council, Her Majesty's Stationery Office, London, 1956.

McCutchan, J. W., & Taylor, C. L. Respiratory heat exchange with varying temperature and humidity of inspired air. *Journal of Applied Physiology*, 1951, *4*, 121-135.

Milan, F. A. Cold water tests of USAF anti-exposure suits. Arctic Aeromedical Lab., TR-64-31, Fort Wainwright, Alaska, 1965.

Mills, A. W. Tactile sensitivity in the cold. In F. R. Fisher (Ed.) *Protection and functioning of the hands in cold climates*. Washington, D.C.: NAS-NRC, 1957.

Molnar, G. W. Survival of hypothermia by men immersed in the ocean. *Journal of the American Medical Association*, 1964, *131*, 1046-1050.

Nelson, N., Eichna, L. W., Horvath, Sm. M., et al. Thermal exchanges of man at high temperatures. *Journal of American Physiology*, 1947, *151*, 627-632.

Newburgh, L. H. (Ed.) *Physiology of heat regulation and the science of clothing*. Philadelphia: W. B. Saunders, 1949.

Parker, F. A., Ekberg, D. A., Withey, D. J., et al. Atmosphere selection and control for manned space stations. General Electric Co., Missile and Space Division, Valley Forge, Pa., presented at the International Symposium for Manned Space Stations, Munich, September 1965.

Pepler, R. D. Extreme warmth and sensorimotor coordination. *Journal of Applied Physiology*, 1959, *14*, 383-386.

Pitts, G. C., Johnson, R. E., & Consolazio, F. C. Work in heat as affected by intake of water, salt, and glucose. *American Journal of Physiology*, 1944, *142*(2), 253-259.

Pfleidere, H., & Buettner, K. *Bioklimatologie, Lehrbuch d. Baeder und Klimaheilkunde* Berlin: Julius, Springs, 1940.

Randall, W. C., & Hertzman, A. B. Dermatomal recruitment of sweating. *Journal of Applied Physiology*, 1953, *5*, 399-409.

Robinson, S. Circulatory adjustments of men in hot environments. *Temperature, its measurement and control in science and industry*. Vol. 3. New York: Reinhold, 1963.

Robinson, S., Turrell, E. S., Belding, H., et al. Rapid acclimatization to work in hot climates *American Journal of Physiology*, 1943, *140*, 168-176.

Roth, E. M. Bioenergetics of space suits for lunar exploration. NASA-SP-84, 1966.

Roth, E. M. Space-cabin atmospheres. Part IV. Engineering trade-offs of one-versus-two gas systems. NASA-AP-118, 1967.

Roth, E. M. (Ed.) *Compendium of human responses to the aerospace environment*. NASA-CR-1205, National Aeronautics and Space Administration, Washington, D.C., 1968.

Sanders Nuclear Corp. Technical proposal for a radioisotope fueled diving suit heating system (U). Sanders-Prop-86 HX, Nashua, New Hampshire, 1966.

Secord, T. C., & Bonura, M. S. Life support systems data from sixty-two days of testing in a manned space laboratory simulator. In AIAA Fourth Manned Space Flight Meeting, St. Louis, Mo., October 1965. *American Institute of Aeronautics and Astronautics*, New York, 1965.

Siple, P. A., Passel, C. F. Measurements of dry atmospheric cooling in subfreezing temperatures. *Proceedings of the American Philosophical Society*, 1945, *89*, 177-199.

Smith, F. E. Indices of heat stress. MRC-Memo-29, Medical Research Council, Her Majesty's Stationery House, London, 1955.

Smith, G. B., Jr., Hames, E. F. Estimation of tolerance times for cold water immersion. *Aerospace Medicine*, 1962, 33(7), 834-840.

Spector, W. S. (Ed.) *Handbook of biological data*. WADC-TR-56-273, Wright Air Development Center, Wright-Patterson AFB, Ohio, 1956.

Stoll, A. M. The role of the skin in heat transfer. American Society of Mechanical Engineers Paper 59-A-138. *Journal of Heat Transfer, American Society of Mechanical Engineers, Trans. Sec. C*, 1960, *82*, 239-241.

Stoll, A. M., Greene, L. C. Relationship between pain and tissue damage due to thermal radiation. *Journal of Applied Physiology*, 1959, *14*(3), 373-382.

Stolwijk, J. A. J., Hardy, J. D. Temperature regulation in man – A theoretical study. *Pflugers Archives*, 1966, *291*, 129-162.

Strydom, N. B., Wyndham, C. H. Natural state of heat acclimatization of different ethnic groups. *Federal Proceedings*, 1963, 22(3), 801-809.

Taylor, C. L., & Buettner, K. The evaporative effect on human perspiration. WADC-TR-53-345, Wright Air Development Center, Wright-Patterson AFB, Ohio, 1953.

Teichner, W. H., Kobrick, J. L. Effects of prolonged exposure to low temperature on visual motor performance, flicker fusion and pain sensitivity. Tech. Rep. EPD 230, Quartermaster Research and Development Center, Natick, Mass., 1954.

Teichner, W. H. Manual dexterity in the cold. *Journal of Applied Physiology*, 1957, *11*, 333-338.

Teichner, W. H. Reaction time in the cold. *Journal of Applied Physiology*, 1958, *42*, 54-59.

Teichner, W. H. Temperature, humidity, and ventilation (preliminary draft). Guggenheim Center for Aviation Health and Safety, Harvard School of Public Health, Boston, Mass., 1961.

Thompson Ramo Wooldridge, Inc. Propellant-atmosphere study. W-ADD-TR-60-622, March 1961. (AD-268768)

Trumbull, R. Environmental modification for human performance. ONR-ACR-105-11, Office of Naval Research, Washington, D.C., 1965. Submarine Medical Practice, NAVMED-P-5054. Bureau of Medicine and Surgery. Government Printing Office, Washington, D.C., 1956.

United States Navy. Medical Newsletter 31: 12. 1958.

Waligora, J. M., & Michel, E. L. Application of conductive cooling for working men in a thermally isolated environment. (abstract). *Aerospace Medicine*, 1966, 37, 306.

Weaver, J. A. Calculation of time-temperature histories and prediction of injury to skin exposed to thermal radiation. NADC-MR-6623, Naval Air Development Center, Warminster, Pa., June 1967.

Webb, P. Pain limited heat exposures. In J. D. Hardy (Ed.) *Temperature, its measurement and control in science and industry*. Vol. 3. *Biology and Medicine*, New York: Reinhold Publishing Co., 1963.

Webb, P. (Ed.) *Bioastronautics data book*. NASA-SP-3006, Washington, D.C., 1964.

Webb, P. Human water exchange in space suits and capsules. NASA-CR-804, National Aeronautics and Space Administration, Washington, D.C., 1967.

Webb, P. Heat loss from the respiratory tract in cold project no. 7-7951. Rept. 3, Arctic Aeromedical Lab., Ladd AFB, Alaska, April 1955.

Webb, P., & Annis, J. F. Bio-thermal responses to varied work programs in men kept thermally neutral by water cooled clothing. NASA-CR-739, 1966.

Webb, P., Garlington, L. N., & Schwarz, M. J. Insensible weight loss at high skin temperatures. *Journal of Applied Physiology*, 1957, *11*, 41-44.

Welch, B. E. Chief, Environmental Systems Branch, USAF School of Aerospace Medicine, Aerospace Medical Div., Air Force Systems Command, Brooks AFB, Texas, personal communication, March 1966.

Winslow, C. -E. A., Herrington, L. P., & Gagge, A. P. Physiological reactions of the human body to varying environmental temperatures. *Journal of American Physiology*, 1937, *120*, 1-22.

Winslow, C. -E. A., Herrington, L. P., & Gagge, A. P. Reactions between atmospheric conditions, physiological reactions and sensation of pleasantness. *Journal of American Hygiene*, 1937, *26*, 103-115.

Wortz, E. C., Diaz, R. A., Green, F. H., et al. Reduced barometric pressure and respiratory water loss. SAM-TR-66-4, School of Aerospace Medicine, Brooks AFB, Texas, 1966.

Wortz, E. C., Edwards, D. K., III, Diaz, R. A., et al. Study of heat balance in full pressure suits. *Aerospace Medicine*, 1967, *38*, 181-188.

Wyndham, C. H., Bouwer, W., Devine, M. G., et al. Examination of use of heat exchange equations for determining changes in body temperature. *Journal of Applied Physiology*, 1952, *5*, 299-307.

Wyndham, C. H., Strydom, N. B., Morrison, J. F., et al. Responses of unacclimatized men under stress of heat and work. *Journal of Applied Physiology*, 1954, *6*, 681-686.

Zollner, G., Thauer, R., Kaufmann, W. Der insensible gewichtsverlust als funktion der umweltbedingungen. Die Abhangigkeit der Hautwasserabgabe von der Hauttemperatur bei Verschiedenen Temperaturen und Wasserdampfdrucken der umgebenden Luft. *Arch. Ges. Physiology*, 1955, *260*, 261-273.

Selected and Recent Books

Fanger, P. O. Calculation of thermal comfort: Introduction of a basic comfort equation. *Transactions of the American Society of Heating, Refrigerating and Air Conditioning Engineers, Inc.*, 1967. Vol. 73, Part III.

Fourt, L., & Hollies, N. R. S. The comfort and function of clothing. Technical report 69-74-CE, U.S. Army Natick Laboratories, Natick, Mass., June 1969.

Gagge, A. P. Man, his environment, his comfort. *Heating, Piping and Air Conditioning*, 1969, 209-224.

Gagge, A. P., Stolwijk, J. A. J., & Hardy, J. D. Comfort and thermal sensations and associated physiological responses at various ambient temperatures. *Environmental Research*, 1967, *1*(1), 1-20.

Gagge, A. P., Stolwijk, J. A. J., & Nishi, Y. The prediction of thermal comfort when thermal equilibrium is maintained by sweating. American Society of Heating, Refrigerating and Air Conditioning Engineers, Inc. Paper number 2116, 1969.

Gagge, A. P., Stolwijk, J. A. J., & Nishi, Y. An effective temperature scale based on a simple model of human physiological regulatory response. Paper presented at American Society of Heating, Refrigerating and Air Conditioning Engineers, Inc. semiannual meeting, Philadelphia, January 1971.

APPENDIX

A TWO-NODE Model of Human Temperature Regulation in FORTRAN

by A. P. Gagge

The following is an Annoted FORTRAN Program which includes the most recent concepts of the regulation of body temperature during rest and exercise and during the transient and steady states. The general principles described are presented in NASA Report CR-1855, A Mathematical Model of Physiological Temperature Regulation in Man by J. A. J. Stolwijk (1971). The present model (A. P. Gagge, J. A. J. Stolwijk and Y. Nishi, ASHRAE TRANSACTIONS, Vol. 77, Part I, 1971) is a simplified version, which considers the control of body temperature to be accomplished primarily by the mean skin temperature and a central core temperature; the latter may be measured either in the rectum or in the esophagus. The present model also includes an analysis of the seven independent environmental factors necessary to make a complete partition of the heat exchange. Definitions are indicated for the new Effective Temperature (ET*) of the American Society of Heating, Refrigerating and Air-Conditioning Engineers, as well as the new Standard Effective Temperature (SET*), by which it is possible to compare on a commonly experienced temperature scale the expected physiological heat stress caused by use of clothing, by radiant heat, by air movement and by barometric pressure. Modifications of the model for water immersion are also indicated.

The independent variables are:

- MR = metabolic rate in W/m^2 (REAL)
- WK = work rate accomplished in W/m^2
- CLO = intrinsic clothing insulation in clo units [0.155 $m^2 \cdot C^o/W$]
- CHR = linear radiation exchange coefficient in $W/(m^2 \cdot {}^oC)$
- CHC = convective heat transfer coefficient in $W/(m^2 \cdot {}^oC)$ at sea level

and varies with both air movement (VELA) and activity (VEL) (see Nishi and Gagge, 1971)

- BARO = barometric pressure (mm Hg)
- TA = ambient air temperature ^oC
- TR = mean radiant temperature ^oC
- PPHG = ambient vapor pressure in mm Hg and may be found

from wet bulb (TWET) or dew point (TDP) measurements

The dependent variables are:

- TSK = temperature of skin shell ($\sim \bar{T}_{sk}$) in ^oC
- TCR = central core temperature ($\sim$ rectal or esophageal) in ^oC
- ALPHA = ratio of mass skin shell to mass central core (N.D.)
- SKBF = skin blood flow in $l/(m^2 \cdot hr)$
- EV = total evaporative heat loss in W/m^2

Characteristics of an Average Man

- 70. = body weight in kg
- 1.8 = body surface in sq. meters
- 0.72 = ratio of body's radiating area to total surface area
- 5.28 = minimum skin conductance in $W/(m^2 \cdot {}^oC)$
- 6.3 = normal skin blood flow in $l/(m^2 \cdot hr)$

The assigned coefficients are

1.163= specific heat of blood in W·hr/(l·°C)
0.68 = latent heat of water W·hr/g
0.97 = specific heat of body in W·hr/(kg·°C)
2.2 = Lewis Relation at sea level in °C/mm Hg
760. = sea level barometric pressure in mm Hg
5.67E-08 = Stefan-Boltzmann Constant in $W/(m^2 \cdot K^4)$

Initial Conditions (TIM = 0) are those for physiological thermal neutrality:

```
TSK  = 34.
TCR  = 37. (for rectal) or 36.6 (for esophageal)
CHR  =  5.0
CTC  = CHR+CHC
SKBF =  6.3
ALPHA=  0.1
EV   =  5.0
```

For sedentary case (1 met):

```
MR   = 58.2
RM   = MR
WK   =  0
CHC  = 2.9
```

For exercise:

```
CHC = 5.4  (bicycle ergometer at 50 RPM)
CHC = 6.0  (  "        "       " 60 RPM)
CHC = 6.51*VEL**0.391   (treadmill walking for VEL in m/sec)
CHC = 8.60*VEL**0.531   (free walking at VEL in m/sec; still air)
CHC = 8.60*VEL**0.531 + 1.96*VELA**0.86 (where VELA is a head wind in m/sec)
```

Initial Definitions

Respired Evaporative Heat Loss (ERES) (Fanger, 1970)

```
ERES = 0.0023*RM*(44.-PPHG)
```

Respired Convective Heat Loss (CRES) (Fanger, 1970)

```
CRES = 0.0012*RM*(34.-TA)
```

Burton Clothing Efficiency Factor (FCL)

```
FCL  = 1./(1.+0.155*CTC*CLO)
```

Operative Temperature (TO)

```
TO   = (CHR*TR+CHC*TA)/CTC
```

The above definitions are entered by READ and DO statements

The Simulation Program for Human Temperature Regulation

starts here:

```
100  CONTINUE
```

Clothing Surface Temperature

```
TCL  = TO+FCL*(TSK-TO)
```

Factor (FACL) increases radiation area of body by 15%/clo (Fanger, 1970)

```
FACL = 1.+0.15*CLO
```

The coefficient CHR varies with TSK or TCL during regulation

```
CHR  = 4.*5.97E-08*((TCL+TO)/2.+273.)**3.*FACL*0.72
CTC  = CHR+CHC
FCL  = 1./(1.+0.155*CTC*CLO)
DRY  = CTC*FCL*(TSK-TO)
```

Heat Flow (HFCR) from body core to skin shell

```
HFCR = RM-ERES-CRES-WK-(5.28+1.163*SKBF)*(TCR-TSK)
```

Heat Flow (HFSK) from skin shell to environment at TO

```
HFSK = (5.28+1.163*SKBF)*(TCR-TSK)-DRY-(EV-ERES)
```

Thermal Capacity of body core (TCCR)

```
TCCR = 0.97*(1.-ALPHA)*70.
```

Thermal Capacity of skin shell (TCSK)

```
TCSK = 0.97*ALPHA*70.
```

Change in core temperature (DTCR) caused by HFCR

```
DTCR = (HFCR*1.8)/TCCR
```

```
Change in skin shell temperature caused by HFSK
      DTSK =  (HFSK*1.8)/TCSK
Iteration to simulate regulation will be at one minute intervals
or by DTSK and DTCR not greater than ± 0.1°C.
      DTIM =  1./60.
      U = ABS(DTSK)
      IF(U-0.1)5, 10, 10
 10   DTIM=0.1/(U*60.)
  5   CONTINUE
      U=ABS(DTCR)
      IF(U-0.1)105,110,110
110   DTIM=0.1/(U*60)
105   CONTINUE
TIM is in hours
      TIM  = TIM+DTIM
      TSK  = TSK+DTSK*DTIM
      TCR  = TCR+DTCR*DTIM


Definition of the Control Signals (SKSIG, CRSIG)
from skin shell:- "cold" (COLDS);  +"warm" (WARMS)
      SKSIG=TSK-34.0
      IF(SKSIG)15,15,20
 15   COLDS=-SKSIG
      WARMS=0.0
      GO TO 25
 20   COLDS=0.0
      WARMS=SKSIG
 25   CONTINUE
from body core: - "cold" (COLDC);  +"warm" (WARMC)
      CRSIG=TCR-37.0
      IF(CRSIG)30,30,35
 30   COLDC=-CRSIG
      WARMC=0.0
      GO TO 40
 35   WARMC=CRSIG
      COLDC=0.0
 40   CONTINUE
Control of Skin Blood Flow (STRIC-vasoconstriction;  DILAT-vasodilation)
      STRIC= 0.5*COLDS
      DILAT= 150.*WARMC
The coefficients 0.5 and 150., which change during acclimatization, may vary
± 50% without significantly changing resulting thermal equilibrium but they do
affect time to equilibrium.
      SKBF  = (6.3+DILAT)/(1.+STRIC)


Sweating is controlled both by the mean body temperature (Snellen, 1966) and the
peripheral skin temperature (Nadel, Bullard and Stolwijk, 1971)
      REGSW=250.*(ALPHA*SKSIG+(1.-ALPHA)*CRSIG)*EXP(SKSIG/10.7)
      IF(REGSW) 45, 45, 50
 45   REGSW=0
 50   CONTINUE
The evaporative heat loss caused by sweating (ERSW)
      ERSW =  0.68*REGSW
The Nishi Permeation Efficiency Factor (FPCL) for clothing
      FPCL =  1./(1.+0.143*CHC*CLO)
The E_max of the body skin surface
      EMAX = 2.2*CHC*(SVP(TSK)-PPHG)*FPCL
SVP is a FUNCTION relating saturated vapor pressure to temperature T

Skin wettedness due to sweating (PRSW)
      PRSW = ERSW/EMAX
Total skin wettedness (PWET)
      PWET = 0.06+0.94*PRSW
Skin diffusion (EDIF)
      EDIF=PWET*EMAX-ERSW
```

```
Total evaporative heat loss (EV)
      EV=ERES+ERSW+EDIF
      IF(PWET)60,60,55
   65 EV=ERES+EMAX
      ERSW=EMAX
      EDIF=0.0
      PRSW=1.0
Unevaporated sweat (DRIP) in g/(m2·hr)
      DRIP=(ERSW-EMAX)/0.68
   60 CONTINUE
Change in skin blood flow affects ALPHA causing skin shell to become thicker
or thinner (Ashoff, 1956)
Hyperbole used to fit (ALPHA,SKBF) at three points (0.05,60)(0.1,6.3) and (0.4,1.0)
      ALPHA=0.0442+0.3509/(SKBF-0.01386)
Protection from cold by shivering (Stolwijk and Hardy, 1967)
      RM=MR+19.4*COLDS*COLDC
A time of exposure (TIME) of 0.25 hr or greater should be selected
Iteration now begins
      IF(TIM-TIME)100,101,101
  101 CONTINUE
```

After exposure (TIME), the following dependent variables have now been evaluated by iteration: CHR, CTC, FCL, TSK, TCR, REGSW, EMAX, ERSW, EDIF, EV, DRIP, PRSW, PWET, ALPHA, and a new RM, if shivering has occurred.

Rate of body heat storage (STORE) in W/m^2 and rate of change of mean body temperature (RTBM) in $^{o}C/hr$ at end of exposure TIME are:

```
      STORE = RM-CRES-WK-EV-DRY
      RTBM  = STORE*1.8/(70.*0.97)
```

For any environment:

```
The resultant dry and humid heat transfer coefficients are
      A=CTC*FCL
      B=2.2*1.92*CHC*FPCL
The linear "dew" temperature is given by
      TDEW=(25.3+PPHG)/1.92
Operative Temperature (TC) is
      TO=(CHR*TR+CHC*TA)/CTC
Humid Operative Temperature (TOH) at end of time (TIME) is
      C=A+PWET*B
      TOH=(A*TO+PWET*B*TDEW)/C

Calculation of new ASHRAE Effective Temperature (ET*)
      ET*TOH
   80 DEWS=(25.3+0.5*SVP(ET))/1.92
      TOHS=(A*ET+PWET*B*DEWS)/C
      ERROR=TOH-TOHS
      IF(ERROR)70,70,75
   75 ET=ET+0.1
      TO TO 80
   70 CONTINUE
```

For the Sedentary Case only, when RM=58.2 or 1 met:

```
The Standard Environment is defined by
      CHCS=2.9
      CLOS=0.6
      CHRS=CHR
      CTCS=CHRS+CHCS
      FPLS=1./(1.+0.155*CTCS*CLOS)
      FPCLS=1./(1.+0.143*CHCS*CLOS
The standard resulting dry and humid heat transfer coefficients are
      AS=CTCS*FCLS
      BS=2.2*1.92*CHCS*FPCLS
Standard Operative Temperature (STO)
      STO=(A/AS)*TO+(1-A/AS)*TSK
```

```
Standard Humid Operative Temperature (STOH)
      CS=AS+PWET*BS
      STOH=(C/CS)*TOH+(1-C/CS)*TSK

Calculation of Standard Effective Temperature (SET)
      SET=STOH
   90 TDEW5=(25.3+0.5*SVP(SET)/1.92
      STOH5=(AS*SET+PWET*BS*TDEW5)/CS
      ERR=STOH-STOH5
      IF (ERR)80,80,85
   85 SET=SET+0.1
      GO TO 90
   80 CONTINUE
```

Prediction of Warm discomfort DISC (positive)

```
      DISC=4.7*PRSW
```

Prediction of Temperature sensation (TSENS) + warm, - cold

```
      TSENS=0.245*SET+0.033*0.5*SVP(SET)-6.471
```

See ASHRAE Handbook of Fundamentals (1972) for sensory data.

Prediction of Cold DISCOMFORT (negative)

A TABLE function is used to relate DISC to TSK:

TSK	28.0	28.5	29.0	29.5	30.	30.5
DISC	-4.6	-4.1	-3.6	-3.1	-2.6	-2.1

TSK	31.0	31.5	32.0	32.5	33.0	33.5	34.0
DISC	-1.68	-1.25	-0.95	-0.7	-0.5	-0.3	0.0

The desired output statements now follow, END of Program.

The above program can be used with reasonable accuracy for exercise and work. The Standard Conditions may be set at any other desired value.

For environments different from sea level, the Lewis factor [2.2] is replaced by [2.2*760./BARO] and the sea level value for CHC by [CHC*(BARO/760.)**0.55], wherever they occur in the program.

In a water environment CHR = 0, and CHC values in range 70 - 150 $W/(m^2 \cdot {}^{o}C)$ should be used. Under these conditions, the Lewis factor [2.2] is set to zero as there is no evaporation.

In Fig. A-1, the model has been used to calculate loci of constant TSENS, TSK, DISC, PWET in terms of a uniform TA and ambient vapor pressure in mm Hg. They are drawn for a sedentary normally clothed subject.

In Fig. A-2, the model has been used to calculate lines of constant physiological strain (SET*) for the same resting subject.

In Fig. A-3, the expected thermal responses of a sedentary subject to the new ET* or SET are indicated.

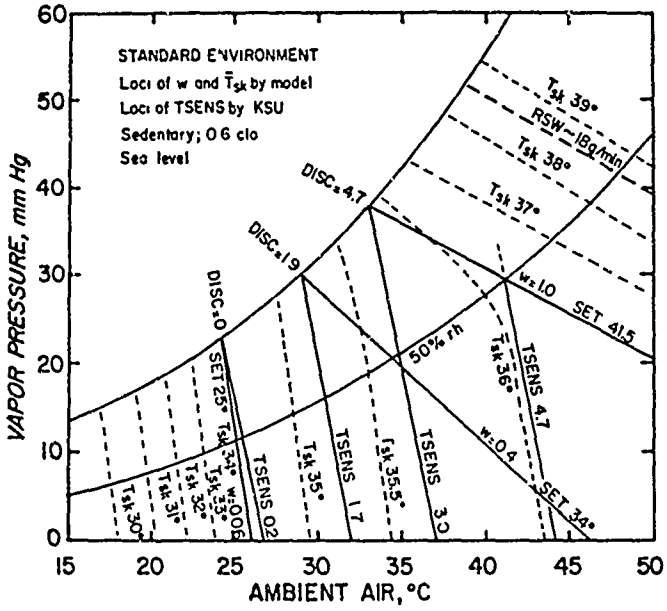


Figure A–1. Loci of constant $\bar{T}_{sk}$, w, TSENS and DISC for a Standard Environment in terms of ambient vapor pressure and air temperature.

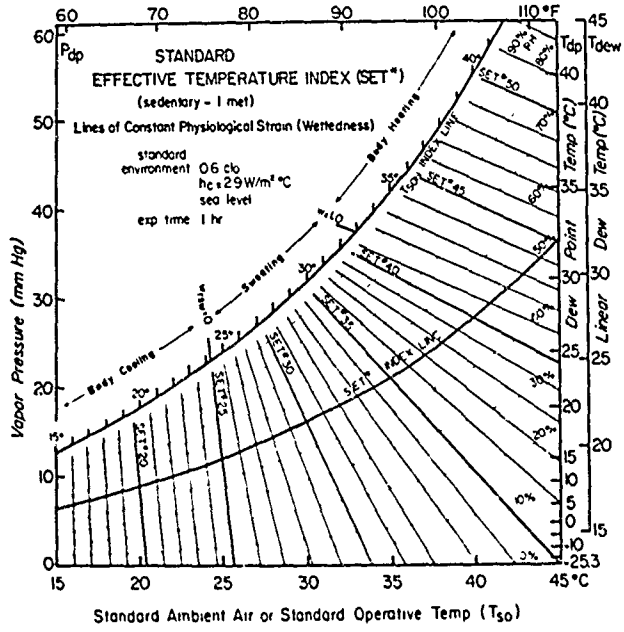


Figure A–2. Standard Operative Temperature or Dry Bulb Temperature (T_a') in a Standard environment. The relative humidity lines apply to the uniform T_a', not to T_{so} when used on the abscissa.

ET° °C	Temperature Sensation	Discomfort	Regulation of Body Temp.	Health	ET° °F
40	Very hot	Limited tolerance Very uncomfortable	Failure of free skin evap.	Increasing danger of heat stroke	
	Hot	Uncomfortable	↑ Increasing vasodilation sweating		100
35	Warm	Slightly uncomfortable			90
30	Slightly warm				
25	Neutral	Comfortable	No reg. sweating	Normal health	80
	Slightly cool		Vasoconstriction		70
20	Cool	Slightly uncomfortable	↓ Behavioral changes	Complaints from dry mucosa	60
15	Cold		Shivering begins	Impairment peripheral circulation	
10	Very cold	Uncomfortable	↓	↓	50

Figure A–3. Human thermal responses to the new Effective Temperature ET or SET. SET is the uniform ambient temperature at 50% relative humidity of an enclosure with air movement 0.15 m/sec or 30 fpm in which a clothed subject (0.6 clo) would exchange the same heat by radiation, convection, and evaporation as in the actual environment defined by TA, TR, PPHG, CIIR, CHC, and BARO.

CHAPTER 4
SUSTAINED LINEAR ACCELERATION

by

T. Morris Fraser, M.Sc., M.D.
University of Waterloo
Waterloo, Ontario, Canada

By definition, acceleration is a rate of change and can occur in any or all of three related, but differing, maneuvers. Linear acceleration is the rate of change of velocity of a mass, the direction of movement of which is kept constant. Acceleration acting on a mass will produce a force exerting a pressure on the mass and causing it to move if movable or to deform if not.

Angular acceleration is the rate of change of direction of a mass, the velocity of which is kept constant. In this regard, the acceleration is directly proportional to the square of the velocity and inversely proportional to the radius of the turn. By common usage, where the axis of rotation is external to the body, as in an aircraft turn or a centrifuge, the acceleration is frequently termed "radial" acceleration, while the term "angular" is retained for situations where the axis of rotation passes through the body. Where the radius is long, the effects of radial acceleration on man approximate those of linear acceleration.

In its third form, acceleration occurs as a component of the attraction between masses. The resulting force is directly proportional to the product of the masses and inversely proportional to the square of the distance between them. The proportionality constant is the gravitational constant g which represents an acceleration of 32.24 feet per second (fps) within the terrestrial field of reference. This is the accepted unit of measurement of acceleration.

When a mass is acted upon by the acceleration of gravity, the resulting force, acted vectorially, represents its weight. When the acceleration is other than gravitational, it interacts with gravity, if present, to produce a resultant which effectively increases the weight of the mass in the direction of the resultant. It is this effective increase in weight which, in one form or another, is largely responsible for the physiological and other changes found in the body exposed to sustained acceleration.

Reviewed by Randall M. Chambers, Ph.D., NASA Langley Research Center

In this regard, it must be remembered that the body is essentially a fluid system and reacts accordingly. Pascal, in the 17th century, showed that in ideal fluids at rest: (a) fluid pressure is equal in all directions, (b) pressures at points lying in the same horizontal plane are equal, and (c) pressure increases with depth under the free surface. This increase is equal to ρgh dynes/cm^2, where ρ is the density of the fluid, g the gravitational constant, and h the depth. These laws apply to the vascular system and, after a fashion, to the body as a whole.

The descriptive nomenclature for acceleration used herein is the system defined in chapter 6, *Impact*.

Terminology for duration of acceleration depends on the fact that there is a difference in body response to accelerations of duration below and above approximately 0.2 second, related to the latent period for development of hydrostatic effects. Thus, *abrupt acceleration* is considered as ranging to 0.2 second, while *sustained acceleration* is prolonged beyond 0.2 second.

Subjective Effects of Sustained Acceleration

In the operational situation, it is unusual, if not impossible, for acceleration stress to occur in a simple form. One is rarely, if ever, exposed to a simple unvarying $+G_z$ stress. Instead, acceleration may vary in its resultant vector, magnitude, and type, and may be accompanied by complex oscillations and vibrations. For purposes of analysis, however, it is simpler to consider the response to a continuous resultant vector without additional complexities. The following compilation is derived from the study by Fraser (1966).

Positive Acceleration Effects ($+G_z$)

1 G_z:	Equivalent to the erect or seated terrestrial posture.
2 G_z:	Increase in weight, increased pressure on buttocks, drooping of face and soft body tissues.
2 1/2 G_z:	Difficult to raise oneself.
3 – 4 G_z:	Impossible to raise oneself, difficult to raise arms and legs, movement at right angles impossible; progressive dimming of vision after 3 to 4 seconds, progressing to tunneling of vision.
4 1/2–6 G_z:	Diminution of vision, progressive to blackout after about 5 seconds; hearing and then consciousness lost if exposure continued; mild to severe convulsions in about 50 percent of subjects during or following unconsciousness, frequently with bizarre dreams; occasionally paresthesias, confused states and, rarely, gustatory sensations; no incontinence; pain not common, but tension and congestion of lower limbs with cramps and tingling; inspiration difficult; loss of orientation for time and space up to 15 seconds postacceleration.

Negative Acceleration Effects ($-G_z$)

$-1\ G_z$: Unpleasant but tolerable facial suffusion and congestion.

-2 to $-3\ G_z$: Severe facial congestion, throbbing headache; progressive blurring, graying, or occasionally reddening of vision after 5 seconds; congestion disappears slowly, may leave petechial hemorrhages, edematous eyelids.

$-5\ G_z$: Five seconds, limit of tolerance, rarely reached by most subjects.

Forward Acceleration Effects ($+G_x$)

$2-3\ G_x$: Increased weight and abdominal pressure; progressive slight difficulty in focusing and slight spatial disorientation, each subsiding with experience; 2 G_x tolerable at least to 24 hours, 4 G_x up to at least 60 minutes.

$3-6\ G_x$: Progressive tightness in chest (6 G_x, 5 minutes), chest pain, loss of peripheral vision, difficulty in breathing and speaking, blurring of vision, effort required to maintain focus.

$6-9\ G_x$: Increased chest pain and pressure; breathing difficult, with shallow respiration from position of nearly full inspiration; further reduction in peripheral vision, increased blurring, occasional tunneling, great concentration to maintain focus; occasional lacrimation; body, legs, and arms cannot be lifted at 8 G_x; head cannot be lifted at 9 G_x.

$9-12\ G_x$: Breathing difficulty severe; increased chest pain; marked fatigue; loss of peripheral vision, diminution of central acuity, lacrimation.

$15\ G_x$: Extreme difficulty in breathing and speaking; severe vise-like chest pain; loss of tactile sensation; recurrent complete loss of vision.

Backward Acceleration Effects ($-G_x$)

Similar to those of $+G_x$ acceleration with modifications produced by reversal of force vector. Chest pressure reversed, hence breathing easier; pain and discomfort from outward pressure toward restraint harness manifest at about $-8\ G_x$; with forward head tilt cerebral hemodynamic effects manifest akin to $-G_z$; distortion of vision at -6 to $-8\ G_x$; feeling of insecurity from pressure against restraint.

Lateral Acceleration Effects ($\pm G_y$)

(Little Information Available)

$3\ G_y$: Discomfort after 10 seconds; pressure on restraint system, feeling of supporting entire weight on clavicle; inertial movement of hips and legs, yawing and rotation of head toward shoulder; petechiae and bruising; engorgement of dependent elbow with pain.

$5\ G_y$ (14.5 sec): External hemorrhage, severe postrun headache.

Table 4-1 shows the most common symptoms which occurred during $+G_z$ and $+G_x$ acceleration on the centrifuge of the U. S. Naval Air Development Center, Johnsville, Pennsylvania, during the period 1961 through 1965.

Table 4–1
Human Response to $+G_z$ and $+G_x$ Accelerations on a Centrifuge

Vector	Symptom	Instances	Runs
$+G_z$	Grayout	351	2380
	Blackout	167	2380
	Motion sickness	40	2380
$+G_x$	Chest pain	104	2557
	Motion sickness	97	2557
	Dyspnea	29	2557
	Arrhythmia	29	2557
Miscellaneous	Abdominal pain		17 cases
	Headaches		15
	Syncope		15
	Limb myalgia		12
	Paresthesia		7

(York et al., 1968)

Physiological Effects of Sustained Acceleration

The fundamental stimulus influencing the physiological effects of sustained acceleration arises from the effective increase in weight of the body, and particularly its fluid components, along the acceleration vector. This is illustrated in figure 4-1. The center sketch of the figure, illustrating the vascular effects at +1 G_z, indicates that with a mean arterial pressure of 120 mm Hg, the mean pressures at head and foot levels are calculated to be 96 and 170 mm Hg, respectively. At +5 G_z, while maintaining mean arterial pressure at heart level of 120 mm Hg, the theoretical pressure at the base of the brain will be zero, while at the feet it will be 370 mm Hg. Under these circumstances, the subject would be unconscious, and an additional venous pressure of 250 mm Hg would be required to return blood from feet to heart. In fact, unconsciousness does not necessarily occur at +5 G_z because of physiological compensatory adjustments.

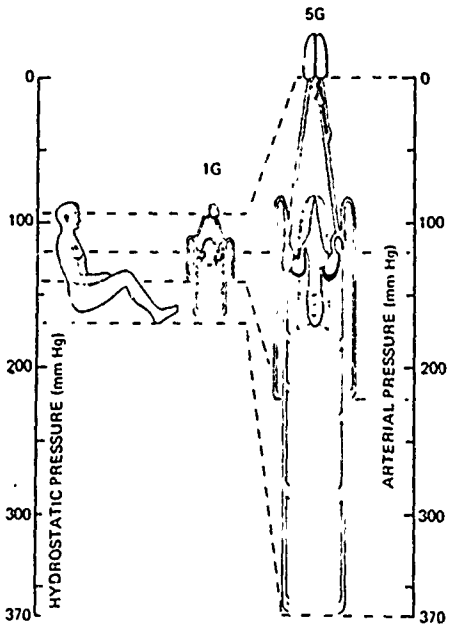
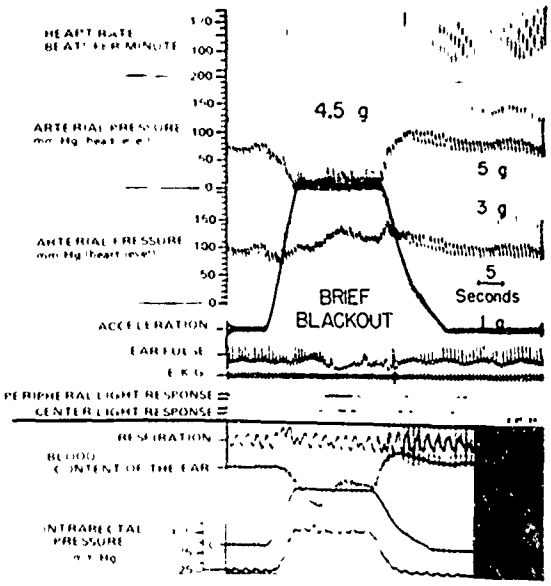


Figure 4–1. Hydrostatic pressures in vascular system of a man in upright sitting position at 1 G and during headward acceleration at 5 G. (After Wood et al., 1963)

During +G_z acceleration with rates of onset from 1 to 2 G/sec, and of magnitude sufficient to produce loss of vision, there is an immediate decrease in blood pressure at head level, an increase in heart rate, a decrease in blood volume at the ear, and a decrease in the amplitude of the arterial pulse at ear level (Lindberg & Wood, 1963). Recovery of blood pressure and ear pulse begins before the acceleration episode is complete, indicating compensatory physiological adjustments. The fall in blood pressure at head level is proportional to the magnitude of the acceleration. Blood pressure at heart level, however, is maintained near normal and in fact may actually increase during exposures to the level of +5 G_z. These effects are illustrated in figure 4-2. Some of the general cardiovascular responses are tabulated in table 4-2.



Reproduced from best available copy.

Figure 4–2. Sequence of physiological events during exposure of normal subject to positive acceleration at +4.5 G_z for 15 sec. Note initial period of progressive failure: there are, in order of occurrence, decrease in blood pressure at head level, increase in heart rate, loss of blood volume in the ear, and failure of peripheral vision. This is followed by a period of compensation despite continuance of exposure. (After Lindberg & Wood, 1963; reprinted by permission of Academic Press, Inc. Copyright 1963 by Academic Press, Inc.)

Table 4–2

Cardiovascular Responses to +G_z Acceleration

CV Response	Percentage Increase (+) or Decrease (–)		
	+2 G_z	+3 G_z	+4 G_z
Cardiac output	– 7	–18	–22
Stroke volume	–24	–37	–49
Heart rate	+14	+35	+56
Mean aortic pressure	+ 9	+21	+27
Systemic vascular resistance	+17	+41	+59

(Wood et al., 1961)

In the -G_z vector, the direction of the increased hydrostatic pressure is reversed. With the onset of acceleration, the arterial and venous pressure rise some 70 to 90 mm Hg as measured in the carotid artery and jugular vein (Gamble et al., 1949).

Gauer and Henry (1964), describing work carried out between 1947 and 1949, showed that the venous pressure developed under $-G_z$ acceleration, as measured in the supraorbital vein, depended on the degree of tilt of the head because of the geometrical relations of the vertical axes of the head and the eyes. Figure 4-3 illustrates the resulting effects at -2 G_z during rotation from the full prone to the full supine position.

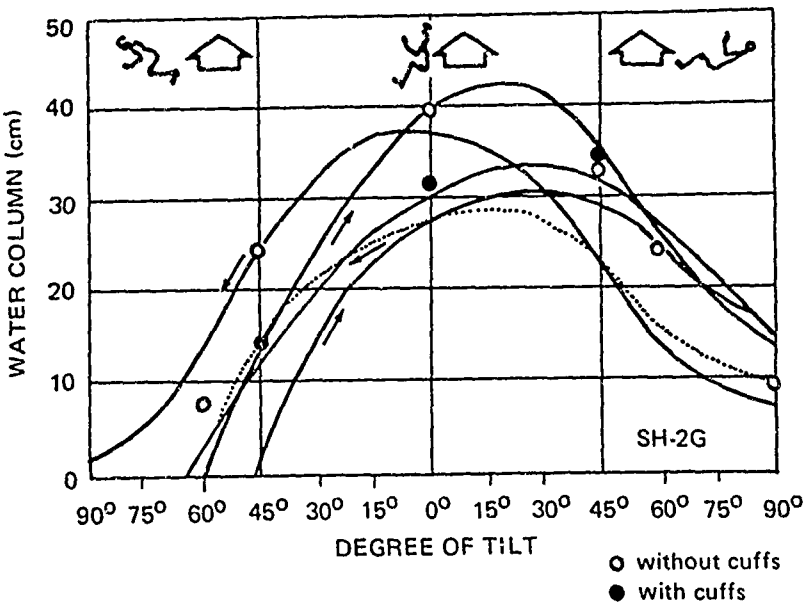


Figure 4–3. Venous pressures during exposure to $-G_z$ acceleration in different positions of body tilt. Light line and O = data obtained normally; heavy line = theoretically calculated pressures; broken lines = pressures obtained when rotating subject with tourniquets about legs to prevent reflux of blood. Venous pressure was measured in forehead vein. (After Gauer & Henry, 1964)

Change in heart rate has been inconsistent in different studies. Brow. e and Fitzsimmons (1957), in an ECG study of 53 subjects with 366 exposures in the range of +3 to +5 G_z for 15 seconds duration, found a progressive increase in pulse rate with increase in acceleration level.

Electrocardiographic changes under sustained acceleration are largely nonspecific and chiefly manifest as alterations in the electrical axis, along with some S-T segment and T-wave changes. Arrhythmias are not uncommon and occur under all vectors.

Retinal and Visual Response

Vision is markedly affected by alteration in hydrostatic pressure. The symptoms, namely, grayout or loss of peripheral vision and blackout or total loss

of vision, manifest themselves at levels below those producing unconsciousness, since intraocular pressure is some 20 mm Hg higher than intracerebral pressure. Consequently, blood supply to the retina fails before failure of cerebral circulation (Andina, 1937).

Visual effects occur in all vectors but, because of the vertical position, are more common in the G_z vectors. Because of the forward position of the eye with respect to the midline, the force experienced at the eye is not the same as that applied to the midline.

Duane (1954) obtained illustrations of the retina during $+G_z$ accelerations to blackout level. A correlation between visual change and change in the fundus oculi was established, as indicated in table 4-3.

Table 4–3

Correlation Between Changes in Vision and Fundus Oculi Changes

Stage	Subjective Response	Objective Response
I	Loss of peripheral vision	Arteriolar pulsation — i.e., recurrent exsanguination
II	Blackout	Arteriolar exsanguination and collapse
III	Return of central peripheral vision	Return of arteriolar pulsation and temporary venous distension

(Duane, 1954)

Newsom and his colleagues (1968) conducted retinal photography and fluorescence angiography during 10-second plateaus of blackout from $+G_z$ acceleration in human subjects. Some of the findings are shown in figure 4-4.

On exposure to $-G_z$ acceleration, local hydrostatic pressure is increased at the eyeball and gives rise to pain and a feeling of fullness. The occurrence of "red-out," or reddening of the visual fields has been reported experimentally in centrifuge work (Ryan et al., 1950), but it is doubtful if it occurs consistently or operationally. It has been suggested that red-out is a distortion of vision caused by obstruction from the conjunctiva of the lower lid.

Visual Thresholds. The general range of visual threshold in relation to unconsciousness is shown in table 4-4. There would appear to be a change in the absolute threshold of vision under acceleration, that is, the minimum light intensity at which a stimulus can be perceived. White (1960) showed that for a given stimulus intensity to be perceived as of equal intensity with a probability of 50 percent under increased acceleration, the actual intensity had to be increased according to the ratios shown in table 4-5. Foveal and peripheral thresholds as a function of acceleration are illustrated in figures 4-5 and 4-6.

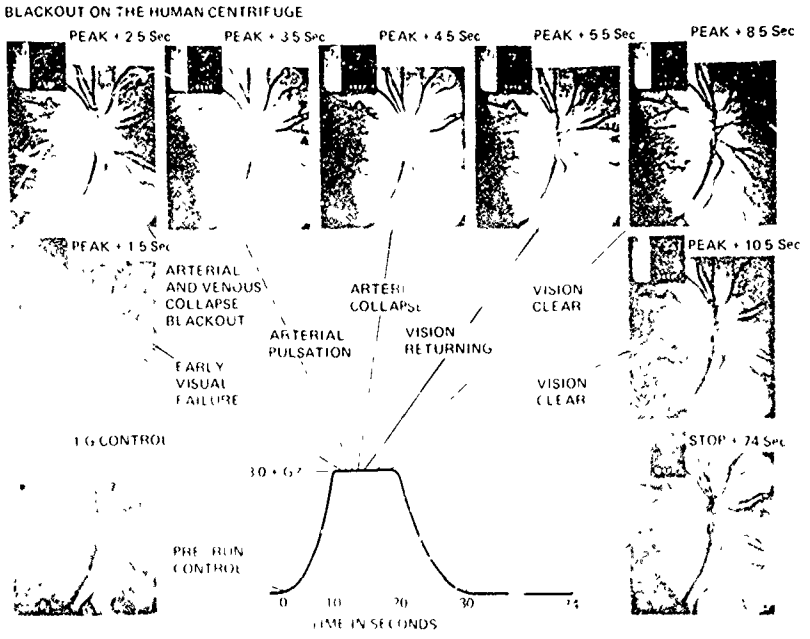


Figure 4–4. Serial photographs of fundus of right eye in a human subject during blackout. Read from left, up, right, and down. (After Leverett, 1968, from work of Newson et al., 1968)

Reproduced from best available copy.

Table 4–4

Range of Visual Thresholds in Relation to Unconsciousness

Criterion	Mean Threshold (G)	Standard Deviation (G)	Range (G)
Loss of peripheral vision	4.1	±0.7	2.2 – 7.1
Blackout	4.7	±0.8	2.7 – 7.8
Unconsciousness	5.4	±0.9	3.0 – 8.4

(After Cochran et al., 1954)

The effect of acceleration on brightness discrimination is shown in figure 4-7. The minimal detectable difference in intensity between a test patch and its lighted surround has long served as a test of visual sensitivity. The threshold difference has been found to be a function of basic energy level as well as contrast between the patch and its reference illumination. Thus, the greater the background intensity, the smaller the ratio between the patch and the background required for detection. The data compiled in the graphs in figure 4-7 illustrate an interaction between acceleration and the minimal discernible differential intensity (ΔI). The stimulus display used to collect the

data consisted of a background subtending 8°4′ visual angle positioned 28 inches from the eye and viewed monocularly through a circular aperture 17.5 inches from the eye. The test patch, projected upon the background, subtended a 1°28′ visual angle (Braunstein & White, 1962).

Table 4–5

Increase in Visual Stimulus Intensity* Required to Perceive a Stimulus as Equalling that at +1 G_z (P = 50%)

Acceleration (+G_z)	Required Increase in Stimulus Intensity	
	Fovea	Periphery
1	1	1
2	–	1.5
3	2	3
4	3,4	4

*Expressed as a ratio of that at +1 G_z.

(Data of White, 1960)

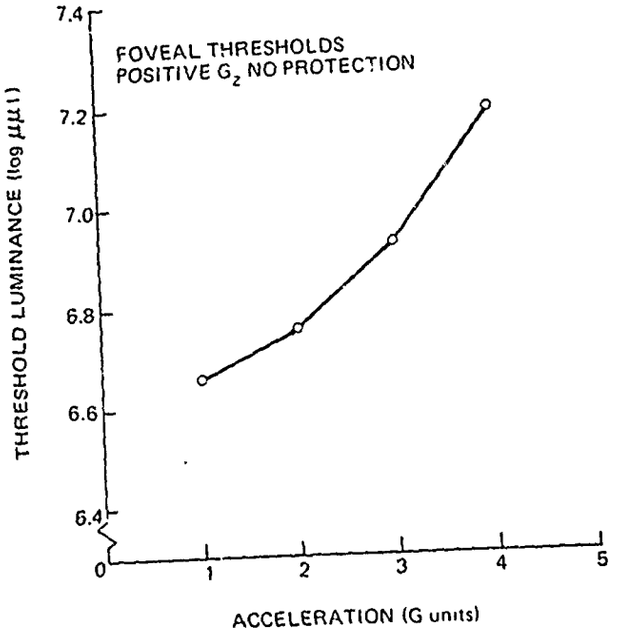


Figure 4–5. Threshold of foveal vision under +1 to +4G_z acceleration. (After White, 1960)

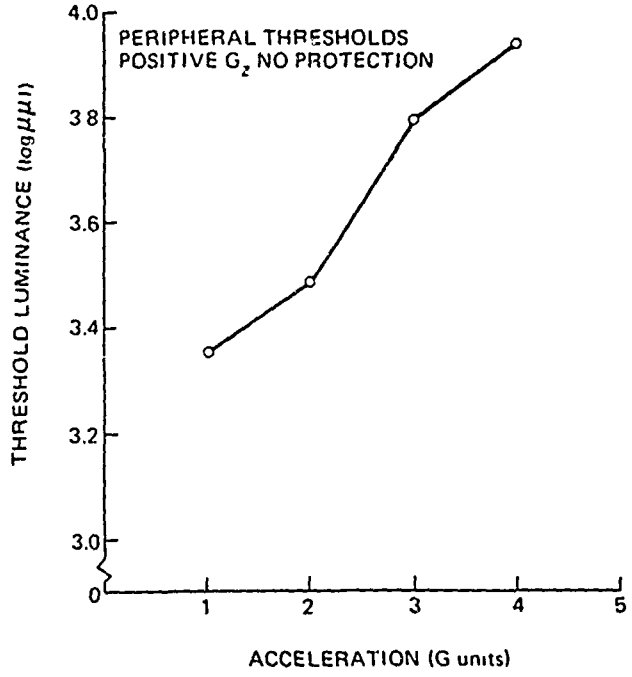


Figure 4–6. Threshold of peripheral vision under +1 to +4 G acceleration. (After White, 1960)

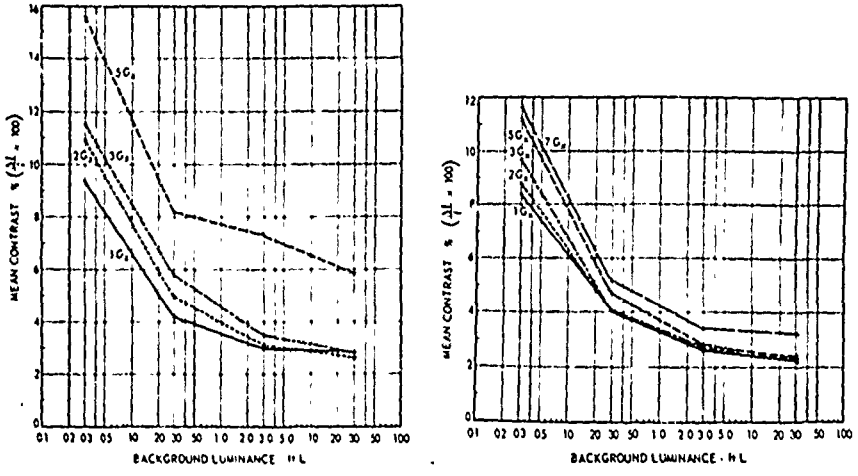


Figure 4–7. Relationship between brightness discrimination and background luminance under four levels of posttive ($+G_z$) (top) and five levels of transverse ($+G_x$) (bottom) acceleration. (After Braunstein & White, 1962)

The effects of oxygen on brightness discrimination are illustrated in figure 4-8, from work by Chambers and Kerr (1962).

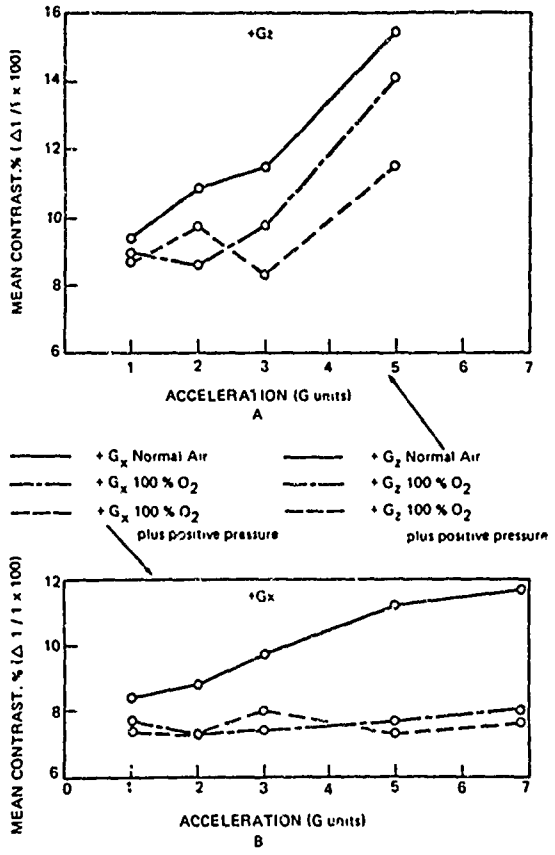
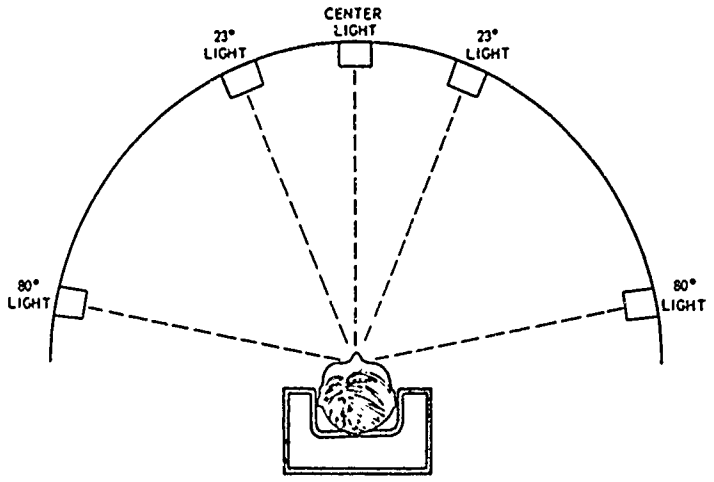


Figure 4–8. Brightness discrimination with different breathing gasses at different acceleration levels. (After Chambers & Kerr, 1962)

Visual Distortion. In the $-G_x$ vector, distortion becomes marked at -6 to -8 G_x. Smedal and his colleagues (1963) showed that this was not due to corneal distortion in the bulging eye but was associated with intermittent watering occurring at about the -6 G_x level.

Visual Fields. Limitation in the visual field under acceleration exposure is, of course, related to the occurrence of grayout. At about [illegible] the field is narrowed to an arc of less than 46°. Figure 4-9 indicates the effect of the retinal position of a signal on the acceleration response. In the study which the figure illustrates, 115 subjects were exposed to $+G_z$ acceleration with a light array above. Almost invariably, subjects lost the 80° light before loss of the 23° light. In 30 subjects, the 80° light loss occurred at a mean of 4.2 G_z, standard deviation ±0.7 G. In the same subjects, the 23° light loss occurred at a mean of 4.5 G_z, standard deviation ±0.8 G. Central light loss occurred at 5.3 G_z, standard deviation ±0.8 G.



Comparison of 80° Light Loss, 23° Light Loss, and 0° Light Loss

	Symptoms			
	Clear	80° LL	23° LL	CLL
Mean (G_z level)	3.8	4.2	4.5	5.3
Range (G_z level)	2.3 – 5.1	2.7 – 5.7	2.9 – 6.4	3.6 – 7.0
Standard deviation	0.7	0.7	0.8	0.8
Duration of symptom-mean (sec)		5.4	5.1	6.8
Duration of symptom-range (sec)		1.9 – 17.0	1.9 – 11.9	2.1 – 23.4

Figure 4–9. Effect of retinal position of a signal on the perception of light signals under acceleration. (From Zariello et al., 1958)

Pupillary Reactions. Pupillary dilation begins with loss of peripheral vision (Beckman et al., 1961). Accommodation is unaffected by acceleration (Smedal et al., 1963).

Unconsciousness and Cerebral Function

Loss of consciousness and complete impairment of cerebral function occur between +3 G_z and +8 G_z, the specific level depending chiefly on biological factors and duration and rate of onset. Figures 4-10 and 4-11 indicate the range of responses found. In the other vectors, the subject normally reaches a tolerance threshold of another sort before unconsciousness occurs. On return to consciousness, there is usually a short (5 to 15 second) period of confusion (Franks et al., 1945).

Convulsions with characteristic EEG changes are a common accompaniment of unconsciousness, having been found in 52 percent of 230 subjects (Franks et al., 1945). Sem-Jacobsen (1959, 1960) has recorded and photographed them in pilots in flight. Brent and coworkers (1960) have found that certain combinations of hyperventilation, hypoglycemia, and +G_z acceleration will produce convulsions in all subjects.

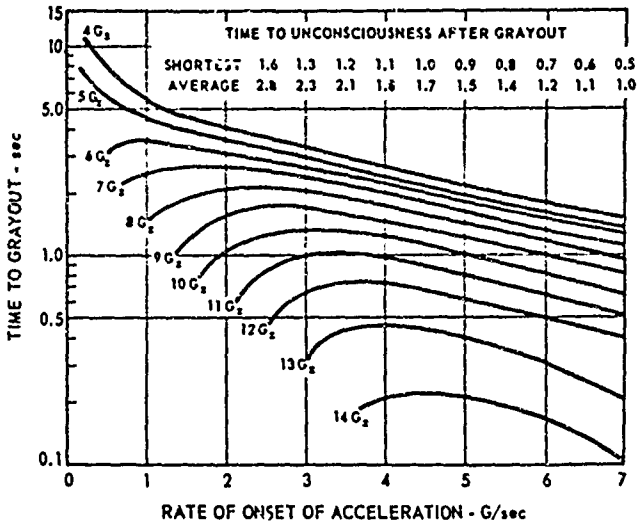


Figure 4–10. Time to unconsciousness as a function of rate of onset of positive acceleration (G_Z). (After Stoll, 1956)

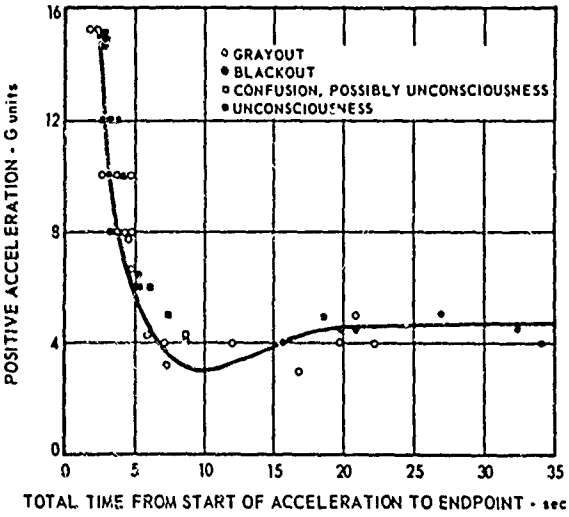


Figure 4–11. Time to unconsciousness as a function of varying rates of positive acceleration (G_Z) onset, G amplitudes, and exposure times. (After Stoll, 1956)

Pulmonary Response

A naturally occurring pressure gradient exists even at 1 G between the apex and the base of the lung in the vertical subject and between the front and the back of the lung in the supine subject (Glaister, 1967; Wood, 1967; Rutishauser et al., 1967, and others). With increase in acceleration, there is an increase in perfusion of the pulmonary vessels in the dependent portions of the lung and a

decrease in the upper zone (Bryan & MacNamara, 1964, and other workers). Figure 4-12 shows the relationships at +3 G_z, while figure 4-13 shows the relationships at 0, +1, and +3 G_x. Individual relationships are shown in figure 4-14.

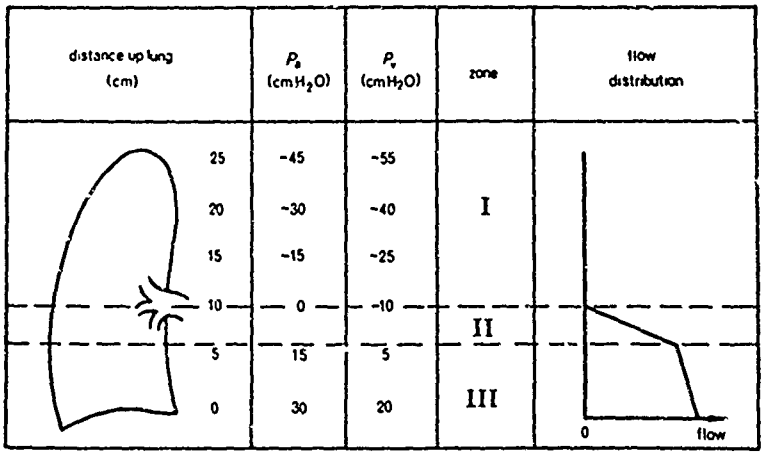


Figure 4–12. Theoretical pressure-flow relationships in vertical lung at +3 G_z; P_a, mean pulmonary arterial pressure; P_v mean pulmonary venous pressure. Hydrostatic indifference plane is taken to be 5 cm below the lung hilum; arteriovenous pressure difference is assumed to remain constant at 10 cm water. (After Glaister, 1967; reprinted by permission of the Controller of Her Britannic Majesty's Stationery Office)

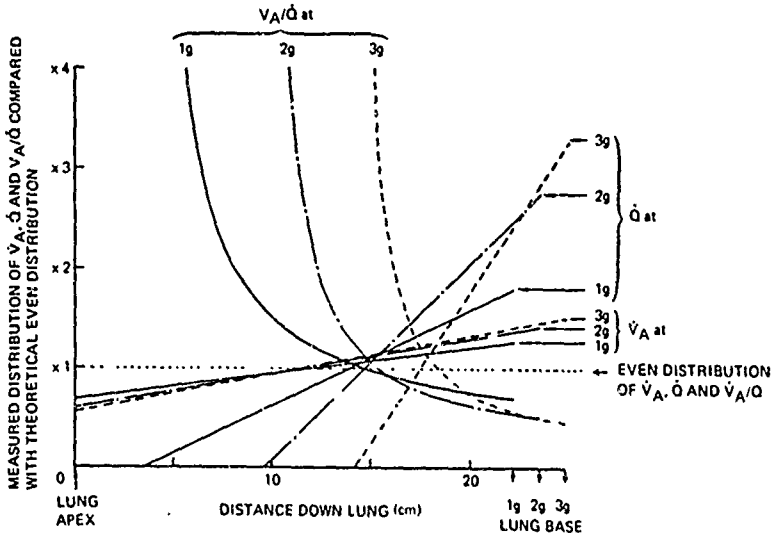


Figure 4–13. Distributions of ventilation ($\dot{V}_A$), perfusion ($\dot{Q}$), and ventilation/perfusion ratio ($\dot{V}_A/\dot{Q}$) down the lung at positive accelerations of +1, +2, and +3 G_z, averaged from four subjects. Mean position of diaphragm at each level of acceleration is also indicated. (After Glaister, 1967; reprinted by permission of the Controller of Her Britannic Majesty's Stationery Office)

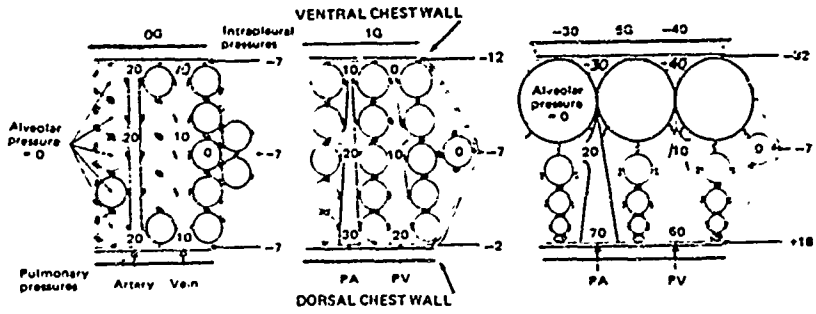


Figure 4–14. Effects of forward ($+G_x$) acceleration on intrathoracic pressures (dorsal-ventral dimension of lung is 20 cm). Numerals indicate pressures as cm H_2O, and zero reference level is atmospheric pressure at midthoracic coronal plane. (After Wood et al., 1963)

Lung Volumes and Mechanics of Breathing. Respiratory rate increases almost linearly with acceleration. Minute volume increases initially, but levels off at about +8 G_x, when acceleration is applied in that vector. Tidal volume, although increasing initially up to about +5 G_z, or +8 G_x, decreases with still greater acceleration. Positive pressure breathing (30 cm H_2O) diminishes the changes in lung volumes resulting from acceleration, and, in particular, allows a relative increase in ventilation of the lower lung. This effect, however, is abolished by the increase in abdominal pressure induced by wearing an inflated G-suit (Glaister, 1965), as shown in table 4-6. Glaister (1961) also showed that there was no change in lung stiffness or air resistance, at least up to +3 G_z. This was confirmed up to +4 G_x by Watson and his colleagues (1960), who further demonstrated an increase in the resting relaxation pressure amounting to 5 mm Hg/G as illustrated in figure 4-15.

The oxygen cost of acceleration in the G_x vector was examined by Zechman and coworkers (1960) and by Glaister (1963). These investigators confirmed, with experiments at +2 to +3 G_z for 1/2 to 5 minutes, that at the lower levels of acceleration oxygen uptake does not increase during the exposure, and may even fall, although an oxygen debt is built up. This debt is, however, repaid on return to 1 G. These findings are summarized in table 4-7 and figure 4-16.

Arterial Oxygen Saturation. The effect of the changed ventilation/perfusion relationships is to produce a progressive decrease in arterial oxygenation with increase in acceleration. Figure 4-17, from the work of Wood et al. (1963), shows the average and range of changes in arterial oxygen saturation in four healthy men exposed to $+G_z$ acceleration, as indicated, breathing air.

Alexander and his colleagues (1965) measured arterial oxygen saturation in a group of 25 pilots breathing air while exposed to $+G_x$ accelerations representative of Apollo operations. The results are illustrated in figure 4-18.

Table 4–6

Effect of Positive-Pressure Breathing (PPB) on Mean Lung Volumes During Increasing Forward Acceleration*

Accel.** (G)	With PPB (mm Hg)	Vital Capacity		Tidal Volume		Inspiratory Reserve		Expiratory Reserve	
		cc	% of 1 G Value	cc	% of 1 G Value	cc	% of 1 G Value	cc	% of 1 G Value
1	0	3875 ±343	—	781 ±107	—	2333 ±171	—	761 ±135	—
4	12	3642 ±535	94	485 ± 56	62	2089 ±343	90	1180 ±121	155
6	16	3121 ±565	81	435 ± 45	56	1681 ±397	72	1005 ±146	132
8	20	2391 ±715	62	510 ±122	65	947 ±407	41	938 ±271	123

*Each figure is the mean for four or five subjects.

**Studies done with an A–13A mask and 12 degree back angle.

(After Watson et al., 1960)

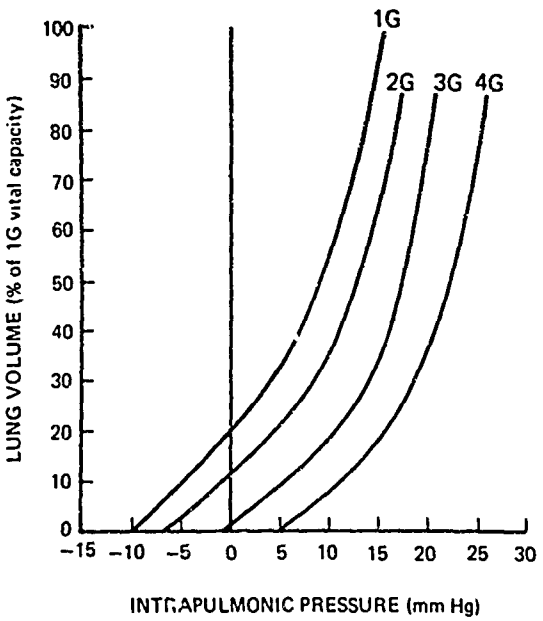


Figure 4–15. Static relaxation pressure-volume curves during control ($+G_x$) and +2, +3, and +4 G_x acceleration. All lung volumes were obtained at 1 G. (After Watson et al., 1960)

Figure 4-19 illustrates a similar experiment with subjects breathing 100 percent oxygen at 5 psi. It will be noted the rate of desaturation is slower and the rate of recovery is even more so.

Arterial desaturation is also evident on exposure to acceleration in the $-G_x$ vector, although the severity is perhaps not so great. Figure 4-20, from the work of Smedal et al. (1963), indicates the results.

In the $+G_z$ vector, the effects of arterial desaturation are overshadowed by other more dramatic responses, but Barr (1962) demonstrated its occurrence and further showed that the rate and degree of desaturation were increased by repeated exposures. Arterial desaturation has also been observed with acceleration in the $-G_z$ vector (Gauer & Henry, 1964).

The "altitude equivalent," representing the extent of hypoxia commensurate with the intensity of $+G_x$ accelerations, is shown in figure 4-21.

Renal Output

Reduction of urine secretion under applied $+G_z$ acceleration, followed by an increased outflow on cessation of acceleration has been demonstrated in human subjects by Stauffer and Errobo-Knudsen (1953), with results shown in figure 4-22.

Table 4–7

Additional Oxygen Consumption (cc/min SPTD) Required During 1 Min Forward ($+G_x$) Acceleration

Subject	+5 G_x		+8 G_x		+10 G_x		+12 G_x	
	Control	Extra	Control	Extra	Control	Extra	Control	Extra
A	324	0	312	174	293	266	330	461
B	311	0			286	594		
C			286	459				
D	271	0			312	124	294	368
E							294	1321
F			352	270	293	569		
G	288	0	311	18				
H	238	55	253	208	239	293		
I			226	0	221	18		
J	292	220						
Mean ±SD	287 ±32	46 ±78	290 ±45	188 ±170	274 ±34	310 ±228	306	716

(After Zechman et al., 1960)

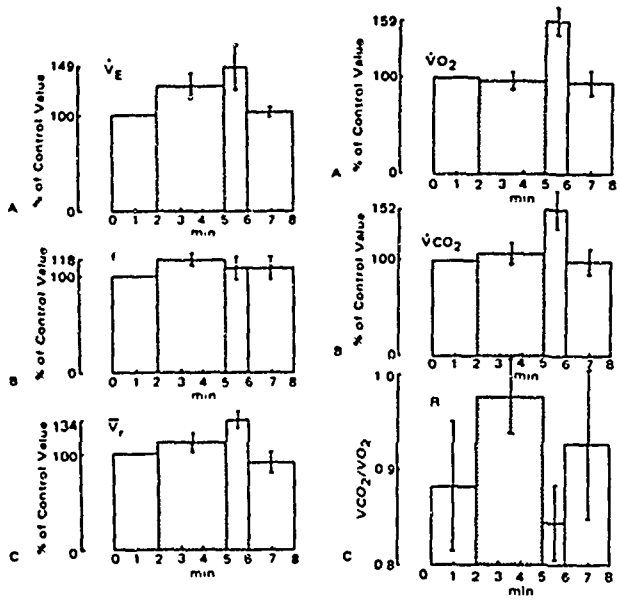


Figure 4–16. Effect of positive acceleration at +3 G_z for 3 min on pulmonary ventilation ($\dot{V}_E$), respiratory rate (f), and tidal volume ($\bar{V}_T$), at left; on O_2 uptake ($\dot{V}_{O_2}$), CO_2 excretion ($\dot{V}_{CO_2}$), and respiratory gas exchange ratio (R), at right. Period of acceleration is shaded. Horizontal lines give mean values for seven runs on five subjects, barred vertical lines indicate ±SD deviation of mean. (After Glaister, 1963; reprinted by permission of the Controller of Her Britannic Majesty's Stationery Office)

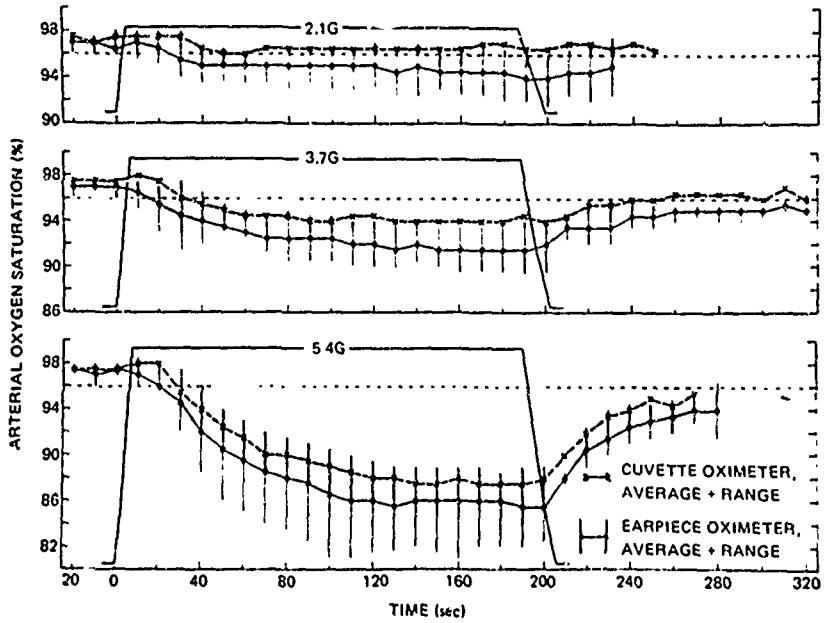


Figure 4–17. Average and range of changes in arterial O_2 saturation of four healthy men, recorded by cuvette and ear oximeters during 3 min at +2.1, +3.7 and +5.4 G_z. (After Wood et al., 1963)

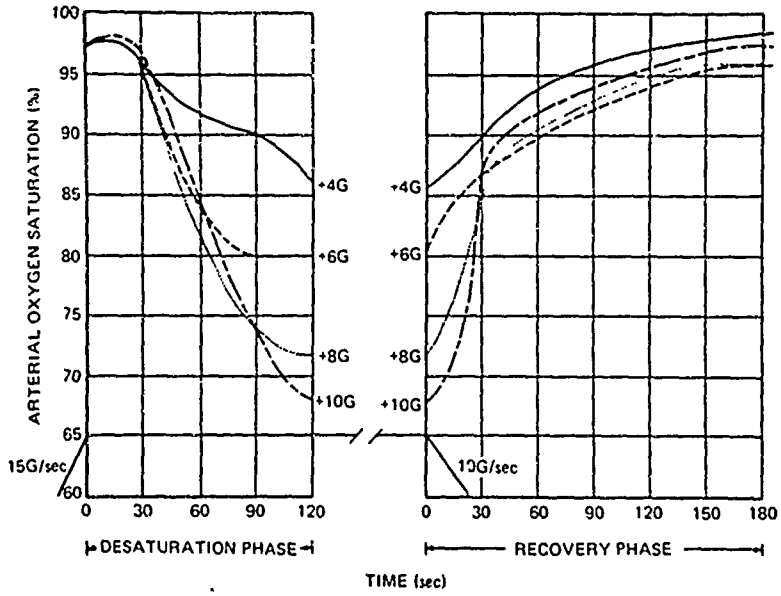


Figure 4–18. Means of arterial saturations in 25 subjects exposed to $+G_X$ acceleration breathing air at 14.7 psia. ΔV = 37 000 fps. (After Alexander et al., 1965)

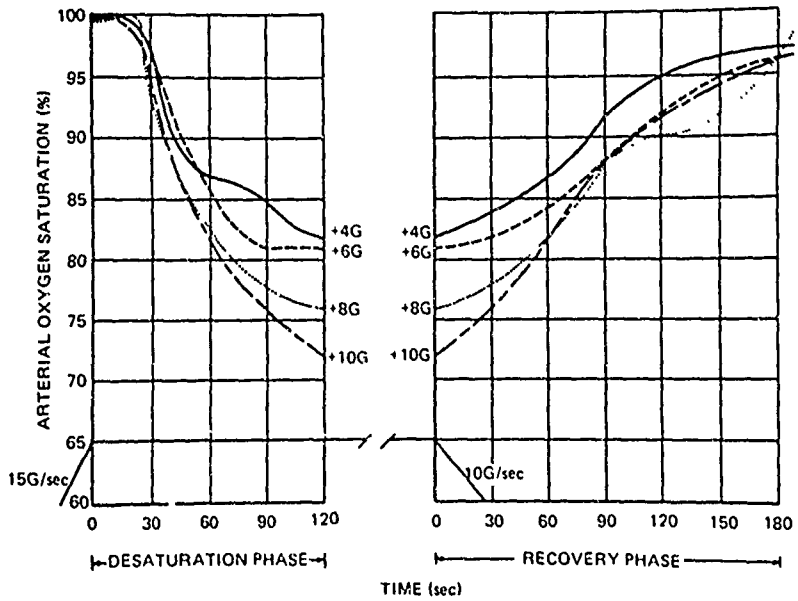


Figure 4–19. Means of arterial saturations in 25 subjects exposed to $+G_X$ acceleration breathing 100% O_2 at 5 psia. ΔW = 37 000 fps. (After Alexander et al., 1965)

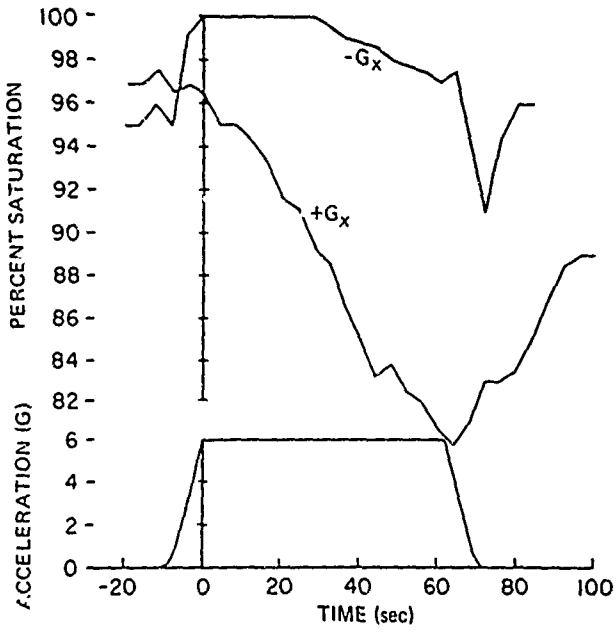


Figure 4–20. Comparison of $-G_x$ and $+G_x$ acceleration exposure on arterial saturation. (After Smedal et al., 1963)

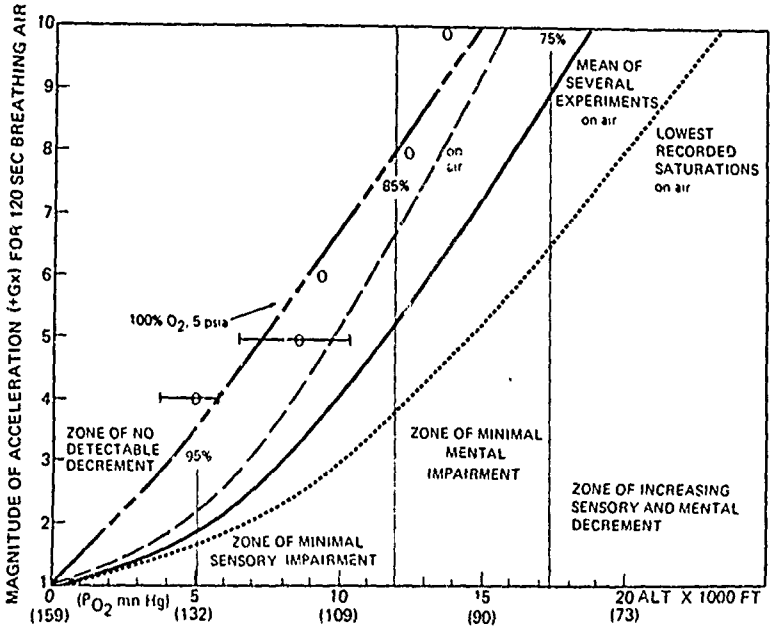


Figure 4–21. Impairment of performance predicted for different $+G_x$ levels breathing air and oxygen at 5 psia, equated to performance at different altitudes. (After Teichner & Craig, 1966; data from many sources)

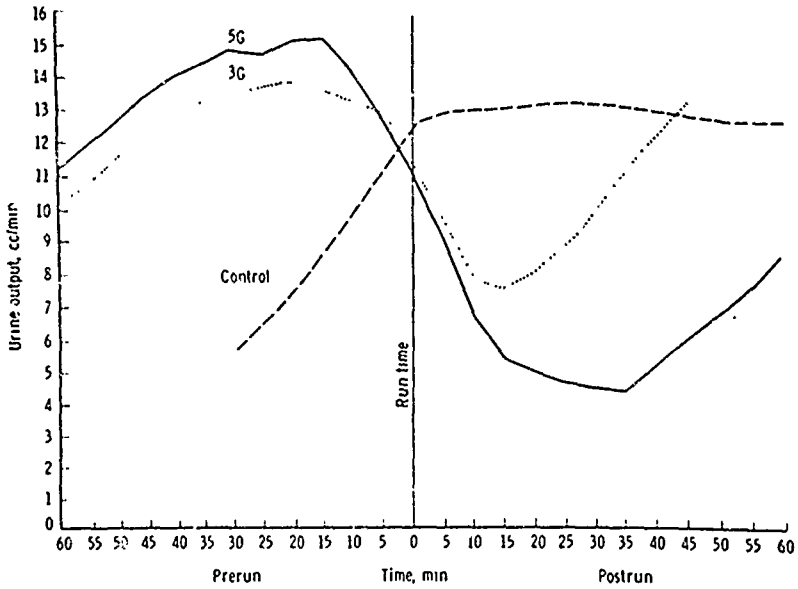


Figure 4–22. Urine output before and after acceleration.
(After Stauffer & Errobo-Knudsen, 1953)

The underlying mechanism has been postulated as involving an increase in secretion of antidiuretic hormone (ADH) as a result of stimulation of fluid volume receptors, or from change in glomerular filtration rate arising from hemodynamic effects on the renal artery. Increase in ADH levels has been noted in human subjects at +2 G_z acceleration for 30 minutes (Rogge et al., 1967).

Mechanical Impedance and Natural Frequency

The fundamental resonant frequency of the human body sitting erect under normal gravitational conditions is approximately 5 Hz (Coermann, 1963). A sustained +G_z acceleration stiffens the seated human body in the direction of the spine and increases the fundamental natural frequency to 7 Hz at +2 G_z and 8 Hz at +3 G_z. During +3 G_z acceleration, at vibrational frequencies up to about 5 Hz, the body tends to respond as though it were a pure mass. The transmission factor decreases under +G_z acceleration, especially at the 5 Hz resonance, but increases considerably above 6 Hz. The damping coefficient of the erect sitting human remains unchanged at about 0.575 during +G_z acceleration. Some of the foregoing factors are illustrated in figure 4-23 from the work of Vogt et al., 1968.

Tolerance to Sustained Acceleration

Tolerance may be defined as the limit of man's capacity to endure the physical and emotional discomfort of a stressful environment. The limit may be difficult to define with certainty, and, in fact, may commonly be an arbitrary cutoff point imposed from without, rather than a subjective endurance

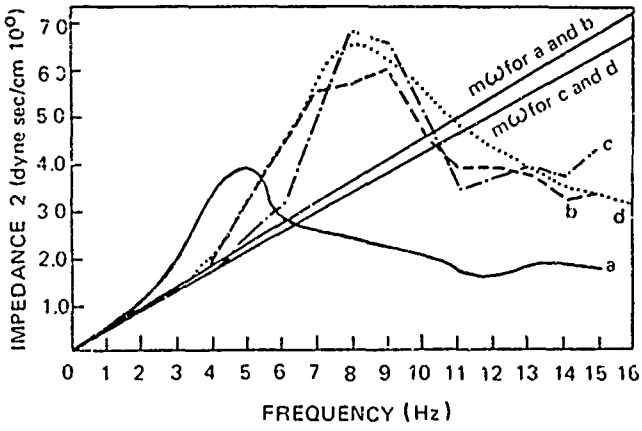


Figure 4-23. Mechanical impedance of sitting human body, under (a) normal gravity, (b) +2 G_z, (c) +3 G_z, and compared with (d) mechanical impedance of simple mass-spring-damper system with f_o = 8 Hz, m = 65 000 dyne sec^2/cm, and δ = 0.575. (After Vogt et al., 1968)

threshold. In $+G_z$ acceleration, the occurrence of grayout, blackout, or unconsciousness can be used as a standard. In $\pm G_x$ acceleration, dyspnea, pain, and discomfort tend to be self-limiting features not amenable to quantification.

Human Acceleration Experience

Figure 4-24 is a compilation by Fraser (1966) from numerous sources, of various human experiences in sustained acceleration. The curves are an estimation of the maximum voluntary tolerance of healthy, well-motivated men but must be considered maximum levels and not operational levels. Higher levels than those indicated in figure 4-24 have been tolerated but not in the form of an acceleration plateau, for example, +20 G_x for a few seconds in the form of a haversine peak (Collins et al., 1958) and +25 G_x for several seconds (Collins & Gray, 1959).

Figure 4-25 compares average G tolerance for several axes (Chambers, 1963).

As contrasted with the average tolerance illustrated in the previous two figures, figure 4-26 demonstrates the upper limits of voluntary tolerance of a group of highly motivated test pilots, preconditioned to the effects of acceleration and suitably restrained.

Rate of Onset

Figure 4-27 illustrates the effect of different rates of onset on the response of 15 subjects to $+G_z$ acceleration (Stoll, 1956). From these data, a monogram was developed (figure 4-28) which, although empirical, indicates the expected duration before grayout at a given plateau and rate of onset.

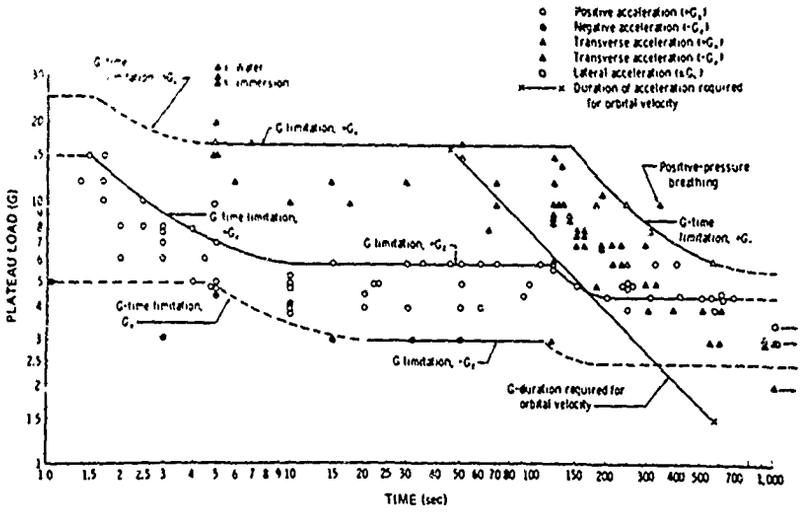


Figure 4–24. Human experience of sustained acceleration. Each datum point represents a plateau of acceleration, not an incidental peak. Curves estimate maximum voluntary tolerance in $+G_Z$, $-G_Z$ and $+G_X$ vectors using restraint harness, couches, or anti-G suits where applicable. Dotted lines are extrapolations on basis of other evidence. (After Fraser, 1966; data from many sources)

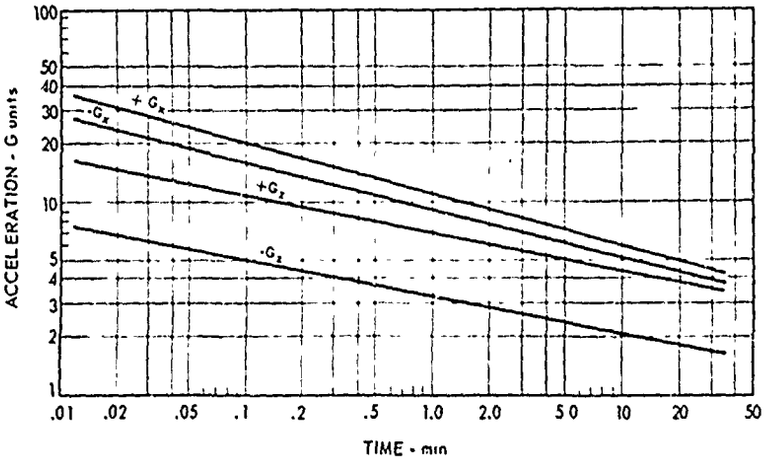


Figure 4–25. Comparison of average G tolerance in four vectors of sustained acceleration. (After Chambers, 1963)

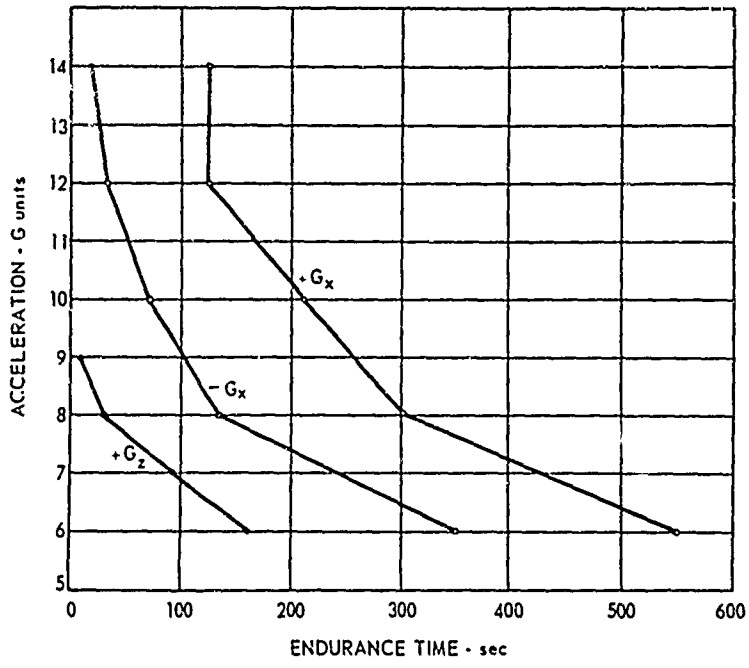


Figure 4–26. Voluntary endurance of acceleration by highly motivated test pilots. (After Chambers & Hitchcock, 1963)

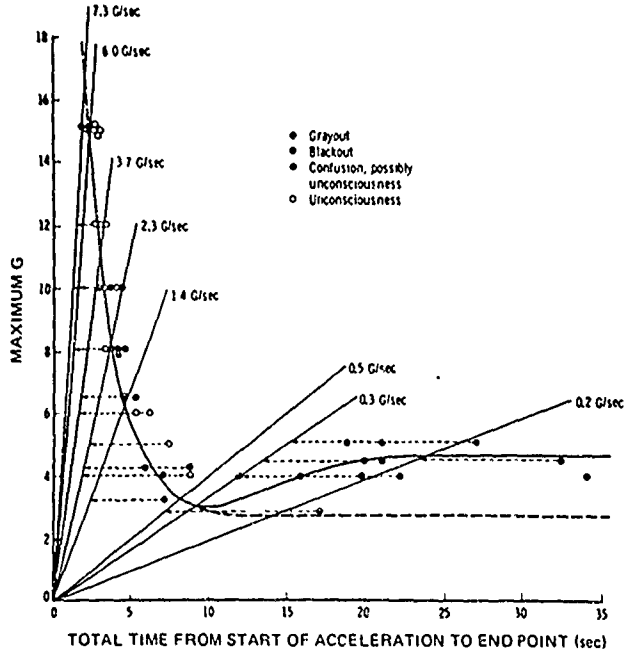


Figure 4–27. Effect of rate of onset of acceleration on G tolerance. (After Stoll, 1956)

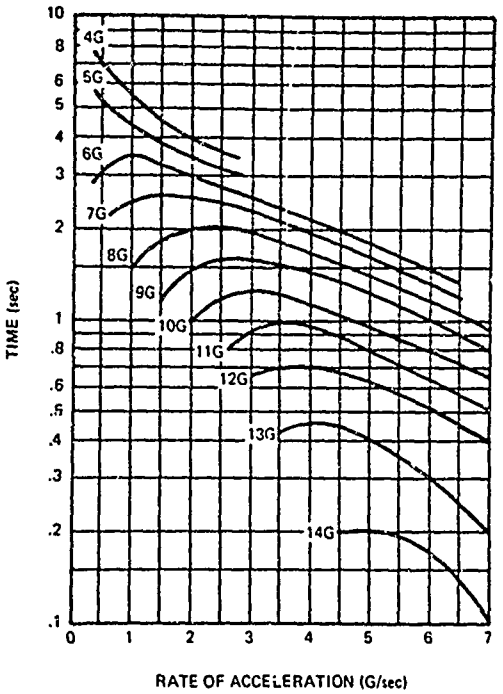


Figure 4–28. Monogram relating rate of onset of acceleration to time to grayout. (After Stoll, 1956)

Posture and Position

Figure 4-29 (Bondurant et al., 1958a) illustrates the effect on tolerance of various positions in the $+G_x$ vector, while figure 4-30 specifies the advantages and disadvantages of a variety of positions. The ideal position for forward ($+G_x$) acceleration is considered to be in a seated posture, forward facing, with the trunk inclined forward 20° from the vertical, hips flexed to bring the knees to eye level, and lower legs extended (position B, figure 4-30).

Very Prolonged Acceleration

Exposure to levels of $+3\ G_x$ and $+4\ G_x$ has been withstood for durations up to 1 hour (Bondurant et al., 1958a; Miller et al., 1959) but there are few instances on record. Clark (1960) describes a 24-hour exposure to $+2\ G_x$ in a reclining seat. It was characterized by rotational illusions and discomfort. Ross and his colleagues (1963) report a study of 4 hours' duration.

Restraint and Protection

Standard aircraft harnesses provide no protection against sustained acceleration except to maintain the subject in general position. The development and usefulness of anti-G devices and clothing is summarized in table 4-8 from the work of Nicholson and Franks (1966).

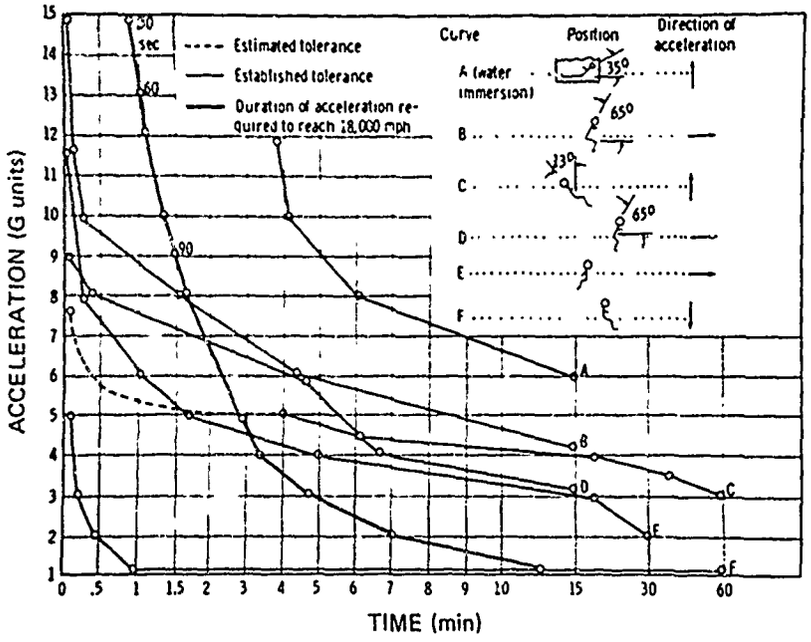


Figure 4–29. Effect of body position and posture on tolerance to acceleration. (After Bondurant et al., 1958a)

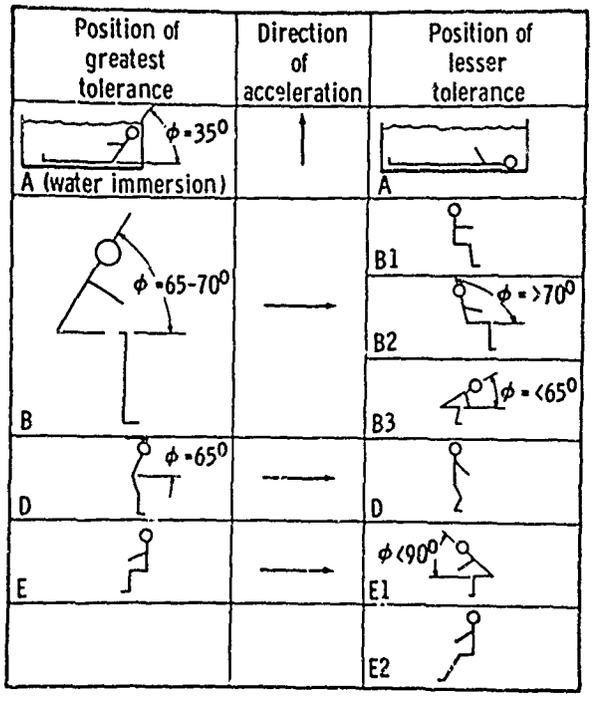


Figure 4–30. Variations in position which influence tolerance to acceleration. (After Bondurant et al., 1958a)

Table 4–8

Devices for Protection Against Positive ($+G_z$) Acceleration

Anti–G Device	Description	Protection Against Visual Symptoms
Abdominal belts	Pneumatic belt connected to inflated bag situated under pilot; belt pressurized at 6 G to approximately 2 psi; additional device, pressurized by hand, exerted 25 mm Hg pressure at 5.8 G	None
	Spencer acceleration belt inflated to 2–3 psi approximately 1 min prior to acceleration	0.5 G
	Hydrostatic belt connected to 2-gal water tank held at head level; during acceleration, belt filled with water and pressurized at the abdomen	0.5 G
Arterial occlusion suit	Activated by G-controlled air pressure, occluding the femoral arteries; another suit occluded the brachial arteries	2.5 G
Bandages	Applied to legs and abdomen	0.5 – 0.8 G
Hydrostatic pressure suits	Water-filled leggings, with pneumatic Spencer acceleration belt	0.5 G
	Franks' flying suit (Canadian water-filled): Thigh, leg, and abdomen bladders were pressurized under gravitational stress and exerted tensing effect on limbs through an inextensible covering	1.0 – 2.0 G 2.1 G 1.4 G 1.5 G
	Franks' liquid-filled suit with superimposed G-graded air pressure	>2.5 G
Pneumatic gradient pressure suits	Cotton aerodynamic anti-G suit (Australian air-filled): Overlapping bags in an inextensible outer covering; bags almost encircled limbs and body from feet to a few inches below the costal margin; provided three levels of pressure	1.5 – 2.0 G
	Spencer-Berger rubber, air-filled suit: Bags partially covered body; ankle bladders pressurized at −1.25 psi/G, calf and abdominal bladders at 1.13 psi/G, bladders at 1.10 psi/G	1.3 – 1.6 G
Single pressure suits	Spencer acceleration belt and stockings (Poppen Belt)	1.0 G
	David Clark single pressure suit inflated at 1.2 psi/G (developed from Spencer acceleration belt and stockings)	1.4 G

Table 4–8 (Continued)

Devices for Protection Against Positive ($+G_z$) Acceleration

Anti–G Device	Description	Protection Against Visual Symptoms
Single pressure suits (Cont'd)	RAF III suit: Essentially a copy of the David Clark single pressure suit, but with a split abdominal bladder and dual air inlet. Present day USAF and RAF suits have single air inlet serving leg and single abdominal bladder	1.4 – 1.5 G
	Pneumatic lever suit: Bladder systems consisting of narrow-bore tubes passing down each side of the body from the low thoracic region to the ankle; inflated bladders applied tension to legs and abdomen through interwoven ribbons using capstan principle; 2.2 psi/G pressure applied, starting with 2.0 psi at 2 G	1.5 G
Water immersion	Mayo bath: Subject immersed in water to third rib level	1.7 G
	G capsule: Total immersion	16.0 G

(After Nicholson and Franks, 1966)

To counter +G acceleration, custom-molded contour couches have been developed and utilized in space flight to provide a body posture with inclination of the head, trunk, thighs, and legs that combines optimum tolerance with useful performance (Clark et al., 1959).

For the -G vector, the "Ames system" is available which incorporates a posterior molded couch with frontal and head support (Vykukal et al., 1962). Seats with raschel nylon net as the primary support surfaces have been developed. These provide good support up to +16.5 G_x but demonstrate an undesirable rebound under severe vibration and impact acceleration (Peterson, 1964).

The possibilities of partial or total water immersion as a protective aid have been explored with some success (Wood et al., 1946; Gray & Webb, 1960, 1961) with exposures to +31 G_z for 5 seconds. Figure 4-31 shows the protection given against the effects of transverse acceleration (G_x) when the subject is immersed in water. Curves are also shown for subjects protected by optimal support and positioning.

Performance Under Sustained Acceleration

Vision

Some of the basic visual responses have already been examined. This section is concerned more with the ability to perform specific activities.

Visual Reaction Time. The majority of workers have found a prolongation in simple reaction time on exposure to severe but tolerable acceleration (Canfield et al., 1949; Brown & Burke, 1957; Frankenhaeuser, 1958; Chambers & Hitchcock, 1963). A typical response time to red signal lights is shown in figure 4-32 (Kaehler & Meehan, 1960). The two curves show mean response times (the time from appearance of a red signal light to the movement of the subject's hand from his lap) for five male college students, 20 to 25 years old, exposed to transverse accelerations. The solid line in the figure shows the combined response times for both right and left hand operation in more than 900 (+G_x) exposures up to +8 G_x. The dashed line shows the combined response times for both right and left hand operation in more than 500 (-G_x) exposures up to -4 G_x. The times required to reach and operate a horizontal lever, a toggle switch, and a pushbutton were longer as the accelerations increased, and variable times were recorded for left and right hand operation. Still longer times were needed for adjusting a rotating knob and a vertical "trim" wheel.

Reading Tasks. In a study by Warwick and Lund (1946), 24 percent of dial readings were erroneous at +3 G_z as compared with 18 percent at 1 1/2 G_z and 0 percent at 1 G. The response under acceleration varies with luminance, as previously noted. This variation in response is reflected in dial reading, as shown in figure 4-33 (White & Riley, 1958).

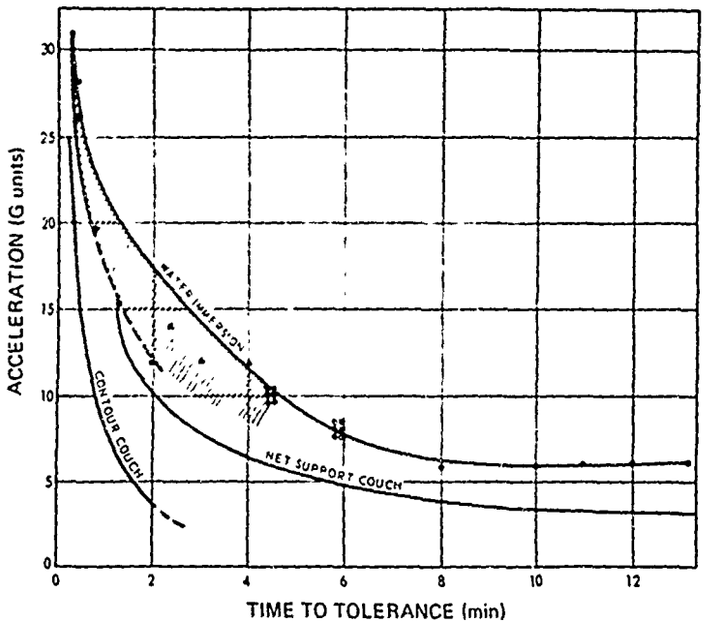


Figure 4–31. Protection against transverse ($+G_x$) acceleration afforded by water imersion, net support, and contour couch. (Bondurant et al., 1958b)

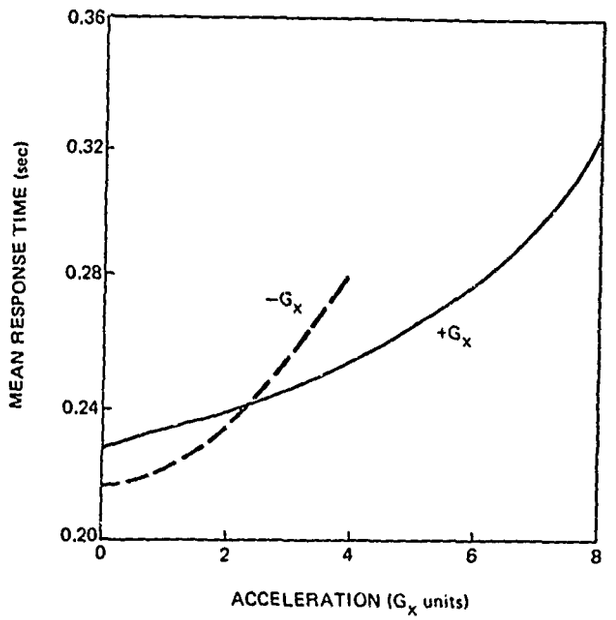


Figure 4–32. Visual reaction time to red signal lights for subjects exposed to $+G_x$ acceleration. (After Kachler & Meehan, 1960)

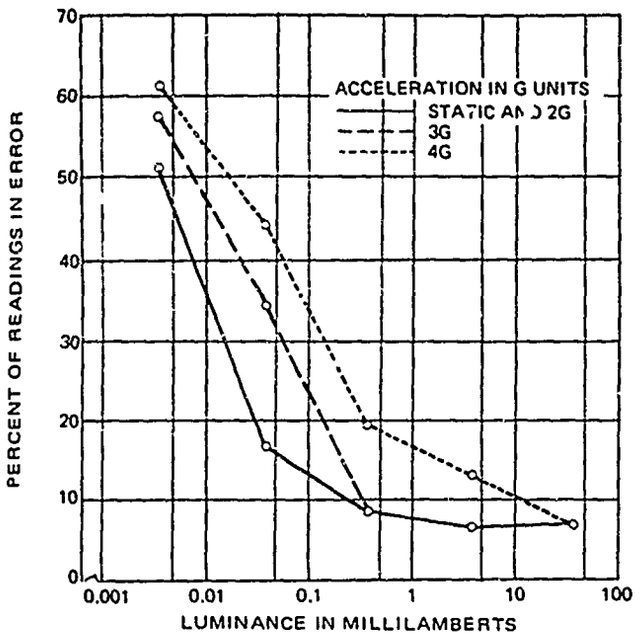


Figure 4–33. Effect of $+G_z$ acceleration on dial reading accuracy as a function of luminance. (After White & Riley, 1958)

Body Motion

Gross body motion is progressively impaired with increasing acceleration as indicated below (Code et al., 1945).

$+2\ G_z$:	Walking and movement along a ladder against acceleration very difficult.
$+3\ G_z$:	Walking, crawling, and movement along a ladder against acceleration impossible; unaided escape from vehicle impossible; parachute donning time increased from 17 to 75 seconds.
$+4\ G_z$:	Movement at right angles to acceleration vector impossible.
$+5\ G_x$:	Difficult to hold feet forward on rudder pedals.
$+6$ to $+7G_z$:	Extremely difficult to reach face curtain ejection seat firing mechanisms (Christie, 1961).
$+8\ G_x$:	Arms, legs, and body cannot be lifted.
$+9\ G_x$:	Unsupported head cannot be lifted although use of counterweighted headgear permits motion up to $+12\ G_x$.
$+25\ G_x$:	Hand and wrist movement still possible (Collins et al., 1958).

Control and Tracking

Control maneuvers involving gross motions of limbs are not practicable above 3 to 4 G, and become impossible, as noted above, as acceleration increases. Movement of hand controls is impaired relatively little, however, at high accelerations. The general characteristics of side-arm controllers and the general response to tracking task are shown in figures 4-34 through 4-42.

Higher Mental Function

Relatively little information is available on higher mental function. Increased time is required to complete multiplication tests at +3 G_z for 2 to 10 minutes as compared with performance without imposed acceleration (Frankenhaeuser, 1958). A decrement in color-naming has been observed during 1-minute trials at +3 G_z, although no decrement was noted in arithmetic ability, number ranking, and word separation tests in the same series (Wilson et al., 1951). According to Chambers (1963), repetitive memorization of a portion of a sequence of random numbers was satisfactorily undertaken at +5 G_x but the subjects involved stated that the concentration required at +5 G_x was much greater than at 1 G. Chambers also found in the same series of experiments that immediate memory was unaffected to +5 G_x but impaired at +7 G_x and above.

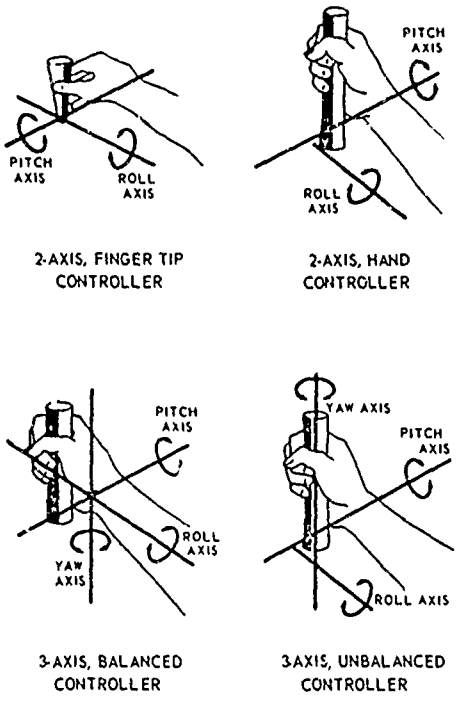


Figure 4–34. Four types of right hand, side-arm controllers. Under acceleration each responds differently Pilot performance is influenced by both acceleration and type of control stick. (Chambers & Hitchcock, 1963)

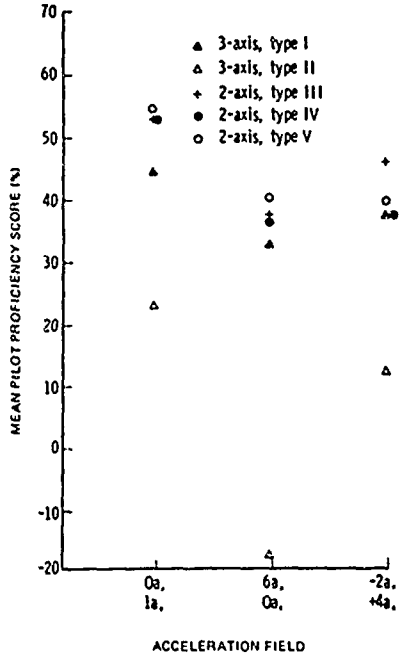


Figure 4–35. Mean pilot efficiency scores using various side-arm controllers in different acceleration fields. (After Chambers, 1961)

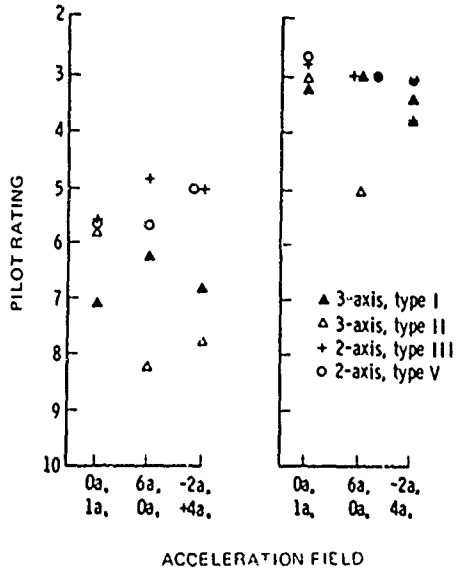


Figure 4–36. Mean pilot ratings of vehicle controllability with different side-arm controllers. (After Chambers, 1961)

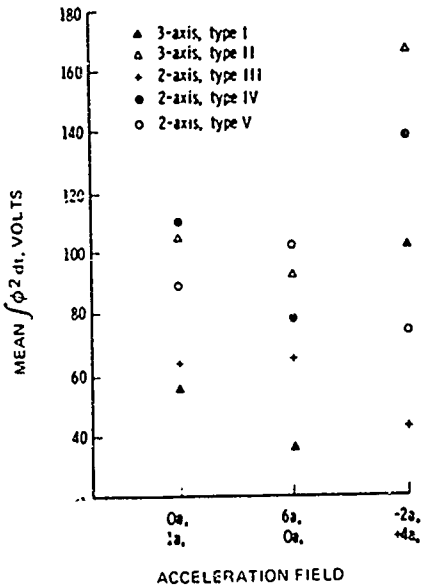


Figure 4–37. Roll error scores for pilots performing tracking task in differing acceleration fields, using differing controllers. (After Chambers, 1961)

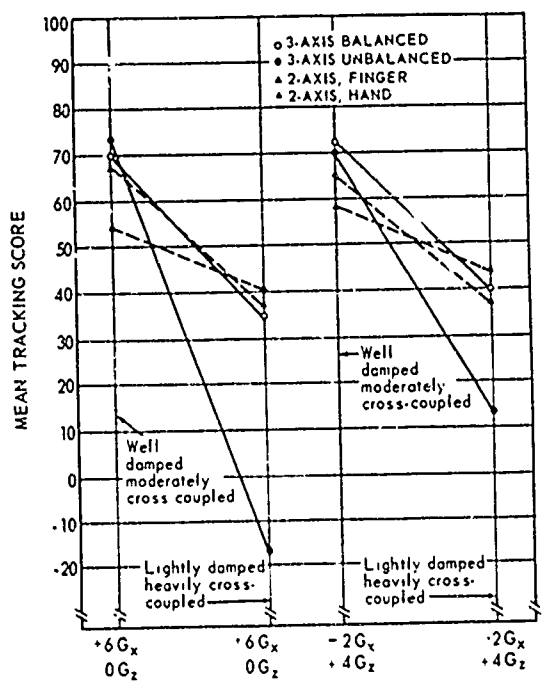


Figure 4–38. Mean tracking efficiency scores, influenced by type of controller, amount of damping and cross coupling, and acceleration vector. (After Chambers & Hitchcock, 1963)

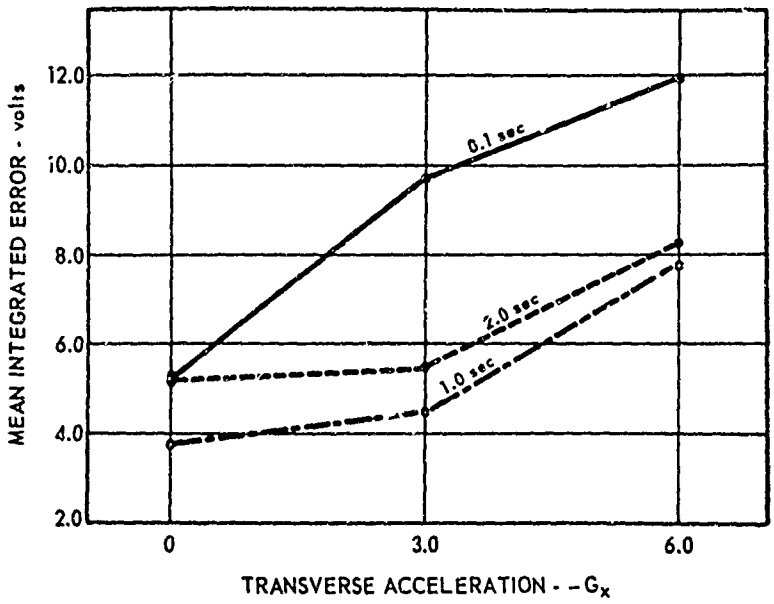


Figure 4–39. Mean integrated error in tracking display varying in x-axis, as a function of increased acceleration and various timelag constants. Error is caused by both changing timelag constants and acceleration. (After Kaehler, 1961)

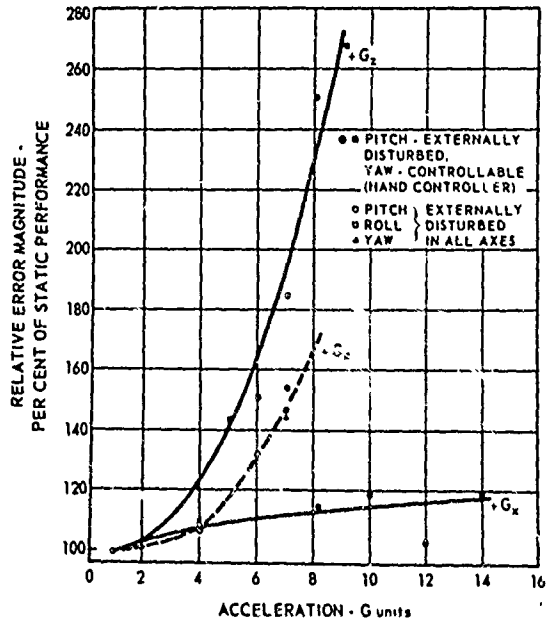


Figure 4–40. Tracking with side-arm controllers; effect of changing pilot task. (After Creer et al., 1962)

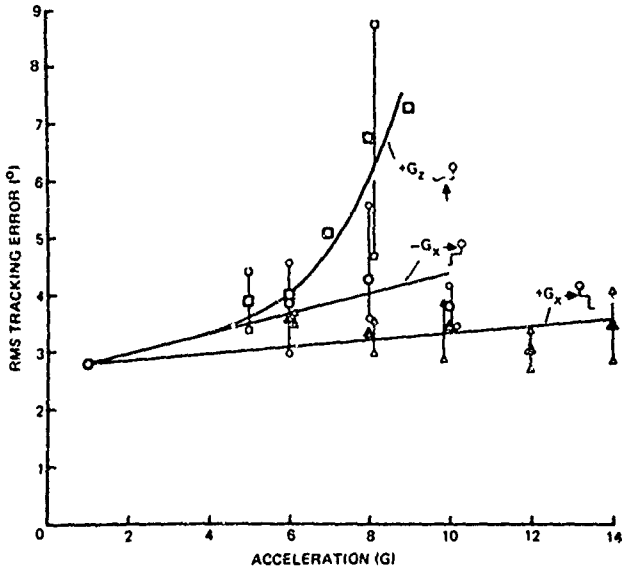


Figure 4–41. Effect of high sustained $+G_Z$ and $\pm G_X$ acceleration on root-mean-square tracking error. (After Creer, 1966)

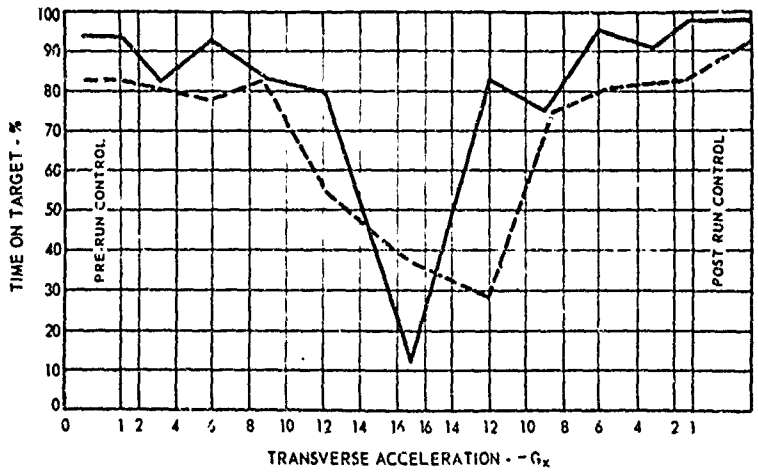


Figure 4–42. Tracking performance decrement, using 3.5 mm target in dual pursuit task, in two subjects exposed to $-16G_X$ acceleration profile simulating reentry. (After Clarke et al., 1959)

References

Alexander, W. C., Sever, R. J., & Hoppin, F. G. Hypoxemia induced by sustained forward acceleration in pilots breathing pure oxygen in a five pounds per square inch absolute environment. NASA-TM-X-51649, National Aeronautics and Space Administration, Washington, D.C., 1965.

Andina, F. "Schwarzsehen" als Ausdruk von Blutdruckschwankungen bei Sturzflugen. *Schweiz. Med. Wchnschn.*, 1937, *67*, 753-756.

Barr, P. O. Hypoxemia in man induced by prolonged $+G_z$ acceleration. *Acta Physiologica Scandinavica*, 1962, *54*, 128.

Beckman, E. L., Duane, T. D., & Coburn, D. R. Limitation of ocular motility and pupillary dilatation in humans due to positive acceleration. NADC-MA-6-140, Naval Air Development Center, Johnsville, Pennsylvania, 1961.

Bondurant, S., Blanchard, W. G., Clarke, N. P., & Moore, F. Effect of water immersion on human tolerance to forward and backward acceleration. WADC-TR-58-290, Wright-Patterson Air Force Base, Ohio, July 1958. (b)

Bondurant, S., Clarke, N. P., Blanchard, W. G., Miller, H., Hessberg, R. R., & Hiatt, E. P. Human tolerance to some of the accelerations anticipated in space flight. *USAF Armed Forces Medical Journal*, 1958, *9*, 1093.(a)

Braunstein, M. L., & White, W. J. The effects of acceleration on brightness discrimination. *Journal of the Optical Society of America*, 1962, *52*, 931-933.

Brent, H. P., Carey, T. M., Powell, T. J., Scott, J. W., Taylor, W. J. R., & Franks, W. R. Synergism between effects of hyperventilation, hypoglycemia, and positive acceleration. *Aerospace Medicine*, 1960, *31*, 101.

Brown, J. L., & Burke, R. E. Effect of positive acceleration on visual reaction time. NADC-MA-5712, Naval Air Development Center, Johnsville, Pennsylvania, 1957.

Browne, M. K., & Fitzsimmons, J. T. Electrocardiographic changes during positive acceleration. FPRC-1009, Royal Air Force, Ministry of Defence, London, 1957.

Bryan, A. C., & MacNamara, W. D. The effect of acceleration on the distribution of pulmonary blood flow. RCAF SAM Rept. 64-RD-8, Institute of Aviation Medicine, Royal Canadian Air Force, 1964.

Canfield, A. A., Comrey, A. L., & Wilson, R. C. A study of reaction time to light and sound as related to positive radial acceleration. *Journal of Aviation Medicine*, 1949, *20*, 350.

Chambers, R. M. Control performance under acceleration with side-arm controllers. NADC-MA-6110, Naval Air Development Center, Johnsville, Pennsylvania, 1961.

Chambers, R. M. Long-term acceleration and centrifuge simulation studies. Aviation Medical Acceleration Laboratory, Naval Air Development Center, Johnsville, Pennsylvania, 1963.

Chambers, R. M. Acceleration. In P. Webb (Ed.), Bioastronautics Data Book. NASA SP-3006, National Aeronautics and Space Administration, Washington, D.C., 1964.

Chambers, R. M., & Hitchcock, L. The effects of acceleration on pilot performance. NADC-MA-6219, Naval Air Development Center, Johnsville, Pennsylvania, 1963.

Chambers, R. M., & Kerr, R. Effects of positive pressure breathing on performance during acceleration. NADC-MA-6308, Naval Air Development Center, Johnsville, Pennsylvania, 1962.

Christie, R. L. Effects of radial and angular accelerations. In: H. G. Armstrong (Ed.), *Aerospace Medicine*. Baltimore: Williams and Wilkins Co., 1961.

Clark, C. C. Observations of a human experiencing 2 G for 24 hours. Paper presented at 31st Annual Meeting of the Aerospace Medical Association, Bell Harbor, Florida, 1960.

Clark, C. C., Gray, R. F., Hardy, J. D., & Smith, F. K. A discussion of restraint and protection of the human experiencing the smooth and oscillating acceleration of proposed space vehicles. NADC-MA-5914, Naval Air Development Center, Johnsville, Pennsylvania, 1959.

Clarke, N. P., Hyde, A. S., Cherniak, N. S., et al. Preliminary report of human response to rearward-facing re-entry accelerations. WADC-TN-59-109, Wright-Patterson Air Force Base, Ohio, 1959.

Cochran, L. R., Gard, P. B., & Norsworthy, M. E. Variation in human G tolerance to positive acceleration. SAM Rept. 001-059.02.10, Naval School of Aviation Medicine, Pensacola, Florida, 1954.

Code, C. F., Wood, E. H., Sturm, R. E., & Lambert, E. H. The sequence of physiological events in man during exposures to positive acceleration. *Federation Proceedings*, 1945, 4,(14).

Coermann, R. R. The mechanical impedance of the human body in sitting and standing positions. In *Human vibration research*. London: Pergamon Press, 1963.

Collins, C. C., Crosbie, R. J., & Gray, R. F. Letter report concerning pilot performance and tolerance study of orbital re-entry acceleration. NADC-LR-64, Naval Air Development Center, Johnsville, Pennsylvania, 1958.

Collins, C. C., & Gray, R. F. Letter report concerning pilot performance and tolerance studies of re-entry acceleration. NADC-LR-90, Naval Air Development Center, Johnsville, Pennsylvania, 1959.

Creer, B. Y. Pilot performance during acceleration. In P. I. Altman and D. S. Dittmer (Eds.), *Environmental biology*. AMRL-TR-66-194, Wright-Patterson Air Force Base, Ohio, 1966.

Creer, B. Y., Stewart, J. D., & Dourullier, J. G. Influence of sustained linear accelerations on certain pilot-performance capabilities. *Aerospace Medicine*, 1962, *33*, 1086-1093.

Duane, T. D. Observations on the fundus oculi during blackout. *A.M.A. Archives of Ophthalmology*, 1954, *51*, 343.

Franks, W. R., Kerr, W. K., & Rose, B. Some neurological signs and symptoms produced by centrifugal force in man. *Journal of Physiology*, 1945, *104*, 10-11.

Frankenhaeuser, M. Effects of prolonged gravitational stress on performance. *Acta Psychologica*, 1958, *14*, 92.

Fraser, T. M. Human response to sustained acceleration. NASA SP-103, National Aeronautics and Space Administration, Washington, D.C., 1966.

Gamble, J. L., Shaw, R. S., Henry, J. P., & Gauer, O. H. Cerebral dysfunction during negative acceleration. *Journal of Applied Physiology*, 1949, *2*, 133.

Gauer, O. H., & Henry, J. P. Negative ($-G_z$) acceleration in relation to arterial oxygen saturation, subendocardial hemorrhage and venous pressure in the forehead. *Aerospace Medicine*, 1964, *35*, 533-545.

Glaister, D. H. Acceleration atelectasis--some factors modifying its occurrence and magnitude. FPRC/Memo 220, Royal Air Force, Ministry of Defence, London, 1965.

Glaister, D. H. Breathing. *Nature*, 1961, *192*, 106-108.

Glaister, D. H. The effect of positive centrifugal acceleration upon the distribution of ventilation and perfusion within the human lung, and its relation to pulmonary arterial and intraoesophageal pressures. *Proceedings of the Royal Society, B*, 1967, *168*, 311-334.

Glaister, D. H. Pulmonary gas exchange during positive acceleration. FPRC-1212, Royal Air Force, Department of Defence, London, 1963.

Gray, R. F., & Webb, M. G. High G protection. NADC-MA-5910, Naval Air Development Center, Johnsville, Pennsylvania, 1960.

Gray, R. F., & Webb, M. G. High G protection. *Aerospace Medicine*, 1961, *32*, 425.

Kaehler, R. C. The effects of transverse accelerations and exponential time-lag constants on compensatory tracking performance. ASD-TR-61-457, Wright-Patterson Air Force Base, Ohio, 1961.

Kaehler, R. C., & Meehan, J. P. Human psychomotor performance under varied transverse acceleration. WADC-TR-60-621, Wright-Patterson Air Force Base, Ohio, 1960.

Leverett, S. D. Biodynamics. USAF SAM *Medical Services Digest*, 1968, *19*, 23.

Lindberg, E. F., & Wood, E. H. Acceleration. In J. H. U. Brown (Ed.), *Physiology of man in space*. New York and London: Academic Press, 1963.

Miller, H., Riley, M. B., Bondurant, S., & Hiatt, E. P. The duration of tolerance to positive acceleration. *Aerospace Medicine*, 1959, *30*, 360.

Newsom, W. A., & Leverett, S. D. Retinal circulation in man during centrifugal acceleration. *Transactions of the American Academy of Ophthalmology and Otolaryngology*, Jan.-Feb. 1968, 39-49.

Nicholson, A. N., & Franks, W. R. Devices for protection against positive (long axis) acceleration. In P. I. Altman and D. S. Dittmer (Eds.), *Environmental biology*. AMRL-TR-66-194, Wright-Patterson Air Force Base, Ohio, 1966.

Peterson, R. L. Personnel seating research for Air Force aerospace vehicles. SAE-85IC, presented at the Air Transport and Space Meeting, New York, April 1964.

Rogge, J. D., Moore, W. W., Segar, W. E., & Fasola, A. F. Effect of $+G_z$ and $+G_x$ acceleration on peripheral venous ADH levels in humans. USAF SAM TR-67-286, School of Aerospace Medicine, Brooks Air Force Base, Texas, 1967.

Ross, B. M., Chambers, R. M., & Thompson, R. R. Effects of transverse acceleration on performance of two running matching memory tasks. NADC-MA-6309, Naval Air Development Center, Johnsville, Pennsylvania, 1963.

Rutishauser, W. J., Banchero, N., Tsakiris, A. G., & Wood, E. H. Effect of gravitational and inertial forces on pleural and esophageal pressures. *Journal of Applied Physiology*, 1967, *22*, 1041-1051.

Ryan, E. A., Kerr, W. K., & Franks, W. R. Some physiological findings on normal men subjected to negative G. *Journal of Aviation Medicine*, 1950, *21*, 173.

Sem-Jacobsen, C. W. Electroencephalographic study of pilots stressed in flight. *Aerospace Medicine*, 1959, *30*, 797-801.

Sem-Jacobsen, C. W. Recording of in-flight stress in jet fighter planes. *Aerospace Medicine*, 1960, *31*, 320.

Smedal, H. A., Rogers, T. A., Duane, T. D., Holden, G. R., & Smith, J. R. The physiological limitations of performance during accelerations. *Aerospace Medicine*, 1963, *34*, 48.

Stauffer, F., & Errobo-Knudsen, E. O. Positive acceleration and urine output. SAM Rept. NM 001.059.02.04, Naval School of Aviation Medicine, Pensacola, Florida, 1953.

Stoll, A. M. Human tolerance to positive G as determined by the physiological end-points. *Journal of Aviation Medicine*, 1956, *27*, 356.

Teichner, W. H., & Craig, R. L. Some human tolerance limits to several environmental stresses of an Apollo mission: Compendium. NASA Grant NGR 22-007-070, Guggenheim Center for Aerospace Health and Safety, Harvard School of Public Health, Boston, Massachusetts, 1966.

Vogt, H. L., Coermann, R. R., & Fust, H. D. Mechanical impedance of the sitting human under sustained acceleration. *Aerospace Medicine*, 1968, *39*, 675-679.

Vykukal, H. C., Gallant, R. P., & Stinnett, G. W. An interchangeable, mobile, pilot-restraint system, designed for use in high sustained acceleration force fields. *Aerospace Medicine*, 1962, *33*, 279-285.

Warwick, M. J., & Lund, D. W. Effect of moderate positive acceleration on ability to read aircraft-type instrument dials. WADC-MR-6[illegible], Wright-Patterson Air Force Base, Ohio, 1946.

Watson, J. F., Cherniak, N. S., & Zechman, F. W. Respiratory mechanics during forward acceleration. *Journal of Clinical Investigation*, 1960, *39*, 1737.

White, W. J. Variations in absolute visual threshold during acceleration stress. WADC-TR-60-34, Wright-Patterson Air Force Base, Ohio, 1960.

White, W. J., & Riley, M. B. Effects of positive acceleration on the relation between illumination and instrument reading. WADC-TR-58-332, Wright-Patterson Air Force Base, Ohio, 1958.

Wilson, R. C., Bryan, G. L., Green, G. A., Willmorth, N. E., Canfield, A. A., & Warren, N. D. After effects of intermittent positive radial acceleration. *Journal of Aviation Medicine*, 1951, *22*, 509-517.

Wood, E. H. Some effects of gravitational and inertial forces on the cardiopulmonary system. *Aerospace Medicine*, 1967, *38*, 225-233.

Wood, E. H., Lambert, E. H., Baldes, E. J., & Code, C. F. Effects of acceleration in relation to aviation. *Federation Proceedings*, 1946, *5*, 327.

Wood, E. H., Nolan, A. C., Donald, E. E., & Cronin, L. Influence of acceleration on pulmonary physiology. *Federation Proceedings*, 1963, *22*, 1024.

Wood, E. H., Sutterer, W. F., Marshall, H. W., Lindberg, E. F., & Headley, R. N. Effect of headward and forward accelerations on the cardiovascular system. WADC-TR-60-634, Wright-Patterson Air Force Base, Ohio, 1961.

York, E., Oleynick, R. J., & Patton, R. M. Human acceleration experience at the Aerospace Medical Research Department, Naval Air Development Center, Johnsville, Pennsylvania, January 1951–30 December 1965. *Aerospace Medicine*, 1968, *39*, 68-71.

Zarriello, J. J., Norsworthy, M. E., & Bower, H. R. A study of early grayout thresholds as an indicator of human tolerance to positive radial acceleratory force. Project NM-11-02-11, Report #1, Naval School of Aviation Medicine, Pensacola, Florida, 1958.

Zechman, F. W., Cherniak, N. S., & Hyde, A. S. Ventilatory response to forward acceleration. *Journal of Applied Physiology*, 1960, *15*, 907.

CHAPTER 5
ROTARY ACCELERATION

by

T. Morris Fraser, M. Sc., M.D.
University of Waterloo
Waterloo, Ontario, Canada

Rotary acceleration is defined as the acceleration which exists during angular motion when the axis of motion passes through some part of the body. Consequently, it is a manifestation of angular acceleration, and is always present during steady state spinning or tumbling, even when the angular velocity is constant. The problems related to the acceleration environment of rotating chambers, rooms, tables, and short radius centrifuges in which the axis of rotation is not through the body are not considered here. These are discussed in chapter 12, *The Vestibular System.*

Rotary acceleration was first noted to be a problem in the tumbling and spinning that occurred during the deployment of early aircraft ejection seats, particularly during ejection at relatively high speeds. In the ejection situation, the problem is more than that of simple tumbling or spinning, since the motion may occur within a decelerative G-field, which, for short durations, may reach a peak or plateau of as much as 50 G. In a space vehicle, or during extravehicular activity, in the null gravity state, problems can arise from simple tumbling or spinning, following imparted motion by, for example, failure of a reaction control system, such as in Gemini 8 where severe tumbling was experienced.

While a specific terminology for rotary acceleration has been suggested (Pesman, 1968), it is more common to use the G terminology defined in chapter 6, *Impact*, along with specification of the axis of rotation, where x refers to rolling, y to pitching, and z to yawing or spinning. The term tumbling is often used in place of pitching and rolling.

Subjective Reactions and Tolerance

Subjective reactions to rotary acceleration vary with the frequency, axis, and duration of rotation. Individual variability in response is marked. Vertigo, as

Reviewed by Randall M. Chambers, Ph.D., NASA Langley Research Center.

manifest subjectively by dizziness, sometimes nausea, and occasionally vomiting, is a common feature of the initial and terminal phases of acceleration to and deceleration from constant angular velocity, but normally ceases after the motion has reached constant velocity, provided head movement is limited. In some individuals, it recurs during prolonged exposure. Vertigo and its associated phenomena are considered in chapter 12.

Tolerance

From the few reports available, tolerance to rotary acceleration does not seem to be a rectilinear function of rotation rate. Most subjects, without prior experience, can tolerate rotation rates up to 6 rpm in any axis or combination of axes. Most subjects cannot initially tolerate rotation rates in the region of 12 to 30 rpm and rapidly become sick and disoriented above 6 rpm unless carefully prepared by a graduated program of exposure (Fletcher, 1968). On the other hand, rotation rates of 60 rpm for up to 3 or 4 minutes around the y-axis (pitch) and around the z-axis (spin) have been described by subjects as being not only tolerable but pleasant (Weiss et al., 1954; Urschell & Hood, 1966). Intolerability becomes manifest again at about 80 rpm in the pitch mode and at about 90 to 100 rpm in the spin mode, although McCabe (1960) relates that one of the Ice Capades skating stars spins around the z-axis for 12 seconds at 420 rpm without manifest discomfort. In the pitch axis, with the center of rotation at the heart level, symptoms of negative acceleration ($-G_z$) are demonstrated at about 80 rpm and are tolerable for only a few seconds. Some effects of positive acceleration ($+G_z$), namely numbness and pressure in the legs, are also observed but develop slowly, with pain being evident at about 90 rpm. No confusion or loss of consciousness is found, but in some subjects disorientation, headache, nausea, or mental depression are noted for several minutes after a few minutes of exposure (Weiss et al., 1954). With rotation in the spin mode, when the head and trunk are inclined forward out of the z-axis, rotation becomes close to limiting at 60 rpm for 4 minutes, although some motivated subjects have endured 90 rpm in the same mode (Courts, 1966). Except for unduly susceptible subjects, tolerance tends to improve with exposure. Long duration runs in the pitch mode have been endured for up to about 60 minutes at 6 rpm in selected subjects (Fletcher, 1968).

The center of rotation within the body determines, to a considerable extent, the nature of the resulting effects, as will be examined in connection with the discussion of physiological mechanisms. Figure 5-1 illustrates the general human tolerance to tumbling in the pitch plane with centers of rotation at the heart level and at the level of the iliac crest. On the basis of extrapolated data from dogs, Weiss and coworkers (1954) calculate that unconsciousness from circulatory effects alone would occur in man after 3 to 10 seconds at 160 rpm with the center of rotation at the heart and at 180 rpm with the center of rotation at the iliac crest.

Tolerance to tumbling in the presence of a superimposed G field is shown in figure 5-2.

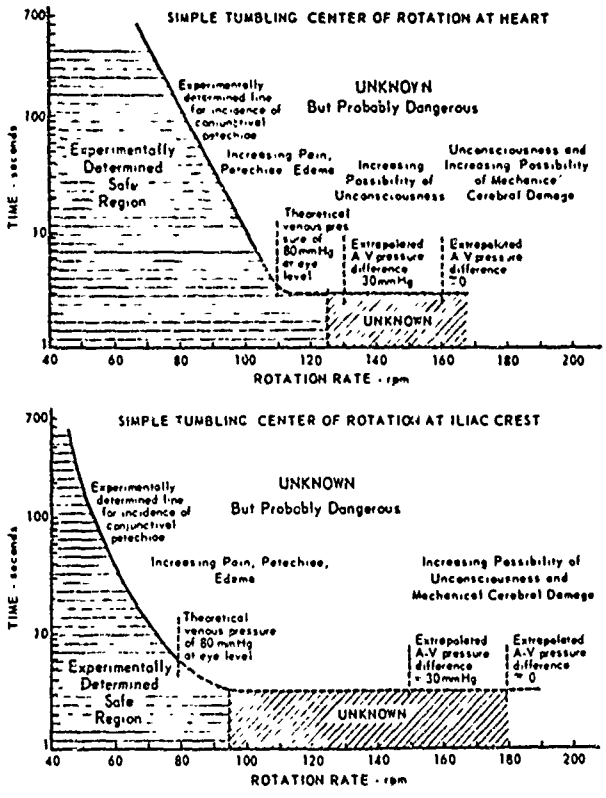


Figure 5–1. Suggested human tolerance to rotation around pitch axis with no superimposed deceleration field (a) with center of rotation at the heart; (b) with center of rotation at the iliac crest. (After Weiss et a., 1954)

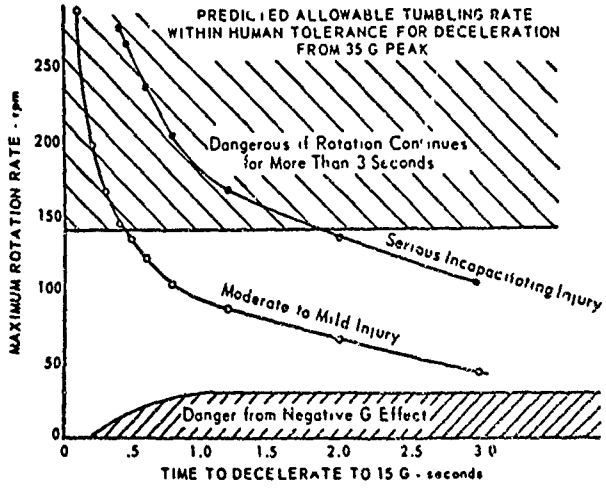


Figure 5–2. Estimate of human tolerance to constant rotation around the pitch axis with a G field decaying from 35 to 15 G. (After Edelberg, 1961)

Tolerance to G_z 100 percent gradient spin is very closely related to tolerance to rotary acceleration, in that in the former the axis of rotation is tangent to the crown of the head. Figures 5-3 and 5-4 illustrate human tolerance to this form of rotary acceleration.

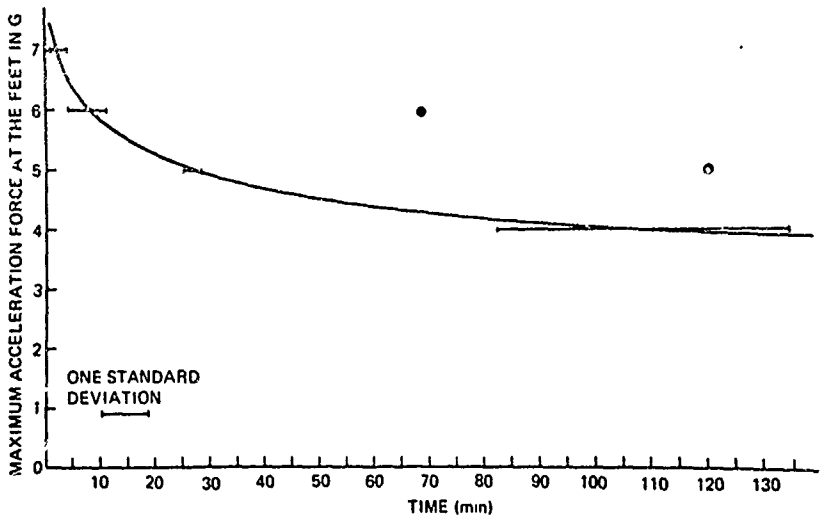


Figure 5–3. Mean tolerance to 100% $+G_z$ gradient spin for seven untrained subjects rotating around x-axis with center of rotation tangential to the head. The two isolated points represent tolerance times of a subject who utilized physiological countermeasures to increase his tolerance. His values are not included in the means. (After Piemme et al., 1966)

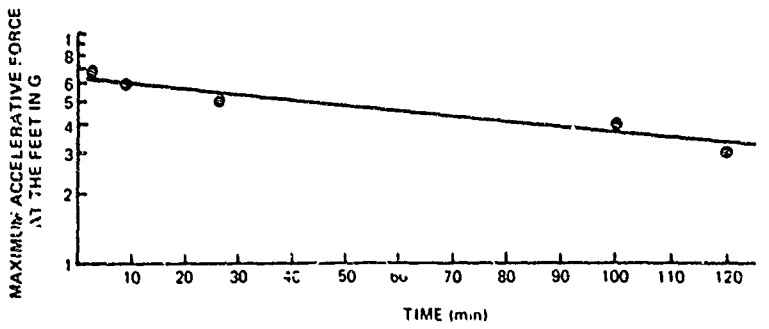


Figure 5–4. Semilogarithmic plot of mean tolerance time vs acceleration at the feet during exposure to $+G_z$ 100% spin around the x-axis with center of rotation tangential to the head. (After Piemme et al., 1966)

Pain and discomfort are not features of slow rotation but begin to be manifest at about 80 rpm in the pitch and roll axes, largely because of fluid swelling of tissues from the imposed +G fields (Wells et al., 1954). Even in the z-axis at these rotation rates, discomfort can be severe in the seated posture because of the hydrostatic gradient that develops along the forearms and thighs (Urschell & Hood, 1966).

Perception

The threshold of perception, or awareness, for rotary acceleration is in fact a measure of vestibular sensitivity, but warrants brief consideration here. Using a one-degree-of freedom simulator that could produce angular accelerations within narrow limits of error, Clark and Steward (1969) examined perception thresholds in the yaw axis in the erect seated position at the center of rotation with head fixed. Figure 5-5 shows the distribution of thresholds in 53 normal male subjects under these conditions.

Table 5-1, from a review by Clark (1967), details the findings of 25 studies on perception of angular acceleration in man. Clark points out that in evaluating the findings in the table, one must bear in mind the miscellany of definitions of threshold, the variation in rotation devices, and psychophysical methods. In general, the results indicate an extreme sensitivity to angular acceleration with perception thresholds varying from $0.035°/sec^2$ to $8.2°/sec^2$

The relationship between a rotational input and a subjective or objective (for example, nystagmus) output may be so tenuous that time must elapse before the threshold of response is reached. Figure 5-6 indicates the latency time for perception of angular acceleration about the yaw axis, as also do figures 5-7 and 5-8.

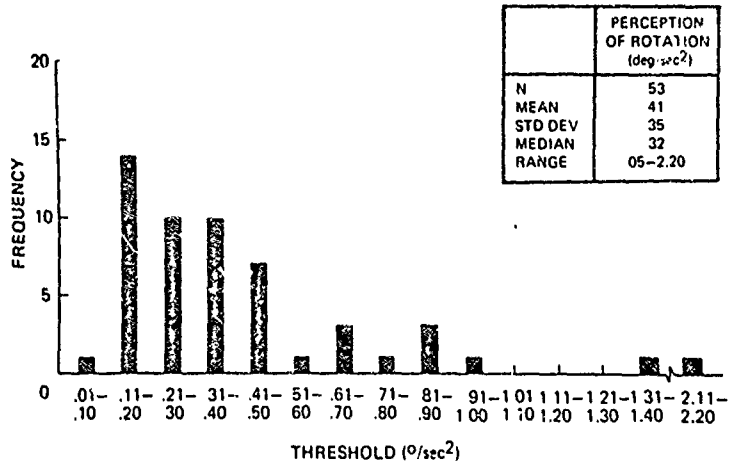


Figure 5–5. Distribution of thresholds for perception of angular acceleration for 53 normal men. (After Clark & Stewart, 1969)

Table 5–1

Thresholds for the Perception of Stimulation by Angular Acceleration in Man

Author and Date	Van Wulfften Palthe[63]* 1922	Dodge[14] 1923	Turnarkin[59] 1937	Christian[5] 1939	Christian[5] 1939	Clark, Graybiel and MacCorquodale[8] 1948	Clark, Graybiel and MacCorquodale[7] 1948
Threshold	~ 2°/sec^2	1°-2°/sec	0.2°/sec^2	0.13°-0.33°/sec^2	0.13°-2.0°/sec^2	~18° bank	~0.2°/sec^2 ~18° of bank
Indicator response							
a) Perceptual mode	Rotation	Rotation	Rotation	Oculogyral illusion	Rotation	Oculogyral illusion	Oculogyral illusion
b) Method of response	Forced-choice	Forced-choice	Yes-No	–	–	Forced-choice	Forced-choice
Canals stimulated	Horizontal and vertical	Horizontal and vertical	Horizontal and vertical	Horizontal and vertical	Horizontal and vertical	Horizontal and vertical	Horizontal and vertical
Head position	Erect	Erect (?)	Erect	Erect (?)	Erect (?)	Erect in cockpit	Erect in cockpit
Stimulus							
a) Duration	Not reported	"Sudden onset"	Variable	–	–	9 - 14 sec	11 - 28 sec
b) Determination of angular acceleration	Computed	Not determined	Computed	Computed (?)	Computed (?)	Not determined	Computed
c) Method of presentation	Constant stimuli	Constant stimuli	Ramp acceleration	–	–	Constant stimuli	Constant stimuli
Subjects	4	5	5 (?)	–	–	4	3
Rotation device	Spyker aircraft	Rotating chair	Rotation in water	Rotating chair	Rotating chair	SNJ-6 aircraft	SNJ-6 aircraft
Definition of threshold	50% above chance report	50% point	Point at which movement perceived	–	–	50% level corrected for guessing	50% above chance

Table 5–1 (Continued)
Thresholds for the Perception of Stimulation by Angular Acceleration in Man

Author and Date	Graybiel, Kerr and Bartley[25]* 1948	Groen and Jongkees[27] 1948	Groen and Jongkees[27] 1948	MacCorquodale[41] 1948	de Vries[60] 1949	Hallpike, Hood and Byford[35] 1952	Hallpike and Hood[34] 1953
Threshold	~0.12°/sec^2	0.28° - 2.0°/sec^2	0.18° - 0.25°/sec^2	0.10°-0.15°/sec^2 15° of bank	0.9°-4.0°/sec^2	0.2°-1.0°/sec^2	0.2°-0.7°/sec^2
Indicator response							
a) Perceptual mode	Oculogyral illusion	Rotation	Rotation	Rotation of aircraft	Rotation	Rotation	Oculogyral illusion
b) Method of response	Forced-choice	–	–	Forced-choice	Yes - No	–	Forced-choice (?)
Canals stimulated	Horizontal	Horizontal	Horizontal	Horizontal and vertical	Horizontal	Horizontal	Horizontal
Head position	20°-25° forward	Head forward	Head forward	Erect in cockpit	Head 30° forward	Head 30° forward	Head 30° forward
Stimulus							
a) Duration	Varied	~30 sec	Varied	Varied	0.1 - 1.0 sec	–	15 - 150 sec
b) Determination of angular acceleration	Computed	Computed	Computed	Computed	Computed average	Computed from oscillograph	Computed
c) Method of presentation	Constant stimuli	–	–	Constant stimuli	Constant stimuli	–	Constant stimuli
Subjects	5	30	2	3	1	5	3
Rotation device	Centrifuge	Rotating chair	Torsion swing	SNJ-6 aircraft	Rotating chair	Rotating chair	Rotating chair
Definition of threshold	50% above chance level on frequency ogive	–	Formula including damping of cupula-endolymph system	50% above chance identification	Number of stimuli perceived corrected for guessing	–	–

Table 5–1 (Continued)
Thresholds for the Perception of Stimulation by Angular Acceleration in Man

Author and Date	Hallpike and Hood[34*] 1953	Hilding[36] 1953	deVries and Schierbeek[61] 1953	Sadoff, Matteson and Havill[55] 1955	Mann and Ray[44] 1956	Montandon and Russback[49] 1956
Threshold	0.6° - 2.0°/sec^2	0.25° - 3.0°/sec^2	0.9° - 1.7°/sec^2	5.3° - 8.2°/sec^2	0 035°-0.13°/sec^2	0.5° - 1.0°/sec^2
Indicator response a) Perceptual mode	Rotation	Rotation	Rotation	Pitch-up of simulator	Rotation	Rotation
b) Method of response	Forced-choice (?)	Forced-choice	Yes - No	Yes - No	Forced-choice	Forced-choice (?)
Canals stimulated	Horizontal	Horizontal	Horizontal	Vertical	Horizontal	Horizontal
Head position	Head 30° forward	Head 30° forward	Head 30° forward	Head erect	Head about 15° forward	Erect (?)
Stimulus a) Duration	15 - 150 sec	Varied	0.4 sec	Varied	4 - 30 sec	Varied
b) Determination of angular acceleration	Computed	Computed (?)	Computed	Computed	Computed	Computed
c) Method of presentation	Constant stimuli	Increasing steps of angular acceleration	Constant stimuli	Ramp acceleration	Up & down time varied	"Liminal"
Subjects	3	26	3	4	4	?
Rotation device	Rotating chair	Rotating chair	Rotating chair	Link trainer	Rotating chair	Rotating chair
Definition of threshold	–	–	75% point with deVries' correction for guessing	Point on graph of increasing acceleration corrected for RT	75% correct identification	–

Table 5–1 (Continued)

Thresholds for the Perception of Stimulation by Angular Acceleration in Man

Author and Date	Roggeven and Nijhoff[54]* 1956	Roggeveen and Nijhoff[54] 1956	Clark and Stewart[9] 1962	Von Diringshofen, Kissel and Osypka[12] 1964	Miery[47] 1965	Miery[47] 1965
Threshold	1.3°/sec^2	1.8°/sec^2	0.12°-0.17°/sec^2	0.26° - 1.0°/sec^2	0.1° - 0.2°/sec^2	0.5°/sec^2
Indicator response						
a) Perceptual mode	Oculogyral illusion	Rotation	Rotation	Rotation	Rotation	Rotation
b) Method of response	Yes - No	Yes - No	Forced-choice	Forced-choice	Forced-choice	Forced-choice
Canals stimulated	Horizontal	Horizontal	Horizontal and vertical	Horizontal	Horizontal and vertical	Horizontal and vertical
Head position	Head 30° forward	Head 30° forward	Head erect in cockpit	"Slightly bent forward"	Head erect	Nose down
Stimulus						
a) Duration	0.8 sec	0.8 sec	10 sec	Varied	Varied	Varied
b) Determination of angular acceleration	Computed	Computed	Angular accelerometer	Computed	Computed	Computed
c) Method of presentation	Constant stimuli	Constant stimuli	Constant stimuli	Ramp acceleration	Constant stimuli	Constant stimuli
Subjects	15	15	5	9	3	3
Rotation device	Rotating chair	Rotating chair	Flight simulator	Flight simulator	Flight simulator	Flight simulator
Definition of threshold	50% correct indication corrected for guessing	50% correct indication corrected for guessing	75% correct identification	Point at which movement perceived for RT	75% correct identification	75% correct identification

*See original references as listed in Aerospace Medicine, May 1967.

(Clark, 1967)

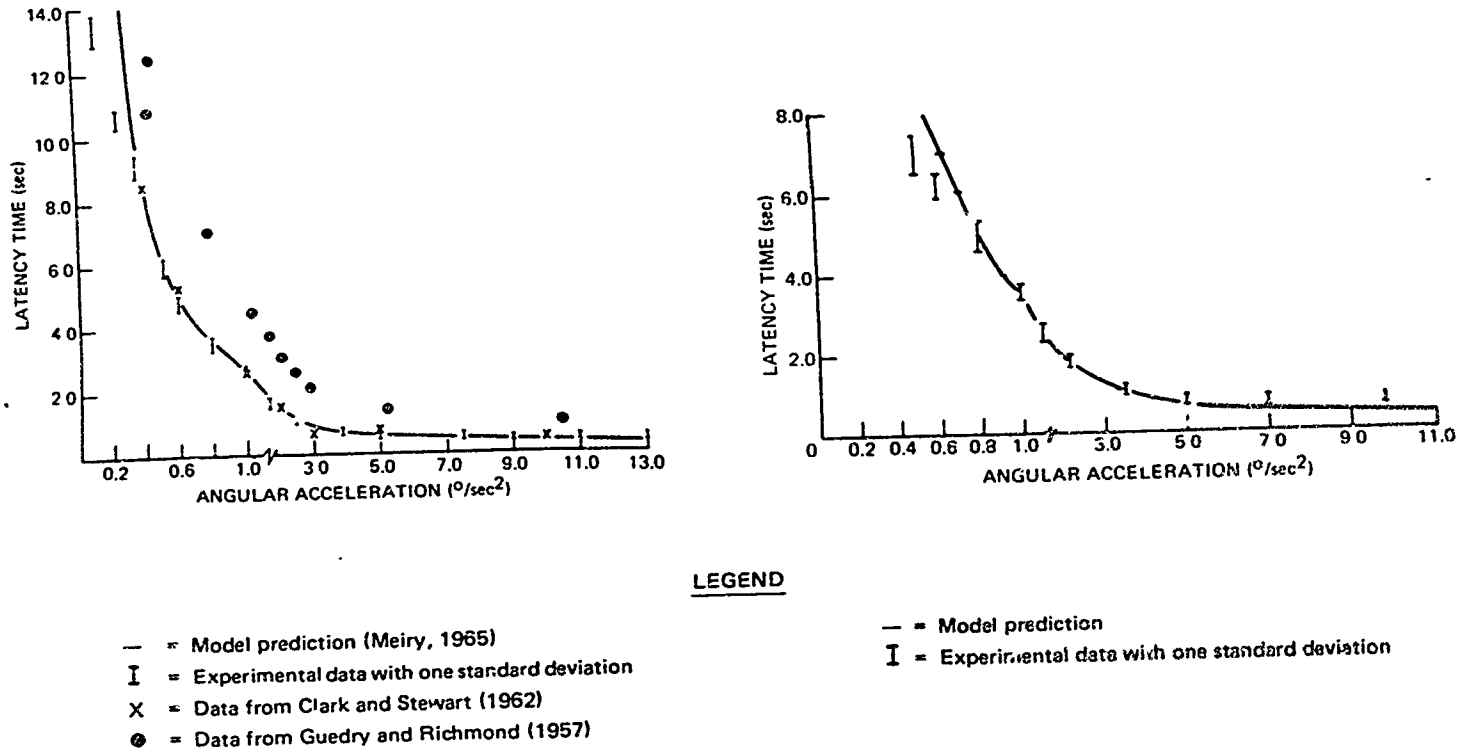


Figure 5–6. Thresholds for sensing rotation about z- and x-axis; at left, latency times for perception of angular acceleration about z-axis; at right, about x-axis. Note scale change of angular acceleration.

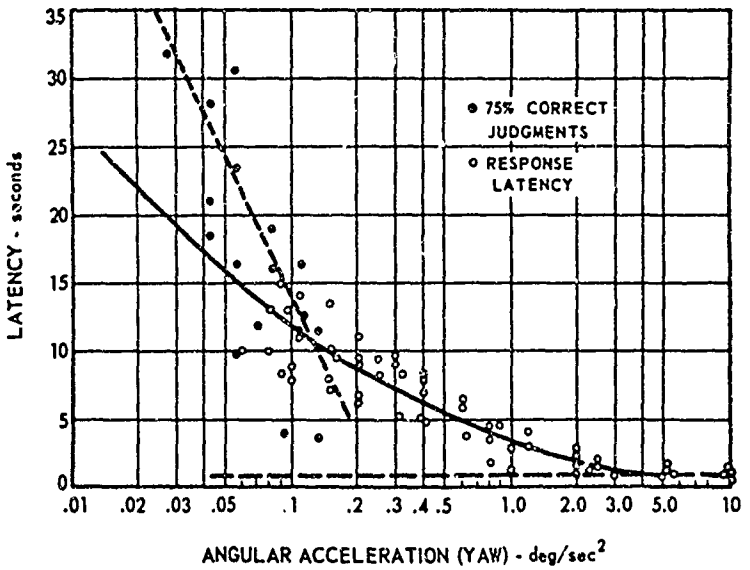


Figure 5–7. Perception of angular acceleration: Time required to judge direction of rotation about yaw axis as a function of angular acceleration. Solid points indicate time to make judgments that are correct 75% of the time; open points = time to make judgments, correct or incorrect. (After Chambers (1964), adapted from others)

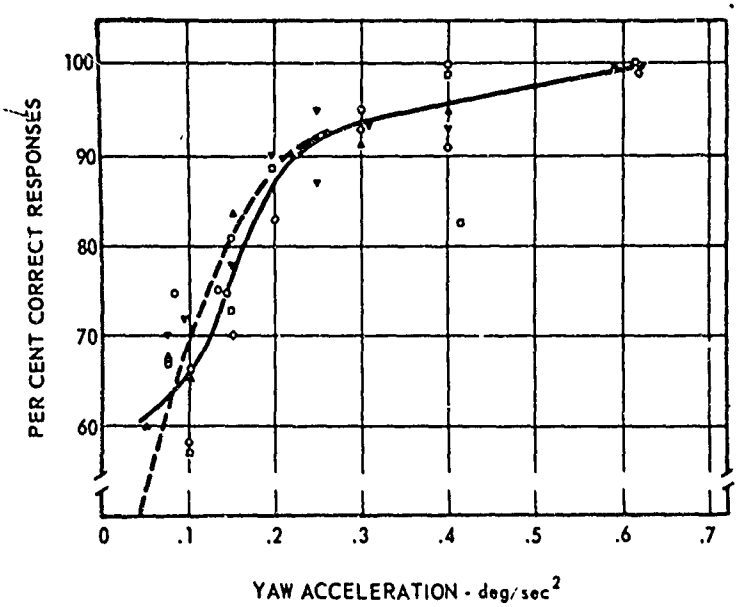


Figure 5–8. Perception of angular acceleration. Correct direction-of-rotation judgments, expressed as percent of total, are plotted as a function of angular rotation (continuous line); 75% correct point is considered threshold. Also included (dashed line) is plot of 75% correct response from figure 5-7. (After Chambers, 1964, from data of others)

Performance During Rotary Acceleration

Relatively few studies have been conducted to determine performance ability during rotary acceleration, that is, with the axis of rotation passing through the body, although numerous investigations have been conducted in rotating rooms and short radius centrifuges. Much of the work on performance has been done in connection with investigation of the vestibular system and is presented in that chapter.

Visual Acuity

During natural turning movements, vestibular and visual sensory inflow act synergistically to maintain clear vision. Guedry (1968) measured visual acuity during rotary acceleration around the z-axis in seated subjects, with particular reference to the presence and intensity of concurrent nystagmus. The results are shown in figure 5-9. Rate of recovery of visual acuity is related to the magnitude of the preceding stimulus, the stronger stimuli requiring longer recovery times. In further testing, subjects were decelerated from an angular velocity of -180°/sec through 0 to +180°/sec at rates of 10°, 15°, or 30°/sec^2 for 18, 12, or 6 seconds, respectively, and visual acuity examined throughout the process. Results are shown in figure 5-10, which indicates the buildup of nystagmus and loss of visual detail during each of the three stimuli, as well as the decline of nystagmus and restoration of visual detail following each stimulus. Considerable individual difference was found among the 18 subjects, as indicated in figure 5-11.

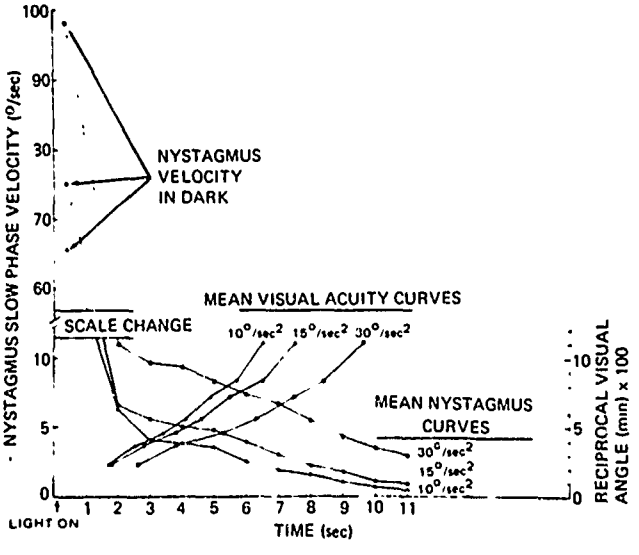


Figure 5–9. Decline of nystagmus and recovery of visual acuity following 10, 15, and 30°/sec^2 stimuli. Values are measures of means taken in initial acceleration and final deceleration of each trial. (After Guedry, 1968)

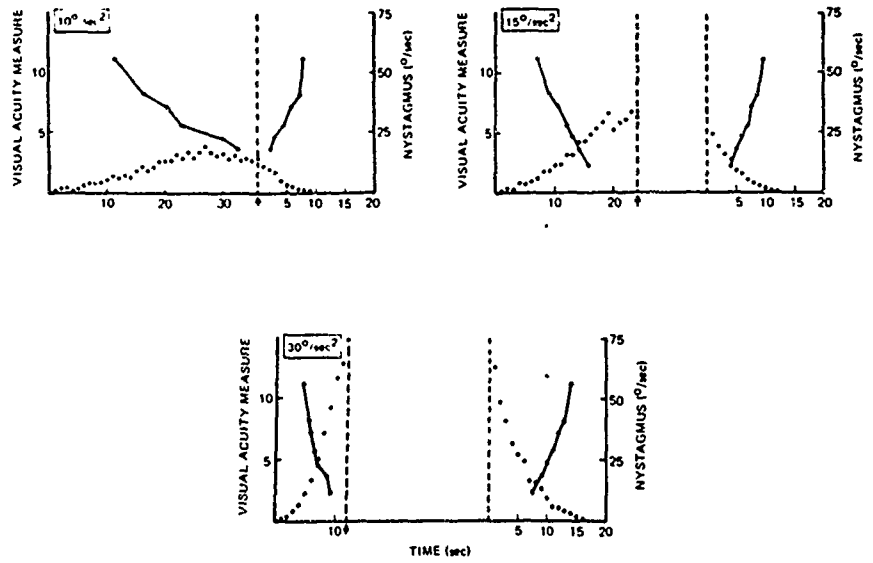


Figure 5–10. Loss of recovery of visual acuity during and after nystagmus from stimuli of different magnitudes. Blank areas were inserted in $15^{\circ}/sec^2$ and $30^{\circ}/sec^2$ results to compensate for differences in duration of stimuli and to aid in visual comparison of results. Dots are nystagmus; solid lines are visual measures; arrow marks end of stimulus. (After Guedry, 1968)

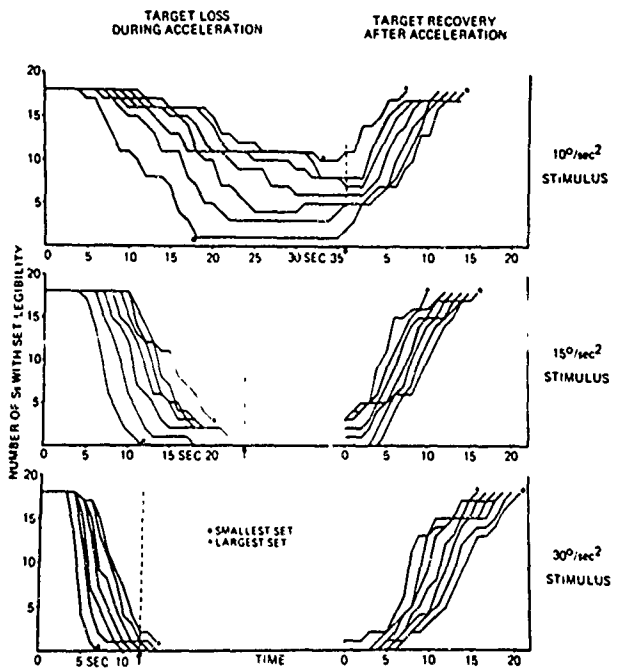


Figure 5–11. Number of subjects seeing each set of visual targets during each second of three different intensities of acceleration stimulus (10, 15, and $30^{\circ}/sec^2$) from -180°/sec through zero to $+180^{\circ}$/sec. (After Guedry, 1968)

Operational Tasks

Using the Rotational Flight Simulator (RFS) of the U. S. Air Force School of Aerospace Medicine, an air-bearing vehicle capable of simulating various rotational profiles, Lim and Fletcher (cited in Rothe et al., 1967) investigated the time required for subjects to restore the simulator to a preset position by means of a joystick after exposure to various rotations. The profiles used were a "slow random" rotation of 4 ±2 rpm and a "fast random" rotation of 12 ±4 rpm for periods of 2, 4, 8, 16, and 30 minutes. Representative results from one subject are shown in figure 5-12. Data from three subjects indicate they had different abilities in righting the RFS, that fast improvement occurred with practice, and that righting time was increased with duration of tumbling and increase of "randomness."

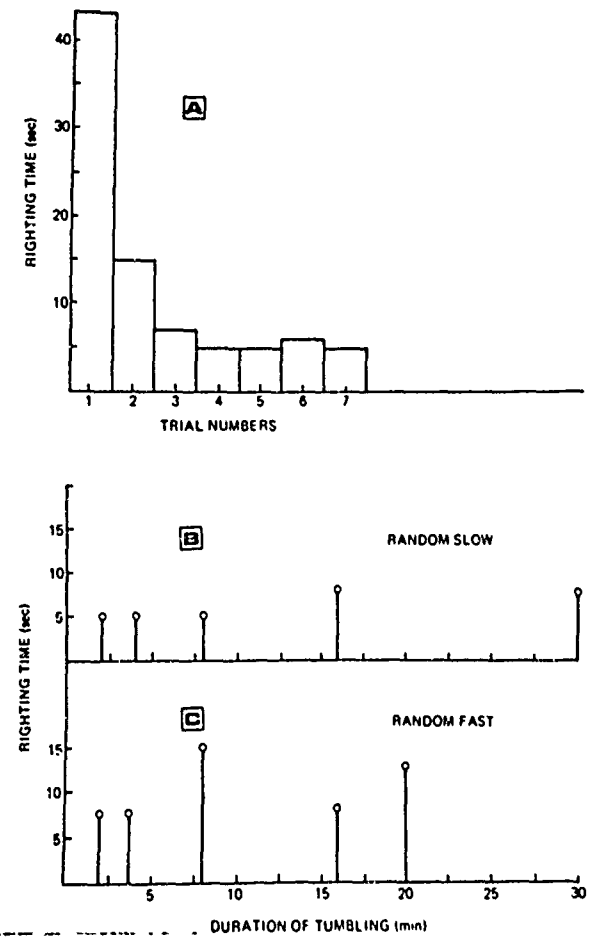


Figure 5–12. Performance of control task during slow and fast random rotation; (A) time required in successive trials to bring back RFS to upright position from initial position; (B) righting time plotted as a function of duration of random tumbling at a slow rate; (C) righting time plotted as a function of duration of random tumbling at a fast rate. (After Lim & Fletcher, cited in Rothe et al., 1967)

It may be that a rotation rate of 6 to 12 rpm is more demanding than some higher rotations, since much higher rotations have been endured with relatively little performance decrement. Using the NASA Multi-axis Test Facility, Useller and Algranti (1963) investigated the ability of pilots to determine and apply corrective torques induced at rates up to 70 rpm. Performance error was determined as a percentage of the total time during which incorrect torque was applied. Error ranged from 6.5 percent to 18 percent, depending on the individual, and was independent of the rate of rotation.

In another form of operational performance task, Weiss and his colleagues (1954) examined the ability of subjects to release a lapbelt (5-lb spring tension) and pull a ripcord (20-lb spring tension) while being exposed to rotations around the y-axis (pitch) of up to 100 rpm with the center of rotation at the heart level, and up to 75 rpm with the center at the iliac crest, or hip. Results are shown in table 5-2. A slight increase in reaction time is observed during the constant speed portion of the run and during the "deceleration" phase. The effect of the deceleration phase is accentuated by requiring the subject to reach out and actuate a toggle switch before releasing the lapbelt. Results of this added test are shown in table 5-3.

Numerical Processing and Coding

Using a sophisticated All-Altitude Air-Bearing Research and Training Simulator (ARTS), Fletcher (1968) examined numerical processing performance during rotations of 3 to 24 rpm in eight individual axes. Tests involved simple arithmetic tasks conducted in four modes: auditory (with verbal response), visual (with remote control of presentation by subject), manipulatory (with digital manipulation of cards by subject), and "flying" (with digital manipulation of cards and instructions to look up and focus on a distant object as though flying, between each numerical task). Task response was measured as time to completion. Table 5-4 indicates overall results of the procedure. Table 5-5 indicates the rank order of speed of performance in the four modes at 3 rpm in the pitch axis, and the rank order of all tasks in eight rotational modes at 3 rpm.

The improved performance at higher rotation rates is shown by the work of Weiss and coworkers (1954) who used coded lights, coded sounds, and verbally presented arithmetic problems as measures of performance. Results of tests during rotation in the pitch axis at about 100 rpm with center of rotation at heart level or 75 rpm at the level of the iliac crest showed "virtually no errors attributable to spinning, and no increase in the time required to answer. Answers to simple arithmetic problems were invariably correct and no subjective confusion was reported."

Physiological Effects of Rotary Acceleration

The primary factor involved in the production of physiological change during rotary acceleration, as with other forms of sustained acceleration, is

the development of a hydrostatic pressure head along the vector of acceleration (see chapter 4, *Sustained Linear Acceleration*). In rotary acceleration, however, with the axis of rotation passing through the body, two opposite vectors exist at the same time, their intensities being dependent on the site of the axis. In addition, rotation has a highly characteristic effect on the vestibular system (see chapter 12).

Table 5–2

Time Required for Release of Lapbelt and Parachute Ripcord During Various Phases of Rotation Around the Pitch Axis at 100 rpm

Subject	Before Spin	During Steady Spin	During Deceleration	After Spin
Time from Switch to Lapbelt Release (sec)				
R.L.	1.68	1.80	1.40	1.10
H.S.	1.04	— —	1.20	1.40
R.E.	1.32	1.10	——	——
H.N.	1.06	1.21	0.87	1.27
R.M.	1.18	1.07	1.27	1.17
J.R.	1.16	0.84	1.37	1.72
E.S.	1.15	1.12	1.08	1.00
J.S.	1.31	1.25	1.87	1.70
H.S.	1.35	1.66	1.63	1.05
AVERAGE	1.25	1.25	1.33	1.30
Time from Lapbelt to Ripcord Pull (sec)				
R.L.	1.16	1.65	1.40	1.10
H.S.	1.09	1.30	1.40	1.30
R.E.	1.30	0.97	——	——
H.N.	1.29	1.36	1.41	1.69
R.M.	1.17	1.13	1.73	1.50
J.R.	1.05	1.43	1.19	1.01
E.S.	1.10	0.95	0.80	1.21
J.S.	0.80	1.00	1.32	1.23
H.S.	1.26	1.45	1.30	1.22
AVERAGE	1.14	1.25	1.32	1.27

(After Weiss et al., 1954)

Cardiovascular–Theoretical Considerations

As noted above, the site of the center of rotation is critical in determining physiological effects. A centrifugal force directed away from the heart produces

Table 5–3

Time (sec) Required to Actuate a Switch at Arm's Length in Front of Chest During Various Phases of Rotation at 100 rpm Around the Pitch Axis

Subject	Before Spin	During Steady Spin	During Deceleration	After Spin
R.L.	0.75	0.80	1.80	0.90
H.S.	1.04	Missed	1.70	1.70
R.E.	0.69	1.29	—	—
H.N.	0.73	0.52	1.27	0.79
R.M.	0.63	0.60	—	0.60
J.R.	0.76	1.72	1.80	1.07
E.S.	0.71	0.88	1.73	0.93
H.S.	1.18	0.90	1.66	0.80
AVERAGE	0.81	0.96 (Discounting miss)	1.66	0.97

(After Weiss et al., 1954)

Table 5–4

Performance of Visual, Auditory, and Manipulatory Tasks During Rotation Around Various Axes

Number of subjects: 17

Number of test runs: 78

Modes tested: Pitch

Pitch forward

Roll

Yaw

Pitch + roll

Roll + yaw

Pitch + yaw

Pitch + roll + yaw

Random

Range: 3 – 24 rpm

Typical results: A 21% performance decrement in four men exposed to 6-rpm rotation in random axes while performing visual, auditory, and manipulating tasks

(After Fletcher, 1968)

an increment of pressure in both the venous and arterial sides of the circulatory system. Flow would continue unabated were it not for the highly distensible venous bed. When pooling in this bed is sufficient, the return of blood to the heart will be inadequate and cardiac output will fall. If this fall produces a pressure drop in the cerebral circulation greater than the increase in hydrostatic pressure occasioned by the rotation, cerebral hypoxia will ensue. When the center of rotation is moved towards the feet, the hydrostatic column to the foot is shortened and a lesser degree of pooling can be expected. Conversely, of course, the negative acceleration ($-G_z$) effects on the cerebral circulation can be expected to increase. Movement of the center of rotation toward the head will increase the positive acceleration ($+G_z$) effects. Thus, final effects are governed by both the rate of rotation and the position of the center of rotation (Edelberg et al., 1954).

Figure 5-13 is a model of hydrostatic pressure variation secondary to rotation in the pitch axis perpendicular to the Earth's gravitational field for a man 67 inches tall. The point of hydrostatic indifference is considered here to be at the level of the diaphragm.

Table 5–5

Performance Decrement in Four Simple Numeric Processing Tasks

Rank order for four tasks at 3 rpm (pitch)

1. Auditory input
2. Simulated visual flying task
3. Visual input
4. Simulated manipulation flying task

NOTES: Largest increase in time taken (auditory): 3.9 sec
Smallest increase in time taken (manipulation): 2.5 sec
Optimum time for test (0 rpm): 20.6 sec
Change: 12% to 19%

Rank order of eight rotational modes at 3 rpm (all tasks)

1. Random
2. Roll + yaw
3. Pitch
4. Roll + pitch
5. Yaw
6. Roll
7. Roll + pitch + yaw
8. Pitch + yaw

NOTES: Largest increase in time taken (random): 4.3 sec
Smallest increase in time taken (pitch and yaw): 2.6 sec
Optimum time for test (0 rpm): 20.6 sec
Change: 12% to 21%

(After Fletcher, 1968)

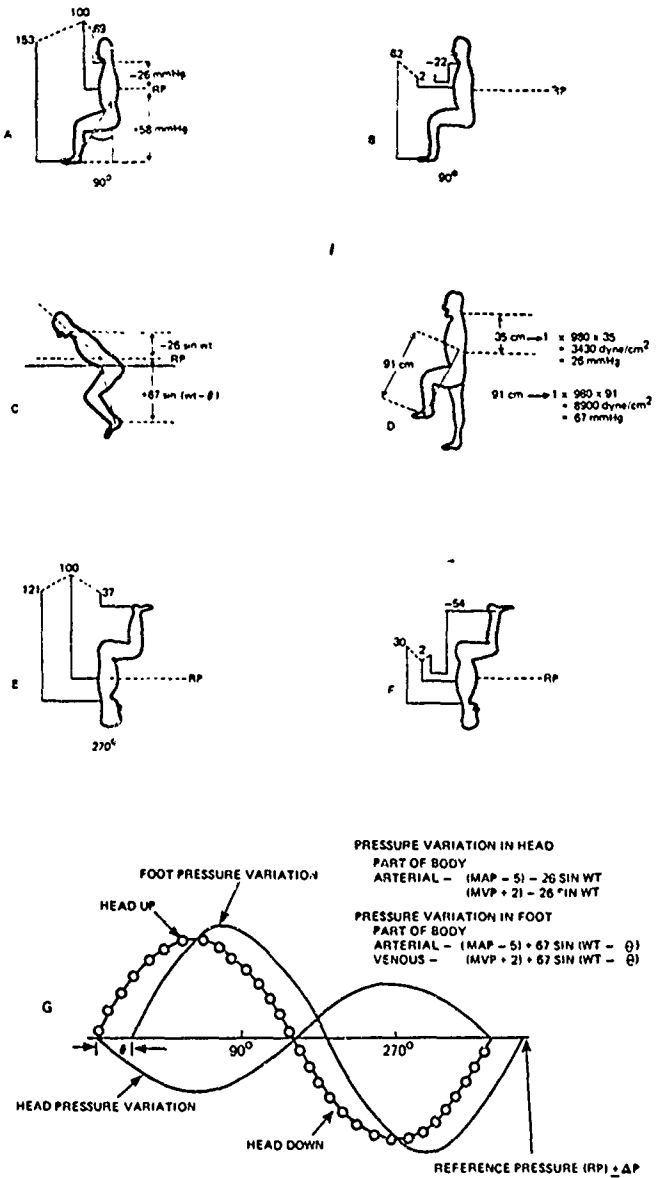


Figure 5–13. Simplified model of hydrostatic pressure variation secondary to rotation in pitch axis. In A, B, E, and F are indicated expected mean arterial pressure (A and E) and venous pressures (B and F) in the neck, diaphragm, and feet levels when subject is at 90° and 270° positions. C and D illustrate calculation of hydrostatic pressure components from anatomical considerations and their sinusoidal variations. In G is shown expected hydrostatic pressure variation in head and feet. Circled sine wave refers to body position where maximum point corresponds to the head-up position and minimum point to head-down position. Maximum hydrostatic pressure at foot area lags head-up position by angle θ since subject is in sitting position. MAP = mean arterial pressure; MVP = mean venous pressure. 5 and 2 are hypothetical pressure drops along arterial and venous vessels, respectively. (After Lim & Fletcher; cited in Rothe et al., 1967)

Cardiovascular Response to Rapid (70 to > 100 rpm) Rotation

Figures 5-14 and 5-15 illustrate some of the cardiovascular findings in human subjects rotated around the z-axis (yaw) with the center of rotation at the heart or the hips. The electrocardiogram (ECG) exhibits changes in the QRS and T vectors, which are probably the result of anatomical motion of the heart within the chest, as well as transient extrasystoles (abnormal beats). Some of these results are delineated in table 5-6. Table 5-7, from the work of Urschell and Hood (1966), shows further aspects of change in blood pressure and heart rate.

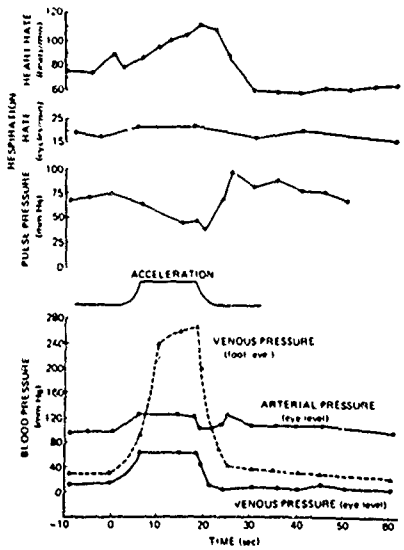


Figure 5–14. Effect on human heart rate, respiration rate, pulse pressure, blood pressure of spinning around z-axis at 106 rpm with center of rotation at the heart. After Weiss et al., 1954)

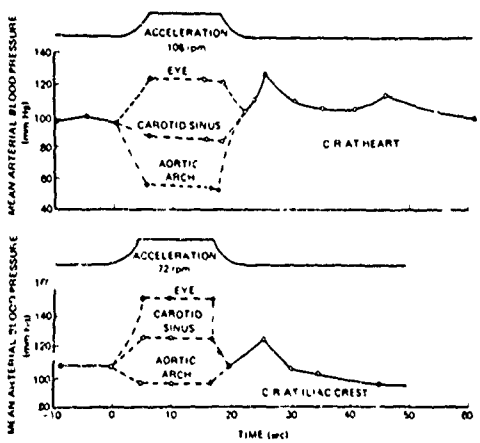


Figure 5–15. Mean arterial blood pressures at eye level, carotid sinus, and aortic arch during rotation around z-axis at 106 rpm with center of rotation at the heart (upper figure); and at 72 rpm with center of rotation at the iliac crest (lower figure). (After Weiss et al., 1954)

Table 5–6

ECG Changes Associated with Rotation Around the Pitch Axis

ECG Component	No. of Subjects	Average Starting Values and SE	Average Change from Starting Values and SE	
		Before Tumbling	During Tumbling (96–118 rpm)	After Tumbling
Center of Rotation at Heart (96–118 rpm)				
Heart rate (bpm)	12	83.0 ±4.2	10.0 ±2.7**	–26.0 ±2.8**
P–R interval (sec)	12	0.18 ±0.011	– 0.01 ±0.006	0.01 ±0.005*
Q–T interval (sec)	12	0.40 ±0.007	0.03 ±0.007**	– 0.04 ±0.006**
QRS–T angle (degrees)	12	14.1 ±3.06	– 4.6 ±3.18	1.8 ±1.49
Center of Rotation at Iliac Crest (75 – 93 rpm)				
Heart rate (bpm)	7	89.0 ±5.6	–22.0 ±3.1**	8.0 ±3.9
P–R interval (sec)	7	0.17 ±0.012	0.0 ±0.005	– 0.01 ±0.005
Q–T interval (sec)	7	0.41 ±0.017	– 0.08 ±0.012**	– 0.03 ±0.016
QRS–T angle (degrees)	7	22.1 ±8.96	6.0 ±2.67	– 2.7 ±2.42

*Significant at the 0.05 level.
**Significant at the 0.01 level.
(After Weiss et al., 1954)

Cardiovascular Response to Slow (1 to 15 rpm) Rotation

Lim and Fletcher (cited in Rothe et al., 1967) examined the heart rate response to relatively slow rotation with the center of rotation at heart level. They recognized three different types of response in 82 exposures studied. Type I response, where the heart rate from cycle to cycle shows a minimum of scatter, is illustrated in figure 5-16. Superimposed is a sine wave representing the subject body position, 90° being head-up and 270° head-down. It will be noted that heart rate "tracks" the body position curve with increase in the head-up position and decrease in the head-down position. Type I response was observed in all but the very slow and very fast rates of rotation. The maximum heart rate, however, lags the 90° position, and the lag increases as the rotation rate increases. Type II response, with more scatter evident, is found at very low rates (1 to 2 rpm), and is shown in figure 5-17. Type III response, in which little or no correlation is observed between heart rate and body position, is found in those situations where the half cycle period of the rotational rate approaches the maximum heart period. The response is illustrated in figure 5-18. Lim and Fletcher suggest that the type III response may be due to the prolonged time constant of the parasympathetic response as compared with the sympathetic, such that the heart is still under vagal control when the subject comes up to and passes through the head-up position.

Table 5–7

Heart Rate and Blood Pressure Changes at End of Constant Velocity Phase of Exposure (3 min) to Rotation (120 rpm) in the Roll Axis

Slow Onset					
Subject	Pulse	Systolic Pressure	Diastolic Pressure	Mean Pressure	Pulse Pressure
Tu	+40	+13	+18	+13	− 5
H	+74	−20	+ 6	− 8	−26
B	+66	−34	−16	−18	−18
Ta	+67	−45	−20	−24	−15
Te	+70	−55	− 4	−22	−51
Means	+63 ±6 $p < 0.001$	−28 ±12	−3 ±7	−12 ±7	−23 ±8 $p < 0.01$

Fast Onset					
Subject	Pulse	Systolic Pressure	Diastolic Pressure	Mean Pressure	Pulse Pressure
Tu	+62	−21	− 2	− 6	−19
H	+61	−54	−24	−30	−30
B	+30	−30	+ 1	−12	−30
Ta	+74	−43	−16	−23	−27
Te	+76	−35	+ 1	− 6	−36
Means	+61 ±8 $p < 0.005$	−37 ±5 $p < 0.005$	−8 ±5	−15 ±5 $p < 0.01$	−28 ±3 $p < 0.001$

(After Urschell & Hood, 1966)

The cardiac rate tracking phenomenon no doubt reflects carotid sinus stimulus, with phase lags related to complex interrelationships of blood vessel wall impedance, blood fluid inertia, and reflex vasomotor responses. Blood pressure readings taken immediately before and after various runs of 3 minute duration on the roll and pitch axes are presented in table 5-8. No trend can be observed at the rates recorded in either systolic or diastolic levels.

For slow rotation, just as for fast rotation, changes occur in the form of the ECG as the axis of rotation changes (Rothe et al., 1967). The variation is different from one subject to another, but reproducible for the same subject. The changes are more pronounced in random axis rotation than in pure axis rotation. No irregularities or arrhythmias have been observed during slow rotation.

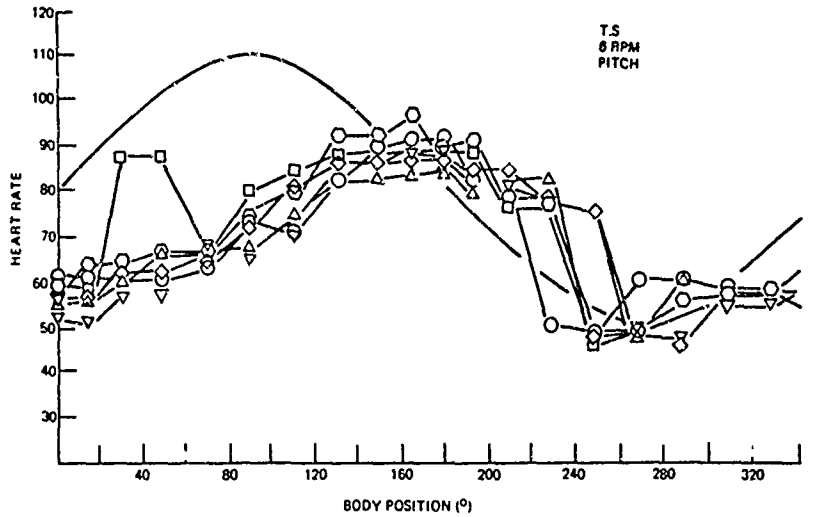


Figure 5–16. Type I heart rate response to rotation (6 rpm in pitch axis) in axis perpendicular to Earth's g field plotted as a function of body position. (After Lim & Fletcher, cited in Rothe et al., 1968)

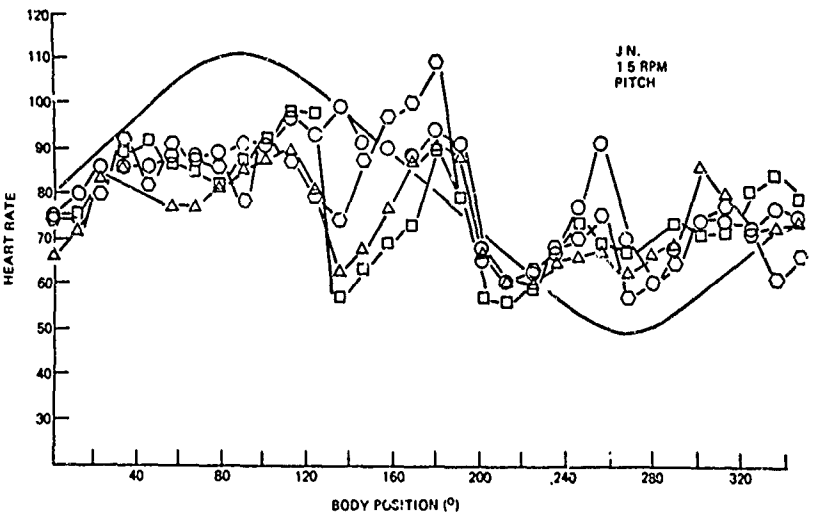


Figure 5–17. Type II heart rate response to slow (1.5 rpm in pitch axis) rotation in axis perpendicular to Earth's g field plotted as a function of body position. (After Lim & Fletcher, cited in Rothe et al., 1968)

Cardiovascular Response to G_z 100 Percent Gradient Spin

While the distribution of vascular pressures is somewhat different during 100 percent gradient G_z spin as compared with rotary acceleration, it is markedly different from that found in long radius sustained acceleration, and is illustrated in figure 5-19. In high gradient spin, pressures in the head and neck

are little altered from normal while in low gradient configurations, central nervous system blood flow is maintained against a large head of pressure. The limitation to CNS blood flow in high gradient spin is not insufficient perfusion pressure but lowered cardiac output occasioned by insufficient venous return, although the impedance to venous return is, in fact, less in high gradient spin than in long arm configuration (Piemme et al., 1966).

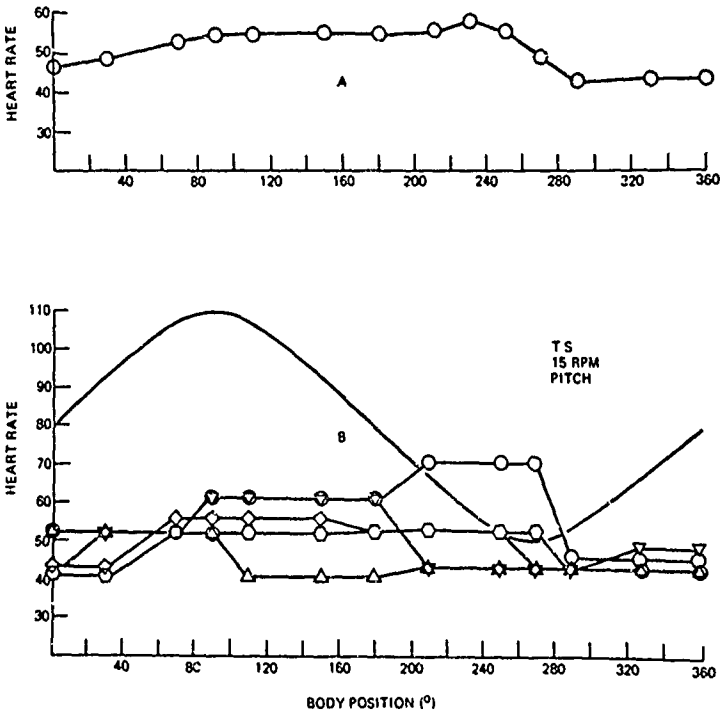


Figure 5–18. Type III heart rate response to fast pitch rotation at 15 rpm; (A) heart rate response of 6 cycles averaged at each body position, (B) cycle to cycle heart rate variation. (After Lim & Fletcher, cited in Rothe et al., 1968)

Mean pulse rates for subjects undergoing 100 percent gradient Gz spin are presented in figure 5-20. At lower G levels, some increase in pulse rate is found with onset of acceleration but this rapidly subsides to control levels. At higher G levels, rates increase progressively to termination of the experiment. No arrhythmias or other cardiac irregularities have been observed (Piemme et al., 1966).

Other Physiological Findings

Apart from investigations of the cardiovascular and vestibular parameters noted above and in the chapter concerning the vestibular system (chapter 12), very little attention has been paid to other physiological effects of rotary acceleration. During high speed rotation in dogs, Edelberg and coworkers (1954) noted that at rates above 140 rpm with the center of rotation at the heart level,

respiration is inhibited. He attributes the apnea to pull on lung stretch receptors. When the center of rotation is moved tailward, however, respiration is maintained. In humans rotating at 106 rpm, respiration is still maintained, according to Weiss and coworkers (1954). Fletcher (1968) also notes that respiration, which tends to be rapid and shallow at 30 rpm, slows and becomes deeper at lower rotation rates. The subject in pitch rotation may, in fact, breathe synchronously with the inversion cycle.

Table 5–8

Blood Pressure Values Before and After Rotation in the Roll Axis

Subject		RPM*								BP Reading
		2	4	6	8	10	12	14	16	
J.N.	Pre-run	130	125	125	105	120	–	125	115	S**
		80	70	75	70	75	–	70	75	D**
	Post-run	125	120	105	130	105	–	115	–	S
		80	75	70	80	70	–	75	–	D
E.O.	Pre-run	125	135	125	125	–	110	115	110	S
		80	75	75	75	–	80	75	70	D
	Post-run	–	125	125	120	–	110	115	125	S
		–	80	75	70	–	70	75	80	D
A.R.	Pre-run	110	115	105	110	120	120	–	–	S
		70	70	75	60	75	75	–	–	D
	Post-run	115	130	115	110	120	120	–	–	S
		70	70	70	70	75	70	–	–	D
A.S.	Pre-run	130	130	130	–	135	130	–	140	S
		85	75	70	–	80	80	–	70	D
	Post-run	130	135	140	130	130	135	–	140	S
		70	65	70	75	70	70	–	80	D
T.S.	Pre-run	115	110	110	110	125	130	135	–	S
		65	65	80	70	80	–	70	–	D
	Post-run	115	115	110	120	115	130	135	–	S
		75	75	65	75	70	80	80	–	D
R.D.	Pre-run	110	–	120	125	125	105	–	–	S
		70	–	75	75	75	75	–	–	D
	Post-run	130	125	125	110	105	120	–	–	S
		90	80	70	75	75	80	–	–	D
V.R.	Pre-run	–	135	125	130	–	125	–	–	S
		–	65	80	70	–	70	–	–	D
	Post-run	–	125	125	135	125	125	–	–	S
		–	75	75	70	70	70	–	–	D

*Revolutions per minute are midpoint rotational rate of class intervals.

**S – systolic; D – diastolic.

(Rothe, et al., 1967)

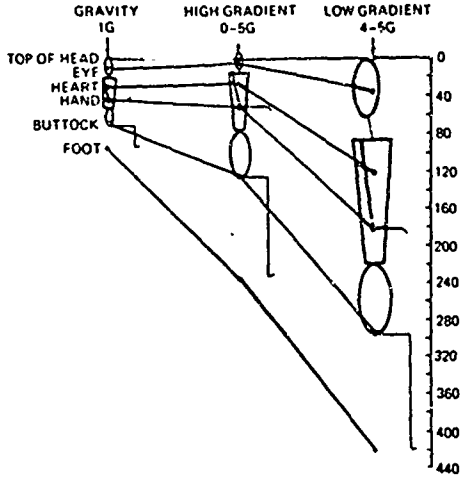


Figure 5–19. Physical pressures (mm Hg) in absence of compensatory vascular reflexes at each level of the body in high gradient vs low gradient acceleration. At the feet, in each of the two figures to the right, a 5 G pressure exists. The difference in pressures against which the heart must perfuse the central nervous system in each case amounts to little if any more than normal physiologic pressures in high gradient acceleration, as opposed to 100 or more mm Hg in the low gradient profile. (After Piemme et al., 1966)

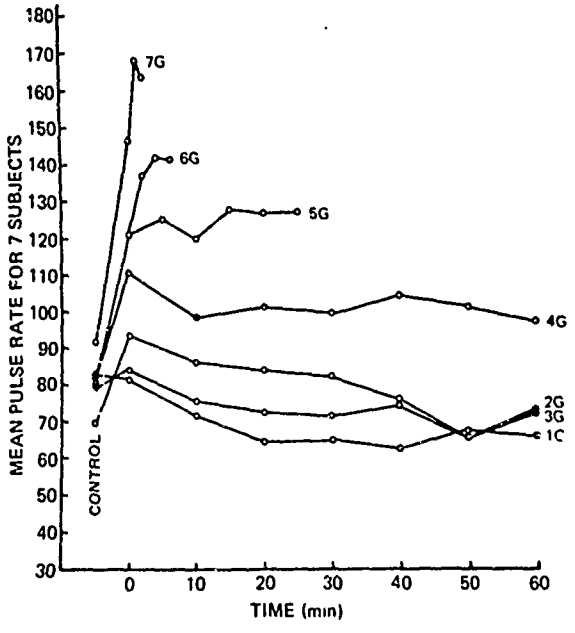


Figure 5–20. Pulse rates of seven subjects as a function of duration of exposure to $+G_z$ 100% spin around the x-axis with center of rotation tangential to the head. Time zero identifies onset of 3 min plateau of constant angular velocity. Each point represents mean for all subject veins at each level. (After Piemme et al., 1966)

Pathological Effects of Rotary Acceleration

The pathological effects of rotary acceleration, that is, those resulting in injury, have been studied to a very slight extent in animals and observed occasionally in man. Table 5-9 presents a summary of postmortem findings in dogs after 1 minute exposures at 195 rpm in the pitch axis. In addition, frequent nasal, oral, and conjunctival hemorrhage have been observed in dogs, occasionally associated with rectal bleeding (Edelberg et al., 1954). Extrapolation of animal findings to man must always be done with caution, but it is reasonable to assume that similar effects might be expected.

Table 5–9

Summary of Results of Postmortem Examination of Eleven Dogs after Rotation Around the Pitch Axis at 195 rpm (one to five runs, 1 min each)

Organ	Description	Positive Cases	Negative Cases
Brain	Macroscopic cerebral hemorrhage	4	7
	Microscopic cerebral hemorrhage	5	6
	Hyperemic	6	5
Heart	Subendocardial hemorrhage	2	9
Lung	Atelectasis	4	7
	Hyperemia or edema	8	9
	Hemorrhage	2	9
Viscera	Hyperemia	7	4
	Rectal hemorrhage	1	10

(After Edelberg et al., 1954)

Humans have not been exposed to the same intensity of exposure, but conjunctival petechiae (pinpoint bleeding into the white of the eye) have been found along with petechiae on the top of the foot. Figure 5-21 illustrates the occurrence of conjunctival hemorrhage at various rotation rates (Weiss et al., 1954). Urschell and Hood (1966) note that all their subjects, spun around the z-axis, developed petechiae on the hands and feet during their rotation at 120 rpm. One experimental subject, following a 4 minute exposure to 60 rpm, developed convulsions 3 hours later. These were attributed to a blood clot in the brain (cerebral embolus), although no other neurological findings were demonstrated (Urschell & Hood, 1966). The incident, although isolated, appears nevertheless to be significant.

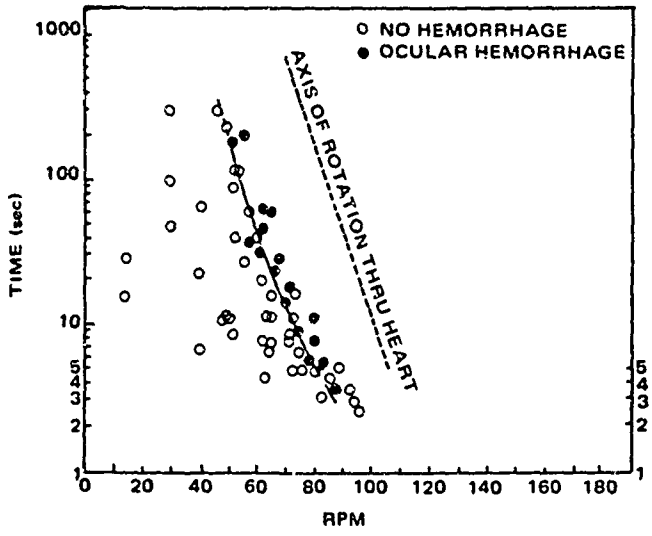


Figure 5–21. Incidence of conjunctival hemorrhage during rotation at various rates around pitch axis. Note that time in ordinate refers to duration of exposure. (After Weiss et al., 1954)

References

Chambers, R. M. Acceleration. In P. Webb (Ed.), Bioastronautics Data Book. NASA SP-3006, National Aeronautics and Space Administration, Washington, D.C., 1964.

Clark, B. Thresholds for the perception of angular acceleration in man. *Aerospace Medicine*, 1967, *38*, 443-450.

Clark, B., & Stewart, J. D. Effects of angular acceleration on man. *Aerospace Medicine*, 1969, *40*, 952-956.

Clark, B., & Stewart, J. D. Perception of angular acceleration about the yaw axis of a flight simulator: Thresholds and reaction latency for research pilots. *Aerospace Medicine*, 1962, *33*, 1426-1432.

Courts, D. E. Tolerance to spinning in ejection escape. *Aerospace Medicine*, 1966, *37*, 133-135.

Edelberg, R. The physiology of combined acceleration. In O. H. Gauer and G. D. Zuidema (Eds.), *Gravitational stress in aerospace medicine*. Boston: Little, Brown, and Co., 1961, Pp. 140-149.

Edelberg, R., Weiss, H. S., Charland, P. V., & Rosenbaum, J. I. The physiology of simple tumbling. (Part I) Animal studies. WADC-TR-53-139, Wright-Patterson Air Force Base, Ohio, 1954.

Fletcher, J. G. Further physiologic research on human tumbling. USAF-SAM-TR-68-109, Brooks Air Force Base, Texas, 1968.

Guedry, F. E. Relations between vestibular nystagmus and visual performance. *Aerospace Medicine*, 1968, *39*, 570-579.

McCabe, B. F. Vestibular suppression in figure skaters. *Trans. Amer. Aero. Ophthal. Otolaryng.*, 1960, *64*, 264-268.

Meiry, J. L. The vestibular system and human dynamic space orientation. NASA CR-64545, National Aeronautics and Space Administration, Washington, D.C., 1965.

Pesman, G. J. Acceleration terminology. In *Principles of biodynamics, prolonged acceleration: Linear and radial.* AGARD, Biodynamics Committee, NATO, 1968, Pp. 1-6.

Piemme, T. E., Hyde, A. S., McCally, M., & Potor, G. Human tolerance to G_z 100% gradient spin. *Aerospace Medicine,* 1966, *37,* 16-21.

Roth, E. M. (Ed.) Compendium of human responses to the aerospace environment. (Vol. II Section 7) NASA CR-1205 (II), National Aeronautics and Space Administration, Washington, D.C., 1968.

Rothe, W. E., Pope, E. E., Lim, S. T., & Fletcher, J. G. Research on the human physiologic response to prolonged rotation and angular acceleration. USAF SAM TR-67-69, Brooks Air Force Base, Texas, 1967.

Urschell, C. W., & Hood, W. B. Cardiovascular effects of rotation in the z-axis. *Aerospace Medicine,* 1966, *37,* 254-256.

Useller, J. W., & Algranti, J. S. Pilot reactions to high speed rotation. *Aerospace Medicine,* 1963, *34,* 501-504.

Weiss, H. S., Edelberg, R., Charland, P. V., & Rosenbaum, J. I. The physiology of simple tumbling. (Part 2) Human studies. WADC-TR-53-139, Wright-Patterson Air Force Base, Ohio, 1954.

CHAPTER 6
IMPACT

by

Richard G. Snyder, Ph.D.
University of Michigan

The limiting factor of all methods of emergency escape and crash survival protection is the tolerance of the occupants to accelerative forces. Abrupt acceleration, deceleration, or impact is characterized by forces of very abrupt onset, short duration, and high magnitude. It is generally considered that impact involves the occurrence of forces of less than 0.2-second duration (Stapp, 1961b). Some abrupt impact conditions to which aerospace or aircrews may be exposed include astronaut pre-lift-off tower escape, lift-off abort, ejection seat or modular capsule firings, launch vehicle staging, escape device parachute deployment, flight instability, clear air turbulence, aircraft or aerospace vehicle crash landing, and capsule water or land touchdowns. In situations such as saw-toothed accelerations produced by successive rockets firing in multistage propulsion systems, in extreme turbulence, or in many crash landings where multiple contacts are made with trees or other objects, the occupants will be exposed to a series of separate impacts. The tolerances of the human component of the abruptly decelerated system are related to the elastic and tensile limits of the tissues involved, as well as to profound physiologic, psychologic, and metabolic effects.

Our current state of knowledge concerning human impact tolerances is very incomplete. While most human volunteer studies have been conducted on young healthy male subjects under rigidly controlled conditions with careful medical monitoring, they have been voluntarily terminated at levels below that of irreversible injury. No experimental impact data are available for females, children, or other segments of the population, and, due to the range of human variability, data derived from volunteer male subjects must be used with caution in other applications.

Animals have been used extensively to obtain physiological data at impact levels above those potentially injurious to the human volunteer. Cadavers offer a

Reviewed by Randall M. Chambers, Ph.D., NASA Langley Research Center

Preceding page blank

means of determining structural limits of tissues, but cannot provide the physiological information which must be obtained on living systems. Accidental free-falls have provided still another means of determining human tolerances to extreme impacts beyond those to which human volunteers may be subjected in the laboratory. Other estimates of impact tolerance are obtained from clinical studies of impact trauma and from reconstruction of automotive, aircraft, or space vehicle accidents. While both mathematical modeling and anthropomorphic dummies are used extensively as tools to provide predictions, particularly of body kinematics and force-mass relationships within the body during impact, such simulations can be no more accurate than the very limited biological input information available.

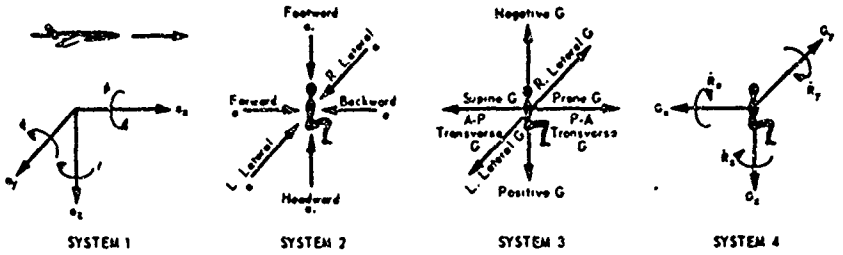
Determination of human tolerances to impact is complicated by many other physical factors influencing the outcome, including tightness and configuration of restraint and support (seat); body orientation; equipment such as helmets or parachute chestpacks, which can alter the force distribution on the body; and the magnitude, direction, distribution, duration and pulse shape of the force resulting from the impact. In addition, biological factors including sex, age, and physical and mental condition have been identified as influencing survival. Individual variability must be considered, for tolerance under identical test conditions will vary in the same individual as well as from person to person. Furthermore, while considerable data are available concerning impact forces in some body orientations, such as in forward or aft-facing positions, less is known of the effects in other orientations, such as in lateral impact. Limited experimental studies of exposure to simultaneous forces or to off-center forces have been conducted. Such conditions also greatly influence tolerance.

It is not possible to state precisely what human tolerance to impact forces is without defining the specific conditions involved. It is the intent of this chapter to present a summary of the known data concerning human tolerance to impact.

Terms and Definitions

The biophysical terminology employed in the field of impact is generally consistent with terms used in the field of sustained acceleration. Some specialized meanings and distinctions have, however, developed. Most work is identified by descriptive terminology, such as forward, rearward or aft, headward, footward, or right or left lateral accelerations. Physiologically, the subject's orientation can be described in relation to the force, and, since 1961, terms using the x, y, z axis (table 6-1) have been recommended by the Biodynamics Committee of the Aerospace Medical Panel, AGARD, as the standard description for simple uniaxial accelerations (Gell, 1961). The physiological standard (System 4 in the table) is recommended as the universal system. Air Force or Navy investigators may use the vernacular description relating "eyeballs" movement in inertial response to the applied acceleration.

Table 6–1
Comparative Table of Equivalents



SYSTEM 1 SYSTEM 2 SYSTEM 3 SYSTEM 4

LINEAR MOTION	TABLE A Direction of Acceleration	
	Aircraft Computer Standard (Sys 1)	Acceleration Descriptive (Sys. 2)
Forward	$+a_x$	Forward accel.
Backward	$-a_x$	Backward accel.
Upward	$-a_z$	Headward accel.
Downward	$+a_z$	Footward accel.
To Right	$+a_y$	R Lateral accel.
To Left	$-a_y$	L. Lateral accel.

LINEAR MOTION	TABLE B Inertial Resultant of Body Acceleration		
	Physiological Descriptive (Sys 3)	Physiological Standard (Sys 4)	Vernacular Descriptive
Forward	(1, 2) Transverse P–A G Prone G Back to chest G	$-G_x$	Eyeballs In
Backward	Transverse A–P G Supine G Chest to Back G	$+G_x$	Eyeballs Out
Upward	Positive G	$+G_z$	Eyeballs Down
Downward	Negative G	$-G_z$	Eyeballs Up
To Right	Left Lateral G	$+G_y$	Eyeballs Left
To Left	Right Lateral G	$-G_y$	Eyeballs Right

Since body orientations and resultant inertial responses in off-axis impacts may involve complex multiaxial accelerations, a three-dimensional description is often used and expressed in terms of degrees of roll, pitch, and yaw relative to horizontal flight on a polar coordinate system. In the neutral position of 0-0-0 the crewman is seated upright facing toward the point of impact (figure 6-1). In the 0-5-180 orientation, a crewman would be seated upright, five degrees back from perpendicular with the back facing the point of impact. Inertail forces in this orientation are directed from anterior to posterior (Hanson, 1965). Similarly, 0-55-90 orientation would indicate a $+G_y$ (eyeballs left) impact, 55 degrees back from the perpendicular, and 0-0-270 would correspond to a $-G_y$ (eyeballs right) impact.

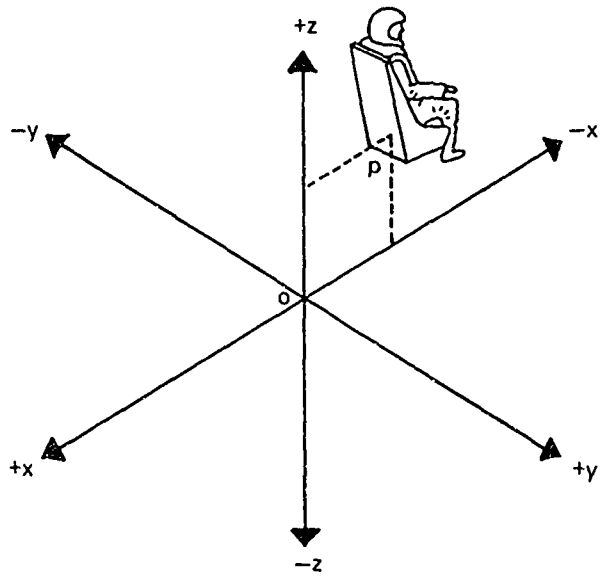


Figure 6–1. Coordinates for describing location of subject within an impact environment. (Modified from Coburn, 1970; Gell, 1961; revised 1966b by AGARD Biodynamics Panel).

Historically, confusion of terminology has existed between researchers in the fields of impact and sustained acceleration. Early impact experimentation was accomplished on deceleration test devices, where the direction of force acting on the test subject is opposite to that which occurs in acceleration, even though the direction of motion is the same. Thus a test described as "forward facing impact" (deceleration) is equivalent to backward acceleration.

Understandably, despite efforts toward standardization, some confusion still exists. One reason for this is the limitation of the term "G" to the inertial reaction of the subject. This poses no problem to the investigator working in steady state acceleration, since the transient response is of minor consequence with most devices capable of producing sustained acceleration. For the investigator concerned with impact, the transient response is of major importance since most end points are established by a transient peak. Because of

the time-varying nature of the transient response, the inertial reaction is continually changing. Moreover, due to the complicated reactions of the biological system, the inertial reaction varies throughout the body during the impact. Thus the specification of a single "inertial response" magnitude as a descriptor of the experiment would be of little value to the researcher in impact tolerance. Some researchers have recognized this limitation but have used the "G" magnitude to indicate the input peak rather than the response. This is advantageous for purposes of experimental control and permits relatively easy measurement with generally available equipment.

Acceleration

Acceleration is defined as the time rate of change of velocity. Since velocity is a vector, acceleration occurs when either the magnitude (speed) or the direction of motion of a body changes. Most impact test devices use a track and sled system, operating either vertically (FAA, NASA, and 6570 AMRL drop towers, or the 6571 ARL HYGE) or horizontally (such as the USAF "Bopper" or "Daisy"). The test pulse is provided either initially, as the sled accelerates to speed, or terminally as the sled is slowed or stopped from a given speed. Impact pulses may be of a variety of waveforms, either as selected by the researcher or limited by the capability of the test device. Figure 6-2 shows an example of a rectangular profile, with a relatively long plateau or "dwell" time. Rise time depends upon how rapidly peak acceleration is reached. The term rate of onset (T) is frequently used synonymously. Jolt describes the rate of change of acceleration (displacement with respect to time), and has been found to be a strong limiting factor in tolerance. A variety of controlled pulse shapes are shown by Chandler (1967). Difficulty is often encountered in describing concisely a complex impact pulse shape, and a number of techniques have been adopted to provide consistent descriptors (the most recent, Mil-S-9479A, 16 June 1967).

The "G" System of Units

Few units of measurement have been more misused and misunderstood than the unit "G." In the strictest sense, it is merely a dimensional representation of the magnitude of acceleration, expressed as a ratio of the magnitude of the measured acceleration to the magnitude of the "standard" acceleration of gravity, $G = |a|/|g_o|$. Since acceleration is a vector quantity, having properties of both magnitude and direction, the capital letter G is used to denote that only magnitudes are being compared, so that the direction of the acceleration of interest does not necessarily coincide with the direction of the acceleration of gravity. The signs and subscripts of the standard terminology, previously discussed, are an attempt to restore directionality to the G nomenclature.

Consideration of Newton's second law, stated in simplified form as F = ma, with weight defined as mass times "standard gravity" (W = mgo), can lead to the conclusion that G is also equivalent to the ratio of the force (required to accelerate the mass m at an acceleration level a) to the weight (under standard

gravitational conditions). This relationship would be stated: G = F/W. Thus G is often thought of as having both force and acceleration significance.

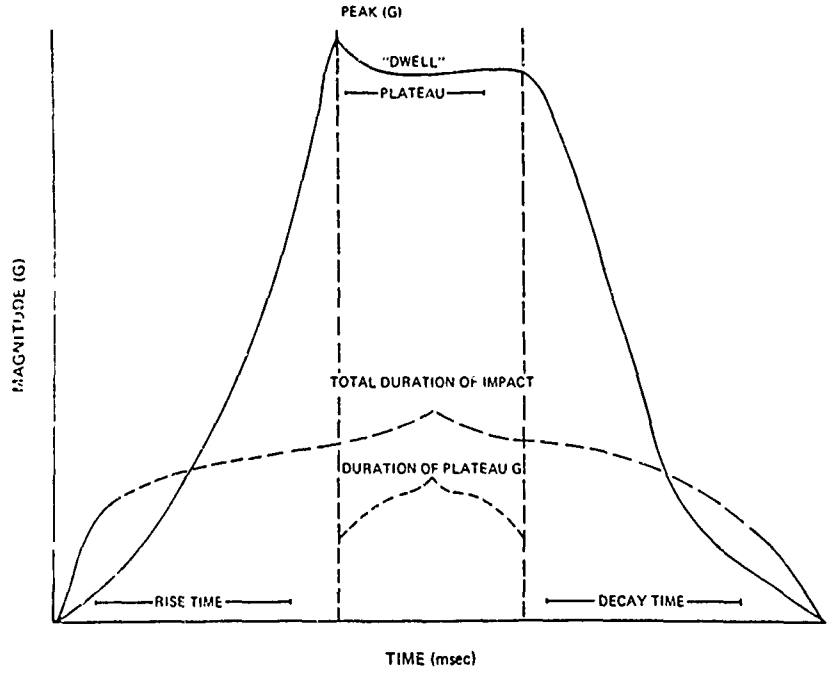


Figure 6–2. Example of rectangular-shaped impulse deceleration profile. (Adapted from Stapp, 1961)

The quantity G is dimensionless, being the ratio of two accelerations or of two forces. However, by definition it is capable of telling how much force is acting and what acceleration is taking place in a given dynamic situation. Thus, if it can be stated that a body is experiencing a certain amount of G, the total amount of force can be determined in ordinary units if the given value of G is multiplied by the standard weight Wo of the body, or F = G Wo. Similarly, G defines magnitude of acceleration, a = Ggo. Although dimensionless, G possesses the same property of direction as do the force and acceleration which it connotes. Thus, it is possible to construct G vector diagrams in place of force or acceleration diagrams when analyzing dynamic problems. G is usually thought of in respect to its "force" aspect (Dixon and Patterson, 1953).

The symbol g has been widely abused in aerospace medical literature. Although g has been rigidly established by physicists as a symbol (go) for a specific physical quantity (32.2 ft/sec^2), the acceleration of gravity, it is often indiscriminately used in place of G in the literature. In contrast to sustained acceleration, in impact a whole body can only be said to experience a certain G when that G refers to the whole body *input*, not response. On impact, each element of the body experiences a different G load, depending upon its

elastic, viscous, and/or plastic relation to the rest of the body, to the parameters of the impact pulse, to the support/restraint system, to the general structural characteristics of the test vehicle, and many other factors. Realistically, six degrees of freedom for motion of each element would have to be measured to accurately assess the force imparted. Although accelerometers have been available for at least five decades, the measurement of force and force distribution during impact has not yet been accomplished. To convert an acceleration measurement to a force measurement, one must know the mass upon which the acceleration is acting (F = ma). Due to the distributed mass and undefined interconnections of tissues encountered in the human body, the effective mass for the acceleration measured is not known. Therefore, investigators cannot yet speak of inertial force based upon body acceleration measurements without making crude guesses.

Interpreting the Data

There are other considerations which pose major problems to the impact engineer. The calibration, placement and attachment of transducers can cause artifacts in the data. Head or chest accelerometers, unless firmly attached or implanted in bone, are subject to distortion of the supporting strap or intervening tissue and result in higher acceleration readings than actually occur (Ewing, 1969). G forces may be recorded on a sled in one study and in various locations on the body in another, yet reported without distinction.

To accurately specify acceleration it would be necessary to utilize three linear accelerometers and three angular accelerometers at the same point, or provide some other means of obtaining these data. Also, acceleration measurements change from point to point on any distributed body element unless it is rigid and moving in only one linear direction without rotation. Thus, one acceleration measure, even if properly made, is not representative of the acceleration distribution over the body (Chandler, 1970). For example, in lateral run No. 2530 programmed for 10 sled G on the Holloman Bopper, peak sled G was 8.48, peak G on subject's chest was 14.47, and head G was recorded as 22.04 (Zaborowski, 1966).

Finally, results are subject to various interpretations depending upon system or computational parameters which may go unreported. For example, while most test results are presented in terms of peak G, some are given as plateau G or average G. Some investigators "round-off" or "average" multiple peaks while others report the peaks. Frequency response and damping characteristics may differ. All of these factors should temper interpretation of reported tolerance limits.

Human Tolerance Limits

Tolerances have been variously defined, and different researchers have established different end points as criteria. Bierman (1947) defined tolerance as "that value of impact or load which produces a painful reaction;" Stapp used a variety of criteria ultimately defining tolerance as the limit beyond which either the subject or the experimenter fears to go lest there be serious injury. Injury has

been termed "reversible" or "irreversible" depending upon whether or not the individual can recover. Aerospace and aviation medical research in impact has been concerned primarily with whole body response to impact forces. Most human tolerance limit data developed to date are based upon the seated, young male subject utilizing maximum body support. In the majority of tests body orientation is in relation to the four main body axes: forward ($-G_x$), rearward ($+G_x$), headward ($+G_z$), and footward ($-G_z$) acting forces. Only one series of right lateral ($+G_y$) tests with human subjects has been conducted (Brown, et al., 1966). Test results can be affected by body position, restraints, instructions given the subject prior to testing (e.g., relax or tense muscles during the test), the subject's task, etc.

In figure 6-3 data from a number of sources have been combined to illustrate impact experience documented to date. It should be noted that numerous biophysical factors influence survival, and the "approximate survival limit" shown is only an estimate.

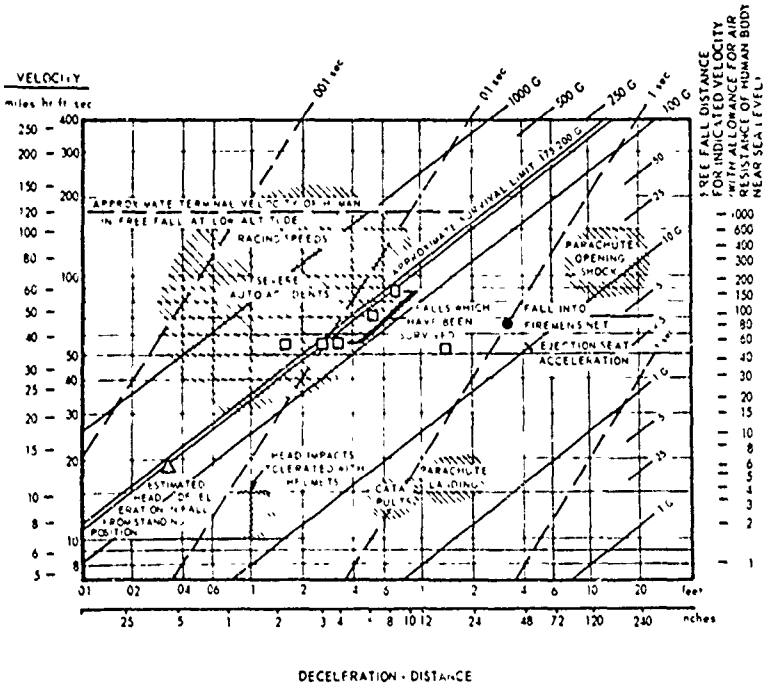


Figure 6–3. Impact documentation. Velocity and deceleration distance are shown on common axes, with magnitude of force and deceleration time shown on secondary scales. Hollow squares mark selected, well documented, free-fall survivals for which impact forces have been calculated. Extent of tissue deformation at impact for these free-falls is not known, thus deceleration distance is not always known. (Modified from Webb, 1964, with data of Snyder, 1963-69)

Tolerance to Transverse ($\pm G_x$) Impact Forces

In forward facing transverse ($-G_x$) impact, tolerance limits for man are approximately 50 G peaks at 500 G/sec rate of onset for 0.25 second's duration, provided there is adequate upper torso restraint (Stapp, 1951a). However, changes in the rate of onset directly affect human response for various impulse durations (Stapp, 1949-1968; Stapp & Hughes, 1956; Stapp & Blount, 1957; Eiband, 1959; Stapp, et al., 1964; Stapp, 1965). Air Force design recommendations are approximately 45 G for a duration of 0.1 second and 25 G for a duration of 0.2 second (U.S. Air Force, 1969). Restraint in the experiments establishing these limits was by means of a double harness with 3 inch wide shoulder straps, a seat belt with thigh straps, and a chest belt. With a less adequate restraint system, some debilitation and injury may occur at these levels and greater tolerance may be found with better protective systems.

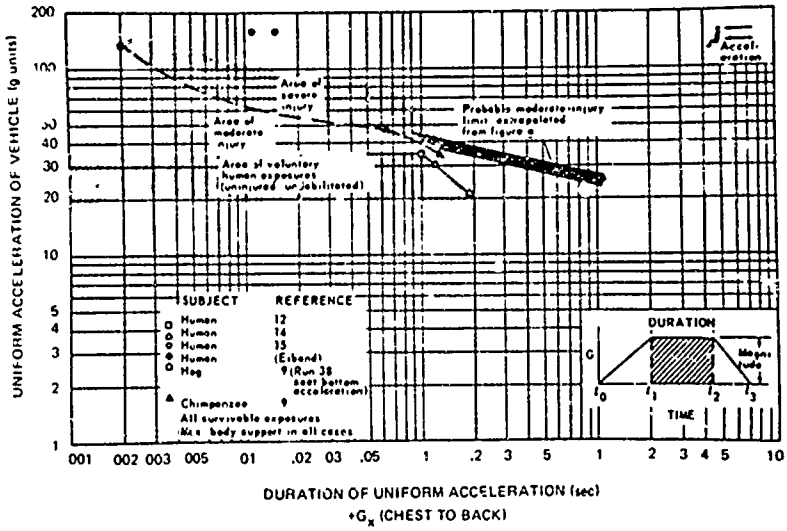
Stapp reported that peak acceleration of approximately 45 G (0.09 second's duration) with a rate of onset of 500 G/sec resulted in no signs of shock. Yet, he found that 38 G's for 0.16 second at onset rates higher than 1300 G/sec produced signs of severe shock (Stapp, 1949; 1968) and 45 G (for 0.23 second) at 413 G/sec produced severe delayed effects (run 215, Stapp, 1949). A higher rate of onset usually implies a higher content of high frequency energy in the acceleration pulse, with a higher energy transfer to the human. Unfortunately, the data are too few and too often uncontrolled with respect to restraint systems for adequate interpretation (Holcomb, 1961; NASA, 1965).

Human tolerance for impact in rearward facing ($+G_x$) body orientation has not been clearly established. Humans have survived impact, with reversible injuries, at a level of 83 G (chest acceleration, not actual input) at 3800 G/sec for 0.04 second's duration (Beeding & Mosely, 1960). The accepted Air Force design limit falls between this and the 45 G for 0.1 second end point for eyeballs out impact (U.S. Air Force, 1969). Stapp (1949) reported human tolerance for $+G_x$ (rearward-facing impact) to be 30 G for 0.11 second's duration with a calculated rate of onset of 1065 G/sec.

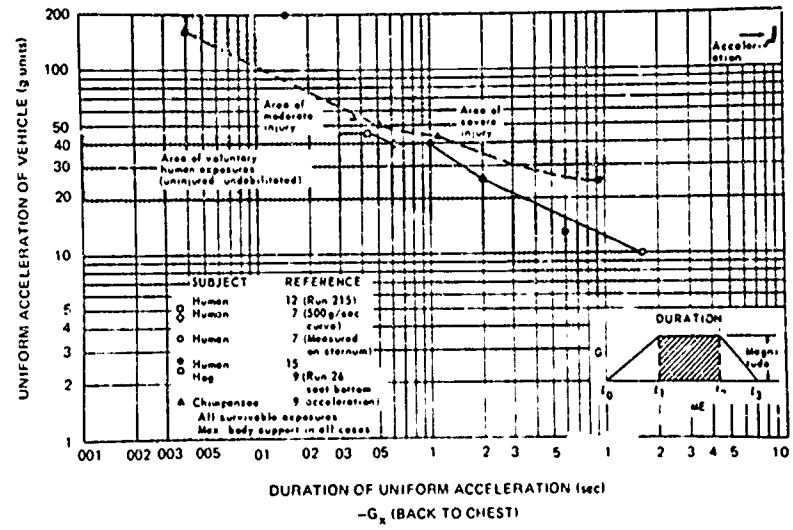
Chimpanzee tests, backed by free-fall data for humans, indicate that limits for survival may be less than 237 G at 11 250 G/sec for 0.35 second's duration in the forward-facing ($-G_x$) body orientation when the subject is restrained by full-body harness, and about 247 G at 16 800 G/sec over 0.35 second's duration (Stapp, 1961a) rate of onset. Persistent injury was found above 5000 G/sec rate of onset, 135 G peak and 0.35 second's duration, although transient injury effects were observed at 60 G at higher than 5000 G/sec rate of onset in the $-G_x$ direction (Stapp, 1958a).

Attempts are being made to expand design criteria regarding the relationship between rate of onset and duration of transverse impact acceleration (U.S. Air Force, 1969). Figure 6-4 gives data related to abrupt transverse ($\pm G_x$) impacts which have been survived by men and animals. In view of these gaps in the data, the general form of the curves in this figure merits some comment (NASA, 1965). It can be seen that for duration times up to 0.01 second, the tolerance level drops off linearly (log-log scale) as duration time increases. This can be

explained in terms of dynamic response, since the critical human response occurs as in a relatively low frequency system. Short duration impacts do not possess sufficient energy to excite maximum response of this low frequency system. When full overshoot is attained (at about 0.01 second) any further increase in the duration of impact does not increase the man's response for a given input level, until the "long" duration regime is approached when hydraulic effects become noticeable and reduce the tolerance level still further (see also figure 6-12).



(a)



(b)

Figure 6–4. Survivable abrupt transverse ($\pm G_x$) impact. Reference numbers are those in original reports. (After Webb, 1964, based on data of Eiband, 1959)

Figure 6-5 presents data for tolerance to $+G_x$ impact as a function of velocity change and average acceleration. The curves of Gurdjian (1954) were calculated to define the dividing line between mild injury (no damage) and severe injury such as shock and retinal hemorrhage in humans, in terms of velocity change and average acceleration force. There are few human experiments at the high accelerations. Animal data support the shape and approximate location of the curve (Kornhauser, 1964). Because of an error found in the original calculations, they were recalculated and plotted as shown. Good agreement is noted except for the 0 to 0.02 region where the earlier model of Gurdjian shows a greater permissible velocity. It can be seen that for exposures of less than 0.02 to 0.06 second, the change in velocity, rather than the acceleration level, determines tolerance (as predicted by figure 6-12). More human data are needed to define the curve at short exposure durations.

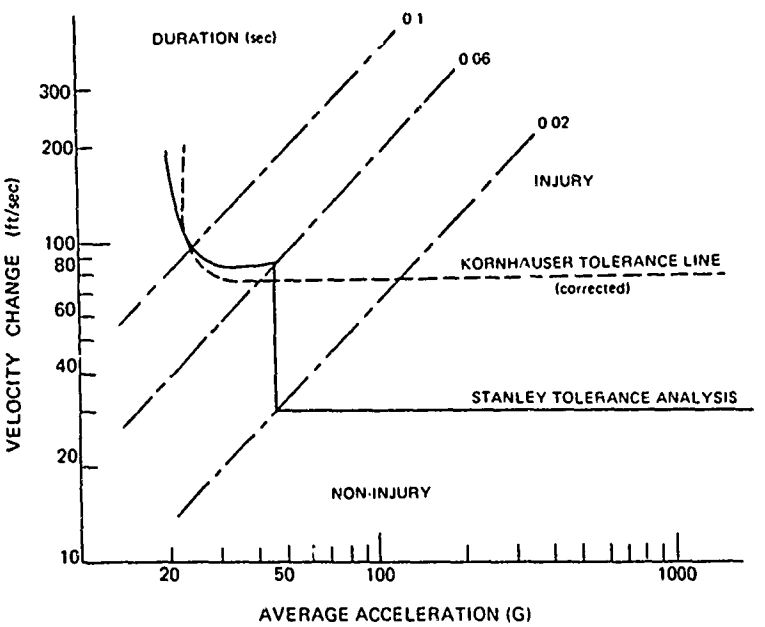


Figure 6–5. Tolerance to rearward $+G_x$ short-duration accelerations as a function of velocity change and average acceleration. Dashed line represents $+G_x$ tolerance curve for injury as determined by Kornhauser and Gold (1961), corrected for errors found in the original duration times. The solid line is the tolerance curve resulting from more recent analysis of available usable impact data by Stanley Aviation Corp. (NASA, 1965). [After NASA (Stanley Aviation Corp.) 1965].

Tolerance to Vertical ($\pm G_z$) Impact Force

Design curves for ejection seat and escape capsules (HIAD, 1960; General Dynamics, 1961) have been vague regarding the relationship between rate of onset and duration, especially in the region of short duration impact (Holcomb, 1961). For example, whole body deceleration of 50-pound chimpanzees at 3 $-G_z$ using a trapezoidal deceleration profile with a plateau of 50- to 60-msec duration resulted in G amplification of 2.0 to 2.5 times the sled G, as detected by a

miniature accelerometer rigidly mounted on the calvarium (Sonntag, 1967). Figure 6-6 gives data which may be helpful in this regard. It shows the durations and magnitudes of abrupt vertical decelerations, in both the tailward ($-G_z$) and headward ($+G_z$) directions, which have been withstood by animals and man.

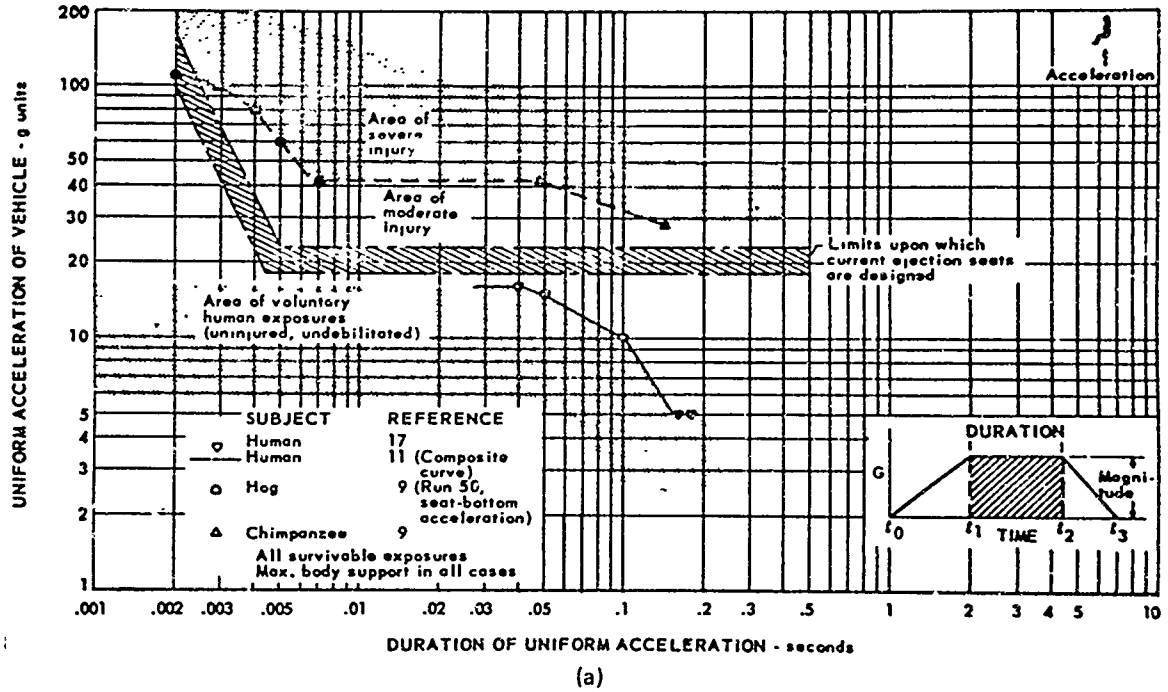
Impact tolerance has been assessed in terms of impact pressure (i.e., force per unit area) as well as from the magnitude-duration point of view. The $+G_z$ (headward) case is illustrated in figures 6-7 and 6-8. There is a considerable area of unknown effect between the region of voluntary human exposure and the region of known injury. The unknown area covers about 20 G in the ordinate in figure 6-7, which includes the region of most interest in space operations. It is clear from the figure that the boundaries of injury versus non-injury are not yet particularly well defined, and a few more reliable points might well change the general shape of the curves, particularly in the impulse region.

Tolerance to Lateral ($\pm G_y$) Forces

Lateral ($\pm G_y$) impact tolerances appear to be considerably lower than is tolerance in either the transverse ($\pm G_x$) or footward ($+G_z$) body orientations, with a maximum of 14.1 peak sled G at 600 G/sec for 0.122 second's duration under full body restraint (Sonntag, 1968). When the subject is restrained by a lap belt only, the voluntary tolerance limit for belt ($-G_y$) lateral impact has been reported to be only 9 G (average) for a duration of approximately 0.1 second (Zaborowski et al., 1965; Zaborowski, 1966). More recent tests with the F-111 restraint system (General Dynamics version) resulted in subjective tolerance levels at 9.2 to 10 sled G's, or 12 to 14 G on the chest (Sonntag, 1968). Few right lateral impact ($+G_y$) tests have been done, but in this orientation with full Mercury mission-type body restraint, the subjective tolerance level has been reported to be above 21.5 G (sled) maximum for 1190 G/sec and 0.121 second's duration (Weis et al., 1963a). With the early Apollo restraint system, 18.7 G (sled) was tolerated with no complaints (Brown et al., 1966).

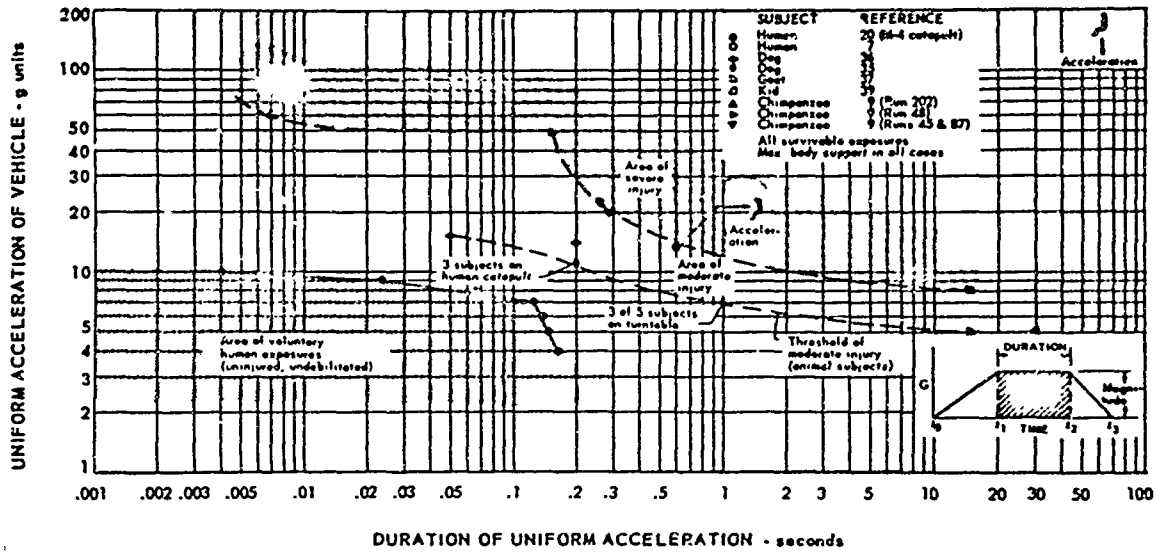
Computer Analyses of Plateau Tolerances

Recent attempts have been made to supplement empirical curves with preliminary computer models employing impedance and resonance techniques (NASA, 1965). An analysis of headward ($+G_z$) accelerations has shown that the maximum plateau input acceleration can probably be taken as 40 G with some degree of confidence. Although essential for computer studies, the selection of an equivalent spinal frequency (ω) is not so well defined. Because of the shortage of results in the impulse region, the most reliable evidence can be taken from the critical velocity change deduced from drop tests which give a value for ω of 225 rad/sec (Swearingen et al., 1960).



(a)

Figure 6–6. Survivable abrupt vertical ($\pm G_z$) impact. Reference numbers are those in original reports. (After Webb, 1964; based on data of Eiband, 1959)



(b)

Figure 6–6. Survivable abrupt vertical ($\pm G_z$) impact. Reference numbers are those in original reports. (After Webb, 1964; based on data of Eiband, 1959) -- *Continued*

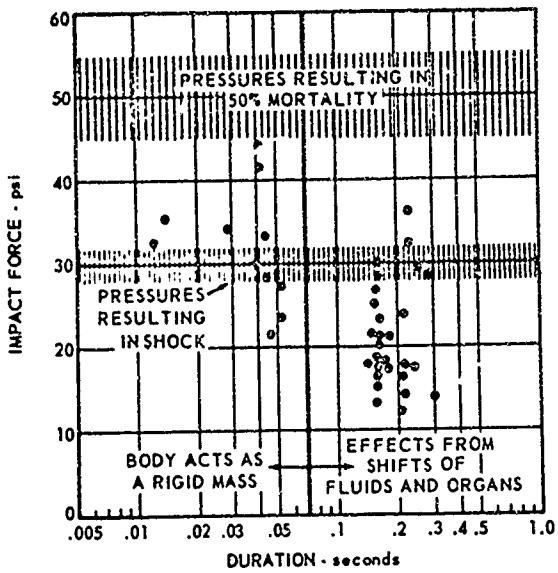


Figure 6–7. Impact sensitivity in terms of force per unit area for $+G_z$ impact. For shorter exposures, the body is believed to act as a rigid mass; for longer exposures, effects are caused by shifts in body fluids and tissues. Data points are taken from human experiments in drop towers, falls, and rocket sleds with various restraint devices. Two shaded areas define approximate areas of effect in terms of impact pressure for any duration. (After Webb, 1964, adapted from Thompson, 1962)

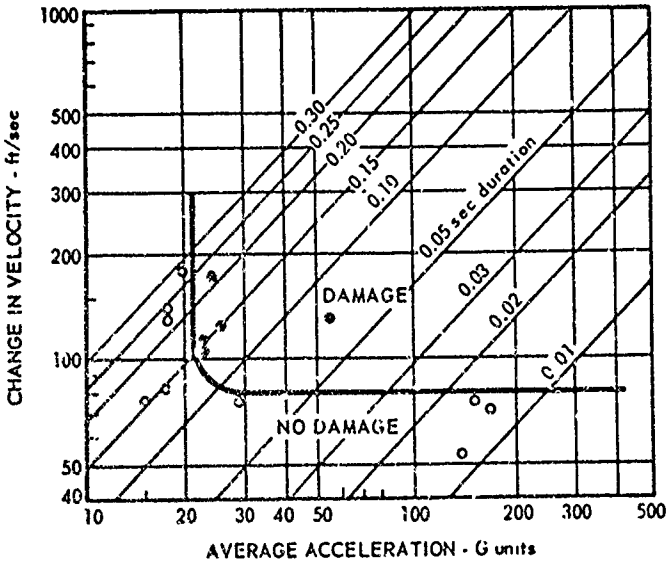


Figure 6–8. Dividing line between mild injury (no damage) and severe injury (shock and retinal hemorrhage) in humans [exposed to $+G_z$ impact, in terms of magnitude and duration of force application.] Data points are from human experiments in several laboratories. Animal data (not shown) support the shape and approximate location of the curve. (After Webb, 1964, adapted from Kornhauser, 1962)

In the transverse, backward direction ($+G_x$) the plateau tolerance line falls at a value of 45 G for the input acceleration, and the most reasonable position for the impulse tolerance line corresponds to an equivalent frequency of 95 rad/sec. This is somewhat higher than the value suggested by the evidence from accident survival. The adoption of the more pessimistic tolerance line appears justified since it satisfies the few sled test points available, and accident cases usually represent extreme end points and cannot be precisely reconstructed. No satisfactory conclusions can be made from the transverse forward data ($-G_x$) but a frequency of 95 rad/sec, as for the backward case, is suggested. From a physiological standpoint, the plateau tolerance level for forward facing impact might be lower than that for the backward direction because of the position of the spine relative to the internal organs, but this also depends upon restraint. Until more relevant tests have been conducted, it is suggested that the allowable peak input acceleration be taken as 35 G.

Tentative impact tolerance parameters suggested for use with the single degree of freedom, undamped dynamic model, are given in table 6-2. It should be remembered that these values are applicable to an undamped model. Damping will introduce changes in the tolerance levels considered to be small enough to be ignored at this stage of model development. Analytic results are also available for two and three degrees of freedom models (NASA, 1965). These bring out the factors determining the drop in tolerance levels at the longer durations of figures 6-4 and 6-6. The exact shapes of the curves are determined sequentially by tolerance of the head, lumbosacral, and spine-abdomen system as the duration of impulse is increased.

Table 6–2

Tentative Impact Tolerance Parameters for Use With Single Degree of Freedom Undamped Dynamic Models

Parameter	Impact Direction		
	Headward ($+G_z$)	Backward ($+G_x$)	Forward ($-G_x$)
Equivalent frequency	225 rad/sec	95 rad/sec	95 rad/sec
Maximum allowable mass acceleration	+80 G_z	+90 G_x	−70 G_x
Impulse region	0 – 0.009 sec	0 – 0.02	0 – 0.02
End of plateau	.00 sec	.06 sec	.08 sec

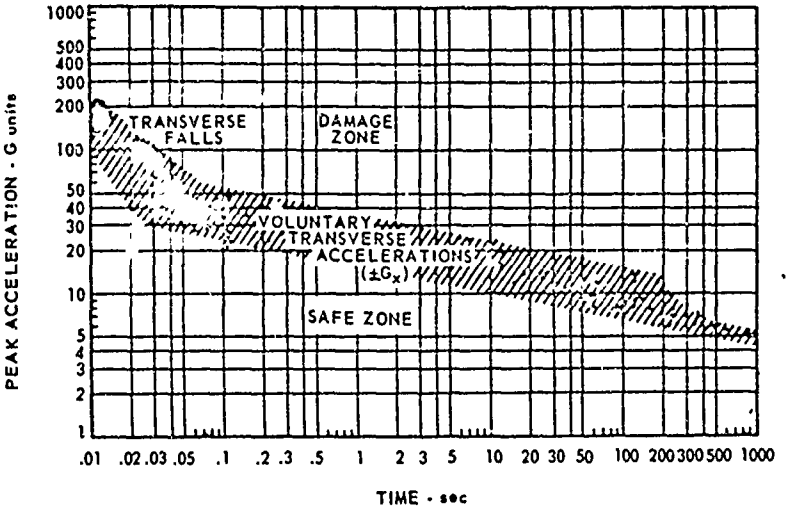
(After NASA, 1965, Stanley Aviation Corp.)

Tolerance to Peak Impact Accelerations

Figure 6-9 indicates the peak accelerations that have been survived without permanent injury. Figure 6-10 shows the greatest vertical impact

subjects would voluntarily endure and the type of symptoms noted at given rates of onset. Free-fall studies have indicated that the critical entrance velocity for human survival of water impact is about 100 ft/sec, feet-first ($+G_z$), and 97 ft/sec in the head-first ($-G_z$) body orientation (Snyder, 1965; Snyder & Snow, 1967). These velocity calculations were corrected for aerodynamic drag and are thus lower than standard values.

(a)



(b)

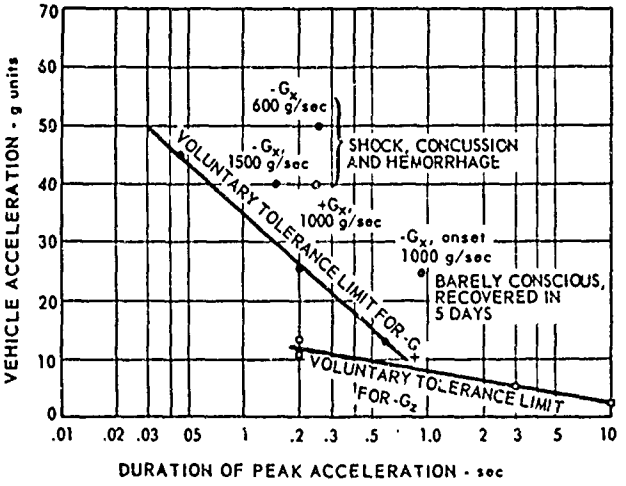


Figure 6–9. Human tolerance to peak accelerations. A: Peak transverse accelerations survived without permanent injury; including data from falls (below 0.03 sec), short tract impact facilitie (0.03 to 0.1 sec), high speed sled runs (0.1 to 1.0 sec), and centrifuge studies (2-1000 sec). Peak accelerations lying below band of data are assumed to be noninjurious, while those above should produce severe injury or death. (After Webb, 1963, adapted from Thompson, 1962). B: The two lines connect data points for highest peak $-G_x$ and $-G_z$ accelerations voluntarily endured without injury by carefully restrained subjects on high speed rocket sleds. Four points above lines show accelerations which produced reversible but serious injury in $\pm G_x$ acceleration. (After Webb, 1964, adapted from Blockley using data of Stapp, 1951; 1955; 1956; 1957; 1964)

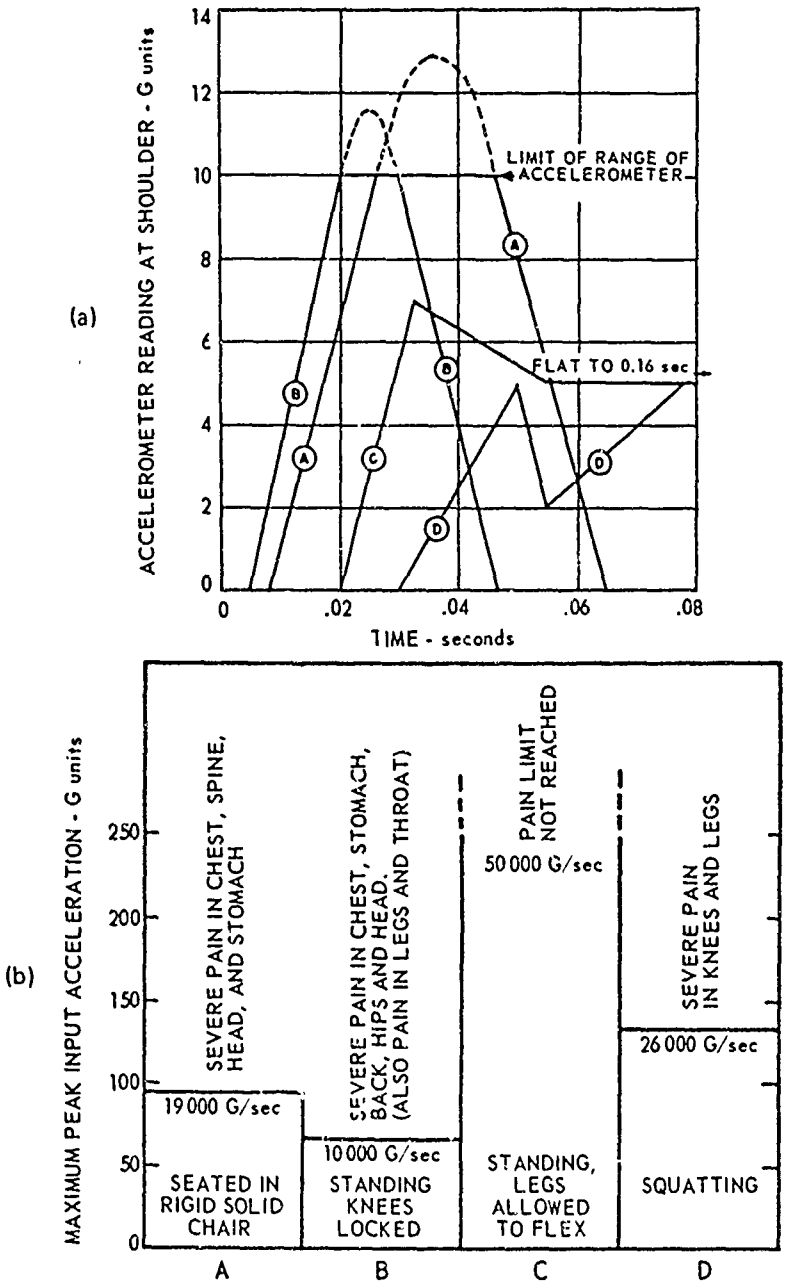


Figure 6–10. Durations and magnitudes of abrupt transverse decelerations endured by various animals and man, showing areas of voluntary endurance without injury, moderate injury and severe injury. A: summarizes $-G_x$ data (chest-to-back impact); B: shows $+G_x$ data (back-to-chest impact). Reference numbers are those in the original reports. (After Webb, 1964; based upon Eiband, 1959) More recent tests with human volunteer subjects confirm in general these early data. The user is cautioned that these tolerances are greatly influenced by the type of restraint protection, which is not specified.

Other Factors Affecting Impact Tolerance

Besides the numerous factors affecting human tolerance to impact which have been indicated in studies to date, new environmental factors encountered in space flight may also exert some degree of influence. In extended space flight, astronauts will be exposed to ionizing radiation which may substantially change the functional state of the organism. However, no information is yet available concerning the effects of ionizing radiation on human impact tolerance and only a little animal data has been gathered. Exposure of mice irradiated in doses of 250 to 750 R to prolonged accelerations of 40 to 42 G for 3 minutes resulted in estimates of the limits of overload resistance of a human subject injured by ionizing radiation of about 52 days (Davydov et al., 1965). Extensive physiological, histological, and biochemical monitoring of two turtles aboard Zond-5,* showed no correlation between radiation and impact effects (Gazenko et al., 1969).

Preliminary acceleration studies (centrifuge) have been initiated relative to the effects of the circadian rhythmicity on impact tolerance, Bolend, 1970, but biological effects upon man's impact or deceleration tolerance have not been reported.

Low-altitude, high-speed flight in turbulent conditions, which exposes crews to random multiple vertical impacts, has been found to result in markedly deteriorating performance after one hour of flight as terrain slopes steepen and airspeed increases from Mach 0.4 to 0.9 (Soliday & Schoban, 1965).

Physiological and Biochemical Response to Impact

Human tolerance criteria are largely physiologically determined, and it must be emphasized that most data related to the human have been obtained at impact levels at or below voluntary tolerance. Very limited human data, generally obtained in connection with accidents, are presently available at higher impact injury levels. Most estimates of lethal impact ranges are extrapolations from animal studies. A large number of environmental factors directly influence physiological responses, including body orientation, direction of application of force, and magnitude, duration, and rate of application of the acceleration pulse shape. In addition, supporting structures and restraint play a major role in variation.

Cardiovascular Response to Impact

Rate of onset has been shown to be a primary limitation and appears to influence clinical shock directly following impact (Stapp, 1955b; Taylor, 1963). The mechanisms of this physiological shock, which involve complex,

*In semilunar flight from 15 – 21 September 1968, splash down landing in Indian Ocean.

simultaneous neural-humoral events, are not yet clearly understood. Post-impact bradycardia, or slowing of the heart rate below 60 beats per minute, has been well documented (Bierman, Wilder, & Hellems, 1946; Stapp, 1949; Ruff, 1950; Rhein & Taylor, 1962; Taylor et al., 1962; Weis et al., 1963a; Brown et al., 1966). At 30 G peak and 100 G/sec, unpleasant pressure sensations, pallor, drop in blood pressure, increased pulse rate, and occasional retinal venous spasms reportedly occur. These transient changes were found in the absence of mechanical failure or tearing of tissues and organs and without bone fracture. Brown et al., (1966) found that bradycardia post-impact is a function of the acceleration profile and the subject orientation, but little additional documented information is available relative to the influence of impact orientation and magnitude on post-impact heart slowing.

Mild bradycardia is produced at 15 G impact in the forward-facing position ($-G_x$) but is not as marked in the rearward-facing ($+G_x$) position. Increasing levels of impact increase both the severity and duration of bradycardia up to the tested voluntary human limits of 30 G (Taylor, 1963). In impact pulses of less than 50 msec and less than 15 G the cardio-inhibitory reflex causing slowing of the heart rate apparently does not occur. At low G forces (7.21 to 15.46 G), a tachycardia, or speeding up of the heart rate, has been reported (Piotrowski, 1968).

A carotid sinus reflex induced by sustained pressure rise in the carotid arteries was subjectively observed following exposure to forward-facing ($-G_x$) impact of 600 G/sec to a plateau of 15 G sustained for 0.60 second (Stapp, 1961a). The cardiovascular shock effect is characterized by pallor, sweating, drop in blood pressure and rise in pulse rate. Mild transient shock has been observed at less than 25 G peaks where duration was less than 0.1 second. Severe shock has resulted from exposure to 38.6 G at a 1370 G/sec onset rate for 0.12 second's total duration (8 to 9 Hz resonant frequency) (Stapp, 1961b).

Hematological and Biochemical Change

In man, various changes in chemical constituents of the blood as well as adrenal gland activity have been reported to occur in conjunction with impact accelerations. Reduction in blood platelets (thrombocytopenia) after forward-facing ($-G_x$) impact at 20 G (peak sled G) was observed one hour post-impact at 400 to 800 G/sec onset rates (Taylor, 1963). Sympathoadrenal response to impact was suggested due to changes found in measurement of urinary excretion of vanelmandelic acid (VMA) (Hanson & Foster, 1966). More precise measurement of norepinephrine, epinephrine, and 17-hydroxycorticosteroid in urine pre- and post-impact showed a definite connection with sympathoadrenal function and emotional stress (Foster & Sonntag, 1969).

Pulmonary and Muscular Effects

In $+G_x$ (rearward-facing) impact levels up to 25 G, no significant impairment of pulmonary function has been found to occur in the restrained $+G_x$ (forward-facing) position (Hanson, 1965).

In lateral ($\pm G_y$) impact, minor physical complaints such as muscle stiffness occurred in approximately 258 G/sec rate of onset for durations of 0.3 to 0.1 second (Zaborowski, 1966).

Physiological Tolerance

Symptoms of various degrees of shock are the first physiological signs limiting human voluntary tolerance to transverse acceleration. A 40 G peak at 331 G/sec onset rate of 0.32 second plateau duration (wearing upper torso restraint) can be tolerated with no indication of cardiovascular shock. Further increase in duration of acceleration (i.e., sustained acceleration) will not affect response (Lewis & Stapp, 1958). However, in seated forward or rearward-facing body orientations ($\pm G_x$), physiological alterations in man have been reported when peak forces exceed approximately 15 G and onset rates are above 100 G/sec. When these levels are exceeded, subjects turn pale, perspire, and exhibit transient rises in blood pressure. More severe loads result in unconsciousness. At the maximum acceleration loads which have been applied, immediate effects are sometimes not pronounced, but delayed effects occur with gradual onset over the next 24 hours (Stapp, 1953, 1965; Pesman & Eiband, 1956; Stapp & Hughes, 1956; Stapp & Blount, 1957; Beeding & Mosely, 1960; Stapp et al., 1964).

The most severe shock observed in human testing occurred in a rearward-facing ($+G_x$) impact of 82.6 G at 3826 G/sec measured on the sternum, or 40.4 G measured on the sled at 2,139 G/sec for 0.04 second's duration (12 to 14 Hz resonant frequency). In this case there was no blood pressure for 30 seconds post-impact, returning to 70 systolic and 40 diastolic within 5 minutes. The subject complained of severe lower back pain, then lost consciousness 10 seconds post-impact. He was hospitalized for 3 days to recover from headache and back pain (Stapp, 1961).

For the lateral body orientation, tolerance has been defined as subject discomfort with prolonged stiffness and soreness in the neck musculature (Zaborowski et al., 1965). Tests reported by Sonntag (1966) have placed voluntary limits in lateral impact with lap belt restraint only at 12 G at which point anal sphincter pain, attributed to vagal effect and acute dilation of the sphincter, has been observed. Two episodes of fainting in shock response are reported, with bradycardia but no nonreversible physiological effects. Earlier, human tolerance determinations, based upon body kinematics, had placed tolerance with lap belt restraint alone as well as lap belt plus shoulder harness at 9 G for 0.1 second's duration.

Apollo Impact Tests

In a study of predicted Apollo command module landing impacts, Stapp and Taylor (1961) observed that impact forces produced effects to the nervous, cardio-respiratory and musculo-skeletal systems. Neurological effects of impact were momentary stunning and disorientation. A consistent effect on the cardiovascular system was transitory post-impact slowing of the heart rate in

those body orientations in which the decelerative force acts in a footward direction (inertial force acts headward). Respiratory effects of impact were momentary shortness of breath and chest pain. Effects to the musculo-skeletal system were soreness and spasm of muscle groups of the neck and back. No effect to the human subject was severe enough to exceed human tolerance or to cause significant incapacitation of undue pain (tables 6-3 and 6-4). In table 6-3 subjects' complaints are compiled into 10 categories. The numbers under the column heading "Category of Complaints" in table 6-3 correspond to the categories listed in the note at the end of the table. In some tests, more than one complaint was registered. The "Complaint G Range" indicates the range of impact at which complaints occurred, as measured on the sled used in the tests.

To date no evidence of cumulative effects due to repeated exposure to impact forces close to voluntary tolerance limits has been reported. However, the number of subjects and exposures are too limited, and physiological and psychological tests do not permit valid differentiation of subtle effects of such stress from the changes which occur with time in individuals unexposed to impact.

Physiological response of man subjected to linear, lateral, vertical, and free-fall impact, along with transient neurological and psychological alterations which have been reported, are summarized in tables 6-5 to 6-12. Changes associated with off-axis impact can be found in table 6-14 at the end of this chapter.

Biomechanical Factors of Impact

The design capability of manned aerospace vehicles is limited by both the biological and the biomechanical "breaking points" of the human body. The body consists of a skeletal structure, held together by tough fibers, which provides both mechanical support and a lever system upon which the muscles act. The basic structural component is the spinal column of vertebrae which has four curvatures. These curvatures are found only in man with his upright posture. The vertebrae act as load carrying elements and are separated by intervertebral discs. These act mechanically as energy absorbers and connecting linkages. The thoracic organs (heart, lungs, and liver), contained in the rib cage, and the abdominal viscera are suspended freely by connective tissues from the muscle and bone framework.

Tissues of the human body show mechanical properties such as compressibility, elasticity, and shear and tensile strength. In general, biological materials are multiphase, nonhomogeneous, anisotrophic, and nonlinear. Fluids are generally non-Newtonian and solids are non-Hookean. Much work has been done to determine the mechanical properties of tissues, but the stress-strain-history law is not known for any tissue (Fung, 1968). Live, whole body response is known to be nonlinear and to exhibit a high degree of rate sensitivity (McElhaney & Byars, 1967). The body responds to impact with considerable variation, both within the same individual and between different individuals.

Table 6–3

Complaints Registered by Volunteers in Apollo Impact Tests

Pos. No.	Seat Orientation (Roll-Pitch-Yaw)	Complaint Tests Total Tests	Category of Complaints	Complaint G Range	Sled G Range
1	000-315-000	2/14	4,9	13.2 – 24.6	5 7 – 26.3
2	000-335-330	3/10	7,8,10,10	17.3 – 21 0	6 0 – 21 0
3	000-005-320	2/14	4,8,9,9,10	17.5 – 25.6	9.2 – 25.6
4	000 035-330	4/12	1,1,4,4,6	18.5 – 25.0	10 5 – 25 0
5	000 045-000	5/14	2,4,4,4 5,5,6,9,9,9	5.9 – 25 0	5 9 – 25 0
6	000 035-030	6/12	2,4,4,5,8,9,9,10	18.5 – 24.5	10 2 – 24 5
7	000 005-040	4/11	2,4,4,6,7,9	14.2 – 23 5	10.0 – 23.5
8	000 335-030	1/14	4,9	19.5	8 0 – 24 7
9	000 085 180	1/2	2,4,10	9 8	9 8 – 11 8
10	000 085 220	2/13	4,10,10	13.9 – 15.4	5 9 – 16.0
11	000 085-270	0/2	No complaints	–	17.4 – 18 7
12	000 085-320	2/21	1,1,4	15.7 – 17.8	6.4 – 19.5
13	000 085 000	0/2	No complaints	–	9.4 – 11.1
14	000 085 040	1/13	4	14 6	5 8 – 18.2
15	000 085 090	0/2	No complaints	–	11.6 – 13 5
16	000 085 140	3/14	4,5,5	15.1 – 16.0	5.5 – 18.9
17	000 045-180	9/17	1,1,2,2,3,3,3,5,5,5, 5,5,6,7,7,7,7,7,8,8, 9,10 10	15.0 – 26.1	15.0 – 26.1
18	000 035-210	8/20	1,1,2,2,3,4,5,6,6,6, 7,7,7,8,9	15 2 – 23.2	10.5 – 28.9
19	000 005-220	5/ 6	1,5,5,6,9,9	16.5 – 28.2	16 5 – 30.0
20	000 335 210	1/6	2	19.8	15.8 – 21.7
21	000 315-180	1/10	2,3	19.0	15 8 – 21.9
22	300 335-150	0/8	No complaints	–	15.0 – 21 9
23	000 005 140	8/19	2,2,4,5,6,8,9,9,9,9, 9,9,10	16.4 – 30.7	16.3 – 30.7
24	000 035-150	8/19	1,1,2,2,5,5,5,6,6,7	11 0 – 29.3	11 0 – 29.3

Note: [1]Headache – Incidence at impact, duration up to several hours. [2]Stunning/disorientation – Incidence at impact but of brief duration. [3]Blurred vision/spots before eyes – Incidence at impact but of brief duration. [4]Neck/back muscle spasm/strain – Delayed onset, lasting up to several days. [5]Chest pain – Incidence at impact but of brief duration. [6]Shortness of breath – Incidence at impact but of brief duration. [7]Abdominal visceral displacement sensation – At impact. [8]Joint pain – Delayed onset and lasting up to several days. [9]Lower extremity muscle spasm/pain – Delayed onset and lasting up to several days. [10]Upper extremity muscle spasm/pain – Delayed onset and lasting no longer than 1 day.

(Brown et al., 1966)

Table 6–4

Significant Physical Findings Post-Impact in Apollo Impact Tests

Significant Physical Findings	Test Position	Test Numbers	Sled G
Harness burns (all first degree)	2	1537	20.0
	7	1552	23.0
Dazed and disoriented (lasting no longer than two minutes post-impact)	17	1163	17.4
		1187	18.9
		1204	21.7
		1205	25.8
		1456	19.6
	19	1295	30.0
	24	1303	28.1
		1182	24.6
		1403	16.5
	9	1387	9.8
	1	1517	17.2
	21	1610	19.0
Respiratory difficulty (lasting no longer than one minute post-impact)	17	1187	18.9
	23	1191	19.5
	18	1215	24.6
		1216	23.2
	24	1217	23.7
		1403	16.5
Blood pressure difference (20 mm Hg at pre and post run physical exam)	19	1295	30.0
Pulse difference (20 beats/min at pre and post run physical exam)	23	1192	19.4
	17	1456	19.6
	24	1441	20.2
	12	1819	19.5
Engorged retinal vessels	17	1204	21.7
	3	1487	9.2
Back and/or neck pain and decreased range of motion	17	1205	25.8
	1	1517	17.2
	5	1559	25.1
		1591	21.0

(Brown et al., 1966)

Table 6–5

Observed Physiological Effects of Impact

Effects	Impact Force	Responses
Bradycardia	5 – 15 $+G_x$	Slowing of heart for at least 5 beats
	15 – 30 $\pm G_x$ 9 – 12 $+G_y$	Slowing of heart rate immediately following impact At higher accelerations slowing is increased. 1.6 mg atropine eliminates slowing, indicating relationship to vagal reflex
Shock	>15 $\pm G_x$, 500 G/sec	Brief disorientation, drop in blood pressure to 90/60 mm Hg 15 – 30 sec post-impact, ECG nodal rhythm
	12 $+G_y$	Faint, pallor
Muscular	>26 $-G_x$, 850 G/sec, 0.002 sec	Chest pains, aches in back and neck muscles, stiff neck 1 – 3 days
Skeletal	>16 $+G_z$, 1160 G/sec	Anterior lip vertebral compression fracture; most observed injury L1 – T7
	>16 $-G_x$, 0.01 – ^{o}.10 sec	Fracture of lumbar vertebrae
	to 83 $+G_x$, 3800 G/sec, ^{o}.04 sec	None
Neurological	$\pm$15 $-G_x$	Increased deep tendon reflexes
	>20 $-G_x$, 400 + 800 G/sec	Appear stunned 10 – 15 sec at 20 G peak accelerations. Euphoria, hand tremor, decreased coordination, loquacity, increased muscle tone, gross involuntary movements in head, arms, trunk
	25 G	Deep tendon tendon reflexes absent for several sec, then hyperactive for about 1 min
	>25 G $-G_x$, 1000 G/sec	Abnormally slow EEG wave patterns observed for several min post-impact
Hematological	20 $-G_x$, 400 + 800 G/sec	Blood thrombocytes reduced 1 hr post-impact. A week later thrombocyte count higher than control value

Table 6–5 (Continued)
Observed Physiological Effects of Impact

Effects	Impact Force	Responses
Psychological	10 to $-G_x$	Kohn symbol arrangement test shows distinctive changes, increasing with force level
General Stress	$>20 + G_x$	Chemical changes in adrenal blood; alterations in adrenal gland activity
		17-OHCS excretion levels increase significantly and are related to anxiety and CNS stimulation of adrenocortical secretion

(Data from Stapp, 1951; 1955; Beeding, 1957b; 1957c; 1960; Beeding & Hessberg, 1958; Lewis & Stapp, 1958; Beeding & Moseley, 1960; Aldman, 1962; Rhein & Taylor, 1962; Taylor, 1962; Taylor, et al., 1962a; 1962b; 1962c; Taylor & Rhein, 1962; Taylor, 1963; Hanson, 1965; Foster & Sonntag, 1969; Klopfenstein, 1969).

Table 6–6

Physiological Effects of Forward-Facing Linear ($-G_x$) Impact

	No. of Subjects [No. of Tests]	Experimental Conditions	Peak G	Rate of Onset G/sec Velocity ft/sec	Duration sec	Physiological Effects	Reference
	Human Tests. Linear Acceleration ($-G_x$), Subjects Forward Facing						
1.	[7]	Oriented ant.-post.; ss; sb, Shh, Hd unsupported	34.3		0.01	Maximum tolerance without symptoms of cerebral concussion, 34.3G	Henschke, 1945
2.	?	ss restrained by steel cable	18-20	250 [57]	0.01-0.10	No ill effects; later tests of 16-19 G caused fractures of lumbar vertebrae	Lovelace, Baldes and Wulff, 1945
3.	5♂[15] 18-21 yrs (8[18] static tests)	Impact decelerator,[1] to test impact loads of 1500 lb & 3000 lb on model-A vest h	(550 lb load to chest)		0.050-0.070 (peak) .15G total	Transient bradycardia, apnea, forced expiration against closed glottic found best protection	Bierman, et al, 1946
4.	>20 yr, >160 lb; [30]	Impact decelerator,[1] to test impact loads of 2000 lb on Shh & sb			0.1-0.2	Cutaneous waves traveled 4-14 ft/sec; long axis of body shortened 2 cm, and transverse axis widened approx. 2 cm, under 2000-lb impact force; body compressed approx. 5 cm ant.-post.; shoulder straps caused abrasions; rates of loading in excess of 0.060 sec result in marked discomfort to subject	Bierman, 1947 (See also, Bierman and Larson, 1946; Bierman, 1946)
5.	13♂, 25-41 yr, 168.9-182.9 cm, 63.9-92.7 kg; [54]	Seated; 2000-ft rocket track	10-46.6	282-1370	0.11-0.42	Tolerance limits approximate 50-G peaks at 500 G/sec rate on onset for 0.25 sec, with adequate restraints[2]	Stapp, 1951

Table 6–6 (Continued)

Physiological Effects of Forward-Facing Linear ($-G_x$) Impact

	No. of Subjects [No. of Tests]	Experimental Conditions	Peak G	Rate of Onset G/sec Velocity ft/sec	Duration sec	Physiological Effects	Reference
	A. Human Tests. Linear Acceleration ($-G_x$), Subjects Forward Facing						
6.	9: [51]	Seated; 2000-ft rocket track	10.9-45.4[3]	281-1370[4]	0.15-0.37	Vasomotor reactions at 30-G peak; shock at 35-G peak, with rate of change of deceleration of 1100 G/sec or more. At 38.6 G with 1370 G/sec rate of onset, fractures, syncope; albuminuria, 2+ for 6 hr. Contusions and muscle soreness due to straps for 2 days post-run.	Stapp, 1951; 1955
7.	2	Crash restraint device	5			Comparison of post-impact escape $+G_x$ and $-G_x$ orientation. .6 sec time differential not significant at this level	Lewis and Stapp, 1957a
8.	♂[19]	Seated; ss; 3-in.-wide lap b	12-23 (Ch); 4-23 (Ab); 4-22 (Kn); 17-32 (s)	160-350 (Ch); 300-600 (Ab); 200-600 (Kn); 350-1600 (s) [15.4-19.6]	0.001-0.003	Minor injury at 10-G peak; abdominal muscle strain and tenderness at 13-G peak, both at 300 G/sec rate of onset for 0.002 sec; back muscle soreness from 26 G with 850 G/sec rate of onset for 0.002 sec	Lewis and Stapp, 1957b; 1958
9.	?	Steering wheel catapult		[16.4]	0.2	Muscle soreness, back of neck	Aldman, 1962

10.	♂, 67.6-78.8 kg. [22]	Hd forward 45°; rocket-propelled trolley	7.9-16.5 (trolley); 10.6-35.1 (b)	[300]	0.19-0.31	No bruising up to 12 G; no protective muscular extensor response in lower limbs in <0.100 sec	Latham, 1958
11.	[18]	80°; daisy track M1A1	12.6-48.0 subj (trans)	400-2500	0.051-0.100	No injuries reported	Beeding, 1959
12.	15[15]	80°; daisy track	19.6-31.8[1]	278-1100	0.065-0.086	No ill effects for 14 subjects. For 1 subject, anterior compression fracture of 5th and 6th thoracic vertebrae, linear fracture of 5th lumbar vertebrae, ECG nodal rhythm and shock 1 min post-impact	Beeding, 1960
13.	7[7]	Daisy track	30.3-34.8		0.034	Burning rectum, sore coccyx 1-5 days; stiff neck 1-3 days	Beeding, 1961
14.	6[6]	Daisy track	35.3-38.4		0.032	Stiff neck 1-10 days; albuminuria, 1+ to 2+, (clear in 24 hr); blood pressure 94/48; blurred vision in left eye; ophthalmoscope examination negative	Beeding, 1961
15.	♂; 22 yr, 190.5 cm, 78.8 kg; [1]	Daisy track	39.8			Syncope:blood pressure, 78/G, ECG nodal rhythm. Anterior compression fracture of 5th and 6th thoracic vertebrae; linear fracture of 5th lumbar vertebrae.	Beeding, 1961
16.	5[35]	Daisy track	8.5-37.5 (Ch)	96-1223	0.070-0.154	Thrombocytopenia at -20 G_x; thrombocyte count almost normal 24 hr after impact; widespread endothelial damage	Taylor, 1962

[1] At various azimuth and elevations

Table 6–6 (Continued)

Physiological Effects of Forward-Facing Linear ($-G_x$) Impact

	No. of Subjects [No. of Tests]	Experimental Conditions	Peak G	Rate of Onset G/sec Velocity ft/sec	Duration sec	Physiological Effects	Reference
	Human Tests. Linear Acceleration ($-G_x$), Subjects Forward Facing						
17.	7♂; 21–43 yr; [35]	Daisy track	8.49-37.46	96-1223	0.070-0.153	Increase in skeletal muscular activity at -20 G_x and at 800 G/sec rate of onset, as compared to 400 G/sec of onset when peak seat G was 20	Rhein and Taylor, 1962
18.	20[20]	Crash demonstrator "bopper"	15	1200	0.052	Relative bradycardia immediately following impact; abolished by 1.6 mg atropine sulfate injected intramuscularly 45-60 min preceding impact	Taylor, Rhein and Beers, 1962
19.	1[2]	Seated; decelerator sled	58 (cart); 35 (sb)	[29;37]	0.017 (cart); 0.061 (sb)	Data projected to 60 ft/sec impact, development of seat belt protections	Ryan, 1962
20.	31♂; [31]	Seated, crash demonstrator "bopper"	5-15 (sled)	[20 (vel chg)]	0.052	Slight bradycardia	Rhein and Taylor, 1962
21.	7[7]	Daisy Decelerator	25	1000 [32.8]		Pre- and post-impact elevated levels of urinary VMA excretion indicating subject anxiety accompanied by sympathoadrenal hyperfunction.	Hanson and Foster, 1966

22.	5 [30]	RAF Swing frame device, F-III IAM and USAF harnesses.	6-14	64 - 310		Subjective reports of collar bone and throat pain, groin tenderness.	Reader, 1967
23.	8[8]	0-13-0 Daisy decelerator F-111 restraint	8-14.0	[30.4-39.6]		No injury reported	Sonntag, 1(.)

Abbreviations: Ab = abdomen; ant. = anterior; Ba = back; b = belt; Ba–Ch = back to chest; Bu = buttocks; Bu 1st = buttocks first; Bu–Hd = buttocks to head; caps. = capsule; Ch = chest; e = ejection; es = ejection seat; ff = free fall(s); Ft 1st = feet first; Ft–Hd = feet to head; h = harness; Hd = head; Hd 1st = head first; Hd–Bu = head to buttocks; Hd–Ft = head to feet; Hdst = head strap; hor. = horizontal; Kn = knees; M1A1 = M1A1 propulsion catapult; par. = parallel; par.–Sp = parallel to spine; pl = platform; post. = posterior; rt = right; s = seat; s–Hd = seat to head; sb = seat belt; Sh = shoulder; shh = shoulder harness; Sp = spine; st = strap; subj = subject; ss = swing seat; trans = transverse(ly); trans–Sp = transverse to spine; uc = upward ejection; vel chg = velocity change.

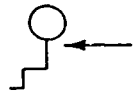
Though investigations have been conducted on other organisms, such as frogs, fish and turtles, data have not been reported. Inertial resultant of body acceleration along x, y, z axis refers to direction of motion of body organs upon impact.

[1]Weights arrested by rod-head which transmits impact up load rod through straps to subject. Subject strapped in restraint seat on back and drop weight jerked against body to simulate forces in aircraft crash. [2]Tolerance to linear decelerations is limited by rate of change, body area involved, and restraints used. No apparent correlation between tolerance and age, weight, height, and backward or forward facing positions. [3]Plateau G of trapezoidal decelerations–time curve calcualted from displacement–time record. [4]Calculated slope.

*For a more complete listing, including all known animal impact data, refer to Snyder, R. G. (1970), Human Impact Tolerances. Society of Automotive Engineers, Inc., N.Y. SAE paper no. 700398.

Table 6–7

Physiological Effects of Rearward-Facing Linear ($+G_x$) Impact

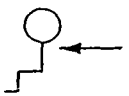


	No. of Subjects [No. of Tests]	Experimental Conditions	Peak G	Rate of Onset G/Sec [Velocity ft/sec]	Duration sec	Physiological Effects	Reference
	Human Tests. Linear Acceleration ($+G_x$), Subjects Backward Facing						
1.	[7]	ss; sb Snh; ld unsupported	20.8		0.01	Maximum tolerance without symptoms of cerebral concussion, 34.3G	Henschke, 1945 Ref.
2.	3[12]	2000-ft rocket track	11.5-31.5[3]	489-1065[4]	0.165-0.405	Safe tolerance, 30-G linear deceleration for 0.11 sec	Stapp, 1949
3.	2[2]	Seated; 2000-ft rocket track	34.8-35.0[3]	1156-1160[4]	0.16	>30-G peak and 100 G/sec resulted in unpleasant pressure sensations, pallor, drop in blood pressure, increased pulse rate, and occasional venous spasms of the retinas	Stapp, 1951; 1955
4.	[19]	Seated; 2000-ft rocket track	10-35	500-1200	0.15-0.42	>30-G peak and 100 G/sec resulted in unpleasant pressure sensations, pallor, drop in blood pressure, increased pulse rate, and occasional venous spasms of the retinas	Stapp, 1955
5.	24	Crash-restraint device	5			Comparison of rearward and forward facing effect upon post-impact escape time. .6 sec not significant at this level	Lewis and Stapp, 1957a

6.	[3]	60°; daisy track	26.7-33.8 (Sh); 26.8-28.6 (Hd)	881.1-924.0 (Sh); 643.2-940.5 (Hd)	0.068-0.070 (Sh); 0.067-0.077 (Hd)	Mild discomforts—skin abrasions, headaches, chest pains, brief disorientation, dull aches in back and neck muscles—persisting to 4 hr; blood pressure dropped	Beeding, 1957c
7.	[3]	75°; daisy track	16.--17.1 (Sh)	328-410 (Sh)	0.083-0.138 (Sh)	1 subject, at 17.1 G for 0.049 sec, skipped systole at 14th and 9th beats, slightly irregular pulse, and blowing and heart sound; no discomfort in other subjects	Beeding, 1957b
8.	2[2]	90°; daisy track	18.- (Sh) 23.9 (Sh)	478.- (Sh) 549.7 (Sh)	0.122 (Sh) 0.112 (Sh)		
9.	♂[7]	15°; daisy track hand-held Hist, vest-type h; leg st; MLA1	7.7-19.4 (Ch); 9.5-21.2 (Hip)	163-552 (Ch); 153-485 (Hip)	0.148-0.150 (Ch); 0.090-0.158 (Hip)	No physical discomfort, normal ECG and urinalysis; pulse average increase was 14.6 counts/min 30 sec after run	Beeding, 1957a
10.	♂[3]	30°; daisy track hand-held Hist, vest-type h; leg st; MLA1	12.7-15.0 (Ch); 15.1-24.5 (Hip)	370-392 (Ch); 528-1687 (Hip)	0.150-0.164 (Ch); 0.055-0.160 (Hip)		
11.	♂[3]	45°; daisy track hand held Hist, vest type h; leg st; MLA1	7.9-13.0 (Ch); 11.8-17.4 (Hip)	210-355 (Ch); 401-587 (Hip)	0.144-0.185 (Ch); 0.133-0.186 (Hip)		
12.	♂[3]	60°; daisy track hand-held Hist, vest-type h; leg st; MLA1	9.2 (Ch); 11.5 (Hip)	175 (Ch); 312 (Hip)	0.097 (Ch); 0.068 (Hip)		
13.	[3]	0°, daisy track	30.0-34.5 (Ch)	1041.0-1622.4 (Ch)	0.051-0.058 (Ch)	Mild discomforts—skin abrasions, headaches, chest pains, brief disorientation, dull aches in back and neck muscels—persisting to 4 hr; blood pressure dropped	Beeding, 1957b
14.		15°; daisy track	27.3-30.5 (Ch)	578.8-1245.6 (Ch)	0.060-0.066 (Ch)		

Table 6–7 (Continued)

Physiological Effects of Rearward-Facing Linear ($+G_x$) Impact



	No. of Subjects [No. of Tests]	Experimental Conditions	Peak G	Rate of Onset G/Sec [Velocity ft/sec]	Duration sec	Physiological Effects	Reference
	A. Human Tests. Linear Acceleration ($+G_x$), Subjects Backward Facing						
15		30°; daisy track	29.2-32.6 (Ch)	1010.6-2144.((Ch)	0.040-0.057 (Ch)		
16.		45°; daisy track	32.5-33.0 (Ch)	1381-2311 (Ch)	0.035-0.065 (Ch)		
17.	†	Supine; 10-lb sandbag dropped 6-12 in. on Ab without warning				Sharp rise in intra-abdominal pressure, then transient rise in frontal and temporal venous pressures after 0.15 sec; 5:1 transmission factor	Latham and Howard, 1958
18.	[13]	Daisy track[1]	37.8-82.6 (Ch trans)	1603-3826 (Ch trans)	0.040-0.052 (trans-Sp)	Back pains from 3rd lumbar vertebra to coccyx for approx. 3 wk	Beeding and Hessberg, 1958
19.	[11]	Daisy track	11.7-31.0	580-1250	0.070-0.162		Beeding, 1959
20.	[17]	100°; daisy track	21-29.2[2]	855-1302	0.052-0.111	None reported	Beeding, 1960
21.	♂, young adults; [50]	Daisy track; Shh lap b, inverted V-strap	37.3-82.6 (Ch)	1603-3826 (Ch)	0.040-0.052	No recognizable permanent damage; tolerance limit for G forces of 0.04-sec duration, 83 G at 3800 G/sec	Beeding and Mosely, 1960

22.	[1]	Daisy track; Convair-B s	25	1000	0.080	No ill effects	Beeding and Cook,
23.	33♂, 21-44 yr; [33]	Seated; crash demonstrator "bopper"	5-15			Bradycardia for at least 5 beats; effect hypothesized as result of vagal exhibition from afferent limb, possibly carotid apparatus or lung (see line 42)	Rhein and Taylor, 1962
24.	20	Northrop sled, molded restraint SR I, SR II	80-87	11,880-12,530	0.03	All survived	Lombard, et al., 1964a
25.	18[18]	Daisy Decelerator 0-5-180 orientation	20	1000 [30]		Impact under these conditions did not produce significant lowering in maximum voluntary ventilation performance	Hanson, 1965

Table 6–8

Physiological Effects of Lateral ($+G_y$) Right Impact on the Human

	No. of Subjects [No. of Tests]	Experimental Conditions	Peak G	Rate of Onset G/sec [Velocity ft/sec]	Duration sec	Physiological Effects	Reference
	A. Human Tests						
1.	15[15]	AMRL Vertical Deceleration Tower Project Mercury. Full torso restraint, rigid fcam couch & semi-rigid "microballoon" couch.	5.21-21.5	200-1190 [9.25-21.9]	0.036-.121	One subject noted pain in right trapezius; one reported "wind knocked out." Tests below subjective tolerance level.	Weiss, et al., 1963
2.	<[2]	Daisy decelerator Apollo restraint OOC-OS5-<70 seated orientation	17.4-18.7 (sled)			No complaints	Brown, et al., 1966

Table 6-9

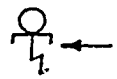
Physiological Effects of Lateral ($-G_y$) Left Impact



	No. of Subjects [No. of Tests]	Experimental Conditions	Peak G	Rate of Onset G/sec [Velocity ft/sec]	Duration sec	Physiological Effects	Reference
	Human Tests. Left Linear Acceleration ($-G_y$), Subjects Sideways Facing						
1.	1[1]	B-58 caps.[2]; upper-torso h		[34]		Small bruises on rt thigh and groin.	Holcomb and Runcey, 1962
		B-58 caps.[3]; upper-torso h		[18]		No injury	
2.	17[17]	AMRL Vertical Deceleration Tower Project Mercury. Full torso restraint, rigid foam couches, and semi-rigid "micro-balloon" couch.	4.27-21.6	62-135 [8-25.5sV]	0.031-.210	One subject noted "wind knocked out" and 2 reported pain in right calf. All tests below subjective tolerance level.	Weiss, et al., 1963
3.	37[70]	Bopper device lap belt left 30° side plate; rt side plate	2.93-9.95 (sled) 4.7-50.8 (chest) 2.3-46.4 (head)	[13.5-16.1]	0.1-0.3	No permanent physiological changes at 9.02 G avg. for 0.1 sec. Minor physical complaints reported by 50% of subjects when exposed to 6.25 avg. G or above.	Zaborowski, 1966; Zaborowski, et al., 1965
4.	2 [2] ♂	Daisy Decelerator 0-85-270 Daisy run 1352, 1353. Cruciform upper torso restraint with lateral chest strap, all 6 straps meeting at sternum. 8" deep headrest, padded 1/2" ensolite. No helmet.	17.1 -18.7 (sled G)	[20 - 20.2]			Chandler, 1966

Table 6–9 (Continued)

Physiological Effects of Lateral ($-G_y$) Left Impact



	No. of Subjects [No. of Tests]	Experimental Conditions	Peak G	Rate of Onset G/sec [Velocity ft/sec]	Duration sec	Physiological Effects	Reference
	Human Tests. Left Linear Acceleration ($-G_y$), Subjects Sideways Facing						
5.	2 [2] ♂	Daisy Decelerator. 0-55-270. Daisy run 1853, 1854 Same as above except 3" head-rest, snug fit Mercury helmet.	12.1 - 13.8 (sled G)	[33.8 -34 7]		Ear of one subject hit helmet.	
6.	10 [10] ♂	Daisy Decelerator 0-13-270 Simulated F-111 seat and restraint helmet. Daisy runs 2205 - 2213, 2410 - 2412.	5.8 - 10.1 (sled G)	[30 6 - 36.9]		Subject complants of sore neck, back pain, harness pain, head motion, eye focus.	
7.	6 [6] ♂	Daisy Decelerator. 0-13-270. Modified F-111 seat and restraint. Lower torso point moved 3" 4", upper lateral straps removed. Daisy runs 2403 - 2408	6 5 - 9.4 (sled G)	[29.3 - 34.7]		All complained of sore neck or head motion.	
8.	4 [4]	Daisy Decelerator. 0-13-270. Lap belt, shoulder straps, inverted V, deep seat. 8" headrest padded with 1/2" [illegible]	14.3 - 17.1 (sled G)	[29.6 - 31.8]		One subject ruptured ear drum.	

9.	9 [9]	Daisy Decelerator. 0-55-90. Daisy runs 1838 - 1842. Standard aircraft harness, shoulder strap, lap, inverted V 3" straps No lateral seat support. 3" head support Mercury type helmet in all but 1st 2 tests. Tests to compare standard harness with previous Apollo harness test	5.2 - 14.1 (sled G) 8.4 - 33.6 (subject vector G summation)	400 - 1100 [26.2 - 35.8] 185 - 710 Subject, onset		No subject complaints in 4 tests, abrasions, burns pain noted in 5 tests.	Rothstein and Brown, 1966
10.	5 [79]	RAF Swing frame device F-111 IAM and USAF GD harnesses	10.5 - 17.7	93 - 390		Tenderness in groin, collar bone and throat discomfort and pain subjectively reported.	Reader, 1967
11.	8[8]	0-15-.70 F-111 Restraint daisy decel.	9.2-10.0 (sled) 12-14 (CK)			Neck muscle strain in one subject.	Sonntag, 1968

Table 6–10

Physiological Effects of Headward ($+G_z$) Vertical Impact



	No. of Subjects [No. of Tests]	Experimental Conditions	Peak G	Rate of Onset G/sec [Velocity ft/sec]	Duration sec	Physiological Effects	Reference
	Human Tests. Upward Linear Acceleration ($+G_z$)						
1.	8[8]	ue, seated; test catapult	28		0.010-0.015	Tolerance with no upper arm support, 23 G; with support, 28 G	Geertz, 1944
2.	5[5]	ue, seated; test catapult; Ba & Ab restraints; no arm supports	20-23		0.010-0.015		
3.	?	ue, seated; test catapult	25-33		0.005	5 types of seat cushions tested; only seat-type parachute reduced acceleration peaks	Geertz, 1944
4.	[2]	ue; catapult seat	10-12			No harmful effects; peak G below injury level	Lovelace, et al., 1945
5.	[27]	ue, inclined track	18-20		0.1-0.2	Physiological limit for seat ejection; minimum injury	Lovelace, et al., 1945
6.	?	s-Hd; catapult of HE-280 jet fighter es	10-12			Compression of spinal column, CNS concussion with contre-coup symptoms; hemostatic effects; inner-ear injury	Richter, 1945
7.	?	Bu-Hd; es, rubber cushion	8-34	6.4-160	0.1-2.5	No injuries reported	Schrenk and Irrgang 1945

8.	[7]	Bu lst; ss; sb, Shh; Hd unsupported	36.5		0.01	Maximum tolerance without symptoms of cerebral concussion, 34.3 G	Henschke, 1945
9.		Ft lst; ss; sb, Shh; Hd unsupported	33.6		0.01		
10.		Ft lst, Kn bent; ss; sb, Shh; Hd unsupported	86.0[15]		0.01		
11.	?	Bu-Hd; es; 2000-ft rocket track	5-33	50-440	0.004-0.03	No injuries reported	Stapp, 1955
12.	[2]	Bu-Hd; 30-ft catapult e; B-14 lap b & Shh	14.9-16.8 (Hd)p 9.8-10.6 (Sh), 19.0-20.8 (Hip); 10.5 11.1(s)		0.08-0.12	High-speed photos showed man appeared to move downward into seat at firing (seat moves faster than man due to compression of body and parachute); movement of unrestrained head	Cofer, et al., 1946
13.	[52]	ue; test tower; Hd rest in varied positions	6-16; 24			Extreme flexion and extension of neck; injury at >12 G if head not held erect	Bavely, et al., 1946
14.	[29]	ue; Naval Air Experimental Station es	17-21	200	0.03-0.14	Recommended maximum hip acceleration, 20 G; time to reach maximum catapult pressure, 0.08 sec or more; dynamic response factor of subject pressure kept to 1.20 maximum	Noble, et al., 1947
15.	[7]	ue; es tower; 2-in. sponge rubber s cver 4-in. wood block	10-14.6(s); 11.3-22.6 (Hd); 10.3-15.6(Sh); 15.9-33.5 (Hip)	[44-48]	0.01	Terminal velocity tolerated for ejection at 14-15 G	Ames, 1947

Table 6–10 (Continued)

Physiological Effects of Headward ($+G_z$) Vertical Impact

	No. of Subjects [No. of Tests]	Experimental Conditions	Peak G	Rate of Onset G/sec [Velocity ft/sec]	Duration sec	Physiological Effects	Reference
			Human Tests. Upward Linear Acceleration ($+G_z$)				
16.	?	ue; es tower; 30-ft track inclined 14°	15	150 [58]			
17.		ue; test tower	12			Flexion of neck, pain, headache; prevented by use of ejection seat headrest	Watts, et al., 1947a Ref. 42
18.	19-53 yr, 45-87.7 kg [61]	ue; Martin-Baker es on 105-ft test tower	9.8-21.7 (Hip); 7.9-24.7 (Sh); 7.9-21.5 (Hd)	709[9] [39.2-71.2[10] 72.5[11]]		No injury, little discomfort from 18-21 G; critical rate of onset, near 100 G/sec imparted to seat for 0.1 sec; acceleration beyond 100 G/sec for 0.02 sec may be excessive	Watts, et al., 1947a Ref. 42
19.	[60]	ue; vertical deceleration test tower; face curtain	16-21	100 (maximum) [56]		Mild pain in buttocks, lumbar, thoracic, or cervical region; more discomfort with armrests at 10- to 12-G ejection than with curtain at 17- to 21-G ejection. 2 subjects noted pain in neck and headaches. At 20-G ejection, 1 subject noted severe pain in 4th and 6th thoracic vertebrae, ich lasted 6 mo.	Watts, et al., 1947b Ref. 442

20.	[7]	ue; vertical deceleration test tower; Martin-Baker aircraft s; face curtain multiple-charge catapult	9-19(Hip) 9.3-16.0 (Sh); 8.3-16.6(Hd)				
21.	7, 60.7-90 kg [13]	ue, test tower	6.2-15			Back relieved by armrest during ejection; 12.4-28% body mass supported by armrest during deceleration to 10 G, 24-56% body mass by lumbar vertebrae	Savely and Ames, 1948 Ref. 431
22.	[10]	Ft 1st; drop tests with torso h	11			Sharp sensation in lower pelvis; discomfort after tests. At 11-G peak, calculated spinal load with harness, 500 lb; without harness, 900 lb	Kalogeris, 1956 Ref. 418
23.		ue; 110-ft Royal Air Force vertical test rig	25	[300]		Anatomical tolerance limits. Ejection at 5 G or more, in first 0.02-0.05 sec, caused discomfort	Latham, 1957 Ref. 421
24.	13 ♂, mean age 22 yr [111]	Seated in rigid chair; vertical drop apparatus	10(Sh); 95 (s)	625(Sh); 19,000(s)	0.057(Sh); 0.0075(s)	Severe pain in chest, spine, head, stomach; general severe shock	Swearingen, et al., 1960 Ref. 75
25.	[121]	Seated in stafoam chair; vertical drop apparatus	9(Sh); 220 (s)	250(Sh); 44,000(s)	0.12(Sh); 0.065(s)	No pain; slight shock in stomach; peak G not maximum tolerance	
26.	[154]	Standing, Kn locked; vertical drop apparatus	10(Sh); 65 (pl)	666(Sh); 10,000(pl)	0.04(Sh); 0.008(pl)	Severe pain in top of head, throat, chest, stomach, lower back, hip joints, legs, feet	

Table 6–10 (Continued)

Physiological Effects of Headward ($+G_z$) Vertical Impact

	No. of Subjects [No. of Tests]	Experimental Conditions	Peak G	Rate of Onset G/sec [Velocity ft/sec]	Duration sec	Physiological Effects	Reference
			Human Tests. Upward Linear Acceleration ($+G_z$)				
27.	[97]	Standing, legs flexed; vertical drop apparatus	7(Sh); 250 (pl)	583(Sh); 50,000(pl)	0.16(Sh); 0.0075(pl)	Shock in feet; slight pain in legs	
28.	[44]	Squatting; vertical drop apparatus	5(Sh); 133 (pl)	250(Sh); 26,600(pl)	0.20(Sh); 0.0075(pl)	Severe pain in legs, heels	
29.	11[46]	Seated; B-70[13]	12-38[14] (caps.); 17-25[14] (Hd)	492-5480 (caps.) 330-1239[14] (Hd) [9.8-30[14]]	0.005 0.038[14] caps.); 0.015-0.055[14](Hd)	Tolerance limit, 24-G peak with 30 ft/sec velocity change at 500 G/sec rate of onset	Headley, et al., 1962
30.	1[1]	Ft lst; B-58 caps.[7]; upper-torso h		[34]		Small bruises on right thigh and groin	Holcomb and Huheey, 1962
31.		Ft lst; B-58 caps.[8-16]; upper-torso h		[32]		Sharp initial pain; X-rays after 9 days showed compression fracture of 3rd thoracic vertebra, with 4-mm loss in height of centrum	

[2]At various azimuth and elevations. [7]Monorail vertical drop 9 ft-9 in. into water. [8]Monorail vertical drop 9 ft-9 in. onto dirt. [9]Maximum rate for any 0.1 second. [10]Velocity from oscillograph record. [11]Maximum velocity record calculated. [12]Cushion deflated for 6 subjects. [13]Drop-test facility with crushable-paper honeycomb impact attenuator. [14]Calculated from author's data.

Table 6–11

Physiological Effects of Footward ($-G_z$) Vertical Impact

	No. of Subjects [No. of Tests]	Experimental Conditions	Peak G	Rate of Onset G/sec [Velocity ft/sec]	Duration sec	Physiological Effects	Reference
	Human Tests. Downward Linear Acceleration ($-G_z$)						
1.	?	Hd-Ft[19]	3-10 estimated	4-60	0.05-2.5	Brain hemorrhages; 3 G for more than 1 sec unsafe	Schrenk and Irregang, 1945
2.	[1]	Hd lst; ss; sb, Shh; Hd unsupported	10		0.01	Maximum tolerance without symptoms of cerebral concussion, 34.3 G	Henschke, 1945
3.	[7]	Hd lst; ss; sb, Shh; Ft supported, Hd unsupported	31		0.01		
4.	[7]	Hd lst, Kn bent, ss; sb, Shh; Hd unsupported	69.5		0.01		
5.	5[12]	Hd-Bu; 30-ft escalator; hor., with s reversed	6.8 (Hd), 10.0 (Bu); 7.5 (s)	[29.4-38.5]	0.27-0.33	Tolerances are 4 G for 0.3 sec at 38 ft/sec for 5-ft acceleration distance; 7 G for 0.17 sec at 37 ft/sec for 3 ft; 10 G at 22 ft/sec for 1 ft	Shaw, 1948

Table 6–11 (Continued)

Physiological Effects of Footward ($-G_z$) Vertical Impact

	No. of Subjects [No. of Tests]	Experimental Conditions	Peak G	Rate of Onset G/sec [Velocity ft/sec]	Duration sec	Physiological Effects	Reference
	A. Human Tests. Downward Linear Acceleration ($-G_z$)						
6	[6] ♂ young adults [60]	Hd-Ft; Mercury couch; 20 s angle, 87°; full-pressure suit and helmet	18.1-31.8	855-1540 (subj); 962-8140 (sled)	0.070-0.150	Tolerance without injury 14.5-G plateau, 18.5-G peak impact tailward for 0.06 sec, with maximum rate of onset 1540 and 31.8-G peak; no apparent effects on CNS	Critz, et al., 1963
7.	5[28] 20-32 yr	Hd-Ft; Mercury couch; 20 s angle, 107°; couch angle, 5° with s	4.3-18.1	6000-8000 [17 (maximum vel chg)]	0.080-0.200	Negative tailward impact of 10.5 G, with subject acceleration of 17 G at 8140 G rate of onset, successfully tolerated	Highly, et al., 1963 Ref. 416

Table 6–12

Biomedical Effects of Free-Fall Impact

	No. of Subjects [No. of Tests]	Experimental Conditions	Peak G	Rate of Onset G/sec [Velocity ft/sec]	Duration sec	Physiological Effects	Reference
	Human Free-Fall Impact						
1.		Ft-Hd ($+G_z$) parachute h	21	[15-20]	0.1-0.2	Dull headache	Ruff, 1942
2.	3♂, 5♀ [8]	4 prone ($-G_z$), 4 supine ($+G_x$); accidenta' ff, 55-185 ft	28.5-209 estimated	780-28,000 [59.4-109] calculated	0.012-0.073	Ranged from no injury to extensive trauma, but all subjects recovered	DeHeven, 1942
3.	1♂, 55 yr; [1]	Prone ($-G_x$); accidental ff	162 estimated	22,600	0.014	Bilateral fractures of ankles and mandible, abdominal rigidity, complaint of chest pain for 36 hr, blood in urine and mouth	DeHaven and Petry, 1948
4.	30[30]	Prone or supine[24] ($\pm G_x$); ff mountain climbing		[32-152]		Velocity of 33 ft/sec calculated as 50% probability of major injury in transverse direction	Stuckman, 1959
5.	♂, 21 yr [1]	Bu-Hd ($+G_z$); suicidal ff, 218 ft onto hard ground	4128 calculated	2,300,608 [103[23]]	0.0023	Extensive trauma to all areas except legs; fatal 10 days after impact; close to maximum level of human survival for vertical impact	Snyder, 1962

Table 6–12 (Continued)

Biomedical Effects of Free-Fall Impact

	No. of Subjects [No. of Tests]	Experimental Conditions	Peak G	Rate of Onset G/sec [Velocity ft/sec]	Duration sec	Physiological Effects	Reference
				Human Free-Fall Impact			
6.	04 ♂, 33 ♀ 1-91 yr [137]	±x,y,z body orientations, accidental ff		[17-116[23]]	0.0006-0.054	Some survivable falls found to involve high-impact velocity, with durations shorter than in previous human experiments	Snyder, 1963
7.	11 ♂, 8 ♀ 16 mo-[illegible] yr[19]	$\pm G_z$, $+G_x$; soil, concrete, snow		[25-61]		7 uninjured in feet-first $+G_z$ impacts. Cerebral concussion and basilar skull fracture common in head-first impacts ($-G_z$)	Snyder, 1963
8.	34[34]	Children, aged 1-12 years		[21-120]			
9.	♂♀, 7-80 yr 36[36]	Ft 1st & Bu 1st ($+G_z$); voluntary & involuntary ff into water		[52-116[23]]		Critical survival velocity, ca. 100 ft/sec[23]; survival up to 116 ft/sec[23] or 133 ft/sec[23] (standard velocity). Feet-first impacts 5-7 times more survivable: 68% had fractures, usually compressions of 1st lumbar or 12th thoracic vertebrae, 14% had internal trauma, and 33% had no clinical trauma; no injuries to feet or ankles	Snyder, 1965

10.	3[3]	Hd lat ($-G_z$); voluntary & involuntary ff into water		[59-97[23]]		Bilateral pneumothorax, chest pain, renal and bladder hematoma; 1 subject uninjured	Snyder, 1965
11.	2[2]	Sppine, ant.-post. position ($+G_x$); voluntary & involuntary ff into water		[87-92[23]]		Contusions, abrasions, lung hemorrhage, compression of 1st lumbar and 12th thoracic vertebrae	
12.	11[11]	$+G_z$ feet just onto concrete, soil, water		[25-120]		No injury below 44 ft/sec; fatal in case at 50 ft/sec onto concrete, but only minor injuries at 74 ft/sec in another water survived at 120 ft/sec	
13.	2[2]	$+G_y$ lateral concrete, soil		[25-28]		Contusions, fall in soil at 25 ft/sec; 2 yr old; 3 yr old falling on concrete at 28 ft/sec compound depressed fracture RT parietal, unconscious 10 min past-impact	
14.	3[3]	$+G_x$ prone, concrete, water		[22-26]		Concussion reported at 22 ft/sec	
15.	3[3]	$-G_x$ supine, soil		[31-53]		Concussion, internal injuries, vertebral fractures	
16.	1[1]	Hands and knees 4 yr old children		[38]		Laceration, ankle sprain	
17.	1[1]	Prone, post.-ant. position ($-G_x$); voluntary & involuntary ff into water		[88[23]]		Multiple contusions, lung ruptures, mediastinal compression syndrome, mediastinal emphysema, left pneumonitis and pleuritis, lacerations	

Table 6–12

Biomedical Effects of Free-Fall Impact

	No. of Subjects [No. of Tests]	Experimental Conditions	Peak G	Rate of Onset G/sec [Velocity ft/sec]	Duration sec	Physiological Effects	Reference
			Human Free-Fall Impact				
18.	2[2]	On rt side ($-G_y$); voluntary & involuntary ff into water		[57-87[23]]		Contusions, basilar skull fracture, rib fracture, renal hematoma, rupture of right tympanic membrane	
19.	[53]	Age 2 mo-14 yrs, selected	35.8-159.0	[24-51]	0.007-0.02	Survival at forces ranging from 1,074-15,264 lb.	Snyder, 1969
20.	14[14]	$-G_z$ headfirst onto concrete soil, snow		[29-64]		48 ft/sec headfirst fatal to 8 mo old; fall in identical conditions produced cerebral concussion contusions to 6 yr child; other impacts to 64 ft/sec survived with cerebral concussions, and/or skull fractures	

[14]Calculated from author's data. [19]Tests included diving in water. [20]On Air Crew Equipment Laboratory, USN, Philadelphia, linear decele ...tors. [21]Wedge impact attenuators. [22]Attenuators of stabilizing fin slicing angles and sliceable cylinders. [23]Corrected for aerodynamic drag. [24]Body position during free-fall assumed in some cases. [25]Euarctos americanus, 4 Selenarctos sp. [26]At abdominal surface. [27]For 300- to 400-G peaks. [28]Estimated from authors data. [29]2 subjects.

In five cases of thirty-four total force calculations were estimated.

For each region of the body, specific tolerance can be defined. The physical properties of bone are best known, but much less information is available concerning physical properties of most soft tissues and organ systems. Such information is important since human tolerance to a specific impact may be limited by the soft tissue damage to a critical organ at levels far below skeletal structural failure. Damage may occur at the cellular level with no gross evidence of shear, tensile, or compressive forces. Such localized trauma may limit whole body tolerance to the lowest threshold of an organ or tissue.

Any attempt at stress analysis of man with respect to impact forces must take into account the responses of the body as a whole: the simultaneous responses of different kinds and states of materials in the body structure, such as the pneumatic and hydraulic behavior of gases and fluids, plastic deformation of soft tissues, the stretching of mesenteries and ligaments by organ masses, and the nonlinearities prevalent throughout the body. Human stress analysis must determine reversible and irreversible, disabling and fatal failure criteria for the human structure, and should relate measurements to points of structural weakness or of load concentrations (von Gierke, 1961). To better understand the mechanics of the body, mechanical analogs have been devised (Coermann et al., 1960; Shapland, 1961; Payne & Stech, 1962; Feder & Root, 1964; Kornhauser, 1964; NASA, 1965; von Gierke, 1967; Stech & Payne, 1968). Eventually, there may be sufficient data about impedence of segments, body masses, coupling, damping, kinetics, and other features of the models so that they may permit accurate predictions about the effects of the random, multivectored, and, often, sequential forces that operate under actual impact environments.

Lastly, biomechanical effects of impact are dependent, as are physiological effects, upon the environmental complex surrounding the impact event, that is, body orientation, velocity, protection, and so forth.

Physical Properties of Human Tissue

Table 6-13 shows some physical properties of human tissue. Data concerning the strength of the vertebrae are also available (Ruff, 1950; Percy, 1957; Gurdjian, 1962; Crocker & Higgins, 1966; Henzel, 1967).

Vertebral Fracture

Escape ejection accelerations from high performance aircraft have resulted in vertebral injury, generally compression of the anterior lips of the lumbar or thoracic vertebrae (Stapp, 1959; Jones et al., 1964; Chubb et al., 1965; Ewing, 1966; Collins et al., 1968; Klopfenstein, 1969). This may be due to poor seat padding, seat contour, inadequate restraint, forced head flexion, poor trunk-thigh angle, or spinal extension or flexion (Jones et al., 1964). Approximately 80 percent of all vertebral injuries occur in the thoracic region. Available literature to 1965 on ejection-related vertebral injuries in aircrew together with basic findings and analysis of the ejection environment are contained in a study by Higgins et al., (1965.)

Table 6–13
Physical Properties of Human Tissue

	Tissue, Soft	Compact Bone	
		Fresh	Embalmed, Dry
Density, g/cm^3	1 – 1.2	1.93 – 1.98	1.87
Young's Modulus, dyne/cm^2	7.5×10^4	2.26×10^{11}	1.94×10^{11}
Volume compressibility,* dyne/cm^2	2.6×10^{10}	–	1.3×10^{11}
Shear elasticity,* dyne/cm^2	2.5×10^4	–	7.1×10^{10}
Shear viscosity,* dyne sec/cm^2	1.5×10^2	–	–
Sound velocity, cm/sec	$1.5 - 1.6 \times 10^5$	3.36×10^5	–
Acoustic impedance, dyne sec/cm^3	1.7×10^5	6.0×10^5	6.6×10^5
Tensile strength, dyne/cm^2	–	9.75×10^8	1.05×10^9
Shearing strength, dyne/cm^2, parallel	–	4.9×10^8	–
perpendicular	–	1.16×10^9	5.55×10^8

*Lamé elastic moduli.
(After Goldman & von Gierke, 1960)

Compressive load analysis of vertebra-disc complexes have demonstrated that the vertebral end-plates are the initial failing structures of the spinal column (Brown et al., 1957; Snyder, 1958; Roaf, 1960; Patrick, 1961; Stech & Payne, 1963; Henzel, 1967). Vertebrae of cadavers fail at loads as low as 435 pounds (Patrick, 1961). Compression fractures of the vertebrae have occurred under experimental test conditions. An experimental impact at 16 mph of a B-58 escape capsule at 43.6 G (spinal) measured on the subject resulted in one reported compression fracture of T-3 (Holcomb & Huheery, 1962).

An ejection seat impact profile of 18.8 peak G for 100 msec with rate of onset of 420 G/sec and body orientation 34° back from the vertical axis ($+G_z$) produced compression fractures to the fourth and fifth thoracic vertebrae in one subject. Others have been exposed to 26 G and velocity change of 8 m/sec in the $+G_z$ orientation (off-axis 45°) under the same conditions with complaint of occasional "mild transient pain" over the area of the second to fifth thoracic vertebrae (Henzel et al., 1965). More recently a human volunteer received a compression fracture of the seventh thoracic vertebra under impact conditions of 16.62 $+G_z$ peak sled G, with an onset rate of 1160 G/sec, entrance velocity of 39.8 ft/sec and braking distance of 26.5 inches (Klopfenstein, 1969).

End-plate and vertebral body injury is much more apt to occur during spinal axial loading than is intervertebral disc disruption (Ruff, 1950; Percy, 1957; Roaf, 1960; Henzel, 1967). Work by Kazarian et al., (1968) has identified the mechanisms of other vertebral body injuries in $+G_z$ vertical impact. There is general agreement that a peak of 20 to 21 G for a duration of less than 0.1 second at a rate of onset of 250 to 300 G/sec is tolerable if the spine is properly positioned for $+G_z$ impact (Watts et al., 1947b; Beckman et al., 1953; Jones et al., 1964). A thorough review of the biomechanical aspects of vertebral injury is found in Henzel (1967). A viscoelastic rod model which includes damping has been used to simulate the spinal column mathematically (Terry & Roberts, 1968).

Head Injury

Injury to the head is the most frequent and severe result of impact, and 75 percent of aircraft crash fatalities may be attributed to head injury. Usually such trauma occurs through head contact with the structure or projections rather than the action of acceleration forces on the head as a whole. The shape and elastic properties of the object injuring the head and exposure time are of prime importance in determining the degree of injury. Dynamic load measurements on the skull and knee bone conducted with less than 1 $in.^2$ penetrators (such as a control knob) show that skull penetration takes place in five steps: initial load build-up as the penetrator loads the entire skull structure; sudden penetration of the outer layer of compact bone, with abrupt falloff in load, in primarily a tensile fracture approximately the circumference of the penetrator; compression of the diploe layer; a cone-shaped shear failure extending to the inner layer of compact bone; and finally fracture of the inner table in the form

of a plug larger than the diameteof the penetrator. Soft tissue does not significantly (10 percent) alter the skull penetration load (Melvin et al., 1969).

The frontal and occipital bones of the skull have been the subject of numerous impact studies (Gurdjian et al., 1949; Lissner & Evans, 1958; Gurdjian, 1962), but limited data are available related to lateral ($\pm G_y$) impact tolerance of the parietal or temporal bones (Nahum et al., 1968). Experimental studies in progress indicate that lateral blows to the parietal or temporal area result in fracture at about half the loads required to fracture a frontal bone. Within the conditions studied, the total energy required for skull fracture of frontal bone varies from 400 to 900 in.-lb, with an average often assumed to be 600 in.-lb (6.8×10^8 ergs) (Roth, 1967).

Experimental studies also indicate that facial bones fracture due to tension, not compression (Huelke, 1962). Hodgson (1967) found that 1000 lb of force was tolerated for durations of 3 msec or less, while impacts lasting beyond 4 msec produced fracture at approxin ly 200 lb for a 1 $in.^2$ area of distribution.

A mathematical model describing the response of the cadaver zygomatic (cheek) bones to blunt impact has been used (Hodgson et al., 1966). Impacts as low as 30 to 40 G for 10 to 40 msec may produce transient unconsciousness. Fracture tolerance for the facial bones is about 30 G for the nose, 50 G cheekbone, 100 G for teeth (3.6 in^2), 40 G mandible, 80 G for 3 msec (1 $in.^2$ area), or 150 G (4 $in.^2$ area) for the forehead (Swearingen, 1965). For a contact area of 1 $in.^2$, fracture tolerance values for the cheekbone have been found to approximate 200 to 225 lb, for the temporal-parietal (side of head) area, 450 to 550 lb,and 900 to 1100 lb, for the frontal area (Nahum et al., 1968). A 600 Hz natural frequency, 0.01 damping factor, 9.5 lb simple system has been found to represent occiput acceleration response to impacts on the forehead for a 1 $in.^2$ area (within 5 percent), for a wide range of pulse durations and acceleration amplitudes in the cadaver (Hodgson & Patrick, 1968). Such results must be used with caution for the living human.

Neck injury, especially to the cervical spinal cord at the first vertebra, appears to occur from hyperextension rearwards followed by abrupt flexion when the whole body is accelerated from back to front without head support. Neck injury may be aggravated by the increased mass of a helmet. Concussion may be accompanied by deformation or fracture of the skull with shear strains throughout the brain. An experimental model of the human head shows the existence of pressure gradients along three orthogonal axes, and at levels of impact to the forehead of less than 80 G, the pressure gradients are linear in shape. Cerebrospinal fluid flow can produce shear stresses previously demonstrated in the region of the brain stem (Roberts et al., 1966). There is a voluminous literature regarding head impact, skull fracture, cervical injury, and the mechanisms of brain injury (Lindgren, 1966; Caveness & Walker, 1966; National Institutes of Health, 1969; Gurdjian et al., 1970; Hodgson, 1970; Thomas, 1970).

Lower Limb Fracture

Mechanical stiffness of the lower limbs (Hirsch & White, 1965) and the fracture tolerance to bending force in impact (Snyder, 1961; Young, 1967; Mather, 1968) have been studied. The lower leg (tibia) can tolerate a concentrated impact of 1000 to 1500 lb prior to fracture (Young, 1967), and the knee and leg voluntary limit is 1030 lb, with the fracture level at about 1500 lb (SAE, 1970).

Soft Tissues

The mechanical properties of soft tissues have had limited study. The skin appears to fail more often in a tensile or cohesive manner than from a shearing or cutting action. Penetration resistance of human skin is thought to be about 15 to 20 lb (Gadd et al., 1967). Data are available relative to mechanical properties of the tendons, muscles, blood vessels (refer to extensive references in Fung, 1958) and the nervous system (Ommaya, 1968).

Visceral motion responses in humans have been measured by cineradiography. Sixteen subjects were exposed to triangular deceleration pulses (velocity change of up to 2.44 m/sec, time duration of about 7.5 msec, peak acceleration up to 654 m/sec) with successive radiographic images (60/sec) obtained during the impulse. A density wave was observed and interpreted as a shear wave (dilation) traveling through the abdomen and torso. It was concluded that voluntary tolerance may be below 4 m/sec (13 ft/sec velocity change) (Weis & Mohr, 1967).

Resonance and Impedance

Studies such as that cited above suggest that the heart, great vessel branches, and associated visceral attachments behave as a spring-mass system with subcritical damping frequency of 7.5Hz for the human diaphragm when the abdominal musculature is relaxed voluntarily at impact (Weis & Mohr, 1967). Whole body vibration studies with humans (von Gierke, 1964) suggest the thoracic viscera may respond as a spring-mass system with viscous damping. In these studies 4.5 Hz is reported for the diaphragm and heart (von Gierke, 1964). Analysis of 29 human impact tests in the G_x position on the Daisy Decelerator indicated that the natural frequency of the response measured by sternum accelerometers varies inversely as the duration of the onset of the input deceleration. The value of the product of response frequency (Hertz) and onset duration (seconds) is approximately 0.5 (Chandler, 1962).

The general impedance concept is ordinarily used in conditions where the motion is rectilinear but applies equally well for angular motions or combinations of rectilinear and angular motions (Weis & Primiano, 1966). Figure 6-11 illustrates some human impedance results. The figure indicates that except for the sitting and standing positions during steady-state vibration, impedance magnitude ranges from zero at low frequencies to higher values at higher frequencies. Critical frequencies are found at 7 and 12 Hz (Weis et al., 1963b, 1964). The locations of resonances obtained from transient data may not

always coincide with those obtained under vibration conditions (Bowen et al., 1966). The human mechanical impedance for a particular experimental condition can be used to determine the motion of the human center of mass in the same condition (Weis & Primiano, 1966), although the effective center of mass for mechanical impendance may not be the center of gravity.

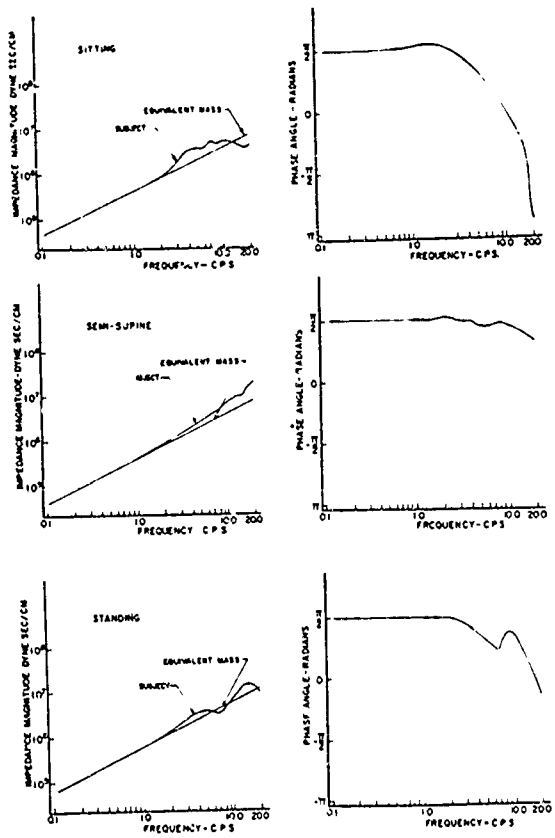


Figure 6–11. Human mechanical driving impedance in the transient (impact) environment. The impedance magnitudes and phase angles reveal critical frequencies at approximately 7 Hz and 12 Hz. The impedance magnitude tends toward zero at low frequencies and toward higher values at higher frequencies. This indicates that man is much like a pure mass over the frequency range of 0 20 Hz, but that resonances in certain frequency ranges depend upon body orientation. (After Weis et al., 1964)

In impact exposure of less than one second when no fluid shifts have time to occur, it is believed that physiological effects are caused by localized pressures and relative tissue displacements. These may develop into pathological trauma if the mechanical stress limits of the tissues involved are exceeded. It has been found that the physical response of the body and its organs, and the impedance of this response on the duration and shape of the acceleration time function, can be calculated when the appropriate mechanical system, representative for the body or the particular situation, is known (Latham, 1957; Shapland, 1961;

Payne, 1961a; Kornhauser, 1961, 1964; Linder, 1962; Feder & Root, 1964; Barrett & Payne, 1965; NASA, 1965; Stech & Payne, 1968). Conditions involving unusual acceleration profiles in accidental or operational situations, nonlinearity in response of tissue, and limitation of complete directional data for the whole body tend to limit use of these models to first order approximations for aerospace design purposes.

If the impact duration is to the same order of magnitude or larger than the natural periods of the body systems, maximum effect of impact functions usually results. Excitation follows a pattern from the dynamic response factor for the transient response of linear structures to shock typical of that shown in figure 6-12. Curves of equal physical displacement of organs are shown as a function of pulse duration and maximum acceleration. In such tolerance curves (see figures 6-5 and 6-12) if the pulse duration is much shorter than the natural period of a system, the response is only dependent on the acceleration time integral, "impulse." It is equal to the differences in velocity of the system before and after impact and ceases to be a direct function of the peak acceleration (NASA, 1965). The curves in figure 6-12 represent undamped responses, but note that the more complex damped responses more realistically represent the actual condition (Barrett & Payne 1965).

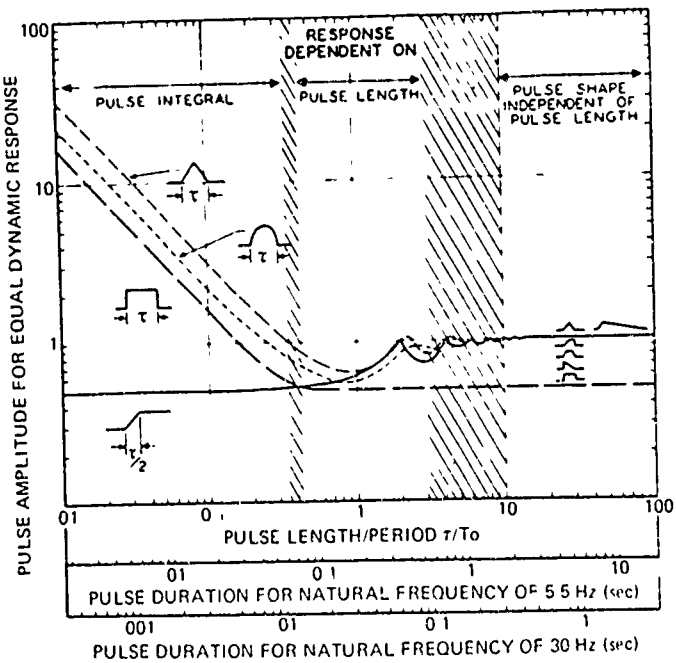
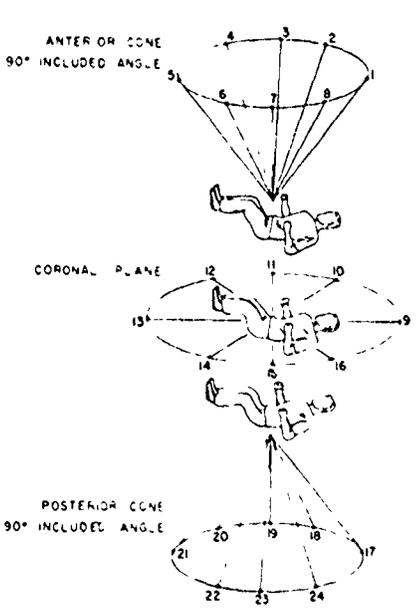


Figure 6–12. Theoretical impact tolerance curves of a one-degree-of-freedom system. Curves of equal physical displacement of organs as a function of pulse duration and max. acceleration. Figure shows, for various types of pulses, pulse height (as a function of ratio of pulse length to natural period of the system) needed to achieve same max. displacement of the system. (T = natural period of system; t = pulse duration). Pulse duration scales on abscissa are for a system with resonance at 5.5 Hz (main body resonance) and for a system with resonance at 30Hz (head resonance). (von Gierke, 1961a, Transient acceleration vibration and noise problems in space flight. In *Bioastronautics*, copyright by the MacMillan Company, 1964, and used with their permission)

In general resonant-response analysis applies to interaction of flexibily linked body masses, and probably to natural frequency characteristics of internally suspended organs, but factors relating to more sustained force application may determine the stress limit. Voluntary tolerance of the lower spinal column in $+G_z$ vertical (longitudinal) impact of less than 6 G amplitude at sustained low-frequency vibrations is in contrast to 20 G, and even 50 G single impact tolerance under well-defined conditions (von Gierke, 1961). This well illustrates the danger in arbitrary conclusions about tolerance, stress limits, and generalized application of criteria beyond their definitions.

Impact Other Than Along Primary Axis ("Off Axis")

The majority of experimental impact studies have been concerned with simple, uniaxial accelerations. Few studies have been conducted of multiaxial acceleration and resultant inertial responses. The orientation of the acceleration vector is a critical factor in human tolerance limitations since the body structures and man's dynamic response characteristics vary with the direction of the applied force. The orientation of the acceleration vector may be random and uncontrolled during aerospace emergency escape, the sequential acceleration environment, and in ground landing impact in closed capsules. The polar coordinate system, in which orientation is expressed in terms of degrees of roll, pitch, and yaw, has been developed to define the precise multiaxial profiles tested (figure 6-13).



SLED POSITIONS

POSITION NUMBER	ROLL	PITCH	YAW
1	0	315	0
2	0	335	330
3	0	005	320
4	0	035	330
5	0	045	0
6	0	035	030
7	0	005	040
8	0	335	030
9	0	085	180
10	0	085	220
11	0	085	270
12	0	085	320
13	0	085	0
14	0	085	040
15	0	085	090
16	0	085	140
17	0	045	180
18	0	035	210
19	0	005	220
20	0	335	210
21	0	315	180
22	0	335	120
23	0	005	140
24	0	035	150

NOTE DECELERATION FORCE ACTS TOWARD SUBJECT

Figure 6–13. Seated subject orientation in 0-0-0 polar coordinates of roll, pitch and yaw relative to direction of sled motion and resultant inertial force. Such a system is used to describe off-axis impacts involving complex multiaxis decelerations. Numbered lines represent direction of forces applied to subject during impact. Columns on right indicate translation of force orientations into seat position. (After Brown et al., 1966; Chandler, 1967b, Stapp, 1968)

To date only one study has been conducted of human response to the acceleration profiles of Project Mercury (Weis et al., 1963a), and two studies have been conducted related to Project Apollo profiles (Stapp & Taylor, 1964; Brown et al., 1966). Table 6-14 provides a summary of other studies in which response of man and animals to impact loads at variable axes is known.

A summary of the acceleration profiles and responses noted in subjects exposed to off-axis accelerations while seated in form-fitting couches used in Project Mercury is presented in figure 6-14 and table 6-15. In these experiments the 20 subjects wore the Mercury pressure suit helmet and sat in a rigid vehicle, restrained with a low elasticity chest and pelvic harness, and were exposed to six deceleration profiles in seven orientations. In the lateral ($\pm G_y$) tests, both rigid foam couches and semirigid "microballoon" couches were used which were molded to the body contour. A vertical drop tower device was employed to decelerate the falling vehicle when a shaped plunger entered the water. In deceleration profiles ranging up to 26 G (peak), 28 ft/sec velocity, and 2000 G/sec rate of onset, subjective tolerance levels were not reached (Weis et al., 1963). Transient premature ventricular contractions were produced, but no injuries occurred.

For Project Apollo, Stubbs (1966, 1967) reviewed impact modes predicted at the couch in Apollo landings. Stapp and Taylor (1964) studied human response to predicted Apollo command module landing impacts in 146 tests of 58 human volunteers, as did Brown et al., (1966) in 288 experiments. In the first series, impact forces were studied in 16 body positions in a combination of pitch and yaw, in seven configurations of onset at 1000, 1500, and 2000 G/sec, at magnitudes of 10, 15, 20, and 25 G, and at durations from 0.060 to 0.130 second. The volunteer subject sat in a seat mounted in three sets of gimbals providing 10° increments in yaw (0° to 360°), pitch (0° to 180°), and roll (0° to 180°), on a sled suspended by four slippers between cylindrical rails. Post-impact bradycardia of less than 30 seconds' duration resulted from headward force vectors exceeding 15 G magnitude. Stomach mobility or displacement occurs during whole body impact when angular force movements exceed 40° or more from the line of motion (in pitch or yaw.) No significant changes in blood or urine were recorded. All body positions and impact configurations studied were within voluntary tolerance limits except the forward-facing 45° reclining position. A forward-facing subject tipped back 45° in pitch sustained simultaneous compression and hyperflexion of the trunk by force vectors at right angles which produced persistent soft tissue injury in the sixth, seventh, and eighth thoracic vertebrae areas, from impact of 25 G at 960 G/sec in 97 msec. Loose restraints contributed to whole body resonance amplification of impact.

With a less sophisticated harness restraint system than the one used in the Apollo study, compression deformities of the fourth and fifth thoracic vertebrae have been reported in a human test subject exposed in laboratory experiments to an impact acceleration profile similar to that produced by ejection seat rockets. This injury was presumed to be the result of an impact profile having a peak acceleration of 18.8 G, a rate of onset of 420 G/sec and a base line duration of approximately 100 msec. The subject's long axis was inclined backward 34°

Table 6–14

Physiological Effects of Off-Axis Impact

	No. of Subjects [No. of Tests]	Experimental Conditions	Peak G	Rate of Onset G/sec [Velocity ft/sec]	Duration sec	Physiological Effects	Reference
	Human Off-Axis Impact Tests.						
1.	[77]	18°, on rt side daisy track	29.9-35.7 (Sh), 22.4-26.7 (Hd); 48.3-55.4 (Ch)	73[illegible]12 (Sh), 761-8.8 (Hd), 1908-3529 (Ch)	0.061-0.076 (Sh), 0.064-0.076 (Hd), 0.060-0.064 (Ch)	Chest pains, headaches up to 18 hr, brief disorientation, or difficult breathing; single case of mild ischemia, hyoid dislocation, shock, albuminuria (1+, later negative). No blood pressure immediately post-run, 80/50 at 2 min, 104/58 at 5 min. 20 G upper limit for no spinal injury in aircraft seat ejection.	Beeding, 1958
		32°, on rt side; daisy track	36.5-51.7 (Sh); 20.3-36.2 (Hd)	8[illegible]1494 (Sh), 5[illegible]24 1.35 (Hd)	0.0[illegible]-0.058 (Sh), 0.047-0.068 (Hd)		
		48°, on rt side; daisy track	46.9-53.7 (Sh), 27.0-36.1 (Hd)	1[illegible]3-1875 (Sh), 1[illegible]-1191 (Hd)	0.048-0.051 (Sh), 0.054-0.047 (Hd)		
		62°, on rt side; daisy track	27.6-36.6 (Sh), 33.3-40.7 (Hd)	1[illegible]-1680 (Ch)	0.050-0.051 (Sh), 0.056-0.059 (Ch)		
		78°, on rt side; daisy track	3[illegible]-45.[illegible] (Ch)	1564-2078 (Ch)	0.042-0.045 (Ch)		
		92°, on rt side, daisy track	45.[illegible]-55.3 (Ch)	1482-2650 (Ch)	0.048-0.053 (Ch)		
2.	[8]	135°, on rt side, daisy track	25.2-30.4[1]	849-1101	0.072-0.098	No injuries reported	Beeding, 1960
3	[17]	Seated, 45° to vertical, B-58 cabs., dropped 22-58 in. into wet sand	$+G_x$, 32.2	[$+G_x$, 11-18[14]]	$+G_x$, 0.045	No injury	Holcomb, 1960
			$-G_x$, -16.3	[$-G_x$, 11-18[14]]	$-G_x$, 0.052		

			$+G_z$, 17.6	[$+G_z$, 12-18[14]]	$+G_z$, 0.060		
			$-G_z$, -39.4	[$-G_z$, 12-18[14]]	$-G_z$, 0.030		
4.	[20]	Seated; Sp par. to ground, B-58 caps.; dropped 34-132 in. into wet sand[21]	$+G_x$, 53.2	[$+G_x$, 15.6-26.6[14]]	$+G_x$, 0.046		
			$+G_z$, 16.9	[$+G_z$, 13.6-26.6[14]]	$+G_z$, 0.015		
			$-G_z$, -21.2	[$-G_z$, 13.6-26.6[14]]	$-G_z$, 0.019		
5.	[13]	Seated; Sp 9.5° from hor.; B-58 caps., dropped 51-132 in. onto hard dirt[22]	60.4 (maximum)	[17-26.6[14]]	0.04-		
6.	[8]	Seated, Sp 9.5° from hor.; B-58 caps.; dropped 60-114 in. onto steel plate over concrete		[18-24.7[14]]			
7.	20[75]	AMRL Vertical Deceleration Tower Project Mercury couch, rigid restraints 7 body orientations. $-G_x$, $-G_z$, $\pm G_y$ and 45° components	≤ 26	200-2000 [5-28]		Tests did not reach voluntary tolerance level at these conditions. In 4 cases EKG alterations noted. No other physiological changes found. Several subjects noted "mild" pain or "wind knocked out."	Weiss, et al., 1963

Table 6–14 (Continued)
Physiological Effects of Off-Axis Impact

	No. of Subjects [No. of Tests]	Experimental Conditions	Peak G	Rate of Onset G/sec [Velocity ft/sec]	Duration sec	Physiological Effects	Reference
			Human Off-Axis Impact Tests (Cont'd)				
8.	58[146]	16 positions in combined pitch and yaw; daisy track; s mounted on sled in 3 sets of gimbals, providing fixation by 10° increments in yaw (0-360°), pitch (0-180°), roll (0-180°)	10; 15; 20; 25	1000; 1500; 2000 [20-45]	0.060-.130	Bradycardia immediately post-impact; heart rate dropped up to 90 beats/min for 30 sec; gastric motility changed with 40° pitch or yaw angles; no significant changes in blood or urine. All body positions and impact configurations were within voluntary tolerance limits except forward-facing 45° reclining position at 25.4 G (sled), with onset rate of 1000 G/sec for 0.060 sec. Pain and stiffness for 60 days due to compression of soft tissues around 6th, 7th, and 8th thoracic vertebrae.	Stapp and Taylor, 1964
9.	28[58, 12]	4 pitch orientations $-G_x$ 45° pitch fwd. from vertical[1]	9.8-26.3[2]	610-1430 [18-32.4][3]	0.072-.128	6 subjects reported no complaints; 3 subjects complained of mild pain for 3 to 6 min post-impact; 3 subjects complained of pain or muscle soreness lasting 1 to 14 days.	Stapp, et al., 1965
10.	[12]	$-G_x$ 45° pitch Back from vertical[4]	8.5-25.0	630-1440 [17.9-31.4][3]	0.068-.140	4 subjects had no complaints; 4 reported mild pain for 2 to 10 min post-impact; 3 reported moderate pain and muscle soreness for 6 to 72 hr after impact; 1 subject sustained severe soft tissue compression injury at 6th, 7th, and 8th thoracic vertebral areas persisting for 60 days post-impact	Stapp, et al., 1965

11.	[8]	$+G_x$ 45° pitch fwd from vertical axis[5]	16.5-22.5	835-2110 [45.8-45.6][3]	.124-.177	1 subject had no complaints; 6 subjects reported mild pains for 3 to 5 min post-impact; 1 subject had moderate pain and muscle soreness lasting 12 hr	
12.	[6]	$+G_x$ seat pitched backward 45° from vertical[6]	15.8-21.9	910-1970 [43.1-45.8][3]	.150-.192	5 subjects had no complaints; 1 subject reported mild pain of 24 hr duration post-impact	
13.	79[288]	24 seat orientations using Apollo restraint	5.5-30.7	300-2500 [9.3]	0.80-.200	Detailed physiological findings are listed in Table V-2	Brown, et al., 1966
14.	5 [18] ♂	RAF Swing frame device. F-111 LAN and USAF CD harnesses. 45° left forward orientation.	6.2 - 8.2	118 - 210		Tenderness in groin, pain in throat, collar bone subjectively reported.	Reader, 1967

from the vertical force vector (Roth, 1967). Stapp and Taylor (1964) recommend head fixation, energy attenuation to keep impact force below 20 G magnitude and above 60 msec pulse duration, and automatic retraction of the harness prior to impact to prevent slack and relative body motion. The most favorable position was found to be backward-facing ($+G_x$), bowing 45° from vertical.

Information relative to the effects of simultaneous multiaxial impact forces combined with other environment conditions are not known. For data on complex multi-environmental stresses, the reader is referred to chapter 19.

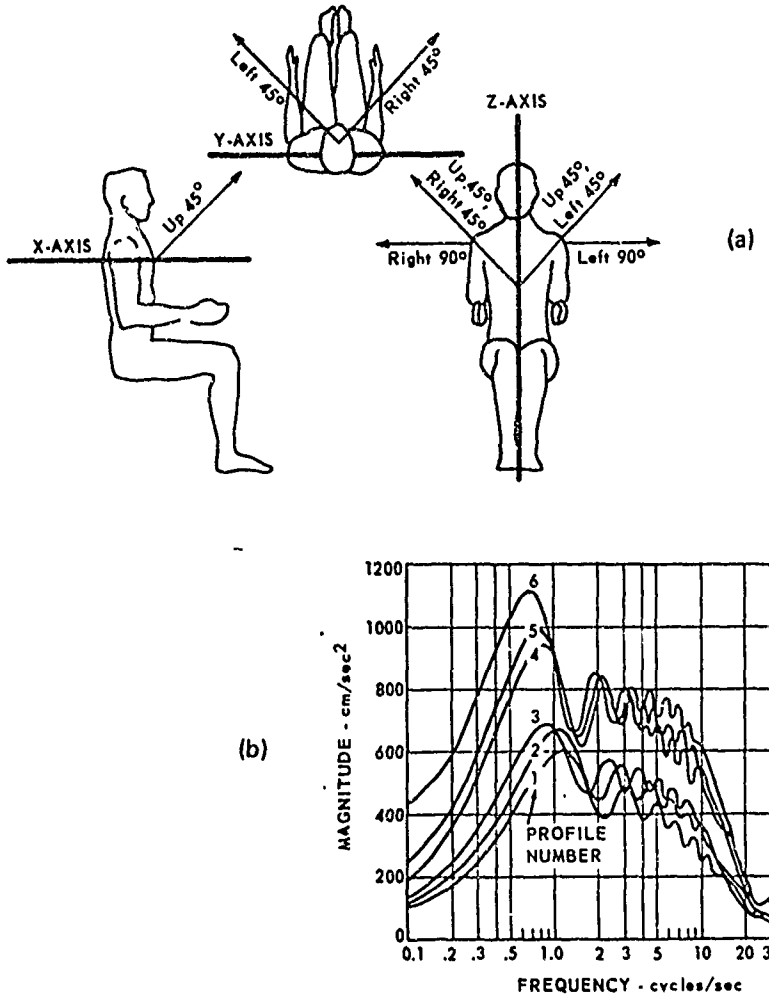


Figure 6–14. Off-axis impact: a Project Mercury profile. Data for tolerability of impacts applied laterally and off major body axes. A: Directions of impact for 5 positions 45° off axis, and for $\pm G_y$ axis. B: Power density spectra of 6 deceleration profiles ranging from 13.4 – 26.6 G with onsets from 426–177 G/sec. No injuries resulted. (Adapted from Weis et al., 1963)

Table 6–15

Responses of Subjects in Project Mercury Deceleration Profile Study

Orientation	Acceleration Profiles					
	1	2	3	4	5	6
Right 45°	None	None	"Slight pain" in center of forehead lasting 5 min	"Slight pain" above left ear in skull	Complained bitterly but diffusely – EKG shows abrupt rhythm changes and four PVCs	Complained bitterly but diffusely
Up 45°	None	Transient pain in occiput	Transient pain in occiput – developed severe pain in neck four hr post-test, gone in a.m.	None	Slight head pain – pain about T2 or T3; transient – developed severe muscle pain at point of left scapula – gone 24 hr	None
Left 45°	Transient pain in occiput moving to temples	None	None	None	None	Mild pain radiating from right midaxillary line at level of 11th rib to left iliac crest, transient
Left 45° up 45°	None	None	None	Fleeting pressure under chest belt	Mild pain beneath chest strap – mild pain about C8 or T1* in midline posterior	None
Right 45° up 45°	None	None	None	None	"Wind knocked out"	"Wind knocked out"
Right 90°	None	None	Skinned right elbow	Pain in right calf	Pain in right calf	"Knocked wind out"
Left 90°	None	None	Pain in right trapezius	None	"Wind knocked out"	One PVC, 2 min post-test and 11 sec pre-test

*T1, T2, T3 – first, second and third thoracic vertebrae; C8 – eighth cervical vertebra.

(Adapted from Weis, 1963)

References

Air Force Systems Command, Headquarters. *Handbook of Instructions for Aircraft Design* (HIAD). Rept. ARCDM-80-1, Andrews AFB, Washington, D.C. 1960.

Aldman, B. Biodynamic studies on impact protection. *Acta Physiologica Scandinavia*, 1962, *56*(192), 1.

Ames, W. H. Tolerance to acceleration in the automatic pilot ejection seat. *U.S. Army Medical Department Bulletin*, 1947, 7(9).

Barrett, S. & Payne, P. R. ,Response of a linear damped dynamic system to selected acceleration inputs. Rept. AMRL TR-65-40, Aerospace Medical Research Labs., Wright-Patterson AFB, Ohio, April 1965.

Beckman, E. L., Ziegler, T. E., Duane, T. D., & Hunter, H. N. Some observations on human tolerance to accelerative stress. Phase II. Preliminary studies on primates subjected to maximum simple accelerative loads. *Journal of Aviation Medicine*, 1953, *24*(5), 377-392.

Beeding, E. L., Jr. Daisy track and supporting systems. Rept. AFADC TR-8, 6571st Aeromedical Research Laboratory, Holloman AFB, New Mexico, June 1957a.

Beeding, E. L., Jr. Daisy track tests. Rept. AFMDC TR-57-6, 6571st Aeromedical Research Laboratory, Holloman AFB, New Mexico, April-June 1957b.

Beeding, E. L., Jr. Daisy track tests. Rept. AFMDC TR-58-7, 6571st Aeromedical Research Laboratory, Holloman AFB, New Mexico, June 1958.

Beeding, E. L., Jr. Daisy tract tests – test numbers 338-519. Rept. AFMDC TR-59-14, 6571st Aeromedical Research Laboratory, Holloman AFB, New Mexico, May–July 1959.

Beeding, E. L., Jr. Daisy decclerator tests. Rept. AFMDC 60-4, 6571st Aeromedical Research Laboratory, Holloman AFB, New Mexico, July 1960.

Beeding, E. L., Jr. Human forward-facing impact tolerance. *Aerospace Medicine*, 1961, *32*(3), 220.

Beeding, E. L., Jr., & Cook, J. E. Correlation tests of animals and humans. 5th Stapp Automotive Crash Field Demonstration Conference, 1962.

Beeding, E. L., Jr., & Hessberg, Jr. Daisy track tests 271-337. Rept. AFMDC TR 28-8, Run 4 Feb.–9 May 1958, 1958.

Beeding, E. L., Jr., & Mosely, J. D. Human deceleration tests. Rept. AFMDC-TN-60-2, Air Force Missile Development Center, Holloman AFB, New Mexico, January 1960.

Bierman, H. R. The protection of the human body from impact forces of fatal magnitude. *Military Surgeon*, 1947, 100-125.

Bierman, H. R., & Larson, V. R. Reactions of the human to impact forces revealed by high speed motion picture technique. *Journal of Aviation Medicine*, 1946, *17*, 407-412.

Bierman, H. R., & Larson, V. R. Distribution of impact forces on the human through restraining devices. Project X-630, Report No. 4, Naval Medical Research Institute, Bethesda, Maryland, March 1946.

Bierman, H. R., Wilder, R. M., Jr., & Hellems, H. K. The principles of protection of the human body as applied in a restraining harness for aircraft pilots. Project X-630, Rept. 6, Naval Medical Research Institute, Bethesda, Maryland, May 1946.

Bierman, H. R., Wilder, R. M., Jr., & Hellems, H. K. The physiological effect of compressive forces on the torso. Project X-630, Rept. 8, Naval Medical Research Institute, Bethesda, Maryland, December 1946.

Boland. (Unpublished test data), 1970.

Bowen, I. G., Fletcher, E. R. et al. Biophysical mechanisms and scaling procedures applicable in assessing responses of the thorax energized by air-blast overpressures or by non-penetrating missiles. DASA-1857, Defense Atomic Support Agency, Washington, D.C., November 1966.

Brown, T., Hansen, R. V., & Yorra, A. S. Some mechanical tests on the lumbosacral spine with particular reference to the intervertebral discs, a preliminary report. *Journal of Bone and Joint Surgery*, 1957, 39(5), 1135-1164.

Brown, W. K., Rothstein, J. D., & Foster, F. Human response to predicted Apollo landing impacts in selected body orientations. *Aerospace Medicine*, 1966, *37*(4), 394-398.

Caveness, W. F., & Walker, A. E. (Eds.) *Head injury conference proceedings*. Philadelphia: J. B. Lippincott Co., 1966.

Chandler, R. F. Unpublished communication. National Bureau of Standards, Washington, D.C., 1970.

Chandler, R. F. The daisy decelerator. Rept. ARL-TR-67, 3, 6571st Aeromedical Research Laboratory, Holloman AFB, New Mexico, May 1967.

Chandler, R. F. Lateral impact data. Unpublished summary, 6571st Aeromedical Field Laboratory, Holloman AFB, New Mexico, January 1966.

Chandler, R. F. Determination of equivalent natural frequency indicated by accelerometers mounted over the sternum during human impact in the G_X direction. Rept. ARL-TDR-62-29, 6571st Aeromedical Research Laboratory, Holloman AFB, New Mexico, December 1962.

Chubb, R. M., Dietrick, W. R., & Shannon, R. H. Compression fractures of the spine during USAF ejections. *Aerospace Medicine*, 1965, *36*, 968-972.

Coburn, K. R. Physiological end points in acceleration research. *Aerospace Medicine*, 1970, *41*(1), 5-11.

Coermann, R. R., Ziegenruecker, G. H., Wittmer, A. L. et al. The passive dynamic mechanical properties of the human thorax-abdomen system and of the whole body system. *Aerospace Medicine*, 1960, *31*, 443-455.

Cofer, F. S., Sweeney, H. M., & Frenier, C. E. History of development since 1941: USAF ejection seats. *ASTIA ATI*, 1946, 9213.

Collins, T. A., Sawyer, C. H., Ferrari, V. J., & Shannon, R. H. Five-year injury experience in escape from USAF ejection seat equipped aircraft. *Aerospace Medicine*, 1968, 39, 627-632.

Cook, J. E., & Mosely, J. D. Visceral displacement in black bears subjected to abrupt deceleration. *Aerospace Medicine*, 1960, *31*(1), 1.

Critz, G. T., Highly, F. M., Jr., & Hendler, E. Determination of human tolerance to negative impact acceleration. Phase II. Paper (2) presented at the 34th Annual Meeting of the *Aerospace Medical Association*, Los Angeles, California, April-May, 1963.

Crocker, J. R., & Higgins, L. S. Phase IV, investigation of strength of isolated vertebrae. TI-1313-66-2, Technology, Inc., Dayton, Ohio, May 1966.

Davydov, B. I., Antipov, V. V., & Saksonov, P. P. Reactivity of the irradiated organism during acceleration of critical magnitude. *Cosmic Research*, 1965, 3(1), 97-102. Translated from *Kosmicheskie Issledovaniya*, 1965, 3(1), 159-166.

DeHaven, H. Mechanical analysis of survival in falls from heights of fifty to one hundred and fifty feet. *War Medicine*, 1942, 2, 586.

DeHaven, H., & Petry, R. M. Informative accident number 7 – Crash injury research. Cornell University, Medical College Crash Injury Research, May 1948.

Dixon, F., & Patterson, J. L. Determination of accelerative forces acting on man in flight and in the human centrifuge. Project NM001 059 04.01, U.S. Naval School of Aviation Medicine, Pensacola, 1953.

Eiband, A. M. Human tolerance to rapidly applied accelerations: A summary of the literature. NASA Memo-5-19-59E, June 1959.

Ewing, C. L. Vertebral fracture in jet aircraft accidents: A statistical analysis for the period 1959 through 1963, U.S. Navy. *Aerospace Medicine*, 1966, *37*(5), 505-508.

Ewing, C. L., Thomas, D. J., Patrick, L. M., Beeler, G. W., & Smith, M. J. Living human dynamic response to $-G_x$ impact acceleration. II. Accelerations measured on the head and neck. Thirteenth Stapp Car Crash Conference Society of Automotive Engineers, Inc., New York, 1969.

Feder, H. C. & Root, E. H. Dynamic response analysis of $+G_x$ impact on man. ARL-TR-64-11, Aeromedical Research Laboratory, Holloman AFB, New Mexico, November 1964.

Foster, P., & Sonntag, R. W., Jr. Urinary excretion of catecholamines and 17-hydroxycorticosteroids following $+G_x$ impact in humans. *Aerospace Medicine*, 1969, *40*(1), 18-23.

Fung, Y. B. Biomechanics: its scope, history, and some problems of continuum mechanics in physiology. *Applied Mechanics Review*, 1968, *21*(1), 1-20.

Gadd, C. W., Peterson, F. J., & Lange, W. A. Strength of skin and its measurement with special application to trauma. American Society of Mechanical Engineers, New York. *Biomechanics Monograph* 1967, 184-191.

Gazenko, O. G., Antipov, V. V., Parfenov, G. P., & Saksonov, P. P. Results of a biological experiment conducted aboard the automatic station "Zond-5". *Aerospace Medicine*, 1969, *40*(11), 1244-1247.

Geertz, A. *Grenzen und sonderprobleme bei der anwendung von sitnkatapulten*. [Limits and special problems in the use of seat catapults], Translation No. U 10-46-22, AAF Aero Medical Center, 1944.

Gell, D. F. Table of equivalents for acceleration terminology: Recommended for general international use by the Acceleration Committee of the Aerospace Medical Panel, AGARD. *Aerospace Medicine*, 1961, *32*, 1109-1111.

General Dynamics/Convair. Capsule escape system specifications, FZC-4-344(G), San Diego, Calif., February 1961.

Goldman, D. R., & von Gierke, H. E. The effects of shock and vibration on man. Lecture and Review Series No. 60-3, Naval Medical Research Institute, Bethesda, Maryland, January 1960.

Gurdjian, E. S. Experiences in head injury and skeletal research. In Impact Acceleration Stress Symposium, Brooks AFB, Texas, November 1961. NAS-NRC-977, National Academy of Sciences, National Research Council, Washington, D.C. 1962.

Gurdjian, E. S., Webster, J. E., & Lissner, H. L. Studies on skull fracture with particular reference to engineering factors. *Journal of American Surgery*, 1949, *78*, 736-742.

Gurdjian, E. S., Lissner, H. R., Webster, J. E., Latimer, F. R., & Haddad, B. F. Studies of experimental concussion. Relation of physiologic effect to time duration of intracranial pressure increase at impact. *Neurology*, 1954, *4*, 674-681.

Gurdjian, E. S., Lange, W. A., Patrick, L. M., & Thomas, L. M. *Impact injury and crash protection*. Springfield: C. C. Thomas, 1970.

Hanson, P. G. Maximum voluntary ventilation after $+G_x$ impact in humans. Rept. ARL-TR-65-22, 6571st Aeromedical Research Laboratory, Holloman AFB, New Mexico, November 1965.

Hanson, P. G., & Foster, P. Urinary excretion of vanilmondelic acid after $+G_x$ impact in humans. Rept. ARL-TR-66-6, 6571st Aeromedical Laboratory, Holloman AFB, New Mexico, March 1966.

Hirsch, C., & White, L. A. Mechanical stiffness of man's lower limbs. ASME Paper No. 65 WA/HUF-4, 1965.

Hodgson, V. R. Physical factors related to experimental concussion. In *Impact injury and crash protection*. Springfield: Charles C. Thomas, 1970.

Hodgson, V. R. Tolerance of the facial bones to impact. *American Journal of Anatomy*, 1967, *120*, 113-122.

Hodgson, V. R., Lange, W. A., & Talwalker, R. K. Injury to the facial bones. Proceedings of the Ninth Stapp Car Crash Conference. St. Paul: University of Minnesota Press, 1966.

Hodgson, V. R., & Patrick, L. M. Dynamic response of the human cadaver head compared to a simple mathematical model. Proceedings of the Twelfth Stapp Car Crash Conference. Society of Automotive Engineers, Inc., New York, 1968.

Holcomb, G. A. Impact studies of the United States aerospace industry, presented at the Symposium on Impact Acceleration Stress, Brooks AFB, San Antonio, Texas, November 1961.

Holcomb, G. A., & Hulsey, M. A minimal compression fracture of T-3 as a result of impact. In *Impact acceleration stress* Publication 977, National Academy of Sciences, National Research Council, Washington, D.C., 1962.

Headley, R. N., Brinkley, J. C., Lokatos, G., & Managan, R. F. Human factors responses during ground impact. *Aerospace Medicine*, 1962, *33*(2), 141.

Henzel, J. H., Clarke, N. P., Mohr, G. C., & Weis, E. B., Jr. Compression fractures of thoracic vertebrae apparently resulting from experimental impact, a case report. Rept. AMRL-TR-65-134, Aerospace Medical Laboratories, Wright-Patterson AFB, Ohio. August 1965.

Henzel, J. H. The human spinal column and upward ejection acceleration: an appraisal of biodynamic implications. Rept. AMRL-TR-66-233, Aerospace Medical Laboratories, Wright-Patterson AFB, Ohio, September 1967.

Henschke, U. Acceleration tolerances of the human body. *ASTIA ATI*, 1945, *59*, 705.

Higgins, L. S., Enfield, S. A., & Marshall, R. J. Studies on vertebral injuries sustained during aircrew ejection. Technology incorporated final report. Office of Naval Research, Washington, D.C., May 1965.

Highly, F. M., Critz, G. T., & Hendler, E. Determination of human tolerance to negative impact acceleration. Paper (1) presented at the 34th Annual Meeting of the Aerospace Medical Association, Los Angeles, California, April-May 1963.

Huelke, D. F. Biomechanical studies of the face. *Impact acceleration stress*, Publication 977, reprint, National Academy of Sciences, National Research Council, Washington, D.C., 1962.

Jones, W. L., Madden, W. F., & Luedeman, G. W. Ejection seat accelerations and injuries. *Aerospace Medicine*, 1964, *35*(6), 559-562.

Kalogeris, J. G. Pilot emergency escape upper torso harness support development test of Model F-106A. *ASTIA AD*, 1956, *144*, 950.

Kazarian, L. E., von Gierke, H. E., & Mohr, G. C. Mechanics of vertebral body injury as a result of G_z spinal impact. Presented at the 39th Annual Meeting, Aerospace Medical Association, Bal Harbour, Florida, 1968.

Klopfenstein, H. W. Compression fracture of the seventh thoracic vertebra caused by experimental impact: a case report. Paper presented at the 40th Annual Scientific Meeting, Aerospace Medical Association, San Francisco, May 1969.

Kornhauser, M. *Structural effects of impact*. Baltimore: Spartan Books, Inc., 1964.

Latham, F. A study in body ballistics: seat ejection. Series B. *Proceedings of the Royal Society*, (London), 1957, *147*, 121-139.

Latham, F. Linear deceleration studies and human tolerance. *Clinical Science*, 1958, *17*(1), 121.

Lewis, S. T., & Stapp, J. P. A crash restraint demonstrator. Report TN 57-9, Holloman AFB, New Mexico, June 1957(a).

Lewis, S. T., & Stapp, J. P. Experiments conducted on a swing device for determining human tolerance to lap belt type decelerations. Report TN 57-1, Holloman AFB, New Mexico, December 1957(b).

Lewis, S. T., & Stapp, J. P. Human tolerance to aircraft seat belt restraint. *Journal of Aviation Medicine*, 1958, *29*(1), 187-196.

Linder, G. S. Mechanical vibration effects on human beings. *Aerospace Medicine*, 1962, *33*, 939-950.

Lingren, S. O. Experimental studies of mechanical effects in head impact. *Acta Chirurgica Scandinavica*, 1966, Supplementum 360, Stockholm.

Lissner, H. L., & Evans, F. G. Engineering aspects of fractures. *Clinical Orthopedics*, 1958, *8*, 310-322.

Lombard, C. F., Close, P., Theide, F. C., & Larmie, F. Impact tolerance of guinea pigs related to orientation and containment. *Aerospace Medicine*, 1964(a), *35*(1), 1-6.

Lombard, C. F., Bronson, D. S., Theide, F. C., Close, P., & Larmie, F. Pathology and physiology of guinea pigs under selected conditions of impact and support restraint. *Aerospace Medicine*, 1964(b), *35*(9), 860-866.

Lovelace, W. R., Baldes, E., & Wulff, V. J. The ejection seat for emergency escape from high-speed aircraft. *ASTIA ATI*, 1945, 7245.

McElhaney, J. H., & Byars, E. F. Dynamic response of biological materials. American Society of Mechanical Engineers, New York. *Biomechanics Monograph*, 1967.

Martinez, J. L., Wickstrom, J. K., & Barcelo, B. T. The whiplash injury—a study of head-neck action and injuries in animals. American Society of Mechanical Engineers, 65-WA/HUF-6, 1965.

Mather, B. S. Observations on the effects of static and impact loading on the human femur. *Journal of Biomechanics*, 1968, *1*(4), 331-336.

Melvin, J., Fuller, P., Daniels, R., & Pavliscak, G. Human head and knee tolerance to localized impacts. Report 690477, Society of Automotive Engineers, Inc., May 1969.

Nahum, A. M., Gotts, J. D., Gadd, C. W., & Danforth, J. Impact tolerance of the skull and face. Proceedings of Twelfth Stapp Car Crash Conference, Society of Automotive Engineers, Inc., New York, 1968.

National Academy of Sciences, National Research Council. Symposium on impact acceleration stress, with a comprehensive chronological bibliography, Brooks AFB, Texas, November 1961. NAS-NRC-977, Washington, D.C., 1962.

National Aeronautics and Space Administration. A study of the dynamic model technique in the analysis of human tolerance to acceleration. NASA-TN-D-2645, Stanley Aviation Corporation, Denver, Colorado, March 1965.

National Institutes of Health. A survey of current head injury research. A report prepared by the subcomittee on head injury, National Advisory Neurological Diseases and Stroke Council for the National Institutes of Health, Bethesda, Maryland, 1969.

Noble, R., Mendelsen, E. S., & Watts, D. T. Dynamic responses in the ejection seat system. Bureau of Aeronautics Report No. 5, TED NAM-255005, Navy Department, August 1947.

Ommya, A. K. Mechanical properties of the tissues of the nervous system. *Journal of Biomechanics*, 1968, *1*(2), 127-138.

Patrick, L. M. Caudo-cephalod static and dynamic injuries to the vertebrae. The Fifth Stapp Automotive Crash and Field Demonstration Conference, The University of Minnesota, Minneapolis, 1961.

Payne, P. R. The dynamics of human restraint systems. In *Impact Acceleration Stress*. Proceedings of the National Academy of Sciences–National Research Council Publication 977, November 1961(a).

Payne, P. R. An analog computer which determines human tolerance to acceleration. Report 101-1, Frost Engineering Development Corp., Denver, Colorado, 1961(b).

Payne, P. R., & Stech, E. L. Human body dynamics under short-term acceleration. Tech. Rept. 115-2, Frost Engineering Development Corp., Denver, Colorado, June 1962.

Perey, O. Fracture of the vertebral end plate in the lumbar spine. *Acta Orthopedica Scandinavica*, Supplement XXV, 1957, Stockholm.

Pesman, G. J., & Eiband, A. M. Crash injury. NACA-TN-3775, 1956.

Piotrowski, J. P. The effects of low-level sub-injury impacts on the heart rates of humans. Masters Thesis, State University of New York at Buffalo, January 1968.

Reader, D. C. The restraint afforded by the USAF and proposed RAF IAM seat harnesses for the F-111 under high forward and lateral decelerations. RAF Institute of Aviation Medicine, Farnsborough, England, September 1967.

Rhein, L. W., & Taylor, E. R. Increased skeletal muscle activity following impact. ARL TDR 62-26, December 1962.

Richter, H., Bateman, J. B., Lovelace, W. R., Baldes, C. J., & Wulff, V. J. Ejection experiments with the catapult seat. *ASTIA ATI* 1945, Appendix 9, 7245.

Roaf, A. A study of the mechanics of spinal injuries. *Journal of Bone and Joint Surgery*, 1960, *42*(4), 810.

Roberts, V. L., Hodgson, V. R., & Thomas, L. M. Fluid pressure gradients caused by impact to the human skull. Paper 66-HUF-1, presented before ASME meeting, 1966.

Robinson, F. R., Hamlin, R. L., Wolff, W. M., & Coermann, R. R. Response of the rhesus monkey to lateral impact. *Aerospace Medicine*, 1963, *34*(1), 56-62.

Roth, E. M. (Ed.) Impact. In *Compendium of human responses to the aerospace environment*. Vol. II, Section 7, 1967. Prepared under Contract No. NASA-115 by Lovelace Foundation for Medical Education and Research for National Aeronautics and Space Administration, Report NASA CR-1205 (11).

Rothstein, J. D., & Brown, W. K. Feasibility study. Lateral impact with standard aircraft harness configuration. Rept. ARL-TR-66-3, 6571st Aeromedical Research Laboratory, Holloman AFB, New Mexico, 1966.

Ruff, S. Human resistance to certain types of uneven acceleration. *ASTIA ATI*, 1942, 47532.

Ruff, S. Brief acceleration: less than one second. *German Aviation Medicine–World War II*, 1950, *1* 122 and 139. Department of the Air Force, Washington, D.C.

Ryan, J. J. Human crash deceleration tests on seat belts. *Aerospace Medicine*, 1962, *33*(2), 167.

Savely, H. E., & Ames, W. H. Arm rests on ejection seats. TSE AA 695-66G, Air Technical Service Command, January 1948.

Savely, H. E., Ames, W. H., & Sweeney, H. M. Laboratory tests of catapult ejection seat using human subjects. *ASTIA ATI*, 1946, 119947.

Schrenk, O., Irrgang, R., Lovelace, W. R. et al. Studies on the catapult seat. *Technische Berichte*, 1941, *8*, 24-30.

Shapland, D. J. The dynamic model, an engineering approach to the problem of tolerance to abrupt accelerations. Stanley Aviation Corporation. Paper presented at the Symposium on Impact Acceleration Stress, Brooks AFB, San Antonio, Texas, November 1961.

Shaw, R. S. Human tolerance to negative acceleration short duration. *Journal of Aviation Medicine*, 1948, *19*(1), 39.

Snyder, R. G. et al. Pathology of trauma attributed to restraint systems in crash impacts. *Aerospace Medicine*, 1968, *39*(8), 812-829. (a)

Snyder, R. G. Impact injury tolerances of infants and children in free fall. Paper presented at Thirteenth Conference of the American Association for Automotive Medicine. University of Minnesota, October 1969.

Snyder, R. G. Terminal velocity impacts into snow. *Military Medicine*, 1966(a), *131*(10), 1290-1298.

Snyder, R. G. Physiological effects of impact: Man and other mammals. In P. L. Altman & D. S. Dittmer (Eds.), *Environmental biology*. AMRL TR-66-194, Aerospace Medical Research Laboratories, Wright-Patterson AFB, Ohio, 1966(b).

Snyder, R. G. Survival of high-velocity free-falls in water. FAA-AM-65-12, Federal Aviation Agency, Oklahoma City, Oklahoma, April 1965.

Snyder, R. G. Human tolerances to extreme impacts in free-fall. *Aerospace Medicine*, 1963, *34*(8), 695-709.

Snyder, R. G. A case of survival of extreme vertical impact in seated position. Civil Aeromedical Research Institute Report 62-19, October 1962.

Snyder, R. G. Tibial fracture in cadaver impacts. Civil Aeromedical Research Institute, Federal Aviation Agency, Washington, D.C., 1961. (Unpublished report)

Snyder, R. G. Unpublished test data, 1958.

Snyder, R. G., & Snow, C. C. Fatal injuries resulting from extreme water impact. *Aerospace Medicine*, 1967, *38*(8), 779-783.

Snyder, R. G., Young, J. W., & Snow, C. C. Experimental impact protection with advanced automotive restraint systems: Preliminary primate tests with air bag and inertial reel/inverted-Y yoke torso harness. Eleventh Stapp Car Crash Conference, Society of Automotive Engineers, Inc., New York, 1968. (b)

Society of Automotive Engineers. Human tolerance to impact conditions as related to motor vehicle design. SAE J885b, Society Information Report (in preparation, revised version of SAE J885a), 1970.

Soliday, S. M., & Schohan, B. Task learning of pilots in simulated low-altitude high-speed flight. *Human Factors*, 1965, 7, 453.

Sonntag, K. W. Intracranial pressure in Macaca speciosa during controlled abrupt deceleration. In *Preprints of Scientific Program*, Annual Scientific Meeting, Aerospace Medical Association, Washington, D.C., April 1967.

Sonntag, R. Unpublished test data with human volunteers. 6571st Aerospace Medical Laboratory, Holloman AFB, New Mexico, 1966.

Stapp, J. P. Human exposures to linear deceleration. Part I, Preliminary survey of aft-facing seated position. AF Tech. Rept. 5915, June 1949.

Stapp, J. P. Human exposures to linear deceleration, Part II, The forward-facing position and the development of a crash harness. December 1951(a).

Stapp, J. P. Human exposure to linear decelerative forces in the backward-facing seated positions. *Military Surgeon*, 1951(b), *109*, 106-108.

Stapp, J. P. Human and chimpanzee tolerance to linear decelerative force. Paper presented at Conference on Problems of Emergency Escape in High Speed Flight. Wright-Patterson AFB, Ohio, September 1952.

Stapp, J. P. Crash protection in air transports. (Notes 1947 pig tests Holloman rocket sled.) *Aeronautical Engineering Review*, 1953, *12*(4), 71-78.

Stapp, J. P. Tolerance to abrupt deceleration. Collected papers on aviation medicine. *Advisory Group for Aeronautical Research and Development, North Atlantic Treaty Organization*, Butterworths Scientific Publications, London, 1955(a).

Stapp, J. P. Effects of mechanical force on living tissues. I. Abrupt deceleration and windblast. *Journal of Aviation Medicine*, 1955(b), *26*, 268-288.

Stapp, J. P. Accelerations of space flight. Preprint No. 700-58, American Rocket Society, November 1958(a).

Stapp, J. P. Biodynamics of manned space flight. *Air University Quarterly Review*, 1958(b), *10*(2), 47-52.

Stapp, J. P. Escape from aircraft. In E. Evard, P. Bergeret, & P. M. Van Wulfften Palthie (Eds.), *Medical aspects of flight safety*. London: Pergamon Press, 1959.

Stapp, J. P. Unpublished manuscript. Jolt effects of impact on man. November 1961(a).

Stapp, J. P. Human tolerance to severe, abrupt acceleration. In Ganer & Zuidema (Eds.), *Gravitational stress in aerospace medicine*. Boston: Little, Brown & Co., 1961(b).

Stapp, J. P., Mosely, J. D., Lombard, C. F., & Nelson, G. A. Part I. Biodynamics of maximal decelerations. Part II. Dynamic response of restrained subject during abrupt deceleration. *Analyzed and biodynamics of selected rocket-sled experiments.* USAF School of Aerospace Medicine, July 1964.

Stapp, J. P. Collected data on 46 rocket sled experiments (Holloman AFB). NSL-65-94, Northrop Space Labs., Hawthorne, Calif., May 1965.

Stapp, J. P. Voluntary human tolerance levels. Paper presented at Wayne State University Centennial–Biomechanics Symposium, Detroit, Michigan, May 1968. (in press)

Stapp, J. P., & Blount, W. C. Effects of mechanical force on living tissues. III. A compressed air catapult for high impact forces. *Journal of Aviation Medicine*, 1957, *28*, 281-290.

Stapp, J. P., & Hughes, C. D. Effects of mechanical force on living tissues. II. Supersonic deceleration and windblast. *Journal of Aviation Medicine*, 1956, *27*, 407-413.

Stapp, J. P., & Taylor, E. R. Space cabin landing vector effects on human physiology. *Aerospace Medicine*, 1964, *35*, 1117-1132.

Stapp, J. P., Taylor, E. R., & Chandler, R. Effects of pitch angle on impact tolerance. In C. C. Thomas, Proceedings of the Seventh Stapp Car Crash Conference, 1965.

Stapp, J. P. Whole body tolerance to impact. In P. L. Altman & D. S. Dittmer (Eds.), *Environmental biology*, AMRL-TR-66-194, Aerospace Medical Research Labs, Wright-Patterson AFB, Ohio, November 1966.

Stapp, J. P. Voluntary human tolerance levels. Paper presented at Wayne State University Centennial–Biomechanics Symposium, Detroit, Michigan, May 1968.

Stech, E. L., & Payne, P. R. The effect of age on vertebral braking strength, spinal frequency and tolerance to acceleration in human beings. Rept. No. 122-101, Frost Engineering Development Corp., Denver, January 1963.

Stech, E. L., & Payne, P. R. Dynamic models of the human body. Rept. AMRL-TR-66-157, Aerospace Medical Research Laboratories, Wright-Patterson AFB, Ohio, 1968.

Stubbs, S. M. Landing characteristics of the Apollo spacecraft with deployed-heat-shield impact attenuation systems. NASA-TN-D-3059, January 1966.

Stubbs, S. M. Dynamic model investigation of water pressures and accelerations encountered during landings of the Apollo spacecraft. NASA-TN-D-3980, September 1967.

Stuckman, E. C. Project Mercury pilot support system development live specimen experiment. McDonnell Aircraft Corporation Report 6875(11), 1959.

Swearingen, J. J., Garner, J. D., McFadden, E. B., & Blethrow, J. G. Human voluntary tolerance to vertical impact. *Aerospace Medicine*, 1960, *31*(12), 989.

Swearingen, J. J. Tolerance of the human face to crash impact. FAA-AM-65-20, Federal Aviation Agency, Oklahoma City, Oklahoma, July 1965.

Taylor, E. R. Thrombocytopenia following abrupt deceleration. ARL-TDR-62-30, Holloman AFB, New Mexico, December 1962.

Taylor, E. R. Biodynamics, past, present and future. Rept. ARL-TDR-63-10, 6571st Aeromedical Research Laboratory, Holloman AFB, New Mexico, March 1963.

Taylor, E. R., Rhein, L. W., & Beers, G. R. Effect of atropine upon the relative bradycardia associated with impact. Rept. No. ARL TDR 62-13, 6571st Aeromedical Research Laboratory, Holloman AFB, New Mexico, August 1962.

Taylor, E. R., Rhein, L. W., Carter, V. L., & Chandler, R. The effects of severe impact on bears. 6571st Aerospace Medical Research Laboratory, Holloman AFB, New Mexico, ARL-TDR-64-6, July 1964.

Terry, C. T., & Roberts, V. L. A viscoelastic model of the human spine subjected to $+G_z$ accelerations. *Journal of Biomechanics*, 1968, *1*, 161-168.

Thomas, L. M. Mechanics of head injury. In *Impact injury and crash protection*. Springfield, Ill.: Charles C. Thomas, 1970.

Thompson, A. B. A proposed new concept for estimating limit of human tolerance to impact acceleration. Paper presented at 33rd Annual Aerospace Medical Association Meeting, Atlantic City, New Jersey, April 1962.

United States Air Force. Crash protection and escape/survival. Section 392, Chapt. 3, Aerospace vehicle safety design. Headquarters, Air Force Systems Command, design handbook, series 1-0, general. AFSC D-H 1-6, System safety. (Second Ed.), July 1969.

von Gierke, H. E. Biomechanics of impact injury. In *Impact Acceleration Stress*, Publication 977, National Academy of Sciences – National Research Council, 1962.

von Gierke, H. E. Transient acceleration, vibration and noise problems in space flight, In K. E. Schaefer (Ed.), *Bioastronautics*. New York: MacMillan, 1964(a).

von Gierke, H. E. Biodynamic response of the human body. *Applied Mechanics Review*, 1964(b), *17*(12), 951-958.

von Gierke, H. E. Response of the body to mechanical forces—an overview. In *Lectures in Aerospace Medicine*, Sixth series, School of Aerospace Medicine, Brooks AFB, Texas, February 1967.

von Gierke, H. E., & Goldman, D. E. Effects of shock and vibration on man. *Shock and vibration handbook*. New York: McGraw-Hill, 1961.

Watts, D. T., Mendelson, E. S., & Hunter, H. N. Evaluation of face curtain and arm rest for use on ejection seats. Bureau of Aeronautics Report No. 4, TED NAM-256005, Navy Department, Washington, D.C., 1947(a).

Watts, D. T., Mendelson, E. S., & Kornfield, A. T. Human tolerance to accelerations applied from seat to head during ejection seat tests; pilot's escape from high performance aircraft mechanism for development and test of. *ASTIA ATI*, 1947(b), 206 052.

Webb, P. Impact and vibration. In P. Webb (Ed.), *Bioastronautics data book*. NASA-SP-3006, 1964.

Weis, E. B., Jr., & Primiano, F. P., Jr. The motion of the human center of mass and its relationship to the mechanical impedance. Rept. AMRL-TR-65-50, Aerospace Medical Research Laboratories, Wright-Patterson AFB, Ohio, June 1966.

Weis, E. B., Jr., Clarke, N. P., & Brinkley, J. W. Human response to several impact acceleration orientations and patterns. *Aerospace Medicine*, 1963(a), *34*(12), 1122-1129.

Weis, E. B., Jr., von Gierke, H. E., & Clarke, N. P. Mechanical impedance as a tool in biomechanics. ASME-63-WA-280, 1963. American Society of Mechanical Engineers, Winter Annual Meeting, Philadelphia, Pa., November 1963(b).

Weis, E. B., Brinkley, J. W., Clarke, N. P., & Temple, W. E. Human response to lateral impact. Paper presented at 34th Annual Meeting of the Aerospace Medical Association, Los Angeles, Calif., April-May 1963(c).

Weis, E. B. Jr., Clarke, N. P., & Brinkley, J. W. Mechanical impedance as a tool in research on human response to acceleration. *Aerospace Medicine*, 1964, *35*(10) 945-950.

Weis, E. B. Jr., & Mohr, G. C. Cineradrographic analysis of human visceral responses to short duration impact. *Aerospace Medicine*, 1967, *38*(10), 1041-1044.

Young, J. W. Unpublished report. Tibial fractures in cadavers. 1967.

Zaborowski, A. Human tolerance to lateral impact with lap belt only. 8th Stapp car crash and field demonstration conference, Wayne State University Press, Detroit, 1966.

Zaborowski, A. V., Rothstein, J. D., & Brown, W. K. Investigations in human tolerance to lateral impact. Paper presented at 36th annual meeting, Aerospace Medical Association, New York, April 1965.

CHAPTER 7
VIBRATION

by

Richard J. Hornick, Ph.D.
Litton Systems, Inc.

Travel in vehicles of all types subjects man to mechanical vibration. This chapter presents the results of investigations concerning vibration that contribute meaningful data which may be applied to the design of future transport systems. Emphasis is placed on data describing man's reactions to vibration rather than on the vibration characteristics of vehicles. Vibration characteristics of future vehicles will vary in accordance with differences in size, propulsion system, mass, and maneuvering envelopes, while man's reactions to vibration intensity and frequency can be expected to remain essentially constant.

Vibration effects described in this chapter are organized into the following areas: performance effects reflected in tracking proficiency, reaction time, visual impairment, and other measures related to man's ability to control a system; physiological reactions; biodynamic responses; subjective reactions; and human "tolerance" limits. Most attention is placed on performance effects because of the importance of human performance in the operation of sophisticated man-machine systems and because a significant amount of performance data has been developed in recent years. Technological refinements in shaker systems, better experimental designs, and better attempts to control other attendant variables have all served to give recent data a greater degree of validity.

Major vehicular resonances generally occur in the range of 1 to 30 cycles per second (Hz)*. Man's performance capability is known to be affected by frequencies in that range. Further, whole body and organic resonances occur in this range with potential adverse effects for physiological responses and subjective tolerance. It is for these reasons that the bulk of human vibration studies have been conducted in this low frequency band.

*Hertz (Hz) has been adopted as the standard notation for cycles/second.

Reviewed by Henning E. von Gierke, Dr. Eng., Wright-Patterson Air Force Base.

Preceding page blank

Certain types of motion are not extensively treated in this chapter. Oscillation below 1 Hz is not usually characterized as vibration since such motion is not known to affect performance or body resonances. Instead, motion sickness associated with otolith stimulation is the most severe effect of motion below 1 Hz. Frequencies above 30 to 60 Hz are not normally a problem for man, and, in any case, are easily damped by body-support cushioning as well as by the tissues of the human body.

Another form of vibration not treated extensively here is localized vibration; that is, vibration applied to a limited body area such as the fingertips or the hand. That type of vibration occurs primarily with the use of hand tools such as pneumatic jackhammers. This problem has become less severe in recent years due to the increasing use of automated power equipment.

Very few animal studies are cited. They have been selected only as they exemplify a need for some consideration important for the human.

The Vibration Environment

Terminology of Motion Axes

Terminology for the vibration environment is generally consistent with that described in chapter 6, *Impact*. However, whereas bias or steady state acceleration is identified with an upper case "G," oscillatory vibration is described with a lower case "g." The complete description of a vibration environment includes identification of the bias acceleration. Figure 7-1 and table 7-1 illustrate the major axes of motion and the terminology involved.

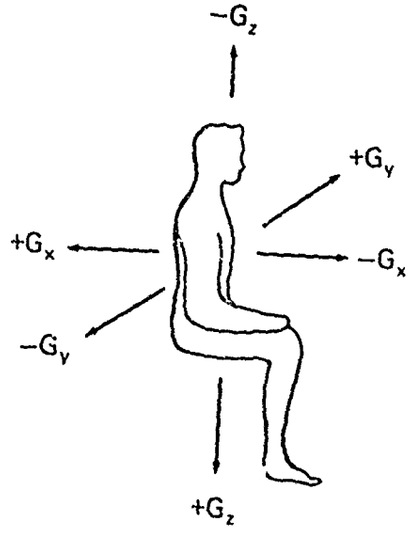


Figure 7–1. Major body axes for acceleration and vibration description.

Table 7–1
Acceleration and Vibration Axis Terminology

Acceleration			Vibration		
Heart Motion Towards	Other Description	Symbol	Heart Motion	Other Description	Symbol
Spine	Eyeballs in	$+G_x$	Spine-sternum-spine	Fore-aft	$\pm g_x$
Sternum	Eyeballs out	$-G_x$			
Feet	Eyeballs down	$+G_z$	Head-feet-head	Head-tail	$\pm g_z$
Head	Eyeballs up	$-G_z$			
Left	Eyeballs left	$+G_y$	Left-right-left	Side-to-side	$\pm g_y$
Right	Eyeballs right	$-G_y$			

To describe completely the vibration environment for a given situation, nondimensional G and g units are used. In the case of a human standing upright in a laboratory on a shake table moving in a direction parallel to the spine, the description would appear as $+1G_z \pm ng_z$ where n would be quantified. In a spacecraft during boost, with the occupants in the usual semisupine position and with vibration being experienced laterally with respect to the body, the dynamic environment might be described as $+3.5G_x \pm 0.5g_y$. An astronaut would be experiencing a 3.5 G boost acceleration force, eyeballs in, with vibration moving him from side to side.

Mathematical Derivations

Vibration is characterized by the periodic displacement of a mass over time and is defined by the amplitude and the frequency of the displacement. Mathematical expressions for sinusoidal vibration are derived from two basic parameters——frequency and amplitude. Frequency can be expressed in any manner related to a time scale——cycles per second (cps), cycles per minute (cpm), Hertz (Hz), etc. The Hz notation will be used in this chapter.

Coupled with frequency is amplitude or intensity. Amplitude is typically expressed by velocity, acceleration, or jerk quantities. The amplitude quantities have been expressed in metric terms and, more often in the United States, in inches or feet per second. A useful quantity is the nondimensional g which can be converted into any kind of expression which the user wishes to employ.

Sinusoidal Vibration. For simple harmonic motion, the following relationships exist between acceleration, velocity, and displacement (Society of Automotive Engineers, 1965):

$$x = x_o \sin (2\pi f)t = x_o (\omega)t$$

where

x = instantaneous displacement from static position, inches

x_o = maximum displacement amplitude from static position, inches

t = time from zero displacement, seconds

f = frequency of oscillation, Hz

ω = $2\pi f$, radians per second

Since the number of gravities of vibration acceleration can be expressed as the following:

$$g = -\frac{(2\pi f)^2 x_o}{G} \sin 2\pi ft$$

where

$G = 386$ inches/sec^2

then

$g = 0.0511Df^2$

where

D is $2x_o$ and is peak-to-peak displacement amplitude

To convert from one numerical system to another, the following equivalent values for g are:

$$g = \frac{\text{acceleration in m/sec}^2}{9.80} = \frac{\text{ft/sec}^2}{32.2} = \frac{\text{in./sec}^2}{386}$$

Occasionally, frequency is expressed in radians, particularly when angular velocity is involved. Angular velocity ω in radians per second = $2\pi f = 6.28$ times the frequency in Hertz. Figure 7-2 illustrates the relations of the parameters in simple harmonic motion.

Random Vibration. Man most often experiences random vibration while traveling in a vehicle. Vibration can be random with respect to frequency and amplitude. At a given frequency, the amplitude may vary from oscillation to oscillation; or amplitude may remain fairly constant and frequency may vary. And, there is motion that varies both with respect to frequency and amplitude.

Amplitude is expressed typically as a root-mean-square (RMS) value in g's. The frequency spectrum (range) is indicated by mean-square spectral density and expressed as power spectral density (PSD), the units being g^2/Hz (Meeder, 1964). Vibration acceleration RMS defines the total energy across the entire frequency band. PSD defines the power at discrete frequencies in the selected bandwidth. A plot of PSD (g^2/Hz) versus frequency illustrates the power distribution of the vibration environment.

In order to equate mathematically a pure sinusoidal amplitude of equivalent RMSg values of random, the peak amplitude of the sinusoid is divided by $\sqrt{2}$.

Vibration Spectra

Data presented here indicate, in general terms, the vibration characteristics of some contemporary vehicles. Future vehicles may well have vibration characteristics which are quite different.

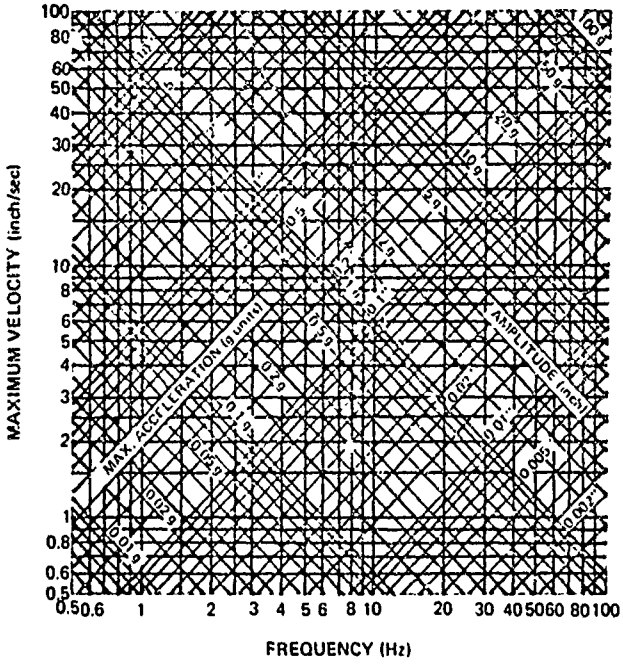


Figure 7–2. Relations in simple harmonic motion. For example, if a mass has an amplitude of 1 in. at a frequency of 1 Hz, the intersection of the vertical line for frequency 1 and the diagonal line for 1 in. amplitude can be used to find velocity and g intensity. Reading horizontally, maximum velocity equals about 6.2 in./sec; reading diagonally, maximum acceleration is about 0.1 g. (From Society of Automotive Engineers, 1965)

Helicopters. Helicopters generate significant vibrations in all major axes. In 1958, Russian helicopters were reported to have significant vibration in a spectrum from 10 to 70 Hz, with amplitudes ranging from 0.4 mm for 70 Hz to 2.4 mm for 10 Hz (Borshchevskiy et al., 1958). Neel (1959) studied the vibration experienced in a suspended litter in the H-13 and H-19 helicopters and found "unpleasant" vibration experienced between 25 and 75 Hz. The UH-1F helicopter, at the base of the pilot seat, shows $\pm g_z$ vibration at 25 Hz with the major frequency components between 100 to 1000 Hz, and a lateral, $\pm g_y$, resonance at 5 Hz at a double amplitude of 0.10 inch. At the seat, the CH-46A has a basic frequency of 4.5 Hz $\pm g_z$, with a major resonance at 12 Hz, and secondary peaks at 28, 38, and 48 Hz (Dean et al., 1964).

In summary, the characteristic helicopter vibration spectrum has a basic low frequency vibration related to the number of overhead rotor blade passes per second. Resonances depend on structural characteristics. The intensity changes of the primary and resonant frequencies depends significantly on load, airspeed, and flight phase.

Aircraft. Prior to jets, the primary source of aircraft vibration was propeller rotation. Vibration was relatively high in frequency (several hundred to several thousand Hertz) and very low in amplitude. While there is a general trend away

from the piston engine/propeller-driven aircraft, it is likely that special applications of such craft, such as the OV-10, will keep them in service for some time to come. Average vibration amplitude for typical propeller-driven military aircraft has been reported to be affected very little by aircraft size, with levels considerably below the envelope at which airborne equipment is tested for military standards (Abeling & Bassett, 1967). Figure 7-3 shows a representative envelope of large aircraft vibration.

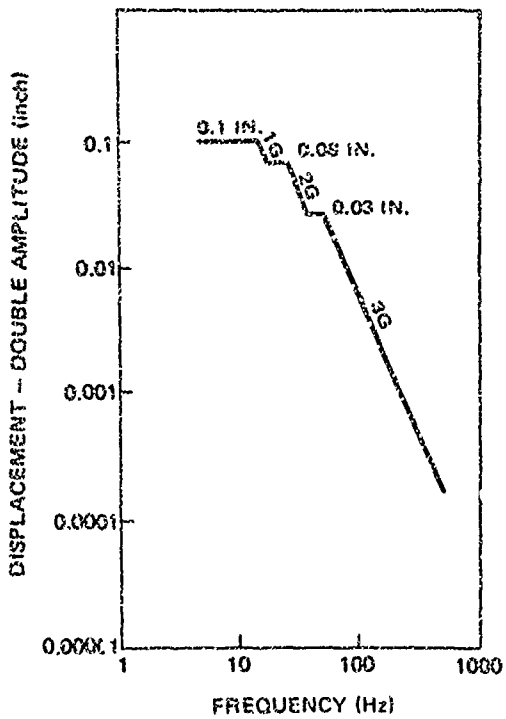


Figure 7–3. Envelope of vibration; B-52, JRB-52B, and YB-52, selected locations. (From Abeling & Bassett, 1967)

When jet aircraft engage in low altitude, high speed flight, the dynamic environment experienced by the pilot is a function of many factors—maneuver loads, wing loading, gust sensitivity, aircraft size, structural bending modes, atmospheric conditions, the type of terrain traversed, and airspeed velocity. Lateral $\pm g_y$ and vertical $\pm g_z$ motion for these aircraft generally have a power peak near 1 Hz, with secondary resonances from 1 to 12 Hz. For a variable, swept-wing configuration, significantly improved ride quality can be achieved by proper design of seating and cushioning; little improvement can be made with fixed-wing configurations (Yamamoto, 1965). Care should be taken, however, that cushioning materials damp rather than amplify the undesirable motion, since the converse is indeed possible.

Primary oscillation for high altitude aircraft is due to atmospheric turbulence. It has been predicted (Notess & Gregory, 1963) that a supersonic transport plane flying above 60 000 feet, would have higher lateral gust sensitivities than propeller aircraft (but lower than current jet aircraft) because of higher speeds with excitation of rigid body and flexible modes. Vertical gust sensitivity, on the other hand, would be very low in an SST, due to the low density of the air at cruise altitude. In general, the probability of encountering periods of turbulence could be expected to be lowest for an SST.

Spacecraft. Relatively little inflight data exist for low frequency vibration for space vehicles. Recording accelerometers typically used have low frequency cutoffs at 20 or 10 Hz. During the first Mercury flights, astronauts complained of vibration during boost which interfered with their vision. A modification was made to the head support padding resulting in more subjectively acceptable vibration levels. A "pogo stick" phenomenon was found in the Titan II rocket engine. This consisted of intense vibration at 11 Hz, experienced along the entire length of the vehicle. A similar problem was detected in an early Saturn V test Fuel pump and engine phasing changes reduced the intensity to acceptable levels.

The only significant vibration levels routinely encountered in spacecraft operations occur during the maximum aerodynamic pressure (max q) portion of boost, with less during atmospheric entry. Since the vibration does occur during boost and entry, it is coupled with a significant bias G acceleration load. Data on the human effects of a coupled vibration-acceleration environment must be obtained from studies conducted with a shaker system coupled with a centrifuge.

Performance Effects

Tracking

A clear statement of the effect of vibration exposure on human tracking performance is not easily achieved for a number of reasons. Paramount is the fact that investigations of vibration stress have used many and diverse tasks, involving a variety of control systems (single axes, multiple axes, fly-to, fly-from, center-stick, side-stick, wheel and column, and steering wheel) in addition to different control system dynamics. However, when similar tasks are used in comparable vibration environments, reasonable agreement of research results is found.

Since most vibration studies have been conducted with seated humans experiencing vertical motion, most data exist for a $+1G_z \pm ng_z$ situation. Considered first are tracking changes found with sinusoidal vibration in the z-axis.

Sinusoidal $\pm g_z$ Vibration. Table 7-2 presents representative findings for the sinusoidal $+1G_z \pm ng_z$ environment. Conclusions for random motion and for tracking effects in other axes are presented at the end of the tracking effects section.

Table 7–2

$+1G_z \pm ng_z$ Vibration Effects on Tracking Ability, Seated Subjects

Vibration Conditions	Tracking Task	Effect	Source
2.5 Hz, ±0.18 and 0.35 g; 3.5 Hz, ±0.15 and 0.30 g, 1.5 hr duration	Subjects and wheel on shaker; static display; single axis compensatory tracking task in horizontal axis	Error a function of frequency and intensity; error greater at 3.5 Hz; incomplete recovery after exposure	Schmitz, Simons, & Boettcher, 1960
0.9 – 5.5 Hz at ±0.15, 0.25, and 0.35 g, 10 min duration	Same	Error elicited, but no effect of frequency or intensity (possibly due to short duration); incomplete recovery after exposure	Schmitz, Simons, & Boettcher, 1960
±0.20 g at 5 Hz, 1 hr duration	Side-arm controller, single axis (horizontal) compensatory tracking	40% decrement in task; incomplete recovery in 15 min postvibration period	Ayoub, c. 1969
1–27 Hz at 4 subjective reaction levels—from "perceptible" to "alarming"	Aircraft wheel and column; 2-axis compensatory: horizontal tracking with wheel, vertical with column	Error related to subjective intensity level; greatest error at 10 – 18 Hz; greater error in horizontal axis in vibration and nonvibration conditions, but vibration has greater relative effect on vertical control	Chaney & Parks, 1964
2, 4, 6, 8, 11, and 15 Hz with single amplitudes of 0.06 and 0.13 in.	2-axis compensatory; static base display, control stick	Slight improvement for 0.06 in.; over 40% error increase at 0.13 in.; greatest error at 8 Hz	Catterson, Hoover, & Ashe, 1962
5 Hz, ±0.26 – 0.36 g; 7 Hz, ±0.29 – 0.41 g; 11 Hz, ±0.55 – 0.77 g; 5 min duration	2-axis compensatory; side-mounted stick controller, second order dynamics	Greatest error produced in vertical tracking axis; 5 and 11 Hz have greatest error in vertical axis; 5 Hz produces greatest error in horizontal; vertical error about 40% greater in vibration compared to static condition; amplitude levels equivalent to 25 – 35% of the 1 min human tolerance level degrades tracking	Buckhout, 1964

Table 7--2 (Continued)

$+1G_z \pm ng_z$ Vibration Effects on Tracking Ability, Seated Subjects

Vibration Conditions	Tracking Task	Effect	Source
5 Hz, ±0.10 – 0.26 g, 20 min duration	2-axis compensatory; side-mounted controller	Horizontal tracking not affected; vertical tracking significantly impaired at and above ±0.21 g, about 40% greater than in a nonvibration condition	Harris, Chiles, & Touchstone, 1964
5 Hz, ±0.10 – 0.26 g; 7 Hz, ±0.15 – 0.30 g; 11 Hz, ±0.25 – 0.62 g; 20 min duration	2-axis compensatory; rate control, side-stick	Horizontal tracking not affected; vertical axis tracking, first impaired at ±0.20 g for 5 Hz, ±0.25 g for 7 Hz, and ±0.37 g for 11 Hz, these levels being about 20% of the 1 min human tolerance limits; decrements in tracking were up to 40% greater than nonvibration error	Harris & Shoenberger, 1966

Sinusoidal versus Random g_z Vibration. Comparatively few studies have investigated the relative effects of sinusoidal and random vibration. In 1961, Parks used a two-axis tracking task with a wheel and column control in random and sinusoidal motion. Of several parameters tested, only the vertical tracking task was affected, at 2.5 Hz sinusoidal at approximately 0.40 g_z. Weisz and coworkers (1965) used a side-stick controller in a two-axis tracking task in sinusoidal 5 Hz, 5 Hz with random amplitude, and a frequency band of 4 to 12 Hz random. Larger errors were reported for vertical tracking than for horizontal tracking. Concerning the relative influence of the vibration environments, error occurred at lower g levels sinusoidal than for random amplitude 5 Hz; and random 4 to 12 Hz vibration did not result in tracking error. These studies tend to establish that random vibration is not as detrimental to tracking performance as is sinusoidal.

Random g_z Vibration. In recent years, knowledge about random g_z vibration effects has come largely from studies which have simulated the low altitude, high speed aircraft response spectrum. For such aircraft, the characteristic motion environment is random, with high energy peaks in the low frequency range. Since many simulations lack a multiaxis motion capability, lateral g_y motion effects (as from lateral gusts) are not fully known. Nevertheless, the lengthy duration of test exposures makes the g_z data quite valuable. Table 7-3 summarizes the studies of long duration random vibration.

Other Axes. The influence of lateral $\pm g_y$ and fore-aft $\pm g_x$ vibration on tracking performance has not been extensively examined. Two studies are indicative, but cannot be applied universally to the $\pm g_y$ and $\pm g_x$ situations. Fraser and coworkers (1961) studied two-axis tracking in the three major axes. Frequencies of 2, 4, 7, and 12 Hz were used, with single amplitudes of 1/16, 1/8, 3/16, and 1/4 inches. No effect of "longitudinal," $+1G_z \pm ng_x$, vibration was detected. Error was greatest in the $\pm g_z$ axis, followed by the side-to-side $\pm g_y$ axis. Hornick and coworkers (1961) studied a horizontal axis tracking task in $+1G_z \pm ng_x$ and $+G_z \pm ng_y$. Frequencies of 1.5, 2.5, 3.5, 4.5, and 5.5 Hz were used at sinusoidal intensities of ±0.15, 0.25, and 0.30 g_x and ±0.15, 0.25, and 0.35 g_y. In the $\pm g_x$ axis, tracking error was related to vibration intensity level. Subjects did not completely recover tracking ability during a 15-minute postvibration period. Finally, there was a slight trend for error to increase as a function of time (during 0.5-hour vibration periods). Similar effects were found for tracking in the $\pm g_y$ axis, with the greatest error rate at the lowest (1.5 and 2.5) frequencies.

Summary of Tracking Effects. The following statements can be made concerning the effects of vibration on the tracking ability of a seated human

1. For the range of 4 to 20 Hz, sinusoidal g_z vibration will significantly impair performance when the double amplitude (D.A.) of 0.05 inches is exceeded. Figure 7-4 indicates the regions of affected and nonaffected performance as delineated by the 0.05 inch D.A. line.

Table 7–3

Effects of Long Duration Random g_z Vibration

Vibration Conditions	Tracking Task	Effect	Source
Aircraft F-111 dynamics; input 0.017 – 0.294 RMSg but closed loop control inputs resulted in 0.028 - 0.291 RMSg; 1.5 hr duration	Center-stick and side-stick controllers, 2-axis terrain following and heading changes	Horizontal control not affected; higher RMSg inputs result in greater pitch control error; no trend for pitch control error to increase as a function of time; pitch error and altitude error for side-stick is about 50% of that with the center-stick, with resulting RMSg reduced by 20% with the side-stick; control error increases as function of task difficulty (displayed terrain)	Soliday & Schohan, 1964
1–5 Hz, shaped PSD	2-axis, with several controller configurations and dynamics	Best performance with side-stick controller with arm support	Torle, 1965
Aircraft, fighter dynamics, input 0.33 RMSg, but closed loop control inputs resulted in 0.40 RMSg; 1 hr duration	Center-stick, simulated terrain following; 3 task difficulty levels—simulated flat, rolling and mountainous terrain	Primary error relationship with tracking task difficulty, greatest error with roughest terrain; altitude error does not increase as function of time	Soliday & Schohan, 1965
Closed loop RMSg levels varied between 0.05 and 0.40 RMSg as function of simulated gust, speed, and pilot inputs; 3 hr duration	Similar to preceding	No altitude control error trend as function of time; increase in simulated "crashes" at end of runs suggesting fatigue	Schohan, Rawson, & Soliday, 1965
1–12 Hz, peak energy at 1 and 7 Hz, with 0.10, 0.15 and 0.20 RMSg; 4 hr duration	Side-stick controller for 2-axis terrain following and avoidance of 3 simulated terrain types—flat, rolling mountainous; open loop platform dynamics	No trend for error to increase as function of time for 2 easiest terrains; error increase as a function of time for only the mountainous terrain after 2.5 hr of exposure; error not related to RMSg intensity; error residual in postvibration period; greatest error for most difficult displayed terrain	Hornick & Lefritz, 1966

1–6 Hz, 0.12 and 0.[illegible] RMSg; two PSD shapes, one with power peak at 2 Hz, one at 5 Hz; 6 hr duration	2-axis, open loop platform dynamics; primarily side-stick controller, with occasional use of center-stick	No trend for error to increase as function of time; error not a function of RMSg intensity; absolute error greater in vertical axis; greater error in spectrum with 5 Hz power peak	Holland, 1967
CH–46A helicopter spectrum, variable RMSg and PSD shapes; seven 40 min tests during 6 hr period	Side-stick controller, 2-axis	No error with this very simple tracking task	Dean, McGlothlen, & Monroe, 1964
UH–1B helicopter spectrum, and frequency sweeps, 4 Hz to over 100 Hz	Variety of controls and servo systems	Greatest tracking error near 5 Hz; position control more accurate in 5–25 Hz range; force control more accurate above 25 Hz	Rosenberg & Segal, 1966

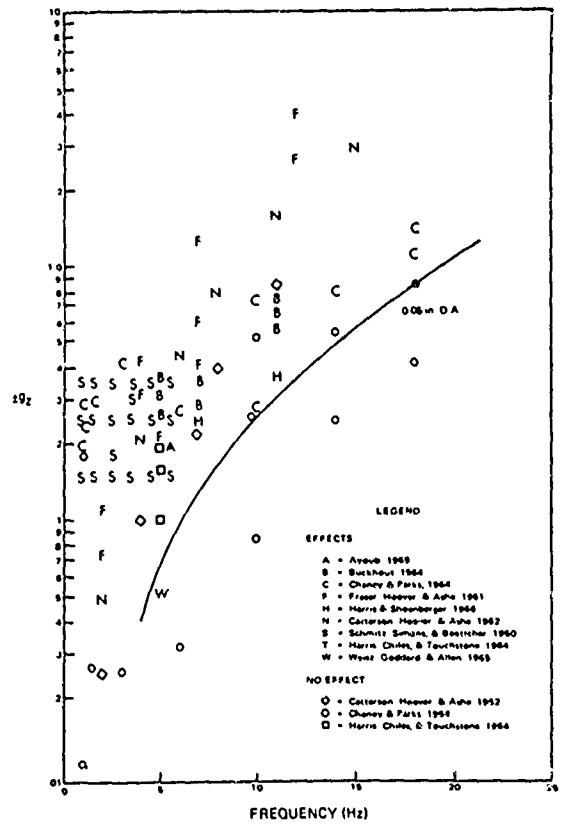


Figure 7-4. Summary of reported effects of $\pm g_z$ vibration on human tracking performance.

2. Sinusoidal low frequency vibration from ±0.20 to ±0.80g_z can produce tracking error up to 40 percent greater than that found in static base conditions. Vehicle control systems must consider the dynamic environment and cannot be designed solely on the basis of static base simulations.

3. Higher RMSg levels are required for random vibration to impair performance as compared to sinusoidal vibration.

4. For sinusoidal vibration, increases in error are related to increases in intensity; for random vibration, tracking error is not related to intensity to approximately 0.40 RMSg. Tracking error during either type of vibration is very much a function of tracking task difficulty, suggesting the use of controls and displays to comprise simplified control task situations.

5. For both random and sinusoidal g_z motion, vertical tracking error is larger than that found for horizontal tracking.

6. For random vibration of long duration, there is no trend for error to increase as a function of time until about 2.5 to 3 hours is reached. Performance deteriorates for difficult tracking tasks at that time, apparently as a result of "fatigue."

7. The type of controller used influences the degree of tracking error experienced. Use of a side-stick and arm support can reduce vibration-induced error in the vertical axis by as much as 50 percent when compared to conventional center-stick controllers.

8. When tracking impairment is experienced during vibration, a residual effect may last up to one-half hour after exposure.

9. Vibration in the $\pm g_x$ and $\pm g_y$ axes is not known to cause decrement greater than that for $\pm g_z$.

Reaction Time

Ability to respond rapidly to a stimulus during exposure to vibration has been subjected to much investigation in a wide variety of vibration conditions. Studies of reaction time for sinusoidal $\pm g_z$ vibration are reported by Schmitz, Simons, and Boettcher (1960), Buckhout (1964), Shoenberger (1967), Johnston and Ayoub (c. 1969); for sinusoidal and random g_z vibration by Parks (1961) and Weisz, Goddard, and Allen (1965); for random g_z vibration by Soliday and Schohan (1965), Schohan, Rawson, and Soliday (1965), Hornick and Lefritz (1966), Holland (1967); and in g_z and g_y axes by Hornick, Boettcher, and Simons (1961). Included in these studies are frequencies from 1 to 20 Hz; intensities to ±0.60g; random vibration intensities to 0.40 RMSg; sitting and standing subjects; hand, foot, and whole body reaction; and simple to complex reaction tasks. The data clearly indicate that (1) vibration does not typically affect human reaction time; (2) when reaction time is affected during or following vibration exposure, only several one-hundredths of a second are added to the static base reaction time, normally 0.02 to 0.05 second; (3) increases in vibration intensity or duration do not produce corresponding change in reaction time.

It is possible, when the task is a secondary monitoring task, that reaction time deterioration can occur. A secondary vigilance task to monitor and detect propulsion thrust changes in a low altitude, high speed piloting simulation was used by Hornick and Lefritz (1966). A change in displayed thrust command occurred randomly once in each half hour during the 4 hour random vibration session. Vigilance response time was markedly impaired, from 2.4 seconds in nonvibration to 8.1 seconds during vibration.

Visual Impairment

When evaluating visual impairment from vibration, the type of vibration, the posture of the man, illumination levels, and the kind of visual task must be considered. Visual impairment is extremely sensitive to the specific

vibration/task situation. To be considered also in any operational setting are whether or not a protective helmet is worn and whether the display is vibrating along with the man or is independently damped.

In general, the range of 10 to 25 Hz is most detrimental to visual performance, though occasionally frequencies above and below this band cause decrement. The relationship of subject and display is important in that lower frequencies (below 10 Hz) more readily cause visual decrement if the display alone or the display and man are vibrating. Above 10 Hz, vibration of the human more frequently results in visual decrement, as compared to motion of the display alone. Decrement increases as a function of amplitude or intensity level.

Visual performance during vibration can be protected by proper design of displayed matter. Cluttered displays result in relatively greater decrement during vibration than do those which are easier to read. At relatively short distances, vibration can be expected to cause errors in viewed numerals or letters subtending about 9 minutes of arc or less.

In the supine position, a helmet can reduce visual error when motion is in the x-axis. Significant error reduction in the z-axis results when the head can move freely. There is some indication that higher frequencies (11 and 15 Hz) in the y-axis may result in larger error when a helmet is worn. Use of any helmet and liner configuration can be expected to modify man's visual response significantly, and each specific configuration should be the subject of dynamic base tests for high performance vehicle application.

The few studies which investigated random vibration effects have not revealed any visual impairment up to levels of 0.40 $RMSg_z$. Table 7-4 presents the major results of primary studies and figures 7-5, 7-6, and 7-7 illustrate selected results.

Miscellaneous Performance Effects

Certain performance effects are related to biodynamic characteristics, though they are not completely biodynamic in nature. For example, typing accuracy can be impaired during vibration because of biodynamic disturbance of the arm rather than a disruption of the basic process of typing *per se*. The influence on speech, auditory, and complex mental processes has also been examined by a number of investigators. Table 7-5 summarizes the results of studies of the influence of vibration on these processes.

Vibration appears to act on the biodynamic and psychomotor properties of man rather than on central neural processes. Tasks which require accurate placement of a limb or movements of controls (figure 7-8) are adversely affected by virtue of leg, arm, hand, or finger displacement (Clark et al., 1965; Schmitz et al., 1960). In cases where accuracy itself does not suffer (figure 7-9), time to complete the task increases during vibration (Guignard & Irving, 1960; Dean et al., 1967; Seeman & Williams, 1966). There is some support of the hypothesis that vibration degrades performance at frequencies where major body resonances occur.

Table 7–4

Summary of Vibration Effects on Visual Performance

Vibration Conditions	Visual Task	Effect	Source
Subject static; display vibrated at 5 Hz, 0.063 in. D.A.	Reading speed	Speed reduced by about 5.3%	Tinker, 1948
$+1G_x \pm ng_z$; 5, 8, 11 Hz	Visual acuity by detection of break in line	Comparison of man vibrating with display static vs man and display vibrating; both conditions result in decrement; for constant displacement, acuity worst at higher frequencies; for constant acceleration, acuity worst at 5 Hz; addition of bite-bar improved vision at 5 Hz	Rubenstein & Taub, 1967
$+1G_z \pm ng_x$ and $\pm ng_y$; 1.5 – 5.5 Hz; 0.15 – 0.35 g	Static display, Landolt C's	No decrement in either axis	Hornick, Boettcher, & Simons, 1961
1 – 30 Hz in combinations of vertical, pitch, and roll motion	Reading printed words, both static and moving display	Visual acuity worst at 4 – 7 Hz; pitch motion caused greatest decrement; roll motion least decrement	Pradko, 1964
$+1G_x \pm ng_x$, $\pm ng_y$, $\pm ng_z$; 6, 11, 15 Hz; ± 0.9 to ± 2.0 g	Read easy and difficult aircraft instrument dials	No effect with easy dial; errors related to intensity; helmet restraint improves performance in x-axis; improves at 6 Hz but degrades at 11 and 15 Hz in y-axis; no effect in z-axis	Taub, 1964 (see figure 7-6)
$+1G_x \pm 1.1g_x$; 6, 11, 15 Hz	Read difficult instrument dials; effect of various types of head restraint	Error greatest at 6 Hz; head damped in x-axis results in error reduction; no consistent effect of z-axis restraint	Taub, 1966

Table 7–4 (Continued)
Summary of Vibration Effects on Visual Performance

Vibration Conditions	Visual Task	Effect	Source
$+1G_z \pm ng_z$; 8, 13, 11, 23 Hz at 0.05 and 0.1 in. D.A. and 10, 20, 30, 40, 50 Hz at 0.05 in.	Read 3-digit numbers, 1/4 in. high	Beginning at 8 Hz, errors increase as a function of frequency; no function of amplitude; errors increase to 40 Hz	Mozell & White, 1958
$+1\ G_z \pm ng_z$; 1 – 27 Hz; 4 subjective intensity levels	Digit reading	Greatest error in 12 – 23 Hz range; errors increase with intensity	Snyder, 1962
$+1G_z \pm ng_z$; 1 – 27 Hz; 4 subjective intensity levels	Digit reading; visual angle 6 to 24 min of arc	Greatest error in 12 – 23 Hz range; errors increase with intensity; error only for 9 and 6 min of arc digits	Teare & Parks, 1963 (see figure 7–5)
$+1G_z \pm ng_z$	Reading aircraft displays	Collimated, head-up display results in fewer errors	Caiger, 1966
$+1G_z \pm 0.25g_z$; 2.4 – 9.5 Hz	Scan letters "c" and count randomly distributed "o's"	Decrement worst at 3.4 and 4.8 Hz; completion time worst at 3.4 Hz	Guignard & Irving, 1960
$+1G_z \pm ng_z$; 1 – 20 Hz; 1/2 short time tolerance limit	Detect diverging lines on static rotating disk	Wide individual differences; greatest decrement at 12 – 18 Hz; error also at 5, 7, and 10 Hz; residual effect following vibration	Lange & Coermann, 1962
$+1G_z \pm ng_z$; 5 – 37 Hz; ± 0.44 – 0.51 g_z and 0.83 – 1.02 g_z; 6 Hz at ± 0.13 – 0.36 g_z; 19 Hz at $\pm 0.16\ g_z$	Read printed numbers, subtending 4.4 min of arc; series of studies to compare subject and display motion influence	Increase in error at 5, 14, and 27 Hz for lower intensity; below 10 Hz, influence of vibrating display greater than vibrating subject; above 10 Hz, the reverse	Dennis, 1965(a)

$+1G_x \pm 1.2g_x$ and $\pm 0.9\ g_y$; 6, 11, 15 Hz	Dial reading; effects of helmet and liner configuration	Error worst in x-axis for 11 Hz; no effect of liner in x-axis; in y-axis performance better with liner at 6 Hz but worse with liner at 15 Hz; total errors higher with helmet than without it	Shoenberger, 1968
$+1G_z \pm ng_y$; 0 to 52 Hz vibration inputed directly to head only	Acuity measured by illumination level required to detect break in line; target static and dynamic base	Acuity decrement above $\pm 0.2\ g_y$; for constant acceleration of $\pm 1.0\ g_y$ acuity worst from 22 – 34 Hz; for constant amplitude of 0.03 cm, acuity worst at 30 Hz; decrements due to target vibration are smaller than those due to head motion	Rubenstein & Kaplan, 1968 (see figure 7–7)
Random vibration, helicopter spectrum, to 0.41 $RMSg_z$ (+1 G_z)	Meter reading, Landolt C's	No effects	Dean, McGlothlen, & Monroe, 1964
Random vibration, LAHS flight spectrum, various turbulence levels to 0.405 $RMSg_z$ (+1 G_z)	Target recognition outside of simulated cockpit	No effects	Schohan, Rawson, & Soliday, 1965
Random vibration, 2 – 7 Hz band, to 0.30 $RMSg_z$ (+1 G_z)	Read aircraft instruments	No blurring or eye strain	Woods, 1967

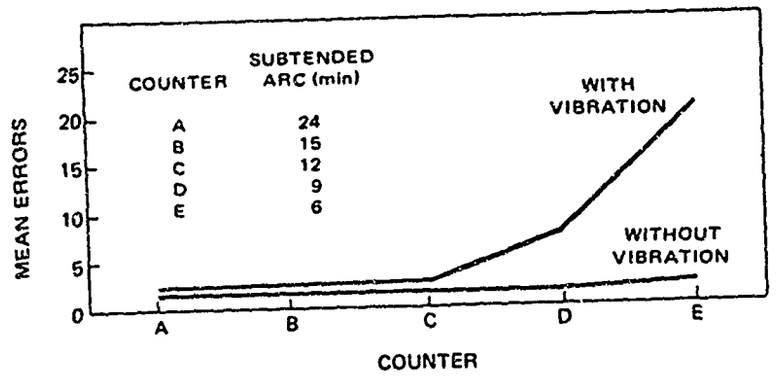


Figure 7–5. Digit reading errors as a function of vibration and digit height. Significant errors occur only for subtended arcs of 9 and 6 min. (From Teare & Parks, 1963)

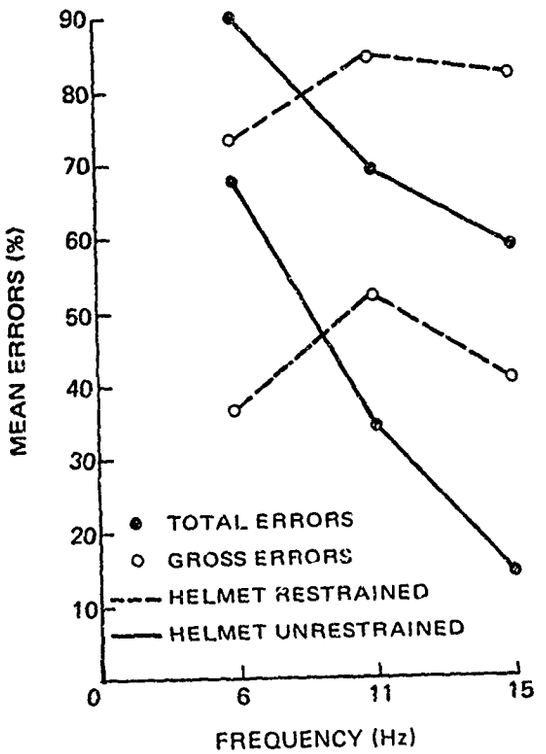


Figure 7–6. Errors on difficult dial reading task (400 range dial) as a function of frequency and helmet restraint conditions for vibration in y-axis. (Taub, 1964)

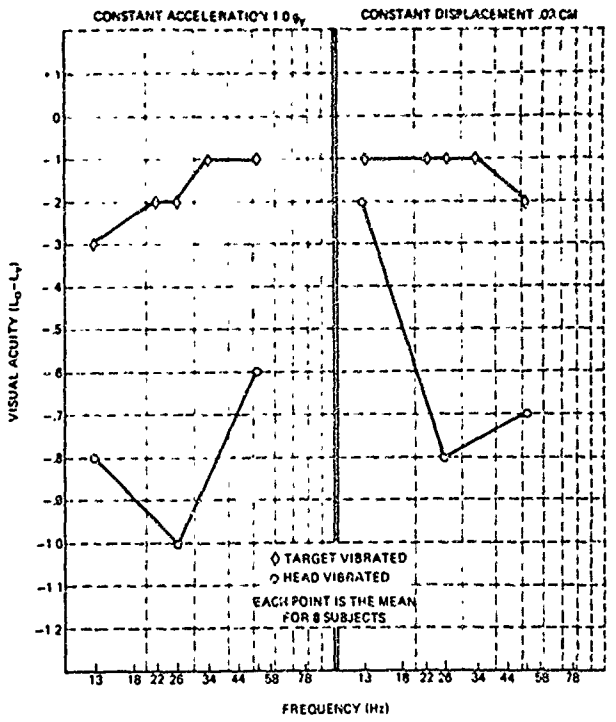


Figure 7–7. Visual acuity as a function of display versus observer vibration. (From Rubenstein & Kaplan, 1968)

While speech intelligibility itself may not be greatly affected, the quality of speech is impaired by vibration. That is, a listener can still understand the spoken material, but does perceive quality loss. No effect on significant hearing ability has been found (Weisz et al., 1965; Holland, 1966). At most, vibration may produce a practically insignificant effect on the auditory thresholds for low frequency sound (Guignard & Coles, 1965).

Tasks involving primarily higher mental processes are not adversely affected by low frequency vibration. Mental addition, pattern recognition and matching, and navigational behavior have been shown not to be impaired below 20 Hz. A single example does exist where vibration at 70 Hz at 4.0 g interfered with "continuous counting" (Ioseliani, 1967).

Physiological Effects

Physiological disturbances which occur during vibration are found at intensity levels much higher than those necessary to cause performance decrement. Further, those changes which do occur are usually very small and have no practical significance. Experimental data for physiologically damaging vibrations are of course, not available for humans. In the operational setting, men have been exposed to extremely intense vibration levels in helicopters when rotor blades are lost in flight. It has been speculated that deaths in these instances have resulted from rupture of the aorta.

Table 7–5

Summary of Effects of Vibration on Biodynamics, Psychomotor Performance, Speech, Hearing, and Higher Mental Processes

Vibration Conditions	Measures	Effect	Source
		Biodynamic Mechanisms	
$\pm 0.15 - 0.35\ g_z$ at 0.9 – 6.5 Hz, low amplitude	Whole body vertical vibration, hand tremor, body equilibrium, foot pressure	Foot pressure constancy impaired at 3.5 to 6.5 Hz (figure 7–8); error increase with intensity; no residual effects	Schmitz, Simons, & Boettcher, 1960
$\pm ng_x$, $\pm ng_y$ for 1/2 hr	Body sway equilibrium	No effects	Hornick, Boettcher, & Simons 1961
$\pm g_z$, 2 – 20 Hz (intensities = 1/3 short-term tolerance limits)	Control of pitch and roll of a chair	Wide individual differences; decrement between 3 and 12 Hz, worst at 6 Hz	Coermann, Magid, & Lange, 1962
$\pm g_z$ at 0, 2, 5, 8 Hz	Orientation (orienting body position to face targets at 15°, 30°, and 60° from reference plane)	Only small decrement in accuracy; mean error $< 0.5°$	Ayoub, c. 1969
$\pm 0.03 - \pm 0.41\ g_z$ at 0, 3, 5, and 8 Hz	Leg muscular power (on bicycle ergometer)	No effects	Harrison, 1969
Various peak-to-peak accelerations at 1 Hz with 3 Hz, and 2 Hz with 6 Hz	Arm-hand steadiness	Positional errors significantly related to RMS and frequency of vibration; 90% of error was periodic; 1 Hz with 3 Hz combination produced larger error; small (0.5 – 1 g) differences in acceleration had no effect	Clarke et al., 1965

Psychomotor Performance			
+0.25 g_z at 2.4 – 9.5 Hz	Time to pick up markers and place in small circular areas	Completion time worst at 3.4 and 4.8 Hz	Guignard & Irving, 1960
+0.5 $RMSg_z$ at 2 – 30 Hz (13 Hz peak power)	Digital decimal input with push-button, toggle switch, rotary switch, and thumbwheel controls	Accuracy unaffected; insert times increasd by 4%; pushbuttons and toggle switches were most rapidly used, with the former preferred; thumb-wheels were most accurate	Dean et al., 1967
0, 0.2, 0.4, 0.6, and 0.8 $RMSg_z$ for 5 min	Same	No effects for 0.2 and 0.4 $RMSg_z$; significant increase in insert time for 0.6 and 0.8 $RMSg_z$ (figure 7–9); speed: pushbuttons $>^*$ rotary switches $>$ thumbwheels; error rate: pushbut-tons highest and thumbwheels lowest for high intensity vibrations	Dean, Farrell, & Hitt, 1967
$\pm g_x$ and $\pm g_y$ at 0.33 and 0.80 Hz at amplitude of ±6.3 and ±7.0 in.	Nut and bolt assembly/disassembly; placement of probe through vari-ous sized holes	No effects at 0.33 Hz; time required increased by 30% at 0.80 Hz with no increase in accuracy	Seeman & Williams, 1966

*Symbol $>$ here indicates faster than.

Table 7–5 (Continued)

Summary of Effects of Vibration on Biodynamics, Psychomotor Performance, Speech, Hearing, and Higher Mental Processes

Vibration Conditions	Measures	Effect	Source
	Speech Intelligibility		
$\pm g_z$ at 10, 20, 30, 40, 50 Hz	Intelligibility	Most effect at 10 and 20 Hz	Nixon, 1962
$0.5 g_z$ sinusoidal at 6 Hz; $0.75 g_z$ at 4 and 8 Hz; $1.0 g_z$ at 2 – 20 Hz	Intelligibility and quality	No effect on intelligibility at 65 dB; "quality" poorer than control condition	Nixon & Sommer, 1963
	Audition		
5 Hz sinusoidal, 5 Hz random amplitude, 4 – 12 Hz random frequency	Frequency (pitch) change (1200 for 1600 Hz) at 86 dB, tones of 0.25 sec duration every sec-detection	No effect	Weisz, Goddard, & Allen, 1965
$\pm g_z$	1200 Hz at 86 dB presented every 0.25 sec for 1 sec against a 74 dB, 30 – 3000 Hz white noise; pitch change at 86 dB (1600 for 1200 Hz) – detection	No effect	Holland, 1966
$+1 G_z \pm 0.7 g_z$ at 15 Hz (amplitude 0.036 in.) for 30 min	TTS determined as function of vibration and noise vs noise alone (acoustical frequencies from 250 – 6000 Hz)	Extremely small vibration effect at low tone frequencies only	Guignard & Coles, 1965

Higher Mental Processes			
$\pm 0.15 - 0.35 g_z$ at 2.5 and 3.5 Hz	Mental addition	No effect	Schmitz, Simons, & Boettcher, 1960
$+g_z$ at 5, 7, and 11 Hz	Pattern matching and discrimination	No effect	Buckhout, 1964
0.40 RMSg_z random vibration	Navigational tasks in simulated low altitude, high speed flight	No effect	Schohan, Rawson, & Soliday, 1965; Soliday & Schohan, 1965
1) No vibration; 2) no noise, no vibration; 3) noise only; 4) vibration plus noise; 5) postvibration $+4.0\ g_z$ at 70 Hz	Continuous counting at a given rate	Decrement, especially during 5 –7 min of exposure; residual effects noted; 70% of decrement attributed to vibration (30% to noise) Ss over 36 showed greater decrement	Ioseliani, 1967

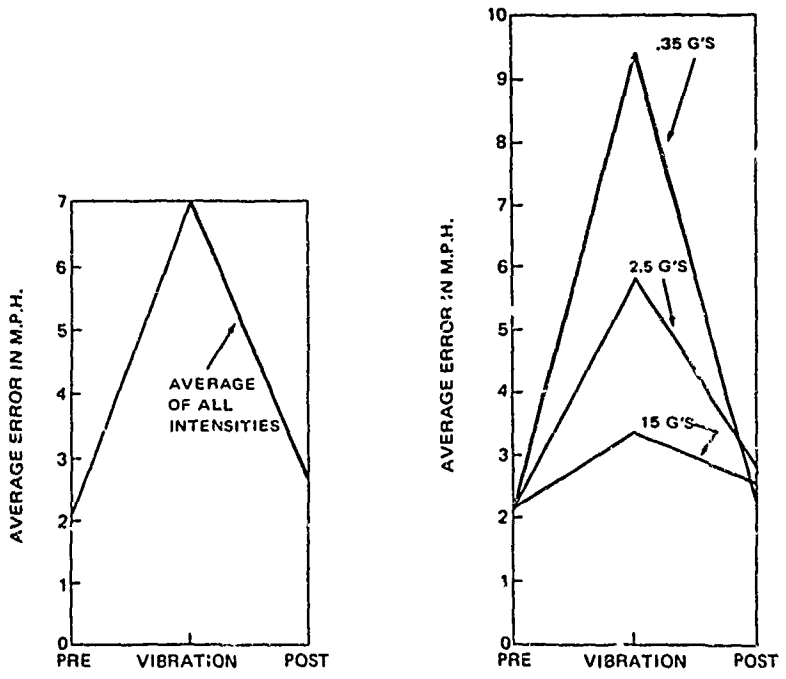


Figure 7–8. Foot pressure error in previbration, vibration and postvibration periods. (From Schmitz et al., 1960)

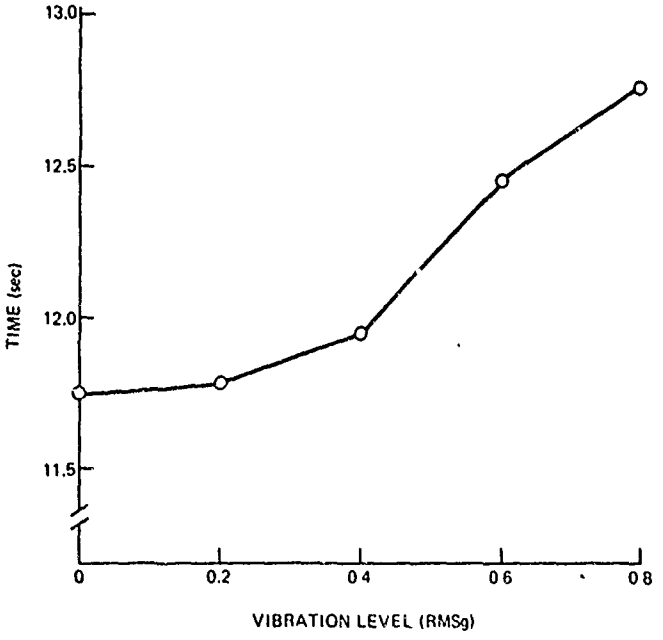


Figure 7–9. Digital input time for vibration intensity level. (From Dean et al., 1967)

Table 7-6 summarizes the known physiological effects of vibration. The experiments summarized in table 7-6 indicate that man does not experience major physiological change while enduring whole body vibration of normal intensity. A slight degree of hyperventilation is suggested, however. No dramatic changes are seen in blood chemistry or endocrine chemical composition. Anesthesia reduces those changes which do occur, suggesting a stress effect of a psychological rather than mechanical nature. There is substantial evidence that heart rate increases occurring in early stages or during short periods of vibration are anticipatory general stress responses, because of a gradual return to resting state levels during continued vibration (Hornick & Lefritz, 1966; Holland, 1967; Ziegenruecker & Magid, 1959; Temple et al., 1964). No clearly consistent blood pressure changes have been identified after exposures to $\pm 1 G_z \pm ng_z$ from 1 to 27 Hz (Chaney, 1965). The conclusion of von Gierke (1965) is yet valid: "...to date these effects in no way characterize vibration as a severe stress nor do the results give us a handle to use these response functions as a basis for criteria."

Biodynamic Effects

Of all recorded vibration effects, there is more agreement in research results in the area of biodynamics than in any other. Biodynamic effects are those phenomena which consist of body movement reactions to vibration inputs. When the human body is vibrated, it does not react in a rigid and passive manner; rather, the body and its organs can be likened to a complex set of masses, springs, and dampers. There have been attempts to derive a mathematical model which could be used to define and predict man's motion responses to vibration inputs. By and large, attempts to develop such a model may be as overambitious as the model would be valuable. Such a model does not yet exist, due primarily to the wide variety of environmental parameters of importance——such as frequency, intensity, randomness, bandwidth, axis, duration, body-support, etc.——as well as of personal parameters——such as body size, weight, posture, age, sex, fatigue, degree of relaxation, and so forth. Discussions to be consulted which treat biodynamic phenomena are the following: Goldman and von Gierke, 1960; Coermann, 1962; von Gierke and Hiatt, 1962; Weis, 1963; von Gierke, 1964; Pradko, Lee, and Kaluza, 1966; Lee and Pradko, 1968.

From a design standpoint, probably the most useful biodynamic data are those dealing with whole body transmissibility——that is, the ratio of output to input motion. Resonances of internal organs, though of value, are not vital to system design because dangerous organ resonances are thought to occur only at severe intensities where subjective tolerance limits (often associated with pain) are reached.

Two terms which are commonly used with reference to biodynamic response to vibration are *mechanical impedance* and *transmissibility*. Mechanical impedance is defined as the ratio of applied force to the resulting body or organ output velocity. Transmissibility is the ratio of body output motion to applied motion in terms of velocity, amplitude, or intensity.

Sinusoidal $\pm g_z$ Vibration

Table 7-7 summarizes results of studies in the g_z axis with seated subjects.

Table 7–6
Summary of Effects of Vibration on Physiological Function

Vibration Condition	Physiological Effects	Source
	Respiration and Heart Rate	
$\pm ng_x$ and $\pm ng_y$, 1.5 – 5.5 Hz	O_2 consumption increased from 7 5 to 11 l/min without increase in breaths/min, at ±0.25 and ±0.35 g	Hornick, Boettcher, & Simons, 1961
$\pm 1G_z \pm ng_z$ (0.13 – 0.25 in. double amplitude), 2 – 15 Hz	No increase in respiration rate; increase in tidal volume at 6, 11, 15 Hz	Ashe, 1961
$\pm 1G_x \pm ng_z$ (1 in. double amplitude), 6.6 Hz	Mild hyperventilation	Lamb & Tenney, 1966
$RMSg_z$	Respiratory rate increased as function of vibration intensity to 0.8 $RMSg_z$, small increase in heart rate	Hornick & Lefritz, 1966
$RMSg_z$	Heart rate increase at onset of vibration, return to resting levels during exposure	Hornick & Lefritz, 1966, Holland, 1967
$+1G_z \pm ng_z$	Same	Ziegenrueker & Magid, 1959
$+1G_x \pm ng_{x, y, z}$	Same	Temple et al., 1964
	Blood, Kidney, Endocrine Effects	
$\pm 1G_z \pm ng_z$, 4 – 9 Hz, 1 min	No evidence of effect on renal function; no change in wbc	Mandel, 1962
0.20 – 0.40 $RMSg_z$	No blood, urine, or stool changes	Dean, McGlothlen, & Monroe, 1964
$\pm 1G_z \pm ng_z$, 1 – 20 Hz, 3 min tolerance level	No effect on 17 – hydroxycorticosteroids; no consistent change in urine or plasma levels	Blivaiss et al., 1964(a)

	Effects in Animals	
9.7 g, 4 – 40 Hz	14 of 60 animals died; effects included high body temperature, kidney degeneration, increased white blood cells, hemorrhage	Nickerson & Paradijeff, 1964
g_z, 4 – 8 Hz	Elevated 17-hydroxycorticosteroids; when anesthetized, not as great; death in some dogs	Blivaiss et al., 1964
	Skin	
$+g_z$	Skin temperature no change	Holland, 1966

Table 7–7

Mechanical Response of Body in $\pm g_z$ Axis, Seated Subjects

Conditions	Results	Source
2 – 60 Hz, unrestrained subjects	Transmissibility acceleration max for shoulders and hips near 5 Hz; ratio of shoulder to table acceleration over 2.5; hip to table, 1.5; attenuation begins at 7 Hz for the shoulder and at 12 Hz for the hip	Guignard, 1960
2 – 13.5 Hz, unrestrained subjects	4.8 Hz max transmissibility measured at shoulder; muscle tensing causes reduction in transmissibility below 4.8 Hz and increases it above 4.8 Hz	Guignard & Irving, 1960
0.9 – 6.5 Hz, wearing lapbelt	4.5 Hz max transmissibility measured at head; 6.5 Hz max transmissibility for hip	Schmitz, Simons, & Boettcher, 1960
2 – 20 Hz, comparison of sitting erect and relaxed	Max "strain" (inches of change/inch of normal circumference of body area) 5.5 to 6.0 Hz for chest and upper abdomen, and 4 Hz for lower abdomen when sitting erect; max strain for chest 5.5 Hz, and abdomen 4.5 Hz when sitting relaxed (see figure 7–10)	Clark, Lange, Coermann, 1962
2 – 20 Hz, unrestrained	Max volumetric pressure changes in rectum at 4 Hz	White, Lange, & Coermann, 1962
5, 7, 11 Hz, subjects with lapbelt and harness	Max transmissibility for sternum at 5 Hz with a 3.8 sternum to table ratio, and 2.3 and 1.5 ratios at 7 and 11 Hz	Buckhout, 1964
Inflight UH-1B helicopter vibration, restrained and unrestrained helmets	Acceleration amplitudes more intense with restrained helmet; different frequencies peak in the different restraint conditions	Rosenberg & Segal, 1966
1 – 10 Hz, unrestrained subjects	Max transmissibility near 4.5 Hz for shoulder, with ratio of 2.5 to table	Woods, 1967

Seated and Standing Subjects. Dieckmann (1958) measured transmissibility and mechanical impedance in comparing the biodynamic effects of sitting and standing postures. He found 4 to 5 Hz to be the resonant frequency at the head and shoulders of the seated subject. When the subject is standing, impedance is greatest at 3 Hz with a secondary peak at about 12 Hz.

Comparing the biodynamic effects of sitting versus standing, Coermann (1962) reported peak impedance at 6 Hz for sitting erect; at 5 to 6 Hz for sitting relaxed; and at 6 and 11 to 12 Hz while standing erect. The data in the Dieckmann and the Coermann studies are for one subject and are, therefore, only suggestive that body resonance differs for the standing person. Coermann further reported that use of an MC-3 pressure suit adversely affects biodynamic as well as subjective response. Edwards and Lange (1964) also reported a standing relaxed resonance near 4 to 5 Hz.

Shoulder transmissibility in standing subjects during 1 to 27 Hz was recorded by Chaney (1965). He reported a maximum transmissibility ratio of 1.5 for the 4 to 6 Hz range, with attenuation below 2 Hz and above 7 Hz (figure 7-10).

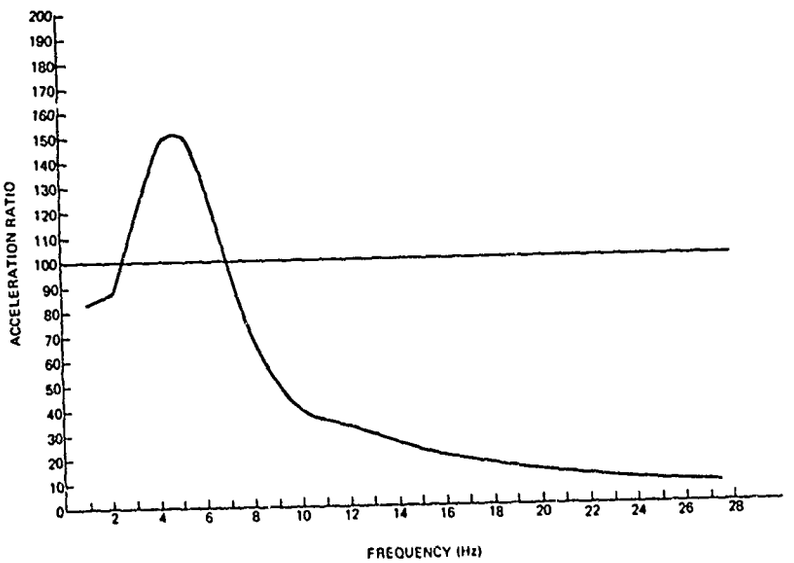


Figure 7–10. Shoulder acceleration expressed as a percentage of table acceleration for standing subjects. (From Chaney, 1965)

To determine whether the bent leg can serve as an effective isolator, Hornick (1962) had subjects attempt to isolate the input motion as much as possible at 2 and 5 Hz. A 1 inch double amplitude was used (±0.21 and ±1.3 g, respectively). Subjects visually fixated on a spot 6 feet forward during 2 minute exposures. The legs effectively attenuated the input vibration as measured at the head, though there was a gradual loss in their ability to do so over time. More effective isolation was achieved at 5 Hz. Figure 7-11 shows that transmissibility

acceleration increases from 68 to 93 percent for 2 Hz and from 25 to 39 percent for 5 Hz during the 2 minute test time.

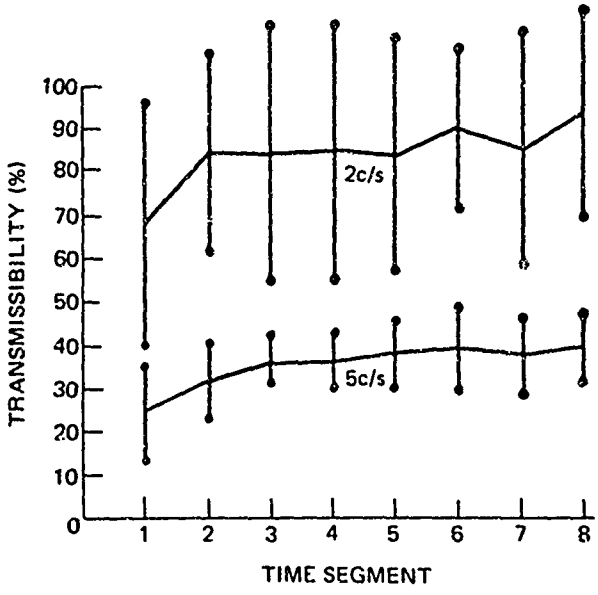


Figure 7–11. Percent of acceleration transmitted to heads of standing persons with knees slightly bent. (From Hornick, 1962)

Random g_z Vibration

In 1966, Hornick and Lefritz recorded acceleration at pilots' heads during simulated LAIIS flight with various RMSg_z levels for a zero to 12 Hz spectrum. It is interesting to note that, for a 10-minute sample, output acceleration is greatest from 4 to 6 Hz, with attenuation below 2.5 Hz and above 11 Hz (figure 7-12). These results agree very well with those obtained during sinusoidal conditions.

Other Axes and Postures

The head motions of seated and standing subjects in $+1G_z \pm ng_x$ conditions were recorded by Dieckmann (1958). Figure 7-13 shows that the head follows the horizontal motion in a flat ellipse at low frequencies. As 5 Hz is reached, the elliptical shape of the head movement becomes vertically oriented for the standing person and becomes circular for the sitting person.

Transmissibility at the head, chest, and pelvic regions was recorded by Hornick, Boettcher, and Simons (1961) in $+1G_z \pm ng_x$ conditions. Figure 7-14 shows that motion at the head level is attenuated through 5.5 Hz, while transmissibility exceeds unity for the chest and belt levels with maximum amplification at 5.5 Hz. In the same experiment, foot pressure constancy was recorded during the $\pm g_x$ motion. Greatest limb motion is experienced at 3.5 Hz.

The loss in control of foot pressure constancy becomes more severe as intensity level increases from ±0.15 to 0.30 g.

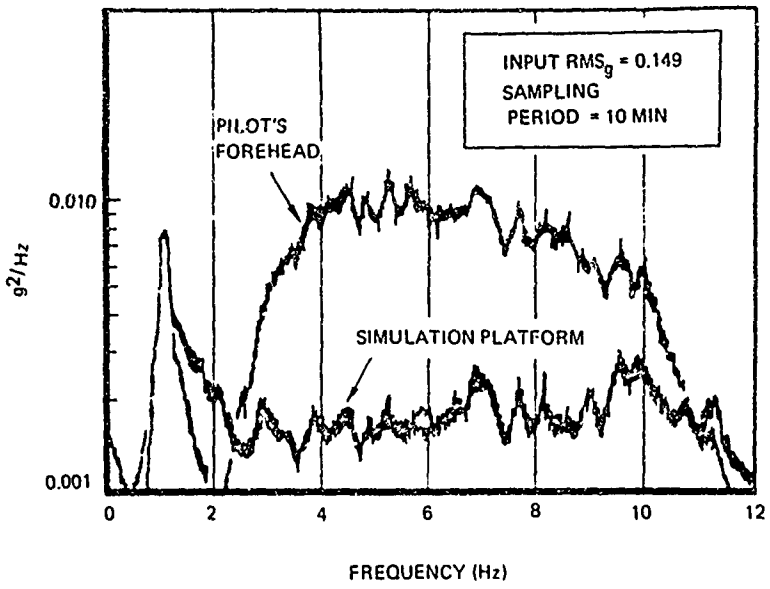


Figure 7–12. Biodynamic transmissibility during random g_z vibration. (From Hornick & Lefritz, 1966)

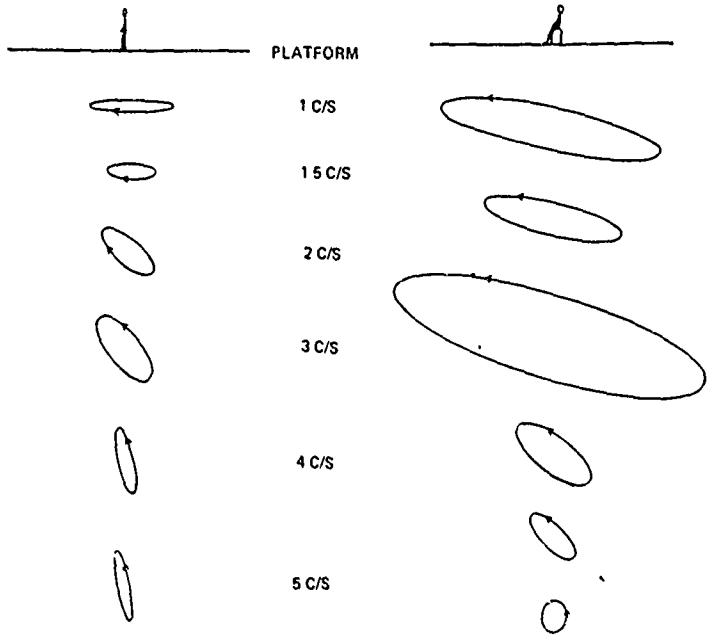


Figure 7–13. Head movement of standing subject (left) and sitting subject (right) with $\pm g_x$ vibration. (From Dieckmann, 1958)

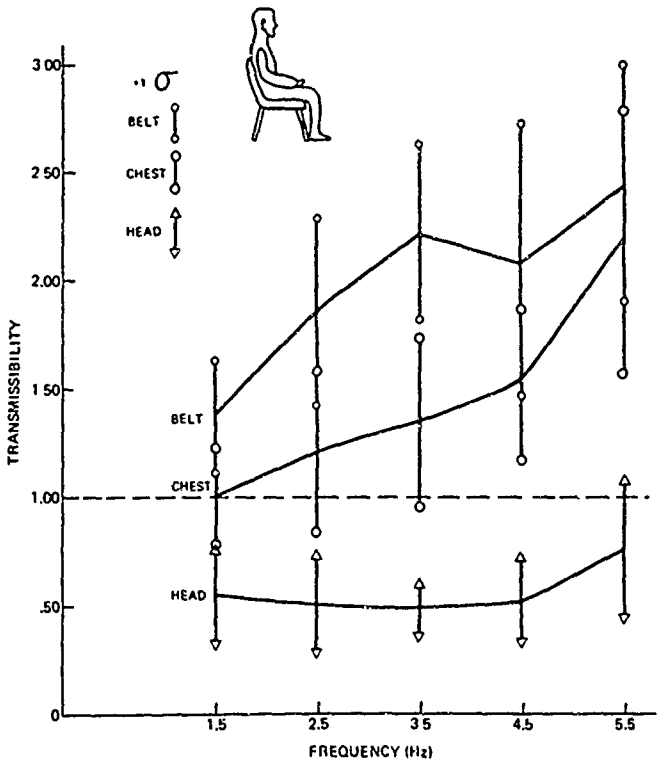


Figure 7–14. Transmissibility at belt, head, and chest levels during $\pm g_x$ vibration. Standard deviations are presented for each mean for 20 subjects. (From Hornick et al., 1961)

Hornick, Boettcher, and Simons (1961) also recorded transmissibility at the head, during $+1G_z \pm ng_y$ conditions. Figure 7-15 reveals that from 1.5 to 5.5 Hz, the body does an excellent job of attenuating motion as recorded at the head during the side-to-side vibration. The least attenuation at 1.5 Hz suggests that $\pm g_y$ resonance lies somewhere near that frequency. Again, foot pressure constancy was recorded, with greatest foot constancy error occurring near 1.5 Hz, the region of greatest head motion. As with the x-axis, foot motion errors are directly related to the $\pm g_y$ intensity levels.

Woods (1967) also studied $+1G_z \pm ng_y$ vibration to 7 Hz with seated subjects. His results confirm those discussed above. Transmissibility is generally below unity above 2.0 Hz for the hip, knee, shoulder, and head. He confirms that $\pm g_y$ resonance is about 1.5 Hz.

Roman, Coermann, and Ziegenruecker (1959) studied the chest-abdomen resonance in supine subjects with $+1G_x \pm ng_z$ conditions. From 2 to 17 Hz, there is amplification in the $\pm g_z$ axis, with highest transmissibility (ratio of 3.5) occurring at 5.9 Hz.

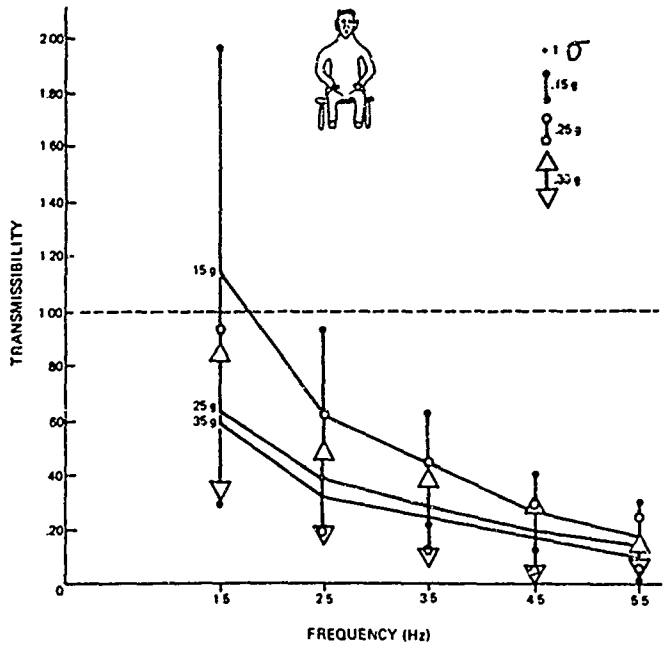


Figure 7–15. Transmissibility at the head during $\pm g_y$ vibration. Standard deviations appear for each mean for 20 subjects. (From Hornick et al., 1961)

Clark, Lange, and Coermann (1962) recorded pelvic, chest, and abdomen motion in supine subjects during $+1G_x \pm ng_x$ conditions, from 2 to 20 Hz. Body deformation "strain" (as described earlier) was employed for measurement. All strains are at a maximum at 6.7 Hz (see figure 7-16).

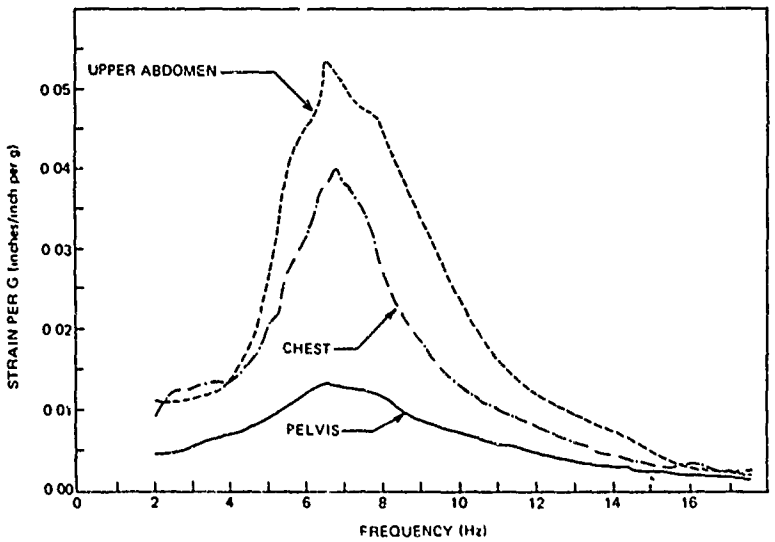


Figure 7–16. Mean strain of 7 subjects exposed to $\pm g_x$ vibrations in semisupine position. (From Clark et al., 1962)

Edwards and Lange (1964) exposed subjects in the supine position and resting on their sides to $+1G_x \pm ng_x$ and $+1G_y \pm ng_y$ vibration from zero to 20 Hz. In the relaxed supine position, it was again found that the first resonance for the chest and abdominal regions occurs between 5.5 to 7.5 Hz. A similar result in impedance peak occurs for subjects resting on their sides, with the peak near 5 Hz.

Summary of Biodynamic Effects

No matter what technique is used to record major body or whole body response to vibration, results are in good agreement.

1. Internal organs have unique resonant frequencies which can differ in each axis.

2. Whole body resonance for seated subjects is in the region of 4 to 6 Hz in the $\pm g_z$ axis.

3. For the seated subject, maximum hip amplification occurs at higher frequencies, about 10 Hz, in the $\pm g_z$ axis.

4. Motion experienced in the seated subject at the upper torso may be amplified from 1.5 to 4.0 times at the resonant frequency.

5. Use of helmets modifies head motion, and it is suggested that the helmet-free condition is better than the helmet-restrained condition.

6. Standing subjects, with motion in the $\pm g_z$ axis, have a major body resonance near 4 to 6 Hz. A secondary resonance occurs near 12 Hz. Standing with the legs bent serves to attenuate the input vibration, but fatigue occurs and effectiveness of this as a damping technique is gradually lowered.

7. When seated and experiencing $\pm g_x$ vibration, the lower body amplifies the motion, but motion is attenuated at the head. Resonance is above 5.5 Hz.

8. When seated and experiencing $\pm g_y$ vibration, motion in the upper torso is attenuated, but maximum response occurs near 1.5 Hz.

9. In subjects who are supine or resting on their sides, chest and abdominal response is greatest in the 5 to 8 Hz region, indicating that man's torso should be protected from such frequencies when in these positions.

Subjective Tolerance Levels

The system designer is confronted with a large body of conflicting data when he attempts to determine vibration levels which are subjectively acceptable to man. It is true that levels which are virtually imperceptible to man can be identified, as well as those where extreme pain or discomfort occur. However, the designer is most often faced with the nebulous area between the extremes. Tolerance limits are treated here along with subjective levels since a tolerance limit may be considered as the uppermost

subjective level. A true tolerance limit would be based on pathological data such as organic damage or actual mortality. Man is not used as an experimental animal for such purposes; therefore, estimates of tolerance limits are based on subjective reactions to pain and anxiety or fear.

The basic problems in defining valid subjective levels are: (1) interpersonal variability——different persons label the same intensity level with different terms; (2) intra-personal variability——the same individual describes an intensity level as "disturbing" at one time, and "hardly noticeable" at another; (3) situation specificity——a particular intensity level is perceived differently depending on whether the individual is in an aircraft, an automobile, or in his home; and (4) semantics——a lack of consistent definitions of terms such as "annoying," "objectionable," "disturbing," etc.

Subjective levels and tolerance limits presented in this section, therefore, should be used with some degree of caution. The system designer should not believe, for instance, that a potential change of 0.10 g suddenly places his system in an "objectionable" range. He must use the described levels advisedly, knowing that while they may be the best data available, limits are quite flexible because of the factors mentioned above.

Historically, subjective studies have largely provided the basis for proposed vibration standards. Various schemes have been used in attempts to provide standards which could be universally applied to the population. Typically, a set of frequency-intensity curves are provided representing different levels of subjective reaction; then conversion functions might be added to arrive at levels for different axes, for random motion, and for duration of exposure.

Two agencies have been active in trying to define acceptable standards. In the United States, Working Group S3-W-39 of the American National Standards Institute (ANSI) is writing standards with respect to annoyance, work interference, and hazard. Technical Committee ISO/TC 108/WG 7 of the International Organization of Standardization (ISO) is determining thresholds of vibration and shock acceptable to man (ISO, 1970; Hornick, 1969).

Probably the first attempt to organize subjective levels was made by Goldman (1948), who summarized several independent studies with curves describing comfort and discomfort regions. These curves were used as design guidelines without distinction for axis, duration, or randomness. In more recent years, studies have been conducted to define more clearly the influence of these factors on subjective reactions.

Sinusoidal $\pm g_z$ Vibration

A short-term tolerance limit from 1 to 15 Hz was established by Ziegenruecker and Magid (1959). Lowest tolerance is the range of 4 to 8 Hz. Subjective symptoms frequently reported included abdominal pain,

chest pain, dyspnea, and general discomfort: with relatively fewer reports of testicular pain, head symptoms, and anxiety. Extending this study, Magid, Coermann, and Ziegenruecker (1960) estimated the g levels which might be tolerated for 1 and 3 minute exposures (figure 7-17).

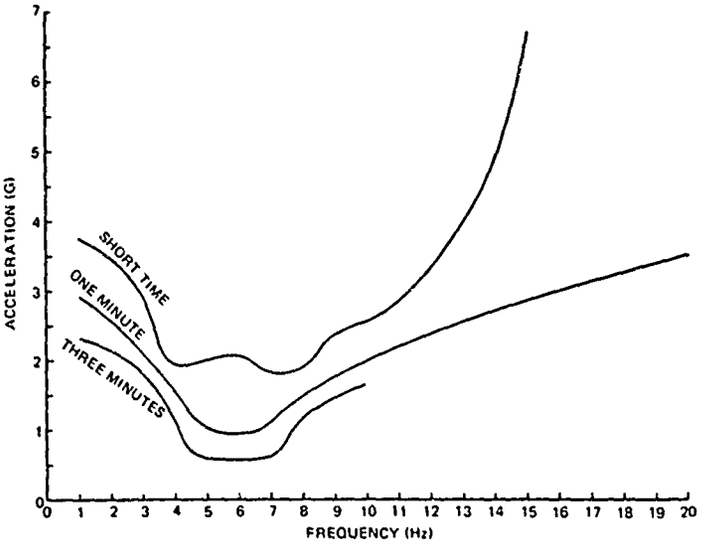


Figure 7–17. Short time, 1 min. and 3 min. tolerance limits. (Magid et al., 1960)

Showing that the manner of respiration affects tolerance, Mandel and Lowry (1962) obtained higher tolerance limits for 1 minute exposures. Subjects were instructed to continue to breathe normally instead of erratically during vibration. Figure 7-18 compares the Mandel and Lowry data with those of Magid, Coermann, and Ziegenruecker (1960). Figure 7-19 illustrates wide variability in subjective tolerance levels reported by subjects exposed to 1 to 27 Hz in studies by Parks and Snyder (1961) and Chaney (1964) using identical facilities.

A psychophysical approach to the quantification of subjective levels has recently been devised by Shoenberger and Harris (1969), whereby magnitude estimation and intensity matching replace qualitative descriptions. For each frequency, results are plotted as straight line functions on log-log graphs of subjective intensity versus physical intensity. Subjects then match the intensity of 9 Hz at 0.08, 0.16, 0.26, 0.36, 0.46, and 0.56 g_z with vibration at each of the other six frequencies. According to Shoenberger and Harris, equal intensity curves from the magnitude estimation data show the same general shape and comparable levels as corresponding curves determined experimentally using the intensity matching procedure. Figure 7-20 shows the derived curves from the intensity matching and magnitude estimation data based upon a value of 0.006 g_z for the threshold of vibration perception at 9 Hz, with the six acceleration levels then corresponding to

the multiples of that base. These results indicate that subjective response to vibration can be assessed by techniques similar to those used in acoustics, and that they could eventually be used for estimating the severity of complex vibration conditions.

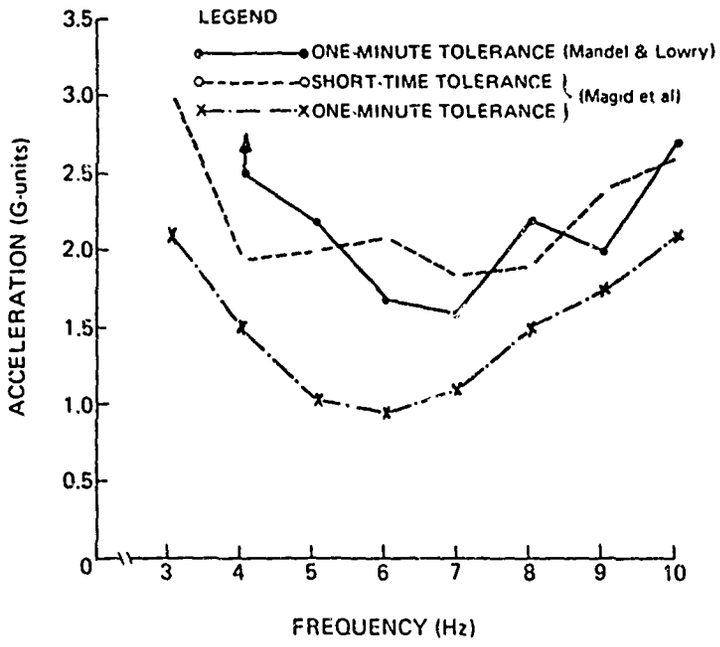


Figure 7–18. Short duration tolerance as a function of respiration technique. (From Mandel & Lowry, 1962)

Subjective levels for dual frequency sinusoidal $\pm g_z$ motion were investigated by Brumaghim (1967). Subjects estimated the severity of 4, 5, 6, 8, and 10 Hz when each was experienced (1) with no other vibration, (2) with 17 Hz at 0.24 RMSg added, and (3) with 17 Hz at 0.43 RMSg added. Subjects were instructed to "ignore" the background 17 Hz motion in identifying perceptible, mildly annoying, and extremely annoying levels for the basic frequencies. When the background intensity was 0.43 RMSg, higher intensity levels of the basic frequency were necessary for the subjects to identify them subjectively. Figure 7-21 shows the change in intensity required for the basic frequencies to be found "perceptible," etc., when paired with the 0.43 RMSg, 17 Hz vibration. It appears that difficulty is experienced in perceiving the primary frequency when a background vibration is present.

In figure 7-22 are data which present subjective levels for sinusoidal vibration.

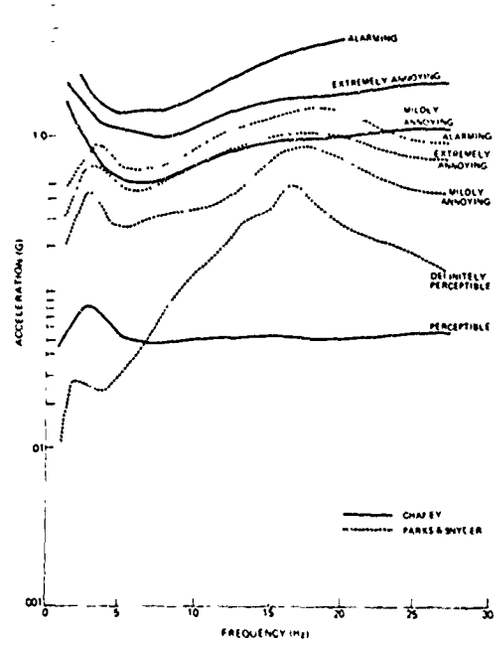


Figure 7–19. Subjective tolerance curves comparison. (Chaney, 1964)

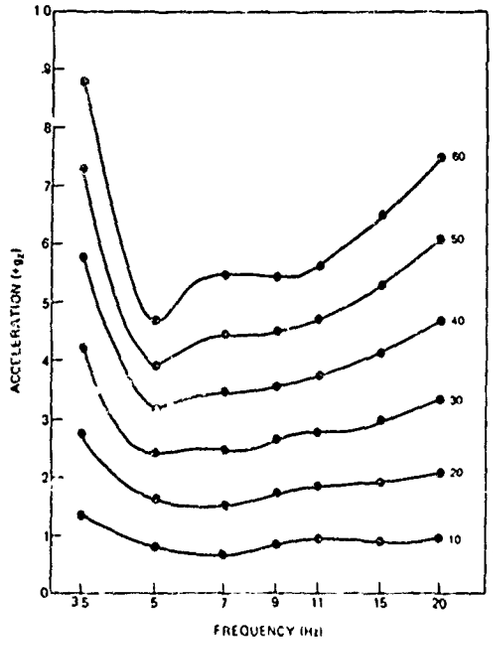


Figure 7–20. Equal subjective intensity curves. (From Shoenberger & Harris, 1969)

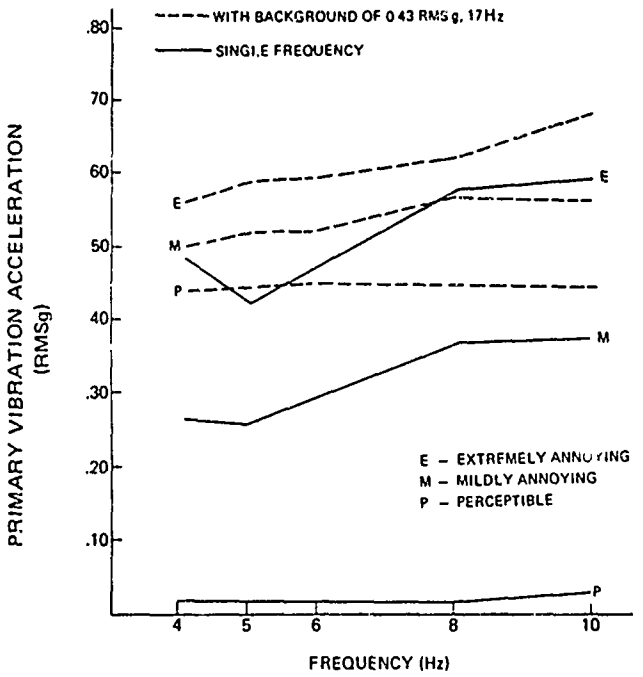


Figure 7–21. Change in intensity required for basic frequency to reach designated subjective thresholds with and without background vibration. (Compiled from data of Brumaghim, 1967)

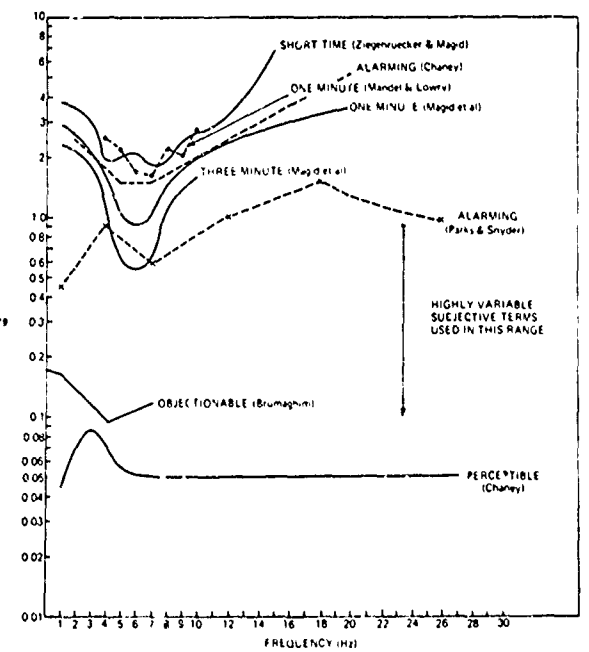


Figure 7–22. Subjective levels and tolerance limits for $\pm g_z$ vibration.

Reports of Pain. Reports of pain are scattered widely in the vibration literature. Most often, these are relatively casual references to general complaints or to pain in some region of the body by some of the participating subjects. These accounts are not treated in detail here because of the typically sporadic character of the reports, though some generalizations may be made. Little is known with respect to the specific causes of pain during vibration. However, it is widely believed that organic resonances and consequent stretching of supportive muscles and tissue is a major contributor. Most reports of pain occur at levels above those necessary to cause performance decrement. As tolerance limits and "alarming" levels are approached, the proportion of complaints can be expected to increase. In the frequency range of 4 to 8 Hz, complaints are often made at levels over approximately $\pm 0.25 g_z$, intensities fairly well below "alarming" levels. Pain and discomfort disappear with the cessation of vibration.

Random g_z Vibration

Table 7-8 summarizes reactions to random g_z vibration.

Absorbed Power Concept. In recent years, a concept of "absorbed power" has been advanced by Pradko and his coworkers which is claimed to correlate subjective and quantified values quite well. Detailed explanations and the mathematical structure of the technique are available in several papers and are, therefore, not presented here (see Pradko & Lee, c. 1965; Pradko et al., 1966; and Lee & Pradko, 1968). The technique involves use of power spectral density (PSD), but with the added measurement of the rate at which the vibration input is used by means of a transfer function of input to output energy The rate of flow of energy characterizes the interaction of the vibrating human and the environment. The energy flow occurs as a result of the complex damped elastic properties of the anatomy, and this flow is designated as "absorbed power." This concept is yet largely a hypothetical approach, and its attempts at correlations with subjective reactions, while mathematically precise, are based on too few subjects to be applicable at this time.

Other Axes

Lee and Pradko data (1968) support the notion that the g_x and g_y axes may not differ much for subjective comfort, and that these axes differ from the g_z axis as follows: below 4 Hz, comfort is lower for the g_x and g_y axes; above 4 Hz, comfort is greater in the g_x and g_y axes.

Earlier, Pradko (1964) used sinusoidal and random vibration from 1 to 30 Hz in several axes and combinations—g_z; pitch; roll; g_z and roll; pitch and roll; and g_z and pitch and roll. With random motion, tolerance is greatest for roll. Overall highest tolerance is to random motion which indicates that generalizing from sinusoidal limits to random vibration is not appropriate and that g_z limits cannot be used for other axes. To do so could result in overly conservative design limits not desirable for system design.

Table 7–8

Subjective Reactions to Random g_z Vibrations

RMSg	Effect	Conditions	Source
0.80	Intense discomfort in abdomen and thorax; pain	5 min duration, 2 – 30 Hz	Dean, Farrell, & Hitt, 1967
0.70			
0.60			
	Refusal to exceed by varying aircraft flight parameters	Flying aircraft through turbulence	Notess, 1963
0.50	Refusal to exceed by reducing the velocity of driven tanks	Driving tanks over rough terrain	Fernstrom, Gschwind, & Horley, 1965
0.40	Occasional complaints of discomfort, fatigue, muscle tightness	3 hr duration	Schohan, Rawson, & Soliday, 1965
	Visual blurring, nose itch, face flutter, teeth chatter	40 min duration, 1 – 1000 Hz	Dean, McGlothlen, & Monroe, 1964
0.30			
	Some unpleasant effects	3 min duration, 2 – 7 Hz	Woods, 1967
0.20	No subjective complaints	4 hr duration, 1 – 12 Hz	Hornick & Lefritz, 1966
	No subjective complaints	6 hr duration, 1 – 6 Hz	Holland, 1967
0.10			

Woods (1967) compared subjective reactions to sinusoidal and random motion in the g_z and g_y axes with 10 seated subjects. Descriptor opinions were: (1) "neutral;" (2) "some unpleasant effects;" (3) "some unpleasant effects cannot be ignored;" (4) "definitely unpleasant;" (5) "most unpleasant;" and (6) "quite unacceptable." Figures 7-23 and 7-24 show the general nature of his findings. Random vibration is better tolerated than is sinusoidal motion in both the g_z and g_y axes.

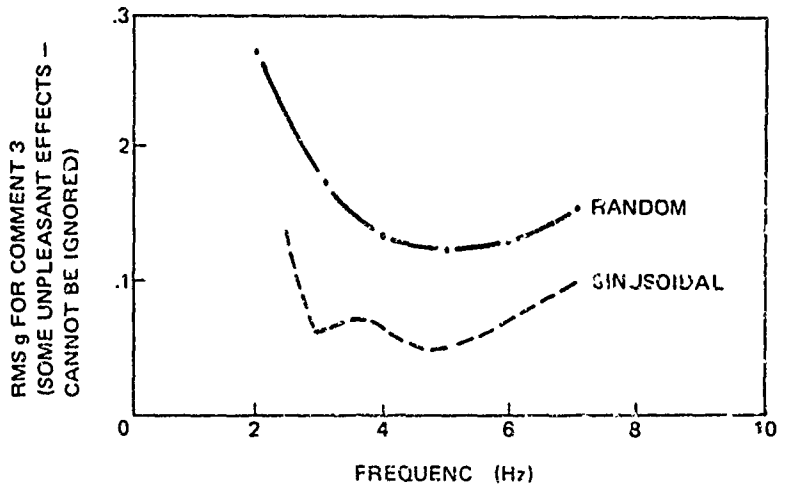


Figure 7–23. Comparison of random and sinusoidal g_z subjective reaction of "some unpleasant effects cannot be ignored". (From Woods, 1967; used by permission of *Aircraft Engineering*)

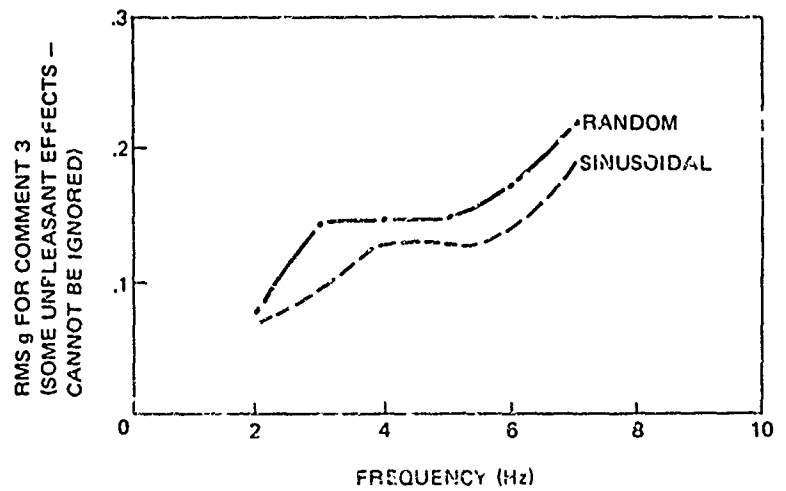


Figure 7-24. Comparison of random and sinusoidal g_y subjective reaction of "some unpleasant effects cannot be ignored". (From Woods, 1967; used by permission of *Aircraft Engineering*)

"Annoying" and "objectionable" levels for aircraft passenger situations were studied by Brumaghim (1969). Subjects were seated in aircraft seats in a simulator and experienced several types of vibration—$\pm g_z$, $\pm g_y$, single and combined frequencies, single and combined axes, and combined frequencies and axes. These results also indicate that lateral $\pm g_y$ vibrations are more objectionable than g_z motion in the range to 3 Hz (figure 7-25). Combined frequency tests were conducted in g_z and g_y axes to determine if reactions to multifrequency vibration could be linearly predicted from the values obtained for each frequency separately. That is, for the 1 and 4 Hz combination, halves of each separate frequency intensity called objectionable were summed as the predicted value for the combined frequencies. Brumaghim found good agreement between predicted and actual values. However, the results for prediction of combined axis vibration reactions were not good, again indicating the nonequivalence of the axes of motion with respect to subjective reaction.

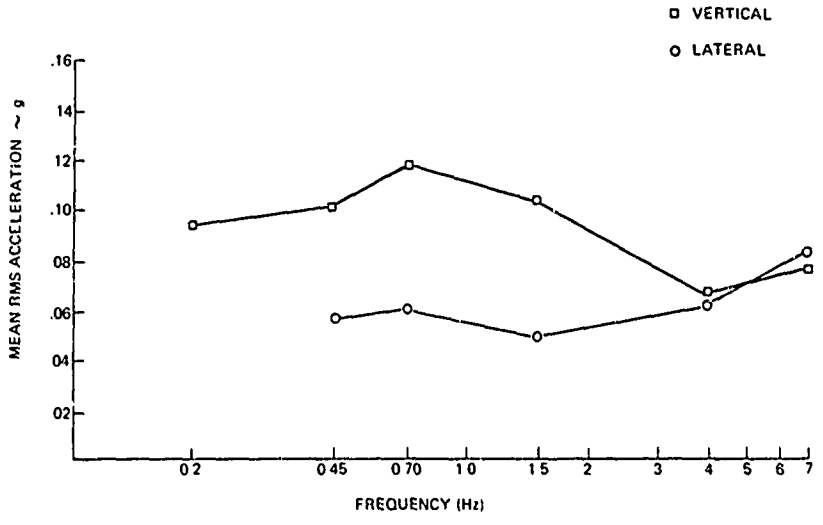


Figure 7–25. Subjective "objectionable" response levels for $\pm g_z$ axes. (From Brumaghim, 1969)

Temple and coworkers (1964) conducted a study with subjects semisupine at $+1\,G_x$ experiencing $\pm g_x$, $\pm g_y$, and $\pm g_z$ vibration from 3 to 20 Hz to evaluate tolerance endpoints for several couch support and head restraint configurations. The data indicate that tolerance is extremely sensitive to the type of support, and that complex interactions exist between type of support system and axis of motion.

Summary of Subjective Responses

Subjective levels and tolerance limits in older literature are not useful for design because they (1) are based on antiquated studies; (2) use grossly

subjective semantics; (3) depend on "data" from one or very few subjects or "observers;" (4) do not account for variability; (5) do not account for duration; (6) do not account for personal variables; and (7) do not differentiate among axes. Certain agencies are in the process of defining limits which may become universally acceptable as design guidelines. However, these are not yet satisfactorily defined.

Two reviews have as their objective the exploration of the limit problem rather than the definition of discrete levels. Bryce (1966) explored the basis of the disagreements in the subjective comfort area and suggests that the most prominent discrepancies are attributable to the amount of restraint afforded by the body support. Gartley and Beldam (1967) explored the feasibility of establishing acceptable exposure criteria and conclude that "the inconsistencies and general lack of agreement...make it impossible to develop realistic vibration exposure criteria..."

Beyond the subjective data reported in figure 7-23 and table 7-6, it can reasonably be stated that subjective comfort to g_y and g_x motion is less than for g_z below 4 Hz; above 4 Hz, g_z is likely to be more disturbing than for the other axes. Further, the small amount of data comparing sinusoidal motion to random suggests that random motion is better tolerated than is sinusoidal. Published exposure limits at this time are difficult to justify and must be applied cautiously.

Interaction of Vibration with Other Environmental Parameters

Limited research has combined vibration stress with other environmental stressors such as acceleration, noise, and altitude. Visual performance during linear acceleration with vibration was studied by Clarke and coworkers (1965). Conditions of $+3.85G_x \pm ng_x$ were used, with vibration intensities ranging from ±0.8 to ±2.4 g at 11 Hz. No effect was found for an easy dial reading task, but increased intensity of vibration was related to increased error scores for a difficult task. In terms of very gross errors, no real effect was noted until ±1.6 g_x was reached.

A similar set of conditions was used by Vykukal and Dolkas (1966) and Vykukal (1968) where tracking, dial reading, and subjective assessment of performance decrement were evaluated during $+nG_x \pm ng_x$ conditions. Acceleration and vibration intensities up to $+4\ G_x$ and $\pm 3.0\ g_x$ in the 2.5 to 20 Hz frequency range were used. Results indicate that decreased visual acuity is the most serious effect. Rapid deterioration of control performance occurred at $\pm 0.7\ g_x$ for 11 Hz. With a $+3.5\ G_x$ bias, vibration levels above $\pm 0.30\ g_x$ at 11 Hz are believed to jeopardize spacecraft mission success. Body resonances were observed at 7 Hz; between 9.5 and 12.5 Hz; and at 15 and 18 Hz. Magnitude of the resonances increases as a function of the bias acceleration for the same level ($\pm 0.4\ g_x$) of vibration. Observance of pain at 7 and 18 Hz suggests a lower tolerance to vibration at resonant frequencies when combined with high linear accelerations.

Typing performance was studied by Rulon, Sampson, and Schohan (1951) during actual flight conditions with turbulence. Steady state acceleration levels ranged from +1 to +3 G_z with turbulence producing added oscillation. Experienced teletypists and "hunt-and-peck" typists were subjects. There was a large practice effect observed, and accuracy of the hunt-and-peck typists actually increased during the flights. However, the high proficiency teletypists experienced more response (wrong finger) and displacement (hand on wrong key) errors during the flights. No data were presented relating errors to vibration intensity or duration.

A complex study concerning pilot control during turbulence was reported by Hitchcock and Morway (1968). In this study, pilots "flew" through turbulent storms in a simulated 720-B cockpit on a centrifuge with a shake platform included to provide 4.7 and 7 Hz associated with aircraft vibration. Flight accelerations ranged to +3.5 G_z with ±0.5 g_z at 7 Hz and ±1.5 g_z at 4.6 Hz. It was noted that under the experimental conditions pilots were willing to follow and capable of following prescribed penetration procedures. They chose, however, to terminate attempts to achieve new headings and altitudes when heavy turbulence was encountered. Finally, the study suggested that use of a "turbulence flight director" enables pilots to maintain better speed control and results in a reduced load factor.

Much additional research is needed in the area of vibration combined with other stresses in order to provide data which can more adequately describe the reactions of man in a dynamic environment.

References

Abeling, A. B., & Bassett, H. L. A study of propeller aircraft vibration. Contract N62269-3112, Project A-866, Technical Report Number 3, Georgia Institute of Technology, Atlanta, Georgia, August 1967.

Ashe, W. F. Physiological and pathological effects of mechanical vibration. Report 862-4, NIH Grant OH-6, Ohio State University Research Foundation, Columbus, Ohio, September 1961.

Ashe, W. F. Physiological and pathological effects of mechanical vibration on animals and man. Report 862-5, NIH Grant OH-00006-06, Ohio State University Research Foundation, Columbus, Ohio, January 1964.

Ayoub, M. M. Performance and recovery under prolonged vibration. Unpublished manuscript, School of Engineering, Texas Technological College, Lubbock, Texas, c. 1969.

Blivaiss, B. B., Litta-Modignani, R., Galansino, G., & Foa, P. P. Endocrine and metabolic response of dogs to whole-body vibration. AMRL-TDR-64-54, Wright-Patterson Air Force Base, Ohio, June 1964.

Blivaiss, B. B., Magid, E. B., & Litta-Modignani, R. Effects of whole-body vibrations on plasma and urinary corticosteroid levels in man. AMRL-TDR-64-53, Wright-Patterson Air Force Base, Ohio, June 1964.

Borshchevskiy, I. Ya., Koreshkov, A. A., Markaryan, S. S., Preobrazhenskiy, V. V., & Terent'yev, V. G. The effect of vibrations of certain types of modern helicopters and airplanes. *Voyenno Meditsinskiy Zhurnal*, 1938, *1*.

Brumaghim, S. H. Subjective reaction to dual frequency vibration. Report D3-7562, Boeing Company, Wichita, Kansas, December 1967.

Brumaghim, S. H. Subjective response to commercial aircraft ride: Passenger ride quality testing. Paper presented to International Symposium on Man Machine Systems, Ergonomic Research Society, United Kingdom, Republic of Ireland, September 1969.

Bryce, W. D. A review and assessment of criteria for human comfort derived from subjective response to vibration. Report No. R. 286, U.D.C. No. 534.1:613.64, National Gas Turbine Establishment, November 1966.

Buckhout, R. Effect of whole body vibration on human performance. *Human Factors*, 1964, *6*(2), 157-163.

Caiger, B. Some effects of vertical vibration on a pilot's head motion and his instrument reading capability. Aeronautical Report LR-463, National Research Council of Canada, Ottawa, Canada, August 1966.

Catterson, A. D., Hoover, G. N., & Ashe, W. F. Human psychomotor performance during prolonged vertical vibration. *Journal of Aviation Medicine*, 1962, *33*, 598-602.

Chaney, R. E. Subjective reaction to whole-body vibration. Report D3-6474, Boeing Company, Wichita, Kansas, September 1964.

Chaney, R. E. Whole-body vibration of standing subjects. Report D3-6779, Military Airplane Division, Boeing Company, Wichita, Kansas, August 1965.

Chaney, R. E., & Parks, D. L. Tracking performance during whole-body vibration. Report D3-3512-6, Boeing Company, Wichita, Kansas, November 1964.

Chaney, R. E., & Parks, D. L. Visual-motor performance during whole-body vibration. Report D3-3512-5, Boeing Company, Wichita, Kansas, November 1964.

Clark, W. S., Lange, K. O., & Coermann, R. R. Deformation of the human body due to uni-directional forced sinusoidal vibration. *Human Factors*, 1962, *4*(5), 255-274.

Clarke, N. P., Mohr, G. C., Brinkley, J. W., Martin, P. J., Wooding, H. C., Henzel, J. H., & von Gierke, H. E. Evaluation of peak vs RMS acceleration in periodic low frequency vibration. *Aerospace Medicine*, 1965, *36*(11), 1083-1089.

Clarke, N. P., Taub, H., Scherer, H. F., Temple, W. E., Vykukal, H. E., & Matter, M. Preliminary study of dial reading performance during sustained acceleration and vibration. AMRL-TR-65-110, Wright-Patterson Air Force Base, Ohio, August 1965.

Coermann, R. R. The mechanical impedance of the human body in sitting and standing position at low frequencies. *Human Factors*, 1962, *4*(5), 227-253.

Coermann, R. R., Magid, E. B., & Lange, K.O. Human performance under vibrational stress. *Human Factors*, 1962, *4*(5), 315-324.

Cope, F. W., & Polis, B. D. Increased plasma glutamic-oxalacetic transaminase activity in monkeys due to nonspecific stress effect. *Journal of Aviation Medicine*, 1959, *30*, 90-96.

Dean, R. D., Farrell, R. J., & Hitt, J. D. Effect of vibration on the operation of decimal input devices. Paper presented at Human Factors Society Annual Meeting, Boston, Massachusetts, September 1967.

Dean, R. D., McGlothlen, C. L., & Monroe, J. L. Performance and physiological effects of six-hour exposure to helicopter noise and vibration. Boeing Company, Seattle, Washington, May 1964.

Dennis, J. P. Some effects of vibration upon visual performance. *Journal of Applied Psychology*, 1965, *49*(4), 245-252.

Dennis, J. P. The effect of whole-body vibration on a visual performance task. *Ergonomics*, 1965, *8*(2), 193-205.

Dieckmann, D. A study of the influence of vibration on man. *Ergonomics*, 1958, *1*(4), 347-355.

Edwards, R. G., & Lange, K. O. A mechanical impedance investigation of human response to vibration. AMRL-TR-64-91, Wright-Patterson Air Force Base, Ohio, October 1964.

Fernstrom, R. W., Gschwind, R. T., & Horley, G. L. Cross-country speed and driver vibrational environment of the M60 main battle tank. Technical Memorandum 7-65, Human Engineering Laboratories, Aberdeen Proving Ground, Maryland, July 1965.

Fraser, T. M., Hoover, G. N., & Ashe, W. F. Tracking performance during low frequency vibration. *Aerospace Medicine*, 1961, *32*, 829-835.

Gartley, C. W., & Beldam, E. M. Feasibility of establishing acceptable vibration exposure criteria. 67-RD-2, Canadian Forces Medical Service, Institute of Aviation Medicine, Toronto, Canada, March 1967.

von Gierke, H. E. Biodynamic response of the human body. *Applied Mechanics Reviews*, 1964, *17*(12), 951-958.

von Gierke, H. E. On noise and vibration exposure criteria. *Archives of Environmental Health*, 1965, *11*, 327-339.

von Gierke, H. E., & Hiatt, E. P. Biodynamics of space flight. In S. F. Singer (Ed.), *Progress in the aeronautical sciences*. Amsterdam: North-Holland Publishing Company, 1962, Pp. 345-401.

Goldman, D. E. A review of subjective responses to vibratory motion of the human body in the frequency range 1 to 70 cps. Project NM 004 001, Report No. 1, Naval Medical Research Institute, Bethesda, Maryland, March 1948.

Goldman, D. E., & von Gierke, H. E. The effects of shock and vibration on man. Lecture and Review Series No. 60-3, Naval Medical Research Institute, Bethesda, Maryland, January 1960.

Guignard, J. C. Physiological effects of mechanical vibration. *Proceedings of the Royal Society of Medicine*, 1960, *53*, 92-96.

Guignard, J. C., & Coles, R. R. A. Effects of infrasonic vibration on the hearing. Fifth Congress International D'Acoustique, Liege, France, September 1965.

Guignard, J. C., & Irving, A. Effects of low frequency vibration on man. *Engineering*. Cardiff, England: British Association, September 1960, Pp. 364-367.

Harris, C. S., Chiles, W. D., & Touchstone, R. M. Human performance as a function of intensity of vibration at 5 cps. AMRL-TR-64-83, Wright-Patterson Air Force Base, Ohio, September 1964.

Harris, C. S., & Shoenberger, R. W. Effects of frequency of vibration on human performance. *Journal of Engineering Psychology*, 1966, *5*(1), 1-15.

Harrison, J. Y. The effect of vibration on the ability to generate human muscle power. Unpublished manuscript submitted to *Human Factors*, 1969.

Hitchcock, L., Jr., & Morway, D. A. A dynamic simulation study of the sweptwing transport aircraft in severe turbulence. Joint Report, NADC-MR-6807, Naval Air Development Center and FAA-DS-68-12, Federal Aviation Agency, October 1968.

Holland, C. L. Performance and physiological effects of long term vibration. AMRL-TR-66-145, Wright-Patterson Air Force Base, Ohio, October 1966.

Holland, C. L. Performance effects of long term random vertical vibration. *Human Factors*, 1967, *9*(2), 93-104.

Hornick, R. J. Vibration effects on man – an overview of recent research. Litton Systems TDOC-690, paper presented to Human Factors Society 13th Annual Meeting, Philadelphia, Pennsylvania, October 1969.

Hornick, R. J. Vibration isolation in the human leg. *Human Factors*, 1962, *4*(5), 301-303.

Hornick, R. J., Boettcher, C. A., & Simons, A. K. The effect of low frequency, high amplitude, whole body, longitudinal and transverse vibration upon human performance. Final report, Contract DA-11-022-509-ORD-3300, Bostrom Research Laboratories, Milwaukee, Wisconsin, July 1961.

Hornick, R. J., & Lefratz, N. M. A study and review of human response to prolonged random vibration. *Human Factors*, 1966, *8*(6), 481-492.

International Standards Organization Technical Committee 108, Working Group 7. Guide for the evaluation of human exposure to whole body vibration: Mechanical vibration and shock. March 1970.

Ioseliani, K. K. The effect of vibration and noise on the mental faculty of man under time stress. NASA TT-F-11-142, National Aeronautics and Space Administration, Washington, D.C., July 1967.

Johnston, W. L., & Ayoub, M. M. Body orientation under low frequency, whole-body vibration. Unpublished manuscript, School of Engineering, Texas Technological College, Lubbock, Texas, c. 1969.

Lamb, T. W., & Tenney, S. M. Nature of vibration hyperventilation. *Journal of Applied Physiology*, 1966, *21*(2), 404-410.

Lange, K. O., & Coermann, R. R. Visual acuity under vibration. *Human Factors*, 1962, *4*(5), 291-300.

Lee, R A., & Pradko, F. Analytical analysis of human vibration. 680091, Society of Automotive Engineers, presented at Automotive Engineering Congress, Detroit, Michigan, January 1968.

Magid, E. B., Coermann, R. R., & Ziegenruecker, G. H. Human tolerance to whole body sinusoidal vibration: Short-time, one-minute and three-minute studies. *Journal of Aviation Medicine*, 1960, *31*, 915-924.

Mandel, M. J. Effect of sinusoidal vertical vibration on the urinary sediment in man. AMRL-TDR-62-63, Wright-Patterson Air Force Base, Ohio, June 1962.

Mandel, M. J., & Lowry, R. D. One-minute tolerance in man to vertical sinusoidal vibration in the sitting position. AMRL-TDR-62-121, Wright-Patterson Air Force Base, Ohio, October 1962.

McClements, A. Operational aspects of helicopter vibration. Paper read at RAS Symposium, Great Britain, January 1951.

Meeder, E. A. Random vibration analysis. *Machine Design*, 10 September 1964, 179-184.

Mozell, M. M., & White, D. C. Behavioral effects of whole body vibration. *Aviation Medicine*, October 1958, 716-724.

Neel, S. H. Noise and vibration exposure of combat zone evacuees. ACAM Report, USAF School of Aviation Medicine, February 1959.

Nickerson, J. L., & Paradijeff, A. Body tissue changes in dogs resulting from sinusoidal oscillation stress. AMRL-TDR-64-58, Wright-Patterson Air Force Base, Ohio, August 1964.

Nixon, C. W. Influence of selected vibrations upon speech: I. Range of 10 cps to 50 cps. *Journal of Auditory Research*, 1962, *2*, 217-266.

Nixon, C. W., & Sommer, H. C. Influence of selected vibrations upon speech (range of 2 cps - 20 cps and random). AMRL-TDR-63-19, Wright-Patterson Air Force Base, Ohio, June 1963.

Notess, C. B., & Gregory, P. C. Requirements for the flight control of a supersonic transport. Society of Automotive Engineers, paper presented at National Aero-Nautical Meeting, Washington, D.C., April 1963.

Oshima, M. The effect of vibration on the visual acuity. *Proceedings of the IVth International Symposium on Space Technology and Science*, Agne Corp., Tokyo, Japan, 1962.

Parks, D. L. A comparison of sinusoidal and random vibration effects on human performance. Report D3-3512-2, Boeing Company, Wichita, Kansas, July 1961.

Parks, D. L., & Snyder, F. W. Human reaction to low frequency vibration. Report D3-3512-1, Boeing Company, Wichita, Kansas, July 1961.

Pradko, F. Human response to random vibration. *The Shock and Vibration Bulletin*, Bulletin 34, Part 4, U.S. Naval Research Laboratory, Washington, D.C., February 1965.

Pradko, F. Human vibration response. *Proceedings of the 10th Annual Conference on Human Factors Research and Development*, Fort Rucker, Alabama, 1964, 154-168.

Pradko, R., & Lee, R. A. Vibration comfort criteria. U.S. Army Tank-Automotive Center, Research and Engineering Directorate, Advanced Systems and Concept Research Division, Systems Simulation Branch, Warren, Michigan, c. 1965.

Pradko, F., Lee, R., & Kaluza, V. Theory of human vibration response. Paper 66-WA/BHF-15, American Society of Mechanical Engineers, New York, November 1966.

Pradko, F., Orr, T. R., & Lee, R. A. Human vibration analysis. U.S. Army Tank-Automotive Center, Research and Engineering Directorate, Systems Simulation Branch, Warren, Michigan, c. 1963.

Roman, J. A., Coermann, R., & Ziegenruecker, G. Vibration, buffeting and impact research. *Aviation Medicine*, February 1959, 118-125.

Rosenberg, B., & Segal, R. The effects of vibration on manual fire control in helicopters. Technical Report 1-168, Franklin Institute Research Laboratories, March 1966.

Rubenstein, L., & Kaplan, R. Some effects of y-axis vibration on visual acuity. AMRL-TR-68-19, Wright-Patterson Air Force Base, Ohio, June 1968.

Rubenstein, L., & Taub, H. A. Visual acuity during vibration as a function of frequency, amplitude and subject display relationship. AMRL-TR-66-181, Wright-Patterson Air Force Base, Ohio, June 1967.

Rulon, P. J., Sampson, P. B., & Schohan, B. The effects of "G" forces on the performance of teletype operators. Technical Report 6568, Educational Research Corporation, Wright-Patterson Air Force Base, Ohio, October 1951.

Schmitz, M. A., Simons, A. K., & Boettcher, C. A. The effect of low frequency, high amplitude, whole body vertical vibration on human performance. Report 130, Contract DA-49-007-MD-797, Bostrom Research Laboratories, Milwaukee, Wisconsin, January 1960.

Schohan, B., Rawson, H. E., & Soliday, S. M. Pilot and observer performance in simulated low altitude high speed flight. *Human Factors*, 1965, 7(3), 257-265.

Seeman, J. S., & Williams, R. B. Deck motion simulator program. Horizontal sinusoidal oscillation effects upon performance of standing workers. NASA TN D-3594, National Aeronautics and Space Administration, Washington, D.C., October 1966.

Shoenberger, R. W. Effects of vibration on complex psychomotor performance. *Aerospace Medicine*, 1967, *38*, 1264-1269.

Shoenberger, R. W. Investigation of the effects of vibration on dial reading performance with a NASA prototype Apollo helmet. AMRL-TR-67-205, Wright-Patterson Air Force Base, Ohio, February 1968.

Shoenberger, R. W., & Harris, C. S. Psychophysical assessment of whole body vibration. Unpublished manuscript, Wright-Patterson Air Force Base, Ohio, 1969.

Snyder, F. W. Effects of low frequency vertical vibration on human performance. Paper presented at Aerospace Medical Association Meeting, Atlantic City, New Jersey, April 1962.

Society of Automotive Engineers. *Ride and vibration data manual*. SAE J6a Information Report, New York, December 1965.

Soliday, S. M., & Schohan, B. A simulator investigation of pilot performance during extended periods of low-altitude, high-speed flight. NASA CR-63, National Aeronautics and Space Administration, Washington, D.C., June 1964.

Soliday, S. M., & Schohan, B. Task loading of pilots in simulated low-altitude high-speed flight. *Human Factors*, 1965, 7(1), 45-53.

Taub, H. A. The effects of vibration on dial reading performance. AMRL-TDR-64-70, Wright-Patterson Air Force Base, Ohio, July 1964.

Taub, H. A. Dial-reading performance as a function of frequency of vibration and head restraint system. AMRL-TR-66-57, Wright-Patterson Air Force Base, Ohio, April 1966.

Teare, R. J., & Parks, D. L. Visual performance during whole-body vibration. Report D3-3512-4, Boeing Company, Wichita, Kansas, November 1963.

Temple, W. E., Clarke, N. P., Brinkley, J. W., & Mandel, M. J. Man's short-time tolerance to sinusoidal vibration. *Aerospace Medicine*, 1964, *35*(10), 923-930.

Tinker, M. A. Effect of vibration upon speed of perception as measured by reading speed. *American Journal of Psychology*, 1948, *61*, 386-390.

Torle, G. Tracking performance under random acceleration: Effects of control dynamics. *Ergonomics*, 1965, *8*(4), 481-486.

Vykukal, H. C. Dynamic response of the human body to vibration when combined with various magnitudes of linear acceleration. *Aerospace Medicine*, 1968, *39*, 1163-1166.

Vykukal, H. C., & Dolkas, C. B. Effects of combined linear and vibratory accelerations on human body dynamics and pilot performance capabilities. Paper presented to XVIIth International Astronautical Congress, Madrid, Spain, October 1966.

Weis, E. B. Experimental analysis of the human body as a mechanical system. AMRL-TR-65-8, Wright-Patterson Air Force Base, Ohio, 1965.

Weisz, A. Z., Goddard, C., & Allen, R. W. Human performance under random and sinusoidal vibration. AMRL-TR-65-209, Wright-Patterson Air Force Base, Ohio, December 1965.

White, G. W., Jr., Lange, K. O., & Coermann, R. R. The effects of simulated buffeting on the internal pressure of man. *Human Factors*, 1962, *4*(5), 275-290.

Wood, J. G. Human response to low frequency sinusoidal and random vibration. *Aircraft Engineering*, July 1967, 6-14.

Yamamoto, T. G. Structural dynamic response of a terrain following vehicle due to turbulence. NA-64-1324, North American Aviation, Los Angeles, California, 22 January 1965.

Ziegenruecker, G. H., & Magid, E. B. Short time human tolerance to sinusoidal vibrations. WADC-TR-59-391, Wright-Patterson Air Force Base, Ohio, July 1959.

CHAPTER 8
WEIGHTLESSNESS

by

Charles A. Berry, M.D.
National Aeronautics and Space Administration

Gravity is a force which is ever present, continuously utilized, and little understood. Its invariant nature underlies our every activity. We walk, we build, we play games–in every instance relying on the constant effect of gravity and seldom realizing that this is the case. The world of unit-gravity is very familiar and very comfortable. A world without gravity would be strange indeed. Yet the designers of space missions and space equipment must plan systems and devices for perfect operation in a world in which there is no gravity.

From the design engineering vantage point, two aspects of the weightless or reduced-weight state are especially important. The first of these, of course, is the absence of weight itself; the second, the tractionlessness which accompanies it. The gravitational weight of the body is a quantity to which the human nervous system has become accustomed to responding over the entire period of development of the species on Earth. The removal of man from Earth's gravitation environment can therefore reasonably be expected to have significant impact on the organism, notably in the areas of perceptual-motor performance, sensory performance, and basic physiological functioning.

Perceptual-motor responses are conditioned to overcoming the existing pull of gravity on both the limbs and on any objects one wishes to lift or move. One learns to judge the weight of objects and to predict their movement by forces in the limbs upon handling various objects. With no gravitational force to overcome, free-floating objects will accelerate with the application of the smallest force. Actual space flight experience fortunately has shown that man's effectiveness in handling objects in that environment is not a problem. On the contrary, one adapts readily to this aspect of the environment, and it has frequently been used to advantage (Berry, 1970). Positioning tools, for example, in "mid-air" at a work site and soaring from place to place are obviously convenient when such behavior is desired.

Certain special senses are subject to functional alterations in the weightless environment. This is particularly true of the body's balance mechanism, the

gravity-dependent otolith organ. The physiology of these responses will be discussed in detail in chapter 17 and will only be mentioned briefly in the present chapter. Since the sense of cutaneous touch depends on stimulation of the touch receptors in the skin, the gravity free environment virtually eliminates this sensation. This seems to create for the inhabitant of the space capsule an unusual but not inconvenient situation.

The satisfactory performance of purely motor functions has posed a more challenging problem in the space environment. The execution of tasks which require push-pull forces and locomotion itself in the weightless state and under lunar gravity conditions has been facilitated through the development of various restraints and specialized tools and preflight astronaut training employing neutral buoyancy and other simulation techniques.

Unfortunately, prediction of physiologic responses during weightlessness is more complicated than prediction of work performance. Many of the problems anticipated have proved to be without foundation. Some, however, have been borne out For example, it was reasonable to expect that head colds would be more troublesome in 0 g than in the Earthbound environment since sinus drainage is gravity dependent. During the Apollo 7 mission, crewmembers who suffered head colds reported considerable discomfort and indicated that the space flight environment was in fact detrimental to relieving cold suffering. Earthbound analogs of weightlessness are available, but these are little more than useful tools. None actually simulates weightlessness since none eliminates gravity effects. At best, these techniques permit long-term study of isolated aspects similar to those which would be experienced in the weightless environment. Bed rest studies, for instance, are useful for more closely examining the effects of prolonged inactivity on such functions as calcium metabolism. The neutral buoyancy technique is unsuitable for the study of long-term physiological change because human subjects obviously can be submerged only for limited periods of time.

Since true weightlessness can be achieved within the influence of Earth's gravity for no longer than 1 min (usually 30 to 40 sec) (Gerathewohl & Ward, 1960), the most reliable predictor of the effects of long-term weightlessness on the human organism is, without doubt, actual orbital space flight experience. To date, this experience is limited to 2 weeks' exposure during the Gemini 7 mission and 24 days in the Soviet Salyut/Soyuz 11 flight. (See appendix for a chronology of U.S. and Soviet space flight mission durations.)

Animal data have been obtained during a 22-day mission where dogs were placed in orbit by Soviet scientists aboard the Kosmos 110 satellite (Parin et al., 1968). This and similar animal experiments are, like ground-based simulation, a valuable, but by no means perfect, tool for studying weightlessness effects. Whereas extrapolation from simulated to actual space flight conditions must be made cautiously because ground-based studies cannot eliminate gravity effects, direct applicability of orbital animal flight data is markedly restricted because of the inherent danger of generalizing results across species. Such experimentation does, however, offer the possibility of performing procedures which could not be ethically applied to man, and animals can be subjected to excessive

environmental exposures in search of threshold tolerances (but still must be instrumented carefully if any results are to be interpretable).

All information available to date indicates that man adjusts well to zero gravity for the periods he has flown. Some reversible physiological changes have been noted, principally in the cardiovascular system. To limit the magnitude of those changes, some countermeasures to weightlessness may be required, but these may be no more complicated than the provision of dietary supplements. With few exceptions, adjustment to weightlessness has been effortless.

Information about weightlessness effects has been gained by increasing man's exposure to the weightless environment in cautious incremental steps. In the Skylab program, scheduled to commence in 1973, this approach will be expanded and systematized. The Skylab space station will permit a much higher level of complexity of medical/behavioral laboratory techniques and equipment as well as longer mission durations of 28 to 56 days. Missions such as these will provide the first steps toward a sound basis for committing man to even longer stays in space, perhaps up to several years' duration.

Data obtained during manned missions in space have done much to dispel speculation concerning the potential hazards of space travel. However, some changes have been seen and although they do not appear to suggest that man is seriously compromised physiologically by space flight experience they nonetheless must be watched carefully to insure that they are not progressive in nature. The necessity for more data is further emphasized by the small number of individuals studied thus far and the inevitable individual variability which exists. Increasing mission length, however, increases the importance of providing an environment for man in space which assures his safe and satisfactory performance. Space vehicles must be designed with all aspects of operation in zero gravity taken into account.

Effects of Weightlessness on Physiological Systems

Prior to actual space flight experience, many legitimate concerns were expressed about man's potential response to the space flight environment. Table 8-1 lists a number of the effects predicted. Some of these involved pure conjecture; others could be more reasonably expected on the basis of early orbital animal flight experience and parabolic aircraft flight experimentation involving both men and animals. Inflight and postflight studies reported for individuals who have lived and worked in space indicate that many predicted problems were baseless, at least for stays up to 2 weeks. Some physiological changes have been consistently noted, but none have been permanently debilitating.

Table 8–1

Predicted Human Response to Space Flight

Dysbarism	Reduced blood volume
Disruption of circadian rhythms	Reduced plasma volume
Decreased g-tolerance	Dehydration
Skin infections and breakdown	Weight loss
Sleepiness and sleeplessness	Bone demineralization
Reduced visual acuity	Loss of appetite
Disorientation and motion sickness	Nausea
Pulmonary atelectasis	Renal stones
High heart rates	Urinary retention
Cardiac arrhythmias	Diuresis
High blood pressure	Muscular incoordination
Low blood pressure	Muscular atrophy
Fainting postflight	Hallucinations
Electromechanical delay in cardiac cycle	Euphoria
Reduced cardiovascular response to exercise	Impaired psychomotor performance
Sedative need	Infectious disease
Stimulant need	Fatigue

Table 8-2 summarizes the responses of the United States astronauts and Soviet cosmonauts to space flight exposure in the Mercury, Gemini, Apollo, Vostok, Voskhod, and Soyuz missions. Observation and measurement of these responses were made possible by a number of techniques, including preflight, inflight, and postflight studies. Television, telemetry and voice communication plus inflight sampling and, in one instance (Voskhod 1), inflight clinical evaluation by a physician, permitted an assessment of real time physiological changes.

Table 8-3 lists the principal techniques employed to monitor minute-to-minute inflight responses.

The sections which follow elaborate the physiological and performance areas which have been or may be expected to be affected by weightless space flight.

Cardiovascular Responses and Hematological Effects

Oxygen and nutrients in the internal environment of the body would be rapidly exhausted if they were not continually replenished by circulating blood. Likewise, the end products of metabolism would soon build up to toxic levels were they not removed from the tissues. This exchange is accomplished in capillary beds. At the arterial end of the capillaries, hydrostatic pressure due to

Table 8–2

Physiological Responses to Manned Space Flight

	UNITED STATES		
	MERCURY	GEMINI	APOLLO
CARDIOVASCULAR RESPONSES AND HEMODYNAMICS			
PULSE RATES	Elevated postflight (76 vs 86 bpm). Normalized 9 - 19 hr. postflight (38)	Peak during reentry, 180 beat/min; resting rate postflight, 18-62% higher than preflight (4)	Elevated postflight in 60% of astronauts (supine) rate, resting; returned to baseline usually 30-50 hours postflight
ORTHOSTATIC TOLERANCE	Decreased postflight 7 - 19 hr; briefly presyncopal (heart rate rose to 188 bpm during egress) (MA-9); greater decrease after 34 hr. flight than after 9 hr. flight (38)	Decreased; postflight increases in heart rate for tilt table test are 17-105% higher than preflight (4)	Significantly decreased (index: elevated heart rate) using LBNP and/or 90° passive stand test
EXERCISE TOLERANCE (WORK CAPACITY)			
INFLIGHT	Not significantly different from preflight (38)	Exercise load revealed no physical or cardiovascular decrement after 14 days (4), unimpaired (19)	Not measured

Table 8-2 (Continued)

Physiological Responses to Manned Space Flight

	UNITED STATES		
	MERCURY	GEMINI	APOLLO
POSTFLIGHT	Not measured	Decreased	Significant decrease in 25/30 astronauts immediately postflight; preflight level reached in 24-36 hours (except Apollo 15)
NET HEMATOLOGICAL CHANGES			
WHITE BLOOD CELLS	Lymphocytosis for 2 weeks postflight (90/80 supine) (38)	Increased (absolute neutrophilia); returned to baseline within 24 hr postflight (4)	Leucocytosis immediately postflight, preflight levels reached after 24 hr (2)
RED BLOOD CELL MASS	Unchanged (38)	Up to 20% decrease (Gemini 5) (4)	No change in Apollo 7 & 8; decrease in Apollo 9; no residual nitrogen 7 to 10 days (2); no measurement Apollo 11, 12, 13. Apollo 14, 15, 16: 16% average loss RBC mass
PLASMA VOLUME		No significant changes (4)	Mean unchanged (9); no measurement Apollo 11, 12, 13. Apollo 14, 15: slight increase over preflight mean: Apollo 16: decrease averaged 9%.
ELECTRICAL ACTIVITY (EKG)	Moderate rightward shift in QRS & T [illegible]ht (38)		

ELECTRIC & MECHANICAL SYSTOLE		Stable (7)	No inflight measurement
ARRHYTHMIAS	Not different from baseline (38)	Rare (4)	Rare ectopic beats; brief episode of supraventicular bigeminy in Apollo 15
BLOOD PRESSURE	Decreased 9 - 19 hr postflight (38)	Normal (4)	Labile for up to 3 days postflight (2)
PULMONARY FUNCTION	Normal (38)	Normal; max 40 b/min during heavy workloads (4), no atelectasis (4)	Normal (2)
GENERAL METABOLISM	-7.75 lb (38)		
WEIGHT LOSS	-7.75 lb (38)	2.5 - 10 lb (Gemini 4 - 7) (1)	-6 lb; range: +1.0 to -12.5
WATER BALANCE	Negative (reduced food and water intake) (38)	Slightly negative (Gemini 4) (4)	Slightly negative
POSTFLIGHT ENERGY EXPENDITURE MEASURED BY O_2 UPTAKE DURING REST	Not measured		Work rate/O_2 consumption at predetermined heart rate decreased postflight
MUSCULO-SKELETAL RESPONSES			
NITROGEN BALANCE	Not measured	Slightly negative nitrogen balance (4)	No data

Table 8–2 (Continued)

Physiological Responses to Manned Space Flight

	UNITED STATES		
	MERCURY	GEMINI	APOLLO
MUSCLE CHANGES			Decreased calf size; cardiac silhouette decreased
BONE DEMINERALIZATION	No evidence of Ca mobilization (39)	12 - 15% decrease in bone density (Gemini 4, 5, 7) (1); calcium balance data confirm negative trend (4, 10)	Minimal density reduction
VESTIBULAR RESPONSES	Sensation of objects rotating 90°, transitory (38)	No alteration (4)	Minimal subjective symptoms of motion sickness in early phase of mission; nausea and/or vomiting in 3 astronauts (of total 30) each on separate missions; tumbling sensation 2 crewmen on donning suits
SLEEP	Total 4.5 hr (in short, sound naps) inflight; subjectively normal (38)	Variation in depth from stage 1 -4 (noted also in ground based data) amount not sufficient to prevent fatigue (4)	Quality and quantity improved when crew slep simultaneously (Apollo 9, 10, 11) (4)
COORDINATION	Normal (39)	Unimpaired (4)	Unimpaired

SENSATIONS			
MOTION SICKNESS	None (39)	None (1)	Slight to severe symptoms (9/30 crewmen)
DISORIENTATION	None (39)	None (4)	None
ILLUSIONS	Transitory; not troublesome (38)		1/30 - sensation of headdown tilt of approximately 30° during recumbency for 5 postflight days
FATIGUE		Expressed, but did not interfere with performance (4)	Expressed, but variable in degree
MISCELLANEOUS		"Fullness of the head" (4)	"Fullness of head"; generally universal during early flight
BIOCHEMICAL CHANGES			
BLOOD			
ELECTROLYTES (Na, K, Cl)	Na elevated postflight (38)	Decreased postflight in command pilot (4)	Consistent slight decrease to moderate decrease in serum potassium. No change in serum sodium, chloride; generally return to preflight levels 24-48 hr postflight
GLUCOSE		Increased postflight (4)	Transient elevation postflight
URIC ACID		Decrease (4)	Generally decreased

Table 8–2 (Continued)
Physiological Responses to Manned Space Flight

	UNITED STATES		
	MERCURY	GEMINI	APOLLO
CREATININE		Slight increase postflight (4)	No significant change
IMMUNOGLOBULINS			Increased (probably related to clinical illness and stress) (2)
HYDROXPROLINE		Marked increase in bound hydroxyproline in plasma (Gemini 7) in 1st postflight sample (4)	
CHOLESTEROL			No significant change
HORMONES	--	ADH and aldosterone elevated (4) 17-hydroxycorticosteroid increased postflight (4)	Hydrocortisone and ACTH decreased. Insulin unchanged. T-3, T-4 unchanged; angiotensin I markedly elevated
URINE			
HYDROXYPROLINE			Increased postflight (9)
ELECTROLYTES (Na, K,C1)	Retention postflight (38)	Na - slightly reduced output inflight, marked retention postflight; Cl - same; K - ambiguous (4)	Diminished excretion immediately postflight (2)

STEROIDS		Aldosterone increased inflight and immediately postflight (4)	Hydrocortisone elevated aldosterone elevated 17-ketosteroids slightly decreased
CATECHOLAMINES			Gemini, elevated, Apollo, elevated
CALCIUM	Elevated postflight (38)	Larger quantities excreted in later phases of flight (4)	No significant trend
UREA NITROGEN		Increased postflight (command pilot Gemini 7) (4)	
CREATININE	Elevated postflight (38)		Apollo 8 through 16: 24-hr urine No significant change from preflight levels
CENTRAL NERVOUS SYSTEM		No evidence of abnormality based on crew mission task performance and EEG (4)	No evidence of abnormality based on crew mission task performance (2)
VISION		Unimpaired (onboard vision tester) (4)	Acuity unimpaired; light flashes noted on most lunar missions

Table 8–2 (Continued)

Physiological Responses to Manned Space Flight

	UNITED STATES		
	MERCURY	GEMINI	APOLLO
PATHOLOGICAL CHANGES			
MICROFLORAL ALTERATIONS	Not measured		Man to man transfer of bacteria; increase in number of individuals and sites individuals infected; growth of opportunist organisms may be favored (2); loss of skin fungi (quantity and quality) oral flora: most drastic changes noted
CLINICAL ILLNESS	None	None related to flight (4)	Correlated with seasonal occurrence and preflight exposure (2); one episode of bacterial urinary tract infection
RADIATION EXPOSURE			No responses noted; average dose less than 1 rad.

Table 8–2 (Continued)
Physiological Responses to Manned Space Flight

	SOVIET UNION		
	VOSTOK	VOSHOD	SOYUZ
CARDIOVASCULAR RESPONSES AND HEMODYNAMICS			
PULSE RATES	Decreased in zero G (33); normalization inhibited; preflight rate reached after 9.5 hr (Vostok 2) and 4.5 hr (Vostok 3) (after centrifuging, normalization took 5 to 10 min for same subjects) (5); 46-80 beats/min (Vostok 5); 54-84 beats/min (Vostok 6) (inflight) (20)	After pronounced increase, normalization occurred within 2 hr of flight; one vagatonic reaction was observed; decrease to 46 beat/min in sleep (11); almost all experienced fluctuation in rate (12); moderate tachycardia in Voskhod 2 (12)	60-76 beats/min toward end of Soyuz 8 mission (3); slowed during flight for 1 cosmonaut, decreased for both during sleep (Soyuz 5) (23)
ORTHOSTATIC TOLERANCE	Decreased heart rate indicated by decreased (26-47%) minute volume, and blood pressure (10-24 mm Hg) on standing (11)	Decreased postflight (11)	Marked decrease (Soyuz 9), reversal required 11 days (25)
EXERCISE TOLERANCE (WORK CAPACITY)			
INFLIGHT	High (Vostok 5, 6) (36)	Somewhat decreased for one cosmonaut; remained high for other (11)	High (Soyuz 9) (22)

Table 8–2 (Continued)
Physiological Responses to Manned Space Flight

	SOVIET UNION		
	VOSTOK	VOSKHOD	SOYUZ
POSTFLICHT		Decreased. Greater increase in heart rate and normalization period than preflight; normal by 3 days postflight (11)	Changes seen after missions lasting more than 5 days; decrease in Soyuz 9 crew lasted 8 days postflight (31)
NET HEMATOLOGICAL CHANGES			
WHITE BLOOD CELLS	Leucocytosis (Vostok 2, 3, 4); lymphopenia and tendency to eosincpenia (Vostok 3, 4) (all quickly reversed: attributed to stress) (8)	Slight leucocytosis and lymphocytosis; normalized in 24 hr postflight (11)	Eosinopenia, leucocytosis, thrombocytopenia 1.5 - 2 hr postflight (Soyuz 9) (26, 31)
RED BLOOD CELL MASS			
PLASMA VOLUME			Decrease indicated by increase in hemoglobin, erythrocytes postflight (31)
ELECTRICAL ACTIVITY (EKG)			

ELECTRIC & MECHANICAL SYSTOLE	Increase in electromechanical delay (6)	Mechanical systole shortened, Voskhod 1 (11); electric systole shortened, Voskhod 2 (12)	Not significantly different from baselines (31)
ARRHYTHMIAS	Noted in Vostok 6 (20)		"Space arrhythmias" (14)
BLOOD PRESSURE	Decrease in zero G (33)	Overall definite decrease (11, 12)	Normal inflight (22); elevated postflight (Soyuz 9) (26)
PULMONARY FUNCTION	No abnormalities (Vostok 3 & 4)(5); normal 12-22 b/min range (Vostok 5 & 6) (inflight) (20)	Somewhat higher rate during entire flight (Voskhod 1) (11); 2 to 3 fold increase in ventilation (in 2 of Voskhod 2 crew) (16)	Normal (3, 22)
GENERAL METABOLISM		Equipment failure precluded data collection (11)	
WEIGHT LOSS		1.9, 2.9, 3.0 kg, Voskhod 1 (11); 1 and 0.9 kg, Voskhod 2 (12)	2.3 and 4 kg for one cosmonaut in Soyuz 4 & 8 (3); 2.7 and 3.9 kg in Soyuz 9 (22)
WATER BALANCE		Increased perspiration (with fatigue) (11); water retention postflight (12)	Slightly negative (Soyuz 9) (26)
POSTFLIGHT ENERGY EXPENDITURE MEASURED BY O_2 UPTAKE DURING REST		Up 6 and 27%, Voskhod 1 (11); up 29 and 13%, Voskhod 2 (12)	
MUSCULO-SKELETAL RESPONSES			
NITROGEN BALANCE			Possibly negative (31)

Table 8–2 (Continued)
Physiological Responses to Manned Space Flight

	SOVIET UNION		
	VOSTOK	VOSKHOD	SOYUZ
MUSCLE CHANGES	Muscular strength decreased in flight (33)		Tonus decreased (Soyuz 6 - 9), pain, atrophy, reflexes decreased postflight (Soyuz 9) (24, 28)
BONE DEMINERALIZATION			Optical density decrease equal to effect of up to 72 days bedrest (29)
VESTIBULAR RESPONSES	Asymmetry of nystagmic movement (Vostok 5 & 6)(18); normal, no asymmetry in oculomotor reaction (by oculogram) (Vostok 3 & 4) (5)	No disagreeable sensations in Voskhod 2, increase in total afferent signals during muscular contraction in active work credited with disappearance of sensations noted in Voskhod 1 (12)	Coriolis-like sensation during period of adaptation to zero g (Soyuz 9) (25)
SLEEP	EEG shifts in excitation-inhibition (8); deep sleep (36)		Deep after several days of adaptation (Soyuz 9) (31)
COORDINATION	Not reduced (15)	Accuracy for slight coordinated movements decreased (11)	Motor functions markedly impaired postflight (Soyuz 9) (27); altered gait (32)

SENSATIONS			
MOTION SICKNESS	Nausea, dizziness (Vostok 2) (37)	After 1.5 to 2 hrs of flight, disappeared after sleep (11)	
DISORIENTATION	Vertigo, rolling sensation (Vostok 2) (17); no spatial disorientation (33)	Mild vertigo in Voskhod 1 (11); none in 2 (12)	Mild coriolis effect (Soyuz 9) (22), disorientation in space in darkness (31)
ILLUSIONS	Inversion of body position (Vostok 1 & 4) (17, 33)	Inversion of body position (Voskhod 1) (11)	
FATIGUE		Marked in Voskhod 1 and 2 (12)	Normal, work related inflight, increased postflight (31)
MISCELLANEOUS			Head fullness and postflight 2.5 g sensation (Soyuz 8, 9) (22, 23)
BIOCHEMICAL CHANGES			
BLOOD			
ELECTROLYTES (Na, K, Cl)		% chlorides unchanged during flight (11)	
GLUCOSE		% unchanged during flight (11)	
URIC ACID		Urea increased (11)	Slight increase postflight (31)

Table 8–2 (Continued)

Physiological Responses to Manned Space Flight

	SOVIET UNION		
	VOSTOK	VOSKHOD	SOYUZ
CREATININE			
IMMUNOGLOBULINS			Moderate decrease indicating depressed immune reaction (Soyuz 9) (22)
HYDROXYPROLINE			
CHOLESTEROL		Up to 260-290 mg % postflight (200-260, normal) (11); normal within 2 weeks (12)	Negligible increase postflight (31)
HORMONES			
URINE			
HYDROXYPROLINE			
ELECTROLYTES (Na, K, Cl)			Diminished excretion postflight (Soyuz 9) (22)

STEROIDS	Noted (Vostok 3 & 4 postflight). Reversed (8)		Elevation postflight indicated no marked stress (31)
CATECHOLAMINES			
CALCIUM	Increased excretion (Vostok 2 & 3) (8); hydroxycorticosteroids increased 2.5 - 10.7 times normal. Reversed (8)		Elevated postflight (Soyuz 9) (29)
UREA NITROGEN			
CREATININE	Increased (Vostok 2 & 3); reversed after 14 days (8)		
CENTRAL NERVOUS SYSTEM	Unimpaired (Vostok 5 & 6) (20); Mental activity remained high (8); EEGs normal (13)		Unimpaired (31)
VISION		Acuity unchanged; negative fusion increased 40, 70% (in 2 of Voskhod 1 crew; no change in 3rd man)	Color vision changes (Soyuz 9) (30)

Table 8–2 (Continued)

Physiological Responses to Manned Space Flight

	SOVIET UNION		
	VOSTOK	VOSKHOD	SOYUZ
PATHOLOGICAL CHANGES			
MICROFLORAL ALTERATIONS	Transient, insignificant changes (Vostok 1 - 4)(34); genetic changes in lysogenic bacteria (Vostok 3 - 6) (35)		Dysbacteriosis (Soyuz 9) (22, 31)
CLINICAL ILLNESS	None (Vostok 3 & 4) (8)		None (Soyuz 9) (26)
RADIATION EXPOSURE			

References for Table 8–2

1. Berry, C. A., Coons, D. O., Catterson, A. D., & Kelly, G. F. Man's response to long-duration flight in the Gemini spacecraft. In Gemini Midprogram Conference. Symposium presented at NASA Manned Spacecraft Center, Houston, Texas, 23-25 February 1966. p. 235-261. (NASA AP-121)
2. Berry, C. A. Summary of medical experience in The Apollo 7 through 11 manned spaceflights. *Aerospace Medicine*, 1970, *41*, 500-519.
3. Mandrovsky, B. The Soyuz-6, Soyuz-7, and Soyuz-8 mission. Prepared by Library of Congress, Reference Department, for NASA, Washington, D.C., January 1970.
4. National Aeronautics and Space Administration. Gemini Summary Conference. Symposium presented at NASA Manned Spacecraft Center, Houston, Texas, 1-2 February 1967. (NASA SP-138)
5. Parin, V. V. (Ed.) *Aviation and space medicine*. NASA, Washington, D.C., December 1964. (NASA TT F-228)
6. Bayevskiy, R. M., & Gazenko, O. G. Reactions of the cardiovascular and pulmonary system in humans and animals under conditions of weightlessness. *Kosmicheskiye issledovaniya*, 1964, *2*, 307.
7. Vallbona, C., Dietlein, L. F., & Judy, W. V. Effect of orbital flight on the duration of the cardiac cycle and of its phases. *Aerospace Medicine*, 1970, *41*, 529-537.
8. Fedorova, T. A., et al. Some metabolic indices in the cosmonauts Gagarin, Titov, Nikolayev, and Popovich. In A. T. D. Press, Special Issue, *Space Medicine*, 1964, *3*(10). *(Library of Congress, N61-26357)*
9. Berry, C. A. Apollo 7 to 11: medical concerns and results. NASA Manned Spacecraft Center, Houston, Texas, November 1969. (NASA TM X-58034)
10. Lutwak, L., et al. Mineral, electrolyte and nitrogen balance studies of the Gemini VII fourteen-day orbital space flight. *The Journal of Clinical Endocrinology and Metabolism*, 1969, *29*(9), 1140-1156.
11. Volynkin, Y. M., & Vasil'yev, P. V. Some results of medical studies conducted during the flight of the Voskhod. In N. M. Sisakyan (Ed.) *Problems of Space Biology*, Vol. VI, NASA, Washington, D.C., July 1969. (NASA TT F-528)
12. Gazenko, O. G., & Gyurdzhan, A. A. Physiological effects of gravitation. NASA, Washington, D.C., August 1965. (NASA TT F-376)
13. Gazenko, O. G., Gurfinkel, V. S., & Malkin, V. B. Electroencephalographic studies in space medicine. In N. M. Sisakyan (Ed.) *Problems of Space Biology*, Vol. VI, NASA, Washington, D.C., July 1969. (NASA TT F-528)
14. Mandrovsky, B. The Soyuz-4 and Soyuz-5 joint space mission. Prepared by Library of Congress, Reference Department for NASA, Washington, D.C., February 1969.
15. Yazdovskiy, V. I., et al. Sensory-motor coordination in conditions of prolonged weightlessness during actual space flight. In A. T. D. Press, Special Issue, *Space Medicine*, 1961, *3*(10). (Library of Congress, N64-26357)
16. Lovelace Foundation. Compendium of human responses to the aerospace environment. Vol. II, Section 7. Prepared for NASA, Washington, D.C., November 1968. p. 7-38-7-55. (NASA CR-1205 II)
17. Gazenko, O. G. Medical studies on the cosmic spacecrafts Vostok and Voskhod. NASA, Washington, D.C., December 1964. (NASA TT F-9207)
18. Gazenko, O. G., Parin, V. V., & Chernigovskii, V. N. Space physiology, some results and outlooks of experimental investigations. ANL Trans-209, Argonne National Laboratory, Argonne, Illinois, July 1965.

19. Dietlein, L. F., & Rapp, R. M. Experiment M-3, inflight exercise–work tolerance. In Gemini Midprogram Conference. Symposium presented at NASA Manned Spacecraft Center, Houston, Texas, 23-25 February 1966, p. 393-396. (NASA SP-121)

20. Yazdovskiy, V. I., & Demsov, V. G. Flights of space vehicles Vostok-5 and Vostok-6. *Vestnik Akademii Nauk SSSR*, Vol. XXXIII, No. 9, Moscow, September 1963, 17-22.

21. Berry, C. A. Preliminary clinical report of the medical aspects of Apollos 7 and 8. NASA Manned Spacecraft Center, Houston, Texas, May 1969. (NASA TM X-58027)

References 22-29 are articles appearing in: Gazenko, O. G. & Gurovskiy, N. N. (Eds.) *Space Biology and Medicine*, Moscow: Meditsina Publishing House. Vol. 4, No. 6, 1970.

22. Vorob'yev, Ye. I. Yegorov, A. D., Kakurin, L. I. & Nefedov, Yu. G. Medical support and principal results of examination of the Soyuz-9 spaceship crew. pp. 26-31.

23. Butusov, A. A., Lyamin, V. R., Lebedev, A. A., et al. Results of routine medical monitoring of cosmonauts during flight on the Soyuz 9 ship. pp. 35-39.

24. Cherepakhin, M. A., & Pervushin, V. I. Space flight effect on the neuromuscular system of cosmonauts. pp. 46-49.

25. Kalnichenko, V. V., Gornago, V. A., Machinskiy, G. V., et al. Dynamics of orthostatic stability of cosmonauts after flight aboard the Soyuz-9 spaceship. pp. 100-112.

26. Molchanov, N. S., Krupina, T. N., Balandin, V. A., et al. Results of clinical examination of A. G. Nikolayev and V. I. Sevast'yanov. pp. 39-42.

27. Petukhov, B. N., Pruakhin, Yu. N., Georgiyevskiy, V. S., et al. Regulation of erect posture of cosmonauts after an 18-day orbital flight. pp. 50-54.

28. Vorob'yev, Ye. I., Nefedov, Yu. G., Kakurin, L. I., et al. Some results of medical investigations made during flights of the Soyuz-6, Soyuz-7, and Soyuz-8 spaceships. pp. 65-73.

29. Biryukov, Ye. N., Krasnykh, I. G. Change in optical density of bone tissue and calcium metabolism in the cosmonauts A. G. Nikolayev and V. I. Sevast'yanov. pp. 42-45.

30. Gazenko, O. G. Personal communication.

31. Kakurin, L. I. Medical research performed on the flight program of the Soyuz-type spacecraft, NASA TT F-14, 026, National Aeronautics and Space Administration, Washington, D.C., November 1971.

32. Chekirda, I. F., Bogdashevskiy, R. B., Yerewin, A. V., & Kilosov, I. A. *Space Biology and Medicine*, 1971, 5(6), 71-77.

References 33-36 are articles appearing in: N. M. Sisakyan (Ed.) *Problems of Space Biology*. Vol. 4, NASA, Washington, D.C., March 1966. (NASA TT-F-368)

33. Kas'yan, I. I., Kopanev, V. I., & Yazdovskiy, V. I. Reactions of cosmonauts to weightlessness. p. 260.

34. Alekseyeva, O. G. Some natural immunity factors and cosmonaut autoflora during the training period and following the flights of Vostok, Vostok 2, Vostok 3, and Vostok 4. p. 278.

35. Zhukov-Verezhnikov, N. N., et al. Results of microbiological and cytological investigations conducted during the flights of Vostok type vehicles. p. 252.

36. Yazdovskiy, V. I., Yemel'yanov, M. D., Vasil'yev, P. V., & Kopanev, V. I. Some results of biomedical investigation conducted during the training period and flights of cosmonauts V. F. Bykovskiy and V. V. Tereshkova. p. 231.

37. Komendatov, G. I., & Kopanev, V. I. Motion sickness as a problem in space medicine. Problems of space biology and medicine. JPRS18395. Joint Publications Research Service, Washington, D.C., 1962.

38. Catterson, A. D., McCutcheon, E. P., Minners, K. A., & Pollard, R. A. Aeromedical observations. Chapter 18 in Mercury project summary, NASA Manned Spacecraft Center, Houston, Texas, 15-16 May 1963. (NASA SP-45)

39. Berry, C. A. Aeromedical preparations. Chapter 11 in Mercury project summary, NASA Manned Spacecraft Center, Houston, Texas, 15-16 May 1963. (NASA SP-45)

Table 8–3

Inflight Biomedical and Performance Measurements

Parameter Measured	Technique Employed	
	American Missions	Soviet Missions
Cardiac activity	2-lead EKG with synchronous phonocardiography	Seismography (myocardial contractility) 2-lead EKG, kineotocardiography, cutaneogalvanography electrocardiophone (pulse rate)
Instantaneous heart rate (arrhythmias)	Cardiotachography	Cardiac contraction monitoring
Blood pressure	Biosensor harness pressure cuff	
Blood vessel permeability		Plethysmometry
Respiratory rate (chest perimeter)	Impedance pneumography	Pneumography
Vestibular functions and CNS	EEG, ocular counter-rolling, overall task performance voice communication	EEG, electrooculography, overall task performance, voice communication, onboard logs, psychophysiological testing by cosmonaut physician
Temperature	Oral thermistor	Rectally inserted sensor*
Muscular fatigability		Central electronic monitoring (not specified)
Muscular strength		Dynamometer
Work capacity	Inflight exercise response; postflight bicycle ergometry	Occupational and graphical analysis and required time for task completion; in Soyuz 9 inflight exercise response was monitored; postflight gas-energy exchange determined by method of Douglas and Holden, minute volume determined by return breathing of CO_2 (Fick Method), bicycle ergometry
Motor activity		Electrooculography
Visual acuity	Onboard vision tester	Examination of ability to focus by cosmonaut physician
Overall clinical profile	Voice communication, television	Voice communication, television, examination by cosmonaut physician

*Temperature sensor was made in form of a "metal olive" inserted into the ampulla of the large intestine by cosmonaut prior to donning spacesuit.
(Soviet data from Kakurin, 1971, and others)

the heart's action drives oxygen and nutrient-bearing fluid into the spaces between the tissue cells. The drop in pressure in the venous end permits depleted fluid to return to the capillaries, thence to the central circulation. To effectively balance these two operations, or maintain homeostasis, blood plasma must be delivered in sufficient volume and with sufficient pressure. The cardiovascular system and all the complex reflexes which govern its function are devoted to maintaining this balance.

In advance of space flight experience, both plasma volume and blood pressure changes were predicted on the basis of extrapolation from bed rest studies (Deitrick, Whedon, & Shorr, 1948) and what could reasonably be expected as a consequence of the reduction in hydrostatic pressure gradients at zero gravity. Reduction of hydrostatic pressure gradients will, for example, greatly diminish pressure exerted on blood vessels; the end result of which can be a reduction in the reactivity or sympathetic tone of the vessels (particularly the veins).

It was thus predicted that over long periods of time the reduced load upon the heart, lowered blood pressure, and reduced hydrostatic pressure differences experienced in weightlessness ultimately might become manifest as a malfunction of one or more of the cardiovascular control loops responsible for homeostatic regulation. The pressure regulation and blood volume loops which are susceptible to hydrostatic effects were expected to be the most likely to deteriorate, if deterioration should occur, since these are subjected to minimal stress during prolonged weightless space flight. The consequences of such phenomena, might, it was thought, diminish or obliterate man's ability to withstand the gravitational load associated with reentry accelerations.

Prior to actual flight, it was not possible to say with any reliability whether weightlessness would alter other aspects of the cardiovascular system. Hence, careful measurements were made to detect any changes in heart rate and electrical conductance. Changes in the formed elements of the blood also were watched closely. The following section describes the principal findings.

Space Flight Results. Cardiovascular indices have been monitored during all United States space flights and have been within expected physiological ranges. No significant changes have been noted in blood pressure while heart rate has tended to stabilize at a lower level. Only in the Apollo 15 crew have any significant irregularities been noted in electrocardiographic recordings. Postflight, reduced orthostatic tolerance has been observed with regularity. It has so far been the most pronounced and consistent finding. This phenomenon has also been seen following Soviet space missions. Orthostatic intolerance accompanied by elevated heart rate was first noted on capsule egress in the Mercury 8 pilot. Cardiovascular function has therefore been extensively investigated following all subsequent flights.

Cardiovascular Profile. The heart function profile has been as follows:

- *Heart Rate.* Peak heart rates (table 8-2) have been observed at launch and at reentry, normally reaching higher levels during the latter. During the

weightless phase of space flight, heart rates have tended to stabilize at lower levels and have responded, at these levels, adequately to physical demands. Soviet investigators (Akulinichev et al., 1964; Volynkin & Vasil'yev, 1969) have reported that normalization of heart rate occurred inflight but that the period of time required to achieve preflight heart rates was considerably extended beyond the period required for normalization following similar accelerative stresses on Earth. Postflight heart rates have been found to be elevated (Berry, 1967a; 1970) and, here again, normalization has been inhibited. Following United States Apollo missions, 30 to 50 hours were generally required for preflight baseline heart rates to be reestablished.

• *Cardiac Electrical Activity.* By far the most serious finding in the sphere of cardiovascular response have been the aberrations in cardiac electrical activity noted in the Lunar Module Pilot and the Commander of Apollo 15. The Apollo 15 crew had engaged in strenuous activity on the lunar surface during which time the arrhythmias were first noted. These were well outside the range of normal. The Lunar Module Pilot experienced numerous premature ventricular contractions both on the lunar surface and during the return to Earth. Twelve bigeminis were recorded, as were premature auricular contractions. The mission Commander experienced four premature ventricular contractions during a sleep period on the morning of reentry when a heart rate of only 28 beats per minute was recorded. This was followed by additional premature auricular contractions and occasional premature ventricular contractions which lasted for about one hour. However, neither crewmember exhibited any evidence of arrhythmia upon postflight examination (Berry, 1972). Extrasystoles had been noted during prior United States and Soviet space missions but these occurred rarely and no individual experienced more than an occasional arrhythmia (Berry, 1967; Akulinichev et al., 1964; Yazdovskiy & Denisov, 1963). Postflight examinations of the Apollo 15 crew revealed potassium deficits which were linked to the irregular heartbeats. Supplementary dietary potassium and less strenuous work schedules eliminated this problem for the Apollo 16 crew (Berry, 1972).

• *Heart Size.* During the Vostok flights, increases were noted in electromechanical delay (Bayevskiy & Gazenko, 1964), while electric and mechanical systole in the Soyuz crews showed no significant difference from preflight baselines inflight (Kakurin, 1971). This parameter has not been measured inflight for U.S. crews. Study of pre- and postflight posterior/anterior chest films from all U.S. flights reveal a decreased cardiac size postflight. Specific studies in Apollo 16 correlating several X-ray views taken at the same time in cardiac cycle, systole or diastole, revealed an apparent decrease in the cardiac silhouette.

• *Blood Pressure Measurements.* Blood pressure recordings, including those taken at reentry, indicate that systolic and diastolic pressures have remained within the envelope of normality (Berry, 1967a). Soviet experience (Volynkin & Vasil'yev, 1969) indicates a definite overall decrease in pulse pressure under the conditions of weightlessness. Pulse pressures following Apollo flights have been found to be quite labile for up to 3 days postflight (Berry, 1970).

• *Orthostatic Tolerance.* Significantly reduced orthostatic tolerance, evidencing cardiovascular deconditioning, to the one g environment has been observed in every United States space mission since the last two Mercury flights. Soviet investigators have also reported the phenomenon in their Voskhod and Soyuz missions (Petukhov et al., 1970; Volynkin & Vasil'yev, 1969; Kakurin, 1971). While there were no noticeable changes in any of the recorded parameters after 2-day flights, all the cosmonauts showed signs of orthostatic instability after 3- to 5-day flights (Kakurin, 1971).

In order to reveal the full extent of cardiovascular deconditioning to 1 g or conditioning to 0 g, several types of postflight cardiovascular provocation are employed while various indicators are monitored. The point of provocative testing is that it often reveals changes otherwise undetectable in resting individuals because compensatory mechanisms may mask any sign of physiological decrement. Gemini astronauts, for example, showed no signs of orthostatic hypotension prior to provocative testing. The methods employed have included the application of lower body negative pressure and passive orthostatic tests. In the U.S. static stand procedure, the subject demonstrates stable heart rate and blood pressure in the resting, supine position for 5 minutes, after which he is assisted to a standing position with minimum delay and movement. He remains motionless in the upright position for 5 minutes while heart rate and blood pressure are again recorded each minute. The Soviet procedure involves 10 minutes of tilting in a rotating chair to a vertical position (88°) after the subject has rested in a supine position for at least 20 minutes, while hemodynamic, gas exchange and respiration measures are made.

Space crews have required, at the longest, 13 days postflight to reach preflight baselines. The Soyuz 9 and Apollo 15 crews' recoveries were markedly slower than those of previous Apollo crews who reached preflight levels within 3 days after space flight.

Whatever the factors causing orthostatic intolerance, heart rate remains the most sensitive index (Berry, 1970). Postflight heart rate increases during tilt table testing for Gemini crewmen were 17 to 105 percent greater than those exhibited preflight. In the Apollo series, 90° passive standing revealed significantly elevated pulse rates in all crewmembers tested. Figure 8-1 indicates representative heart rate changes.

Blood pressure, on the other hand, has not proved to be a consistently reliable index of deconditioning. Decreased pulse pressure has been noted in 15 of 21 Apollo crewmembers tested postflight (Rummel et al., 1972).

Hematological Profile. The folowing paragraphs describe all blood changes for United States missions to date. It should be noted that these changes were completely reversible.

• *Plasma Volume.* Plasma volume changes associated with weightlessness have been variable in direction and temporary, not lasting more than 10 days. This is strikingly different from results of bed rest studies, in which decreases continue for several weeks. Table 8-2 summarizes individual findings. A later

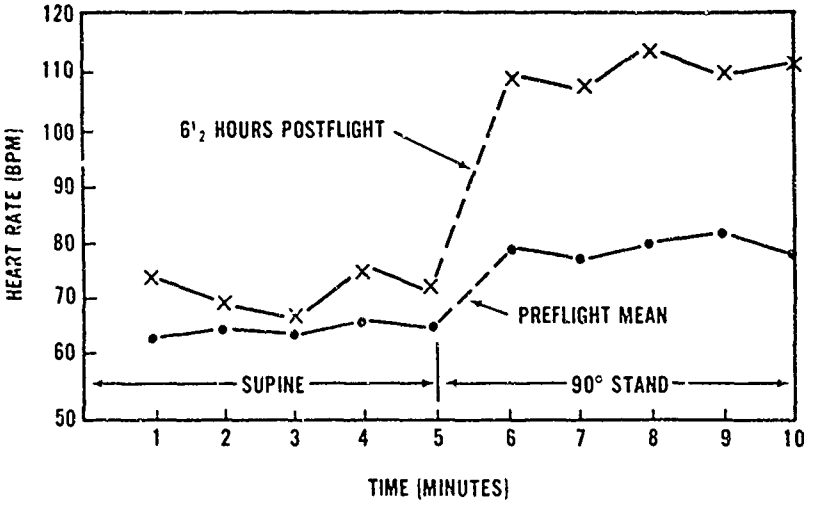


Figure 8–1. Representative changes of heart rate during 90° passive standing preflight and postflight (Berry, 1970)

discussion concerning endocrine and electrolyte response to weightless space flight presents an explanation of this phenomenon.*

• *Red Blood Cell Mass.* Hematological changes have been compared in three Gemini crews (4, 5, and 7) and the crews of Apollo missions 7, 8, 9, 14, and 15 by Johnson & Driscoll (1972). When the Gemini crews were compared with the Apollo crews on missions which did and did not employ the lunar module, a statistically significant difference was noted in the percent change of red blood cell mass (using ^{51}Cr) among the groups; no such change was seen in controls. These results are indicated in table 8-4. No difference was found in the mean survival time of red blood cells, and no difference was found between the two types of Apollo missions compared.

Blood studies of Soyuz 9 cosmonauts indicated increased hemoglobin 1.5 to 2 hours postflight (Molchanov et al., 1970).

Table 8–4

Red Cell Mass Percent Change
(Premission vs Immediately Postmission)

	GEMINI	APOLLO & LM	APOLLO
Crew	−15.6 ±2.3	−7.4 ±1.2	−2.4 ±1.6
Controls		−1.1 ±1.0	+0.1 ±1.6

(From Johnson & Driscoll, 1972)

*Plasma volume decreases are suggested in the Soyuz crew by increases in hemoglobin and red blood cell mass postflight (Kakurin, 1971.)

● *White Blood Cells.* Net increases in the number of white blood cells were consistently noted in Gemini missions and continued to occur during Apollo missions. Similar changes have been reported for Soviet cosmonauts (Molchanov et al., 1970). Soyuz 9 results showed thrombocytopenia for two weeks postflight. Although other leucocytes have decreased in number, substantially elevated neutrophil counts account for the net increase (Berry et al., 1966; 1970). Table 8-5 summarizes changes in hematological responses for the Apollo 7 through 11 missions.

Table 8–5

Apollo Blood Profile Summary

Parameter	Mission					
	Apollo 7	Apollo 8	Apollo 9	Apollo 10	Apollo 11	Overall
Red blood cells	0	▲▲	▼▼	▲▲	0	0
Hematocrit	0	▲▲	0	▲▲	0	0
Hemoglobin	0	▲▲	▲▲	0	0	
Reticulocytes	0	0		0	0	
White blood cells	▲▲▲	▲▲▲	0	▲▲	▲▲▲	▲▲▲
Neutrophils	▲▲	▲▲	0	▲▲▲	▲▲▲	▲▲
Lymphocytes	▼▼	▼▼	0	▼▼	▼▼	▼▼
Monocytes	0	▼▼	0	0	▼▼	▼▼
Eosinophils				▼▼	▼▼	▼
Basophils				▼▼		0
Platelets	0	0	0	0	0	0

LEGEND:

0 No occurrence

▼ Significant trend (negative)

▼▼ -2σ

▼▼▼ -3σ

▲▲ $+3\sigma$

▲▲▲ $+3\sigma$

Simulation Studies. As early as 1948, Deitrick, Whedon, and Shorr noted that hypodynamia, produced by bed rest and standardized by cast immobilization of the pelvic girdle and legs, brought about a definite deterioration in the mechanisms essential for adequate circulation in the erect position. Figure 8-2 shows the percentage change from resting levels of pulse rate and pulse pressure for their subjects during tilt table testing. Increases in pulse rate and decreases in pulse pressure of 40 to 70 percent were noted prior to immobilization. During immobilization, these changes exceed 70 percent. Syncope was also common.

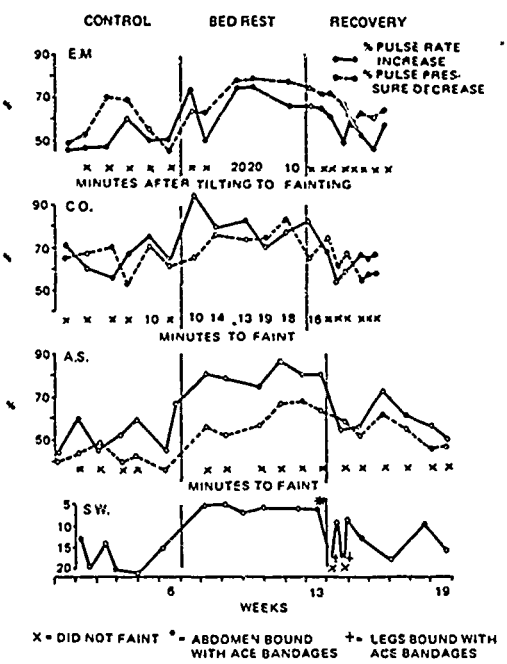


Figure 8–2. Effect of immobilization on the responses of pulse rate and pulse pressure to tilting to 65 degrees feet downward for twenty minutes in four normal male subjects. (From Deitrick, Whedon, & Shorr, 1948)

To examine to what extent bed rest parallels weightlessness, the flight data obtained during the Gemini mission series were compared with data from bed rest studies of equal duration. Figure 8-3 shows resting heart rate changes (expressed as a percentage of preexposure values) for each. Although the two conditions show very similar trends, the magnitude of change is markedly different. This, perhaps, indicates that factors other than those simulated by bed rest are involved in the changes in heart rate noted after exposure to weightlessness.

Conclusions. Cardiovascular deconditioning, as evidenced by diminished orthostatic tolerance, is the most consistently observed and most profound of the effects upon the cardiovascular system following exposure to up to 18 days of weightless space flight. This condition is reversible and appears to have no serious lasting implications. Rare irregularities have been noted in the electrical activity of the heart. These appear to be controllable through maintenance of electrolyte balance. An apparent decrease in cardiac silhouette postflight has been consistently observed in U.S. flights.

The factors accounting for deconditioning of the cardiovascular system are not yet clear. Soviet investigations (Volynkin & Vasil'yev, 1969) suggest that relative hypodynamia and, possibly, physical fatigue observed inflight are related and that these together might be responsible for decrease in myocardial contractility, a breakdown of the mechanisms regulating coordinated activity of

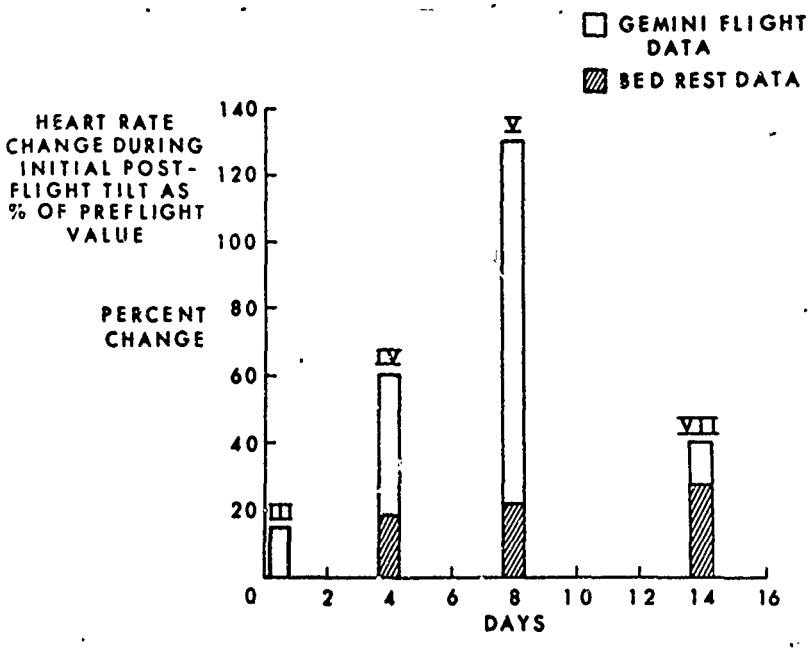


Figure 8–3. Gemini missions and bed rest; resting pulse rate change vs. time.

the heart and vessels, and a decrease in venous tone. Fatigue has not been a feature of any significance during United States missions except when inadequate rest had been obtained or when heavy workloads were imposed on the lunar surface. Weightlessness per se appeared to reduce rather than increase fatigue, since movement seems to require much less work in weightlessness than in the unit gravity environment (Berry, 1970).

Examination of endocrine and electrolyte data offers clues to the nature of the changes that present as orthostatic intolerance postflight. An hypothesis as to the mechanisms involved is presented later in this chapter in conjunction with the discussion of endocrine and electrolyte responses to space flight.

Red blood cell mass decreases which have been noted may be explained by one important difference among missions: the amount of residual nitrogen in the space cabin atmosphere. Hyperbaric oxygen (at 2 atmospheres or greater) is known to have a hemolytic effect. Conclusive data are not available for atmospheres of 100 percent oxygen delivered at 5 psi. A normal ^{51}Cr red blood cell half time indicates that hemolysis did not occur in the Apollo program. The decrease in red blood cell mass noted in the absence of external bleeding suggests that the probable cause for the decrease is inhibited erythropoiesis (Johnson & Driscoll, 1972, cited in Berry, 1972).

The only persistent hematological change, transient increases in the white blood cell count, is probably a consequence of increased blood epinephrine and steroid levels associated with mission stress and is reversible by two days postflight.

Work Capacity (Exercise Tolerance)

In assessing the physiological cost of manned space flight, it is essential to determine to what extent the many factors inherent in the weightless environment affect the capability to do physical work. This capacity can be an index of cardiopulmonary function. Significant deterioration in physical work capacity is a phenomenon noted in individuals subjected to bed rest. For this reason, exercise capacity tests are routinely performed before and after space flights. For the most part, work capacity tests have employed an electronic bicycle ergometer capable of producing a fixed workload. The load is increased in regular increments until elevated heart rates, usually 160 or 180 beats per minute, are reached. Oxygen uptake per kilogram of body weight and systolic blood pressure serve as the indices, with oxygen consumption the more reliable of the two. Cardiac output has also been estimated indirectly by the single breath method requiring instantaneous gas composition and oxygen consumption data.

Space Flight Results. A reduction in work capacity has been noted in both Gemini and Apollo crews. In Gemini 7 work capacity was reduced 19 percent in the Command Pilot and 26 percent in the Pilot. Twenty-five of 30 Apollo astronauts tested have shown a significant decrease in exercise tolerance postflight. Table 8-6 shows typical results, in this case for the Apollo 14 crew. In general, preflight levels have been reattained within 24 to 48 hours postflight. The single exception to this rule was the Apollo 15 crew. In this crew, preflight exercise capacity was not reached in the Command Module Pilot until 3 to 5 days postflight; in the Lunar Module Pilot, until 9 days postflight; and in the Commander, until 13 days postflight. Exercise tolerance was reduced in the Apollo 15 crew by about 44 percent compared with a deficit of 20 percent in the Apollo 16 crew.

Table 8–6

Work Capacity Indicators for Apollo 14 Crew

		O_2 Consumption/ 160 H. R.	Systolic Blood Pressure/160 H. R.
CDR			
	Preflight	2.40 l/min.	233 mm Hg
	R + 0	2.48	238
LMP			
	Preflight	3.05	225
	R + 0	2.86	207
CMP			
	Preflight	2.40	216
	R + 0	1.81 ↓	156 ↓

↓ = statistically significant decrease.

(Berry, 1971)

In conducting a functional test consisting of 30 knee bends during the day after the Voskhod 1 mission (Volynkin & Vasil'yev, 1969), all Soviet cosmonauts showed a greater increase in pulse rate than they did during the preflight period. Soyuz cosmonauts in all flights beyond 5 days' duration exhibited decreased work capacity. In the Soyuz 9 crew, this was ascertained by examination of postflight gas-energy exchange determined by the method of Douglas and Holden and by minute volume determinations (using the Fick method), as well as by bicycle ergometry (Kakurin, 1971).

Conclusions. Significant decrements have been noted in work capacity after space flight. The physiologic mechanisms responsible for the changes observed remain to be identified through further investigation. Hypokinesia leading to decreased muscle tone appears, from Soviet findings, to play a part. Supplementary U.S. data indicate that work performance decrements are not due to altered pulmonary function or to diminished ability to extract oxygen from the atmosphere (Berry, 1970). It is more likely that these changes are in some way associated with cardiovascular deconditioning. To elucidate further the physiological mechanisms underlying the reduction in work capacity, cardiac output assessments are being made to determine whether a decrease in peripheral resistance plays a part. Increases in cardiac output for given oxygen consumption levels were noted in crewmen of Apollos 14 and 15 but not in Apollo 16. No change in peripheral resistance was indicated in Apollo 16 results, and thus the mechanisms still await further study.

Respiratory Responses

The aspects of respiratory function which have been of concern with relation to prolonged weightless space flight include changes in lung volume and airway conductance, and the possibility and consequences of atelectasis. Hypothetically, pulmonary circulation and pulmonary gas diffusion might also be affected. In an extensive review of respiratory physiology in the space environment published in advance of the Apollo missions, the National Academy of Sciences (1967) expressed the opinion that none of these would pose problems of any real consequence.

Space Flight Results. Pulmonary function in weightlessness appears completely unimpaired. Pre- and postflight X-rays during the Gemini mission series have failed to reveal any evidence of atelectasis. Peak respiratory rates were noted during heavy workloads, but even when these rates have exceeded 40 breaths per minute, they have not been accompanied by symptomatology (Berry, 1967a). No respiratory problems were noted during lunar surface activity and Apollo pre- and postflight X-rays have shown no atelectasis.

During the Soviet Voskhod 1 and 2 missions, somewhat higher respiratory rates were noted, as was also the case during preparation for and conduct of the Soyuz spacewalk (Kakurin, 1971).

Conclusions. The weightless environment appears to have no significant impact upon either respiratory mechanics or lung structure. Inflight pulmonary function evaluation in Skylab should further clarify pulmonary status in weightlessness.

Skeletal Responses

Gravity and countergravitational muscular effort are important for the maintenance of skeletal strength. In zero or reduced gravity conditions, elimination or reduction of mechanical forces such as those produced by weight bearing and muscle tension can result in the loss of calcium, and other related elements, from the bones. If such losses were to continue unabated over a long period of time, it is conceivable that demineralization, leading to loss of skeletal strength, could ultimately occur. A 1 to 2 percent per month figure has been predicted as reasonable for the rate of bone loss for persons in the weightless state (Hattner & McMillan, 1968). It is possible, on the other hand, that stabilization may occur at some point in time. Calcium balance does, for example, appear to normalize after some years in paralyzed patient-subjects (Heaney, 1962).

Space Flight Results. To minimize both muscle and skeletal deterioration during weightlessness, rigorous exercise routines have been adhered to by United States astronauts and Soviet cosmonauts. During the 18-day Soyuz 9 flight, cosmonauts exercised twice daily, for 120 minutes a day. Rubber bungee cords attached to the cosmonauts' suits at one end and to the floor at the other provided for increased load during simulated walking and running exercises. The cosmonauts reported a feeling of "muscular exhilaration" after exercise which lasted for the entire work day (Vorob'yev et al., 1970). Similar, but less extensive, exercise routines were followed by United States astronauts. Despite this regimen, both groups experienced loss of bone mass.

Losses in bone mass were observed in the Gemini and Apollo missions. These were directly demonstrable using a bone densitometric X-ray technique. Tables 8-7 and 8-8 indicate bone density changes for the Gemini 7 crew and the Apollo 7 and 8 crews, respectively. When compared with changes observed during bed rest studies, calcium losses for Gemini 7 crewmen were far lower than for Gemini 4 and 5 crewmen. This is illustrated graphically in the case of heel bone density in figure 8-4. The figure also indicates the realtive calcium intake in each mission. In addition to receiving supplementary calcium (approaching 1000 milligrams per day), the Gemini 7 crew routinely exercised.

Although loss of bone density varies considerably from site to site and in individuals, none of the losses noted in either the Gemini 7 or the Apollo 7 and 8 missions approached the maximum 20 percent loss noted in the calcanei and metacarpals of the Command Pilot and Pilot of the Gemini 5 voyage (Mack & LaChance, 1966).

In contrast to earlier findings, Apollo 14 bone mineral content determinations did not reveal bone demineralization. Pre- and postflight examinations of the left central os calcis and the right distal radius and ulna by means of a monoenergetic photon absorption technique revealed no significant mineral losses during the 10-day mission.

Optical density studies of bone tissue of Soyuz 9 cosmonauts after their 18-day flight revealed effects similar to those seen for Gemini and Apollo crews

Table 8–7

Bone Density Changes in Gemini 7
(Percentage Decrease)

	Command Pilot	Pilot
Conventional os calcis scanning section	– 2.91	– 2.84
Overall os calcis involving multiple traces over 60% of bone	– 2.46	– 2.54
Section through distal end of talus	– 7.06	– 4.00
Multiple traces covering hand phalanx 4-2	– 6.55	– 3.82
Multiple traces covering hand phalanx 5-2	– 3.78	– 7.83
Greatest change in any section of os calcis	– 5.17	– 7.66
Greatest change in hand phalanx 4-2	– 9.11	– 8.00
Greatest change in hand phalanx 5-2	–12.07	–14.86

(Mack, Vogt, & LaChance, 1966)

Table 8–8

Bone Density Changes in Apollo 7 and 8

Skeletal Sites	Individual Crewman Percentage Change During Flight					
	Apollo 7			Apollo 8		
Os calcis	–5.35	+0.74	+2.27	–2.13	– 6.95	– 2.93
Hand phalanx 4–2	–9.30	+2.04	–6.50	–2.19	– 2.41	+4.81
Hand phalanx 5–2	–	–	–	–2.07	–3.09	– 1.00
Capitate	–4.07	+3.31	–3.44	–9.60	–12.11	– 6.65
Distal radius	–3.25	+3.34	–3.64	–8.76	–11.06	–11.39
Distal ulna	–3.02	+2.12	–3.41	–6.42	–12.41	–16.17

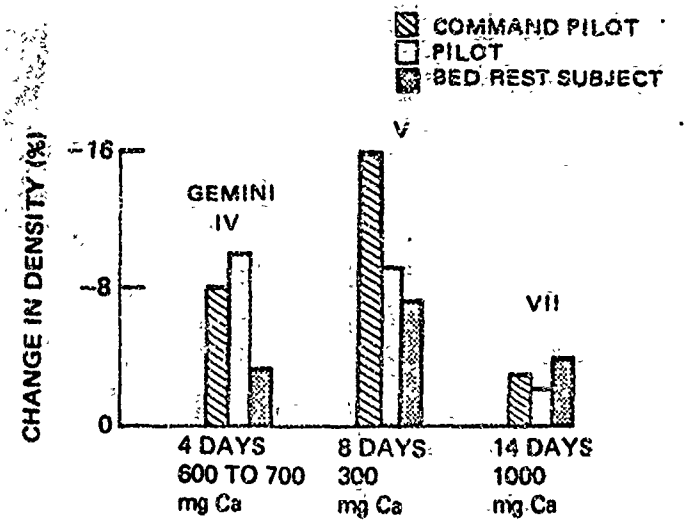


Figure 8–4. Loss of os calcis density on Gemini 4, 5, and 7 missions.

examined by application of the same technique. Table 8-9 summarizes these findings. During the postflight period, optical density levels increased, but by 50-days postflight the initial status of the bone tissue had not yet been restored. The decreases in optical density noted compared to levels characteristic of 62 to 72 days of bedrest confinement. Biryukov and Krasnykh (1970) note that since these decreases in optical density were less than those found in the same bones for the Gemini crewmembers and almost equalled the decreases observed during the 4-day Soyuz 3 flight, some positive effect may have been associated with the use of the inflight exercise routine. The differences between the findings for each of the cosmonauts are thought to be attributable to age and the differences in the nature of the exercise loads performed by each.

Mineral balance studies conducted during the Gemini 7 mission (Berry, 1967a) indicate a slightly negative calcium balance. Soviet investigators report similar findings (Fedorova et al., 1964). Although no overall changes in calcium or magnesium levels have been found, there have been individual instances of elevated urinary calcium and magnesium.

A less equivocal picture of demineralization has been provided by an examination of plasma and urinary hydroxyproline levels. Large amounts of hydroxyproline are present in collagen, which is found in connective tissue and bone. An increased excretion of this substance, it was reasoned, might accompany demineralization and dissolution of bone matrix (Berry, 1967a). Bioassay revealed that bound plasma hydroxyproline levels immediately following the 14-day Gemini mission were elevated, while larger quantities of calcium were excreted later in the flight than during the early phases. Similar changes were noted after the Apollo 8 mission.

Table 8–9

Change in Optical Density of X-Ray Image of Bone Tissue (In Percent of Initial Level) Postflight (Soyuz 9)

Investigated Parts	A. G. Nikolayev		V. I. Sevast'yanov	
	Period of Investigation			
	Day 2	Day 22	Day 2	Day 22
Bone				
2 phalanx (finger)	–	–	–4.1	±0
3 "	–5.0	–2.5	–6.0	–5.0
4 "	–3.1	±0	–4.3	–1.4
5 "	–4.7	–1.6	–8.9	–4.4
Heel bone	–8.5	–4.5	–9.6	–3.4

(Biryukov & Krasnykh, 1970)

Biochemical confirmation for bone demineralization, and partial restoration, was also found for Soyuz 9 cosmonauts. Figure 8-5 indicates urinary calcium excretion on the last day of flight exceeded the first day's level by 29 to 60 percent. During the postflight period, however, calcium excretion in the urine decreased until preflight levels were reached.

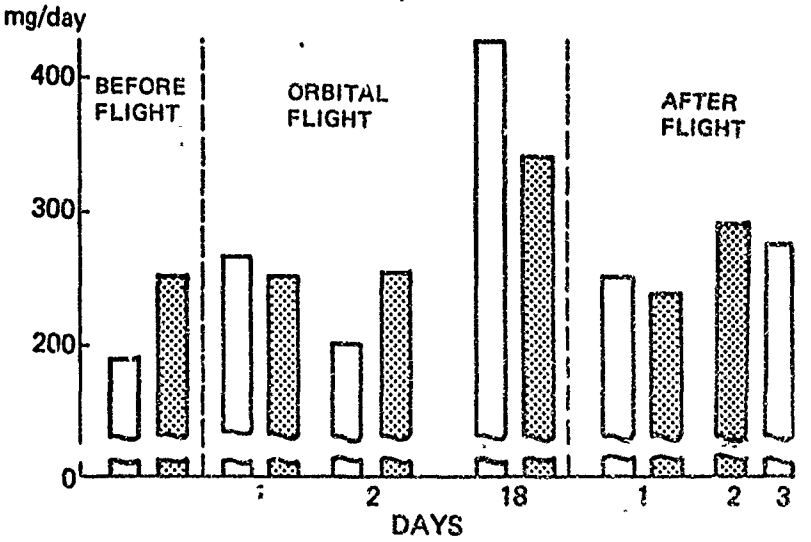


Figure 8–5. Renal excretion of calcium for Soyuz 9 cosmonauts. White bars — calcium excretion for A. G. Nikolayev; shaded bars — for V. I. Sevast'yanov. (Biryukov & Krasnykh, 1970)

Simulation Results. A number of studies (cited in Hattner & McMillan, 1968) indicate that normal, immobilized humans have shown unabated negative calcium balance. Deitrick, Whedon, and Shorr (1948) have demonstrated a net calcium loss of up to 2 percent in healthy subjects immobilized in plaster casts for up to 6 weeks. Their subjects also showed increased excretions of phosphorus, sodium, and nitrogen. All of the changes noted were reversible within about 6 weeks postexposure.

In a more recent study (Donaldson et al., 1969) of longer duration than most previously reported, subjects were confined to bed for periods of 30 to 36 weeks. A regime of supine exercise failed to prevent negative mineral balance. Space flight effects on bone tissue have been more severe than those changes produced by equal periods of bedrest.

Conclusions. Overall, bone density has been minimally reduced after space flight. The reason for the divergence of results is unclear. Mineral balance data have shown a negative balance trend indicative of calcium loss from the bones. Further, although no overall changes in calcium or magnesium levels have been noted, there have been instances of elevated urinary calcium and magnesium. In addition, elevated bound plasma hydroxyproline levels immediately following the 14-day Gemini mission are consistent with resorptive changes in bone matrix. Subsequent mission data will be needed to clarify the reason for the disparity in bone mineral data; it may be simply a matter of altered technique (Berry, 1971a).

One final point regarding reduced bone mineral content should be made. Although functional underloading of skeletal muscle and the decrease in energy expended during muscular work in the weightless state are undoubtedly closely linked to skeletal muscle changes, other possibilities must be taken into account. Biryukov and Krasnykh (1970) suggest that "calcium metabolic mechanisms associated with general impairment in regulatory processes under the influence of space flight stress may be involved." These might include the endocrine mechanisms responsible for regulating the general metabolism of the body. It is possible, for example, that calcium ions are mobilized from the bone cation pool in order to correct the electrolyte balance changes occurring in weightlessness. Changes in parathormone and calcitonin levels will be investigated in subsequent missions to further clarify the mechanisms of mineral loss from the bones (Berry, 1971a).

Neuromuscular Changes

Muscle structure, like bone structure, can reasonably be expected to deteriorate in the absence of gravity and counter-gravitational effort. Deitrick, Whedon and Shorr (1948) noted increased urinary nitrogen excretion and muscle atrophy from 2 to 12.5 percent in the arms and thighs of their bed rested subjects. Because it was an area likely to manifest effects, the neuromuscular system has been examined closely after all manned space flights.

Space Flight Results. Fourteen days of exposure to weightlessness did not cause muscle atrophy or any impairment in coordination (Berry, 1967b).

Mineral balance studies for astronauts exposed to two weeks of space flight, however, indicated slightly negative nitrogen balances which persisted postflight despite increased dietary nitrogen intake (Berry, 1967a). After 18 days of space flight, however, the picture changed radically. Upon return to Earth, the Soyuz 9 cosmonauts exhibited extreme changes in the motor sphere. They reported that their limbs felt unusually heavy and they had difficulty walking and lifting objects. When in the prone position, they sensed "being pressed" into their beds. On the second to the fifth day postflight, muscle pain was reported. Muscle tone and strength, as well as the circumference of the lower extremities were diminished. Reflex excitability of the neuromuscular system, determined by recording the bioelectric activity of muscles during knee tendon reflexes, was increased.

Conclusions. Cherepakhin and Pervushin (1970) surmised that the principal cause of decrease in muscle tone during 18 days of space flight is weightlessness *per se*, since this condition makes it unnecessary to maintain posture, and, as a result, the tonic stress of the muscle tissue through application of effort. This, they feel, is confirmed by the fact that muscle groups subjected to a lesser load showed the highest degree of change. Since neuromuscular tone plays an important part in regulating many body functions, these authors conclude, deterioration of tone following exposure to weightlessness plays an important part in determining the characteristics of the readaptation period. Apparently, too, the longer the space flight the more stressful will be the adaptation to Earth's gravity. Exercise is undoubtedly helpful, but other techniques, for example preventive medications may, these authors suggest, have to be explored.

Vestibular Responses

Information related to body orientation is relayed to the brain via innervation from two structures in the inner ear: the semicircular canals and the otolith apparatus. The semicircular canals respond to angular accelerations, and the otoliths to linear acceleration. In the absence of gravitational force, there is "physiological deafferentation" of the otolith apparatus, but no corresponding dramatic effect on the semicircular canals. Movements of the head will, in weightlessness as in unit gravity, generate angular accelerations sufficient to stimulate the canals. However, the linear accelerations caused by head movement and occasional changes in spacecraft velocity and attitude might not, it was feared, provide sufficient stimulation for the otoliths under extended 0 g (Graybiel et al., 1967). In fact, there was some question as to whether otolithic stimulation would be adequate to provide an appropriate cue concerning the upright of the spacecraft. There is much evidence to indicate that visual cues compensate for vestibular and kinesthetic cues that normally contribute to orientation. Moreover, disorientation rarely occurs without reduction in vision (Clark & Graybiel, 1955), and this does not occur in space. On the other hand, the relationship between the gravity dependent vestibular apparatus and motion sickness is well established. In view of these considerations, close attention has been paid to the function of the vestibular apparatus in weightless space flight.

Space Flight Results. In the Gemini mission series, no disorientation was noted. Crews adjusted easily to the weightless environment and did not observe aberrant sensations during head movements. Visual orientation was achieved with reference to the spacecraft interior and to the Earth. During extravehicular activity, the sky and Earth provided reference points. There were no instances of motion sickness. Apollo crewmen, however, experienced motion sickness symptoms which ranged from mild stomach awareness to nausea and vomiting. Symptoms lasted from 2 hours to 5 days, after which time adaptation occurred (Berry, 1970). Orientation illusions have also been reported. These symptoms, along with the history of motion sickness for Apollo crewmembers, are listed in table 8–10. It should be noted, however, that despite the reported symptoms, specific tests for alteration of vestibular function have been negative (Berry, in press; Graybiel et al., 1967).

Vestibular and vestibular-related aberrations in Soviet cosmonauts have been reported to occur with greater frequency than for United States astronauts. "Space sickness," characterized by a decrease of appetite followed by nausea, has been reported for nearly every Vostok and Voskhod mission (Volynkin & Vasil'yev, 1969; Yuganov, 1964). Illusions of inverted position have also been noted (Volynkin & Vasil'yev, 1969). These were said to affect cosmonauts when

Table 8–10

Illusions and Motion Sickness Symptoms Experienced by Apollo Astronauts

Mission	Astronaut	Motion Sickness History			Illusions/Motion Sickness Symptoms in Space Flight			
		In Land, Air and Sea Vehicles	In Zero G Parabola	In S/C Egress or Egress Training	Tumbling Illusions	Stomach Awareness	Nausea	Vomiting
7	A	X						
	B	X	X	X				
	C	X		X	X			
8	D	X				X	X	X*
	E	X	X	X		X	X	
	F	X	X			X		
9	G							
	H			X	X	X		
	I	X	X	X		X	X	X
10	J	X						
	K	X						
	L	X				X		
11	M	X	X	X				
	N	X	X	X				
	O	X	X					
12	P	X						
	Q							
	R			X				
13	S(E)	X	X	X				
	T					X	X	X
	U					X		
14	V	X						
	W	X						
	X							
15	Y(H)			X				
	Z		X		X	X		
	AA							

*Concomitant illness.
(Adapted from Berry, in press)

their eyes were both open and closed and reportedly lasted for the duration of the effect of weightlessness, disappearing completely only with the onset of reentry accelerations. Changes in the function of the vestibular apparatus are thought to be implicated.

Electrooculograms recorded during the flights of Vostok 3 and 4, sometimes simultaneously with the administration of special tests, revealed no asymmetry of oculomotor reactions or nystagmus (Akulinichev et al., 1964). The otolith apparatus' threshold of sensitivity to galvanic current, examined after the flight of Voskhod 1 (Volynkin & Vasil'yev, 1969) was unchanged.

Soyuz 9 crewmembers reported some Coriolis-like sensations in the earlier portion of their flight which disappeared after the normal adaptation period (third to fifth day). They found, as did Apollo astronauts, that taking care to make no abrupt head movements during this period lessened symptoms. Analysis of the writing of vertical letters inflight, a test of vestibular function, revealed the magnitude of slope angles to be increased threefold over groundbased baselines, indicating an increase in reactivity of the cupuloendolymphatic system of the vestibular analyzer to Coriolis acceleration under weightless conditions (Kakurin, 1971). Postflight, increases were noted in the indices of general center of gravity (GCG) oscillations and the frequency of cardiac contractions when the eyes were closed (Petukhov et al.,1970; Kakurin, 1971).

No perceptual-motor impairment has been observed in conjunction with U.S. space flight. Soviet investigators have noted some changes. During the Voskhod 1 mission, the accuracy of carrying out slight coordinated movements was found to decrease (Volynkin & Vasil'yev, 1969), and in the Soyuz 3 flight, a subjective increase was reported in the pause between the decision to perform a motor activity and the act itself (Kakurin, 1971).

Conclusion. Both Apollo astronauts and Soyuz cosmonauts have reported sensations resembling sea sickness during spaceflight. On the whole, however, U.S. astronauts do not appear to be excessively plagued by motion sickness symptoms. A clue to the ease with which the vestibular system of these individuals appears to adapt to the zero-g environment may be provided in the results of a study conducted by Clark and Stewart (1972). These investigators, in attempting to establish the relationship between reports of motion sickness and selected vestibular tests, found that pilots as a group clearly report less experience with motion sickness than do nonpilots. The pilot's less frequent experience with motion sickness may well be an important contributing factor in his selection of flying as a profession. The U.S. astronaut population to date is comprised entirely of pilots, most of whom have extensive experience as test pilots (Berry, 1972).

Metabolism

Metabolism in the broad sense may be defined as tissue change. This tissue change is the end product of the conversion of small molecules into larger ones, for example, amino acids to proteins, and the breaking down of larger molecules

into smaller ones. In the former process, anabolism, energy is consumed; in the latter, catabolism, energy is given off. All energy used by the body (except that for outside work) finally appears as heat. Since oxygen is used in the process of breaking down nutrients to yield carbon dioxide and water, oxygen consumption and carbon dioxide production are useful indices of metabolic rate.

Direct metabolic measurements have not been made during actual space flight. Metabolic costs have been inferred from examination of total carbon dioxide production by chemical analysis of spent lithium hydroxide canisters. This technique established an average heat production rate during multiman missions. Other, more direct techniques have been used to assess metabolic costs during lunar surface activities. Metabolic rate has been determined from telemetry data by use of three methods: thermal balance, oxygen consumption, and heart rate. Thermal balance was determined by comparing the inlet and outlet temperatures in the water cooled undergarment during lunar surface activity; oxygen usage from the portable life support system was measured; and heart rate during lunar activity was compared to that on an energy cost calibration curve obtained preflight by bicycle ergometry. (For detailed treatment of these methods, the reader is referred to Carson, 1972).

Space Flight Results. Inflight metabolic data from both Soviet and U.S. space flights show close agreement. Figure 8-6 compares the average metabolic rates for the Vostok, Mercury, and Gemini missions. The higher rate observed during the Gemini mission, graphed at the far left of the figure, undoubtedly is due to the fact that these were short flights during which crewmen did not sleep. Metabolic rate, based on carbon dioxide output, for the longest American mission (Gemini 7) was estimated to be 2219 calories per day (figure 8-7). This expenditure was adequately provided for by the diet (2333 calories per day).

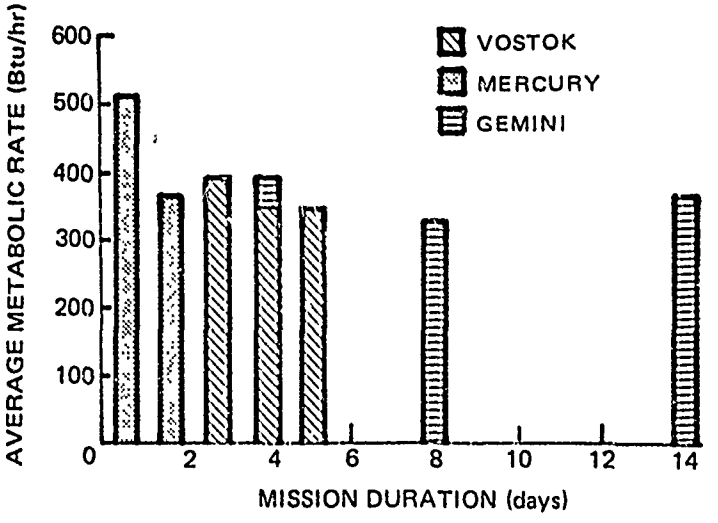


Figure 8–6. Average metabolic rates during actual space flight. (Berry, 1967a)

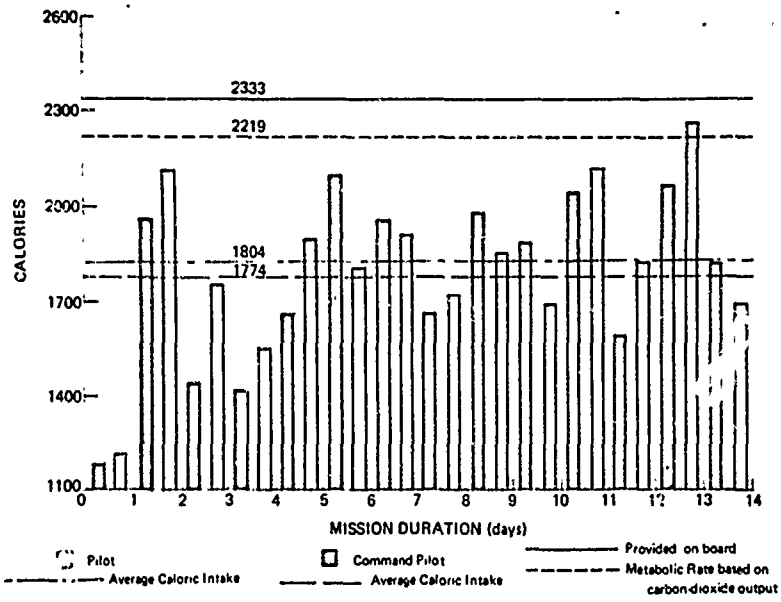


Figure 8–7. Caloric intake on Gemini 7. (Berry, 1967a)

Comparative techniques for metabolic assessment used during Apollo lunar surface activity indicated that monitoring of the temperatures at the inlet and outlet of the liquid cooled undergarment (thermal balance method) was best suited for estimating energy production. For the Apollo 11 mission, the thermal balance and oxygen use methods yielded similar data and accurately reflected the physical activity observed by telemetry. Heart rate data proved the least reliable method for determining metabolic rates (Berry, 1970).

Average expenditure for each task varied for each crewman, with the average hourly energy production between 900 and 1200 BTU's. Table 8-11 compares lunar extravehicular times and metabolic rates for Apollo lunar surface crews.

Conclusions. The techniques used for determining metabolic expenditure inflight admittedly are gross. Nevertheless, the expenditures calculated by this technique indicate that the diet provided for missions is more than adequate for living and working in space for up to 2 weeks. Refined techniques for assessing metabolic costs during lunar surface activity yield accurate data which provide a sound basis for life support system and mission planning.

Endocrine and Electrolyte Responses

Extensive biochemical studies have been a feature of space flight programs. Data gathered through these studies are essential for determining the etiology of clinically demonstrable changes. Attention has been focused in areas where earlier experience has indicated most physiological changes occur, and in areas where it might be reasonably expected that zero gravity exposure could have significant impact. Accordingly, attempts have been made to elaborate the

Table 8–11

Lunar Extravehicular Activity Times and Metabolic Rates

Mission	Crewman	Launch Date	EVA time, min	Average metabolic rate, Btu/hr
Apollo 11	Armstrong	6/69	168	777
Apollo 11	Aldrin		168	1118
Apollo 12	Conrad (EVA-1)	11/69	241	925
Apollo 12	Bean (EVA-1)		241	930
Apollo 12	Conrad (EVA-2)		235	840
Apollo 12	Bean (EVA-2)		235	950
Apollo 14	Shepard (EVA-1)	1/70	288	750
Apollo 14	Mitchell (EVA-1)		288	900
Apollo 14	Shepard (EVA-2)		275	900
Apollo 14	Mitchell (EVA-2)		275	1050
Apollo 15	Scott (EVA-1)	6/71	393	1050
Apollo 15	Irwin (EVA-1)		393	1050
Apollo 15	Scott (EVA-2)		432	950
Apollo 15	Irwin (EVA-2)		432	800
Apollo 15	Scott (EVA-3)		290	1000
Apollo 15	Irwin (EVA-3)		290	850
Apollo 16	Young (EVA-1)	4/72	431	800
Apollo 16	Duke (EVA-1)		431	1050
Apollo 16	Young (EVA-2)		443	750
Apollo 16	Duke (EVA-2)		443	850
Apollo 16	Young (EVA-3)		340	850
Apollo 16	Duke (EVA-3)		340	900

mechanisms involved in weight loss, demineralization, stress, and cardiovascular deconditioning. Insight has been gained into several of these phenomena as a result of analyses of urine and blood samples collected before, during, and after space flight.

Space Flight Results and Conclusions

Electrolytes. Urine and plasma electrolyte studies have revealed postflight retention of electrolytes. Decreases have been noted in potassium levels, indicative of decreases in total body potassium, and in urinary sodium and chloride levels. These changes have paralleled the time course of body weight changes.

Figure 8-8 shows the results of urinary potassium studies for the Gemini 7 pilot. In flight, potassium excretion appeared depressed, and this depression was still apparent by 24 hours postflight. Similar decreases were found in both serum and urinary potassium levels for Apollo crewmen. These changes were, in fact, suggestive of a decrease in total body potassium, an hypothesis that was supported by K^{40} evaluations in the Apollo 13 and 14 crews. Total body gamma spectrometry indicated a significant decrement of total body potassium for Apollo 13 crewmen compared with preflight values. In Apollo 14 crewmen, similar decreases in total body potassium were seen 17 days after recovery versus the astronauts' preflight values. These decreases were noted when control subjects showed increased total body potassium levels. This potassium loss is

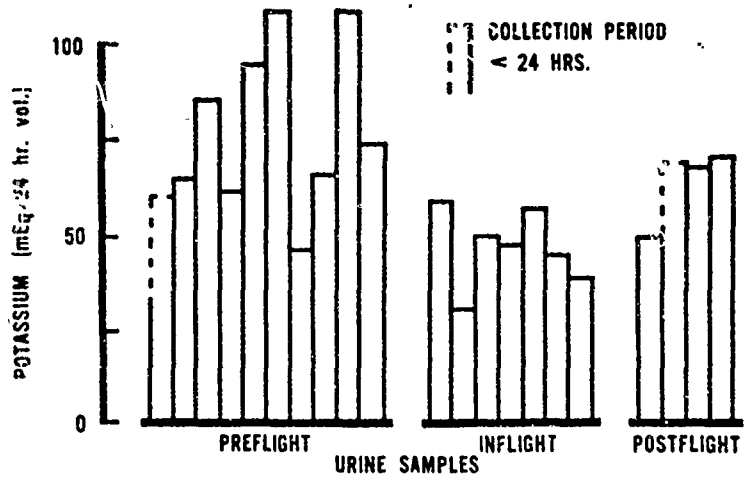


Figure 8–8. Urine potassium, Gemini 7 pilot.

presumptive evidence of intracellular water and cation loss, for which there is other supporting evidence. Decrements in total exchangeable potassium (10 to 15 percent) also were seen in Apollo 15 crewmen when evaluated postflight by K^{42}. No decrements were noted in Apollo 16 crewmen.

Consistently diminished excretions of sodium and chloride have also been observed in the immediate postflight period. Figure 8-9 indicates urinary electrolyte levels for the Command Module Pilot of the Apollo 14 mission. This figure also shows his pre- and postflight potassium levels. Although some individual variation has been observed, these urinary electrolyte measures are typical following space flight exposure and clearly indicate efforts on the part of the body to retain fluid to compensate for inflight fluid volume loss.

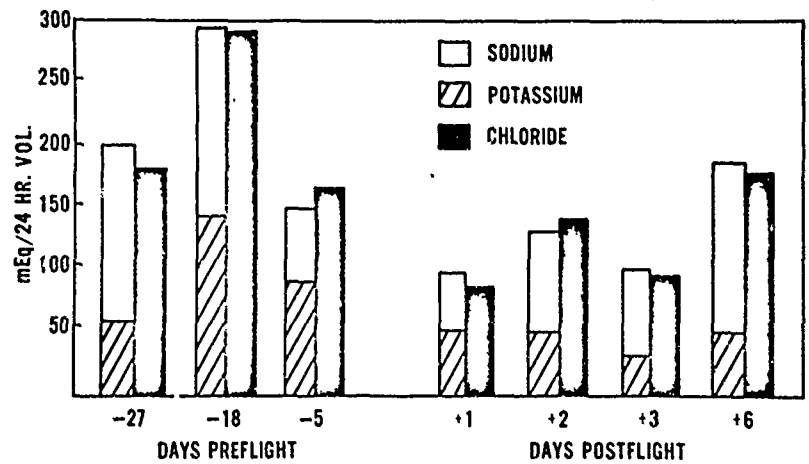


Figure 8–9. Urinary electrolyte levels pre- and postflight for Apollo 14 Command Module Pilot.

Endocrine Responses. Endocrine responses have been evaluated principally to determine whether hormones related to body fluid regulation reflect the observed postflight fluid and electrolyte changes.

Attempts have also been made to evaluate stresses related to space flight by measuring certain postflight steroid levels. These results, based on very limited data, appear to indicate that the reentry and recovery periods may be the most stressful. Inflight steroid levels are, in contrast, low. Figure 8-10 indicates a typical response, noted in the Gemini 7 Command Pilot. Apollo astronauts have exhibited similar responses.

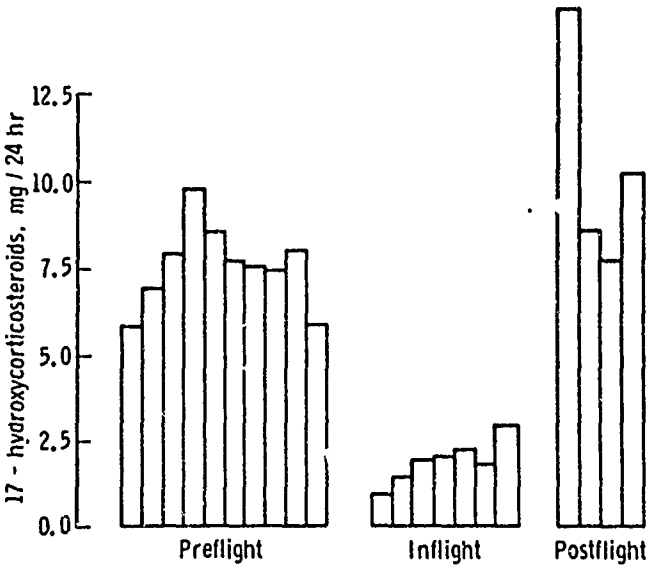


Figure 8–10. Urine 17-hydroxycorticosteroids, Gemini 7 Command Pilot.

It is, however, admittedly difficult to evaluate "stress" on the basis of endocrine assay since many hormones which are believed to be indicative of certain stresses are also related to other physiological functions, for example, vasoconstriction or vasodilation and electrolyte regulation.

Pre- and postflight measures of hormones related to electrolyte and fluid balance support the hypothesis that readily recoverable weight losses immediately postflight are primarily the result of inflight water loss. Postflight elevations have been noted for (1) antidiuretic hormone, (2) aldosterone, (3) plasma angiotensin which indicates renin activity, and (4) catecholamines.

Increased levels of antidiuretic hormone, which regulates water resorption through the distal renal tubule, and increased aldosterone levels resulting in resorption of sodium in the proximal tubule are consistent with the electrolyte retention noted and the rapid weight gain postflight. Plasma angiotensin levels,

an index of renin activity, show significant increases postflight. Since renin stimulates the adrenal gland to secrete aldosterone upon sensing decreased blood volume or salt concentration (which is uncertain) in the kidney, the elevations in aldosterone levels observed postflight are consistent with cardiovascular and fluid/electrolyte findings.

Aldosterone excretion triggered by exposure to zero gravity may explain why elevated plasma volume is not noted in longer duration missions but is in shorter missions. If the high urinary aldosterone excretion is associated with an increased aldosterone secretion rate, one would anticipate elevated plasma volume during longer duration missions since aldosterone expands circulating plasma volume as potassium is diuresed and sodium is retained. If increased aldosterone secretion occurred after plasma volume had been lost in response to an initial redistribution of body fluid volumes upon entering the weightless state, the net result would be a near normal plasma volume (Johnson & Driscoll, 1972, based on data of Lutwak et al., and Leach). Near normal plasma volumes were found postflight in the Apollo 14 and 15 crews (they were not measured for Apollo missions 11, 12, and 13). In fact, these crewmen exhibited plasma volume levels that were slightly elevated above their preflight mean. Apollo 16 crewmembers, however, averaged plasma volume decreases of 9 percent.

Weight Loss

All but one U.S. astronaut has lost weight in space. Weights recorded immediately postflight have ranged from 2 to 14 pounds below preflight levels. The Apollo 14 Commander alone gained 1 pound during his stay in space. Because most astronauts have regained about 60 percent of their weight loss within the first 24 hours after splashdown, it has been presumed that the weight loss is principally a water loss. Soviet cosmonauts exhibited similar weight loss patterns. The Soyuz crews lost 2 to 4 pounds postflight. These body weight losses were rapidly recoverable in all but the Soyuz 9 (18-day) crew. Because postflight urinary nitrogen excretion did not increase, it was presumed that weight loss reflects water loss and not tissue catabolism. After the 18-day flight, some urinary nitrogen excretion was noted although this was within physiological limits. This coupled with the slow reattainment of preflight body weight indicates the possibility of some tissue catabolism (Kakurin, 1971).

Apollo 16 astronauts, like all crews before them, lost weight (the Commander, 7.5 pounds; the Lunar Module Pilot, 5.5 pounds; and the Command Module Pilot, 6.5 pounds). Various indirect measurements made on the Apollo 16 crew, including estimates of the amount of food and drink taken and the amount of excreta produced, coupled with weighings on the recovery ship by scales calibrated with those used before launching, appear to indicate that the astronauts' weight losses did not result from a diuresis alone. Further studies apparently will be needed to clarify all the factors underlying weight loss (Berry, 1972).

Weight losses observed postflight for the Apollo 7 through 16 mission crewmen are shown in table 8-12. The rapidity with which the average weight

Table 8–12
Weight Changes – Apollo 7 thru 16

	Weight Loss	Percent Change	Weight Regained (R + 24 hr)	Percent Change
Apollo 7				
CDR	– 6.3 lbs	–3.2	+2.5 lbs	+1.3
CMP	–10.0 lbs	–6.4	+3.5 lbs	+2.2
LMP	– 8.0 lbs	–5.1	+5.5 lbs	+3.5
Apollo 8				
CDR	– 8.7 lbs	–5.1	+2.7 lbs	+1.6
CMP	– 7.8 lbs	–4.5	+0.7 lbs	+0.4
LMP	– 4.0 lbs	–2.8	+0.5 lbs	+0.3
Apollo 9				
CDR	– 5.2 lbs	–3.3	+2.7 lbs	+1.7
CMP	– 5.7 lbs	–3.2	+8.5 lbs	+4.8
LMP	– 6.1 lbs	–3.8	+4.2 lbs	+2.6
Apollo 10				
CDR	– 2.0 lbs	–1.1	+2.0 lbs	+1.1
CMP	– 5.0 lbs	–3.0	+1.0 lbs	+0.6
LMP	–10.0 lbs	–5.8	+2.0 lbs	+1.2
Apollo 11				
CDR	– 8.0 lbs	–4.7	+6.0 lbs	+3.7
CMP	– 7.0 lbs	–4.2	+0.0 lbs	+0.0
LMP	– 1.0 lbs	–0.6	+4.0 lbs	+2.4

Apollo 12				
CDR	− 4.2 lbs	−2.8	+2.0 lbs	+1.4
CMP	− 7.2 lbs	−4.7	+4.0 lbs	+2.7
LMP	−12.5 lbs	−8.2	+3.0 lbs	+2.1
Apollo 13				
CDR	−14.0 lbs	−8.1	———	———
CMP	−11.0 lbs	−5.6	———	———
LMP	− 6.5 lbs	−4.2	———	———
Apollo 14				
CDR	+ 1.0 lbs	+0.5	+1.0 lbs	+0.6
CMP	−12.0 lbs	−7.2	+7.0 lbs	+4.8
LMP	+ 1.0 lbs	+0.5	+1.0 lbs	+0.6
Apollo 15				
CDR	− 1.2 lbs	−0.7	+1.0 lbs	+0.5
CMP	− 3.0 lbs	−1.9	+2.0 lbs	+1.3
LMP	− 5.5 lbs	−3.4	+5.0 lbs	+3.2
Apollo 16				
CDR	−7.5 lbs	−4.3	+3.5 lbs	+2.0
CMP	−6.5 lbs	−4.0	+3.0 lbs	+1.9
LMP	−5.5 lbs	−4.1	+2.5 lbs	+1.8

loss was regained (and a consistent pattern of retention of electrolytes postflight) indicates that of the average 6.2 lb loss, 3.1 lb may be attributed to water loss. Although slightly negative water balance has been maintained, the situation is within manageable bounds.

The Nature of the Adaptive Response to Space Flight: An Hypothesis

Much information has been gained in American biomedical programs concerning the effects of space flight on man. A number of consistent findings have been observed: some imply a possible alteration of the structure of physiological systems while others indicate merely a change in capacity. These changes, while dealt with as discrete events, undoubtedly are individual elements in a basic adaptive response of the human organism to the unique stresses of space. Sufficient information is presently available to begin to piece together at least a tentative hypothesis concerning the nature of the adaptive process and the manner in which the various changes may be interrelated.

Table 8-13 is a greatly simplified illustration of the hypothesis now being developed and shows the major classes of body response during the period of adaptation. Figure 8-11 presents the same hypothesis in diagrammatic form. In each case, the part of the hypothesis presented is that intended to describe factors influencing fluid shifts within the body.

Table 8–13

Overview of Current Hypothesis Concerning Processes Involved in Man's Adaptation to Zero Gravity

Event		Response of Body
Entry into zero gravity. Redistribution of circulating blood volume.	↓	Body attempts to reduce volume. ADH decreases, aldosterone production decreases.
Loss of water, sodium, potassium (loss of body weight).	↓	Decrease in plasma volume. Aldosterone produced.
Increased sodium. Potassium loss continues. Cell: acidotic; extracellular fluid: alkalotic.	↓	Intracellular exchange of potassium and hydrogen ions. Decrease in bone density and muscle mass, possibly including cardiac muscle.
Respiratory and renal compensation. Halt to weight loss trend.	↓	Stabilizes with new cardiovascular load. New body fluid and electrolyte balance.

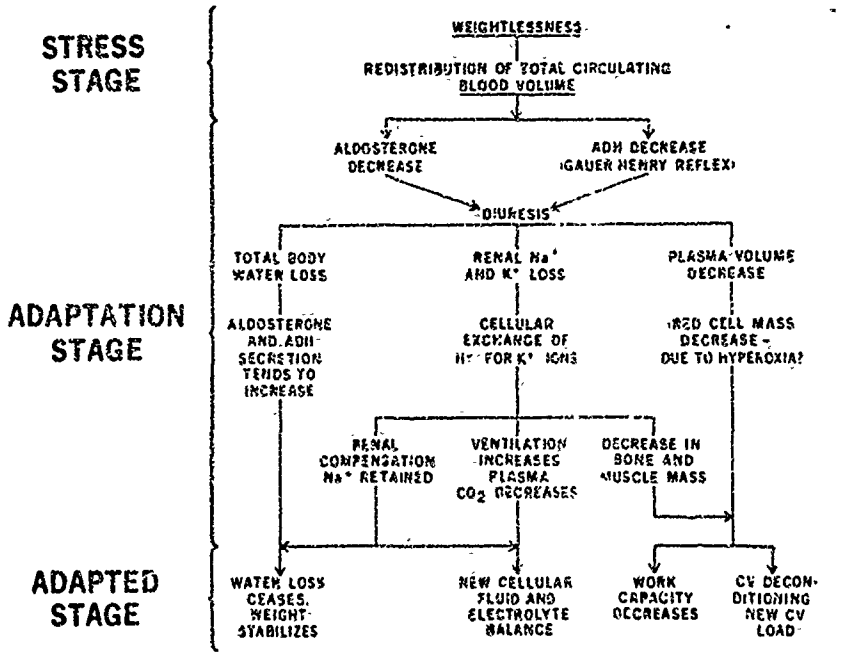


Figure 8–11. Diagram of the hypothesized course of adaptation to weightlessness (Adapted from Leach, Alexander, and Fischer, 1970; used by permission of Academic Press, New York, copyright 1967 by Academic Press, Inc.)

Upon initial entry into weightlessness, an immediate redistribution in the total circulating blood volume occurs. The body interprets the resultant increase in right atrial filling as an indication of a need to reduce total fluid volume by increasing urine output. This event is governed by a decrease in antidiuretic hormone and a decrease in aldosterone production. The result is a loss of water, sodium, and potassium through the kidneys with a resultant loss in total body weight. The concomitant decrease in plasma volume tends to reverse the initial aldosterone decrease. At this point, the body is believed to enter a phase of electrolyte and fluid imbalance in which sodium retention increases while potassium loss continues. Intracellular fluid and potassium loss results in a cellular acidosis with a mild (compensated) hypokalemic alkalosis of extracellular fluids.

In essence, the body's response to lowered total body potassium is an intracellular exchange of potassium for hydrogen ions. Associated with the potassium deficit may be a decrease in bone density and muscle mass. Loss of cellular potassium can include the heart muscle, with resultant increased irritability and tendency toward disorders of cardiac rhythm. This was very likely the series of events which led to the cardiac arrhythmias experienced by the Apollo 15 crew. Postflight decreases of total exchangeable potassium in this crew offer support of this supposition.

In the final phase of the adaptation loop postulated, hyperacidity of the cell stimulates the respiratory system to decrease plasma carbon dioxide by

increasing ventilatory rate. Renal compensation commences as the renal tubules begin to reabsorb potassium. The body weight now stabilizes at a new equilibrium point. This part of the body's overall adaptation process now becomes complete. The new equilibrium establishes an optimal total circulating blood volume or "new load" on the cardiovascular system and a new fluid and electrolyte balance state. It is reasonable to presume that the new stabilized condition is appropriate for long-term performance under space flight conditions, provided it is unperturbed. If factors such as workload, thermal stress, or emotional stress are introduced, the system may be driven beyond the point of equilibrium.* The conceptual model postulated here will be further tested and amplified as new flight data warrant. Information collected in conjunction with the Skylab experiments should be valuable in elucidating the mechanisms of man's response to space flight.

Microbiological Changes

Under Earth's gravitational conditions, airborne particulate matter remains suspended in inverse proportion to its settling velocity: larger particles (a few to several hundred micrometers in diameter) settle out rapidly. In the gravity free environment of the spacecraft, on the other hand, it is presumed that no sedimentation will occur. As a consequence, a considerable range of particles of biological interest on earth, that is $>0.5\mu$ and $<10\mu$ will be stabilized (National Academy of Sciences, 1967). The tremendous number of particles shed by man into the spacecraft atmosphere (talking alone expels 1000 infectious nuclei into the air per minute) will remain suspended. This is of particular significance in future spacecraft where leakage rates will be low. Because this set of circumstances can produce untoward effects, microbiological studies have been conducted before and after space flight missions. In addition to weightlessness, other aspects of the space environment, radiation, for example, have the potential to produce microfloral alterations.

Space Flight Results. Microbiological studies during the Apollo mission series have shown that growth of opportunistic organisms appears to be favored in the space environment (Berry, 1970). In one case, staphylococcus aureus obtained at one preflight sampling site on one crewman, spread to most sites on all three crewmen and produced some clinical infection. Soyuz 9 cosmonauts also exhibited microflora shifts with a number of organisms less resistant to antibiotics postflight (Kakurin, 1971). The etiology of these changes is unclear and factors other than weightlessness, confinement, for example, may be involved.

The Effects of Zero Gravity Upon Performance

The nature of the null gravity environment produces two kinds of change in the human space traveler. Adaptive changes, or those changes which take place in the physiological systems, have been discussed. The second type of change may be referred to as operative or habitational change. Stated simply, when the

*In the Apollo 15 crew, this was evidenced by an absolute rather than relative loss of potassium as well as the loss of sodium measurable postflight.

unit gravity force is removed, the things that man is accustomed to doing one way on Earth must be done quite differently in space. Sleeping, eating, and moving about in zero gravity both inside and outside the spacecraft are all affected in some measure.

Sleep

It is difficult to isolate weightlessness *per se* as a factor influencing the quality of sleep. Sleep disturbances have been common during space flight missions but these appear to be much more profoundly affected by operational factors than by the weightless element of the environment. Cyclic noise disturbances from events such as thruster firings, communications, movement in the spacecraft, staggered sleep periods, alterations from preflight diurnal cycles, and the so-called "command pilot syndrome" all contributed to sleep disturbances during the Gemini missions. Similar problems were experienced by Apollo mission crew members until the time of the Apollo 11 lunar landing flight, when increased confidence in spacecraft systems permitted scheduling of simultaneous sleep periods for crew members. This resulted in rest periods which were close to ideal prior to lunar orbit insertion (figure 8-12). These sleep periods, described only from the study of telemetered heart and respiration rates and crew reports, were deemed adequate for medical approval of earlier extravehicular activity on the lunar surface than was originally planned. Environmental aspects of the lunar module, however, once again disrupted sleep. This has been the case for astronauts on missions subsequent to Apollo 11 and has in some cases necessitated the prescription of sleeping medication.

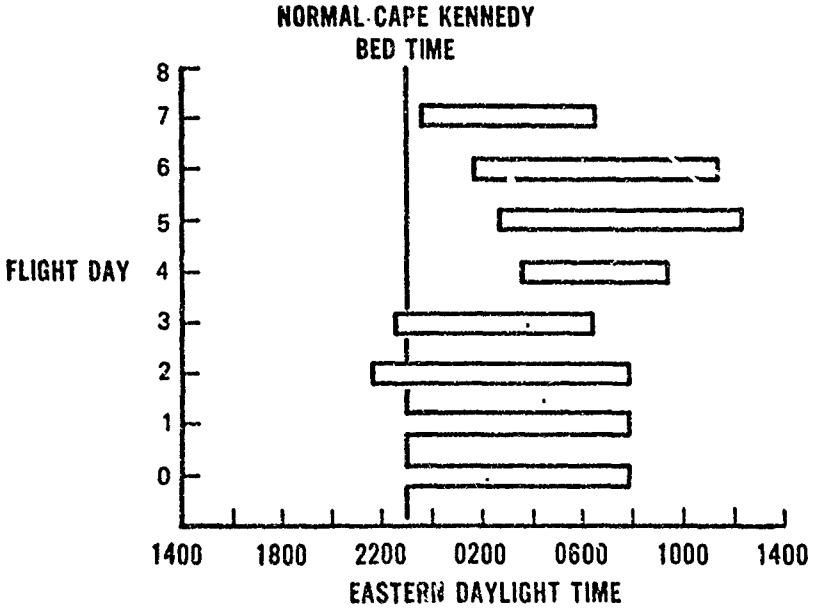


Figure 8–12. Crew sleep periods during Apollo 11 mission.

Sleeping in the weightless environment is accomplished by many astronauts most comfortably if a fetal position is assumed. Consistent reports of backache among astronauts may well be linked to the tendency to assume the fetal position. The use of improved sleep restraint systems on future missions may alleviate this problem.

Mission constraints have thus far precluded the collection of inflight EEG sleep data, although pre- and postflight baseline data were obtained for the Apollo 16 crew (Berry, 1972). Sleep experiments scheduled for the Skylab program will permit the first inflight monitoring of sleep patterns by EEG and EOG and undoubtedly help to clarify the effects of weightlessness on sleep (Berry, 1971a; 1972).

Kakurin (1971) reports that after several days of adaptation during the 18-day Soyuz 9 flight, sleep lasted 7 to 9 hours and "always brought freshness and good humor." Crewmembers fell asleep rapidly in about the same manner as on Earth. One crewmember appeared to adapt so well to sleeping in the weightless condition that he preferred to sleep without being tied into his cot.

Eating in Weightlessness

Space diets have consisted principally of freeze dehydrated food that is easily reconstituted inflight with both cold and hot water. This diet has been augmented by the inclusion of thermostabilized meat dishes of high moisture content as well as drinks and snacks containing dietary potassium supplements. Initially, these foods were eaten through tubes incorporated into the food container, but it was later found that eating foods with sufficient moisture could be easily accomplished in zero gravity with a conventional spoon utensil.

Regardless of the diet provided for any given mission, space crews have indicated in postflight debriefings that hunger occurred less frequently in space and that food requirements are only about two-thirds of "normal." Based on these observations, menus have been designed to provide approximately 2300 to 2500 kilocalories per man per day in U.S. missions. Soviet space dietary allowances are considerably higher; 2800 kcal were provided in the daily diet for the Soyuz 9 crew members (Kakurin, 1971). These latter diets which initially comprised principally freeze dehydrated foods have, like American diets, been supplemented by other types of foods because of the "low rating" given by cosmonauts to dehydrated food products. With consideration given to individual tastes, these diets have been reported to satisfy cosmonauts' requirements "completely" (Kakurin, 1971). Sensations of thirst have been reported to be slightly reduced in Soviet cosmonauts during flight and increased considerably postflight.

Intracabin Movement

The absence of gravity has been found to represent a bonus for locomotion within the spacecraft cabin. Locomotion in zero g appears to require much less work than in the unit gravity environment. Movement is accomplished with

minimal effort, frequently in a swimming manner. Acrobatic maneuvers, such as rolling, tumbling, and spinning, are done without difficulty. An additional feature of the zero gravity environment, the capability to impart minimal velocities to objects, also has been used repeatedly by crewmen as an aid in performing inflight activities.

The ability to move freely through all parts of a space cabin during weightlessness has implications for general vehicle habitability. Apollo astronauts have commented that the Command Module, which seemed rather cramped during ground tests, was more comfortable in flight due to the increase in usable living and working space. This observation has raised the question of the validity of volumetric studies which attempt to extrapolate from habitation in other confined areas such as submarines or low pressure chambers the volume of living space required for astronauts in long duration missions. Locomotion in three dimensional space, as opposed to two, appears to be a positive factor in determining vehicle habitability.

Extravehicular Activities

The first extravehicular activities, performed by cosmonaut Aleksei Leonov in March 1965, and by astronaut Edward White in June 1965, demonstrated that man is capable of reasonable activity in space while operating without the protection of a space capsule. These first ventures, while quite short, clearly were the forerunners of later periods of lunar exploration and of useful maintenance and equipment assembly operations during longer space missions. In subsequent EVA attempts during Gemini flights, however, astronauts experienced considerable difficulty in actually accomplishing what had been considered to be a normal EVA work assignment prior to launch. As matters stood at that time, the demands of EVA exceeded the capabilities of an astronaut. It was not until the final flight of the Gemini series that these difficulties were resolved through intensive study that resulted in partial redesign of EVA work stations and support equipment. This series of events provided very dramatic demonstration of the requirement that information concerning human capabilities be reflected in the design of space equipment. At the root of the problem was a paucity of useful data concerning the effects of weightlessness on man's performance capabilities. Subsequent flight experience, however, has done much to provide the information needed by space system designers.

EVA History. Table 8-14 summarizes extravehicular activity in United States space missions. Problems associated with early EVA were eradicated, principally through the development of energy saving techniques and work aids and the opportunity for rehearsal afforded by underwater simulation experience.

Energy Expenditure in Extravehicular Activity. The principal problem with early EVA flights was, as noted earlier, the exhaustion which was suffered by the astronaut, at times even before the completion of the assigned tasks. This exhaustion was due principally to the unique character of working in the weightless environment where difficulties are encountered in producing reactions to actions once momentum had been imparted and maintaining position in the

Table 8–14

U.S. Extravehicular Summary – Free Space and Lunar Surface

Mission	Time of Exposure (hr min)	Principal Tasks Accomplished	Proolems	Comments
		Free Space		
Gemini 4	0:36	Dynamics of 25-ft tether evaluated, hatch ingress and egress assessed	Metabolic heat output exceeded cooling capacity of ventilation, control module	EVA successful although energy required exceeded anticipated levels
Gemini 9-A	2:07	AMU* evaluated, photography	Overheating, exhaustion; attitude maintenance difficult; loss of traction, visor fogging	EVA terminated due to visor fogging and fatigue
Gemini 10	1:29	Experiment package retrieved, photography, CP assisted by EVP in formation flying with Agena vehicle	Grip difficult to maintain, eye irritation; 50-ft umbilical difficult to control	Eye irritation believed due to use of both O_2 compressors
Gemini 11	2:43	100-ft tether attached between spacecraft and Agena vehicle, photography	Overheating, exhaustion	EVA terminated due to fatigue
Gemini 12	4:30	Restraints and workload assoc. with photography and equipment use evaluated, experiment package retrieved	None	EVA completely successful as a result of underwater simulation practice and body restraints
Apollo 9	0:37	System tests	None	EVA successful
Apollo 15	0:35:12	Inflight EVA performed out of Earth orbit	None	EVA successful
Apollo 16	1:24			
		Lunar Surface		
Apollo 11	5:36	First manned lunar landing, photography, survey, sampling of lunar soil	No major problems	Loping g-fit used
Apollo 12	15:52	Demonstrated point landing capability, sampled more area, deployed ALSEP, investigated Surveyor 3 spacecraft, and obtained photographs of candidate explorations sites.	No major problems	Metabolic production values lower than predicted
Apollo 14	18:46	Experiment package deployment. Sample collection	First indication of excessive workload	Overall metabolic production within satisfactory limits
Apollo 15	37:10	First to carry Lunar Roving Vehicle; extended exploration	Lunar surface workload overtaxed crew (arrhythmias)	EVA successful
Apollo 16	40:28	Most comprehensive sampling	None	EVA successful

* AMU = Astronaut Maneuvering Unit

absence of traction. Additional problems were imposed by the increased effort involved in moving in a pressurized space suit (3.5 psi). This created a heat load in the space suit and unacceptably high carbon dioxide levels.

Reduction of effective work load in the Gemini 12 mission EVA was due, at least in part, to realistically simulated weightlessness training and, in part, to improved work aids. Additional energy conservation resulted from the astronaut's ability to condition himself to relax completely on occasion within the neutral position of the space suit (Kelly and Coons, 1967). The Gemini 12 astronaut reported that he systematically monitored each muscle group. When a group of muscles was found to be tense while performing no useful work, he was able to relax these muscles consciously. All of his movements were slow and deliberate. When a task could be performed by small movement of the fingers, he would use only those muscles necessary for this small movement.

Planning for EVA missions in either 0 g or 1/6 g and the development of equipment for use during these missions has and must continue to take into account work load. The Lunar Roving Vehicle is one example of equipment designed for conservation of energy.

Counteracting the Physiological Effects of Weightlessness

Considering the trepidations expressed a decade ago about possible effects of long term exposure to weightlessness, man has weathered his entry into this new domain in surprisingly good shape. Not only have most of the predicted problems been negligible, but certain benefits have been found to be associated with living and working in zero gravity. However, certain changes in major body systems have been observed. Space flight results to date tend to substantiate the belief that these changes are largely adaptational responses to the new environment. However, one can not be absolutely certain that some of these changes do not in fact represent the first stages of a gradual deterioration process. Countermeasures to weightlessness have therefore been and are continuing to be investigated. Table 8-15, from a survey by Vinograd and Manganelli (1972), lists approaches which have been explored with mixed results.*

A limited number of countermeasures to weightlessness effects have been employed in conjunction with past space missions. Inflight exercise regimes have been a feature of both U.S. and Soviet space missions. These regimes and their effects have been discussed in an earlier section of this chapter. Because it was believed that potassium deficits were responsible for the arrhythmias suffered by the Apollo 15 crew, dietary countermeasures were employed during the Apollo 16 mission. A diet high in potassium was provided (105 milliequivalents, versus a normal 70, in the command module diet, and 135 milliequivalents in the lunar module diet). Potassium enriched beverages and snack supplements were

*This survey, entitled Literature Summary on Countermeasures, may be consulted for details on experiments which have been attempted and for efficacy rating. (See *References* for full citation)

Table 8–15

Potential Countermeasures to Weightlessness

Exercise	Tumbling
Medication	Electrical stimulation of muscles
Diet	Exercise and LBNP
LBNP	Exercise and venous occlusion cuffs
Gradient positive pressure	Exercise and positive pressure breathing
G-Suit	Exercise and bone stress
Venous occlusion cuffs	Exercise and hypoxia
Positive pressure breathing	Venous occlusion cuffs and medication
Valsalva maneuver	Venous occlusion cuffs and leotards
Bone stress	Hypoxia, LBNP and exercise
Double trampoline	Centrifugation

(Vinograd & Maganelli, 1972)

also stocked. Potassium enriched meals were also consumed for 72 hours prior to launch to guarantee adequately high potassium levels at launch time. The provision of a high potassium diet, coupled with better planned work-rest cycles, proved to be a successful technique for countering the cardiac problems experienced by the prior crew. Lower body negative pressure was used by the Salyut crewmen inflight.

Another approach which has been suggested for countering the effects of the weightless environment is the provision of some system of artificial gravity in space vehicles. Two approaches have been suggested: rotation of the entire space vehicle or station and inclusion of an onboard centrifuge.

Table 8-16 shows the rotation radii and angular velocities necessary to achieve 3 gravity levels currently considered acceptable. The Coriolis force created is also indicated. A maximum Coriolis force of 20 percent of man's apparent weight is thought to be the limit which can be obtained without resulting discomfort. With higher angular velocities than those shown and shorter radii of rotation, even simple head movements can cause severe Coriolis forces with the associated discomfort. In addition, with a short radius of rotation, a gravity gradient (a difference in gravity between head and feet) exists which, if sufficiently large, can also produce discomfort. The Coriolis forces indicated in the table are based on a man's moving at a velocity of 3 feet per second.

It should be pointed out that medical and performance data available at the present time do not support a requirement for artificial gravity systems in spacecraft. In the view of space crews to the present time, artificial gravity systems are unnecessary for task performance. Crews have learned to live in a zero gravity environment and feel very confident in this state. Many have, in fact, expressed a preference for a zero g environment since the absence of gravity

Table 8–16

Generation of Artificial Gravity by Rotation

	Apparent Gravity								
	.28*			.57			1.0**		
Radius of rotation (feet)	95	200	600	48	200	600	88	200	600
Gravity gradient (6/r)*** (percent)	7	3	1	13	3	1	7	3	1
Angular velocity (RPM)	3	2	1.2	6	2.9	1.8	6	3.9	2.2
Angular velocity (radians/sec)	.32	.22	.13	.62	.30	.18	.63	.41	.24
Coriolis force (percent)	20	14	8	20	10	5	11	7	2

*Anticipated minimum acceptable (Thompson, 1965).

**Recommended maximum.

***Computed for a 6-ft-tall person.

increases the effective volume of what would otherwise be rather confined work spaces. On the other hand, the provision of artificial gravity would undoubtedly increase the habitability of spacecraft. Eating would become a simple affair, and locomotion could proceed nearly as it does in the Earth-bound environment. Everyday activities could be carried out about as easily and simply as they are in one's own home. Where engineering considerations are concerned, design tasks would be simplified in that restraint systems and locomotion aids would no longer be required. On the other hand, the engineering tasks associated with designing the artificial gravity system itself are formidable and could be costly.

The issue of the need for artificial gravity in spacecraft of the future is no more clearly resolved among Soviet scientists than it is in the United States. Valyavski (1969) states that until it becomes clear whether man forms adaptive mechanisms in the weightless state, technology will continue in the Soviet Union to attempt to create artificial gravitation. This is a problem which is "much in the forefront of modern cosmonautics." Members of the Soviet medical community had indicated to the author that they find no basis for requiring artificial gravity, but that it is still a question of concern to Soviet space system designers.*

References

Akulinichev, I. T., et al. Results of physiological investigations on the space ships Vostok 3 and Vostok 4. V. V. Parin (Ed.), *Aviation and Space Medicine.* NASA TT F-228, December 1964, National Aeronautics and Space Administration, Washington, D.C.

Bayevskiy, R. M., & Gazenko, O. G. Reactions of the cardiovascular and pulmonary system in humans and animals under conditions of weightlessness. *Kosaicheskiye isskdovaniya*, 1964, 2, 307.

Berry, C. A., et al. Man's response to long-duration flight in the Gemini spacecraft. In Gemini Midprogram Conference. Manned Spacecraft Center, Houston, Texas, 23-25 February 1966. NASA SP-121, 1966, National Aeronautics and Space Administration, Washington, D.C.

Berry, C. A. Pre-Gemini medical predictions versus Gemini flight results. In Gemini Summary Conference. Symposium presented at the Manned Spacecraft Center, Houston, Texas. February 102, 1967. NASA SP-138, 1967, National Aeronautics and Space Administration, Washington, D.C. (a)

Berry, C. A. Space medicine in perspective. *Journal of the American Medical Association*, 1967, *201*, 86-95. (b)

Berry, C. A. Preliminary clinical report of the medical aspects of Apollo VII and VIII. *Aerospace Medicine*, 1969, *40*, 245-254. (a)

Berry, C. A. Status report on space medicine in the United States. *Aerosapce Medicine*, 1969, *40*, 762-769. (b)

Berry, C. A. Summary of medical experience in the Apollo 7 through 11 manned space flights. *Aerospace Medicine*, 1970, *41*, 500-519.

*Personal communication.

Berry, C. A. Biomedical findings on American astronauts participating in space missions. Paper presented at the Fourth International Symposium on Basic Environmental Problems of Man in Space, Yerevan, Armenia, 1-5 October 1971. (a)

Berry, C. A. Medical results of Apollo 14-implications for longer duration space flights. Paper presented at XXIInd International Astronautical Congress, Brussels, Belgium, 25 September 1971. (b)

Berry, C. A. Effects of weightlessness in man. Paper presented at XVth COSPAR Meeting, Madrid, Spain, 23 May 1972.

Berry, C. A. Findings on American astronauts bearing on one issue of artificial gravity for future manned space vehicles. In press.

Biryukov, Ye. N., & Krasnykh, I. G. Change in optical density of bone tissue and calcium metabolism in the cosmonauts A. G. Nikolayev and V. I. Sevast'yanov. In O. G. Gazenko and N. N. Gurovskiy (Eds.) *Kosmicheskaya Biologiya i Meditsina* (Space Biology and Medicine), Moscow: Meditsina Publishing House, 1970.

Busby, E. Clinical space medicine: A perspective look at medical problems from hazards of space operations. NASA CR-856, July 1967. Prepared by Lovelace Foundation for Medical Education and Research for National Aeronautics and Space Administration, Washington, D.C.

Carson, M. A. Apollo portable life-support system. Proceedings of the Second Conference on Portable Life-Support Systems. NASA SP302, National Aeronautics and Space Administration, Washington, D.C., 1972.

Cherepakhin, M. A. & Pervushin, V. I. Space flight effects on the neuromuscular system of cosmonauts. In O. G. Gazenko and N. N. Gurovskiy (Eds.) *Kosmicheskaya Biologiya i Meditsina* (Space Biology and Medicine), Moscow: Meditsina Publishing House, 1970.

Clark, B., & Graybiel, A. Disorientation: A cause of pilot error. *Rev. Med. Aeronautics*, 1955, *18*, 219. Cited in J. F. Parker, Jr. (Ed.) *U.S. Naval Flight Surgeon's Manual*. Washington, D.C.: U.S. Government Printing Office, 1968.

Clark, B., & Stewart, J. D. The relationship between motion sickness experience and vestibular tests in pilots and nonpilots. Paper presented at Aerospace Medical Association Annual Scientific Meeting, Bal Harbour, Florida, 8-11 May 1972.

Deitrick, J. E., Whedon, G. D., & Shorr, E. Effects of immobilization upon various metabolic and physiologic functions of normal men. *American Journal of Medicine*, 1948, *4*, 3-36.

Dietlein, L. F., & Harris, E. Experiment M-5 bioassay of body fluids. In Gemini Midprogram Conference. Manned Spacecraft Center, Houston, Texas, 23-25 February 1966. NASA SP-121, National Aeronautics and Space Administration, Washington, D.C.

Donaldson, C. L., et al. The effects of long-term bed rest on mineral metabolism. Paper presented at Symposium on Hypogravic and Hypodynamic Environments. French Lic, Indiana, 16-18 June 1969.

Faget, M. A., & Olling, E. H. Orbital space stations with artificial gravity. Paper presented at Third Symposium on the Role of the Vestibular Organs in Space Exploration, Pensacola, Florida, 24 January 1967. NASA SP-152, 1968. National Aeronautics and Space Administration, Washington, D.C.

Fedorova, T. A., et al. Some metabolic indices in the cosmonauts Gagarin, Titov, Nikolayev, and Popovich. In A. T. D. Press, Special Issue, *Space Medicine*, 1964, 3(10). Library of Congress, N64-26357.

Fischer, C. L., Johnson, P. C., & Berry, C. A. Red blood cell mass and plasma volume changes in manned space flight. *Journal of The American Medical Association* 1967, *200*, 579-583.

Fraser, T. M. The intangibles of habitability during long-duration space missions. Lovelace Foundation, Albuquerque, New Mexico. NASA CR-1084, June 1968. National Aeronautics and Space Administration, Washington, D.C.

Gerathewohl, S. J., & Ward, J. E. Psychophysiological and medical studies of weightlessness. In O. Benson, Jr., & H. Strughold (Eds.), *Physics and Medicine of the Atmosphere and Space*. New York: John Wiley & Sons, 1960.

Graybiel, A., Miller, E. F., Billingham, J., Waite, R., Berry, C. A., & Dietlein, L. F. Vestibular experiments in Gemini flights V and VII. *Aerospace Medicine*, 1967, *38*, 360-370.

Haldane, J. S. *Respiration*. New Haven: Yale University Press, 1922.

Hatch, T. T., & Gross, P. *Pulmonary deposition and retention of inhaled aerosoles*. New York: Academic Press, 1964.

Hattner, R. S., & McMillian, D. E. Influence of weightlessness upon the skeleton: A review. *Aerospace Medicine*, 1968, 39, 849-855.

Heaney, R. P. Radiocalcium metabolism in disuse osteoporosis in man. *American Journal of Medicine*, 1962, *33*, 188.

Johnson, P. C., & Driscoll, B. S. Red cell mass and plasma volume changes found in selected Apollo missions. Paper presented at Aerospace Medical Association Annual Scientific Meeting, Bal Harbour, Florida, 8-11 May 1972.

Jones, W. L. The human factors systems program. Office of Advanced Research and Technology, National Aeronautics and Space Administration. Presented before the Committee on Science and Astronautics, House of Representatives, Washington, D.C., 1968.

Kalinichenko, V. V., Gornago, V. A., Machinskiy, G. V., et al. Dynamics of orthostatic stability of cosmonauts after flight aboard the Soyuz-9 spaceship. In O. G. Gazenko and N. N. Gurovskiy (Eds.) *Kosmicheskaya Biologiya i Meditsina* (Space Biology and Medicine), Moscow: Meditsina Publishing House, 1970.

Kakurin, L. I. Medical research prepared on the flight program of the Soyuz-type spacecraft. NASA TTF-141026, National Aeronautics and Space Administration, Washington, D.C., November 1971.

Kakurin, L. I., et al. The effect of hypokinesia on some indices of work capacity and respiratory function of man. In A. T. D. Press, Special Issue, *Space Medicine*, 1964, *3*(10), Library of Congress, Washington, D.C.

Kelly, G. F., & Coons, D. O. Medical aspects of extravehicular activity. In R. M. Machell (Ed.), Summary of Gemini extravehicular activity. NASA SP-149, 1967, National Aeronautics and Space Administration, Washington, D.C.

Lebedinskiy, A. V., et al. As cited in Petukhov, B. N., Purakhin, Yu. N., Georgiyevskiy, V. S., et al., 1964. Regulation of erect posture of cosmonauts after an 18-day orbital flight. In O. G. Gazenko and N. N. Gurovskiy (Eds.) *Kosmicheskaya Biologiya i Meditsina* (Space Biology and Medicine), Moscow: Meditsina Publishing House, 1970.

Mack, P. B., & LaChance, P. A. Effects of recumbency and space flight on bone density. Second Annual Biomedical Research Conference, Houston, Texas, 1966.

Mack, P. B., Vogt, T. B., & LaChance, P. A. Experiment M-6, bone demineralization. In Gemini Midprogram Conference. Manned Spacecraft Center, Houston, Texas, 23-25 February 1966. NASA SP-121, 1966, National Aeronautics and Space Administration, Washington, D.C.

Molchanov, N. S., Krupina, T. N., Balandin, V. A., et al. Results of clinical examination of A. G. Nikolayev and V. I. Sevast'yanov. In O. G. Gazenko and N. N. Gurovskiy (Eds.) *Kosmicheskaya Biologiya i Meditsina* (Space Biology and Medicine), Moscow: Meditsina Publishing House, 1970.

National Academy of Sciences, National Research Council. Physiology in the space environment. Vol. II, Respiration. Report of a conference conducted by the Space Science Board of the National Academy of Sciences, National Research Council, Woods Hole, Massachusetts, June-July, 1966. Publication 1485B, Washington, D.C., 1967.

National Academy of Sciences, National Research Council. Infectious disease in manned space flight. Space Science Board, Washington, D.C., 1970.

Parin, V. V., et al. Some results of a medical-biological experiment on the biological satellite Kosmos 110. In *Space Biology and Medicine*, Joint Publications Research Service Report No. 45798, USSR, 1968.

Petukhov, B. N., Purakhin, Yu. N., Georgiyevskiy, V. S., et al. Regulation of erect posture of cosmonauts after an 18-day orbital flight. In O. G. Gazenko and N. N. Gurovskiy (Eds.) *Kosmicheskaya Biologiya i Meditsina* (Space Biology and Medicine), Moscow: Meditsina Publishing House, 1970.

Rummel, J. A., Hoffler, G. W., Sawin, C., Wolthuis, R. A., Buderer, M. C., Johnson, R. L., & Michels, E. L. Cardiopulmonary responses to space flight. Paper presented at Aerospace Medical Association Annual Scientific Meeting, Bal Harbour, Florida, 8-11 May 1972.

Valyavski, Y. Some compensation reactions during extended weightlessness. Paper presented at the Third International Symposium on the Basic Environmental Problems of Man in Space, Geneva, Switzerland, 15-19 November 1968. NASA TT-F-12094, National Aeronautics and Space Administration, Washington, D.C., January 1969.

Vinograd, S. P., & Manganelli, L. A. Literature summary on countermeasures. George Washington University Medical Center, Washington, D.C., January 1972.

Volynkin, Yu. M., Vasil'yev, P. V. Some results of medical studies conducted during the flight of the Voskhod. In N. M. Sisakyan (Ed.), *The problems of space biology*, Vol. VI, NASA TT F-528, July 1969. National Aeronautics and Space Administration, Washington, D.C.

Vorob'yev, Ye. I., et al. Medical support and principal results of examination of the Soyuz-9 spaceship crew. In O. G. Gazenko and N. N. Gurovskiy (Eds.) *Kosmicheskaya Biologiya i Meditsina* (Space Biology and Medicine), Moscow: Meditsina Publishing House, 1970.

Yazdovskiy, V. I., & Denisov, V. G. Flights of space vehicles Vostok 5 and Vostok 6. In the Russian language, *Herald of the Academy of Sciences of the U.S.S.R.*, 1963, *33*(9), 17-22.

Yazdovskiy, V. I., et al. Sensory-motor coordination in conditions of prolonged weightlessness during actual space flight. In A. T. D. Press, Special Issue, *Space Medicine*, 1964, 3(10). Library of Congress, N64-26357.

Yegorov, B. B. Physiological reactions and possible means of protection during long term exposure to weightless conditions. NASA TT F-12095, January 1969, National Aeronautics and Space Administration, Washington, D.C.

Yuganov, Ye. M. Physiological reactions in weightlessness. In V. V. Parin (Ed.), *Aviation and space medicine*. NASA TT F-228, December 1964, National Aeronautics and Space Administration, Washington, D.C.

APPENDIX

History of U.S. and Soviet Manned Space Flights

Spacecraft	Launch Date	Crew	Flight Time	Highlights
Vostok 1	Apr. 12, 1961	Yuri A. Gagarin	1 hr. 48 mins.	First manned flight.
Mercury-Redstone 3	May 5, 1961	Alan N. Shepard, Jr.	15 mins.	First U.S. flight; suborbital.
Mercury-Redstone 4	July 21, 1961	Virgil I. Grissom	16 mins.	Suborbital; capsule sank after landing.
Vostok 2	Aug. 6, 1961	Gherman S. Titov	25 Hrs. 18 mins.	First flight exceeding 24 hours.
Mercury-Atlas 6	Feb. 20, 1962	John H. Glenn, Jr.	4 hrs. 55 mins.	First American to orbit.
Mercury-Atlas 7	May 24, 1962	M. Scott Carpenter	4 hrs. 56 mins.	Landed 250 miles from target.
Vostok 3	Aug. 11, 1962	Andrian G. Nikolayev	94 hrs. 22 mins.	First dual mission (with Vostok 4).
Vostok 4	Aug. 12, 1962	Pavel R. Popovich	70 hrs. 57 mins.	Came within 3.1 miles of Vostok 3.
Mercury-Atlas 8	Oct. 3, 1962	Walter M. Schirra, Jr.	9 hrs. 13 mins.	Landed 5 miles from target.
Mercury-Atlas 9	May 15, 1963	L. Gordon Cooper, Jr.	34 hrs. 20 mins.	First long U.S. flight.
Vostok 5	June 14, 1963	Valery F. Bykovsky	119 hrs. 6 mins.	Second dual mission (with Vostok 6)
Vostok 6	June 16, 1963	Valentina V. Tereshkova	70 hrs. 50 mins.	First woman in space; within 5 miles of Vostok 5.
Voskhod 1	Oct. 12, 1964	Vladimir M. Komarov Konstantin P. Feoktistov Dr. Boris G. Yegorov	24 hrs. 17 mins.	First 3-man crew.
Voskhod 2	Mar. 18, 1965	Aleksei A. Leonov Pavel I. Belyayev	26 hrs. 2 mins.	First extravehicular activity (Leonov, 10 minutes).
Gemini 3	Mar. 23, 1965	Virgil I. Grissom John W. Young	4 hrs. 53 mins.	First U.S. 2-man flight; first manual maneuvers in orbit.

Gemini 4	June 3, 1965	James A. McDivitt Edward H. White, II	97 hrs. 56 mins.	21-minute extravehicular activity (White).
Gemini 5	Aug. 21, 1965	L. Gordon Cooper, Jr. Charles Conrad, Jr.	190 hrs. 55 mins.	Demonstrated long-duration flight and rendezvous capacity.
Gemini 7	Dec. 4, 1965	Frank Borman James A. Lovell, Jr.	330 hrs. 36 mins.	2-Week duration flight; demonstrated controlled reentry.
Gemini 6-A	Dec. 15, 1965	Walter M. Schirra, Jr. Thomas P. Stafford	25 hrs. 51 mins.	Rendezvous within 1 foot of Gemini 7.
Gemini 8	Mar. 16, 1966	Neil A. Armstrong David R. Scott	10 hrs. 41 mins.	First docking of 2 orbiting spacecraft (Gemini 8 with Agena target rocket).
Gemini 9-A	June 3, 1966	Thomas P. Stafford Eugene A. Cernan	72 hrs. 21 mins.	Extravehicular activity; rendezvous.
Gemini 10	July 18, 1966	John W. Young Michael Collins	70 hrs. 47 mins.	First dual rendezvous (Gemini 10 with Agena 10, then Agena 8).
Gemini 11	Sept. 12, 1966	Charles Conrad, Jr. Richard F. Gordon, Jr.	71 hrs. 17 mins.	First initial-orbit rendezvous; first tethered flight; highest Earth-orbit altitude (853 miles).
Gemini 12	Nov. 11, 1966	James A. Lovell, Jr. Edwin E. Aldrin, Jr.	94 hrs. 35 mins.	Longest extravehicular activity (Aldrin, 5 hours 37 minutes).
Soyuz 1	Apr. 23, 1967	Vladimir M. Komarov	26 hrs. 40 mins.	Cosmonaut killed in reentry accident.
Apollo 7	Oct. 11, 1968	Walter M. Schirra, Jr. Donn F. Eisele R. Walter Cunningham	260 hrs. 8 mins.	First U.S. 3-man mission.
Soyuz 3	Oct. 26, 1968	Georgi Beregovoy	94 hrs. 51 mins.	Maneuvered near unmanned Soyuz 2.
Apollo 8	Dec. 21, 1968	Frank Borman James A. Lovell, Jr. William A. Anders	147 hrs.	First manned orbit(s) of Moon; first manned departure from Earth's sphere of influence; highest speed ever attained in manned flight.
Soyuz 4	Jan. 14, 1969	Vladimir Shatalov	71 hrs. 22 mins.	Soyuz 4 and 5 docked and transferred two cosmonauts from Soyuz 5 to Soyuz 4.
Soyuz 5	Jan. 15, 1969	Boris Volynov Alecksey Yeliseyev Yevgeniv Khrunov	72 hrs. 40 mins.	

APPENDIX — Continued

History of U.S. and Soviet Manned Space Flights

Spacecraft	Launch Date	Crew	Flight Time	Highlights
Apollo 9	Mar. 3, 1969	James A. McDivitt David R. Scott Russel L. Schweickart	241 hrs. 1 min.	Successfully simulated in Earth orbit operation of lunar module to landing and takeoff from lunar surface and rejoining with comand module.
Apollo 10	May 18, 1969	Thomas P. Stafford John W. Young Eugene A. Cernan	192 hrs. 3 mins.	Successfully demonstrated complete system, including lunar module descent to 47,000 feet from the lunar surface.
Apollo 11	July 16, 1969	Neil A. Armstrong Michael Collins Edwin E. Aldrin, Jr.	195 hrs. 19 mins.	First manned landing on lunar surface and safe return to Earth. First return of rock and soil samples to Earth, and manned deployment of experiments on lunar surface.
Soyuz 6	Oct. 11, 1969	Georgiv Shonin Valeriy Kubasov	118 hrs. 21 mins.	Soyuz 6, 7 and 8 operated as a group flight without actually docking. Each conducted certain
Soyuz 7	Oct. 12, 1969	Anatoliy Filipchencko Vladislav Volkov Viktor Gorbatko	118 hrs. 43 mins.	experiments, including welding and Earth and celestial observations.
Soyuz 8	Oct. 13, 1969	Vladimir Shatalov Aleksey Yeliseyev	118 hrs. 51 mins.	
Apollo 12	Nov. 14, 1969	Charles Conrad, Jr. Richard F. Gordon, Jr. Alan L. Bean	244 hrs. 36 mins.	Second manned lunar landing. Continued manned exploration and retrieved parts of Surveyor III spacecraft which landed in Ocean of Storms on April 19, 1967.
Apollo 13	Apr. 11, 1970	James A. Lovell, Jr. Fred W. Haise, Jr. John L. Swigert	142 hrs. 54 mins.	55 hours and 54 minutes into flight pressure in oxygen tank No. 2 rose, mission aborted.
Soyuz 9	June 1, 1970	Adrian W. Kojayev Vitaly Sevastyanov	424 hrs. 59 mins.	Longest duration manned mission to date. Also first nighttime manned launch.

radiation energies lie betweem 10^{-3} and 10^{13} million electron volts (MeV). The identifying term "ionizing" is used because these radiations penetrate matter and, in their interactions with matter, cause pairs of positive and negative ions to be formed along the path of the incident particle or photon by loss or gain of an electron. The less energetic radiations may penetrate only a fraction of a millimeter, while the more energetic can penetrate many inches of dense material such as lead. Penetration implies entry to at least 10 microns, which is slightly beyond the thickness of most cells.

This chapter introduces the reader to the ionizing radiations in space and the general biological effects of ionizing radiation, but makes no attempt to establish or recommend standards of operational safety. Similarly, shielding against radiation, being an operational problem, is not discussed, though the matter is introduced because of the perturbations produced in any radiation field by any mass. (See also Radiobiological Factors in Manned Spaceflight, Langham, 1967.)

The space radiations can be broadly defined as falling into one of three categories: the primary cosmic radiations, the geomagnetically trapped radiations (Van Allen belts), and the solar flare events. The solar events vary considerably from one event to the next in the differential energy spectrum and the intensity of the protons of which they are predominantly composed. The energy spectrum of solar flares also varies with time. The reader is referred to the Solar Proton Manual (McDonald, 1963) and Webber (1963) for a more thorough treatment of these potentially hazardous radiation events.

The profuse and various secondary radiations generated when primary particles are stopped, and the importance of these secondaries are discussed. Common terms in radiation are defined and the concept of relative biological effectiveness (RBE) or the related quality factor (QF) is introduced. A word of warning here is appropriate. By definition (National Committee on Radiation Protection Handbook 59, 1954), the biologic response to radiation is standardized to the effects produced by 200 kVp X-rays. Radiations that have the same effect are said to have an RBE of unity. Radiations with a greater effect per rad (radiation absorbed dose)—such as neutrons, low energy protons and alpha particles—are said to have an RBE greater than unity in accordance with the ratio of doses that produce the same response.

RBE values are shown later, some of which are quite firmly established. Since they are generally to be applied to occupational radiation safety considerations, additional safety factors have been built in. Thus, they may be of only limited value for the evaluation of space radiations. There is also, at present, some controversy concerning the "best estimate" RBE for protons of energies equal to or greater than 100 MeV. These vary from about 0.6 (Sondhaus, 1962) to 1.6 (Pickering, 1963). The higher figure, derived from primate studies, may be more like that for man, since the exposure "geometry" is more typical. The reader is advised, however, not to accept any RBE value as rigorous.

Attention also is given to the question of tissue depth dose, since a heterogeneous or heterochromatic radiation flux will not penetrate any mass

uniformly at all depths. In addition, every solar flare event will have its own characteristic depth dose distribution. In this regard, it is suggested that the mean dose to the bone marrow be estimated wherever possible, and employed as a best estimate of the biologically significant dose.

The balance of the radiation effects sections present a rather broad delineation of the expected human response to the ionizing radiations. The data assume that depth dosage is nearly uniform and that exposure of the whole body has occurred. The summary of acute radiation illness has been derived from a number of sources, as indicated in the legends; but for the most part, well-documented accident cases, cases treated with therapeutic radiation, and the Hiroshima-Nagasaki survivors form the bulk of existing experience. Dose estimates are, therefore, uncertain. Individual biologic variations in response also occur. Therefore, indicated dose-response relationships must be considered to have at least a 20 percent error of estimate in either direction. A field where as yet figures cannot be provided for the engineer is that of the behavioral aspects and the possibility of effects of damage to the central nervous system by radiation alone or radiation combined with emotional and physical stress.

All existing experience supports the assumption that man is comparatively radiosensitive. He has a lower median lethal dose (~450 R) than observed in most rodents (500-750 R) but is somewhat more resistant than the average canine (250-400 R). Man shows a long slow course of events in the typical hematopoietic or bone marrow syndrome. Injury develops slowly, and reaches a maximum in 3 to 6 weeks. The testis, highly sensitive to radiation, is damaged promptly, but since this injury is done to immature cells the damage may not appear for some days and if not too severe will slowly recover. Recovery, in general, from the more acute manifestations may be protracted over many months or even years. Some efforts have been made to evaluate residual or long-term injury, but these have to employ many simplifying and therefore inaccurate assumptions, because of our general inability to detect critical recovery mechanisms and rates. The ERD (equivalent residual dose) concept is presented later, but the user should *not* attempt to employ any derived values for engineering design criteria. The concept is given more to enable the nonspecialist in radiation effects to gain better appreciation of the nature of the time-intensity dose variables in radiation biology. In general, if doses are kept small enough and sufficient time is allowed for recovery from earlier injury, the radiation "status" of an individual can be kept in a fairly steady state.

Dose-response estimates for the eyes and skin are largely based on clinically determined responses to standard radiation sources. The space radiations are more difficult to evaluate for these effects for several reasons. They include (a) particles that produce very dense ionization tracks which are more effective in inducing lens damage, (b) large numbers of low energy particles that can produce high surface doses with negligible deep tissue dosage, and (c) the capability of inducing diverse secondary particulate and bremsstrahlung radiations that can add significantly to the burden of surface-damaging ionization.

Apollo 14	Jan. 31, 1971	Alan B. Shepard Steward A. Roosa Edgar D. Mitchell	216 hr. 42 mins.	Used mobile equipment transporter on moon; record time on moon of 31 hours 33 minutes; first lunar highlands exploration. Lunar material weighing 96 pounds returned to Earth.
Soyuz 10	Apr. 22, 1971	Vladimir A. Shatalov Alexei Yeliseyev Nikolai Rukavishnikov	47 hrs. 46 mins.	Linked for 5.5 hours with Salyut; mission aborted early; first nighttime recovery.
Soyuz 11	June 6, 1972	Georgi T. Dobrovolsky Vladislav N. Volkov Viktor I. Patsayev	570 hrs. 22 mins.	New regenerative life support systems used; extensive biomedical data collected; plants grown. Crew died of hypoxia and dysbarism due to hatch seal failure resulting in rapid decompression of spacecraft prior to reentry.
Apollo 15	July 26, 1971	David Scott Alfred Worden James Irwin	295 hrs. 11 mins. 58 sec.	28-mile coverage of moon's surface, using the first self-powered transport system for the surface of the moon; subsatellite launch; deep-space walk; approximately 170 pounds of moon rock returned to Earth.
Apollo 16	Apr. 16, 1972	John W. Young Thomas K. Mattingly Charles M. Duke	265 hrs. 51 mins.	5th manned lunar landing; exploration using Lunar Rover; 213 pounds of lunar samples returned.

Adapted from: Aeronautics and Space Report of the President. Transmitted to the Congress January 1970. Executive Office of the President, National Aeronautics and Space Council, Washington, D.C.

CHAPTER 9
IONIZING RADIATION

by

Shields Warren, M.D.
New England Deaconess Hospital
Boston, Massachusetts

and

Douglas Grahn, Ph.D.
Argonne National Laboratory
Argonne, Illinois

Concern over the effects of exposure to radiation is uniquely a product of the twentieth century. Within this period, machines capable of producing or releasing many kinds of radiation particles have been developed. Man also has taken the first steps into space, a radiation environment altogether different from that found on Earth. Medical and dental personnel now use radiation sources as diagnostic and therapeutic tools. It is with respect to space travel, however, that the most dramatic issues concerning radiation exposure have been raised. It has been known for some time that the Earth's atmosphere shields man from higher levels of solar and galactic radiation. Only now is information being obtained as to the effects of deliberate penetration into these regions of increased radiation. The findings from these early space missions will aid in determining the feasibility of long-term space voyages. Also, and perhaps of even greater importance, these findings will aid in determining the tolerance of man to the ever-proliferating radiation sources now being encountered on Earth.

The penetrating ionizing space radiations are extremely diverse in the energy range of both their particulate and their electromagnetic components. The particulate radiation component includes all subatomic particles such as protons, neutrons, electrons, atomic nuclei stripped of orbital electrons (the heavy primaries), mesons, etc. The pi meson is a charged or neutral particle and reacts to form new mesons with release of energy which in turn form electrons or positions with release of energy. K-mesons are also present in cosmic radiation. The electromagnetic portion includes the X- and gamma radiations. The

Preceding page blank

It is not yet possible to present a clear picture of the expected effects of partial-body exposure. Any degree of partial-body shielding and any protraction or fractionation of exposure can be advantageous. It is particularly beneficial to shield the sensitive organs or tissues, such as the gastrointestinal tract, eyes, and significant portions of the bone marrow. It should be understood that dose-response estimates of the acute radiation syndrome following partial-body exposures are impossible to make at this time; but if the major portion of the main torso is in the exposure field, the response would probably grade toward the whole-body exposure case.

Lastly, some consideration is given to the general questions of long-term effects—both for the exposed individual and for subsequent generations. With the exception of the leukemia incidence estimate, the data are all based on animal experimentation. Errors of estimate are therefore unknown, and could certainly involve a factor of 2. Long-term injury is also a population phenomenon in many respects, and all statements must, therefore, be given in probability terms. Probability statements for selected individuals are thus not appropriate and can be extremely misleading.

Basic references that will be found useful are: D. E. Lea, *Actions of Radiations on Living Cells* (1955); W. D. Claus, editor, *Radiation Biology and Medicine* (1958); A. Hollaender, editor, *Radiation Biology* (1954); U.S. Atomic Energy Commission, *Proceedings of the Symposium on the Protection Against Radiation Hazards in Space* (1963); United Nations Scientific Committee, *Report on the Effects of Atomic Radiation* (1962); United Nations Scientific Committee, *Ionizing Radiation: Levels and Effects (1972).*

Radiation Terms and Measures

Basic Units

There are several units in use for describing radiation intensity and human exposure. These are interrelated as follows (Nuclear Radiation Guide, 1962):

Roentgen. The basic indicator of quantity of radiation is the roentgen unit. Inasmuch as radiation cannot be measured directly, its magnitude is determined by the ionization produced by the passage of radiation through a medium. The roentgen refers to the ionization produced in air by the passage of X- or gamma radiation, specifically, that amount of radiation required to produce 0.001293 grams of air ions carrying one electrostatic unit of electricity of either sign.

Rad. The rad (radiation absorbed dose) is the measure of exposure in most common use. One rad of any type of radiation corresponds to the absorption of 100 ergs per gram of any medium. Because the rad does not specify the medium, a medium should be stated unless clearly implied. For example, the term "tissue rad" should be used in the case of exposure of soft human tissue.

Biological Effectiveness

The RBE (Relative Biological Effectiveness) expresses the effectiveness of a particular type of radiation in producing the same biological response as X- or gamma radiation having a linear energy transfer (LET) equivalent to 3 kilovolts per micron of water and delivered at the rate of about 10 rads per minute. For applied radiation protection, QF (quality factor) is the preferred term under most practical circumstances.

Figure 9-1 shows the manner in which the RBE factor is used to translate an exposure expressed in rads into one expressed in REM's. The REM (Roentgen Equivalent, Man) is the most accurate unit for expressing exposure of man. The REM refers to the absorbed dose of any ionizing radiation which produces the same biological effects in man as those resulting from the absorption of 1 roentgen of X-rays. As seen in figure 9-1, each type of radiation must be converted by a specific factor, the RBE, in order to equate the biological effects.

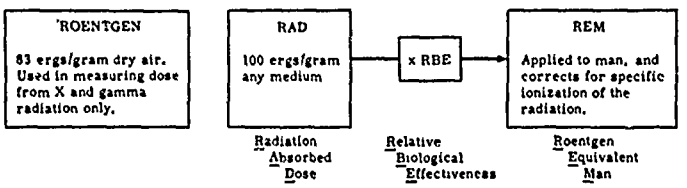


Figure 9–1. Relationship among principal units used in describing radiation exposure.

Table 9-1 presents RBE factors for a number of types of radiation. The standard RBE values are based on the most detrimental chronic biological effect (for example, cataract induction by neutrons) for continuous low dose exposures that might be met in industrial situations. However, the RBE for many acute high dose rate exposures may be very much lower. The RBE for a large acute lethal dose of fast neutrons may be less than 1.0 for man, as against the values of 5 to 10 shown in table 9-1. Also, as a given particle degrades in tissue, the RBE will rise as its energy transfer per micron (LET) rises. At the same time, a heterogeneous beam of protons will have an average RBE that tends to drop with increasing depth in tissue as the lower energy component becomes fully absorbed and the higher energy component continues its traverse. Figure 9-2 shows instantaneous and mean RBE's for protons of different energies, corresponding to the instantaneous linear energy transfer at energy E, and the mean RBE for dissipation of the entire energy from E down to zero.

Table 9-2 illustrates the manner in which the RBE (QF) value changes as a result of increasing power of X-rays or electron radiation. The relation between RBE (QF) and LET in terms of keV/μ in water can be employed for virtually all end points to compensate for differences in radiation quality.

Table 9–1
RBE Values for Various Types of Radiation

Type of Radiation	RBE
X-rays	1
Gamma rays and bremsstrahlung	1
Beta particles, 1.0 MeV	1
" " 0.1 MeV	1
Neutrons, thermal energy	2.8
" 0.0001 MeV	2.2
" 0.005 MeV	2.4
" 0.02 MeV	5
" 0.5 MeV	10.2
" 1.0 MeV	10.5
" 10.0 MeV	6.4
Protons, greater than 100 MeV	1-2
" 1.0 MeV	8.5
" 0.1 MeV	10
Alpha particles, 5 MeV	15
" " 1 MeV	20

(From Barbiere et al., 1958; U.S. Atomic Energy Commission, 1962; Saenger, 1963.)

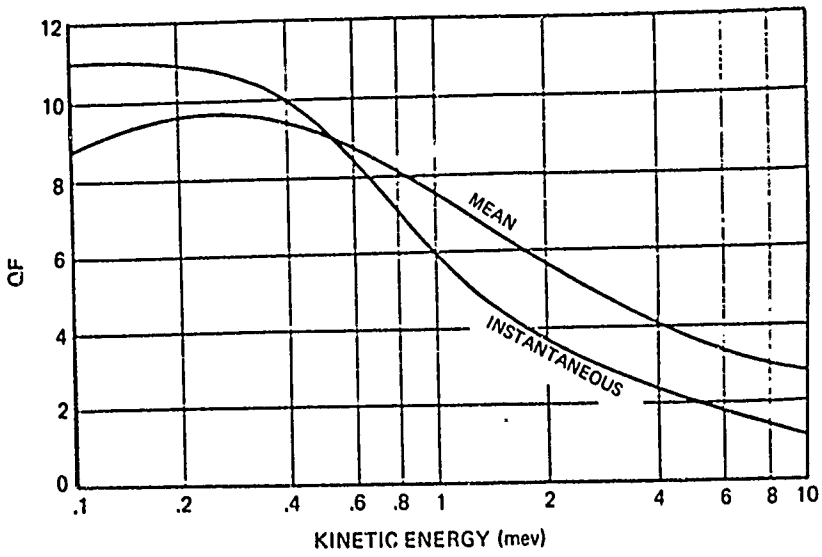


Figure 9–2. Instaneous and mean RBE's for protons of various energies. (Schaefer, 1961; Sondhaus & Evans, 1969)

Table 9–2

Values of RBE (QF) for Late or Delayed Effects as a Function of Average LET

LET_∞ (keV/μ in Water)	RBE (QF)
X-rays and electrons of any LET	1
3.5 or less	1
3.5–7	1–2
7–23	2–5
23–53	5–10
53–175	10–20

(National Committee on Radiation Protection and Measurements, 1954)

Equivalent Residual Dose (ERD) is a concept used in estimating what residual acute radiation injury persists for a period of weeks and months after an exposure to radiation. Thus a person exposed to radiation on Monday can be said to have a certain amount of that injury on the next Monday, something less on the next after that, and so forth. The ERD at any time, t days, after onset of exposure can be calculated on the basis of the following assumptions:

1. 10 percent of the injury attributed to the dose is considered to be irreparable.

2. The body repairs the remaining 90 percent at the rate of 2.5 percent per day.

3. Recovery is continuous during protracted exposure. The ERD at t days may be expressed as:

$$ERD = D_0[0.1 + 0.9(1.000-0.025)^{t-4}] + \dot{D}\int_4^t [0.1 + 0.9(1.000-0.025)^t]dt,$$

where

D_0 = brief dose in r received during first 4 days,

$\dot{D}$ = protracted daily dose at a constant rate, r/day, received after the 4th day, and

t = time in days after onset of initial exposure.

Classes and Sources of Ionizing Radiation

The radiation encountered in space, and to a lesser extent on Earth, may be attributed to three principal sources: geomagnetically trapped radiation, galactic cosmic radiation, and solar particle radiation. Space radiation levels vary substantially both with time and with distance from the Earth. These temporal and spatial fluctuations must be taken into account in the planning of space missions if radiation exposures are to be held to an acceptable level. Table 9-3 shows the nature and location of electromagnetic and particulate ionizing radiations found in space. As indicated, most of the various radiations can be found within each of the three radiation sources noted above. Principal exceptions are alpha particles and heavy primary nuclei which are not generally associated with the radiation emanating from solar events.

Table 9–3

Nature and Location of Electromagnetic and Particulate Ionizing Radiations in Space

Name	Nature of Radiation	Charge	Mass	Where Found
Photon	Electromagnetic	0	0	Radiation belts, solar radiation (produced by nuclear reactions and by stopping electrons), and everywhere in space
X-ray	Electromagnetic	0	0	
Gamma ray	Electromagnetic	0	0	
Electron	Particle	−e	1 m_e	Radiation belt and elsewhere
Positron	Particle	+e	1 m_e	Cosmic rays, radiation belt, solar flares
Proton	Particle	+e	1840 m_e or 1 amu*	Primary cosmic rays, radiation belt, solar flares
Neutron	Particle	0	1841 m_e	Secondary particles produced by nuclear interactions involving primary particle flux
Pi meson	Particle	+,−, or 0	273 m_e	Cosmic rays, radiation belt, solar flares
Alpha particle	Particle	+2e	4 amu	Primary cosmic radiation (nucleus of helium atom)
Heavy primary nuclei	Particle	≥+3e	≥6 amu	Primary cosmic radiation (nuclei of heavier atoms)

*amu = atom mass unit

(Newell & Naugle, 1960; Sondhaus & Evans, 1969; Glasstone, 1958)

The following sections describe the sources of the principal ionizing radiation of biological significance in space.

Primary Radiation

Geomagnetically Trapped Radiation. There are two belts of geomagnetically trapped radiation around the Earth, as shown in figure 9-3. These belts, known as the Van Allen belts, are separated by a region of relatively low intensity. Figure 9-3 shows the relative intensities of both electrons and protons within the trapped radiation belts. Electrons are shown to the left, protons to the right. Both, of course, are intermingled and are separated only for clarification of the values.

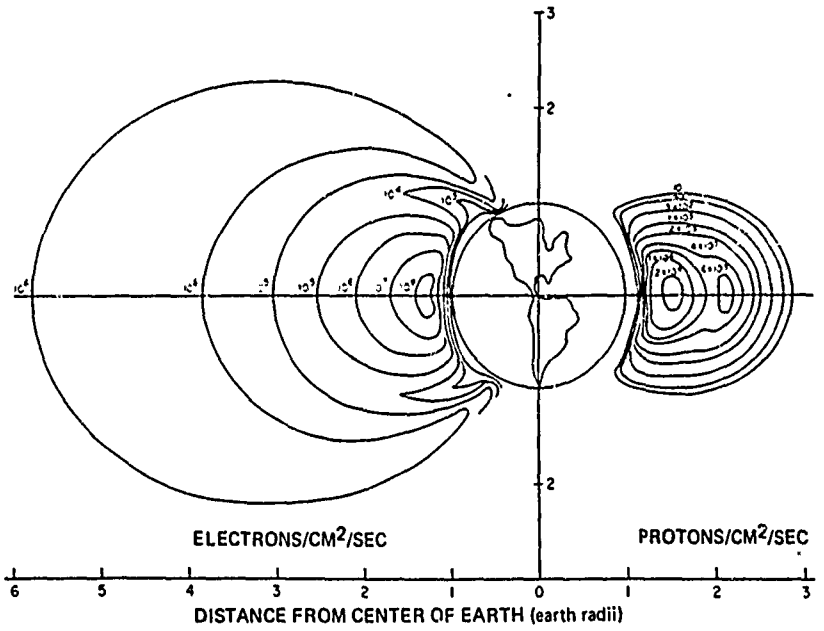


Figure 9–3. Representation of the radiations trapped in the Earth's magnetic field, known as the "Van Allen belts". (Adapted from White et al., 1969)

The Van Allen radiation belts are not entirely symmetrical. In the South Atlantic Anomaly, extending from about 0 to 60 degrees west longitude and 20 to 50 degrees south latitude, the trapped proton intensity for energies more than 30 MeV is the equivalent at 100 to 200 miles altitude to that at 800 miles altitude elsewhere. This is due to a perturbation or asymmetry of the Earth's geomagnetic field. For trajectories of space vehicles of 30 degrees inclination from the equator or greater, there will be approximately five traverses through this anomaly in each day. Experience with earth orbital missions to date indicates that nearly all of the accumulative radiation exposure has been attributable to passage through this geomagnetic anomaly.

Table 9-4 compares the total radiation exposures for Apollo missions 7 through 14. Most of this exposure, it is believed, took place during the period while the vehicle was within the Van Allen belts. It is apparent that the Apollo 14 crew received a higher radiation dose than crews on any prior Apollo mission,

but still a dose of no hazard or biological significance (Berry, 1971). In fact, the crewmembers on this flight received the largest dose experienced on any manned mission to that point in time. The Apollo 14 trajectory, particularly the outbound portion, took the spacecraft close to the heart of the trapped radiation belts. Since the mission occurred at a time of solar minimum, the cosmic ray flux was relatively higher than for previous missions.

Table 9–4

Radiation Exposure for Apollo 14

Comparison of Apollo Missions

	Rad		Rad
Apollo 7	.16	Apollo 11	.18
8	.16	12	.58
9	.20	13	.24
10	.48	14	1.14

Apollo 14 Exposure (Rad)

	Chest	Thigh	Ankle
CDR	.996	1.095	1.073
CMP	1.126	1.145	1.279
LMP	1.078	1.204	1.248

(Berry, 1971)

Galactic Cosmic Radiation. Galactic cosmic radiation, frequently referred to simply as galactic radiation, originates outside the solar system. This radiation consists of atomic nuclei which have been completely ionized and accelerated to very high energies. Protons of 10^{18} electron-volt energy have been identified from this source. Protons (hydrogen nuclei) constitute about 85 percent of this radiation; alpha particles (helium nuclei), about 13 percent; and heavier nuclei ranging up to tin, the remaining few percent (Jones, 1968).

Cosmic activity in space is reasonably constant. Measures obtained with deep-probe rockets show little difference in intensity between 1.0 and 1.5 astronomical units from the sun. This would indicate that cosmic ray intensity in the vicinity of planets such as Venus and Mars is quite similar to that found near the Earth.

The galactic cosmic radiation received on Earth varies substantially both as a function of the level of solar events occurring at that time and as a function of position on the Earth's surface. Figure 9-4 shows the galactic radiation received at varying altitudes up to 120 000 feet during periods of minimum and maximum solar activity. The two curves are based on estimated whole-body dose to an unshielded man at about 40 degrees north latitude. These curves show that, whereas the dose rate is essentially negligible at sea level, at higher altitudes

the exposure during periods of solar minimum is approximately twice that found during solar maximum.

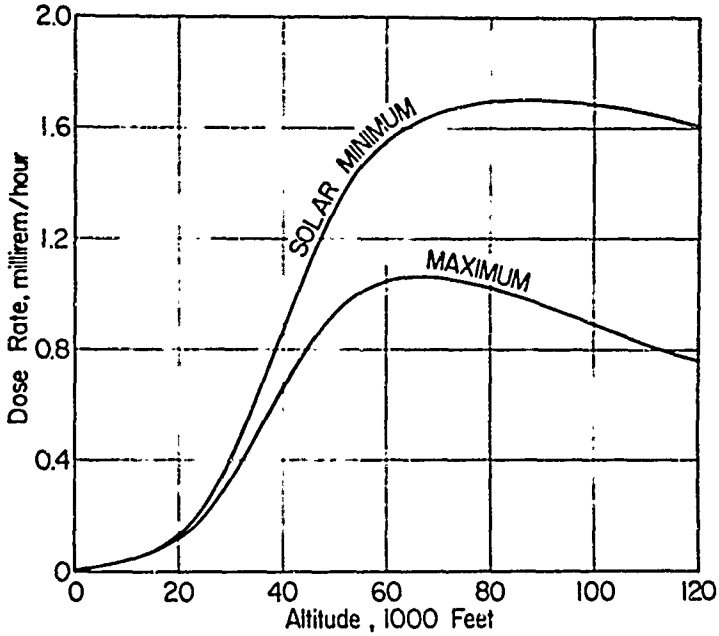


Figure 9–4. Altitude profiles of galactic radiation level in the atmosphere. (Foelsche et al., 1969)

As seen in figure 9-5 distance from the equator has a very significant effect on exposure to galactic radiation at altitudes above 30 000 feet. Highest exposures are recorded in the polar region. At polar latitudes and at altitudes in excess of 70 000 feet, radiation levels are more than triple those found at a latitude of 30 degrees.

Solar Particle Radiation. Solar activity increases in rather regular 11 year cycles and is characterized by giant eruptions from the surface of the sun, termed "solar flares." Solar flares develop rapidly and generally last only 30 to 50 minutes, during which time intense radiation activity occurs. Table 9-5 shows the major solar events occuring during the period from 1956 through 1961. The peak events of this solar cycle were recorded in 1958 and 1959. This was the period showing the greatest solar particle radiation reaching the Earth.

The electromagnetic radiation from a solar flare is emitted only during the visible activity. However, the solar particles continue to arrive near the Earth for a few hours to several days after the visible activity has ceased. High energy protons, alpha particles and a few heavy nuclei of Z up to 9 or 10 emitted during the flare activity constitute the radiation hazard to space travellers outside of the trapped radiation (Van Allen) belts. Neutrons have not been detected in the primary solar flare radiation.

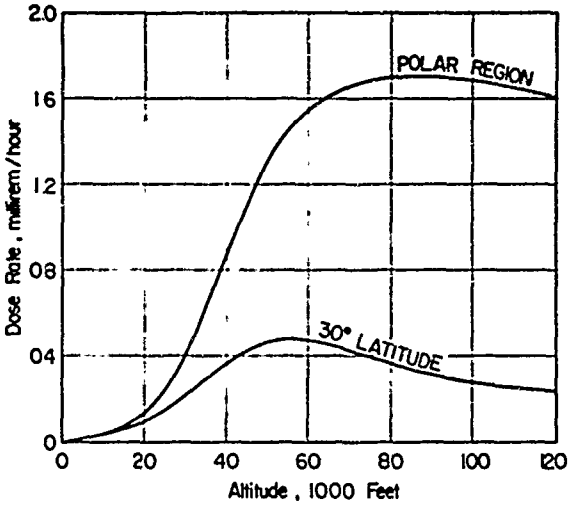


Figure 9–5. Altitude profiles of galactic radiation level at solar minimum. (Foelsche et al., 1969)

Table 9–5

Major Solar Cosmic Ray Outbursts Occurring 1956 – 1961

Solar Flare Data			Integrated Skin Dose (rad)	
Date		Importance	≥30 MeV	≥100 MeV
1956	Feb 23	3+	120	28
1957	Jan 20	3+	60	1.2
	Aug 29	Uncertain flare,		
	to 31	possibly two events)	15	
1958	Mar 23	3+	50	0.7
	Jul 07	3+	80	1.0
	Aug 22	3	20	0.15
	Aug 26	3	17	
1959	May 10	3+	440	10
	Jul 10	3+	148	11
	Jul 14	3+	177	7.4
	Jul 16	3+	125	19
1960	May 04	3+	16	0.07
	Nov 12	3+	205	33
	Nov 15	3+	100	12
1961	Jul 18	3+	27	3

(Modified from McDonald, 1963)

Evidence indicates that two classes of protons are produced during flare activity. The highest energy particles, 200 to 300 MeV, arrive first, within 5 to 20 minutes after the onset of the optical flare, and consist of high-velocity particles, about 0.6 times the velocity of light.

After about one-half hour, the second class of protons arrives, the average energy of which has fallen to below 100 MeV. Maximum intensity is reached one-half hour to one day after the beginning of the solar disturbance. The intensity slowly decreases over a period of several days. The variation with time of the spectral energy distribution and the flux density (number of particles/cm^2) is unpredictable.

During the period of solar activity between 1956 and 1962, about 30 flares occurred which would have produced a total tissue dose of more than one rad (as measured with plastic phantom material placed behind approximately 0.5 gm/cm^2 of aluminum) at 3000 kilometers or greater above the surface of the Earth. In four events, the potential tissue dose approached 1000 rads and exceeded 200 rads in 13 other flares. With the thickness of shields on present day spacecraft, the probability of a crewmember receiving a tissue dose of greater than 100 rads during a manned 30 day mission appears to be between 5 and 10 percent. However, this calculation must be tempered by the fact that crewmembers of all manned space missions to date have received total doses considerably less than this (see table 9-4).

The matter of variable solar particle radiation is of great importance for the selection of launch dates, particularly for long-term space missions. Table 9-6 shows the maximum and minimum doses calculated as a function of mission duration for the worst and best launch dates during a single period of solar activity. Fortunately, the selection of dates so far has been quite good since astronauts have received only nominal radiation exposures.

With the thrust presently available for spacecraft, it is impractical to provide the extensive shielding which would be required against high-energy protons. Thin shielding is of little value, inasmuch as protons and other charged particles give up increasingly more energy as they are slowed. The most intensive zone of ionization is at the end of their path, where it may be up to several orders of magnitude greater than at the beginning. The proton does not produce ionization having about the same LET (linear-energy-transfer) throughout the irradiated material, as would be produced by X- or gamma rays, but would produce a LET value a hundred times greater at the end of its path than at the beginning. The solar electrons encountered in space, as well as most of the remaining electromagnetic radiations, are of sufficiently low energy that they should not present a great hazard inside a vehicle, but could be hazardous during extravehicular activities.

The radiations that are constantly being given off from the sun, between periods of flare activity, consist of a large number of protons and electrons of low energy, ranging from a few electron volts for the electrons to approximately 5 MeV for the protons. The protons do not exist as simple

monoenergetic sources. They are found in complex spectra of energies and intensities.

Table 9–6

Maximum and Minimum Mission Doses*
for Best and Worst Launch Dates During Active Period of Cycle 19

Mission Duration	Maximum Dose (rads)	Minimum Dose (rads)
4 years	3492	2439
3 years	3229	974
2 years	2781	526
1.5 years	2415	176
1 year	2110	15
9 months	1963	2
6 months	1963	0
3 months	1962	0
1.5 months	1492	0
1 month	1452	0
2 weeks	1452	0
1 week	1452	0

*Surface dose inside 1 g/cm^2 uniform aluminum shielding.
(Langham, 1967)

Secondary Radiations

One of the principal problems in developing effective shielding for the occupants of space vehicles concerns secondary radiations. Whenever primary particles strike a spacecraft and its shielding material, secondary radiations are produced. Figure 9-6 illustrates the fates of particles meeting a manned vehicle. Electrons and positrons are stopped by the vehicle wall, which then emits the bremsstrahlung (gamma rays). Protons and heavy ions may hit a target in the wall, or within the cabin, or may pass right through the structures. Wherever a target is hit, these particles produce characteristic showers of secondary particles as shown. Whenever a primary particle with an energy of 300 MeV or greater hits a nucleus of target material, secondary particles and electromagnetic radiations are generated in great variety, as shown in figure 9-7.

The absorption of radiation in matter involves the transfer of all or some portion of the incident radiation energy to an electron or nucleus in the absorber mass. This may lead, as illustrated in figure 9-7 to the production of recoil protons, neutrons, electrons, X- or gamma radiation, or many other secondary particles. The space radiations are not qualitatively different from conventional radiations in this regard, but quantitatively the production of secondaries is somewhat unique. This is due to the presence in space of particles of unusually

high energies that can generate a cascade of secondary photons and particles. The exact nature of the secondaries will be a function of the incident particle and its charge and energy, the density of the absorbing or shielding material and its thickness, and the proximity of masses of different composition or elemental form (i.e., laminated shielding, capsule wall, and black boxes).

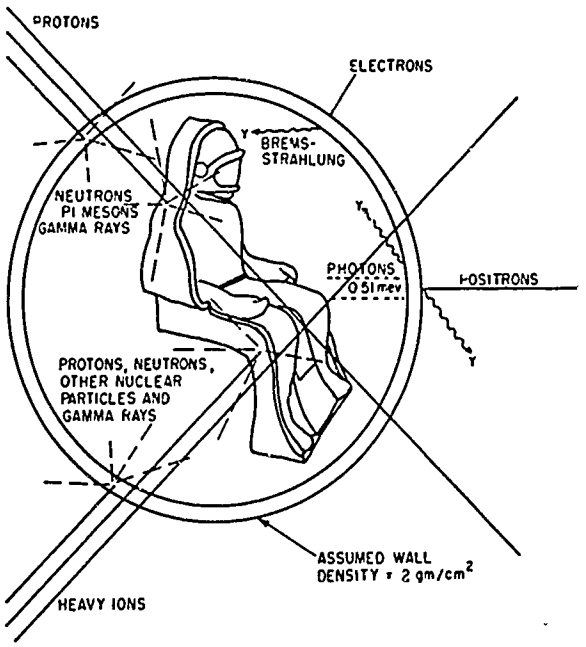


Figure 9–6. The fates of radiation elements striking a manned spacecraft. (Modified from Grahn, 1964)

Several studies have been initiated on the shielding problem, and these can be reviewed in the *Proceedings of the Symposium on the Protection against Radiation Hazards in Space* (1963). The biological importance of the problem is illustrated in figure 9-7 which demonstrates the buildup of secondary radiation dose in shielding material. In other words, while shielding is certainly an effective countermeasure, it does modify the quality of the radiation, which must then be considered the radiation of interest for biological consideration (Keller, 1962).

The complexity of the secondary radiation and shielding problem is illustrated further in figures 9-8a and 9-8b. These show the differential effectiveness of aluminum shielding against trapped protons and solar protons. Even heavy shielding is seen to be inefficient with regard to trapped protons although fairly effective with regard to solar protons. Still other shielding problems arise with intracapsular radiation sources such as might be found with isotopic power units or small reactors.

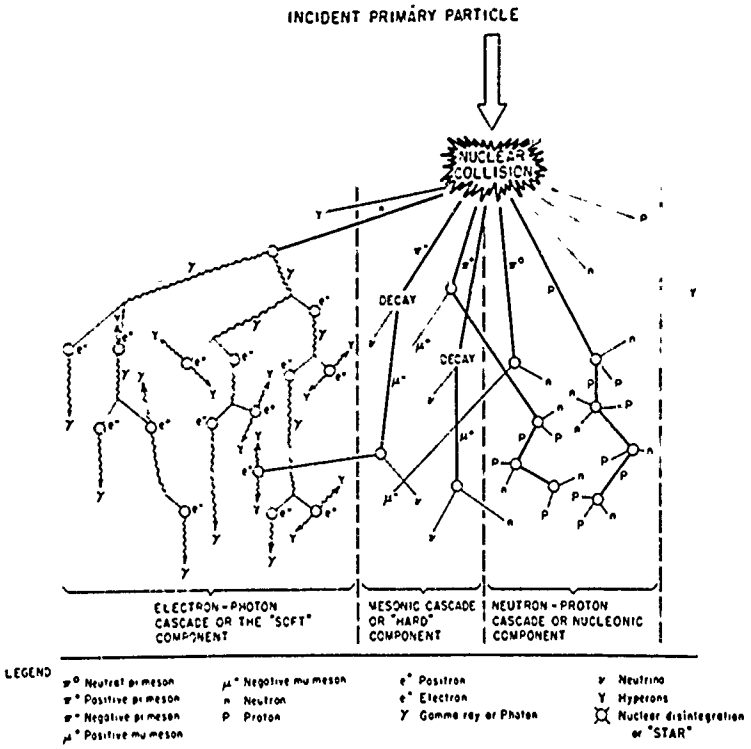


Figure 9–7. Generation of secondary particles and electromagnetic radiations following nuclear collision. (Saylor et al., 1962)

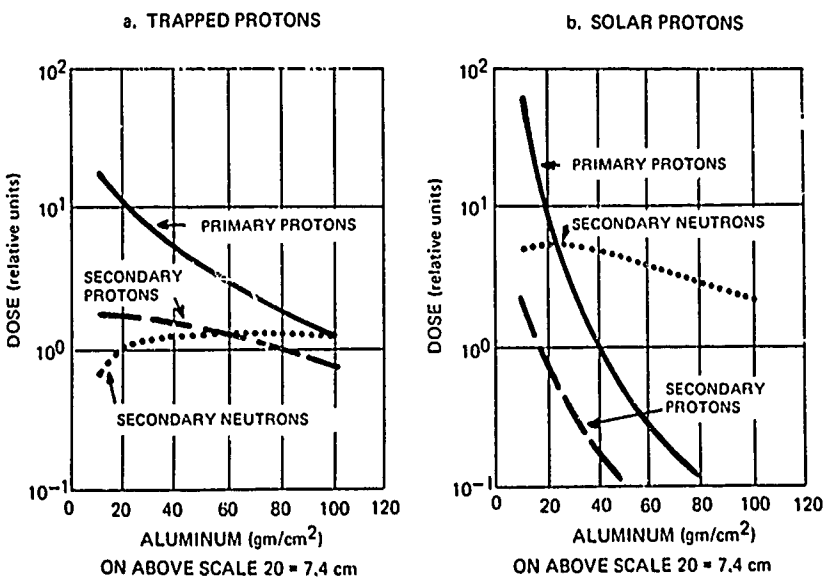


Figure 9–8. Effectiveness of aluminum shielding of varying weight against trapped and solar protons. (Keller, 1962)

Whole Body Radiation Effects

There is only limited information available concerning the effects of whole body radiation on man. Data on Japanese victims of World War II nuclear explosions constitute one source, although the relationship between exposure and aftereffects is in this case not a simple matter to interpret. Many other factors, such as the medical condition of the survivors at the time of exposure plus the complications of other injuries, make the issue a difficult one. Other data, from accidents involving radiographic equipment, industrial X-ray machines, cyclotrons, and nuclear reactors, are easier to interpret but are quite sparse.

In examining the whole body radiation effects, it should be noted that reliable information has been obtained for doses from 52 to 100 rem. As the dose increases from 200 to 600 rem, the data from exposed humans decrease rapidly and must be supplemented by extrapolations based on animal studies. Nevertheless, the conclusions drawn can be accepted with a reasonable degree of confidence. Beyond 600 rem, however, observations on man are so sporadic that the relationship between dose and biological effect must be inferred or conjectured, almost entirely from observations made on animals exposed to ionizing radiations (Glasstone, 1962).

Radiation Intensity

Figure 9-9 shows the relationship between median survival time and acute radiation dose for mice, rats, monkeys, and man. It can be seen that man is slightly more resistant to radiation effects than the animals until the dose rate reaches a level where death is a certainty within several days or less.

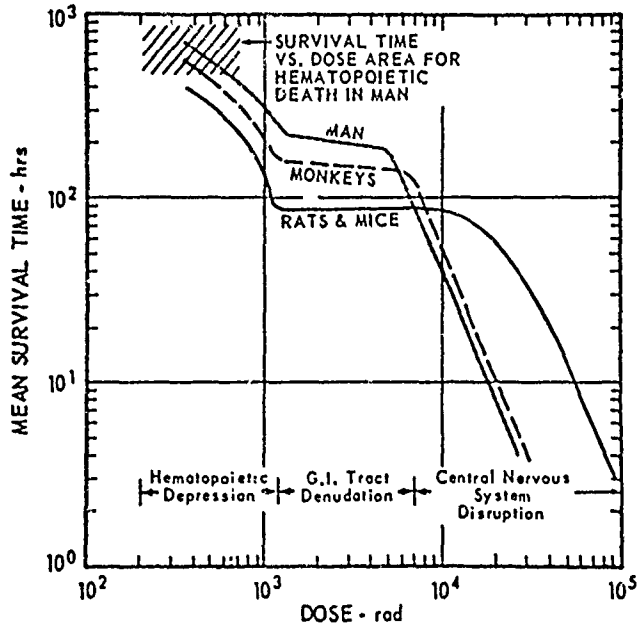


Figure 9–9. Relationship between median survival time and acute radiation dose for different species. (Langham, 1963)

Figure 9-10 shows the probability of death, for man, within a finite period (60 days) as well as the probability of initial symptomatology (nausea and vomiting). The relation is plotted for whole body radiation dosage and first symptoms of death. For exposures in the mid-lethal range and above, nearly all persons will experience severe nausea and vomiting within 5 hours of the time of exposure with a mean time of onset of about 2 hours. These probability plots are estimates based on accumulated experience from Japanese casualties, accidental exposure to fallout, reactor incidents and clinical experience.

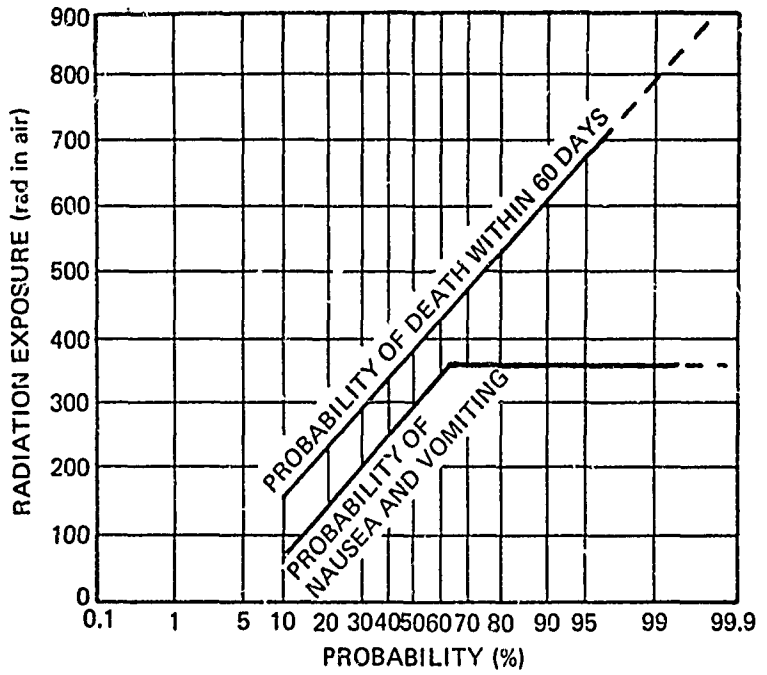


Figure 9–10. Relationship of whole body radiation dose and first symptoms of death. (Langham, 1967)

Changes in the probability of death as a function of radiation dose level and dose rate are shown in table 9-7. This table also shows the difference in the dose level producing a given probability of death as the time during which the radiation is received ranges from 1 day to 1 year.

The short term effects to be expected from acute whole body radiation are described in table 9-8. Dose levels discussed range from 10 rads, an easily survivable one-time event, to 5000 rads, an event in which ensuing death is certain for all individuals exposed. In examining table 9-8, it is of interest to note that doses of 100 to 200 rads were common in survivors of the Hiroshima and Nagasaki nuclear attacks, particularly among persons who were at some distance from the nuclear explosion (Glasstone, 1962).

Table 9–7

Some Conjectured Human Tolerances

	Day	Week	Month	4 Months	Year
A. Exposure dose (midline rads), Subcommittee No. 14 (NCRP)					
LD_0/time period	100	100	135	200	250
LD_{5-10}/time period	165	165	200	270	
LD_{50}/time period	300	300	340	370	
B. Dose* rate (R/min), Subcommittee No. 14 (NCRP)					
LD_0/time period	0.069	0.0099	0.0031	0.0012	
LD_{5-10}/time period	0.115	0.0164	0.0046	0.0016	
LD_{50}/time period	0.208	0.0298	0.0079	0.0021	

*Dose = R in air in phantom midline.
(National Council on Radiation Protection, 1962)

Table 9-8 shows that vomiting is one of the principal reactions to acute whole body radiation. A more clear definition of the incidence of vomiting as a function of dose level is shown in figure 9-11. The line represents the most likely given dose in hundreds of rads following acute exposure and indicates the 10 percent incidence when the radiation has been protracted over one day.

An idealized description of the time course of symptomatology of acute radiation illness following a mid-lethal acute exposure is shown in figure 9-12. The symptoms shown in this figure are predicated upon a radiation level of 250 to 500 rad. Of particular interest in figure 9-12 is the period around 10 days following exposure when an individual for a short period may be entirely free of any symptoms of radiation illness.

Rate-Effectiveness Factors

It is apparent that a low radiation dose rate, if received over a sufficient period of time, can have consequences as severe as those following a high dose rate for a short period of time. Table 9-9 presents rate-effectiveness factors (f_r) which can be used to equate radiation exposures for the production of three classes of symptomatology: erythema and skin desquamation, prodromal signs, and hematological depression and lethality. In general, this table shows that a low dose must be administered for 2 to 3 times as long as that considered a high dose rate if the same biological effects are to be produced.

Table 9–8

Expected Short-Term Effects From Acute Whole-Body Radiation

Dose in Rads	Probable Effect
10 – 50	No obvious effect, except, probably, minor blood changes.
50 – 100	Vomiting and nausea for about 1 day in 5%–10% of exposed personnel. Fatigue, but no serious disability. Transient reduction in lymphocytes and neutrophils.
100 – 200	Vomiting and nausea for about 1 day, followed by other symptoms of radiation sickness in about 25%–50% of personnel. No deaths anticipated. A reduction of approximately 50% in lymphocytes and neutrophils will occur.
200 – 350	Vomiting and nausea in nearly all personnel on first day, followed by other symptoms of radiation sickness, e.g., loss of appetite, diarrhea, minor hemorrhage. About 20% deaths within 2–6 weeks after exposure; survivors convalescent for about 3 months, although many have second wave of symptoms at about 3 weeks. Up to 75% reduction in all circulating blood elements.
350 – 550	Vomiting and nausea in most personnel on first day, followed by other symptoms of radiation sickness, e.g., fever, hemorrhage, diarrhea, emaciation. About 50% deaths within 1 month; survivors convalescent for about 6 months.
550 – 750	Vomiting and nausea, or at least nausea, in all personnel within 4 hours from exposure, followed by severe symptoms of radiation sickness, as above. Up to 100% deaths; few survivors convalescent for about 6 months.
1000	Vomiting and nausea in all personnel within 1–2 hours. All dead within days.
5000	Incapacitation almost immediately (minutes to hours). All personnel will be fatalities within 1 week.

*Author's change.
(Langham, 1967)

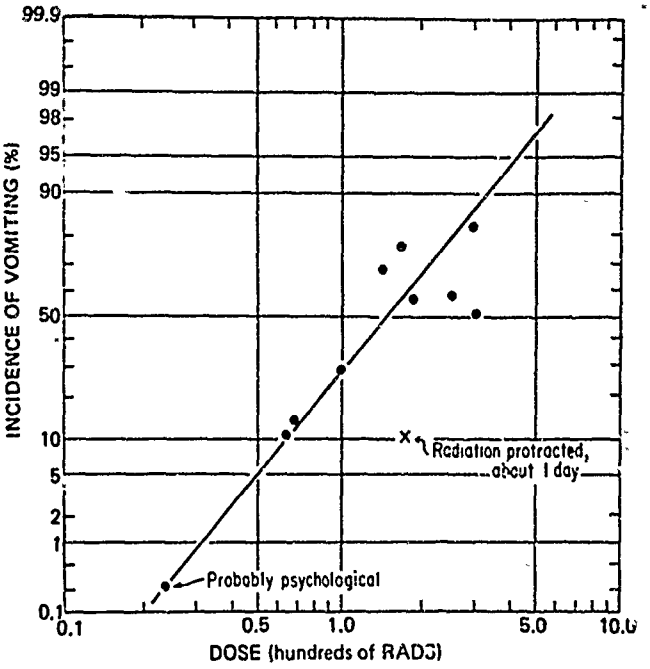


Figure 9–11. Incidence of vomiting as a function of radiation dose. (Langham, 1967)

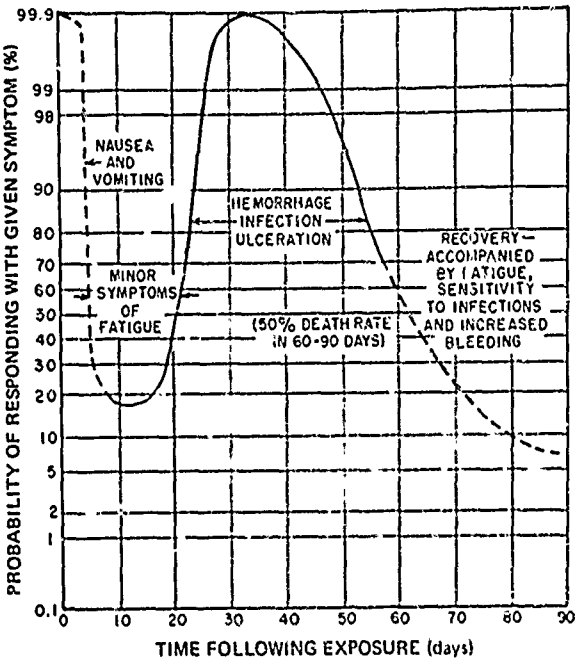


Figure 9–12. Changing symptomatology during acute radiation illness (From Glasstone, 1962; Saenger, 1963; and Cronkite et al., 1956)

Table 9–9

Suggested Dose-Rate or Rate-Effectiveness Factors (f_r) for Early Responses Following Exposure to Low-LET Radiations

	Duration of Exposure to Produce Same Response Level		
	Erythema and Skin Desquamation	Prodromal Signs	Hematological Depression and Lethality
High Dose Rate			
Duration of exposure for maximum effectiveness	1–2 hr or less	2–4 hr or less	1–2 days or less
Low Dose Rate			
Duration of exposure for minimum effectiveness	4–6 days or longer	2–4 days or longer	3–4 weeks
Ratio of total doses to produce same response level (B/A)	3	2.5	2
Rate-effectiveness factor (f_r)	1/3	1/2.5	1/2

(Adapted from National Committee on Radiation Protection and Measurements, 1962; Langham, 1967)

Radiation Effects on Specific Body Systems

Tissue

When radiation particles are absorbed in human tissue, there is an irradiation effect as a particle is slowed. Figure 9-13 presents a longitudinal section of the isodose line field in tissue for the terminal section of a cosmic ray heavy nucleus of Z = 20 (Ca). In this figure, the section from 280 to 0 micron residual range is the "thindown" part.

Figure 9-14 shows the calculated dose which might have been received from protons at various depths in tissue from Inner Van Allen belt and the solar proton event of 12 May 1959, assuming a spacecraft cabin providing only 2 gm/cm^2 of shielding. The greater drop of tissue depth-dose from flare protons as compared to inner belt protons is a function of the differences in the integral energy spectra; the greater frequency of higher energy protons in the inner belt increases the dose rate in deep tissues. Note the importance of knowing the integrated energy spectrum of the proton radiation when considering the critical targets–i.e., bone marrow, spleen, and intestinal locations beneath the surface.

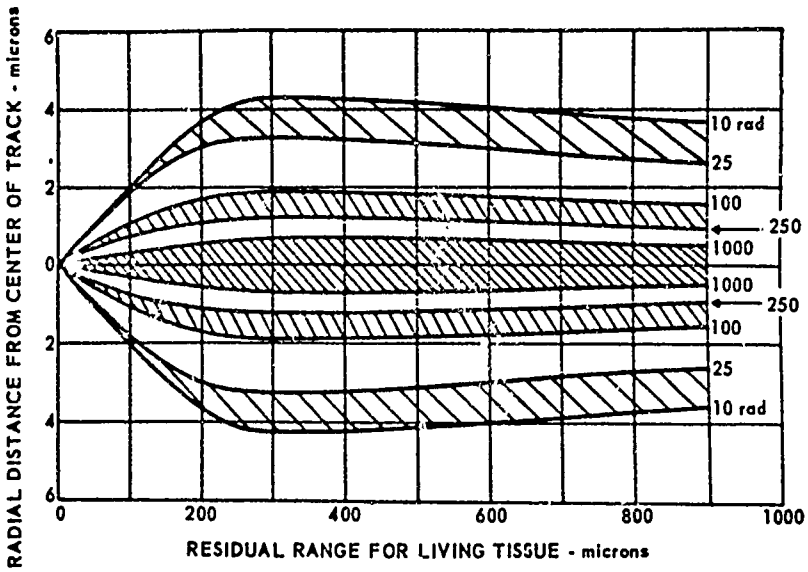


Figure 9–13. Longitudinal section of isodose line field for terminal section of cosmic ray nucleus of Z = (Ca). (Schaefer & Golden, 1960)

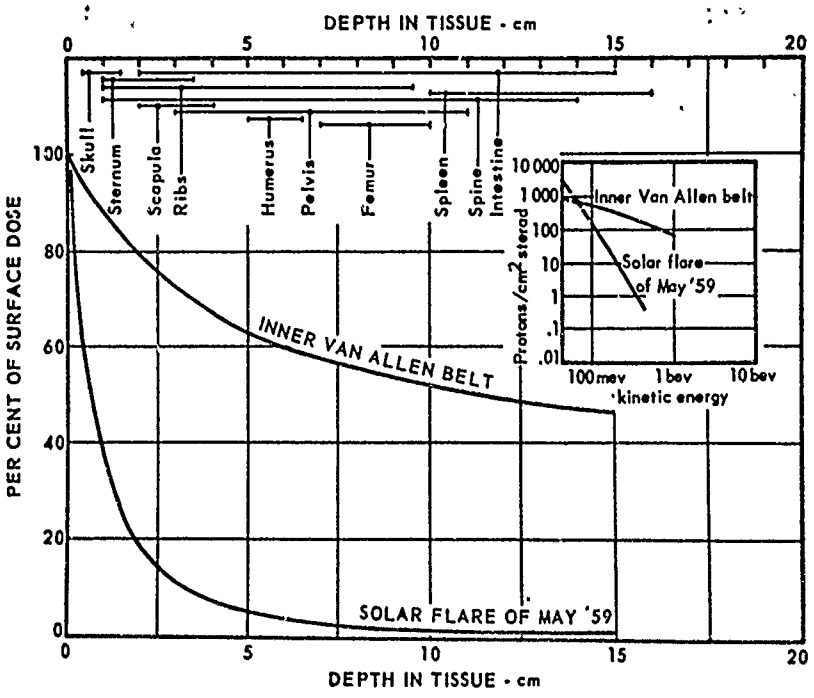


Figure 9–14. Calculated radiation dose from protons at various tissue depths – assuming shielding of 2 gm/cm2. (Schaefer, 1960)

Blood System

Radiation exposure produces a number of significant changes in the various elements of the blood. The extent of these changes is shown dramatically in figure 9-15 which presents average values of blood elements for five individuals exposed to estimated doses of 250 to 350 rads at the Oak Ridge Criticality Accident of 16 June 1958. Note that, whereas initial changes are seen in virtually all blood elements, the full extent of the damage may not be apparent until 25 to 40 days following the event. In view of the observed drops in red cell mass assumably due to oxygen effect, the effect of radiation on hematocrit and hemoglobin shown in figure 9-15 may be exaggerated.

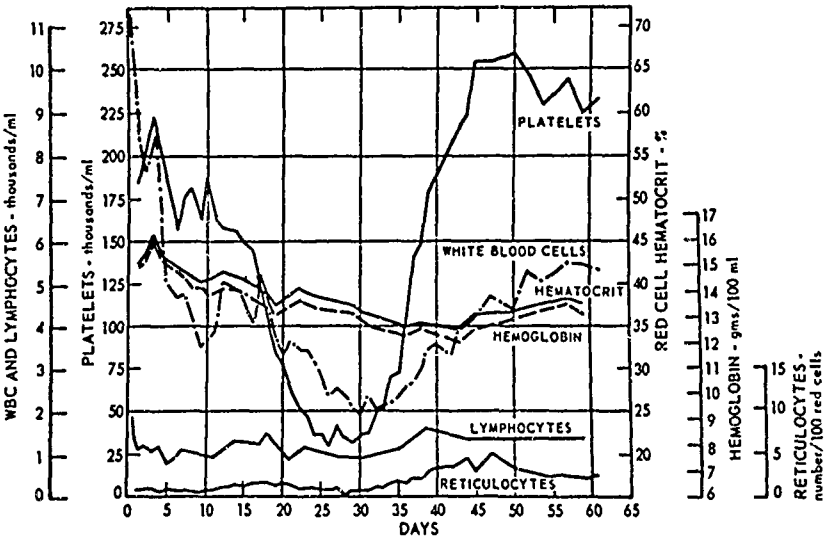


Figure 9–15. Change in blood elements for five individuals exposed to 250 to 350 rads. (Saenger, 1963)

The response of one individual to a brief whole body exposure of about 130 rads of fission gamma radiation is shown in figure 9-16. The curves in this figure emphasize the long persistence of radiation injury in man. The cellular elements of the blood show an early rapid decline in number, but do not reach a minimum for 4 to 5 weeks. The blood cell count remains at about 50% of normal for over a year, yet the affected individual, in this case, expressed no outward signs or symptoms of this injury. The individual was, undoubtedly, more susceptible to infection and his general response capability to any additional stress was probably depressed throughout the period of observation. Although no direct test was made for this individual, victims of other radiation accidents have complained of a persistent fatigue for many months after exposure.

Figure 9-17 shows the limits for receipt of radiation by a human without clinically detectable damage to the hematopoietic system. Individuals receiving continuous dose rates indicated on figure 9-17 would be expected

to show no overt symptoms relating to injury of blood forming tissues at the accumulated doses, dose rates, and times shown on the figure.

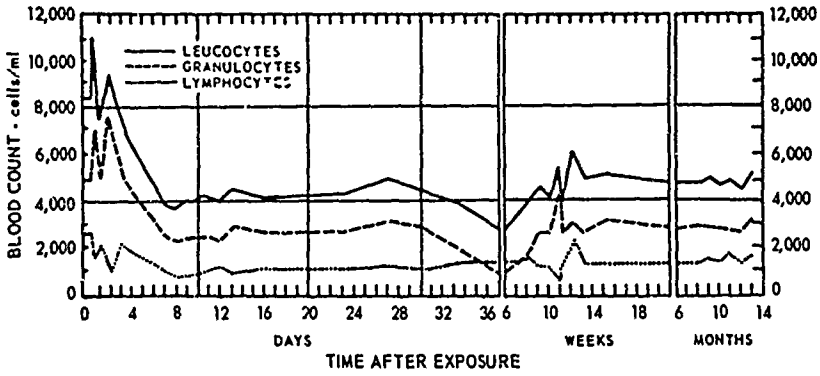


Figure 9–16. Blood element changes for one individual exposed to 130 rads. (Langham, 1963)

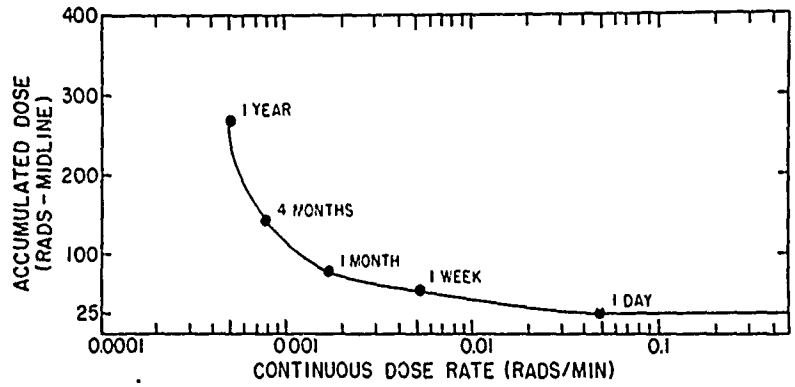


Figure 9–17. Continuous radiation exposures at the above level should produce no injury clinically measurable to the hematopoietic system. (Modified from Langham, 1967)

Radiation injury, by virtue of its effect on specific blood elements, could make an individual more susceptible to disease. This is shown in figure 9-18 which shows the depression of normal neutrophil count following exposure to acute radiation. Schematized levels of neutrophils in the blood are shown for varying exposures and are related to the times when infections are most prevalent. Only neutrophils are shown here as the predominant white blood cell involved in combating acute infections. Other white blood cells (lymphocytes and monocytes) also would be depressed as a result of radiation damage.

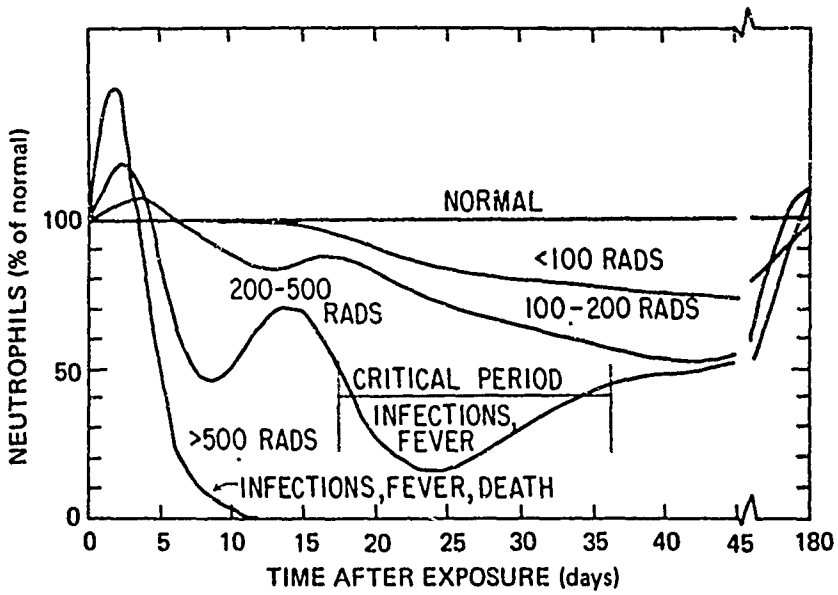


Figure 9–18. Schematized levels of blood neutrophils following different radiation exposures. (Adapted from Cronkite et al., 1956; Andrews, 1962; and Langham, 1967)

The effect of radiation on platelets formation is shown in figure 9-19. These curves indicate, for various exposure levels, the observed course of platelet counts over a 180 day period. Whenever platelet count falls below 40 to 50 percent of normal, bleeding and oozing from minor wounds and scrapes is hard to stop and hemorrhage is likely from such radiation-damaged tissues as the intestine.

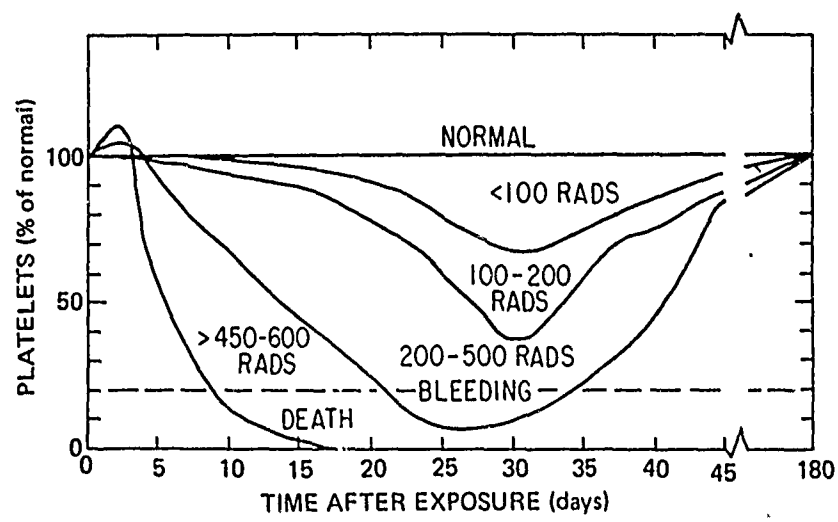


Figure 9–19. Observed course of platelet counts following different radiation exposures. (Langham, 1967)

One of the most dramatic demonstrations of the effect of radiation on blood systems comes from the increase in cases of leukemia recorded for survivors of the Hiroshima nuclear explosion, as shown in figure 9-20. This figure shows that leukemia in Hiroshima rose from a number of approximately one case per 100 000 people in 1946 to almost 18 per 100 000 by 1951, but has decreased in recent years (Ishimaru, 1971). This can be compared with only a slight increase (about double in 1960) in leukemia incidence for the rest of the Japanese population.

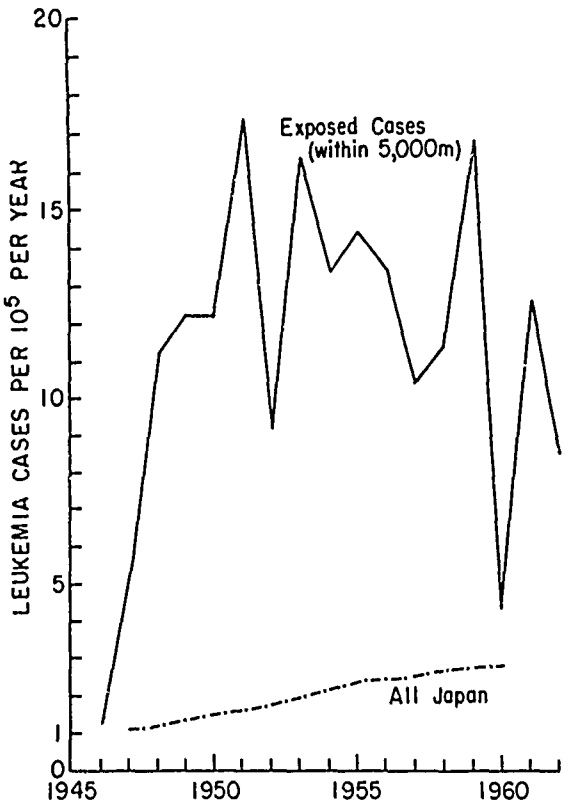


Figure 9–20. The incidence of leukemia cases reported in Hiroshima in the period 1946 to 1962. (Modified from data of Watanabe, 1961 by Brill et al., 1962; United Nations Committee on the Effects of Atomic Radiation, 1964)

A calculated probability of death from leukemia is about 10^{-6}/R/year for the first 15 to 20 years after brief exposure to whole body radiation. This probability is based on experience at rather high exposure dose rates (>25 R/min). Animal data clearly indicate that the response is less at low dose rates (<R/min), and assumably man would respond in a like manner. Experience of the A-bomb survivors suggests that most cases of leukemia develop within 15 or 20 years of exposure.

Since the astronauts are healthy adult males, their susceptibility can be assumed to be less than that of the general population. The probability of achieving doses high enough to induce cancer other than leukemia or cancer of the thyroid in astronauts is slight. With doses of 50 R and above, the probability of induction of leukemia is on the order of 10^{-6}/rad/year; that for cancer of the thyroid is in the same range, and that for other cancers is less by at least a factor of 10 (Brill et al., 1962; United Nations Committee on the Effects of Atomic Radiation, 1964).

The Skin

Radiation damage to the skin is of interest since this is the initial point of penetration for the radiation and also since changes are easily assessed. In general, it is found that higher radiation dose levels are required to produce demonstrable damage to the skin than is the case for the hematopoietic system. Table 9-10 shows four levels of damage occurring from acute exposure to X and gamma radiation. Note that approximately 350 rads must be received before significant changes begin to appear. In all cases, with the exception of extreme levels in excess of 2000 rads, the principal effect is not immediate but appears instead after an interval of several days to several weeks.

Table 9–10

Acute Radiation Damage to the Skin From X- and Gamma Rays

Epilation - loss of hair	Erythema (first degree burns)	Wet dermatitis and blistering (second degree burns)	Ulceration (third degree burns)
Rare at less than 200 r			
Partial epilation at 350-450 r	Response is dependent on energy, dose rate, area exposed, & complexion of the individual. Full effect in 1 to 3 weeks after:		
Complete epilation in 16-18 days at > 450 r	200-400 r (<150 kev)		
	500-600 r (200-400 kev)		
Permanent epilation at > 700 r	800-1000 r (>400 kev)		
	Response in first hours at 1000 r	Effect in 1-2 weeks at >1000 r	
			Rapidly progressive effect at > 2000 r

Note: 1 r ≅ 1 rad since these statements are based on air doses.
(From Grahn, 1964, adapted from Saenger, 1964 & Cronkite et al., 1956.)

Table 9-11 shows the dose level of high intensity radiation necessary to achieve a given probability level for the production of erythema and

desquamation of the skin. Note that with each of the clinical signs it is necessary to essentially double the dose rate in order to progress from a 10 percent probability of the symptom appearing to a 90 percent probability level. In either case, a high dose rate is required in order to produce the given symptoms. Figure 9-21 shows the effect of single and fractionated radiation in producing erythema and also moist desquamation, either of which would be partially or completely disabling, particularly in the wearing of a space suit.

Table 9–11

Estimated Absorbed Doses of High-Intensity Reference Radiation for Production of Erythema and Desquamation of the Skin*

Clinical Sign	Absorbed Dose for Probability of Response (rads)**		
	10%	50%	90%
Erythema	400	575	750
Desquamation	1400	2000	2600

*See Early Skin Effects, p. 60, Langham, 1967.

**Site of interest for dose estimation, 0.1 mm depth; area exposed, 35–100 cm^2.

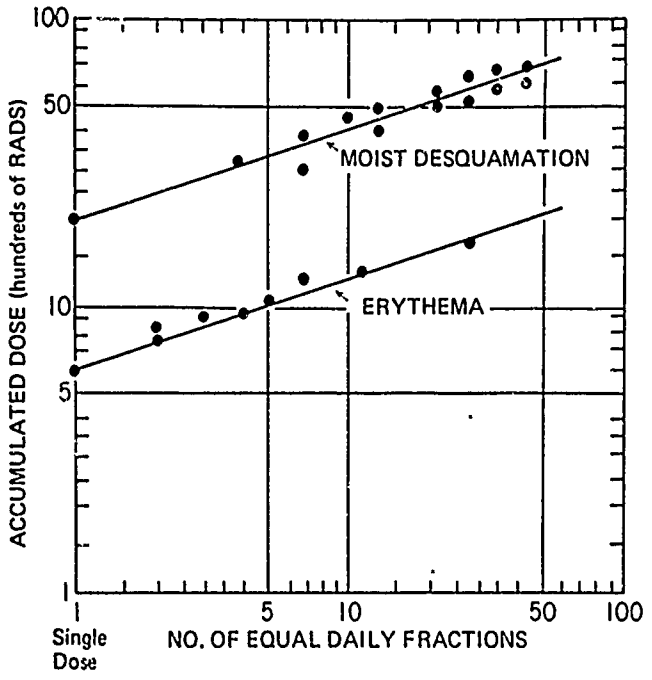


Figure 9–21. Effect of single and fractionated radiation in producing erythema and moist desquamation. (Modified from Langham, 1967)

Skin effects produced by exposure to electron radiation are indicated in figure 9-22. Electron radiation is of importance during extravehicular activity, the wall of the capsule being sufficiently dense for shielding. The space suit alone provides some protection. However, the abrasive and pressure effects of the space suit may make the skin more susceptible to radiation injury as is indicated in the figure (Langham, 1967; U.S. Air Force–National Aeronautics and Space Administration, 1969).

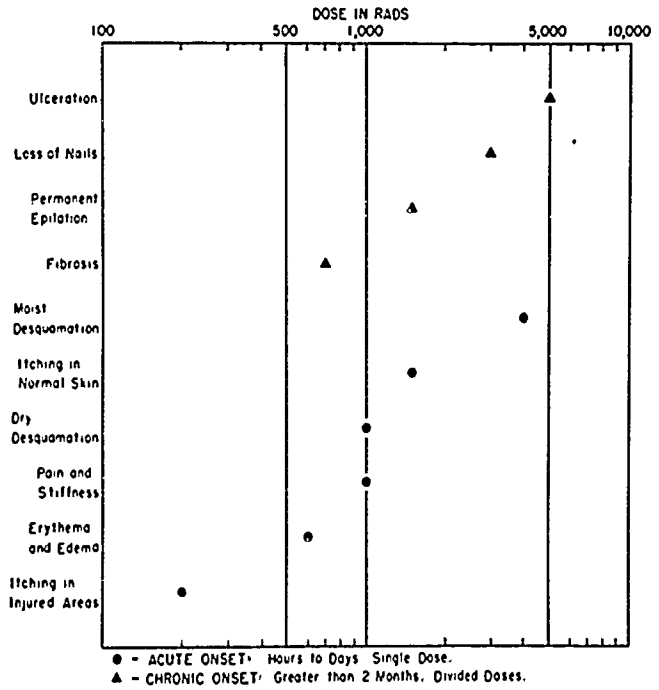


Figure 9–22. Skin effects produced by exposure to electron radiation. (U.S. Air Force–National Aeronautics and Space Administration, 1969)

Visual System

Data regarding the effect of ionizing radiation on the visual system come largely from reactions noted clinically following exposure to standard radiation sources. These data, as noted earlier, may underestimate the impact of space radiations for several reasons. First, solar or cosmic ray particles can produce very dense ionization tracks which would cause greater lens damage. Second, there are in space large numbers of low energy particles that can produce high surface damage. Third, there is the matter of induced secondary particulate and bremsstrahlung radiations that can augment the damage pattern. Figure 9-23 shows the incidence of lens opacities in man as a function of dose for X- and for gamma radiation delivered over a period of 3 weeks or less. This could be considered an acute exposure. Figure 9-24 shows the time-dose relationship for the

production of both cataract and non-cataract changes in the ocular lens for chronic exposures in which the exposure time is extrapolated for periods as long as 3 years.

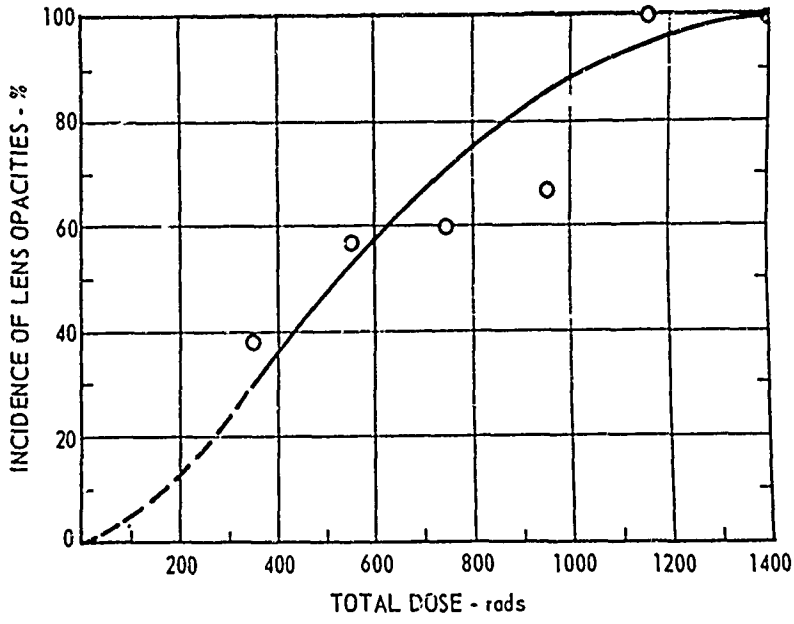


Figure 9–23. Incidence of lens opacities in man as a function of dose for X and gamma radiation delivered over three weeks or less. (Merriam & Focht, 1957)

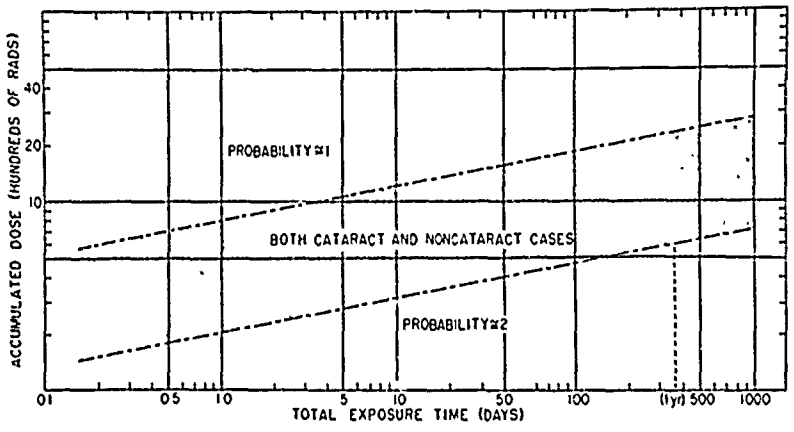


Figure 9–24. Extrapolated relationship for the production of late indication changes in the ocular lens. (Langham, 1967)

Reproductive System

The extent to which radiation exposure produces temporary or lasting damage to the reproductive system is an issue of concern for the planning of long duration space missions. Table 9-12 presents a summary of observations concerning the effects of high intensity X-ray exposure on spermatogenesis. In essence, it appears that at exposures of 15 to 100 rads, the response will probably be reduced fertility. From 100 to 300 rads, there will probably be temporary sterility for approximately one year or longer. Over 500 rads, the individual will probably not survive but, if so, permanent sterility would probably result.

Table 9–12

Summary of Observations of Effects of High-Intensity Doses of X-Rays on Spermatogenesis

Dose (rads)	Observed Effect on Sperm Count
15	Moderate oligospermia
20	Moderate oligospermia
50	Pronounced oligospermia
100	Marked oligospermia and azoospermia
200	Azoospermia
300	Azoospermia
400	Azoospermia
600	Azoospermia

(From Heller, 1966)

There is little information available on the effects of protracted radiation, but it is probable on the basis of studies in dogs that a dose of 0.5 rem/day will produce radiation damage within one year. Exposure at an average daily rate of 0.2 rem continued for 2 to 5 years will probably produce some temporary infertility. However, this would be without effect on libido or potency.

Late Effects of Radiation

It is characteristic of radiation damage that significant effects may not be evident for long periods of time, frequently years after the event or, as would be the case with genetic damage, even into subsequent generations. One of the most important long term features of radiation damage is a shortening of life expectancy. Figure 9-25 shows the estimated life expectancy of a 20-year old population exposed to fixed daily doses of whole body radiation, continued until time of death. Deaths would be from natural causes. While comparisons have been drawn between the effects of radiation and the normal process of

aging, the analogy is not complete. When radiation is delivered over a long period, there will be approximately a 1% shortening of the life span per 100 rads of exposure. For short periods of exposure at rates above 2 rads per hour, the life shortening effect will be multiplied by 5 (Storer, 1969).

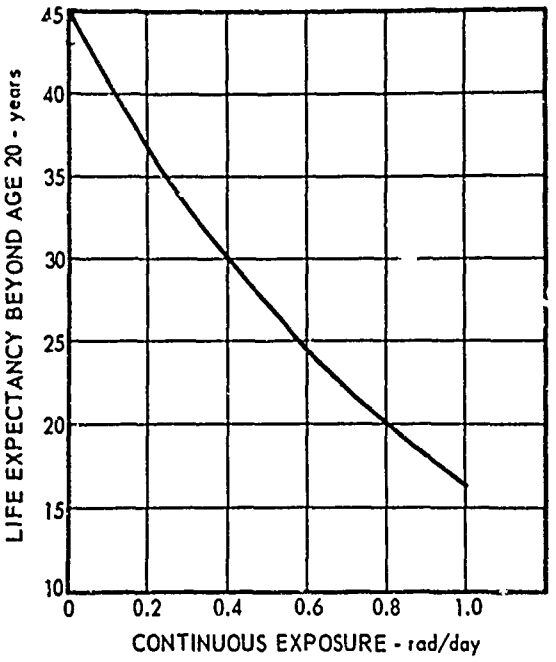


Figure 9–25. Estimated life expectancy of 20-year old population exposed to fixed daily doses of whole body radiation. (Adapted from Sacher & Grahn, 1964)

The effect of radiation intensity on life shortening is shown in figure 9-26. These projections, based on accumulated doses of penetrating ionizing radiation, show that high intensity radiation is appreciably more damaging than is low intensity with respect to anticipated life span.

Of a special concern with respect to radiation damage are possible genetic effects. Figure 9-27 shows the frequency of anticipated mutation for a total exposure dose delivered at two dose rates. The genetic effect is expressed as the probability of induction of recessive mutations in the male germ cell, since dominant lethals have relatively limited clinical significance in this selected population. Two probabilities are given: (a), for high dose-rate exposure, 25×10^{-8}/R/gene; (b), for low dose-rate exposure, 5×10^{-8}/R/gene. Although these data were obtained from mice, man is expected to respond similarly. If he has 10^4 genes per germ cell, then the probability of occurrence of a new recessive mutation is that shown in the figure. Additional information on mutation rate estimates is presented in table 9-13. Again, these estimates are derived from data obtained from the mouse and extrapolated to the human.

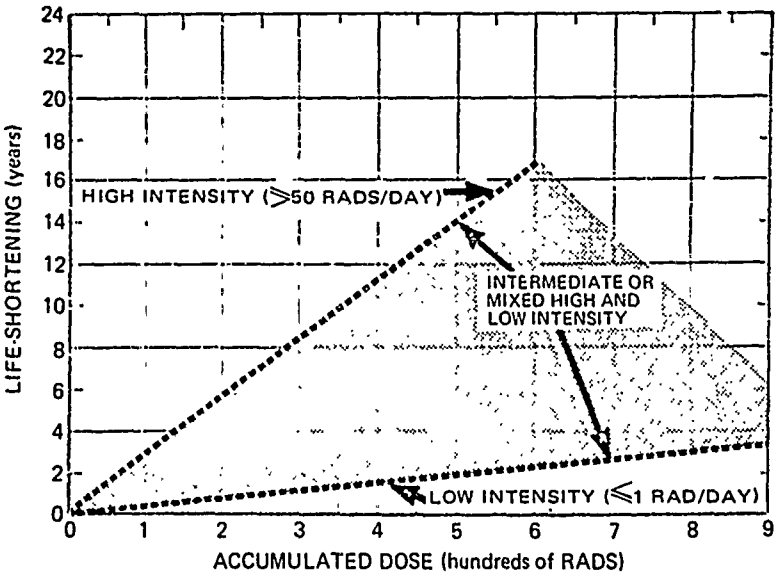


Figure 9–26. Life-shortening effect for low and high intensity radiation. (Langham, 1967)

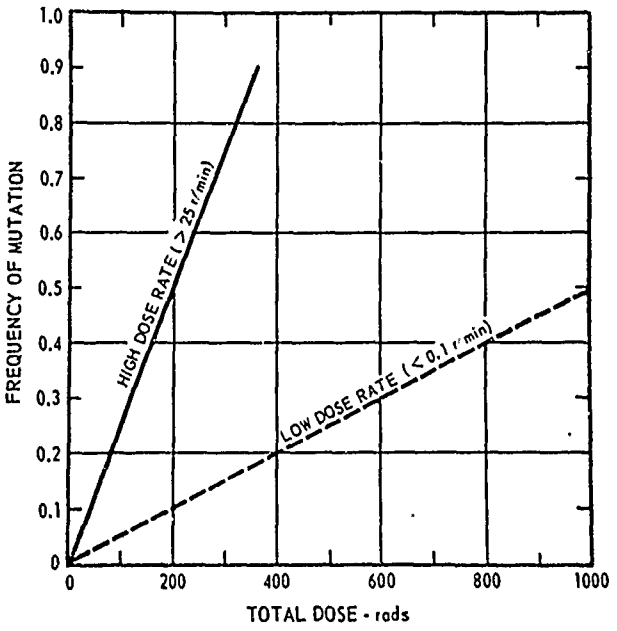


Figure 9–27. Probability of induction of recessive mutations in the male germ cell for different radiation exposures. (Russell et al., 1958)

Table 9–13

Mutation Rate Estimates for Males (Derived from the Mouse)

Mutation Type	Germ Cell Stage	
	Mature	Immature
A. High dose rate (>25 R/min)		
Dominant Lethal	1×10^{-3}/R/gamete	1×10^{-4}/R/gamete
Recessive Visible	5×10^{-7}/R/locus*	25×10^{-8}/R/locus*
Recessive Lethal	—	1×10^{-4}/R/gamete
B. Low dose rate (<1 R/min)		
Recessive Visible	Not applicable	5×10^{-8}/R/locus*
Recessive Lethal	Not applicable	2×10^{-5}/R/gamete

*Based upon 7 selected recessive visible mutant loci. The range of induced mutations is estimated to be on the order of $6–40 \times 10^{-5}$/gamete/R.

(Adapted by Grahn from available data)

References

Andrews, G. A. Criticality accidents in Vinca, Yugoslavia, and Oak Ridge, Tennessee. *Journal of the American Medical Association*, 1962, *179*, 191-197.

Barbiere, R. E., Sweeton, R. F., Sakalosky, G. P., & Klatt, P. E. A radiobiology guide. WADC TR 57-118 (I), Wright Air Development Center, Wright-Patterson Air Force Base, Ohio, June 1958.

Berry, C. A. Medical results of Apollo 14 – implications for longer duration space flights. Paper presented at XXIInd International Astronautical Congress. Brussels, Belgium, September 1971.

Brill, A. B., Tomonaga, M., & Heyssel, R. M. Leukemia in man following exposure to ionizing radiation, a summary of the findings in Hiroshima and Nagasaki and a comparison with other human experiences. *Annals of Internal Medicine*, 1962, *56*, 590-609.

Claus, W. D. (Ed.) *Radiation biology and medicine*. Reading, Mass.: Addison-Wesley Publishing Company, 1958.

Cronkite, E. P., Bond, V. P., & Dunham, C. L. (Eds.) Some effects of ionizing radiation on human beings. U.S. Atomic Energy Commission, TID-5358, Washington, D.C., 1956.

Foelsche, T., Mendell, R., Adams, R. R., & Wilson, J. W. Measured and calculated radiation levels produced by galactic and solar cosmic rays in SST altitudes and precaution measures to minimize implications at commercial SST-operations. RIF-FAUSST 7.3.3.02. NASA Langley Research Center, Hampton, Virginia, 1969.

Glasstone, S. (Ed.) *Source book on atomic energy*. (2nd ed.) Princeton, New Jersey: D. Van Nostrand Company, Inc., 1958.

Glasstone, S. (Ed.) *The effects of nuclear weapons*. Washington, D.C.: U.S. Atomic Energy Commission, 1962.

Grahn, D. Radiation. In P. Webb (Ed.) *Bioastronautics data book*. NASA SP-3006. Washington, D.C.: National Aeronautics and Space Administration, 1964.

Grahn, D. Late effects of external irradiations in animals and the prediction of low-dose effects. In *Biological implications of the nuclear age*. Proceedings of symposium held at Lawrence Radiation Laboratory, Livermore, California, U.S. Atomic Energy Commission, Division of Technical Information, Symposium Series CONF-690303, 1969.

Heller, C. G. Radiation damage to the germinal epithelium of man. Work in progress, reported to the Space Radiation Study Panel, 1966.

Hollaender, A. (Ed.) *Radiation biology*. Volumes I, II, and III. New York: McGraw-Hill, 1954.

Ishimaru, T., Hoshino, T., Ichimaru, M., Okada, H., Tomiyasu, T., Tsuchimoto, T., & Yamamoto, T. Leukemia in atomic bomb survivors, Hiroshima and Nagasaki, 1 October 1950–30 September 1966. *Radiation Research*, 1971, *45*, 216-233.

Jones, W. L. Space flight. In *U.S. Naval Flight Surgeon's Manual*. Washington, D.C.: Government Printing Office, 1968.

Keller, J. W. Long range NASA shielding requirements. In proceedings of the symposium on the protection against radiation hazards in space. U.S. Atomic Energy Commission, TID-7652, Washington, D.C., 1962.

Langham, W. H. Some radiobiological aspects of early manned space flight. Paper presented at the 4th International Space Science Symposium (COSPAR), Warsaw, Poland, 1963.

Langham, W. H. (Ed.) *Radiobiological factors in manned space flight*. Pub. 1487. Washington, D.C.: National Academy of Sciences–National Research Council, 1967.

Lea, D.E. *Actions of radiations on living cells*. (2nd ed.) Cambridge, England: Cambridge University Press, 1955.

McDonald, F. B. (Ed.) *Solar proton manual*. NASA Technical Report R-169. Goddard Space Flight Center, Greenbelt, Maryland, December 1963.

Mayo, A. M. Human activity in space cabin design. Personal equipment. Douglas Aircraft Company TP No. 540, Santa Monica, California, 1958.

Merriam, G. R. & Focht, E. F. A clinical study of radiation cataracts and the relationship to dose. *American Journal of Roentgenology and Radiation Therapy*, 1957, 77, 759-785.

National Committee on Radiation Protection and Measurements. Exposure to radiation in an emergency. NCRP Handbook No. 29, National Bureau of Standards, U.S. Department of Commerce, Washington, D.C., January 1962.

National Committee on Radiation Protection and Measurements. Permissible dose from external sources of ionizing radiation. NCRP Handbook No. 59, National Bureau of Standards, U.S. Department of Commerce, Washington, D.C., September 1954.

Newell, H. E., & Naugle, J. E. Radiation environment in space. *Science*, 1960, *132*, 1465-1472.

Pickering, J. E. Biological effects of whole-body proton irradiation. *Aerospace Medicine*, 1963, *34*, 942-943.

Russell, W. L., Russell, L. B., & Kelly, E. M. Radiation dose rate and mutation frequency. *Science*, 1958, *128*, 1546-1550.

Sacher, G. A., & Grahn, D. Survival of mice under duration-of-life exposure to gamma rays. I. The dosage-survival relation and the lethality function. *Journal of the National Cancer Institute*, 1964, 32, 277-321.

Saenger, E. L. (Ed.) *Medical aspects of radiation accidents*. Washington, D.C.: U.S. Atomic Energy Commission, 1963.

Saylor, W. P., Winer, D. E., Eiwen, C. J., & Carriker, A. W. Space radiation guide. AMRL TDR 62-86, 6570th Aerospace Medical Research Laboratories, Aerospace Medical Division, Wright-Patterson Air Force Base, Ohio, August 1962.

Schaefer, H. J. Tissue ionization dosages in proton radiation fields in space. *Aerospace Medicine*, 1960, *31*, 807-816.

Schaefer, H. J. A note on the RBE of proton radiation in space. USN AMC 61-18, U.S. Naval School of Aviation Medicine, Pensacola, Florida, January 1961.

Schaeffer, H. J., & Golden, A. Solar influences on the extra-atmospheric radiation field and their radiobiological implications. In Otis O. Benson, Jr., & Hubertus Strughold *Physics and medicine of the atmosphere and space*. New York: John Wiley & Sons, 1960.

Sondhaus, C. A. Biological effects of high energy protons. In Proceedings of the symposium on the protection against radiation hazards in space. TID-7652, U.S. Atomic Energy Commission, Washington, D.C., 1962.

Sondhaus, C. A., & Evans, R. D. Dosimetry of radiation in space flight. In F. H. Attix, W. C. Roesch, & E. Tochilin *Radiation dosimetry, sources, fields, measurements and applications*. Vol. III. (2nd ed.) New York & London: Academic Press, 1969.

Storer, J. B. Late effects: extrapolation to low dose rate exposures. *Health Physics*, 1969, *17*, 3-9.

Report of the United Nations Scientific Committee on the Effects of Atomic Radiation. General Assembly Official Records: 17th Session, Supplement No. 16 (A/5216), New York, 1962.

Report of the United Nations Scientific Committee on the Effects of Atomic Radiation. General Assembly Official Records: 19th Session, Supplement No. 14 (A/5814), New York, 1964.

United Nations Scientific Committee. Ionizing Radiation: Levels and effects. *Effects.* Vol. 2. United Nations Publication No. E72IX18, Annex 8, 1972.

U.S. Air Force–National Aeronautics & Space Administration *Ad Hoc* Committee on Electron Therapy. Final Technical Documentary Report. Brooks Air Force Base, Texas, December 1969.

U.S. Atomic Energy Commission. Proceedings of the symposium on the protection against radiation hazards in space, Gatlinburg, Tennessee, November 1962. AEC TID-7652, Book 1: *Radiation environment in space; effects of space radiation on radiosensitive objects; biological effects of space radiation*, Washington, D.C.: U.S. Atomic Energy Commission, 1963.

U.S. Atomic Energy Commission. Proceedings of the symposium on the protection against radiation hazards in space, Gatlinburg, Tennessee, November 1962. AEC TID-7652, Book 2: *Shielding against space radiations*, Washington, D.C.: U.S. Atomic Energy Commission, 1963.

Watanabe, S. On the incidence of leukemias in Hiroshima during the past fifteen years from 1946 to 1960. *Journal of Radiation Research*, 1961, 2(2), 131-140.

Weber, W. R. In *An evaluation of the radiation hazard due to solar particle events.* Aerospace Division, Boeing Company, Seattle, Washington, 1963.

White, T. T., Robbins, D. E., & Hardy, A. C. Radiation environment for the 1975-1985 space station program. MSC Document No. MSC-00183, NASA Manned Spacecraft Center, Houston, Texas, October 1969.

CHAPTER 10

TOXICOLOGY

by

J.D. MacEwen, Ph.D.
SysteMed Corporation
Dayton, Ohio

Rapid advances in the United States manned spacecraft programs have emphasized the importance of careful environmental control of space cabin atmospheres. The need for control applies not only to the concentrations of breathing gases at various cabin pressures but also to the levels of contaminants present in the environment. A unique aspect of toxicology has been developed in an attempt to provide the information necessary for the establishment of safe levels of space cabin contaminants.

Both facilities and techniques have been developed in recent years to explore the toxicological problems of space flight under simulated flight conditions, with the exception of weightlessness. These research programs are designed to establish safe limits for environmental contaminants under continuous exposure conditions of space flight and to define emergency tolerance limits for accidental situations. The information derived from these programs unfortunately lags behind the general advances of the space program and consequently many atmospheric limits have had to be established by committee action to provide engineering guidelines. The selection of limits by any committee is based on available toxicological information for each material considered. This information, frequently sparse, has been based on acute exposures of short duration or, at best, chronic daily exposures simulating industrial working conditions. The circumstance of the immediate need for contaminant limits for non-comparable conditions frequently causes selection of limits having extremely large safety factors for use until better information can be obtained. Provisional limits for a number of space cabin contaminants, with such safety factors, have been established for 90 and 1000 day continuous exposures by the Panel on Air Standards for Manned Space Flight (1968).

A discussion of the terminology of the units of contaminant concentration is in order since the conventional units of parts per million (ppm) is applicable

Reviewed by Ralph Wands, M.D., National Academy of Sciences.

only at the normal atmospheric pressure of 760 mm Hg experienced here on Earth. NASA has chosen to define contaminant concentrations as millimoles per 25 cubic meters (m mole/25M^3) since the number before the unit is essentially the same as for ppm, which is based on standard temperature and pressure conditions. In addition to other reasons, the use of molarity permits direct interpretation of the standards in the light of available biochemical knowledge. Other groups have selected the unit of milligrams per cubic meter (mg/M^3) which expresses the concentration in terms of volume regardless of absolute pressure. The latter term also is comparable with units in use by toxicologists for setting industrial threshold limits on contaminants. The experimental data presented in this chapter are given with units of ppm or mg/M^3 wherever applicable since these are the terms used in the research cited.

Oxygen Toxicity and The Effects of Variations In Oxygen Partial Pressure on Toxicity

The advent of manned space flight brought about a need for information concerning the physiological and toxicological response of animals and humans to prolonged exposure in enriched oxygen environments at reduced pressure. While considerable information had been obtained concerning the toxicity of oxygen at atmospheric pressure by Bert (1878), Bean (1953), Comroe and Dripps (1945), Ohlsson (1947), and Weir et al. (1965) and at hyperbaric pressures by Bean (1945) and Smith et al. (1932), little was known concerning the toxic response of man or other species to oxygen under hypobaric conditions.

Herlocher et al. (1964) measured the physiological response of men exposed to essentially pure oxygen at 258 mm Hg pressure (5 psia) for a 30-day period. Their clinical observations indicated that no significant changes occurred which were not associated with the prolonged confinement of these men. Robertson et al. (1964) described respiratory studies conducted on the human subjects used in the experiment reported by Herlocher. The most significant result of this study was that vital capacities decreased on depressurization to 250 mm Hg. The entire gas supply to the chamber was essentially pure oxygen, which resulted in an alveolar pO_2 of 177 mm Hg as opposed to the normal alveolar pO_2 of 100 mm Hg cited by Dittmer and Grebe (1958). These investigators found that the vital capacity of the individual test subjects returned to normal immediately upon repressurization to ambient atmospheric conditions.

Since hematopoietic decreases at increased partial pressures of alveolar oxygen tension had been previously reported (Helvey et al., 1963, Mammen et al., 1963, and Morgan et al., 1963), Zalusky et al. (1964) studied the hematopoietic parameters of the subjects included in the study reported by Herlocher et al. (1964). These investigators found that no significant decreases occurred during a 30-day exposure period with the exception of a slight change in hematocrit values.

Continuous exposure studies on animals conducted in reduced pressure chambers at Wright-Patterson Air Force Base showed increased mortality in rats

exposed to 100 percent oxygen at 5 psia pressure. McNerney and MacEwen (1965) reported that the rodent mortality was uniform in all chambers whether a contaminant was present or not. Ambient air control rats did not exhibit a similar mortality pattern. Subsequent experiments conducted by MacEwen and Haun (1966) determined that this was a strain-specific effect of the Wistar rats used and was not related to reduced pressure–enriched oxygen environments. The more important finding of those studies was the clearer understanding of oxygen toxicity at near ambient pressures. The mortality observed at various absolute oxygen pressures is illustrated in figure 10-1. While dogs and mice exhibit essentially a similar pattern of oxygen toxicity response, the albino rat is shown to be much less susceptible to oxygen toxicity than any of the other three species tested, as had been reported earlier by Smith et al. (1932) and by Boycott and Oakley (1932). Rhesus monkeys were not as consistent as the other species in their mortality response but no mortality was seen at total oxygen pressures below 600 mm Hg.

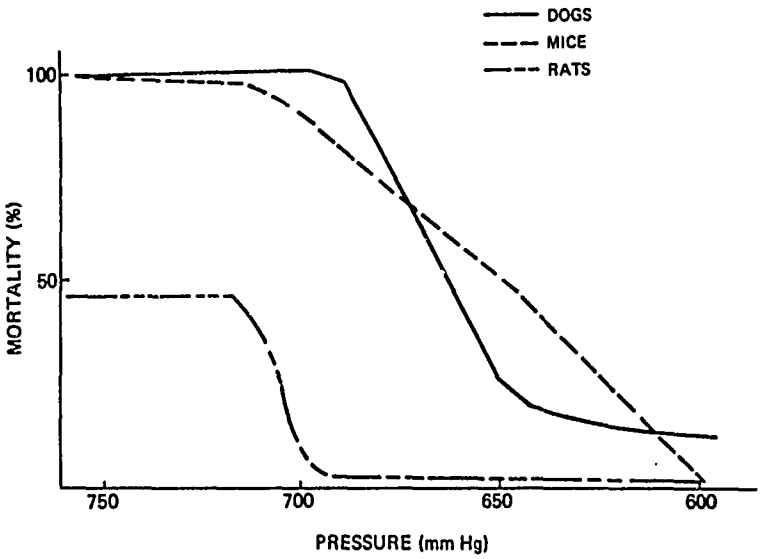


Figure 10–1. Oxygen toxicity mortality at varying absolute near-ambient pressures in experimental animals.

Kistler et al.(1967) described the pathological picture of oxygen toxicity at 760 mm Hg pO_2 to be one of pulmonary edema with resolution of the edema resulting in morphometic changes in the air-blood barrier. Death appears to result from the acute pulmonary edema formed. Dickerson (1964) and Kydd (1967) have shown that the lowest oxygen pressure that will produce acute pulmonary edema in the rat is about 650 mm Hg although rats surviving a 30-day exposure to oxygen at 516 mm Hg pressure were found to have thickening of the walls of small blood vessels of the lungs associated with pulmonary hypertension. Kydd (1968) showed that preexposure of rats to 518 mm Hg total oxygen pressure decreased the mortality expected at

760 mm Hg pO_2. He postulated that this protective effect was due to development of maximal lymphatic drainage of lung fluids formed at the lower pressure so that drainage was still in excess of fluid formation even at 760 mm Hg pO_2.

Continuous long-term exposures of four animal species to 100 percent oxygen at 5 psia pressure was reported by Kaplan et al. (1968). This exposure of dogs, monkeys, mice, and rats conducted for 8 months, produced no evidence of systemic oxygen toxicity. Electron microscopy showed changes in the lungs of these dogs and rats that could be related to the oxygen exposure as reported by Lewerenz et al. (1967). The change seen was minimal in nature and could not be associated with any apparent pulmonary functional deficit.

A similar study of continuous exposure of the same animal species to a mixture of 68 percent oxygen and 32 percent nitrogen at 5 psia was described by Fairchild (1967). In these studies, verified by a second 8 month continuous exposure to the same conditions one year later, the only significant and repeatable finding was the depression of growth of male rats in the test environment. The prolonged breathing of pure oxygen at near ambient or hyperbaric pressure has been shown to produce pathologic changes, such as pulmonary edema, and death. However, none of the controlled laboratory experiments with animals or humans breathing pure oxygen at reduced pressures (pO_2 less than 400 mm Hg) has shown any harmful effect.

Effects of Oxygen on the Toxicity of Ozone and Nitrogen Dioxide

The effect of variation in oxygen partial pressure upon the acute toxicity of inhaled ozone and nitrogen dioxide has been reported by MacEwen (1966). One-hundred percent oxygen at 253 mm Hg was shown to be protective against the acute effects of ozone exposure. Table 10-1 shows the results of a series of experiments in which animals were exposed continuously to 8.0 mg/M^3 ozone for a 14-day period. Increased partial pressure of oxygen resulted in reduced mortality among mice, rats, dogs and monkeys. Differences were also observed in the lung weight to body weight ratios, shown in table 10-2 for the various test environments. The intermediate pO_2 of the mixed gas environment resulted in the highest weight ratio while exposure of monkeys at near ambient pressure resulted in an essentially normal pattern.

These studies demonstrated differences in time of onset and severity of toxic responses in animals to O_3 and NO_2. While a beneficial protective effect of increased O_2 partial pressure against O_3 toxicity was shown, it was only demonstrated up to a pO_2 of 260 mm Hg. Higher O_2 concentrations may not be protective, as shown by Mittler (1958), and in fact, may be synergistic in action.

A protective action of O_2 against NO_2 toxicity was not clearly shown, although increasing pO_2 to 260 mm Hg appeared to prolong the life of animals exposed to lethal concentrations. There was, however, a reduction of mortality response in both mixed gas and 100 percent O_2 reduced pressure (5 psia) environments compared to ambient pressure conditions.

Table 10–1

Mortality Produced During 14-Day Continuous Exposure to Ozone – 8.0 mg/M^3

Exposure Conditions					
Total pressure (mm Hg)	700	260	260	720	700
pO_2 (mm Hg)	140	175	260	260	260
Gas supply	Air	68% O_2- 32% N_2	100% O_2	36% O_2- 64% N_2	36% O_2- 64% N_2
Species (No. deaths/No. Controls)					
Mice	33/40	32/40	33/40	—	16/40
Rats	50/50	45/50	45/50	—	15/50
Guinea pigs	8/8	9/9	8/8	—	—
Dogs	5/5	6/8	2/8	0/8	2/8
Monkeys	2/4	1/4	0/4	0/4	0/9

Toxicity of Fuels and Oxidizers

One criterion for the selection of compounds as suitable propellant fuels and oxidizers is that their combustion exhaust gases consist of low molecular weight species since the specific impulse (thrust/unit mass of fuel) is an inverse function of that molecular weight. Therefore compounds selected as fuels must be highly reactive materials containing elements of low atomic weight. Usually the more reactive fuels and oxidizers are more reactive with one another than they are with biological materials. This high reactivity generally results in a high order of toxicity in the more useful fuels and oxidizers.

Hydrazines

Hydrazine and its methylated derivatives meet the criteria for propellant fuels and are used as such. The Titan II rocket uses a mixture of hydrazine and unsymmetrical dimethylhydrazine (UDMH) as a fuel while both the Gemini and Apollo space vehicles use monomethylhydrazine (MMH) in their attitude control systems.

A comprehensive review of research on the pharmacology and toxicology of propellant hydrazines by Clark et al. (1968) reports 273 studies on these compounds. Further studies on MMH toxicity have been reported by Haun et al. (1968) and MacEwen and Vernot (1970).

The acute toxicity of all the propellant hydrazines manifests itself on the central nervous system resulting in convulsions and death. Death usually occurs during or immediately following a severe convulsive seizure. The principal difference between these compounds in their acute effects is the dose required

Table 10–2

Effect of Ozone on Lung Weight to Body Weight Ratio for a 14-Day Continuous Exposure (Chamber Concentration – 8.0 mg/M^3)

	Exposure Conditions					Unexposed Controls
Total pressure (mm Hg)	700	260	260	720	700	
O_2 (mm Hg)	140	175	260	260	260	
Gas supply	Air	68% O_2- 32% N_2	100% O_2	36% O_2- 64% N_2	36% O_2- 64% N_2	
	Lung Weight/Body Weight					
Beagle dogs						
Males (4) test	.033	.041	.029	.019	.026	.012
Females (4) test	.039	.053	.020	.018	.014	.010
Monkeys						
Males (2) test	.016	.021	–	.011	.012	.009
Females (2) test	–	.018	.010	.012	.009	.007
Rats						
Males (25) test	.026	.024	.021	–	.021	.006
Females (25) test	.027	.025	.025	–	.019	.008

to initiate the convulsive action. Jacobson et al. (1955) reported the relative order of toxicity for hydrazine and its methylated derivatives as shown in table 10-3. Similar data were reported by Weir et al. (1964). MMH is approximately twice as toxic as UDMH and symmetrical dimethylhydrazine (SDMH) and is at least five times more toxic than hydrazine. In general, there is a species gradient for the acute toxicity of the propellant hydrazines with rats and monkeys least susceptible and mice and dogs most susceptible. Since susceptibility of the various species to these compounds does not show a consistent pattern based on progression in size, it is impossible to predict where man falls in this order. Therefore, any use of such toxicity data in establishing safety standards must utilize the results of the most susceptible species.

Table 10–3

LC_{50} Values of Rats and Mice Exposed Four Hours to Hydrazine Derivatives

Compound	LC_{50}			19/20 Confidence Limits (ppm)	Slope	S.E. of Slope
	Species	(ppm)	(mg/M^3)			
Hydrazine	Rats	570	750	504 – 649	7.32	1.8
	Mice	252	330	–* – 305	3.79	1.6
Methylhydrazine	Rats	74	139	71 – 78	28.50	7.9
	Mice	56	105	50 – 110	4.96	2.2
uns-Dimethylhydrazine	Rats	252	618	219 – 290	8.65	2.8
	Mice	172	423	150 – 194	8.52	1.9
s-Dimethylhydrazine	Rats	280–400**		–	–	–

*Lower limit is not calculable from the data.

**Rough estimate.

(Jacobson et al., 1955)

Subacute exposures to monomethylhydrazine have been shown to produce decreased performance in trained primates at subconvulsive doses by Reynolds and Back (1966). Similar changes in the learned performance of cats have also been reported by Sterman et al. (1968). Reynolds and others (1963, 1964) reported changes in primate learned behavior and discrete avoidance tasks. Kidney damage has been reported from hydrazine exposure by Weatherby and Yard (1955) and by Krop (1954). MMH-induced kidney damage was described by Pinkerton et al. (1967), George et al. (1968), and Sopher et al. (1968). A decrease in renal blood flow resulting from hydrazine exposure was also described by Coe and Korty (1967).

Acute effects and death from severe propellant hydrazine exposures may be prevented by rapid therapeutic treatment using barbiturates or barbiturates in combination as suggested by Azar et al. (1970). Phenobarbital or other barbiturate preparations will suppress the convulsant seizures and provide protection through the acute intoxication phase until the propellant hydrazine has metabolized. It has been shown that pyridoxine, a form of vitamin B, will prevent fatty liver changes from hydrazine. A method of pyridoxine treatment has been recommended by Back et al. (1963).

The chronic effects of UDMH exposure have been reported by Rinehart et al. (1960). They exposed three dogs daily to a 5 ppm UDMH concentration for a 6-month period. The exposed dogs were lethargic throughout the exposure period and exhibited a mild hemolytic anemia (approximately a 15 percent depression of hematologic values) which persisted. A similar 3-month exposure of dogs to 25 ppm UDMH resulted in a more profound hemolytic anemia with one death. The 6-month exposure of the dogs to 5 ppm UDMH is the basis for the current threshold limit value (TLV) of 0.5 ppm used for occupational health conservation as cited in the Documentation of the Threshold Limit Values (1971).

A recent 6-month chronic toxicity study on MMH (TLV of 0.02 ppm) was reported by MacEwen and Vernot (1970). This study exposed dogs, rats, mice, and monkeys to 5 ppm and 2 ppm concentrations on a 6 hour/day, 5 day/week basis. Definite dose-related responses were shown in mice with 29 percent mortality at 5 ppm and 17 percent at 2 ppm. Similar dose-related effects were seen in rats with significant depression of growth rate and increased liver and kidney organ-to-body weight ratios. Both dogs and monkeys exhibited methemoglobinemia and Heinz body formation. A moderate hemolytic anemia was seen in dogs (approximately 15 percent depression of hematologic values) and increased red blood cell fragility. Only a marginal hemolytic response was seen in monkeys. The response seen in these chronic exposures of dogs to MMH was almost identical with that seen by Rinehart with UDMH. Most important, a no-effect level was not achieved, which suggests that further consideration should be given to the safety margin of the industrial TLV values.

Propellant Oxidizers

The oxidizers of most interest in propellant reactions that have been used or have a high potential for use are oxygen, fluorine, nitrogen trifluoride (NF_3), chlorine trifluoride (ClF_3), chlorine pentaflouride (ClF_5), oxygen difluoride (OF_2) and the dimer of nitrogen dioxide, nitrogen tetroxide (N_2O_4). Since oxygen toxicity is primarily a function of O_2 partial pressure (and total pressure) creating biological damage only when either too high or low, it will not be discussed further.

Fluorine. Fluorine and FLOX (a mixture of fluorine and oxygen) have been used as oxidizers for rocket fuels. The acute toxicity of fluorine in animals has been described by Stokinger (1949), Eriksen (1945), and Keplinger and Suissa (1968). Human experience with this compound has been reported by Machle and Evans (1940), Lyon (1962), Rickey (1959), Belles (1965) and Keplinger

(1959). The signs of fluorine toxicity below lethal concentrations are irritation of the eyes, nose and lungs. According to Keplinger, this effect begins at an air concentration of approximately 25 ppm F_2. When lethal exposure occurs, the degree of irritation is increased with coughing, wheezing, and severe lacrimation. Death usually occurs within 12 to 18 hours after severe exposure from pulmonary congestion. Experimentally, animals that survived any exposure level for 48 hours went on to recovery.

Repetitive animal exposures to fluorine at sublethal levels have produced increased fluoride content of the long bones in all species tested. Thus the signs associated with chronic fluorosis may be expected to occur if toxic levels of fluoride are built up and released systemically. The industrial TLV is based on this effect.

Oxygen Difluoride. An important member of the family of fluorine containing gaseous oxidizers is OF_2 which has been reported to be a severe pulmonary irritant. Rodent exposures to as little as 10 ppm for 10 minutes have been shown by LaBelle (1945) and Lester and Adams (1965) to cause death. Death results from asphyxiation subsequent to severe pulmonary edema and hemorrhage. The odor of OF_2 resembles garlic and is perceptible somewhere between 0.1 and 0.5 ppm. Since a TLV for this gas has been established at 0.5 ppm, its odor is thought to be a safe warning property. There have been reports of OF_2 exposure of research chemists at three different industrial plants. All of these people were sufficiently aware of the hazard of breathing OF_2 and, when its odor was noticed, they immediately left the exposure area. Each of the men exposed to OF_2 complained of soreness of the chest which disappeared within 3 days with no further effects. Their estimated exposure levels were below 10 ppm in each case.

A human exposure to OF_2 was investigated by MacEwen and Vernot (1969) who concluded that the man had been briefly subjected to an air concentration of approximately 1000 ppm. His survival and complete recovery after several days of severe respiratory distress were inconsistent with the toxicity data derived from rodent inhalation exposures. Therefore, more comprehensive studies on OF_2 toxicity were undertaken. These studies reported by MacEwen and Vernot (1970) showed that dogs and monkeys were less sensitive to the effects of OF_2 by a factor of 10, having a 1-hour LC_{50}* value of 26 ppm as compared with approximately 2 ppm for rats and mice. If this difference in toxicity levels is related to the difference in size, then it would help to explain the survival of the man exposed to 1000 ppm OF_2.

Chronic exposures of rodents to 0.1 ppm OF_2 for 5 weeks were conducted by LaBelle (1945) with no measurable effect.

Chlorine Trifluoride. Chlorine trifluoride (ClF_3) is a highly reactive compound with strong oxidizing properties approaching that of fluorine itself. This compound, characterized by Grisard et al. (1951), has been successfully used as a fluorinating agent in numerous reactions which customarily require elemental fluorine.

*Lethal concentration which kills 50 percent of animals by inhalation route.

One of the earliest studies on the toxicity of ClF_3 was made by Horn and Weir (1955). Chronic inhalation studies were made on dogs and rats exposed to sublethal concentrations of the gas for periods up to 6 months. Acute effects of ClF_3 on rodents have been reported by Dost et al. (1968). The reactivity of ClF_3 is such that it is highly unlikely that it reaches the lung of exposed subjects unchanged. One of the major breakdown products of this chemical compound in air is hydrogen fluoride (HF), and their biological effects are identical. ClF_3 is very irritating to the eyes and nose and, in animals, has been shown to produce pulmonary edema, hemorrhages, and emphysema, frequently leading to death. Experiments reported by MacEwen and Vernot (1970) showed essentially no difference in response between animal species and a reasonable correlation between LC_{50} levels for HF and ClF_3 on an equimolar fluorine basis. It is reasonable, then, that the health and safety limits for ClF_3 are one third those of HF.

Nitrogen Trifluoride. The acute toxicity of nitrogen trifluoride (NF_3) has been shown by Ruff (1931), Torkelson et al. (1962), Dost et al. (1968), and Vernot and Haun (1969) to be due to massive formation of methemoglobin, with death ensuing from the resulting anemia. Death seldom occurs unless the methemoglobin level exceeds 75 percent, beyond which the oxygen carrying capacity of the blood is reduced below that required to supply the needs of body tissues, particularly the brain. Animal experiments conducted by Vernot and Haun showed that survivors of near-lethal exposures (50 to 75 percent methemoglobin formed) have a Heinz body type of hemolytic anemia with destruction of approximately 35 percent of the red blood cells (RBC). In healthy animals the RBC loss stimulates reticulocyte activity and new cells begin forming. The time of lowest RBC values occurs about 10 days after exposure, and full recovery to normal RBC levels requires approximately 40 days. There is little species variation in response to NF_3 exposure, as shown in table 10-4, with the exception of the dog which is more susceptible to Heinz body anemia regardless of etiology than the others.

Table 10-4

Nitrogen Trifluoride LC_{50} Values for Various Species (ppm)

Time (min)	Rats	Mice	Dogs	Monkeys
15	26 700	19 300	38 800	24 000
30	11 700	12 300	20 200	14 100
60	6700	7500	9600	9200

From a toxic hazard point of view, NF_3 is probably the safest of the fluorinated oxidizers and would be the chemical of choice if other factors, such as specific impulse, were equal.

Chlorine Pentafluoride. There is very little known about the biological action of chlorine pentafluoride (ClF_5). Dost and his associates (1969) have studied its effects on plants and fish and report it to be chemically less reactive

with air and water vapor than ClF_3. It is also slightly less toxic than ClF_3 to plants, microorganisms, and fish. The only animal exposure data available, reported by Weinberg and Goldhamer (1967), is limited both in the variety of species tested and in the scope of inhalation toxicity studied. From the data available, it may be estimated that ClF_5 is slightly more toxic to animals than ClF_3. Necropsy results were similar to those seen from most strong oxidizing chemicals, marked pulmonary edema and hemorrhage with congestive changes in other visceral organs. During the subacute exposure of rats to 100 ppm ClF_5 for 15 minutes per day for 6 days, respiratory enzyme activity (glutamic oxaloacetic transaminase) was absent in the lungs, but all other criteria of physiological status were normal. Ten-minute exposures to ClF_5 of 400 ppm concentration produced 100 percent mortality, while 200 ppm produced only a partial lethal response in rats.

Nitrogen Tetroxide. Nitrogen tetroxide is an equilibrium mixture of nitrogen tetroxide (N_2O_4) and nitrogen dioxide (NO_2). This equilibrium shifts toward NO_2 at lower pressure and increased temperature, and NO_2 is, therefore, the more common form to which man is exposed. Health and safety limits for N_2O_4 are one-half what they are for NO_2 since the dimer form is exactly twice as reactive with biological materials. Nitrogen dioxide can be identified by its distinct odor in concentrations as low as 5 ppm, its current threshold limit value. It is mildly irritating to the eyes, nose, and upper respiratory mucosa at concentrations of 10 to 20 ppm, and, unfortunately, higher concentrations cannot be distinguished since no further irritation is experienced until significant pulmonary injury has been produced.

Concentrations of NO_2 above 100 ppm will cause death after a relatively short exposure. Death results from asphyxia subsequent to massive pulmonary edema. Exposures to concentrations of NO_2 as low as 40 ppm for periods of 4 to 6 hours have produced death in all common experimental animal species.

NO_2 is probably the most dangerous to man of all irritant gases because it is so commonly found. Its release in industrial accidents has caused many deaths. As is often the case in accidental exposures to toxicants, the NO_2 concentrations producing death in man have never been quantitatively identified but have been estimated to be slightly in excess of 100 ppm. Experimental evidence of acute NO_2 toxicity in primates and other species suggests, however, that exposure to 50 ppm for 6 to 8 hours might be fatal to man. It is because of the increasing evidence that NO_2 acute toxicity effects may occur at such low atmospheric concentrations that the threshold limit value has been reduced several times since it was first established at 25 ppm, to the current 5 ppm level. A safety factor of 10 below the lethal dose level is relatively small, when one considers that the safety factors used for many other industrial chemicals or contaminants are greater than 10 below nonlethal effect levels. It should also be noted that persons with chronic respiratory disease—asthma, chronic bronchitis, and emphysema—are more adversely affected by NO_2 than are healthy individuals.

There are many conflicting reports regarding the effect of NO_2 on animals under conditions of either repeated or continuous exposure. Wagner et al. (1965) exposed six species of animals 6 hours per day, 5 days per week to three

concentrations of NO_2 (1, 5 and 25 ppm) for 18 months without producing any demonstrable morphologic changes or significant changes in any of the usual indices of normal physiological status. Grey et al. (1952), however, reported emphysema and pneumonitis in rats exposed 4 hours per day, 5 days per week for 6 weeks to 9 to 13 ppm NO_2.

The results of reported continuous NO_2 exposures are also conflicting. Freeman and Haydon (1964) exposed rats to 25 ppm of NO_2 for about 150 days and produced strikingly voluminous lungs, a 50 percent reduction in growth rate, and eventual death. At 12.5 ppm, these investigators reported an 11 percent mortality after 213 days which was associated with 20 percent decrement in growth and increased respiration rate in the survivors. Haydon et al. (1965) reported no mortality or evidence of pulmonary disease or abnormality in body or lung weight in rats exposed for 16 weeks to 4 ppm, although the rats sacrificed exhibited the early histopathologic changes associated with higher concentrations. Rats exposed for 90 weeks to 0.8 ppm showed only a slight increase in respiration rate. Freeman et al. (1968) reported continuous 3 ppm NO_2 exposures of rats for 2 years produced pulmonary changes. Terminal and bronchiolar epithelium was affected by a loss of exfoliative activity, loss of cilia, and the appearance of crystalloid cellular inclusion bodies. They believed that the morphologic evidence suggested a reduction of the pulmonary cleansing function of the lungs particularly in the peripheral regions.

Continuous exposure to 0.5 ppm NO_2 for 3 months or longer has been shown by Ehrlich and Henry (1968) to significantly increase the susceptibility of mice to airborne *Klebsiella pneumoniae*. Henry et al. (1969) also reported that a single 2 hour exposure of mice to 3.5 ppm NO_2 either before or after the inhalation of an aerosol of *Klebsiella pneumoniae* resulted in significantly increased mortality.

A significant epidemiologic study of the effects of exposure to NO_2 was reported by Shy et al. (1970a, b). They found an increased rate of respiratory illness in families and a reduced forced expiratory pulmonary volume in children exposed to an average NO_2 concentration ranging from 0.062 to 0.109 ppm.

Conversely, Steadman et al. (1966) exposed animals continuously to five concentrations of NO_2 ranging approximately from 0.5 ppm to 11.5 ppm for a period of 90 days. Although 20 to 50 percent mortality was seen in several species at the higher concentration, 0.5 and 5 ppm exposures produced no significant effect on any biological parameters measured (nor were any morphologic changes attributable to the NO_2 exposure seen). Similar 90 day continuous exposures of rats, mice, monkeys, and dogs to 5 ppm NO_2 were reported by MacEwen and Geckler (1968) in which only transient signs of stress were seen with no significant morphologic or biochemical changes.

Data from chronic human exposure are equally confusing. Patty (1963) reported that exposures of men to average NO_2 concentrations ranging from 10 to 20 ppm for 18 months produced no ill effects. Vigdortschik et al. (1937),

on the other hand, reported symptoms of NO_2 toxicity after 5 years of daily exposures at approximately 2.5 ppm. The symptoms included possible bronchitis and emphysema.

There are numerous other liquid propellant fuels and oxidizers that have either been used or seriously considered for use that are not discussed in this chapter. For the convenience of the users of this handbook, some of the physical and chemical properties of these compounds, along with toxicity data and safety limits, are listed in table 10-5, in increasing order of toxicity. Additional information on the properties and handling procedures for these propellant chemicals may be found in the report of the JANNAF Hazards Working Group (1970).

Table 10–5

Some Physical and Toxic Properties of Propellant Fuels and Oxidizers

Compound	Boiling Point (°C)	Vapor Pressure at 80°F (mm Hg, approx)	Rat 60 Min LC_{50} (ppm)	Industrial TLV (ppm)
Nitrogen Trifluoride (NF_3)	−129	—	6700	10
Hydrazine (N_2H_4)	113.5	16	2280	1
Hydrogen Fluoride (HF)	19.7	985	1275	3
1, 1-Dimethylhydrazine (UDMH)	63	104	1410	0.5
Chlorine Pentafluoride (ClF_5)	−13.1	3790	<400	0.1*
Chlorine Trifluoride (ClF_3)	11.8	1375	300	0.1
Nitrogen Dioxide ($NO_2 - N_2O_4$)	21.2	1158	120	5
Monomethylhydrazine (MMH)	87.5	52	245	0.2
Flucrine (F_2)	− 188	–	185	0.1
Diborane (B_2H_4)	− 93	–	160**	0.1
Oxygen Difluoride (OF_2)	− 145	–	2.6	0.05
Pentaborane (B_5H_9)	600	207	10	0.005

*Proposed.
**Estimated from partial data.

Carbon Monoxide

This colorless and odorless gas is still the subject of scientific controversy, even though it was one of the earliest of the toxic gases to be recognized. The toxicity of carbon monoxide (CO) arises from its great affinity for hemoglobin (approximately 200 times greater than is the affinity of hemoglobin for oxygen),

resulting in oxygen starvation of body tissues. The concentrations of CO that are dangerous to life are shown in figure 10-2. It is not the lethal effects that are the basis of the scientific controversy, however, but the level of CO which will produce impairment of human mental functions. It is generally believed that subjective symptoms of CO intoxication rarely occur below blood carboxyhemoglobin (COHb) levels of 20 percent, while acute signs of central nervous system embarrassment occur at COHb levels greater than 30 percent (Haldane, 1927).

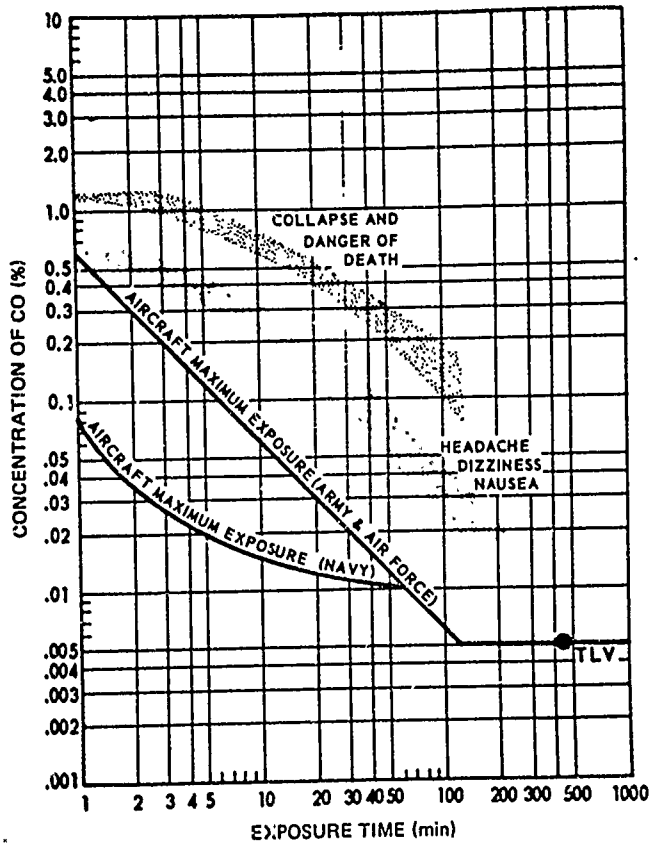


Figure 10–2. Effects of CO on man as a function of concentration and exposure time. Lightly shaded band shows region of milder effects; heavily shaded band, dangerous or lethal region. Solid lines indicate exposure limits set by military services for aircraft. The point marked at 0.005% CO (50 ppm) and 480 min is current TLV for 8-hr/day exposure in industry. (Department of Defense, 1958; Haldane, 1895; Henderson & Haggard, 1922; Sayers et al., 1922)

Recently, a number of investigators have suggested that the central nervous system is impaired at COHb levels as low as 2 to 5 percent. MacFarland et al. (1944) demonstrated impairment of visual discrimination with COHb levels of 4 percent. Trouton and Eysenck (1961) reported decrement in limb coordination at the same COHb levels. Schulte (1963) reported consistent impairment in cognitive and psychomotor performance at COHb levels of

5 percent with beginning tendencies for disruption as low as 2 percent COHb, while Beard and Wertheim (1967) reported a decrement in auditory discrimination of tone signal duration at estimated COHb levels from 4 to 5 percent.

Contradictory findings have been reported by equally competent scientists. Clayton et al. (1960) found no association between COHb level and automobile accidents, although Rockwell and Ray (1967) reported a possible effect of CO exposure on estimation of distances between following automobiles in fatigued, CO-exposed drivers with COHb levels of 5 to 10 percent. Mikulka et al. (1969) reported no observable impairment on a battery of psychomotor performance tasks in young men with COHb levels up to 12 percent. These findings were confirmed by Hanks (1970). Stewart et al. (1970) found no untoward effects on central nervous system function in sedentary males at COHb levels below 15 percent, while exposures resulting in higher blood COHb levels caused delayed headaches, changes in visual evoked response, and impairment of manual coordination.

Current standards for emergency exposures to carbon monoxide are based on air concentrations which will not produce COHb levels greater than 15 percent. When sufficient data are accumulated to settle the controversy on the possible influence of lower COHb levels, these standards may be lowered. In order to clarify the relationship between CO atmospheric concentrations and COHb blood levels, blood saturation rate curves are shown in figure 10-3 for rest and light work. An increase in work effort decreases the time required to reach the equilibrium level. Both sets of equilibrium curves originate from 0.5 percent COHb, which is about the normal level resulting from catabolism. An increase in CO concentration will produce a corresponding increase in COHb to a new equilibrium value that is not additive with the previous level.

Prolonged exposures of experimental animals to CO have shown that environmental adaptation occurs. Back and Dominguez (1968) and Back (1969) reported a series of experiments in which monkeys were continuously exposed to CO for periods up to 105 days to CO concentrations of 50, 200, and 400 ppm. No detectable effect on learned performance was seen in reaction time to visual and auditory signals or in work output of the monkeys. The failure of CO to impair these functions in monkeys having COHb levels up to 33 percent was thought to be due to a concomitant increase in red blood cells and total hemoglobin, which was shown by Vernot et al. (1970) to occur in other species as well. The increase of total hemoglobin resulted in sufficient oxygen delivery to tissues to prevent cellular hypoxia.

While sudden exposures to high atmospheric concentrations of CO may cause impairment of human ability to perform tasks critical for survival, it is believed that the slow buildup of CO concentration in a closed environment, such as a spacecraft, while not desirable, will cause an adaptive increase in hemoglobin and red blood cells that will permit normal functioning at elevated COHb levels and, more important, survival.

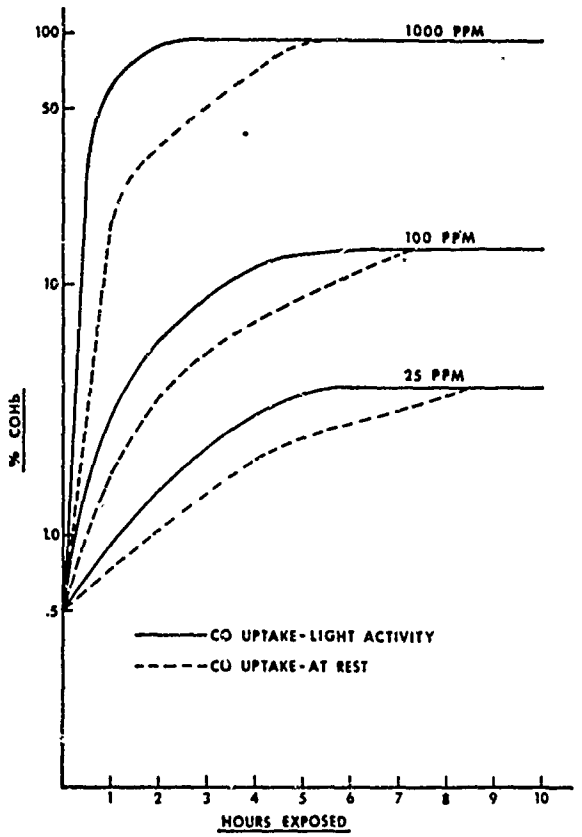


Figure 10–3. Carbon monoxide uptake in man.
(Derived from data of Forbes et al., 1945)

Spacecraft Threshold Limit Values

Experimental data for establishing spacecraft continuous exposure limit values are extremely limited. The continuous exposure of animals to contaminants is a difficult and expensive task and therefore has been done only with a few materials. The needs and problems associated with this type of research has been described by Back et al. (1962) and Thomas (1968). The first reports of results of continuous prolonged exposures of animals to probable spacecraft contaminants were given by Sandage (1961a,b) and by House (1964). Additional studies have been reported by MacEwen and Geckler (1968) and by Jones et al. (1970).

As a beginning step in establishing spacecraft exposure limit values, the Panel on Air Standards for Manned Space Flight of the Space Science Board-National Academy of Sciences proposed provisional limits for a few materials identified as spacecraft contaminants. The provisional long-term exposure limit values are shown in table 10-6. The panel decided that U.S. Navy submarine standards were suitable as guidelines for space mission limits for 90-day exposures but could not

be extrapolated for longer missions since interplanetary flight is not easily aborted, and return to Earth may take weeks or months. A list of chemical contaminant submarine TLV values is given in table 10-7. For simple alaphatic hydrocarbons not listed, the 90-day limit is 60 mg/M^3 and for simple aromatic hydrocarbons other than benzene, it is 10 mg/M^3. MacEwen and Geckler (1968) recommended 90-day spacecraft exposure limit values of 1 ppm for NO_2, 0.01 ppm for ozone and 0.5 ppm for carbon tetrachloride.

Table 10–6

Provisional Limits for Space Cabin Contaminants for 90 and 1000 Days

Air Contaminant	Air Limit in PPM	
	90 Days	1000 Days
n-Butanol	10	10
2-Butanone	20	20
Carbon monoxide	15	15
Chloroform	5	1
Dichloromethane	25	5
Dioxane	10	2
Ethyl acetate	40	40
Formaldehyde	0.1	0.1
2-Methylbutanone	20	20
Trichloroethylene	10	2
1, 1, 2-Trichloro, 1, 2, 2-trifluoroethane & related congeners	1000	200

(Data from National Academy of Sciences, Space Science Board, 1968)

Emergency Exposure Limits (EEL)

Provisional emergency limits for spacecraft contaminants were established by the NAS Panel on Air Standards for Manned Space Flight for five materials as shown in table 10-8. These limits are intended only as guidelines for a single exposure which does not reoccur during the flight.

Emergency exposure limits for use in fuel manufacturing, storage, and handling have been established by the NAS/NRC Committee on Toxicology for a number of chemicals including some propellant fuels and oxidizers. Some of these EEL values are shown in table 10-9. EEL values are intended only as guidelines for selection of engineering criteria for storage limitations. By definition, an EEL is a limit for an accidental exposure which would normally not be repeated in a lifetime. It is based on a contaminant dose which is not

expected to produce any irreversible physiologic changes and will permit the conduct of emergency duties and escape from the environment. EEL's are closely related to specific circumstances of exposure and should not be used for different conditions without first verifying their applicability. These values should never be exceeded since they contain little or no safety factor.

Table 10–7

U.S. Navy Submarine Contaminant Concentration Limits
(ppm)

	1 Hr	24 Hr	90 Day	ACGIH TLV*
Acetone	–	2000	30	1000
Acetylene	–	2500	2500	2500
Ammonia	400	50	25	50
Benzene	–	100	1	25
Carbon Monoxide	200	200	25	50
Chlorine	–	1	0.1	1
Dichlorodifluoromethane	30 000	20 000	1000	1000
1, 1, 2, 2-Tetrafluoro-1,2-Dichloroethane	30 000	20 000	1000	1000
Ethyl alcohol	–	500	100	1000
Hydrogen	–	3000	3000	–
Hydrogen Chloride	10	4	1	5
Hydrogen Fluoride	8	1	0.1	3
Methane	–	5000	5000	–
Methyl alcohol	–	200	10	200
Methyl Chloroform	350	1000	500	200
Monoethanolamine	50	1	0.5	3
Nitrogen Dioxide	10	1	0.5	5
Ozone	1.0	0.1	0.02	0.1
Phosgene	1.0	0.1	0.05	5
Sulfur Dioxide	10	5	1	200
Toluene	–	100	–	200
1, 1, 1-Trichlorethane	1000	500	200	350
Xylene	–	100	–	100

*American Conference of Governmental Industrial Hygienists, 1966.

Spacecraft Contaminants

The appearance of contaminants in space cabins during flight is caused by several factors, none of which can be completely eliminated. The factors are: (1) outgassing of cabin construction materials under reduced pressure conditions, (2) volatile metabolic waste products of the crew, (3) volatile components of spilled food, and (4) leaks from the environmental or flight

control systems. Contaminants found in submarines differ only in the area of outgassing from construction materials but have additional sources due to the increased amount of operational machinery. Many of the contaminants found in manned spacecraft simulation tests were also found in some of the Mercury and Apollo space flights.

Table 10–8

Provisional Emergency Limits for Space Cabin Contaminants

Air Contaminant	Air Limit for 60 Min	
	(ppm)	(mg/M^3)
2-Butanone	100	294
Carbonyl fluoride	25	68
Ethylene glycol	100	254
2-Methylbutanone	100	352
1, 1, 2-Trichloro, 1, 2, 2, 2-trifluoroethane and related congeners	30 000	2320

(Data from National Academy of Sciences, Space Science Board, 1968)

A type of spacecraft contaminant which has received little notice consists of particulate pollutants which are not easily removed from the air under conditions of weightlessness. Although a spacecraft cabin is cleaned many times before use, some dust may remain in inaccessible places and become airborne by mechanical means during flight. Other sources of particulate contamination are foodstuffs, abraided flight uniforms, and powdering from painted surfaces. Particles have been seen by astronauts in flight but information is lacking on particle size and concentration. Particulate removal is accomplished to a limited degree in the filter section of the air handling system. Additional sources of particulate contamination in future space flights may be found when regenerative life support systems are placed in operational spacecraft.

A comprehensive list of contaminants found in space flight to date, in submarines, and in some of the simulated space flight tests conducted at the USAF School of Aerospace Medicine is given in table 10-10. This list also includes the contaminants found in Sealab II and in the McDonnell Douglas Corporation's 60-day manned test of a regenerative life-support system (1968). This list, although not complete, contains 88 contaminants that were common to many of the space flights and spacecraft simulator runs and are also found in cabin material off-gassing studies. Although the presence of these contaminants has been verified, little or no information is yet available about the concentrations present in the spacecraft. Until the contaminant concentrations can be assessed, no judgments can be made concerning the toxic hazard of a space cabin environment.

Table 10–9

Emergency Exposure Limits of the Committee on Toxicology NAS/NRC (ppm)

Compound	10 Min	30 Min	60 Min
Acrolein			0.2 ppm
Aluminum fluoride	25 mg/M^3	10 mg/M^3	7 mg/M^3
Aluminum oxide	50 "	25 "	15 "
Ammonia (anhydrous)	500 ppm	300 ppm	300 ppm
Boron trifluoride	10	5	2
Bromine pentafluoride	3	1.5	0.5
Carbon disulfide	200	100	50
Carbon monoxide			
(normal activity)	1500	800	400
(mental acuity)	1000	500	200
Chlorine pentafluoride	3	1.5	0.5
Chlorine trifluoride	7	3	1
Diborane	10	5	2
1, 1-Dimethylhydrazine	100	50	30
Ethylene oxide	650	400	250
Fluorine	15	10	5
Formaldehyde	—	—	3
Hydrazine	30	20	10
Hydrogen chloride	30	20	10
Hydrogen fluoride	20	10	8
Hydrogen sulfide	200	100	50
JP-5	5 mg/l	5 mg/l	2.5 mg/l
Monomethylhydrazine			
(MMH)	90 ppm	30 ppm	15 ppm
Nitrogen dioxide	30	20	10
Nitrogen trifluoride	—	100	50
Oxygen difluoride	0.5	0.2	0.1
Perchloryl fluoride	50	20	10
Sulfur dioxide	30	20	10
Sulfuric acid	5 mg/M^3	2 mg/M^3	1 mg/M^3
Tellurium hexafluoride	1 ppm	0.4 ppm	0.2 ppm
1, 1, 2-Trichloro-1, 2, 2-trifluoroethane (Refrigerant 113)			1500 ppm

Table 10–10

Contaminants Found in Confined Spaces During Actual or Simulated Space Flights

Contaminant	Sources*															
	1	2	3	4	5	6	7	8	9	10	11	12	13	14	15	16	17
Acetaldehyde	x	x						x	x	x	x	x	x	x	x		x
Acetic Acid						x		x	x				x	x	x		
Acetone	x	x	x	x	x	x	x	x	x	x	x	x	x	x	x	x	
Acetylene	x	x	x										x		x		
Allyl Alcohol								x	x	x							
Ammonia			x			x			x		x			x	x		x
Amyl Acetate									x	x							
Benzene	x		x	x		x		x	x	x			x	x	x	x	
1-3 Butadiene				x		x		x									
n-Butane	x	x	x	x		x		x			x	x	x		x	x	
2-Butanone	x	x				x		x	x	x	x			x	x		
1-Butene	x		x		x			x					x		x		
2-Butene cis, trans	x	x				x		x							x		
n-Butyl Alcohol	x	x						x		x			x	x			
iso-Butyl Alcohol		x				x		x	x	x				x			
iso-Butylene								x			x		x		x		
Butyraldehyde								x	x	x							x
Carbon Disulfide		x		x					x					x			
Carbon Monoxide			x	x				x	x	x				x	x	x	x
Chlorobenzene								x	x	x							
Chlorofluoroethylene			x				x										
Chloroform			x			x		x	x	x				x			
Chloromethane			x				x	x			x						
Cyclohexane	x	x	x	x		x	x	x	x	x						x	
Cyclopentane			x	x				x	x							x	
1-2, Dichloroethane	x	x		x	x	x	x	x	x	x			x				
2-2, Dimethylbutane	x	x	x			x		x	x	x							
2-3, Dimethylbutane								x	x	x							
Dioxene	x	x	x	x													
Ethane		x	x	x	x	x	x	x	x								
Ethanethiol		x		x						x							
Ethyl Acetate	x	x	x			x		x	x	x		x	x	x			
Freon 12	x					x	x		x						x		
Freon 22	x	x	x					x	x	x						x	
Freon 113						x		x		x							
Freon 114	x	x						x	x	x					x		
Furan				x				x	x	x							
n-Heptane						x		x	x	x				x	x	x	
n-Hexane	x	x	x				x	x	x	x				x	x	x	
Hexene	x								x								
Ethyl Alcohol	x	x	x	x	x	x	x	x	x	x	x	x	x	x	x	x	x
Ethyl benzene								x	x	x				x	x	x	
Ethylene	x	x				x		x	x	x			x		x		
Ethyl Ether			x	x				x	x	x	x						

*See notes at end of table.

Table 10–10 (Continued)

Contaminants Found in Confined Spaces During Actual or Simulated Space Flights

Contaminant	Source*																
	1	2	3	4	5	6	7	8	9	10	11	12	13	14	15	16	17
Ethyl Formate								x	x	x			x				
p-Ethyl Toluene									x					x	x		
Formaldehyde	x	x											x	x	x		x
Freon 11	x	x	x			x		x	x	x					x		
Hydrogen		x							x				x		x		
Hydrogen Fluoride									x						x		
Hydrogen Sulfide			x						x						x		
Indene						x		x	x								
Isoprene						x		x	x	x				x		x	
Isopentane	x	x						x	x	x					x	x	
Methane		x	x	x		x	x	x	x	x				x	x	x	
Methyl Alcohol	x	x	x	x		x		x	x	x	x	x			x		
2-Methylbutanone-3	x									x							
Methyl Chloride			x				x	x			x						
Methyl Chloroform	x							x	x	x					x		
Methyl Cyclopentane									x							x	
Methylene Chloride	x	x		x	x	x	x	x	x	x			x			x	
Methyl Cyclohexane								x	x	x					x	x	
Methyl Ethyl Benzene									x					x	x		
Methyl Ethyl Ketone	x	x				x		x	x	x	x			x	x		
Methyl Isobutyl Ketone								x	x	x				x	x		
Methanethiol						x		x	x								
2 or 3-Methyl Pentane	x								x	x			x			x	
Methylsiloxane Polymers								x	x	x				x	x		
Methyl Thiophene						x		x									
Nitrogen Oxides								x							x		x
Pentafluoroethane	x	x						x		x							
Pentane	x	x						x	x	x					x	x	
iso-Pentane	x	x						x	x	x	x				x	x	
iso-Pentene								x			x						
Perchloroethylene		x						x	x	x			x				
Propane	x		x	x		x	x	x	x	x					x		
Propene					x		x										
Propionic Acid								x	x						x		
n-Propyl Alcohol	x	x						x	x	x			x				
iso-Propyl Alcohol			x	x	x	x		x	x	x				x	x		
Propylene	x	x						x	x	x					x		
Sulfur Dioxide		x									x				x		x
Toluene	x	x	x	x		x		x	x	x			x	x	x	x	x
1, 1, 1-Trichloroethane	x							x	x	x					x		

*See notes at end of table.

Table 10–10 (Continued)

Contaminants Found in Confined Spaces
During Actual or Simulated Space Flights

Contaminant	Source*																
	1	2	3	4	5	6	7	8	9	10	11	12	13	14	15	16	17
Trichloroethylene	x	x						x	x	x	x		x	x			
Trimethyl Pentane			x					x	x								
Vinyl Chloride	x	x						x		x					x	x	
Xylene	x					x		x	x	x				x	x	x	

*Note: Data originally reported in publication of the National Academy of Sciences' Space Science Board (1968) from the following sources:

SOURCE LIST

1. Mercury Spacecraft: Saunders (1962), Samonski (1967)
2. Apollo GT-3: Panel on Air Standards for Manned Space Flight (1968)
3. Apollo GT-4: Panel on Air Standards for Manned Space Flight (1968)
4. Apollo GT-5: Panel on Air Standards for Manned Space Flight (1968)
5. Apollo GT-7: Panel on Air Standards for Manned Space Flight (1968)
6. Apollo GT-10: Panel on Air Standards for Manned Space Flight (1968)
7. Apollo GT-12: Panel on Air Standards for Manned Space Flight (1968)
8. SAM-I: Conkle et al. (1967)
9. SAM-II: Conkle (1966)
10. SAM-III: Adams et al. (1966)
11. MESA I: Saunders (1967A), Cotton et al. (1966)
12. MESA II: Cotton et al. (1966)
13. Integrated Life Science Systems Tests: Hodgkiss et al. (1967), Toliver et al. (1966)
14. Offgassing Tests: Hodgson et al. (1966), Pustinger et al. (1966)
15. Submarines: Naval Research Lab Reports
16. SeaLab II: Saunders (1967B)
17. Life Support System: McDonnell Douglas (1968)

Another possible source of future contaminant generation may be the thermal reaction products formed by small electrical fires or contaminant removal systems. One such material was identified in a manned life support test (MESA I) when 1, 2-dichloroacetylene was found to result from the reaction of trichloroethylene with lithium hydroxide. The lithium hydroxide is used as a scrubber for removal of metabolically produced CO_2. The production of dichloroacetylene caused the experiment to be stopped with resulting loss of time and money. This contaminant has caused other expensive delays (Saunders & Williams, 1969) and the circumstances causing its formation should not be allowed to reoccur. *Specifically, trichloroethylene should not be introduced into a spacecraft in any form at any time.*

Outgassing studies have been conducted on a large number of spacecraft construction materials to identify possible contaminants. Animal experiments also have been conducted to screen the candidate space cabin materials used in

the Apollo series. Results of the screening studies made under reduced pressure–100 percent oxygen conditions have shown the outgassed contaminants of most cabin materials to be nontoxic under the test condition used, as reported by Culver (1966) and Haun (1967). Of several hundred tested, one material proved to be toxic when heated. Carboxynitroso rubber, which was selected as a candidate spacecraft material because it was nonflammable, was found to decompose at 300°C and to form highly toxic decomposition products. MacEwen (1968) estimated that the decomposition of 15 grams of carboxynitroso rubber in an Apollo space cabin would be fatal if inhaled for 2 minutes.

Water Quality Standards for Space Missions

Standards for the quality of potable water aboard spacecraft are as important as those for air quality. The amount of water needed for drinking and personal hygiene is sufficiently great on extended space missions to make storage prohibitive. Therefore, water used by the crew for personal or cabin hygiene and body waste water and water produced by spacecraft equipment must be collected, treated, and reused.

Water quality standards need not be as stringent as those used for municipal water supplies since the latter are established to protect a broad population, including young and old, and sick and healthy, for a lifetime, not just a limited period. However, whereas it is true that spacecraft water will not be contaminated by soil leachates and industrial pollution, it may contain concentrated impurities (because of recycling) released by the water treatment system and the crew itself.

The requirements for spacecraft water quality standards are based on aesthetic or physical criteria, trace chemical content, and microbiological impurities. From the crew viewpoint, the aesthetic criteria may be most important since unpleasant odors or taste may discourage normal use of the water which may in turn cause adverse effects on health. The aesthetic standards recommended by the National Academy of Sciences' Space Science Board (1967) are listed in table 10-11. Chemical standards are listed in table 10-12.

Table 10–11

Spacecraft Water Quality Standards for Physical Properties

Quality	Spacecraft Limit	Municipal Limit
Turbidity (Jackson units)	Not to exceed 10	Not to exceed 5
Color (platinum – cobalt units)	Not to exceed 15	Not to exceed 15
Taste	None objectionable	–
Odor	None objectionable	Odor No. 3
Foaming	None persistent more than 15 sec	–

(National Academy of Sciences, Space Science Board, 1967; Public Health Service, 1962)

Table 10–12

Spacecraft Water Quality Standards for Chemical Content (mg/l)

Chemical	Spacecraft Limit	PHS (Upper Limit)
Arsenic	0.50	0.05
Barium	2.00	1.00
Boron	5.00	–
Cadmium	0.05	0.01
Chemical Oxygen Demand (dichromate method)	100.00	–
Chloride	450.00	250.00
Chromium (hexavalent)	0.05	0.20
Copper	3.00	1.00
Fluoride	2.00	1.00
Lead	0.20	0.05
Nitrate and nitrite (as nitrogen)	10.00	0.001
Selenium	0.05	0.01
Silver	0.50	0.05
Sulfate	250.00	250.00
Total solids	1000.00	–

(National Academy of Sciences, Space Science Board, 1967; Public Health Service, 1962)

Recirculation or reuse of bodily and hygienic waste waters requires consideration of biological contamination. The nature of a water reclamation system is such that microbiological organisms of body of air origin may find many suitable physical and nutritional support sources. Although the biological forms of bacteria, molds, fungi, and viruses would be limited to those with which the bodies of the crewmembers are familiar, there is ample opportunity for overgrowth which may overwhelm the normal tolerance to small numbers of these organisms. Furthermore, biological growths in the water system may add byproduct toxins or unwanted taste and odor. The recommended standard of the National Academy of Sciences' Space Science Board (1967) is stated as follows:

> Because of the diverse natures and modes of hazard of possible biological contaminants in water-recovery systems for space use, the Panel found no justification for the establishment of standards based on individual types of microorganisms. It was considered that the goal should be essential sterility and that total counts of aerobic, facultative and anaerobic organisms would be the best indications of attainment of this condition. A maximum of 10 viable microorganisms per milliliter was considered to be a realistic criterion for "essential sterility."

It was considered essential, moreover, that this criterion of essential sterility be applied to all parts of the recovery system beyond the initial phase separation step and not simply to the finished product water.

The Panel felt strongly that some positive form of sterilization was needed at some point in the recovery-storage-delivery system immediately after phase separation. In addition, it was felt that there should be provision for periodic heat treatment of the subsequent portions of the system to forestall hazards of possible bacterial or fung ' growth.

It will be difficult to monitor the quality of the drinking water under actual space flight conditions. Therefore, any water reclamation system should be thoroughly use-tested in simulator runs to establish that it meets required chemical, biological, and physical standards. Some sampling may be feasible during flight but could by necessity be limited to simple indicator tests of single ions and simple biological cultures on multipurpose media. Research from the Apollo program has produced rapid techniques for identifying the presence of living forms through the reaction of their ATP content with the "fire fly" enzymes to give a visible signal. This test will not distinguish pathogenic organisms from nonpathogens but would be applicable to the Space Sciences Board's recommendation of 10 microorganisms per milliliter without regard to their identity or pathogenicity.

References

Adams, J. D., Conkle, J. P., Mabson, W. E., Watson, J. T., Wolf, P. H., & Welch, B. E. Study of man during a 56-day exposure to an oxygen-helium atmosphere at 258 mm Hg total pressure. II., Major and minor atmospheric components. *Aerospace Medicine*, 1966, *37*, 555.

American Conference of Governmental Industrial Hygienists. *Documentation of the threshold limit values.* (3rd ed.), 1971.

Azar, A., Thomas, A. A., & Shillito, F. H., Pyriodoxine and Phenobarbital as treatment for aerozine-50 toxicity. *Aerospace Medicine*, 1970, *41*, 1.

Back, K. C. Effects of carbon monoxide on the performance of monkeys. In Proceedings of the 5th Annual Conference on Atmospheric Contamination in Confined Spaces, AMRL-TR-69-130, Aerospace Medical Research Laboratory, Wright-Patterson AFB, Ohio, 1969.

Back, K. C., Sandage, C., & Thomas, A. A. Development of space cabin tolerance criteria to trace contaminants. *Aerospace Medicine*, 1962, *33*, 1438.

Back, K. C., Pinkerton, M. K., & Thomas, A. A., Therapy of acute UDMH intoxication. *Aerospace Medicine*, 1963, *34*, 1001.

Back, K. C., & Dominguez, A. M., Psychopharmacology of carbon monoxide under ambient and altitude conditions. AMRL-TR-68-175, Aerospace Medical Research Laboratory, Wright-Patterson AFB, Ohio, 1968.

Bean, J. W. Effects of oxygen at increased pressure. *Physiology Review*, 1945, *25*, 1-47.

Bean, J. W. Hypophyseal and adrenocortical factors in pulmonary damage induced by oxygen at atmospheric pressure. *Journal of American Physiology*, 1953, *172*, 169-174.

Beard, R. R., & Wertheim, G. A. Behavioral impairment associated with small doses of carbon monoxide. *American Journal of Public Health*, 1967, *57*, 11.

Belles, F. *Fluorine handbook*. Lewis Research Center, National Aeronautics and Space Administration, Cleveland, Ohio, 1965.

Bert, P. *La Pression Barometric: Recherches de Physiologie Experimental*. Paris: G. Masson, 1878.

Boycott, A. F., & Oakley, C. L. Oxygen poisoning in rats, *Journal of Pathology and Bacteriology*, 1932, *35*, 468.

Clark, D. A., Barrington, J. D., Bitter, H. L., Coe, F. L., Medina, M. A., Merritt, J. H., & Scott, W. N. Pharmacology and toxicology of propellant hydrazines. Review 11-68, USAF School of Aerospace Medicine, Aerospace Medical Division, Brooks AFB, Texas, 1968.

Clayton, G. D., Cook, W. A., & Frederick, W. G. A study of the relationship of street carbon monoxide concentrations to traffic accidents. *Journal of American Industrial Hygiene Association*, 1960, *21*, 46.

Coe, F. L., & Korty, P. R. The effect of hydrazine upon renal blood flow. SAM-TR-67-46, USAF School of Aerospace Medicine, Aerospace Medical Division, Brooks AFB, Texas, 1967.

Comroe, J. H., Drippe, R. D., & Deming, M. Effects produced in man by inhalation of high concentrations of oxygen for 24 hours. *Journal of the American Medical Association*, 1945, *128*, 710-717.

Conkle, J. P. Contaminant studies in closed ecological systems at the USAF School of Aerospace Medicine. In Proceedings of the 2nd Annual Conference on Atmospheric Contamination in Confined Spaces, AMRL-TR-66-120, Aerospace Medical Research Laboratory, Wright-Patterson AFB, Ohio, 1966.

Conkle, J. P., Mabson, W. E., Adams, J. D., Zeft, H. J., & Welch, B. E. Detailed study of contaminant production in a space cabin simulator at 760 mm of mercury. *Aerospace Medicine*, 1967, *38*, 491.

Cotton, J. E., Fosberg, T. M., Monteith, L. E., & Olsen, R. L. An integrated program approach to the control of space cabin atmospheres. In K. Kammermeyer (Ed.), *Atmosphere in Space Cabins and Closed Environments*. New York: Appleton-Century Crofts, 1966.

Culver, B. D. Toxicological screening of space cabin materials. In Proceedings of the 2nd Annual Conference on Atmospheric Contaminants in Confined Spaces, AMRL-TR-66-120, Aerospace Medical Research Laboratory, Wright-Patterson AFB, Ohio, 1966.

Department of Defense. Military standard procedure for carbon monoxide detection and control in aircraft. MIL-STD-800, U.S. Government Printing Office, Washington, D.C., July 1958.

Dickerson, K. H. Pathophysiology of pulmonic toxicity in rats exposed to 100 percent oxygen at reduced pressures. NADC-ML-6403, Aerospace Medical Research Department, Naval Air Development Center, Johnsville, Pennsylvania, 1964.

Dittmer, D. S., & Grebe, R. M. *Handbook of Respiration*. Philadelphia: Saunders, 1958.

Dost, F. N., Reed, D. J., Finch, A., & Wang, C. H. Metabolism and pharmacology of inorganic and fluorine containing compounds. AMRL-TR-67-224, Aerospace Medical Research Laboratory, Wright-Patterson AFB, Ohio, August 1968.

Dost, F. N., Reed, D. J. & Wang, C. H. Studies on environmental pollution by missile propellants. AMRL-TR-68-85, Aerospace Medical Research Laboratory, Wright-Patterson AFB, Ohio, 1969.

Ehrlick, R., & Henry, M. C. Chronic toxicity of nitrogen dioxide. I., Effect on resistance to bacterial pneumonia. *Archives of Environmental Health*, 1968, *17*, 860-865.

Eriksen, N. A study of lethal effects of the inhalation of gaseous fluorine (F_2) at concentrations from 100 PFM to 10 000 PPM. Report 435, United States Atomic Energy Commission, University of Rochester, Rochester, New York, 1945.

Fairchild, E. J., II. Eight-month continuous exposure of animals to an oxygen-nitrogen atmosphere at 5 psia. In Proceedings of the 3rd Annual Conference on Atmospheric Contamination in Confined Spaces, AMRL-TR-66-120, Aerospace Medical Research Laboratory, Wright-Patterson AFB, Ohio, December, 1967.

Forbes, W. H., Sargent, F., & Roughton, F. J. W. The rate of carbon monoxide uptake by normal men. *Journal of American Physiology*, 1945, *143*, 594.

Freeman, G. & Haydon, G. B. Emphysema after low level exposure to NO_2. *American Medical Association Archives of Environmental Health*, 1964, *8*, 125.

Freeman, G., Stevens, R. J., Crane, S. C., & Furiosi, N. J. Lesion of the lung in rats continuously exposed to two parts per million of nitrogen dioxide. *American Medical Association Archives of Environmental Health*, 1968, *17*, 121.

George, M., Mautner, W., & Back, K. C. Nephro toxic effects of monomethylhydrazine in monkeys. AMRL-TR-68-110, Aerospace Medical Research Laboratory, Wright-Patterson AFB, Ohio 1968.

Grey, E. LeB., MacNamee, J. K., & Goldberg, S. B. Toxicity of NO_2 vapors at very low levels. *American Medical Association Archives of Industrial Hygiene*, 1952, *6*, 20.

Grisard, J. W., Bernhardt, H. A., & Oliver, G. D. Thermal data, vapor pressure and entropy of chlorine trifluoride. *Journal of the American Chemical Society*, 1951, *73*, 5725.

Haldane, J. S. The action of carbonic acid on man. *Journal of Physiology*, 1895, *18*, 201.

Haldane, J. S. Carbon monoxide as a tissue poison. *Journal of Biochemistry*, 1927, *21*, 1068.

Hanks, T. H. Analysis of human performance capabilities as a function of exposure to carbon monoxide. Presented at the Conference on Biological Effects of Carbon Monoxide, New York Academy of Sciences, February, 1970.

Haun, C. C. Toxicological screening of 100 space cabin materials. In Proceedings of the 3rd Annual Conference on Atmospheric Contamination in Confined Spaces, AMRL-TR-66-120, Aerospace Medical Research Laboratory, Wright-Patterson AFB, Ohio, December, 1967.

Haun, C. C., MacEwen, J. D., Vernot, E. H., & Egan, G. F. The acute inhalation toxicity of monomethylhydrazine vapor. AMRL-TR-69-169, Aerospace Medical Research Laboratory, Wright-Patterson AFB, Ohio, 1968.

Haydon, G. B., Freeman, G., & Furiosi, N. J. Covert pathogenesis of NO_2 induced emphysema in the rat. *American Medical Association Archives of Environmental Health*, 1965, *11*, 776.

Helvery, W. M., Albright, G. A., Benjamin, F. B., Peters, J., Gail, L., & Rand, H. The effects on man of prolonged exposure to pure oxygen. *Aerospace Medicine*, 1963, *34*, 257.

Henderson, Y. & Haggard, H. W. The physiological principles governing ventilation when the air is contaminated with carbon monoxide. *Journal of Industrial and Engineering Chemistry*, 1922, *14*, 229.

Henry, M. C., Ehrlich, R., & Blair, W. H. Effect of nitrogen dioxide on squirrel monkeys to Klebsiella pneumoniae infection. *Archives of Environmental Health*, 1969, *18*, 580-587.

Herlocher, J. E. Quigley, D. G., Behar, V. S., Shaw, E. G., & Welch, B. E. Physiologic response to increased oxygen partial pressure. I., Clinical observations. *Aerospace Medicine*, 1964, *35*, 613.

Hodgkiss, W. S., Johns, R. H., & Swinehart, J. S. Environmental testing of contaminant producing materials from the integrated life support system. Contract No. NASI-4425, Atlantic Research Corporation, Alexandria, Virginia, 1967.

Hodgson, F. N., & Pustinger, J. V., Jr. Gas-off studies of cabin materials. In Proceedings of the 2nd Annual Conference on Atmospheric Contamination in Confined Spaces, AMRL-TR-66-120, Aerospace Medical Research Laboratory, Wright-Patterson AFB, Ohio, 1966.

Horn, J. H., & Weir, R. J. Inhalation toxicology of chlorine trifluoride. *American Medical Association Archives of Industrial Health* 1955, *12*, 515.

House, W. B. Tolerance criteria for continuous inhalation exposure to toxic materials. III., Effects on animals of 90-day exposure to hydrazine, unsymmetrical dimethylhydrazine (UDMH), decaborane and nitrogen dioxide. ASD-TR-61-519 (III), Aerospace Medical Research Laboratory, Wright-Patterson AFB, Ohio, 1964.

Jacobson, K. H., Clem, J. H., Wheelwright, H. J., Jr., Rinehardt, W. E., & Mayes, N. The acute toxicity of the vapors of some methylated hydrazine derivatives. *American Medical Association Archives of Industrial Health*, 1955, *12*, 609.

JANNAF Hazard Working Group. Chemical rocket/propellant hazards. Volume III. Liquid propellant handling, storage and transportation. Chemical Propulsion Agency, Information Agency Publication Number 194, 1970.

Jones, R. A., Jenkins, L. V., Jr., Coon, R. A., & Siegal, J. The effects of long-term continuous inhalation of ozone on experimental animals. *Toxicology and Applied Pharmacology*, 1970, *17*, 189.

Kaplan, H. P., Thomas, A. A., Back, K. C., & Robinson, F. R. Evaluation of animals continuously exposed to a 5 psia pure oxygen space cabin atmosphere for eight months. *Aerospace Medicine*, 1968, *39*, 63.

Keplinger, M. L., & Suissa, L. W. Toxicity of fluorine short-term inhalation. *Journal of American Industrial Hygienical Association*, 1968, *29*, 10.

Keplinger, M. L. Effects from repeated short-term inhalation of fluorine. *Toxicology and Applied Pharmacology*, 1969, *14*, 192.

Kistler, G. S., Caldwell, P. R. B., & Wiebel, E. A. Development of fine structural damage to alveolar and capillary living cells in oxygen-poisoned rat lungs. *Journal of Cellular Biology*, 1967, *32*, 605.

Krop, S. Toxicology of hydrazines, a review. *American Medical Association Archives of Industrial Health*, 1954, *9*, 199.

Kydd, G. H. Lung changes resulting from prolonged exposure to 100 percent oxygen at 550 mm Hg. *Aerospace Medicine*, 1967, *38*, 918-923.

Kydd, G. H. Survival of rats exposed to 10 psia oxygen to further exposure at one atmosphere oxygen. *Aerospace Medicine*, 1968, *39*, 739.

Labelle, C. W. Studies on the toxicity of oxygen difluoride levels of exposure from 10 to 0.1 ppm by volume. Pharmacology Report No. 478, Manhattan Project Contract W-7401 eng 49, The University of Rochester, January, 1945.

Lester, D. & Adams, W. R. The inhalation toxicity of oxygen difluoride. *Journal of American Industrial Hygienical Association*, 1965, *26*, 562.

Lewerenz, M., Schwinger, G., Weibel, E. R., & Kaplan, H. P. Electron microscopic and morphometric evaluation of lungs from animals exposed continuously for eight months to 5 psia, 100 percent oxygen. In Proceedings of the 3rd Annual Conference on Atmospheric Contamination in Confined Spaces, AMRL-TR-67-200, Aerospace Medical Research Laboratories, Wright-Patterson AFB, Ohio, December, 1967.

Lyon, J. S. Observations on personnel working with fluorine at a gaseous diffusion plant. *Journal of Occupational Medicine*, 1962, *4*, 199.

MacEwen, J. D. The acute toxicity of thermal decomposition products of carboxy nitroso rubber (CNR). In Proceedings of the 4th Annual Conference on Atmospheric Contamination in Confined Spaces, AMRL-TR-68-175, Wright-Patterson AFB, Ohio, 1968.

MacEwen, J. D., & Geckler, R. P. Comparative studies of 90-day continuous exposure to O_2, NO_2 and CCl_4 at reduced and ambient pressures. AMRL-TR-67-68, Aerospace Medical Research Laboratory, Wright-Patterson AFB, Ohio, 1968.

MacEwen, J. D., & Haun, C. C. Oxygen toxicity at near ambient pressures. In Proceedings of the 2nd Annual Conference on Atmospheric Contamination in Confined Spaces, AMRL-TR-66-120, Aerospace Medical Research Laboratories, Wright-Patterson AFB, Ohio, December, 1966.

MacEwen, J. D., & Vernot, E. H. Toxic hazards research unit annual technical report. AMRL-TR-68-133, Aerospace Medical Research Laboratory, Wright-Patterson AFB, Ohio, October, 1968.

MacEwen, J. D., & Vernot, E. H. Toxic hazards research unit annual report. AMRL-TR-69-84, Aerospace Medical Research Laboratory, Wright-Patterson AFB, Ohio, September, 1969.

MacEwen, J. D., & Bernot, E. H. Toxic hazards research unit annual technical report: 1970. AMRL-TR-70-77, Aerospace Medical Research Laboratory, Wright-Patterson AFB, Ohio, 1970.

MacFarland, R. A., Roughton, F. J. W., Halperin, M. H., & Niven, J. I. The effects of carbon monoxide and altitude on visual thresholds. *Journal of Aviation Medicine*, 1944, *15*, 381.

McDonnell Douglas Astronautics Company Report. 60-day manned test of a regenerative life support system with oxygen and water recovery. NASA-CR-98500, National Aeronautics and Space Administration, 1968.

McNerney, J. M., & MacEwen, J. D. Comparative toxicity studies at reduced and ambient pressures. I., Acute Response. *Journal of American Industrial Hygiene*, 1965, *26*,568.

Machle, W., & Evans, E. E. Exposure to fluorine in industry. *Journal of Industrial Hygiene and Toxicoloty*, 1940,*22* 213.

Mammen, R. E., Critz, G. T., Dery, D. W., Highly, F. M., & Hendler, E. Effects of sequential exposure to acceleration and space capsule atmospheric conditions. *Aerospace Medicine*, 1963 *34*, 260, (Abstract)

Mikulka, P. J., O'Donnell, R. D., Heinig, P. E., & Theodore, J. The effect of carbon monoxide on human performance. In Proceedings of the 5th Annual Conference on Atmospheric Contamination in Confined Spaces, AMRL-TR-69-130, Aerospace Medical Research Laboratory, Wright-Patterson AFB, Ohio, 1969.

Mittler, S. Toxicity of ozone IV, silicone aerosols and alcohol vapor therapy in ozone poisoning. *Industrial Medicine and Surgery*, 1958, *27*, 43.

Morgan, T. E., Jr., Cutler, R. G., Shaw, E. G., Ulvedal, F., Hargraves, J. J., Moyer, J. E., McKenzie, R. E., & Welch, B. E. Physiologic effects of exposure to increased oxygen tension at 5 psia. *Aerospace Medicine*, 1963, *34*, 720.

National Academy of Sciences. Space Science Board, Panel on Air Standards for Manned Space Flight. Atmospheric contaminants in spacecraft. Washington, D.C., October, 1968.

National Academy of Sciences. Space Science Board, Panel on Water Quality Standards Report of the Ad Hoc Panel on Water Quality Standards for Long Duration Manned Space Missions. Washington, D.C., 1967.

Naval Research Laboratory Reports. The present status of chemical research in atmosphere purification and control on nuclear-powered submarines. NRL Report 5465, Naval Research Laboratory, Washington, D.C., 1960, NRL Report 5630 (1961); NRL Report 5814 (1962); NRL Report 6053 (1963); NRL Report 6251 (1965); NRL Report 6491 (1967).

Ohlsson, W. T. L. A study on oxygen toxicity at atmospheric pressure. *Acta Medica Scandinavica*, 1947, *128*, Supplement 190.

Patty, F. A. Inorganic compounds of oxygen, nitrogen and carbon. In D. W. Fassett and D. D. Trish (Eds.), *Industrial Hygience and Toxicology*. Volume II. Interscience Publishers, 1963.

Pinkerton, M. K., Hagan, E. A., & Back, K. C. Distribution and excretion of ^{14}C-Monomethylhydrazine. *Toxicology and Applied Pharmacology*, 1967, *10*, 401.

Public Health Service. Drinking water standards. Public Health Publications Number 956, U.S. Department of Health, Education and Welfare, Washington, D.C., 1962.

Pustinger, J. V., Jr., Hodgson, F. N., & Ross, W. D. Identification of volatile contaminants of space cabin materials. AMRL-TR-66-53, Aerospace Medical Research Laboratory, Wright-Patterson AFB, Ohio, 1966.

Rinehart, W. E., Donati, E., & Greene, E. A. The sub-acute and chronic toxicity of 1, 1-dimethylhydrazine vapor. *Journal of American Industrial Hygiene*, 1960, *21*, 207.

Reynolds, H. H., Rohles, F. H., Fineg, J., Back, K. C., & Thomas, A. A. The effect of UDMH on learned performance in the Java monkey. *Aerospace Medicine*, 1963, *34*, 920.

Reynolds, H. H., Rohles, F. H., Prine, J. R., & Back, K. C. The effects of 1, 1-dimethylhydrazine (UDMH) on complex avoidance behavior in the Java monkey. *Aerospace Medicine*, 1964, *35*, 377.

Reynolds, H. H., & Back, K. C. Effect of injected monomethylhydrazine on primate performance. *Toxicology and Applied Pharmacology*, 1966, *9*, 336.

Rickey, R. P. Decontamination of large liquid fluorine spills. United States Air Force Flight Training Command, Technical Report 59-21, 1959.

Robertson, W. G., Hargraves, J. J., Herlocher, J. E., & Welch, B. E. Physiologic response to increased oxygen partial pressure. II., Respiratory studies. *Aerospace Medicine*, 1964, *35*, 618.

Rockwell, T. H., & Ray, A. M. Subacute carbon monoxide poisoning and driving performance, a selected review of the literature and discussion. January, 1967. A report to the National Safety Council.

Ruff, O., Zur Kenntnis der Stickstoff-3-fluoride. Zeitschrift für anorganische und allgemeine Chemie, 1963, *197*, 273.

Samonski, F. H., Jr. Technical history of the environmental control system for Project Mercury. NASA-TN-4126, National Aeronautics and Space Administration, Washington, D.C., 1967.

Sandage, C. Tolerance criteria for continuous inhalation exposure to toxic material. I., Effects on animals of 90-day exposure to phenol, CCl_4 and a mixture of indole, skatole, H_2S and methyl mercaptan. ASD Technical Report, 61-519 (I), Aerospace Medical Research Laboratory, Wright-Patterson AFB, Ohio, October 1961.

Sandage, C. Tolerance criteria for continuous inhalation exposure to toxic material. II., Effects on animals of 90-day exposure to H_2S, methyl mercaptan, indole, and a mixture of HeS; methyl mercaptan, indole and skatole. ASD Technical Report 61-519 (II), Aerospace Medical Research Laboratory, Wright-Patterson AFB, Ohio, December 1961.

Saunders, R. A. Analyses of the spacecraft atmosphere. NRL Report 5816, Naval Research Laboratory, Washington, D.C., 1962.

Saunders, R. A. A new hazard in closed environmental atmospheres. *American Medical Association Archives on Environmental Health*, 1967, *14*, 380.

Saunders, R. A., Umstead, M. E., Smith, W. D., & Gammon, R. H. The atmospheric contaminant pattern of SeaLab II. In Proceedings of the 3rd Annual Conference on Atmospheric Contamination in Confined Spaces, AMRL-TR-67-200, Aerospace Medical Research Laboratory, Wright-Patterson AFB, Ohio, 1967.

Saunders, R. A., & Williams, F. W. Another incident of dichloracetylene contamination. In Proceedings of the 5th Annual Conference on Atmospheric Contamination in Confined Spaces, AMRL-TR-69-130, Aerospace Medical Research Laboratory, Wright-Patterson AFB, Ohio, 1969.

Sayers, R. R., Meriwether, E. V., & Yant, W. P. Physiological effects of exposure to low concentrations of carbon monoxide. U.S. Public Health Report 37, 1922.

Schulte, J. H. Effects of mild carbon monoxide intoxication. *American Medical Association Archives of Environmental Health*, 1963, 7, 524.

Shy, C. M., Creason, J. P., Pearlman, M. E., McLain, K. E., & Benson, F. B. The Chattanooga school children study: effects of community exposure to nitrogen dioxide. I., Methods, description of pollutant exposure, and results of ventilatory function testing. *Journal of Air Pollution Control Association*, August, 1970, *20*, 539-545.

Shy, C. M., Creason, J. P., Pearlman, M. E., McLain, K. E., & Benson, F. B. The Chattanooga school children study: effects of community exposure to nitrogen diozide. II., Incidence of acute respiratory illness. *Journal of Air Pollution Control Association*, September 1970, *20*, 582-588.

Smith, F. J. C., Heim, J. W., Thompson, R. M., & Drinker, C. K. Body changes and development of pulmonary resistance in rats living under compressed air conditions. *Journal of Experimental Medicine*, 1932, *56*, 63.

Sopher, R. L., Esparza, A. R., & Robinson, F. R. The effect of methylhydrazine by inhalation or injection in dog's kidneys. In Proceedings of the 4th Annual Conference on Atmospheric Contamination in Confined Spaces, AMRL-TR-68-175. Aerospace Medical Research Laboratory, Wright-Patterson AFB, Ohio, 1968.

Steadman, B. L., Jones, R. A., Rector, D. E., & Siegel, J. Effects on experimental animals of long-term continuous inhalation of nitrogen dioxide. *Toxicology and Applied Pharmacology*, 1966, *9*, 160.

Sterman, M. B., Fairchild, M. D., & VanTwyver, H. E. Subconvulsant effects of monomethylhydrazine in runway performance in the cat. AMRL-TR-68-183, Aerospace Medical Research Laboratory, Wright-Patterson AFB, Ohio, 1968.

Stewart, R. D., Peterson, J. E., Baretta, E. D., Bachand, R. T., Hosko, M. J., & Herrmann, A. A. Experimental human exposure to carbon monoxide. *American Medical Association Archives of Environmental Health*, 1970, *21*, 154.

Stokinger, H. E. Toxicity following inhalation of fluorine and hydrogen fluorine. In C. Voegtlin and H. C. Hodge (Eds.), *The Pharmacology and Toxicology of Uranium*. National Nuclear Energy Series, Volume 6. New York: McGraw-Hill, 1949.

Thomas, A. A. Man's tolerance to trace contaminants. AMRL-TR-67-146, Aerospace Medical Research Laboratory, Wright-Patterson AFB, Ohio, 1968.

Toliver, W. H., Sr., & Morris, M. L. Chemical analysis of permanent and organic gases in a 30-day manned experiment. *Aerospace Medicine*, 1966, *37*, 233.

Torkelson, T. R., Oyen, F., Sadek, S. E., & Rowe, V. K. Preliminary toxicologic studies on nitrogen trifluoride. *Toxicology and Applied Pharmacology*, 1962, *4*, 776.

Trouton, D., & Eysenck, H. J. The effects of drugs on behavior. In H. J. Eysenck (Ed.), *Handbook of Abnormal Psychology*. New York: Basic Books, Inc., 1961.

Vernot, E. H., & Haun, C. C. Acute toxicology and proposed emergency exposure limits of nitrogen trifluoride. In Proceedings of the 5th Annual Conference on Atmospheric Contamination in Confined Spaces, AMRL-TR-69-130, Aerospace Medical Research Laboratory, Wright-Patterson AFB, Ohio, 1969.

Vernot, E. H., Back, K. C., George, M. E., Chikos, P. M., Jr., & MacEwen, J. D. Hematologic effects of long-term animal exposure to high concentrations of carbon monoxide. In Proceedings of the Conference on Environmental Toxicology, AMRL-TR-70-102, Aerospace Medical Research Laboratory, Wright-Patterson AFB, Ohio, 1970.

Vigdortschik, N. A., Andreeva, E. C., Matussentch, I. Z., Nikulina, M. M., Fiumina, L. M., & Striter, V. A. Symptomatology of chronic poisoning with oxides of nitrogen. *Journal of Industrial Hygiene and Toxicology*, 1937, *19*, 469.

Wagner, W. D., Duncan, B. R., Wright, P. G., & Stokinger, H. E. Experimental study of the threshold limit of NO_2. *American Medical Association Archives of Environmental Health*, 1965, *10*, 455.

Weatherby, J. H., & Yard, A. S. Observations on the subacute toxicity of hydrazine. *American Medical Association Archives of Industrial Health*, 1955, *11*, 413.

Weinberg, M. S., & Goldhamer, R. E. Pharmacology and metabolism of compound A. AMRL-TR-66-238, Aerospace Medical Research Laboratory, Wright-Patterson AFB, Ohio, 1967.

Weir, F. W., Memenzo, T. H., Bennett, S., & Meyers, F. H. A study of the mechanisms of acute effects of hydrazine, UDMH, MMH and SDMH. AMRL-TR-64-26, Aerospace Medical Research Laboratory, Wright-Patterson AFB, Ohio, 1964.

Weir, F. W., Batl., D. W., Yevich, P., & Oberst, F. W. Study of effects of continuous inhalation of high concentrations of oxygen at ambient pressure and temperatures. *Aerospace Medicine*, 1965, *36*, 117.

Zalusky, R., Ulvedal, F., Herlocher, J. E., & Welch, B. E. Physiologic response to increased oxygen partial pressure. III., Hematopoiesis. *Aerospace Medicine*, 1964, *35*, 622.

CHAPTER 11
RESPIRATORY SYSTEM

by

Roscoe G. Bartlett, Jr., Ph.D.
International Business Machines Corporation

This chapter presents a treatment of the topic of human respiration intended primarily for use by persons who are not professionals in the biologic sciences. It discusses developments in the field where these are relevant to problems faced by engineers and designers of life support equipment. Essentially all of the relevant data concerning respiration have been known for some time; the problem has been one of application, not acquisition of information. There is a growing appreciation of a gap in effective dialogue between biologists (including those in medicine) and engineers and physical scientists. This chapter represents an attempt to present material in a form that should bridge this gap in the area of respiratory physiology. To the skilled biologist, the presentation will perhaps appear condescending and to the theoretical engineering scientist the engineering and physics naive; the presentation is not really meant for either of these. Rather it is meant for the engineers and designers who must face and solve the myriad of small and large problems in the development of any man-rated system.

It is beyond the scope of this book to present a description of the basic anatomy of the respiratory system, and length constraints also necessitate an abbreviated treatment of the physiology of respiration. For a better understanding of the data presented, it is recommended that the reader who is unfamiliar with these topics consult any one of the following texts for background material:

Best, C. H., & Taylor, N. B. *The physiological basis of medical practice.* (8th ed.) Baltimore: The Williams & Wilkins Company, 1966.

Comroe, J. H., Jr., Forster, R. E.,II, Dubois, A. B., Briscoe, W. A., & Carlsen, E. *The lung: clinical physiology and pulmonary function tests.* (2nd ed.) Chicago: Year Book Medical Publishers Inc., 1962.

Ruch, T. C., & Fulton, J. F. (Eds.) *Medical physiology and biophysics.* Philadelphia: W. B. Saunders Co., 1960.

Preceding page blank

The following list of terms may also be helpful:

Apnea–no breathing activity

Dyspnea–labored breathing, especially if not warranted by physical exertion

Eucupnea–normal level of body CO_2

Hypercapnea–Higher than normal level of body CO_2

Hyperventilation–correctly, a level of lung ventilation in excess of that required to maintain CO_2 at eucupnea levels: sometimes incorrectly used to describe the labored breathing produced by exercise or stress

Hypocapnea–lower than normal level of body CO_2, produces hypercapnea

Minute Volume–volume of air moved in and out of the lungs in one minute, may be either inhalation or exhalation volumes, which are rarely the same. The fact is usually ignored when this term is used.

Respiratory Exchange Ratio (R)–CO_2/O_2 ratio as determined from inhaled exhaled gas composition comparisons. Will deviate from R. Q. with hypoventilation and hyperventilation.

Respiratory Quotient (R Q)–CO_2/O_2 ratio as a result of tissue metabolism

Respiratory Rate–frequently used by physicians and physiologists as a synonym for breathing frequency, used by biochemists to indicate the rate of tissue metabolism.

General Anatomy of Chest and Lungs

The relations of chest and lungs are shown in figure 11-1, which schematically shows the grosser features and the position of the heart, which shares the chest cavity with the lungs. The major divisions of the "respiratory tree" and a schematic of the micro anatomy are shown in figure 11-2. The branching and rebranching of the bronchi and bronchioles gives rise to a very large number of respiratory bronchioles and alveoli. The total surface contact between alveolar air and lung capillary blood is approximately 100 square meters (about half a singles tennis court) in the healthy adult male.

Accumulating evidence indicates that microscopic lung structure is deleteriously affected by a number of pollutants. Since the life support engineer may be called upon to provide respiratory protection and support equipment for use in environments where the atmosphere cannot be economically cleansed of pollutants some knowledge of the microscopic anatomy of the lung may be useful.

Intrathoracic Pressure

During development of the fetus and during the growth of the child, the chest cavity enlarges faster than the lung increases in size. Consequently, the lung pulls away from the chest wall with greater and greater pressure. This pressure is referred to as the intrapleural pressure or intrathoracic pressure. Because intrathoracic pressure is applied directly to the heart and major thoracic blood vessels, changes in intrathoracic pressure have effects on the circulation.

Increased intrathoracic pressure prevents venous return to the heart. Cardiac output rapidly falls reducing blood pressure and blood supply to the brain, and, since it has no ability to accumulate an oxygen debt, the brain ceases to function and unconsciousness ensues. The engineer and designer of life support equipment must be careful not to produce or require changes in this pressure that compromise the circulation.

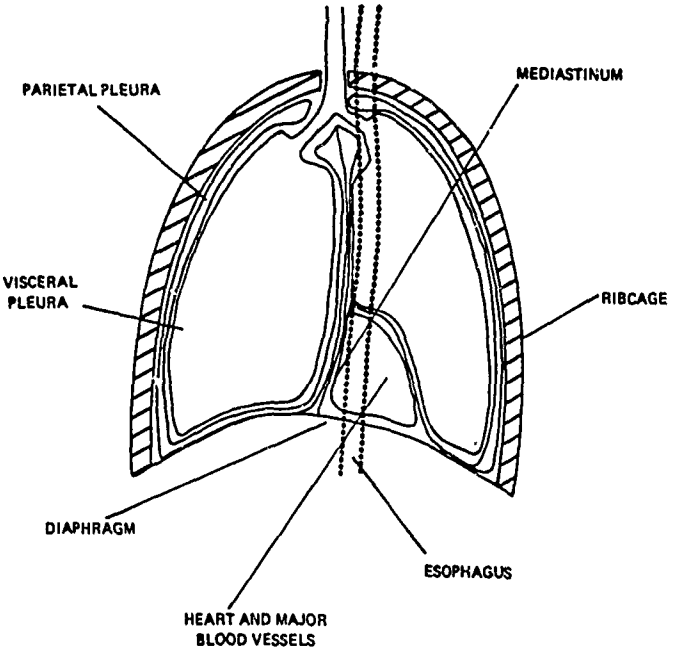
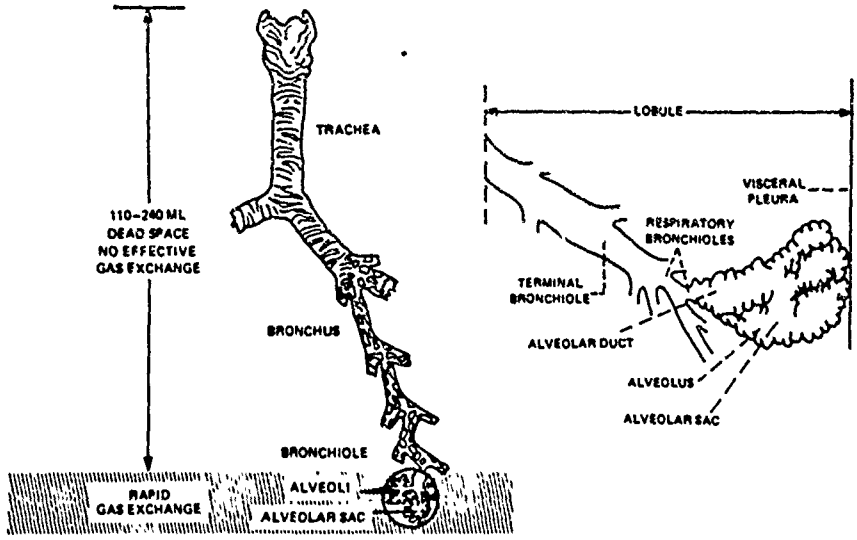


Figure 11–1. Gross anatomical relations of chest and lungs.

General Function of Respiration

In the majority of people during routine activities, the depth and rate of breathing movements are regulated for the maintenance of carbon dioxide in the arterial blood. Oxygen want can be regulating, but only when the oxygen content of the inspired gases is reduced to nearly half that in air at sea level. Oxygen partial pressure, except in some unusual circumstances, should always be high enough so that the breathing will be regulated by the body requirements for CO_2.

The oxygen content of lung air will be determined by the oxygen content of the inspired gases, the flushing of the lungs required for CO_2 regulation, and the rate of oxygen uptake by the blood as it passes through the lungs.



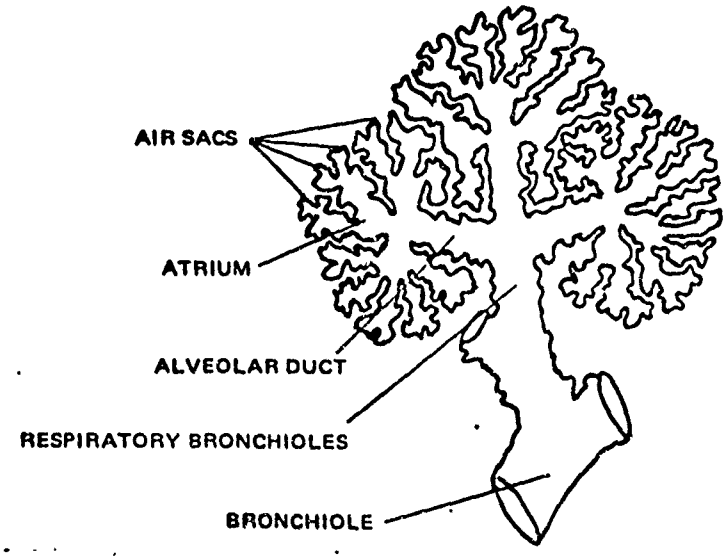


Figure 11–2. Micro-anatomical relations of chest and lungs. Terminal bronchiole gives rise to 10 to 20 respiratory bronchioles, each of which widens into alveolar ducts with many hundreds of alveoli. The alveolar duct often has several major partitions, the so-called alveolar sacs. Interalveolar septa are shown extending into the sacs; the irregular small spaces thus formed are the alveoli.

Respiration

Strictly speaking, respiration refers to the tissue enzyme oxidation processes that utilize oxygen and produce carbon dioxide. More generally this term designates the phases of oxygen supply and carbon dioxide removal. The following annotated outline shows the general subdivisions of the overall process:

1. *Breathing*—Movement of chest/lung complex to ventilate the alveoli

2. *External respiration*—Exchange of gas (O_2 and CO_2) between lung (alveolar) air and blood

3. *Internal respiration*—Exchange of gas between tissue blood and the tissue cells

4. *True respiration*—Ultimate utilization of oxygen by the cells with the coincident release of carbon dioxide.

To the biochemist respiration refers to the enzymatic processes in the tissues which use oxygen and produce carbon dioxide. Figure 11-3 shows the general function of the blood in tissue gas supply and removal.

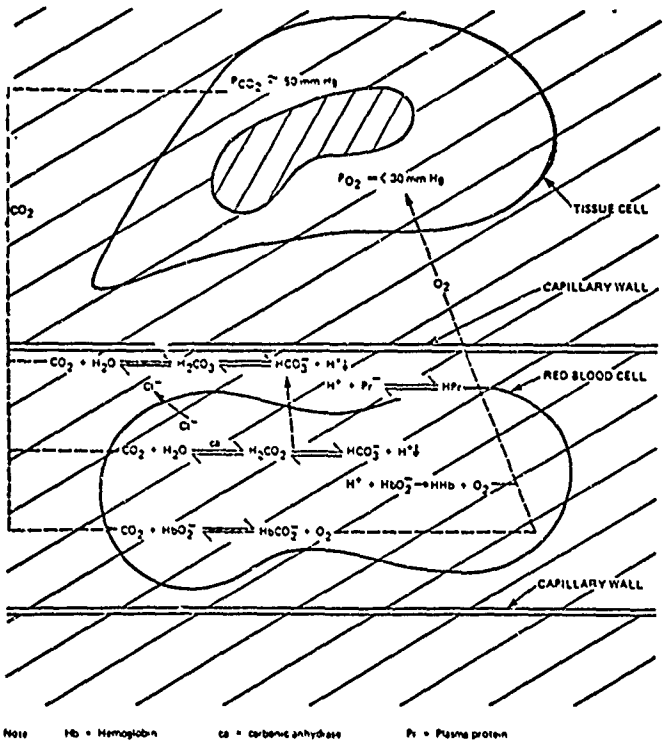


Figure 11–3. Gas exchange between the capillary blood and tissue cells.

Breathing Movements

The volume of the lungs is determined by the balance between the elastic recoil of the lungs and the elasticity of the chest structure in the resting position. From this midposition appropriate muscular action will produce either an exhalation or an inhalation. Breathing motion during space flight, as on Earth, is produced by active inhalation (increasing lung volume above of midposition). Subsequent passive exhalation is produced by the elastic recoil of the chest/lung complex releasing potential energy stored during the active inhalation. Figure 11-4 depicts the balance of forces establishing midposition and the mechanism of passive exhalation during normal breathing. Any system design or use that requires forced exhalation (e.g., pressure breathing in high altitude flying) will produce rapid discomfort and fatigue. Therefore, low exhalation resistance is required.

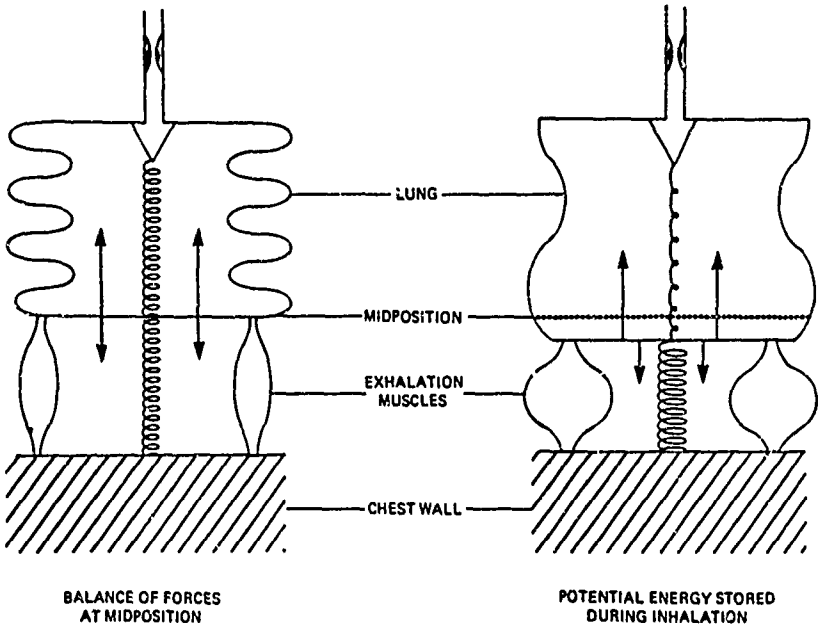


Figure 11–4. Balance of forces at midposition and mechanism of passive exhalation.

Inhalation Movements

The mechanism of inhalation may be an important consideration in support equipment design because any circumstance which tends to deform the usual mechanism will be both limiting and fatiguing.

The expansion of the chest in the lateral diameter is produced by movement of the lower full ribs (6 to 10). They are bowed downward, and, during inhalation, move up and out much as the bail on a bucket is raised. The chest is increased in its anterior/posterior diameter by movement of ribs 2 and 5, which elevate the sternum. In adults, the ribs have a downward slant from their attachment to the vertebral column.

The chest is increased in the head-foot dimension by descent of the diaphragm.

Exhalation Movements

In most breathing activity, exhalation is entirely passive. The relaxation of the inhalation muscles permits the forces of gravity and stored elastic energy to return the chest/lung complex to its normal midposition. In weightlessness, only elastic recoil remains as a passive force for exhalation; but it is adequate. In active exhalation the ribs move down, decreasing both the anterior/posterior and lateral dimension of the thorax. This compression is a usual concomittant of parturition (childbirth), micturition, defecation, and vomiting.

Control of Breathing

Frequency and Depth Variations

To understand the effects on breathing of various conditions of space flight, it is well to know the basic mechanisms by which the body regulates the rate and depth of breathing. Normal resting rates may vary from 5 to more than 30 breaths per minute and little is known about the mechanisms that determine individual differences. Slower breathing rates are related to greater breathing depths. This relationship is a very constant one. There is, on the other hand, a very narrow normal range for alveolar ventilation. The rate and depth of respiration produces, in the average individual, an alveolar CO_2 concentration of 40 mm Hg; thus, deeper breaths accompany slower breathing rates.

To differentiate alveolar ventilation from total lung ventilation the following terminology is used:

1. *Pulmonary ventilation*—The total amount of air moved by the breathing movements

2. *Alveolar ventilation*—The volume of inspired gas which reaches and ventilates the alveoli, i.e., total ventilation minus dead space ventilation.

Table 11-1 shows the relations to produce a 6.0 liter per minute alveolar ventilation with 150 ml dead space.

Table 11–1

Breathing Rate Breaths/min	Dead Space Ventilation ℓ/min	Total Ventilation ℓ/min	Alveolar Ventilation ℓ/min
5	0.75	6.75	6.0
10	1.50	7.50	6.0
20	3.00	9.00	6.0
30	4.50	10.50	6.0

When equipment dead space is added to body dead space, the breaths at any one breathing frequency must be correspondingly deeper. Considerable difference of opinion exists as to the effects of added dead space. Some investigators believe that there are compensating mechanisms that tend to keep CO_2 at the desired level. Others do not. Thus, engineers and designers may have to decide between added support system complexity and dead space increases. A brief description of some of the mechanism of breathing control will be presented so that the dead space effects can be better appreciated.

Mechanisms of Breathing Control

Normal rhythmic breathing is controlled by the requirement to ventilate the lungs to remove CO_2 as fast as it is produced by metabolic activity. There are, however, other factors effective in the control of breathing. These are illustrated schematically in figure 11-5 and described briefly below.

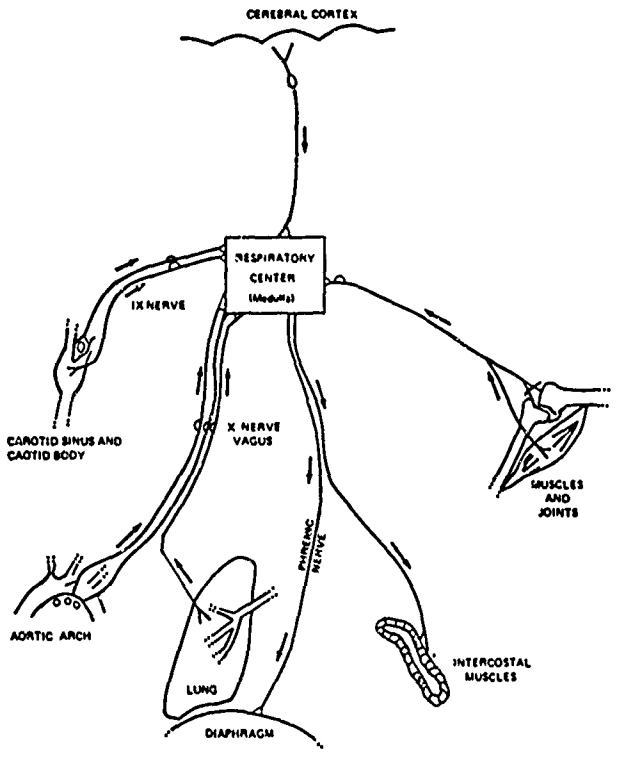


Figure 11–5. Respiratory control elements.

Cerebral Cortex Control. Physical exercise results in an immediate increase in pulmonary ventilation. Impulses originating in the cerebral cortex stimulate the respiratory center to greater activity, so that breathing is increased in anticipation of exercise. Breathing is also regulated by the

cerebral cortex to accommodate talking, swimming, etc. Within limits, there is also a voluntary control of breathing that is cerebral in origin.

Under heavy exercise, maximum pulmonary ventilation can reach 110 to 120 liters per minute, as compared to a resting rate of 6 liters per minute. In aviation, however, extremes of physical activity are not encountered, with the metabolic oxygen consumption seldom exceeding 2 to 3 times the resting rate. On this basis, the provision of oxygen in military aircraft is based on a pulmonary ventilation rate of 25 liters.

Blood Pressure Effects. Pressoreceptors in the carotid sinus respond to blood pressure changes with impulses that regulate breathing rate as well as blood pressure. Increased blood pressure results in a lowered respiratory rate and falling blood pressure increases the rate.

Chemoreceptor Reflexes. The primary receptors for chemical control of breathing are located within the respiratory system. There are, however, chemoreceptors adjacent to the aortic and carotid arteries that reflexively affect breathing regulation. Two reflexes are involved. Increases in the P_{CO_2} and hydrogen ion concentration stimulate breathing to make it faster and deeper; decreases depress breathing. Falling oxygen/blood tensions (oxygen want) also stimulate breathing. With a falling oxygen content of inspired air, the blood is better oxygenated with increased alveolar ventilation. This mechanism produces hypocapnia at high altitudes without supplemental oxygen. Under these conditions, the hypoxic drive overrides the usually precise P_{CO_2} control. The resulting hyperventilation decreases the carbon dioxide concentration, thereby effecting an increase in oxygen concentration since water vapor pressure remains constant.

Lung Stretch Receptors. There are three types of stretch receptors in the lung that are stimulated progressively as the lung is inflated. One set of receptors increasingly inhibits further inhalation and finally terminates it. Passive exhalation then follows. When inhalation is deeper and more forceful than usual, another set excites the inspiratory center of the medulla to further intensity of inspiration. The response of these receptors is short lived and inhalation inhibitory receptors come into play, abruptly terminating inhalation. Lastly, when inhalation is very deep, for example, during heavy exercise or emotional stress, a third set of receptors produces a forced, active exhalation.

Reflexes from Muscles and Joints. Increases in breathing activity during exercise cannot be explained by chemical or blood pressure changes since arterial blood P_{CO_2} is usually lower and P_{O_2} elevated during exercise compared to values at rest. A very important factor in increased breathing activity during exercise is the reflex stimulation from joint and muscle movement. Even movement of the arm or leg stimulates breathing.

Lung Volumes and Capacities

For descriptive convenience the total capacity of the lung at full inspiration is divided into several functional subdivisions. These are defined below and illustrated in figure 11-6.

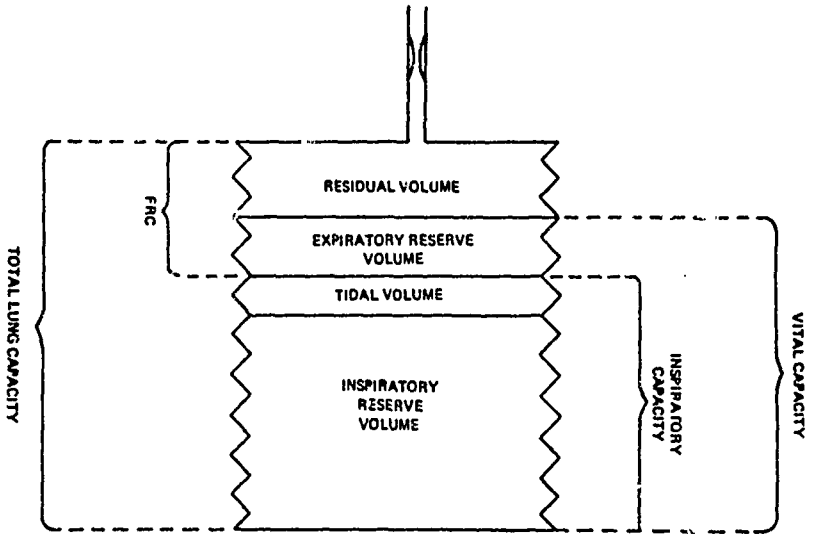


Figure 11-6. Inspiratory capacity and tidal capacity.

The four primary lung volumes which do not overlap are:

1. *Tidal Volume* (TV)–the volume of gas inspired or expired during each respiratory cycle.

2. *Inspiratory Reserve Volume* (IRV)–the maximal volume that can be forcibly expired following a normal inspiration (from the end-inspiratory position).

3. *Expiratory Reserve Volume* (ERV)–the maximum amount of air that can be forcibly expired following a normal expiration.

4. *Residual Volume* (RV)–the amount of air remaining in the lungs following a maximum expiratory effort.

Each of the four following capacities includes two or more of the primary volumes.

1. *Total Lung Capacity* (TLC)–the sum of all four of the primary lung volumes.

2. *Inspiratory Capacity* (IC)–the maximum volume by which the lung can be increased by a maximum inspiratory effort from midposition.

3. *Vital Capacity* (VC)–the maximum amount of air that can be exhaled from the lungs following a maximum inspiration. It is the sum of the inspiratory reserve volume, tidal volume, and expiratory reserve volume.

4. *Functional Residual Capacity* (FRC)–the normal volume at the end of passive exhalation, i.e., the gas volume which normally remains in the lung and functions as the residual capacity.

The lung volumes and capacities are frequently determined by use of a spirometer (a volume displacement device into which the subject breathes). From this instrument a spirogram (volume change versus time) is obtained.

Significance of Lung Volumes for Equipment Design

Functional Residual Capacity. FRC is important in equipment design for two principal reasons. First, when a closed-loop breathing system is used, the total gas volume will be the sum of the gas volumes of the rebreather loop and FRC and the tidal volume. (The tidal volume will be contained in either the lungs or the rebreather bellows or will be distributed between them during inhalatory or exhalatory activity.) This total system gas volume is important in considerations of inert gas dilution, expansions or contractions with pressure change, inert gas washout, etc. Secondly, should the expanding gases exceed tolerable pressures, the designer must assure that a breathing apparatus will not so impede the flow of these rapidly expanding gases as to increase lung pressures above these critical levels.

Residual Volume. Because the residual volume is that portion of lung volume that remains in the lung after a forced exhalation, to reduce lung volume below this level will require compression of the chest/lung complex or an increased trans-lung (intrapleural pressure to alveolar air pressure) pressure gradient as the result of reduced external breathing apparatus pressure acting through the airway. Regardless of the mechanism, lung collapse (atelectasis), lung blood vessel rupture, pulmonary edema, or any combination of these three effects may occur. It is therefore, important to assure that system operation over every possible range of pressure changes never produces such pressure differentials as to require a lung volume less than residual volume.

Inspiratory Capacity and Inspiratory Reserve Volume. Inspiratory capacity represents the maximum volume of air that can be forced into the lung by changes in system volume, without producing overexpansion of the lungs. The volume of the inspiratory reserve capacity is progressively reduced during an inhalation, and the remaining volume that can be inhaled is referred to as the inspiratory reserve volume. Thus, during a breathing cycle, the permissible increase in lung volume imposed by system pressures is reduced by the tidal volume. When system pressures are such as to require a lung volume increase greater than that represented by the inspiratory capacity (or inspiratory reserve volume, as appropriate), the lungs are overextended, and lung rupture is possible. It is, therefore, important to

assure that system pressure changes will never require an increase in lung volume above what could be produced by a maximum inhalation.

Tidal Volume. A closed-loop system must have a rebreather bellows that will accommodate the largest expected tidal volume. Such a tidal volume could, of course, be as large as the vital capacity. But it might not be practical to provide so large a rebreather bellows. In such a case a rebreather bellows of reasonable size should be provided (determined by expected level of exercise, etc.). In this case increased inhalation volumes can be provided from oxygen storage and increased exhalation volumes can be accommodated by venting through a spring loaded exhalation pressure safety valve.

Total Lung Capacity. In an extreme case, the maximum amount of gas the lungs could contain, which must be considered for total system volume calculations and accommodation for gas expansion, is the total lung capacity. Although such a circumstance is unlikely, a conservative design must use this volume as the basis for the design.

Average Lung Capacities, Volumes, and Function Capabilities for Healthy Adult Males

There is considerable individual variability in lung volumes and capacities. This variability is somewhat decreased if the data are shown with size and age relationships. Figures 11-7 through 11-11 presents these data. One should note, however, that because of individual variations, the values presented must be used only as approximations when applied to individuals or small groups of individuals.

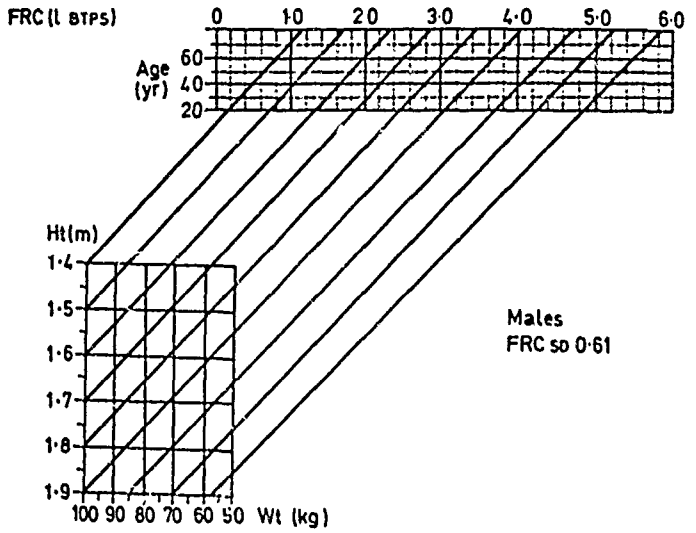


Figure 11–7. Functional residual capacity (FRC) in normal adult males. (Cotes, 1968)

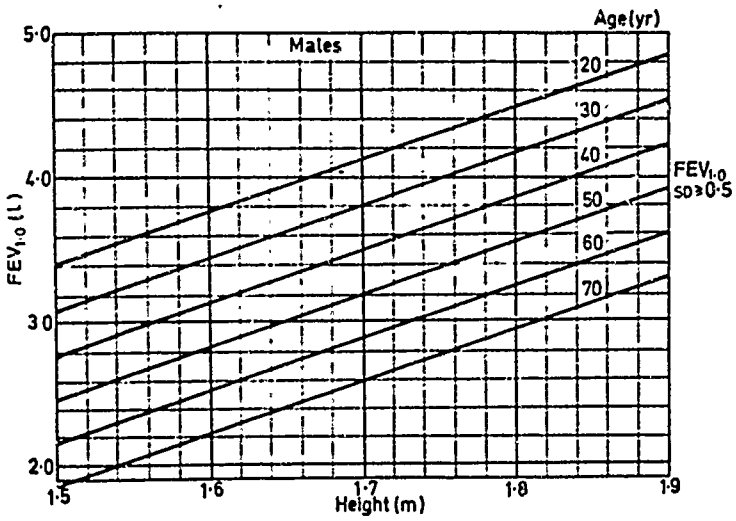


Figure 11–8. Forced expiratory volume in normal adult males. (Cotes, 1968)

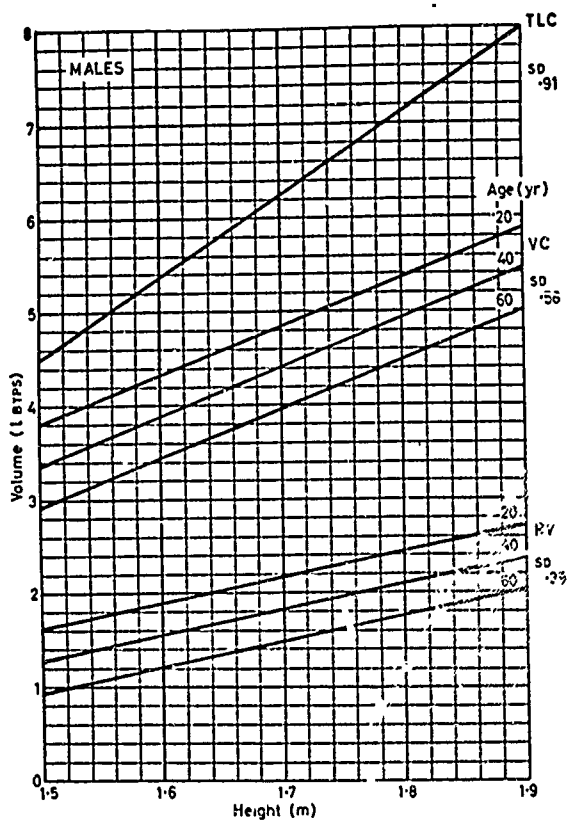


Figure 11–9. Total lung capacity (TLC), vital capacity (VC), and residual volume (RV) in normal adult males. (Cotes, 1968)

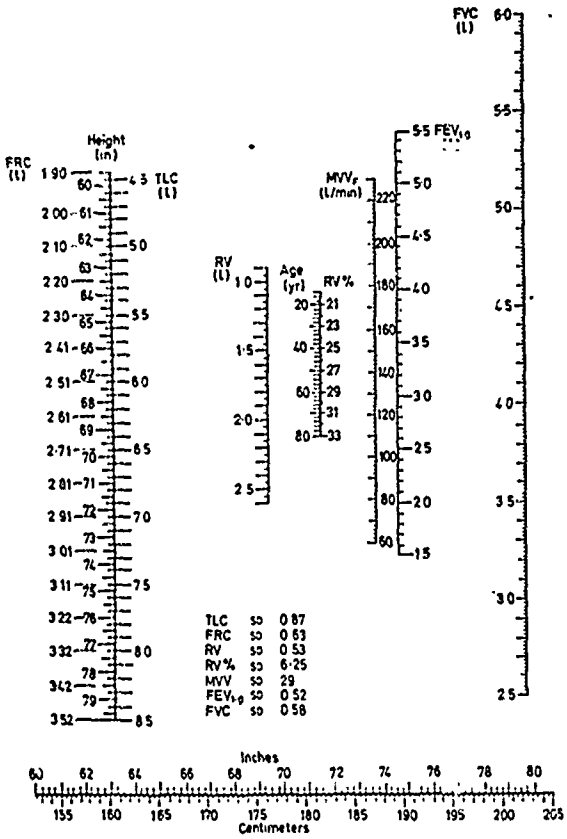


Figure 11–10. Nomogram relating indices of ventilatory capacity to weight and height for normal adult males. (MVV = max voluntary ventilation; FEV 22 = forced expiration velocity at one second from start of forced exhalation from full lung). (Cotes, 1968)

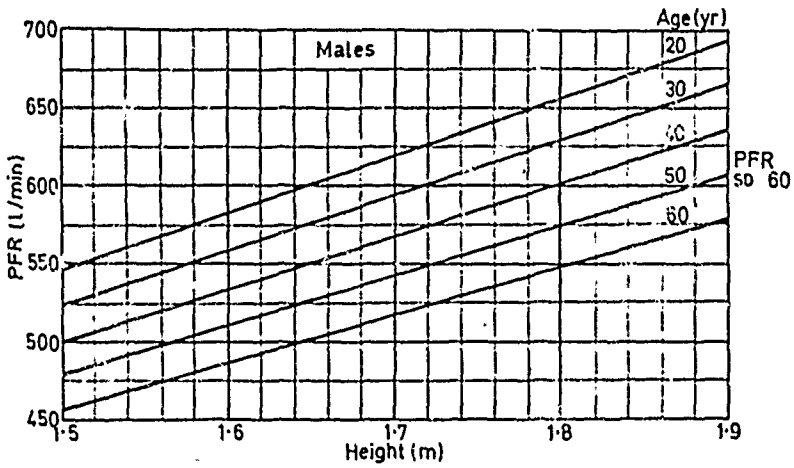


Figure 11–11. Expiratory peak flow rate in normal adult males. (Cotes, 1968)

Mechanical Relations

Pressure/Volume Relations

A knowledge of the pressure/volume relationships is important in the design of life-support equipment. Figure 11-12 presents the relationship in its simplest form. *Maximum inspiratory* (at the left of the figure) represents the negative inspiratory pressure that can be exerted with lung volume varying from 0 to 100 percent of vital capacity and the maximum inhalation volume exchange over a range of negative pressures to nearly 100 mm Hg. For example, with the lung completely emptied, when only residual air remains (Point 1), a maximum inspiratory effect of approximately 90 mm Hg can be exerted. Also, if the pressure in an external breathing loop is 90 mm Hg negative, no inspiratory volume can be moved. In fact, this negative pressure will empty the lung to this point. If the negative pressure were greater, i.e., more negative, there would be marked engorgement of the lung vascular bed with imminent threat of blood vessel rupture.

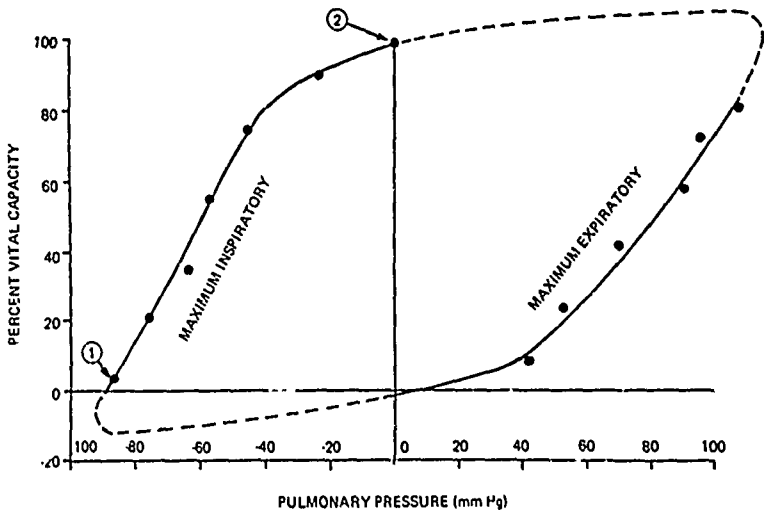


Figure 11–12. Pressure/volume relations of chest/lung complex.

With the lung as full as possible (Point 2) no additional inspiratory effort can be exerted. It also can be seen that, if the pressure in the external breathing loop is the same as lung pressure, a full vital capacity can be exchanged.

The points establishing the curve labeled *maximum expiratory* are obtained in a like manner using exhalation efforts and positive rather than negative pressures. Thus, at 100 percent vital capacity a maximum exhalation effort can be made, and at 0 percent, no exhalation effort made. Likewise, with about 100 mm Hg positive pressure the lung is completely filled in spite of a maximum exhalation effort so that no air can be moved. If more pressure

is exerted there is the danger that the lung may be stretched to the rupture point with tearing of tissue, bleeding, and loss of effective gas exchange surface.

The reader is cautioned that these curves present average values for maximum breathing efforts. For any one person danger may exist at much lesser pressure values. These figures, then, represent extremes that should never be approached as design points.

The maximum pressure/volume loop takes on new meaning if an additional dimension, the pressure volume relations for the relaxed chest-lung complex, is included (figure 11-13). The point at which the relaxation pressure curve crosses the zero pressure line is the midposition; the volume below it is the expiratory reserve volume, and the volume above it is the inspiratory capacity. The figure shows that at about 20 mm Hg negative pressure the lung is collapsed to the residual volume, if there is no competing muscle force. At about 20 mm Hg positive pressure the lung is completely filled, if there is no competing exhalation muscle force.

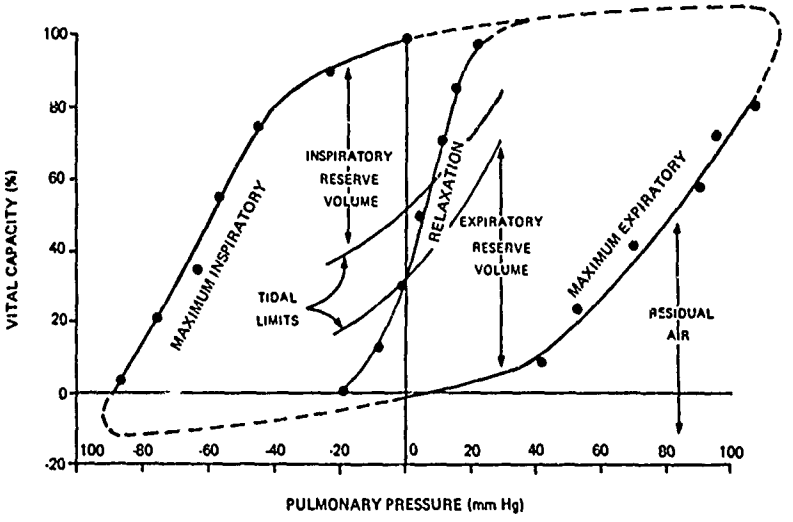


Figure 11–13. Pressure/volume relations of chest/lung complex (including relaxion relations and pressure breathing); cross hatched triangle is elastic work of breathing at zero pressure differential.

Since the pressure/volume loop has the dimensions of work (AREA = volume x pressure = cm^3 x gm/cm^2 = gm centimeters), one can also show diagrammatically the mechanical work done at different breathing loop pressures. This is shown in figure 11-13 for zero pressure differential and for a positive 30 mm Hg differential.

The mechanical work at zero pressure differential is done by the inspiratory muscles because exhalation is passive. At 30 mm Hg positive

pressure, the mechanical work is done by the expiratory muscles. The fatigue effect is even greater than the relative increase in mechanical work so that such breathing can be endured only during an emergency.

Pressure breathing is employed in emergency situations in aircraft flight and might be a desirable fallback capability for some space flight contingencies. The limit of tidal pressure/volume loops over a range of negative to positive breathing loop pressures can be superimposed on figure 11-13. Because there is an inherent, reflex, muscular counterforce applied to the differential breathing loop pressures, the limit envelope for the tidal pressure/volume loops deviates from the relaxation pressure curve. Thus, whenever the applied pressure is positive, relaxation of the exhalation muscles does not occur at any phase of the breathing cycle. The same is true for inspiratory muscles if negative pressures are applied. The position of the curves determining the pressure/volume loops over a range of breathing loop pressures is shown in figure 11-13.

Breathing Resistance and Mechanical Work of Breathing

Breathing equipment, no matter how well designed, provides some flow resistance. "Safety pressure" may be employed to remove inhalation resistance, but then exhalation resistance is correspondingly increased. Increased flow resistance increases the work of breathing. Mechanical work over a range of breathing resistance is shown in figure 11-14. The pressure/volume loops shown were obtained at uniform breathing rates of 40 breaths per minute and with maximum or near maximum effort.

Note that at low resistance (50 mm H_2O pressure to produce 100 liters per minute flow) the area, and therefore mechanical work, is small. As pressures are increased (125 and 225 mm Hg), the volume moved is not appreciably lessened, but the pressures exerted are much higher so that the mechanical work done is greater. With still higher pressures (675 mm), the work lessens because the respiratory muscles cannot exert higher pressures. Thus the volume decreases because breathing in all cases is at 40 breaths per minute. As far as work output is concerned, there is an optimal loading of the breathing mechanism. This is shown in the figure 11-15. The oxygen cost of breathing through these resistances was relatively flat across the range of breathing resistances.

With mechanical work done and the coincident oxygen cost, one can calculate the efficiency. These relations are shown in figure 11-16.

Oxygen consumption for the subjects in the study illustrated in the figures that follow is very high compared to oxygen consumption during space flight. Also, highest efficiencies occurred with relatively high airway resistances. One can conclude, therefore, that there is a very large breathing reserve that can be called on in an emergency. Breathing this reserve may be fatiguing, but the reserve is available for emergencies of short duration.

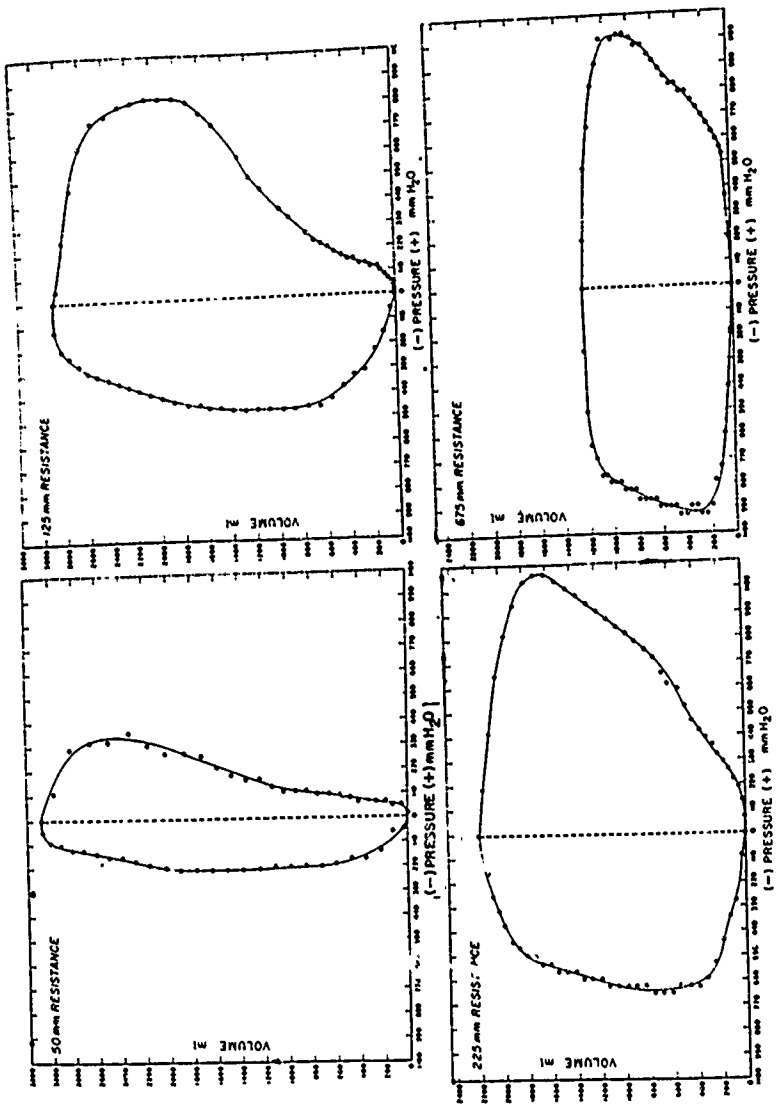


Figure 11–14. Pressure/volume loops for maximum breathing effort with four levels of airway resistance. (Reprinted from Journal of Applied Physiology, 1958, 13(2), 194-204)

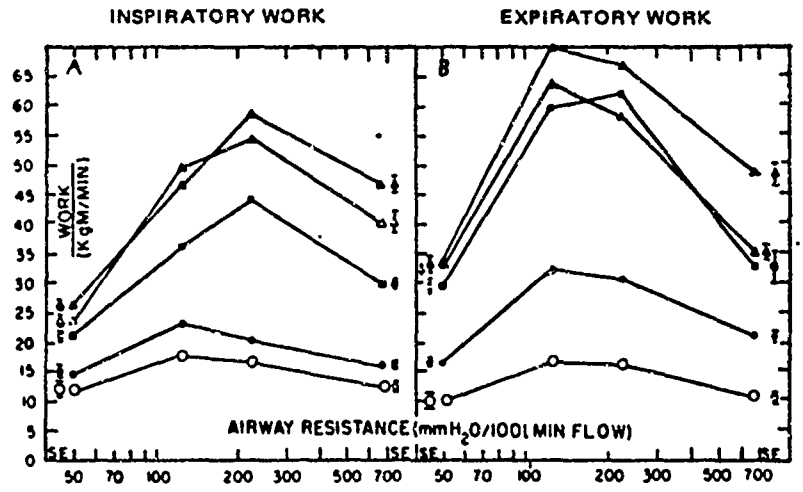


Figure 11–15. Mechanical breathing work output with maximum breathing effort at several airway resistance levels. Symbols represent different subjects. (Reprinted from Journal of Applied Physiology, 1958, 13(2), 194-204)

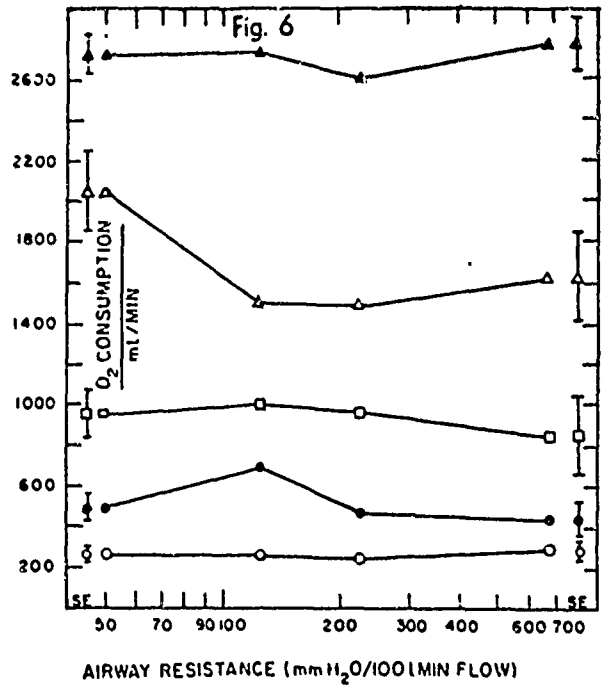


Figure 11–16. Breathing efficiency with maximum breathing effort at several airway resistence levels. (Reprinted from Journal of Applied Physiology, 1958, 13(2), 194-204)

Velocity/Volume Loop

If breath velocity is plotted against breath volume, and if inspiratory volumes are equal, a closed loop is generated. When maximum inspiratory and expiratory efforts are exerted, a closed loop is formed. For adult males the velocity/volume ($\dot{V}/V$) loop has the form presented in figure 11-17. This contour is markedly changed with respiratory diseases and aging. The figure also shows lung volumes and capacities usually obtained from a spirogram by superimposing the resting $\dot{V}/V$ loop on the maximum $\dot{V}/V$ loop *O*.

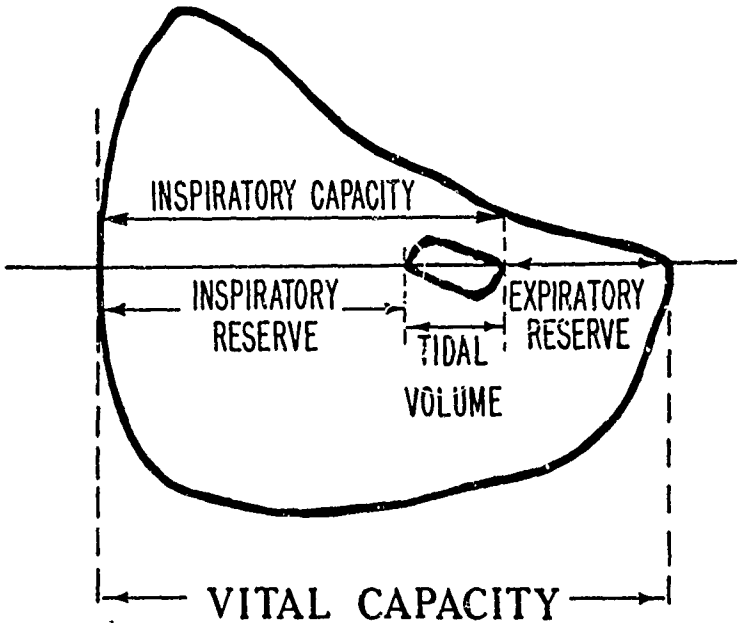


Figure 11–17. Maximum velocity/volume ($\dot{V}/V$) loop.

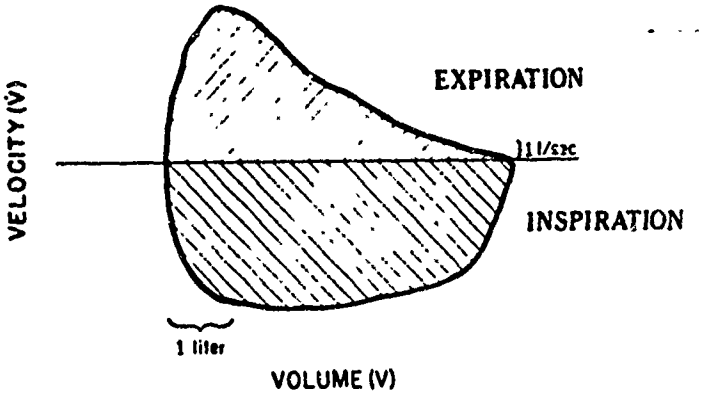
Because time elements can be determined, it is feasible to use the maximum $\dot{V}/V$ loop for obtaining any of the frequently used timed vital capacities of forced expiratory volumes, as they may be called. Figure 11-18 illustrates the technique for full inspiratory and expiratory efforts.

The $\dot{V}/V$ loop can be determined during space flight by use of a pneumotachograph and appropriate transducers (figure 11-19). These are lightweight and can be integrated into the life-support equipment. Because the pneumotachograph produces only a velocity signal, the coincident volume values are obtained by integration under the velocity trace. This is conveniently done by using an onboard or ground-based computer.

Gas Density, Airway Resistance, and Flow Rates

The reduced pressures during space flight produce a reduced gas density. If helium were used as the inert gas in a two-gas atmosphere, there would be an

additional reduction in gas density. Reduced gas density results in lesser airway resistance for a given flow rate. Airway resistance is also determined by gas viscosity and gas density; but over wide ranges of density differences, viscosity effects will be small. If increased airway resistance slows the transit time of gas from the alveoli to the mouth, a measure of the lag between alveolar pressure production and resultant air flow at the mouth will reflect relative resistance to air flow.



$$\text{For Expiration EVCT} = \frac{V^2}{A} = \frac{5^2}{20.75} = 1.20 \text{ sec.}$$

$$\text{For Inspiration IVCT} = \frac{V}{A} = \frac{5^2}{34.15} = 0.73 \text{ sec.}$$

Figure 11–18. Use of the maximum $\dot{V}/V$ loop for calculating inspiratory vital capacity time (IVCT) and expiratory vital capacity time (EVCT).

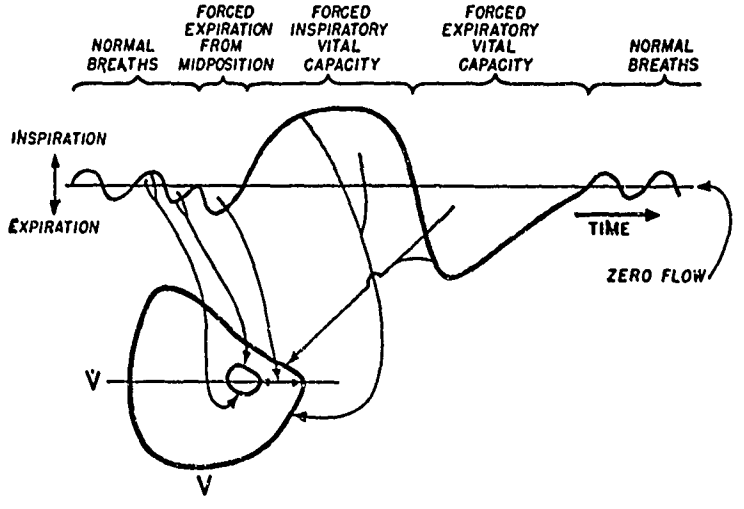


Figure 11–19. Construction of $\dot{V}/V$ loop from pneumatogram.

To understand the effects on the astronaut of engineering expediencies that may compromise the exchange of gases between alveolar air and capillary blood, it is helpful to note the partial pressures of gases in this exchange (table 11-2). The only active process in the exchange is transportation (the circulation of the blood and the ventilation of the lungs). There is no secretory process. The gases move along concentration gradients as seen in the table.

Table 11–2

Partial Pressure and Gas Exchange Breathing Air at Sea Level

	Gas Partial Pressure				
	O_2	CO_2	N_2	H_2O	Total
Inspired air	158	0.3	596	5.7	760
Expired air	116	32	565	47	760
Alveolar air	100	40	573	47	760
Arterial blood	100	40	573	47	760
Venous blood	40	46	573	47	706
Tissues	30 or less	50 or more	573	47	700

A study of this table raises three questions that should be answered:

1. Why is the alveolar/venous blood gradient so much larger for O_2 than for CO_2? Although O_2 is a smaller molecule than CO_2, and therefore diffuses faster, CO_2 is approximately 30 times more soluble in body tissues than is O_2. Therefore, the effective diffusability is approximately 20 times greater for CO_2 than O_2, and a concentration gradient for CO_2 of 6 mm Hg results in a more complete equilibration than does a concentration gradient of 60 mm Hg for O_2. This general relationship is important in design. Oxygen supply to the tissues is much more sensitive to derangement than is CO_2 removal, thus the necessity for assuring equipment and physiological O_2 supply adequacy.

2. Why is nitrogen partial pressure lower in lung air and blood than in inspired air? Actually if gas composition is calculated on a dry basis, percentage of nitrogen is higher in alveolar air (and blood) than in inspired air. This is because more oxygen is picked up by the blood than CO_2 released. This reflects metabolic activity in the tissues when varying combinations of fat, carbohydrate, and proteins are burned producing ratios of CO_2 production to O_2 consumption (called Respiratory Quotient (RQ) in the tissues or Respiratory Exchange Ratio (R) for exhaled air).

3. Why is total gas pressure, including water vapor pressure, less in venous blood and tissue than in arterial blood and respiratory gases? As is apparent from the gas partial pressure table 11-2 this difference reflects the difference in partial pressure for oxygen uptake by the tissues (60 mm Hg for venous blood) and carbon dioxide increase as a result of CO_2 release by tissue metabolic activity

(6 mm Hg for venous blood). Implicit in this comparison is the observation that for binding of a given quantity of gas there must be a much larger change in O_2 partial pressure than in CO_2 partial pressure. This reflects the very large binding (or buffering) capacity of blood and other body fluids for CO_2. Indeed, as discussed later in this section, hypoventilation and hyperventilation can move enormous quantities of CO_2 in and out of body storage, respectively. The lower total partial pressure of dissolved gases in venous blood and tissue assures that gas injected into the body or leaked from the lung by rupture will be quickly absorbed by the blood. Thus, there are no permanent gas pockets in any tissue in the body.

Oxygen Dissociation Curve of Hemoglobin

The requirements for maintaining oxygen partial pressure at specified levels is better understood if the mechanism of oxygen transport is understood. Almost all of the oxygen transported by the blood is carried by the hemoglobin. (Hemoglobin carries approximately 19 ml per 100 ml of blood. At usual O_2 tensions only about 0.3 ml per 100 ml of blood is carried in the dissolved state.) The relation between O_2 partial pressure and hemoglobin saturation with oxygen is usually described as the oxygen dissociation curve of hemoglobin and is presented as a curve on P_{O2} – percent saturation coordinates. The general shape of the curve is shown in figure 11-20.

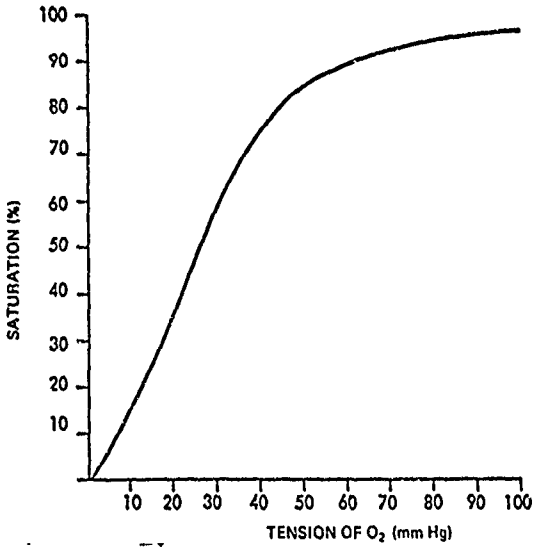


Figure 22–20. Oxygen dissociation curve of hemoglobin.

The shape of this curve has great significance. Note that above 50 mm Hg P_{O2}, there is little increase in hemoglobin carrying capacity for oxygen. Therefore a lowered alveolar P_{O2} concentration will not materially reduce the O_2 available for tissue use as long as the partial pressure remains above 50 mm Hg. However, at the tissue level where the P_{O2} is kept low by

metabolic activity, the hemoglobin will hold little oxygen. This means that large amounts of oxygen are reduced for tissue use. Table 11-2 shows average values of O_2 concentrations in alveolar air, arterial blood, venous blood, and tissues. Figure 11-21 indicates the usual conditions of hemoglobin saturation in the lungs and desaturation at the tissue level. Note the markedly increased amounts of O_2 released to the tissues with high metabolic rates that may reduce the tissue P_{O_2} level to near zero.

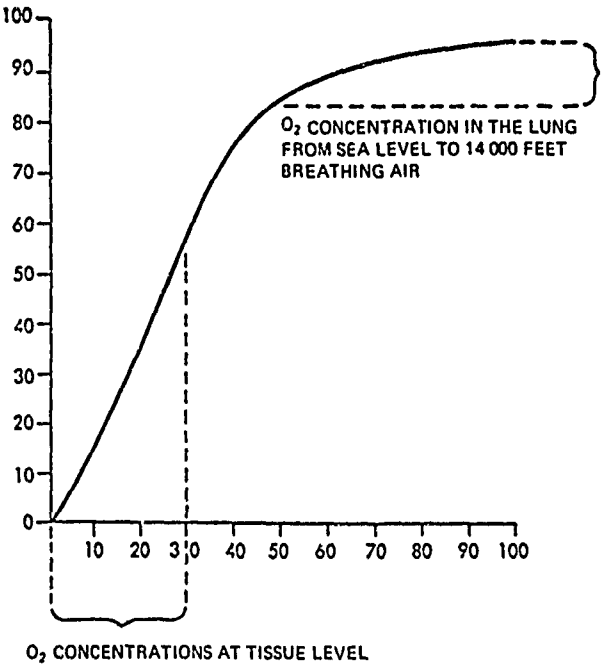


Figure 11–21. Oxygen dissociation curve of hemoglobin and the facilitation of O_2 uptake and release.

An additional facility further increases the efficiency of oxygen supply to the tissues: the oxygen dissociation curve of hemoglobin is not fixed but is different at the tissue level as compared to lung blood. The extent of this shift is shown in figure 11-22. Examination indicates the great efficacy of this shifting of the curve: hemoglobin/oxygen association is much facilitated in the lung blood and hemoglobin/oxygen dissociation is much enhanced at the tissue level. For instance, at 25 mm Hg O_2 tension and with the curve at the far left position, the hemoglobin would be 62 percent saturated, but with the curve at the extreme right position the hemoglobin is only 35 percent saturated. Thus an additional 27 percent of total saturation volume of O_2 is released to the tissues.

To convert the percent of saturation to the actual quantity of O_2 carried by hemoglobin, multiply the grams of hemoglobin per 100 ml of blood by 1.34, which is the milliliters of O_2 that will combine with one

gram of hemoglobin. Because normal adult male blood contains about 15 grams of hemoglobin, each 100 ml of blood will carry about 20 ml of O_2 (called 20 ml percent, i.e., percent by volume). But, because of venous admixture (some blood in the lungs is not adequately exposed to ventilated alveoli), the hemoglobin of mixed arterial blood is only about 95 to 97 percent saturated. The curves above show the percent of saturation plateauing at this level. Higher O_2 (e.g. 100 percent at sea level) will not much increase the percent saturation. More O_2 is carried in simple solution. But for space cabin pressures, even 100 percent O_2 will not much increase this carrying capacity because O_2 solution in blood is small.

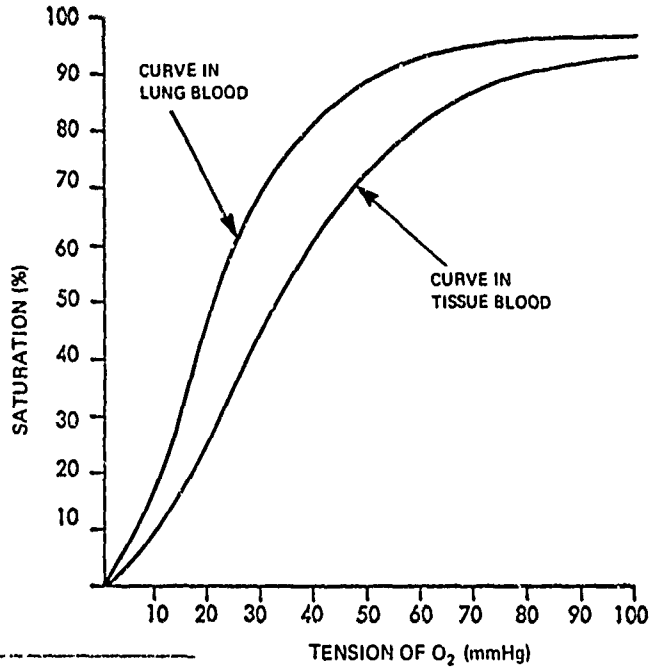


Figure 11–22. Oxygen dissociation curve of hemoglobin shift and lung blood as compared to tissue blood.

The conditions of blood in the lungs (as compared to those of tissue blood) that cause the curve to be shifted to the left are:

1. Lower temperature
2. Lower pH
3. Lower ionic concentration
4. Lower P_{CO_2}.

Opposite conditions exist at the tissue level and cause the curve to be shifted to the right.

Denitrogenation

Saturation, Tissue Types, and Nitrogen Elimination. Ambient air contains approximately 79 percent physiologically inert gases of which nearly all (78 percent) is nitrogen. The body is saturated with nitrogen when breathing air. When lung nitrogen is removed by flushing with oxygen, the nitrogen that is dissolved in the body tissues moves along concentration gradients to the lungs where it is in turn flushed out. If the decrease in lung partial pressure is too precipitous, the dissolved gases are expanded and collect in body tissues and structures to produce a variety of symptoms. This syndrome has many names, such as bends, chokes, decompression sickness, and caissons disease, which are based on the more conspicuous complaints.

To determine the likelihood of decompression sickness resulting from inadvertent decompression, one must know: (1) the extent of denitrogenation at the time of decompression and (2) the absolute level of inhaled nitrogen immediately preceding the decompression. Continued exposure to an inhalation mixture containing nitrogen at a low partial pressure, e.g., 35 mm Hg, will produce a relative denitrogenation with ultimate equilibrium at this level rather than at 0 mm Hg N_2 partial pressure, which would obtain if denitrogenation were accomplished by inhalation of 100 percent oxygen (or a mixture of gases containing no nitrogen). At sea level, breathing air, the body is equilibrated with nitrogen solution at a partial pressure of approximately 670 mm Hg. Therefore, when oxygen is breathed, nitrogen elimination proceeds with the initial gradient for nitrogen movement being approximately 670 mm Hg. If, instead of denitrogenation with 0 mm Hg N_2 pressure, a mixture containing 35 mm Hg N_2 partial pressure is inhaled, the initial driving force for nitrogen elimination will be a pressure gradient of approximately 635 mm Hg. Such a small reduction in the total gradient would not meaningfully slow the rate of nitrogenation, particularly since N_2 elimination is generally perfusion (i.e., blood flow) limited rather than diffusion (i.e., gas diffusion) limited. Even small changes in lung perfusion rate would affect the rate of nitrogen elimination much more than would the small difference in driving force.

The other consideration is the absolute pressure of nitrogen in the inhaled mixture immediately preceding the decompression. If alveolar P_{N_2} is high in the few minutes before decompression, the probability of bends, or another manifestation of decompression sickness, will be determined largely by the long term alveolar P_{N_2} levels rather than the short-term effects. This is true for two reasons. First, the high levels of P_{N_2} inhaled for a short time will affect N_2 solution primarily only in the lowest tissue component, and the nitrogen from this component will be released very quickly on decompression. Second, bends manifestation is believed to be largely restricted to the higher tissue components with long half-times for clearing. Because it takes many hours to clear this tissue (see table 11-3) and because even the highest P_{N_2} levels expected will not materially slow the nitrogen elimination from these tissues, short-term exposure to the higher P_{N_2} levels should have little effect on bends production.

Table 11–3

Tissue Types for Nitrogen Clearance

Tissue Component	Tissue Types	Time for Removal of Half Previous Level (Approximate)
I	Lungs Circulatory system	1.5 min
II	Viscera	8 min
III	Muscle Fascia Skin	30 min
IV	Adipose tissue Bone	150 min
V N	(There is evidence for even longer half-time tissues, perhaps in excess of 940 min)	

The importance in bends production of nitrogen dissolved in the tissues with long clearance half-times is further suggested by the following comparison. Even though long-term exposure to an altitude of 4700 feet theoretically removes only about 15 percent of dissolved nitrogen and one hour of denitrogenation removes about 60 percent of dissolved nitrogen, still the protection provided against bends production is about equal.

This discussion has been related to decompression sickness only and not to hypoxia. It is clear that inhalation of essentially 100 percent O_2 during decompression above 35 000 feet is required and this will not be less efficacious if predecompression P_{N_2} levels have been 70 mm Hg rather than 35 mm Hg.

Breathing Equipment Design and Nitrogen Elimination. Because nitrogen solution in body tissues (at pressures of 1 or 2 atm and lower) is directly proportional to lung concentration, the relative amount of nitrogen contained in lung air at saturation equilibrium, as compared to that dissolved in the body tissues, is constant over this pressure range with varying nitrogen percentages in the respired gases. Therefore, we can consider elimination of nitrogen after equilibrium, at sea level, and breathing air and then extrapolate to indicate elimination relations for other conditions.

At sea level breathing air, the lungs contain about 2 liters of nitrogen (at midposition FRC). The total dissolved nitrogen in the body is not much more than 1 liter. If closed-loop breathing equipment is employed and if denitrogenation is desired, then the nitrogen must be removed from the lungs and from the tissues.

Nitrogen elimination from the lungs is quite rapid. Considering N_2 elimination from the tissues, it is apparent from the curve in figure 11-23 that N_2 elimination from the lungs has essentially asymptoted at about 1.5 minutes.

If one considers N_2 elimination as a function of number of breaths, rather than on a time basis, a theoretical elimination curve can be constructed (figure 11-24). It is apparent from this curve that lung N_2 elimination is about 90 percent complete in 15 breaths.

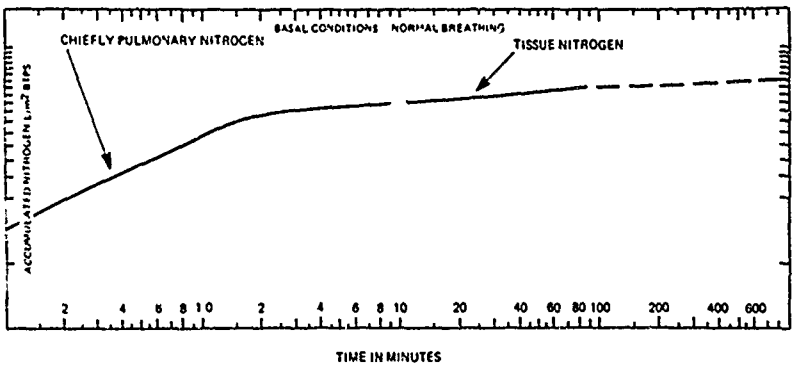


Figure 11–23. Accumulated nitrogen elimination.

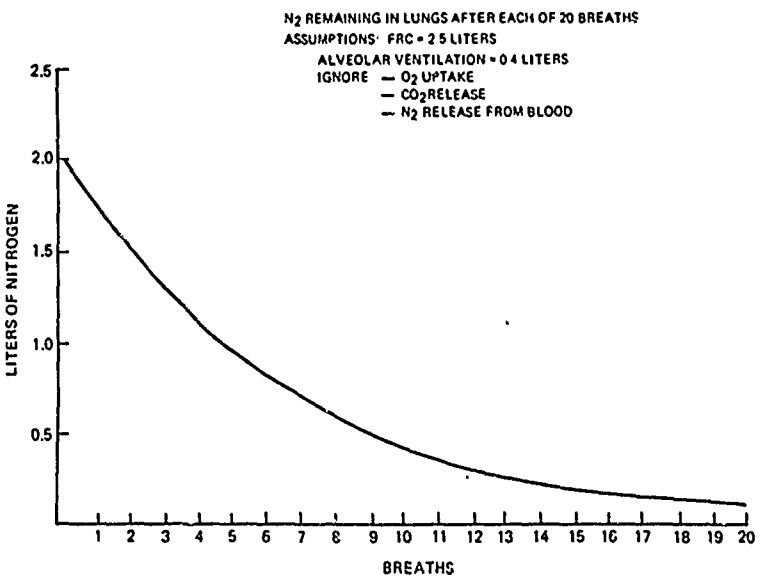


Figure 11–24. N_2 remaining in lungs after each of 20 breaths.

The importance of these observations to respiratory support equipment design relates to the requirement for nitrogen purging from closed-loop systems. It is clear that the purging must be rapid at first to clear the lungs and then slower over a protracted time to keep equipment P_{N_2} levels low enough to permit relatively unimpeded nitrogen elimination from the tissues without extravagant use of gas for flushing.

Ventilation, Perfusion, Dead Space, and Shunts

In the normal adult male at rest there is an alveolar ventilation of about 5 liters per minute and a cardiac output (perfusion) of about 5 liters per minute. Thus, the ventilation/perfusion ratio for the lung as a whole is approximately unity. However, ventilation and perfusion are not evenly distributed, so that some alveoli/capillary units are relatively over ventilated (under perfused) while others are over perfused (under ventilated) (see figure 11-25). In addition, some of the inhaled air never reaches the alveolar surface, so that it does not take part in gaseous exchange. Thus the total lung complex may be subdivided into the following functional compartments so far as gas exchange is concerned:

1. Air in the lung and air conducting passages
2. Ventilated and non-perfused alveoli
3. Perfused and non-ventilated alveoli
4. All variations between 2 and 3, including those with balanced ventilation/perfusion ratios.

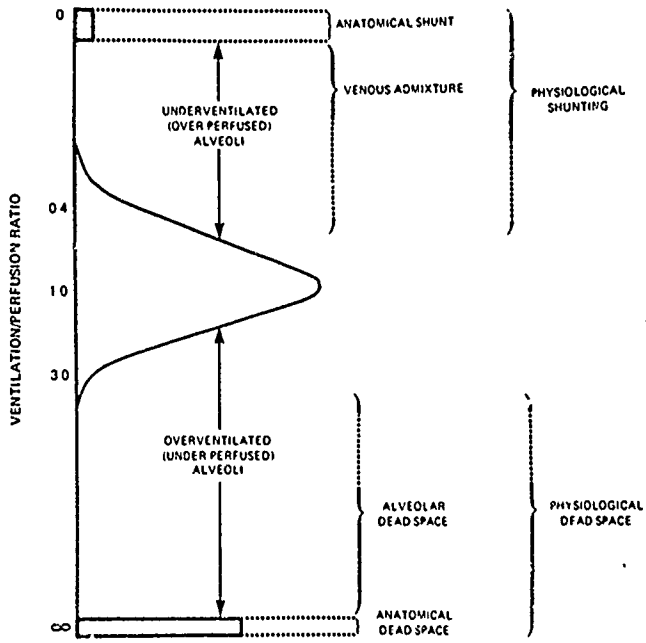


Figure 11–25. Range of ventilation/perfusion ratios.

The relations shown in figure 11-25 are discussed in the order of the lowest to the highest ratios of ventilation to perfusion.

Anatomical Shunt. Some blood passes from artery to vein in the lung without ever going through a capillary bed. The effect is the same as that which occurs with perfused but non-ventilated alveoli. Anatomical shunting, then, is the sum of actual blood shunting and effective shunting when some alveoli are collapsed or plugged and not ventilated at all.

Venous Admixture. Other alveoli are relatively under ventilated, so that the blood perfusing them is only partly replenished with oxygen and has only a portion of the CO_2 that was picked up in the tissues. This blood is only partly arteriolized and to a lesser or greater extent remains venous blood. The effect of this on the mixed arteriolized blood leaving the lungs is referred to as venous admixture. In the normal lung it is small, reducing potential O_2 carrying capacity from about 20 to about 19 volumes percent and reducing hemoglobin saturation with oxygen from the potential of 100 percent to 95 to 97 percent.

Normally Ventilated and Perfused Alveoli. In the normal lung most of the alveoli fall into this category. Because of the shape of the oxygen dissociative curve of hemoglobin, the hemoglobin is essentially 100 percent saturated over the range of ventilation/perfusion ratios shown in the central hatched area in figure 11-25. In some diseased states, a much smaller percentage of the alveoli will fall in this range.

Alveolar Dead Space. Still other alveoli are relatively underperfused. The blood that passes through these capillary beds reaches complete equilibrium with the air. Because the reduced blood flow could have been redistributed to fewer alveoli to produce normal ventilation/perfusion ratios, the effect is as if some alveoli were adequately perfused and others not perfused at all. These non-perfused alveoli constitute alveolar dead space. The effective alveolar dead space is the same whether the inadequate perfusion is evenly distributed or selectively distributed to some alveoli, with other alveoli completely non-perfused. Alveolar dead space may be very large in some disease states.

Anatomical Dead Space. If alveoli had no perfusion, the ventilation/perfusion would be zero. The inspired gas that remains in the anatomical dead space (the air conducting passages) is equivalent to this. In the normal adult male the anatomical dead space is approximately 160 ml; the alveolar dead space is very small with quiet breathing but increases with increased breathing effort.

Physiological Dead Space. The combination of anatomical and alveolar dead space is called the physiological dead space. It is the effective dead space. To this space must be added equipment dead space if a mask or helmet is worn. Thus it can be seen that added anatomical dead space is the equivalent of added alveolar dead space. Many individuals have markedly increased alveolar dead space in certain diseases (e.g., emphysema). If the disease process is arrested, the patient adapts to the increased dead space, as long as it is not too large, with no great adverse effects. What, then, of added equipment dead space? Perhaps, if it is not too large, an astronaut would accept it and adapt to it with no noticeable effect.

But what is too large? Certainly a few hundred milliliters would not appear to be. It should be cautioned that there is no agreement on this point. But, the above logic is intended to guide the engineer and designer in his assessment of the varying opinions.

O_2/CO_2 Diagram and the Alveolar Equations

O_2/CO_2 Diagram. The O_2/CO_2 diagrams for oxygen breathing are relatively simple. Because the alveolar and expired points fall on a straight line, it is easy to determine the effects of hypoventilation and hyperventilation. If the alveolar concentration of one gas and the total ambient pressure are known, the alveolar concentration of the other can be easily calculated. The formula is

$$P_{CO_2} + P_{O_2} + P_{H_2O} = P_{AMBIENT}$$

Figure 11-26 shows these relations at sea level and several altitudes.

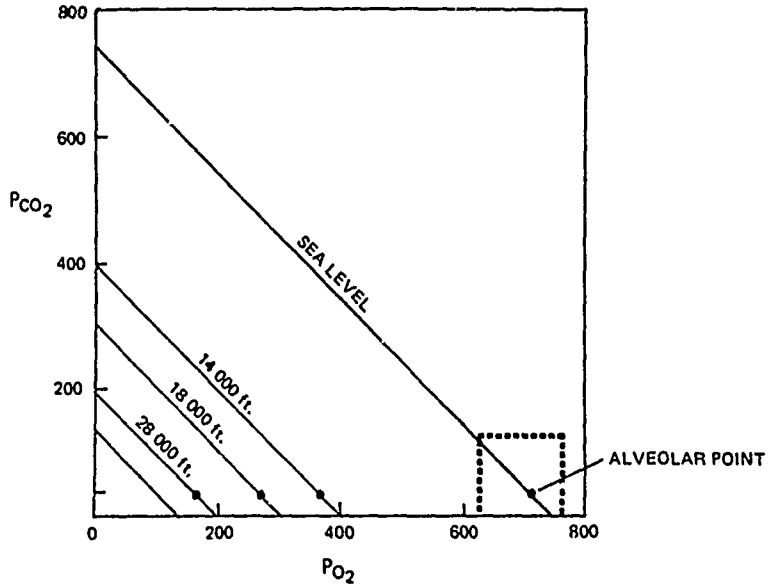


Figure 11–26. O_2/CO_2 diagram breathing pure O_2.

With usual breathing the breath is warmed to body temperature and completely saturated so that P_{H_2O} is 47 mm Hg. This is independent of ambient pressure. And since the body, also independent of ambient pressure, strives to maintain alveolar P_{CO_2} at 40 mm Hg, these two gases (CO_2 and H_2O) exert a combined pressure of 87 mm Hg. Thus, at high altitude, even breathing 100 percent oxygen, the lungs will not contain adequate oxygen to saturate the blood. In the event, as shown in figure 11-27, the body compromises the P_{CO_2}

stability as the low O_2 (hypoxia) creates a strong respiratory drive through reflexes from the chemo receptors. This compromise makes more oxygen available at the expense of a stable CO_2, and the pH is elevated with the untoward effects of this acid base balance derangement.

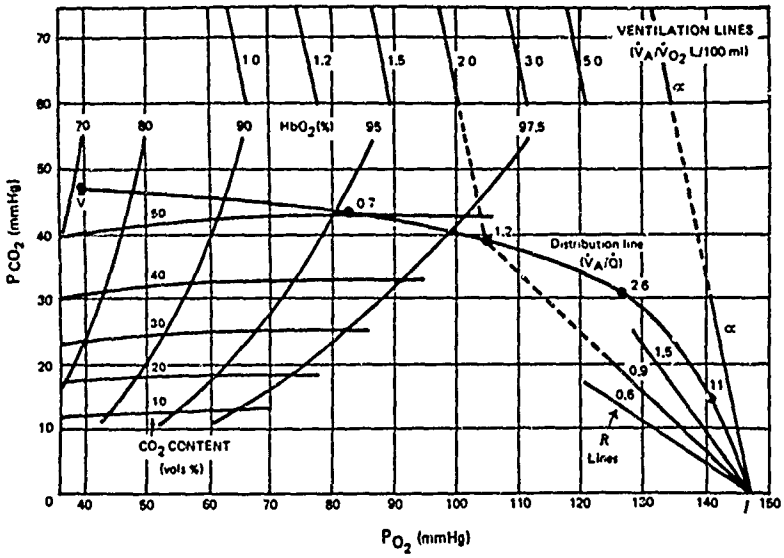


Figure 11–27. O_2/CO_2 diagram breathing air.

When air is breathed the alveolar gas concentrations are not so simply related. As shown in figure 11-27, there is a family of curves, specific relationships being determined by the Respiratory Exchange Ratio.

The basic diagram is represented by the grid of curved lines and relates the tensions of O_2 and CO_2 to the hemoglobin saturation and the total content of carbon dioxide in the blood. It is constructed from the dissociation curves for oxygen and carbon dioxide in a subject with a normal hemoglobin concentration and may be used to predict any two of the variables when the other two are known.

Superimposed on the basic diagram are two sets of co-ordinates and a curved line. The co-ordinates for the respiratory exchange ratio (R) radiate from a point (I) which describes the inspired gas (in this case air). The co-ordinates for the alveolar ventilation in the units/min per 100 ml/min of oxygen uptake are represented by sets of parallel lines of which that for infinite ventilation is also that for an R value of infinity. The curved distribution line illustrates the combinations of oxygen and carbon dioxide tension which may occur for different ventilation-perfusion ratios in one particular subject: the distribution line is defined at its lower end by the composition of the inspired gas ($\dot{V}_A/\dot{Q} = \infty$) and at its upper end by that of the mixed venous blood ($\dot{V}_A/\dot{Q} = o$). The dashed lines converge on a point on the distribution line where the $\dot{V}_A/\dot{Q}$

ratio is 1·2. For an alveolus having this ratio of ventilation to perfusion the alveolar ventilation may be expected to be 2·0 l/100 ml, the respiratory exchange ratio os 0·9 and the tensions of oxygen and carbon dioxide are respectively 104 and 39 mm Hg. The corresponding values for the oxygen saturation and the total content of carbon dioxide may also be read off the diagram.

Alveolar Equations. In space flight with two gas atmospheres and reduced total pressures, neither air nor oxygen will be breathed. It will, therefore, be of frequent interest to the engineer and designer to determine alveolar gas concentrations under various conditions. At times it will be inconvenient to measure all of the gaseous constituents. A set of equations called the alveolar equations has been developed that permits the calculations of some variables if others are known. The equations are derived as follows:

General Symbols	Symbols for Gas Phase
$\dot{V}$ – Velocity	I – Inspired gas
V – Gas volume per unit time	E – Expired gas
P – Gas pressure or partial pressure	A – Alveolar gas
F – Fractional concentration in dry gas phase	B – Barometric
R – Respiratory exchange ratio CO_2/O_2	

Two assumptions must be made:

1. There is no gas exchange in the dead space; therefore, all gas exchange is through the alveolar membranes.

2. The inspired volume of nitrogen is equal to the expired volume (therefore the equations do not apply during denitrogenation or renitrogenation).

$$\dot{V}IFI_{N_2} = \dot{V}EFE_{N_2} \tag{1}$$

Because inspired and expired total volumes are not the same (except when R = 1), one must be expressed in terms of the other.

$$\dot{V}I = \dot{V}E \frac{FE_{N_2}}{FI_{N_2}} \tag{2}$$

Similarly for CO_2 release

$$\dot{V}CO_2 = \dot{V}EFE_{CO_2} - \dot{V}IFI_{CO_2}$$

and substituting from equation (1)

$$\dot{V}CO_2 = \dot{V}EFE_{CO_2} - \left(\dot{V}E \frac{FE_{N_2}}{FI_{N_2}}\right) FI_{CO_2}$$

$$\dot{V}CO_2 = \dot{V}E \left(FE_{CO_2} - FI_{CO_2} \frac{FE_{N_2}}{FI_{N_2}}\right). \quad (3)$$

Similarly for O_2 uptake

$$\dot{V}O_2 = \dot{V}IFI_{O_2} - \dot{V}EFE_{O_2}$$

Substituting from equation (1)

$$\dot{V}O_2 = \left(\dot{V}E \frac{FE_{N_2}}{FI_{N_2}}\right) FI_{O_2} - \dot{V}EFE_{O_2}$$

$$\dot{V}O_2 = \dot{V}E \left(FI_{O_2} \frac{FE_{N_2}}{FI_{N_2}} - FE_{O_2}\right) \quad (4)$$

Since $R = \dot{V}CO_2/\dot{V}O_2$ = Respiratory exchange ratio

Substituting equations (3) and (4)

$$R = \frac{FE_{CO_2} - FI_{CO_2} \frac{FE_{N_2}}{FI_{N_2}}}{FI_{O_2} \frac{FE_{N_2}}{FI_{N_2}} - FE_{O_2}}$$

FE_{N_2} and FI_{N_2} can be eliminated by substituting

$$FE_{N_2} = 1 - FE_{O_2} - FE_{CO_2} \text{ and}$$

$$FI_{N_2} = 1 - FI_{O_2} \left(\text{when } FI_{CO_2} \text{ is negligible}\right)$$

P can be substituted for F since

$$F_x = \frac{Px}{PB - 47}, \quad x = O_2, CO_2, N_2$$

(PH_2O = 47mm Hg at body temperature)

With these substitutions one can solve for

$$PA_{CO_2}, PA_{O_2} \text{ and } R$$

On the other hand, it is incumbent upon the engineer and designer to assure that an individual will not be exposed to levels of oxygen much increased over sea-level concentrations. The effect of oxygen in increased partial pressures (hyperoxia) is tissue poisoning. The effect is especially pronounced in the lungs, and breathing an atmosphere composed primarily of oxygen for a day may result in death. When the P_{O_2} is raised to three atmospheres or more, the effects on the central nervous system are so sudden that lung edema seldom is the critical problem. The subject may collapse or experience convulsions which may precipatate death. These considerations obviously limit the therapeutic uses of oxygen and call for care in the design of respiratory support equipment and facilities.

Factors Relevant to Respiratory Support Equipment Design

Temperature, Humidity, and Respiratory Water Loss

Humidity, Temperature, and Comfort. The humidity standards for air conditioning have been set at approximately 50 percent Relative Humidity (RH), a level which subjective data indicate to be generally comfortable for the

entire body. Respiratory system comfort, however, demands considerably higher humidity levels (viz. speakers in climate-controlled auditoriums who must take frequent drinks of water to maintain respiratory system comfort).

At very high whole-body environmental temperatures, low humidity is comfortable because of the cooling effect produced by evaporation of water from the mucous membranes, in spite of the discomfort occasioned by drying of these membranes. The discomfort associated with breathing dry oxygen is well known among aviators. If the temperature of the inspired gases can be kept low enough, the respiratory system experiences (within limits) greater comfort at higher humidity. Because the gases are always essentially 100 percent saturated by the time they reach the lungs, saturation of the inspired gases is of little importance to the welfare of the mucous tissues deep in the respiratory system.

Humidity and Engineering Considerations for Respiratory Support Equipment Design. Expired breath is at body temperature, i.e., 37°C, and essentially saturated. Because it is desirable to maintain the temperature of the inspired gases considerably below this, there is a condensation of moisture in respiratory equipment from the expired breath as it is cooled. High humidity level has at least two implications for engineering consideration. First, wet surfaces are more susceptible to all types of corrosion, particularly when bathed in an atmosphere of essentially pure oxygen. Also, the higher the level of humidity the greater the tendency for valves or flow orifices to freeze.

From an engineering viewpoint then, it is desirable to keep the humidity as low as possible. This consideration has resulted in the requirement for the maintenance of essentially dry oxygen derived from compressed or liquid oxygen. Because of the great cooling occasioned by the expansion of these gases, even a small amount of moisture would result in the freezing of the valves and orifices.

The optimum level of humidity must be determined by a resolution of the opposing physiological and engineering considerations. Freezing and corrosion problems may well dictate that relative humidities be kept below levels that might be optimally desirable from a physiological viewpoint. It is therefore recommended that no arbitrary upper or lower levels of humidity be specified for breathing support equipment, but that the final level of humidity be determined by the temperature of the inspired gas, which relates to comfort, and by the engineering requirements to limit corrosion and freezing. To require specific levels of humidity without regard to the several parameters which will ultimately dictate the level of humidity is to place artificial constraints on the engineering design, and this may produce an undue complication in the final system implementation.

Standardization of Gas Volumes for Temperature and Humidity. Gas volumes are usually measured at the ambient temperature and pressure of the recording instruments and variable relative humidities. Because these conditions are not constant from one test to another, the volumes need to be converted to some standard form for interpretation or comparison with other data.

The conversion usually employed is the following:

- Volumes which relate to uptakes or evolution of gas by the body are converted to standard conditions, i.e., 760 mm Hg and 0° C
- Other gas volumes are reported saturated and at body temperature and ambient pressure.

These notations are usually abbreviated:

- ATP Ambient Temperature, Pressure, and humidity
- ATPS Ambient Temperature and Pressure and Saturated with water vapor
- STPD Standard Temperature and Pressure and Dry, i.e., 0°C, 760 mmHg
- BTPS Body Temperature and Pressure and Saturated with water vapor.

The relationship between them can be expressed:

$$V_{STPD} = V_{ATP} \times \frac{273}{273 + t} \times \frac{P_b - P_{H_2O}}{760}$$

$$V_{BTPS} = V_{ATP} \times \frac{310}{273 + t} \times \frac{P_b - P_{H_2O}}{P_b - 47}$$

With these equations one can convert from one set of notations to another. The use of table 11-4 makes the process simpler.

Respiratory Water Loss. Respiratory water loss can be calculated for any given condition if minute volume of pulmonary ventilation, inspired gas temperature, and the relative humidity of inspired gases are known. For usual minute volumes, one can assume near saturation of the inspired gases at body temperature.

Energy Cost of Breathing

Whenever respiratory-protective equipment is used, the work of breathing increases. This increase may be expressed in three ways, the first two quantitative and the last one qualitative:

1. The Physical Work of Breathing. This can be expressed as foot-pounds per minute or, more commonly (using the pressure-volume loops), as gram-centimeters per breath or per minute.

Table 11–4

Factors for Conversion of Volumes from ATPS to STPD and BTPS

Ambient Temperature °C	Aqueous Vapor Pressure (mmHg) at Saturation	Factor to Convert to:	
		STPD	BTPS
14	12.0	0.936	1.133
15	12.8	0.932	1.128
16	13.6	0.928	1.123
17	14.5	0.924	1.118
18	15.5	0.920	1.113
19	16.5	0.916	1.108
20	17.5	0.911	1.102
21	18.7	0.906	1.096
22	19.8	0.902	1.091
23	21.1	0.897	1.085
24	22.4	0.893	1.080
25	23.8	0.888	1.075
26	25.2	0.883	1.069
27	26.7	0.878	1.063
28	28.3	0.874	1.057
29	30.0	0.869	1.051
30	31.8	0.864	1.045
31	33.7	0.859	1.039
32	35.7	0.853	1.032
33	37.7	0.848	1.026
34	39.9	0.843	1.020
35	42.2	0.838	1.014
36	44.6	0.832	1.007
37	47.1	0.826	1.000
38	49.7	0.821	0.994
39	52.4	0.816	0.987
40	55.3	0.810	0.980

2. The Physiological Work of Breathing. This is the energy cost of breathing. With an appropriate apparatus it is easy to measure. It is the real cost of breathing and is easily related to respiratory gas storage requirements.

3. Fatigue Effects. Increased breathing work loads of identical increased energy costs can produce vastly different fatigue effects. As an example, pressure breathing produces fatigue effects out of all proportion to the relative increase in energy cost.

The simplest way of determining the energy cost of breathing is to determine the increased oxygen consumed coincident with the increased breathing activity. Figure 11-28 shows the typical effects of increased ventilation. The scatter diagram shows the relation of pulmonary minute volume to minute oxygen consumption with increased external respiratory dead space in a single subject. Both parameters were plotted as increases over resting values. The curve was visually fitted to the points. Points in the areas marked A, B, C, and D were determined with 2780 cc, 2280 cc, 1780 cc, and 780 cc externally added dead space, respectively. Extrapolation into lower left quadrant permits an estimate of the energy cost of breathing at resting ventilation volumes. It can be seen further that total cost of moving a given volume of air may be determined from the curve by adding 6 cc to a value indicated on the *ordinate*. The *triangle* and *star* represent the average of 10 tests on each of 2 additional subjects. To obtain an estimate of the calorie cost, assume an R value and multiply by the appropriate calorie equivalent. If R is 0.825, the calorie equivalent of a liter of oxygen is 4.825. Note the estimate of the oxygen cost of resting ventilation (0.5 ml O_2 per liter ventilation, which is in agreement with the generally cited figure).

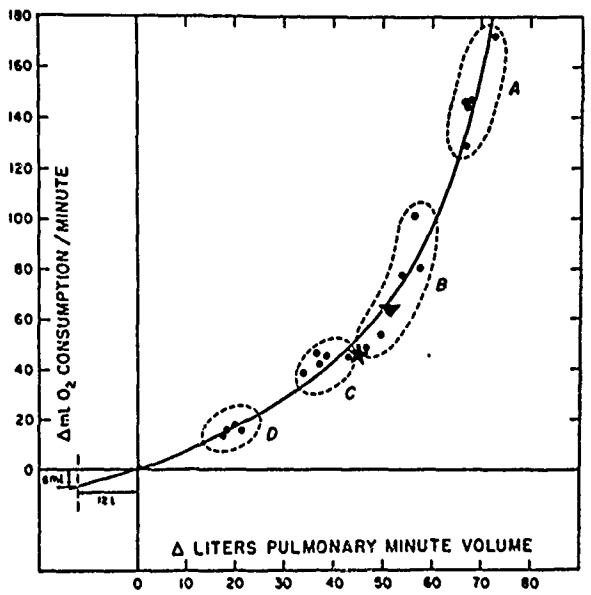


Figure 11–28. Oxygen cost of increased ventilation produced by breathing through four different added dead spaces. (Reprinted from Journal of Applied Physiology, 1957, 11(1), 84-86)

The data for the above curve were obtained using a breathing rate of 26 breaths per minute. Minute volumes approaching 80 liters per minute require very large tidal volumes. Figure 11-29 shows the oxygen cost of breathing over a range of breathing frequencies using only the data for the more efficient breathing, i.e., the lowest oxygen cost for a given minute volume of ventilation. There is good reason to believe that the body will inherently choose the optimum combination of rate and depth of breathing for a given circumstance. This curve should, therefore, be reliable for design purposes.

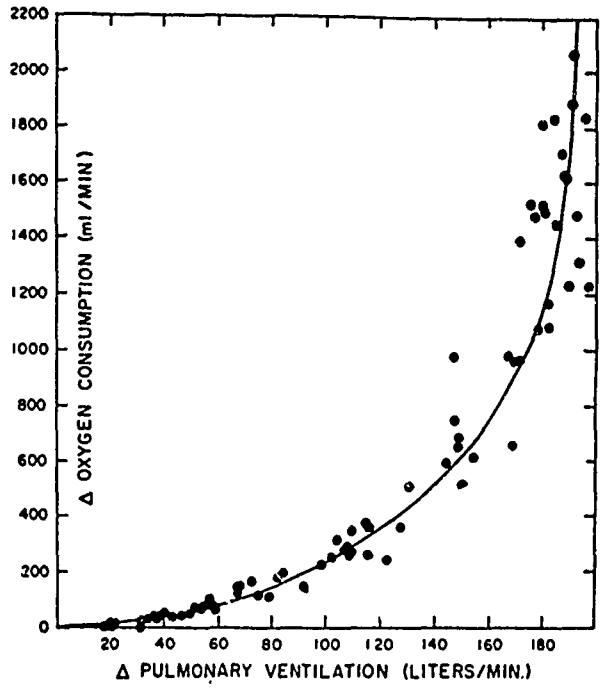


Figure 11–29. Relation of increased pulmonary ventilation and O_2 cost of increased ventilation for "efficient" breathing. Curve was visually fitted to points. (Reprinted from Journal of Applied Physiology, 1958, *12*(3), 413-424)

Because even very hard work rarely increases ventilation above 120 liters per minute, the energy cost of breathing is a very small portion of the total energy cost of work. At 120 liters, it is just over 300 ml O_2 per minute. A work load to produce such a large increase in pulmonary ventilation will produce a total oxygen consumption of well over 4 liters per minute. Thus, the oxygen cost of breathing is less than 8 percent of the total cost of the work. Because the relationship is not linear, the percentage of energy cost is much lower at lower work loads. Table 11-5 shows this relationship for a single subject. It should be noted that there may be considerable variability among individuals. The table illustrates the point that any increased breathing work load that can be easily tolerated will not result in meaningful increases in oxygen consumption.

Table 11–5

Oxygen Cost of Breathing as Related to Total Oxygen Cost of Exercise

Total O_2 Cost of Exercise (l/min)	O_2 Cost of Ventilation (ml/min)	O_2 Cost of Ventilation (%/min of Total O_2 Cost)
Rest 0.30	6	2.0
1.17	24	2.1
1.60	36	2.25
2.38	58	2.3
5.37	430	8.0

Some Physiologic Parameters Relevant to Respiratory Support Equipment Design

Because breathing is regulated (under all normal circumstances) to maintain a constant arterial blood P_{CO_2}, the amount of oxygen in the respired gas mixture (so long as it is above 120 or so mm Hg), has little effect on the amount of oxygen removed by the blood or on the pulmonary minute volume. Even 100 percent oxygen at sea level, therefore, does not reduce the breathing. Ordinarily about 25 liters of air are moved in and out of the lungs for each liter of oxygen removed. This is called the Oxygen Ventilation Equivalent.

Because only about 4 percent of the respired volume is removed by the lung blood, a closed-loop breathing support system, when the exhaled breath is purged of CO_2 and rebreathed, will represent a considerable economy compared to conventional open-loop systems. Table 11-6 shows these relationships with engineering implications. It should be noted, however, that the comparison shown does not represent the real tradeoff. A closed system must also remove CO_2 and provide an exhalation volume accumulation. The table shows only the stored gas requirements.

Average astronaut activity requires about 2 lb of oxygen per day. In table 11-6 this falls above midway between rest and light work. There may, however, be short bouts of physical exertion with markedly increased metabolic activity. This is more likely to occur with extravehicular activity when the astronaut is being supported by portable breathing gear. (See also chapter 18, *Work, Heat and Oxygen Cost*.)

Physiological and Engineering Considerations of CO_2 Levels in Respiratory Protective and Support Equipment Design

Long-Term P_{CO_2} Effects. Long-term CO_2 effects are defined here as those effects that might be produced by exposure to elevated P_{CO_2} tensions over a maximum 15-hour period. In considering the effects of altered P_{CO_2} levels on the body, it might be worthwhile to note that in certain disease processes the body P_{CO_2} is considerably elevated and the body seems to adapt without noticeable deterioration in the performance of the individual. Similarly, persons living at high altitudes have a significant decrease in alveolar and arterial P_{CO_2} without any measurable detrimental effects on general performance levels.

Table 11–6

Gas Storage Requirements for Closed-Loop and Open-Loop Systems

Open System			Closed System	
Metabolic Level	Minute Volume (l)	Lb Air/Hr (With 150% Container Weight)	O_2 Uptake (1/min)	Lb O_2/Hr (With 150% Container Weight)
Sleep	6.0	2.46	0.24	0.13
Rest	9.3	3.97	0.37	0.17
Light work	19.7	8.55	0.79	0.37
Medium work	29.2	12.4	1.17	0.55
Med. heavy work	40	17.1	1.60	0.75
Heavy work	59.5	25.3	2.38	1.10
Maximum work	132.0	56.5	5.37	2.45

In a number of studies animals and humans have been exposed for prolonged periods to various levels of elevated carbon dioxide. Although elevated levels produced noticeable physiological changes, particularly in the renal activity necessary for elimination of the buffered acid, no studies have defined any debilitating or compromising effects of modest increases (i.e., up to 3% at sea level) in CO_2 on performance. The reader interested in a detailed treatment of this topic should consult:

> Greenbaum, L. & Hoff, E. (Eds). *A bibliographic source book of compressed air diving and submarine medicine*, Vol 3. Office of Naval Research & Bureau of Medicine, Department of Navy, Washington, D.C., 1966.
>
> Comroe, J. *Physiology of respiration*. Yearbook Medical Publisher, 1966.

CO_2 Levels in Rebreather Systems. It would seem desirable to maintain P_{CO_2} at as low a level as practicable because we ordinarily inspire an atmosphere in which P_{CO_2} is a small fraction of one percent. However, considerable studies and operational experience have indicated that there are no subjective or performance effects when P_{CO_2} is allowed to increase to as much as 22 mm Hg partial pressure. It is therefore recommended that for rebreather systems, P_{CO_2} be kept as low as practicable in terms of engineering requirements. However, if the engineering penalty necessary to keep P_{CO_2} at 8 mm Hg or below is exorbitant as compared with that required to maintain P_{CO_2} with no excursions going above 22 mm Hg, it is then suggested that these higher levels should be allowed.

A study report from the U.S. Naval School of Aviation Medicine (1962) indicates that for the full pressure suit helmet or the partial pressure suit helmet with the conventional face seal, CO_2 levels run between 1-1/2 and 3 percent at sea level (i.e., up to 22 mm Hg partial pressure). Subsequent studies by the Air Force and NASA have indicated similar levels of carbon dioxide in helmets of space suits and full or partial pressure suits with no detrimental effect on the wearers.

CHAPTER 12

THE VESTIBULAR SYSTEM

by

Ashton Graybiel, M.D.
Naval Aerospace Medical Center

The material presented here represents an attempt to provide the reader with some comprehension of the role that the vestibular system may play in manned space missions involving rotation of a portion of the space vehicle. The "vestibular problem" is one item to be considered, along with others, in reaching a compromise that determines vehicle design criteria. Among the interested parties are (1) specialists knowledgeable in regard to the other human element problems; (2) engineers who must ensure inertial stability of the vehicle, taking into account "cost"; (3) astronauts who must assume partial responsibility not only in self-prevention of vestibular side effects but also, along with astroscientists, participate as subjects or observers in validation experiments; (4) biomedical personnel in charge of long-range and specific-mission plans; and (5) investigators conducting ground-based supporting experimentation. The operational objective of concern is the prevention of vestibular side effects, which encompasses the selection process, adaptation, education and experience, and the use of various countermeasures, including drugs. The greater the understanding of the events and processes underlying the side effects, the better this operational objective will be achieved.

A systematic review of the vestibular system is complicated by the many gaps in knowledge resulting from the fact that the vestibular system only recently has come under intensive study. In areas where information is available, it is mostly of a descriptive nature. For these reasons, the vestibular system will be discussed first in general terms, where the issues are quite clear, before proceeding to more specific features, where our understanding may not be as precise.

In primitive fish the "ear," containing acoustic and nonacoustic sensory organs, developed in association with the hindbrain. The organ of hearing long

---

Opinions or conclusions contained in this chapter are those of the author and do not necessarily reflect the views or endorsement of the U.S. Navy

Reviewed by G. Melvill Jones, M.D., McGill University, Montreal, Canada.

Preceding page blank

remained in a rudimentary state, and the evolutionary development of the acoustic system had to await the expansion of the primitive forebrain in higher vertebrates. In striking contrast, the nonacoustic portion of the ear, containing otolith organs and semicircular canals, developed early because these organs of equilibrium were essential. With the appearance of the cerebellum, an outgrowth of the hindbrain, the basic componentry of the vestibular system was complete. Thus, as we view the phylogenetic scale from fish to man, the essential structure and the cardinal purpose of the vestibular system remain unchanged.

The otoliths and canals are uniquely designed to sense linear and angular accelerations; to convert this energy into neural impulses, and, mainly through influencing motor behavior, to aid in orientation to the upright and in eye-head-body coordination. Because the sensory inputs from the vestibular organs are destined mainly for lower portions of the central nervous system, we are not familiar, through personal experience, with the functions they subserve, as in the case of vision or hearing. Indeed, not until the turn of the century was it generally recognized that the organs of equilibrium comprise a portion of the labyrinth of the inner ear.

Under natural stimulus conditions, the behavioral responses to which the vestibular system contributes are characterized by automaticity, reliability, and egality among members of a species or subspecies. There is little if any awareness of vestibular influences when man is engaged in natural activities, implying that the incredibly complex integrative mechanisms intercalated between sensory input and motor output have been effected in elegant fashion. This "silent elegance" is of such importance to the organism that it could only have evolved through natural selection and survival of the fittest. A backward look at our evolutionary development is enormously important in appreciating both the harmony that characterizes functions subserved by the vestibular organs under natural physiological conditions and the inherent limitations in making rapid adjustments to abnormal patterns of accelerative stimuli under artificial conditions.

Long before man was aware that he had organs of equilibrium, he learned to extend his natural powers of locomotion by various means. In these motion environments, he was exposed to abnormal patterns of accelerations to which he could not quickly adapt, and motion sickness resulted. Prior to the "discovery" of the vestibular organs, reports dealing with the etiology and treatment of motion sickness were of little or no value. Subsequently, the major advances were made in the light of the role of the vestibular organs and the institution of studies under laboratory conditions.

Only recently has there been a concerted attempt to study the vestibular system in a comprehensive manner, greatly aided by the new techniques of morphologists, neurophysiologists, psychophysiologists, and others. While most investigations of structure necessarily must be conducted on animals, many behavioral studies are easier to carry out on man than animal and have the unrivaled advantage of using the definitive experimental subject.

Almost all experiments on man depend on using an unnatural stimulus that elicits a response that is always unnatural and usually abnormal. This is done in order to manipulate and measure the stimulus to canal or otolith or both, and to evoke specific measurable responses. Most responses imply that the vestibular system is disturbed and that these disturbances fall into two categories, depending on whether they are system-bound or not. System-bound responses include abnormal eye motions, "sensations," and eye-head-body incoordination, and have characteristics of reflex disturbances. Non-system-bound responses include the symptomatology of motion sickness and do not have the characteristics of reflex disturbances.

The advantages that the investigator gains by eliciting abnormal responses are offset generally by some amount as a result of the departures from natural stimulus conditions. These handicaps include individual differences in susceptibility to a disturbing stimulus and individual differences in the rate of acquisition and decay of adaptation effects. All of these individual differences are more prominent in dealing with motion sickness than with reflex disturbances.

With regard to useful servation, the importance of the vestibular organs to man's performance is far less than in marine forms of life which must remain upright when free-swimming, in birds that fly, and even in subhuman primates. In man there seems to be a disparity between the great potentialities of the vestibular system he inherited and its useful servation. This disparity disappears, however, when we come to consider reflex disturbances and motion sickness which may, as a result of exposure to a physically harmless stimuli, create turmoil throughout the body.

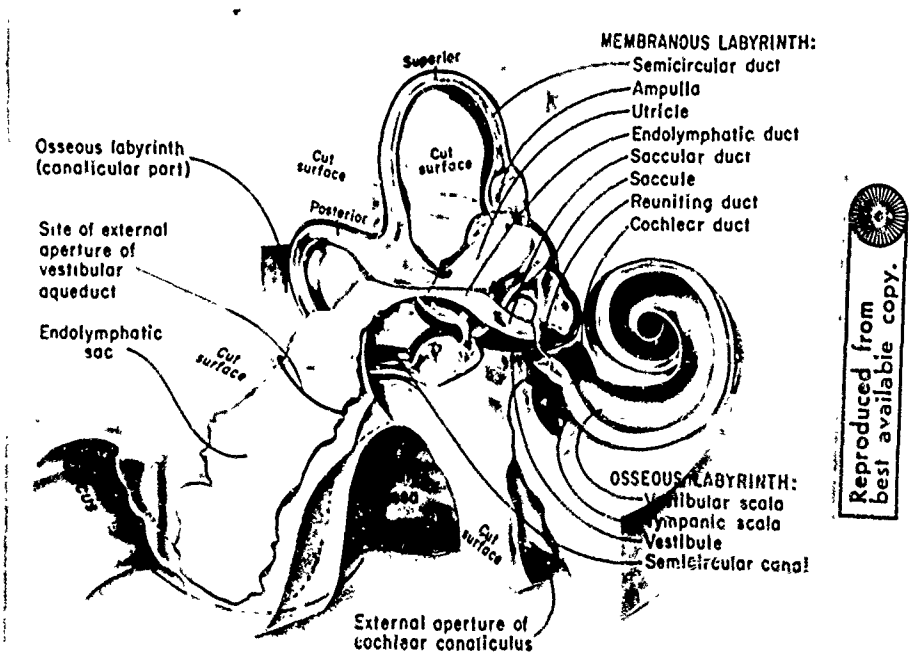
In research bearing on the design of a rotating space vehicle, laboratory studies have indicated that vestibular side effects tend to increase as a log function of angular velocity (generating cross-coupled angular accelerations) and that other physiological side effects are the result of short radius and high angular velocities. Thus, it seems that an effective design approach will involve assigning relative weighting factors to the cross-coupled angular acceleration, Coriolis accelerations, and subgravity level (short radius effects would not be involved if the other conditions were satisfied). Observations in space flight and parabolic flight, however, indicate that persons change in their susceptibility to motion sickness in weightlessness, complicating the "vestibular problem." An important missing bit of information concerns the change in susceptibility as a function of subgravity level, an issue presently under study. Inasmuch as nearly all of our information on the vestibular system has been obtained under laboratory conditions, the extrapolation to space flight conditions must be made with appropriate reservations.

The End Organs

Among the organs of special sense that are stimulated by physical means, the vestibular organs are unique in that, under physiological conditions, they are stimulated exclusively by the gravitoinertial force environment; the semicircular

canals (largely if not entirely gravity independent) respond to angular or cross-coupled angular accelerations and the otolith organs to gravity and to linear or Coriolis accelerations. Man has no control over a gravitoinertial force comparable to that of blocking a visual stimulus by closing the eyes in a lighted room or blocking the entry of sound waves to the cochlea. The only control man has is that of manipulation, for example, the nullification of gravity in orbital flight or control over the generation of impulse accelerations.

The paired vestibular end organs are situated in hollowed-out channels in the petrous portion of the temporal bone (figure 12-1) (Anson, Harper, and Winch, 1968). Within the bony labyrinth, the membranous labyrinth is surrounded by perilymph and filled with endolymph. Thus the sensory receptor mechanisms are protected from the effects of superimposed body weight by the bony labyrinth and, by virtue of the contained fluids, from the effects of accelerations except for displacements due to differences in specific weight among fluid and solid tissues and displacement due to inertial lag in fluid-filled ducts which resemble a torus. This "protection" is illustrated by the findings on animal subjects exposed to high peak- and sustained-linear acceleration. In table 12-1 are shown some findings on squirrel monkeys tested at a wide range of linear accelerations immediately after exposure to sustained accelerations. At levels below 60G (Igarashi and Nagaba, 1968), none demonstrated abnormal eye motions and only a few manifested slight ataxia. Moreover, none sustained any damage to the vestibular organs, as revealed by histologic study of the gross and fine structure. At levels of 60G and above fragmentation appeared in the otolithic zone.



Reproduced from best available copy.

Figure 12–1. Reconstruction of membranous labyrinth and related anatomy. (Anson, Harper, & Winch, 1968)

Table 12–1

Gross Ataxia and Spontaneous Eye Movement Immediately After Exposure to High-Intensity Acceleration Stimuli

g-Level	Number of Animals	Ataxia		Spontaneous Eye Movement
		Floor	Bar	
20.....	2	—	—	—
30	3	±	±	—
40	2	+	—	—
50	3	+	+	—
60	4	++	++	—
75	2	+	+	—
80	1	±	—	±
100	3	++	++	±
125	3	++	++	±
150	6	+++	+++	+
175	4	+++	++	+
200	6	+++	++	+
		—	—	—
200 p.....	1	—	—	—
250 p	1	+	++	+
300 p	1	—	+	+
350 p	3	++	+++	+
400 p	3	++	+++	++
450 p	4	++	+++	±
500 p	1	+++	+++	++

[p, peak-g exposure; +++, severe; ++, moderate; +, slight; ±, questionable; —, negative].

The Otolith Apparatus

The four otolith organs appear as thickened portions, termed macular plates, on the inner walls of the paired utricle and saccule (figure 12-2). Taken together, these four curved macular plates occupy, without overlap, a significant portion of a sphere. A cross section of the saccular macula of a squirrel monkey, which is similar to that in man, is shown in figure 12-3, and a sketch of the zonal structure is shown in figure 12-4 (Igarashi, 1966).

The otolithic membrane contains otoconia (figure 12-5) (Lindeman, Ades, and West, 1970), concretions of calcium carbonate with a specific weight of about 2.71, embedded in a gelatinous material. This membrane is the only tissue within the bony labyrinth that differs much from the specific gravity of the lymph fluids. The otolith membrane rests on the cupular membrane into which protrude the hair-like projections of the sensory cells. It is the movement of the otolithic membrane relative to these sensory "hairs," or cilia, that constitutes the effective stimulus to the organ (figure 12-6) (Lindeman, Ades, and West, 1970).

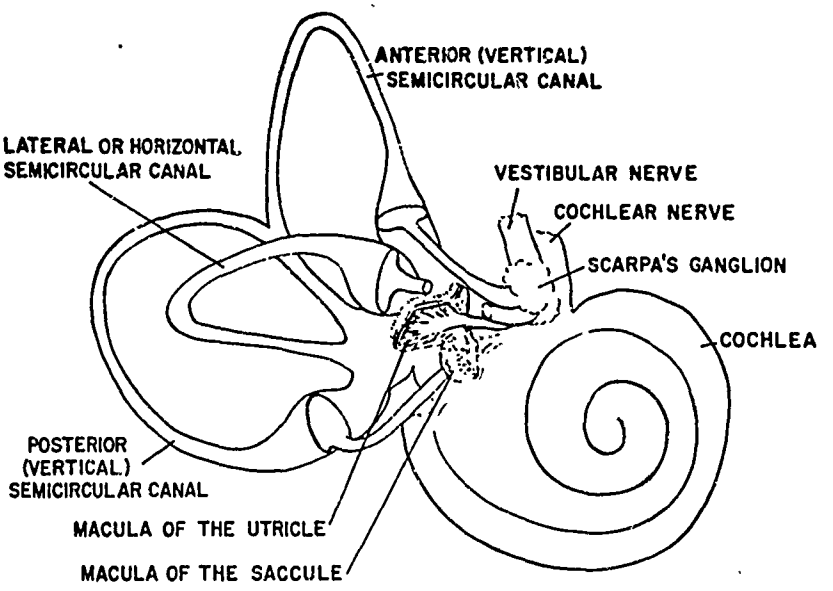


Figure 12–2. Labyrinth of left ear as viewed from medial aspect.

Reproduced from
best available copy.



Figure 12–3. View of macula saccula from squirrel monkey.
Zonal structure is clearly seen. (Igarashi, 1966)

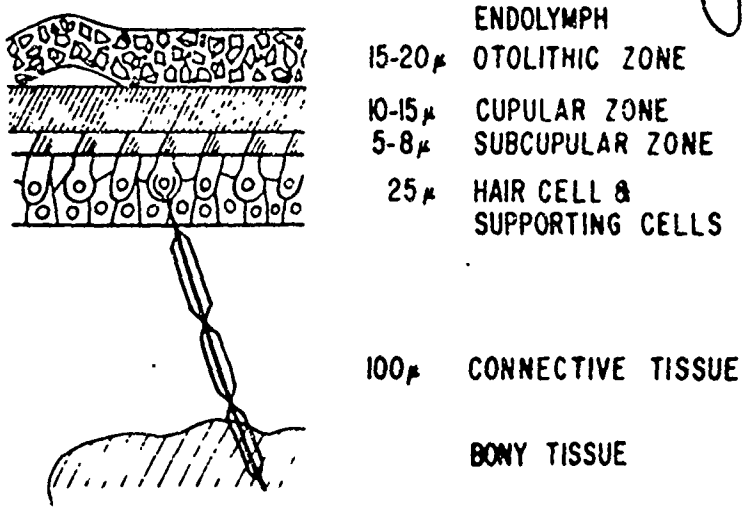


Figure 12–4. Schematic of zonal structure of macula sacculi in squirrel monkey. (Igarashi, 1966)



Reproduced from best available copy.

Figure 12–5. Scanning micrograph showing statoconia from macula utriculi in cat. (Lindeman, Ades, & West, 1970)



Reproduced from best available copy.

Figure 12–6. Bundles of sensory hairs at periphery of macula utriculi in chinchilla. (Lindeman, Ades, & West, 1970)

The sketch in figure 12-7 was drawn from electronmicrographs of the sensory epithelium of the utricular macula of the squirrel monkey (Spoendlin, 1966). Two types of hair cells, each with two types of cilia, are depicted. Each cell has 60 to 70 stereocilia and one kinocilium laid out in strict geometrical arrangement. It is considered likely that the kinocilium plays the major role in the energy transfer. In different regions of the macula, kinocilia are polarized in different directions (figure 12-8); hence, a shearing force in one plane will result in kinocilia moving in different directions with reference to the kinociliar pole (Spoendlin, 1965).

The "power train," constituting the cilia-otolith mechanism, is initiated by the acceleration of gravity and by impulse linear accelerations so directed as to cause a shearing displacement between the otolithic membrane and the membrane supporting the hair cells. The result is mechanical deformation of the cilia (kinocilium) which, in turn, causes chemical changes affecting the generation of bioelectricity (nerve action potentials). After a suprathreshold stimulus, the resting spike discharge is altered in its temporal and spatial patterning, constituting the propagated discharge which, traveling along nerve fibers to the central nervous system, is the way in which otolith sensory inputs affect behavior. Most receptor cells have a resting discharge but some do not. An example of typical responses is shown in figure 12-9 (Wersäll and Lundquist, 1966); i.e., deviation toward or away from the kinociliar pole has opposite effects. In some cells stimulation may result in abolition of the resting discharge.

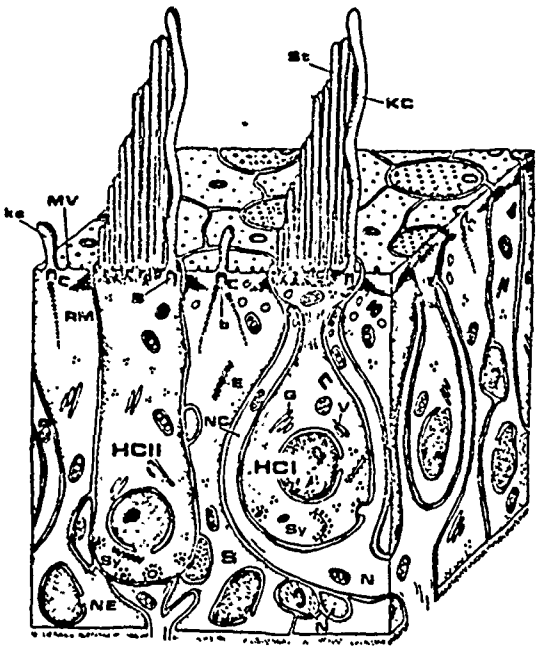


Figure 12–7. Schematic drawing of an area from a vestibular sensory epithelium, with haircell of type I (HC I) and type II (HC II). Typical arrangement of the stereocilia (St) and kinocilia (KC), modified kinocilia (kc) with their basal bodies and roots (b) in the supporting cells (S) and (B) in the hair cells, Nerve fibres (N), Nerve-chalice (NC) and Nerve endings (NE), Synaptic structures (Sy), Golgimembranes (G), Multivesicular bodies (V), and endoplasmic reticulum (E). Reticular membrane (RM) Microvilli (MV). (From Spoendlin, 1966, p. 41)

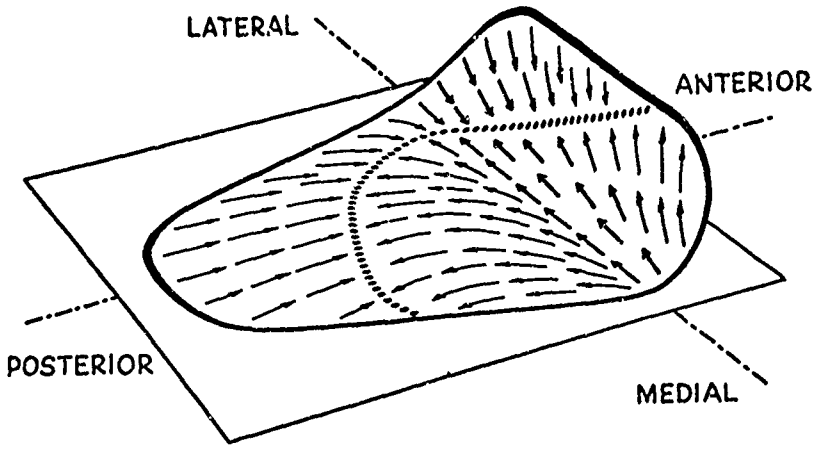


Figure 12–8. Schematic representation of polarization pattern of sensory cells in macula utriculi of guinea pig. Arrows indicate direction of polarization showing fanlike spread from one side of macula up to line beyond which polarization is reversed. Kinocilia on either side of dividing line face each other. (Spoendlin, 1965)

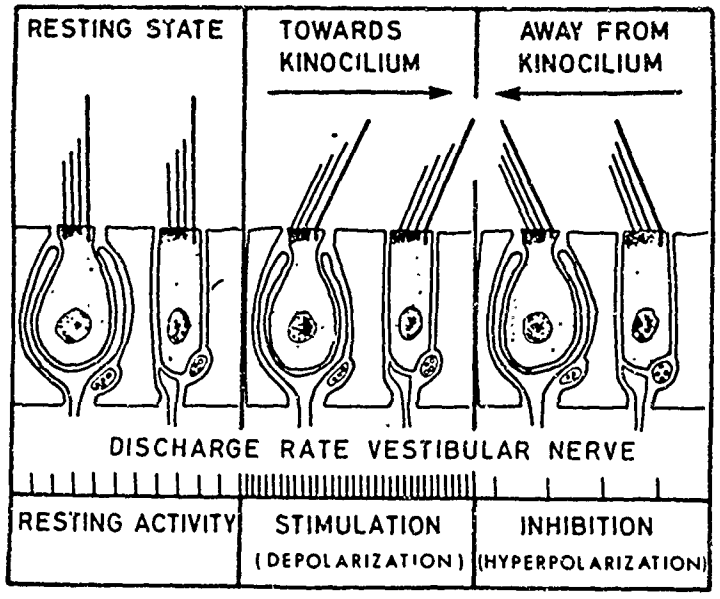


Figure 12–9. Electrical discharge rate of hair cells as function of displacement of the sensory hairs. (From Wersäll & Lundquist, 1966)

The Semicircular Canals

The orientation of the six semicircular canals with reference to the head is shown in figure 12-10. It will be noted that, although the three canals on one side lie approximately in mutually perpendicular planes, only the horizontal canals lie close to one of the coordinate planes of the skull, the superior and posterior canals deviating by 45 degrees from the sagittal and frontal planes. Thus, rotary motions in the horizontal plane, generating impulse angular accelerations, would stimulate the horizontal pair of canals, although not maximally. Rotation in the sagittal and frontal planes would generate angular accelerations in planes almost 45 degrees from the planes of vertical (superior and posterior) canals. The operational significance is seen when the canals are stimulated in a pilot during pitch, roll, and yaw of the aircraft (Clark and Stewart, 1962; Hixson, Niven, and Correia, 1966).

The so-called "semicircular" canals form a complete circuit by virtue of their connections with the utricle (figure 12-1). One extremity of each canal is dilated to form the ampulla, which contains the sensory receptors. A cross section of the ampulla of a horizontal canal of the squirrel monkey is shown under low magnification in figure 12-11 (Igarashi, 1966). The crista is a transverse ridge of tissue covered with the sensory epithelium containing sensory cells whose cilia extend into the cupula. This structure completes a fluid-tight gate across the ampulla, hinged at the crista and free to move back and forth in response to movements of the endolymph. This constitutes the so-called cupula-endolymph system. Clockwise rotation about an axis at right angles to the plane shown in figure 12-11 would result in an inertial lag of the endolymph in the torus-like canal, causing the cupula to be displaced counterclockwise. The fine structure of the sensory epithelium is provided with hair cells similar to those of the macula. The kinocilia in the hair cells

are uniformly polarized; in the horizontal canals they are toward the utricle (utricular pole) and in the vertical canals toward the opposite pole.

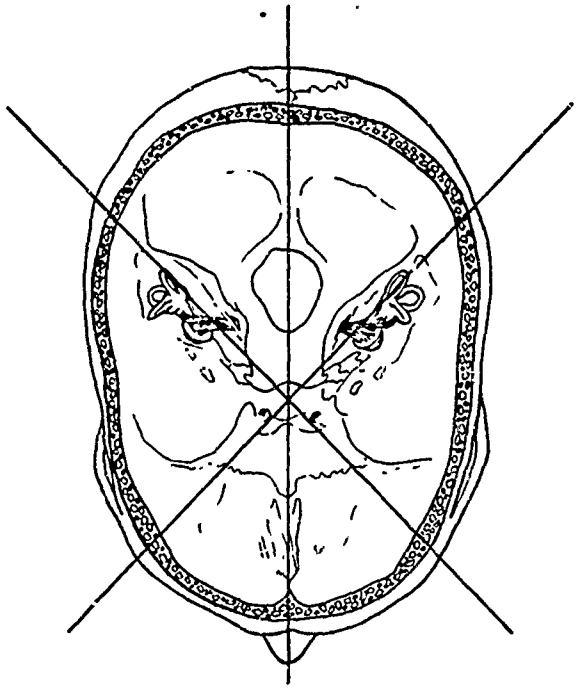


Figure 12–10. Orientation of semicircular canals (enlarged) as viewed in skull from above.

It is apparent that the power train involved in the transformation of angular acceleration forces to electrical energy in the semicircular canals is quite different from the corresponding mechanisms in the otolith organs. In the first place, the acceleration of gravity, which plays the major role under natural stimulus conditions in the cilio-otolith system, may be neglected. The cupula-endolymph system, responding to impulse angular accelerations in the plane of the canal, has been likened to a fluid-filled torus, with the cupula responding to movements of the endolymph in the manner of a spring-mass system with viscous damping. Head motions under natural conditions generate a high angular acceleration with the onset of rotation, transient in character, followed by a very brief period of rotation approaching constant velocity, and ending with another transient acceleration of opposite sign. The duration of angular accelerations is usually measured in fractions of a second and, inasmuch as the areas under the curves depicting acceleration and deceleration are the same, the cupular deflection is immediately restored to, or almost to, its natural resting place. In sharp contrast to the otolith organs, the variations in G-loading encountered in space flight may be neglected in dealing with the stimulus to the canals. In the absence of angular or Coriolis accelerations (cross-coupled angular accelerations) there is no accelerative stimulus present. The resting discharge presumably is of chemical origin.



Reproduced from best available copy.

Figure 12–11. View of crista-cupula system of horizontal canal from squirrel monkey. (Igarashi, 1966)

Central Nervous System Connections

This section summarizes the exceedingly complex vestibular reflex mechanism, and points out some of the important functional neuroanatomical relations. Figure 12-12, indicating the principal nervous pathways (Rasmussen, 1952), and figure 12-13 (Graybiel, 1969), indicating some additional features, will serve as visual aids.

Afferent impulses from sensory receptors in the canals and otolith organs are propagated along first-order neurons that terminate in the vestibular nuclear complex, cerebellum, reticular formation, and, according to one authority at least (Camis, 1930), some primary fibers reach the motor nuclei of the extraocular muscles, although not verified in a more recent investigation (Carpenter, 1960). These terminations are sites of origin for monosynaptic vestibular pathways and receiving sites for reciprocal or outside influences. The widespread distribution of these neuronal chains and networks, along with the less well-known efferent fibers terminating in the receptor cells of the canals and otolith organs, constitutes the reflex vestibular system.

The vestibular nuclear complex is the chief center, both with regard to anatomical organization and functional control of the vestibular system. The vestibular nuclei have important reciprocal linkages with the cerebellum and

reticular formation; they send out major projections that ascend, descend, and cross the neuraxis; they contain sites for interconnection with other sensory systems and other neural mechanisms coordinating reflex activity (Fredrickson and Schwarz, 1970; Gernandt, 1967, 1968; Ito, 1970; Nyberg-Hansen, 1970; Pompeiano, 1970; Snyder and Lowy, 1970; Wilson, 1970)

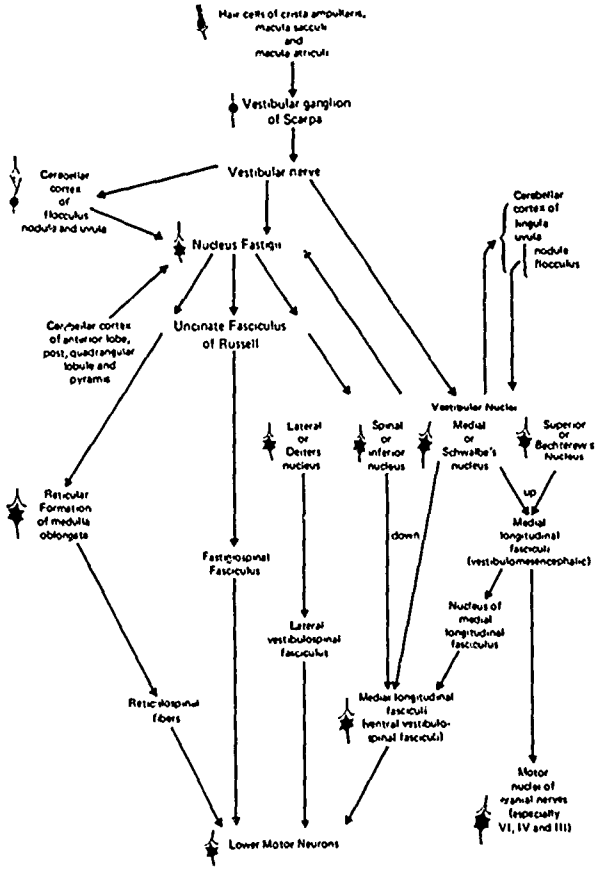


Figure 12–12. Vestibular or equilibratory system. (Rasmussen, A.T., The Principal Nervous Pathways. Copyright 1952 by MacMillan Company and used with their permission)

In addition to well-defined vestibular pathways, there is evidence that vestibular activity reaches areas to which specific tracts have not yet been identified. Representation in the cerebral cortex of the brain has been established using the evoked potential method (Mickle and Ades, 1953, 1954; Spiegel et al., 1970). Connections between the vestibular system and visceral nervous system have been demonstrated, using electrophysiological methods upon animal subjects (Megirian and Manning, 1967; Tang and Gernandt, 1969) and behavioral indicators for man exposed to unusual periodic accelerations.

The vestibular system, almost entirely concerned with the control of movement, is subject to strong modulating influences. Specific control over

afferent impulses may be in the nature of gating mechanisms subserved by efferent vestibular fibers (Gacek, 1960, 1968; Smith and Rasmussen, 1968). The cerebellum, which contributes greatly to the fine control of movement, exercises a strong tonic inhibitory control over vestibular reflexes. Cortical influences also are inhibitory, as are those having their origin in the reticular formation.

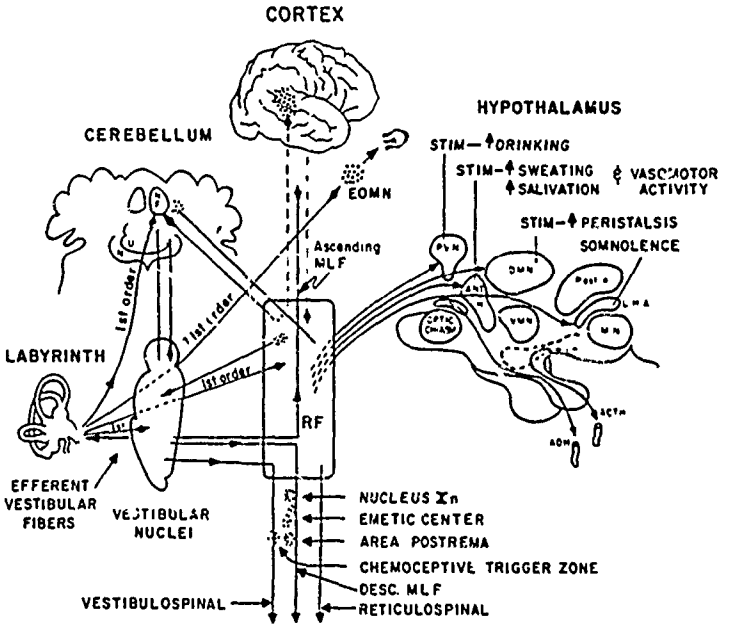


Figure 12--13. Depicting possible (abnormal) irradiation of vestibular activity (dotted lines) following strong Coriolis acceleration; first order refers to effects. NF = fastigial nucleus; U = uvula; N = nodulus; F = flacculus; EOMN = extraocular motor nuclei; MLF = medial longitudinal fasciculus; RF = reticular formation; PVN = paraventricular nucleus; SN = supraoptic nucleus; Ant. H. = anterior hypothalamic area; DMN = dorsomedial hypothalamic nucleus; VMN = ventromedial hypothalamic nucleus; Post. N. = posterior nucleus; L.H.A. = lateral hypothalamic area; M.N. = medial nucleus.

The extensive connections of the vestibular system with the motor nuclei of the extraocular muscles deserve special attention. Stimulation of a branch of the vestibular nerve supplying a single canal in the cat may result in conjugate deviation of the eyes (Fluur, 1959). Such a movement, involving agonists and antagonists, implies that messages with highly specific physiological "meanings" are sent to the extraocular motor nuclei. The close relation between the vestibular system, on the one hand, and vision and control over eye motions, on the other, has a firm foundation in the underlying neuroanatomical relations.

Extensive connections, some of them monosynaptic (Wilson, 1970), also exist between some of the vestibular nuclei and the spinal cord, particularly to those portions controlling movement of the head and trunk. These underlying neuroanatomical relationships provide the foundation for the

powerful control exerted by the vestibular system upon coordinated movements of eyes, head, and trunk.

The reciprocal influences between canalicular and otolithic inputs and the integration between right and left vestibular inputs are of great importance, and some of the anatomical pathways and sites of interaction have been identified and studied in detail. With regard to the advantages of having paired organs, the benefits must lie in synergism effected in the central nervous system, inasmuch as loss or even damage to one labyrinth results not only in loss of servation but also in severe vestibular disturbances. These disturbances, that may be severe in man, would be fatal in many animals and stand in sharp contrast to the little or no disturbance following unilateral loss of visual or auditory function. Inasmuch as vestibular influences do not reach the neocortex to any great extent, the possibility of right-left differences based on learning would be negligible, a matter of practical significance.

Static and Dynamic Characteristics

There is an important body of information dealing with the class of phenomena under this heading, much of recent date. This information is widely scattered in scientific journals, ranging through publications devoted to the medical, psychological, engineering, and even mathematical sciences. A relatively large amount of this information is in the nature of "facts," but a very important amount represents attempts to formulate theories based on these facts and, insofar as possible, express them in the form of nomographs or in mathematical notation. There are reasons why this is difficult even for the simplest of all input-output responses; i.e., those due to stimulation of the horizontal pair of horizontal canals. The basic difficulty is that this cannot be done based on information obtained under natural stimulus conditions (although Nashner's sophisticated experiments, mentioned in the next section, approach near-normal stimulus conditions). As soon as one departs from natural stimulus conditions he is usually dealing with perturbed responses, representing instability of the canalicular system, that may implicate the otolithic system; in any event, there is an attempt to restore stability through the adaptation process.

If one attempts to extend the scope of his theory to include the vertical pairs of canals by using facts obtained by exposure to angular accelerations in the sagittal and frontal planes of the head (body), which is commonly done, none of the canals lie in these planes; indeed, they are 45 degrees from this "ideal." Central nervous system processing somehow compensates for this anatomical state of affairs, but the underlying mechanisms have not been fully elucidated.

Much less information is available with regard to the otolithic system, and here one must contend with nonvestibular somatosensory receptors that constitute, in effect, a second system. It is further complicated by the constant stimulus due to gravity. Finally when all systems are operating and interacting under abnormal stimulus conditions, the input-output relations are difficult to stabilize, and the question of relevance is raised. Insofar as they simulate an operational situation they have relevancy, but extrapolation to natural stimulus conduction must be done with caution.

Natural Stimulus Conditions

Under natural stimulus conditions the semicircular canals are stimulated only as a result of angular accelerations with reference to the skull. Under these conditions, a person does not perceive a true sensation of rotation or visual illusions or manifest nystagmus, all of which are used as indicators under many experimental conditions. Positional nystagmus observed in some normal persons is an exception. The canals furnish information with regard to angular velocity and displacement, and some investigators are of the opinion that they furnish information at two or three higher derivatives than angular velocity. Head motions under natural conditions generate a high angular acceleration with the onset of rotation, transient in character, followed by a very brief period of rotation approaching constant velocity, and ending with another transient acceleration of opposite sign. Although the acceleration and deceleration magnitude may be different, the time-integral of angular acceleration at the onset and offset are equal (area under the curves). Thus under most natural conditions the end organ is thought to respond as an integrating accelerometer.

The otolith organs pose an interesting question that would seem to be of more than academic interest: namely, whether they always act as accelerometers. This relates to the fact that even if the head is "fixed" in the gravitational field, the receptors are stimulated, giving rise to a tonic input over and above the resting discharge. There is general agreement that if the head is rotated in the gravitational field in such a manner as to cause relative motion between otolithic and cupular membranes, this constitutes an effective stimulus, in addition to whatever suprathreshold tangential accelerations are generated. In the head-fixed situation, the question arises whether receptor elements continually fire (respond) due to the weight or pressure of the otoconia, or whether the fixation is sufficiently imperfect, as in the case of the eye, to stimulate receptor elements as a result of fine or imperceptible motions of the head relative to the direction of gravity.

There are a number of stimulus conditions which meet or nearly meet the criterion of natural terrestrial conditions, as will be discussed later.

Unnatural Stimulus Conditions

This section is devoted mainly to experimental findings in subgravity states, which are of operational and theoretical interest. The central feature in all of the findings pertains to the role of the otolith system. Additional information is presented in a later section dealing with unnatural stimuli in "Vestibular Servation in Man" as well as in Appendix A, which contains a summary of vestibular modeling efforts.

Ocular Counterrolling. Ocular torsion may be defined as the involuntary conjugate rolling movement of the eyes around their lines of sight in the direction opposite to the leftward or rightward tilted position of the head (and body) with respect to the gravitional upright. The measurements are made by comparing the position of a metal frame, to which the subject is thoroughly secured (head secured by individually fitted dental appliance), and the relative

position of the uncovered eye from colored photographs made in the upright and tilt positions. The amount of the roll is measured in degrees of arc. Findings on a large number of subjects are shown in figure 12-26, presented in the section on functional tests.

One experiment dealt with the problem of response decline as function of length of exposure. The findings, figure 12-14, indicate fluctuations in the amount of roll but no significant decline over a period of about 8 hours (Miller & Graybiel, 1970 c). These findings bear on the question raised above regarding the nature of the stimulus responsible for the tonic output. In figure 12-15 (Miller, Graybiel & Kellogg, 1966) the amount of roll as a function of G-loading is compared in seven normal and six labyrinthine-defective (L-D) subjects; the decline manifested in the L-D subjects may have been due to residual otolithic function. In figure 12-16 is shown a log plot with extensions into the supragravity range based on data from other experiments (Miller & Graybiel, 1965). It is seen that the S-shaped curve becomes linear at around 0.6 G, i.e., proportional to the log of the stimulus; the upper limit to this logarithmicity has not been determined.

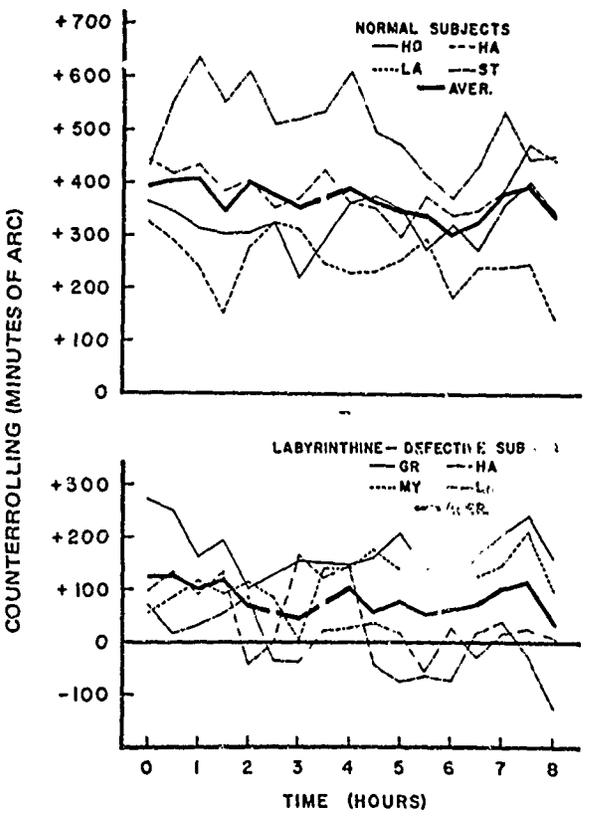


Figure 12–14. Counterrolling manifested by normal and labyrinthine-defective subjects during 8-h period of sustained tilt.

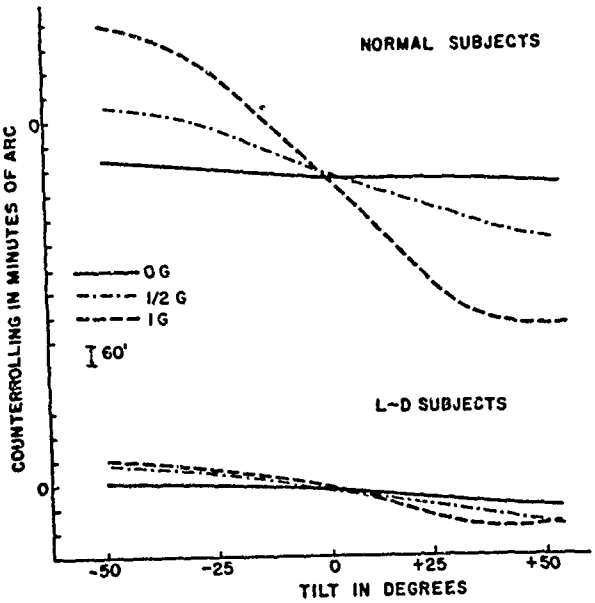


Figure 12–15. Counterrolling as a function of magnitude of gravitational force (zero g, 1/2 g, 1 g) and body position with respect to direction of force in normal and labyrinthine-defective subjects. (Miller, Graybiel, & Kellogg, 1966)

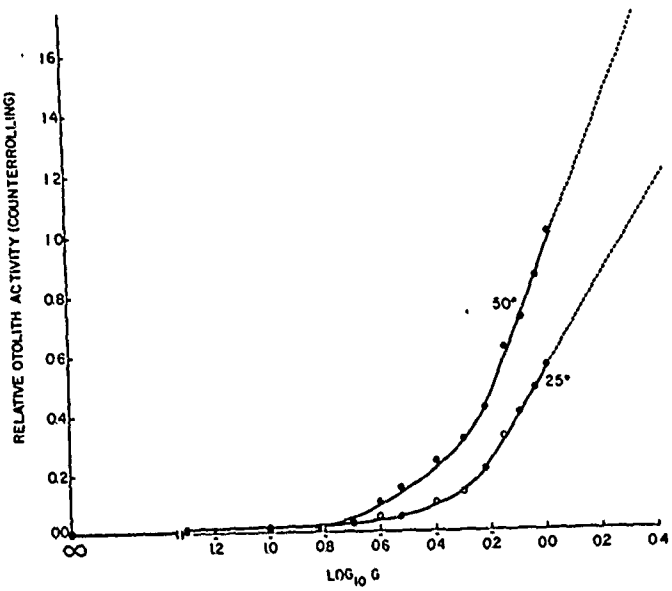


Figure 12–16. Relative otolith activity (mean counterrolling response of 3 subjects) as a function of logarithm of gravitational stimulus. (Miller & Graybiel, 1965)

Oculogravic Illusion. When a person is subjected to a change in direction of the gravitoinertial vertical with reference to himself, this is rightly interpreted as body tilt away from the upright, and the visual framework tends to tilt concordantly. The latter has been termed the oculogravic illusion (Graybiel, 1952). It is mainly dependent on the integrity of the otolith system, although nonvestibular proprioceptors may contribute to its perception. When a person views an objectively vertical luminous line in the dark, it will appear to tilt when the direction of the resultant force vector has inclined about 1.5 degrees from the Earth vertical. The observer's estimates of the tilt correspond closely to the change in direction of the resultant vector up to about 30 degrees, but beyond this the subject increasingly overestimates the angular change. In figure 12-17 are shown estimates made of the illusion by normal and L-D subjects under dry and head-out water immersion conditions on a human centrifuge (Graybiel et al., 1968a). There was greater individual variation in the settings made by the L-D compared to the normal subjects, but the contribution of (mainly) nonotolith gravireceptors under dry conditions in the case of the L-D subjects is evident. Water immersion simulated to some extent the weightless condition with regard to nonotolith but not to otolith receptors.

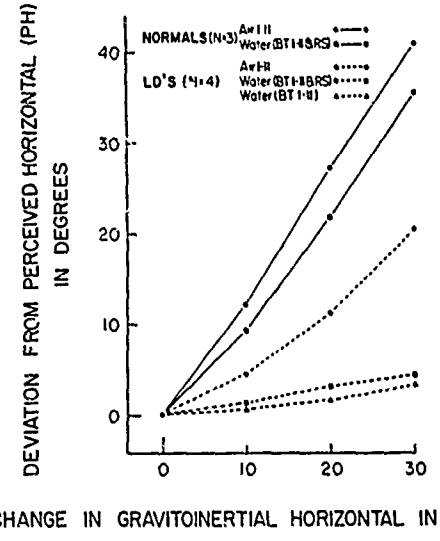


Figure 12–17. Comparison between mean settings of a target line to the horizontal of extrapersonal space made by normal and labyrinthine-defective subjects under wet and dry (air) conditions. BT = bathing trunks; RS = rubber suit; I, II = series of trials. (Graybiel et al., 1968a)

In figure 12-18 are shown the settings made by normal subjects during prolonged exposure on a human centrifuge (Clark & Graybiel, 1963a). The body was restrained and the head fixed by means of a fiberglas helmet. As in the case of ocular counterrolling, there was little or no decay in the magnitude of the illusion during periods measured in hours.

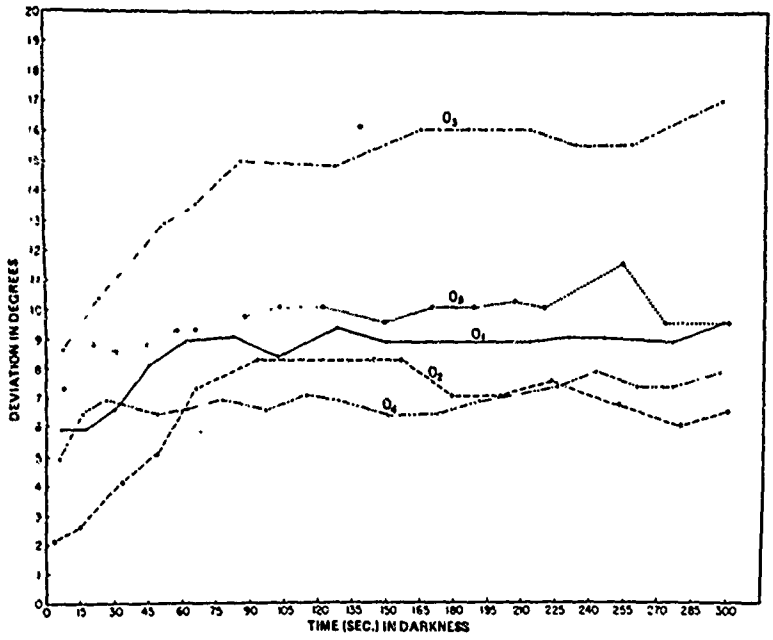


Figure 12–18. Change in perception of horizontal following prolonged exposure to a visual framework. (Experimenter offset the line.) (Clark & Graybiel, 1963a)

Up to this point the illustrations of the oculogravic illusion suggest that it falls into the near-normal type of vestibular response, but in some circumstances this is not the case. One is when the strength of the stimulus is increased while the subject is riding in a lighted circular room at the end of the arm of the centrifuge. Everything in the field of vision appears to tilt 90 degrees to the Earth vertical. Visual cues to the Earth vertical are literally overpowered by the strength of the stimulus to the otoliths, receptors, and other gravireceptors.

A and E Phenomena. Wade (1968) has recently reviewed the literature dealing with visual orientation to the upright, and how it is influenced by body position with reference to the gravitational vertical, and has analyzed the contributory role of postural mechanisms in terms of the otolith, neck, and trunk systems. In brief, it is readily demonstrated that when man is upright, orientation of a visual target to the gravitational vertical and horizontal, in the absence of visual cues to the upright, is accurate and that with rightward or leftward tilt, a bias appears first in a gradual displacement of the visual vertical to the opposite side of the gravitational vertical, the Müller (1916) or E effect; after tilting through 65 degrees the bias reverses and eventually is displaced toward the same side, the Aubert (1861) or A effect.

The curves in Figure 12-19 A and B demonstrate differences between normal and L-D subjects, respectively, in perceiving the A and E effects,

which clearly point to a contributory influence of the otolith apparatus. Some evidence that this bias is lost in weightlessness was demonstrated in Gemini flights V and VII (Graybiel et al., 1967), suggesting its dependence under terrestrial conditions on otolithic and nonotolithic gravireceptors.

Inversion Illusion. In space flight the inversion illusion has been experienced by some cosmonauts on making the transition into weightlessness (Billingham, 1966; Yuganov et al., 1966). Its probable dependence on physiological deafferentation of the otolith receptors is suggested by the observation in parabolic flight that some normal subjects but none of the L-D subjects experienced the illusion (Graybiel & Kellogg, 1967).

Nystagmus. Caloric nystagmus has been elicited in parabolic flight missions (Kellogg & Graybiel, 1967). With eyes open, nystagmus was manifested during pushover and pullup but not during the weightless phase. An experiment was repeated (Graybiel et al., 1970a) using a similar procedure except that the subject's eyes were closed. Figure 12-20 illustrates typical findings. Note that in the first two parabolas, nystagmus (velocity of the slow phase) declines but is present; that, in the third parabola, the primary gives way to a secondary nystagmus in the weightless phase; and that during the pullout, primary nystagmus reappears. In the last three parabolas only secondary nystagmus is seen. The modulating influences of changing strength of the caloric stimulus and changing G-loadings on the otolith receptors are apparent. Under laboratory conditions secondary nystagmus did not appear.

Motion Sickness. In a later section, the problem of motion sickness experienced in orbital flight and in the weightless phase of parabolic flight is discussed. Symptoms are elicited as a consequence of head motions generating angular accelerations that stimulate the canals, despite the fact that these stimuli are normal. The tonic afferent impulse from the otolith receptors is absent in weightlessness; hence, the normal integration in the (combined) vestibular system has been altered. Thus the basic cause is physiological deafferentation of the otolith receptors, yet the events triggering the abnormal response are natural head motions.

Not easily explained are the great individual differences in susceptibility to motion sickness in weightlessness, resulting not only from normal stimulation of the canals but also from cross-coupled angular accelerations that would result from head motion in a rotating vehicle. It would appear that some persons have unusually low and some unusually high susceptibility. Thus, the subgravity level is a parameter that must be taken into account as well as the angular velocity. The curves describing susceptibility to motion sickness as a function of subgravity level can be determined from experiments in parabolic flight but require validation under actual space flight stimulus conditions. The American experience with regard to motion sickness in space missions has recently been reviewed in detail (Berry & Dietlein, 1970).

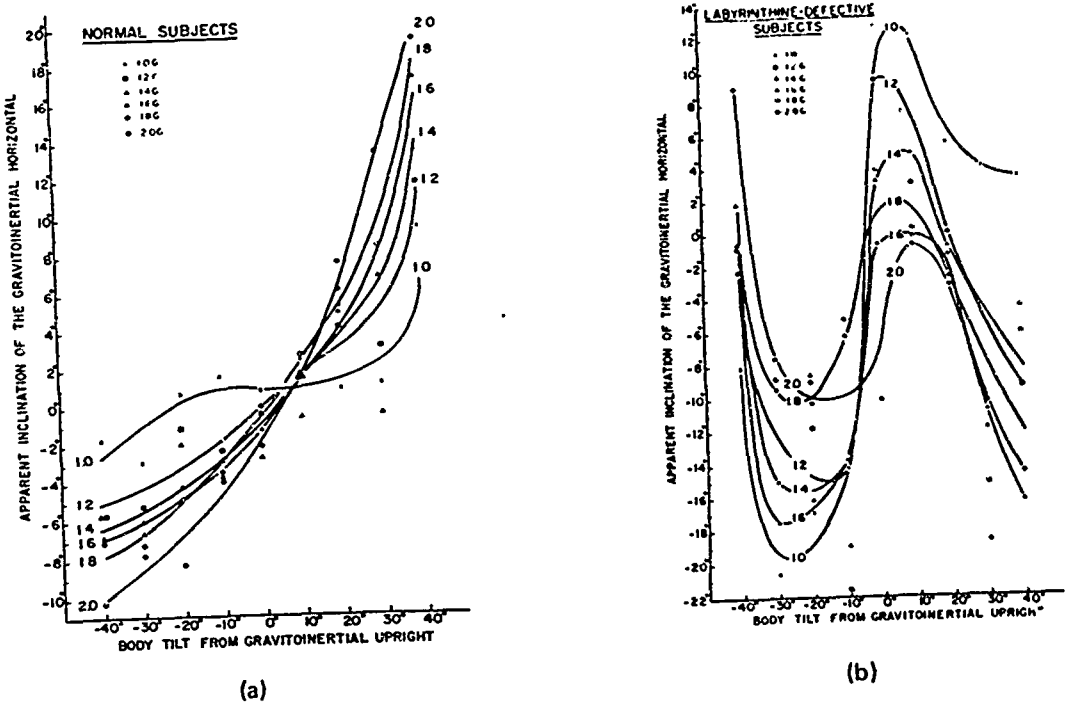


Figure 12–19. A: Change in E-phenomenon as a function of increasing g level in normal subjects; B: Change in E- and A-phenomena as a function of increasing g level in L-D subjects. (Graybiel et al., 1967)

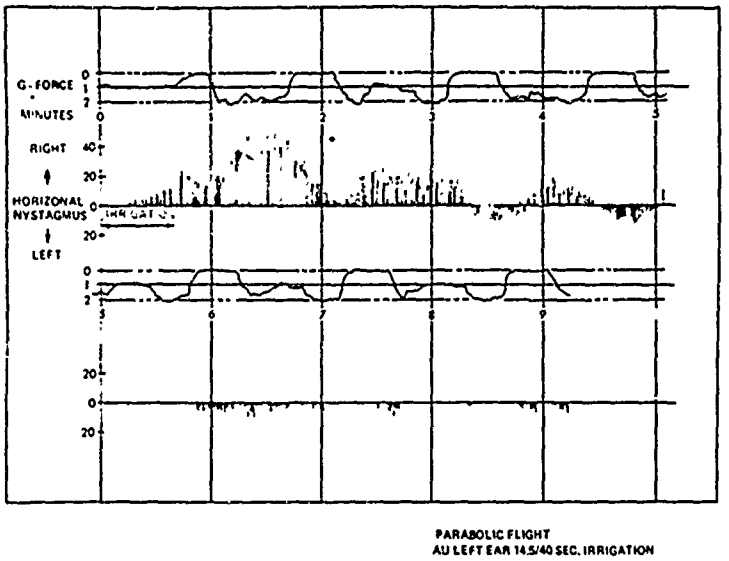


Figure 12–20. Effect of varying g values during parabolic flight on caloric induced nystagmus. Caloric nystagmus is reduced, then suppressed, and, finally, reversed in repeated periods of weightlessness, while caloric nystagmus is increased during periods of g values above 1.0.

Vestibular Servation In Man

Under Natural Stimulus Conditions

Astonishingly little is known concerning the normal functions of the vestibular system in man under natural conditions. The canals and otoliths serve mainly as "participants" in motor functions, and it is exceedingly difficult to elucidate their contributory roles. A classical experimental approach to this question involves the use of human or animal subjects with bilateral loss of canalicular and otolithic functions. Experiments on animals alone, however, will never suffice, because the findings are not directly applicable to man. The identification of human subjects with bilateral loss of vestibular functions has been accomplished by screening groups of deaf persons, but experimentation on subjects identified in this way is complicated by the great differences between persons who hear and those who do not. Moreover, in all such subjects not only is there the need to make sure that the pathologic changes are quiescent and that adaptive changes are complete following any loss of function, but also there is the need to take into account the unmeasurable factor of "compensatory adjustments." Despite these limitations, the best information we have has been derived from a comparison of performance of persons with and without vestibular defects.

Clinical Studies. Under ordinary present-day living conditions, severe losses of vestibular function have gone undetected. This is dramatically illustrated by the rare cases in which there has been loss of vestibular function early in life but

retention of hearing (Graybiel et al., 1970b). Two such persons, discovered fortuitously, revealed that neither they, their families, nor their physicians was aware of the loss. Despite the fact that loss of function was readily revealed in our laboratory, this takes little away from the fact that they met not only the ordinary demands of present day living but also were proficient above the average in a variety of sports. When apprised of their loss, it was brought out that they had experienced difficulties under circumstances in which visual cues were inadequate and, possibly, in eye-head-body coordination when visual cues were adequate.

Laboratory Studies. Although a variety of behavioral tests has been proposed to demonstrate the effects of loss of vestibular function, only a few well-controlled systematic investigations have been conducted.

The postural equilibrium test battery. These tests have a limitation in the sense that many systems in addition to the vestibular reflexes are challenged, but a great advantage is that they test natural behavioral mechanisms. Findings in the case of subjects with partial loss of vestibular function (Graybiel & Miller, 1970a) suggest that postural equilibrium is more dependent upon canalicular than on otolithic function. A useful test battery, described elsewhere in detail (Graybiel & Fregly, 1966), comprising six individual items, requires the subject to stand or walk in the stringent position of body erect, arms folded against chest, wearing shoes with flat heels and leather soles. The below-listed test items constitute this battery:

Sharpened Romberg (SR): Stand on floor, eyes closed, feet in heel-to-toe position. Maximum score 240.

Walk eyes open (E/O): Walk heel-to-toe, eyes open, on ¾-inch wide rail. Maximum score 15.

Stand eyes open (E/O): Stand heel-to-toe, eyes open, on ¾-inch rail. Maximum score 180.

Stand on leg eyes closed (SOLEC): First right leg (SOLEC-R), then left leg (SOLEC-L). Maximum score 150.

Walk a straight line heel-to-toe on floor (WALEC). Maximum score zero.

The scores are normalized in percentile equivalents. Some comparative scores are shown in table 12-2. Scores below the 6th percentile are regarded as abnormal, and above the 40th, in the typical normal range. In general, improvement in scores suggests normality, and its absence, abnormality.

Nashner (1970) has just published the results of a sophisticated study on postural sway under near-normal baseline conditions. Based on available information, he developed a general postural control model that, in turn, was used in devising a series of experiments dealing with postural sway resulting from rotation about the ankle. The experimental findings were combined with the

Table 12–2

Group Differences in the Percentage of Abnormal Ataxia Test Battery Scores

Subject Groups	N	Walk E/O (%)	Stand E/O (%)	Stand E/C (%)	SR (%)	SOLEC-R (%)	SOLEC-L (%)	WALEC (%)
Normals	240*	1	5	4	7	3	4	3
Patients with vertigo	76**	18	26	22	37	23	35	29
Congenitally deaf	3	0	0	33	67	33	67	67
Head injury deaf	5	60	60	80	60	80	80	40
Unilateral labyrinthine-defective	11	18	18	18	64	46	64	100
Meniere's patients	4***	25	50	75	100	100	100	100
Bilateral labyrinthine-defective	26	72	96	96	100	100	100	100

*N = 198 on SOLEC-R and SOLEC-L; N = 147 on WALEC.

**N = 31 on SOLEC-R and SOLEC-L; N = 38 on WALEC.

***N = 3 on SOLEC-L and WALEC.

general model to develop specific models for the sensory-motor interfaces. Three normal subjects and one L-D subject participated. The latter was 20 years of age and had compensated "to the extent possible" following bilateral transection of the VIIIth nerve, 2 years prior to testing. Four types of tests were conducted:

1. Reflex response gains. In normal subjects the average gain of the stretch reflex response induced by small rotations was about one-third that necessary for postural stability. In the L-D subject with eyes open the gains were larger than in the normals but below those necessary for postural stability; with eyes closed the average gain increased markedly, and, for extensor muscles, resulted in "rigid" postural stability.

2. Induced sway: thresholds for perception with eyes open. Threshold values in terms of response time and body angle are shown in figure 12-21 (Nashner, 1970).

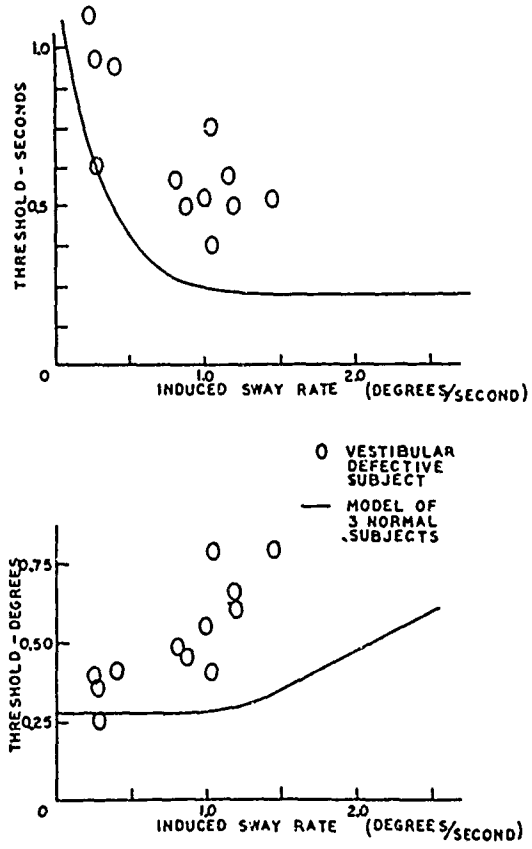


Figure 12–21. Response threshold to induced sway motion of vestibular defective subject. (Nashner, 1970)

3. Continuous recording of postural response and body angle motion. With eyes open the "control strategy" is the same for the L-D subject and normal controls, but in making corrections for transient disturbances (higher center

commands). performance was better for the normals than the L-D subjects. With eyes closed the strategy remains the same for normal subjects (periods of reflex stability and transient disturbances), but changes for the L-D subject in that reflex stability gives way to continuous oscillation.

4. Frequency spectra of body angle motions. Con.parative values are shown in figure 12-22A and B (Nashner, 1970).

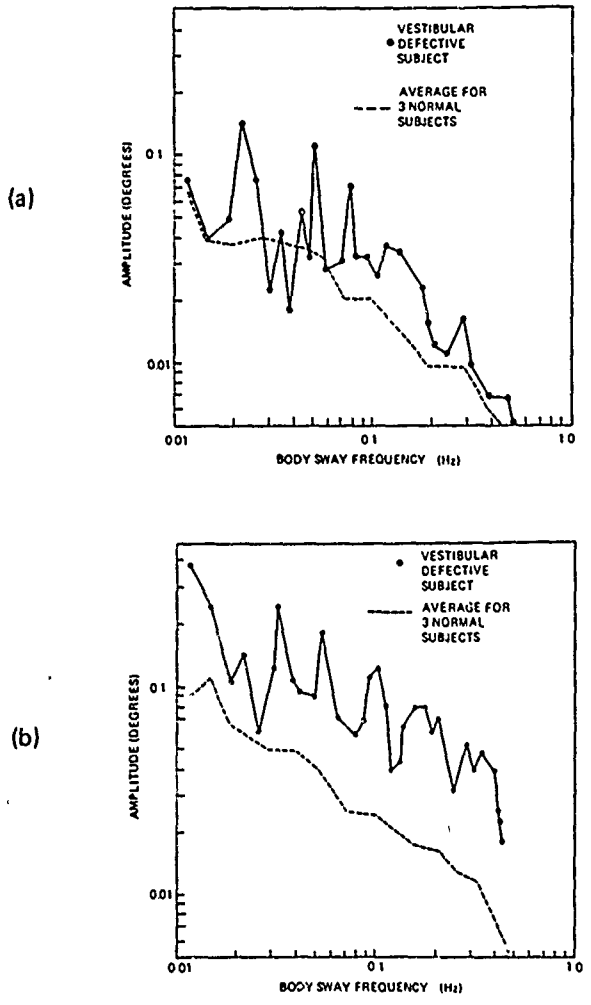


Figure 12–22. Fourier coefficients of body sway motion for vestibular defective subject standing on rigid, flat surface–A: with eyes open; B: with eyes closed. (Nashner, 1970)

In summary, the normal subject regulates posture with a combination of high-frequency (canal and somatosensory receptors) stabilization and low-frequency (otolith and optic receptors) stabilization; with eyes closed he still has otoliths functioning. The L-D subject with eyes closed is without low-frequency stabilization, resulting in a "rigid" stability.

Perception of postural vertical. Perception of the postural vertical was compared in normal and L-D subjects (eyes closed) immediately after right or left displacement of 30 degrees from the upright in a series of 30 trials. The findings in figure 12-23 (Clark & Graybiel, 1963b) show that although the normal subjects exhibited smaller average errors than the L-D subjects, the differences between these groups were not statistically significant. Moreover, the improvement with practice was about the same for both groups.

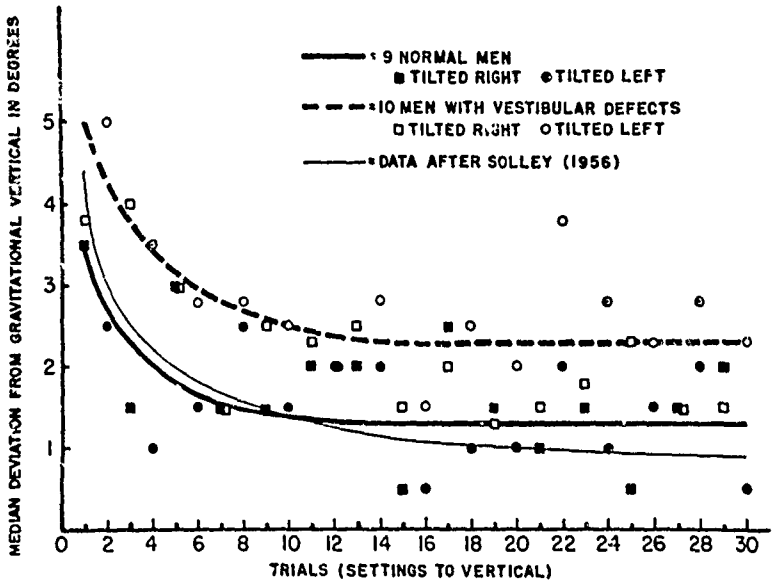


Figure 12–23. Errors in setting to postural vertical. (Clark & Graybiel, 1963b. Copyright 1963 by the American Psychological Association and reprinted with their permission)

In another study the same subjects were tested under four conditions of tilt and two conditions of delay before setting themselves to the upright. The findings in table 12-3 (Clark & Graybiel, 1964) indicate the somewhat greater average errors in the L-D compared with normal subjects and suggest that the error in setting is a function of both the degree of tilt and length of delay.

Table 12–3

Average Errors in Degrees in Setting to the Postural Vertical

Delay in Setting	Normal Subjects (S = 9) Tilt				Labyrinthine Defective Subjects (S = 10) Tilt			
	10°	20°	30°	40°	10°	20°	30°	40°
0	1.2	1.5	2.0	1.9	2.4	2.7	3.0	3.3
2 min	2.2	3.5	3.8	4.2	3.7	6.1	6.5	6.8

Taken together, these findings emphasize that the vestibular contribution to nonvisual perception of the upright was relatively small under the conditions of the experiment. These findings are in accord with those of Schock (1960) who demonstrated large decrements in the ability of normal subjects to set a luminous rod, in darkness, to the vertical or horizontal when under water, compared with settings made out of water.

Tentative Conclusions Based on a Review of Clinical and Laboratory Studies.

1. In young persons with normal hearing, severe losses of vestibular function have gone undetected under ordinary living conditions. Handicaps can be demonstrated, however, under challenging situations, especially in the absence of visual cues.

2. Loss of otolithic function is well tolerated, inasmuch as nonotolithic proprioception subserves quite adequately some of the same functions.

3. Loss of canalicular function is less well tolerated than loss of otolithic function, partly because it subserves more important and unique functions.

Under Unnatural Stimulus Conditions

The schema in figure 12-24 represents an attempt to identify important elements determining input-output relations in which the vestibular organs play either the essential or a contributory role. The main chain of events involves: (1) the accelerative stimuli; (2) the cili-otolith and cupula-endolymph systems: (3) the sensory inputs to the canalicular and otolithic systems; (4) their integration to form the vestibular system; (5) interactions of vestibular and nonvestibular systems, notably the visual system; (6) normal and abnormal system-bound responses; and (7) non-system-bound responses that involve not only a facultative linkage but also nonvestibular servation systems. Listed in the figure are: (1) a categorization of etiologic factors resulting in normal and abnormal sensory inputs, (2) an attempt to illustrate typical sensory input activity patterns, and (3) a listing of important secondary etiologic factors affecting susceptibility to reflex vestibular disturbances and motion sickness. Not shown in the figure are the many important events and processes involved in the acquisition and decay of adaptation effects. Exposure to unnatural accelerations may stimulate canals, otoliths, or both. The extremely important contribution made by head motions in otherwise stress-free motion environments needs emphasis. In a rotating environment the cross-coupled angular accelerations constitute an ever-changing bizarre stimulus pattern for the canals that do not vary significantly with changes in radius. The otolith organs are stimulated by Coriolis accelerations which are affected by change in radius, but their "positive" contribution, i.e., abnormal sensory input pattern, must be small, inasmuch as susceptibility to motion sickness does not seem to vary within radii ranging from 0 to 19 feet in a rotating environment. Stated differently, any otolith contribution to a disturbance in otolith-canal integration would appear to be independent of a disturbance in the otolithic system caused by the vectorial sum of radial, gravitational, and Coriolis accelerations.

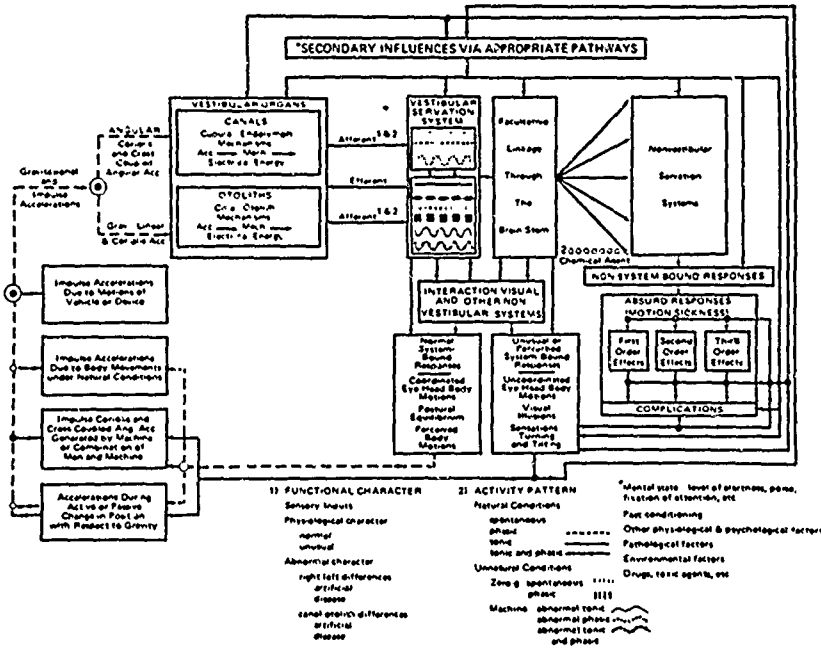


Figure 12–24. Conceptual framework showing important elements and their interactions underlying system-bound vestibular disturbances and non-system-bound disturbances (motion sickness).

In weightlessness the tonic* sensory output of the otolith organs due to gravity is abolished, thus altering the sensory input to the otolithic system. The semicircular canals, however, are stimulated by angular accelerations generated by head (body) motions that differ little if at all from those generated by making similar head motions under terrestrial conditions. The loss in stability in the (combined) vestibular systems would appear to be due to normal canalicular inputs encountering an otolithic input consisting only of the spontaneous discharge. The resulting disturbance is sufficient to elicit symptoms of motion sickness in some persons but not in others.

Many unnatural patterns of accelerative stimuli elicit only abnormal system-bound responses; i.e., do not evoke the symptomatology of motion sickness. In general, they have the characteristics of reflex phenomena and vary greatly in their departure from normal stimulus conditions. Adaptation may not be manifested under near-normal or under certain abnormal stimulus conditions. If adaptation occurs during continual exposure, it is an indication that the response was elicited as a consequence of insufficient adaptive capacity to cope (immediately) with the stressful stimuli.

*For the purpose of clarity, a distinction is made between a spontaneous discharge and one resulting from stimulation which, in the case of the otolith organs, may be either tonic or periodic or both.

Many reflex vestibular disturbances have the following characteristics in common: (1) short latencies, (2) maximal response to the initial stimulus, (3) possible modulation by secondary influences, (4) little or no evidence of temporal perseveration based on sensory input (some exceptions here), (5) variable time course of adaptation, and (6) possible need for readjustment on change to the initial or a different gravitoinertial force environment.

In the case of stimulus patterns that have the potential for precipitating motion sickness, these symptoms may be avoided, e.g., by short exposure, making it possible to elicit reflex vestibular disturbances as "isolated" vestibular responses. Much of what follows under the etiology of motion sickness applies to stimuli in this category.

The typical overt symptoms of motion sickness are well known, and systematic studies reveal that they have the following characteristics: (1) delay in appearance of symptoms after the onset of the stressful stimuli, (2) gradual or rapid increase in severity of symptoms, (3) modulation by secondary influences, (4) perseveration after sudden cessation of stimuli, and (5) response decline indicating recovery. Further abstractions reveal: (1) great individual differences in susceptibility and in the acquisition and decay of adaptation, (2) transfer of adaptation effects, (3) learning, and (4) conditioning.

The appearance of symptoms always indicates that the adaptative capacity of the person has been exceeded. Indeed, even prior to the appearance of overt responses it can be demonstrated that the individual's susceptibility has risen. Moreover, the order of appearance of symptoms is affected by the strength of the stressful stimuli and length of exposure.

Under all stimulus conditions, secondary etiologic influences, categorized in figure 12-24, are present, tending either to raise or lower susceptibility. Vision plays an important role. A pilot, for example, free of symptoms in the cockpit, may experience motion sickness in the navigator's closed compartment. Mild symptoms of motion sickness have disappeared under the influence of experimenter directed tasks that may have preempted central nervous system pathways used by irradiating vestibular influences. Covert factors may come into play. Covert factors include defects, disease, and functional disturbances that either are not diagnosed or wrongly considered unimportant. Examples are personality defects, which render a person unwilling or unable to cope with functional disorders of vestibular origin, prodromal stages of disease, and undiagnosed vestibular disease or functional disorder.

Little is known concerning the precise nature of the facultative linkage. The fact that irradiating vestibular activity is demonstrably open to modulating influences points to the use of common pathways in the brain-stem reticular formation. This common meeting ground between somatic and visceral systems is essential not only for coordination at the reflex level but also to provide for some voluntary control over otherwise autonomic responses. What makes the vestibular linkage unusual (but not unique) is the readiness with which vestibular activity may get "out of bounds" and elicit the widespread responses that include the typical symptoms of motion sickness. The sometimes long delay

between the onset of stimulation and appearance of motion sickness suggests that a chemical linkage also may be involved.

Recovery during continual exposure to stress is complicated. At some point in time, the tendency toward restoration of homeostasis in nonvestibular systems exceeds the influences having a contrary tendency. At another point in time, nonvestibular systems are freed from vestibular influences (adaptation in the vestibular system and disappearance of any neurohormones released). Then restoration takes place spontaneously through homeostatic events and processes, not only in the systems responsible for first-order effects but in all systems involved in higher order effects and complications. Curves depicting the time course of adaptation in the vestibular system, the disappearance of vestibular influences, and the restoration in the nonvestibular systems tend to overlap and have not been clearly defined. Thus the engagement and disengagement between the vestibular and nonvestibular systems is difficult to follow but an interesting object of study.

Investigations dealing with reflex vestibular disturbances and motion sickness in man may be directed to the solution of an operational problem, or to the accumulation of facts, the synthesis of which would be applicable to any operational problem.

Individual Assessment

The distinction among functional, provocative, and simulation tests is useful although somewhat arbitrary. Only simulation tests will be discussed in detail, partly because some of the material is not readily accessible elsewhere but mainly because they comprise the most important kinds of tests in the assessment of astronauts.

Functional Tests. There is evidence that functional test scores within the normal range have no value in predicting individual differences in susceptibility to reflex vestibular disturbances and motion sickness (Khilov, 1969a, b; Miller & Graybiel, 1970a). They are valuable nevertheless from the clinical standpoint (to rule out overt and, if possible, cryptic defect or disease) and from the standpoint of making comparative measurements, the astronaut serving as his own control. The reliability of most vestibular tests is not high compared with vision or hearing tests; hence, the need or desirability for repeated measurements on astronauts serving as experimental subjects. Functional tests should be used not only in the selection of aviators and astronauts but also in the selection of subjects used in vestibular experimentation.

Clinicians have described test batteries (Aschan, Bergstedt, & Stahle, 1956; Henriksson et al., 1966; Jongkees, 1967; McNally, 1969; McNally & Stuart, 1942; Spector, 1967) to which reference might be made for details, but nearly all batteries include tests for spontaneous and positional nystagmus, a modified Hallpike test, and some clinicians use a visual tracking "pendulum test." The latter is not widely used, hence will be described briefly. Eye motions are recorded while the subject "tracks" an oscillating target. The displacement and frequency of the pendulum device can be varied. Normal persons begin to have

difficulty in tracking the target with displacements greater than 20 degrees and a frequency greater than 0.8 Hz (oscillation time = 1.2 sec), and this is declared by the appearance of saccadic perturbation in the record. The testing procedure can be exploited by using one eye for fixation. Some typical results are shown in figure 12-25.

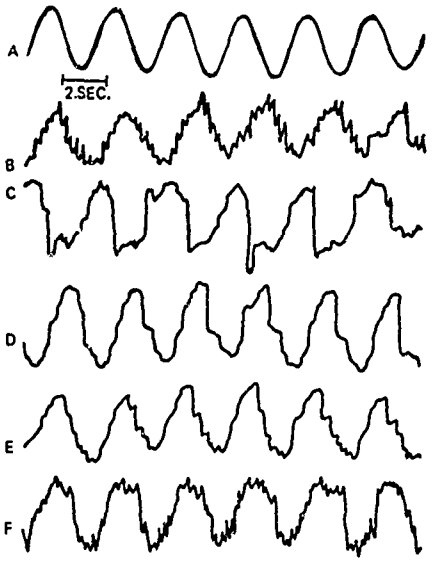


Figure 12–25. Eye movements recorded during pendulum test.

Semicircular Canals. Thermal stimulation consists of delivering a jet of water of known temperature against the ear drum at a predetermined rate and volume. The subject's head is positioned so that the horizontal pair of canals are vertical. Differences in specific weight of endolymph at body temperature and that portion of the canal influenced by the irrigating water causes a displacement of the cupula. The thermal stimulus to one ear is grossly abnormal because of the disturbance created in the delicate right-left synergistic mechanisms underlying normal canalicular function. The great advantage is that each horizontal canal can be stimulated individually (vertical canals also can be stimulated). The nystagmic response may be observed, but nystagmographic recordings are recommended for reasons of objectivity and better opportunity for analysis.

With the well-known Hallpike test (Fitzgerald & Hallpike, 1942), irrigating temperatures of 30 degrees and 44 degrees C are used, which may induce nausea in highly susceptible persons. It has the great advantage of determining what is termed right-left labyrinthine and directional preponderance. We have used the threshold caloric test (McLeod & Meek, 1962). It has advantages for screening purposes and comparative measurements, a person serving as his own control, and the vestibular disturbance is brief and recovery quick. Irrigating temperatures just below body temperature usually suffice, but if not, stepwise

decreases are made until a response is obtained. If irrigating temperatures below 35 degrees C are required to elicit a response, some abnormality should be suspected.

Angular Acceleration Thresholds. Rotating devices have been fabricated that provide not only a stimulus of a physiological character, albeit unusual, but may have excellent performance characteristics, including preprogramming. The most sensitive indicator is the oculogyral illusion, but "sensations" and nystagmus are also used routinely.

The oculogyral illusion is a form of apparent motion that has its genesis in the cupula-endolymph mecha- ..n and may be viewed under many different circumstances (Graybiel & Hupp, 1946). In measuring "thresholds," favorable conditions include a dimly lighted three-dimensional target viewed in darkness and fixed with respect to the subject. The expected apparent motion is in the direction of acceleration. In a recent report by Clark and Stewart (1969), the mean threshold for the perception of the oculogyral illusion in 32 normal subjects was found to be $0.11^{\circ}/sec^2$ when they were exposed to rotation in the vertical axis for 10 seconds.

Tests of Otolith Function. Ocular counterrolling, described above, has the advantage of not disturbing the vestibular system; hence, it qualifies as a test conducted under near-normal stimulus conditions. The values obtained with different degrees of rightward and leftward tilt describe curves that can be examined for left-right symmetry. The "index" (one-half the sum of the maximal left and right roll) values obtained in a group of 550 presumably normal persons and 10 L-D subjects are shown in figure 12-6 (Miller, 1970). The rare instances when values fall below 120 seconds of arc are unexplained.

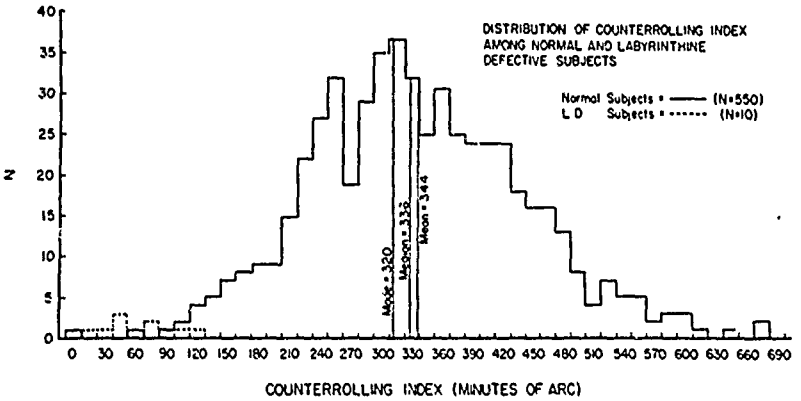


Figure 12–26. Distribution of counterrolling index among normal and labyrinthine-defective subjects. (Miller, 1970; reprinted by permission of Pergamon Press, Oxford)

There are a variety of other tests available, but none recommended as a substitute for ocular counterrolling; sometimes a second test is desirable if facilities for counterrolling are not available. Among the other tests are: (1) the

oculogravic illusion test described above, (2) the elicitation of compensatory eye motions by exposing a person to horizontal oscillations on a horizontal swing or other device, (3) the elicitation of nystagmus in a device that rotates a person about an axis other than the Earth vertical or revolves a person in a counterrotating capsule or room that exposes him to a rotating linear acceleration vector.

As part of our routine, we always include audiometry and the postural equilibrium test battery.

Provocative Tests. Provocative tests serve the important purpose of evaluating a person's susceptability to reflex vestibular disturbances and to motion sickness and may, in addition, measure his ability to cope with such disturbances either with or without the aid of countermeasures, including the use of drugs. Factors of etiologic significance in addition to the gravitoinertial force environment, may be introduced to simulate more completely the anticipated operational conditions or to explore their role in affecting an individual's susceptibility to novel circumstances. The distinctions between provocative and simulation tests involve primarily their duration and, secondarily, their specificity in terms of the global exposure conditions; thus, the predictive value of provocative tests is less than that of simulation tests. The validity of the findings, as in the case of functional tests, is compromised if the person tested either is suffering from active disease involving the vestibular systems or, indeed, has not compensated completely following permanent injury that is no longer active.

In conducting and interpreting the results of provocative tests, difficulties are encountered and precautions must be taken, which are not unrelated. Difficulties have their origin in: (1) the individual differences in susceptibility with regard to a given test; (2) intraindividual differences in susceptibility, when exposed in different gravitoinertial force environments; (3) preternaturally high susceptibility if insufficient time has not elapsed between exposures; (4) the fact that adaptation occurs as an inevitable consequence of every test, with much individual variation in the rate of acquisition and of loss of adaptation; and (5) the difficulty in expressing the results in absolute values. Great advantage would occur from the use of normalized scores and standardization of techniques.

Some advantages of provocative tests include: (1) the low "cost" in terms of time and equipment that makes a "test battery" feasible, (2) individual testing, and (3) their use in studying vestibular mechanisms and in evaluating countermeasures.

A large number of provocative tests are in use, but brevity dictates limiting what follows to the description of a few representative tests relevant to space flight operations.

The Dial Test. A standardized test has been devised for determining susceptibility to motion sickness in the slow rotation room (SRR), and this came to be known as the "dial test." The stressful Coriolis accelerations are generated

by simultaneous rotations of room and subject. Five dials are so placed in relation to the subject that, to set the needle number on each dial, he is required to move his head and trunk to five different extreme positions, which maximizes the rotation of the head out of the plane of the room's rotation. A "sequence" consists in setting the five dials in accordance with a tape recording, one every 6 seconds, followed by a rest period of 6 seconds. The subject, usually with eyes open, continues the task until either a definite endpoint is reached, usually M111 (severe malaise) (table 12-4) (Graybiel et al., 1968b), or (usually) until 20 sequences or 100 settings have been made. If the original rate of rotation, say, 7.5 rpm, is too stressful, the velocity is reduced, or if too weak, the velocity is increased. With few exceptions, normal persons reach the endpoint at some velocity between 5 rpm and 20 rpm. The results are scored in terms of angular velocity, number of head motions, and level of symptom (e.g., 10 rpm, 78, M111, respectively).

The Coriolis Sickness Susceptibility Index. This represents a modification of the dial test, but a rotating Stille or Litter-chair is used, the subject making standardized head motions ususally with eyes closed (Miller & Graybiel, 1970b). Higher angular velocities than those in the SRR are required to reach the same endpoint. A noteworthy feature of this test is the method of scoring, which yields a single value, the "index," enabling the investigator to make comparisons within and among subjects.

Off-Vertical Rotation Test. In contrast to the two tests just described, which mainly "disturb" the canalicular system, a rotating linear acceleration vector mainly stresses the otolithic system. The off-vertical rotation (OVR) test is one of many and may be scored in "duration," which has some but not all of the advantages of an index. The device consists of a rotating chair (figure 12-27) (Graybiel and Miller,1970b) mounted on a platform that can be tilted either by a hand crank or by an electric motor, and the degree of tilt read from a large protractor. The subject's head, held rigidly against the headrest by adjustable straps across his forehead, is maintained precisely over the center of rotation, with smooth rotation ensured by proper counterbalancing. The rotation, programmed on a time axis, involves periods of acceleration at $0.5^{\circ}/sec^2$ for 30 seconds, followed by periods of constant velocity for 6 minutes, until either the endpoint is reached or 6 minutes completed at 25 rpm, the cut-off point. In effect, this program represents unit increases of 2.5 rpm every 6.5 minutes after the initial step. The endpoint can be expressed in terms of elapsed time at terminal velocity, as total elapsed time at terminal velocity, or as total elapsed time, which serves as an index of susceptibility to motion sickness. With each revolution of the OVR device, the subject continually changes position with respect to the gravitational upright. Thus, receptors in the paired maculae of utricle and saccule and nonvestibular proprioceptors are continually exposed to an unusual stimulus pattern. The findings in a group of healthy men, the great majority attached to a naval air station, are shown in figure 12-28 (Graybiel and Miller, 1970b). All but twelve men reached the predetermined endpoint (M11A) at a 10-degree tilt; all but five of the remainder reached it only when the angle of tilt was increased to 20 degrees. Thus, the scores ranked 95 subjects in terms of their susceptibility to this unusual gravitoinertial force environment and demonstrated that five were highly insusceptible.

Table 12–4

Diagnostic Categorization of Different Levels of Severity of Acute Motion Sickness

Category	Pathognomic 16 Points	Major 8 Points	Minor 4 Points	Minimal 2 Points	AQS* 1 Point
Nausea syndrome	Vomiting or retching	Nausea+ II, III	Nausea I	Epigastric discomfort	Epigastric awareness
Skin		Pallor III	Pallor II	Pallor I	Flushing/Subjective warmth ≥ II
Cold sweating		III	II	I	
Increased salivation		III	II	I	
Drowsiness		III	II	I	
Pain					Headache ≥ II
Central nervous system					Dizziness Eyes closed ≥ II Eyes open III

Levels of Severity Identified by Total Points Scored				
Frank Sickness (S)	Severe Malaise (M III)	Moderate Malaise A (M IIA)	Moderate Malaise B (M IIB)	Slight Malaise (M I)
≥ 16 points	8 – 15 points	5 – 7 points	3 – 4 points	1 – 2 points

*AQS = Additional qualifying symptoms. + III = severe or marked, II = moderate, I = slight.

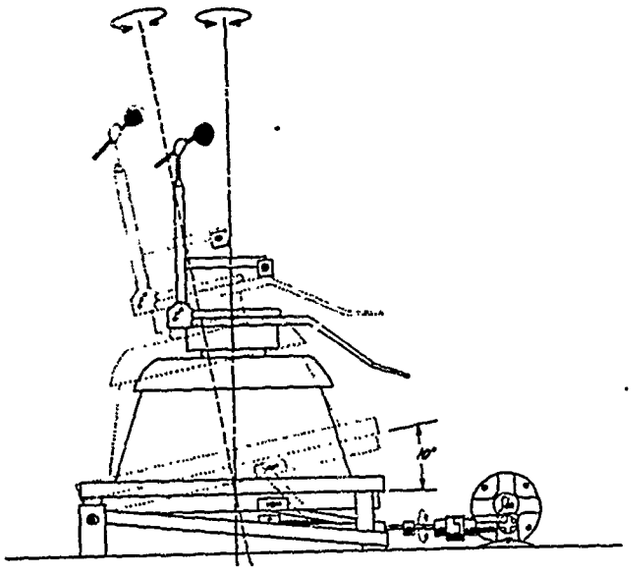


Figure 12–27. Off-vertical rotating chair device. Slide mechanisms for positioning subject now shown. (Graybiel & Miller, 1970b)

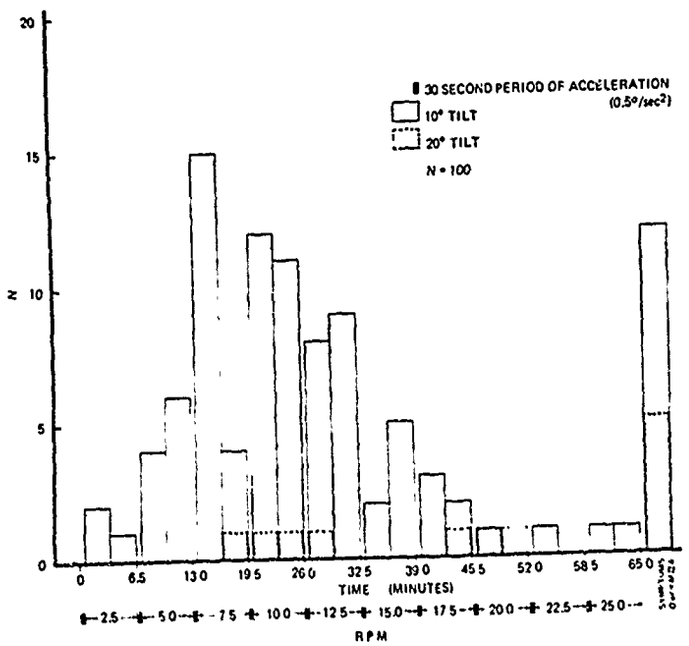


Figure 12–28. Susceptibility index in subjects exposed to off-vertical rotation according to programmed stress indicated on abscissa. (Graybiel & Miller, 1970b)

Figures 12-29 and 12-30 are plots comparing susceptibilty to motion sickness with scores obtained in testing, respectively, the function of the semicircular canals and otolith organs (Graybiel and Miller, 1970b). Although it appears that significant relationships were not found between functional test scores and susceptibility to motion sickness, it is worth adding that when extreme values are compared, susceptibility was higher in subjects with low rather than high oculogyral illusion threshold test values, and susceptibility was lower in subjects with high rather than low values for the counterrolling index.

Simulation Tests Some of the problems posed in attempting to predict susceptibility to vestibular side effects under the novel conditions in a rotating space base are pointed out in figure 12-31. The slow rotation room (SRR), which can be used to simulate the angular velocity, is a completely enclosed space and provides for prolonged exposures and sudden transitions between the rotating and nonrotating state. The SRR fails to simulate space-base conditions in such notable aspects as weightlessness, subgravity levels, man's orientation when upright with regard to the axis of rotation, and the Coriolis forces while walking and handling objects. Stated differently, the SRR provides a very useful simulation device for the important study of the effects of cross-coupled angular accelerations, except for the fractional subgravity levels and man's orientation with respect to the axis of rotation. The SRR is useful in demonstrating the qualitative aspects of the role of the vestibular organs in postural equilibrium and in walking, but nonvestibular factors play a greater role. The necessary use of small rotating devices poses limitations in terms of visual reference, length of exposure, and postural equilibrium. Parabolic flight offers the opportunity to study the effects of weightlessness and fractional subgravity levels for brief periods. Orbital flights prior to the establishment of a space base offer the opportunity to use small or even fairly large rotating devices for validation of ground-based experimental findings and the advantages of prolonged exposure to study adaptation effects.

It is convenient, although somewhat arbitrary, to distinguish between experiments designed to elicit responses that have their genesis mainly in the vestibular system and those designed to prevent such responses by means of stepwise incremental increases in the stressful stimuli.

The studies now to be reported for *elicitation* of vestibular side effects, were selected for their operational relevance and were conducted for the most part either in the SRR or in parabolic flight.

Slow Rotation Room. A series of experiments was carried out in the SRR to determine if there were differences in susceptibility to vestibular side effects dependent upon man's orientation to the axis of rotation and if the acquisition of adaptation effects acquired in one orientation mode transferred to the other. A unique feature of this experiment was the provision for subjects to walk on the "wall" of the circular SRR and carry out their tasks while horizontal with respect to the Earth vertical (Graybiel et al., 1968c). This was made possible by the use of air-bearing supports and custom-fitted articulated fiberglass molds. Four subjects participated in two different experiments involving adaptation to the stimulus conditions with the room rotating at 4 rpm

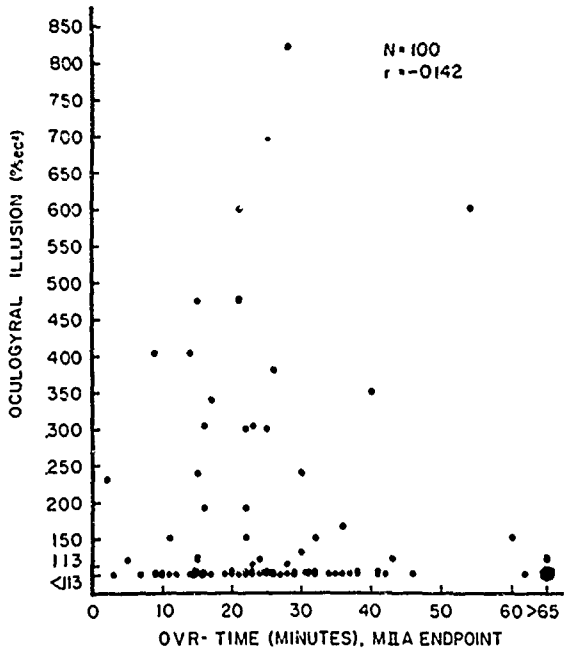


Figure 12–29. Comparison of motion sickness susceptibility with scores on test of semicircular canal function (oculogyral illusion). (Graybiel & Miller, 1970b)

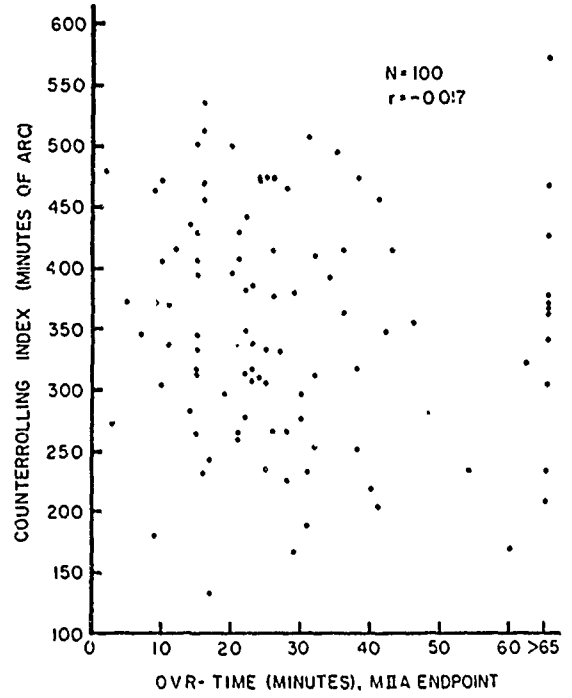


Figure 12–30. Comparison of motion sickness susceptibility with scores on test of otolith function (counterrolling index). (Graybiel & Miller, 1970b)

for a period of either 4 or 5 days. One pair of subjects initially in the horizontal mode was changed to the vertical mode near the middle of the perrotation period when symptoms of motion sickness had disappeared; in the second experiment they began in the vertical mode. The order was reversed for the second pair. When in the horizontal mode, the subjects spent approximately 6 hours a day in the airbearing device, 6 to 10 minutes upright, and the remainder of the time recumbent on a bunk. The findings, summarized in figure 12-32, indicate that there is no significant difference in susceptibility in the two modes and that transfer of adaptation is excellent. On cessation of rotation only mild symptoms of motion sickness were manifested. A by-product of the experiment was the demonstration of important differences between motion sickness and postural disequilibrium during adaptation to the rotating environment and subsequent return to the stationary one. In the start-horizontal mode, adaptation ensuring freedom from symptoms of motion sickness on change to the vertical mode did not prevent ataxia. In the start-vertical mode, the adaptation resulted in a great decrease in ataxia; this adaptation perseverated throughout the finish-horizontal mode and as long as 36 hours afterward. This implied that the dynamic processes underlying postural homeostasis involved muscular activities largely rendered static when subjects were in the horizontal mode.

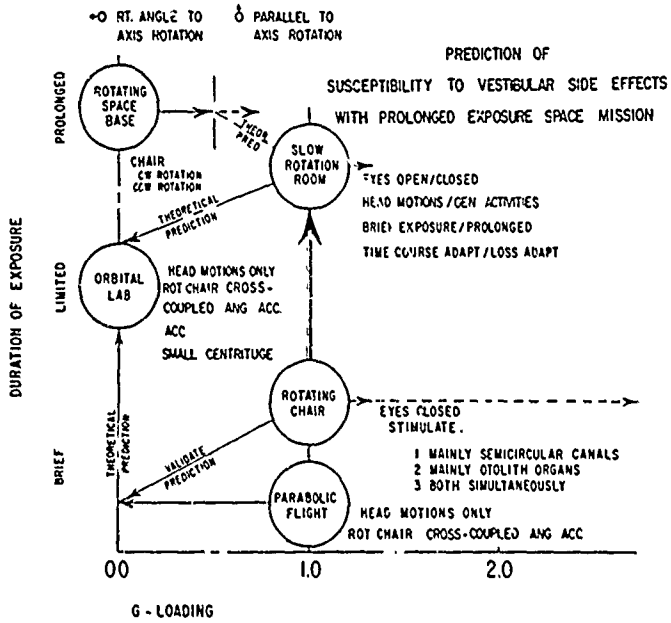


Figure 12–31. Prediction of susceptibility to motion sickness with prolonged exposure space mission.

In the light of the experiment just described, earlier studies involving prolonged exposures in the SRR were reviewed, particularly from the standpoint of manifestations of motion sickness on cessation of rotation. The experiment in which four subjects were exposed at 10 rpm over a period of 12 days was

notable in this regard (Graybiel et al., 1965). Despite the fact that severe symptoms were experienced, especially in the first half of the perrotation period, manifestations of motion sickness on cessation of rotation were trivial or absent.

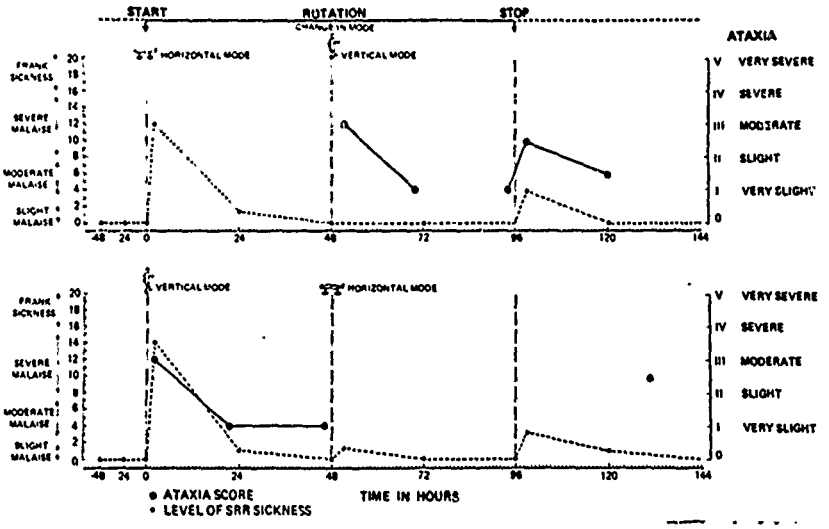


Figure 12–32. Appropriate mean changes in level of symptoms of motion sickness and in postural disequilibrium in 4 young healthy subjects exposed to continual rotation at 4 rpm.

Adaptive Capacity Tests. These tests measure individual differences in the rate of acquisition and decay of adaptation in a rotating environment. They qualify as simulation tests, and measure at once susceptibility to reflex vestibular disturbances and motion sickness and ability to adapt and to retain adaptation effects. Repeated exposures are required to measure retention of adaptation effects, and the best schedule is yet to be determined. These tests have various options open (Reason & Graybiel, 1969; 1970a, b), but all rely on exposure to stepwise increases in the stressful accelerations.

The findings in one test of this sort are summarized with the aid of table 12-5 (Reason & Graybiel, 1970a). Ten young subjects executed controlled head (and body) motions at each of ten 1-rpm increases in velocity of the slow rotation room. Eight discrete head motions at 2-second intervals comprised a sequence, and 4 seconds elapsed between sequences. At the end of each head motion the subject responded with a yes or no; yes indicated that he experienced one or more reflex vestibular disturbances or symptoms of motion sickness. The adaptation criterion was a negative response during three sequences, at which point the angular velocity of the SRR was increased by 1 rpm. The number of head movement sequences required at different step increases of the subjects are shown in table 12-5. The individual differences in performance were great. Four of the ten subjects experienced motion sickness and dropped out; one at 5 rpm, two at 6 rpm, and one at 10 rpm. One subject

required only nine sequences (72 head motions) to reach 10 rpm, and these were made at velocities below 3 rpm. At the other extreme, one subject required 390 sequences (3120 head motions) to achieve the adaptation criterion at 10 rpm.

Table 12–5

Number of Movement Sequences Prior to Achieving Adaptation Criterion at Each rpm*

Subject	1	2	3	4	5	6	7	8	9	10 rpm
RE	0	1	2	9	10	20	33	64	94	157
TA	0	2	3	2	3	9	10	5	8	8
HA	1	2	4	4	7	11	18	34	48	22
JE	5	4	0	0	0	0	0	0	0	0
HU	0	1	2	1	1	2	4	5	6	6
DI	0	0	0	2	2	2	2	3	3	4
HE	0	0	0	0	0	0	3	15	31	T**(45)
JA	0	0	1	12	6	T(23)				
SY	8	7	1	1	1	T(10)				
WE	23	44	33	22	T(225)					

*This value represents the total number of movement sequences executed at each rpm less the three movement sequences, eliciting negative sensation, which constituted the adaptation criterion.

**T indicates that rotation was terminated without achieving the adaptation criterion. The figures in parentheses show the number of sequences completed prior to termination.

This type of procedure stands somewhere between brief susceptibility tests and incremental adaptation tests designed to prevent reflex vestibular disturbances and motion sickness. Tests of adaptive capacity, however, are the best available for revealing individual differences in ability to cope with operational stimulus conditions.

Parabolic Flight. Studies dealing with the susceptibility to motion sickness in the weightless phase of parabolic flight have been mainly of two types (Miller, et al., 1969). In one kind, subjects were restrained in their seats and required to make standardized head motions during the weightless phase only. The findings are summarized in figure 12-33 and demonstrate that, among the twelve subjects tested in this manner, six were asymptomatic. Five of the remaining six experienced symptoms only when making head motions; the last subject demonstrated increased susceptibility when making head motions as compared to the head restraint (control) condition. These findings are concordant with those of Russian investigators utilizing parabolic flights (Kas'yan et al., 1965) and with the findings on astronauts (Berry &

Dietlein, 1970) and cosmonauts (Yuganov et al., 1966) who experienced motion sickness in orbital flight.

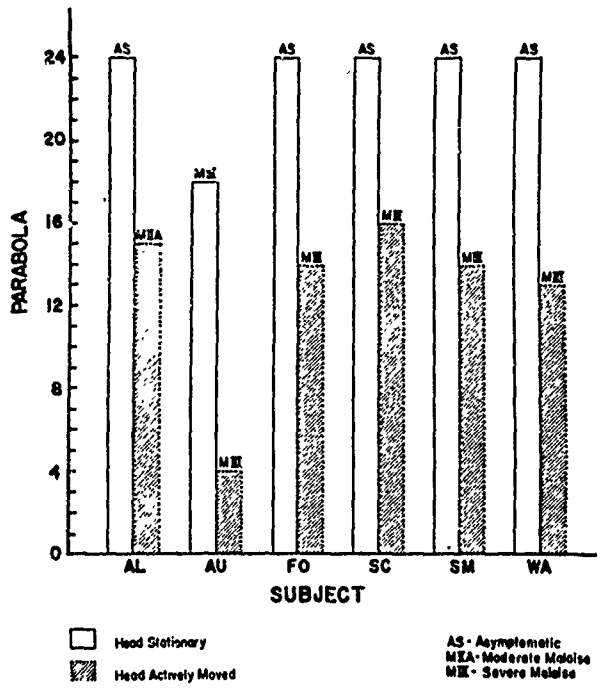


Figure 12–33. Effect among 6 susceptible subjects of active head movements relative to restrained condition upon sickness susceptibility measured in terms of number of parabolas required to provoke severe malaise. (Miller et al., 1969)

The second kind of experiment involved the use of a rotating chair device, with subjects required to make standardized head motions similar to those used in the dial test but with eyes blindfolded. Each subject served as his own control, and comparisons were made between susceptibility under terrestrial conditions and during parabolic flight, using similar periods of rotation and nonrotation. The findings summarized in figure 12-34 (Miller, et al., 1969) indicate that some subjects experienced a significant increase in susceptibility aloft while others manifested a decrease. When subjects were ranked in terms of their susceptibility under terrestrial conditions, the higher the susceptibility, the greater the likelihood that there would be an increase aloft, although there were exceptions to this generality.

The following studies were aimed at defining techniques and procedures for the *prevention* of vestibular side effects.

Incremental Adaptation Tests. Programming the acquisition of adaptation effects is good only in the sense that it is the best means to an end. Although there are a number of factors and trade-offs involved, the basic

operation consists of establishing new integrative patterns in the nervous system in response to changes in stimulus conditions. One object is to confront the nervous system with the largest change in stimuli possible, short of eliciting unwanted responses. In the absence of any response, there is no guide as to whether the nervous system is being fully tasked; i.e., operating at high efficiency. In practice, however, there are, ofttimes, responses in the nature of delicate indicators. If these indicators are not present spontaneously, they may be evoked with caution, and the degree of provocation required serves as a monitoring guide. However, only persons with experience in this kind of testing can safely task the nervous system to the limit without risk. The smaller the experience, the greater the margin of safety required.

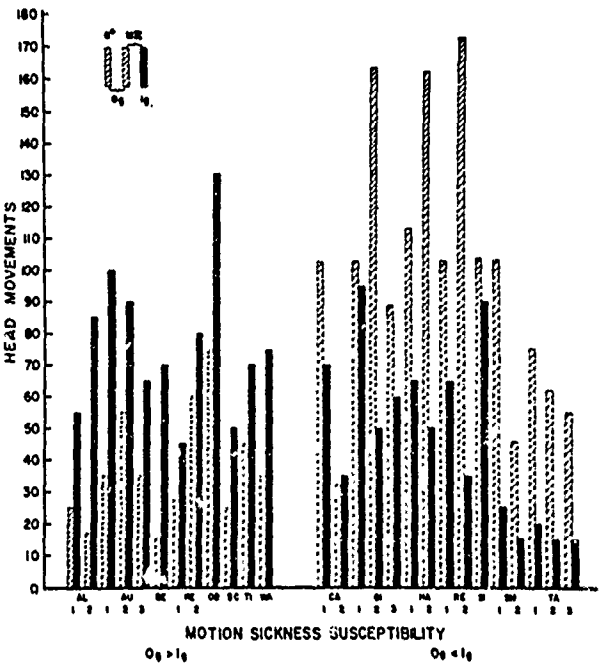


Figure 12–34. Comparison of Coriolis (motion) sickness susceptibility of 15 subjects measured in weightlessness and under terrestrial conditions. 0* = no symptoms, except in subject HA who experienced moderate malaise (M11A) on only his first test at 0 g; M111 = severe malaise. (Miller et al., 1969)

A brief review of early experiments representing attempts at incremental adaptation to a given terminal velocity in the SRR is worthwhile, partly to indicate the problems involved and partly to draw abstractions from the findings.

Three attempts to prevent motion sickness by step increases to a terminal velocity of 10 rpm were unsuccessful; two involved three incremental steps over a period of approximately three days, and the third a series of 40 incremental

steps over a period of 40 hours. In the next attempt (Graybiel, Deane, & Colehour, 1969) overt motion sickness symptoms, with the exception of drowsiness, on exposure to otherwise intolerable accelerations were prevented solely by means of nine stepwise increases in rotational speeds over a period of 16 days to a terminal velocity of 10 rpm. The stress profile and the symptomatology are summarized in figure 12-35. The four subjects had a busy schedule, and experimenter-paced head motions were required only for brief periods in connection with provocative tests. On cessation of rotation, ataxia was the most prominent and lasting complaint, and symptoms of motion sickness were either absent or of small significance. The on-board experimenter who was quite susceptible to SRR sickness spent his "nights" at home. He gradually adapted however, and could make the sudden transitions between the rotating and nonrotating states "without malaise or motion sickness". He did require about 30 minutes to adjust to the change. Important implications include: (1) the feasibility of adapting to 10 rpm, although the "cost" in time was high; (2) the remarkable freedom from symptoms of motion sickness on cessation of rotation, implying that efferent vestibular activity may have played an important role; and (3) the feasibility of making sudden transition between 0 and 10 rpm on a daily basis.

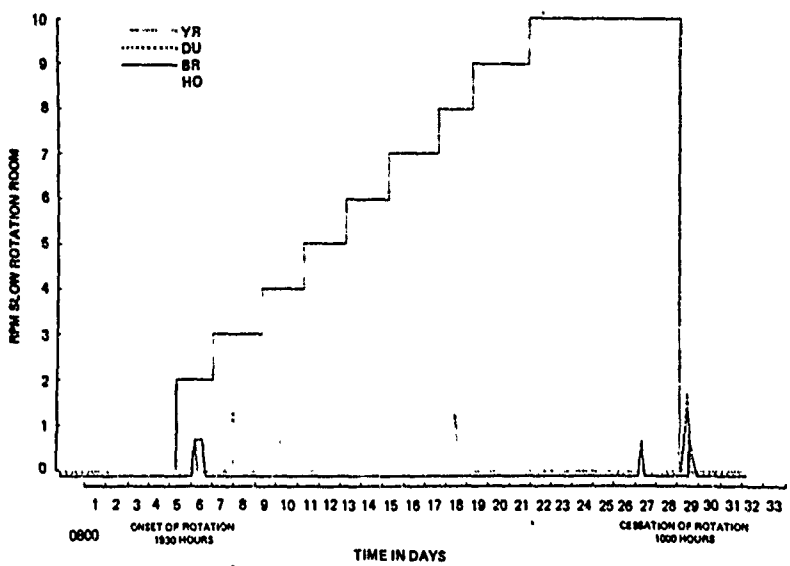


Figure 12–35. Stress profile and symptomatology in exposing 4 healthy subjects to stepwise increases in rotational speed to a terminal velocity of 10 rpm.

An attempt then was made to effect symptomatic incremental adaptation in an experiment in which the three subjects were required to execute experimenter-paced head-body motions (front, back, left, right). The actual time spent making 1000 head motions was a little over half an hour. In figure 12-36 (Graybiel & Wood, 1969) are shown the stress profile, the number of head motions made at each step, each up-down counting as one motion, and the level

of symptoms experienced by the subjects. One subject, TA, was quite susceptible, becoming very drowsy at 2 rpm, experiencing epigastric discomfort at 5 rpm, and minimizing or refraining from making head motions at the higher rpm. The two remaining subjects experienced mild symptoms at terminal velocity, which became more severe on cessation of rotation. TA resorted to the use of an antimotion sickness drug. Noteworthy features were: (1) the inability of TA to keep up with the schedule, (2) the appearance of symptoms resulting from inadequate adaptation in the remaining two subjects, and (3) the increase in symptoms experienced by all subjects on cessation of rotation.

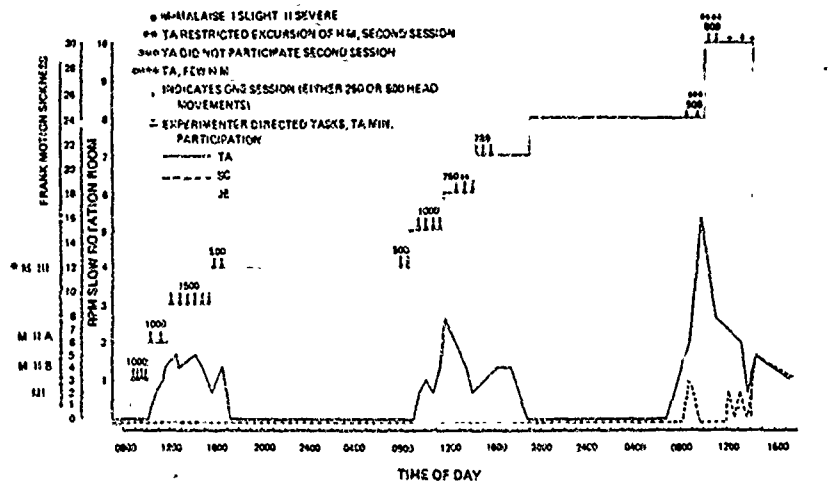


Figure 12–36. Stress profile in the SRR and manifestions of motion sickness in 3 healthy subjects exposed to rotation for over 2 days. (Graybiel & Wood, 1969)

In figure 12-37 (Graybiel & Wood, 1969) are shown the findings in a similar test, except that more head motions were made at the higher angular velocities. Symptoms of motion sickness were trivial except in subject RO who experienced very mild symptoms at 8 rpm and 9 rpm and on cessation of rotation. Except for ataxia, which was aggravated by head motions, complaints were minimal on cessation of rotation. These findings confirmed inferences drawn from the earlier studies and demonstrated that the time required to effect adaptation can be greatly shortened through control over head motions as well as angular velocity and by setting up an adaptation schedule. It should also be pointed out that the problems encountered were greater at relatively high velocities compared with relatively low ones and that, except in one instance, problems were not experienced if the unit increase was 1 rpm.

The above findings stimulated intensive studies centering on: (1) the best manner to execute a discrete head-body motion, (2) the spacing between head motions, (3) the size of unit increases in velocity, (4) the number of head motions as a function of 1-rpm increases in angular velocity, and (5) the individual differences in rate of acquisition and decay of adaptation effects mentioned above.

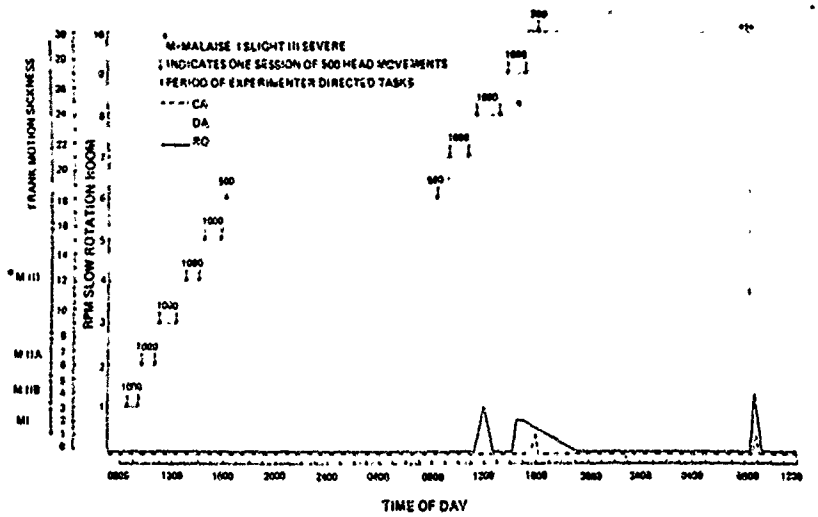


Figure 12–37. Stress profile in SRR and manifestations of motion sickness in 3 healthy subjects exposed to rotation for about 2 days. The large number of head motions accounted for rapid adaptation. (Graybiel & Wood, 1969)

The findings in an experiment to be reported (Reason & Graybiel, 1970b) can be briefly summarized with the aid of figure 12-38. Three subjects participated, and the adaptation schedule was the same for all subjects; the procedure was essentially the same as that described above in connection with table 12-5. On Day 1, while rotating counterclockwise, subjects executed 40 head movement sequences at 2 rpm, 50 at 3 rpm, 70 at 4 rpm, 90 at 5 rpm, and 110 at 6 rpm. The subjects, while rotating, then were shifted to highly stressful generalized activities in an attempt to evoke motion sickness. Their performance indicated that the head motions had produced a substantial degree of protection both with respect to reflex vestibular disturbances and motion sickness. On Day 2 the subjects executed 130 head movement sequences at 7 rpm, 150 at 8 rpm, 180 at 9 rpm, and 80 at 10 rpm. The subjects were again transferred to generalized activities and their performance was similar to that on Day 1. On the morning of Day 3 after 120 head movement sequences at 10 rpm, the room was brought to a stop, and the subjects executed the same head motions as during rotation. There were no symptoms of motion sickness, and all reflex effects quickly disappeared.

In figure 12-39 are shown findings obtained on the same three subjects when they executed an incremental adaptation test before and after participating in the 3-day experiment just described. This test is also identical with the incremental adaptation test described in connection with table 12-5. The noteworthy findings are: (1) the small number of affirmative responses 6 hours after the 3-day experiment ended; (2) weekly exposures led to increasingly better performance; and (3) when the subjects were rotated in the opposite direction (clockwise), their performance was far better than on the first pre-experimental test, indicating transfer of adaptation effects acquired during counterclockwise rotation. Again these findings support the conclusion that sudden transfers between the rotating and nonrotating environments are not only feasible in the SRR, but also that the adaptation effects may not decay rapidly and with weekly practice may not only be retained but improved.

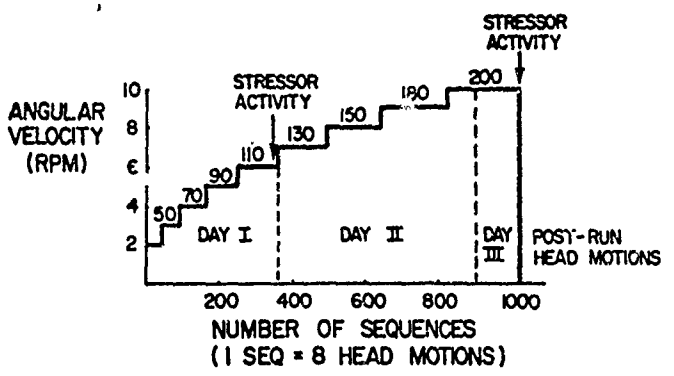


Figure 12–38. Stimulus profile for a 3-day adaptation schedule on SRR.

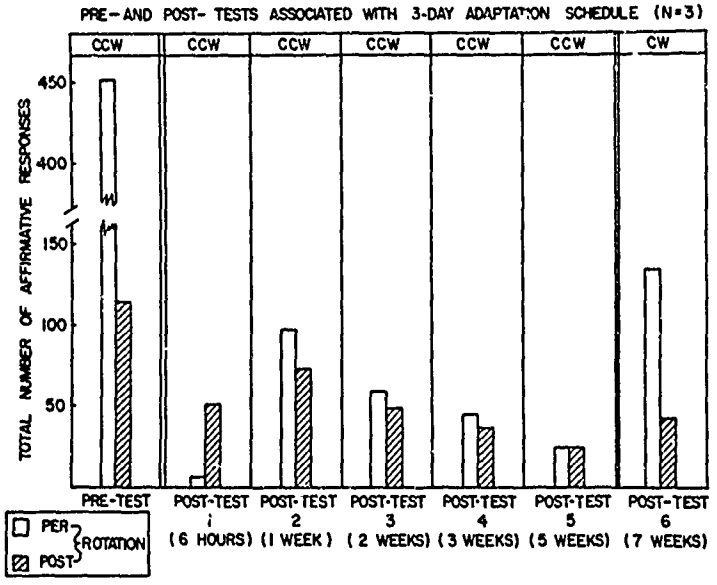


Figure 12–39. Pre- and post-tests associated with 3-day adaptation schedule for 3 subjects on SRR.

Postural Disequilibrium. Nonvestibular factors are of greater importance than vestibular factors in connection with postural stability while standing or walking in a rotating environment, and this problem is considered along with others in Appendix B. Not considered, however, is the acquisition of adaptation effects (along with skill) readily demonstrable in the SRR.

The ataxia manifested in the rotating room resembles that experienced aboard ship, and it is possible to demonstrate the contributing role of the vestibular organs by comparing the responses of normal and of labyrinthine defective (L-D) subjects (figure 12-40 A, B). With the onset of rotation, both normal and L-D subjects experience difficulty in walking, which is maximal initially and becomes progressively less over a period of days, after which there is little further change. This may be

shown by a test for postural disequilibrium designed to reveal small differences between the normal and L-D subjects in a stationary environment. One significant difference between the normal and L-D subjects is that the former, on sudden movement of the head, is more disturbed in his postural equilibrium than is the L-D subject. On cessation of rotation, both normal and L-D subjects manifest ataxia on walking. The sensations differ from those experienced on disembarking after a sea voyage in that the subjects report that they feel unstable on a stable platform, whereas after a voyage the platform seems to be unstable too. Again, the normal subject on quickly rotating the head, experiences disequilibrium and may experience dizziness; these are not experienced by the L-D subject.

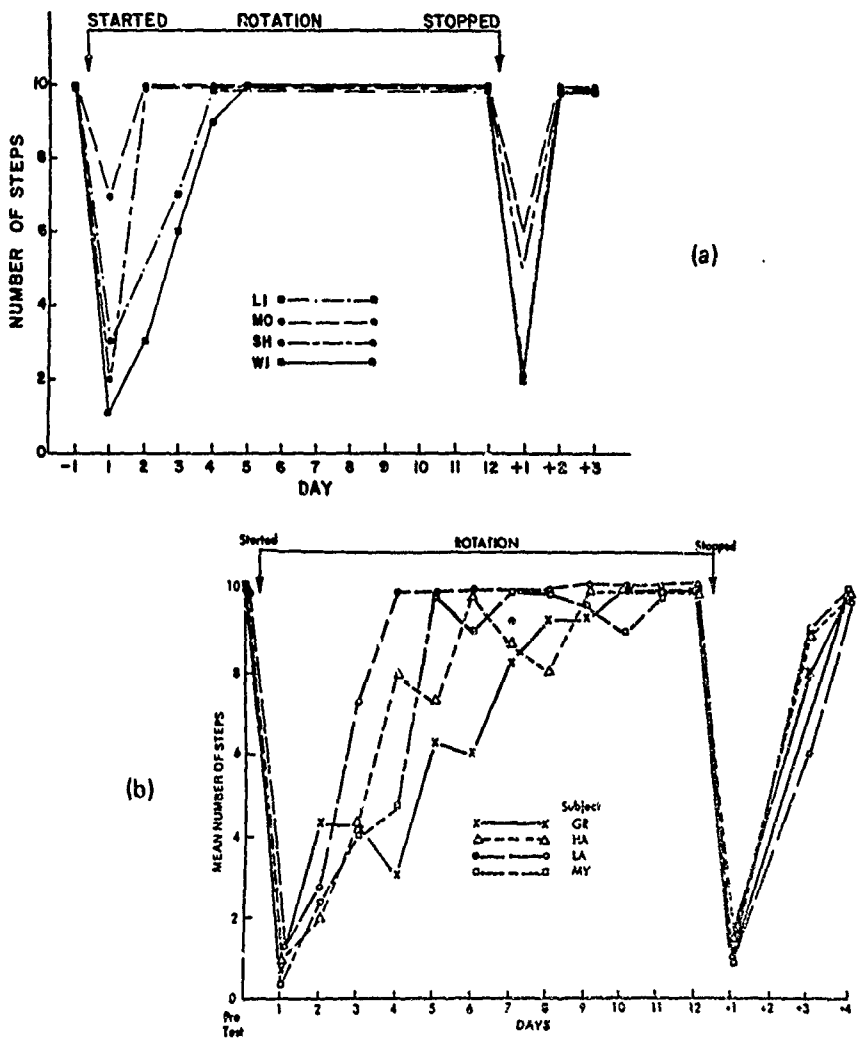


Figure 12–40. A: Heel-to-toe walking scores for four normal subjects; B: Individual test performance of 4 L-D subjects on a 3-inch wide rail along time axis of rotation. (Fregly & Kennedy, 1965)

Drugs. The dial test has also been used on the SRR in the evaluation of antimotion sickness drugs; a summary of the findings is shown in figure 12-41 (Wood & Graybiel 1970a). It was found that only those drugs with a parasympatholytic or sympathomimetic action and some of the antihistamines were notably effective under the stimulus conditions. Recently it was demonstrated (Wood & Graybiel, 1970b) that a combination of promethazine 25 mg with d-amphetamine 10 mg had the same range of effectiveness as that found for scopolamine 0.6 mg plus d-amphetamine 10 mg and that the substitution of ephedrine 50 mg for the amphetamine, while slightly less effective, was the best combination in terms of freedom from side effects. The drowsiness (sophite) syndrome and nausea and vomiting require different therapy. Coffee or its alkaloids have long been used to increase alertness, and the amphetamines should be reserved for "contingences." Once the nausea syndrome is well established, which should be a rarity, drugs taken by mouth may either remain in the stomach or be regurgitated. The combination of preventing head motions and the injection of an antimotion sickness remedy should suffice. The most effective measure would involve the use of a soporific or an antimotion sickness drug in an amount to ensure sleep.

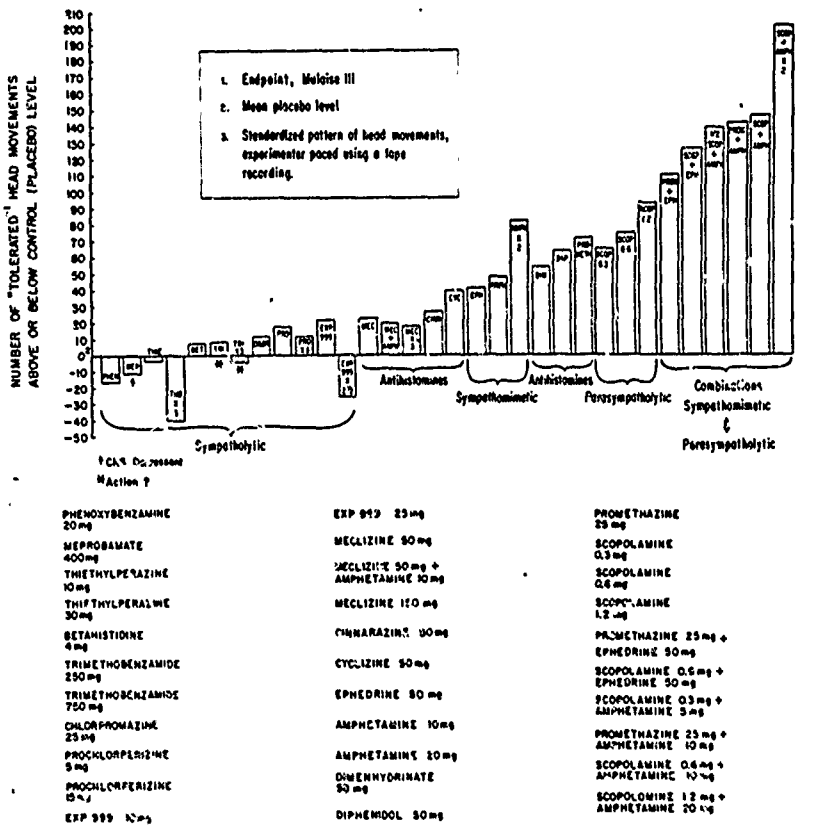


Figure 12–41. Effectiveness of antimotion sickness drugs in preventing SRR sickness in 60 subjects exposed on 500 occasions in rotating environment, using Dial Test. (Wood & Graybiel, 1970a)

Early Guidelines in the Prevention of Vestibular Side Effects on Space Missions Involving The Generation of Artificial Gravity

The limitations in simulating such novel stimulus conditions as those involved in making sudden transitions between rotating and nonrotating portions of a space base force an extension of ground-based studies to include validating observations and experiments conducted aloft. The astronaut necessarily plays the key role in this integration. In the role of subject he can serve as his own control in validating studies; in the role of onboard experimenter he is essential in conducting experiments and making observations aloft; in the role of astronaut he has responsibilities in connection with the prevention of vestibular side effects during the mission. As indicated earlier, prevention involves taking charge rather than responding to events, and this will require close cooperation between the astronaut in the space base and the biomedical representatives in the ground-based control center during the period of adjustment.

Ground-based activities involving the astronaut center around the individualization of the problem in preventing vestibular side effects and the astronaut's somewhat complementary role as subject and onboard experimenter. Major elements include selection (or secondary selection), instruction, preflight adaptation, monitoring his progress during the mission, and postflight assessment. The astroscientist, who does not double as an astronaut, presents somewhat different considerations. He would not be under the same time-load stress as the astronaut prior to launch, and presumably there would be little restriction in terms of participation in prelaunch assessment, indoctrination, and adaptation. Inasmuch as his tasks aloft would not include items critical for life support, rapid adjustment to stimulus conditions would not be a necessity, which in turn would permit greater freedom in the selection process.

The lines of direction of the ground-based experimental program would be determined in large part by the findings obtained under space flight conditions. Until that time, all guidelines are tentative in nature. A brief status report serves to point up gaps in our knowledge.

In order to keep the discussion within manageable limits it will be assumed that the rotating portion of the space base will have a radius of about 80 feet and that its maximal angular velocity will be 4 rpm. The problem posed by postural instability will not be discussed inasmuch as nonvestibular factors are of chief importance in this case. Only the worst-case situation will be considered; namely, initial transition into weightlessness, subsequent (initial), transition to rotation at 4 rpm with one-third fractional G loading, and sudden transitions between the rotating and nonrotating portions of the space base.

Transition Into Weightlessness

Information presently available indicates that it is possible by means of selection procedures not only to distinguish among astronauts and astroscientists who are or are not susceptible to vestibular side effects in weightlessness, but

also to rank those who are, according to their degree of susceptibility. In other words, rarely, if ever, should one be surprised by unexpected responses from astronauts making their initial transition into weightlessness and seldom surprised even in the case of astroscientists.

Transition Into The Rotating Environment

The principal unknown element of this novel experience concerns the effect of the fractional G load. This information will soon be available, but until then a conservative approach would serve to avoid the selection of persons who are susceptible to motion sickness in weightlessness. Present findings indicate that, with few exceptions, persons who are relatively insusceptible to motion sickness in weightlessness are in the group that is relatively insusceptible to motion sickness in the SRR. Consequently, persons with high adaptive capacity in the SRR and low susceptibility to motion sickness in weightlessness should not have a problem in making a sudden transition to 4 rpm in a space base if prelaunch adaptation has been carried out. This does not obviate the necessity for small rotating devices to permit incremental adaptation in case of need.

Sudden Transitions Between Rotation and Weightlessness

Here too we are dealing with novel stimulus conditions, and again it would be helpful to know the shape of the curves depicting susceptibility to vestibular side effects as a function of subgravity levels. The evidence available strongly indicates that it is possible to rank persons with regard to their acquisition and retention of adaptation to 4 rpm in the SRR and that persons fully adapted can make the transition between the stationary and rotating environments without experiencing either motion sickness or reflex vestibular effects, except insofar as they contribute to ataxia. What is not known is the extent to which adaptation effects acquired in the SRR would transfer to the space base condition. Again this points to the necessity of making provision for incremental adaptation in case of need. In weightlessness, incremental adaptation is more difficult to program than in a rotating environment, unless there are means for substituting passive for active motions.

Frequent transitions (measured in days) are necessary to preserve adaptation to both rotating and nonrotating environments under terrestrial conditions, and this would be a reasonable expectation under space base conditions.

References

Anson, B. J., Harper, D. B., & Winch, T. G. The vestibular and cochlear aqueducts: Developmental and adult anatomy of their contents and parietes. In *Third symposium on the role of the vestibular organs in space exploration.* NASA SP-152. Washington, D.C.: U.S. Government Printing Office, 1968. Pp. 125-146.

Aschan, G., Bergstedt, M., & Stahle, J. Nystagmography. Recording of nystagmus in clinical neuro-otological examination. *Acta oto-laryngologica*, Stockholm, 1956, Supplement 129.

Aubert, H. Eine scheinbare bedeutende Drehung von Objekten bei Neigung des Kopfes nach rechts oder links. *Archiv für pathologische Anatomie und Physiologie*, 1861, *20*, 381-393.

Berry, C. A., & Dietlein, L. F. Findings on astronauts bearing on the problem of artificial gravity. Presented at the *Fifth symposium on the role of the vestibular organs in space exploration*, Pensacola, Florida, August 19-21, 1970.

Billingham, J. Russian experience of problems in vestibular physiology related to the space environment. In *Second symposium on the role of the vestibular organs in space exploration.* NASA SP-115. Washington, D.C.: U.S. Government Printing Office, 1966. Pp. 5-11.

Camis, M. *The physiology of the vestibular apparatus.* Oxford, England: Clarendon Press, 1930.

Carpenter, M. B. Experimental anatomical-physiological studies of the vestibular nerve and cerebellar connections. In G. L. Rasmussen and W. F. Windle (Eds.) *Neural mechanisms of the auditory and vestibular systems.* Springfield, Ill.: Charles C. Thomas, 1960. Pp. 297-323.

Clark, B., & Graybiel, A. Contributing factors in the perception of the oculogravic illusion. *American Journal of Psychology*, 1963a, *76*, 18-27.

Clark, B., & Graybiel, A. Perception of the postural vertical in normals and subjects with labyrinthine defects. *Journal of Experimental Psychology*, 1963b, *65*, 490-494.

Clark, B., & Graybiel, A. Perception of the postural vertical following prolonged bodily tilt in normals and subjects with labyrinthine defects. *Acta oto-laryngologica*, Stockholm, 1964, *58*, 143-148.

Clark, B., & Stewart, J. D. Perception of angular acceleration about the yaw axis of a flight simulator. *Aerospace Medicine*, 1962, *33*, 1426-1432.

Clark, B., & Stewart, J. D. Effects of angular acceleration on man: Thresholds for the perception of rotation and the oculogyral illusion. *Aerospace Medicine*, 1969, *40*, 952-956.

Fitzgerald, G., & Hallpike, C. S. Studies in human vestibular function. I. Observations on the directional preponderance ("nystagmusbereitschaft") of caloric nystagmus resulting from cerebral lesions. *Brain*, 1942, *65*, 115-137.

Fluur, E. Influences of semicircular ducts on extraocular muscles. *Acta oto-laryngologica*, Stockholm, 1959, Supplement 149.

Fredrickson, J. M., & Schwarz, D. Multisensory influence upon single units in the vestibular nucleus. In *Fourth symposium on the role of the vestibular organs in space exploration.* NASA SP-187. Washington, D.C.: U.S. Government Printing Office, 1970. Pp. 203-208.

Fregly, A. R., & Kennedy, R. S. Comparative effects of prolonged rotation at 10 rpm on postural equilibrium in vestibular normal and vestibular defective human subjects. *Aerospace Medicine*, 1965, *36*, 1160-1167.

Gacek, R. R. Efferent component of the vestibular nerve. In G. L. Rasmussen and W. F. Windle (Eds.) *Neural mechanisms of the auditory and vestibular systems.* Springfield, Ill.: Charles C. Thomas, 1960. Pp. 276-284.

Gacek, R. R. Anatomical evidence for an efferent vestibular pathway. In *Third symposium on the ... of the vestibular organs in space exploration*. NASA SP-152. Washington, D.C.: U.S. Government Printing Office, 1968. Pp. 203-211.

Gernandt, B. E. Vestibular influence upon spinal reflex activity. In A. V. S. de Reuck & J. Knight (Eds.) *Myotatic, kinesthetic and vestibular mechanisms*. London: Churchill, 1967. Pp. 170-183.

Gernandt, B. E. Interaction between extraocular myotatic and ascending vestibular activities. *Experimental Neurology*, 1968, *20*, 120-134.

Graybiel, A. Oculogravic illusion. *Archives of Ophthalmology*, 1952, *48*, 605-615.

Graybiel, A. Structural elements in the concept of motion sickness. *Aerospace Medicine*, 1969, *40*, 351-367.

Graybiel, A., & Fregly, A. R. A new quantitative ataxia test battery. *Acta oto-laryngologica*, Stockholm, 1966, *61*, 292-312.

Graybiel, A., & Hupp, D. I. The oculogyral illusion: A form of apparent motion which may be observed following stimulation of the semicircular canals. *Journal of Aviation Medicine*, 1946, *17*, 3-27.

Graybiel, A., & Kellogg, R. S. The inversion illusion in parabolic flight: Its probable dependence on otolith function. *Aerospace Medicine*, 1967, *38*, 1099-1103.

Graybiel, A. & Miller, E. F., II. The otolith organs as a primary etiological factor in motion sickness: With a note on "off-vertical" rotation. In *Fourth symposium on the role of the vestibular organs in space exploration*. NASA SP-187. Washington, D.C.: U.S. Printing Office, 1970a. Pp. 53-64.

Graybiel, A., & Miller, E. F., II Off-vertical rotation: A convenient precise means of exposing the passive human subject to a rotating linear acceleration vector. *Aerospace Medicine*, 1970 b, *41*, 407-410.

Graybiel, A., & Wood, C. D. Rapid vestibular adaptation in a rotating environment by means of controlled head movements. *Aerospace Medicine*, 1969, *40*, 638-643.

Graybiel, A., Deane, F. R., & Colehour, J. K. Prevention of overt motion sickness by incremental exposure to otherwise highly stressful Coriolis accelerations. *Aerospace Medicine*, 1969, *40*, 142-148.

Graybiel, A., Kennedy, R. S., Knoblock, E. C., Guedry, F. E., Jr., Mertz, W., McLeod, M. E., Colehour, J. K., Miller, E. F. II, & Fregly, A. R. The effects of exposure to a rotating environment (10 rpm) on four aviators for a period of twelve days. *Aerospace Medicine*, 1965, *36*, 733-754.

Graybiel, A., Miller, E. F., II, Billingham, J., Waite, R., Berry, C. A., & Dietlein, L. F. Vestibular experiments in Gemini flights V and VII. *Aerospace Medicine*, 1967, *38*, 360-370.

Graybiel, A., Miller, E. F., II, Newsom, B. D., & Kennedy, R. S. The effect of water immersion on perception of the oculogravic illusion in normal and labyrinthine-defective subjects. *Acta oto-laryngologica*, Stockholm, 1968a, *65*, 599-610

Graybiel, A., Wood, C. D., Miller, E. F., II, & Cramer, D. B. Diagnostic criteria for grading the severity of acute motion sickness. *Aerospace Medicine*, 1968b, *39*, 453-455.

Graybiel, A., Thompson, A. B., Deane, F. R., Fregly, A. R., & Colehour, J. K. Transfer of habituation of motion sickness on change in body position between vertical and horizontal in a rotating environment. *Aerospace Medicine*, 1968c, *39*, 950-962.

Graybiel, A., O'Donnell, R. D., Smith, J. J., & Sansing, J. C. Nystagmic responses in subjects with eyes closed during parabolic flight. NAMRL Report. Naval Aerospace Medical Research Laboratory, Pensacola, Fla., 1970a, in preparation

Graybiel, A., Smith, C. R., Guedry, F. E., Jr., Miller, E. F., II, Fregly, A. R., & Cramer, D. B. Idiopathic progressive vestibular degeneration in a young man. Loss of vestibular servation not a basis for detection. *Annals of Otology, Rhinology and Laryngology*, 1972, *81*, 165-168.

Henriksson, N. G., Lundgren, A., Lundgren, K., & Nilsson, A. New techniques of vestibular examination. I. Analysis of eye-movements for oto-neurological diagnosis. Ciba Foundation, 1966.

Hixson, W. C., Niven, J. I., & Correia, M. J. Kinematics nomenclature for physiological accelerations with special reference to vestibular applications. Monograph 14. Naval Aerospace Medical Institute, Pensacola, Florida, 1966. Pp. 47-53.

Igarashi, M. Dimensional study of the vestibular end organ apparatus. In *Second symposium on the role of the vestibular organs in space exploration*. NASA SP-115. Washington, D.C.: U.S. Government Printing Office, 1966. Pp. 47-53.

Igarashi, M., & Nagaba, M. Vestibular end-organ damage in squirrel monkeys after exposure to intensive linear acceleration. In *Third symposium on the role of the vestibular organs in space exploration*. NASA SP-152. Washington, D.C.: U.S. Government Printing Office, 1968. Pp. 63-81.

Ito, M. The cerebellovestibular interaction in cat's vestibular nuclei neurons. In *Fourth symposium on the role of the vestibular organs in space exploration*. NASA SP-187. Washington, D.C.: U.S. Government Printing Office, 1970. Pp. 183-199.

Jongkees, L. B. W. The examination of the vestibular organ. *Progress in Brain Research*, 1967, *23*, 155-168.

Kas'yan, I. I., Kolosov, I. A., Lebedev, V. I., & Yurov, B. N. Reaction of cosmonauts during parabolic flight in aircraft. *Izv. Akad. Nauk SSSR*, Series B., No. 2, Mar-April 1965. (Translation.)

Kellogg, R. S., & Graybiel, A. Lack of response to thermal stimulation of the semicircular canals in the weightless phase of parabolic flight. *Aerospace Medicine*, 1967, *38*, 487-490.

Khilov, K. L. Function of the vestibular analyzer in space flights. *Archives of Otolaryngology*, 1969a, *90*, 152-160.

Khilov, K. L. (*The function of the equilibrium organ and motion sickness.*) Leningrad: Izdatel'stvo Meditsina, 1969b, 280 pp.

Lindeman, H. H., Ades, H. W., & West, R. W. Scanning electron microscopy of the vestibular end organs. Presented at the *Fifth symposium on the role of the vestibular organs in space exploration*, Pensacola, Florida, August 19-21, 1970.

McLeod, M. E., & Meek, J. C. A threshold caloric test: Results in normal subjects. NSAM-834. Naval School of Aviation Medicine, Pensacola, Fla., 1962.

McNally, W. J. An evaluation of vestibular testing. *Archives of Otolaryngology*, 1969, *89*, 57-63.

McNally, W. J., & Stuart, E. A. Physiology of the labyrinth reviewed in relation to seasickness and other forms of motion sickness. *War Medicine*, 1942, *2*, 683-771.

Megirian, D., & Manning, J. W. Input-output relations of the vestibular system. *Archives italiennes de biologie*, 1967, *105*, 15-30.

Mickle, W. A., & Ades, H. W. Spread of evoked cortical potentials. *Journal of Neurophysiology*, 1953, *16*, 608-633.

Mickle, W. A., & Ades, H. W. Rostral projection pathway of the vestibular system. *American Journal of Physiology*, 1954, *176*, 243-252.

Miller, E. F., II Evaluation of otolith organ function by means of ocular counterrolling measurements. In J. Stahle (Ed.) *Vestibular function on earth and in space*. Oxford, England: Pergamon Press, 1970. Pp. 97-107.

Miller, E. F., II & Graybiel, A. Otolith function as measured by ocular counterrolling. In *The role of the vestibular organs in the exploration of space*. NASA SP-77. Washington, D.C.: U.S. Government Printing Office, 1965. Pp. 121-130.

Miller, E. F., II, & Graybiel, A. The semicircular canals as a primary etiological factor in motion sickness. In *Fourth symposium on the role of the vestibular organs in space exploration*. NASA SP-187. Washington, D.C.: U.S. Government Printing Office, 1970a. Pp. 69-82.

Miller, E. F., II, & Graybiel, A. A provocative test for grading susceptibility to motion sickness yielding a single numerical score. *Acta oto-laryngologica, Stockholm* 1970b, Suppiement (in press).

Miller, E. F., II, & Graybiel, A. Ocular counterrolling measured during eight hours of sustained body tilt. NAMRL-1154. Naval Aerospace Medical Research Laboratory, Pensacola, Florida, 1972, (in preparation).

Miller, E. F., II, Graybiel, A., & Kellogg, R. S. Otolith organ activity within Earth standard, one-half standard, and zero gravity environments. *Aerospace Medicine*, 1966, *37*, 399-403.

Miller, E. F., II, Graybiel, A., Kellogg, R. S., & O'Donnell, R. D. Motion sickness susceptibility under weightless and hypergravity conditions generated by parabolic flight. *Aerospace Medicine*, 1969, *40*, 862-868.

Müller, G. E. Über das Aubertsche Phänomen. *Zeitschrift für Sinnesphysiologie*, 1916, *49* (Part II), 109-244.

Nashner, L. M. Sensory feedback in human posture control. MVT-70-30. Man-Vehicle Laboratory, Massachusetts Institute of Technology, Cambridge, Mass., 1970.

Nyberg-Hansen, R. Anatomical aspects on the functional organization of the vestibulospinal projection, with special reference to the sites of termination. In *Fourth symposium on the role of the vestibular organs in space exploration*. NASA SP-187. Washington, D.C.: U.S. Government Printing Office, 1970. Pp. 167-180.

Pompeiano, O. Interaction between vestibular and nonvestibular sensory inputs. In *Fourth symposium on the role of the vestibular organs in space exploration*. NASA SP-187. Washington, D.C.: U.S. Government Printing Office, 1970. Pp. 209-235.

Rasmussen, A. T. *The principal nervous pathways*. (4th ed.) New York: The MacMillan Co., 1952.

Reason, J. T., & Graybiel, A. An attempt to measure the degree of adaptation produced by differing amounts of Coriolis vestibular stimulation in the slow rotation room. NAMI-1084. Naval Aerospace Medical Institute, Pensacola, Florida, 1969.

Reason, J. T., & Graybiel, A. Progressive adaptation to Coriolis accelerations associated with 1-rpm increments in the velocity of the slow rotation room. *Aerospace Medicine*, 1970a, *41*, 73-79.

Reason, J. T., & Graybiel, A. The effectiveness of a three-day adaptation schedule to prevent motion sickness in a slowly rotating device. NAMRL Report. Naval Aerospace Medical Research Laboratory, Pensacola, Florida, 1970b (in press).

Schock, G. J. D. Perception of the horizontal and vertical in simulated subgravity conditions. *U.S. Armed Forces Medical Journal*, 1960, *11*, 786-793.

Smith, C., & Rasmussen, G. L. Nerve endings in the maculae and cristae of the chinchilla vestibule, with a special reference to the efferents. In *Third symposium on the role of the vestibular organs in space exploration*. NASA SP-152. Washington, D.C.: U.S. Government Printing Office, 1968. Pp. 183-200.

Snyder R. S., & Lowy, K. Evoked potentials and microelectrical analysis of sensory activity within the cerebellum. In *Fourth symposium on the role of the vestibular organs in space exploration*. NASA SP-187. Washington, D.C.: U.S. Government Printing Office, 1970. Pp. 245-257.

Solly, C. M. Reduction of error with practice in perception of the postural vertical. *Journal of Experimental Psychology*, 1956, *52*, 328-333.

Spector, M. (ed.) *Dizziness and vertigo*. New York: Grune and Stratton, 1967.

Spiegel, E. A., Szekely, E. G., Moffett, H., & Egyed, J. Cortical projection of labyrinthine impulses: Study of averaged evoked responses. In *Fourth symposium on the role of the vestibular organs in space exploration*. NASA SP187. Washington, D.C.: U.S. Government Printing Office, 1970. Pp. 259-268.

Spoendlin, H. H. Ultrastructural studies of the labyrinth in squirrel monkeys. In *The role of the vestibular organs in the exploration of space*. NASA SP-77. Washington, D.C.: U.S. Government Printing Office, 1965. Pp. 7-21.

Spoendlin, H. H. Ultrastructure of the vestibular sense organs. In R. J. Wolfson (Ed.) *The vestibular system and its diseases*. Philadelphia, University of Pennsylvania Press, 1966. Pp. 39-68.

Wersäll, J., & Lundquist, P.-G. Morphological polarization of the mechanoreceptors of the vestibular and acoustic systems. In *Second symposium in the role of the vestibular organs in space exploration*. NASA SP-115. Washington, D.C.: U.S. Government Printing Office, 1966. Pp. 57-71.

Wilson, V. J. Vestibular and somatic inputs to cells of the lateral and medial vestibular nuclei of the cat. In *Fourth symposium on the role of the vestibular organs in space exploration*. NASA SP-187. Washington, D.C.: U.S. Government Printing Office, 1970. Pp. 145-156.

Wood, C. D., & Graybiel, A. A theory of motion sickness based on pharmacological reactions. *Clinical Pharmacology and Therapeutics*, 1970a, *11*, 621-629.

Wood, C. D., & Graybiel, A. Evaluation of antimotion sickness drugs: A new effective remedy revealed. *Aerospace Medicine*, 1970b, *41*, 932-933.

Yuganov, E. M., Gorshkov, A. I., Kasian, I. I., Brianov, I. I., Kolosov, I. A., Kopanev, V. I., Lebedev, V. I., Papov, N. I., & Solodovnik, F. A. Vestibular reactions of cosmonauts during the flight in the "Voskhod" spaceship. *Aerospace Medicine*, 1966, *37*, 691-694.

APPENDIX A

Vestibular Models*

The input-output relationships for the vestibular system relating linear and angular acceleration and gravitational forces to eye movements, perceived orientation, postural reflexes and control commands are shown schematically in figure A-1 (Young, 1969). Models have been developed for semicircular canal and otolith function, and to a limited extent for their interactions on the basis of behavioral experiments. Typically, subjects are rotated through known angular velocity patterns, and the resulting eye movements (usually angular velocity of slow phase nystagmus) or subjective sensation of velocity and perceived orientation with respect to the apparent vertical are monitored. A control engineering model for subjective sensation and slow phase nystagmus velocity for rotation about a vertical axis is shown in the adaptation model for horizontal semicircular canals given in figure A-2 (Young & Oman, 1969). The torsion pendulum canal dynamics represents the second-order equation describing semicircular canal action summarized by van Egmond, Groen, & Jongkees (1949). The differential equation relating angular deviation of the cupula to angular acceleration normal to the plane of the canal is given by:

$$\theta \ddot{\xi} + \pi \dot{\xi} + \Delta \xi = a\theta$$

where

θ = moment of inertia of the endolymph

π = moment of friction at unit angular velocity of the endolymph with respect to the skull

Δ = stiffness, or torque moment per unit angular deflection of the cupula

ξ = angular deviation of the endolymph with respect to the skull

a = component of angular acceleration of the skull, with respect to inertial space, normal to the plane of the semicircular canal.

In Laplace transfer notation the cupula deflection is related to the angular acceleration by the relationship:

$$\frac{\xi(S)}{a(S)} = \frac{1}{S^2 + (\pi/\theta)S + (\Delta/\theta)}$$

*The material in this section was kindly furnished by Professor L. R. Young, Massachusetts Institute of Technology.

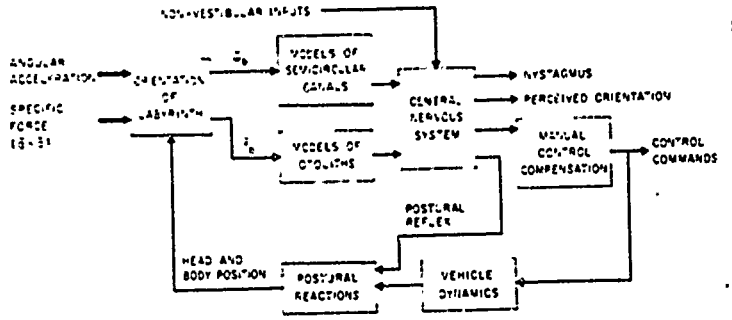


Figure A–1. Framework for systems analysis of vestibular function. (Young, 1969)

Reproduced from best available copy.

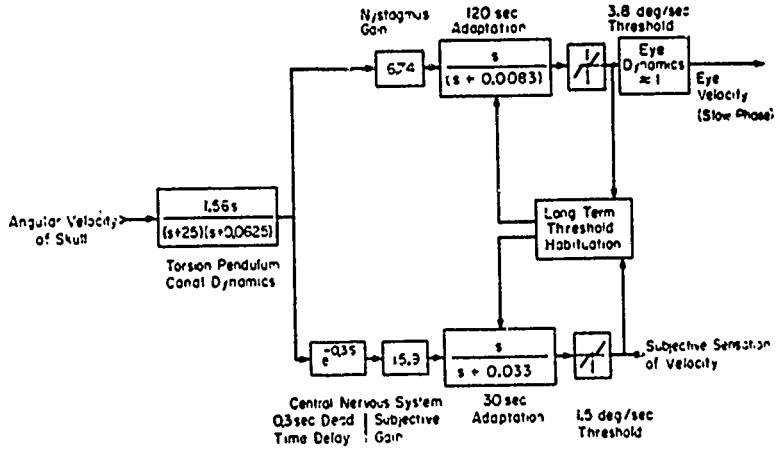


Figure A–2. Model for subjective sensation and slow phase nystagmus velocity for rotation about a vertical axis. (Young & Oman, 1969)

If the roots of the denominator are real and widely separated, i.e., the system overdamped and $\Delta/\pi \ll \pi/\theta$, the equation may be approximated as

$$\frac{\xi(S)}{\alpha(S)} = \frac{1}{(S + a)\ (S + b)}$$

where

$$a = \frac{\Delta}{\pi}\,(0.04 - 0.02\ \text{rad/sec})$$

$[a_{nominal}$ = 0.1 rad/sec for lateral canals,
0.14 rad/sec for posterior and superior canals]

corresponding to the long time constant of the cupula return phase

and

$$b = \frac{\pi}{\theta}\,(4 - 300\ \text{rad/sec})$$

$[b_{nominal}$ = 10 rad/sec]

corresponding to the short time constant of the system

The existence of a nystagmus reversal following an impulse of acceleration and the reduction in nystagmus and sensation during sustained constant angular acceleration led to inclusion of central adaptation blocks for both nystagmus and sensation of angular velocity. The response of this model to an acceleration impulse (velocity step) of 1.0 deg/sec is shown in figure A-3 (Young & Oman, 1969). Notice the apparently shorter time constant for subjective angular velocity than for nystagmus slow phase velocity as has been observed in cupulometry. The model response to a step of constant acceleration is shown to agree with experimental data in figure A-4 (Young & Oman, 1969). Latency to detection of low-level constant angular accelerations is shown in figure A-5 (Young & Oman, 1969). Finally, the semicircular canal model can be used to predict nystagmus and subjective sensation responses to sinusoidal stimuli. For nystagmus, the concept of "cumulative" eye position is used, derived by eliminating all fast phases and piecing together the slow phase nystagmus as in figure A-6 (Young, 1969). The resulting frequency response for nystagmus is shown in figure A-7 (Young & Oman, 1969). It is seen that over a wide range of frequencies (within 0.1 rad/sec-10 rad/sec), the eye angular velocity tends to compensate for head angular velocity with relatively little phase lag or phase lead, but with a gain significantly less than 1. The complementary frequency response for subjective sensation of velocity is shown in figure A-8 (Young & Oman, 1969). The break frequencies are noted in terms of τ_a (adaptation time constant) and Δ/π.

The nonlinear model for otolith function relates specific force (gravity minus linear acceleration) to perceived linear acceleration or tilt, as shown in figure A-9 (Young, 1969). The step response of this model shows a rapid rise, an overshoot, and decay of the resting level to about 40 percent of the peak response with a time constant of approximately 5 seconds. The model frequency response is shown in figure A-10 (Young, 1969). It is supported by data on sensation of linear velocity during sinusoidal horizontal acceleration and by the phase angle of dynamic counterrolling during continuous rotations. The model can be interpreted as perceived velocity with respect to actual velocity, or perceived tilt with respect to actual tilt. Figure A-11 (Young, 1969) shows the latency to perception of constant linear acceleration as a function of acceleration level. The

model assumes an absolute threshold of approximately 0.005 g's for gravitioertial force in the plane of the utricular otolith. Figure A-11 is for horizontal acceleration with the head upright which places the latency at 0.01 g's.

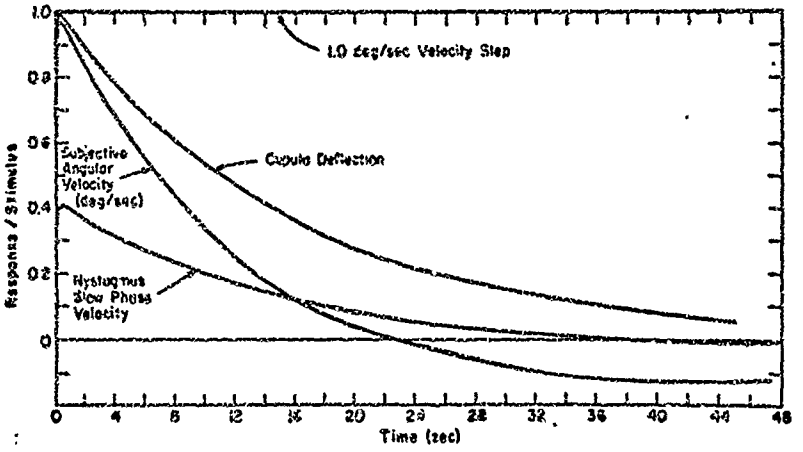


Figure A–3. Velocity step response of MIT semicircular canal linearized model to 1.0 deg/sec velocity step. (Young & Oman, 1969)

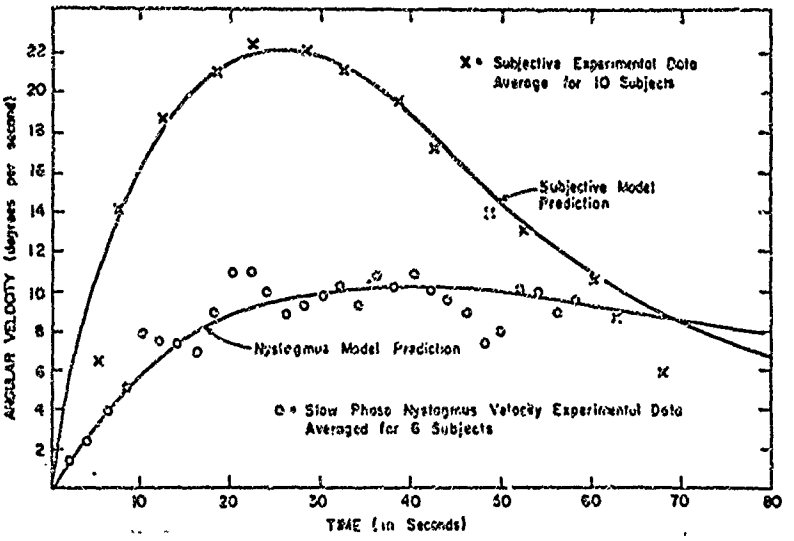


Figure A–4. Comparison of adaptation model for vestibular response with Guedry and Lauver (1961) experiments for an angular acceleration step (1.5 deg/sec2). (Young & Oman, 1969)

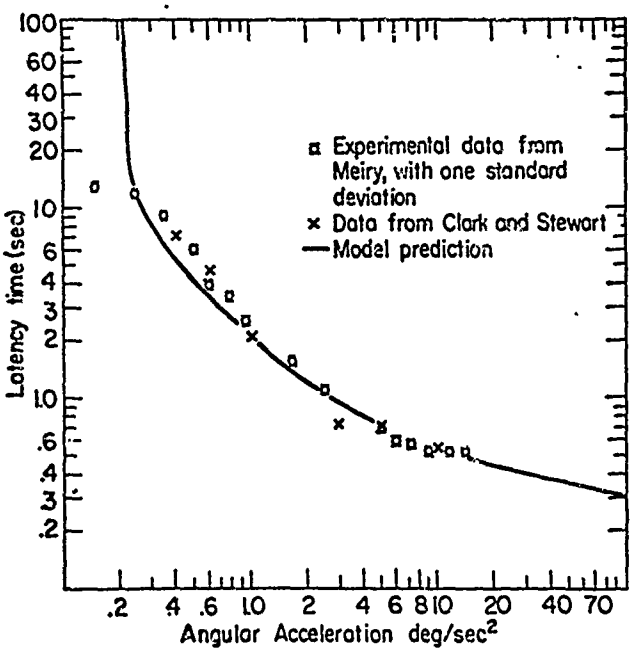


Figure A–5. Adaptation model for subjective response latency to constant angular acceleration. (Young & Oman, 1969)

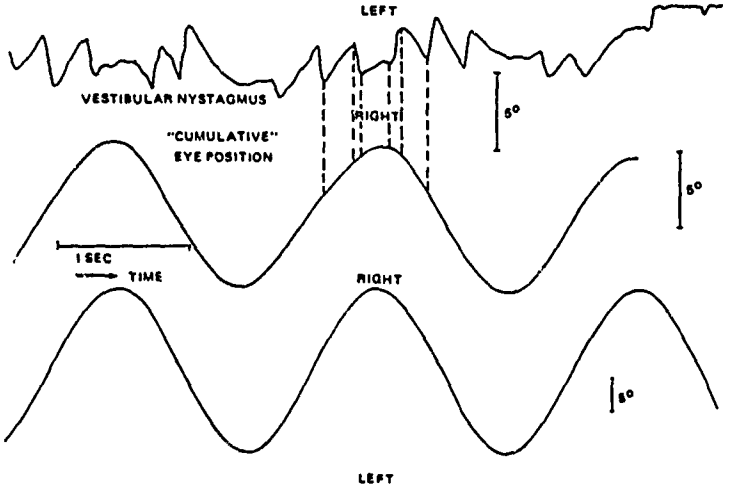


Figure A–6. Vestibular nystagmus and "cumulative" eye position ($f = 0.5$ Hz). Note correspondence of slow phase vestibular nystagmus and "cumulative" eye position. (Meiry, 1965)

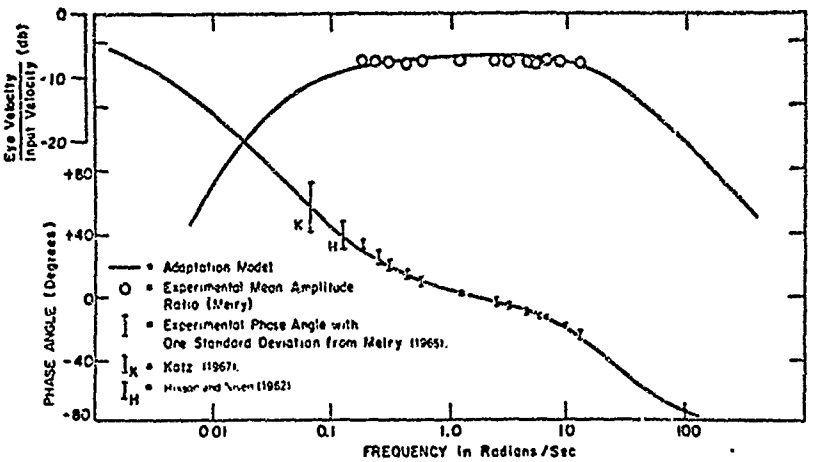


Figure A–7. Frequency response of compensatory eye movements for linearized model: eye velocity/input velocity = $10.5s^2/(s+-25)(s+.0625)(s+.008)$. (Young & Oman, 1969)

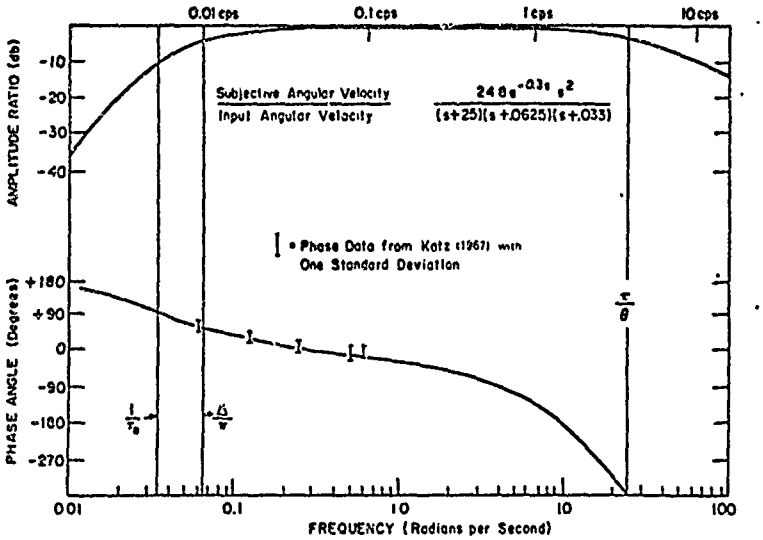


Figure A–8. Frequency response of adaptation model for subjective sensation. (Young & Oman, 1969)

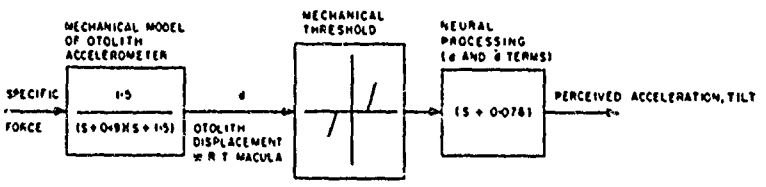


Figure A–9. Revised nonlinear otolith model. (Young, 1969)

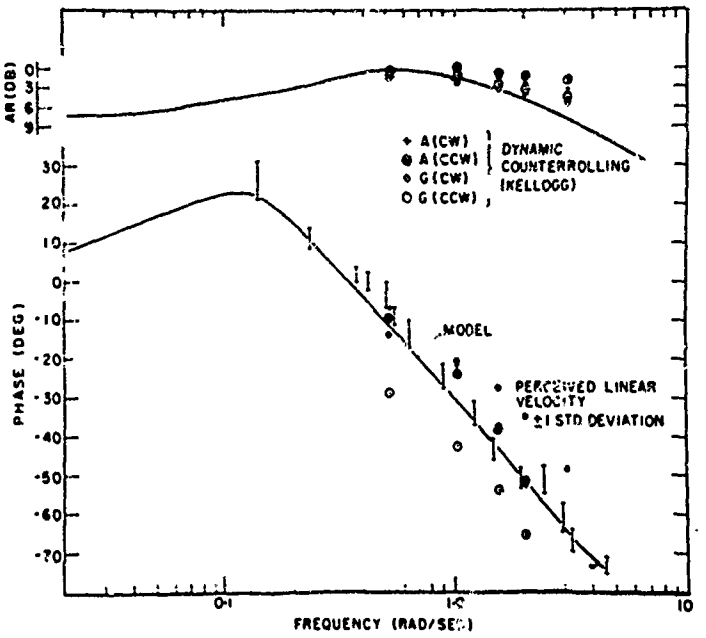


Figure A–10. Perceived velocity frequency response. (Young, 1969)

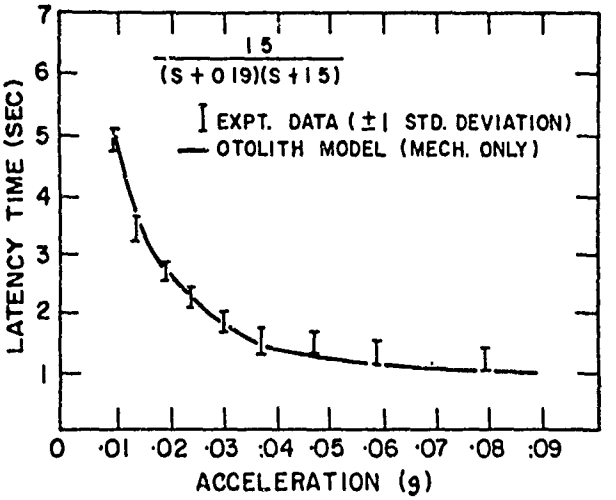


Figure A–11. Time for perception of constant linear acceleration—model and experiment. (Young, 1969)

Cross-coupling between linear and angular sensors has also been a subject of input-output modeling. A preliminary structure of this cross-coupling is shown in figure A-12 (Young, 1969) in which linear acceleration affects nystagmus

both through modification of semicircular canal nystagmus and through "L nystagmus" based on otolith stimulation. Numerous examples of "barbeque spit" nystagmus have been observed, both by constant angular velocity rotation about a longitudinal horizontal axis and by counterrotating a subject on a centrifuge. In each case the "steady state" angular acceleration at the semicircular canals is zero, and yet a consistent nystagmus pattern persists. The nystagmus contains both a bias (steady level) component and a sinusoidal component with period equal to that of the rotation. The sensitivity of this bias and sinusoidal component (as well as the predication of Steer's "roller pump" model) is shown in figure A-13 (Young, 1969).

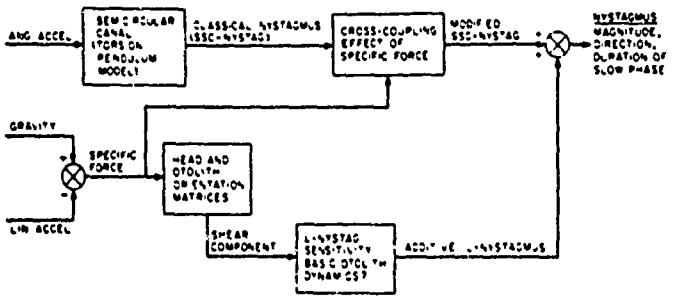


Figure A–12. Preliminary structure–model of influence of linear acceleration on nystagmus. (Young, 1969)

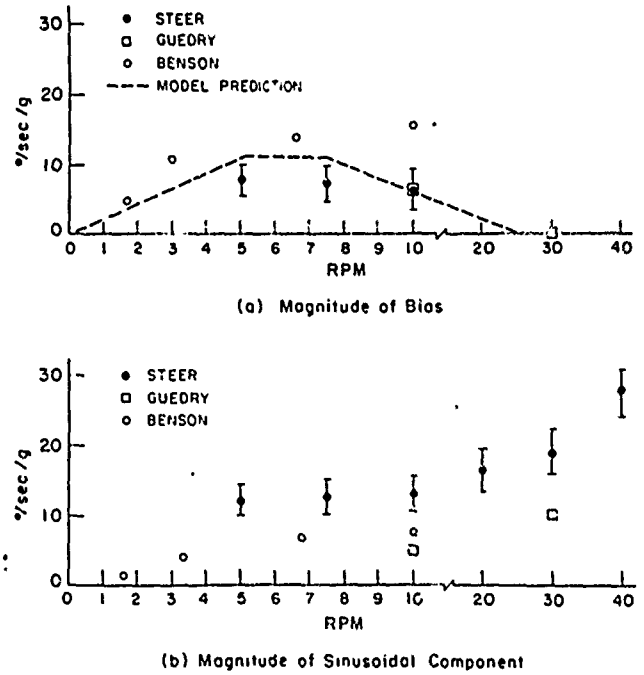


Figure A–13. Summary of available data of normalized bias and sinusoidal amplitude of vestibular nystagmus fromrotationin a 1-g field (L-nystagmus). (Young, 1969)

An overall summary diagram of the vestibular model is given in figure A-14 (Young, 1969).

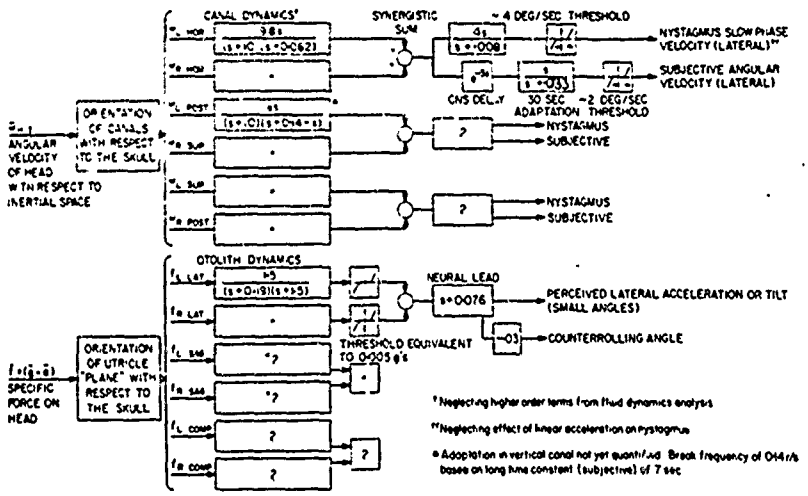


Figure A–14. Summary diagram. Biocybernetic model of vestibular system. (Young, 1969)

References

Benson, A.S. Modification of per-and post-rotational responses by the concomitant linear acceleration. In *Second symposium on the role of the vestibular organs in space exploration.* NASA SP-115. Washington ,D.C.: U.S. Government Printing Office, 1966. Pp. *199-211.*

Clark, B., & Stewart, J.D. Perception of angular acceleration about the yaw axis of a flight simulator. *Aerospace Medicine,* 1962, *33,* 1426-1432.

Guedry, F.E. Influence of linear and angular acceleration on nystagmus. In *Second symposium on the role of the vestibular organs in space exploration.* NASA SP-115. Washington, D.C.: U.S. Government Printing Officer, 1966. Pp. 185-196.

Guedry, F.E., & Lauver, L.S. Vestibular reactions during prolonged constant angular acceleration. *Journal of Applied Physiology,* 1961, *16,* 215-220.

Hixson, W.C., & Niven, J. I. Frequency response of the human semicircular canals. II. Nystagmus phase shift as a measure of nonlinearities. NSAM-830. Naval School of Aviation Medicine, Pensacola, Fla., 1962.

Katz, G.B. Perception of rotation–Nystagmus and subjective response at low frequency stimulation. S.M. Thesis. Massachusetts Institute of Technology, Cambridge, Mass., 1967.

Meiry, J.L. The vestibular system and human dynamic space orientation. T-65-1. Massachusetts Institute of Technology, Cambridge, Mass., 1965.

Steer, R.W., Jr. The influence of angular and linear acceleration and thermal stimulation on the human semicircular canal. MVT-67-3. Massachusetts Institute of Technology, Cambridge, Mass., 1967.

Steer, R.W., Jr. Response of semicircular canals to constant rotation in a linear acceleration field. In *Fourth symposium on the role of the vestibular organs in space exploration.* NASA SP-187. Washington, D.C.: U.S. Government Printing Office, 1966. Pp. 353-360.

van Egmond, A.A.J., Groen, J.J., & Yongkees, L.W.B. The mechanics of the semi-circular canal. *Journal of Physiology*, London, 1949, *110*, 1-17.

Young, L.R. The current status of vestibular models. *Automatica*, 1969, *5*, 369-383.

Young, L.R., & Oman, C.M., Model for vestibular adaptation to horizontal rotation. *Aerospace Medicine*, 1969, *40*, 1076-1080.

APPENDIX B

Design Criteria for Rotating Space Vehicles*

Mathematical expressions for the unique static and dynamic characteristics (and associated derivatives) in rotating environments are listed in table B-1. Certain aspects of man's performances are influenced by these characteristics. They are as follows:

Self-locomotion, either walking or climbing, and material handling are, of course elements of gross motor performance; other gross motor performances of concern are force and torque applications. Fine motor performance involves dexterity and eye-hand coordination involving head motions. Postural balance may be influenced by reduced gravity and the Coriolis forces acting due to body motions necessary in the act of balancing or moving. Transition from artificial gravity to zero gravity and return, as may be required in space base operations, can possibly degrade performance because of developed adaptations to either condition. Passive radial locomotion, as with an elevator on a space base, may be influenced by the Coriolis forces involved, dependent on the rate of elevator movement. In addition, the potential rapid onset of g when increasing radius could have an acute influence on orthosatic tolerance as any rapid onset of g might. Work-rest cycles involve the time lines of general and specific performance and the energies involved for performance, and could influence the extent of work and rest periods.

The remainder of this material involves the considered influence of the unique characteristics of artificial gravity on specific elements of performance. A number of criteria have been suggested that relate to these characteristics and the potential influence on performance (table B-2). These criteria are used to draw boundaries on plots of the two independent variables of artificial gravity, radius and rate of rotation, and thus depict areas of these variables where acceptable performance may be expected. It must be remembered that these boundaries are currently based on judgment, as little data exist. It is necessary, therefore, to verify the validity of the criteria and to establish appropriate magnitudes for them. The criteria (table B-2) relate to the gravity level, Coriolis forces, gravity gradient, and cross-coupled angular accelerations. The gravity-level criteria are bounded by 1 g and 0.1 g while moving in the vehicle. There is clearly no need to exceed 1 g and 0.1 g is considered a minimum value for adequate traction. The Coriolis forces relate to human or object motion tangentially and radially and with the annoying factor that objects do not fall where expected. The gravity gradient criteria relate to changes of weight of objects when their radical position is changed, to the gradients along the body, and to variations of hydrostatic pressure along the body relative to that on Earth. The cross-coupling angular acceleration criteria relate to the rotation of objects and to the rotation of the human head in the rotating environment.

*The material under this heading was kindly furnished by Mr. R. W. Stone, Jr., NASA Langley Research Center.

Table B–1

Mathematical Expressions of the Characteristics of Artificial Gravity

Characteristic	Mathematical Expression
g level	$a_{cg} = r_{cg}\,\omega_v^2$
g gradient	$da_{cg}/d_r = \omega_v^2 = a_{cg}/r_{cg}$
g ratios	$a_1/a_2 = r_1/r_2$
Object weight change	$\Delta W/W = (r_1 - r_2)/r_2$
Gravity variations along body	$h\left(\omega_v^2\right) = (h/r)\,a_{cg}$
Coriolis acceleration (radial)	$\ddot{x} \cdot \gamma - \underline{r}\left(\omega_1^2 + 2\omega_1\,\omega_v + \omega_v^2\right)$
Coriolis acceleration (tangential)	$\ddot{y} = \underline{2\dot{r}}\left(\omega_1 + \omega_v\right) + r\dot{\omega}_1$
Angular cross coupling	$\dot{\omega}_{h_x} = \dot{\omega}_{h_\phi} - \underline{\omega_v}\left(\omega_{h_\theta} \sin\theta + \omega_{h_\psi} \cos\theta \sin\psi\right)$
	$\dot{\omega}_{h_y} = \dot{\omega}_{h_\theta} - \underline{\omega_v}\left(\omega_{h_\psi} \cos\theta \cos\psi - \omega_{h_\phi} \sin\theta\right)$
	$\dot{\omega}_{h_z} = \dot{\omega}_{h_\psi} + \underline{\omega_v}\left(\omega_{h_\theta} \cos\theta \cos\psi + \omega_{h_\phi} \cos\theta \sin\psi\right)$
Hydrostatic pressure variation	$P_{Hs} = \rho/2\left(r_2^2 - r_1^2\right)\omega_v^2$
Distance objects fall from expected position	$d = r_F\left(\sqrt{r_F^2 - r_1^2/r_1} - \tan^{-1}\left(\sqrt{r_F^2 - r_1^2/r_1}\right)\right)$

Table B–2
Potential Criteria for Artificial Gravity

Gravity Level

$$32.2 \geq r\omega_1^2 + 2r\omega_1\omega_v + r\omega_v^2 \geq 3.22$$

Coriolis Forces

Tangential movement	$(1 + C_1)\, r\omega_v^2 \geq r\omega_1^2 \pm 2r\omega_1\omega_v + r\omega_v^2 \geq (1 - C_1)\, r\omega_v^2$
Radial movement	$2r/r\omega_v \leq C_2$
Dropped objects	$r\sqrt{r^2 - r_1^2}/r_1 - \tan^{-1}\sqrt{r^2 - r_1^2}/r_1 \leq C_3$

Gravity Gradient

Change in object weight	$(r - r_1)/r \leq C_4$
Along body	$(r - r_h)/r \leq C_5$
Hydrostatic pressure	$(r_{heart} + r_h)/(r + r_h) \geq C_6$

Cross-Coupled Angular Accelerations

$$\omega_v \leq C_7/\omega_1$$

$$\omega_v \leq C_8/\omega_h$$

Figure B-1 is a graphic representation of the influence of these characteristics on man moving within a rotating spacecraft. There is radical movement toward and away from the center of rotation with the tangential components of Coriolis forces acting. There is tangential movement with and against the direction of rotation with alterations in the radial forces (weight) shown. Axial motion causes no Coriolis forces except for those created by lateral movement of limbs or lateral body sway. The least influence of the characteristics of artificial gravity on human mobility probably occurs during axial motion.

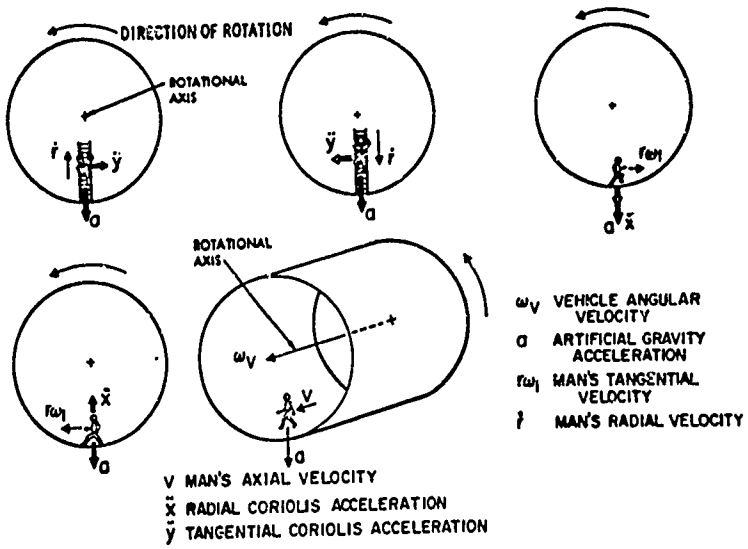


Figure B–1. Graphical representation of influence of artificial gravity on self-mobility.

Figure B-2 shows four boundaries expected to influence walking on the floors of rotating vehicles. The 1 g limit is one below which, when walking at 3 ft/sec, the body will never exceed 1 g. Below the leg weight boundary, the feet, when walking at 3 ft/sec, will not exceed 1 g. Above the 0.1 g traction limit, traction is expected to be adequate. The fourth boundary, $\Delta W/W$, often referred to as the ratio of Coriolis force to artificial weight, is one above which, when walking 3 ft/sec, the change in weight due to the relative motion will not exceed 0.5 of the artificial weight. Also shown in this figure are data for walking in simulated artificial gravity at nominal values of artificial gravity of 1/6 g, 0.2 g, 0.3 g, and 0.5 g. While walking against the rotation at 1/6 g, traction became difficult which tends to verify the traction boundary. At 0.5 g, while walking with the rotation, subjects complain of leg heaviness, indicating that the boundary for leg heaviness may be somewhat high. Walking at 0.3 g seems to be the most amenable g of those studied. The $\Delta W/W$ boundary has not essentially been established at 0.5. It should be noted that these data were obtained for curved floors having a constant value of radius. Flat floors, depending on the radius, can impose difficulties not indicated on this figure.

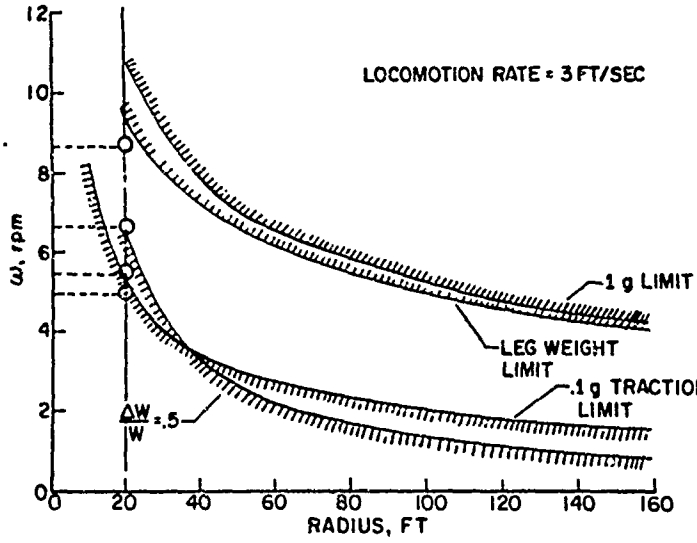


Figure B–2. Rate of rotation and radium boundaries for acceptable tangential self-locomotion in artificial gravity. Boundaries are for speed of locomotion of 3 ft/sec.

Figure B-3 shows two boundaries for radial motion of the astronaut, as when climbing toward or away from the center of rotation, one for which the Coriolis forces due to 2 ft/sec radial motion does not exceed 0.30 the artificial weight, and the other where it does not exceed 0.30 the Earth weight. There are no data to support either criteria or the magnitude of 0.30. As these are forces not supported by the legs, the boundary that relates to Earth weight may have significance. Clearly, studies to establish proper values are needed.

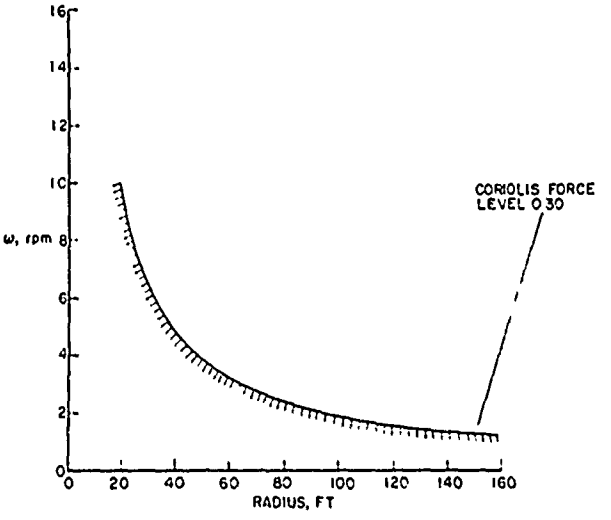


Figure B–3. Rate of rotation and radius boundaries for acceptable self-locomotion in artificial gravity. Boundaries are for a speed of locomotion of 2 ft/sec.

Figure B-4 shows boundaries for material handling. Three boundaries are shown: one for tangential movement above which the change in weight due to 4 ft/sec of motion will not exceed 0.25 of the artificial weight; a second for radial motion where the tangential Coriolis forces do not exceed 0.25 of the artificial weight; beyond the third boundary, the weight of an object when raised 6 feet does not decrease below 0.50 of its original artificial weight. A fourth possible boundary is not shown but would relate to the rotation of an object out of the plane of rotation. It has been assumed that a torque caused by angular cross-coupling probably can be 0.50 of the applied torque. Rate of vehicle rotation for this value could be rather large, greater than 10 rpm. Research to establish the validity of any of these criteria and proper magnitudes for them are required.

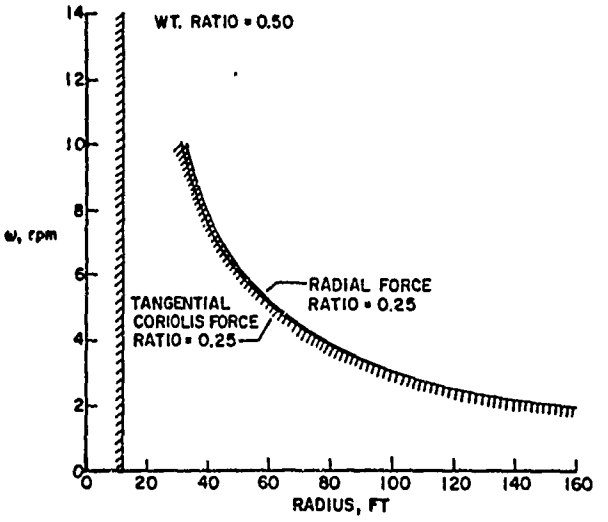


Figure B–4. Rate of rotation and radius boundaries for acceptable material handling in artificial gravity. Boundaries are for speed of material movement of 4 ft/sec.

Figure B-5 relates to boundaries for postural balance. The first is a static boundary or neutral stability, beyond which the vestibular mechanism would sense falling before an unbalance angle for a stationary man would be exceeded. It is felt that this is not a significant boundary for normal man. Two dynamic boundaries are shown, one for the vertical motions and the other for lateral motions present when walking. In both instances, these could have more critical influence when walking axially as the unusual Coriolis accelerations would act in a lateral direction about which man is least stable. When man is walking tangentially, the accelerations act in the saggital plane. It is assumed that these Coriolis accelerations should not exceed 0.25 of the artificial weight.

Figure B-6 is a plot that relates angular head motions and vehicle rate of rotation. The stimulus that causes disturbances in a rotating environment is the cross-coupling that exists between these two angular velocities. The product of these two values gives the maximum stimulus from cross-coupled angular

acceleration. Shown on this figure are curves of constant values of this cross-coupling, ranging from 0.5 to 4.0 rad/sec^2. Based on current experience, a value of this cross-coupling of 2.0 rad/sec^2 (deg/sec^2) seems to be a conservative tolerance criterion. A range of rapid head motions possible for man is from 2.5 to 3.5 rad/sec (140 deg/sec to 200 deg/sec). Vehicle rpm boundaries of 4 (a conservative value), 6 (a nominally acceptable value), and 10 (a tolerable value) are shown. Generally, of course, adaptation is required to attain continued exposure to such rotation.

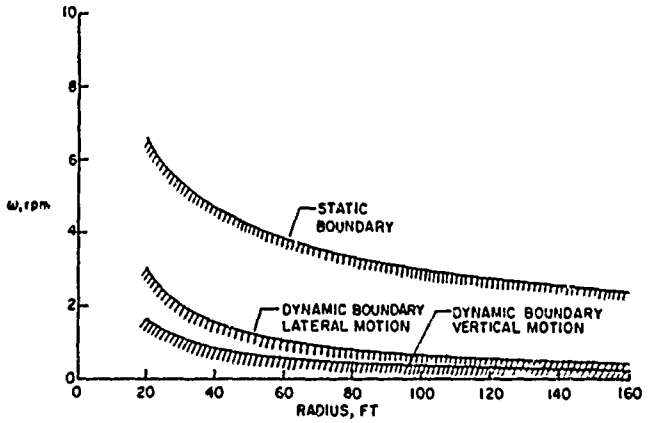


Figure B–5. Rate of rotation versus radius boundaries for acceptable postural balance in artificial gravity.

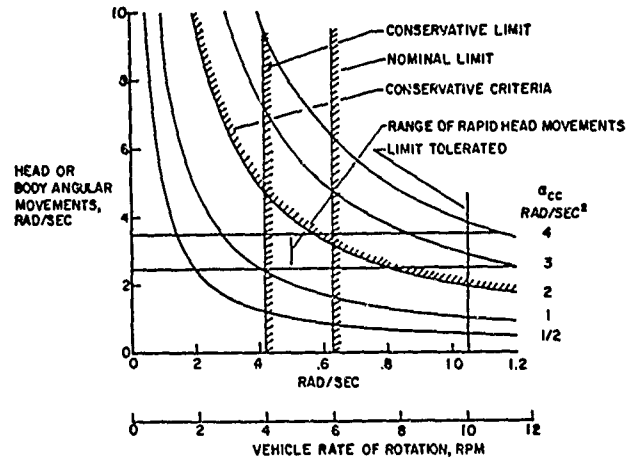


Figure B–6. Possible criteria for acceptability of cross-coupled angular accelerations in vehicles with artitifial gravity.

Figure B-7 is a compilation of all the previous boundaries shown, superimposed on plots of artificial gravity. The area encompassed by all

boundaries shows a minimum radius between 50 and 55 feet. The material handling boundaries are the critical elements. These boundaries are, of course, not well established and must be validated numerically and for analytical form by experiments. If these are not valid, a much smaller radius may be possible. It must be noted, of course, that all other boundaries require similar verification. The Coriolis force to artificial gravity ratio (W/W), which is plotted as 0.5 on this figure, has often been considered to have a maximum desirable value of 0.25. Such a value would impose a radius of the order of 50 feet, as has been noted previously.

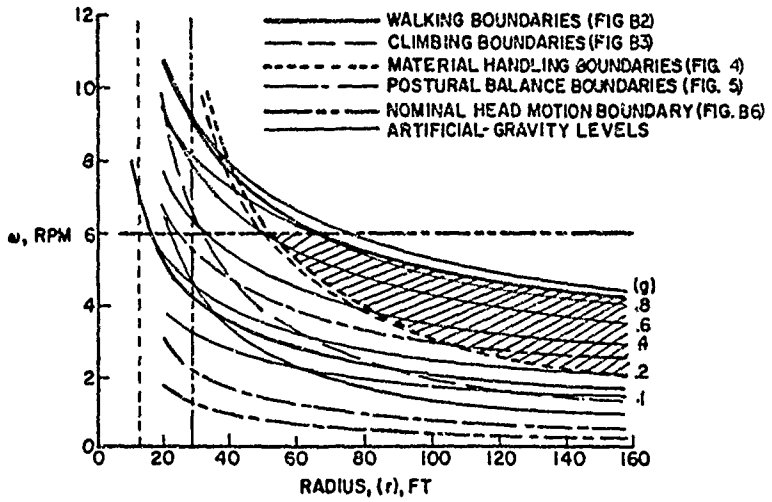


Figure B–7. Compilation of boundaries for acceptable human performance in artificial gravity.

Figure B-8 is a log plot based on the material in Figure B-7.

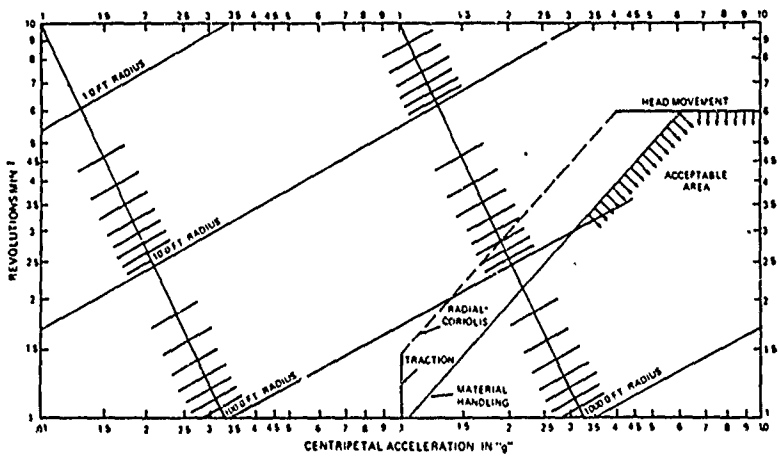


Figure B–8. Log plot of material in figure B-7. (Courtesy of D. B. Cramer)

SYMBOLS

a	acceleration, feet per second squared
α	angular acceleration, rad/sec
r	radius, feet
ω	rate of rotation, radians per second
W	artificial weight, pounds
ΔW	change in artificial weight due to radius change or relative velocity, pounds
g	acceleration of Earth's gravity
h	distance or height along body, feet
x	instantaneous radial distance, feet
y	instantaneous tangential distance, feet
θ, ϕ, ψ	Euler angles, radians
P_{Hs}	hydrostatic pressure pounds per square foot
d	tangential distance, feet

Subscripts

cg	center of gravity
v	vehicle
1 and 2	radial positions
1	incremental
h_x, h_y, h_z	head or object relative to inertial space
h_θ, h_ϕ, h_ψ	head or object relative to vehicle axis
F	floor
cc	cross coupling
	Dot represents the first derivation with respect to time
	Double dot represents the second derivation with respect to time

CHAPTER 13
VISION

by

John H. Taylor, Ph.D.
Scripps Institution of
Oceanography

The extreme importance of the human visual system in ordinary life is obvious, and the necessity for an intact functional visual apparatus in the performance of ever more critical tasks when man and machine must interact has become increasingly evident. Man is no longer a mere passenger aboard a space vehicle—he is an active element in the system, able to perform intricate tasks, to make scientific observations, to exercise judgment, and to modify the course of a mission. The most important sensory input which he requires for nearly all such activity is visual, and it is therefore imperative that every phase of operation in space be considered in regard to the optimization, maintenance, and protection of man's vision.

This chapter presents some of the facts of human vision which are believed to be important in present and projected space activities. Even though it is limited to the case of normal or superior visual capabilities, as may be assumed to pertain to the astronaut group, the information is necessarily sketchy. For this reason, and because new data are always becoming available, it is to be hoped that the reader will seek supplementary information in the current literature.

Units and Definitions

The quantitative description of the visual process requires a set of meaningful units, and because of the nonlinearity of the eye as receiver, these units differ from the units of physics in that they reflect the properties of the underlying physiological and psychophysical mechanisms of vision. Radiant energy in the band of electromagnetic wavelengths between about 380 and 750 nanometers is capable of stimulating the eye, and that

Reviewed by John Lott Brown, Ph.D., University of Rochester.

Preceding page blank

which does so is called light. While the measurement of radiant energy in general is called radiometry, the measurement of light is called photometry, and photometric units are based upon the potential of light for stimulating vision. An adequate discussion of the relationship between radiometric and photometric concepts and quantities is beyond the scope of this chapter, and the reader should consult one or more of the available contemporary references (Walsh, 1958; Kaufman, 1966; Meyer-Arendt, 1968). Some of the units most frequently used are shown in table 13-1. The function which relates radiometric quantities to their photometric counterparts is called the luminous efficiency curve, and is shown in figure 13-1. This curve is, in fact, the spectral sensitivity function for the eye at high energy levels, and the photometric units which depend upon it are rigorously appropriate only to the case of daylight vision. It will be seen later that the maximum of the curve is shifted toward the shorter wavelengths as light levels drop, and that for night vision the peak has moved from its daylight position at 555 nanometers (nm) down to 505 nm. There have been efforts to establish photometric units which apply to the low-level case (scotopic, as opposed to photopic vision), but for most purposes the units based on the data of figure 13-1 continue to be used. A notable exception occurs in the treatment of colored stimuli at low levels, where the correction is absolutely mandatory.

Most of the data provided in this chapter are expressed in terms either of luminance or of a kind of ratio of luminances called contrast. Luminance is the photometric term corresponding to radiance, and refers to the amount of visible light coming from an extended surface which is illuminated or self-luminous. In the former (much more usual) case it is the product of the illuminance falling on the surface and the luminous reflectance of the surface, and will generally be dependent on the lighting and viewing geometries. There are many units of luminance which have been used from time to time, and the present trend is to reduce their number to a single unit in the M.K.S. system; the candela per square meter ($cd \cdot m^{-2}$), or nit. But almost none of the data of vision are reported in terms of nits, and it is safe to say that almost none of the engineers who deal with light are yet able to visualize a luminance of, say, 10 $cd \cdot m^{-2}$. By far the most used and most familiar units of luminance, at least in English-speaking countries, are the foot-lambert (ft-L) and the millilambert (mL). These two quantities are close enough in magnitude (1 ft-L = 1.076 mL) so that they may be considered equal in most engineering applications, and these are the units which will be used here. Interconversions between some of the more common luminance units and illuminance may be accomplished by use of the values in tables 13-2 and 13-3. Other units and concepts will be defined as needed in the text.

Concept of the Threshold

The quantitative description of visual performance is usually made in terms of that useful construct called the threshold. Simply put, the threshold is some value of stimulus magnitude, or interstimulus difference,

Table 13–1

Radiometric and Photometric Terms, Symbols, and Units

Physical			Psychophysical		
Radiator (source of radiant energy) Radiation (process)			Luminator (source of luminous energy) Lumination (process)		
Radiometry	Symbol	M.K.S. Units	Photometry	Symbol	M.K.S. Units
Radiant energy	U	joule	Luminous energy	Q	talbot
Radiant density	u	joule/m^3	Luminous density	q	talbot/m^3
Radiant flux	P	watt	Luminous flux	F	lumen
Radiant emittance	W	watt/m^2	Luminous emittance	L	lumen/m^2
Radiant intensity	J	watt/ω	Luminous intensity	I	lumen/ω(candle)
Radiance	N	watt/ω X m^2	Luminance	B	lumen/ω X m^{2*}
Irradiance	H	watt/m^2	Illuminance	E	lumen/m^2 (lux)
Spectral reflectance	ρ		Luminous reflectance	r	
Spectral transmittance	τ		Luminous transmittance	t	

Ratio of photometric quantity to corresponding radiometric quantity (standard units) = luminosity, K (luminous efficiency, lumens/watt) of radiant energy involved.

*cd m^{-2}.

(From Biberman et al., 1966)

to which an observer responds with some selected probability. The general case is suggested by figure 13-2. As the magnitude of the stimulus is increased from low values where seeing never occurs to high values where seeing is essentially certain, the curve of point probabilities rises in an ogival fashion. Since the inflection of the curve (which is commonly believed to be a normal Gaussian integral) occurs at a probability level of 0.50, this value is usually selected for reasons of statistical precision, and the value of stimulus magnitude which elicits the response 50 percent of the time is called the threshold.

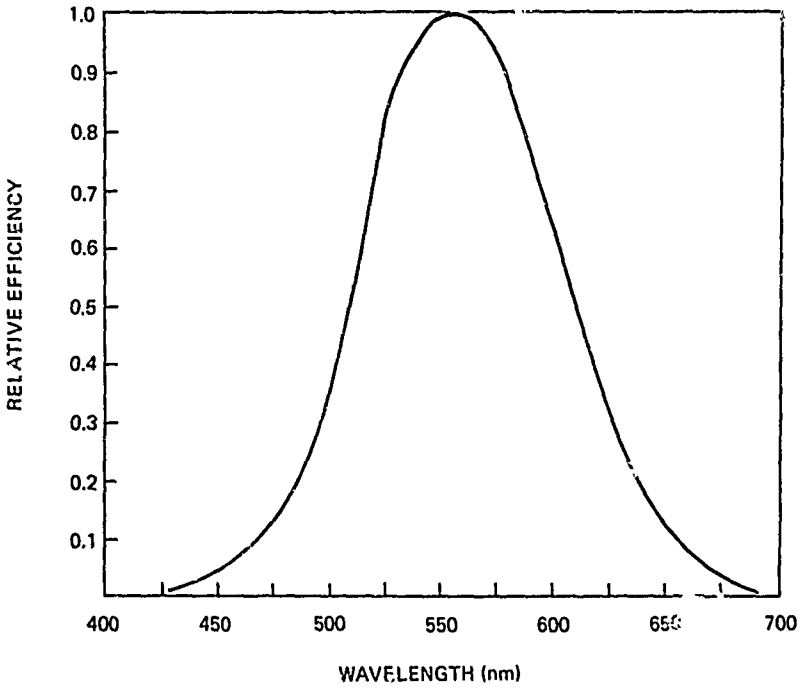


Figure 13–1. Spectral sensitivity of the human eye for daylight conditions.

In most engineering applications, of course, one is concerned with performance levels other than 50 percent—usually with such probabilities as 0.95 or 0.99 or even higher. Conversion to probabilities other than 0.50 can be made with confidence in some cases; the degree of risk depends heavily upon the manner in which the basic data were collected. Useful approximations can be made, for example, in the data for contrast discrimination and visual acuity, where doubling the value of threshold at P = 0.5 yields magnitudes where P is close to 1.0.

Visibility

The term visibility has been used in a number of ways; by meteorologists in evaluating seeing conditions in the atmosphere, by airframe

Table 13–2

Conversion Factors for Units of Luminance

Number of Multiplied by Equals Number of	cd/m^2 (nit)*	cd/cm^2 (stilb)	cd/ft^2	cd/in^2	apostilb (blondel)	millilambert	foot-lambert
cd/m^2 (nit)*	1	10 000	10.764	1550	0.3183	3.183	3.426
cd/cm^2 (stilb)	0.0001	1	0.001076	0.155	0.00003183	0.0003183	0.0003426
cd/ft^2	0.0929	929	1	144	0.02957	0.2957	0.3183
cd/in^2	0.000645	6.452	0.00694	1	0.0002054	0.002054	0.002211
apostilb (blondel)	3.1416	31 416	33.82	4869	1	10	10.764
millilambert	0.31416	3 141.6	3.382	486.9	0.1	1	1.0764
foot-lambert	0.2919	2919	3.1416	452.4	0.0929	0.929	1

*The name "nit" is not in widespread use.

designers to describe a pilot's field of view, and others. Used in its more technical sense, visibility refers to the total process of seeing and thus reflects the interaction between man's visual apparatus and his physical environment. The description of visibility, therefore, requires data which relate to the properties of the visual stimulus (usually an object seen against a background, illuminated in a specific way), the optical transmission properties of the path of sight (whether it be air, or water, or through an intervening element such as a window or an optical device), and to the visual performance capabilities of the observer. A general treatment of the topic may be found in the papers by Duntley et al. (1964). By and large the solution of problems of visibility of greatest interest has been laborious and slow. Recent developments by the University of California's Visibility Laboratory are leading to the use of high-speed computers which are able to cope with the tremendous numbers of interactions between the dozen or more variables which must be taken into account.

Table 13–3

Conversion Factors for Units of Illuminance

Number of Multiplied by Equals Number of ↓	Foot-candles	lm/m^2 (lux)*	Phot	Millilphot
Foot-candles	1	0.0929	929	0.929
lm/m^2 (lux)*	10.764	1	10 000	10
Phot	0.00108	0.0001	1	0.001
Milliphot	1.076	0.1	1000	1

*The symbol for lux is lx.

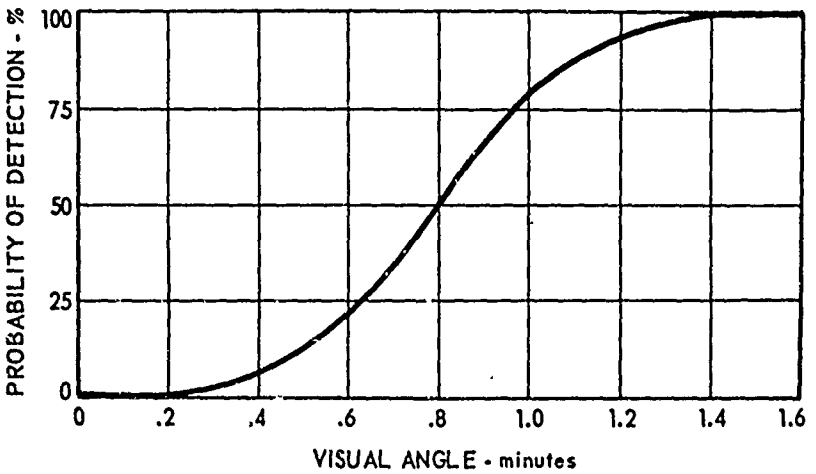


Figure 13–2. General case of a response curve used to define "threshold." (From the *Human factors in air transport design* by R. A. McFarland. Copyright 1946 by The McGraw-Hill Book Company. Used by their permission)

The Visual Environment

Earthbound man's visual environment has been determined by the quantity and quality of natural and artificial illuminations available to him, and by the reflectance characteristics of materials present in his world. His visual system has evolved in such a way that he enjoys useful vision over a range of more than ten million to one in natural illumination, by means of a relatively narrow band of wavelengths in the electromagnetic spectrum. The great range of luminances over which the human visual system can function is shown in table 13-4.

Natural illumination reaching the Earth's surface depends upon solar altitude, lunar altitude and phase angle, and cloud cover. An extensive study by Brown (1952) is summarized in figure 13-3. The original reference should be consulted for large scale plots relating to different latitudes and declinations, which show illumination as a function of local apparent time. A more conveniently-sized and readily obtainable version of Brown's charts may be found in Biberman et al. (1966).

The inherent luminance of objects in the visual field depends upon the intensity of the illumination and the reflectance of the objects, each having directional properties. Contrast between object and background will be governed by the same quantities in the case of palpable backgrounds, or by background luminance alone in the case of objects of fixed luminance seen against the sky. The optical properties of objects and backgrounds have been discussed in detail by Gordon (1964), and the reflectance of many natural terrains has been measured by Krinov (1947). The range of luminances in average outdoor scenes on Earth is about 160:1, although extremes of 27:1 and 760:1 were noted by Jones and Condit (1941). In the special case of self-luminous or specularly reflectant objects being included in the field of view, these ratios can become very much higher.

In space the visual environment will differ significantly from that on Earth. In flight, and on the surface of celestial bodies without atmospheres, natural illumination will come from the sun, planets, stars, planetary satellites, galactic light, and the zodiacal light. The lunar surface normal to the sun's rays receives (as does the top of the Earth's atmosphere) about 12 700 foot-candles (ft-c) of solar illumination. But in the absence of atmospheric scattering, this highly directional light will produce extremely high contrasts between lunar features in sunlight and those in shadow. The lunar visual environment has been discussed by Taylor (1967), and some of the photometric properties of the moon's surface, measured during the Surveyor program, have been described by Rennilson et al. (1968). Owing to the absence of atmospheric scattering and the generally low reflectance of lunar surface materials, it may be expected that the range of luminances on the moon may extend from about 1000 ft-L for sunlit rock down to about 10^{-6} ft-L for areas in shadow. During lunar night, when both sun and Earth are below the local horizon, the only illumination will come from the space background elements noted above. Thus, in the absence of twilight, airglow and aurorae, illumination in the lunar night will fall considerably below the minimum value shown in figure 13-3 for Earth night, and is estimated to be 10^{-6} ft-c. Average luminance of the nighttime lunar landscape can therefore fall below 10^{-7} ft-L, a level at which the human eye performs as if the luminance were zero.

Table 13–4

Range of Luminance for Visual Performance

Luminance in mL		Object	Notes
1×10^{9}	7×10^{8}	Sun	Viewed from outside earth's atmosphere
	4.4×10^{8}	Sun	Viewed from the earth
1×10^{8}	8×10^{7}	A-Bomb	Fireball 4 miles from point of detonation of an 800 KT weapon.
1×10^{7}			
1×10^{6}			
1×10^{5}			
	1.58×10^{4}	Venus	Assume albedo (r) of 0.59 viewed from outside atmosphere
	9.4×10^{3}	Earth	Viewed from space with cloud cover (r = 0.8)
1×10^{4}	6.4×10^{3}	Mercury	Viewed from outside atmosphere (r = 0.069)
	4.3×10^{3}	Earth	Viewed in January from outside atmosphere, no clouds (r = 0.39)
	2.8×10^{3}	Jupiter	Viewed from outside atmosphere (r = 0.56)
	2×10^{3}	Sky	Average sky on clear day
	1.2×10^{3}	Moon	Full moon viewed from outside of atmosphere (r = 0.073)
1×10^{3}	9.6×10^{2}	Saturn	Viewed from outside atmosphere (r = 0.63)
	9×10^{2}	Mars	Viewed from outside atmosphere (r = 0.15)
	8×10^{2}	Moon	Full moon viewed from earth
	5×10^{2}	Sky	Average sky on cloudy day
	2.4×10^{2}	Uranus	Viewed from outside the earth (r = 0.63)
1×10^{2}	1.1×10^{2}	Neptune	Viewed from outside atmosphere (r = 0.73)
	2×10^{1}	White paper in good reading light	
	1.6×10^{1}	Movie screen (indoors)	
1×10	1×10^{1}	TV screen	
	7×10^{0}	Pluto	Viewed from outside the atmosphere
1×10^{0}	8×10^{-1}	Snow in light of full moon	
1×10^{-1}			
	2×10^{-2}	Lower limit for useful color vision	
1×10^{-2}	7.5×10^{-3}	Earth	Viewed from outside atmosphere with full moon
	1×10^{-3}	Upper limit for night vision	
1×10^{-3}			

Table 13–4 (Continued)
Range of Luminance for Visual Performance

1×10^{-4}			
	3×10^{-5}	Earth	Viewed from outside atmosphere at night with airglow, starlight, and zodiacal light providing illumination
	1×10^{-3}	Absolute threshold for dark adapted human eye, lower limit for night vision	
1×10^{-5}			
5×10^{-6}	1×10^{-5}	Sky	Moonless nigh. sky viewed from earth
4×10^{-6}			
3×10^{-6}			
2×10^{-6}			
1×10^{-6}	1×10^{-6}	Space background	Background luminance formed by starlight, zodiacal and galactic light.

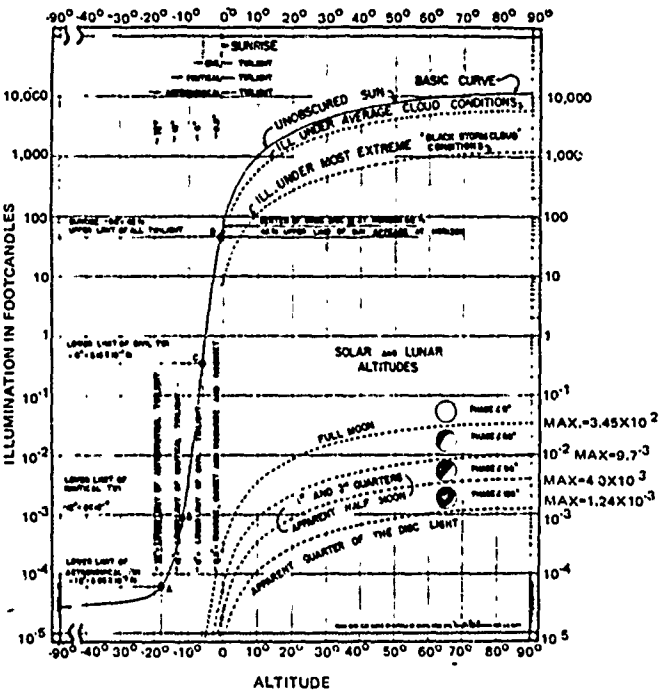


Figure 13–3. The range of natural illumination falling on the surface of the Earth. (Brown, 1952)

Between these extreme values of sunlit lunar day and Earthless lunar night, illumination on the moon is due to light from the Earth. The maximum value occurs with the full Earth at the zenith, which will provide approximately 10 ft-c—with minor variations caused by rotation and differences in cloud cover As Earth's phase angle increases from zero (full) to 180° (dark), illumination levels will drop in conformity with the curve shown in figure 13-4 which refers to the case of the Earth at the zenith.

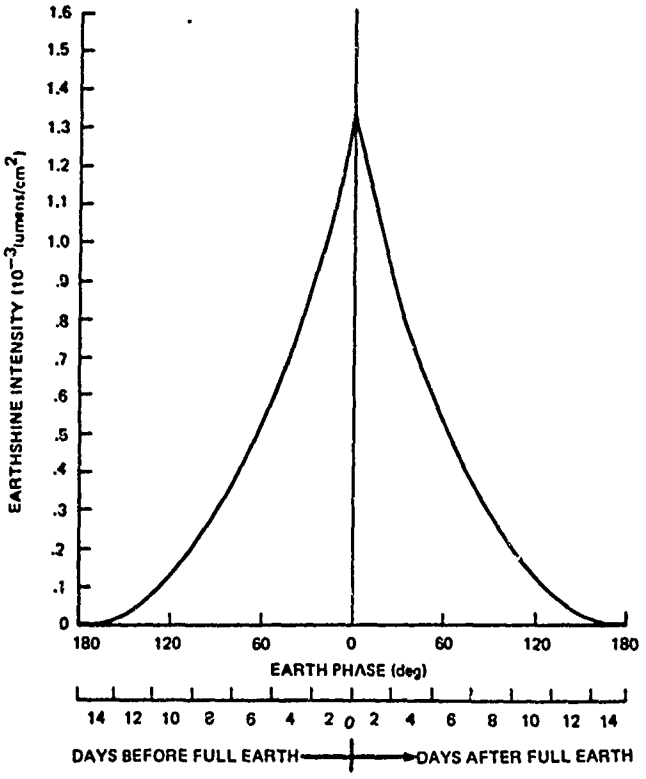


Figure 13–4. Earthshine intensity on the moon as a function of Earth phase. (Jones, 1967; taken from Koval, 1964)

Variations in illumination due to altitude of the Earth in the lunar sky may be expected to follow the cosine law of illumination very closely. A more detailed consideration of the lunar visual environment is given by Jones (1967) and by Kuiper (1954). The report of Shoemaker et al. (1967) indicates that there are only minor local color differences to be found in the lunar surface materials, at least for the local Surveyor regions. Earthshine is somewhat variable in color, but is predominantly bluish.

Farther out in space, in interplanetary travel and planetary surface exploration, the visual environment will be determined by distance from the sun, the properties of planetary atmospheres, the presence of natural satellites, and the character of the planetary materials. Solar illumination will vary with the square of the distance, so that average values may be summarized (for the normal plane) as indicated in table 13-5.

The values in the table refer to illumination at the top of the planet's atmosphere, if present, and vary with distance from the sun. Conditions within and beneath the atmospheres will depend upon the characteristics of the planetary aerosols. At present only scant data exist; the cloud cover enshrouding Venus, as well as Jupiter and Saturn, precludes measurement except by remote

probes. Koval (1964) has summarized the data for Mars, and considers both its atmosphere and the properties of the Martian surface with its observed seasonal variations.

Table 13–5

Illumination Levels in Space

Planet	Mean Solar Illumination (Foot-Candles)
Mercury	84 600
Venus	24 400
Earth	12 700
Mars	5430
Jupiter	470
Saturn	138
Uranus	34
Pluto	8

The directional luminous reflectances of some selected terrain backgrounds are given in table 13-6. These values not only exemplify the range of luminances, but also their variation with angles of both illumination and path of sight. After correction for transmission losses along appropriate paths of sight, these values may be used in predicting visibility for such activities as reentry (e.g., for the Apollo landmark problem), and the evaluation of Earth resources from earth orbit and other sorts of visual reconnaissance.

Structure of the Visual System

The principal parts of the human eye are shown in figure 13-5 and figure 13-6. Figure 13-5 shows some of the muscles that move the eyeball in its orbit. The superior rectus muscle elevates the front of the eyeball; the lateral rectus muscle pulls the eye to the right (outward). Inferior and medial rectus muscles, not seen in this drawing, balance or oppose these movements. The superior muscle, passing through a pulley, and the opposing inferior oblique, rotate the eyeball, also moving the front surface up or down and laterally. These movements allow the visual image to be consistently aligned on the retina when the head is moved or tilted. Inside the eyeball, the lining of the major cavity behind the lens is the retina, the light-sensitive neural layer (that is detailed diagrammatically in figure 13-7). Arteries and veins to supply this active retinal tissue come through the back of the eyeball with the fibers of the optic nerve, thence to be distributed over the front surface of the retina. Light rays enter the transparent cornea, and in so doing are refracted at the curved interface between air and the tear fluid which bathes the cornea. Most of the optical power of the eye inheres in this initial refraction. After passing through the cornea and the

clear liquid (the aqueous humor) contained in the anterior chamber, the bundle of rays is restricted by a circular variable aperture, the pupil, whose size is changed through action of the muscles of the iris. The rays are further refracted by passage through the lens, traversing the clear, jellylike vitreous humor of the posterior chamber, so that, in a properly focused eye, a sharp image is formed on the retina. Scattering of light within the eye is minimized by a darkly pigmented layer of tissue underlying the retina, called the choroid. The shape of the eye is maintained by reason of its enclosure in an elastic capsule, the sclera, and the fact that the fluids within are maintained at positive pressure.

Figure 13-6 and table 13-7 give dimensions and optical constants of the human eye. Values in brackets shown in the table refer to state of maximum accommodation. The horizontal and vertical diameters of the eyeball are 24.0 and 23.5 mm, respectively. The optic disk, or blind spot, is about 15 degrees to the nasal side of the center of the retina and about 1.5 degrees below the horizontal meridian.

Changes in focus are accomplished by altering the shape of the lens; relaxation of the ciliary muscle results in a thickening of the lens, with a consequent shortening of the focal length so that nearby objects are brought into focus. The action is termed accommodation.

The retina is a thin membrane lining rear of the posterior chamber and containing the light-sensitive cells. These cells are of two functionally discrete types, called rods and cones. Rod cells are the more abundant, there being about 120 million in each eye. They subserve night vision, and are incapable of yielding the information necessary for color discrimination, since they contain a single common photosensitive pigment. Cone cells are both less numerous (6 million or so in each eye) and less sensitive to low levels of luminance. Human cones are of three types, each containing a different photopigment with peak response to a particular part of the visible spectrum. Thus, by differential transmission of nerve impulses upon stimulation, the cones are able to encode information about the spectral content of the image so that the observer experiences the sensation of color.

In addition to the rods and cones, the retina contains other nerve cells of various function. Some of these enable the impulses from many rods to be converged upon relatively few optic nerve fibers; others permit many sorts of excitatory and inhibitory cross-innervations within the retina. Through this arrangement of bipolar cells, ganglion cells, and their various interactions, impulses which arose in the photoreceptors are transmitted to the visual cortex of the brain. A vastly simplified diagram of the retina is shown in figure 13-7. Light must traverse the various layers of cell bodies and synapses before reaching the photosensitive pigments which are contained in the outer segments of the rods and cones. The darkly pigmented choroid serves to absorb unused light and thus to reduce the amount of intraocular scattering. Although there are many more rods (around 125 000 000) than cones (about 6 500 000), the impulses from many rods converge upon relatively few bipolar cells. This convergence is significantly less in the case of the cones, and is one reason for the fact that visual acuity is best at luminance levels high enough to permit adequate cone function, especially in the fovea where only closely-packed cones are found.

Table 13–6

Directional Luminous Reflectance of Terrain

Description	Sun Zenith Angle	Azimuth of the Path of Sight Relative to the Sun	Zenith Angle of Path of Sight 180	165	150	135	120	105	100	95
1. Pine trees, small, uniformly spaced. Data are for unresolved terrain over which atmospheric data given in Sec. VI were collected.	41.5	0	0.0333	0.0241	0.0214	0.0214	0.0261	0 0379	0.0463	0.0859
		45		0.0222	0.0202	0.0194	0.0210	0.0303	0.0387	0 0549
		90		0.0315	0.0311	0.0317	0.0317	0.0337	0 0387	0.0463
		135		0.0335	0 0382	0.0392	0.0387	0.0438	0.0163	0.0572
		180		0.0402	0.0444	0.0578	0.0640	0.0711	0.0758	0.0825
2. Grass, thick, rather long, pale green, dormant, dryish, little ground showing.[a]	41.5	0	0.088	0.081	0.076	0 077	0.088	0.094	0.096	0.094
		180		0 098	0.119	0.146	0.150	0.153	0.153	0.160
3. Asphalt, oily, with dust film blown onto oil.[a]	42.0	0	0.061	0.057	0.058	0.060	0.068	0.090	0.104	0.127
		180		0.067	0.080	0.101	0.090	0.086	0.086	0.088
4. "White" concrete, aged.[a]	42.2	0	0.266	0.263	0.254	0.254	0.266	0.298	0.320	0.374
		180		0.289	0.313	0.343	0.367	0.350	0.343	0.320
5. Calm water, infinite optical depth.[b]	41.5	0	0.0222	0.0234	0.0297		0.0569	0.139	0.267	0.461
		45		0.0230	0.0240	0.0272	0.0357	0.107	0.199	0.325
		90		0.0221	0.0222	0.0234	0.0293	0.0711	0.121	0.214
		135		0.0213	0.0212	0.0220	0.0270	0.0665	0.113	0.203
		180		0.0214	0.0212	0.0216	0.0267	0.0718	0.125	0.254

Table 13–6 (Continued)

Directional Luminous Reflectance of Terrain

Description	Sun Zenith Angle	Azimuth of the Path of Sight Relative to the Sun	Zenith Angle of Path of Sight							
			180	165	150	135	120	105	100	95
6. Grass, lush green, closely mowed thick lawn.[c]	40.4	0	0.100	0.096	0.098	0.108	0.120	0.149	0.168	
	39.6	90		0.103	0.110	0.121	0.138	0.159	0.168	
	39.6	135		0.107	0.125	0.148	0.166	0.178	0.178	
	39.9	180		0.109	0.109	0.119	0.122	0.125	0.125	
7. Macadam, washed off and scrubbed.[c]	48.5	0	0.113	0.115	0.119	0.128	0.148	0.194	0.229	
	60.1	90		0.110	0.109	0.116	0.122	0.139	0.147	
	46.0	180		0.126	0.141	0.156	0.166	0.172	0.176	
8. Dirt, hard packed, yellowish.[c]	53.2	0	0.243	0.230	0.229	0.239	0.252	0.300	0.330	
	56.5	90		0.243	0.258	0.260	0.276	0.300	0.304	
	51.1	180		0.272	0.313	0.370	0.422	0.432	0.434	
9. Mixed green forest, deciduous (oak) and evergreen (pine).[d]	39.0	0	0.0360	0.0325	0.0291	0.0205	0.0205	0.0342		
	37.0	180		0.0410	0.0493	0.0493	0.0820	0.263		
10. Pine forest.[d]	33.5	0	0.0385	0.0385	0.0308	0.0246	0.0246	0.0200		
11. Grass, dry meadow, dense, mid-summer.[c]	45	0	0.0955	0.0897	0.0960	0.0952	0.108	0.129		
	45	90		0.0778	0.0890	0.101	0.111	0.130		
	45	180		0.116	0.131	0.143	0.153	0.170		
	45	270		0.107	0.121	0.134	0.137	0.132		

12. Ilyas, sparse and dry, yellowish grass on sand at end of summer.[a]	40	0	0.231		0.320		0.342	0.356
	40	90			0.163		0.176	0.198
	40	180			0.295		0.353	0.359
	40	270			0.262		0.237	0.229
13. Sand dunes, sharply expressed micro-relief, dry.[c]	40	0	0.288		0.183		0.337	0.353
	40	90			0.284		0.329	0.306
	40	180			0.246		0.259	0.276
	40	270			0.278		0.410	0.281
14. Podsol, ploughed, moist.[d]	50	0	0.0600	0.0680	0.0646		0.0555	
	50	90		0.0662	0.0953	0.0715	0.0614	0.0761
	50	270		0.149	(0.180)[f]	0.168	0.168	(0.189)[f]

[a]These terrains were measured on the ground by means of a goniophotometer.

[b]Computed from equations by Duntley (1952) for the lighting condition prevailing for items 1 and 2 in this table.

[c]Data taken with a goniophotometer, 10 October 1956.

[d]Data taken with a photoelectric telephotometer from a helicopter at 300 ft (91.4-m) altitude, mountain forested area near Julian, California, 23 September 1959.

[e]Luminous directional reflectance for terrains 11 through 14 were computed from spectrophotometric data by Krinov (1947) using C.I.E. Illuminant B. Disparity between data for azimuths 90° and 270° "is explained apparently by the direction of shallow furrows in relation to the sun" (Krinov-Belkov, 1953, P. 75).

[f]Parentheses indicate estimates based on incomplete spectral data.

(From Gordon, 1964)

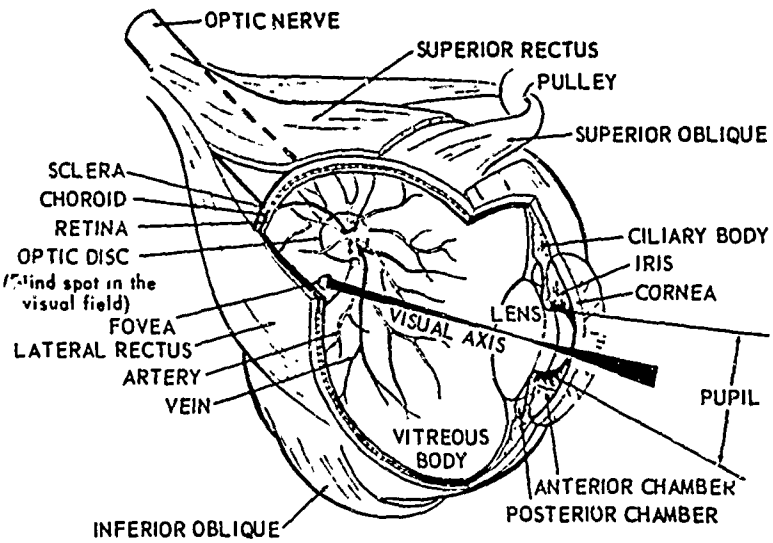


Figure 13–5. Right eye, viewed from outer side, showing visual axis passing through center of lens to point of sharpest vision at fovea, where cones are concentrated. (White, 1964)

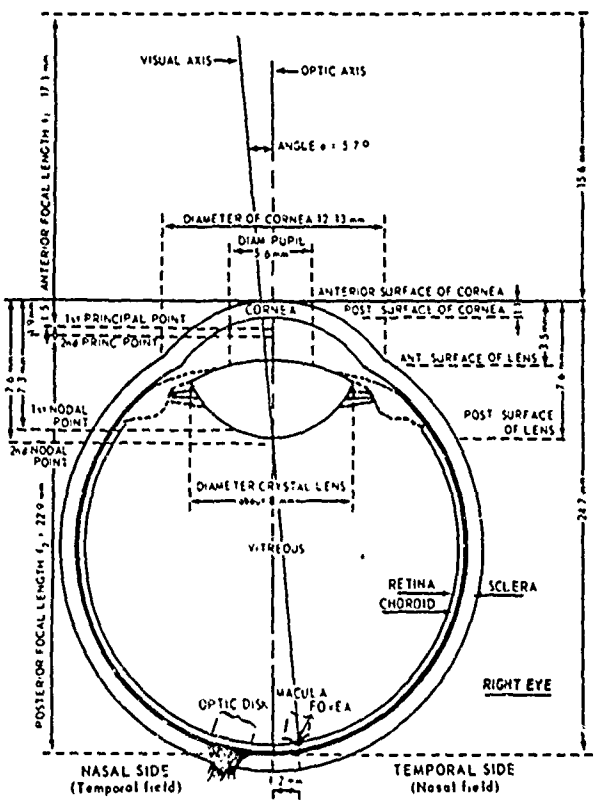


Figure 13–6. Dimensions of the human eye. (Spector, 1956)

Table 13–7
Optical Constants for the Human Eye

Constant	Eye Area or Measurement	
Refractive index	Cornea	1.37
	Aqueous humor	1.33
	Lens capsule	1.38*
	Outer cortex, lens	
	Anterior cortex, lens	
	Posterior cortex, lens	
	Center, lens	1.41
	Calculated total index	1.41
	Vitreous body	1.33
Radius of curvature, mm	Cornea	7.7
	Anterior surface, lens	9.2 - 12.2
	Posterior surface, lens	5.4 - 7.1
Distance from cornea, mm	Posterior surface, cornea	1.2
	Anterior surface, lens	3.5
	Posterior surface, lens	7.6
	Retina	24.8
Focal distance, mm	Anterior focal length	17.1 [14.2] **
	Posterior focal length	22.8 [18.9]
Position of cardinal points measured from corneal surface, mm	1. Focus	−15.7 [−12.4]
	2. Focus	24.4 [21.0]
	1. Principal point	1.5 [1.8]
	2. Principal point	1.9 [2.1]
	1. Nodal point	7.3 [6.5]
	2. Nodal point	7.6 [6.8]
Diameter, mm	Optic disk	2-5
	Macula	1-3
	Fovea	1.5
Depth, mm	Anterior chamber	2.7 - 4.2

*Cortex of lens and its capsule.
**Values in brackets refer to state of maximum accommodation.

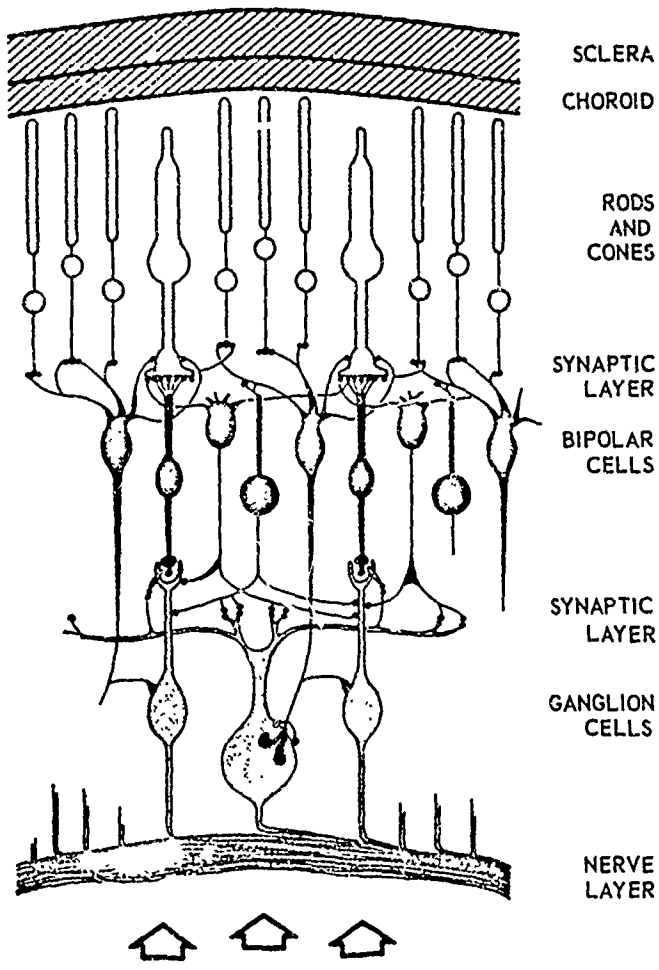


Figure 13–7. Simplified diagram of retina. (White, 1964)

The distribution of rods and cones over the retina is by no means uniform. The cones are most numerous at the center of the visual field, and are most densely packed in the region just at the fixational center. In this small central region, whose diameter is about 0.5 mm or 1°40′ of arc, there are no rods at all. This is the region of best visual acuity and best color vision. The rods are most dense in a band lying about 20° from the fixational center, and it is for this reason that night vision (at levels when the cones are inoperative) is best for averted vision. The distribution of rods and cones is shown in figure 13-8. Note that there is a hiatus in a region of about 5° diameter centered at about 15° in the nasal retina; this is the "blind spot", where the optic nerve fibers leave the retina.

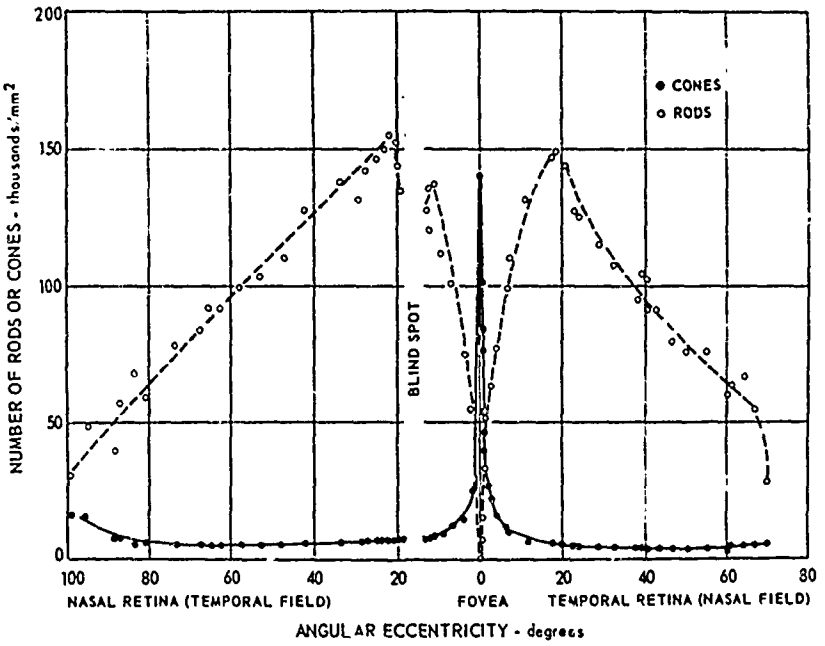


Figure 13–8. Typical distribution of rods and cones. (Østerberg, 1935; used by permission of Ejnar Munksgaard, publisher)

Rods and cones differ in their response to light of different wavelengths, as well as in their overall sensitivities. Figure 13-9 shows the spectral response curves for each. It will be noted that the sensitivity maximum for rods lies at 505 nm, while that for cones is at 555 nm. For this reason, colors of long wavelength become rapidly darker in appearance as the luminance is decreased.

The distribution of rods and cones in the retina is such that the extent of the visual field for a single eye is as shown in figure 13-10(a). The foveal fixation point lies at the center of the figure. The absolute limits of the visual field are bounded by the black portion of the polar plot, while the limits for the appreciation of various colors are shown by the indicated contours. The chromatic contours are subject to fluctuation with changes in luminance and size of the test patch, while the outer limit is stable and set by anatomical features such as the brow, nose, and cheek. When both eyes are open, the field of view is increased, as shown in figure 13-10(b) and there is a considerable region over which both eyes are operative, that is, there is binocular vision. The central white area is the field of stereoscopic vision. The cross-hatched region in the figure is seen only by one eye, and the blackened area is not seen. Binocular vision is an important factor in good depth discrimination, as well as having other advantages. The visual field represented is for a stationary eye or pair of eyes. Movement of the head and eyes and of the whole body will, of course, extend the limits of the visual field. On the other hand, the use of optical instruments almost always restricts the field. For certain space applications where whole-body movement may be restricted, it is instructive to note the extent of the binocular visual field under various conditions of restraint, as is shown in table 13-8, taken from the data of Hall and Greenbaum (1950).

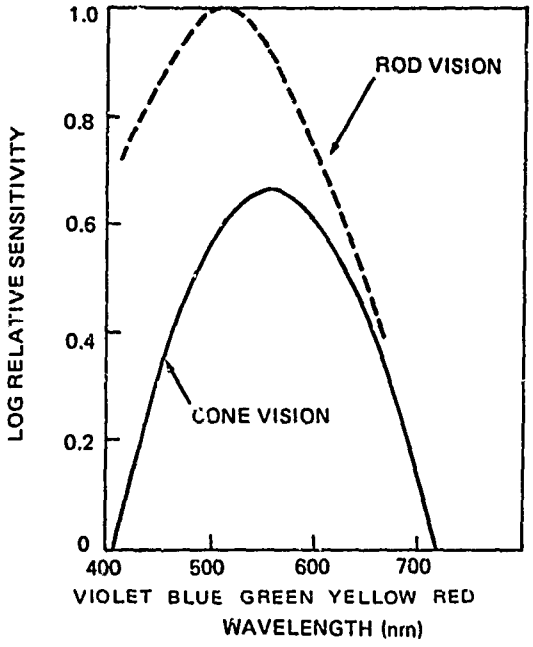
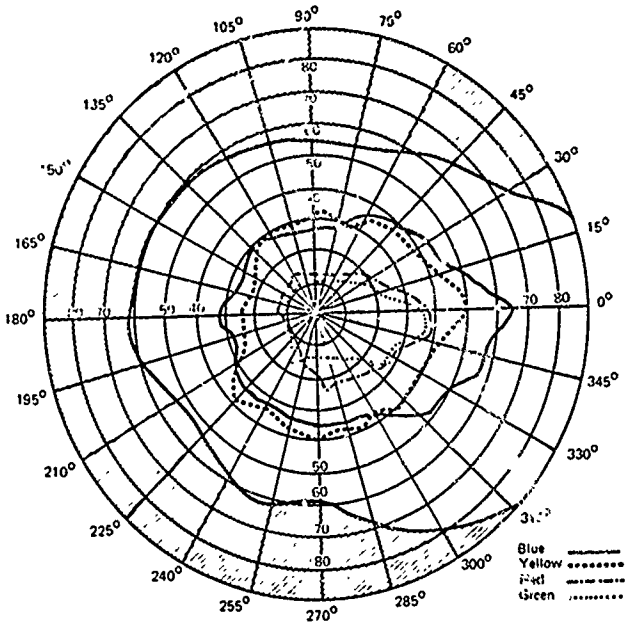


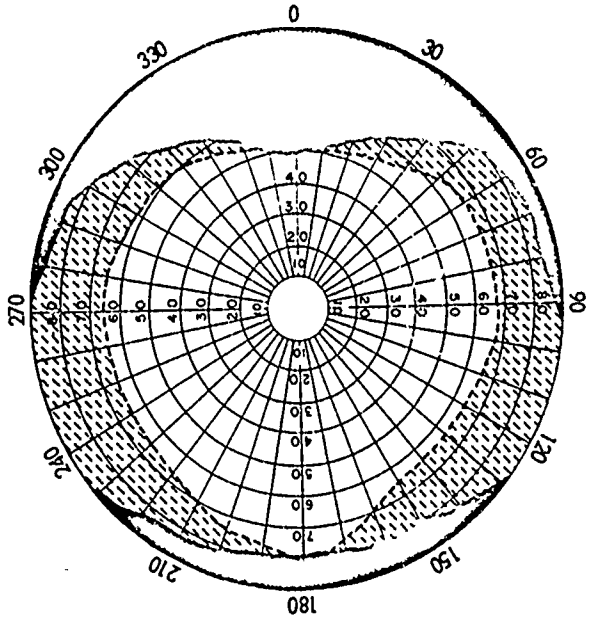
Figure 13–9. Spectral response of rods and cones, with relative amount of radiant energy for vision at absolute threshold shown as a function of wavelength of light. (Hecht & Williams, 1922)

Detailed description of the structure of the visual pathways to the brain, and the muscles responsible for eye movements is beyond the scope of this chapter. Reference should be made to any good contemporary texts in physiology and anatomy, or to the general references cited (e.g., Davson, 1962).

The size of the pupil of the eye is of concern, especially in the design of optical instruments wherein it may be the limiting aperture of the device. Under conditions of steady illumination, pupillary diameter depends upon the prevailing luminance level, as is indicated in figure 13-11. The dynamics of pupillary change are indicated by figure 13-12. The left part of the figure shows the contraction of a dark-adapted pupil with 8 mm diameter when exposed to bright light, and indicates that the pupil has stabilized at about 3 mm after 4-5 seconds. The right portion of the figure shows that dilation upon going into darkness is a slower process, and that even after 5 minutes the pupil has not reached its fully dark-adapted diameter. It should be noted that the change in diameter is responsible only for about a seven-fold change in the amount of light entering the eye, and hence plays only a miniscule role in the whole process of light and dark adaptation.



(a)



(b)

Figure 13–10. Human field of vision. (a) Field of view from right eye. (b) Binocular field of vision. (Boring et al., 1948)

Table 13–8
The Limits of the Visual Field Under Various Kinds of Restraint

Movement Permitted	Type of Field and Factors Limiting Field	Horizontal Limits		Vertical Limits	
		Temporal Ambinocular Field (each side)	Nasal Binocular Field (each side)	Field Angle Up	Field Angle Down
Moderate movements of head and eyes assumed as:	Range of fixation	60°		45°	
Eyes: 15° right or left 15° up or down	Eye deviation (assumed)	15°	15°	15°	15°
	Peripheral field from point of fixation	95°	(45°)	46°	67°
Head: 45° right or left 30° up or down	Net peripheral field from central fixation	110°	60°***	61°	82°
	Head rotation (assumed)	45°	45°	30°*	30°*
	Total peripheral field (from central body line)	155°	105°	91°	112°**
Head fixed Eyes fixed (central position with respec. to head)	Field of peripheral vision (central fixation)	95°	60°	46°	67°
Head fixed Eye maximum deviation	Limits of eye deviation (= range of fixation)	74°	55°	48°	66°
	Peripheral field (from point of fixation)	91°	Approx (5°)	18°	16°
	Total peripheral field (from central head line)	165°	60°***	66°	82°

		60°		45°	
Head maximum movement Eyes fixed (central with respect to head)	Limits of head motion (= range of fixation)	72°	72°	80°*	90°*
	Peripheral field (from point of fixation)	95°	60°	46°	67°
	Total peripheral field (from central body line)	167°	132°	126°	157°**
Maximum movement of head and eyes	Limits of head motion	72°	72°	80°*	90°*
	Maximum eye deviation	74°	55°	48°	66°
	Range of fixation (from central body line)	146°	127°	128°	156°**
	Peripheral field (from point of fixation)	91°	Approx (5°)	18°	16°
	Total peripheral field (from central body line)	237°	132°	146°	172°**

*Estimated by the authors on the basis of a single subject.
**Ignoring obstruction of body (and knees if seated). This obstruction would probably impose a maximum field of 90° (or less, seated) directly downward; however, this would not apply downward to either side.
***This is the maximum possible peripheral field; rotating the eye in the nasal direction will not extend it, because it is limited by the nose and other facial structures rather than by the optical limits of the eye. The figures in parentheses on the line above are calculated values, chosen to given the maximum limit thus indicated.

Notes: 1. All data except as noted are from Hall and Greenbaum (1950). 2. The ambinocular field is defined here as the total area that can be seen by either eye; it is not limited to the binocular field, which can be seen by both eyes at once. That is, at the sides, it includes monocular regions visible to the right eye but not to the left, and vice versa. 3. The term binocular is here restricted to the central region that can be seen by both eyes simultaneously (stereoscopic vision). It is bounded by the nasal field-limits of the eyes.

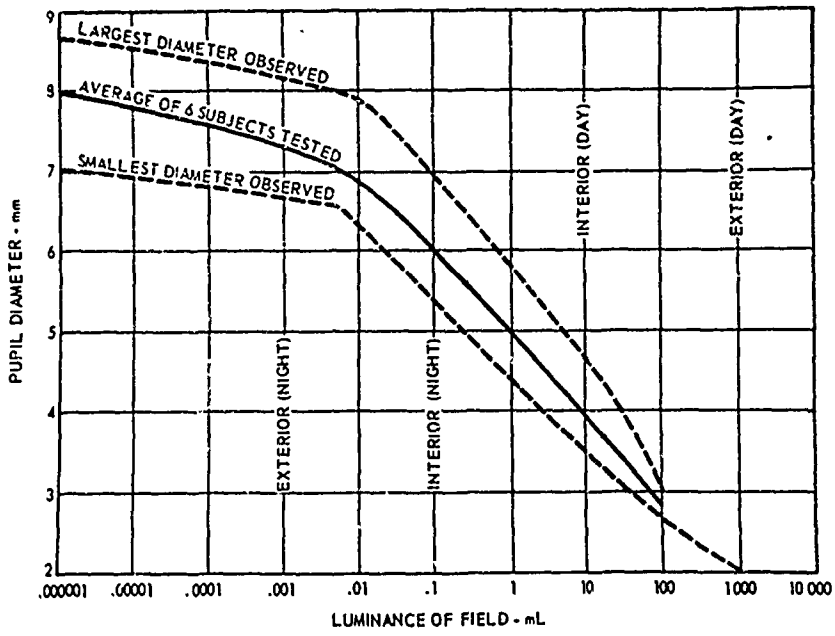


Figure 13–11. Pupil diameter as a function of luminance of adapting field. (Kaufman, 1966; *I.E.S. lighting handbook*. New York: Illuminating Engineering Society, 1966)

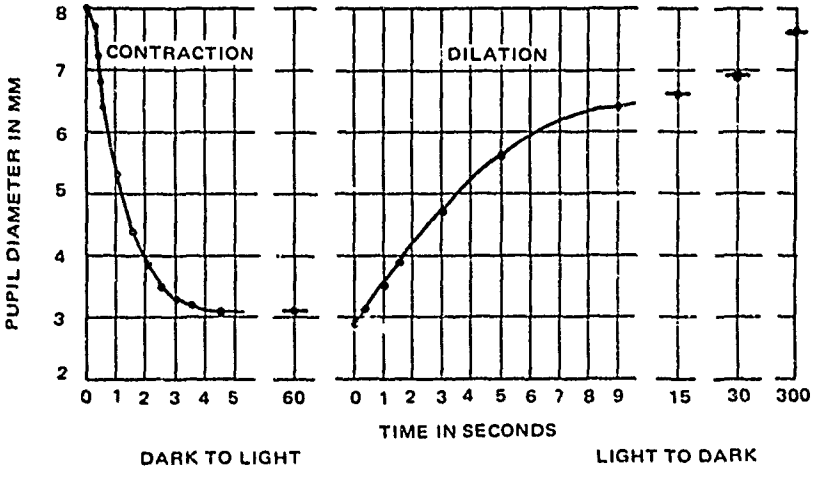


Figure 13–12. Pupillary response to light and darkness. (Reeves, 1918; copyright 1918 by the American Psychological Association)

The Stiles-Crawford Effect

A ray of light will be maximally effective if it reaches the retina via the center of the pupil. An identical ray which traverses a peripheral part of the aperture may, according to its eccentricity, need to be made several times more intense in order to produce the same result. This phenomenon is called the Stiles-Crawford effect, after its discoverers. It is primarily of concern for photopic vision, and has been shown experimentally to be related to the structure and optical properties of the cones.

The quantitative aspect of the Stiles-Crawford effect is shown in figure 13-13. It should be noted that the maximum of the curve is displaced nearly a millimeter toward the nasal side, and that the effect therefore is neither strictly symmetrical, nor exactly concentric with the pupil. The magnitude of the effect is dependent upon the wavelength of light, with more diminution in intensity for blue and red than for the center of the spectrum. There are also changes in hue and saturation of colors as the entrant ray is moved across the pupil. In general, most peripheral rays undergo a change toward some longer wavelength, although greens in a narrow band around 520 nm appear to shift toward blue (Stiles, 1939).

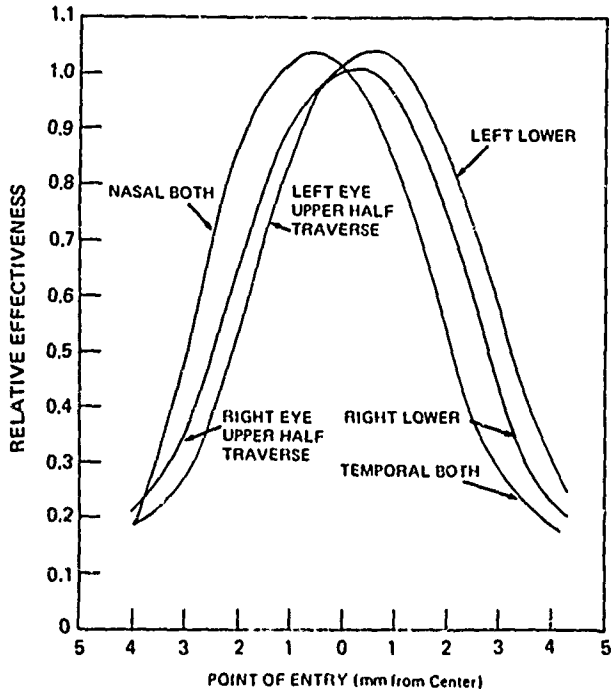


Figure 13–13. Stiles-Crawford effect. Light falling on different parts of pupil is not equally effective in producing sensory end result, even though light reaches same point on retina. Data are those for B. H. Crawford's eye. (Stiles & Crawford, 1933; reprinted by permission of the Controller of Her Britannic Majesty's Stationery Office)

There are two practical cases in which the Stiles-Crawford effect is of concern. The first of these relates to the design of optical instruments, where it is evident that distribution of the light flux at the eyepiece should be such that neither instrument nor operator performance is penalized. An example may be found in the case of certain binoculars and monoculars which use reflecting optics. In these instruments light emerges from the eyepiece as a hollow cylindrical beam, so that the most efficient central part of the pupil is not used, and the annular rays may suffer both loss of luminance and distortion of color. The second consequence of the effect is that it is critically necessary, in the determination of retinal illumination, to allow for the fact that simple enlargement of either the natural or an artifical pupil will not produce as large an increase in visual effect as would be expected on the basis of the increase in pupil area. The troland unit of retinal illumination thus has limited utility, for it matters to the retina from what part of the pupil it receives its light. An approximate correction for the Stiles-Crawford effect has been attempted (LeGrand, 1957), but even so the troland remains an imprecise unit.

Chromatic Aberration

The eye is unable to bring rays of all wavelengths to focus at the same retinal plane simultaneously. As in other simple optical systems, light of short wavelengths being more strongly refracted by the lens, is focused at a plane in front of that for the longer, less deviated ones. The eye tends to maintain focus for the wavelengths near the photopic sensitivity maximum, so that, in the white light case, the red and blue components of an image will lie behind and in front of the plane of best focus, respectively. This effect is quite large, and chromatic differences of focus over the spectrum amount to approximately three diopters.

Measurements of chromatic aberration in the human eye have been made by several investigators, and the results are in good agreement (Ivanoff, 1949; Hartridge, 1950; Wald & Griffin, 1947). The data of figure 13-14 are typical.

The consequences of chromatic aberration are many, and although much of ordinary visual activity is affected little or not at all, there are some important implications for engineering design. Normal visual acuity is best for conditions where the color of the illuminant for the task is confined to the spectral region near the peak of the luminosity curve, at least at low to moderate levels of illumination (Schober, 1937; Schober & Whittman, 1938). The effect may be bothersome in certain optical instruments using polychromatic fields, although this may be corrected by incorporation of a specially designed lens (Wright, 1947). It is often impossible to discriminate between white and yellow stimuli of small angular extent, since the eye tends to focus on the yellow-green component of the white and allows the blue and red to blur out so that they are ineffective in the discrimination (Wilmer, 1946). Finally, it is clear that small colored stimuli, such as signal lights, will be perceived to be at different distances according to their spectral composition and that, further instances may occur when critical detail of displays shows serious chromatic disparities, leading to operator error.

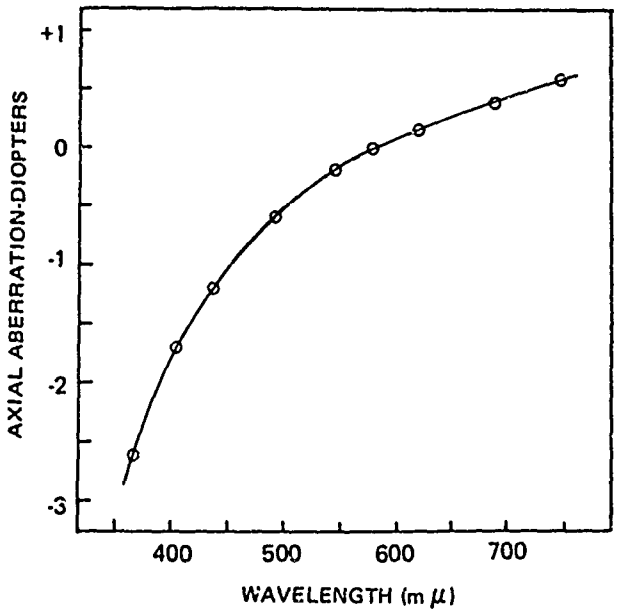


Figure 13–14. Axial chromatic aberration of human eye. Averages of measurements on 14 observers. Ordinates show lens correction in diopters needed to give each eye same refractive power it possesses when accommodated for distance vision at 578 mμ (Wald & Griffin, 1947)

Visual Performance

Normal visual performance involves a number of interdependent discriminations which are made in response to factors in the visual environment and mediated by the structure of the visual system. Principal among these discriminations are the appreciation of detail (visual acuity), contrast, color, form, distance, movement and certain temporal aspects of the object of regard. The limiting capabilities of the human observer have been extensively investigated in all of these areas, usually in laboatory studies which isolate the function of interest. It must be recognized, therefore, that the data do not take into account the interactions between functions which are known to occur. Rather, they should be taken as indicative of the limiting case, modifiable for better or worse in accordance with other factors.

Visual Acuity

There are many definitions of the term "visual acuity;" all, however, incorporate the notion of the resolution of detail. A variety of test patterns has been used to measure acuity, from simple single dots to twin stars, gratings, broken rings, checkerboards, and letters. It is unfortunate that no general agreement as to the choice of a test has been reached, and that results from the different patterns are often at odds. The Snellen Letter Test is probably the most familiar, and is widely used in clinical practice, despite the fact that it is a

test of letter recognition rather than of retinal resolution. The most satisfactory expression for visual acuity is in terms of the angular subtense of the critical detail which can just be discriminated. (In the Snellen notation, the width of the letters of the 20/20 line is such that they subtend one minute of arc at 20 feet.) A well-entrenched popular misconception is that 20/20 ,or 1', represents "perfect" vision. Acuity depends upon the character of the test, and resolutions of a few seconds of arc are not uncommon. Some results from use of various test patterns are shown in figure 13-15.

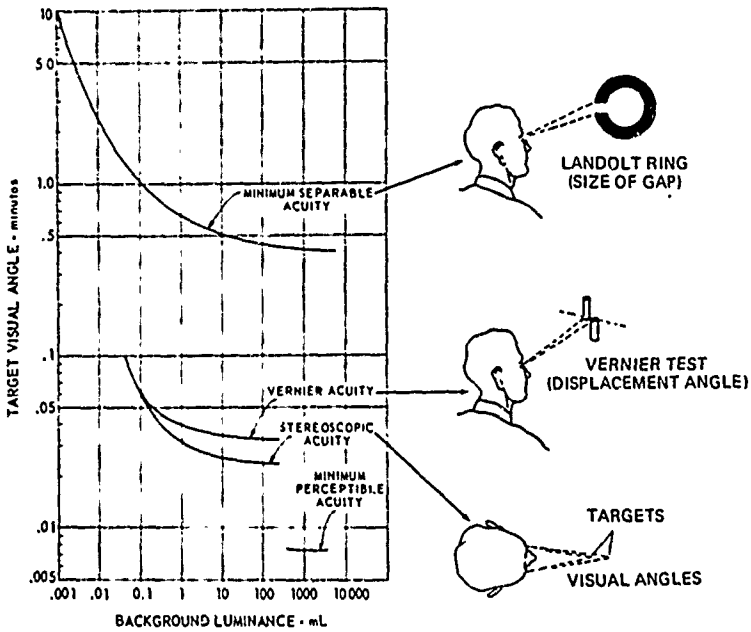


Figure 13–15. Approximate relationship between various measures of visual acuity and background luminance. Uppermost curve is obtained using a broken ring (Landolt C) test object, and data are values of angular gap size discriminable over range of luminances tested. Vernier acuity task: discrimination of discontinuity in otherwise smooth edge, or of small linear displacement. Stereoscopic acuity angle: difference in subtense between two test objects of identical size whose distances from eye are just discriminably different. Minimum perceptible acuity: smallest detectable spot, with contrast limited to -1.0. (Adapted from White, 1964)

There are some important variables which affect visual acuity, and which must be taken into account in operational planning terms:

Luminance. The level of adaption of the eye has a profound effect upon visual acuity, as might be expected. This dependency is shown for two different test patterns in figure 13-16.

Position In The Field. At photopic levels, acuity is best at the fovea, and drops off as the retinal periphery is approached, owing to receptor population differences. Nocturnal acuity is quite poor, with essential blindness at the fovea

and best resolution appearing in the periphery where rod packing is densest. The variation of visual acuity is indicated in figure 13-17.

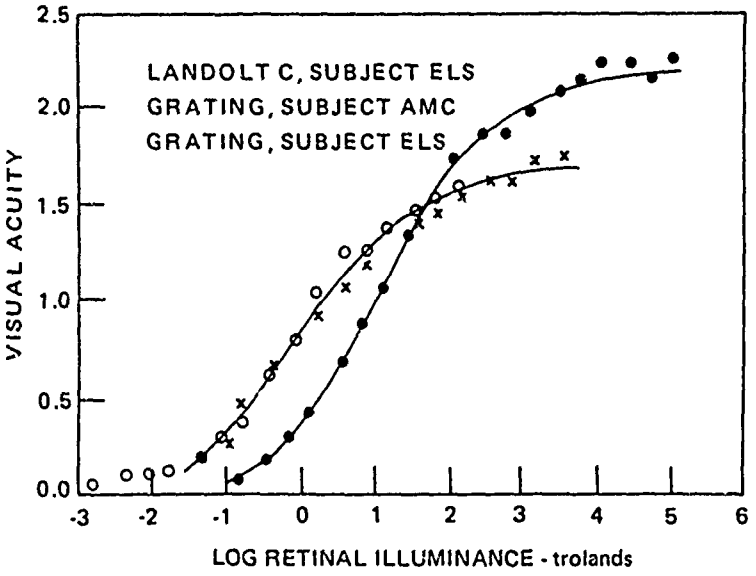


Figure 13–16. Variation of acuity with retinal illuminance for resolution of a grating and for recognition of orientation of a Landolt C test object. (Schlaer, 1937)

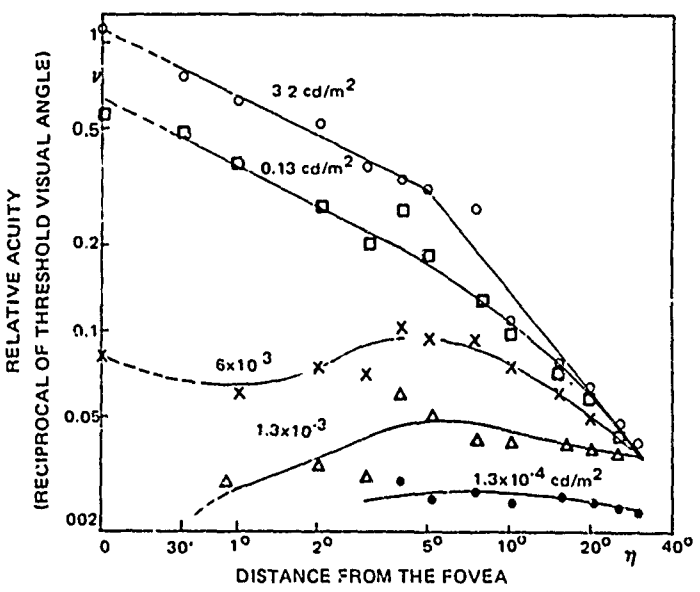


Figure 13–17. Change in visual acuity (reciprocal of Landolt C gap size) as a function of position on retina for 5 luminances. Eccentricity shown in degrees from foveal center. (Mandelbaum & Sloan, 1947)

Duration. When the pattern is exposed for only a short time, measured acuity diminishes in accordance with the function shown in figure 13-18. It is evident from this figure that the duration effect is related to the luminance of the test.

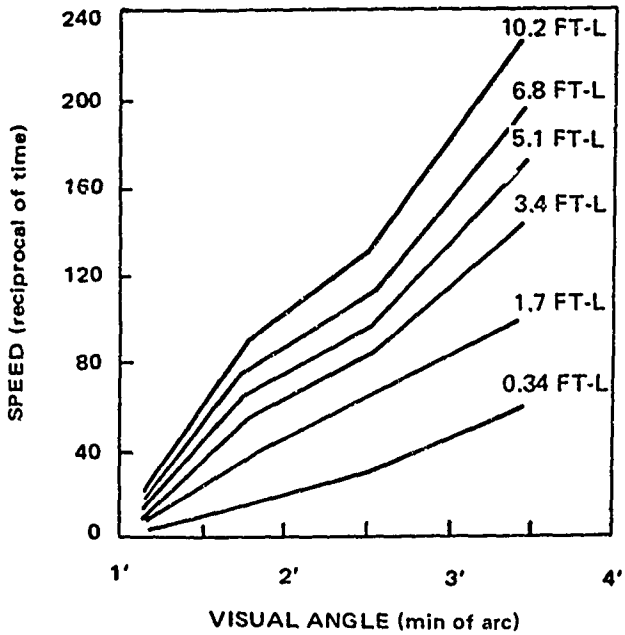


Figure 13–18. Visual acuity as a function of time of exposure for several luminance levels. At any given level less time is needed to see larger objects, and, for any given object size, less exposure time is required at higher luminances. (Ferree & Rand, 1922)

Color. For tasks illuminated by monochromatic or narrow-band sources, there is a small but measurable difference in acuity as a function of the dominant wavelength used, provided that all colors have been equated for luminance. In comparison with acuity measured in white light, there is a nominal improvement when sodium vapor lamps are used, while with blue or violet light acuity is poor (Moon, 1961). These statements apply only to photopic vision.

Contrast. Visual acuity decreases as the contrast between pattern and background is diminished. The form of this relationship depends upon the adapting luminance, as was shown by Connor and Ganoung (1935) and by Cobb and Moss (1928), whose results are combined in figure 13-19.

Movement. Detail vision for moving objects is called dynamic visual acuity. Investigations of this problem have been reported by Miller (1958), whose results are summarized in figure 13-20. These data must not be used uncritically, for it was shown by Ludvigh and Miller (1958) that wide differences exist between observers, and that thes. are not correlated with their measured static visual acuities.

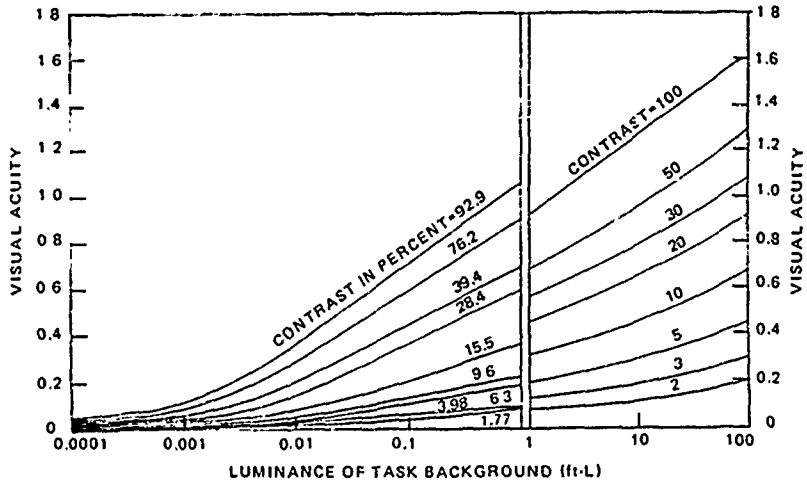


Figure 13–19. Visual acuity as a function of background luminance for a number of contrast levels, here expressed as percentages. (Data on left from Conner & Ganoung, 1935; on right from Cobb & Moss, 1948)

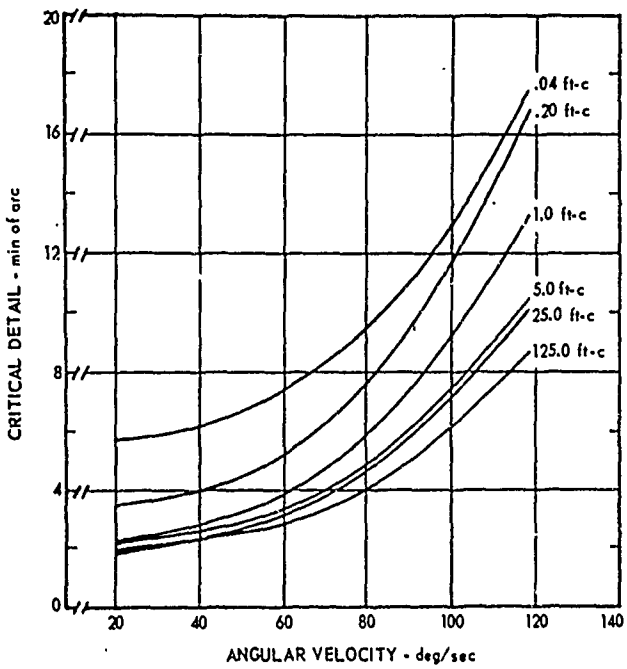


Figure 13–20. Dynamic visual acuity. Note decrease as velocity increases, for 6 levels of test chart illumination. (Miller, 1958)

Contrast Discrimination

Vision requires that there be differentiation of the luminances (or colors) in the field of view. Without these gradients of energy across the retinal image, there can be no information received from the environment by visual means, at least in the ordinary sense. The luminance gradients which we use are distributed both in space and in time, and man is sensitive to both spatial and temporal differences. Simple contrast discrimination is conventionally discussed in terms of the static case, with the phenomena of movement, intermittency and color being treated as separate entities. In a sense, nearly all of visual activity (visual acuity included) may be regarded as contrast discrimination. Here, however, we will restrict its meaning to refer to the simplest case of the appreciation of a luminance difference--generally in white light.

Contrast is defined as the ratio of a luminance change ascribable to the presence of an object, or target, to the luminance of the background. If the luminances of target and background are b_t and b_o, respectively, then the luminance contrast, C, is:

$$C = \frac{B_t - B_o}{B_o} = \frac{\Delta B}{B_o}$$

It is evident that the contrast of targets brighter than their backgrounds can vary between zero and infinity, while those darker than their backgrounds can vary from zero to minus one. In many cases it has been found (e.g., Blackwell, 1946) that targets of equivalent numerical contrast are equally visible irrespective of sign. This generalization has recently been questioned by Patel and Jones (1968) who find higher thresholds for positive than for negative targets; the effect becoming significant at low luminance levels.

The most important variables affecting contrast discrimination are luminance of the background, size and duration of the target, and the portion of the visual field used. Color is relatively unimportant in simple target detection if a luminance gradient exists (MacAdam, 1949), although color is important in many other visual tasks.

Background Luminance And Target Size. These two variables have been investigated quite thoroughly for the case of simple circular targets on uniform backgrounds (e.g., Blackwell, 1946; Blac' well & Taylor, 1970). Their influence on contrast discrimination is seen in figures 13-21 and 13-22, taken from the earlier study. These data have been used extensively in the construction of nomograms for predicting the visibility range of objects under a variety of viewing conditions (Middleton, 1952; Duntley, 1960).

Duration. For very brief exposure times, contrast discrimination depends on the product of the luminous flux and the duration of the flash, that is,

$\Delta B \times t$ = a constant at threshold. This is Bloch's law, and it holds for values of t up to a critical duration, t_c, which varies from 0.002 to 0.1 second, depending upon conditions (Baumgardt & Segal, 1946) although the latter figure is more typical under conditions of practical interest. At exposure times longer than a few tenths of a second, threshold is independent of duration and ΔB = a constant. The character of the transition from $\Delta B \times t$ = C and ΔB = C is sometimes abrupt, sometimes gradual, depending upon the conditions. (For details, see, e.g., Kishto, 1968.) Data relating duration to contrast discrimination have been published by Graham and Kemp (1938), by Blackwell and McCready (1958), and by Blackwell and Taylor (1970). Data from the first study are shown in figure 13-23.

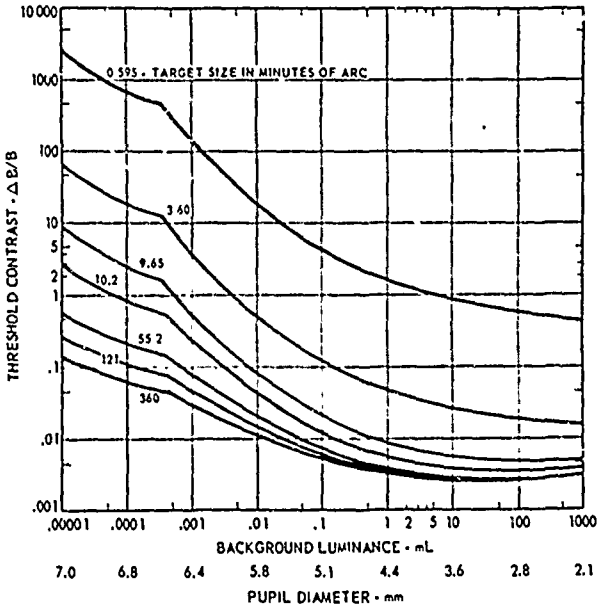


Figure 13–21. Contrast thresholds as a function of adaptation luminance for 7 sizes of uniform circular targets. (Blackwell, 1946)

Position In The Visual Field. In the light-adapted eye contrast discrimination is best at the fovea, where the density of cone receptors is highest, and deteriorates as the target moves out toward the periphery of the visual field. Under dark-adapted conditions, foveal vision is inoperative and optimum discrimination is achieved by use of averted vision, usually at about 10° away from the visual axis. Some data for the daytime case for targets in the near periphery are shown in figure 13-24, from a study by Taylor (1961).

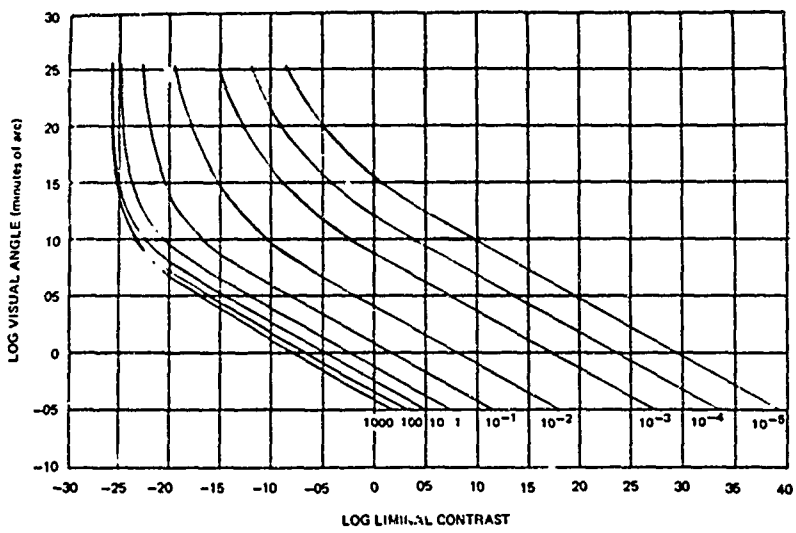


Figure 13–22. Interpolations made from curves of figure 13-21, plotted to show relationship of target size to threshold contrast. Individual curves refer to adaptation luminances over 1000 ft-L–10^{-6}ft-L range. (Blackwell, 1946)

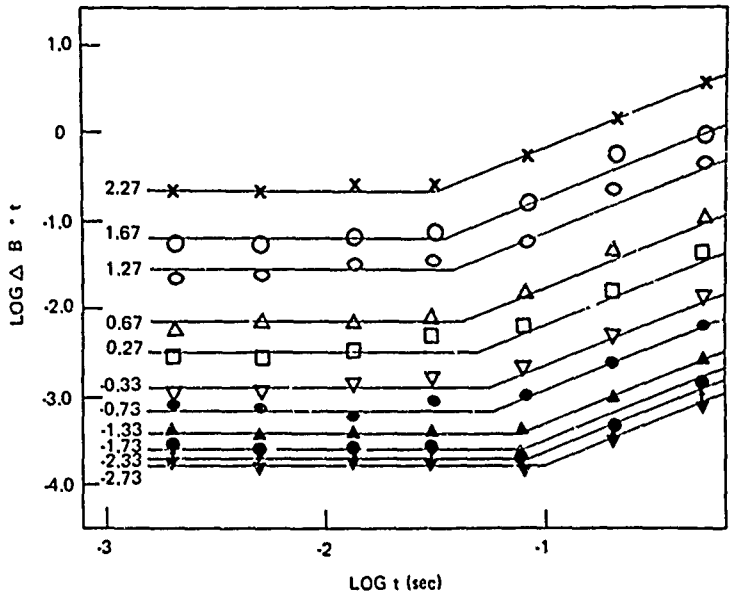


Figure 13–23. Relation between ΔB and t. Individual curves are labeled with values of log B, adapting luminance, in m-L. Horizontal lines represent equation Log B·t = constant; the inclined lines, ΔB = constant. Critical duration, t_c, is shown to decrease with increase in adapting luminance. (Graham & Kemp, 1938)

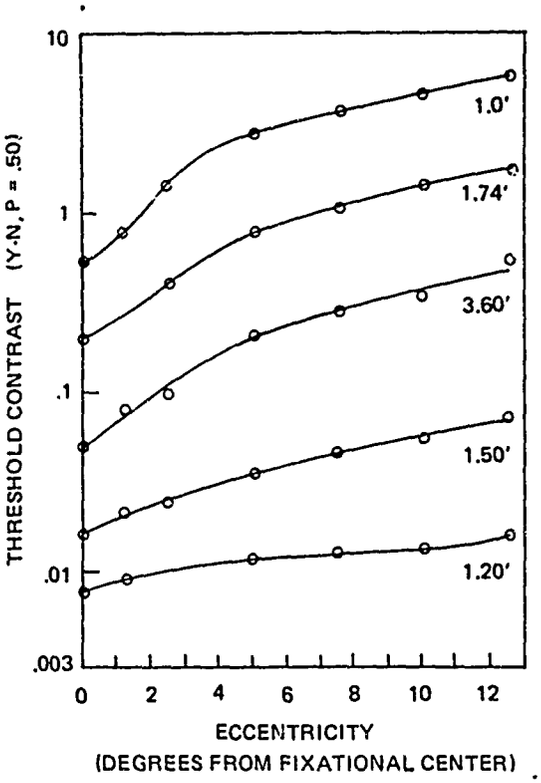


Figure 13–24. Threshold contrast as a function of retinal position and target size for binocular photopic vision. Adaptation level, 75 ft-L (257 cd/m^2); target duration, 0.33 sec. Curves labeled to indicate angular diameter of uniform circular stimuli; 4 observers, for which plotted average values represent 0.50 probability of detection in "yes-no" experiment; each data point based upon 2400 observations. (Taylor 1961)

Depth and Distance Discrimination

The estimation of depth and distance in ordinary terrestrial seeing is accomplished by use of a number of cues which are available to the experienced observer. Some of these cues are provided by the nature of the scene of interest, while others inhere in the observer himself. Some of the important external and internal cues are indicated in table 13-9. But a number of these cues may be absent in the space environment, and it will be necessary to evaluate any visual task which requires critical judgment of depth or distance in terms of the available information.

In cases where only internal cues to distance are available, that is to say when the objects of interest are of unknown size and shape, and none of the external aids such as aerial perspective or interposition is of help, it is evident that the observer must depend upon his stereoscopic acuity, accommodation and convergence, and, where possible, movement parallax. Accommodation is only an effective cue to distances at ranges of a meter or less, and even here it is inaccurate. Convergence alone is a somewhat

more useful cue, but is limited to a range out to about 20 meters. Stereoscopic acuity, however, provides a powerful cue to distance. Experimentally determined values of stereoscopic acuity are in the range from about 10" to 2" arc. An observer with a stereoscopic acuity of 5", for example, can discriminate that an object at 2600 meters is closer than one at infinity (LeGrand, 1967).

Table 13–9

External and Internal Cues to Depth and Distance

External Cues	
Linear perspective	Apparent convergence of parallel lines and related effects
Apparent size	A strong cue to distance of objects of known size, and texture
Motion parallax	Relative angular motion as either head or objects move
Interposition	Nearer objects eclipse more distant ones
Aerial perspective	Contrast and color loss due to aerosols; useless in free space
Shading	A cue to three-dimensional form of objects (not to distance)
Apparent intensity	A cue only to distance of effective "point sources"
Internal Cues	
Accommodation	Relatively unimportant (see text)
Convergence	Useful limit is about 20 meters (see text)
Binocular disparity	Most important intrinsic cue to depth and distance

Note: All cues excepting last two can be utilized by a single eye, and by extension, in uniocular optical devices.

(Adapted from Gibson, 1950)

Movement parallax is another important cue to depth and distance, especially where binocular vision is impossible, as in the use of uniocular optical instruments. The accuracy of this cue depends upon the luminance level, the rate of angular movement, and the direction of movement across the visual field (Graham et al., 1948). Under optimum conditions (high luminance levels, orthogonally-oriented movement, and an angular rate of about 0.1 radian/second of time), the resulting acuity is about 40"/second of time. Thus, even slight side-to-side or up-and-down movements of the head can provide an accurate cue to relative distance.

Temporal Discrimination

The temporal resolution of the visual system is occasionally of concern in space operations. Examples include the discrimination of temporally coded

displays, differentiation between steady and flashing lights, and the time-varying visual signals received from a sunlit, tumbling space object seen against a black background. Experimental data regarding temporal discriminations are exceedingly voluminous, and the reader should consult the general references noted at the end of this chapter for details. Only a small sample of these results will be given here.

As the rate of intermittency of a flashing light is gradually increased, there is a rather sharply defined point at which the light begins to appear as a steady one. The rate at which this transformation occurs depends upon a host of conditions, but two of the most important are the luminance of the background and the position in the visual field. (Size, of course, is an important variable, but it may be assumed that intermittent stimuli in the space environment will be angularly small.) The transition point between steady and intermittent appearance is called the "critical frequency of fusion", and is often abbreviated "CFF." In figure 13-25 the value of the CFF is plotted as a function of background luminance, for a 2° circular test target located at the fovea and at 5° and 15° above the fovea. Had the target subtended 0.3°, the CFF values would have been about 5 Hz lower for the foveal case (Hecht and Verrijp, 1933).

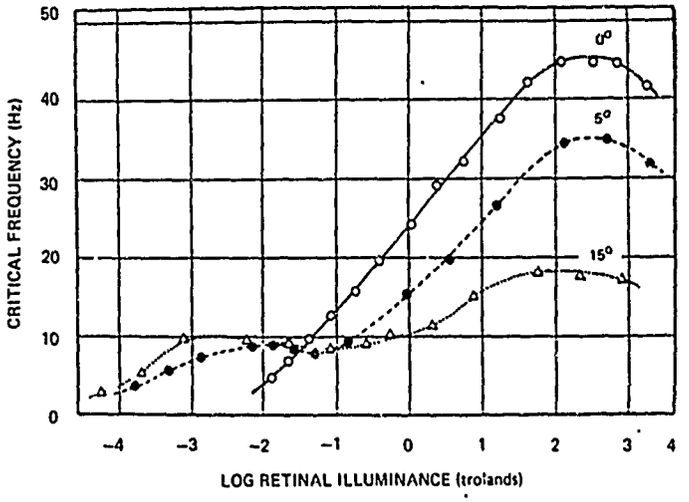


Figure 13–25. Relation between critical frequency and log retinal illuminance for white light for three different retinal locations: at the fovea and 5 and 15° above the fovea. (Hecht and Verrijp. Reprinted by permission of The Rockefeller Institute Press from *The Journal of General Physiology*, 1933, *17*, 251-265; Fig. 2, p. 257)

There are other considerations regarding intermittent illumination. Spacecraft internal illumination, for example, should not exhibit perceptible flicker, owing to possible performance decrements suffered by the crew. Temporally-coded display systems, likewise, should be designed so that the crewman's temporal resolution capabilities are never exceeded.

Movement Discrimination

Several sorts of tasks are subsumed under this category, and several modes of movement must be considered. The more common cases of interest may be listed as follows:

1. Movement across the visual field in the fronto-parallel plane, with or without stationary reference objects in the field of view.

2. Movement in depth, toward and away from the observer and with or without reference objects.

3. A combination of the above.

4. A change in the rate or direction of movement.

5. The discrimination of rotational movement, usually centered on the line of sight, but not always.

In space operations, movement discrimination is especially critical in instrument reading, rendezvous and docking maneuvers, and in spacecraft landing procedures. It is abetted by the presence of reference objects in the field (especially familiar ones), high luminance levels, and optimum rates of movement.

The variables influencing movement discrimination of any sort are identical with those affecting other visual functions (luminance, size, contrast, and retinal position), but with the additional factors of velocity and rate of change of velocity as complications. The recent book by Spigal (1965) should be consulted for detailed treatment of the subject, as should the general references.

Some specimen data are shown in figures 13-26 to 13-28.

Color Discrimination

Color vision is mediated by the retinal cones, and is therefore best at photopic luminance levels and in those parts of the visual field where the cones are most densely packed. Color discrimination may be general, as in differentiating between different colors, or it may be specific, as in the appreciation of some one color characteristic such as hue, saturation, or luminance. When color is used in coding and in displays, only general discrimination is usually required (wiring, signals, pipelines, warning and clearance lights, etc.). In space tasks involving naturally occurring colors, however, it may be necessary to make subtle discriminations of chromatic differences (lunar and planetary exploration, spacecraft landing, vehicular maintenance, and observations of the terrestrial surface from orbit).

Hue, the psychophysical counterpart of the physical dominant wavelength of a stimulus, can be discriminated very well under conditions of adequate luminance (10 ft-L or more) provided that the angular size is large enough. The data of figure 13-29 refer to the case of a 2° field and photopic luminance (Wright and Pitt, 1934). About 150 hues can be discriminated under these conditions; with larger fields, the number of hues would be larger (Wright, 1947).

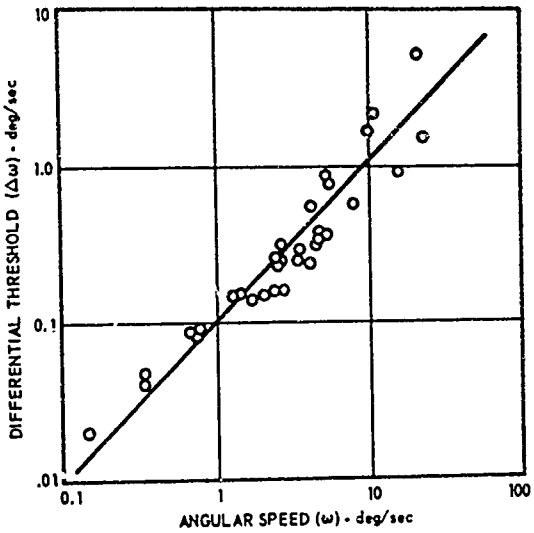


Figure 13–26. Sensitivity to change in velocity of a moving ($\Delta\omega$) as a function of angular speed (ω). Formula for straight line with unit slope: $\text{Log}_{10}\Delta\omega = -1.00 + \text{Log}_{10}\omega$. (Brown, R. H., 1960; copyright 1960 by The American Association for the Advancement of Science)

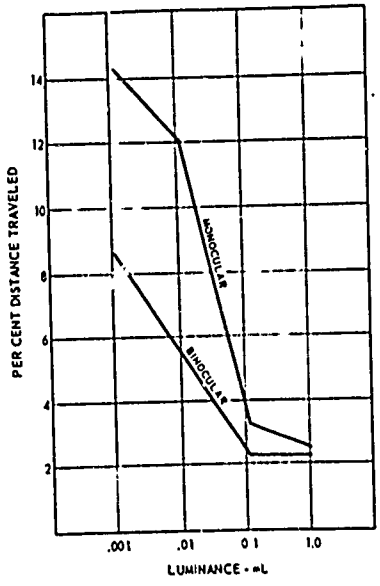


Figure 13–27. Sensitivity to movement in depth, expressed in terms of percent distance traveled by a 3.5 in. luminous disc at mean distance of 25 ft against dark background, as a function of luminance of disc. Both monocular and binocular curves refer to 75% level of movement detection. Target was a lamp 3.5 in. in diameter, moved back and forth on a tract from an initial distance of 25 feet. At the initial distance, the lamp subtended 40 min. at the eyes. 2% change in distance represents a 2% change in visual angle, or about 0.8 min. Target speeds ranged from 1.65 to 13.2 in./sec producing initial changes in visual angle from about 0.25 to 2 min of arc. (Baker & Steedman, 1961)

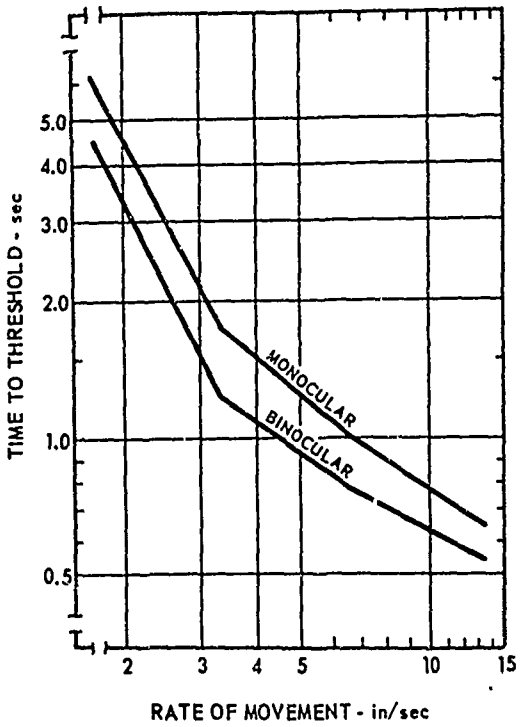


Figure 13–28. Sensitivity to movement in depth as a function of rate of movement. Conditions as in figure 13-27, but target luminance was fixed at 1 ft-L while target speed was varied. Values on ordinate are times required to detect movement at probability 0.75. (Baker & Steedman, 1961)

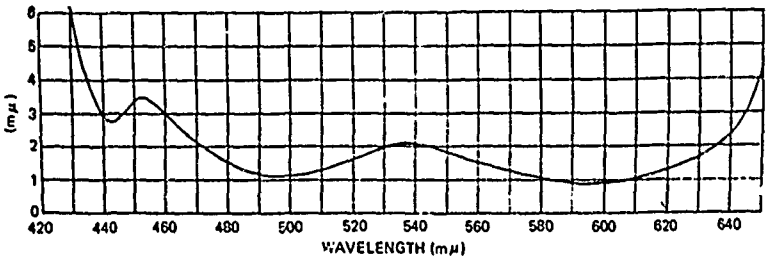


Figure 13–29. Hue discrimination. Shows the amount of change in wavelength ($\Delta\lambda$) needed to produce a noticeable change in hue for various parts of the visible spectrum. (Wright, 1947)

Saturation, the psychophysical equivalent of spectral purity, refers to the degree to which a color of given hue differs from white. Pale pink, for example, is a red of low saturation. Discrimination of saturation is best at the center of the visible spectrum (570 nm), as seen in figure 13-30.

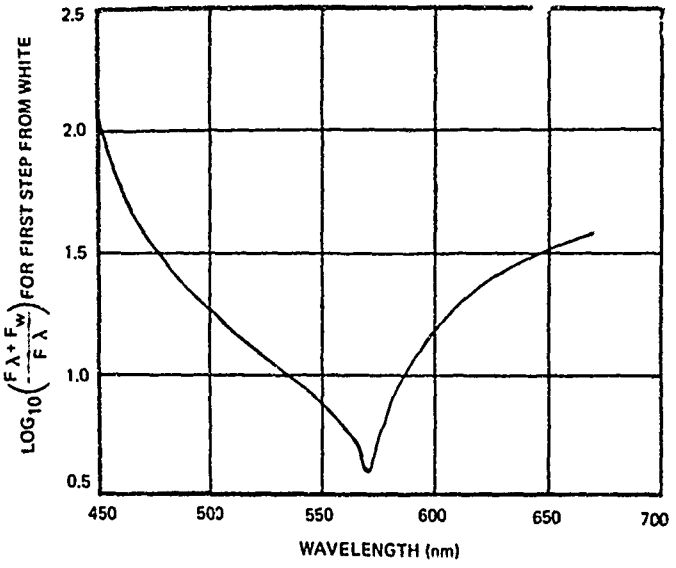


Figure 13–30. Saturation discrimination. Values on ordinate represent amount of color added to white for color change to be discriminable, assuming equality of luminance for the two conditions. The expression $F\lambda/F\lambda + F_W$, where $F\lambda$ is light flux of wavelength and F_W is flux of white illuminant, is called colorimetric purity. (Wright, 1947)

In most practical cases one is interested in the discrimination of a combination of hue and saturation - a quantity known as chromaticity. Investigations of chromaticity discrimination by MacAdam (1942) have yielded data of the sort shown in figure 13-31, in which the ellipses indicate the fineness of this discrimination in various parts of the chromaticity diagram. (For a discussion of the chromaticity diagram, see Wright, 1947, or other general reference.)

There are some special considerations which should be taken into account in the design of systems and in the planning of missions if color discrimination is to be successful. Some of these have already been alluded to (chromatic aberration, luminance level); others should be noted.

Small Subtense Color Vision. The ability to discriminate colors is drastically reduced in the case of angularly small targets. Under this condition, only three colors may be reliably differentiated: red, green, and another color which may be yellow, or white, or gray. For this reason, the coding of signal lights is restricted to three colors whenever they are to be seen at any appreciable distance.

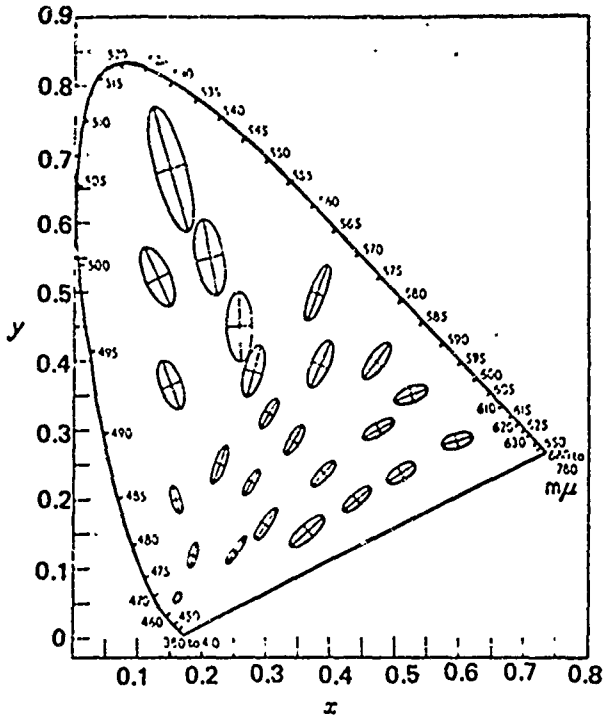


Figure 13–31. Ellipses representing 10 times S.D. of color matches made at constant luminance. Each ellipse is based on matches made with variation restricted in direction in the diagram. These variations were taken in 5 to 9 directions, and 50 matches were made for each direction of variation, so that each ellipse is based on 250 to 450 color matches. (MacAdam, 1942)

Peripheral Color Vision. Best color vision occurs at and near the center of the field. As stimuli are moved toward the periphery, discrimination becomes poor, and colors are not seen (although the loss of color occurs at different distances from the fovea). Some typical data are shown in figure 13-32, from the report of the Committee on Colorimetry (1953). This figure shows in a very general way the limits of color discrimination in the parafoveal retina for the colors shown. The use of larger or more luminous stimuli would cause expansion of these fields; perhaps to the outer limit shown for achromatic (white) luminance discrimination.

Visual Search

The visual acquisition of objects in the field of view when their location is unknown is called visual search. The important variables in the search process include size and structure of the field, characteristics of the target object, including its size and complexity, luminance level, contrast, uniqueness, and so on. Although a great deal of work has been done on the problem, there is no simple set of rules which may be used to formulate optimum search procedures.

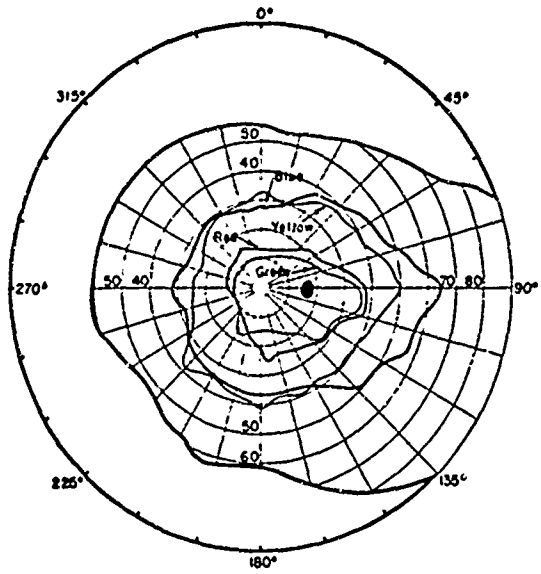


Figure 13–32. Visual fields for color in a right eye. (Committee on Colorimetry, 1953)

From the standpoint of engineering design for space operations it may be assumed that the usual objective will be to assist the search process (as opposed to concealment and camouflage). Accordingly, it will be desirable to increase the probability of visual acquisition by careful attention to the factors which are known to assist in the search process. A number of such factors have been summarized by Taylor (1969), and a collection of papers edited by Morris and Horne (1960) should be consulted for additional suggestions.

Size Discrimination

The size of an object is usually discriminated by the aid of such cues as known distance, comparison with other objects of known size, and such factors as perspective and familiarity. In space operations, however, these cues may be lacking, or conditions may be such as to deceive the observer. A very important phenomenon is that called irradiation. Simply put, two objects of identical size and at the same range will appear of the same size if they are illuminated equally. If one is very much more intensely lit, it will appear larger. The effect is especially great in the case of angularly small objects. Recent work by Haines (1967) should be consulted for the quantitative aspects of the irradiation phenomenon as it affects both size and shape discrimination.

Form Discrimination

The form of an object is of undoubted interest in all phases of space exploration, and especially so in the discrimination and description of planetary and lunar surface features as well as in the differentiation of

orbiting objects and terrestrial formations. The many variables which affect the form discrimination process are discussed in Wulfeck and Taylor (1957). Observer experience and training are important, and the task will depend upon the level of discrimination desired.

Dark Adaptation

Optimal visual discrimination under conditions of very low luminance can be made only if the visual system is adapted to the level of the prevailing photic environment, or even lower. If a fully light adapted eye is suddenly plunged into darkness, its sensitivity is initially very poor. With time, however, sensitivity begins to increase as a result of photochemical regeneration, certain functional neural changes, and (to a much smaller degree) enlargement of the pupil of the eye. If the eye remains in total darkness for 30 to 60 minutes, the adaptation process will be nearly complete and the sensitivity of the eye in those parts of the retina where both rods and cones are present will have increased by a factor of 10 000 for white light.

The course of dark adaptation is influenced by many factors, such as the intensity, duration, and color of the preadapting light, the size and area of the retinal area stimulated, and the nature of the visual stimulus used to test the effect. Summaries of the many parametric studies of dark adaptation may be found in Graham et al. (1966), Davson (1962), LeGrand (1957) and in Jayle and Ourgaud (1950). A general curve, obtained with white light, is shown in figure 13-33. The early portion of the curve, extending to about 10 minutes, is here reflecting the adaptation of cones. The subsequent increase in sensitivity is due to activity of the rods. The curve is an average from the data of 101 observers. It clearly indicates that adaptation of the cones is complete after about 10 minutes. Later increase in sensitivity is caused by activity of the rods.

There are several important operational consequences of the dark adaptation process and its properties:

1. Best performance on a task at low luminance requires that the eye be preadapted to an appropriately low level for sufficient time so that maximum sensitivity obtains.

2. Since the rods are more sensitive than the cones at low luminances, best detection capability will occur on those parts of the retina where rods abound (10 to 30 degrees from the fovea), and averted vision is required for optimal performance.

3. Since the rods are relatively insensitive to extreme red wavelengths, dark adaptation will proceed if the observer dons suitable red goggles or if the illumination provided, in a spacecraft for example, is very deep red. By this means it is possible to continue to use the high-acuity capability of the central fovea at elevated luminance levels for reading instruments, etc., while the adaptation process goes on; although vision will naturally be monochromatic in this case.

4. Because the two eyes are essentially independent as regards adaptation, it is possible to maintain dark adaptation in one (e.g., by means of an eye patch) while the other is used for tasks at high luminance.

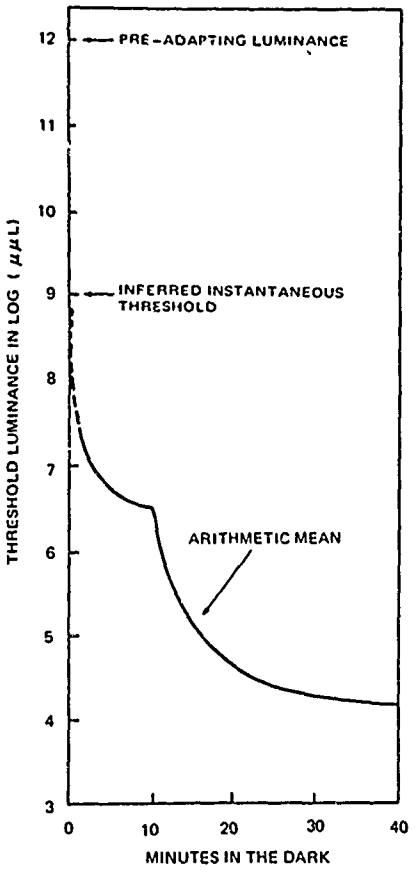


Figure 13–33. Course of dark adaptation following exposure to a luminance of about 1000 ft-L. Measurements made using a test spot 1° in diameter imaged on a retinal region 15° in nasal periphery where both rods and cones are present. (Sloan, 1947; adapted from *How we see: A summary of basic principles*, by A. Chapanis, in *Human factors in undersea warfare*, by permission of the National Academy of Sciences)

Vision Under Stress

Environmental stresses to which astronauts may be subjected have been studied in some detail. Most of these are of a transient nature, occurring only during some relatively short part of the mission, such as launch, extravehicular activity, or reentry. Others, however, will be a necessary part of extended missions, and a potential part of system malfunctions. Added to environmental factors may be individual stresses induced by anxiety, boredom, interpersonal

frictions or sensory deprivation*. The latter class of stresses has been only partially amenable to test, and the practical importance of these factors remains a matter of conjecture. The physical environmental stresses thought to be important may, however, be quantitatively evaluated in many instances.

Acceleration

The effects of acceleration on vision have been summarized by White and Monty (1963). As is well known, the decrement in performance is a function of the g vector, and less impairment is incurred in the case of transverse g loads. Central and peripheral contrast discrimination are affected differentially, and central losses in acuity are suffered. Figure 13-34 shows the nature of these effects, and their implications for system design and mission profile planning are clear.

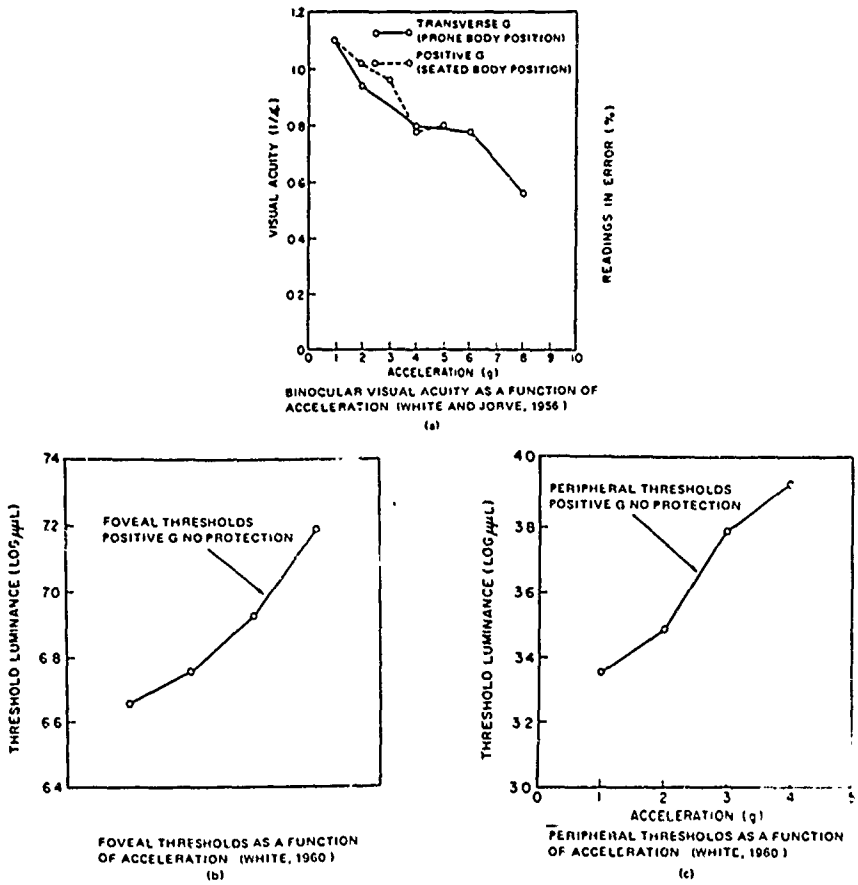


Figure 13–34. Binocular visual acuity as a function of transverse g-forces. Note that effect is independent of body position in these data. (White & Jorve, 1956)

*Sensory deprivation refers to the condition wherein the individual is kept in an environment with drastically reduced sensory input. Laboratory experiments in which subjects were immobilized (e.g., in a tank of water at skin temperature) and isolated from all visual and auditory stimuli, have led to bizarre behavior, hallucinations, delusions, etc. It is no longer believed that these phenomena are of any interest in biotechnology, even for extended interplanetary missions.

Vibration

Whole body vibration produces a loss in visual acuity and the accuracy of dial reading. The effects are related to the axis of vibration, the nature of the task, and the frequency, but appear to be relatively independent of the amplitude, at least over the range from 0.025 to 0.05 inches (Mozell and White, 1958). Recent studies have shown visual performance decrements to depend upon the kind of head restraint used (Taub, 1966) and the use of various helmet and liner combinations (Schoenberger, 1968). Y-axis vibration applied to the head alone (Rubinstein and Kaplan, 1968) shows acuity to be a U-shaped function of frequency, with poorest acuity in the range from 25 to 35 Hz. The same study showed that acuity gradually returns to normal as frequency is increased, and that the effect has vanished at 78 Hz. It should be noted that the decrement in acuity could be overcome by increasing the contrast of the resolution pattern used. The data for both constant acceleration ($1.0g_y$) and constant displacement (0.03 cm) are shown in figure 13-35.

Weightlessness

As it is impossible to simulate zero-g conditions in the laboratory, or for long periods in parabolic aircraft flights, the effects of prolonged weightlessness on vision are only imperfectly known. The existing data were collected on Gemini flights, GT5 and GT7, of approximately 7 and 14 days' duration, respectively. Visual acuity was the only task which was evaluated, and no significant differences were found between preflight, inflight, and postflight results (Duntley et al., 1968).

Hypoxia

The effects of oxygen lack on vision are well known from many studies. Some of the effects of G-forces may be attributed to the fact that blood supply to the head is diminished, and that an anoxia is thereby produced both in the retina and the visual cortex. The effects of oxygen lack on the visual threshold are exemplified by figure 13-36 (McFarland, 1946), which also shows the effect of cigarette smoking on this function.

Glare

Visual performance is degraded when a source of high luminance intrudes upon the field of view. The disability and discomfort which result are functions of the size and intensity of the glare source, and its position in relationship to the object of regard. Whether the glare source is small and intense, as when the sun is in the field of view, or large and diffuse, as in looking through a spacecraft window which is scratched or dirty and illuminated by a strong source, the effect is to reduce the apparent contrast of the desired object. The quantitative expression of glare is usually done in terms of an hypothetical uniform veiling luminance which would produce the same performance decrement, although this is at best only an approximation. (For a discussion, see LeGrand, 1957).

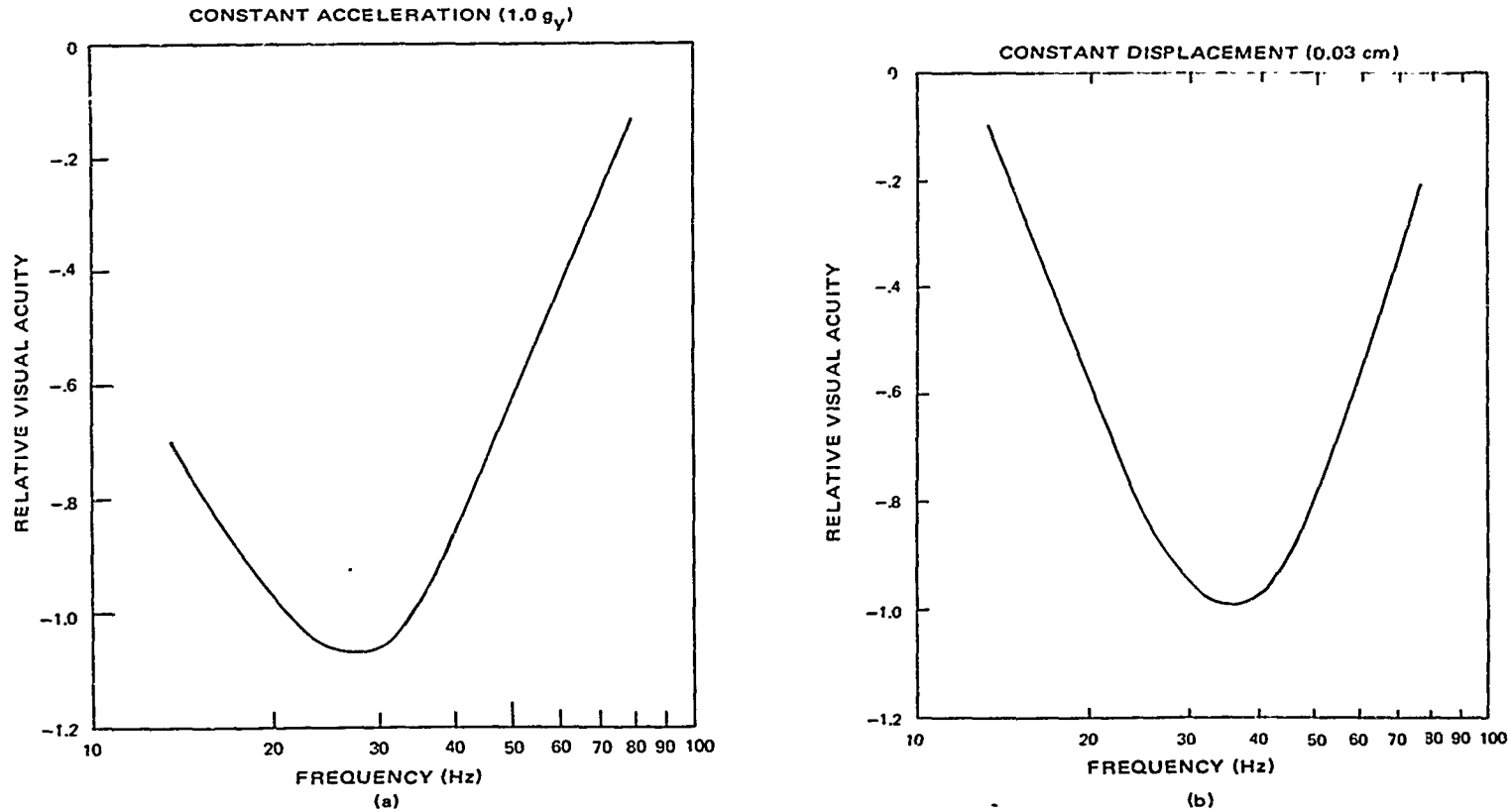


Figure 13–35. Vibration effects on visual acuity at (a) constant acceleration and (b) constant displacement. (Rubinstein & Kaplan, 1968)

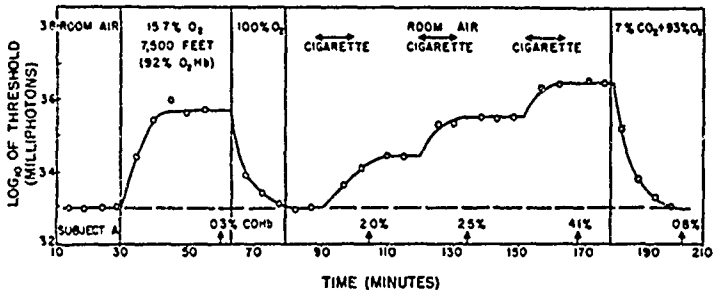


Figure 13–36. Effects of altitude, smoking, and oxygen inhalation on luminance sensitivity. (From *Human factors in air transport design* by R. A. McFarland. Copyright 1946 by The McGraw-Hill Book Company. Used by their permission)

Empty Fields and Low Luminance Levels

It has been noted that the refractive power of the resting eye changes significantly (in the direction of myopia) when the visual field is unstructured, as in a dense fog, or when the average luminance level is very low, as in dark night conditons. This effect is not insignificant, and typically results in refractive errors from 0.75 to 1.5 diopters in the negative direction. The importance of these phenomena in space operations is not clear except in the case of foglike atmospheres and darkened environments where no cues to distance exist. The empty field problem has been discussed by Whiteside (1954), and the night myopia effect by LeGrand (1967). The possibility of crew disorientation from this cause should be considered.

Flash Blindness

Momentary exposure to a very intense flash of light results in a loss of visual sensitivity which may take some time to be restored. Such exposures are likely to be accidental through loss of a protective visor, inadvertant looking at the sun, or chance reflections from the polished metal surfaces of space vehicles. Recovery time depends upon the intensity and duration of the flash and on the nature and luminance of the task of interest. For any given task, recovery time can be shortened by increasing the task luminance in the period immediately following the flash, as may be seen in figure 13-37. A detailed study of the flash blindness problem may be found in Brown (1965).

Visual Tasks in Space Operations

It is evident, from the experiences gained in manned spaceflight by both the United States and the USSR, that the human operator can be relied upon to perform a number of visually mediated tasks. The trend, therefore, has been toward giving the man ever greater responsibility in the conduct of

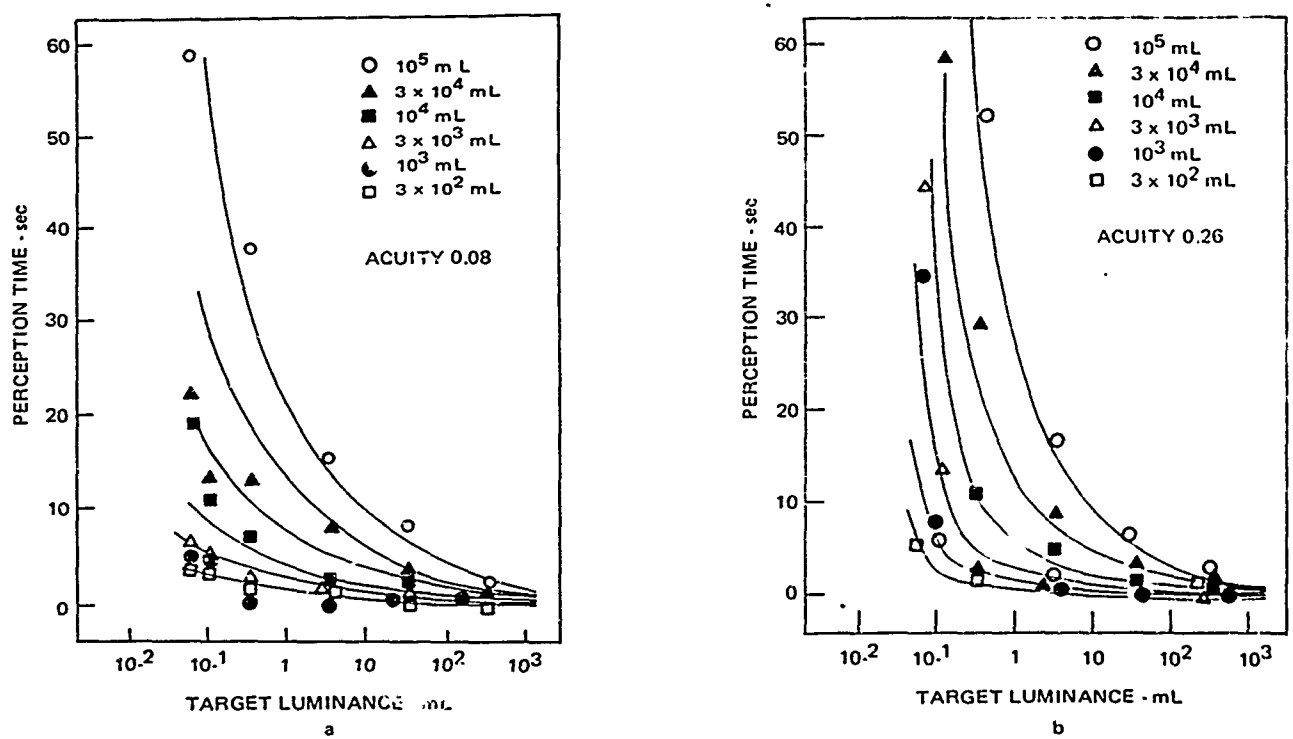


Figure 13–37. Recovery time in flash blindness. Ordinate values are times required to discriminate test objects after brief exposure to flash luminances indicated on the individual curves, for various values of luminance of target shown on abscissa. Correct discrimination required visual acuities of 0.08 (a) and 0.26 (b). Note that disabling effect of flash blindness at all levels used was overcome by use of sufficiently bright targets. (Brown, 1961)

space missions. It is now thought that any or all of the following activities will depend significantly upon vision, either in a primary sense, or in a backup mode:

1. Orientation, both personal and vehicular
2. Rendezvous and docking, including detection and interception; estimates of distance and closure rates
3. Navigation, including star tracking and angle measurements
4. Observation, from the upper atmosphere, of the Earth, other planets, and the Moon
5. Astronomical observations from space
6. Lunar surface observation from lunar orbit
7. Planetary surface observation from orbit
8. Lunar landing, including estimates of distances and closure rates
9. Observation of the lunar surface from the lunar surface
10. Planetary landing, including estimates of distance and closure rates
11. Translation on the lunar surface
12. Extravehicular maintenance and other activity.

The effects of certain environmental variables upon the ability of man to perform the above tasks, as well as the visual functions necessary in each, have been discussed by Taylor (1964), and that document should be referred to for detailed consideration of the list.

References

Allen, C. W. *Astrophysical quantities.* (2nd ed.) London: The Athlone Press, 1963.

Baker, H. D. Initial stages of light and dark adaptation. *Journal of the Optical Society of America*, 1963, *53*, 98-103.

Baker, C. A. & Steedman, W. C. Perceived movement in depth as a function of luminance and velocity. *Human Factors*, 1961, *3*, 166-173.

Baumgardt, E. & Segal. *Compt. Rend. Soc. Biol.*, 1946, *140*, 231.

Bedford, R. E. & Wyszecki, G. Axial chromatic aberration of the human eye. *Journal of the Optical Society of America*, 1957, *47*, 464-465.

Biberman, L. M., Dunkelman, L., Fickett, M. L., & Fink, R. G. Levels of nocturnal illumination. Research paper P-232, Institute for Defense Analysis, 1966.

Blackwell, H. R. Contrast thresholds of the human eye. *Journal of the Optical Society of America*, 1946, *36*, 624-643.

Blackwell, H. R., & McCready, D. W., Jr. Foveal contrast threshold for various durations of single pulses. USN BuShips Contract NObs 72038, ERI Report No. 2455-13-F, University of Michigan, 1958.

Blackwell, H. R., & Taylor, J. H. Consolidated set of foveal contrast discrimination data for normal binocular vision. *Journal of the Optical Society of America*, 1970, *60*, 736A. (Full paper in press)

Boring, E. G., Langfield, H. S., & Weld, H. P. *Foundations of psychology*. New York: John Wiley & Sons, 1948.

Brown, D. R. E. Natural illumination charts. USN BuShips Report No. 374-1, 1952.

Brown, J. L. Flash blindness. *General Electric Technical Information Series*, 61SD129, November 1961.

Brown, J. L. Flash blindness. *American Journal of Ophthalmology*, 1965, *60*, 505-520.

Brown, R. H. Weber ratio for visual discrimination of velocity. *Science*, 1960, *131*, 1809-1810.

Burns, N. M., Chambers, R. M., & Hendler, E. (Eds.) *Unusual environments and human behavior*. Glencoe: The Free Press, 1963.

Chapanis, A. How we see. In a survey report of human factors in undersea warfare. Prepared by the Panel on Psychology and Physiology of the Committee on Undersea Warfare of the National Research Council. Washington: NRC, 1949.

Cobb, P. W., & Moss, F. K. Four fundamental factors in vision. *Transactions of the American Illuminating Engineering Society*, 1928, *23*, 496.

Committee on Colorimetry, Optical Society of America *The science of color*. New York: Thomas Y. Crowell, 1953.

Conner, J. P., & Ganoung, R. E. An experimental determination of the visual thresholds at low values of illumination. *Journal of the Optical Society of America*, 1935, *25*, 287-294.

Davies, J. M., & Randolph, D. T. (Eds.) *Proceedings of the U.S. Army Natick Laboratories flash blindness symposium*. NAS-NRC Committee on Vision, Washington, 1967.

Davson, H. (Ed.) *The eye*. New York: Academic Press, 1962.

Duntley, S. Q. Final report of Contract N5ori-07864 MIT, Scripps Institution of Oceanography, 1952.

Duntley, S. Q. Improved nomographs for predicting visibility by swimmers. Report No. 5-3, USN BuShips Contract NObs 72039, 1960.

Duntley, S. Q., Austin, R. W., Harris, J. L., & Taylor, J. H. Experiments on visual acuity and the visibility of markings on the ground in long-duration earth-orbital space flight. Report No. 68-8, University of California, Scripps Institution of Oceanography, 1968.

Duntley, S. Q., Gordon, J. I., Taylor, J. H., White, C. T., Boileau, A. R., Tyler, J. E., Austin, R. W., & Harris, J. L. Visibility. *Applied Optics*, 1964, *3*, 549-598.

Ferree, C. E., & Rand, G. The effect of variation of visual angle, intensity, and composition of light on important visual functions. *Transactions of the American Illuminating Engineering Society*, 1922, *17*, 69-102.

Gibson, J. J. *The perception of the visual world*. Cambridge: The Riverside Press, 1950.

Gordon, J. I. Optical properties of objects and backgrounds. *Applied Optics* 1964, *3*, 556-562.

Graham, C. H., & Kemp, E. H. Brightness discrimination as a function of the duration of the increment in intensity. *Journal of General Physiology* 1938, *21*, 635-650.

Graham, C. H., Bartlett, N. R., Brown, J. L., Hsai, Y., Mueller, C. G., & Riggs, L. A. (Eds.) *Vision and visual perception*. New York: John Wiley & Sons, 1966.

Graham, C. H. (Ed.) *Vision and visual perception*. New York: John Wiley & Sons, 1965.

Haines, R. F. Size matching accuracy under very high target luminances. Published in Proceedings of 1967 Aerospace Medical Association Meeting, Washington, D.C., April 10-13, 1967, Pp. 278-279.

Hall, M. V., & Greenbaum. L. J., Jr., Area of vision and cockpit visibility. *Transaction of the American Academy of Ophthalmology and Otolaryngology* September-October, 1950.

Hartridge, H. *Recent advances in the physiology of vision*. Philadelphia: Blakiston, 1950.

Hecht, S., & Verrijp, C. D. Intermittent stimulation by light. III: The relation between intensity and critical fusion frequency for different retinal locations *Journal of General Physiology*, 1933, *17*, 251-265.

Holladay, L. L. The fundamentals of glare and visibility. *Journal of the Optical Society of America*, 1926, *12*, 271-319.

Ivanoff, A. Chromatic aberration of the eye. *Documents of Ophthalmology*, 1949, *3*, 322-323.

Jayle, G.-E., & Ourgaud, A.-C *La vision nocturne et ses troubles*. Paris: Masson et Cie, 1950.

Jones, L. A., & Condit, H. R. Brightness scale of exterior scenes and the computation of correct photographic exposure. *Journal of the Optical Society of America*, 1941, *31*, 651.

Jones, R. L. An investigation of earthshine lighting conditions for lunar-surface operations. NASA Technical Memorandum TM X-58011, 1967.

Jones, W. L., Allen, W. H., & Parker, J. F. Advanced vision research for extended spaceflight. *Aerospace Medicine*, 1967, *38*, 475-478.

Kaufman, J. E. (Ed.) *I.E.S. Lighting handbook*. New York: Illuminating Engineering Society, 1966.

Kinney, J. S., & Connors, M. M. Recovery of foveal acuity following exposure to various intensities and durations of light. *American Journal of Psychology*, 1965, 432-440.

Kishto, B. N. The photometric evaluation of flashing light sources. PhD Thesis, University of London, 1968.

Koval, I. K. On the study of the optical properties of the atmosphere and surface of Mars. In I. K. Koval (Ed.), *Physics of the moon and planets*. Kiev: Naukova Dumka. (Translation by Israel Program for Scientific Translations, Ltd., IPST Catalogue No. 1548, Jerusalem 1964.)

Krinov, E. L. Spectral reflectance properties of natural formations. *USSR Academy of Science*, Translation by G. Belkov, National Research Council of Canada, 1947.

Kuiper, G. P. *The earth as a planet*. Chicago: The University of Chicago Press, 1954.

LeGrand, Y. *Light, colour and vision*. New York: John Wiley & Sons, 1957.

LeGrand, Y. *Form and space vision*. Bloomington:Indiana University Press, 1967.

Ludvigh, E. J., & Miller, J. W. Study of visual acuity during the ocular pursuit of moving test objects. I., Introduction. *Journal of the Optical Society of America*, 1958, *48*, 799-802.

MacAdam, D. L. Visual sensitivities to color differences in daylight. *Journal of the Optical Society of America*, 1942, *32*, 247-274.

Mandelbaum, J., & Sloan, L. L. Peripheral visual acuity. *American Journal of Ophthalmology*, 1947, *30*, 581-588.

McFarland, R. A. *Human factors in air transport design*. New York: McGraw-Hill, 1946.

Meyer-Arendt, J. R. Radiometry and photometry: Units and conversion factors. *Applied Optics*, 1968, *7*, 9-12.

Middleton, W. E. K. *Vision through the atmosphere*. Toronto: The University of Toronto Press, 1952.

Miller, J. W. Study of visual acuity during the ocular pursuit of moving test objects. II. Effects of direction of movement, relative movement, and illumination. *Journal of the Optical Society of America*, 1958, *48*, 803-808.

Moon, P. *The scientific basis of illuminating engineering*. (Rev. ed.) New York: Dover Publications, 1961.

Morris, A., & Horne, E. P. (Eds.) *Visual search techniques*. NAS-NRC Publication No. 712, 1960.

Mozell, M. M., & White, D. C. Behavioral effects of whole body vibration. *Journal of Aviation Medicine*, 1958, *29*, 716-724.

Østerberg, G. Topography of the layer of rods and cones in the human retina. *Acta Ophthalmology*, 1935, *13*, Supplement 6.

Patel, A. S., & Jones, R. W. Increment and decrement visual thresholds. *Journal of the Optical Society of America*, 1968, *58*, 696-699.

Reeves, P. Rate of pupillary dilation and contraction. *Psychology Review* 1918, *25*, 330.

Rennilson, J. J., Holt, H. E., & Morris, E. C. *In situ* measurements of the photometric properties of an area on the lunar surface. *Journal of the Optical Society of America*, 1968, *58*, 747-755.

Rubinstein, L., & Kaplan, R. Some effects of Y-axis vibration on visual acuity. USAF AMRL-TR-68-19, 1968.

Schlaer, S. The relation between visual acuity and illumination. *Journal of General Physiology*, 1937, *25*, 553-569.

Schober, H. Neuere untersuchungen über sehscharfe, auflosungsvermögen der optischen instrumente und besonders des menschlichen auges. *Zeitschrift für Physik*, 1937, *19*, 343-344.

Schober, H., & Wittman, K. Untersuchungen über die sehscharfe bei verschiedenfarbigen licht. *Das Licht* 1938, *8*, 199-201.

Schoenberger, R. W. Investigation of the effects of vibration on dial reading performance with a NASA prototype Apollo helmet. USAF AMRL-TR-67-205, 1968.

Shoemaker, E. M., Bateson, R. M., Holt, H. E., Morris, E. C., Rennilson, J. J., & Whitaker, E. A. Surveyor V: Television pictures. *Science*, 1967, *158*, 642-652.

Sloan, L. L. Rate of dark adaptation and regional threshold gradient of the dark-adapted eye. Physiologic and clinical studies. *American Journal of Ophthalmology*, 1947, *30*, 705-719.

Spector, W. S. (Ed.) *Handbook of biological data*. Philadelphia: W. B. Saunders Co., 1956.

Spigal, I. M. (Ed.) *Readings in the study of visually perceived movement*. New York: Harper & Row, 1965.

Stiles, W. S. The directional sensitivity of the retina and the spectral sensitivities of the rods and cones. *Proceedings of the Royal Society*, (London), 1939, *127B*, 64-105.

Stiles, W. S., & Crawford, B. H. The luminous efficiency of rays entering the pupil at different points. *Proceedings of the Royal Society*, (London), 1933, *B 116*, 428-450.

Taub, H. A. Dial reading performance as a function of frequency of vibration and head restraint system. USAF AMRL-TR-66-57, 1966.

Taylor, J. H. Contrast thresholds as a function of retinal position and target size for the light-adapted eye. USN BuShips Contract NObs 72092, REport No. 61-10, 1961.

Taylor, J. H. Survey of research relating to man's visual capabilities in space flight. USN Contract NObs 86012, Final report, Lot III, 1964.

Taylor, J. H. Visual performance on the moon. In F. J. Malina (Ed.), *Life sciences and lunar medicine*. Oxford: Pergamon Press, 1967.

Taylor, J. H. Factors underlying visual search performance. S.I.O. Ref. 69-22, Pp. 23, University of California, San Diego, 1969.

Wald, G., & Griffin, D. R. The change in refractive power of the human eye in dim and bright light. *Journal of the Optical Society of America*, 1947, 37, 321-336.

Walsh, J. W. T. *Photometry*. London: Constable, 1958.

Whiteside, T. C. D. *The problems of vision in flight at high altitude*. London: Butterworth's, 1957.

White, W. J. Vision. In P. Webb (Ed.), *Bioastronautics data book*. Washington: National Aeronautics and Space Administration, 1964.

White, W. J., & Jorve, W. R. The effects of gravitational stress upon visual acuity. WADC Technical Report 56-247, Wright Air Development Center, Wright-Patterson Air Force Base, Ohio, 1956.

White, W. J., & Monty, R. A. Vision and unusual gravitational forces. *Human Factors*, 1963, 5, 239-262.

Wilmer, E. N. *Retinal structure and colour vision*. Cambridge: University Press, 1946.

Wright, W. D. *Researches on normal and defective colour vision*. St. Louis: C. V. Mosby Co., 1947.

Wright, W. D., & Pitt, F. H. G. Hue discrimination in normal colour vision. *Proceedings of the Physical Society*, (London), 1934, *46*, 459.

Wulfeck, J. W., & Taylor, J. H. (Eds.) *Form discrimination as related to military problems*. NAS-NRC Publication No. 561, 1957.

CHAPTER 14
AUDITORY SYSTEM

by

Harlow W. Ades, Ph.D.
University of Illinois

The importance of effective communication cannot be overstated. Progress in all facets of civilization depends on the exchange of ideas, messages, and commands. The orderly flow and management of information has become a *sine qua non* in all the complex activities of a modern world.

Communications, whether occurring between humans in normal day-to-day association or occurring during the operation of complex man-machine systems, depend primarily on the auditory and visual systems. This chapter deals with the former. In designing any system in which communications plays some part, the unique characteristics of any auditory system must be considered. An understanding of its structure and eccentricities will allow this receptor system to be matched with other system elements to achieve efficient system design. However, the responsibility of the designer does not end here. He must attend not only to system efficiency but to the impact of system operation on the environment of which it becomes a part. In this regard, noise pollution has become an issue of major concern. While noise-free systems are usually not feasible, the design engineer still bears the responsibility for understanding the noise characteristics of his system and their likely effects on audition.

This chapter is divided into three major sections. The first deals briefly with the physical correlates of hearing, i.e., the acoustic stimulus. In working with a psychophysical phenomenon such as hearing, one must be able to define and measure the stimulus parameters with precision since the stability of measurement for any psychophysical relationship generally comes from the physical (or stimulus) side; however, the reader is referred to other recent works for most of the detail.

The second section describes in some detail the auditory system itself. Here one is confronted with the time-honored question, "How much information should a designer have concerning the morphology and neurology of a body

Reviewed by William D. Neff, Ph.D., Indiana University

Preceding page blank

system in order to work with it effectively?" Although it is possible to work in a system design dealing only with input-output relationships, a certain level of sophistication concerning system elements will provide confidence to the designer if nothing else. Here again, except for the inner ear itself, the reader is referred to recent works on the subject.

The third section of this chapter presents recent data concerning hearing loss and structural change caused by carefully controlled over-stimulation of the auditory system. The main purpose of this section is to provide information concerning the physiological response of the auditory system, as evidenced by physical damage. The section serves further as a caution against subjecting the auditory system to stimulation for which it was not designed. It also sets the stage for the next chapter which deals with the response of the auditory system under conditions of noise and overload.

Physical Correlates of Hearing

Hearing is the sum total of the transmission of sound from the external environment to the brain. It involves the conversion of mechanical impulses to neural impulses, the transmission of these impulses to the brain, and their "perception" by the brain. The sensation of airborne sound is produced when vibrations of the molecules of air strike the ear drum in alternating phases of condensation and rarefaction. A graph of these movements as changes in pressure on the tympanic membrane per unit of time shows a series of waves. The speed of sound increases with temperature and with altitude. Water also conducts sound, at speeds over four times as fast as air (775 mph versus 3215 mph), but here we are concerned mostly with airborne sound. The loudness of a sound correlates with the amplitude of a sound wave. The pitch of a sound correlates with the frequency or number of waves per unit of time, with greater amplitude meaning louder sound and greater frequency, i.e., higher pitch.

The presence of one sound decreases an individual's ability to hear other sounds. This phenomenon is known as masking. It is believed to be due to the relative or absolute refractoriness of previously stimulated auditory receptors. The degree to which a given tone masks other tones is related to its frequency. (For curves of masking effect as a function of frequency, see chapter 15, *Noise and Blast.*) The masking effect of a background noise raises the auditory threshold a definite and measurable amount.

In describing an auditory stimulus, one must specify the frequency of the sound and its intensity. When dealing with pure tones, frequency is expressed as "cycles per second" or the preferred synonymous term "Hertz" (Hz). The intensity of a sound wave is a function of the amplitude of the wave and is measured in pressure units. Three terms are widely used in referring to intensity. These are decibels (dB), perceived noise (PNdB), and effective perceived noise (EPNdB).

The decibel is based on the ratio of the acoustic energy being measured to a reference energy. The standard sound reference level adopted by the Acoustical

Society of America is 0.0002 dynes per square centimeter, a value just at the auditory threshold for the average human. The ratio of the two energy or intensity measures is transformed into a logarithmic scale for greater manageability. A value of zero decibels does not mean the absence of sound, but a sound level equal to that of the arbitrary standard, the least sound the average human ear can hear. Zero to 140 dB, a range extending from threshold intensity to an intensity generally assumed to be painful to the ear, actually represents a 10^{14} or 100 million million-fold increase in sound intensity.

The perceived noise (PNdB) is a calculated unit used to express unwanted or unacceptable sound; that is, noise. The unit, used frequently to describe aircraft noise, is calculated by combining actual sound level with a weighted annoyance factor based on a variation in frequencies since some frequencies are more troublesome to the human ear than others. Kryter (1970) feels that the relationship between the sound pressure level and judged perceived noisiness, or annoyance, as a function of the frequency content of random noise is reasonably well established. Frequency weightings for noisiness and for loudness given by a number of investigators are in close agreement. Weightings given by Stevens' loudness index contours (1961) are similar to the equal noisiness contours developed by Kryter and Pearson (1963), and Wells (1967).

The effective perceived noise decibel (EPNdB) is also a calculated unit, which is little used, and which carries the weighting concept further by accounting for the effects of pitch and duration of noise.

A concept which is gaining rapidly in usefulness is the use of the noise exposure forecast (NEF) in conjunction with the compatible noise exposure limit (CNEL). In these terms, the noise around an airport, for example, may be expressed. All of the foregoing terms are expressed in the NEF which can be monitored and checked periodically and, in addition, can be predicted for the future by computer calculation. Kryter (1970) describes these terms in much more detail.

The Auditory System

The process of sound transmission can be very briefly summarized as follows. Sound waves impinge upon the tympanic membrane and are transformed by this organ and the bones of the middle ear into mechanical waves, and, by the action of the footplate of the stapes into fluid-borne waves, since the inner ear is fluid-filled. The action of these waves on the organ of hearing proper, the organ of Corti, in the inner ear, triggers impulses in nerve fibers which supply the organ. These nerve fibers transmit coded information regarding sound to the brain.

The audible range of frequencies for humans is generally given as 20 to 20 000 Hz, though few individuals can hear as high as 20 000. In other animals, much higher frequencies can be heard. The greatest sensitivity is in the range of 1000 to 3000 Hz. Pitch discrimination is less sensitive at frequencies outside this range.

stapes. These bones functionally connect the ear drum with the inner ear, transmitting the waves imposed on the drum across the middle ear to the footplate of the stapes which rocks to and fro, delivering the agitation to the perilymph of the cochlea.

The ear bones of the middle ear function as a lever system. A small mechanical advantage is gained because the handle of the malleus is longer than the long crus of the incus. Much more important, however, is the ratio of the area of the tympanic membrane to the footplate of the stapes at the oval window. This ratio is effectively 14 to 1, and corresponds to an increase of 23 dB. The total force at the oval window is about the same as at the tympanic membrane, but it is concentrated in a much smaller area. Pressure exerted on the fluid of the inner ear is therefore only 3 to 5 dB less than that exerted by the sound pressure wave on the tympanum.

The Inner Ear

The inner ear is a closed fluid-filled chamber. It communicates with the middle ear at the oval and round windows (see figure 14-1). The oval window, closed by the stapes which is fixed by means of an annular ligament, links the middle ear with the vestibule of the inner ear. The round window provides the means of relieving the pressure imparted to the cochlea by connecting the middle ear with the basal turn of the cochlea through a flexible membrane. The cochlear wall is rigid and incompressible.

The cochlear partition, including basilar membrane and Reissners' membrane, ends a little short of the apical end of the cochlear canal. There the scala vestibuli and the scala tympani join through the helicotrema while the cochlear duct ends blindly. At the other end of the scala tympani is the round window. The scala vestibuli opens into the central chamber of the labyrinth, the vestibule, close to the oval window. The length of the cochlear partition in man, from its origin between the oval and round window to the helicotrema, is about 35 mm. The sensory surface of the cochlea is thus a long narrow ribbon, coiled in spiral form, mounted on an elastic membrane, between two fluid-filled channels. This membrane is moved by the fluid which is driven acoustically at the oval window by the stapes.

The Organ of Corti

The organ of Corti occupies the cochlear duct between the scala vestibuli and the scala tympani (see figure 14-2a). The cochlear duct is bounded by the thin vestibular (Reissners') membrane and the basilar membrane on which the organ of Corti is situated. The organ of Corti, otherwise known as the acoustic papilla, consists of hair cells, supporting structures, and nerve endings, the hair cells being the sound sensitive elements (figure 14-2b).

The organ of Corti is divided by one variety of the supportive elements, the inner and outer pillar cells, which slant toward each other to meet at the free

surface, forming a triangular space, the tunnel of Corti. On the medial (modiolar) side of this, the inner hair cells are situated, and on the outer side are the three rows of outer hair cells. The pillar cells are stiffened by bundles of tonofibrils. The outer hair cells reach the surface of the epithelium, but not the base, being supported underneath and held in place above by the phalangeal cells (also called Deiters' cells). Outside the outer tunnel is a solid bank of less differentiated cells, the cells of Hensen. These gradually diminish in height to merge with the cells of Claudius which form a simple epithelium merging, in turn, with the stria vascularis at the side of the cochlear duct.

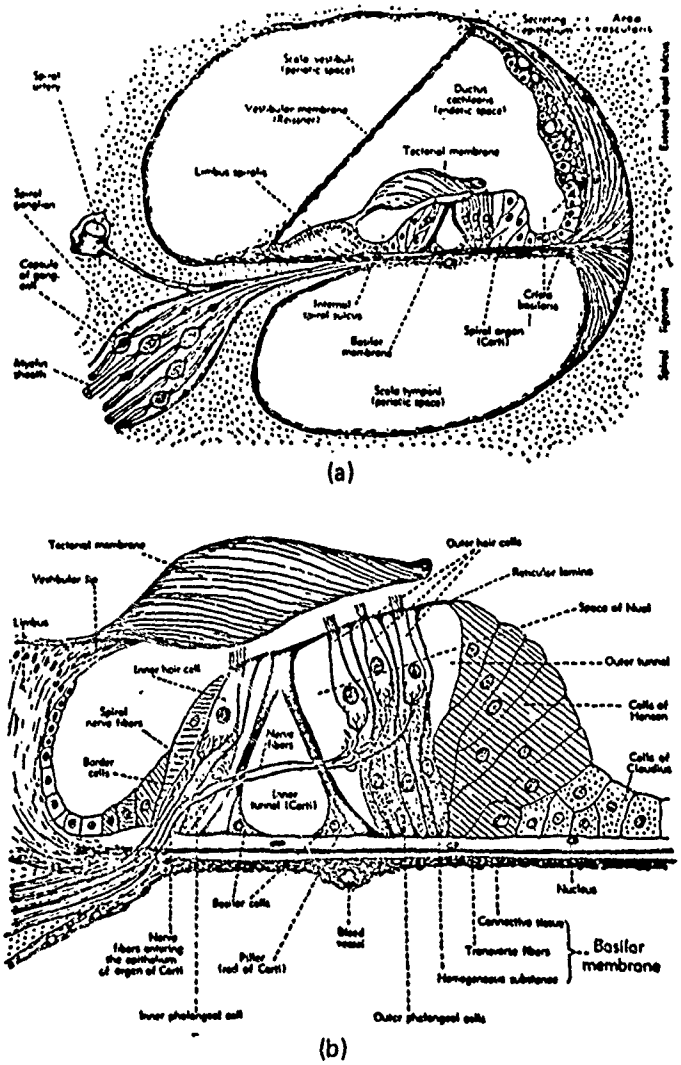


Figure 14–2. A: Drawing of section through one turn of cochlea. B: Enlarged drawing of section of acoustic papilla showing all essential parts. (From Rasmussen, 1943)

Medial to the inner hair cells is a comparable, though more abrupt, bank of cells which are called border cells, and which diminish rapidly to a simple epithelium composed of cuboidal cells comparable to the cells of Claudius, covering the surface of the limbus spiralis. The limbus has a projection, the tectorial membrane, an acellular organ which extends outward, covering, and in contact with, the hairs of the hair cells.

The structure of the organ of Corti might be summed up as being an organization in which the hair cells are suspended in a fluid-filled space supported by their accessory cells, sitting on a membrane (basilar membrane) which is capable of passive movement, and covered by a membrane (tectorial membrane) which is capable of exerting a shearing action on the tips of the hairs upon such movement. The space in which the hair cells hang is open throughout the length of the organ of Corti. It is filled with a fluid, the cortilymph, and it is covered top and bottom by the surfaces of hair cells and phalangeal cells, and by the basilar membrane. This is significant because the electric potential of the endolymph within the cochlear duct, according to Davis (1959), has been determined to be +80 relative to the cortilymph, which is -70, which means about a 150 mV differential.

The organ of Corti is the organ by which the complex sound waves are analyzed into their component frequencies. A mechanical disturbance beginning at the oval window becomes a wave which moves from the base to the apex of the cochlea along the basilar membrane. This in turn moves the entire acoustic papilla in such a way that a shearing force is exerted on the hairs by their motion against the tectorial membrane. In some way, this is translated into excitation of the hair cells, which is transmitted to the nerve endings at the base of the cells, and transmission of what are now no longer mechanical, but electrical impulses to the brain.

The Basilar Membrane

The basilar membrane (figure 14-2b) has distinct properties which enable it to participate in the analysis of complex sounds. First, the membrane is much wider at the apex than at the base, the ratio being between five-fold and eight-fold in man (Wever, 1949). This characteristic is related to the fact that the membrane is a low-pass filter, permitting low frequency sounds to travel further along than high frequency sounds. The question of how sound waves move along the membrane was once thought to be explained by a theory that suggested that the entire membrane resonated. This theory presupposed that the membrane was under tension, which has been proven not to be the case. The membrane does, however, vary in stiffness along its length, and is about one hundred times stiffer at the basal than at the apical end (Bekesy, 1947). This characteristic is the one primarily responsible for movement of energy waves.

Relying on mechanical models, Bekesy (1960) determined that when periodic forces are applied to a system with a stiffness gradient, traveling waves are generated. He had earlier demonstrated the existence of such waves in the cochlea by stroboscopic illumination. Figure 14-3 shows the amplitude and

phase relations of the vibrating membrane at various points. At low frequencies, the membrane vibrates in phase. At higher frequencies, the rate of change in phase increases with distance. The result is a wave train of several cycles. Also as frequency is increased, the amplitude envelope, described by the dotted lines in figure 14-3, moves toward the basal end of the basilar membrane.

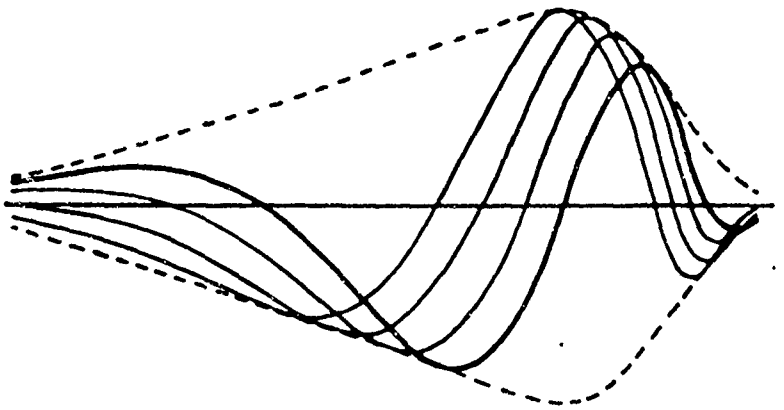


Figure 14–3. Successive positions of the traveling wave along the basilar membrane. The dotted envelope shows the maximum amplitude of vibration at each point. (From Whitfield, 1967; after Bekesy, 1953)

One final point should be made concerning propagation of waves along the basilar membrane. Although the waves always travel from the base to the apex, this property is independent of the direction of the mechanical driving force. If this were not the case, conduction of sound through the bones of the skull, bypassing the stapes entirely, would not be possible. The driving force results from pressure changes in the fluid surrounding the cochlear duct; it is not provided directly by movement of the stapes. This has been confirmed experimentally by Wever and Lawrence (1954); however, since the time of transmission of waves along the entire length of the cochlea is only 10 to 20 msec, any pressure is applied almost simultaneously to all points along the length of the membrane, setting a considerable fraction of the membrane in motion.

Hair Cells

The ear converts sound waves to nerve impulses. It is relatively clear how sound waves become mechanical vibrations of the basilar membrane and that nerve impulses are generated in the cochlear nerve. The transducer mechanism involves the hair cells of the organ of Corti, but how it does so is a more difficult question. These cells are illustrated diagrammatically in figure 14-2, as they appear to the scanning microscope (figure 14-4), and when specimens have been prepared by the surface specimen technique (Engström, Ades, & Andersson, 1966) as seen in figure 14-5. The sensory cells are known as hair cells because of

the tufts of stereocilia which extend from the free ends of the cells. The cilia are embedded in the cuticle and make contact with the overlying tectorial membrane. There are some 25 000 hair cells in the human ear (Guild, 19..) which are arranged in a regular mosaic as a single row of inner hair cells and three to five rows (the number increases toward the apical end of the cochlea) of outer hair cells.

Reproduced from best available copy.

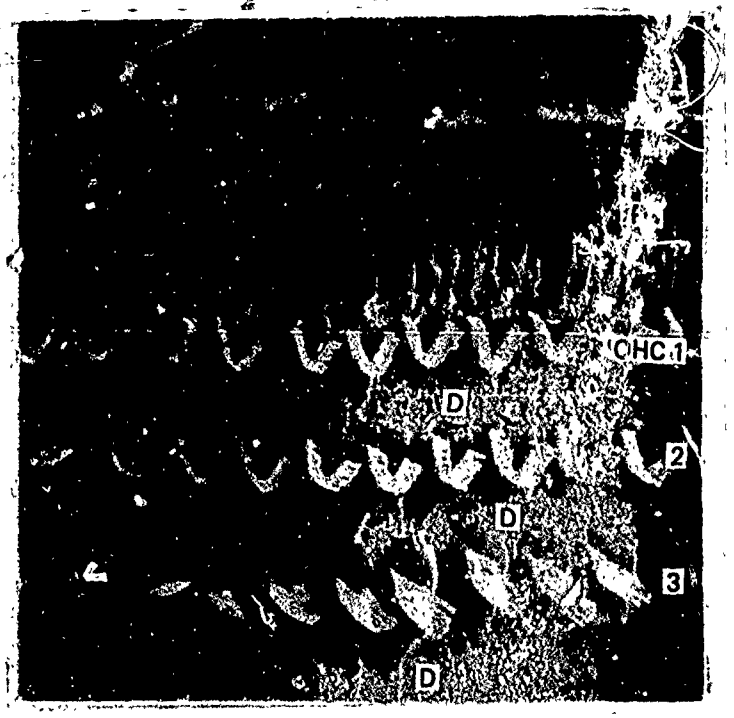


Figure 14–4. Scanning photomicrograph of a segment of organ of Corti of guinea pig. IHC= inner hair cell row; OHC 1, 2, 3 = outer hair cell rows as numbered; PC = pillar cells; D = Deiters' (phalangeal) cells.

Inner Hair Cells

The upper surface of the inner hair cell is bounded by a membrane with an underlying cuticle in which the roots of the stereocilia are embedded. The stereocilia have different lengths and form three or four slightly irregular lines. Each inner hair cell is provided with a single basal body placed at the side of the rows of stereocilia away from the modiolus. The inner hair cells have a characteristic shape with a relatively slender upper portion terminating in the cuticular plate, a bent neck and a thicker cell body containing the nucleus. They are slanted toward the tunnel of Corti (figure 14-2b).

Reproduced from best available copy.

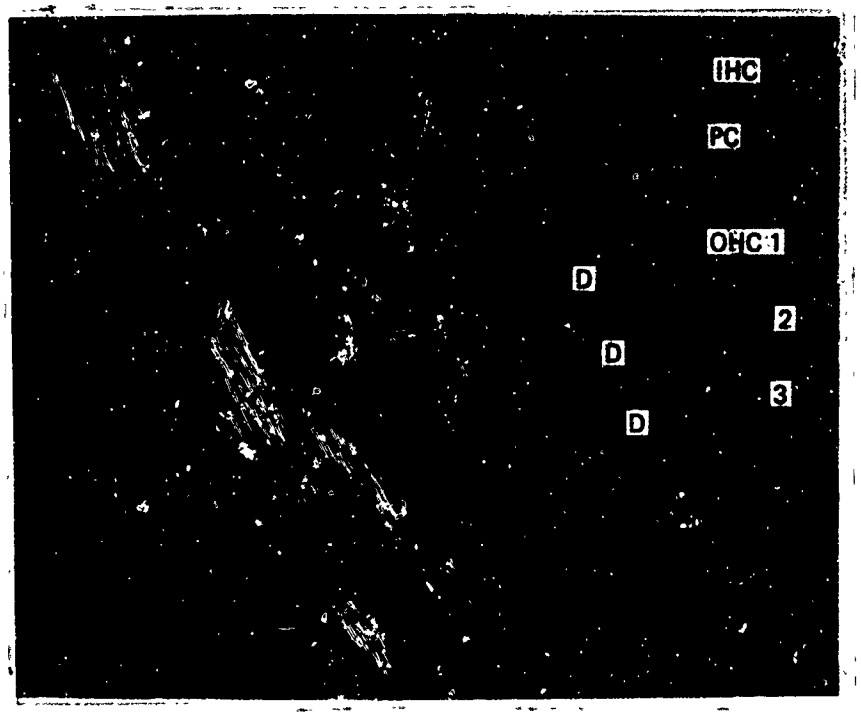


Figure 14–5. Surface preparation of organ of Corti of guinea pig. Symbols as in Figure 14–4.

Outer Hair Cells

The outer hair cells form three regular rows. They slant inward, that is, toward the modiolus, at an angle of 25 to 30 degrees (figure 14-2b). They have a flat upper surface with a thick cuticle, a cylindrical body, and a rounded base. It is customary to distinguish a cuticular, an infracuticular, a supranuclear, and an infranuclear region. On their cuticular surfaces the cells are provided with about 120 stereocilia and one modified kinocilium consisting only of the basal body. The stereocilia of the outer hair cell form a regular W-pattern with a basal body located below the W (figure 14-4). The angle between the outer ends of the W is wide (120 to 130 degrees) in the basal coil of the cochlea and narrows gradually to about 70 degrees in the apical coil. The rootlets of the stereocilia are inserted in the cuticular plate which is thicker toward the modiolus and thinner toward the basal body. Surrounding the basal body is a region where there is no cuticular plate at all, but only a plasma membrane. The infracuticular region contains many mitochondria and other organelles grouped around the basal body. Among these structures are rounded granules containing osmiophilic particles which increase in size in old animals and animals that have been exposed to intense noise (Engström, & Ades, 1960).

The central part of the supranuclear region is rather homogeneous in structure containing few mitochondria or cytoplasmic organelles. The nucleus is rounded or slightly ovoid in shape. The infranuclear region contains large groups of mitochondria. The base of the hair cell is surrounded by the cup-shaped Deiters' cell and by the nerve endings. The cochlear sensory cells are provided with two kinds of nerve endings at their base. One type has a centripetal or afferent, and the other a centrifugal or efferent, conducting property (figure 14-6). The afferent fibers form a major part of the acoustic nerve and consists of a large number of myelinated fibers, their myelin sheaths being continuous with the myelin coating of the spiral ganglion cells. This sheath continues along the peripheral dendrite of the neuron to the region immediately below the medial attachment of the basilar membrane where the myelin ends.

Each ganglion cell in the spiral ganglion is surrounded by a distinct myelin coating. The myelin of the ganglion cell is much less regular than that of the nerve. The myelin coating is externally bordered by the nuclear region of the Schwann cell. After prolonged treatment with neomycin, the ganglion cells demonstrate varying stages of degeneration and the myelin and Schwann cells show a highly pathological structure with irregular myelin folds and vacuolated mitochondria. Similar severe destruction may also occur after exposure to high intensity noise.

At the outer margin of the spiral osseous lamina the myelinated nerves all shed their myelin sheaths within a very restricted zone. The Schwann cell protoplasm follows the nerve fibers all the way to the basilar membrane whereas the nerve fibers, surrounded only by their axolemma, penetrate the basal layer and enter the organ of Corti where they run as unmyelinated fibers.

Innervation of Hair Cells

The afferent neurons of the auditory nerve are bipolar cells. They are arranged in a long spiral ganglion parallel to the organ of Corti but within the bony modiolus. The axon-like dendritic processes pass outward through the sieve-like bony and fibrous habenula perforata into the organ of Corti. They are myelinated up to the habenula. Some of them pass directly to the inner hair cells, innervating the outer hair cells. There is a spiral bundle under each row of outer hair cells. These fibers may then pass great distances in the spiral bundle and innervate many outer hair cells. Thus there is a great difference between the innervation of inner hair cells and outer hair cells. The inner hair cells are innervated directly – no fiber passes to more than three to six cells and no cell is innervated by more than three to six fibers. The outer hair cells may be innervated by fibers which pass for considerable distances under them, and great segments of outer hair cells may be innervated by the same fiber. Each cell receives typically more than one fiber.

Reproduced from best available copy.



Figure 14–6. Electron photomicrogram of base of outer hair cell (OHC) with two kinds of nerve endings, NE1 and NE2. Dc is a part of a Deiters' cell. (Engström, Ades, and Hawkins, 1965; used by permission of Academic Press, Inc. Copyright 1965 by Academic Press, Inc.)

In addition to the afferent fibers, an efferent olivo-cochlear bundle runs lengthwise of the organ of Corti as the intraganglionic bundle within the modiolus just peripheral to the spiral ganglion. These fibers end as highly granulated endings on the base of the hair cells. Some of them may end as well on afferent fibers. There are fewer of them than there are hair cells

innervated, so that each one ends on many hair cells. They innervate particularly the inner hair cells and the first row of outer hair cells. Their function is not well known, but is tentatively assumed to be inhibitory.

A detailed explanation of the physiology of the central auditory pathways is beyond the scope of this chapter. For additional information, the reader is referred to the chapter entitled "Central Auditory Mechanisms" in the *Handbook of Physiology* (Ades, 1959).

Transducer Mechanisms

The ear, as stated above, converts the mechanical energy of sound waves to nerve impulses in the auditory nerve. It is clear that the basilar membrane of the organ of Corti is displaced as a result of the force imparted to the fluid in the inner ear by the action of the stapes moving in and out at the oval window. It is also clear that nerve impulses are discharged in the nerve endings surrounding the base of the hair cells. The mechanism of stimulation of the hair cells is not known, although it is now generally assumed that a shearing force is exerted by the tectorial membrane on the stereocilia and that this somehow results in stimulation. It may be because of the displacement imparted by the stereocilia to the basal body, the residue of the kinocilium, which is all that remains on cochlear hair cells (although a kinocilium is present on vestibular hair cells and fetal cochlear hair cells).

The phenomena of electrical potentials associated with the cochlea during stimulation and at rest are germane to this discussion, but not to the main emphasis of this chapter. For the interested reader, they are summed up in Davis' (1959) chapter in the *Handbook of Physiology*.

Hearing Loss

Damage to or lesions of any one or several elements of the hearing chain can result in reduced or complete loss of sensitivity to sounds of various frequencies. This loss of sensitivity, referred to as threshold shift, is treated in some detail in chapter 15. In this section we shall discuss some of the physiological changes which accompany hearing loss. Loss of hearing can be either temporary or permanent and is considered, practically speaking, total when the threshold is 85 to 90 dB above normal.

Two broad types of hearing loss are generally identified. These are conductive hearing loss and perceptive hearing loss. Hearing loss that is hysterical in origin will not be treated here, since obviously there is no question of demonstrable damage. Conductive hearing loss involves the external ear, the tympanic membrane, and/or the auditory ossicles. Perceptive or sensorineural hearing loss involves the organ of Corti or any one of a number of sites along the auditory pathway, that is, the cochlear nerve or the auditory centers of the brain. Figure 14-7 indicates the audibility curve in man under ideal conditions (solid line) and under conditions

(broken line) of audiometry. The threshold for feeling is also shown. At sound pressure levels in excess of 130 or 140 dB, sensations in addition to hearing are perceived. These can include discomfort, tickling, and, finally, pain.

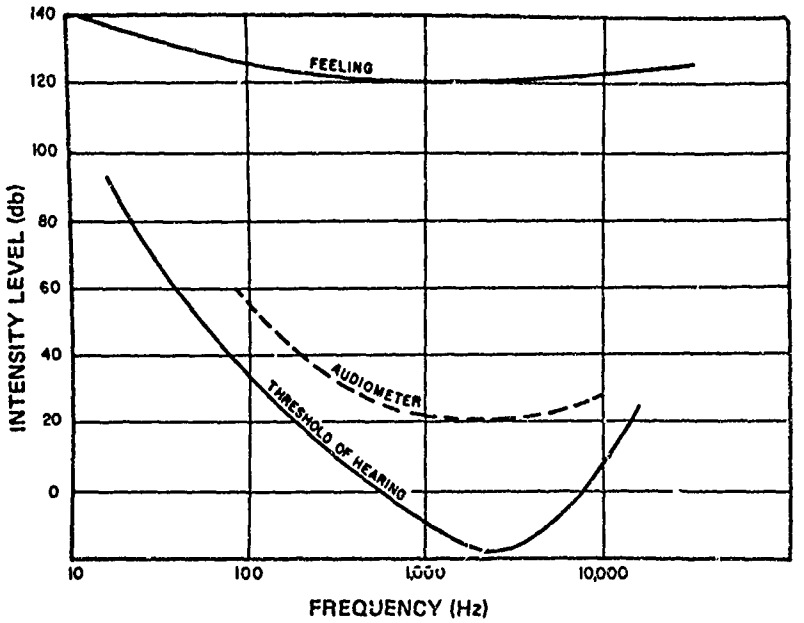


Figure 14–7. Audibility curve in man, showing thresholds of feeling and hearing. (After Licklider, 1951; reprinted from Naval Flight Surgeon's Manual, 1968)

Conductive Hearing Loss

Persons with pure conductive hearing loss have normal inner ears. The hearing decrement in these instances results from the fact that sound cannot reach the cochlea for one reason or another. The abnormality may be in:

1. the external canal
2. the ear drum
3. the middle ear bones, including the footplate of the stapes.

Hearing loss can result from obstruction of the auditory canal. The canal may be impacted with wax or foreign bodies or be swollen during infection. In the case of a birth defect, the external ear may be closed or the canal missing entirely. Damage to the drum by blast injury, for example, causes hearing loss either by perforation or scarring. Repeated middle ear infections also leave the drum scarred or perforated.

Hearing loss related to the bones of the middle ear is the most common type of conductive hearing loss. Figure 14-8 shows hearing loss in otosclerosis. In this

hereditary defect, the footplate of the stapes may become progressively fixed. If the disease is purely conductive and does not involve sensorineural elements as well, hearing can be improved by surgery.

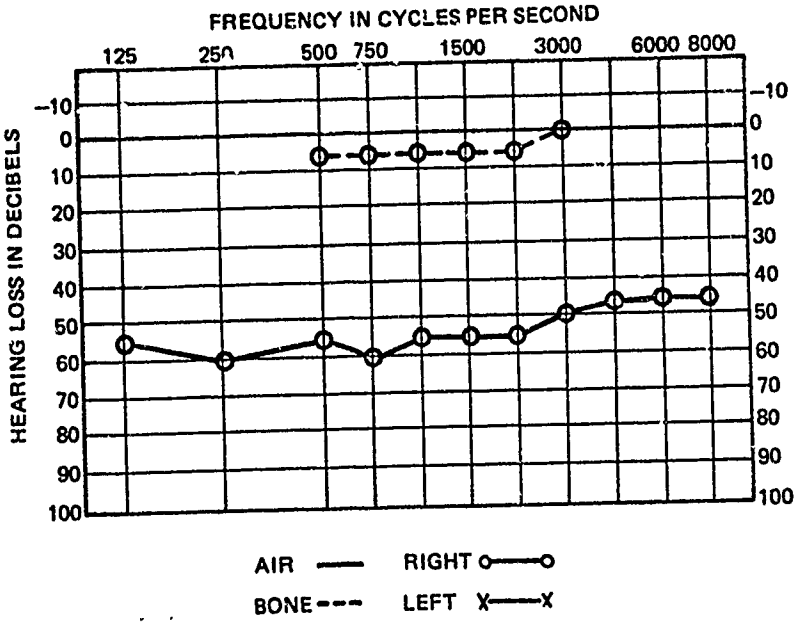


Figure 14–8. Audiogram of otosclerosis. Fixation of the stapes is nearly complete. (From DeWeese, D. D., & Saunders, W. H. *Textbook of Otolaryngology* (3rd ed.) St. Louis: C. V. Mosby Co., 1968)

The conductive apparatus of the ear is equipped with a feature that provides a limited amount of protection from prolonged intense noise. The mechanism is called the stapedial reflex. Two muscles, one attached to the malleus and the other to the stapes, act synergistically to limit the amount of stimulation reaching the inner ear. The muscles contract, after a brief latency, in response to loud sound. It is, at best, poor protection.

Finally, conductive hearing loss can never be total since sound can bypass the middle ear entirely and be conducted to the inner ear through the bones of the skull.

Sensorineural Hearing Loss

Sensorineural hearing loss is caused primarily by loss of hair cells or acoustic ganglion cells or both. It may be caused by lesions to the central auditory pathway also, although this is an unlikely cause due to the fact that beyond the first synapse the pathway is essentially doubled, with elements

for both ears ascending in right and left tracts. Unlike conductive loss, sensorineural loss can be complete.

Sensorineural loss comes about by a variety of agencies or events. These include hereditary and congenital conditions, disease, drug toxicity, presbycusis, and exposure to noise. Of these, the latter may well be far and away the greatest single cause. It may, indeed, include "presbycusis." Sensorineural hearing loss affects high frequency perception primarily, with ultimate progression to lower frequencies. Figure 14-9 is an audiogram showing hearing loss characteristic of the gradual degenerative process in "presbycusis." High tones are lost first.

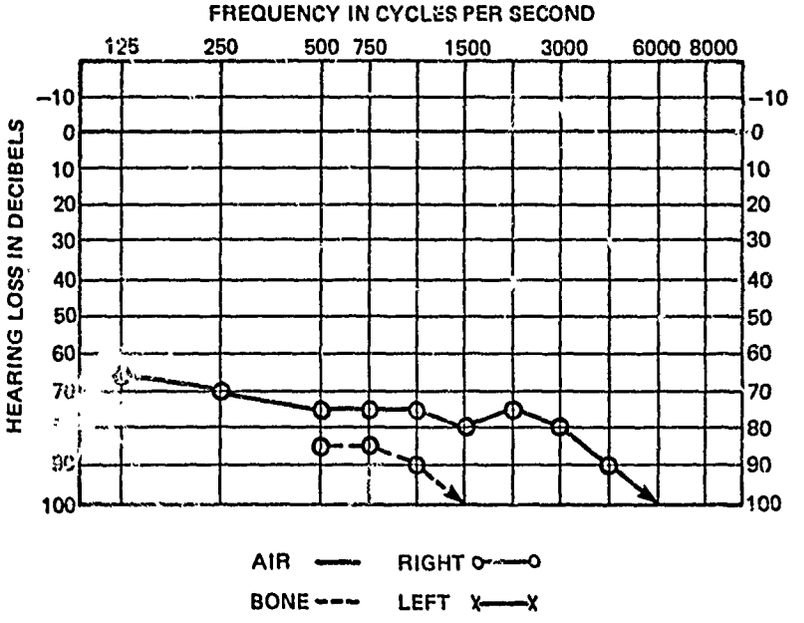


Figure 14–9. Audiogram of profound sensorineural hearing loss. (From DeWeese, D. D., & Saunders, W. H. *Textbook of Otolaryngology* (3rd ed.) St. Louis: C. V. Mosby Co., 1968)

When the human ear is exposed to excessively loud sounds, it shows a loss of acuity to sound, that is, a rise in threshold. This is called "temporary threshold shift," and it will return to normal over a time regulated by the parameters of the sound causing it. If the sound is repeated, the return to normal may be less than complete and this may progress with repeated exposure, the residual hearing loss being designated as "permanent threshold shift." We presume that this is due to loss of hair cells in the organ of Corti.

There is reason to believe that repetition of exposure over many years causes a gradual loss of hair cells, and consequent loss of hearing. This is known as

boilermakers' disease, a tribute to a bygone profession, the like of which is reduplicated many times over in modern industry. The same thing has been noted to occur among individuals who have engaged in frequent small arms fire, such as soldiers, persistent hunters, skeet shooters, and the like. Significantly, Bredberg (1968) found many examples of a similar affliction in his review of a large number of elderly cases whose ears he examined at autopsy. Although he had relatively few whose noise-exposure history was known, there were enough to create the definite suspicion that he was dealing with chronic acoustic trauma rather than merely the ravages of age.

Effects of High Intensity Pure Tones

Total or partial deafness can result from damage to the hair cells of the cochlea. It is widely believed that there is a relationship between tonal frequency and position on the cochlear partition at which it vibrates with maximum amplitude. This vibration, if great enough, is believed to cause mechanical injury to hair cells. Further, it is believed that there is an approximately inverse relation between the logarithm of frequency and the distance from the base of the cochlea with relation to the site of damage. Greenwood's function is probably the best available expression for this relationship. It may be stated as follows:

$$f = 253\,(10^{0.105x} - 1)$$

Since stress equals mass times acceleration per unit area, and the mass of the cochlear partition is thought to be the same over its entire length (Schuknecht & Tonndorf, 1960), the stress on any segment of the cochlear partition during displacement will be directly proportional to its acceleration. Since acceleration varies directly with frequency, high frequencies will produce greater stress in the region of maximum amplitude than do lower frequencies. High frequencies should, therefore, cause greater hair cell damage.

In addition to mechanical stress, it is thought that prolonged exposure to acoustic stimuli damages the hair cells by exhausting cytochemical or enzymatic materials in the cells (Beagley, 1965; Engström & Ades, 1960). Outer hair cells are more sensitive to this type of destruction.

Recently, Stockwell, Ades, and Engström (1969) studied the effects of high intensity noise (130 to 150 dB) on the hair cells of the guinea pig cochlea, which is similar in all important respects to the human cochlea. Various aspects of both the mechanical and chemical theories of hair cell destruction were investigated as were the relationship between exposure frequency and the site of hair cell damage and the effects of exposure time on damage. Table 14-1 shows the plan of exposure for the animals in this experiment.

The study reconfirmed that maximum damage bears some relation to exposure frequency, but as frequency increases, the position of maximum damage tends to move in the basalward direction. Figure 14-10 shows mean damage curves for animals exposed to 130 dB. (The arrows indicate the position

of maximum stimulation for exposure frequency calculated with Greenwood's formula.) Figure 14-11 shows mean damage curves for 150 dB exposures. These indicate that inner hair cell damage is complete after 1 hour, but outer hair cell damage increases between 1 and 4 hours.

Table 14–1
Plan of Exposures

Frequency	Exposure Duration	
	1 Hour	4 Hours
	130 dB	
4000 Hz	16 ears/10 animals	
2000 Hz	2 ears/1 animal	8 ears/4 animals
1000 Hz	4 ears/2 animals	6 ears/3 animals
500 Hz	6 ears/3 animals	6 ears/3 animals
125 Hz	4 ears/2 animals	4 ears/2 animals
	150 dB	
2000 Hz	4 ears/2 animals	2 ears/1 animal
1000 Hz	1 ear	2 ears/1 animal
125 Hz	18 ears/9 animals	1 ear

(From Stockwell, Ades & Engström, 1969)

These results suggest that at higher frequencies, mechanical stress is the important mechanism of hair cell damage; furthermore, outer hair cells are more affected than inner hair cells. At lower frequencies, the same sound pressure levels produce less mechanical stress, so hair cell damage may result from gradually accumulating effects of stimulation, that is, enzyme exhaustion. Outer hair cells also appear to be more sensitive than inner hair cells to this latter type of damage.

Effect of Impulse Noise

Impulse noise (see also chapter 15) is the type of noise produced, for example, by small arms fire and certain children's toys, notably cap pistols. This type of noise, considered dangerous when it exceeds 140 dB at a distance of less than 20 cm (NAS, 1965), produces mechanical destruction of hair cells comparable in severity to that produced by prolonged exposure to high intensity pure tones. Figure 14-12 shows hair cell damage demonstrated by Poche, Stockwell, and Ades (1969) in a guinea pig exposed to impulse noise and one exposed to pure tone. Distribution of damage along the organ of Corti is indicated. Table 14-2 indicates overall hair cell damage. The figure shows considerable variation in susceptibility to damage. In ears that did sustain damage in this study, outer hair cells (OHC) were more susceptible than inner

hair cells (IHC) (a finding one might expect when the mechanism of damage is mechanical stress). When damage due to cap gun exposure is plotted against damage caused by pure tone noise (figure 14-13), it is clear that cap gun exposures produce damage equal in severity to a 4-hour exposure to 2000 Hz tone of 125 to 130 dB.

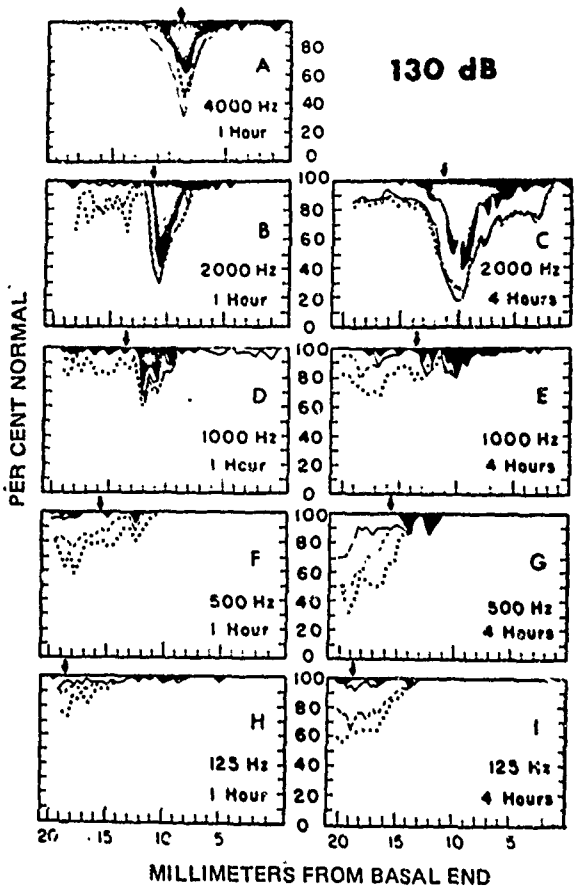


Figure 14–10. Mean damage curves for groups exposed to 130 dB SPL. The small arrow above each curve indicates the position of maximum stimulation for the exposure frequency. (Stockwell, Ades, & Engström, 1969; reprinted by permission of the Annals of Otology, Rhinology, and Laryngology)

The scanning electron microscope has been a further blessing for the study of the structure of the ear. For example, this device has made it possible to see changes in the surfaces of hair cells not visible by other means. We have observed the hair cells of the cochlea alongside a serious lesion, that is, one in which the acoustic papilla had been reduced to a simple epithelium (figure 14-14). On either side of the lesion, numbers of hair cells are distorted in that the hairs are fused, overgrown, or both (figure 14-15). It is not known to what extent these cells are functional, but it seems probable that they are not, inasmuch as the

damage to hearing is considerably wider in terms of frequency than would be true if only the cells visibly damaged in surface specimen (Engström, Ades, & Andersson, 1966) were functionally impaired. This then, would represent an intermediate stage of damage in which the hair cell was not completely destroyed, but was functionally impaired while retaining its viability.

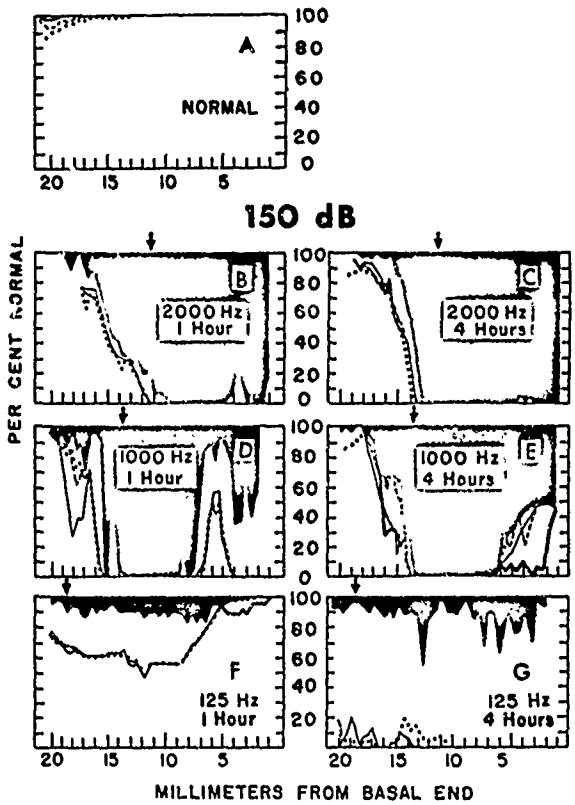
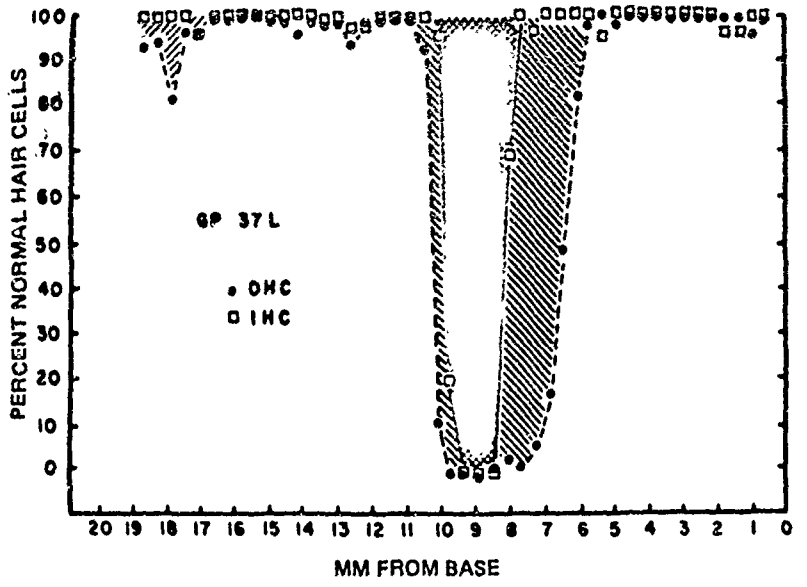
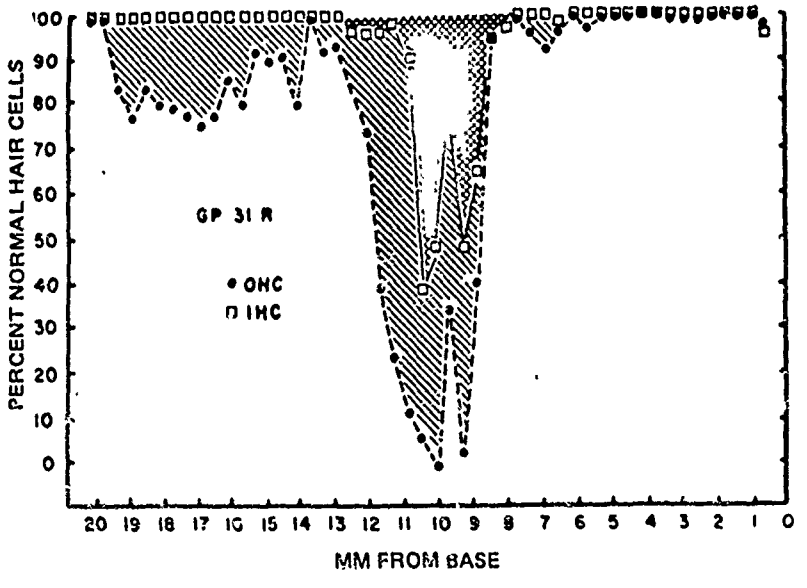


Figure 14–11. Mean damage curves for groups exposed to 150 dB SPL. The small arrow above each curve indicates the position of maximum stimulation for the exposure frequency. (Stockwell, Ades, & Engström, 1969; reprinted by permission of the Annals of Otology, Rhinology, and Laryngology)

It is important to note that in these experiments, among the methods of light/phase contrast, electron, and scanning electron microscopy, each has its place in the study of the pathological cochlea, and none will stand alone. Similarly, in the study of the noise-damaged cochlea, it is imperative that each cell be seen in its proper place in relation to the other hair cells, for otherwise, it is impossible to observe all the damage and relate it appropriately to the intact regions.



(a)



(b)

Figure 14–12. Percent hair-cell damage plotted as a function of distance from basal end of the organ of Corti. (a) Left ear of an animal exposed to 500 rounds of cap-gun fire at 30 cm. (b) Right ear of an animal exposed for 4 hours to a 2000-Hz tone at 130 dB. (Poche, Stockwell, & Ades, 1969)

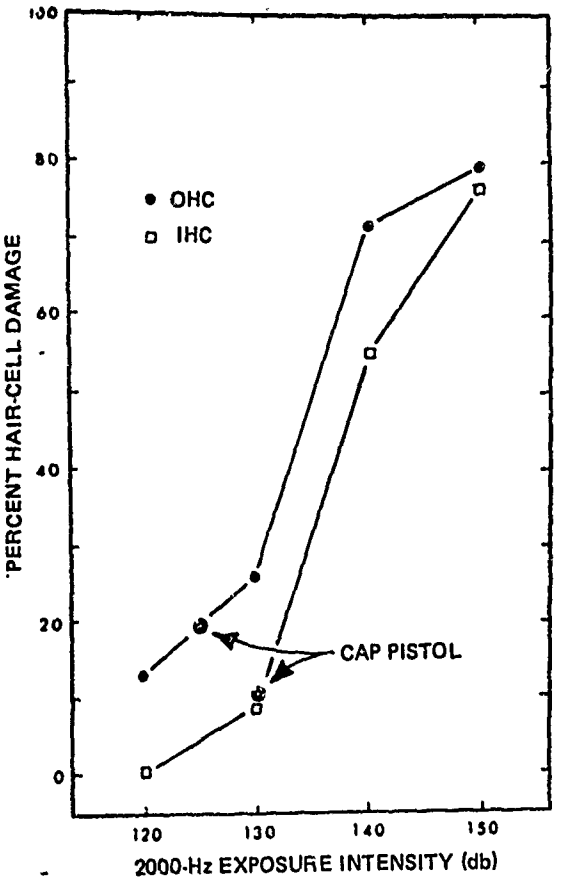


Figure 14–13. Comparison of overall hair cell damage produced by a 2000-Hz tone and by cap-pistol fire. Damage is plotted separately for IHC and OHC as a function of pure-tone exposure intensity. (Poche, Stockwell, & Ades, 1969)

Table 14–2

Overall Hair Cell Damage (Percent) in Ears From Unexposed Animals and From Animals Exposed to 500 Rounds of Cap gun Fire

	IHC	OHC 1	OHC 2	OHC 3
		Normals (12 ears)		
Maximum	0.73	1.39	2.11	3.30
Minimum	0.00	0.19	0.33	2.40
Mean	0.29	0.58	1.21	3.08
		Cap Gun (27 ears)		
Maximum	33.04	55.19	56.84	54.18
Minimum	0.05	0.23	0.93	2.53
Mean	10.37	17.80	18.86	21.50

(From Poche, Stockwell, & Ades, 1969)



Figure 14–14. Scanning electron micrograph of one-quarter turn of cochlea of guinea pig exposed to 4000 Hz. MO = modiolus; OC = organ of Corti; TM = tectorial membrane; lesion between arrows. Note abrupt character of lesion, and simple epithelium replacing acoustic papilla. (Bredberg, Ades, & Engström, in press)

Reproduced from best available copy.



Figure 14–15. Highly magnified scanning electron micrograph of ten outer hair cells of guinea pig, showing abnormal stereocilia. Arrow points to a giant stereocilia. Other cells show varying degrees of abnormality. (Bredberg, Ades, Engström, in press)

References

Ades, H. W. Central auditory mechanisms. In J. Field, H. W. Magoun, and V. E. Hall (Eds.), *Handbook of physiology*. Washington, D.C.: American Physiological Society, 1959.

Beagley, H. A. Acoustic trauma in the guinea pig: Electrophysiology and histology. *Acta Oto-Laryngologica*, 1965, *60*, 437.

Bekesy, G. V. Experiments in hearing. In E. G. Wever (Ed.), New York: McGraw-Hill Book Co., Inc., 1960.

Bekesy, G. V. Shearing microphonics produced by vibrations near the inner and outer hair cells. *Journal of the Acoustical Society of America*, 1953, *25*, 783-790.

Bekesy, G. V. The variation of phase along the basilar membrane with sinusoidal vibrations. *Journal of the Acoustical Society of America*, 1947, *19*, 452-460.

Bredberg, G. Cellular pattern and nerve supply of the human organ of Corti. *Acta Oto-Laryngologica Supplement 136*, 1968.

Bredberg, G., Ades, H. W., & Engström, H. in press.

Davis, H. Excitation of auditory receptors. In J. Field, H. W. Magoun, and V. E. Hall (Eds.), *Handbook of physiology*. Washington, D.C.: American Physiological Society, 1959.

Department of the Navy, Bureau of Medicine and Surgery. *U.S. naval flight surgeon's manual*. Washington, D.C.: U.S. Government Printing Office, 1968.

DeWeese, D. D., & Saunders, W. H. *Textbook of otolaryngology*. St. Louis: C. V. Mosby Company, 1968.

Engström, H., & Ades, H. W. Effect of high intensity noise on inner ear sensory epithelia. *Acta Oto-Laryngologica Supplement 158*, 1960.

Engström, H., Ades, H. W., & Andersson, A. *Structural pattern of the organ of Corti*. Stockholm: Almqvist and Wiksell, 1966.

Engström, H., Ades, H. W., & Hawkins, H. E., Jr. Cellular pattern, nerve structures and fluid spaces of the organ of Corti. In W. D. Neff (Ed.), *Contributions to sensory physiology*. New York: Academic Press, 1965.

Guild, S. R. Correlations of histologic observations and the acuity of hearing. *Acta Oto-Laryngologica*, 1932, *17*, 207-249.

Kryter, K. D. Possible modifications to the calculation of perceived noisiness. NASA-CR-1636, National Aeronautics and Space Admininstration, Washington, D.C., August 1970.

Kryter, K. D., & Pearson, K. S. Some effects of spectral content and duration on perceived noise level. *Journal of the Acoustical Society of America*, 1963, *35*, 866-883.

National Academy of Sciences, National Research Council, Committee on Hearing and Bioacoustics, Working Group 46. *Hazardous exposure to intermittent and steady state noise*. Washington, D.C.: National Academy of Sciences, 1965.

Poche, L. B., Stockwell, C. W., & Ades, H. W. Cochlear hair-cell damage in guinea pigs after exposure to impulse noise. *Journal of the Acoustical Society of America*, 1969, *46*, 947-951.

Rasmussen, G. L. *Outlines of neuro-anatomy*. (3rd ed.) Dubuque, Iowa: William C. Brown, Co., 1943.

Schuknecht, H. F., & Tonndorf, J. Acoustic trauma of the cochlea from ear surgery. *Laryngoscope*, 1960, *70*, 479.

Stevens, S. S. Procedure for calculating loudness: Mark VI. *Journal of the Acoustical Society of America*, 1961, *33*, 1577-1585.

Stockwell, C. W., Ades, H. W., & Engström, H. Patterns of hair cell damage after intense auditory stimulation. *Annals of Otology, Rhinology, and Laryngology*, 1969, *78*, 1144.

Wells, R. J. Recent research relative to perceived noise level. *Journal of the Acoustical Society of America*, 1967, *42*, 1151.

Wever, E. G. *Theory of hearing*. New York: John Wiley & Sons, 1949.

Wever, E. G., & Lawrence, M. *Physiological acoustics*. Princeton: Princeton University Press, 1954.

Whitfield, I. C. *The auditory pathway*. Baltimore: Williams & Wilkins Company, 1967.

CHAPTER 15
NOISE AND BLAST

by

David C. Hodge, Ph.D.

and

Georges R. Garinther
Aberdeen Proving Ground

Noise and blast problems may occur in all phases of aerospace activities. Tremendous quantities of acoustical energy are developed by rocket engines on the launch pad and during lift-off, and this may affect ground personnel as well as the crew on board the space vehicle. As payloads become larger and boosters increase in size and power, significant increases in noise and blast problems may be expected. Noise from equipment used in assembling and static testing of boosters and payloads may adversely affect ground-support personnel. In mission-control centers, noise from computers and monitoring devices may interfere with voice communications. Current evidence suggests that noise and blast problems in future space operations may be more severe at ground-service crew locations and in nearby communities than in the space vehicles themselves. However, control of noise levels inside spacecraft will still require consideration in assessing the likelihood of mission success.

The most significant effects of noise and blast on man are damage to hearing, masking of speech and warning signals, and annoyance. In addition, noise interferes with some of man's sensory and perceptual capabilities and thereby may degrade critical task performance. Noise also produces temporary or permanent alterations in body chemistry.

This chapter describes the noise and blast environment. It provides a definition of units and techniques of noise measurement and gives representative booster-launch and spacecraft noise data. It reviews the effects of noise on hearing sensitivity and performance and discusses briefly community response to noise exposure. Physiological, or nonauditory, effects of noise exposure are also

Reviewed by Henning E. von Gierke

Preceding page blank

treated, as are design criteria and methods for minimizing the effects of noise on hearing sensitivity and on communications. The references cited in this chapter relate primarily to research conducted during the past 10 years in the United States and several foreign countries.

Description of the Noise and Blast Environment

Definitions and Units

Airborne sound refers to a rapid variation in ambient atmospheric pressure. By definition, noise is unwanted sound. *Steady-state* noise is a periodic or random variation in atmospheric pressure which has a duration in excess of 1000 milliseconds. *Impulse* noise is a nonperiodic variation in atmospheric pressure which has a duration of less than 1000 msec, and a peak to root-mean-square (RMS) ratio greater than 10 decibels (dB). Blast is an anomalous term, but is most frequently used to describe very large amplitude and/or long duration pressure waves accompanying the discharge of large-caliber weapons, the ignition of rocket motors, or the detonation of conventional and nuclear explosives. Taken together, sound, noise, and blast all refer to airborne acoustical phenomena whose energy may be described both in terms of their physical characteristics (amplitude, frequency content, and/or duration) and their effects on man's physiology and behavior.

Amplitude The amplitude of sound at any given point is expressed as sound-pressure level (SPL). Its physical unit is the decibel which is given as:

$$SPL = 20 \log (p/p_o) \text{ in dB}$$

where p = the sound pressure being measured; and p_o = a reference pressure, usually 20 micronewtons per square meter ($\mu N/m^2$). The reference pressure of 20 $\mu N/m^2$ is approximately equal to the lowest pressure which a young person with normal hearing can barely detect at a frequency of 1000 Hertz (Hz). Other measures of sound pressure may be encountered in the literature, such as dynes per square centimeter (dyn/cm^2), microbar (μbar) and pounds per square inch (psi). Table 15-1 shows the relationship between four such measures.

Common examples of representative SPL include:

A business office	50 dB
Speech at 3 feet	65
Subway at 20 feet	95
Jet aircraft at 35 feet	130
Atlas launch at 150 feet	150
On gantry during Saturn V launch	172.

Table 15–1

Relationship Between Decibels, Newtons/Meter^2, Microbar*, and Pounds/Inch^2

dB	N/m^2	μbar	PSI
0	0.00002	0.0002	2.94×10^{-9}
14	0.0001	0.001	14.70×10^{-9}
34	0.001	0.01	147.0×10^{-9}
54	0.01	0.1	1.47×10^{-6}
74	0.1	1	14.70×10^{-6}
94	1	10	147.0×10^{-6}
114	10	100	1.47×10^{-3}
134	100	1000	14.70×10^{-3}
154	1000	10 000	147.0×10^{-3}
174	10 000	100 000	1.47

*Also note that 1 μbar = 1 dyn/cm^2.

Velocity. The speed of sound is dependent only upon the absolute temperature of the air, assuming that air behaves as an ideal gas. The equation for the speed of sound (C) in meters per second is:

$$C = 20.05 \sqrt{T} \text{ m/sec}$$

where T is the absolute temperature in degrees Kelvin (273.2° plus the temperature in degrees Centigrade). Thus the speed of sound at 21.1° C is about 344 m/sec.

In English units:

$$C = 49.03 \sqrt{R} \text{ ft/sec}$$

where R is the temperature in degrees Rankine (459.7° plus the temperature in degrees Fahrenheit). Again, at 70°F, the speed of sound is about 1128 ft/sec.

Wavelength. The wavelength (λ) of a sound is the distance the wave travels during one period or cycle. It is related to the speed of sound and to frequency by the equation:

$$\lambda = \frac{c}{f}$$

where c = speed of sound (m/sec or ft/sec), and f = frequency (Hz). For example, during one period a 100 Hz wave would move 3.44 meters or 11.3 feet at 70°F (21.1°C). It is helpful to keep in mind that as frequency increases, wavelength becomes shorter.

Frequency. The unit of frequency is Hertz (Hz) or cycles per second (cps). Nominally, the range of aurally detectable sounds is 20 to 20,000 Hz. Pressure oscillations at frequencies above this range are called ultrasonic. These frequencies cannot normally be heard by man but they do produce some biological effects and will be discussed in a later section. The effects of infrasonic frequencies (<20 Hz) will also be discussed briefly. The terms supersonic and subsonic, which are related to the speed of sound, should not be confused with those terms which describe frequency range.

When describing sound, noise or blast, it is not sufficient to measure only the overall SPL. The noise must also be analyzed to determine how the sound energy is distributed over the frequency range. A noise is usually analyzed by passing it through a constant-percentage bandwidth filter, such as an octave-band analyzer, in which each passband has upper and lower limiting frequencies having a ratio of 2:1. An octave-band analysis is usually sufficient to determine the effect of steady-state noise upon humans and the surrounding community. A 1/3-octave (or narrower) analysis is required when it is desired to localize which component in a system is the major contributor to a noise problem, or if the noise contains a pronounced narrow-band frequency component.

The preferred series of octave bands for acoustical measurements are identified as multiples and submultiples of 1000 Hz which describe the center frequency of each band. Another series of octave bands which has been widely used in the past are the commercial octave bands. These are normally described by their band-limiting frequencies.

Another type of frequency analysis which is gaining importance is the "weighting network" which is included in all sound-level meters which meet the requirements of the current American National Standards Institute's (ANSI) specification for sound level meters (ANSI, 1971). The weighting networks consist of three alternate frequency response characteristics, designated A-, B-, and C-weighting. Whenever one of these networks is used, the reading obtained must be identified properly. For instance, if an A-weighted sound pressure level of 90 is obtained, it would be reported as 90 dBA. The A-weighting network is particularly valuable if a quick estimate of the interference of noise upon speech is required (Klumpp & Webster, 1963). Also there has been a recent movement toward using the A-weighting network for evaluating the hearing hazard of steady-state noise when it is not possible or practical to perform a complete octave-band analysis (Botsford, 1967).

Definitions Peculiar to Impulse Noise and Blast.

Peak Pressure is the highest pressure achieved, expressed in dB *re* 20 $\mu N/m^2$, or in psi.

Rise Time is the time taken for the single pressure fluctuation that forms the initial or principal positive peak to increase from ambient pressure to the peak pressure level.

Pressure Wave Duration (A-Duration) is the time required for the pressure to rise to its initial or principal positive peak and return momentarily to ambient pressure.

Pressure Envelope Duration (B-Duration) is the total time that the envelope of pressure fluctuations (positive and negative) is within 20 dB of the peak pressure level. Included in this time would be the duration of that part of any reflection pattern that is within 20 dB of the peak pressure level.

Psychological Terms. The measures of loudness are the phon and the sone. Sones are obtained by a conversion of eight octave bands into sones from an appropriate table. The phon is merely a transformation of the sone into a logarithmic scale. Sounds that are perceived as equally loud to the human ear will have the same sone or phon value. The mel is used as a subjective measure of the pitch differences in frequency between sounds.

Propagation of Sound

In an ideal, homogeneous, loss-free atmosphere SPL decreases, through spherical divergence, inversely with distance in the far field. That is, there is a 6 dB decrease in SPL for each doubling of distance from the source. In addition, when sound travels through still, homogeneous air, a significant amount of energy is extracted through "molecular absorption" which is related to the relaxation behavior of the oxygen molecules. This excess attenuation depends not only on frequency, but also on temperature and humidity and is in addition to losses resulting from spherical divergence. Figure 15-1 shows engineering estimates of excess attenuation as a function of distance and frequency for air temperatures ranging from 0° to 100°F and over a relative humidity range from 10 to 90 percent. Data are given for the preferred octave bands ranging from 500 to 8000 Hz. While there is some absorption in the lower bands, it can usually be neglected. A more complete discussion of atmospheric absorption is provided by the Society of Automotive Engineers (SAE) (1964).

In certain cases "classical absorption" should also be considered. Classical absorption is proportional to the frequency squared, is independent of humidity, and its effects typically are much less than those of molecular absorption (Nyborg & Mintzer, 1955).

In addition to the preceding, the refraction of sound waves produced by meteorological conditions between the earth's surface and altitudes of 3 to 5 kilometers must be considered. This phenomenon may cause sound waves produced at or near the surface of the earth to be focused near residential areas adjacent to rocket launch sites (Perkins et al., 1960). This refraction is due to changes in velocity of sound with altitude, and it is caused by variations in temperature, humidity and wind with altitude. The SPL for various refraction

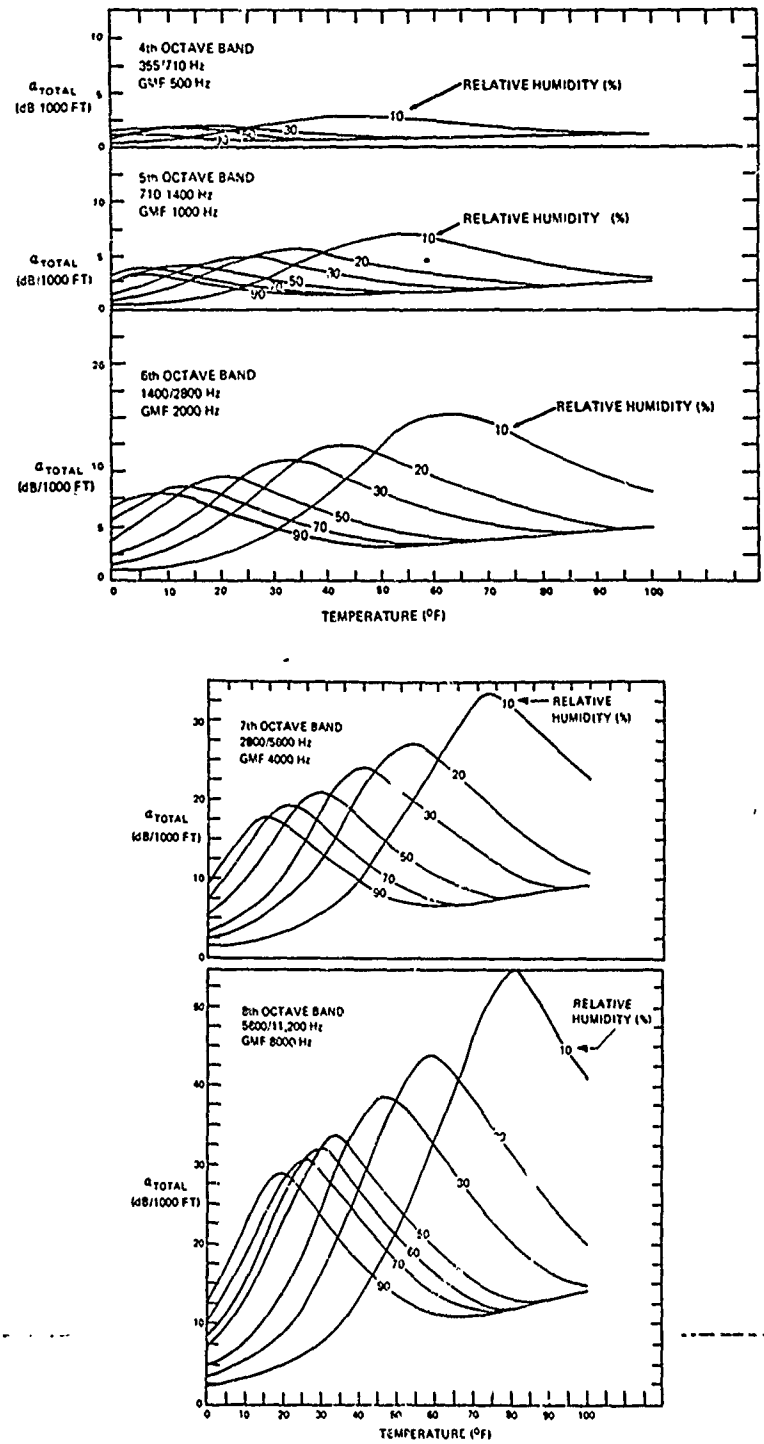


Figure 15–1. Atmospheric absorption coefficients for octave bands of noise for different temperatures. (Society of Automotive Engineers, 1964)

conditions and their focal points may be calculated by a modified ray acoustic method if the directivity characteristics of the source are known. Experience has shown, though, that quite often the effects of refraction and focusing do not occur and the SPL approaches that predicted for a homogeneous medium. Although those conditions causing focusing do sometimes occur in the Cape Kennedy area, they are not prevalent (Chenoweth & Smith, 1961).

Noise Measurement.

The basic measuring system for evaluating the physical characteristics of noise to relate them to their effect on man consists of the following elements:

1. transducer (microphone)
2. electronic amplifier and calibrated attenuator
3. data storage
4. octave-band analyzer
5. read-out.

The choice of instrumentation for a particular situation must be based upon a knowledge of the limitations and capabilities of the various types of instrumentation available. Normally, the weakest item of a measuring system is the transducer (microphone). Most of the discussion will, therefore, center around the selection of transducers and the techniques to be used in measuring steady-state and impulse noise. The associated equipment will naturally require characteristics which are as good as, or better than, those of the microphone selected.

Steady-State Noise. Microphones are available in a variety of sensitivities. When very low noise levels are to be measured, the minimum SPL to which a microphone can respond should be the determining factor in selection. It must also be ascertained that the self-noise of the microphone (and the entire measuring system for that matter) is at least 10 dB below the noise that is to be measured *in each octave band of interest.* On the other hand, for measuring high-level noises such as those produced by rocket engines, the choice of microphone to be used will be limited by the maximum SPL to which the microphone can respond without excessive distortion or failure. After the preceding two considerations have narrowed the selection, the microphone that should be selected is the one having the smoothest frequency response over the range of interest.

The frequency response of most microphones varies with the direction of arrival of the sound wave. At low frequencies (below 1 kHz), where the size of the microphone is small in relation to the wavelength of sound, microphones are omnidirectional. However, at higher frequencies the direction in which the microphone is pointed, or its incidence angle*, must be carefully considered.

*The incidence angle for most microphones is that angle subtended between its longitudinal axis and a line drawn between the noise source and the microphone.

The manufacturer's specifications should be consulted to obtain the incidence angle which provides the smoothest possible frequency response.

If a moving noise source is to be measured, a microphone which has its best response at 0° (normal) incidence should not be used since the measured spectrum will change with noise-source location. Therefore, in this case, it would be desirable to select a microphone with good response at 90° (grazing) incidence and to position it so the moving noise source is always at 90° incidence to the microphone.

Impulse Noise and Blast. The measurement of impulse noise presents several problems which must be discussed separately. The principal limitations in the measurement of impulse noise lie in the ability of the transducer and its associated equipment to respond to the pressure pulse accurately (Garinther & Moreland, 1965; Coles & Rice, 1966). The minimum qualities of the transducers and associated equipment for such measurements are:

1. A good phase response.

2. A uniform amplitude response characteristic over a wide frequency range. [A bandwidth of from 100 Hz to 70 kHz is adequate for measuring most short duration impulses such as from small arms, but longer duration impulses such as from large caliber weapons and sonic booms require an extension of the low frequency response, and may permit relaxation of the upper limit (Crocker, 1966).]

3. Less than 1.5 dB ringing and overshoot at the pressure being measured (ringing should be completely damped after 100 μsec).

4. Rise time capability of 10 μsec or less *at the pressure being measured.*

5. Sufficient robustness to withstand damage from the pressure pulse being measured.

6. Mounting of all apparatus to eliminate microphonics.

7. Sufficient sensitivity to allow a signal-to-noise ratio of 25 dB or greater.

8. Minimum drift caused by temperature instability.

The *angle of microphone incidence* is even more important for measuring impulse noise than for measuring steady-state noise. Garinther and Moreland (1965) have shown that at 0° (normal) incidence, the measured peak pressure level of various microphones may differ by as much as 10 dB. Since the peak readings obtained from various microphones should theoretically be, and were in fact found to be, in good agreement at 90° incidence, the transducer should be oriented for impulse-noise measurements at an angle of 90° (grazing incidence) between the longitudinal axis of the transducer and the direction of travel of the pressure pulse or shock wave.

With the transducer positioned at grazing incidence, rise-time characteristics will be affected by the transit time of the wave across the sensing element. Therefore, it is necessary that the transducer selected have a sensitive diameter of about 4mm or less.

Two precautions must be stated regarding the measurement and analysis of short-duration impulse noise. First, great care must be taken in interpreting the results of a frequency analysis. [Pease (1967) has published a computer program for spectrum analysis of impulse noises.] Second, in tape recording impulse noise it has been found necessary to use FM recording equipment. "Direct" (AM) tape recording produces phase shift of frequency vs. time which distorts the pressure-time history of an impulse noise.

Prediction of Launch Noise

The primary sources which must be considered in assessing mission-associated noises are: (1) static and preflight tests, (2) launch, and (3) flight operations. Consideration must be given to how each of these phases of propulsion system noise affects the crew, ground-support personnel, and the surrounding community.

In addition to the propulsion system, noise generated within the command module must be carefully assessed with regard to its long-term effects upon the crew. In space, the only sources which need to be considered are those generating noise within the capsule and any structure-borne noise.

The potential noise environment should be defined as early as possible in the development of a system. Techniques are available for predicting from a knowledge of certain parameters the sound spectrum of a propulsion system. These have been shown to be accurate to within a few decibels. A brief discussion of these follows, but the reader should consult Wilhold et al. (1970) to obtain an understanding of the computations.

The area surrounding the rocket must be divided into three regions to be properly analysed. In the acoustic *near field* (within 1 λ) no accurate predictive technique exists. The second region is the *mid-field* (3-5λ). Here it is possible to calculate a dimensionless spectrum function and source position which is dependent upon frequency, using techniques outlined in Dyer (1958). From these, and the known parameters of the propulsion system, the acoustic environment may be determined. The *far field* of the noise produced by the launch of a rocket is the area with which we are most concerned in dealing with the effects of noise upon man. The predictive method for this region is quite involved and is described in detail by Wilhold et al. (1963). Excess attenuation and meteorological effects described in an earlier section must, if appropriate, be included in computation. This technique has proven to be very accurate in predicting the band pressure levels of several rocket systems.

The acoustic environment of advanced Saturn V vehicles has been calculated for strap-on configurations having 13.1 million and 32 million pounds of thrust (Wilhold et al., 1970). These are shown in figures 15-2 through 15-5.

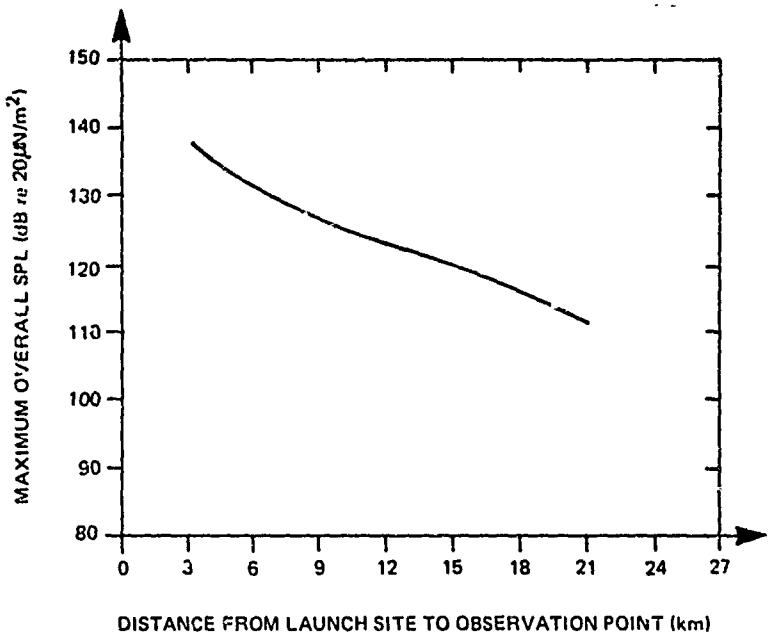


Figure 15–2. Maximum anticipated overall SPL for Saturn V MLV configuration of 32.0 million lb of thrust, as a function of distance from launch pad. (Wilhold et al., 1970)

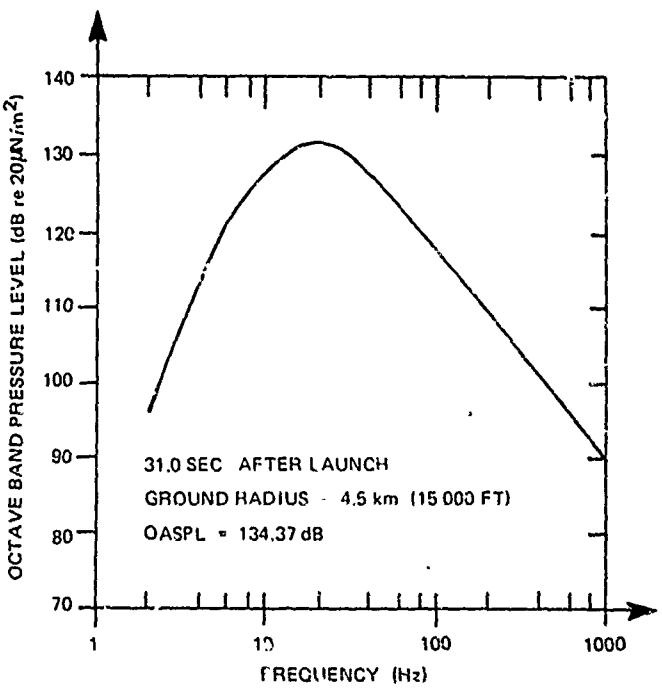


Figure 15–3. Predicted octave band pressure level spectrum at 4.5 km from Saturn V MLV launch (32 million lb thrust). (Wilhold et al., 1970)

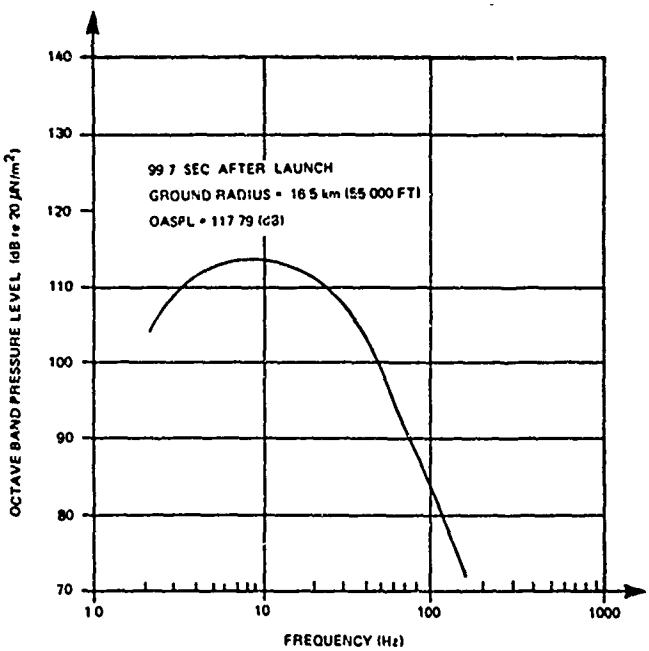


Figure 15–4. Predicted octave band pressure level spectrum at 16.5 km from Saturn V MLV launch (32 million lb thrust). (Wilhold et al., 1970)

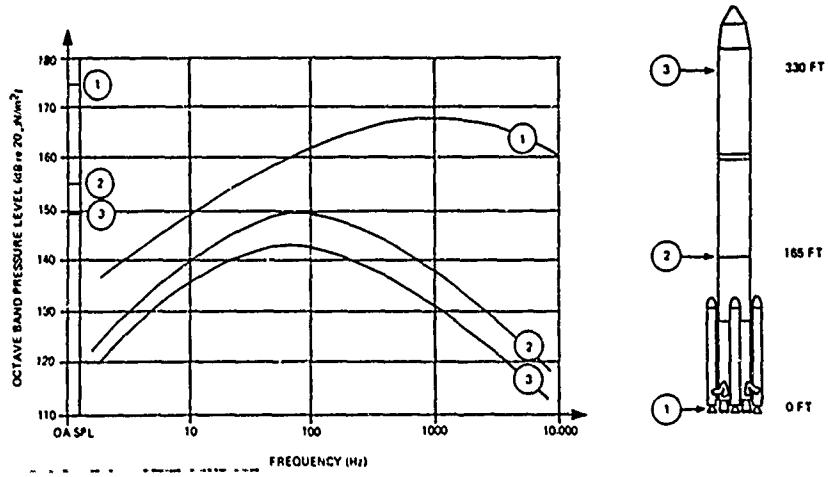


Figure 15–5. Predicted spectra for 3 vehicle stations for a 13.1 million lb thrust configuration. (Saturn V with four 1.4 million lb thrust strap-on units.) (Wilhold et al., 1970)

Apollo Launch Noise

Detailed measurements of Apollo launch noise have been made at many positions in and around Cape Kennedy Launch Complex 39A. The range of octave-band SPL around the vehicle at a distance of 400 meters is shown in table 15-2. Also shown are the maximum levels achieved on the side of the gantry closest to the rocket 10 m above ground.

Table 15–2

Octave Band Pressure Levels Around an Apollo Launch at a Distance of 400 Meters and on the Gantry 10 Meters Above Ground

Center Frequency (Hz)	Sound Pressure Level (dB)*	
	At 400 Meters	On the Gantry
2	122 – 143	158
4	136 – 155	163
8	141 – 157	162
16	136 – 158	159
31	135 – 158	159
63	130 – 152	164
125	129 – 149	166
250	127 – 146	168
500	125 – 142	164
1000	120 – 139	161
2000	116 – 138	158
4000	118 – 136	156
8000	110 – 131	152

*re 20 $\mu N/m^2$.

(J.F. Kennedy Space Center, 1969a)

The SPL to which the Apollo astronauts are exposed remains above 85 dB for about 80 seconds during liftoff (French, 1967). The maximum SPL achieved at the crew position is shown in table 15-3. Since the crew will be wearing helmets and space suits during launch, a conservative estimate of the actual SPL at the ear is also shown in table 15-3.

It is important to note that the maximum SPL for the Apollo system occurs at very low frequencies, below 100 Hz. This noise, which is produced by the turbulent mixing of the booster propulsive flow with the surrounding atmosphere, will continue to become higher in intensity, and lower in frequency, as boosters increase in size and thrust. The very large boosters, such as Nova, will probably produce their maximum noise energy in the infrasonic region (below 20 Hz) (National Aeronautics and Space Administration, Marshall Space Flight Center, 1961).

Table 15–3

Sound Pressure Level in Crew Area and at Ear Position of Apollo Astronauts at T + 60 Seconds

Center Frequency (Hz)	Sound Pressure Level (dB)	
	Crew Area	Ear Position
63	123	119
125	123	116
250	126	112
500	125	106
1000	122	96
2000	120	89

(French, 1967)

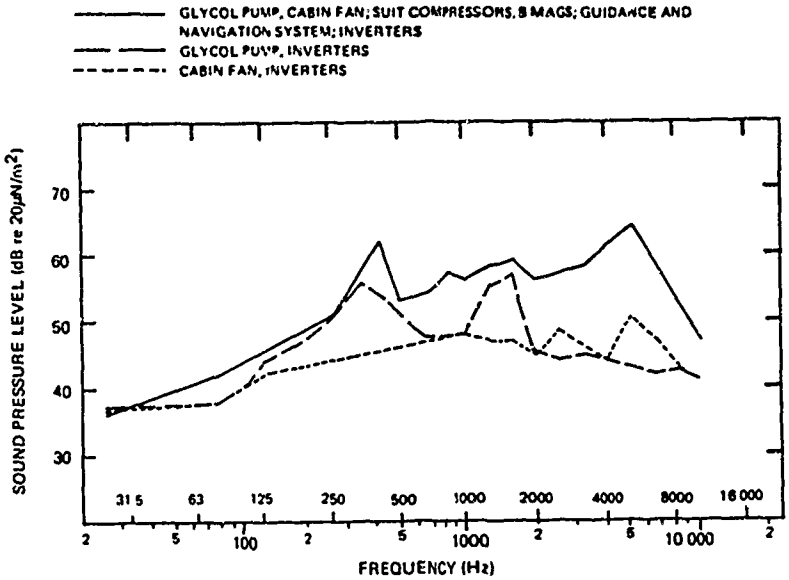
Low-frequency sounds must be measured accurately so research may be continued on the effects of these sounds on man. Hearing protective devices, such as helmets and circumaural muffs, provide their poorest protection at low frequencies (discussed further in a later section), so research must be continued on providing more efficient means of protecting man from the possible damaging effects of low-frequency sound. Also, as was discussed in the section on propagation of sound, low-frequency energy is least affected by excess attenuation. Therefore, these are the frequencies which are most likely to produce both physical and psychological effects in the communities surrounding launch areas.

Spacecraft Noise Levels During Non-Powered Flight

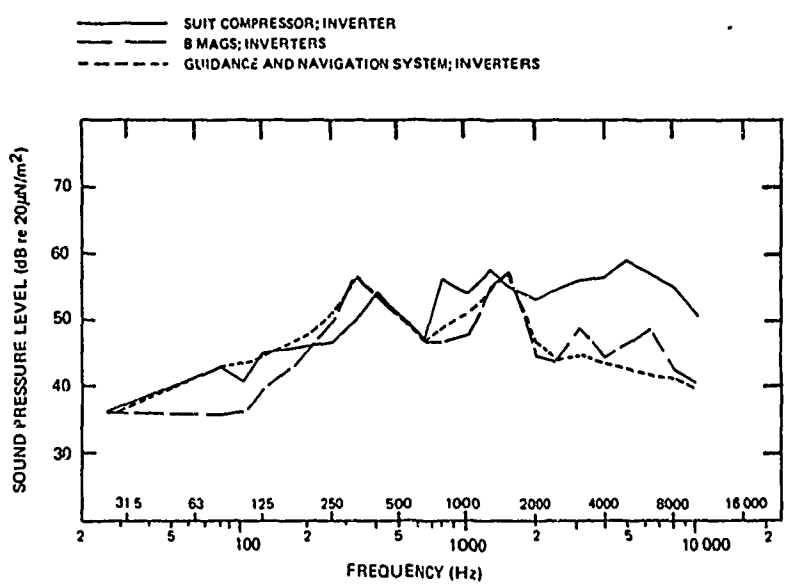
Apollo crew compartment noise measurements are shown in figure 15-6 for non-powered flight. These data were acquired in the 2TV-1 command module which was used for combined thermal/vacuum tests at the NASA Marshall Space Flight Center (MSFC) facility. Measurements were made with the internal environment controlled by the spacecraft life support system, and compartment pressure was maintained at about 5 psia. During this simulated flight, the interior noise sources included the glycol pumps, cabin fans, suit compressors, B mags, inverters, and guidance and navigational systems.

Effects of Noise and Blast on Hearing

This section treats the factors influencing the acquisition and recovery of hearing loss for steady-state and impulse noise, and for blast (a special case of impulse noise). A basic understanding of the anatomy, physiology and functioning of the human auditory system is assumed. Readers not possessing this background may find a preliminary reading of chapter 14 helpful.



(a) 1/3 octave band pressure level in command module crew area.



(b) 1/3 octave band pressure level in command module crew area.

Figure 15–6. Apollo crew compartment noise.

Types of Hearing Loss

The sensitivity of human hearing at a particular test frequency is referred to as the threshold of audibility. Thresholds stated with reference to standard criteria [such as ANSI-1951 or ISO-1964 audiometric zero (International Standards Organization)] are called hearing levels re the appropriate reference level. When a loss of sensitivity is temporary, i.e., returns to baseline after a suitable recovery interval, it is referred to as a temporary threshold shift, or TTS. A loss of sensitivity which does not return to baseline is called a permanent threshold shift, PTS. TTS is usually measured at 2 minutes or longer after exposure, and is referred to as $TTS_{2\ min}$ or, simply, TTS_2.

Relation Between TTS and PTS

Some relation is assumed to exist between TTS_2 experienced on a near-daily basis and the likelihood of eventual accumulation of PTS. CHABA (Committee on Hearing, Bioacoustics and Biomechanics) Working Group 46 (1965) assumed that 10 years of near-daily exposure would result in $PTS_{10\ yr}$=$TTS_{2\ min}$. TTS measures are widely used in assessing noise effects on hearing because (1) TTS is a valid measure of the temporary effects of noise exposure, and (2) TTS can affect man's ability to perform tasks requiring maximum hearing sensitivity. In fact, where life-or-death decisions rest on the acuteness of man's hearing, as in astronauts' reception of speech signals, or in the perceiving of auditory warning signals, prevention of excessive TTS is the most important consideration. Absence of TTS may be responsible for saving a life or many lives. TTS will be used here as the primary indicant of noise effects on hearing threshold sensitivity.

Susceptibility to TTS

The concept of susceptibility refers jointly to the fact that for a given noise exposure, different ears demonstrate varying amounts of TTS, and for a given sample of ears, different noise conditions may produce varying distributions of TTS. Because of the unpredictable and uncontrollable variability in ears' responses to noise--between days and among noise conditions--the possibility of developing criteria for protecting *specific* ears from excessive TTS is at best slim (Ward, 1968; Hodge & McCommons, 1966). As a result, criteria for determining what constitutes hazardous vs. nonhazardous noise exposures are, in reality, a form of actuarial or statistical tables in which the responses of certain proportions of noise-exposed populations are predicted.

Steady Sounds and Noise

Acquisition of TTS. The many factors influencing the acquisition of TTS from steady sound and noise exposure have been reviewed by Ward (1963, 1969) and Nakamura (1964). Some of the salient aspects are summarized below. When reading these, it should be kept in mind that the *interaction* of variables is a most important consideration. The present discussion will be limited primarily to TTS measured 2 minutes or longer after exposure.

Stimulus Amplitude. TTS_2 increases linearly with average SPL over the range of 75 to 120 dB and possibly higher. The difference between TTS produced by 85- and 90-dB noise is about the same as the difference between that produced by 90- and 95-dB SPL. This relationship is illustrated in figure 15-7.

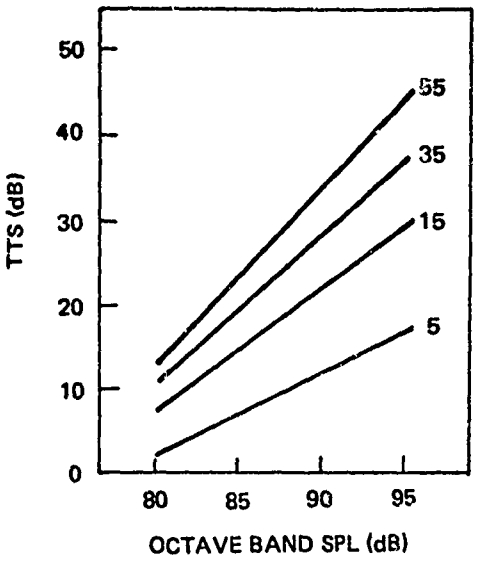


Figure 15–7. TTS at 4 kHz as a function of SPL for exposure to octave band of 2–4 kHz. Parameter is exposure time in minutes. (Shoji et al., 1966)

Exposure Frequency. For equal SPL in octave-bands of noise, low frequencies present less hazard to the ear than higher frequencies up to 4 kHz. This is due to the frequency-response characteristics of ma 's ear. Figure 15-8 illustrates the general relation betwee: exposure frequency and TTS for octave bands of noise.

Pure tones produce more TTS than corresponding octave bands of noise of the same amplitude. Carter and Kryter (1962) showed that the overall level of an octave band had to be about 5 dB higher than a pure tone at the octave center frequency to produce an equal amount of TTS; this 5 dB correction was later adopted for use in the CHABA (1965) steady-state noise damage-risk criterion.

Cohen and Bauman (1964), investigating TTS from broad-band noise, showed that when pure tones below 2 kHz were present the combined tone and noise condition produced more TTS than noise alone, even though the overall SPLS for the two conditions were equated.

Jerger et al. (1966), and Alford et al. (1966) investigated TTS from infrasonic tones, concluding that the most hazardous conditions were at or above 141 dB SPL in the range of 10 to 12 Hz.

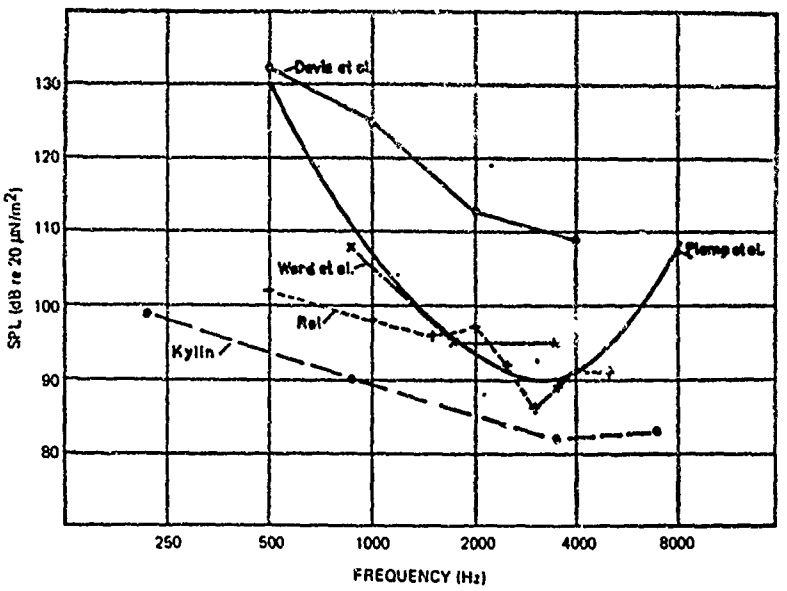


Figure 15–8. Relation between exposure of frequency and TTS for octave bands of noise: comparison of some iso-traumatic lines, all based on TTS. Within any one set of data, the same exposure time or TTS criterion was used. (Plomp et al., 1963)

There is evidence that exposure to ultrasonic tones up to 120 dB SPL is unlikely to produce TTS (Acton & Carson, 1967). No clear evidence exists upon which to assess the effect of higher SPL.

Duration of Exposure. TTS_2 from steady noise grows linearly with the logarithm of exposure time, as illustrated in figure 15-9. Most experiments have involved relatively short exposures (8 hr), but Yuganov, et al. (1967) have suggested that the rule is valid for exposure times of up to 720 hours.

The effects of intermittent noise exposure have been reviewed by Ward (1963, 1966) and Cohen and Jackson (1969), and others have compared the effects of continuous and intermittent exposures. In general, intermittent exposures produce less TTS than continuous exposures.

Test Frequency. TTS involves areas, not points, on the basilar membrane (Ward, 1963). Thus, virtually any type of tone or noise exposure affects auditory thresholds at a range of test frequencies. For SPL above 60 dB, maximum TTS occurs at a frequency on the order of one-half to one octave above the stimulating frequency for pure tones and bands of noise. The relative TTS occurring at various frequencies with a broad-band ("white") noise exposure is shown in figure 15-10.

Preexposure Hearing Level. The foregoing discussion has been based almost entirely on ears with *normal* sensitivity. Impaired ears may demonstrate different results. Ears with conductive hearing losses, for

example, would be expected to show less TTS because less energy is transmitted to the cochlea. Ears with pure sense organ losses should also show less TTS than normals, but this is due to their having less remaining sensitivity to lose.

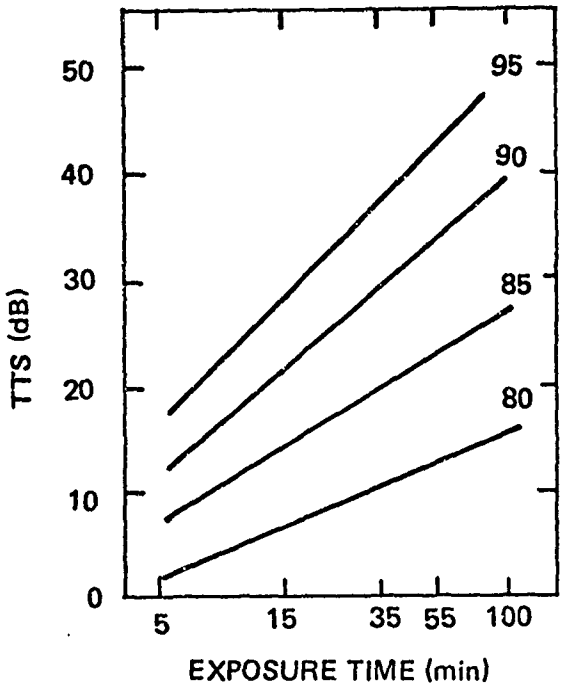


Figure 15–9. TTS at 4 kHz from exposure to 2–4 kHz octave band noise. Parameter is noise level in SPL. (Shoji et al., 1966)

Sex and Age. No systematic difference in TTS as a function of sex and age have been reported (Ward et al., 1959b; Loeb & Fletcher, 1963), nor have any systematic trends in TTS growth been reported solely as a function of age. For a discussion of the PTS which normally accompanies the aging process (presbycusis), see chapter 14.

Monaural vs. Binaural Exposure. Ward (1965) showed that monaural exposures were accompanied in general by about 5 dB more TTS than binaural exposure to the same condition.

Recovery of TTS. When TTS_2 does not exceed about 40 dB, and is induced by relatively short exposures to continuous blocks of steady-state noise, TTS recovers linearly in log time and occurs within a maximum of 16 to 48 hours (Ward, 1963; Smith & Loeb, 1969). Under these conditions recovery rate is also independent of test frequency. The slope of the recovery function may, however, vary as a function of the amount of TTS_2. Representative recovery functions are shown in figure 15-11.

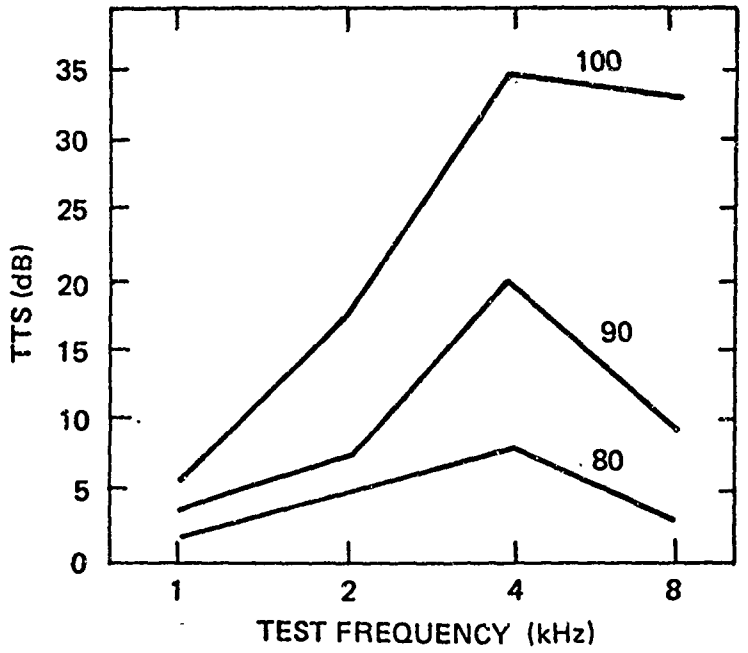


Figure 15–10. Distribution of TTS resulting from 5-min exposure to broad-band noise. Parameter is amplitude in sensation level. (Nakamura, 1964)

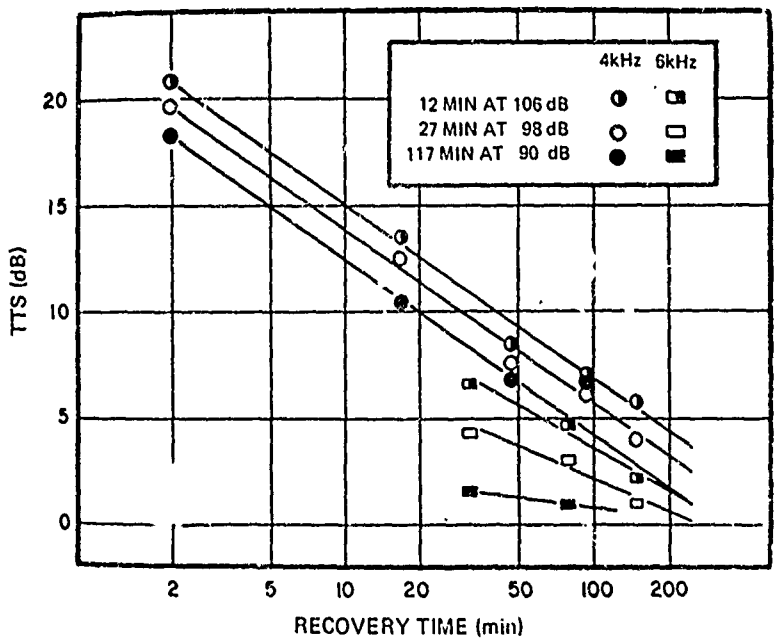


Figure 15–11. Course of recovery at 4 and 6 kHz following 3 different exposures to 1.2 – 2.4 kHz octave band noise. (Ward et al., 1959a)

Since subsequent recovery is usually quite predictable once the value of TTS_2 is known, generalized recovery functions can be developed for $TTS_{||}40$ dB. Such functions permit TTS measured at various times after exposure to be converted backward or forward to TTS_2 for purposes of direct comparison. Kryter (1963) published such a graph for converting TTS_t to TTS_2 as shown in figure 15-12.

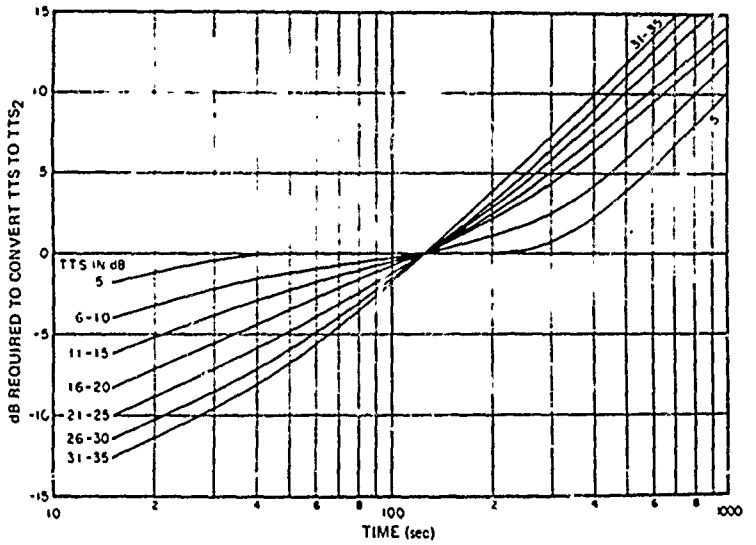


Figure 15–12. Graph for conversion of TTS to TTS_2 with TTS as the parameter. Example: for TTS of 25 dB measured 500 sec after exposure, add 10 dB to arrive at TTS_2 = 35 dB. Graph is based on exposure of subjects to continuous periods of steady-state noise, and is probably invalid for application to TTS induced by other types of exposures. (Kryter, 1963)

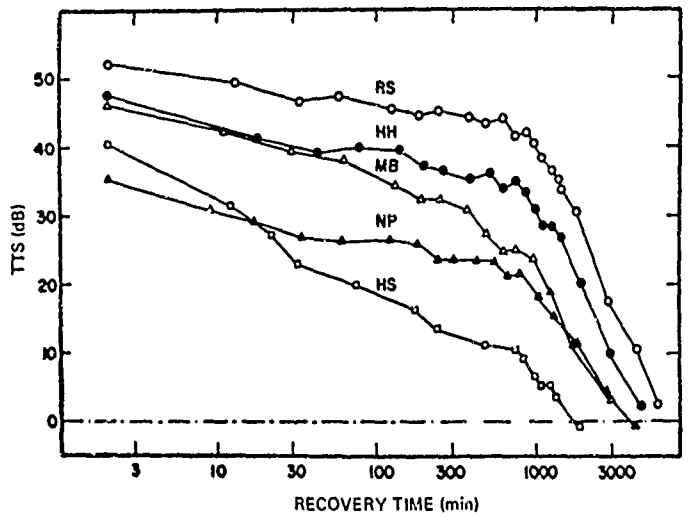
When TTS is induced by exposures to steady noise longer than 8 hours, or by intermittent noise, these generalized recovery functions are probably invalid. Ward (1970) found that intermittent noise caused a significant increase in recovery time, for equal TTS, and Yuganov et al. (1967) and Mills et al. (1970) reported similar findings for exposures of 12 to 720 hours.

As TTS_2 exceeds about 40 dB a change in the recovery function may be noted. Recovery from high values of TTS is linear in time, rather than linear in log time, as illustrated in figure 15-13.

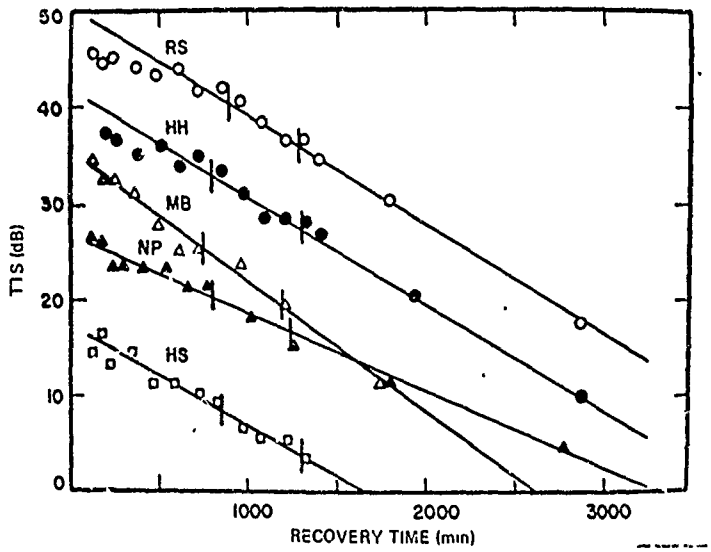
Impulse Noise

An impulse may be defined as an aperiodic pressure phenomenon of less than 1000 msec duration, having a fast rise time and a peak-to-RMS ratio greater than 10 dB. Such a definition leaves much to be desired, including a 'gray' area of pressure phenomena which may be considered either as long impulses or short, steady sounds. Impulses are, however, characteristic of many working

environments, and common examples include the sound of gunfire, impact and power-operated tools, drop forges, pile drivers, etc.



(a)



(b)

Figure 15–13. (a) Average course of recovery at 3 and 4 kHz following exposure to 105 dB SPL 1.2–2.4 kHz noise whose duration was sufficient to produce 50 dB TTS_2. Time is represented logarithmically. (b) Data replotted in terms of time, rather than log time (abscissa). (Ward, 1960)

The literature on impulse noise effects has been reviewed by Ward (1963), Chaillet et al. (1964), Coles et al. (1967, 1968), and Rice (1968). Some of the more important findings are summarized below. As was the case with steady noise, the interaction of variables is an extremely important consideration.

Acquisition of TTS..

Peak Pressure Level. The higher the peak pressure level, the greater is the risk of TTS, other parameters being equal. This relation is illustrated in figure 15-14 by data from the classic studies of Murray and Reid (1946), and in figure 15-15 by data from Ward et al. (1961). The peak pressure level where TTS is first produced depends in part on other parameters such as impulse duration or the number of impulses presented, as well as on individual susceptibility.

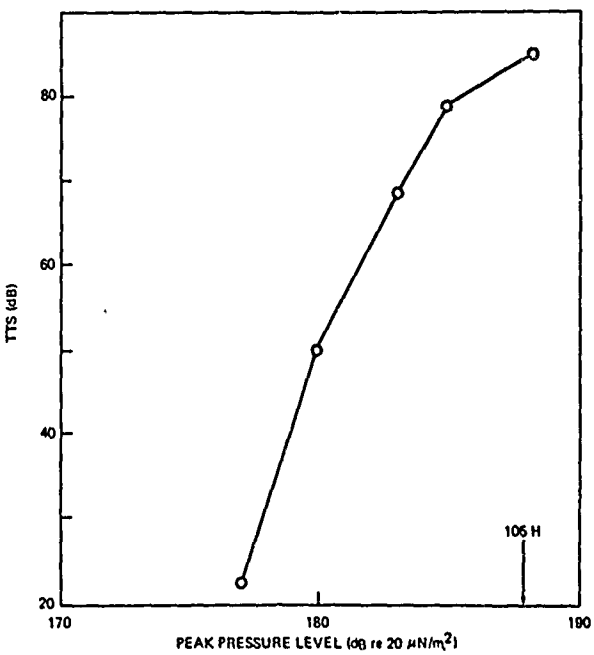


Figure 15–14. TTS as a function of peak pressure level for ears exposed to 10 impulses produced by various weapons. Notation "105 H" on abscissa indicates peak pressure level found in crew area of a current Army howitzer. Graph underscores need for protection of personnel exposed to high noise levels. (Murray & Reid, 1946)

Impulse Duration. Fletcher and Loeb (1967) have shown that, for a peak level of 166 dB, 10 to 25 impulses of 92 μsec duration had about the same effect as 75 tto 100 impulses of 36 μsec duration. Similar results were later obtained by the same investigators (1968). Acton et al. (1966) showed that 0.22 caliber rifles fired in the open (short duration) did not constitute a hazard to hearing, whereas the same rifles fired in an indoor reverberant range (long duration) did constitute a borderline hazard. The relation between impulse

duration and risk of TTS is best described by reference to the CHABA damage-risk criterion for impulse-noise exposure (discussed later).

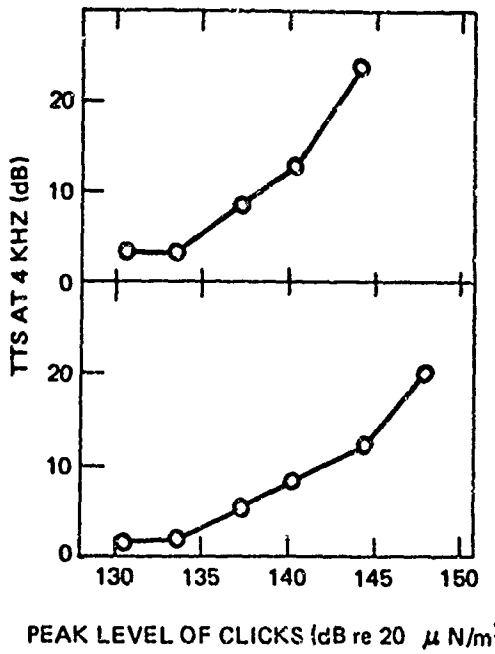


Figure 15–15. TTS at 4 kHz as a function of peak level of clicks. Upper curve: 3 min exposure at 25 clicks/min. Lower curve: 1 min exposure at 25 clicks/min. (Ward et al., 1961)

Rise Time. Many impulses have rise times less than 1 μsec since a shock wave is a major component of the event. To date, however, no serious attempt has been made to relate impulse rise time to the risk of TTS, and this variable is not treated systematically in damage-risk criteria.

Spectrum. Recently it has become possible to perform spectral analyses of impulses with a computer (Pease, 1967). There are, however, few data relating the spectrum of impulses to risk of TTS, and considerably more investigation will be required before such information will be of any real benefit.

Number of Impulses., TTS appears to grow linearly with the number of impulses, or linearly in time for a constant rate of presentation, as illustrated in figure 15-16.

Rate of Impulse Presentation. TTS growth rate from impulses does not differ significantly when the inter-pulse interval is between one and 9 seconds. At less than one second between pulses, TTS growth rate is reduced because of the protective action of the aural reflex. Also, when as much as 30 seconds elapses between successive impulses, TTS grows more

slowly because of the recovery which takes place between impulses (Ward, 1962; Ward et al., 1961).

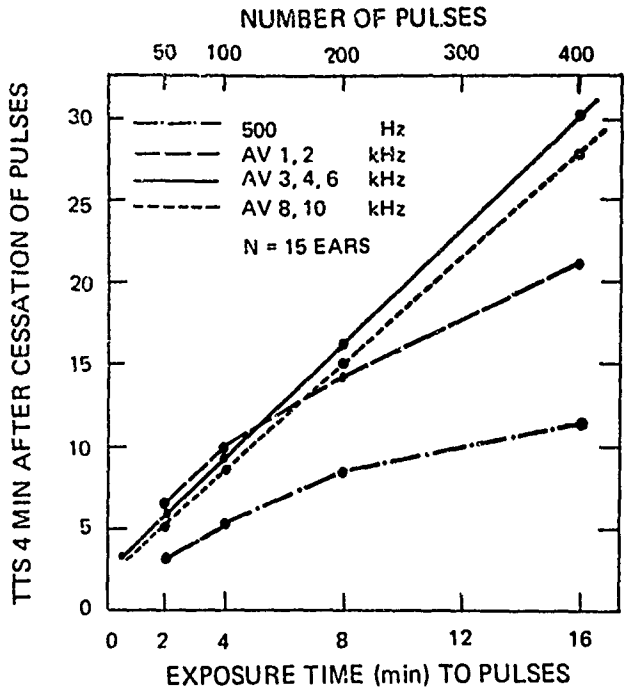


Figure 15–16. Average growth of TTS from pulses as a function of exposure time (lower abscissa), or of number of pulses (upper abscissa) when pulses are presented at a constant rate. TTS from impulses increases linearly with time or with number of pulses. (Ward et a., 1961)

Ear Orientation. When the impulse noise includes a shock wave, the orientation of the external ear with respect to the shock front is of considerable importance. Hodge et al. (1964) showed that when the ear is at normal incidence to the shock wave, the TTS produced is approximately equivalent to that produced by an impulse having 5 dB greater amplitude but arriving at grazing incidence. Golden and Clare (1965) reported a similar difference. Hodge and McCommons (1967b) have also shown that when the shockwave strikes one ear at normal incidence, the other ear, which is shadowed (protected) by the head, evidences considerably less TTS. This explains why it is usually found that right-handed rifle shooters demonstrate more TTS in the left, than right, ear: the right ear is at least partially protected by the head's shadow.

Test Frequency. TTS from impulse-noise exposure occurs at a wide range of frequencies, with the maximum TTS usually occurring in the region of 4 to 6 kHZ. This effect is illustrated in figure 15-17. Note that whereas mean and median TTS was between 0 and +10 dB at all frequencies, the *range* of

effect was from -25 dB (sensitization) at 3 kHz to +55 dB (loss) at 4 kHz. Also note that this exposure produced TTS at frequencies up to 18 kHz. Loeb and Fletcher (1968) believe that high-frequency TTS is a precursor of speech range TTS, and they suggest that when speech range TTS exceeds the CHABA (1968) allowable limits there is a chance of producing permanent high-frequency hearing loss.

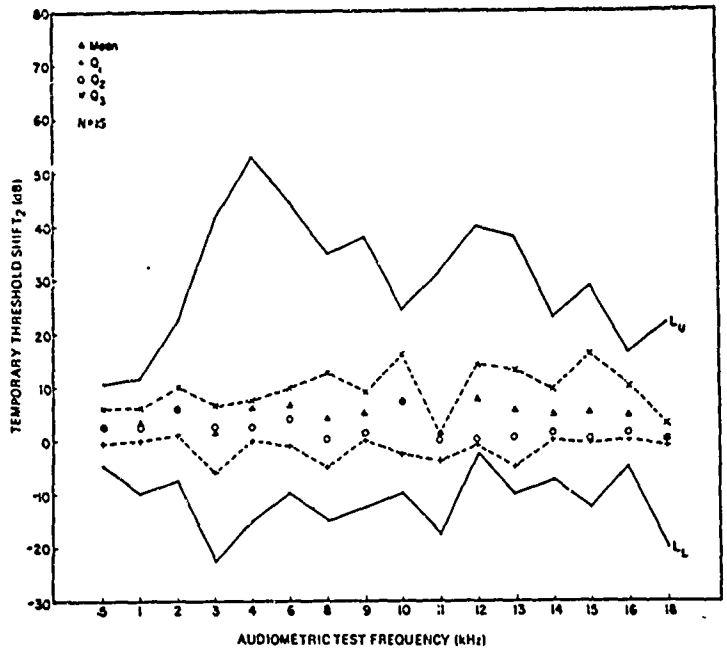


Figure 15–17. Distributions of TTS_2 following exposure to 25 gunfire impulses. (Hodge & McCommons, 1966)

Monaural vs. Binaural Exposure. Hodge and McCommons (1967a) found that, on the average, TTS growth rates for binaural and monaural exposure did not differ significantly when the interpulse interval was 2 seconds. There were large individual differences among the subjects, but no consistent trend favoring either type of exposure.

Recovery of TTS. A growing body of data indicates that recovery from TTS induced by various types of intermittent noise differs radically from that caused by steady noise exposure. Rice and Coles (1965) observed instances of individual subjects with $TTS_2 \approx 25$ dB who showed little or no recovery for periods of up to one hour after exposure, but thereafter recovery became approximately linear in log time. Luz and Hodge (1971) have found four types of recovery curves for impulse-noise-induced TTS in humans and monkeys: (1) recovery linear in log time; (2) no apparent recovery for periods of up to one hour, followed by linear in log time recovery; (3) slight recovery followed by an *increase* in TTS; and (4) slight recovery followed by a long plateau of no change, and then further recovery. These diverse functions occur to TTS 30 dB in humans, and suggest

that considerable further research will be required to derive averaged, generalized recovery functions for impulse noise induced TTS.

For TTS_2 40 dB recovery may be very slow; Fletcher and Cairns (1967) suggest that 6 months of recovery may be necessary to accurately assess residual PTS from excessive exposure to gunfire noise.

Blast

Blast differs little from impulse noise so far as the hearing mechanism is concerned. The term "blast" is typically used to refer to much higher pressures and/or longer durations than are usually associated with common impulse-noise sources. However, so far as the development of TTS is concerned, the preceding discussion of impulse-noise paramters is equally applicable to the parameters of blast.

Single, large-amplitude blast waves may rupture the eardrum. The threshold for eardrum rupture is about 5 psi; at 15 psi 50 percent of eardrums will probably be ruptured (Hirsch, 1966). When the eardrum is ruptured loss of hearing is severe in the affected ear, although after healing (2 to 6 weeks), the ear's sensitivity may return to normal, particularly if the middle ear ossicles are intact (Hamberger & Liden, 1951; Akiyoshi et al., 1966). Rupture of the eardrum thus serves as a "safety valve." If the eardrum is not ruptured by the blast, profound PTS may result from a single exposure, particularly at the higher frequencies of hearing (Ward & Glorig, 1961; Singh & Ahluwalia, 1968).

Long-Term Exposure to Spacecraft Noise

Short-term exposure to the high level, low frequency noise of spacecraft launch will not likely adversely affect astronauts, especially when earmuffs, helmets, and other protective gear are worn (Mohr et al., 1965). On the other hand, the relatively lower level steady background noise to which they will be exposed could adversely affect astronauts' hearing. Such background noise is produced by the life support system and other items of onboard equipment, such as glycol pumps, cabin fans, suit compressors, guidance and navigation systems, and inverters.

Yuganov et al. (1967) reported an extensive series of studies of the effects of spacecraft background noise on hearing. Their studies were conducted in a simulated spacecraft environment (complete with confinement and hypoactivity) during ground static testing. Figure 15-18 illustrates the growth of TTS resulting from successively longer exposures to 75 dB levels.* Yuganov et al. reported that recovery time for noise-induced TTS became progressively longer with increased exposure time. This phenomenon has been verified by NASA-sponsored studies conducted under the Gemini program, and was also reported by Mills et al. (1970).

*Although it is not clearly stated in their report, it is assumed from the description of procedure and instrumentation that the noise levels stated refer to dBA.

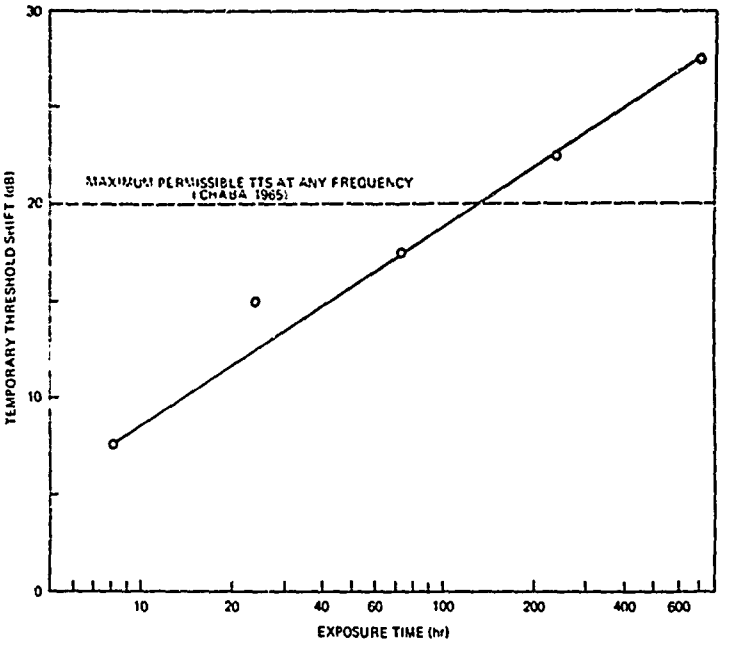


Figure 15–18. Growth of TTS with time for overall exposure level of 75 dB. Growth rate was linear in log time, and compares favorably with other data for higher levels and shorter durations (see figures 15-8 and 15-10). CHABA (1965) limit of 20 dB maximum TTS at any frequency was exceeded at about 130 hr exposure. (Yuganov et al., 1967)

In followup studies with 60 to 65 dB noise levels, Yuganov et al. found no evidence of TTS (or behavioral or physiological alterations) in astronauts exposed up to 60 days (1440 hours). Thus these authors concluded, and recommended, that for extended space flights of up to 60 days the background noise levels inside spacecraft should not exceed 65 dB. The 65 dB overall background noise limit recommendation compares favorably with the design criterion for background noise for Apollo spacecraft, indicated by Dr. B. O. French of the Manned Spacecraft Center (personal communication) to be NC-55, or approximately 60 dBA.

Effects of Hearing Loss on Performance

Some persons are likely to suffer TTS or PTS from noise exposure in spite of the application of safety criteria or the use of protective equipment. Other persons may have PTS from disease or trauma. Accordingly, in this section the effects of TTS and PTS on performance will be briefly considered.

Detection of Low-Level Sounds

Earlier, it was noted that an ear's threshold sensitivity (hearing level) is stated with reference to audiometric zero, such as the ANSI-1951 or ISO-1964 values. Audiometric zero at various test frequencies represents the lowest SPL

which can be detected, on the average, by listeners having "normal" hearing. Table 15-4 shows the SPL representing ISO-1964 audiometric zero at selected frequencies and the "allowable TTS" permitted by the CHABA (1965, 1968) damage-risk criteria for steady and impulse noise. The column at the far right shows the minimum SPL detectable, on the average, by a listener whose baseline hearing sensitivity equals ISO audiometric zero and who has CHABA-limit TTS at the various frequencies. These values are also descriptive of the detection limits for a listener who has PTS of the amounts shown in column 3.

Table 15–4

SPL Representing ISO Audiometric Zero and Minimum Detectable SPL for a Listener Having CHABA-Limit TTS

Frequency (Hz)	SPL for ISO Zero (dB re 20 $\mu N/m^2$)	CHABA Allowable TTS (dB)	Minimum Detectable SPL (dB re 20 $\mu N/m^2$)*
500	11	10	21
1000	6.5	10	16.5
2000	8.5	15	23.5
3000	7.5	20	27.5
4000	9	20	29
6000	8	20	28
8000	9.5	20	29.5

*This interpretation assumes that the listener's preexposure hearing sensitivity was equal to ISO audiometric zero.

Given a knowledge of the spectral characteristics of a low-level sound which must be detected, and the lowest SPL at various test frequencies which a particular listener can detect, predictions can be made of the listener's ability to detect the low-level sound. A convenient example from a military context, well-known to the authors, may be cited. It has been shown that sounds created by people walking over various types of terrain contain energy primarily in the 3 to 8 kHz range. Knowing this, it would be hypothesized that persons having TTS or PTS in this range of frequencies would be less able to detect such sounds than persons with normal hearing sensitivity. This hypothesis has been confirmed by experimental test, and these results suggest that, for example, military personnel receiving TTS from daytime exposure to weapon noise should not be assigned nighttime duty as perimeter sentry where the preservation of a life, or many lives, may depend on maximum hearing sensitivity, unimpaired by slowly-recovering TTS. These results further suggest that in *any* detection situation the listeners selected should have the most sensitive hearing possible, free of TTS or PTS.

Reception of Speech

The spectral characteristics of speech must be considered in assessing the effects of TTS or PTS on speech reception. Speech sounds range in frequency from 0.2 to 7 kHz; peak energy occurs at about 0.5 kHz. Speech sounds are of two basic types: vowels and consonants. Vowel sounds fall roughly into the frequencies below 1.5 kHz, and consonants are above 1.5 kHz (Sataloff, 1966). Vowels are thus more powerful (i.e., contain more energy) than consonants. Vowel sounds indicate that someone is saying something, but consonants aid in discriminating what is being said. Thus, consonants may be said to convey more information than vowels.

A person with TTS or PTS in the range of 0.2 to 1.5 kHZ has difficulty hearing speech unless it is quite loud, and is unable to hear soft voices. If the talker raises his voice level the listener will be able to understand what is being said.

The person with TTS or PTS in the range of 1.5 to 7 kHz, on the other hand, hears vowels normally but finds it difficult to discriminate consonants. Increasing the speech level aids little, but careful enunciation by the talker is of great benefit. This type of TTS or PTS is a particularly severe problem in occupational deafness since the loss of hearing sensitivity frequently occurs first in the 3 to 6 kHz range. The problem is compounded by the presence of background masking noise, since the low-level consonant sounds are masked to a greater extent by broad-band noise than the higher-level vowel sounds. This fact has led some hearing conservation groups to develop criteria for protecting hearing at frequencies up to 4 kHz (e.g., Piesse et al., 1962). In the United States, however, this has not been done: only frequencies of 0.5 to 2 kHz are considered in assessing occupational hearing impairment (Bonney, 1966).

Table 15-5 shows classes of hearing handicap which are defined by the average of PTS at 0.5, 1, and 2 kHz, as recommended by the Committee on Conservation of Hearing (1969). In general it may be said that TTS of the same amount will constitute an equivalent degree of impairment, although of course the impairment disappears when the individual has recovered from the TTS.

Subjective and Behavioral Responses to Noise Exposure

An earlier section considered the effects of noise demonstrated after exposure and indicative of a decrease in the responsiveness or neural activity in the auditory receptors. In this section, by contrast, noise effects which occur currently with exposure and result in increased neural activity will be considered. These responses will be discussed in terms of (1) general observations, (2) masking of auditory singals, (3) masking of speech, and (4) annoyance. Methods for measuring speech intelligibility and assessing the effect of noise on speech intelligibility will be presented. The treatment of annoyance will introduce the notion of "community response" to noise exposure.

Table 15–5

Chart for Determining Class of Hearing Impairment

Class	Degree of Handicap	Average Hearing Level (dB re ISO 1964) at 500, 1000, and 2000 Hz in Better Ear*		Ability to Understand Ordinary Speech
		At Least	Less Than	
A	Not significant		25	No significant difficulty with faint speech
B	Slight	25	40	Difficulty with faint speech only
C	Mild	40	55	Frequent difficulty with normal speech
D	Marked	55	70	Frequent difficulty with loud speech
E	Severe	70	90	Can understand only shouted or amplified speech
F	Extreme	90		Usually cannot understand even amplified speech

*If average of poorer ear is 25 dB or more greater than that for better ear, add 5 dB to average for better ear.

(Committee on Conservation of Hearing, 1969, p. 43)

General Observations

Broadbent and Burns (1965) and Cohen (1969) have reviewed the effects of noise on behavior and psychological state. In some respects the existing literature does not yet support firm conclusions, but representative subjective and behavioral responses are summarized in table 15-6.

Masking of Auditory Signals

The amount of masking is the number of decibels that the quiet threshold of a signal must be raised to be intelligible because of the presence of masking sound. Masking effects may be classed as monaural or interaural. Monaural masking occurs when the signal and noise reach the ear(s) at the same time; this type of masking is most critical in working environments where personnel are not wearing earphones, and will be discussed below. (Interaural masking occurs when the signal reaches one ear and noise the other ear. No interaural masking occurs unless the noise exceeds about 40 to 50 dB SPL, since below this level the listener can readily distinguish between the sounds heard separately in his two ears. At higher levels the noise is transmitted to the "signal" ear via bone conduction; thus this situation may be regarded as a special case of monaural masking with the head serving as an attenuator. Interaural masking is a particular problem when the telephone is used in a noisy environment, and when the SPL in one ear is much higher than in the other.)

The monaural masking effect of a pure tone, or of a noise having a strong pure tone component, is greatest near the frequency of the tone but also extends to frequencies adjacent to the masking tone. Curves of masking effects as a function of frequency are shown in figure 15-19. Audible beats near the frequency of the masking tone increase the audibility of the signal and thus reduce the degree of masking at these frequencies. For tones of low intensity masking is confined to a region near the masking tone; for higher intensities the masking is extended, particularly at frequencies above the masking tone. The masking effect of narrow-band noise is quite similar to that for pure tones, except that the dips due to audible beats are absent. Masking of signals by wide-band noise whose level does not exceed about 60 to 70 dB SPL is governed by the critical band concept. At low noise levels pure tones are masked by only a narrow range of frequencies whose width defines the critical band for that signal frequency. The width of the critical band varies from about 40 to 200 Hz, over the tonal range of 0.5 to 8 kHz. Within this range, and for low noise levels, an increase of 10 dB in noise level results in about 10 dB additional masking of tones within the critical band. Above masking levels of about 70 dB SPL, however the width of the critical band increases markedly in both directions. A 10 dB increase in noise level will still cause about 10 dB more masking of frequencies within the noise band, but it may also increase the masking effect at more distant frequencies by as much as 20 dB.

Table 15–6
Representative Subjective and Behavioral Responses to Noise Exposure

Conditions of Exposure			Reported Disturbances	Reference
SPL (dB)	Spectrum	Duration		
150*	1 – 100 Hz	2 min	Reduced visual acuity; chest wall vibrations; gag sensations; respiratory rhythm changes	Mohr et al., 1965
120	Broadband		Reduced ability to balance on a thin rail	Nixon et al., 1966
110	Machinery noise	8 hr	Chronic fatigue	Cohen, 1969
105	Aircraft engine noise		Reduced visual acuity, stereoscopic acuity, near-point accommodation	Panian, 1963
90	Broadband	Continuous	Vigilance decrement; altered thought processes; interference with mental work	Broadbent & Burns, 1965
85	1/3-octave @ 16 kHz	Continuous	Fatigue, nausea, headache	Acton, 1968
75	Background noise in spacecraft	10 – 30 days	Degraded astronauts' performance	Yuganov et al., 1967
60	SIL	80 sec/hr	Annoyance reactions in 50% of community residents	Borsky, 1958

*In this study subjects wore protective devices to prevent hearing loss.

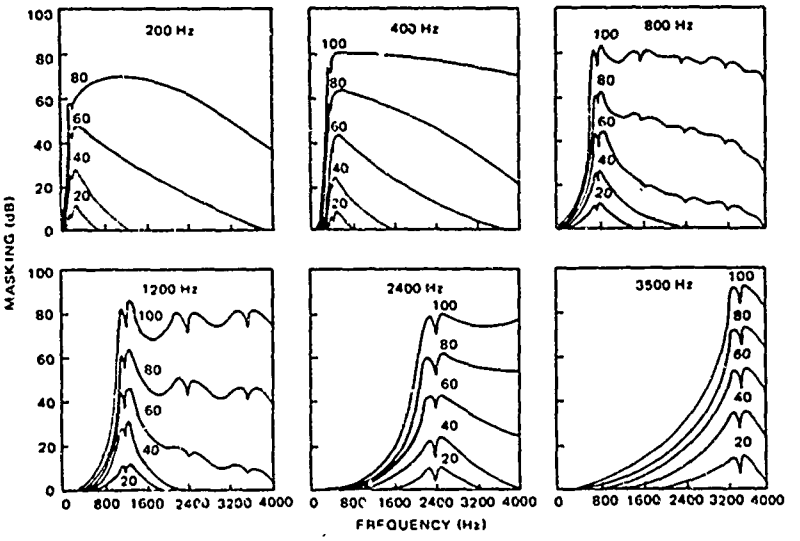


Figure 15–19. Masking as a function of frequency for masking by pure tones of various frequencies and levels. Number at top of each graph is frequency of masking tone. Number on each curve is level above threshold of masking tone. (Wegel & Lane, 1924)

Masking of Speech by Noise

Most of the energy required for near-perfect speech intelligibility is contained in the range of 0.2 to 7 kHz. This range may be narrowed to 0.3 to 4.5 kHz without significant loss in intelligibility. (In reducing the frequency range it must be remembered that 1.5 kHz constitutes the "center of importance" of speech, and narrowed pass bands of a communications system should be centered on about 1.5 kHz.) Consonants contain energy at frequencies above 1.5 kHz, whereas vowels contain lower-frequency energy. Unfortunately, the consonants, which convey most of the information in English speech, contain very little energy. Thus, they are more subject to interference (masking) from noise than are vowels. Conversely, vowels contain more energy but transmit less information.

Communication System Design. It is desirable to maintain as high a speech signal-to-noise ratio as possible in each frequency band, with particular emphasis on those bands which contribute most to intelligibility. Another consideration is the point of overload of the hearing mechanism: the level above which intelligence is no longer extracted from the stimulus. The overload effect can be demonstrated quite readily in a noisy environment when a voice comes over a loudspeaker at a very high level. A listener will find the amplified speech more intelligible when his ears are plugged than when listening without earplugs. This effect occurs because with the ears plugged the speech signal does not overload the hearing mechanism and, at the same time, the signal-to-noise ratio remains constant. Overloading of the ear due to speech amplitude begins to occur when the overall RMS level of the speech signal is about 100 dB at the listener's ear. (The average overall RMS level of speech in a quiet environment may be

approximated by subtracting 3 dB from the arithmetic average of the peak levels observed on a sound level meter set for slow meter damping on the C-scale.) In addition to not contributing to intelligibility, higher levels of speech signals produce discomfort and possible hearing loss.

Factors in Speech Intelligibility. Two types of communications must be considered in discussing speech intelligibility: electrically-aided, and direct. The effectiveness of both types of coice communication are determined by the following parameters: (1) level and spectrum of ambient noise at the ear (includes both acoustical noise, and electronically-induced noise); (2) voice level and spectrum of speech; (3) distance between the speech source and the listener's ear; and (4) the complexity and number of alternative messages available to the listener. Electrically-aided speech more specifically also depends upon the characteristics of all of the components of the transmission and receiving systems.

Recommended Approaches to Measurement of Speech Intelligibility. Speech intelligibility is measured by determining the percentage of words correctly received by listeners. This may be done by conducting subjective tests with talkers and listeners, or by calculations based on the signal-to-noise ratio in various frequency bands. The choice of approach will be determined by the amount of time, personnel and/or instrumentation available.

PB Word Intelligibility Test. In the bioastronautics field one usually attemps to discriminate among, or evaluate, highly effective communications systems. This requires a sensitive test of speech intelligibility—one that is capable of detecting small differences between systems. Therefore, the use of the "Phonetically Balanced (PB) Monosyllabic Word Intelligibility Test" (ANSI Standard S3.2-1960) is recommended for applications requiring maximum accuracy.

Some aspects of the test procedure are as follows. The test material consists of 20 lists of 50 phonetically-balanced words each. Each list is of approximately the same difficulty. The talker reads the words in a "carrier sentence" at 4-second intervals and the listener writes down each key work. The hearing level of both talkers and listeners must average no more than 10 dB overall, with no more than 15 dB at any of the frequencies 0.25, 0.5, 1, 2, and 4 kHz (*re* ANSI Standard Z24.5-1951). Talkers must have no obvious speech defects or strong regional or national accents. Test personnel must be completely familiar with each of the 1000 words and with the speech characteristics of the talkers. The test must always be given in its entirety (i.e., all 1000 words must be used), and if the test is to be repeated several times with the same personnel, it is recommended that the order of words within lists be randomized for each presentation. Normally, 8 to 10 hours of talker and listener training are required to properly utilize the PB intelligibility test.

PB intelligibility score may be acceptable in certain instances with values as low as 50 percent (of words correctly received). Only rarely is an intelligibility score of 90 percent required. Single digits may be transmitted with greater than 99 percent reliability with a system providing a PB score of 60 to 70 percent,

since the listener has only 10 alternatives from which to choose. The criterion of acceptability for communication systems should be a *mandatory score of 70 percent* and a *desirable score of 80 percent* when the ANSI PB method is followed.

Modified Rhyme Test. If testing time is limited, or time is not available to thoroughly train subjects for the PB method, the second recommended choice is the Modified Rhyme Test (MRT) described by House et al. (1963). The test material consists of 300 words which are printed on an answer sheet in 50 groups of six words each. The talker reads one of the six words in the first group and each listener selects one word from the closed set of six alternatives. Unlike the PB test, little account is taken of word familiarity or of the relative frequency of occurrence of sounds in the language. This test has the advantage of requiring little or no training, and does not require a written response as is the case with PB tests. A chart for converting MRT scores to PB test scores is shown in figure 15-20.

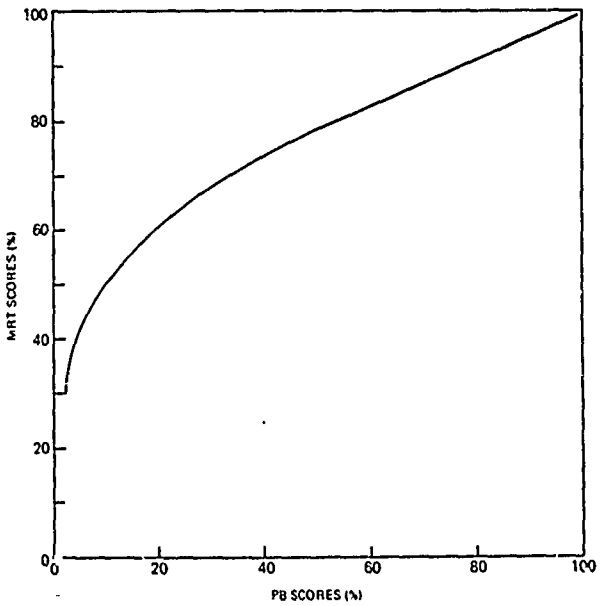


Figure 15–20. Relationship between MRT test scores and PB test scores. (Based on unpublished data from K. D. Kryter, 1964)

Articulation Index Calculation. Intelligibility of speech in noise may also be calculated from measures of the speech and noise levels through use of the Articulation Index (AI) (Kryter, 1962). AI can be calculated from octave-band measurements using the worksheets shown in figure 15-21 and table 15-7, provided the noise does not have any severe pure tone components and is steady in character without an extremely sloping spectrum. (Additional worksheets are available in the source document if the situation requires the use of 1/3-octave band measurements.)

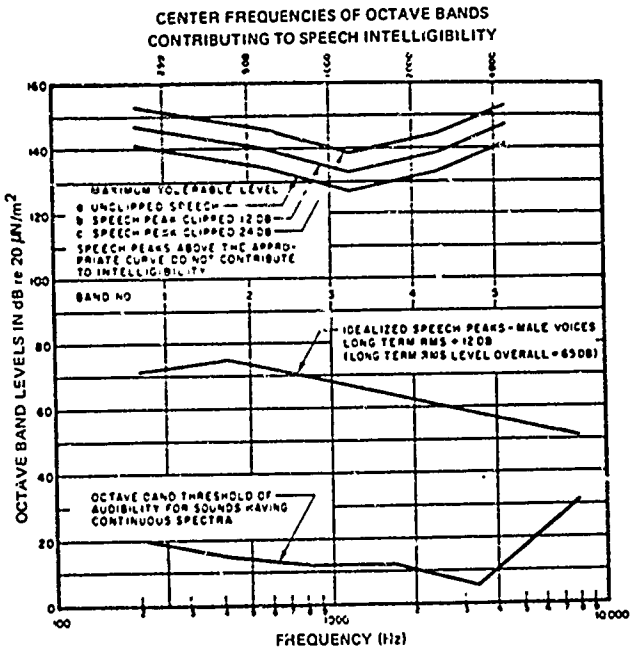


Figure 15–21. Worksheet for calculating Articulation Index by the octave band method using ANSI preferred frequencies. (Kryter, 1962)

Table 15–7

Worksheet for Calculating Articulation Index by the Octave Band Method (Preferred Octave Bands)

Col 1		Col 2	Col 3	Col 4
Octave Band	Frequency	Speech Peak-to-Noise Difference in dB	Weight	Col 2 X Col 3
1. 180– 355 Hz	250 Hz	_____	0.0018	_____
2. 355– 710	500	_____	0.0050	_____
3. 710–1400	1000	_____	0.0075	_____
4. 1400–2800	2000	_____	0.0107	_____
5. 2800–5600	4000	_____	0.0083	_____
			AI =	_____

(Kryter, 1962)

The octave band method of calculating AI is as follows: (1) Plot the measured octave band SPL of the noise. (2) Adjust the idealized speech spectrum shown on the worksheet to reflect its actual level. (3) Measure the difference between the speech and noise in each band, and assign a value between zero and 30 dB. (4) Multiply this assigned value in each band by the appropriate weighting factor (this accounts for the difference in the importance among the several bands) and add the resultant numbers. This number, which is between zero and one, is the AI which may then be converted to PB intelligibility score through the use of figure 15-22.

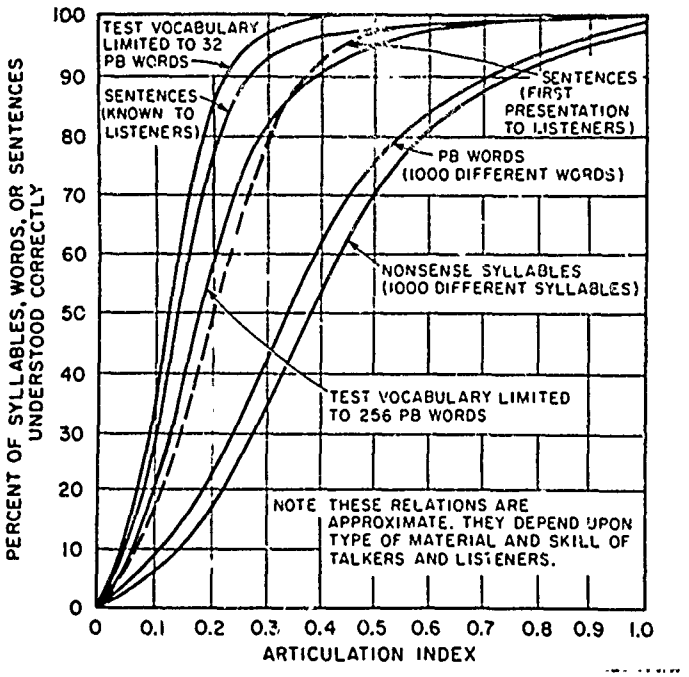


Figure 15–22. Relation between Articulation Index and various measures of speech intelligibility. (Kryter, 1970b)

The AI method of calculating speech intelligibility may be used for either direct or electrically-aided communication, provided only that the speech signal and noise levels at the ear are known.

Annoyance: Community Response to Noise Exposure

The term annoyance refers to the perceived noisiness, unwantedness, objectionableness, or unacceptableness of noise. Communities of noise-exposed residents may be annoyed and may respond collectively, or as individuals, in attempts to rid themselves of the intruding noises. Individual differences among group members make it very difficult to predict individual responses; however, group response prediction has achieved a high degree of sophistication and reliability.

Quantification and prediction of community response to noise exposure involves identification and/or measurement of many variables, including level, spectrum, duration, time of day, frequency of occurrence, type of residential neighborhood and amount of previous noise exposure. Integrating these data, with appropriate weighting, into a predictive scheme results in a single "composite" rating of the annoyance reaction to be expected. Such reactions range from no response, through occasional complaints by individuals, to concerted legal action by groups.

Two general approaches to the prediction of annoyance reactions enjoy wide acceptance. The first approach, typified by the Composite Noise Rating of Rosenblith and Stevens (1953), results in a qualitative prediction of community response without attaching to it a precise numerical value. Botsford (1969) has simplified this approach, as illustrated in figure 15-23, by reducing the measurement of level and spectrum to A- and C-weighted sound levels. This figure can thus be used to predict community responses to noise levels up to 95 dBA and 110 dBC.

The second approach involves computation of a numerical index of perceived noisiness which is then used to predict community response. Kryter's (1968) Effective Perceived Noise Level (EPNL) expressed in EPNdB, has found particular application in the evaluation of community response to aircraft noise [although, as Kryter (1970) indicates, the method is applicable to all types of community noise exposure]. The general relationship between EPNL and annoyance reactions is illustrated in figure 15-24.

It is not practical to recommend a single, optimum procedure for calculating EPNL since many new developments are rapidly taking place. The various existing procedures differ primarily in terms of the weighting to be assigned to the highest SPL during an occurrence of a noise, and the length of the integration time used in calculating perceived noise level. Sperry (1968) presents the calculation procedure used for Federal Aviation Agency certification of new commercial aircraft. Kryter (1968) reviews a variety of computation procedures, and (Kryter, 1970) describes his latest recommendations for EPNL calculation, including a discussion of its application to sonic boom problems. Department of Defense (1964) reports related procedures helpful in land use planning. Cole and von Gierke (1957) discuss community response to noise from missile static testing and launch operations.

Physiological (Nonauditory) Responses to Noise Exposure

Low Level Stimulation

It is now well established that noise exposure can affect human physiological processes and that measureable effects are obtained with noise exposure conditions involving little or no risk of TTS. The main concern of researchers is whether these effects of noise, which in some instances appear to be correlated with pathological effects and/or behavioral alterations, may represent a real hazard to the health and well-being of exposed persons.

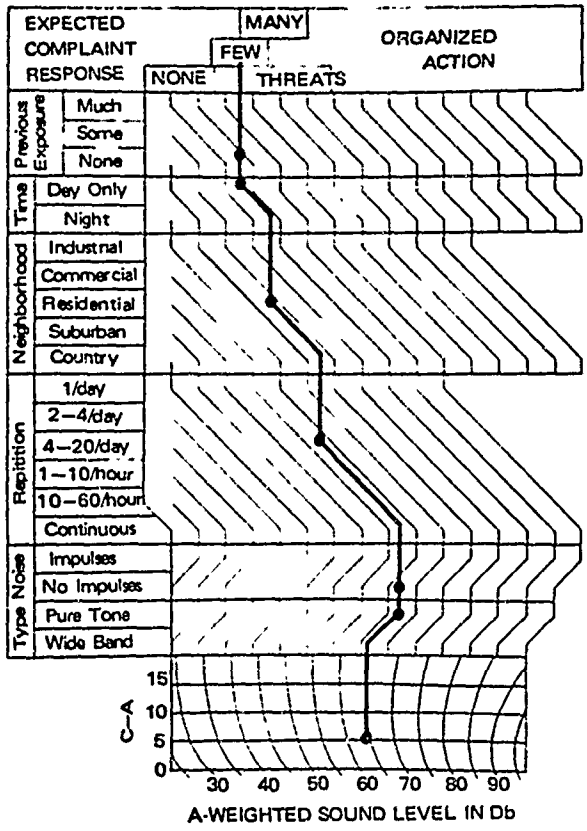


Figure 15–23. Annoyance of neighborhood sound levels. To use graph, locate in curved grid at bottom, point corresponding to sound levels of neighborhood noise under consideration and project directly above it into first of the 6 correction sections bounded by horizontal lines. Follow correction lane entered until reaching position opposite condition listed at left which applies to noise under consideration, and then proceed vertically, disregarding lanes, until next section is reached. Work upward through lanes of correction sections until reaching response to be expected at the top, e. g., if truck movements at a new loading station are to be cued by a whistle that will produce 65 dBA and 70 dBC at the nearest homes 10 to 15 times/day, then few complaints would be expected according to the line traced through the chart above. (Botsford, 1969)

Jansen (1969) dichotomizes physiological responses to noise into stress reactions and vegetative reactions. Stress reactions to unfamiliar stimuli, in general, show adaptation with repeated exposure as the stimuli become familiar and gain meaning to man, and hence are of less concern in the present context. It is the vegetative reactions to meaningless noise stimulation which is of primary concern here. Meaningless noise refers, for example, to the background noise found in industry, in the community and in the home. Adaptation to such noises has not been reported in many instances, and continued exposure may involve some risk of eventual interference with the health and well-being of workers.

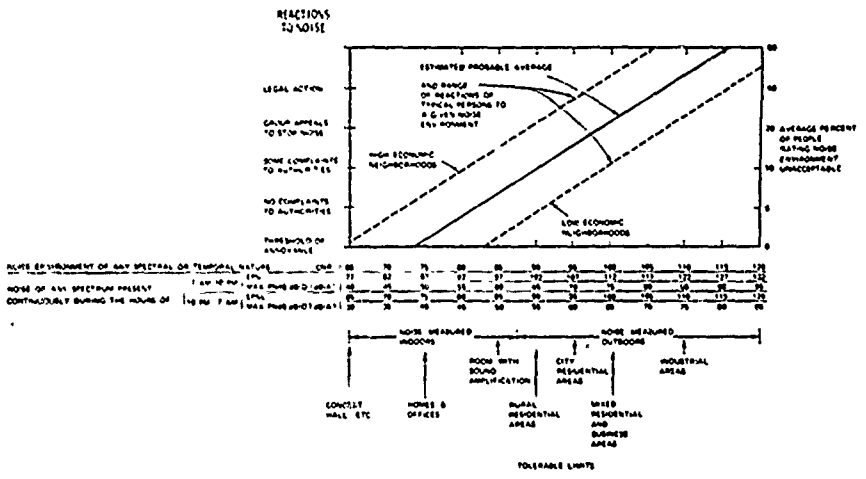


Figure 15–24. General reactions of people and communities to environmental noise. (Kryter, 1970)

Representative observations from studies cited by Anticaglia and Cohen (1969) and Jansen (1969) are summarized below:

- Noise exposure causes increases in the concentration of corticosteroids in the blood and brain and affects the size of the adrenal cortex. Continued exposure is also correlated with changes in the liver and kidneys and with the production of gastrointestinal ulcers.
- Electrolytic imbalances (magnesium, potassium, sodium and calcium) and changes in blood glucose level are associated with noise exposure.
- The possibility of effects on sex-hormone secretion and thyroid activity is indicated.
- Vasoconstriction, fluctuations in blood pressure, and cardiac muscle changes have been reported. Vasoconstriction in the extremeties, with concomitant changes in blood pressure, have been found for noises of 70 dB SPL, and these effects become progressively worsened with higher levels of exposure.
- Abnormal heart rhythms have been associated with occupational noise exposure and this and other evidence supports the tentative conclusion that noise may cause cardiovascular disorders.
- Panian (1963) states that in Russia the cardiovascular symptoms outlined above are collectively referred to as "noise sickness."
- Yuganov et al. (1967) found that 10 to 30 days of exposure to noise levels of 75 dB produced electroencephalographic and cardiovascular alterations in astronauts similar to those described above. Reduction of the noise level to 65 dB resulted in no such observations at all for exposures of up to 60 days.
- With respect to *impulse*-noise exposure, Yuganov et al. (1966) reported that repeated exposure to simulated sonic booms having peak levels up to 9 kg/m^2 (133 dB *re* 20 $\mu N/m^2$) caused alterations in electrocardiogram and

electroencephalogram traces as well as moderate bleeding in tympanic membrane epithelium, and they said that subjects reported headache, tinnitus and "fullness" in their ears.

Risk of Injury or Death from Steady Noise

Studies of very intense steady acoustic stimulation have been carried out primarily with animals, and few data are available for human exposures. Three relevant observations follow:

- One instance of a ruptured human eardrum has been reported for exposure to 159 dB SPL at 6.5 kHz for 5 minutes (Davis et al, 1949).
- Mohr et al. (1965) reported no risk of bodily injury to astronauts from the intense, low-frequency noise simulating a space rocket launch, but a number of questions remain unanswered in this regard. Exposure to tones in the 1 to 100 Hz range should not exceed 2 minutes or 150 dB SPL, as these values appear to be close to the limits of human tolerance.
- Parrack (1966) calculated that for a 2 kHz whole-body exposure (probably not attainable in a practical situation) human lethality from overheating would require from 5 minutes at 167 dB SPL to 40 minutes at 161 dB. At 6 to 20 kHz the exposures required for lethality range from 5 minutes at 187 dB to 40 minutes at 181 dB SPL. Parrack's paper further indicates that ultrasonics pose no special hazard to man's life until the SPL exceeds 180 dB.

Blast and Impulse Noise Effects

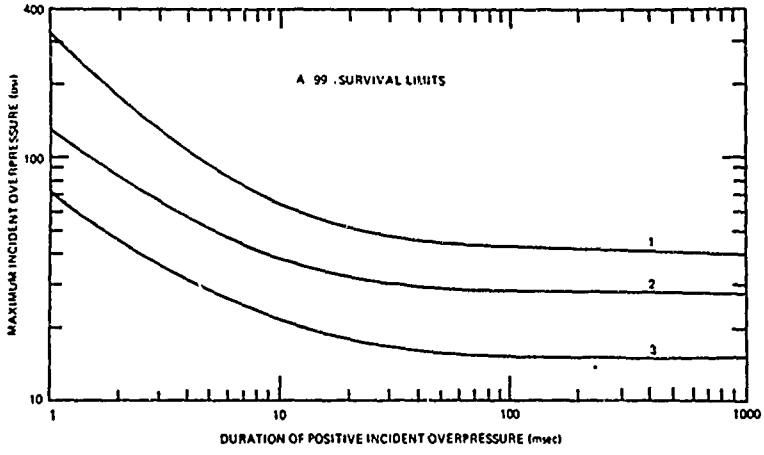
The effects of high-intensity blast waves on man are classed as primary, secondary and tertiary: primary effects are those resulting from the impact of blast waves on tissues; secondary effects are caused by flying debris set in motion by the blast; tertiary effects result from propulsion of the body. Only the primary effects of blast will be briefly summarized here.

The following extrapolations of animal data to human exposures are valid only for exposure to single, fast-rising blast waves involving classical or near-classical waveforms:

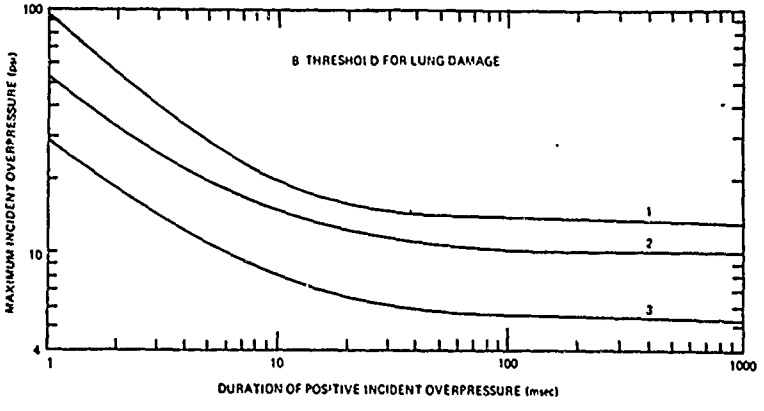
- Risk of injury or death increases with increased pressure and/or duration, and with the presence of nearby reflecting surfaces.
- Risk of injury is lessened with increased rise time, and higher-than-normal ambient pressures.
- Gas-containing organs (ears, lungs, intestines) are very susceptible to blast injury.
- The eardrum is most susceptible: its threshold for rupture is about 5 psi.
- The lungs are most critical with regard to possible lethality: the threshold for lung damage (minor hemorrhage) is about 10 psi.

• Animals exposed to blast show evidence of central nervous system (concussive) damage--ataxia, paralysis, convulsions, dazed appearance, and lethargy--and often do not respond to noxious stimuli.

• Figure 15-25 shows 99 percent survival limits and lung damage thresholds as a function of peak overpressure and blast duration.



(a)



(b)

Figure 15–25. Blast exposure limits as a function of peak overpressure and duration. (A: 99% survival limits; B: threshold for lung damage; 1: long axis of body parallel to blast wave; 2: long axis of body perpendicular to blast wave; 3: thorax near a reflecting surface which is perpendicular to blast wave.) All curves relate to subjects facing any direction. (Bowen et al., 1968)

Few studies have been made of the effect of repeated, high-amplitude blast waves and impulse-noise waves. De Candole (1967) states that repeated blast exposure is responsible for the syndrome known as "battle fatigue." Anecdotal reports indicate that large caliber weapon instructors exposed to 50 impulses per day at about 10 psi complain of chest pains, nausea, and sleeplessness. Jacobson

et al. (1962) felt that it was necessary for subjects exposed to repeated impulses from a howitzer to wear a foam rubber "chest protector" at levels of 6 psi and higher. Tanenholtz (1968) recommends that artillery crewmen not be exposed to repeated blast at pressures above 7 psi, even when utilizing protection.

Design Criteria

Design Goals

It seems unlikely that noise and blast will ever be completely eliminated from man's environment. Therefore, steps must be taken to insure that the noise which reaches man's receptors is tolerable. The term "tolerable" may be interpreted in several ways. (1) It refers to the prevention of excessive hearing loss and unpleasant subjective sensations: criteria for this purpose are discussed below. (2) Prevention of injury from blast is also considered. (3) Further, tolerable noise exposure refers to limiting background noise levels to the extent required to minimize masking of speech communications, and (4) to providing noise levels in work areas that do not interfere with the performance of duties. (5) Also, community noise levels must be limited to prevent annoyance, complaints or threats of legal action.

Finally, one method of achieving tolerable noise levels at a person's ear is by the use of hearing protectors. Various protective devices and techniques are presented at the end of this section.

Noise Exposure Limits

Documents developed to aid in specifying noise exposure limits are variously referred to as damage-risk criteria (DRC), damage risk contours, and hearing conservation criteria. The first two names point to a consideration which must not be ignored. "Damage risk" implies just that: there is always the risk of some TTS or PTS in a portion of the noise-exposed population. Because of the wide range of susceptibility to hearing loss (discussed earlier), it is neither philosophically realistic nor economically feasible to enforce DRC which will protect everyone (Cohen, 1963). Always, there is a risk that someone will lose a portion of his hearing sensitivity either temporarily or permanently. Thus, it is incumbent upon the user of any DRC to insure that he understands the risks involved.

It should be noted that the noise limits imposed by DRC refer to the noise which actually enters the ear canal. If the environmental noise exceeds the allowable limits, several means are available for reducing the levels to or below acceptable limits.

Steady-State and Intermittent Noise DRC.

CHABA DRC. The CHABA Damage Risk Criteria (DRC) (1965) was developed through the efforts of Working Group 46 of the NAS-NRC Committee on Hearing, Bioacoustics and Biomechanics. The acceptable limits

for end-of-day TTS_2 are: 10 dB at or below 1 kHz, 15 dB at 2 kHz, and 20 dB at or above 3 kHz, in 50 percent of exposed ears. These TTS limits are considered to be equal to the maximum acceptable amounts of PTS after about 10 years of near-daily exposure. The allowance of less TTS in the lower frequencies is designed to provide additional protection for the speech-range frequencies, and the 10-15-20 dB TTS limits are related to the borderline criteria for compensable hearing loss. It is not safe to attempt to extrapolate the criteria to prevent PTS at intermediate number of years, nor the protection of different amounts of hearing. For such individualized applications, special criteria should be developed.

The CHABA steady noise DRC is presented in the form of 11 graphs relating the trade-offs among (1) spectrum, (2) exposure time up to 8 hours and, (3) SPL. Figure 15-26 shows the exposure limits for octave (and narrower) bands of noise, and figure 15-27 gives the limits for exposure to pure tones.

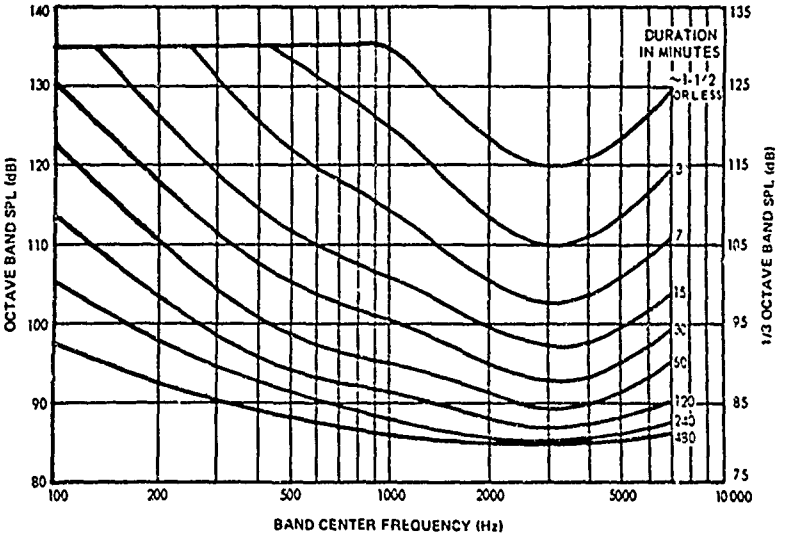


Figure 15–26. Damage risk contours for 1 exposure/day to octave (left-hand ordinate) and 1/3 octave or narrower (right-hand ordinate) bands of noise. Graph can be applied to individual band levels present in broad band noise. (CHABA, 1965)

The CHABA DRC's 8-hour exposure limit makes it inapplicable as a design criterion for extended space flight, but it is applicable to the protection of ground-service crews and other personnel who typically work 8-hour shifts each day. (See below for design criteria for extended space flight.)

Those regulations, which apply to noise, under the Occupational Safety and Health Act of 1970 include the limits on occupational noise

exposure. Noise exposure limits are stated in terms of A-weighted sound levels, and table 15-8 shows the permissible levels for exposures of 15 minutes to 8 hours per day. For octave band SPL data, a graph is provided for determining equivalent A-weighted sound levels, as shown in figure 15-28.

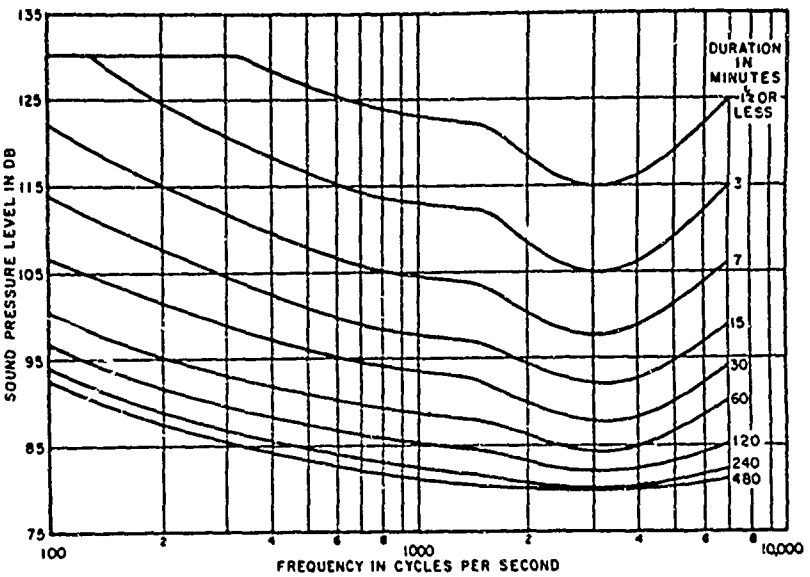


Figure 15–27. Damage risk contours for 1 exposure/day to pure tones. (CHABA, 1965)

Table 15–8

Occupational Safety and Health Act
Permissible Daily Noise Exposure*

Duration (hr)	Sound Level (dBA)
8	90
6	92
4	95
3	97
2	100
1.5	102
1	105
0.5	110
0.25	115

*When the exposure is intermittent at different levels the fraction $C_1/T_1 + C_2/T_2 \ldots C_n/T_n$ should not exceed unity to meet the exposure limit.

C_n = total exposure time at the specified noise level.

T_n = total exposure time permitted at the specified level.

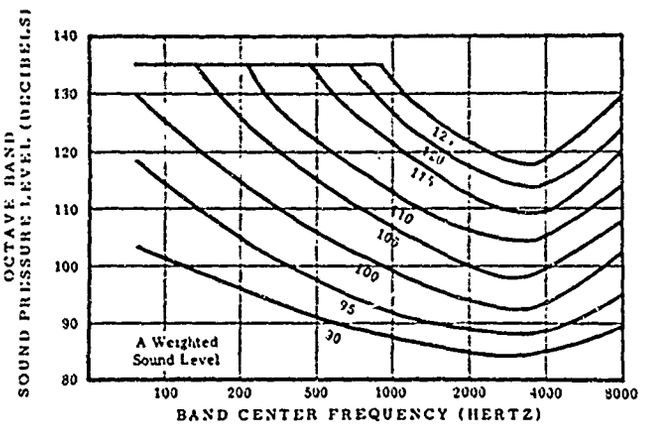


Figure 15–28. Contours for determining equivalent A-weighted sound level. Graph is used in interpreting octave-band sound levels according to the provisions of Occupational Safety and Health Act. (OSHA, 1970)

Noise Limits for Extended Space Flight. To obviate the possibility of TTS during extended space flights (up to 60 days) the background noise level inside spacecraft should not exceed 65 dB overall (Yuganov et al., 1967).

Ultrasonic Noise Limits. To prevent TTS and unpleasant subjective responses to ultrasonic noise, the SPL must not exceed 75 dB in 1/3-octave bands centered at 8 to 16 kHz or 110 dB at 20 to 31.5 kHz (Action, 1968).

Low-Frequency and Infrasonic Noise Limits. To prevent physiological injury from low-frequency and infrasonic noise (1 to 100 Hz) the limits shown in table 15-9 must not be exceeded. Even at these limits, experienced astronauts may report transient unpleasant sensations. Above these levels wearing of hearing protective devices is *mandatory*.

Table 15–9

Low-Frequency and Infrasonic Noise Exposure Limits

Frequency* (Hz)	SPL (dB)	Duration** (min/day)	Notes
1 – 7	150	4	Use of ear plugs will reduce unpleasant sensations
8 – 11	145	4	
12 – 20	140	4	
21 – 100	135	20	Without protection
21 – 100	150	20	With ear plugs

*Refers to pure tones or to octave bands with center frequencies as indicated.
**Refers to one exposure per day with at least .4 hr elapsing between successive exposures. (Wilhold et al., 1970)

Impulse-Noise Limits. The most comprehensive DRC for impulse noise exposure is that published by CHABA (1968) and based on the formulations of Coles et al. (1967, 1968). This DRC assumes the same TTS limits as does the CHABA (1965) steady noise DRC. However, the impulse noise DRC is designed to protect 95 percent of ears exposed. The basic DRC (figure 15-29) assumes a daily exposure of 100 impulses distributed over a period of from 4 minutes to several hours and that the impulses reach the ear at normal incidence.

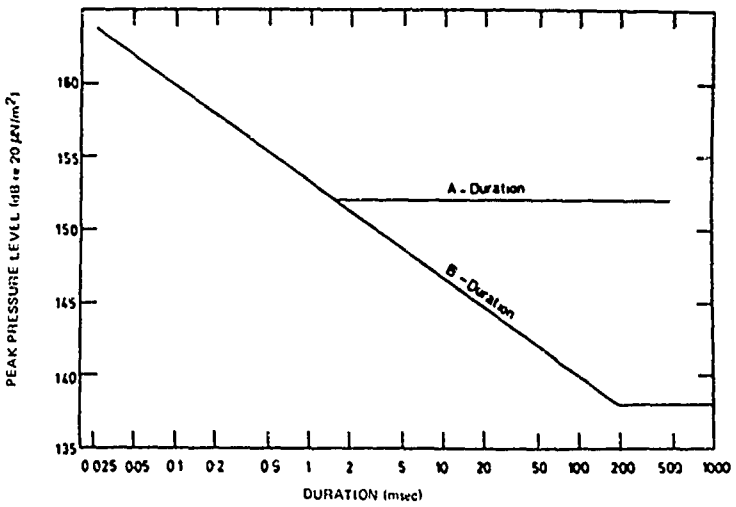


Figure 15–29. Basic limits for impulse noise exposure assuming 100 impulses/day and other conditions as stated in text. (CHABA, 1968)

Two correction factors are included in the DRC. First, if the pulses reach the ear at grazing incidence (rather than normal) the curves can be shifted upward by 5 dB. Second, if the number of impulses in a daily exposure is some value other than 100 (i.e., 1 to 1000) an adjustment can be made according to the curve shown in figure 15-30.

Blast Exposure Limits

To minimize temporary or permanent hearing loss from blast, the impulse noise criteria stated above should be used. To avoid other physiological injury from fast rising, long duration blast waves, the following pressures must not be exceeded:

5 psi (unprotected) to prevent eardrum rupture

10 psi (ears protected) to prevent lung damage. (See figure 15-25)

Speech Interference Criteria

In a preceding section, calculation of the Articulation Index was discussed. AI, as a method of estimating the masking effect of noise on speech

intelligibility, is quite involved. A relatively simple method was devised by Beranek (1947) and later modified by Webster (1969). Webster's method, called the three-band preferred octave speech-interference level (PSIL), is obtained by averaging the noise levels in the 500, 1000, and 2000 Hz octave bands.

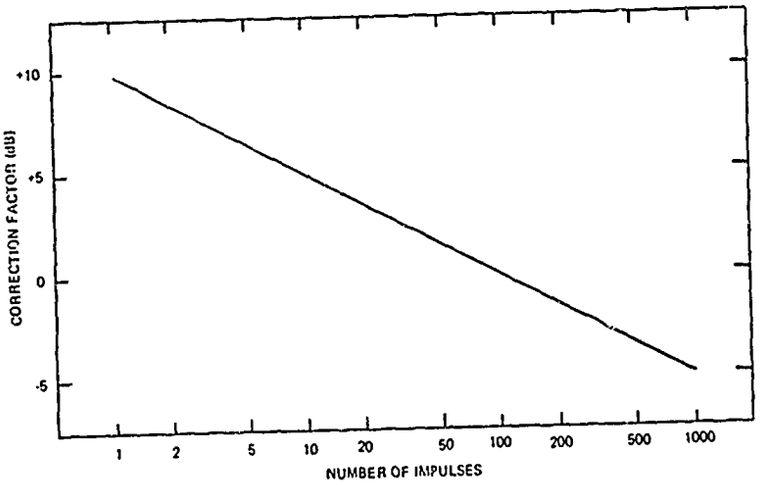


Figure 15–30. Correction factors to be added to ordinate of figure 15-29 to allow for daily impuse noise exposures different from 100 impulses. (CHABA, 1968)

Once the PSIL value has been calculated, reference to figure 15-31 may be made to determine what voice level is required to provide acceptable intelligibility at a given talker-to-listener distance. "Acceptable intelligibility" here corresponds to a PB intelligibility score of 75 percent and assumes that no lipreading occurs. The "expected voice level" results from the fact that a speaker tends to raise his voice level about 3 dB for each 10 dB increase in ambient noise starting at about 50 dB PSIL when he receives no feedback from the listener. The "communicating voice" is that effort produced when a talker receives instantaneous feedback of success or failure from the listener.

Workspace Noise Criteria

Beranek (1960) presents criteria for limiting workspace background noise where communications interference, loudness, or annoyance of noises are an important design consideration. These noise criterion curves, or "NC" curves, are widely used as workspace d sign criteria. Figure 15-32 shows the allowable octave-band SPL (for both commercial and preferred octave bands) and table 15-10 identifies typical work spaces with the appropriate NC curves. These curves were derived in such a way that each octave band contributes about equally to the loudness of the background noise. To be acceptable, the noise level in each octave band must not exceed the level permitted by the selected NC curve. It should be noted that when using commercial frequencies the NC number is also the SIL for that particular spectrum.

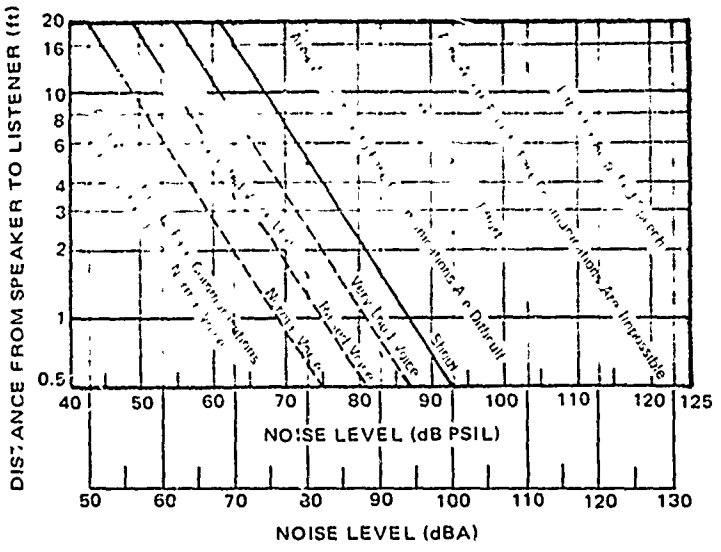


Figure 15–31. Voice level and distance between talker and listener for satisfactory face-to-face speech communications, as limited by ambient noise level. Along abscissa are two generally equivalent objective measures of noise level: average octave-band level in octaves centered at 500, 1000, and 2000 Hz, called the three-band preferred octave speech-interference level (PSIL), and A-weighted sound level meter reading (dBA). Example: Jet aircraft cabin noise is roughly 80 ±2 dBA. At 80 dBA with raised voices, seatmates can converse at 2 ft, and, by moving a little, can lower their voices to normal level and converse at 1 ft. To ask the stewardess for an extra cup of coffee from the window seat (4 ft), one would need to use his communicating (very loud) voice. (Webster, 1969)

The recommended NC level inside a spacecraft without engines operating is NC-55.

Community Noise Criteria

It should be clearly recognized that the final decision as to criteria for community noise exposure is an administrative one. Scientific and technical data may aid in answering questions, but it remains the province of society and legal administrative officials to make ultimate decisions (Galloway & von Gierke, 1966). Only society, and its official representatives, can decide what price it is willing to pay for community noise control.

FAA (1969) lists EPNL limits for new commercial aircraft. Department of Defense (1964) recommends PNL limits for land use planning around airports. Fredrikson (1970) discusses zoning ordinances for limiting community noise.

Hearing Protection

Four general approaches may be taken to prevent sound from reaching the ear: (1) The person may be removed to a distance from the noise source such that spherical divergence and excess attenuation reduce the noise level to an

acceptable extent. (2) A physical barrier may be placed between the noise or blast source and the man. (3) The natural "aural reflex" action of man's middle-ear muscles may be stimulated as a means of protection. (4) A mechanical hearing protector may be placed over, or in, the ear canal to attenuate sound energy. Discussion of this latter approach to noise reduction will occupy the bulk of this section.

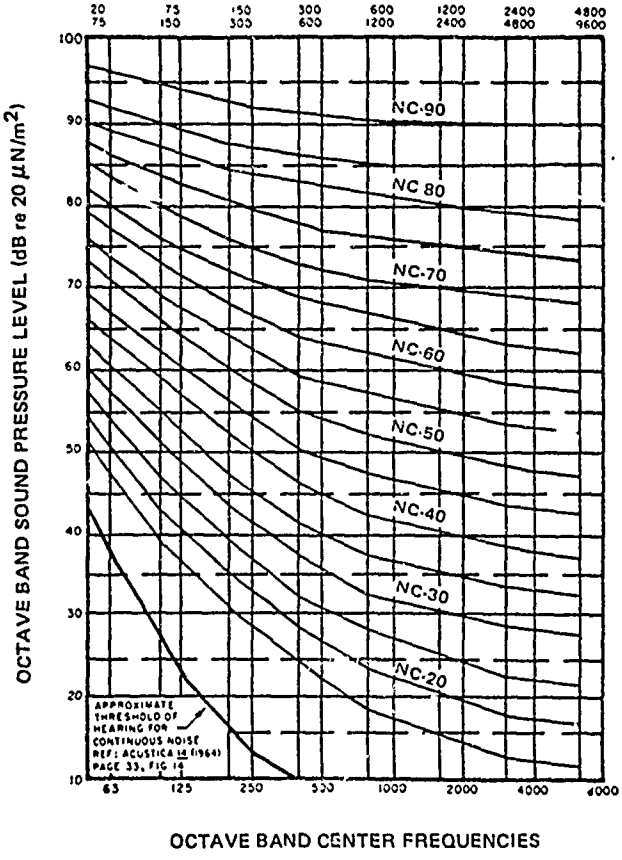


Figure 15–32. Noise criteria (NC curves) referred to preferred octave bands (lower abscissa) and commercial octave bands (upper abscissa). (From Schultz, 1968) NC 75-90 curves are present authors' own extrapolations which have been found to be very useful in practical applications. NC-55 is design criterion for Apollo spacecraft during nonpowered flight.

Mechanical Hearing Protection. Situations often arise in which it is neither economical nor practical to remove people to a distance from a noise source or to place a barrier between them and the source. In such cases the use of mechanical hearing protection is recommended to reduce the noise to a level which is not hazardous to hearing and/or will permit effective communication.

Table 15–10
Recommended NC Curves for Various Work Spaces

NC Curve	Type of Work Space	Communication Equivalent	Office Application
90		Noise-attenuating headset required	Not recommended
80		Communication very difficulty; telephone use unsatisfactory	Not recommended
70 – 80		Raised voice range 1–2 ft; shouting range 3–6 ft; telephone use very difficult	Not recommended
60 – 70		Raised voice range 1–2 ft; telephone use difficult	Not recommended
55 – 60		Very noisy; not suited for office; telephone use difficult	Not recommended
55	Spacecraft during nonpowered flight		
50 – 55		Unsatisfactory for conferences of over 3 people; telephone use slightly difficult; normal voice at 2 ft; raised voice at 3 ft	Areas with typists and accounting machines
40 – 50	Restaurants, sports coliseums	Conferences at 4–5 ft table; telephone use slightly difficult; normal voice at 3–6 ft; raised voice at 6–12 ft	Large drafting rooms
35 – 40		Conferences at 6–8 ft table; telephone use satisfactory; normal voice at 6–12 ft	Medium sized offices
30 – 35	Libraries, hospitals, motion picture theatres, home sleeping areas, assembly halls	Quiet office; conferences at 15 ft table; normal voice at 10–30 ft	Private or semi-private offices; reception rooms; conference rooms for up to 20 people
25 – 30	Courtrooms, churches, home sleeping areas, assembly halls, hotels and apartments, TV studios, music rooms, schoolrooms	Very quiet offices; large conferences	Executive offices; conference rooms for 50 people
20 – 25	Legitimate theatre, concert halls, broadcasting studios		

(Modified from Beranek 1960)

Hearing protectors will often improve person-to-person and loudspeaker-to-person communication in noise (Acton, 1967). The same speech signal-to-noise ratio reaches the ear with and without protection in such cases, but the use of protection may cause the speech signal to reach the ear at a level in the optimum range for speech intelligibility (i.e., overall RMS level of about 70 dB). This effect may, therefore, influence the selection of hearing protection for use in a given situation. It would be undesirable to recommend a highly effective hearing protector for use in a relatively low noise level, for example, since this might reduce the speech signal to below the optimum speech level.

Mechanical hearing protectors fall into four general categories: earplugs, semi-inserts, earmuffs, and helmets.

Earplugs are available in two forms: (1) preformed rubber or plastic plugs supplied in up to seven sizes, and (2) disposable plugs, such as wax-impregnated cotton, or "glass down" (a very fine, nonirritating glass wool).

Dry cotton is not recommended for use since it provides negligible sound attenuation (2 to 5 dB in the lower frequencies; 6 to 10 dB at the higher frequencies) and may provide a false sense of security.

In order to be maximally effective, earplugs must be properly fitted for size. It is not unusual to find people who require a different size plug for each ear. Furthermore, the plugs must be properly inserted each time they are used: they must be tight to be effective. Finally, the plugs must be kept clean to minimize the possibility of ear infections.

Semi-inserts are available in one size only and are pressed against the entrance to the ear canal by a light, spring-loaded headband. If frequent donning and doffing are required they are very convenient and, unlike bulky earmuffs, may easily be hung around the neck when not in use. On the other hand, semi-inserts may not provide as effective a seal against sound as either earplugs or earmuffs.

Earmuffs are made in one size only and almost everyone can be fitted satisfactorily with little difficulty. They attenuate sound as well as, or better than, earplugs at high frequencies but are slightly poorer than plugs below 1 kHz. The primary disadvantages of earmuffs are their bulk and relative expense. They do not, however, entail the fitting and insertion problems of earplugs. Another advantage, in certain situations, is that a supervisor can readily determine from a distance that all of his personnel are wearing their hearing protectors. Where very intense noise levels exist, it may be desirable to wear *both* earplugs and earmuffs. The total sound attenuation does not, of course, equal the sum of the individual protector attenuations, but this combination will ordinarily provide increased attenuation at most frequencies, with particular benefit being derived at the low frequencies (Webster & Rubin, 1962).

Helmets can provide more attenuation than the aforementioned devices if they cover the greater portion of the head. The acoustical importance of a helmet increases when the SPL reaches a point where bone-conducted sound

transmission through the skull becomes a controlling factor. In cases other than this the use of helmets for hearing-protective purposes alone is not justified. The maximum attenuation which can be provided by a plug, muff or semi-insert is about 35 dB at 250 Hz and is greater at higher frequencies (Zwislocki, 1955). After reductions of this magnitude, the remaining sound is conducted through the bones of the skull directly to the inner ear (Rice & Coles, 1966). An astronaut's helmet, which seals off the whole head, can provide an additional 10 dB of protection. Beyond this point, conduction of sound by the body is the limiting factor.

References

Acton, W. I. Effect of ear protection on communications. *Annals of Occupational Hygiene*, 1967, *10*, 423-429.

Acton, W. I. A criterion for the prediction of auditory and subjective effects due to air-borne noise from ultrasonic sources. *Annals of Occupational Hygiene*, 1968, *11*, 227-234.

Acton, W. I., & Carson, M. B. Auditory and subjective effects of air-borne noise from industrial ultrasonic sources. *British Journal of Industrial Medicine*, 1967, *24*, 297-304.

Acton, W. I., Coles, R. R. A., & Forrest, M. R. Hearing hazard from small bore rifles. *Rifleman*, 1966, *74*, 9-12.

Akiyoshi, M., Amemiya, A., Sato, K., Takeda, T., & Shoji, T. On the pathogenesis of acoustic trauma of the cochlea in rabbits and guinea pigs due to explosion. *International Audiology*, 1966, *5*, 270-271.

Alford, B. R., Jerger, J. F., Coats, A. C., Billingham, J., French, B. O., & McBrayer, R. O. Human tolerance to low frequency sound. *Transactions of the American Academy of Ophthamology and Otolaryngology*, 1966, *70*, 40-47.

American National Standards Institute. *American National Standard specification for audiometers for general diagnostic purposes, Z24.5.* New York: American National Standards Institute, 1951.

American National Standards Institute. *American National Standard specifications for an octave-band filter set for the analysis of noise and other sounds, Z24.10.* New York: American National Standards Institute, 1953.

American National Standards Institute. *American National Standard preferred frequencies for acoustical measurements, S1.6,* New York: American National Standards Institute, 1960a.

American National Standards Institute. *American National Standard method for measurement of monosyllabic work intelligibility, S3.2.* New York: American National Standards Institute, 1960b.

American National Standards Institute. *American National Standard specification for sound level meters, S1.4.* New York: American National Standards Institute, 1971.

Anticaglia, J. R., & Cohen, A. Extra-auditory effects of noise as a health hazard. Paper presented to American Industrial Hygiene Association, Denver, May 1969.

Beranek, L. L. The design of speech communication systems. *In Proceedings of the Institute of Radio Engineers*, 1947, *35*, 880-890.

Beranek, L. L. *Noise reduction.* New York: McGraw-Hill, 1960.

Bonney, T. B. (Ed.) *Industrial noise manual.* (2nd ed.) Detroit: American Industrial Hygiene Association, 1966.

Borsky, P. Some of the human factors underlying community reactions to Air Force noise. Paper presented to NRC Committee on Hearing and Bioacoustics, Washington, D.C., 1958.

Botsford, J. H. Simple method for identifying acceptable noise exposure. *Journal of the Acoustical Society of America*, 1967, *42*, 810-819.

Botsford, J. H. Using sound levels to gauge human response to noise. *Sound and Vibration*, 1969, *3 (10)*, 16-28.

Bowen, I. G., Fletcher, E. R., & Richmond, D. R. Estimate of man's tolerance to the direct effects of air blast. DASA Report 2113, Lovelace Foundation, Albuquerque, New Mexico, October 1968.

Broadbent, D. C., & Burns, W. Effect of noise on hearing and performance. RNP Report 65/1057, Royal Naval Personnel Research Committee, Medical Research Council, United Kingdom, April 1965.

de Candole, C. A. Blast injury. *Journal of the Canadian Medical Association*, 1967, *96*, 207-214.

Carter, N., & Kryter, K. D. Equinoxious contours for pure tones and some data on the "critical band" for TTS. Report 948, Bolt Beranek and Newman, Inc., Cambridge, Massachusetts, August 1962.

CHABA Hazardous exposure to intermittent and steady-state noise. Report of Working Group 46, NAS-NRC Committee on Hearing, Bioacoustics and Biomechanics, Washington, D.C., January 1965.

CHABA Proposed damage-risk criterion for impulse noise (gunfire). Report of Working Group 57, NAS-NRC Committee on Hearing, Bioacoustics and Biomechanics, Washington, D.C., July 1968.

Chaillet, R. F., Garinther, G. R., Hodge, D. C., & Newcomb, F. R. High-intensity impulse noise: A major problem. Technical Note 4-64, Human Engineering Laboratories, Aberdeen Proving Ground, Maryland, August 1964.

Chenoweth, H., & Smith, O. Frequency of atmospheric conditions producing acoustical focusing over Cape Canaveral, Florida. Report MTP-AERO-61-61, Manned Spaceflight Center, July 1961.

Cohen, A. Damage risk criteria for noise exposure. Aspects of acceptability and validity. *Journal of the American Industrial Hygiene Association*, 1963, *24*, 227-238.

Cohen, A. Effects of noise on psychological state. In W. D. Ward & J. E. Fricke (Eds.), *Noise as a public health hazard*. Proceedings of the conference. Washington: American Speech and Hearing Association, 1969.

Cohen, A., & Bauman, E. C. Temporary hearing losses following exposure to pronounced single-frequency components in broad-band noise. *Journal of the Acoustical Society of America*, 1964, *36*, 1167-1175. 75.

Cohen, A., & Jackson, E. Threshold shift in hearing as a function of bandwidth and mode of noise exposure. Report RR-12, Bureau of Occupational Safety and Health, U.S. Public Health Service, Cincinnati, Ohio, February 1969.

Cole, J. N., & von Gierke, H. E. Noise from missile static firing and launch sites and the resultant community response. Technical Report 57-547, Wright Air Development Center, Ohio, September 1957.

Coles, R. R. A., & Rice, C. G. Speech communications effects and temporary threshold shift reduction provided by V-51R and Selectone-K earplugs under conditions of high intensity impulsive noise. *Journal of Sound and Vibration*, 1966, *4*, 172-186.

Coles, R. R. A., Garinther, G. R., Hodge, D. C., & Rice, C. G. Criteria for assessing hearing damage-risk from impulse-noise exposure. Technical Memo 13-67, Human Engineering Laboratories, Aberdeen Proving Ground, Maryland, August 1967.

Coles, R. R. A., Garinther, G. R., Hodge, D. C., & Rice, C. G. Hazardous exposure to impulse noise. *Journal of the Acoustical Society of America*, 1968, *43*, 336-343.

Committee on Conservation of Hearing. Guide for conservation of hearing in noise. Supplement to Transactions of the American Academy of Ophthamology and Otolaryngology, 1969.

Crocker, M. J. Measurement of sonic booms with limited frequency response instrumentation. Report WR 66-20, Wyle Laboratories, Huntsville, Alabama, 1966.

Davis, H., Parrack, H. O., & Eldredge, D. H. Hazards of intense sound and ultrasound. *Annals of Otology, Rhinology and Laryngology* 1949, *58*, 732-738.

Department of Defense Land use planning with respect to aircraft noise. Air Force Manual 86-5, Dept. of the Army Tech. Manual 5-365, Dept. of the Navy Manual NAVDOCKS P-98, October 1964.

Dyer, I. Estimation of sound-induced missile vibrations. In S. H. Crandall (Ed.), *Random vibrations*. New York: John Wiley, 1958.

FAA Noise standards: Aircraft type certification. Federal Register, 1969.

Fletcher, J. L., & Cairns, A. B. Recovery from impulse noise induced acoustic trauma. *Journal of Auditory Research* 1967, 7, 35-39.

Fletcher, J. L., & Loeb, M. The effect of pulse duration on TTS produced by impulse noise. *Journal of Auditory Research*, 1967, 7, 163-167.

Fredrikson, H. M. Noise control on the local level. *Archives of Environmental Health*, 1970, *20*, 651-654.

French, B. O. Appraisal of Apollo launch noise. *Aerospace Medicine*, 1967, *38*, 719-722.

Galloway, W. J., & von Gierke, H. E. Individual and community reactions to aircraft noise: Present status and standardization. Paper presented to London Noise Conference, 1966.

Garinther, G. R., & Moreland, J. B. Transducer techniques for measuring the effect of small arms' noise on hearing. Technical Memo 11-65, Human Engineering Laboratories, Aberdeen Proving Ground, Maryland, July 1965.

Golden, P. M., & Clare, R. The hazards to the human ear from shock waves produced by high energy electrical discharge. Report E-1/65, United Kingdom Atomic Energy Authority, Atomic Weapons Research Establishment, Aldermaston, Berks, England, 1965.

Hamberger, C. A., & Liden, G. The prognosis in hearing injuries following acoustic shot trauma. *Acta Otolaryngologica*, 1951, *39*, 160-165.

Hill, R. E. Space Division, North American Rockwell Corporation, Downey, California, 20 November 1969. (Unpublished data)

Hirsch, F. G. Effects of overpressure on the ear—A review. DASA Report 1858, Lovelace Foundation, Albuquerque, New Mexico, November 1966.

Hodge, D. C., & McCommons, R. B. Reliability of TTS from impulse-noise exposure. *Journal of the Acoustical Society of America*, 1966, *40*, 839-846.

Hodge, D. C., & McCommons, R. B. Growth of temporary threshold shift from impulse noise: A methodological study. Technical Memo 10-67, Human Engineering Laboratories, Aberdeen Proving Ground, Maryland, May 1967(a).

Hodge, D. C., & McCommons, R. B, A behavioral study of the sound-shadow effect in impulse noise. Technical Memo 12-67, Human Engineering Laboratories, Aberdeen Proving Ground, Maryland, July 1967(b).

Hodge, D. C., Gates, H. W., Helm, C. P., Soderholm, R. B., & Blackmer, R. F. Preliminary studies of the impulse-noise effects on human hearing (Project HumIN). Technical Memo 15-64, Human Engineering Laboratories, Aberdeen Proving Ground, Maryland, December 1964.

House, A. S., Williams, C., Hecker, M. H., & Kryter, K. D. Psychoacoustic speech tests: A modified rhyme test. TDR 63-403, Electronic Systems Division, L. G. Hanscom Field, Bedford, Mass., June 1963.

International Standards Organization. Standard reference zero for the calibration of pure-tone audiometers. Recommendation 389, International Organization for Standardization, 1964.

Jacobson, B., Dyer, E. M., & Marone, R. J. Effectiveness of the V-51R earplug with impulse pressures up to 8 psi. Technical Memo 1-63, Human Engineering Laboratories, Aberdeen Proving Ground, Md., November 1962.

Jansen, G. Effects of noise on physiological state. In W. D. Ward & J. E. Fricke (Eds.), *Proceedings of the conference on noise as a public health hazard*. Washington: American Speech and Hearing Association, 1969.

Jepger, J., Alford, B., Coats, A., & French, B. Effects of very low frequency tones on auditory thresholds. *Journal of Speech and Hearing Research*, 1966, *9*, 150-160.

J. F. Kennedy Space Center. Results of AS-503 facilities and environmental measurements, Vol. 1. Technical Report 927, January 1969.

Kryter, K. D. Methods for the calculation and use of the articulation index. *Journal of the Acoustical Society of America*, 1962, *34*, 1689-1697.

Kryter, K. D. Exposure to steady-state noise and impairment of hearing. *Journal of the Acoustical Society of America*, 1963, *35*, 1515-1525.

Kryter, K. D. Personal communication with D. C. Hodge, 1964.

Kryter, K. D. Concepts of perceived noisiness, their implementation and application. *Journal of the Acoustical Society of America*, 1968, *43*, 344-361.

Kryter, K. D. Possible modifications to the calculation of perceived noisiness. Report CR-1636, National Aeronautics and Space Administration, Langley Research Center, 1970a.

Kryter, K. D. *The effects of noise on man*. New York: Academic Press, 1970b.

Klumpp, R. G., & Webster, J. C. Physical measurements of equally speech interfering Navy noises. *Journal of the Acoustical Society of America*, 1963, *35*, 1328-1338.

Loeb, M., & Fletcher, J. L. Temporary threshold shift for "normal" subjects as a function of age and sex. *Journal of Auditory Research*, 1963, *3*, 65-72.

Loeb, M., & Fletcher, J. L. Impulse duration and temporary threshold shift. *Journal of the Acoustical Society of America*, 1968, *44*, 1524-1528.

Luz, G. A., & Hodge, D. C. Recovery from impulse-noise induced TTS in monkeys and men: A descriptive model. *Journal of the Acoustical Society of America*, 1971, *49*, 1770-1777.

Mills, J. H., Gengel, R. W., Watson, C. S., & Miller, J. D. Temporary changes of the auditory system due to prolonged exposure to noise. *Journal of the Acoustical Society of America*, 1970, *47*, 85.

Mohr, C. G., Cole, J. N., Guild, E., & von Gierke, H. E. Effects of low frequency and infrasonic noise on man. *Aerospace Medicine*, 1965, *36*, 817-824.

Murray, N. E., & Reid, G. J. Temporary deafness due to gunfire. *Laryngoscope*, 1946, *61*, 91-121.

Nakamura, S. Some of the basic problems in noise trauma. Paper presented to 65th symposium of Japan Ear, Nose and Throat Science Association, May 1964. (Tech. Transl. FSTC-HT-23-869-68, U.S. Army Foreign Science and Technology Center, Washington, D.C.)

NASA-Marshall Space Flight Center. Safety and design considerations for the static test and launch of large space vehicles. Part II-B: Acoustic hazards and design data, Joint Air Force–NASA Hazards Analysis Board, 1961.

Nixon, C. W., Harris, C. S., & von Gierke, H. E. Rail test to evaluate equilibrium in low-level wideband noise. AMRL Tech. Report 66-85, Wright-Patterson Air Force Base, Ohio, 1966.

Nyborg, W. L., & Mintzer, D. Review of sound propagation in the lower atmosphere. WADC Tech. Report 54-602, Wright-Patterson Air Force Base, 1955.

Occupational Safety and Health Administration. Occupational Safety and Health Act, Part 1910.95, *Federal Register*, 1970, *36*, (105), 10518.

Panian, Z. Influence of noise on certain functions of the eye, Vojnosanitetski Pregled, 20, 19-26. 1963. (Transl. No. J-1397, Office of Assistant Chief of Staff for Intelligence, Department of the Army, Washington, D.C., [illegible]-67).

Parrack, H. O. Effects of air-borne ultrasound on humans. *International Audiology*, 1966, *5*, 294-308.

Pease, C. G. Obtaining the spectrum and loudness of transients by computer. Tech. Report I, Institute of Sound and Vibration Research, University of Southampton, England, December 1967.

Perkins, B., Lorrain, P. H., & Townsend, W. H. Forecasting the focus of air blast due to meteorological conditions in the lower atmosphere. Report 1118, Ballistics Research Laboratories, Aberdeen Proving Ground, Md., 1960.

Piesse, R. A., Rose, J. A., & Murray, N. E. Hearing conservation in industrial noise. Report 19, Commonwealth Acoustic Laboratories, Sydney, Australia, June 1962.

Plomp, R., Gravendeel, D. W., & Mimpen, A. M. Relation of hearing loss to noise spectrum. *Journal of the Acoustical Society of America*, 1963, *35*, 1234-1240.

Rice, C. G. Deafness due to impulse noise. *Philosophical Transactions of the Royal Society of London*, 1968, *A* 263, 279-287.

Rice, C. G., & Coles, R. R. A. Impulsive noise studies and temporary threshold shift. Paper B67 presented at 5th International Congress on Acoustics, Liege, Belgium, 1965.

Rice, C. G., & Coles, R. R. A. Design factors and use of ear protection. *British Journal of Industrial Medicine*, 1966, *23*, 194-203.

Rosenblith, W. A., & Stevens, K. N. Handbook of acoustic noise control. Vol. II: Noise and man. Tech. Report 52-204, Wright Air Development Center, June 1953.

Sataloff, J. *Hearing loss*. Philadelphia: Lippincott, 1966.

Schultz, T. J. Noise-criterion curves for use with the USASI preferred frequencies. *Journal of the Acoustical Society of America*, 1968, *43*, 637-638.

Shoji, H., Yamamoto, T., & Takagi, K. Studies on TTS due to exposure to octave-band noise. *Journal of the Acoustical Society of Japan*, 1966, *22*, 340-349.

Singh, D., & Ahluwalia, K. J. S. Blast injuries of the ear. *Journal of Laryngology*, 1968, *82*, 1017-1028.

Smith, R. P., & Loeb, M. Recovery from temporary threshold shifts as a function of test and exposure frequency. *Journal of the Acoustical Society of America*, 1969, *45*, 238-239.

Society of Automotive Engineers. Standard values of atmospheric absorption as a function of temperature and humidity for use in evaluating aircraft flyover noise, ARP 866, Society of Automotive Engineers, 1964.

Sperry, W. C. Aircraft noise evaluation. Tech. Report 68-34, Federal Aviation Agency, Washington, D.C., September 1968.

Tamenholtz, S. D. Research on acoustic problems of the military: A review and future aspect. Tech. Report 69-ff-PR, U.S. Army Natick Laboratories, Natick, Mass., October 1968.

Ward, W. D. Recovery from high values of temporary threshold shift. *Journal of the Acoustical Society of America*, 1960, *32*, 497-500.

Ward, W. D. Effect of temporal spacing on temporary threshold shift from impulses. *Journal of the Acoustical Society of America*, 1962, *34*, 1230-1232.

Ward, W. D. Auditory fatigue and masking. In J. Jerger (Ed.), *Modern developments in audiology*. New York: Academic Press, 1963.

Ward, W. D. Temporary threshold shift following monaural and binaural exposures. *Journal of the Acoustical Society of America*, 1965, *38*, 121-125.

Ward, W. D. Susceptibility to auditory fatigue In W. D. Neff (Ed.), *Advances in sensory physiology*. Vol. 3. New York: Academic Press, 1968.

Ward, W. D. Effects of noise on h aring thresholds. In W. D. Ward & J. E. Fricke (Eds.), *In proceedings of the conference on ..oise as a public health hazard*. Washington: American Speech and Hearing Association, 1969.

Ward, W. D. Temporary threshold shift and damage risk criteria for intermittent noise. *Journal of the Acoustical Society of America*, 1970, *in press*.

Ward, W. D., & Glorig, A. A case of firecracker-induced hearing loss. *Laryngoscope*, 1961, *61*, 1590-1596.

Ward, W. D., Glorig, A., & Sklar, D. L. Relation between recovery from temporary threshold shift and duration of exposure. *Journal of the Acoustical Society of America*, 1959a, *31*, 600-602.

Ward, W. D., Glorig, A., & Sklar, D. L. Susceptibility and sex. *Journal of the Acoustical Society of America*, 1959b, *31*, 1138.

Ward, W. D., Selters, W., & Glorig, A. Exploratory studies on temporary threshold shift from impulses. *Journal of the Acoustical Society of America*, 1961, *33*, 781-793.

Webster, J. C. SIL–Past, present, and future. *Sound and Vibration*, 1969, *3*, (8), 22-26.

Webster, J. C., & Rubin, E. R. Noise attenuation of ear protection devices. *Sound*, 1962, *1*, 34-46.

Wegel, R. L., & Lane, C. E. The auditory masking of one pure tone by another and its probable relation to the dynamics of the inner ear. *Physics Review*, 1924, *23*, 266-285.

Wilhold, G. A., Guest, S., & Jones, J. A technique for predicting farfield acoustic environments due to a moving rocket sound source. Technical Note D-1832, National Aeronautics and Space Administration, August 1963.

Wilhold, G. A., Jones, J., Guest, S., Cole, J., & Parrack, H. O Acoustic energy hazards. In Chemical rockets/propellent hazards, Vol. 1, Chapter 7, Publication No. 194, Chemical Propellent Information Agency, Johns Hopkins University Applied Physics Laboratory, Silver Spring, Md., May 1970.

Yuganov, Ye. M., Krylov, Yu. V., & Kuznetsov, V. S. Standards for noise levels in cabins of spacecraft during long-duration flights. In V. N. Chernigovskiy (Ed.), *Problems in space biology, Vol. 7: Operational activity, problems in habitability and biotechnology*. Moscow: Nauka Press, 1967. (Tech. Transl. F-529, National Aeronautics and Space Administration, Washington, D.C., 1969.)

Yuganov, Ye. M., Mirzoyev, B. M., Krylov, Yu. V., & Kuznetsov, V. S. Material on the physiological-hygienic basis of the allowable levels of impulse noises (sound shocks). In V. V. Parin (Ed.), *Problems of space medicine: Data on the conference of 24-27 May 1966*. Moscow: Ministry of Public Health, 1966. (Tech. Transl. 66-34698 (JPRS 38-272), Clearinghouse for Federal Scientific and Technical Information, Washington, D.C. 1966.)

Zwislocki, J. Design and testing of earmuffs. *Journal of the Acoustical Society of America* 1955, *27*, 1154-1163.

CHAPTER 16
HUMAN CONTROL CAPABILITIES

by

Laurence Retman Young, Sc.D
Massachusetts Institute of Technology

This chapter concentrates on the capabilities and limitations of man as an element in a closed loop control system under normal environmental conditions. Only by careful consideration of the engineering aspects of man as a control element can performances of man-vehicle systems be assessed, stability and power assists be designed, and trade-offs between manual and automatic functions be determined objectively.

The usual breakdown of man's functions in a piloting task is shown in figure 16-1. The human operator uses his various senses to gain information on vehicle state and the command situation, integrates this information centrally where the appropriate control actions are decided upon, and through the use of effectors such as control sticks, changes the inputs to the vehicle or plant which is being controlled. In the typical piloting application, man participates in two levels of this man-machine system; control and guidance. In his *control* function, man establishes an equilibrium state of vehicle motion and regulates departures of the vehicle from equilibrium. In *guidance* man determines the appropriate course and speed to reach a desired point under constraints of time, fuel, position error, and accelerations. Typically the progression from control to guidance involves manual control functions which are successively slower in their characteristics but requi a higher level of decision-making. The remainder of this chapter considers the human controller, controls, and displays. The effects of other-than-normal environments on the human senses and effectors are discussed in other chapters of this book.

Controller Characteristics

Nature of Manual Control

The controller characteristics considered in this section correspond to continuous piloting tasks. Information is received by observing meters, CRT

Reviewed by Duane T. McRuer, M.S., Systems Technology, Inc.

displays, or other continuous information presentations, and responses are made by continuous movements of control sticks, rudder pedals, or other manual devices. This section includes empirical data on performance limitations and relative ease of controlling in different types of situations. It also summarizes mathematical models for the human operator proposed as attempts to make engineering approximations to the pilot which can be used in systems design. Some of the more important variables which affect the human controller characteristics are: *task variables* (dynamics of the controlled element, characteristics of the manipulator, command inputs), *environmental variables* (temperature, vibration, acceleration), *operator-centered variables* (experience, training, alertness, fatigue, motivation), and *procedural variables* (instructions, order of presentations in competing configurations, analysis procedures).

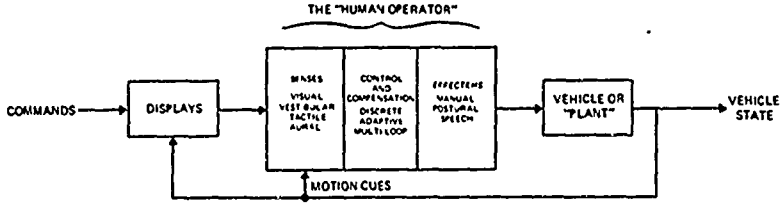


Figure 16–1. Human operator in a control task.

Modes of Tracking: Compensatory, Pursuit, and Precognitive

Three major modes of human tracking are distinguished and illustrated in figure 16-2.

In *compensatory tracking* the operator observes only the system error or the difference between the system command and the actual system output. He has no explicit information on whether changes in this error result from a change in the command or a change in the vehicle output. Of course he may always estimate the contribution of changes in vehicle output to the observed error changes on the basis of the controls he has applied. Typical examples of compensatory situations are tracking a target through a telescopic sight or following a glideslope descent schedule by nulling ILS needles. In the next stage of manual control, *pursuit tracking*, the human operator has explicit displays of system command and vehicle output separately. He can derive system error by direct comparison of the two. The pursuit situation simplifies the problem of stability by allowing the operator to observe the vehicle output directly without interference from changing inputs. It also enables him to somewhat predict input by extrapolating from the current input and its derivatives. Examples are following a descent schedule in which command altitude and actual altitude are displayed simultaneously on the same altimeter, or tracking a moving object in which the azimuth and elevation of both the target and the tracking device are simultaneously displayed on the same instrument using different symbols. Finally, for *precognitive tracking* the operator has explicit or implicit information about *future values of the input*. Thus for driving an automobile on a curved road or lining up an airplane for a landing on a runway, the future

required path as well as the current position of the vehicle are explicitly available. Similarly, displays, which show where obstacles or desired paths will be in the future, lead to precognitive tracking. In addition, the operator may perform precognitive tracking if he is able to extract reliable predictive information about input or disturbance from the periodicities or predictability of these signals. In general, the operator is able to overcome most of the limitations associated with his decision times and neuromuscular dynamics in the cases of precognitive or preview tracking.

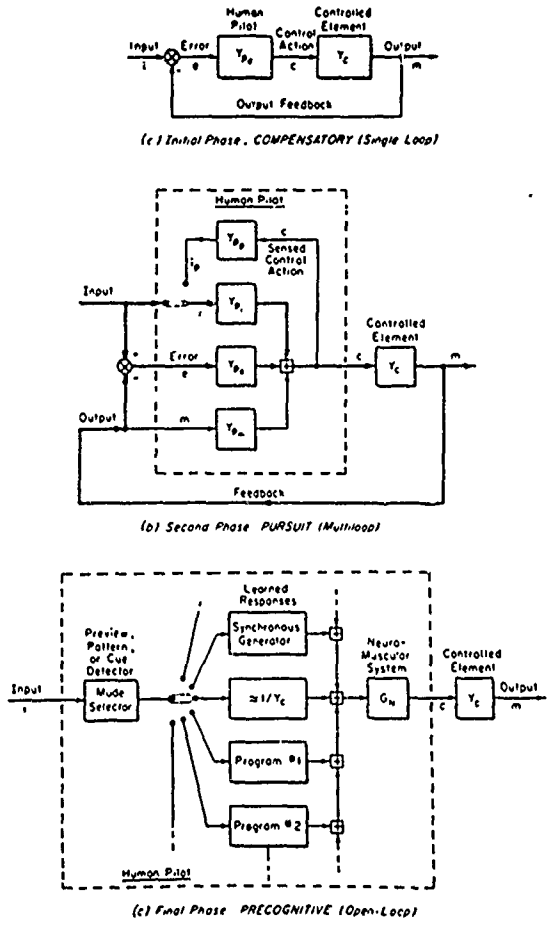


Figure 16–2. Successive organization of perception. (McRuer et al., 1968)

Quasilinear Models

Precision and Approximate Models. The most generally applied model of the human operator used in analysis of man-machine performance is the quasilinear model, so named because it represents the human operator as a "best linear approximation" plus a remnant to account for the human control outputs other than those predicted by the linear approximation (figure 16-3).

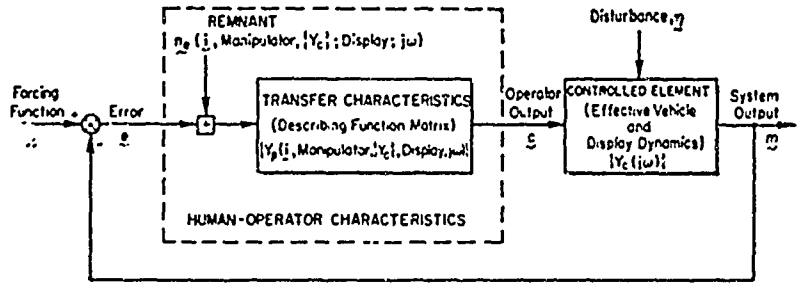


Figure 16–3. Quasilinear human operator model. (McRuer & Weir, 1969)

The linear approximation generally used is the Gaussian input describing function. It varies significantly with the dynamics of the controlled element, as well as with the nature of the display and the bandwidth of the input. It is applicable only for tracking situations involving random or random appearing continuous inputs or disturbances and without additions, does not accurately predict responses to transient input such as steps or impulses, or in situations where one can preview he input. The most detailed form of this model is the *precision model* of McRuer et al. (1965), leading to a human operator describing function given in the following equation:

$$Y_p(j\omega) = K_p\left(\frac{T_L j\omega + 1}{T_I j\omega + 1}\right)\left(\frac{T_K j\omega + 1}{T_K' j\omega + 1}\right)\frac{1}{\left(T_{N_1} j\omega + 1\right)\left[\left(\frac{j\omega}{\omega_N}\right)^2 + \frac{2\zeta}{\omega_N} j\omega + 1\right]} e^{-j\omega\tau} \qquad (1)$$

H.O. Describing Function	Variable Gain	Adjustable Lead-Lag Equalization	Approximation to Low Frequency Gain and Phase	High Frequency Neuromuscular Characteristics	Delay Time

The use of this equation in systems design is limited to cases where accurate characterization at very high frequencies (>4 rad/sec) or very low frequencies are required (McRuer et al., 1965). Primary adjustment of operator characteristics is through the gain (K_p) and the lead and lag time constants (T_L and T_I). The neuromuscular characteristics change primarily with forcing-function bandwidth and with manipulator (control stick) restraints. A typical Bode plot for the neuromuscular system portion is shown in figure 16-4.

$$Y_p(j\omega) = K_p \frac{(T_L j\omega + 1)}{(T_I j\omega + 1)} e^{-j\omega\tau_e} \qquad (2)$$

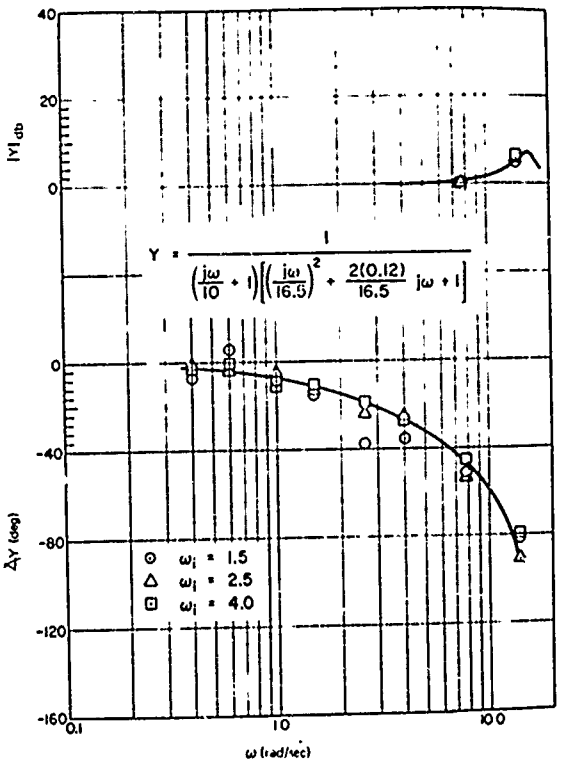


Figure 16–4. High frequency neuromuscular characteristics $Y_c = K_c/(j\omega - 2)$. (McRuer et al., 1965)

For practical systems design purposes, the above simplified model is generally adequate. τ_e is the effective time delay comprising the delays associated with reading and interpreting the display, deciding upon the appropriate control motion, and the high frequency neuromuscular lags. T_L, the *lead time constant*, expresses the ratio of the weight the operator attributes to the displayed velocity compared to the displayed position. T_I, the *integr' time constant*, represents the amount of data smoothing the operator applies

There have been a number of attempts to generate empirical and theoretically based *adjustment rules* for selecting the variable parameters of the pilot describing function appropriate to each compensatory tracking case. The simplest of these is the *crossover model* popularized by McRuer and his associates.

The Crossover Model. The crossover model is based on the notion that the human operator adjusts his parameters so that the open loop frequency response $[Y_p\ (j\omega)\ Y_c\ (j\omega)]$ satisfies conditions for closed loop stability and reasonably low error. The pilot adjusts his own transfer function to compensate, insofar as

possible, for the transfer function of the controlled element. To quote from McRuer and Jex (1967, p. 234):

> The pilot adopts sufficient lead or lag equalization so that the slope of $|Y_{OL}| = |Y_p Y_c|$ lies very close to -20dB/decade in the region of crossover frequencies. Besides the -90 deg phase shift associated with the 20dB/decade amplitude ratio, there is an accumulation of additional lags due to transport delays and high frequency neuromuscular dynamics. All of these can be represented (near crossover frequencies) by an effective time delay τ_e.

[The crossover frequency (ω_c) is the frequency at which the open loop amplitude ratio is unity, or zero dB.] The *crossover model* is:

$$Y_{OL}(j\omega) \doteq Y_p Y_c = \frac{\omega_c e^{-j\omega\tau_e}}{j\omega}; \text{ near } \omega_c. \tag{3}$$

Thus the open loop transfer function approximates an integrator and time delay in the region of the crossover frequency. Notice that in this simplified model only two parameters, ω_c and τ_e, are functions of the task variables; plant dynamics, Y_c, input bandwith, ω_i, and manipulator characteristics. In situations involving rotational motion, the first-order effects of motion can also be accounted for in τ_e.

Using the simple human operator describing function model of Equation 2, the parameters are varied according to the form of Y_c, such that the system is stable, the magnitude ratio $Y_p Y_c$ has a slope of approximately -20 dB/decade near ω_c, and the low frequency amplitude ratio is much greater than 1. Forms of the pilot's describing function for a variety of common controlled elements are given in table 16-1.

Selection of actual values of ω_c and τ_e for particular values of plant dynamics and input bandwidths is somewhat empirical.

$$\omega_c(Y_c, \omega_i) \doteq \omega_{c_0}(Y_c) + \Delta\omega_c \text{ and}$$
$$\tau_e(Y_c, \omega_i) \doteq \tau_0(Y_c) - \Delta\tau(\omega_i) \tag{4}$$

The following are useful linear approximations to the dependency of crossover frequency and time delay on input bandwidth:

$$\Delta\omega_c = 0.18\,\omega_i \text{ and}$$
$$\Delta\tau = 0.08\,\omega_i$$

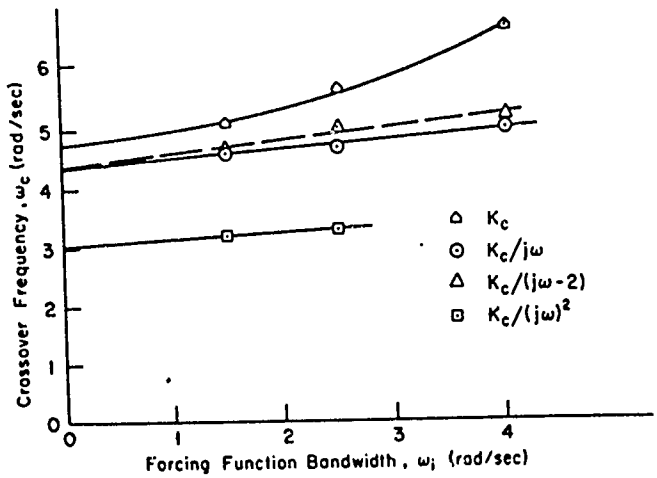
Table 16–1

Pilot Equalization Adjustment for Various Controlled Elements

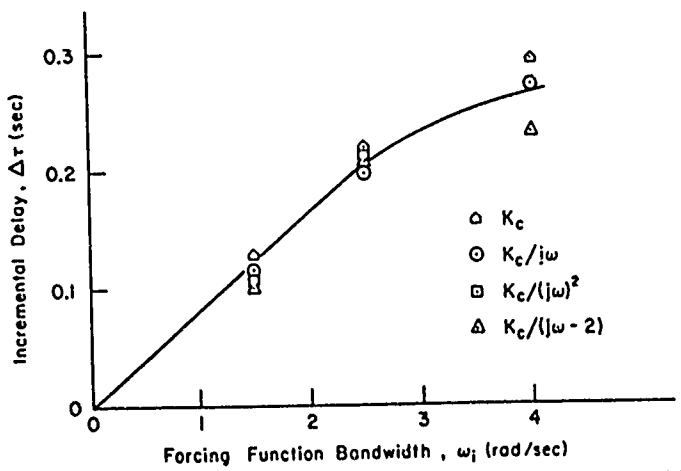
Controlled Element Approximate Transfer Function in Crossover Region $Y_c(s)$	Pilot's Equalizer Form	Pilot's Describing Function $Y_p(j\omega)$	Location of Equalization Break Frequency
K_c	Lag-lead	$\frac{K_p e^{-j\omega\tau e}}{(T_l j\omega + 1)}$	$\frac{1}{T_l} \ll \omega_c$
$\frac{K_c}{s}$	High-frequency lead	$K_p e^{-j\omega\tau e}$	—
$\frac{K_c}{s^2}$	Low-frequency lead	$K_p(T_L j\omega + 1)e^{-j\omega\tau e}$	$\frac{1}{T_L} \ll \omega_c$
$\frac{K_c}{s(Ts + 1)}$	If $T > \tau_e$ use mid-frequency lead	$K_p(T_L j\omega + 1)e^{-j\omega\tau e}$	$\frac{1}{T_L} \doteq \frac{1}{T}$
	If $T < \tau_e$ use high-frequency lead	$K_p e^{-j\omega\tau e}$	—
$\frac{K_c}{\left(\frac{s}{\omega_n}\right)^2 + \frac{2\zeta}{\omega_n} s + 1}$	If low natural frequency ($\omega_n \ll 1/\tau_e$) use low-frequency lead	$K_p(T_L j\omega + 1)e^{-\omega j \tau e}$	$\frac{1}{T_L} \ll \omega_c$
	If high natural frequency ($\omega_n > 1/\tau_e$) use lag-lead	$\frac{K_p e^{-j\,\omega\tau e}}{(T_l j\omega + 1)}$	$\frac{1}{T_l} \ll \omega_c$

(McRuer & Jex, 1967)

The crossover frequency increases with input bandwidth until $\omega_i \cong 0.8\omega_{c0}$, when it is again reduced. Data on ω_c and $\Delta\tau$ is given in figure 16-5. The dependency of ω_{c0} and τ_0 (the values for crossover and effective time delay with no forcing function) for several plants are summarized in table 16-2. The value of $\overline{\omega}_c$ can be used if the effect of input bandwidth on ω_c is ignored. Note that the operator effective time delay also varies with the amount of lead equalization he must supply. When the pilot is acting as a pure amplifier with a delay ($Y_c = K/j\omega$), the effective time delay is of the order of 0.36 second. As more lead is required [$Y_c = K_c/(j\omega)^2$] then the operator's effective time delay also increases. When the operator introduces lag, however, in the case of controlling a pure gain, his effective time delay is slightly reduced.



(a) Variations of crossover frequency with forcing function bandwidth



(b) Dependence of incremental time delay on forcing function bandwidth

Figure 16–5. Variation of describing function parameters with forcing function bandwidth. (McRuer et al., 1965)

Table 16–2

Summary of Crossover Parameters

Y_c	τ_0 (sec)	ω_{t_0} (rad/sec)	$\overline{\omega}_c$ (rad/sec)
K_c	0.33	4.8	5.8
$K_c/j\omega$	0.36	4.4	4.75
$K_c/(j\omega - 1/T)$	0.36	4.4	4.9
$K_c/(j\omega)^2$	0.51	3.0	3.25

(McRuer et al., 1965)

The performance expected of a closed loop system including a human operator using the crossover model can be approximated very simply on the basis of the crossover model. If the input spectrum is assumed to be rectangular and band limited (maximum frequency ω_i, uniform power spectral density ϕ_{ii}, and mean square input power σ_i^2), then the ratio of mean square error to mean square input is easily found by use of figure 16-6.

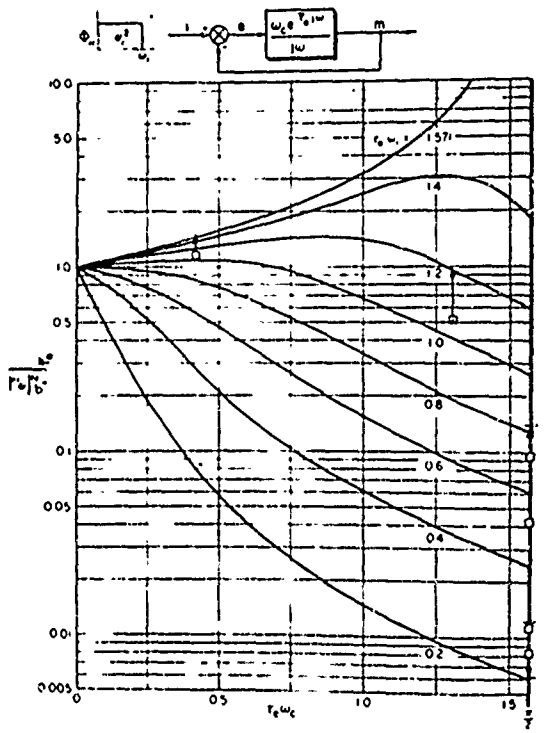


Figure 16–6. Mean square error calculated from the crossover model.

A typical example of measured open loop frequency response for a simple rate control plant at three input bandwidths is shown in figure 16-7.

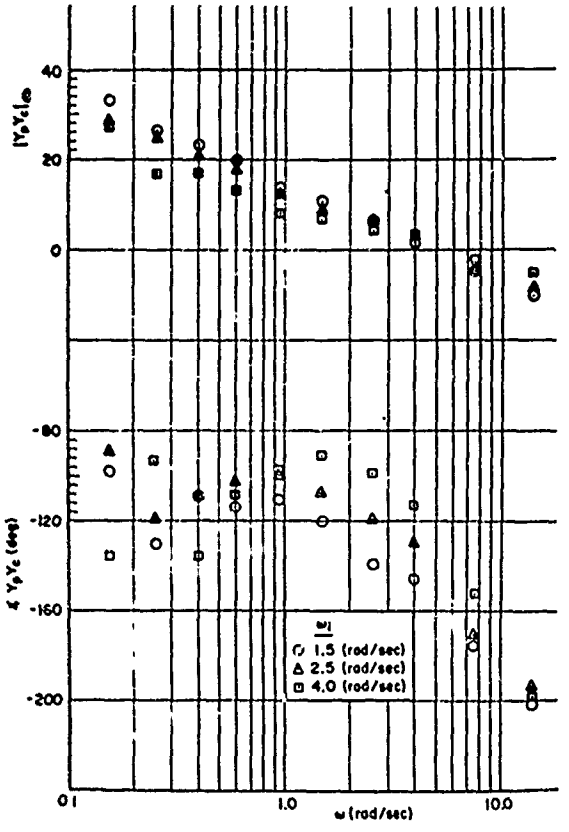
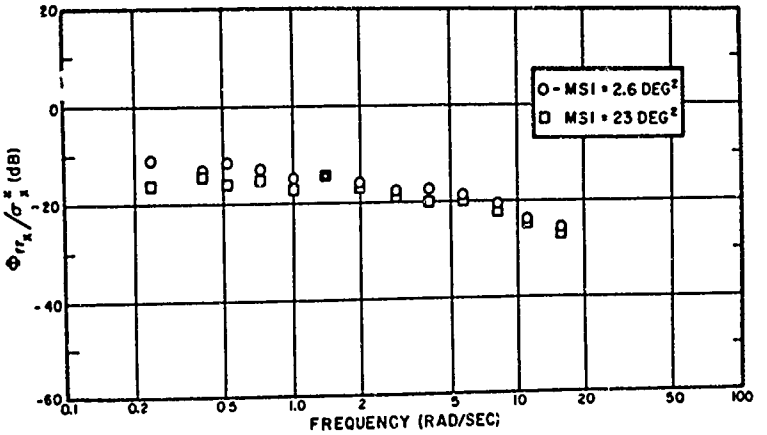


Figure 16–7. Measured open loop frequency response data. Averaged open loop describing function for $Y_c = K_c/j\omega$ with ω_i as parameter. (McRuer et al., 1963)

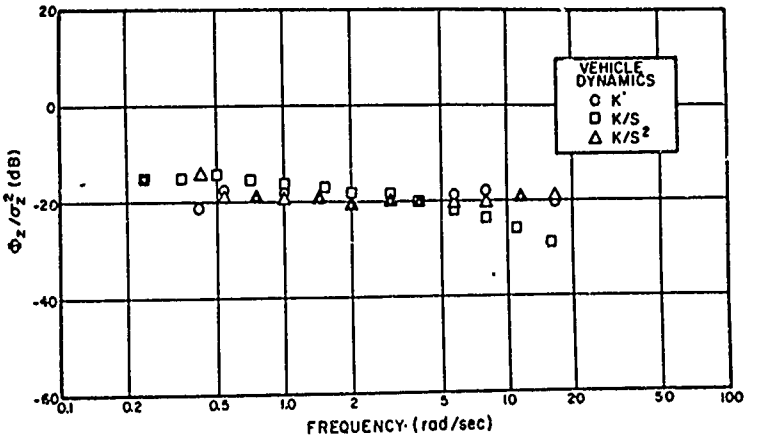
Remnant. In addition to the quasilinear portion of describing functions, the remnant, or added disturbance injected by the operator, must be considered to establish the total error in a tracking loop. For certain conditions in which pilot behavior is particularly nonstationary and nonlinear (especially in tracking high order systems requiring pulsatile control), the contribution of remnant to error may be very significant. Levison et al., (1969) have shown certain simplifications if the remnant is referred to equivalent observation noise appearing at the operator's input, that is, added to the system error. (In most literature prior to 1968, the remnant is given as additive noise at the operator's output.) By normalizing the observation noise spectrum with respect to the input noise spectrum, the injected observation noises seem to be relatively constant at approximately (-20 dB) and independent of frequency, input amplitude, vehicle dynamics, or input bandwidth (figure 16-8). The observed remnant in terms of

normalized observation noise spectrum increases significantly when the display is used peripherally rather than foveally. The effect of remnant on system error can be minimized by control design which does not require the operator to generate low frequency lead. Optimum controlled element gain and filtering of the operator's output can further reduce the contribution of remnant to error or to exciting high order system modes.



(a) Effect of mean squared input on the normalized observation noise spectrum.

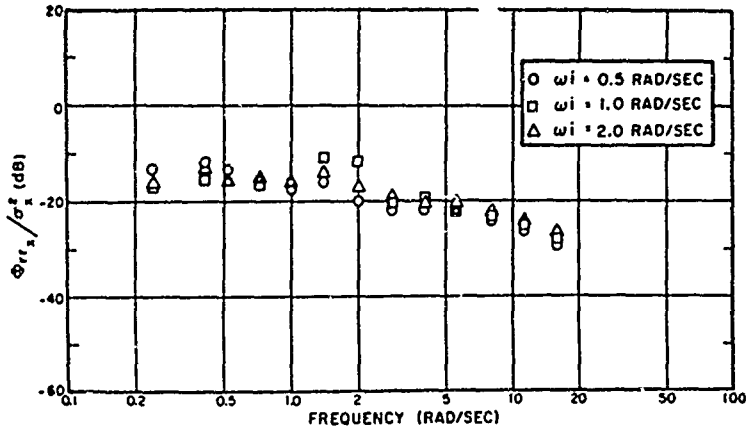
Vehicle dynamics = K/s
Input bandwidth = 0.5 Rad/Sec
Average of 3 subjects



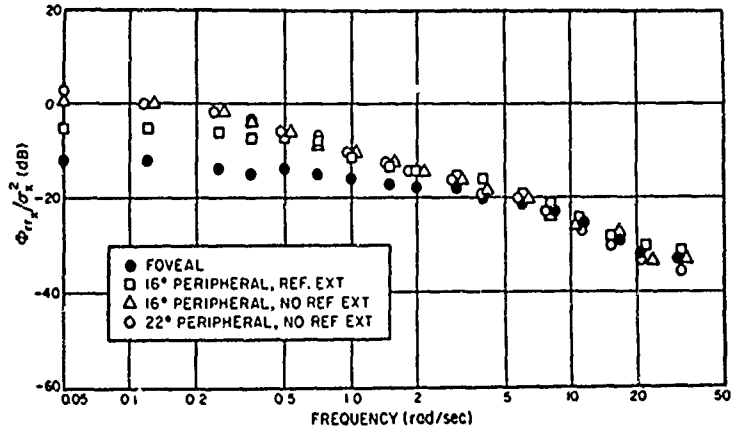
(b) Effect of vehicle dynamics on the normalized observation noise spectrum.

Average of 3 subjects (K and K/s^2)
Average of 4 subjects (K/s)

Figure 16–8. Remnant expressed as normalized observation noise spectrum. (Levison et al., 1969)



(c) Effect of input bandwidth on the normalized observation noise spectrum.
Vehicle dynamics = K/s
Average of 3 subjects



(d) Effect of viewing conditions on the normalized observation noise spectrum.
Vehicle dynamics = K/s
Average of 4 subjects

Figure 16–8. Remnant expressed as normalized observation noise spectrum. (Levison et al., 1965) — *Continued*

Pursuit Tracking. Little experimental data on pursuit tracking is available. It is surmised that the pilot uses information on input alone to attempt open loop tracking. To this extent, he can be considered to operate on the input signal with a transfer function Y_{pi}, which is just equal to the reciprocal of the controlled element ($Y_{pi} = 1/Y_c$). The remaining errors associated with inaccuracies in open loop tracking and injected remnant are compensated by closed loop compensatory tracking. The effect of pursuit tracking is to permit the operator to overcome

internal delays and reduce his phase lag, thereby producing higher gains than for compensatory tracking at frequencies above 0.4 Hz. Figure 16-9 shows some compensatory-pursuit frequency response comparisons for $Y_c = K$.

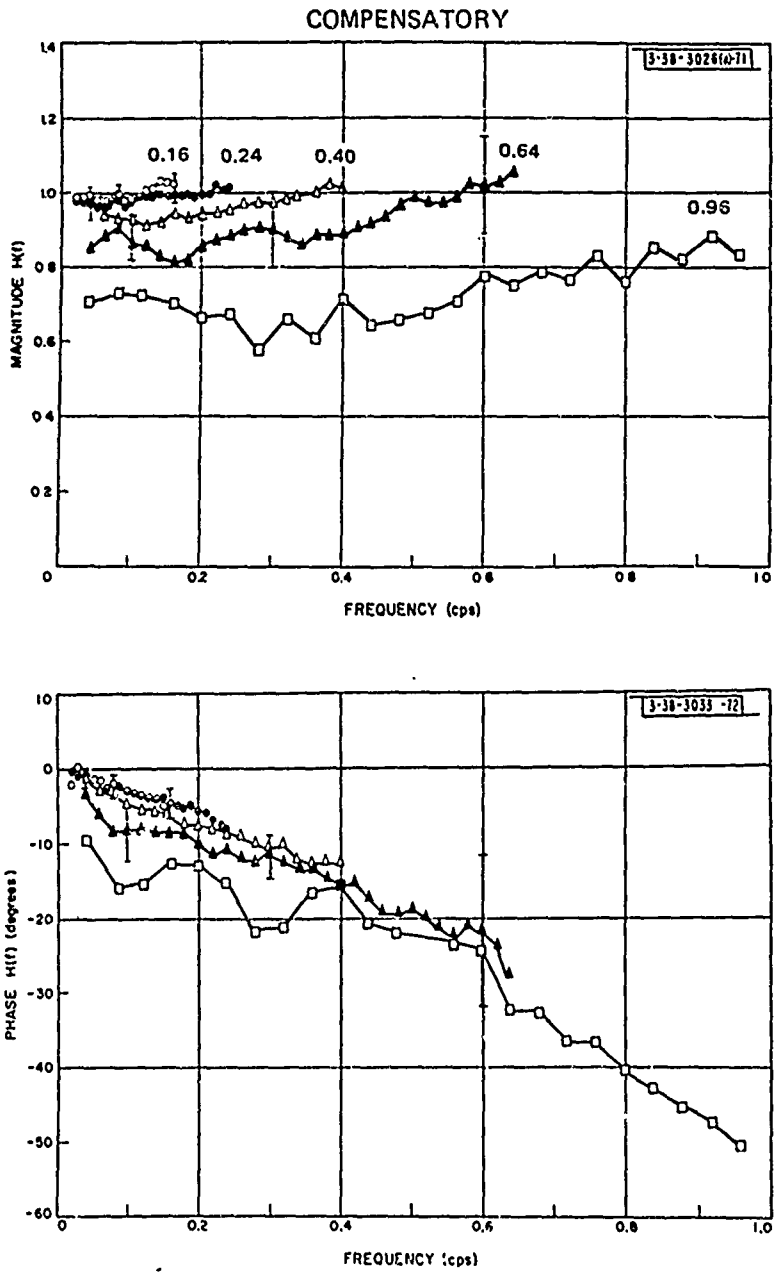
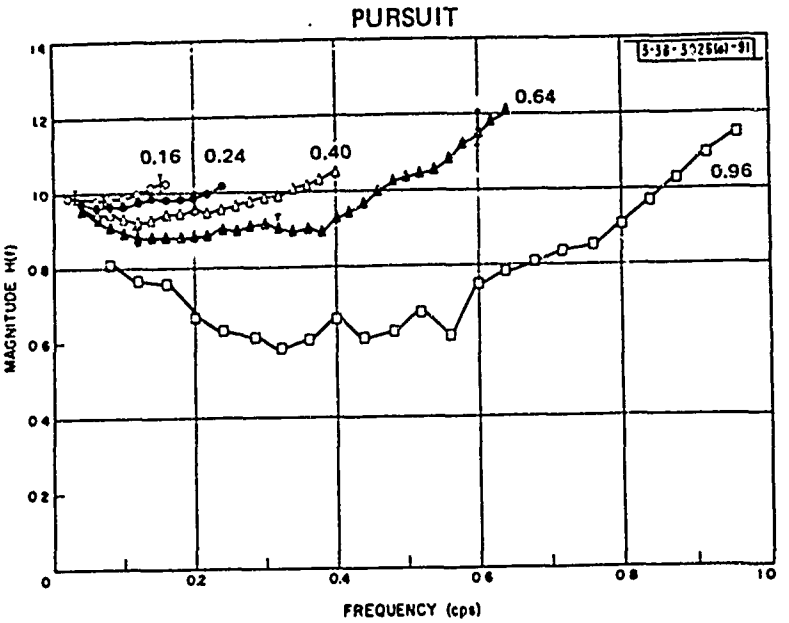


Figure 16–9. Pursuit and compensatory $Y_c(j\omega)$ frequency characteristics for $Y_c = K$ and various input bandwidths. (Elkind, 1956)

(c)



(d)

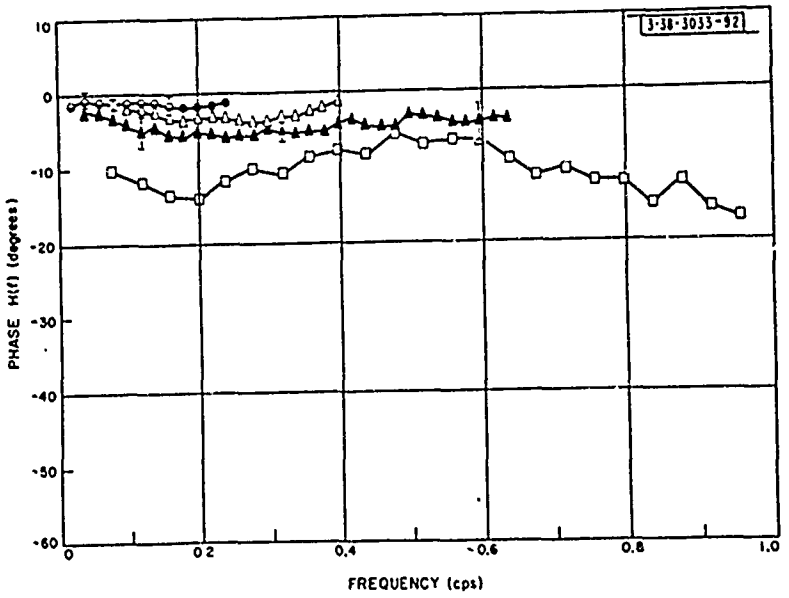


Figure 16–9. Pursuit and compensatory Y_c ($j\omega$) frequency characteristics for Y_c = K and various input bandwidths. (Elkind, 1956) – *Continued*

Further study of pure pursuit tracking with input only [i (t)] or pursuit plus disturbance [g(t)], shown in figure 16-10, has explored pursuit behavior as the sum of an operation on the inputs, output, and error. Precision pilot model

parameters, using the model of Equation 1, are given for the various cases in table 16-3. The use of pursuit tracking in the presence of disturbances yielded no improvement in performance over simple compensatory tracking.

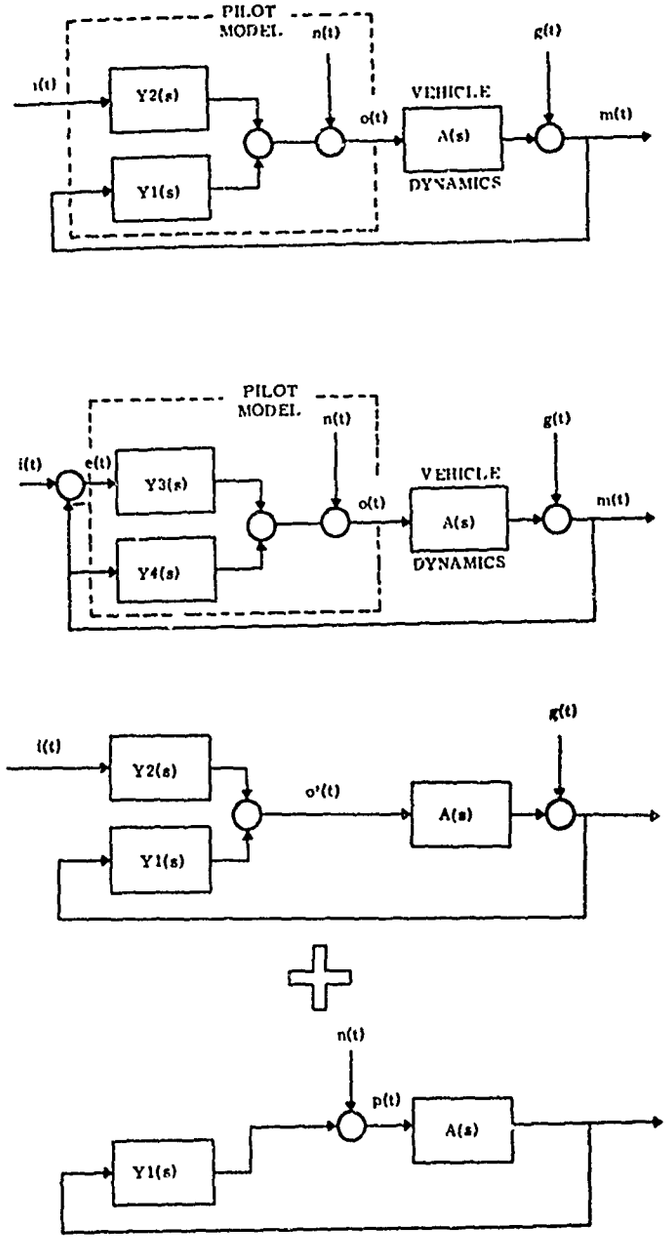


Figure 16–10. Pure pursuit tracking: a. with input only [i (t)]; b. plus disturbance [g (t)]. (Reid, 1969)

Table 16–3

Pilot Model Parameters

Experimental Conditions	K_p	τ	a	$1/T_L$	$1/T_I$	$1/T_K$	$1/T_{K'}$	$1/T_{N_I}$	ω_N	ζ_N
VL CK Y	114.6	0.035	0.05	2.70	1.67	–	0.67	12.5	17.0	0.10
VL PDK Y_1	−106.0	0.030	0.08	2.78	1.67	–	0.63	12.5	15.9	0.10
VL PDK Y_2	105.0	0.010	0.08	2.78	1.67	–	0.67	12.5	15.4	0.10
VL PDK Y_4	1.43	0.300	0.25	−1.00	–	12.5	–	–	3.0	2.0
L CK Y	55.7	0.045	0.08	2.70	1.50	–	0.71	12.5	17.0	0.10
L PDK Y_1	− 48.9	0.060	0.03	2.70	2.00	–	0.59	12.5	17.0	0.10
L PDK Y_2	48.5	0.075	0.03	2.70	2.18	–	0.59	12.5	15.9	0.10
L PDK Y_4	0.16	0.300	–	−0.10	2.00	7.15	2.00	2.00	15.1	0.05
M CK Y	44.6	0.055	0.04	–	0.83	–	–	11.1	17.5	0.12
M PDK Y_1	− 39.0	0.055	0.06	–	0.91	–	–	11.1	17.5	0.12
M PDK Y_2	36.4	0.068	0.08	–	1.11	–	–	11.1	17.0	0.12
M PDK Y_4	1.10	0.400	0.25	−1.00	–	12.5	–	–	3.0	2.0
H CK Y	79.7	0.060	−0.02	0.20	2.18	–	0.05	12.5	18.1	0.08
H PDK Y_1	− 74.2	0.070	–	0.20	2.00	–	0.05	12.5	17.5	0.08
H PDK Y_2	23.8	0.090	0.04	2.00	5.00	–	0.83	12.5	17.0	0.08
H PDK Y_4	4.40	0.350	–	−2.00	0.20	7.15	–	10.0	16.7	0.10
VL C 1/s Y	16.8	0.087	0.04	3.30	1.82	–	–	16.7	14.9	0.07
VL PD 1/s Y_1	− 3.22	0.10	0.15	2.86	1.25	0.17	1.11	17.0	15.4	0.07
VL PD 1/s Y_2	4.85	0.115	0.06	2.86	1.11	0.25	1.11	17.0	17.0	0.07
VL PD 1/s Y_4	0.69	0.020	0.40	1.50	4.00	–	–	–	–	–

L C 1/s Y	10.3	0.129	0.08	4.00	2.78	–	–	16.7	17.0	0.07
L PD 1/s Y_1	– 2.5	0.150	–0.04	3.00	2.22	0.05	0.20	14.3	17.5	0.07
L PD 1/s Y_2	2.18	0.180	–0.04	3.00	2.22	0.05	0.20	14.3	17.5	0.07
L PD 1/s Y_4	0.38	0.200	0.20	1.50	10.00	–	–	–	–	–
M C 1/s Y	8.75	0.110	0.05	0.89	1.21	–	–	11.1	16.6	0.10
M PD 1/s Y_1	– 7.43	0.120	0.25	0.20	1.00	0.17	0.05	11.1	16.1	0.10
M PD 1/s Y_2	6.68	0.150	0.25	0.20	1.00	0.17	0.05	11.1	16.1	0.10
M PD 1/s Y_4	0.61	0.260	0.40	1.50	–	–	–	–	–	–
H C 1/s Y	5.52	0.110	0.05	1.39	3.22	–	–	11.1	17.0	0.10
H PD 1/s Y_1	– 3.24	0.115	0.25	0.63	2.22	–	–	11.1	15.9	0.10
H PD 1/s Y_2	2.13	0.145	0.25	0.50	2.50	–	–	12.0	15.6	0.09
H PD 1/s Y_4	0.73	0.270	0.40	5.0	–	5.0	–	–	–	–

Display:	C – Compensatory PP – *Pure pursuit (no disturbance)* PD – Pursuit tracking with additional disturbance	
A(s) dynamics	K – Pure gain 1/s – Rate control	
Input Power Spectra (ω_{ie} = equivalent input bandwidth)	VL – Very low L – Low M – Medium H – High	ω_{ie} = 1.28 rad/sec ω_{ie} = 1.41 rad/sec ω_{ie} = 2.80 rad/sec ω_{ie} = 4.30 rad/sec

(Reid, 1969)

Pilot Opinion and Ratings

In addition to satisfying specifications on performance (e.g., stability and error) it is important to consider the operator acceptability of a given vehicle system. Pilot rating for aerospace vehicles is usually given in terms of the Cooper rating shown in table 16-I. In general the pilot can make wide compensation for controlled element dynamics resulting in equivalent performance but with varying Cooper ratings.

A review of pilot rating scales to eliminate uncertainty in definitions and increase the reliability of ratings led to the handling qualities rating scale proposed by Cooper and Harper (1969) shown in figure 16-11.

Particular emphasis in flight and ground base simulation has been paid to pilot opinion and aircraft handling qualities. Handling qualities for longitudinal aircraft attitude control are governed by the short period natural frequency ω_{sp}, the short period damping ratio ζ_{sp}, the numerator time constant $T\theta_2$, and the airplane gain. Figure 16-12 shows approximate boundaries of pilot opinion for one value of $T\theta_2$ as a function of ω_{sp} and ζ_{sp}. These boundaries would be different for other values of $T\theta_2$. Figure 16-13 shows similar trends of acceptable and controllable regions plotted in a somewhat different format for longitudinal control of a reentry vehicle. A discussion of lateral handling qualities is beyond the scope of this chapter. Pilot rating depends upon gain, roll mode time constants, spiral mode time constant, and dutch roll mode natural frequency and damping. (For further discussions, see Harper, 1961; Ashkenas & McRuer, 1962.)

Pilot ratings can also be related to parameters of the pilot model. The gain which the pilot adapts for a particular application affects his rating. Although the absolute level of the optimum gain depends upon a great number of factors, including the type of control stick, deviations from this optimum result in poorer ratings, as shown in figure 16-14. Pilot ratings also suffer when the pilot is forced to introduce lead compensation (figure 16-15). No particular penalty is apparently associated with increased lag compensation. Pilot rating also has been observed to show a decrement of 2 to 3 points as the pilot's effective time delay τ_e decreases, associated with greater lead generation, as discussed earlier.

To handle multiaxis tracking situations it has been suggested that the decrements in pilot rating (relative to optimum) for each axis individually be added to indicate the resulting decrement in the multiaxis rating (McRuer and Jex, 1967). A recent attempt to predict pilot ratings for VTOL on the basis of weighted sums of performance and pilot lead time constants shows some promise. The empirical relationship is

$$R = R_1 + R_2 + R_3 + 1.0 \qquad (5)$$

Table 16–4

Original Cooper Rating Scale

	Adjective Rating	Numerical Rating	Description	Primary Mission Accomplished	Can Be Landed
		1	Excellent, includes optimum	Yes	Yes
Normal operation	Satisfactory	2	Good, pleasant to fly	Yes	Yes
		3	Satisfactory, but with some mildly unpleasant characteristics	Yes	Yes
		4	Acceptable, but with unpleasant characteristics	Yes	Yes
Emergency operation	Unsatisfactory	5	Unacceptable for normal operation	Doubtful	Yes
		6	Acceptable for emergency condition only*	Doubtful	Yes
		7	Unacceptable even for emergency condition*	No	Doubtful
No operation	Unacceptable	8	Unacceptable - Dangerous	No	No
		9	Unacceptable - Uncontrollable	No	No
	Unprintable	10	"Motions possibly violent enough to prevent pilot escape"		

*Failure of stability augmenter.

(Cooper, 1957)

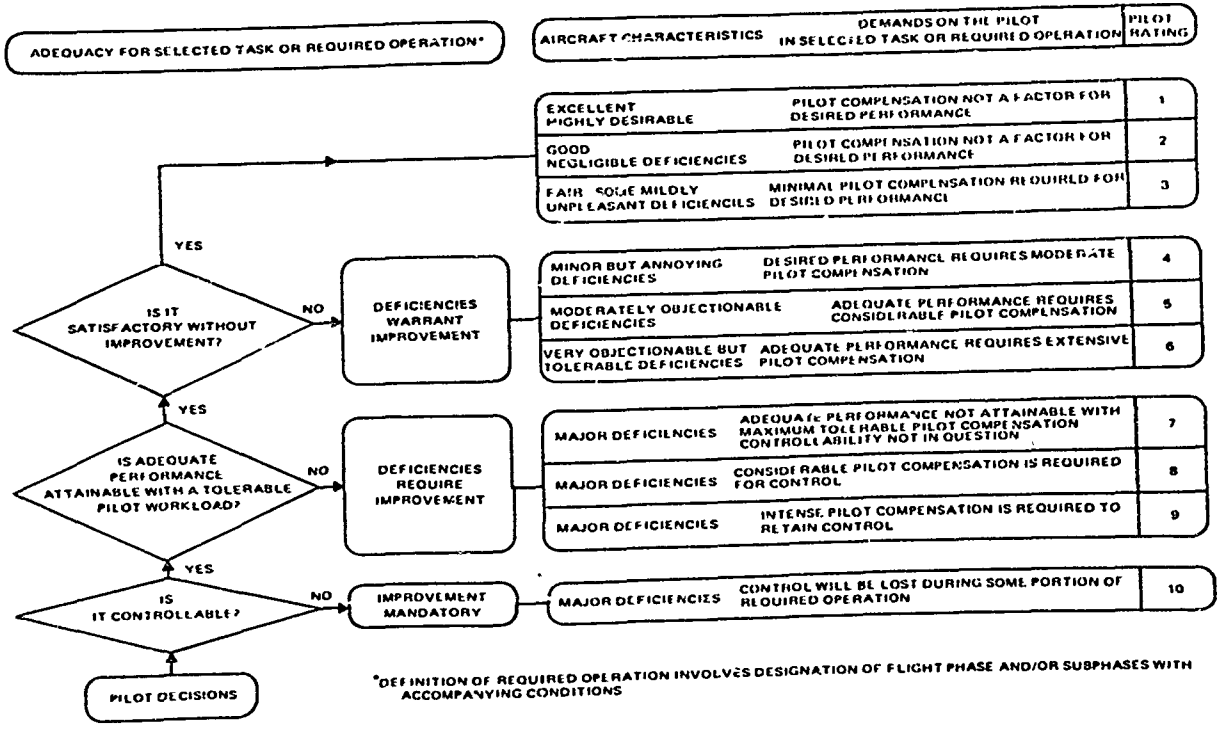


Figure 16–11. Proposed handling qualities rating scale. (Cooper & Harper, 1969)

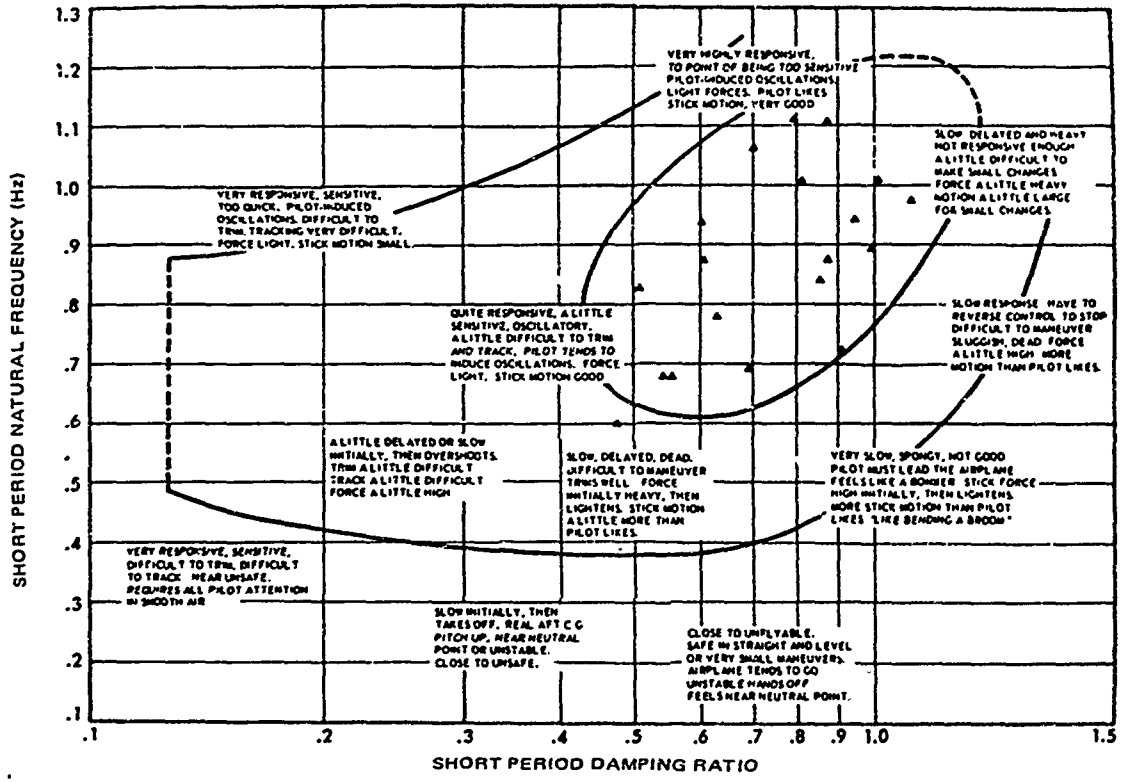


Figure 16–12. Pilot opinion vs. vehicle dynamic response – second order system.
(Adapted from Chalk, 1958)

R_1 is the weighted sum of pitch and displacement errors relative to a criterion level

$$0 \leq R_1 \leq 2.50$$

$$R_2 = 2.5(T_{L_\theta})$$

and is limited to $R_2 \leq 3.25$. T_{L_θ} is the pilot lead time constant in the inner pitch loop.

$$R_3 = 1.0(T_{L_x})$$

is limited to $R_3 \leq 1.20$. T_{L_x} is the pilot lead time constant in the outer displacement loop (Anderson & Dillow, 1970).

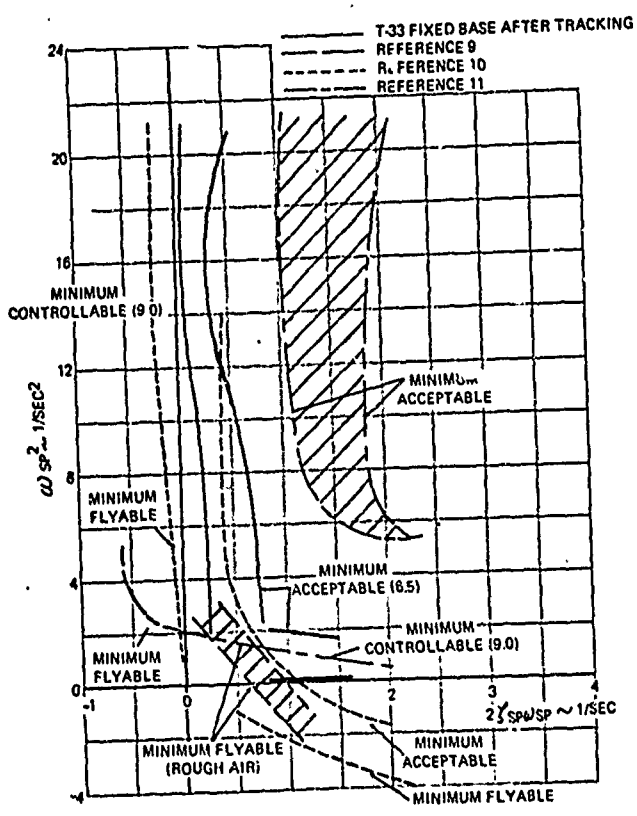


Figure 16–13. Pilot opinion boundaries for longitudinal control. (Kidd & Harper, 1964)

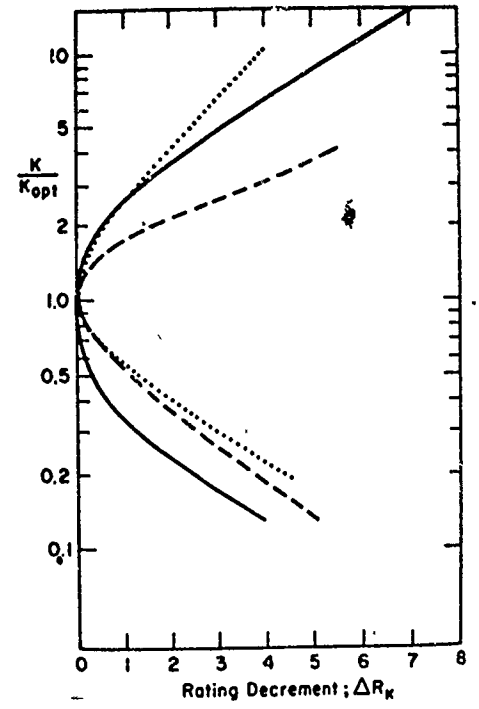


Figure 16–14. Decrement in pilot rating for off-optimal gain. (McRuer & Jex, 1967; used by permission of the Institute of Electrical and Electronics Engineers)

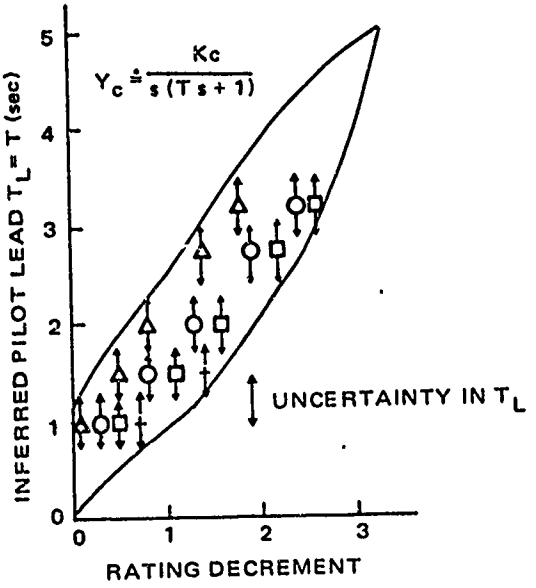


Figure 16–15. Decrement in pilot opinion due to pilot lead. (Ashkenas, 1965; symbols refer to various cases within the reference)

"Rule of Thumb" for Compensatory Tracking

A useful rule of thumb which includes some aspects of the dependence of pilot workload on lead and lag equalization as well as the easily achieved levels of crossover frequency for single axis compensatory tracking may be stated as follows: Design the controlled element and display so that the controlled element is approximately a pure integrator, input frequencies are limited to less than 0.5 Hz, and the human can act as a simple amplifier with a time delay.

Although the optimum control and display depends upon input spectrum and performance criteria in a somewhat complex way, it is generally true that a pure integral plant is easily controlled for low frequency inputs. By the same token, without special training or assistance in display, men should not be expected to control elements with dynamics containing more phase lag than $Y_c=K/s^2$. (Under certain conditions, using pulsatile control, plants as high as $Y_c=K/s^3$ may be controllable for short periods.)

Optimum Control Models

Several attempts have been made to reduce some of the arbitrariness of the quasilinear describing function model for describing human operator characteristics by substituting the techniques of optimal control theory. The goal is still to estimate loop closures, pilot dynamics, crossover frequencies, etc., but the desire is to substitute the systematic optimal control calculation techniques for the previously described artistic conventional methods. This requires that a cost function to be minimized be specified. The peculiar nature of this function must be such that when the input and vehicle dynamics are given, the minimization of the cost function results in control law(s) which mimic those the human would adopt. The artistry has now shifted to the selection of the cost function. A promising approach using optimal control is shown schematically in figure 16-16. The block (e^{-sT}) represents an approximation to the human operator's invariant equivalent simple time delay. State feedbacks for the human are assumed to be only gains and first derivatives of explicitly displayed information. The effect of the usual remnant, including motor uncertainties, and the effects of visual scanning are represented by a vector observation noise $\underline{V}_\omega(t)$. Because of his inherent delay and the observation noise, the human operator must estimate the true state which had existed T seconds ago [estimated state $\hat{\underline{x}}(t-T)$], predict the current state [$\hat{\underline{x}}(t)$], and generate the optimum control law control vector [u(t)] which minimizes the cost functional, subject to the constraints on state variables fed back. Although the application of optimal control techniques to estimation of human operator dynamics is still a very new art, reasonable agreement with conventional results for several simple plants and a V/STOL vehicle in hovering flight has been achieved (Elkind et al., 1968).

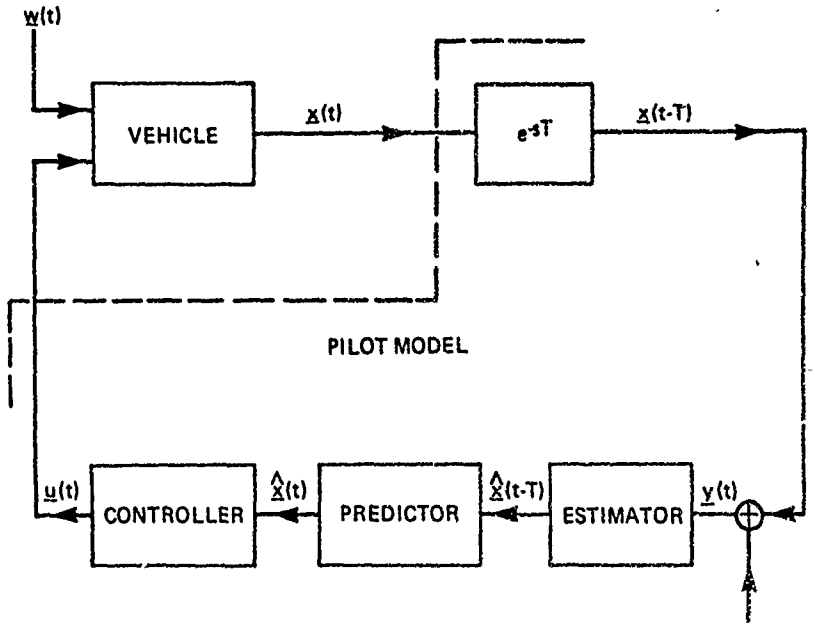


Figure 16–16. Optimum control model for manual control. (Elkind et al., 1968)

Motion Cues

Describing function data for human operators gathered in laboratory fixed base experiments frequently must be extrapolated to moving base or flight tests. The presence of motion cues in flight, as sensed by the vestibular and tactile senses, influences the describing functions. At extremes of high vibration and acceleration levels it results in important performance decrements; for moderate motions, however, the information is generally useful to the pilot. In particular, angular rate information sensed by the semicircular canals may be used to generate additional lead compensation and reduce the effective reaction time. Graviceptor cues help alignment to the apparent vertical. Roll motion cues are most useful at high frequencies and for plants in which high frequency variations in roll can occur. The effect of roll motion cues in allowing the operator to exhibit additional lead, and thereby increase his crossover frequency and reduce RMS error, is shown schematically in figure 16-17.

Table 16-5 gives approximate linear models of the human operator describing function for a wide variety of controlled elements under fixed base or roll motion. (The 0.1 sec delay in all controlled elements approximates the dynamics of the simulator utilized). When motion is in yaw rather than roll or pitch, presumably the linear acceleration sensors of the body are not stimulated. Experiments indicate that although the additional linear acceleration contributes to a higher gain of the human operator, the contribution is relatively less significant than that attributable to sensation of rotation (Dinsdale, 1968).

Multiple-Input Tracking

When multiple inputs are presented on separated displays the operator tends to adopt an optimal scanning pattern, devoting most time to those displays having the most information and linking scans between related displays. The implications for display layout and details of optimization are beyond the scope of this chapter (see Carbonell et al., 1968, and Clement, Jex, & Graham, 1968). One of the effects of multiple inputs on separated displays is a net increase in effective time delay associated with the scanning time.

When multiple inputs can be displayed on a single integrated display, the effects of more than one input can be assessed according to the following cases: (a) homogeneous dynamics and homogeneous input, (b) homogeneous dynamics and heterogeneous inputs, and (c) heterogeneous dynamics. Two-axis tracking performance is nearly as good as single-axis performance with compatible integrated displays, when the dynamics in the two axes are the same, whether or not the inputs are identical. However, when the dynamics are different in the two axes, requiring different operator equalization, significant increases in normalized mean square error occur, ranging from 15 to 125 percent (Levison and Elkind, 1966). The equalization associated with one axis seems to affect that used on the other, resulting in an increase in error on both axes. Figure 16-18 shows the describing function for tracking with dynamics K in one axis, with and without a second axis task of K/s^2 dynamics.

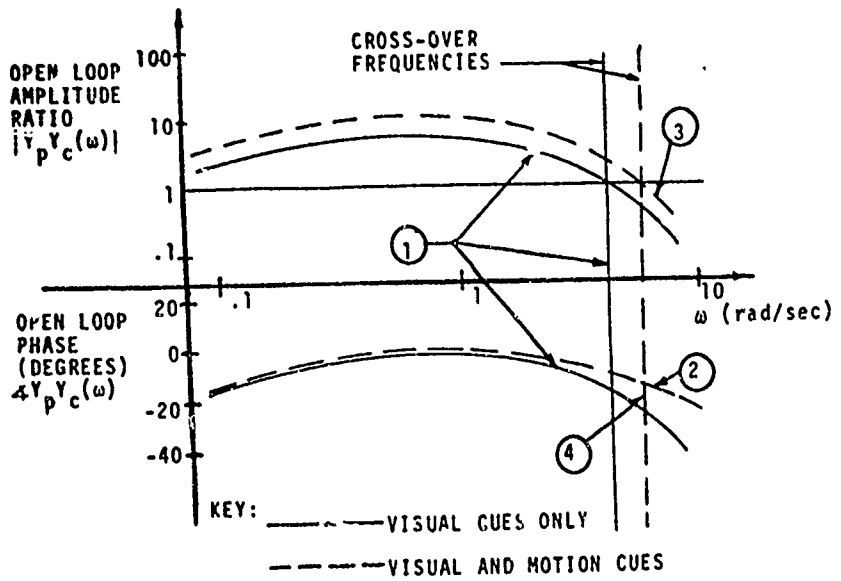


Figure 16–17. Schematic indication of effects of roll motion cues. (Shirley & Young, 1968; used by permission of the Institute of Electrical and Electronics Engineers)

Table 16–5

Human Operator Describing Functions for Various Dynamics – Compensatory Roll Tracking

Controlled Element Y_c	Fixed Base Pilot Model Y_p	Roll Moving Base Pilot Model Y_p
$\frac{e^{-.1s}}{s}$	$\frac{4.5e^{-.08s}(7s+1)(1.9s+1)}{(15s+1)(1.75s+1)(.08s+1)}$	$\frac{4.5(7s+1)(5s+1)}{(15s+1)(1\ 75s+1)(.08s+1)}$
$\frac{20e^{-.1s}}{s(s+20)}$	$\frac{10e^{-.07s}(6s+1)(1.1s+1)}{(27s+1)(.55s+1)(.08s+1)}$	$\frac{10(6s+1)(2.5s+1)}{(27s+1)(.9s+1)(.08s+1)}$
$\frac{5e^{-.1s}}{s(s+5)}$	$\frac{8e^{-.1s}(7s+1)(.85s+1)}{(31s+1)(.13s+1)(.08s+1)}$	$\frac{8(7s+1)(1.6s+1)}{(31s+1)(.29s+1)(.08s+1)}$
$\frac{4e^{-.1s}}{s(s+4)}$	$\frac{16e^{-.1s}(7s+1)(1.55s+1)}{(31s+1)(.15s+1)(.08s+1)}$	$\frac{16(7s+1)(4s+1)}{(31s+1)(.6s+1)(.08s+1)}$
$\frac{2e^{-.1s}}{s(s+2)}$	$\frac{10.5e^{-.1s}(7s+1)(2s+1)}{(31s+1)(.23s+1)(.08s+1)}$	$\frac{15(7s+1)(2s+1)}{(31s+1)(.23s+1)(.08s+1)}$
$\frac{e^{-.1s}}{s(s+1)}$	$\frac{4.3e^{-.1s}(7s+1)(3.8s+1)}{(31s+1)(.12s+1)(.08s+1)}$	$\frac{5.5(7s+1)(3.8s+1)}{(31s+1)(.12s+1)(.08s+1)}$
$\frac{e^{-.1s}}{s^2}$	$\frac{.15e^{-.25s}(10s+1)(3s+1)}{(.01s+1)(1.5s+1)(.08s+1)}$	$\frac{.18e^{-.15s}(10s+1)(3s+1)}{(.01s+1)(1.5s+1)(.08s+1)}$
$\frac{-e^{-.1s}}{s(s-1)}$	$\frac{.2e^{-.2s}(10s+1)(3s+1)}{(.01s+1)(1.5s+1)}$	$\frac{.4e^{-.15s}(10s+1)(3s+1)}{(.01s+1)(1.5s+1)}$
$\frac{5e^{-.1s}}{s^2+5}$	$\frac{3e^{-.38s}(1.75+1)(s^2+2s+5)}{5(12s+1)(.08s+1)}$	$\frac{5e^{-.25s}(1.75s+1)(s^2+2s+5)}{5(12s+1)(.C8s+1)}$
$\frac{20e^{-.1s}}{s^2+20}$	$\frac{9e^{-.3s}(1.5s+1)(s^2+s+20)}{20(14s+1)(.08s+1)}$	$\frac{20e^{-.2s}(1.5s+1)(s^2+s+20)}{20(14s+1)(.08s+1)}$
$\frac{-2.5e^{-.1s}}{s^2+s-2.5}$	$\frac{3e^{-1.5s}(s^2+1.5s+2.5)}{2.5(.2s+1)(.25s+1)}$	$\frac{5e^{-.05s}(s^2+1.5s+2.5)}{2.5(.38s+1)(.3s+1)}$
$\frac{5e^{-.1s}}{s^2+ss+5}$	$\frac{11.5e^{-.25s}(1.9s+1)(s^2+4s+5)}{5(7.5s+1)(.5s+1)}$	$\frac{20e^{-.14s}(1.9s+1)(s^2+4s+5)}{5(7.5s+1)(.5S+1)}$
$\frac{10e^{-.1s}}{s^2+2s+10}$	$\frac{19e^{-.3s}(2.5s+1)(s^2+2s+10)}{10(10s+1)(.43s+1)}$	$\frac{23e^{-.2s}(2.5s+1)(s^2+3s+10)}{10(10s+1)(.43s+1)}$

Table 16–5 (Continued)

Human Operator Describing Functions for Various Dynamics – Compensatory Roll Tracking

Controlled Element Y_c	Fixed Base Pilot Model Y_p	Roll Moving Base Pilot Model Y_p
$\frac{5e^{-.1s}}{s^2+5s+5}$	$\frac{19e^{-.28s}(4.3s+1)(s^2+5s+4.5)}{4.5(10s+1)(.65s+1)}$	$\frac{30e^{-.15s}(4.3s+1)(s^2+5s+4)}{4.5(10s+1)(.8s+1)}$
$\frac{25e^{-.1s}}{s^2+5s+25}$	$\frac{4.5e^{-.3s}(1.75s+1)(s^2+5s+24)}{25(9s+1)(.17s+1)}$	$\frac{6.8e^{-.2s}(1.75s+1)(s^2+5s+2)}{25(9s+1)(.17s+1)}$
$\frac{10e^{-.1s}}{s(s^2+10)}$	$\frac{.9e^{-.4s}(3s+1)(s^2+s+5)}{(12s+1)}$	$\frac{1.5e^{-.35s}(3s+1)(s^2+s+5)}{(12s+1)}$
$\frac{4e^{-.1s}}{s^2(s+4)}$	$\frac{.4e^{-.32s}(10s+1)(3s+1)}{(1.2s+1)(.01s+1)}$	$\frac{.48e^{-.25s}(10s+1)(3s+1)}{(1.2s+1)(.01s+1)}$
$\frac{10e^{-.1s}}{s(s^2+2s+10)}$	$\frac{.45e^{-.43s}(.8s+1)(s^2+4s+10)}{(.15s+1)(.15s+1)}$	$\frac{.8e^{-.43s}(.8s+1)(s^2+4s+10)}{(.15s+1)(.15s+1)}$
$\frac{10e^{-.1s}}{s(s^2+4s+10}$	$\frac{e^{-.35s}(.9s+1)(s^2+4s+10)}{(.15s+1)(.25s+1)}$	$\frac{1.15e^{-.35s}(.9s+1)(s^2+4s+1)}{(.15s+1)(.25s+1)}$

(Adapted from Shirley, 1968)

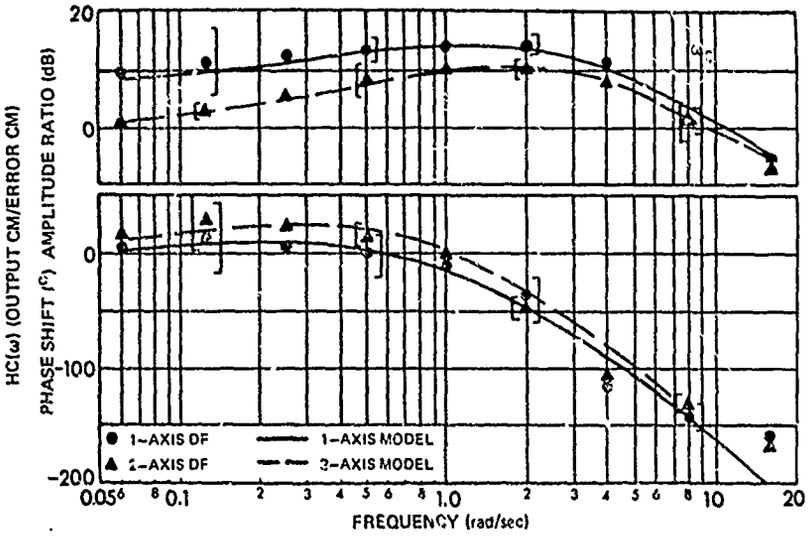


Figure 16–18. One- and two-axis describing functions $Y_c = K$ (other axis = K/s^2). (Levison & Elkind, 1966)

Multiple Loop Tracking

On many occasions, the operator is faced with a multi-loop control task in which he must participate in one or more coupled loops. Examples are control of aircraft pitch angle and angle of attack which, in turn, affects the control of airspeed and altitude. As another example, control of VTOL roll angle affects lateral position. A discussion of the extension of the single-axis models to multi-loop situations is given in McRuer and Jex (1967). A cascade model of the human operator suffices as an example of VTOL control (figure 16-19). The pilot adopts an inner loop equalization to stabilize pitch attitude and a separate slower outer loop equalization for commanding altitude to achieve the desired longitudinal position.

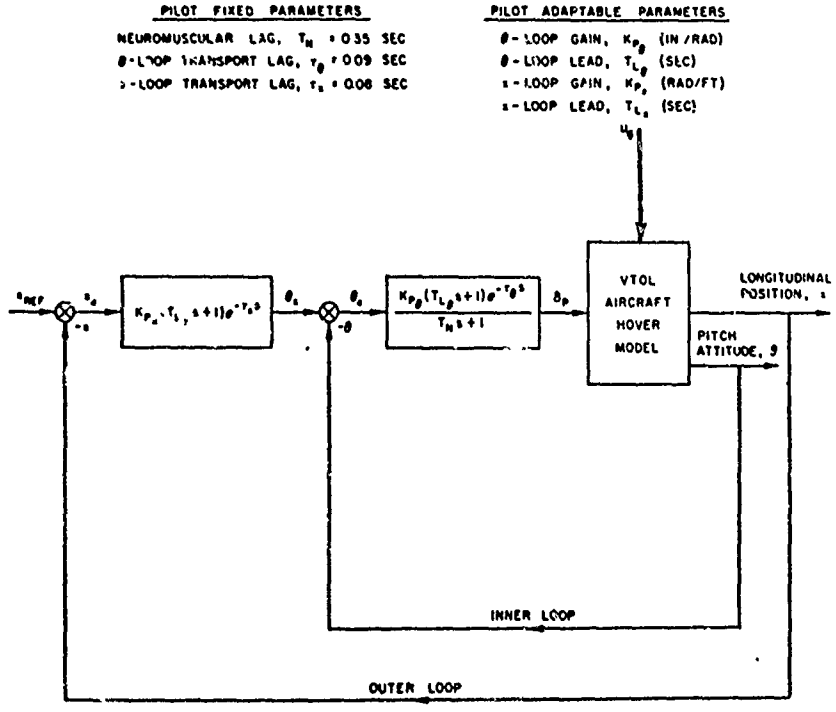


Figure 16–19. A multi-loop pilot model. (Vinje & Miller, 1967)

Transmission Delays

Manual control with transmission delays is a practical problem for remote manipulation across great distances. Delay in transmission of command information to the remote element and delay in receiving feedback information from the remote element forces manual controllers to adopt a move and wait strategy to cope with the delay. (The round trip delay from earth to moon is 2.6 seconds.) The time to complete a task depends on the delay and the number of discrete moves required.

Completion time can be lowered by reducing the number of discrete motions (making larger open loop steps) at the expense of accuracy. For delayed manipulation, Ferrell (1965) uses two approximations (t_{c1} and t_{c2}) to total movement time:

$$t_{c1} = t_0 + N(t_d + t_r) + t_d \tag{6}$$

$$t_{c2} = t_N + (N + 1)t_d$$

where

t_0 = time to complete a task with no time delay

N = number of open loop steps required to perform the task

t_d = transmission delay

t_r = reaction time

t_N = average time to perform the task with no delay and no feedback between looks.

Completion time estimates for t_{c1} are consistently lower than average times, and for t_{c2} are consistently higher. The average of these two

$$t_{ca} = \frac{t_{c1} + t_{c2}}{2} \tag{7}$$

is a good predictor of actual completion time.

The average number of times feedback is required is nearly independent of the delay time and depends only on the difficulty of the task. Task difficulty may be measured by the information index of difficulty proposed by Fitts (Fitts & Peterson, 1964).

$$I = \log_2 \frac{\text{distance moved}}{\text{average clearance of final placement}} \tag{8}$$

Both task difficulty and delay increase completion time, as seen in figure 16-20. For more complex remote manipulation tasks, involving movement and operation of tools, the same accuracy of prediction of completion time as a function of delay time seems to hold. The average number of open loop moves to perform a task depends on the task difficulty and can be estimated for simple one dimensional tasks from figure 16-21.

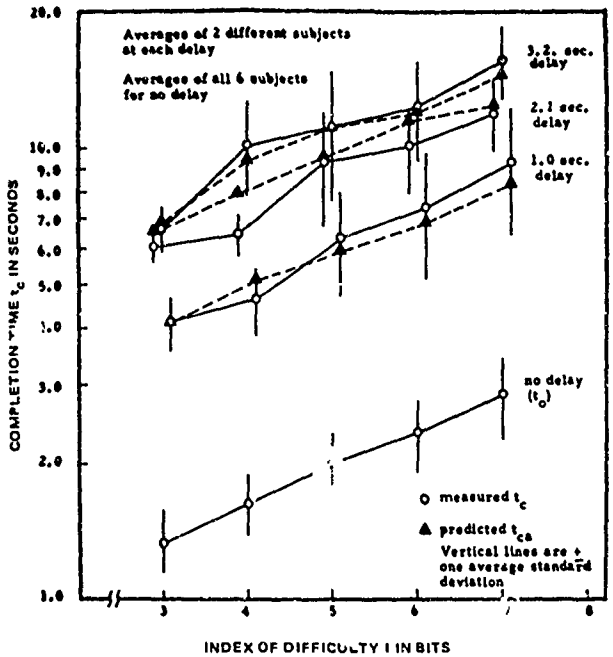


Figure 16–20. Effects of transmission delay and task difficulty on completion time. (Ferrell, 1965; used by permission of the Institute of Electrical and Electronics Engineers)

For continuous control of a dynamic system with transmission delay, phase lags associated with human operator and system delay would lead to instability unless the human reduced his gain and the crossover frequency. For a fixed input spectrum tracking errors increase with transmission time delay. To maintain a constant error level the input bandwidth must be reduced. Stated in terms of operating a remotely controlled vehicle, the vehicle speed must be reduced with increasing time delay for a constant path spatial frequency of path. Experiments on remotely controlled vehicles with variable time delay and two types of control (velocity and acceleration control) are summarized in figure 16-22. Notice that the curves indicate a relative trade-off between time lag and speed or speed and accuracy, as in the remote manipulation experiments referred to above.

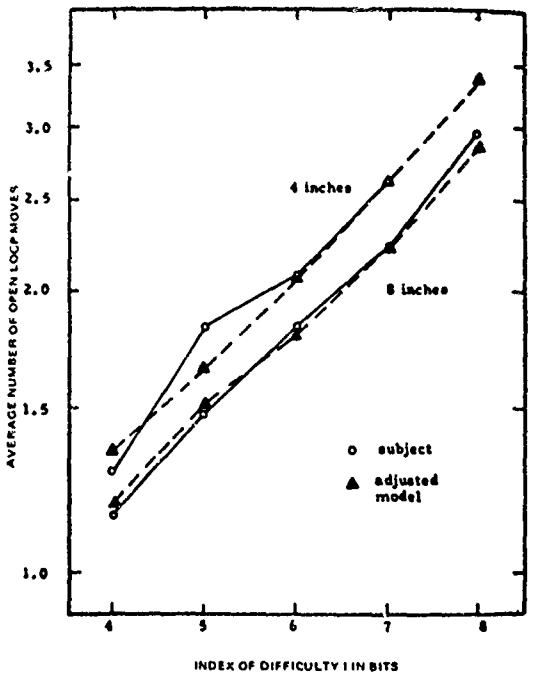


Figure 16–21. Number of open loop moves as a function of task difficulty. (Ferrell, 1965; used by permission of the Institute of Electrical and Electronics Engineers)

Adaptive Manual Control

The ability of the human controller to adapt his control according to requirements in changing conditions constitutes one of his major virtues as an element in closed loop systems. The major classes of adaptation of interest are shown in figure 16-23.

Input adaptation and prediction refer to man's ability to detect familiar or repeated patterns in the input and track these in a predictive or open loop fashion.

Controlled element adaptation refers to the well-known ability of men to adapt different control strategies appropriate to changing dynamics of the system being controlled.

Task adaptation encompasses the complex matter of optimization of the manual control loop on the basis of various control objectives. Thus, the human changes his strategy, for the same input and controlled elements, depending on the relative penalties associated with system error, vehicle accelerations, time to reach a terminal state, fuel penalties, or control effort.

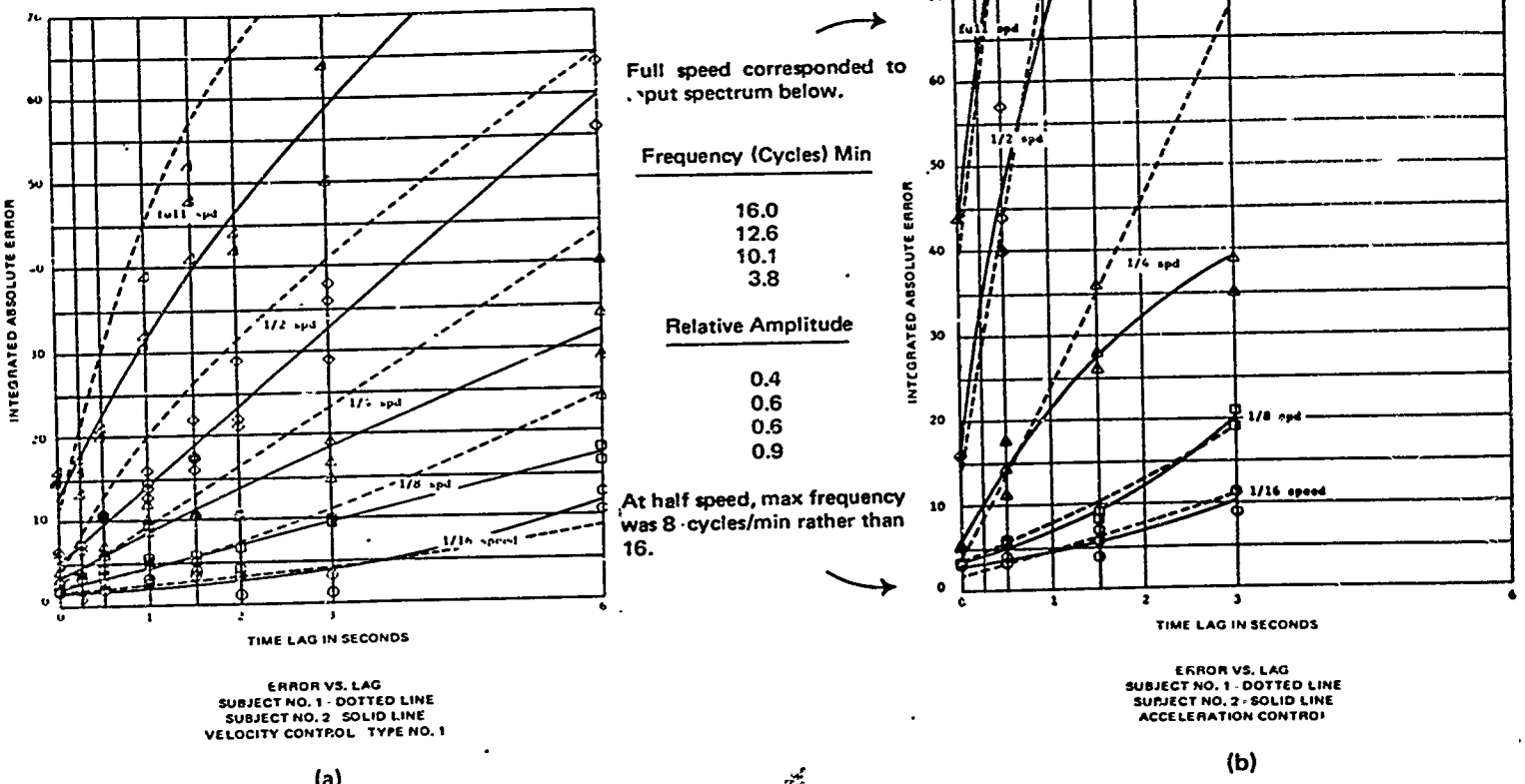


Figure 16–22. Effects of transmission delay upon remote control. (Adams, 1961)

Programmed adaptation, or open loop adaptive control, and the role it plays must not be overlooked. In this mode the environmental status, for example, attitude, road surface condition, sea state, or time-to-go, is used by the human to adopt control strategies which he has been taught (programmed) are appropriate for that situation.

Behavior of the human operator following sudden failures of the controlled element is fundamental to assessing the overall reliability of a manual, automatic, or manual backup system. The process of adaptive control is thought to consist of four phases: retention of prefailure dynamics, detection of the failure, identification of the failure and adaptation of appropriate dynamic form for the postfailure situation, and, finally, optimization of postfailure control. In the model reference schema, detection occurs when the observed change in error deviates from the expected change in error (based upon an internal model) by more than some threshold level. Typical detection times for laboratory experiments with sudden changes in gain or velocity range from 0.5 to 3 seconds. Times to detect failures involving higher order plants are increased to several seconds and may be considerably longer if emergency training is insufficient.

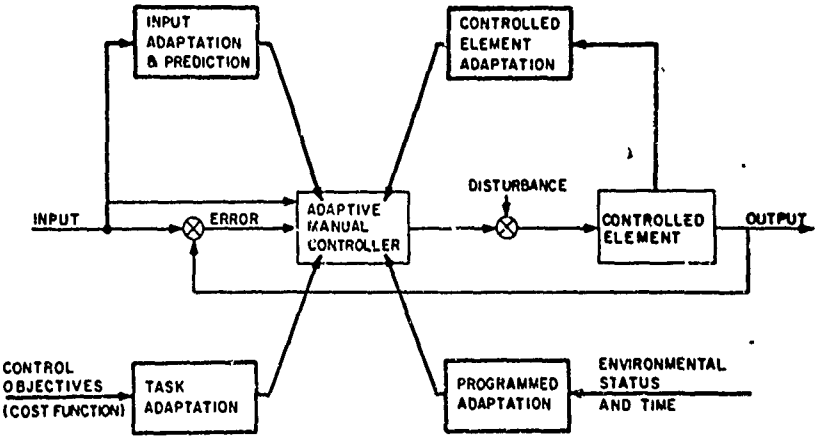


Figure 16–23. Major adaptive functions in manual control. (Young, 1969)

Controls and Manipulators

Control-Display Compatibility

A control function and the corresponding display should be geometrically compatible. Linear translations of the controls should correspond to colinear translations of the displayed variable. (The direction of display motion is opposite to control motion in a "fly-to" or inside-out display.) Rotations of controls corresponding to translation of a display are inherently ambiguous.

In certain cases, a rotation between display axes and control axes is unavoidable. The resulting ambiguity can be overcome partially by indicating the instantaneous deflection of the control stick resolved in display axes on the display itself, as in configuration c of figure 16-24. Controls should be in conventional positions, well separated, associated with the task, and easily distinguished by touch (see figure 16-25).

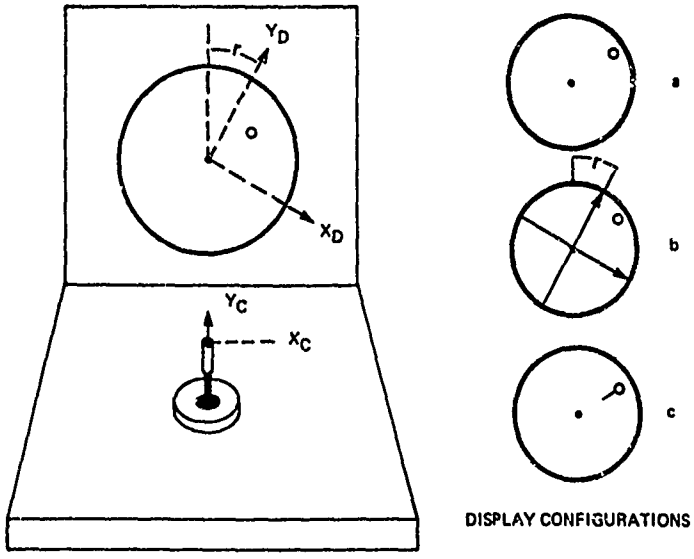


Figure 16–24. Display configurations for rotated display reference. (Bernotat, 1969)

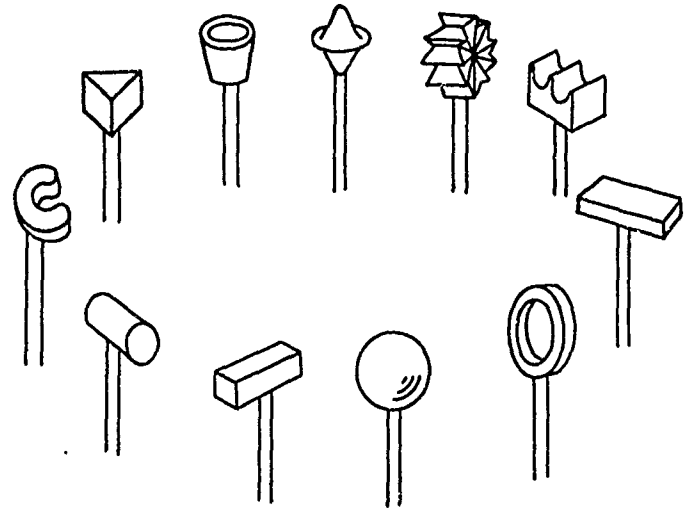


Figure 16–25. Control knob shapes. (Chapanis, Garner, & Morgan, 1955)

Control Forces

A wide variety of manipulators are in common use in vehicle control, including steering wheels, "joy sticks," pencil controllers, and pedals. (Less commonly used are head position and eye position.) As a general rule, satisfactory control feel requires the normal use of forces well below maximum without being so sensitive that inadvertent muscular movements or tremors result in errors in control. Control stick specifications include consideration of flexibility, springback, minimum control increment, friction, preload and hysteresis. For a review of this problem see Glenn (1963).

Control Stick Characteristics

The two basic modes of control stick operation are *position control*, in which the displacement or angle of the control stick is the control signal, and *force control* (or pressure control), in which the force on the control stick (which is usually maintained nearly stationary) is the control signal. Pressure control yields significantly less phase lag at high frequencies and is consequently preferable for use in situations such as control of high order systems, where excessive delay is a problem. Pressure control, spring restrained position control, and free moving control yield similar tracking results at low frequencies. For spring restrained position control sticks, an optimum value of spring constant usually exists. Increasing the moment of inertia of the control stick decreases the crossover frequency and increases tracking error for high order controlled elements (Magdaleno & McRuer, 1966).

Effects of Control Stick Nonlinearities

Common control stick nonlinearities include coulomb friction, control stick preload, control displacement limits, nonlinear gearing, control system hysteresis and backlash, and control stick velocity limits. In a vibrating environment, low levels of static friction may improve tracking performance. In controlled fixed base simulations using fore and aft motion of a light center stick and simple rate control, control stick friction and preload are found to have no significant effect on tracking performance.

For the case of control velocity limits, however, the effects on error are quite noticeable and show a marked decrement in performance as the control velocity limit is lowered, accompanied by rapid deterioration of the pilot rating. Graham (1967) concludes that human operators tend to linearize the nonlinearities of control sticks where possible by use of dither and high gain feedback around the nonlinearity. However, in the case of velocity limit, this linearization is not possible and performance degrades.

Quantization and Pulsatile Control

Deliberate quantization of the control stick output into relatively few discrete levels may be desirable for stability and ease of operation. For example, a common five-position control stick would permit fast slewing or slow control

to left or right, as well as null. The three-level controller of either the on-off or the pulse modulated type is useful for tracking situations requiring considerable operator lead. In controlling systems containing several integrators, for example, operators may prefer counting pulses to integrating their continuous control output (Young and Meiry, 1965).

Displays

This section discusses techniques for visual displays. Hardware, including developments in cathode ray tubes, electroluminescence, holographic displays, and other new techniques, is discussed fully in NASA SP-159 (1967), Poole (1966), and Luxenberg and Kuehn (1968). Some interesting aerospace applications of audio and tactile displays for control have been explored, but these are mostly in the research stage and are not, therefore, discussed here.

Compensatory and Pursuit Displays

Pursuit and compensatory displays correspond to pursuit and compensatory tracking, as discussed previously. In a pursuit display, the commanded state of the system (input) as well as the actual system state (output) is displayed separately, and the operator's task is to control the actual output so that it tracks the command. An example of a pursuit display is shown in figure 16-26(a). When only the error between ordered and actual system state is displayed, as in figure 16-26(b), the display is compensatory.

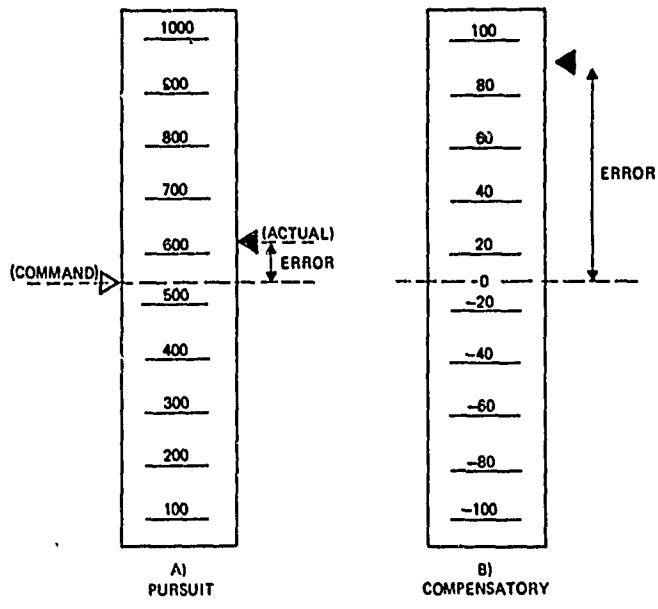


Figure 16–26. Pursuit and compensatory displays.

As mentioned earlier, the pursuit display permits the pilot to generate greater lead and anticipate the input, and consequently is of particular use for high frequency inputs or for controlling high order plants. On the other hand, error magnification can be far greater in a compensatory display, since the scale need only accommodate maximum tracking error rather than maximum output. Thus, highly accurate null readings can be achieved for low frequency inputs and well controlled vehicles.

Inside-Out versus Outside-In

The inside-out display, which is the conventional attitude instrument for aircraft, takes the aircraft as the fixed frame of reference and shows vehicle motion by movement of external reference lines or grids: the view from the inside of the vehicle looking out at the horizon.

The alternative view takes the external reference frame as fixed and shows the moving vehicle motion with respect to this frame. This approach is the outside-in method and corresponds to the view of a moving vehicle seen by an observer on the earth. Both are shown in figure 16-27. An interesting alternative suggestion by Fogel (1963) is the "Kinalog display," in which the pilot's sensation of rotation in a turn, attributable to interpretation of vestibular stimuli, is made compatible with the display format, so that both the aircraft symbol and the horizon rotate in conformity with the pilot's kinesthetic adaptation to a turn.

Where problems of vertigo may be present, general practice is to rely upon inside-out displays and to train pilots to suppress or ignore motion cues.

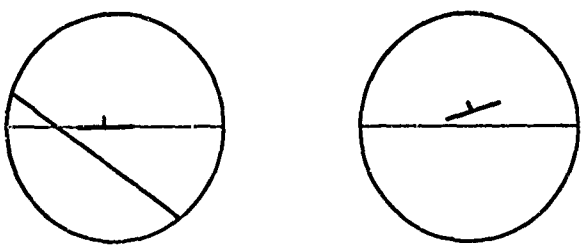


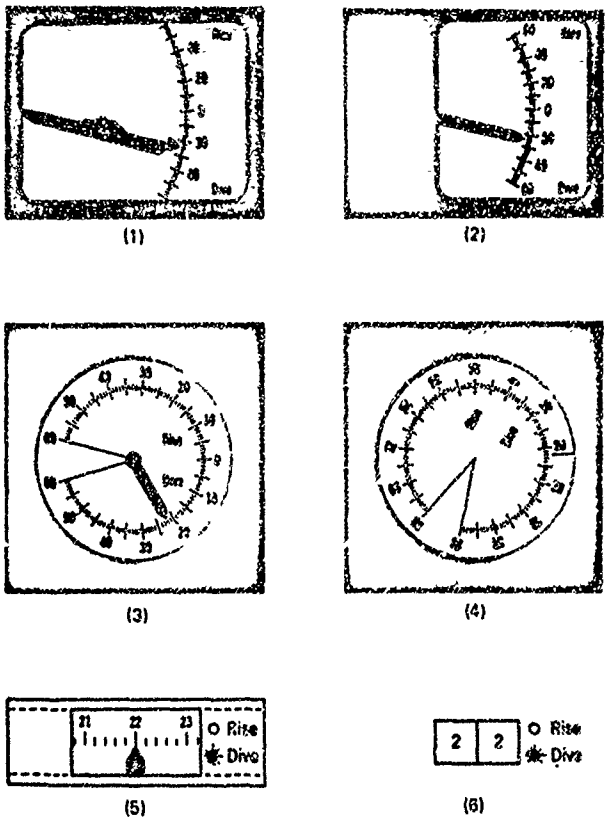
Figure 16–27. Inside-out and outside-in attitude displays.
(The aircraft is pitched nose-up and rolled left.)

Display Formats

Information is usually displayed in either a digital format, as numbers on a counter, or in a pure analog format such as length of a line or position of a pointer. There are, however, a number of mixed analog-digital displays, in which information is either presented both ways or in which the slowly changing portion is displayed digitally for unambiguous readout (as in the case of

altimeters) and the rapidly moving portion is shown in an analog fashion. A variety of single quantitative instrument displays is shown in figure 16-28. Some of the pros and cons of various indicators are summarized in table 16-6.

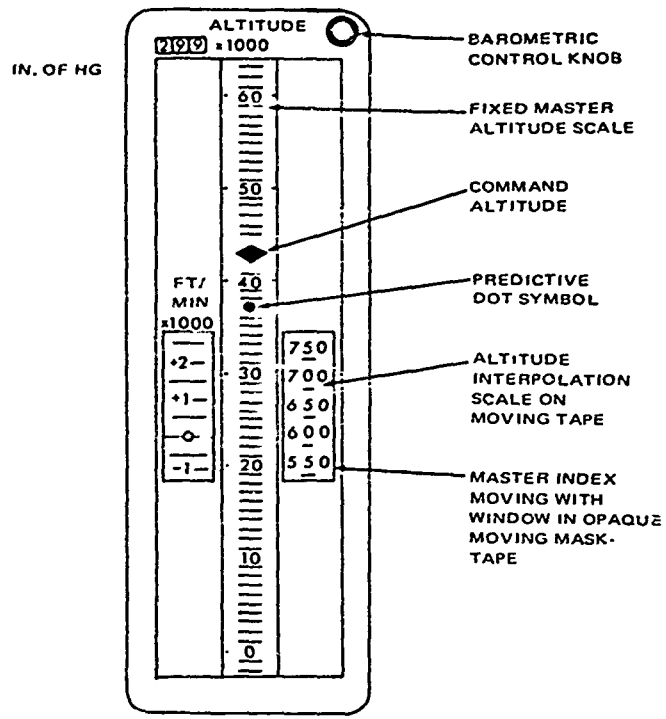
Moving tape displays have the advantage of permitting a very wide range of readings to be displayed (as in the case of pursuit displays) while still offering a large magnification or error between command input and actual output. However, they may be difficult to read when they are in motion.



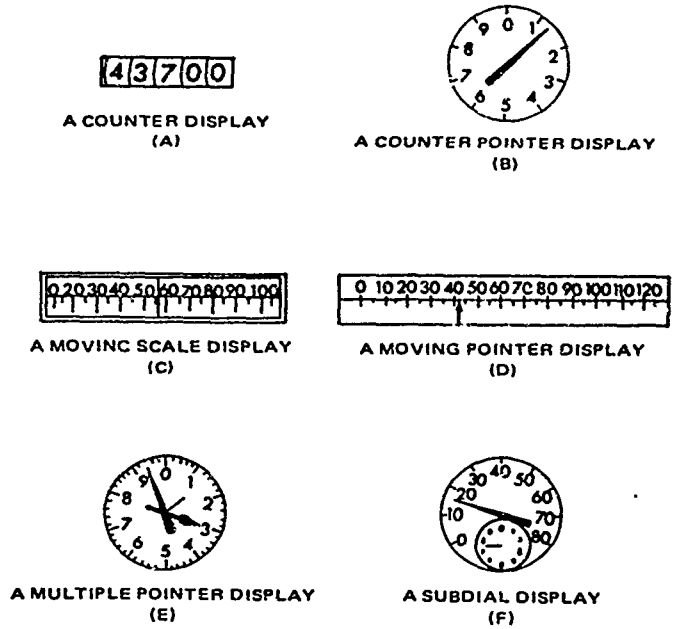
Combined analog and symbolic displays of submarine pitch angle with an increasingly symbolic emphasis: (a) pictorial; (b) moving pointer (angular correspondence preserved); (c) moving pointer (angular correspondence distorted); (d) rotating scale; (e) moving dial; (f) electronic digital display.

(a) (Kelley, 1968)

Figure 16–28. Various display formats.



(b) (Fogel, 1963)



(c) (Fogel, 1963)

Figure 16–28. Various display formats. — *Continued*

Table 16–6

Recommended Indicators According To Use

Method of Use	Counter	Moving Scale	Moving Pointer
Quantitative reading	Good Minimum time and error in obtaining exact numerical value	Fair	Fair
Qualitative and check reading	Poor Numbers must be read. Position changes not easily detected	Poor Difficult to judge direction and magnitude of deviation without reading numbers and scale	Good Location of pointer easily detected. Numbers and scale need not be read. Change in position easily detected
Setting	Good Most accurate monitoring of numerical setting. Relation to motion of setting knob less direct than for moving pointer. Not readable during rapid setting	Fair Somewhat ambiguous relation to motion of setting knob. No pointer position change to aid monitoring. Not readable during rapid setting	Good Simple and direct relation of pointer motion to motion of setting knob. Pointer position change aids monitoring
Tracking	Poor No gross position changes to aid monitoring. Ambiguous relation to control motion. Not readable during rapid changes	Fair No pointer position changes to aid monitoring. Somewhat ambiguous relation to control motion. Not readable during rapid changes	Good Pointer position readily monitored and controlled. Most simple relation to manual control motion

(Baker & Grether, 1954)

Peripheral Displays

While most conventional displays are designed for foveal viewing, and require fixation and accommodation for accurate reading of the instrument, there are a number of applications for displays which can be read in peripheral vision. Peripheral displays may be used to avoid interference with the primary scan pattern and to present additional information outside the central instrument display area. Although the rods of the eye are capable of poorer resolution than are the cones, they respond well to motion. Several examples of motion displays are shown in figure 16-29. Peripheral motion displays are particularly appropriate for displaying vehicle rates of turn or linear velocities. Flashing lights are useful principally as warning indicators.

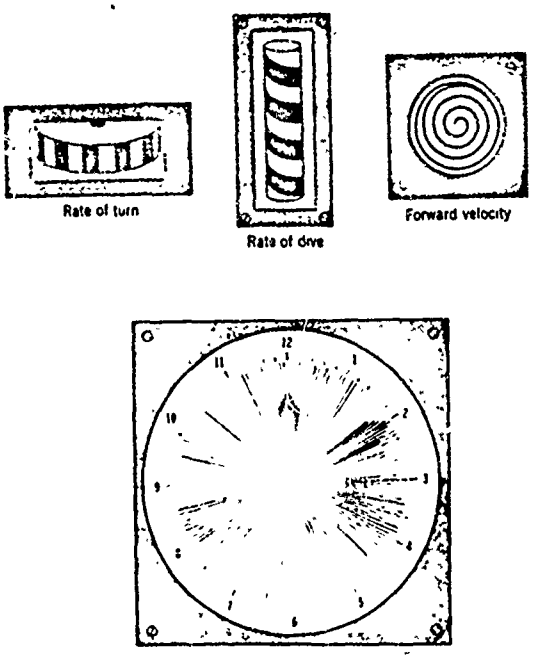


Figure 16–29. Motion displays. (Kelley, 1968)

Coding of Visual Information

Further information can be added to the two dimensions of a displayed point by appropriate coding of the symbol. Coding may help in identifying the particular point (as in the case of air traffic control displays) or giving information on other dimensions. Use of alphanumeric identification tags is of great value, providing there is sufficient room to present legible alphanumerics without cluttering. A summary of other coding dimensions is given in table 16-7.

Integrated Displays, Contact Analog Displays, and Head-up Displays

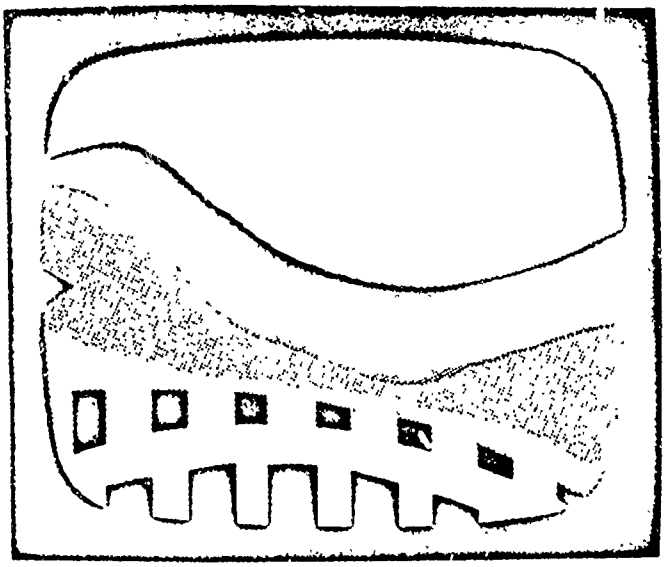
In complex multi-axis control tasks, such as are typical of piloting aircraft or space vehicles, considerable assistance can be given the pilot by integrating related information on a single display. Generally, integrated displays show the rates of change of variables in proximity to the variable itself. Integrated displays permit the pilot to view a single display containing all relevant information and simplify his problem of reconstructing the geometrical status of a vehicle.

If the integrated display contains symbols or lines unrelated to real geometrical variables it is a *symbolic display*. If the elements of the display bear some relation to a picture of the outside reference frame, such as a pilot might view looking through a window, then the display is of the *contact analog* variety. (This is analogous to flying in "contact" or under visual flight rule conditions.) Examples of contact analog displays for terrain avoidance and for submarine control are given in figure 16-30.

Table 16–7
Summary of Coding Dimensions

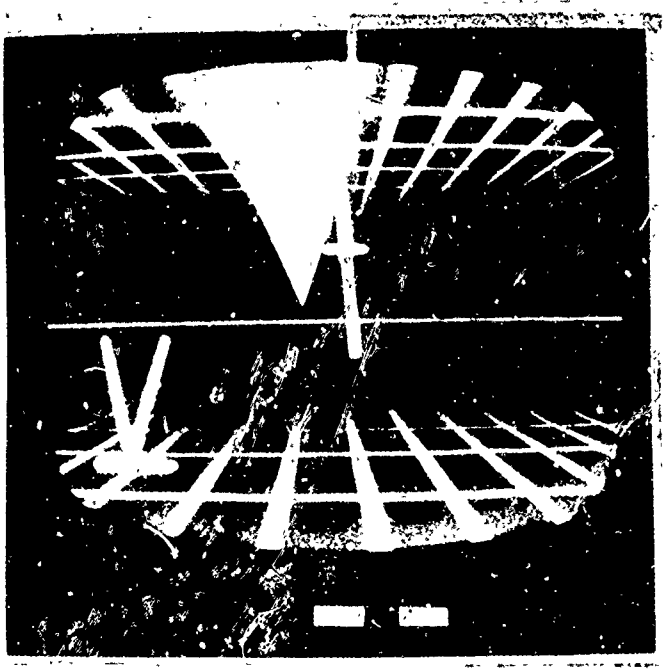
Dimension	Number of Steps	Evaluation	Combines With	Remarks
Size	4 – 5	Fair	Shape, color, brightness	Requires considerable display space. Limited usefulness. Best when used in combination codes
Shape	15	Excellent	Size, color, motion, flash brightness	Certain shapes easily recognized. Requires good contrast and resolution. Combines well with other codes
Alphanumerics	Unlimited	Excellent	Color, brightness	Requires good contrast and resolution. Easily learned
Color	11	Excellent	Size, shape, alphanumerics, motion, flash	Recognizable colors on CRTs limited to 4 – 7. Combines well with other codes
Motion	1 – 2	Poor	Shape, color, brightness	Hard to discriminate. Not recommended except for getting attention or to supplement other codes
Flash	1 – 3	Poor	Shape, color	Distracting and fatiguing. Not recommended except for getting attention
Brightness	7	Fair – good	Size, shape, alphanumerics, motion	Requires good contrast. Best when combines with other codes, as in shades of gray

(Ketchel & Jenney, 1968)



(a) Terrain avoidance display. (Ketchel & Jenney, 1968, from Kaiser Aerospace and Electronics data)

Reproduced from best available copy.

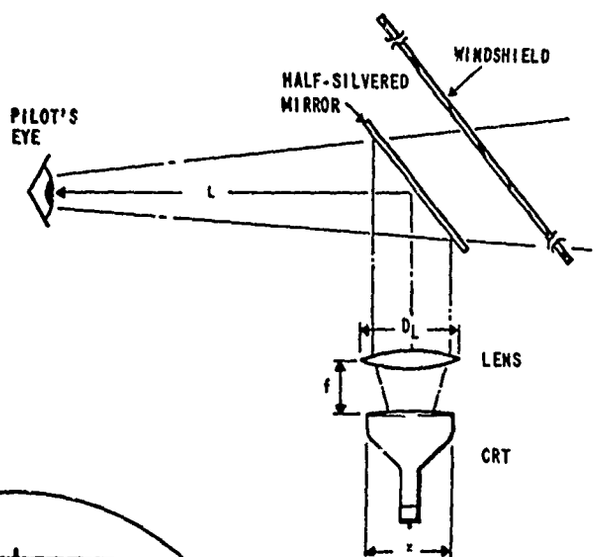


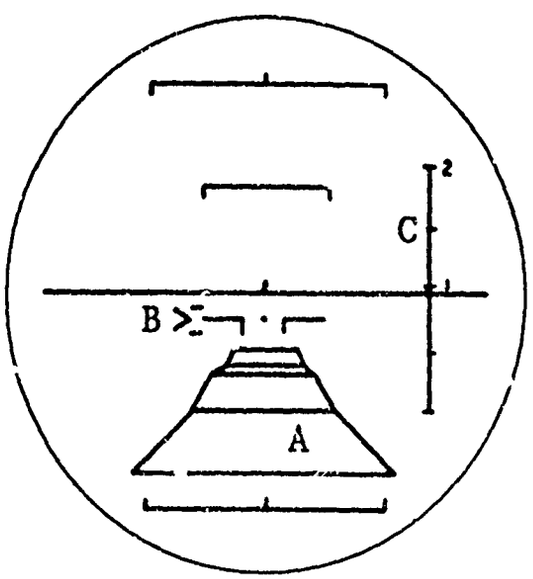
(b) Simulation of the Norden contact analog perspectively quickened display. (McLane & Wolf, 1968)

Figure 16–30. Contact analog displays.

An integrated display presented by reflecting a CRT-generated picture at optical infinity, so the operator can view the display while continuing to look out the window, is known as a *head-up display*. This configuration and an example are shown in figure 16-31. Integrated displays of the schematic or contact analog variety have been used with integration of pictures of the outside environment, which may be gathered from T.V., sonar, or radar data. Displays which emphasize attitude and position in a vertical plane may be thought of as forward-looking for a vehicle in level flight, and are known as vertical situation displays. Those which emphasize geographical information or position over the ground are horizontal situation indicators. Examples of each are given in figure 16-32.

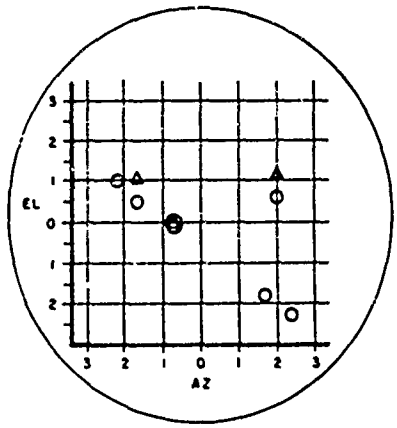
(a) (Poole, 1966)



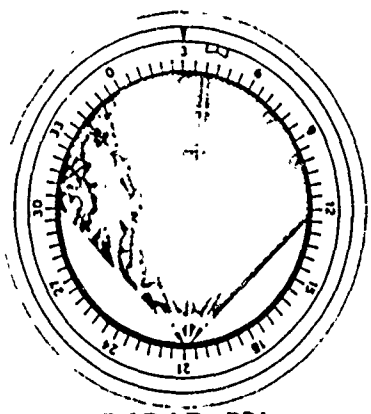


(b) (Ketchel & Jenney, 1968, after Sperry)

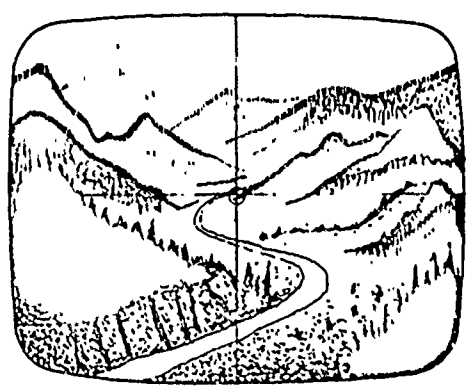
Figure 16–31. Head-up display.



MULTISENSOR (RADAR/IR)



RADAR–PPI



TV DISPLAY

Figure 16–32. Vertical situation, horizontal situation and pictorial displays. (Ketchel & Jenney, 1968)

Control Augmentation and Display Quickening

The human operator has difficulty controlling systems which contain more than two integrations, and operates best in systems approximating a single integration. When the controlled element is of a higher order than desired from a point of view of manual control, the designer can improve the dynamics of the total man-machine loop by control augmentation or quickening, as shown in figure 16-33. In control augmentation the dynamic compensation is performed on the man's output, by feedback of system output and its derivatives to the controlled element. Position and rate feedback in stability augmentation systems is a common technique to change the handling qualities of vehicles. As a consequence of control augmentation, however, man loses his direct control over the controlled element actuators, and controls the vehicle only indirectly through a servomechanism. Typically, with control augmentation the man has full information on vehicle output and operates with a status display.

An alternative method of improving the loop dynamics by derivative feedback is adding lead through the addition of output derivatives in the display, thereby operating on the operator's input. When the displayed signal is a weighted sum of output and several of its derivatives, the technique is known as *quickening* (figure 16-34a). If some derivative signal is added to the display but the human operator must still generate lead equalization to perform the task, then it is known as a *partially quickened display*. If, on the other hand, just enough derivative feedback is added to the display so that the operator need merely move the control stick in proportion to the deflection on the display, then the display is *fully quickened*.

The appropriate gains on the output derivatives for fully quickened displays are selected by assuming that the operator is a pure time delay of 0.2 to 0.3 second for single axis tracking. The principal disadvantage of the display quickening technique is that the operator functions merely as a control amplifier and no longer has status information on the vehicle output. He is thus deprived of his ability to exercise choice in the method of control. The pros and cons of display augmentation versus control augmentation are summarized in table 16-8.

Command and status displays are closely related to the question of control display quickening and control augmentation. A *status display* presents

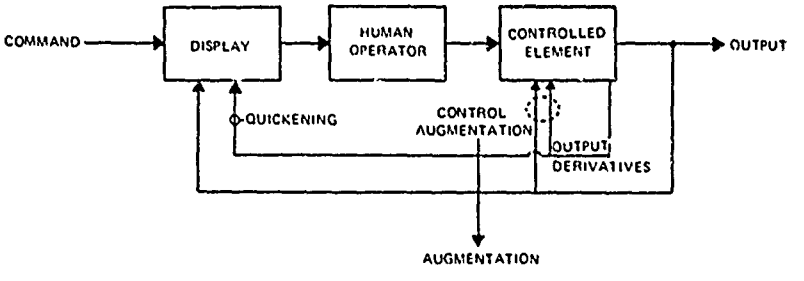


Figure 16–33. Control augmentation.

information on the ordered system output, the current system output, and whatever additional state variables may be necessary to help its operator control the system. The additional status information may include derivatives or integrals of system output, or settings of intermediate control variables, such as rocket gimbal angles or aerodynamic surfaces. The operator uses the status display to choose an appropriate control action, which may take into account many additional constraints, such as acceleration, fuel, or time. By having

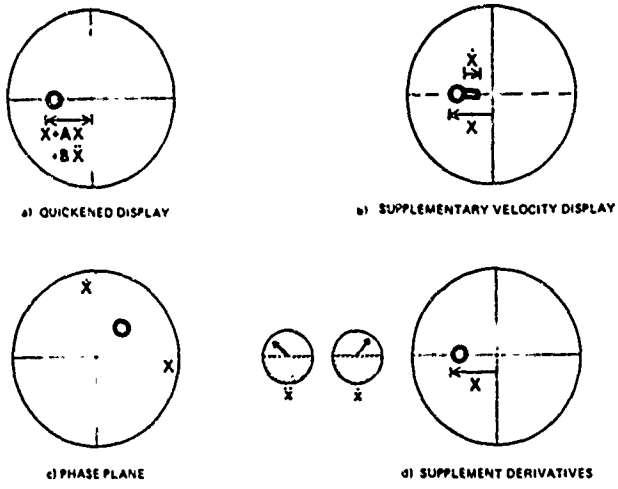


Figure 16–34. Display quickening.

Table 16–8

Display vs. Control Augmentation

Display Augmentation	Control Augmentation
Operations performed on man's input	Operations performed on man's output
Attention is transferred from outer-loop goal to inner-loop functioning	Attention is transferred from inner-loop functioning to outer-loop goal
Can employ man's muscular strength at the control junction in the inner loop to move a control surface, open a hydraulic valve, etc	Can employ man's senses in the outer loop to observe the controlled variable and the environment
Man is kept aware of control signal	Man is kept aware of system output
Requires higher frequency, more complex human output	Requires simpler, lower frequency output.

(Kelley, 1968)

complete status information the operator can exercise his judgment in selecting a control sequence. To help him in this control, he may be assisted by varying degrees of control augmentation, as discussed above.

In the case of a pure command display, the operator is given information on required control action to achieve the desired system output. The display may be quickened or include other computation to ease the operator's task and, in the extreme, he need merely act as a proportional controller. Although the results may be satisfactory according to the computed response, the operator loses the ability to adapt to changing situations.

Frequently, command and status displays are combined, so that the pilot can follow the commanded control if he wishes or take alternative action based on the status information.

Supplementary Velocity Indication

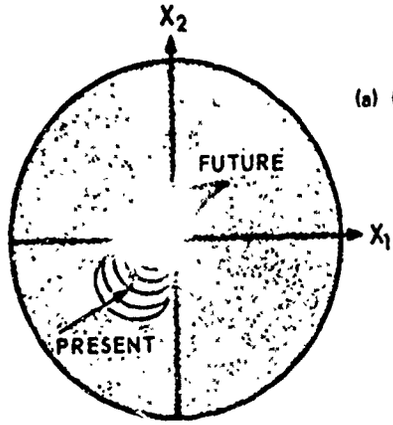
Several techniques have been used to present supplementary velocity indication without the loss of output state or error information associated with quickening. For example, supplementary velocity may be displayed by a variable length vector attached to the display spot, as shown in figure 16-34(b) or by use of a second axis to indicate velocity, as in the phase plane of figure 16-34(c). Finally, separate needle indicators on the derivatives for a two-axis display when appropriately arranged can yield supplementary velocity information to be used by the pilot, as shown in figure 16-34(d).

Predictor Displays

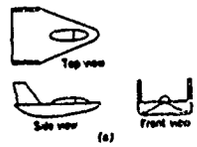
A powerful technique for stabilizing man-machine loops by putting lead information into the display, without removing the human operator from his role as an adaptive controller, is the use of a predictor instrument. A trace extends from the current output or error into the future. The trace representing future output is generated rapidly and repeatedly by use of a fast time model of the controlled element, which has the same initial conditions and control signals as those being applied to the actual controlled element. When used with systems having several integrations or with very slowly responding systems, the predictor display is of great value. It allows the operator to experiment with several different control possibilities off-line before actually applying one to the controlled element. Possible formats for the predictor display are shown in figure 16-35.

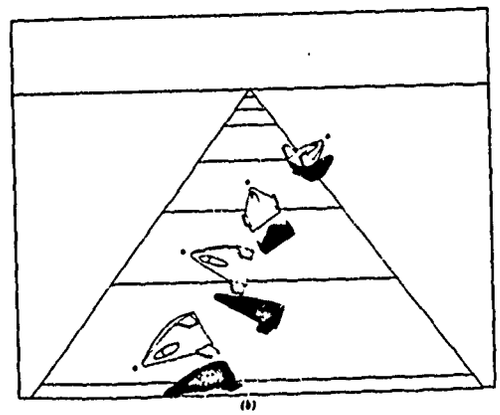
Preview Displays

Preview displays are related to predictor displays. In most control applications involving human operators, some explicit information concerning the input which will reach him in the future is available, and his control actions are based to a great extent on this preview. A view of the road and obstacles ahead or of the runway on which he will be landing is used by the operator in his role as a preview controller. Displays which can incorporate information on

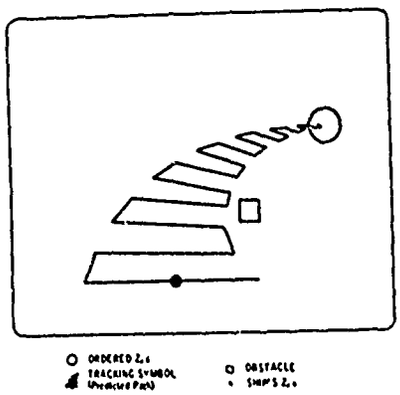


(a) (Senders et al., 1964, from Kelley, 1960)





(b) (Kelley, 1968)



(c) (McLane & Wolf, 1966)

Figure 16–35. Predictor displays.

future inputs may be presented in a manner analogous to those of predicted future outputs for the predictor display. Models of the human controller, developed for compensatory tracking situations and extendable to pursuit tracking, are clearly inappropriate for the preview situations so common in controlling vehicles with a view of the external surround. Some optimal control models applicable to the preview situation have been developed and tested (Sheridan, 1966).

Display Intermittency

Intermittent flashing of a display, or low frequency updating of a display, may lead to increased tracking errors. Well below the theoretical limits of sampling (twice the highest input frequency), tracking degrades because of interference with the ability to extract rate information and the appearance of flicker. The on-time of the display as well as the flash rate influences the performance, as shown in figure 16-36.

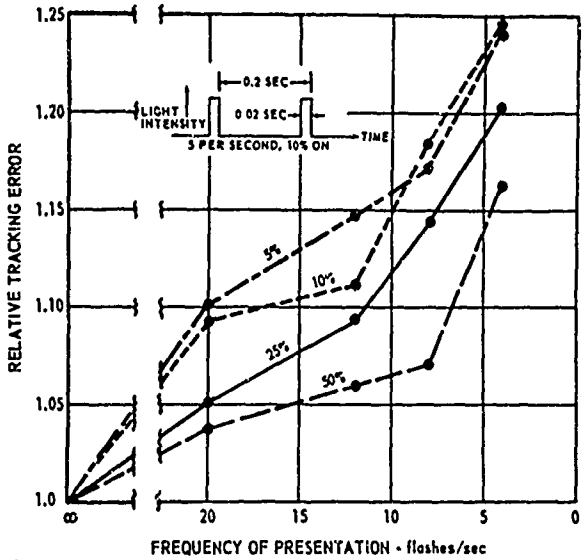


Figure 16–36. Display intermittency. (Senders et al., 1966)

Display Layout

Most display layouts follow usual workspace guidelines and common sense. Related instruments should be grouped together. Instruments requiring frequent attention should be in the optimum viewing zone. Null indicating instruments should be oriented so that the pointers are all directed the same way for normal conditions, to assist monitoring. Recommended console dimensions and viewing angles for a seated operator are given in figure 16-37. Other such layout considerations exist for aircraft panel design (for example see A. F. Systems Command, 1969).

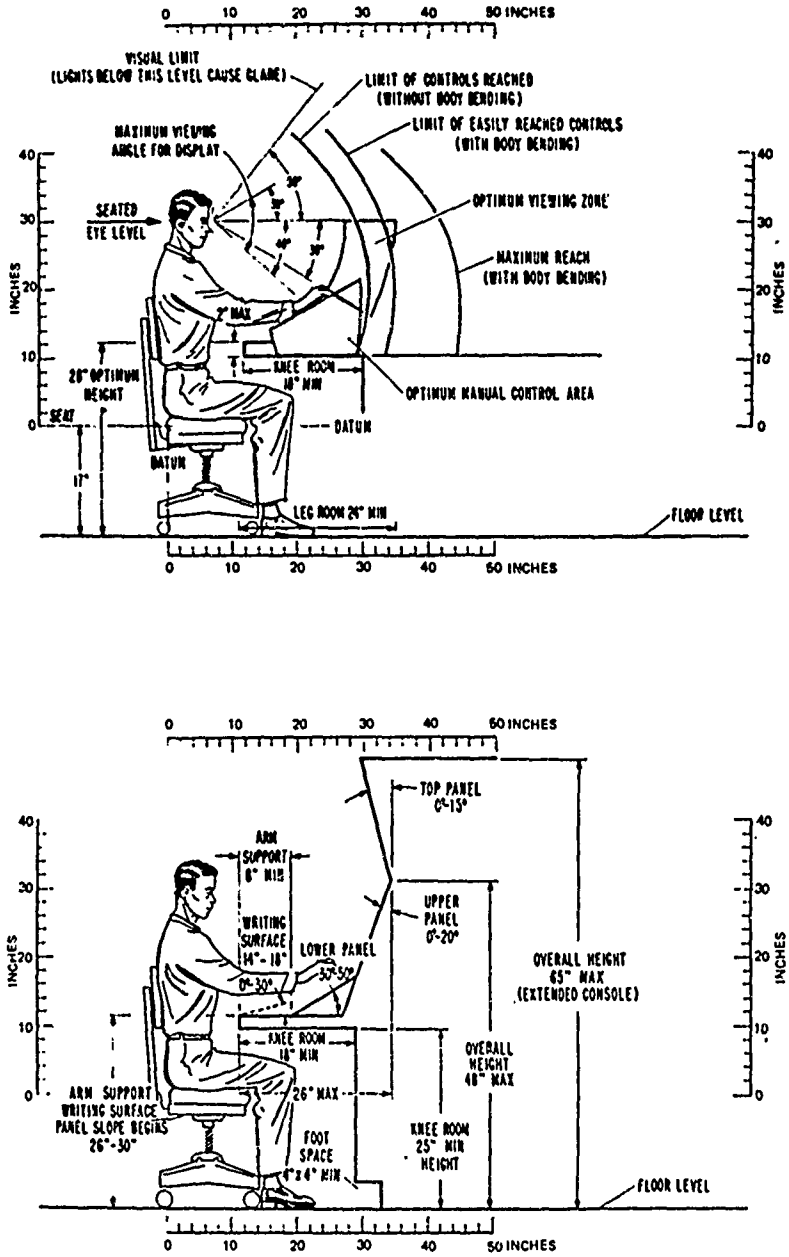


Figure 16–37. Recommended console dimensions and viewing angles. (Kubokawa, 1968; used by permission of the Institute of Electrical and Electronics Engineers)

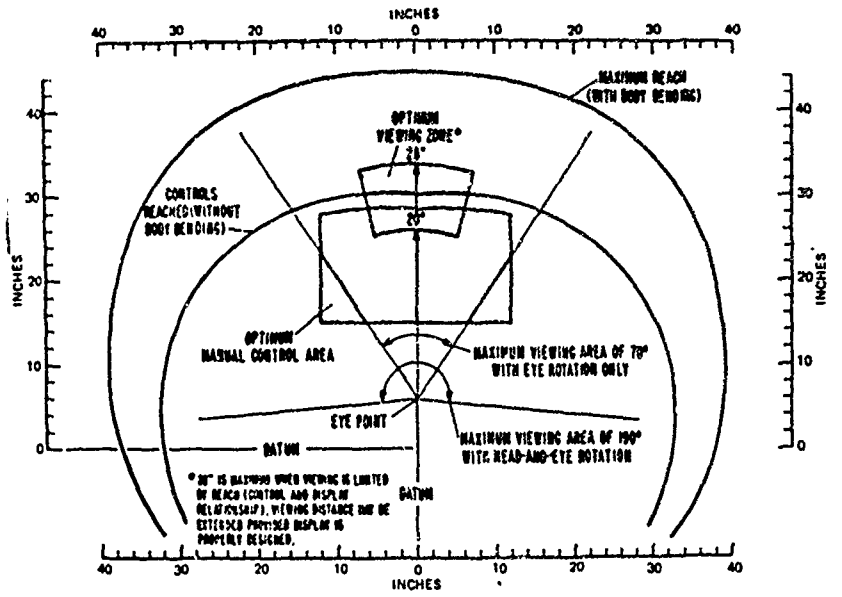


Figure 16–37. Recommended console dimensions and viewing angles. (Kubokawa, 1968; used by permission of the Institute of Electrical and Electronics Engineers) – *Continued*

References

Adams, James L. An investigation of the effects of the time lag due to long transmission distances upon remote control: Phase I–tracking experiments. NASA TN D-1211, Stanford University, Stanford, Calif., December 1961.

Air Force Systems Command. Crew stations and passenger accomodations. Design handbook 2-2. Wright-Patterson AFB, Ohio, May 1969.

Anderson, R. O., & Dillow, J. D. "Paper pilot"–an application of pilot models to predict VTOL flying qualities in precision hover. Sixth Annual Conference on Manual Control, Air Force Institute of Technology, Wright-Patterson AFB, Ohio, April 1970.

Ashkenas, I. L. A study of conventional airplane handling qualities requirements. I: Roll handling qualities. AFFDL TR-65-138-I, Air Force Flight Dynamics Laboratory, Wright-Patterson AFB, Ohio, October 1965.

Ashkenas, I. L., & McRuer, D. T. A theory of handling qualities derived from pilot vehicle system consideration. *Aerospace Engineering*, 1962, *21*(2), 60-102.

Baker, C. A., & Grether, W. F. Visual presentation of information. WADC TR-54-160, Wright Air Development Center, Wright-Patterson AFB, Ohio, August 1954.

Bernotat, R. Rotation of visual reference systems and its influence on control quality. Fifth Annual NASA-University Conference on Manual Control, NASA SP-215, Massachusetts Institute of Technology, Cambridge, Mass., March 1969.

Bull, Gifford. Minimum flyable longitudinal handling qualities of airplanes. Cornell Aeronautical Laboratory Report No. TB-1313-F-1, December 1959.

Carbonell, J. R., Ward, J. L., & Senders, J. W. A queueing model of visual sampling: Experimental validation. *Institute of Electrical and Electronic Engineers Transactions on Man-Machine Systems*, 1968, *MMS-9* (4), 82-87.

Chalk, Charles R. Additional flight evaluations of various longitudinal handling qualities in a variable-stability jet fighter. WADC TR 57-719, Wright Air Development Center, Wright-Patterson AFB, Ohio, Part I, January 1958; Part II, July 1958.

Chalk, C. R. Additional flight evaluations of various longitudinal handling qualities in a variable-stability jet fighter, Part II. Wright Air Development Center Technical Report 57-719, Part II, July 1958 (also published as Cornell Aeronautical Laboratory Report No. TB-1141-F-2).

Chapanis, A., Garner, W. R., & Morgan, C. R. *Applied experimental psychology: Human factors in engineering design*. New York: John Wiley & Sons, Inc., 1955.

Clement, W. F., Jex, H. R., & Graham, D. A manual control display theory applied to instrument landings of a jet transport. *Institute of Electrical and Electronic Engineers Transactions on Man-Machine Systems*, 1968, *MMS-9*(4), 93-110.

Cooper, George E. Understanding and interpreting pilot opinion. *Aeronautical Engineering Review*, 1957, *16*(3), 47-51, 56.

Cooper, G. E., & Harper, R. P. The use of pilot rating in the evaluation of aircraft handling qualities. NASA TN D-5153, Washington, D.C., April 1969.

Dinsdale, P. B. Relative effects of roll and yaw motion cues in manual control. S.M. Thesis, Massachusetts Institute of Technology, Cambridge, Mass., September 1968.

Elkind, J. I. Characteristics of simple manual control systems. Report 111, M.I.T. Lincoln Laboratory, Lexington, Mass., April 1956.

Elkind, J. I., Falb, Peter L., Kleinman, David, & Levison, W. H. An optimal control method for predicting control characteristics and display requirements of manned-vehicle systems. TR AFFDL-67-187, Air Force Flight Dynamics Laboratory, Wright-Patterson AFB, Ohio, June 1968.

Ferrell, W. R. Remote manipulation with transmission delay. *Institute of Electrical and Electronic Engineers Transactions on Human Factors in Electronics*, 1965, *HFE-6*(1), 24-32.

Fitts, P. M., & Peterson, J. R. The information capacity of discrete motor responses. *Journal of Experimental Psychology*, 1964, *67*, 103-112.

Glenn, J. Manual flight control system functional characteristics. *Institute of Electrical and Electronic Engineers Transactions on Human Factors in Electronics*, 1963, *HFE-4*.

Graham, Dunstan. Effect of some control system nonlinearities on single-loop compensatory tracking. Third Annual NASA-University Conference on Manual Control, NASA SP-144, University of Southern California, Los Angeles, Calif., March 1967.

Harper, R. P. In-flight simulation of the lateral directional handling qualities of entry vehicles. WADC TR 61-147, Wright Air Development Center, Wright-Patterson AFB, Ohio, 1961.

Kelley, Charles R. *Manual and automatic control: A theory of manual control and its application to manual and automatic systems*. New York: John Wiley & Sons, Inc. 1968.

Ketchel, J. L., & Jenney, L. L. Electronic and optically generated aircraft displays: A study of standardization requirements. JANAIR Report No. 680505, Washington, D.C., May 1968.

Kidd, E. A., & Harper, R. P., Jr. Fixed-base and in-flight simulations of longitudinal and lateral-directional handling qualities for piloted re-entry vehicles. ASD-TDR-61-362, Air Force Flight Dynamics Laboratory, Wright-Patterson AFB, Ohio, February 1964.

Kubokawa, C. C. Instant modular 3-D mockup for configuring control and display equipment. *Institute of Electrical and Electronic Engineers Transactions on Man-Machine Systems*, 1968, *MMS-9*(3), 72-81.

Levison, W. H., Baron, Sheldon, & Kleinman, David L. A model for human controller remnant. Fifth Annual NASA-University Conference on Manual Control, Massachusetts Institute of Technology, Cambridge, Mass., NASA SP-215, March 1969.

Levison, W. H., & Elkind, J. I. Studies of multi-variable manual control systems: Two axis compensatory systems with compatible integrated display and control. NASA CR-554, Bolt Beranek and Newman, Inc., Cambridge, Mass., August 1966.

Luxenberg, H. R., & Kuehn, R. L. *Display systems engineering*. New York: McGraw-Hill, 1968.

Magdaleno, R. E., & McRuer, D. T. Effects of manipulator restraints on human operator performance. AFFDL-TR-66-72, Air Force Flight Dynamics Laboratory, Wright-Patterson AFB, Ohio, December 1966.

McLane, R. C., & Wolf, J. D. Symbolic and pictorial displays for submarine control. Second Annual NASA-University Conference on Manual Control, NASA SP-128, Massachusetts Institute of Technology, Cambridge, Mass., May 1968.

McRuer, D. T., Graham, G., Krendel, E., & Reisener, W. Human pilot dynamics in compensatory systems—theory, models and experiments with controlled element and forcing function variations. AFFDL-TR-65-15, Air Force Flight Dynamics Laboratory, Wright-Patterson AFB, Ohio, July 1965.

McRuer, D. T., & Jex, H. R. A review of quasi-linear pilot models. *Institute of Electrical and Electronic Engineers Transactions on Human Factors in Electronics*, 1967, *HFE-8*(3), 231-249.

McRuer, D. T., & Weir, D. H. Theory of manual vehicular control. *Ergonomics*, 1969, *12*(4), 599-633.

NASA SP-169. Recent advances in display media. Symposium, Cambridge, Massachusetts, September 1967.

Poole, H. H. *Fundamentals of display systems*. Washington: Spartan Books, 1966.

Reid, L. D. An investigation into pursuit tracking in the presence of a disturbance signal. Fifth Annual NASA–University Conference on Manual Control, NASA SP-215, Massachusetts Institute of Technology, Cambridge, Mass., March 1969.

Sadoff, M., McFadden, N. M., & Heinle, D. R. A study of longitudinal control problems at low and negative damping and stability with emphasis on effects of motion cues. NASA TN D-348, January 1961.

Senders, John, Frost, George, & Crocker, Jeremy. The human operator. *Bioastronautics data book*. NASA SP-3006, 1966.

Sheridan, T. B. Three models of preview control. *Intitute of Electrical and Electronic Engineers Transactions on Human Factors in Electronics*, 1966, *HFE-7*(2), 91-102.

Shirley, Richard S. Motion cues in man-vehicle control. S.M. Thesis, Massachusetts Institute of Technology, Cambridge, Mass., January 1968.

Shirley, R. S., & Young, L. R. Motion cues in man-vehicle control: Effects of roll-motion cues on human operator's behavior in compensatory systems with disturbance inputs. *Institute of Electrical and Electronic Engineers Transactions on Man-Machine Systems*, 1968, *MMS-9*(4), 121-128.

Vinje, E. W., & Miller, D. P. Interpretation of pilot opinion by application of multiloop models to a VTOL flight simulator task. Third Annual NASA–University Conference on Manual Control, NASA SP-144, University of Southern California, Los Angeles, Calif., March 1967.

Young, L. R. On adaptive manual control. *Ergonomics*, 1969, *12*(4), 635-675.

Young, L. R. Some effects of motion cues on manual tracking. *Journal of Spacecraft and Rockets*, 1967, *4*(10), 1300-1303.

Young, L. R., & Meiry, J. L. Bang-bang aspects of manual control in high order systems. *Institute of Electrical and Electronic Engineers Transactions on Automatic Control*, 1965, *AC-10*(3), 336-341.

CHAPTER 17
ATMOSPHERE CONTROL

by

Walton L. Jones, M.D.

and

A. L. Ingelfinger

National Aeronautics and Space Administration

The life support system regulates the temperature, pressure and humidity of the spacecraft atmosphere. In addition, the system controls the constituents of the atmosphere, removing carbon dioxide and trace contaminants; supplying oxygen to replace that lost by leakage and metabolic consumption; and supplying nitrogen to replace that lost by leakage. In order to design an acceptable life support system a number of design parameters must be established. Many of these parameters are related to the requirements of the crew and, therefore, are established in large degree by medical personnel. In addition, vehicle configuration will significantly influence the requirements for the life support system. When the man, mission and vehicle characteristics are established, however, then subsystem parameters must be selected which best integrate into the most effective life support/environmental control system. This chapter examines all functions of the atmosphere control system and presents representative performance data and physiological data for the most promising subsystems developed to date.

Figure 17-1 indicates schematically the principal functions of an atmosphere control system and the interconnection of the various subsystems. An operational system is, of course, greatly more complicated than the schematic suggests, but the figure is included as an aid to those who may be unfamiliar with the essentials of providing breatheable atmospheres in spacecraft. Very briefly stated, the system operates as follows. Cabin air laden with humidity is dried, and trace gas contaminants generated by the crew and equipment are removed. Carbon dioxide is then extracted and concentrated in the carbon removal unit and purified air is returned to the cabin. The concentrated carbon

Reviewed by Karl H. Houghton, M.D., and Mouhoud M. Yakut, McDonnell Douglas Astronautics Company, Huntington Beach, California

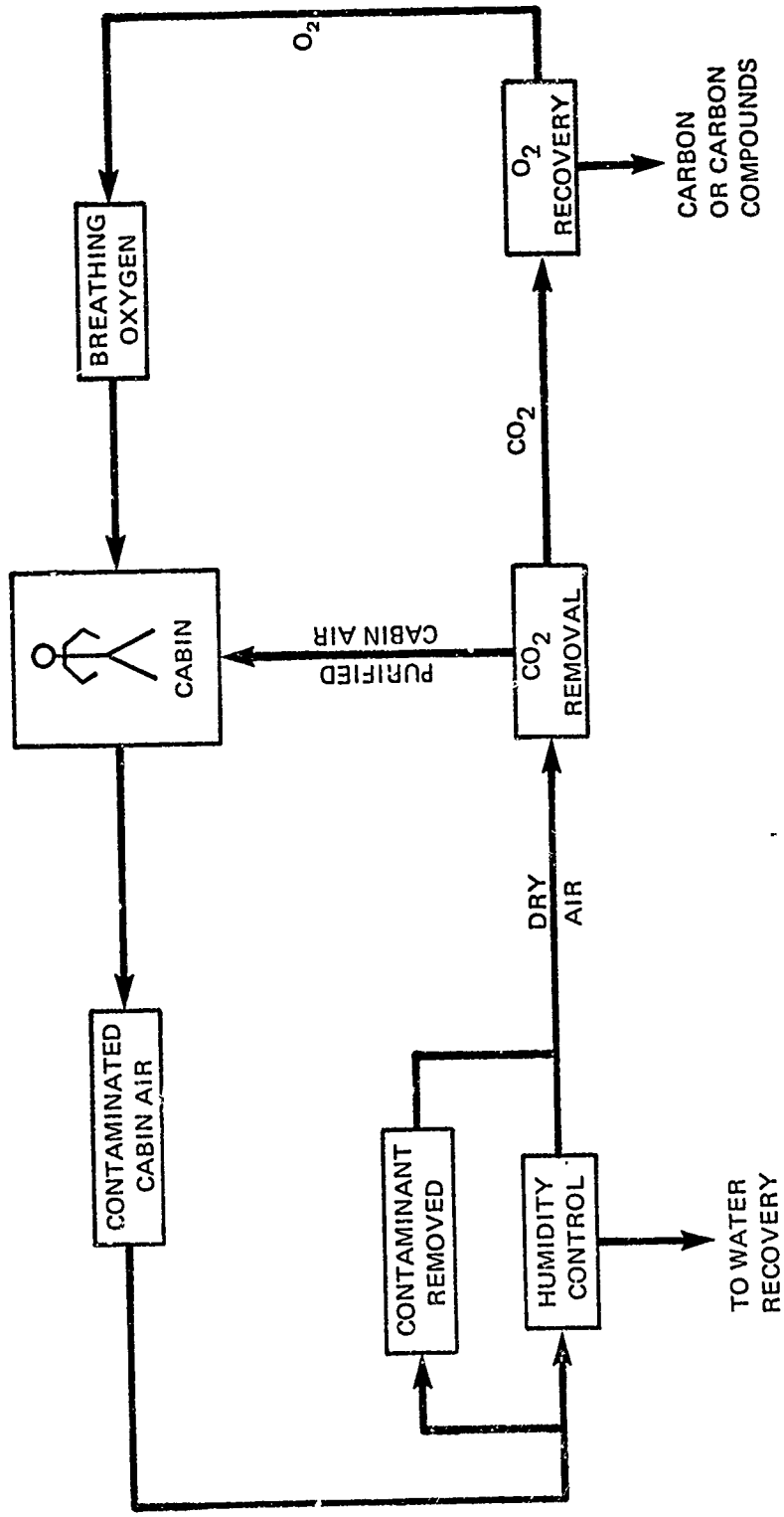


Figure 17–1. Schematic atmosphere control system for space vehicle application.

dioxide is then processed to recover oxygen, and carbon compounds are dumped overboard (or, in future systems, possibly cracked or used in attitude control). It should be emphasized that a typical system is being illustrated here. Particular processes will depend upon both mission parameters and available technology.

Table 17-1 shows a materials mass for a one-man life support system. It also includes urine and wash water reclamation units (Jackson, 1971).

Table 17–1
Space Cabin Mass Balance
(Pounds/Man-Day, Based On
2800 KCal/Day)

Potable Water Recovery	
Output	3.45 lb urine
	3.08 ib respiration and perspiration
	.25 lb feces and H_2O
Total Output	6.78 lb H_2O
	- .66 lb metabolic H_2O from 1.3 lb dry food
Total required	6.12 lb/man for drinking and rehydrating food
Oxygen Recovery	
	2.12 lb CO_2 from concentrator
	.24 lb H_2 (electrolysis and stores—Sabatier reactants)
To produce	1.01 lb H_2O from Sabatier
	1.06 lb H_2O from storage
Total	2.07 lb H_2O electrolyzed
To produce	1.83 lb O_2
Wash Water	
	25 lb recovered and recycled
Oxygen and Nitrogen leakage	
	1-5 lb/day

(Jackson, 1971)

Carbon Dioxide

Man functions as a combustion heat engine, continuously consuming oxygen and producing carbon dioxide and water vapor as a part of the life processes. In closed atmospheres, the concentrations of these waste products must be controlled. Carbon dioxide management implies its removal from the breathing

gas supply and its disposal. The removal process can be accomplished by a variety of different methods, including adsorbents, solid and liquid absorbents, diffusion cells, and electrochemical cells. The carbon dioxide which is separated from the breathing gas can be dumped overboard, stored onboard, or processed to recover the oxygen contained therein for reuse. Presented in this section are representative data for the most promising carbon dioxide removal and/or collection methods, discussed in the following order:

1. Lithium Hydroxide
2. Solid Amines
3. Hydrogen-Depolarized Cells
4. Molecular Sieves

Lithium Hydroxide

Of all the CO_2 removal methods, lithium hydroxide has been used most in spacecraft application. This choice was based on the relatively high CO_2 absorption capacity of LiOH per unit mass of material, coupled with a lower-than-average heat of absorption. Table 17-2 compares the performance of LiOH with a number of other CO_2 absorbents.

Table 17–2

Theoretical Performance of Carbon Dioxide Absorbents

Substance	Formula	Theo. CO_2 Capacity (lb CO_2/lb Absorbent)	Heat of Absorption (Btu/lb CO_2)	Carbonate Decomposition Temperature (°F)
Lithium oxide	Li_2C	1.47	2210	
Lithium hydroxide	LiOH	0.92	875	
Sodium oxide	Na_2O	0.71	3140	1290
Sodium hydroxide	NaOH	0.55	1228	1290
Potassium oxide	K_2O	0.47	3820	1340
Potassium hydroxide	KOH	0.39	1395	1340
Magnesium oxide	MgO	1.09	1150	840-1020
Magnesium hydroxide	$Mg(OH)_2$	0.76	358	840-1020
Calcium oxide	CaO	0.79	1738	1345-1515
Calcium hydroxide	$Ca(OH)_2$	0.60	670	1345-1515
Silver oxide	Ag_2O	0.19	151	250-300
Cadmium oxide	CdO	0.34	975	660

(Coe et al., 1962)

LiOH absorbs CO_2 from a gas mixture and in the presence of water vapor. A cabin relative humidity of 50 to 70 percent usually provides sufficient water

vapor for the absorption reaction to take place. The reaction is given by the following equation:

$$2LiOH + CO_2 \longrightarrow Li_2CO_3 + H_2O$$

This reaction is exothermal, producing 875 BTU per pound of CO_2 absorbed, assuming the water of reaction is evolved as vapor. Table 17-3 lists some of the properties of LiOH as a CO_2 absorbent.

Table 17–3

Properties of Lithium Hydroxide

Chemical formula	LiOH
Molecular weight	23.95
Melting point	862°F
Density of crystals	0.0918 lb cu in.
Bulk density of granular LiOH	0.0145-0.0162 lb/cu in.
Theoretical CO_2 absorption capacity	0.917 lb CO_2/lb LiOH
Heat of absorption (H_2O gas)	875 Btu/lb CO_2
Water of reaction	0.409 lb/lb CO_2 (or 0.375 lb/lb LiOH)

(Coe et al., 1962)

The dynamic removal efficiency which expresses the reduction in CO_2 concentration across the bed varies with time in the operation of a LiOH canister as the absorbent is used up. Usually, as shown in Figure 17-2, removal efficiency remains high (in excess of 70 percent) until the "breakthrough" point in time is approached. The breakthrough point is defined as the time when the CO_2 concentration in the effluent gas from a given canister reaches a specified value. It is apparent that utilization efficiency to some extent will be a function of the breakthrough point specified. Typically, a breakthrough point corresponding to a P_{CO_2} of 8.0 mm Hg is used for rating or performance comparison purposes.

Figure 17-3 shows the temperature rise across a lithium hydroxide canister assuming that all of the water of reaction is evolved as vapor.

Inspection of a psychrometric chart shows that, for any case where the temperature of the air is not lower than 32°F and the pressure is not higher than one atmosphere, the slope of the process line in the LiOH bed is such that the increase in temperature of the air will be ample to provide vaporization of all the moisture produced in the chemical reaction. Operation of the LiOH canister with inlet gas temperatures around 120°F appears to result in higher utilization efficiencies than does operation at lower temperatures.

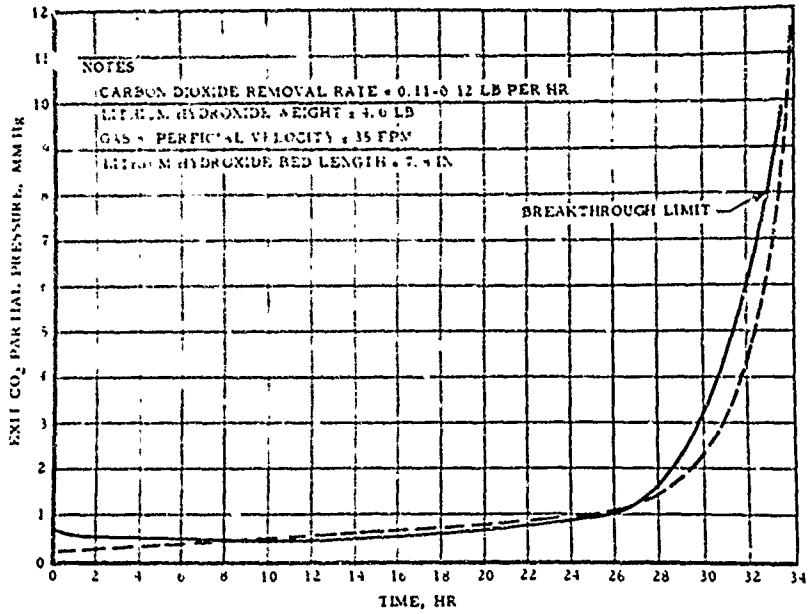


Figure 17–2. Typical curve showing LiOH canister performance. (Coe et al., 1962)

Solid Amines

Another type of chemical CO_2 absorption is based on the use of organic amines. These compounds are highly basic and react with CO_2 to form carbonates. At elevated temperatures, the reaction can be reversed, enabling the use of amines in a regenerative system. Liquid amines have been used in industrial applications and on submarines. These systems usually employ monoethanol amine (MEA), although other members of the same chemical series are also effective. The attractive regenerative properties of the aliphatic amines have led to research on the possibility of employing solid amines, preferably in the form of resins, in order to avoid the zero-g liquid handling problems associated with solutions.

Investigations of the use of amine resins for CO_2 absorption have been carried out using both commercially available ion exchange resins and special resins synthesized for this purpose. Tests of the commercial resins have indicated that the strongly basic resins absorb CO_2 at relatively rapid rates, but that only limited regeneration is possible with the application of heat. The weakly basic resins, on the other hand, exhibit slow CO_2 absorption rates but permit greater thermal regeneration. Specially prepared amine resins, in which excess aliphatic amines are added to epoxy resins, in certain cases yield resins that can be regenerated completely by heating and that show rapid CO_2 absorption rates. Solid amine systems remove CO_2 from cabin air by means of cyclic absorption/desorption in suitable granular amine resins. The chemical nature of the bonding between CO_2 and these resins provides a CO_2 removal method which is feasible for cabin P_{CO_2} levels of 3 mm Hg or less.

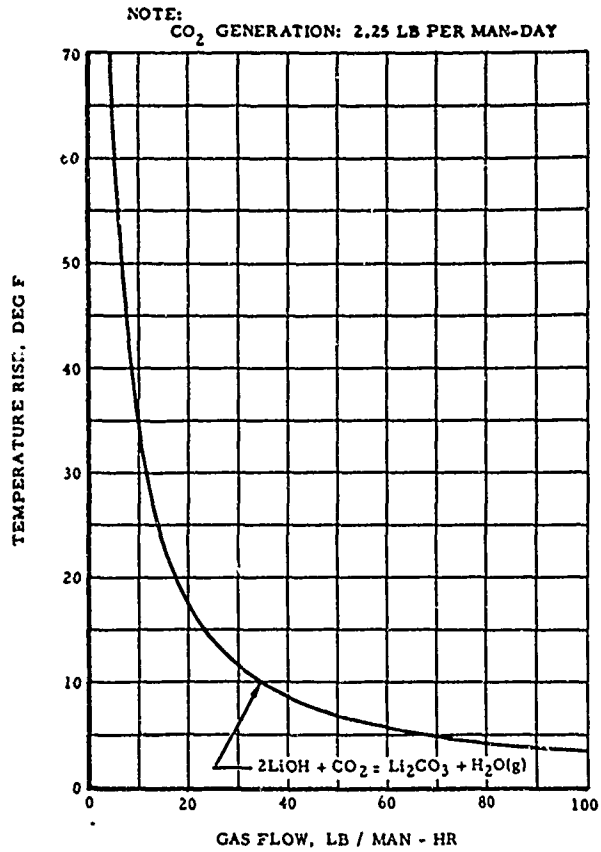


Figure 17–3. Temperature rise across LiOH canister. (Coe et al., 1962)

Dynamic CO_2 absorption and desorption processes, as well as equilibrium CO_2 bed loading conditions, are extremely sensitive to the amount of water present. For example, for Rohm and Haas IR-45 resin, increases in bed water content up to as high as 40 percent weight result in correspondingly increased absorption efficiencies. However, for this resin, water vapor content higher than 25 percent causes excessive pressure drop and flooding. Table 17-4 lists some of the physical and chemical characteristics of IR-45. Also shown in Figure 17-4 is the transient outlet P_{CO_2} as a function of time and bed water content. Representative dynamic removal efficiency curves and the overall time integrated removal efficiency, which may be used in sizing IR-45 beds, are also presented in Figure 17-4.

With the solid amines bed cooler than approximately 140°F, the absorption process takes place according to the following relationship:

$$R * NH_2 + CO_2 + H_2O \rightarrow RNH_3^+ + HCO_3^-$$

Table 17–4
Manufacturer's Data on Rohm and Haas IR-45 Resin

Physical Characteristics	
Physical form	Uniform, beadlike particles
Density	39-43 lb/ft^3
Moisture content	37-45%
Screen grading	20-50 mesh
Effective size	0.35-0.50mm
Uniformity coefficient	1.6 max
Voids	35-45%
Chemical Characteristics	
Exchange capacity	43 Kg/ft^3 max as $CaCo_3$ (27 Kg dynamic capacity)
pH Range	0-7
Chemical stability	Excellent; completely insoluble and inert in strong acids (except nitric), concd alkalies, aliphatic and aromatic hydrocarbons, alcohols, ethers and all other common solvents; prolonged exposure to strong oxidixing agents should be avoided
Stability at elevated temperatures	Outstanding; exchange capacity unchanged after prolonged exposure to boiling water

(Martin & Brose, 1970)

The desorption of solid amines may be accomplished by the application of heat and/or vacuum, or steam. For the case of steam desorbed resins, desorption is accomplished by flowing superheated steam into the bed in the axial direction. The steam condenses on the resin, heats the resin and displaces the CO_2 and air. The process occurs in "chromatographic" fashion. That is, steam, CO_2, and air are found in individual zones which travel along the length of the bed. The displaced CO_2 is reabsorbed immediately ahead of the steam zone and the air is displaced ahead of the CO_2-rich zone. This chromatographic feature of the desorption process facilitates separation of CO_2 from air and steam. Flows of the separate quantities of gas in each of the zones have associated physical properties which can be sensed and used in control schemes for diverting the CO_2-rich flow to the CO_2 accumulator and also for diverting the air and steam flows back to the cabin via a condensing heat exchanger. Figure 17-5 shows representative performance data for the steam desorbed resin CO_2 concentrator used in the NASA Langley Research Center/McDonnell Douglas 90-day manned test. The lower curve shows the mixed P_{CO_2} downstream of the two absorption

beds. As shown, the effluent P_{CO_2} drops rapidly at the start of the absorption phase, reaches a minimum value, and then rises with a plateau characteristic observed partway through the P_{CO_2} rise.

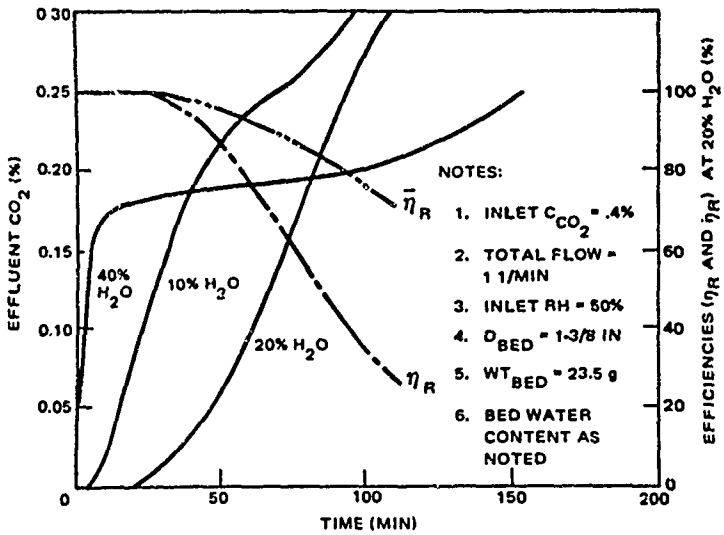


Figure 17–4. Transient outlet P_{CO_2} and removal efficiences for IR-45. (Tepper et al., 1968)

Hydrogen-Depolarized Cells

Hydrogen-depolarized cells are basically electrochemical concentration cells which employ an aqueous carbonate electrolyte to transfer CO_2 from the cathode side of the cell, where CO_2-laden cabin atmosphere is introduced, to the anode side where hydrogen is introduced. The chemical and electrochemical reactions occurring in the cell are as shown in Figure 17-6.

The necessary number of hydrogen-depolarized cells should be series connected. Tests (Heubscher & Blakely, 1970) have indicated that uniform distribution of hydrogen flow could not be continuously achieved when the cells were in a parallel H_2 flow configuration. On the other hand, when a series configuration was used in which the first of 10 cells received pure hydrogen and the last cell received 70 percent hydrogen and 30 percent CO_2, stable performance was obtained. Figure 17-7 shows performance curves for the series connected hydrogen-depolarized cell module tested in the study referred to here. Cesium carbonate was much more desirable in the CO_2 collection application than other electrolytes with lesser solubility in water (Heubscher & Blakely, 1970). Electrochemical devices that employ aqueous electrolytes are especially sensitive to water balance. When the electrolyte becomes too concentrated as a result of a water imbalance, precipitates form at the anode of the cell, reducing cell voltage and CO_2 transfer rate and may even result in gas crossover from anode to cathode. Consequently, electrolytes with high solubility in water are favored. The physical characteristics of a hydrogen-depolarized cell module currently undergoing development testing are shown in Table 17-5. The hydrogen-depolarized cell system readily lends itself to zero gravity operation

since mass transfer occurs only in the gaseous state. There are no free liquids or components dependent upon gravity operation.

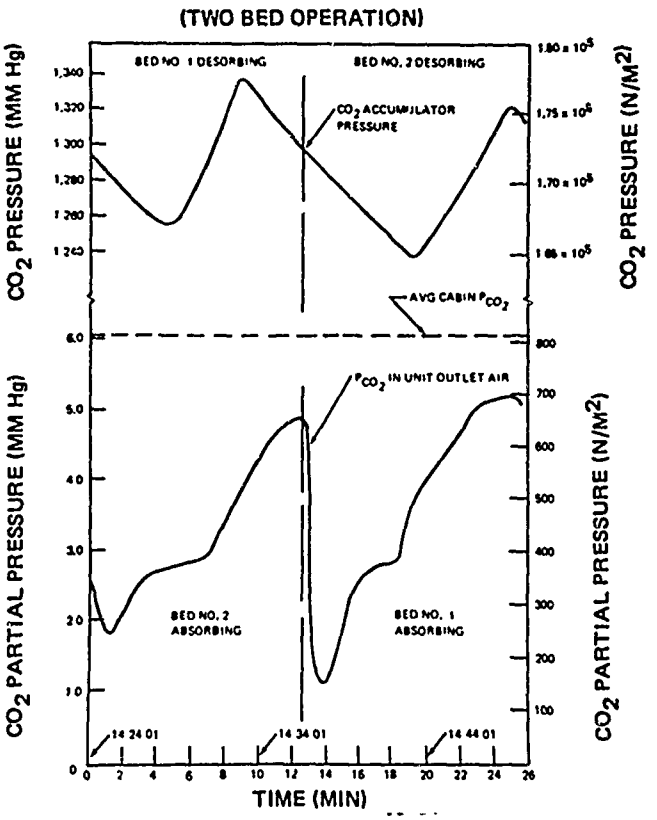


Figure 17–5. NASA Langley Research Center/McDonnell Douglas manned test: amine resin CO_2 concentrator performance. (Jackson, 1971)

Molecular Sieves

Regenerative molecular sieve units use granular synthetic zeolites as the basic CO_2 collecting material. The zeolites are metal ion-alumino silicates which have a relatively high affinity for CO_2, but a still higher affinity for water. Thus, desiccants must be used to reduce the moisture content in the cabin atmosphere before it is introduced into the zeolite beds. Desiccant materials may be either silica gel or another synthetic zeolite. Molecular sieve units usually include air coolers to lower the temperature of the atmosphere being fed to the zeolite canisters to increase the CO_2 adsorption capacity of these beds. The synthetic zeolites of interest for CO_2 adsorption have a heat of adsorption of 300 BTU/lb of CO_2, a specific heat of 0.25 BTU/lb°F, a thermal conductivity of 0.34 BTU/hr ft°F, and a density of approximately 45 lb/ft^3. Figures 17-8 and 17-9 show equilibrium adsorption isotherms for molecular sieves and silica gel.

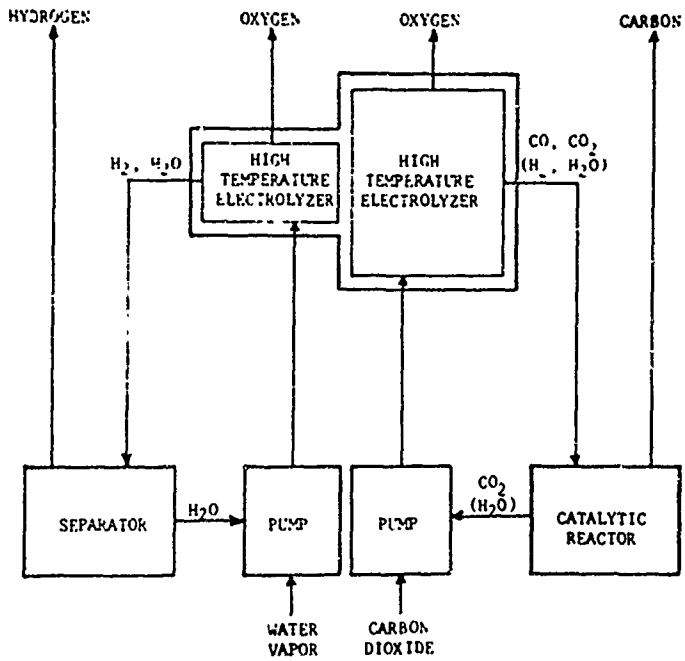


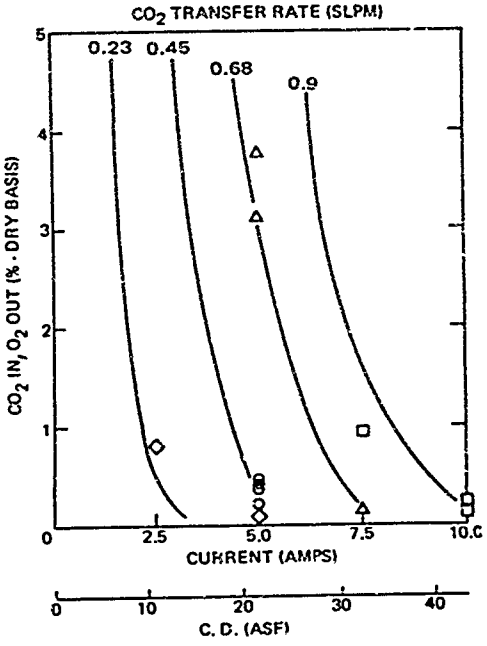
Figure 17–6. Hydrogen depolarized cell. (Wynveen & Quatrone, 1971)

Table 17–5

Physical Characteristics of Developmental Hydrogen Depolarized Cell

Electrode area	35 in^2 (per cell)
Electrode type	AB-6
Electrolyte matrix	Asbestos
Electrolyte	Cs_2CO_3
Cell material	Injection molded polysulfone
Gas cavity spacer	Expanded titanium
Heat removal plates (current collectors)	Titanium-clad copper
Seals	Flat, ethylene-propylene gaskets
Cell size (overall)	7.7 x 13.7 x 0.15
Current density (max)	40 ASF
No. of cells per module	15
Module size (overall)	7.7 x 13.7 x 4.5
CO_2 transfer rate	0.234 lb/hr
CO_2 partial pressure	3.8 mm Hg

(Huebscher & Babinsky, 1970)



MODULE DATA	18	15
NUMBER OF CELLS		
CELL AREA		0.242 SQ. FT.
OPERATING CONDITIONS		
CURRENT		N/A
TRANSFER RATE		N/A
TEMPERATURE		110°F
DEW POINT TEMP. O_2 & H_2 IN		100°F
H_2 FEED RATE		1.7 SLPM
O_2 RECYCLE RATE		3.5 SCFM
PRESSURE		20" H_2O GAGE
DILUENT GAS, CATHODE SIDE		N/A

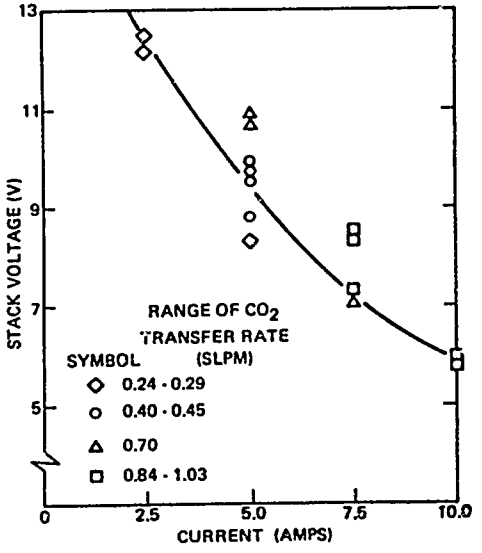


Figure 17–7. Performance of H_2-depolarized cell module showing CO_2 transfer rate, P_{CO_2} at cathode, stack current and voltage. (Heubscher & Babinsky, 1970)

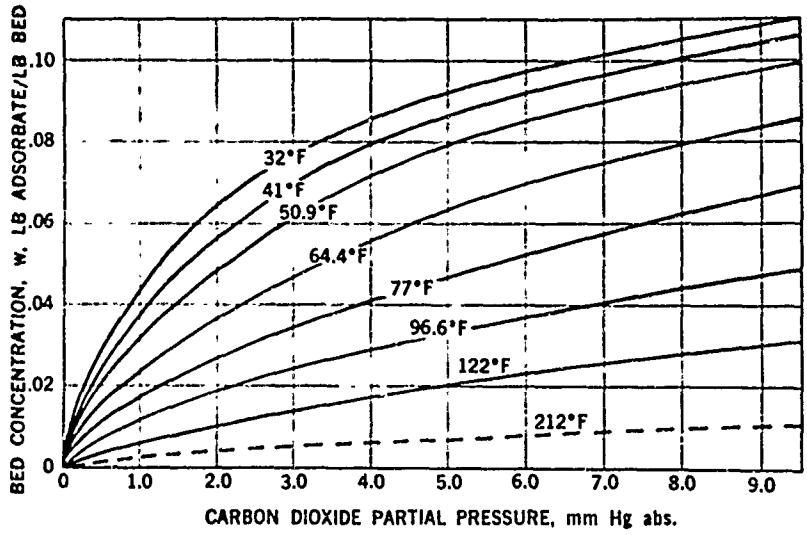


Figure 17–8. Adsorption isotherms for Type 5A molecular sieve. (Jackson & Blakely, 1967)

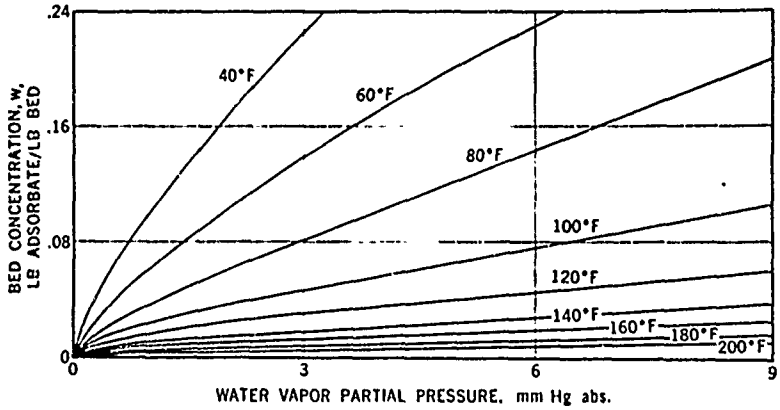


Figure 17–9. Adsorption isotherms for silica gel. (Jackson & Blakely, 1967)

Three typical methods of CO_2 removal by molecular sieve materials which may be used for different spacecraft applications are considered here. These are all of the regenerative type. They are: (1) a two-bed adiapatic system utilizing two types of sieve material within each bed (one type for water adsorption, one for CO_2 adsorption); (2) a two-bed system similar to the first type but having silica gel as the desiccant and a fluid heat exchanger in the silica gel; and (3) an isothermal four-bed system whereby the silica gel and molecular sieve materials are contained in separate beds and in which each bed is provided with integral fluid heat exchangers. The first two methods vent both water and CO_2 to space. The third provides water recovery and, if desired, CO_2 collection for oxygen recovery. The operating characteristics for each of these methods are discussed in the following paragraphs.

Two-Bed Molecular Sieve – Water Adsorption/CO_2 Adsorption. This type system is primarily for low gas flow rate application. It has a small pressure drop and high removal efficiency. The molecular sieve beds are provided with a Linde Type 13X zeolite for water removal and a Linde Type 5A zeolite for CO_2 removal. Electrical heaters are provided for bakeout of the beds should they become "poisoned" with water; otherwise, normal regeneration simply involves venting the beds to the space environment. This system usually operates on a 15-minute adsorption/desorption cycle. Inlet process air is 45° to 55°F and saturated.

Two-Bed Molecular Sieve – Silica Gel Desiccant and Fluid Heat Exchanger. This system utilizes silica gel as a desiccant in each bed. The silica gel bed contains an integral fluid heat exchanger to improve its water adsorption and desorption characteristics. The molecular sieve portion of the bed also contains electrical heaters to aid adsorption and desorption of the molecular sieve bed if it becomes "poisoned" with water. This system is also a low gas flow, small pressure drop, high removal efficiency type. Operation usually involves a 30-minute adsorption/desorption cycle, 120°F heating fluid, 60°F cooling fluid, and 45 to 55°F saturated inlet air.

Isothermal, Four-Bed Sieve. In this method, the silica gel and molecular sieve materials are packaged in separate beds. Each bed is provided with an integral heat exchanger to improve adsorption and desorption characteristics. A schematic of the system is shown in Figure 17-10. In the operational mode shown in the schematic, silica gel bed No. 1 and molecular sieve bed No. 1 are being cooled and are in their adsorption cycle. The gas from molecular sieve bed No. 1 is then passed through silica gel bed No. 2 which is concurrently heated to desorb trapped water and return it to the cabin. At this time, molecular sieve bed No. 2 is being heated and desorbed. The CO_2 may be vented to space. If, however, an oxygen recovery subsystem is used, recovered CO_2 is pumped into an accumulator or recovery unit. When pumps are used, a higher temperature is required for CO_2 desorption because of the pump limitations. The isothermal, four-bed molecular sieve system usually operates on a 30-minute adsorption/desorption cycle, with process air supplied saturated at 40°F. Cooling fluid is supplied at approximately 40°F, and heating fluid at approximately 300°F.

Experimental work with molecular sieves (Houck et al., 1970) shows that as the heating fluid temperature decreases, the equilibrium chamber CO_2 concentration increases. This fact is illustrated in Figure 17-11. Heating fluid temperature in the study represented was varied over a range of 200° to 338°F.

The high weight penalties associated with providing fluids at the elevated temperatures required for efficient molecular sieve operation led to the search for other CO_2 concentration methods, notably solid amines and hydrogen-depolarized cells. Another factor militating against the use of molecular sieves is their decreased adsorptive capacity at low CO_2 partial pressures (negligible at 1.0 mm Hg) which is incompatible with the current trend toward low cabin P_{CO_2} levels.

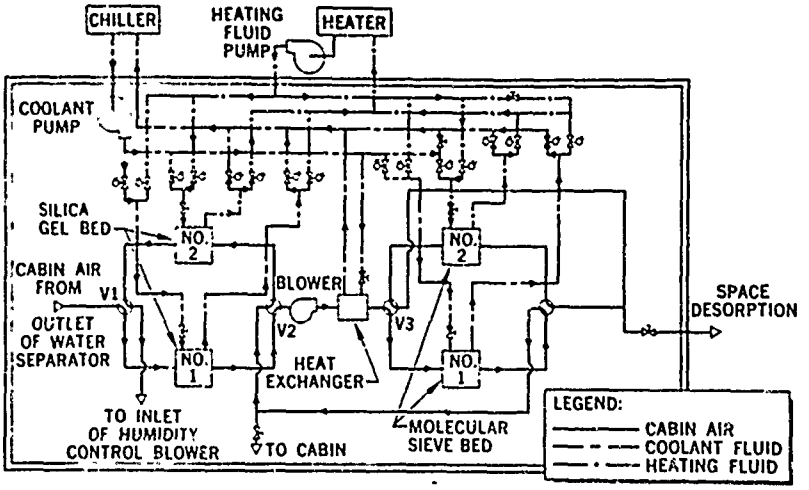


Figure 17–10. Four-bed isothermal regenerative molecular sieve system. (Jackson & Blakely, 1967)

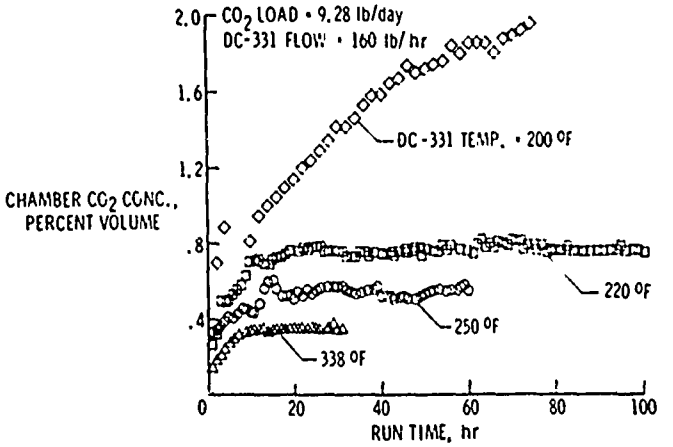


Figure 17–11. Effect of heating fluid temperature on molecular sieve system performance. (Houck et al., 1970)

Oxygen Regeneration

The recovery of oxygen from exhaled carbon dioxide is essential for long-duration space flights. The recovery process of choice involves, first, carbon dioxide reduction, and, second, electrolysis of the product water to liberate oxygen. Several techniques for the reduction of CO_2 have been under consideration. The four methods which have received the most intensive study and development efforts are described in this section. These are: the Sabatier, Bosch, solid electrolyte, and molten carbonate processes.

Carbon Dioxide Reduction

Sabatier Process. The Sabatier process involves the hydrogenation of CO_2 over a 400° to 700°F catalyst in a reactor. The Sabatier reaction is summarized by the following equation:

$$CO_2 + 4H_2 \rightarrow CH_4 + 2H_2O$$

The Sabatier water product is electrolyzed to oxygen, for breathing, and to hydrogen for return to the Sabatier reactor. The methane produced may be disposed of in one of the following ways:

1. Overboard dumping.

2. Decomposing the methane to carbon and hydrogen, with return of the hydrogen to process streams and collection of solid carbon.

3. Converting the methane to a compound containing a smaller proportion of hydrogen (e.g., acetylene), separating the gases, dumping the acetylene overboard, and returning hydrogen to process streams.

From the equilibrium equation for the Sabatier reaction, Gibb's free energy relation, enthalpies and standard heat of formation, the theoretical degree of CO_2 conversion can be related directly to the equilibrium temperature (Jackson, 1971). This relationship is depicted in Figure 17-12, which shows the maximum possible CO_2 conversion at atmospheric pressure and any given temperature for a stiochiometric H_2:CO_2 ratio of 4:1. From this curve it can be seen that, from equilibrium considerations, it is desirable to operate the reaction at temperatures approximating 300°F for 100 percent CO_2 conversion, or up to 400°F for 99 percent conversion; operation at temperatures higher than these prohibits this high degree of CO_2 conversion. At low temperatures (300° to 500°F), conversion occurs only with the proper choice of catalyst. The precious metals ruthenium, rhodium, and iridium are the most effective catalyzing materials for promoting the reduction reaction, with 0.5 percent ruthenium-on-alumina the best of these (Thompson, 1964–1967).

The Sabatier stoichiometric H_2:CO_2 ratio of 4:1 for complete conversion of CO_2 to methane is not optimum in an actual unit. Optimum reaction rates have been experimentally determined to be a molar ratio of 4.35:1 (Yakut & Barker, 1969). However, the ratio used should be based on mission tradeoffs, including water availability, stored O_2 and H_2 gas weight penalties and water electrolysis penalty. For some mission applications, it may be advantageous not to store H_2 onboard but to use a CO_2-rich mixture to insure maximum conversion of hydrogen. Such a mission application was simulated in a 90-day manned test conducted by the NASA Langley Research Center and McDonnell Douglas Astronautics Company. Figure 17-13 shows the Sabatier feed gas mixture ratio for this test.

Hydrogenation catalysts are poisoned by halogen or sulfur-containing compounds, so these must be excluded from the feed gas. The effect of contaminants on the conversion of CO_2 to CH_4 is shown in Figure 17-14. As

the figure indicates, halogen-containing compounds are more poisonous than sulfur-containing compounds.

$CO_2 + 4H_2 \rightarrow CH_4 + 2H_2O$

R = H_2:CO_2 ratio, volumetric

π = REACTION PRESSURE, psia

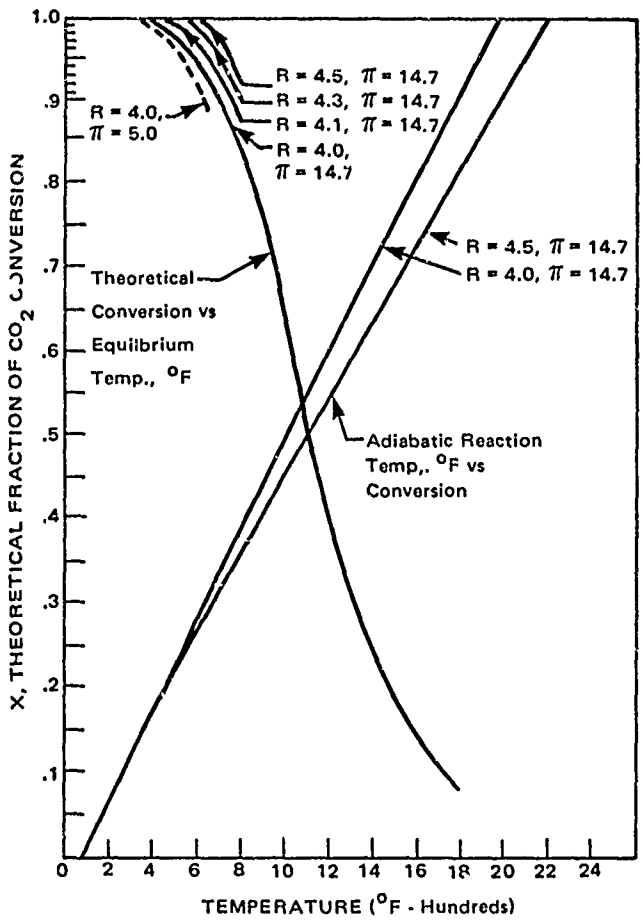


Figure 17–12. Theoretical CO_2 equilibrium conversion vs temperature for Sabatier reaction. (Remus et al., 1965)

Other factors also influence the efficiency of CO_2 conversion. Extremely short reactor beds may introduce channeling and extremely long beds result in a large pressure drop, both of which reduce conversion efficiency. Space velocity appears to have a much greater negative influence on the reaction rate than mass velocity. Space velocity is volume-dependent and is characterized by the volume of feed in a unit time per volume of catalyst. The reaction products, CH_4 and water, have little effect on the Sabatier reaction rate.

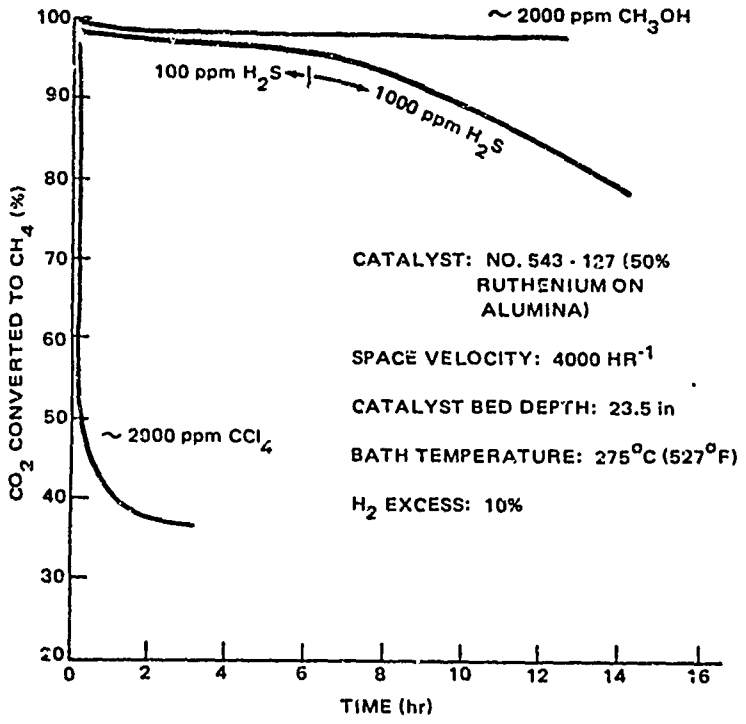


Figure 17–13. NASA Langley Research Center/McDonnell Douglas 90-day test Sabatier mixture ratio. High mixture ratios resulted from reducing the catalyst with hydrogen to overcome poisoning. (Jackson, 1971)

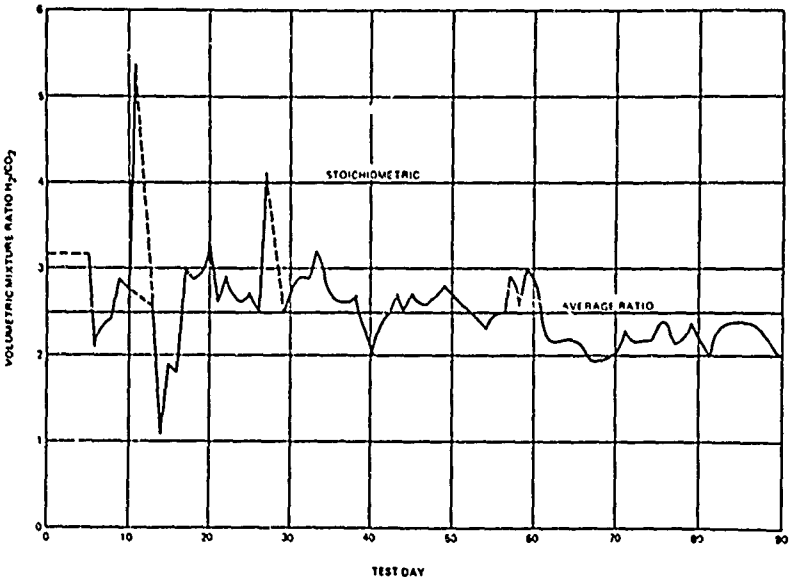


Figure 17–14. Effect of contaminants on the conversion of CH_2 to CH_4. (Adlhart & Hartner, 1967)

A summary material balance for the 90-day test Sabatier reactor is presented in Table 17-6. The table shows that the overall conversion of H_2 to water and CH_4 was 95 percent and overall CO_2 conversion was 66 percent.

Table 17–6

Sabatier Subsystem Material Balance for 90-Day Test

Material In		Material Out	
Carbon dioxide	636.9 lb	Water to electric cell	332.0 lb
Hydrogen	81.0	Methane	152.5
Nitrogen	16.6	Carbon dioxide	217.6
Oxygen	8.1	Nitrogen	16.6
Water vapor	5.5	Oxygen	.5
		Hydrogen	3.8
		Water exhausted	25.1
TOTAL	748.1 lb	TOTAL	748.2 lb

Bosch Reaction. The Bosch carbon dioxide reduction reaction is usually summarized by the following equation:

$$CO_2 \; 2H_2 \rightarrow C + 2H_2O + 595 \text{ W-hr/kg } CO_2$$

The reaction occurs in the presence of an iron catalyst at temperatures of 1100° to 1800°F. Partial conversion is achieved, ranging from 30 percent at the lower temperatures up to 98 percent at higher temperatures. Unfortunately, maximum carbon formation occurs in the Bosch reaction temperature range. Within this range, additional reaction also occur. This results in the production of carbon monoxide and methane, as follows:

$$CO_2 + C \rightarrow 2CO$$

$$2H_2 + C \rightarrow CH_4$$

The gases resulting from the side reactions above are usually recycled to achieve a higher degree of conversion.

The rate of the Bosch reaction is controlled by many apparently independent but nonetheless interrelated variables. The most important variables relate to the conditions in the reactor. Reaction kinetics are, for example, influenced by reactor temperature and gas flow rate or recycle rate, which is

controlled by the recycle compressor. Increasing the flow rate through the reactor increases the probable number of collisions per unit time, thereby increasing the reaction rate, and this, in turn, calls for higher compressor power requirements. Experiments conducted to investigate the effects of reactant gas H_2:CO_2 volume ratio on conversion rates (Clark, 1967) have shown that conversion rates are somewhat insensitive to gas ratios. However, a hydrogen-rich ratio appears more conducive to higher conversion rates.

One of the major development problems encountered with the Bosch reactor is that of solid carbon collection. Two catalyst configurations have been utilized. One consists of an expendable static cartridge of steel wool and the other is a rotating assembly of low-carbon steel plates. Emphasis is placed at the present time on developing a Bosch CO_2 reduction unit with expendable catalyst cartridges. Typical test data from a Bosch system are shown in Table 17-7. The data in the table were taken after a 12-hour leadtime for warm-up.

Solid-Electrolyte System. The solid electrolyte system utilizes a solid electrolyte reactor and a carbon monoxide disproportionation reactor for the complete reduction of carbon dioxide to carbon and oxygen. A typical solid electrolyte reactor (Weissbart & Smart, 1970) is comprised of a number of two-cell drums. Each drum consists of two electrolyte disks, each having 20-cm^2 electrodes, sealed to a 6.3-cm diameter zirconia-calcia ring body. Disks (0.08 to 0.22 cm thick) are made from hot-pressed compacts of scandia-stabilized zirconia. Typical electrolyzer modules are assembled by connecting drums to alumina manifold tubes by means of metal gas-feed tubulations. Modules incorporate parallel gas flow through the drums and series electrical connection between the cells. For a gas stream including CO_2 and water vapor the following reactions occur at the cathode:

$$2CO_2 + 4e^- \rightarrow 2CO + 2O^=$$

$$H_2O + 2e^- \rightarrow H_2 + O^=$$

At temperatures of 525° to 700°C (1000° to 1300°F), the $O^=$ ions are transported across the oxide film by the potential gradient. (The reactions are enhanced by the presence of water in the gas stream.) The oxygen ion then migrates through vacancies in the crystal lattice of the solid electrolyte material to the anode, where the ion is converted to an oxygen atom. The cell material is essentially impermeable to non-ionic species (in particular to CO) so that pure O_2 is formed at the anode and may be sent to the cabin with no further processing other than cooling. The cell consumes power for decomposition of CO_2 and resistance heating of the solid electrolyte. The unit must be well insulated to prevent heat leakage which would decrease performance. An auxiliary heater in the cell is designed to bring it to operating temperature.

The free energy change involved in the decomposition of CO_2 to CO and to O_2 is 123 kcal/gram-mole of O_2. This corresponds to a theoretical power requirement for a cell of 136 W/kg of CO_2 per day. The mixture of CO and CO_2

from the cell cathode is passed through a catalytic reactor which converts CO to CO_2 (returned to the electrolytic cell) and to solid carbon. The free energy change in this reaction is 29 kcal/gram-mole of carbon. This corresponds to a heat dissipation requirement of 735 W/kg of CO_2 per day.

Table 17–7

Typical Bosch Carbon Dioxide Reduction System Test Data*

Data Collection Time	1535	1600	1630	1700	1730
CO_2 Feed Rate, lb/day	9.7	10.2	10.8	11.2	11.1
H_2 Feed Rate, lb/day	0.900	0.960	1.02	1.02	1.02
Recycle Rate, cfm	2.25	2.25	2.25	2.25	2.25
Purge Rate, cfm	0.005	0.005	0.005	0.005	0.005
Water Separator Pressure, psig	2.20	2.18	2.10	2.00	1.95
Bosch Reactor Pressure, psig	9.6	9.3	9.2	9.1	8.9
Temperature, °F					
Bosch Reactor	1230	1240	1240	1240	1240
Carbon Collector	115	115	120	125	125
Water Separator	47.3	47.0	46.0	44.7	44.0
Compressor Discharge	150	150	150	150	148
Bosch Reactor Inlet	800	810	820	820	820
Bosch Reactor Power, watts					
Main Heater**	200	200	200	200	200
Auxiliary Heater	610	610	320	320	620
Gas Analysis, volume %					
H_2	43.0	69.4	-	56.0	-
CO_2	11.7	6.4	-	9.8	-
CH_4	12.0	5.7	-	13.0	-
CO	12.0	6.0	-	11.0	-
N_2	18.0	11.0	-	9.2	-
O_2	3.0	1.5	-	0.7	-
Water Rate, lb/day	5.8	5.8	5.8	7.2	7.4
Theoretical Water Rate, lb/day	7.91	8.31	8.88	8.94	8.94

*NASA/Langley ILSS Bosch reactor operated at 10 psia.
**Main heater started at 500 W and reduced gradually to 200 W as reactor came up to temperature.
(Armstrong, 1966)

A flow diagram of a typical solid electrolyte system is presented in Figure 17-15. The regenerative heat exchanger pictured cools the gas products to approximately 950°F, which is the operating temperature of the catalytic reactor. The catalyst used in the reactor is nickel or stainless steel. Carbon build-up is sensed by a pressure switch which signals for a

change of catalyst bed when necessary. The catalytic reaction is exothermic and no heating is needed once the system has reached operating temperature.

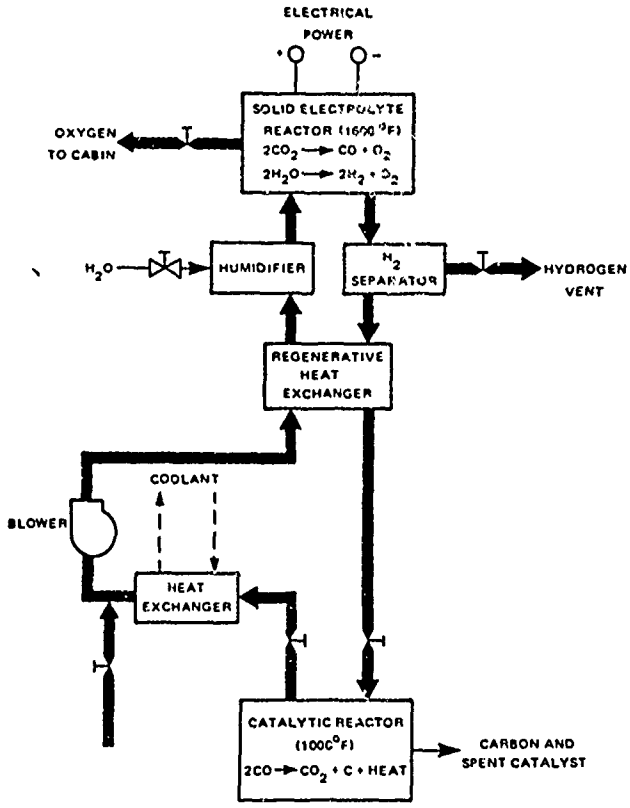


Figure 17–15. Solid electrolyte system schematic. (Weissbart et al., 1971)

A comparison of a number of solid electrolyte reactors is presented in Table 17-8.

Molten Carbonate Process. The molten carbonate process involves both chemical and electrochemical reactions. When CO_2 is introduced into a molten lithium carbonate electrolysis cell, first, Li_2CO_3 is electrolyzed to Li_2O, carbon, and O_2. Lithium oxide then reacts with CO_2 to reform Li_2CO_3. Carbon, from the first reaction, is deposited on the cathode, while the O_2 to be collected is generated at the anode. Electrolysis of pure molten carbonate can be satisfactorily accomplished in a gravity field (Stein, 1965); however, a satisfactory solution for phase separation of the gases from the molten salts in zero gravity has not been found. The high operating temperature also requires heat-resistant materials and accelerates corrosion of the equipment.

Table 17–8

Components and Performance Characteristics of Several Solid Oxide Electrolyte Electrolysis Units

Unit Description	No. Z-8 8-Amp Module	No. J-1 127-Amp Electrolyzer-Reactor, 1-Man Unit[1]	No. J-10 24-Amp Module
Drums unit[2]	1	18	6
Cells/unit	2	36	12
Joint sealant	Au and Au-Pd[3]	Au and Au-Pd[3]	Au and Au-Pd[3]
Electrolyte configuration	Disk	Disk	Disk
Disk thickness, cm	0.09	0.08 – 0.22	0.15
Electrical connection	Series	Series	Series
Gas flow pattern	Parallel	Parallel	Parallel
Active area/cell, cm^2	20	20	20
Operating temperature, °C	870	880	870
Electrolyte composition	$(ZrO_2)_{0.92}(Sc_2O_3)_{0.08}$	$(ZrO_2)_{0.92}(Sc_2O_3)_{0.08}$ & $(ZrO_2)_{0.93}(Sc_2O_3)_{0.07}$	$(ZrO_2)_{0.93}(Sc_2O_3)_{0.07}$
Current density, mA/cm^2	200	175	100
Initial average cell voltage, V	1.94	1.88	1.61
Final average cell voltage, V	2.29	2.04	1.84
Time in operation, hr	750[4]	250[4]	1800[5]
Oxygen purity, %	100[6]	96[7]	100[8]
Oxygen current efficiency, %			
Initial	100	100	100
Final	100	95	100
Electrolysis power, W/man[9]			
Initial	246	239	204
Final	291	259	233
Conversion of CO_2, %	43	40 – 55	24

[1]Reactor for disproportionation of CO from electrolyzer gas stream to carbon and CO_2 was operated at 556°C and reactor exit gas stream was vented. [2]Two-cell basic building block of electrolyzer modules, consisting of 2 electrode disks attached to a ceramic body or ring, containing metal gas inlet and outlet tubes, and current collector leadthroughs. [3]Gas-tight, gold and gold-palladium alloy brazed to platinum plated surfaces. [4]Operation discontinued to allow examination of unit. [5]Unit continued on life test with constant performance characteristics. [6]Less than 0.01% of CO_2 in oxygen by gas chromatographic analysis. [7]For first 110 hrs, O_2 purity remained at 96%, after which a large leak developed in one 42-amp module. Only a gradual rise in CO_2 content by a factor of 2 to 3 occurred in the other two modules. [8]0.3% CO_2 in O_2. [9]O_2 generation rate of 2 lb/day or 127 amp.

(Weissbart & Smart, 1970)

Water Electrolysis

An electrolysis unit is required in the oxygen recovery system to convert water generated in either the Sabatier or Bosch carbon dioxide reduction process to oxygen and hydrogen, so that oxygen can be returned to the atmosphere for breathing. With an electrolysis cell available, water can be used for making up oxygen lost through leakage or extravehicular operations, which simplifies the resupply process.

Commercial electrolysis units have been used reliably for many years, but they cannot operate in zero-g. The phase separation problems of the space environment complicate the design and make more difficult the achievement of a reliable system. The design of a flight-type electrolysis unit for long duration usage has been one of the most difficult technological problems to solve. Yet it is a major "key" to both low-weight oxygen supply, ease of resupply, and recovery.

The several most attractive concepts under development are discussed in this section.

Static Feed Electrolysis Unit. This electrolysis cell uses a potassium hydroxide electrolyte (35 percent KOH in water) which is contained in an asbestos matrix held between electrodes. O_2 and H_2, generated at the anode and cathode, respectively, are collected in cell cavities and passed into integral gas manifolds. Water is fed to the water pocket behind the water transport matrix, which also contains a potassium hydroxide solution. Water is transported to the electrolyte matrix by diffusion of water vapor across the H_2 gas cavity to the more concentrated electrolyte solution. Zero-g capability of the electrolysis cell design is provided by containing the electrolyte and water feed in asbestos matrices. Capillary retention of the liquid at the matrix interfaces prevents mixing of the gases and liquids. In addition, the matrix prevents O_2 and H_2 from mixing as they are produced.

The unit operates at about 150°F and consists of a number of modules, a condenser-separator, current controllers (one for each module), back-pressure regulators, and necessary plumbing, wiring, and control devices. Major development problems encountered with the unit include difficulties in startup, shutdown, automatic electronic control, cell flooding with KOH in startup and shutdown, and cell drying. Data from a representative life test and performance tests of a static-feed water electrolysis system are given in Figures 17-16 and 17-17, respectively.

Circulating Electrolyte Electrolysis Unit. In this unit, the alkaline (potassium hydroxide) is circulated between the dual asbestos matrix of the cell and is cooled by a heat exchanger external to the cell. The electrolyte temperature is well regulated with the external heat exchanger and, consequently, so is the water vapor content of the O_2 and H_2 gases generated in the cell. The circulation of the electrolyte helps to minimize concentration polarization and decrease the time required to reach steady-state operation after either starting up or adding makeup water to the electrolyte. The purposes for the asbestos matrix were previously described.

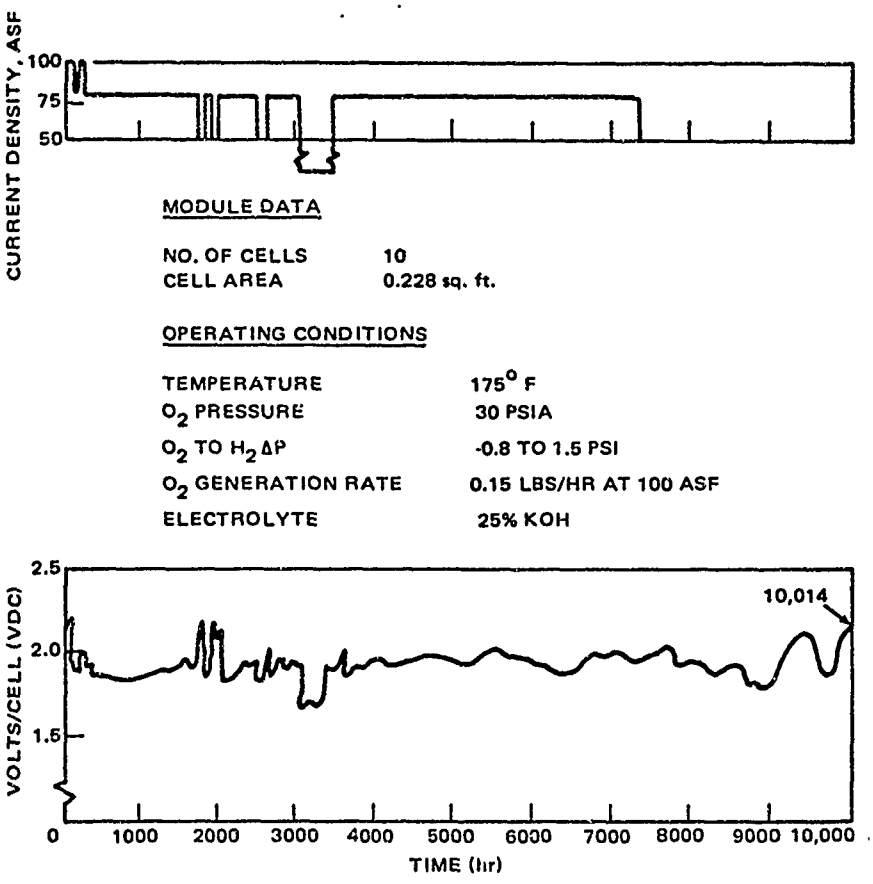
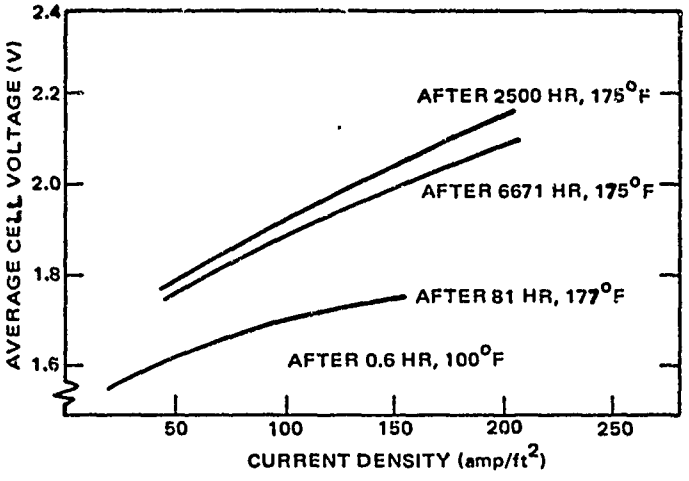


Figure 17–16. Representative life test of a static-feed water electrolysis module. (Babinsky & O'Grady, 1970)

A typical continuous flow electrolysis system uses 30 percent KOH diluted in water, operates at near-ambient temperature and pressure, and has the following design features. The body and matrix screen and spacers are cast of epoxy resin. The dual matrix located on either side of the electrolyte pocket consists of an asbestos fuel cell sandwiched between a nickel matrix-support screen and a fuel cell electrode (type AB). Spot-welded to the electrodes are nickel electrode support screens and electrical leads. The electrical lead is nickel sheet cut in a picture frame configuration and spot-welded around the edge of an electrode. The modules are sealed by O-rings and fastened together by end plates and bolts. The electrodes from adjacent cells are supported by four intercell spacers. A liquid-level sensor in the electrolyte reservoir, located external to the cell, provides the signal for adding makeup water to the module when it is in operation. To prevent the electrolyte from passing through the matrix and into the gas manifolds, a differential pressure controller maintains the pressure in the gas manifolds higher than the electrolyte pressure (ΔP = 3 psig).



NOTE:

MODULE DATA	
NO. OF CELLS	10
CELL AREA	0.228 ft^2
OPERATION CONDITIONS	
O_2 PRESSURE	30 psia
ELECTROLYTE	25% KOH

Figure 17–17. Representative performance tests of static-feed water electrolysis module after 0.6, 81, 2500, 6671 hr of operation. (Schubert, 1969)

Some of the more serious development problems encountered with the unit have included: (1) difficulty in maintaining differential pressure control; (2) a small increase in cell voltage required at startup to maintain a constant current; (3) slow deterioration in cell performance; and (4) some degradation of the epoxy resin plates. A continuous flow KOH electrolysis unit was tested in the NASA Langley Research Center/McDonnell Douglas 90-day test. Figure 17-18 shows the O_2 generation characteristics of the unit during the test (Jackson, 1971).

Vapor Feed Electrolysis Unit. The vapor feed cell is unique among electrolysis cell concepts because it is designed to operate directly off humid cabin air. Therefore, the cell can assist the cabin air-conditioning system in controlling humidity. Furthermore, since the vapor cell uses expired and perspired water vapor for its water supply, it is not contaminated by dissolved solids normally present in undistilled, liquid water. The vapor cells have an acid rather than alkaline electrolyte and, thus, are not contaminated by expired CO_2. The vapor cell utilizes a wicking material which holds the electrolyte, usually sulfuric acid, between the anode and cathode. The unit is made of a number of cells, each consisting of anode and cathode screens with a pad of microporous rubber,

or the like, acting as the wicking material. Electrolysis dehydrates the electrolyte and delivers H_2 at the cathode and O_2 at the anode. New moisture then rehydrates the electrolyte, and the process is continued. Theoretically, 1520 amp-hr are required for the electrolysis of water to produce one pound of O_2. On a 24-hour operational basis, this corresponds to 63.3 amp/lb of O_2 per day. The corresponding theoretical reversible voltage necessary to electrolyze liquid water at room temperature is 1.23 V, an unusually high operational voltage (Figure 17-19). As figure 17-19 illustrates, the observed voltage, E_{cell}, between the connecting terminals of the electrolysis cell is the summation of E_o, the theoretical minimum reversible potential, and the polarization voltages. The following equation expresses this relationship.

$$E_{cell} = E_o + E_{aa} + E_{ca} + E_{ac} + E_{cc} + E_{IR}$$

where,

E_{aa} = Activation polarization at anode

E_{ca} = Activation polarization at cathode

E_{ac} = Polarization at the anode created by concentration (diffusion) gradient at the anode

E_{cc} = Polarization at the cathode created by concentration (diffusion) gradient at the cathode

E_{IR} = (Ohmic) polarization, the voltage loss due to ohmic resistance of the electrolyte or electrolyte media, leads, and electrode metal.

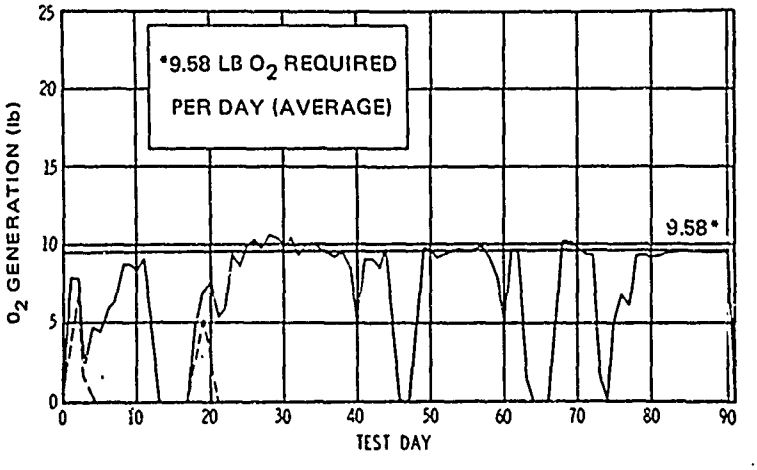


Figure 17–18. Oxygen generation characteristics of a continuous flow KOH electrolysis unit operated in the NASA Langley Research Center/McDonnell Douglas 90-day test. (Jackson, 1971)

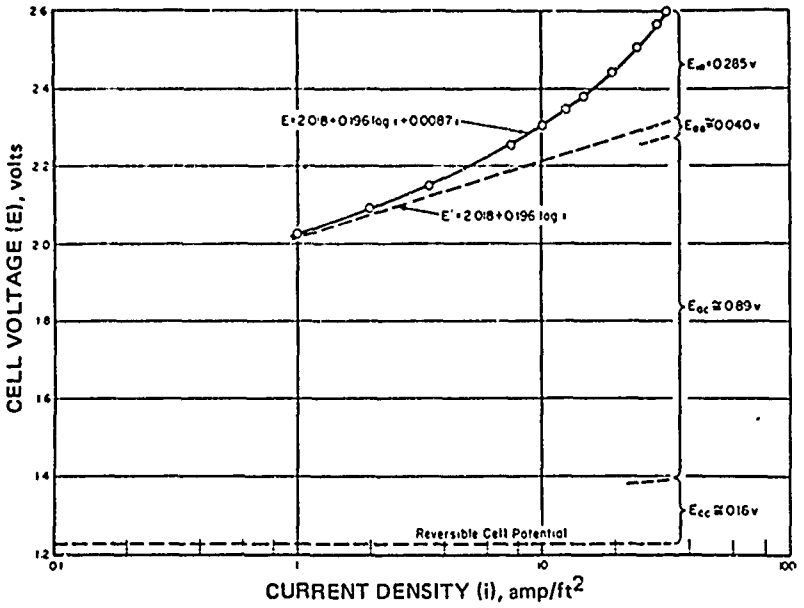


Figure 17–19. Voltage characteristics for vapor electrolysis at 1074 hr (polarization voltage shown at current density of 33 amp/ft^2). (Clifford, 1967)

Solid Polymer Electrolysis. Solid polymer electrolysis utilizes an ion-exchange membrane (cation exchange membrane about 12 mils thick) which, when saturated with water, is the only electrolyte used. The system uses no free acid or alkaline liquids. Water is supplied to the O_2 evolution electrode (anode) where it is electrochemically decomposed to provide oxygen, hydrogen ions, and electrons. The hydrogen ions move to the hydrogen-evolving electrode (cathode) by migrating through the solid polymer electrolyte (SPE). The electrons pass through the external circuit to reach the hydrogen electrode, where hydrogen ions and electrons recombine electrochemically to produce hydrogen gas. An excess of water is usually supplied to the system and recirculated to remove any waste heat. The gases are generated at a stoichiometric ratio of H_2 and O_2 at any pressure required of the system. The SPE can withstand large differential pressures (>1000 psia) as well as high generating pressures which can easily be attained simply by back-pressuring the system.

The ion-exchange membrane in a system under development is a perfluorinated sulfonic acid which meets the stability and performance requirements of a long-lived electrolysis system. The development of electrocatalysts, made of platinum-iridium or other noble metals, has reportedly (Nuttal & Fiterington, 1971) reduced cell voltage from values over 2.0 VDC at 200 amp/ft^2 to less than 1.60 VDC at 200 amp/ft^2 in an acid SPE electrolysis cell (figure 17-20), thereby reducing power

consumption. Figure 17-21 indicates the performance capability of a one-man SPE module developed for the NASA Langley Research Center with current density inputs up to 260 amp/ft^2, which were obtained prior to subjecting the unit to life testing.

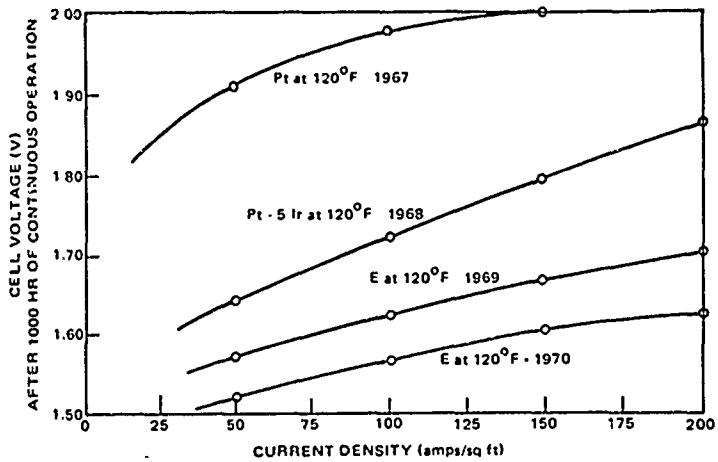


Figure 17–20. Solid polymer electrolyte electrolysis performance at ambient pressure as a function of anode catalyst and temperature. (Nuttal & Fiterington, 1971)

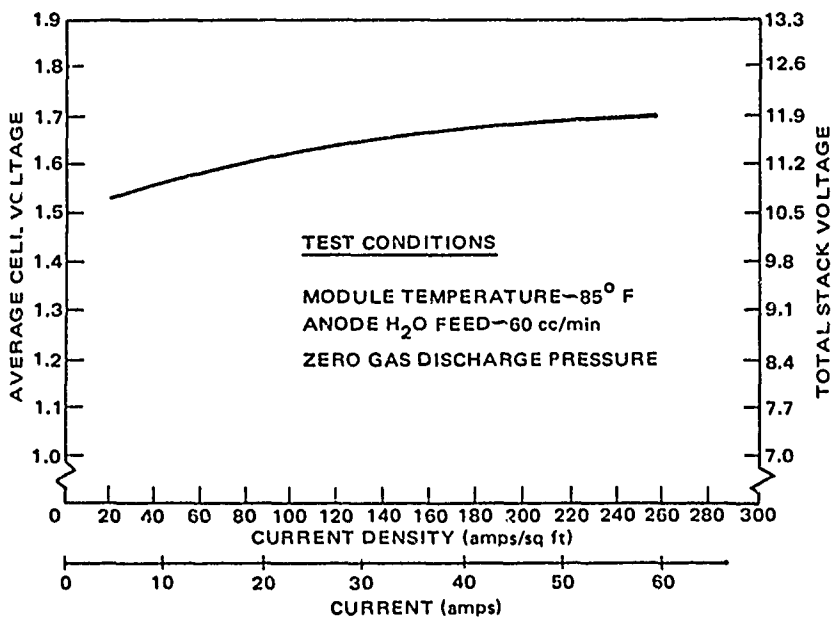


Figure 17–21. Performance data for a seven-cell module solid polymer electrolyte tested for the NASA Langley Research Center. (Nuttal & Fiterington, 1971)

Trace Contaminants Removal

Trace contaminant removal equipment maintains atmospheric contaminants at a physiologically acceptable level. Contaminants may be separated into the broad categories of particles and gases. Particles include solids such as dust and small liquid droplets. Those gases which have been identified as potential contaminants and those which have been detected in the Mercury and Gemini space vehicles, submarines, Apollo outgassing tests, and Earth-based space cabin simulator tests are rather extensive. Discussions of these gases and the measured generation rates are available in the literature (Olcott, 1970; see also Chapter 10, *Toxicology*). Table 17-9 shows the major trace contaminants identified in the NASA/McDonnell Douglas 90-day test (Jackson, 1971). Contaminant levels during the test were at all times below the allowable levels established by the National Academy of Sciences.

Trace contaminant removal equipment includes particulate filters, activated charcoal, sorbent beds, and catalytic burners. Particulate filters may include not only a debris filter but also an absolute filter used in conjunction with charcoal or other sorbent beds. The debris filter traps coarse particles entering the atmosphere purification loop and the absolute filter removes particles as small as 0.3 μ.

Trace Contaminant Removal by Solid Adsorbents

Activated charcoal is used primarily to remove trace contaminant gases having high molecular weights, including many hydrocarbons, alcohols, ketones, aldehydes, mercaptans, organic acids, halogenated materials, and ozone. Figure 17-22 shows adsorption capability of activated charcoal for NO_2. Most of the odor-causing and toxic materials expected to accumulate in a space cabin are effectively adsorbed by charcoal. Activated charcoal, however, is a poor adsorbent of CO_4, CO_2, and CO. Water is adsorbed but not retained. Activated charcoal is sometimes impregnated with phosphoric acid for the removal of ammonia and basic (i.e., high pH) compounds.

Other solid adsorbents, notably molecular sieves and silica gel, have been shown to adsorb most of the organic contaminants found in low concentrations in a space cabin simulator as well as those normally adsorbed by activated charcoal (Mader, 1969). However, they have a great affinity for CO_2 and/or water and, thus, cannot be used effectively without prior removal of these compounds.

Trace Contaminant Removal by Catalytic Oxidation

Catalytic burners are used to oxidize various low molecular weight gases in the cabin atmosphere to CO_2, water vapor, or other compounds. Catalytic burners are not necessary for short missions (of the Mercury, Gemini, and Apollo type) but they are likely to be included in life support systems for future, long-term missions in which contaminant level buildup could become a problem.

Table 17–9

Major Atmospheric Contaminants in Space Station Simulation

Contaminant	Accuracy	Normal Operations	Lower End of Contingency Operations	Abort Level	Allowable Level Specified By NAS/NRC Committee
CO (ppm)	±2.0	12.0	100	200	X
CO_2 (mm Hg)	±0.4	4.0	8	[illegible]	
Hydrocarbons (ppm)	±2.0	4.0	60	300	
NH_3 (ppm)	±1.0	4.0	75	150	
Aldehydes (ppm)	±0.005	1.0	[illegible]	25	
SO_2 (ppm)	±0.25	0.5	7	12	
H_2S (ppm)	±1.0	1.0	15	30	
$(NO)_x$ (ppm NO_2)	±0.1	0.5	1.5	15	
O_3 (ppm)	±0.001	0.03	0.15	1.5	
Chlorine (ppm)	±0.04	0.1	0.7	1.5	
Cyanides (ppm)	±1.0	1.0	3.0	15	
Phosgene (ppm)	±0.2	0.07	0.15	1.5	
Ethanol (ppm)	±0.2	2.5	300	1,500	
Toluene (ppm)	±0.2	0.5	30	300	
2-Ethyl butanol (ppm)	±0.2	1.0	20	60	
N-Butanol	±0.2	1.0	15	150	X
2-Butanone	±0.2	2.0	30	300	X
Chloroform	±0.2	0.5	7	70	X
Dichloromethane	±0.2	2.5	40	700	X
Dioxane	±0.2	1.0	15	150	X
Ethylacetate	±0.2	4.0	60	600	X
2-Methylbutanone	±0.2	2.0	30	300	X
Trichloroethylene	±0.2	1.0	15	150	X
1,1,2-Trichloro; 1,2,2-Trifluoroethane and related congeners	±0.2	20	150	1,500	X
Formaldehyde	---	0.05	0.15	3.0	X
Dichlorolacetylene	---	0	Detected	0.1	X
Vinylidene Chloride	---	2.0	10	25	X

[illegible] >60 (3 min), 60 to 40 (10 min), 40 to 30 (30 min), 30 to 20 (60 min), 20 to 15 (48 hours)

(Jackson, 1971)

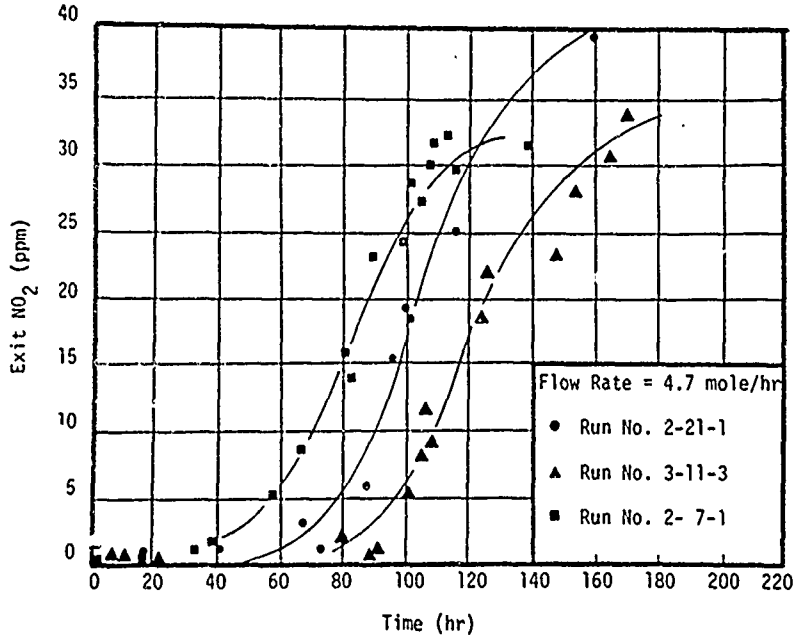


Figure 17–22. Breakthrough curves for NO_2 adsorbed on activated carbon. (Gully et al., 1969)

A typical catalytic burner includes a catalytic bed, electrical heaters, and a regenerative heat exchanger, all contained within an insulated jacket. The pre- and post-sorbent bed filters are connected to the catalytic burner with tubing, and the filter canisters and catalytic burner are assembled on a lightweight structural frame. A number of catalysts have been used in catalytic burners, including 0.5 to 1.0 percent palladium or platinum deposited on alumina, Hopcalite, and other proprietary materials. Hopcalite, a mixture of the oxides of manganese, copper, cobalt, and silver, has been used for many years as a catalyst for removal of CO in air. Pre- and post-sorbent beds are used to prevent catalyst poisoning and to remove undesirable oxidation products. These beds utilized acid-impregnated activated charcoal, Linde-type 13 zeolite, and lithium hydroxide sorbents. Of these, LiOH is the most desirable. During use, the presorbent LiOH is partially converted to $LiCO_3$ as it absorbs CO_2. The combination of LiOH and $LiCO_3$ presorbent effectively removes such compounds as SO_2, H_2S, HCl, and HF. As a postsorbent, LiOH-$LiCO_3$ removes such acid gases as HCl and HF resulting from the catalytic oxidation processes.

Figure 17-23 shows the concentration of CH_4 and CO_2 during a 90-day test referred to previously. The catalytic burner was purposely turned off between test days 68 to 82. After test day 68, the CO level had increased from about 16 ppm to 26 ppm. When the catalytic burner was reactivated, the level was gradually reduced to 17 ppm by the end of the test.

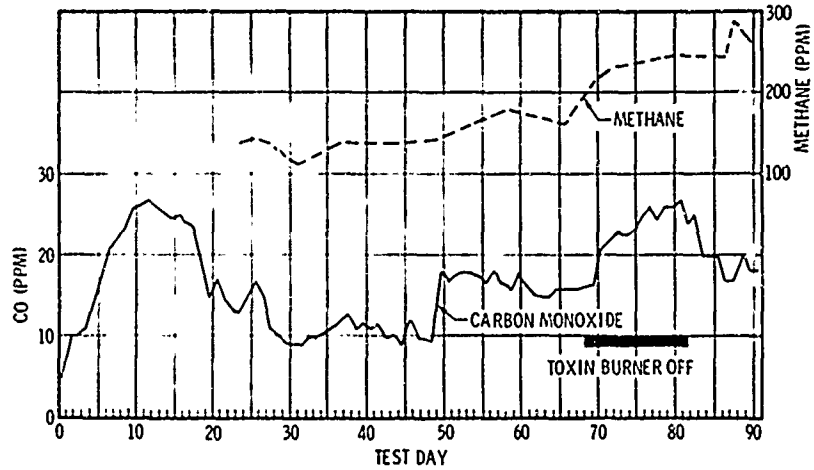


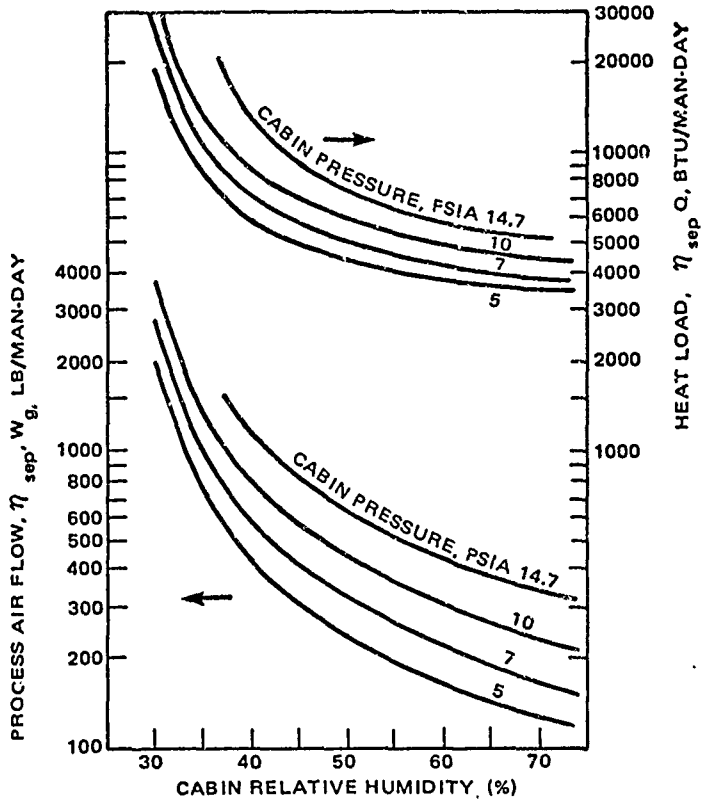
Figure 17–23. Methane and CO concentration during the NASA Langley Research Center/McDonnell Douglas 90-day test showing effects of toxin burner operation. (Jackson, 1971)

Humidity Control

Humidity control in spacecraft may be achieved by one of two methods: (1) condensation of atmospheric water vapor, followed by phase separation of condensate from the air, or (2) drying of cabin air by passage through a bed of granular material. The moisture in this case is either absorbed chemically, by, for example, sodium hydroxide, or adsorbed physically by silica gel or molecular sieves. However, because of the high penalty associated with drying air over granular material, this method is used only in low flow, essential applications, such as drying air prior to CO_2 adsorption on molecular sieves.

Humidity control by condensation/water separation is now universally used in spacecraft. In this method, a heat exchanger cools the cabin air below its dew point, thus condensing water from the moist airstream. Most of the water droplets are then separated from the main airstream in a water separator and channeled to the water management equipment. The air, now reaching the saturation state, is returned to the cabin or routed to another subsystem for further processing. Airflow through the condenser is a function of (1) the inlet and outlet water concentrations in the process airstream; (2) the cabin pressure; and (3) the water separator efficiency. Figure 17-24 is a graphic presentation of the flow requirement and heat load for a humidity control condenser utilized to collect 2.2 lb/man-day of water and operating with a 35°F process airflow. Figure 17-24 also shows a sharp rise in flow requirement and cooling load at low cabin relative humidity with a flattening characteristic at about 60 percent relative humidity. This points to the desirability of maintaining high cabin humidity. It also indicates the savings ensuing from low condenser outlet temperatures. The latter is, however, more difficult to satisfy than the former. Heat sink

temperatures lower than about 40° to 45°F normally impose very high weight penalties on space vehicle liquid cooling loops. These penalties result from the large radiator areas required to cool the heat transport fluid to the temperature level desired for operation of the humidity control system.



(*) NOTES:

1. Condenser temperature = 35 °F
2. η_{sep} = Water Separator efficiency;
3. Wg=Process air flow, Lb. man-day.

Figure 17–24. Flow requirement and heat load for humidity control. (Rousseau, 1963)

Water separation may be accomplished in a number of ways. These include wick condenser/separators, hydrophobic-hydrophilic types and centrifugal, porous plate, elbow, and vortex separators. Of these, the hydrophobic-hydrophilic and the wick condenser separators are considered superior.

Hydrophobic-Hydrophilic Separator

The hydrophobic-hydrophilic separator unit is based on two capillary concepts, the hydrophobic (non-wetting) and hydrophilic (wetting) liquid/gas separation phenomena. The moist gas stream contacts a conical-shaped screen, with the apex of the cone facing the gas stream. The screen cone is coated with a hydrophobic material. The free water droplets are deflected to the base of the cone while the gas flows through the screen. A hydrophilic sump is provided at the base of the cone around its circumference. A pressure differential maintained across the sump by a pressure-controlled pumping system transfers the water to storage tanks. A hydrophobic-hydrophilic water separator was tested in a 60-day chamber study where it operated for the full 60 days with free water separation of 99 percent or better (Lamparter, 1970).

Wick-Type Condenser/Separator

In wick-type condenser/separators, wicking material is located in the unit between layers of heat exchanger surfaces. Moisture condenses on the fins and coolant passage surfaces of the heat exchanger. The condensed water is transferred along the fins by surface tension forces to the wick material. The flow of water within the wick occurs by a combination of capillary action and pressure gradient. If the pressure gradient is kept below a certain value, there is no air leakage through the wick. If the pressure gradient is not large enough (i.e., either the pressure source is too weak or the wick material is not dense enough), a cellular material may be installed at the wick-drain interface. The wick material acts in a manner similar to the hydrophilic screen. This type of water separator was used in Gemini and Apollo spacecraft.

Table 17-10 presents an excellent compilation of data on the important characteristics of existing water separators including those already flight-tested in the Gemini and Apollo programs.

Storage Systems for Atmospheric Constituents

Three methods for storing atmosphere gases in the gaseous phase are considered for spacecraft applications:

1. High-pressure storage at ambient temperature
2. Supercritical storage at cryogenic temperature
3. Subcritical storage at cryogenic temperature

High-pressure gaseous storage is usually heavier than cryogenic storage because of the heavy vessels dictated by the high storage pressure (about 6000 psi). The primary advantages of high-pressure storage are that the equipment is relatively simple and the gas is readily available for the requirements of rapid repressurization and emergency operation.

Storage of atmospheric constituents at cryogenic temperatures generally entails lower tankage weight. This reduction in weight is attributed mainly to two effects: (1) smaller volumes because the gas is stored as a fluid, and

Table 17–10
Comparison of Existing Water Separators

Parameter \ Unit	Lockheed Separator	Hamilton Standard LM	AiResearch Gemini	AiResearch Apollo	Hamilton Standard PLSS
Type	Hydrophobic/hydrophilic static	Centrifugal-hydrophobic screen with pilot pickup	Integral heat exchanger water separator	Integral heat exchanger water separator	Elbow type
Associated equipment required (All have valves and fans)	1. Heat exchanger 2. Water pump 3. Pressure switch	1. Heat exchanger 2. Power supply		1. Cyclic accumulators	1. Sublimator
Most likely failure modes	1. Pump bearings 2. Pressure switch malfunction	1. Shaft bearings	1. Clogging of porous plate	1. Clogging of porous plate 2. Accumulator seal leakage	1. Wick saturation
Efficiency $\frac{H_2O \text{ in} - H_2O \text{ out}}{H_2O \text{ in (Condensed)}}$	99+%	99+%	99+%	99+%	Below 98%
Qualification status	Ground development test completed	Flown in LM	Flown in Gemini	Flown in Command Module	Flown in PLSS
Envelope (Does not include assoc. equipment)	4 in. dia X 8 in. long (Approximate)	5.6 in. dia X 7.25 in. long	8 in. X 10 in. X 7 in. (Heat exchanger included)	8 in. X 10 in. X 7 in. (Approximate)	1.5 in. dia X 4 in. long
Weight	5 lb (Approximate)	2.2 lb	19.32 lb, dry (Includes heat exchanger)	36 lb, dry (includes heat exchanger)	0.20 lb

Table 17–10 (Continued)

Comparison of Existing Water Separators

Parameter \ Unit	Lockheed Separator	Hamilton Standard LM	AiResearch Gemini	AiResearch Apollo	Hamilton Standard PLSS
Porous material	*Hydrophobic* 230 mesh X 0.014 in. wire. CRES with teflon coating. *Hydrophilic* same without teflon coating	CRES	Fabric wick with glass plates	Fabric wick with sintered metal plates	Fabric wick with glass plates
Gas inlet flow	2.16 lb/min air at 7.3 psia and 36°F	0.75 lb/min O_2 at 5.3 psia and 40°F	0.626 lb/min O_2 at 5 psia and 135°F	0.632 lb/min O_2 at 3.71 psia and 138°F	0.12 lb/min O_2 at 80°F and 3.85 psia
Inlet gas humidity	108 grains H_2O/lb dry gas	336 grains H_2O/lb dry O_2	346 grains H_2O/lb dry O_2	438 grains H_2O/lb dry O_2	614 grains H_2O/lb dry O_2
Gas ΔP	0.6 in. H_2O	1.20 in. H_2O	3.5 in. H_2O max (Includes heat exchanger ΔP)	0.20 in. H_2O (Includes heat exchanger ΔP)	0.2–0.6 in. H_2O
H_2O removal rate	0.8 lb/hr (Above conditions)	0.5 lb/hr (Above conditions) (Approximate	0.90 lb/hr with 8 in. H_2O ΔP across plates	1.2 lb/hr (Above conditions)	0.54 lb/hr (Maximum) (Above conditions)

(2) lower working pressures which permit thinner pressure vessel walls. On the other hand, cryogenic systems have the relative disadvantages of more complex control systems, more sophisticated hardware, loss by boiloff, greater electrical power requirements, lower reliability and higher maintenance requirements.

References

Adlhart, O. J., & Hartner, A. J. Experimental evaluation of precious metal carbon dioxide catalysts. Report No. AFFDL-TR-67-80, Engelhard Industries, Inc., Newark, New Jersey, May 1967.

Armstrong, R. C. Life support systems for space flight of extended time periods. NASA-CR-614, National Aeronautics and Space Administration, Washington, D.C., November 1966.

Babinsky, A. D., & O'Grady, T. P. Aircrew oxygen system development: Water electrolysis subsystem report. NASA-CR-73394, National Aeronautics and Space Administration, Washington, D.C., May 1970.

Clark, L. G. Carbon dioxide reduction unit operation with Bosch reaction. Langley Working Paper No. LWP-387, Langley Research Center, Hampton, Virginia, 31 March 1967.

Clifford, J. E. Water vapor electrolysis cell with phosphoric acid electrolyte. SAE Paper No. 670851, presented to Society of Automotive Engineers Aeronautic and Space Engineering Manufacturing Meeting, Los Angeles, California, 2 October 1967.

Coe, C. S., Roseaux, J., & Shaffer, A. Analytical methods for space vehicle atmospheric control processes. Report No. ASD-TR-61-162, AiResearch Manufacturing Division, Los Angeles, California, November 1962.

Gully, A. J., Betha, R. M., Graham, R. R., & Meader, M. C. Removal of acid gases and oxides of nitrogen from spacecabin atmospheres. NASA-CR-1388, National Aeronautics and Space Administration, Washington, D.C., July 1969.

Heubscher, R. G., & Babinsky, A. D. Aircrew oxygen system development – carbon dioxide concentrator subsystem. NASA-CR-73397, National Aeronautics and Space Administration, Washington, D. C., 1970.

Houck, O. K., Wilson, C. H., Clark, L. G., & Hypes, W. D. Recent development and tests of integrated systems hardware. ASME Paper No. 70-Av/SpT-13, American Society of Mechanical Engineers, New York, 21 June 1970.

Jackson, J. K. Test results, operational ninety-day manned test of a regenerative life support system. NASA-CR-111881, National Aeronautics and Space Administration, Washington, D. C., May 1971.

Jackson, J. K., & Blakely, R. L. Application of adsorption beds to spacecraft life support systems. SAE Paper No. NR-670-842, presented to Society of Automotive Engineers Aeronautic and Space Engineering Manfacturing Meeting, Los Angeles, California, 2 October 1967.

Lamparter, R. A. Development of zero gravity hydrophobic/hydrophilic bubble separators. NASA-CR-66922, National Aeronautics and Space Administration, Washington, D.C., May 1970.

Mader, P. P. Evaluation of desorbates from a regenerative carbon dioxide removal system used in a sixty-day manned test. NASA-CR-106214, National Aeronautics and Space Administration, Washington, D.C., October 1969.

Martin, R. B., & Brose, H. F. An amine polymer carbon dioxide concentrator for the ninety-day LRC/MDAC manned chamber test. Presented at the American Society of Mechanical Engineers Space Technology and Heat Transfer Conference, Los Angeles, California, 21 June 1970.

Nuttal, L. J., & Fiterington, W. A. Status of the General Electric solid polymer electrolyte water electrolysis system. ASME Paper No. 71-Av-9, presented at the American Society of Mechanical Engineers Conference on Environmental Control/Life Support, San Francisco, California, 12 July 1971.

Olcott, T. O. Study and preliminary design of an isotope-heated catalytic oxidizer system. NASA-CR-66346, National Aeronautics and Space Administration, Washington, D.C., 1970.

Remus, G. A., et al. Catalytic reduction of carbon dioxide to methane and water. Report No. FDL-TR-65-12, Wright-Patterson AFB, Ohio, April 1965.

Rousseau, J. Atmospheric control systems for space vehicles. Report No. ASD-TDR-62-527, AiResearch Manufacturing Division, Los Angeles, California, March 1963.

Schubert, F. H. Long term operation of a water electrolysis module. SAE Paper No. 690613, Society of Automotive Engineers, New York, October 1969.

Smith, R. W. Zero-G water separator selection: A performance trade-off. Report No. MDC-69-018, McDonnell Douglas Astronautics Company, Eastern Division, St. Louis, Missouri, October 1969.

Stein, P. J. Research and development program for a combined carbon dioxide removal and reduction system. Contract No. NAS1-4154, National Aeronautics and Space Administration, Washington, D.C., October 1965.

Tepper, F., Vancheri, F., Samuel, W., Udavacak, R. Development of a regenerable carbon dioxide removal system. NASA-CR-66571, National Aeronautics and Space Administration, Washington, D.C., January 1968.

Thompson, E. B., Jr. Investigation of catalytic reactions for carbon dioxide reduction. Report No. FDL-TDR-64-22, Wright-Patterson AFB, Ohio, 1964-1967.

Yakut, M. M., & Barker, R. S. Parametric study of life support systems. NASA-CR-73283, National Aeronautics and Space Administration, Washington, D.C., January 1969.

Weissbart, J., & Smart, W. H. Development of a carbon dioxide-water solid electrolyte electrolysis system. Contract No. NAS2-4843, National Aeronautics and Space Administration, Washington, D.C., May 1970.

Wynveen, R., & Quatrone, P. Electrochemical carbon dioxide concentrating system. Paper presented at the American Society of Mechanical Engineers Conference on Environmental Control/Life Support, San Francisco, California, 12 July 1971.

CHAPTER 18

WORK, HEAT, AND OXYGEN COST

by

Paul Webb, M.D.
Webb Associates, Inc.
Yellow Springs, Ohio

Human energy exchange is discussed in this chapter in terms of the whole man. The physical work a man does, the heat he produces, and the quantity of oxygen he takes from the air to combine with food, the fuel source of his energy, are described. Work, heat, and oxygen all are closely tied together in animal energetics, as Kleiber (1961) has written in a historically interesting review, *The Fire of Life*. At the cellular level, not dealt with here, Lehninger's *Bioenergetics* (1965) is an excellent and readable introduction to the biochemistry involved.

The human animal, like most machines which do work, oxidizes fuel to obtain energy. But unlike man-made engines that convert the heat of combustion into work, the body oxidizes fuel at a low temperature, 37°C, and converts chemical energy directly into work. In other words, humans are chemical engines.

The work man does is not impressive. A man cannot generate a lot of power. Humans fancy themselves as thinkers and manipulators of tools. Machines do the heavy work. Nevertheless, man is a muscular animal, with some 40 percent of his weight in skeletal muscles. He moves about under his own muscle power, and does some mechanical (external) work in certain activities.

Whether performing mechanical work or not, just staying alive requires energy. Cells do chemical work in biosynthesis; there is work involved in active transport of solutes across cell membranes; and there is osmotic work in concentrating solutes. Some cells, especially muscle, do mechanical work, much of which is internal and only visible from outside as heat. For example, the work done by heart muscle in pumping blood against the resistance of the vascular distribution network, and the work done by skeletal muscle in supporting ourselves upright in Earth's gravity field, are all internal.

Reviewed by John B. West, Ph.D., University of California, San Diego.

Preceding page blank

There is continual energy exchange in living and doing things. Quantifying energy exchange is important in designing life support equipment since it determines food supplies, the oxygen to be carried, waste products to be removed, and the heat to be dissipated. The design of respiratory equipment and oxygen supplies must allow the man to do the heaviest work a mission may require, and the cooling of protective clothing, e.g. a space suit, must carry off the greatest amount of heat he can generate.

Heat is the dominant expression of human energy exchange. Heat is generated within the body while one sleeps and during all waking hours. The more active one is, the more heat there is to be dissipated. When a task is carried out in which mechanical work is done, 10 to 30 percent of the energy expenditure is applied to the external load; the rest comes out as heat.

The rate of energy exchange varies over a wide range. A man asleep may operate at a level as low as 1.1 kcal/min (77 watts, or 262 BTU/hr). When doing sustained hard work he may operate at 15 kcal/min (1046 watts, or 3571 BTU/hr).

Units for the description of energy exchange are varied. Physiologists think in terms of kilogram calories (kcal); the calories used in nutrition are kcals, and body heat production is generally expressed as kcal/min. In international convention the basic energy unit is the joule, or its rate derivative, the watt (W), which is 1 joule/sec. Older units which have been in common use are the met (1 met = 50 kcal per square meter of body surface an hour), and the BTU, or BTU/hr.

1 kcal = 4184 joules = 1.162 watt-hours = 3.968 BTU
1 kcal/min = 69.7 watts = 238 BTU/hr
100 watts = 1.43 kcal/min = 341 BTU/hr
100 BTU/hr = 0.42 kcal/min = 29.3 watts

In this chapter the energy unit will be the kcal, with rates expressed in both kcal/min and watts.

It has been noted that living involves heat production as a major by-product of the oxidation of fuel to supply energy for "work." The work of staying alive is hard to measure since it takes place in a closed and hidden system—the body—but the total heat produced by all the separate activities is known and measurable. It is possible to estimate the internal work done individually by the heart, the kidneys, the brain, and other organs and tissues. Data of this kind based on measuring blood flow and oxygen use appear in table 18-1.

Some organs, particularly the brain, oxidize fuel at a high and steady rate throughout the 24 hours; the liver is typical of organs which oxidize fuel at slowly changing levels depending on the work required; some tissues oxidize at a slow pace, like the skin. Skeletal muscle changes its level of fuel consumption and heat production manyfold between quiescent and active states. Since skeletal muscle is 40 percent of the body mass, this change in muscle heat production is the dominant factor when total heat production varies over a 10:1 range.

Table 18–1

Oxygen Consumption and Heat Production of Organs in Man

Organ	Oxygen Consumption (ml/min – 100 gm)	Typical Organ Weight (gm)	Heat Production (kcal/min)
Heart	9.5 (7.8 – 10.5)	320	0.15
Brain	3.6 (3.3 – 3.9)	1380	0.25
Kidneys	10.2 (6.2 – 16.0)	300	0.15
Muscle			
Rest	0.17	28 000	0.24
Exercise	11.2	28 000	15.7

(Based on averaged data from Altman & Dittmer, 1968)

Measuring total body heat production is called direct calorimetry. The technique is complex and the machinery for doing it has always in the past confined and restrained the subject unnaturally. A new and less constraining method is evolving from research done with water cooled garments, about which more will be said later. But our body of knowledge about human work and energy exchange rests on a small number of direct calorimetric measurements, and a very large number of indirect calorimetric measurements.

Indirect calorimetry measures energy exchange by seeing how much oxygen a man uses to burn fuel, and how much carbon dioxide, water, and nitrogen he excretes as the chemical residues of oxidation. By measuring these material exchanges in the respired air, and nitrogen in urine, one may estimate with reasonable accuracy the amount and type of fuel burned, hence the total energy being released.

Given the three measured quantities of O_2 consumed, CO_2 produced, and urinary N excreted, Consolazio et al. (1963) show that the three types of fuel, carbohydrate (CHO), fat (F), and protein (Pro), and the energy (H) released in their oxidation are directly calculable from:

$$\text{CHO} = 2.909\ O_2 + 4.115\ CO_2 - 2.539\ N\ .$$
$$\text{F} = 1.689\ O_2 - 1.689\ CO_2 - 1.943\ N$$
$$\text{Pro} = 6.25\ N$$
$$\text{H} = 3.78\ O_2 + 1.16\ CO_2 - 2.98\ N$$

It is also feasible to do an energy exchange analysis by counting fuel calories. One can measure food intake, and any residues in urine and feces which are not oxidized, and know a man's daily energy exchange. But the measurement does not discriminate in usefully short time intervals since a man eats only about three times a day, and he stores his fuel rather than burning it as consumed.

Thus a 24-hour period is the shortest time we use for this type of data (see figure 18-1). To further complicate matters, a man can store great quantities of fuel as fat, and can live and work for days without eating at all. Body weight reflects storage and expenditure of stores, but it reflects other things as well, such as dehydration, growth, and atrophy.

The energetic equivalents of oxygen consumed and of carbon dioxide excreted are standard numbers in physiology. Every liter of oxygen consumed indicates that 5 kcal of energy has been released from stored fuel. The same 5 kcal is the caloric equivalent of 1 liter of CO_2 produced. These caloric equivalents were first described in experiments in a direct calorimeter while O_2 and CO_2 exchange were also monitored. There are small variations of the caloric equivalents of O_2 and CO_2 which reflect variations in the type of foodstuff being used. The range is from 4.7 to 5.0 kcal, but for most purposes 5 kcal is sufficiently accurate (Maxfield & Smith, 1967; Weir, 1949).

One way to visualize these basic work and energy relationships is shown in figure 18-1.

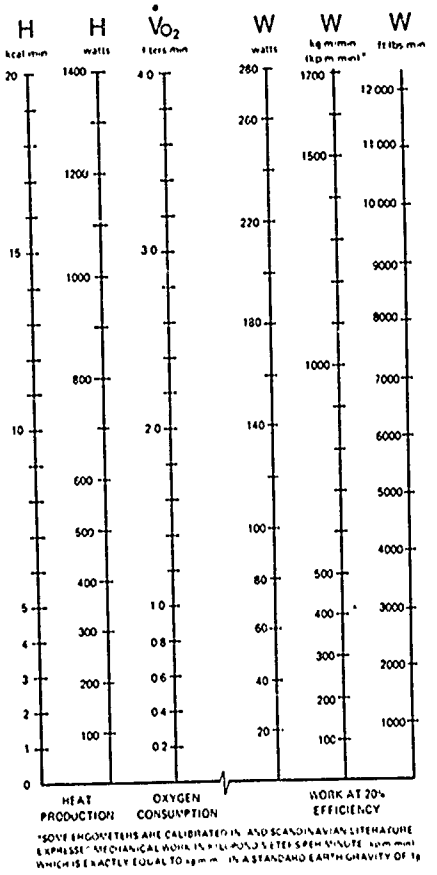


Figure 18–1. Relationship of heat production (H) to O_2 consumption ($\dot{V}_{O_2}$), and of these to mechanical or external work (W), when a man performs at 20% efficiency. H and W are shown in various common units.

Daily Energy Exchange

Consider now the energetics of just staying alive, with no physical activity at all. This is, to use an old and imprecise term, the basal metabolism, or better, the cost of tissue maintenance. Figure 18-2 shows the oxygen cost and heat production for tissue maintenance. The ranges shown for periods of 4, 8, and 24 hours show how size and biochemical individuality affect such data. The three diagonal lines on the graph show how particular dietary mixtures would alter the values.

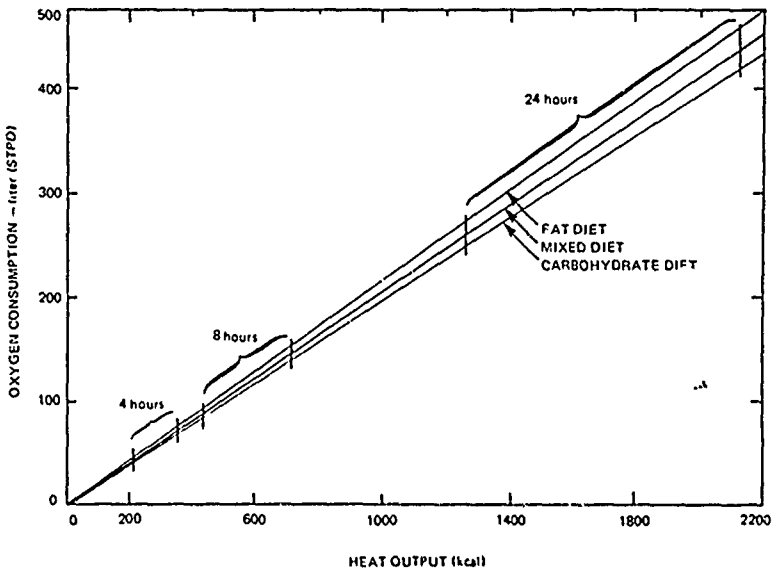


Figure 18–2. O_2 cost and heat production of tissue maintenance, calculated for men of astronaut size and age under basal conditions. (Redrawn from Fletcher, 1964; based on standard values from Diem, 1962)

The total daily energy level is the cost of tissue maintenance plus the cost of activities. Assuming standard activity, the smaller the person the smaller his daily oxygen need, his food requirement, and his heat production. This is shown in the figure 18-3, which gives total daily energy levels for normally active people of various sizes. These daily levels are about twice as high as the daily cost of tissue maintenance. Note that the values for men of astronaut size and age, (3400 to 3800 kcal/day), imply considerable daily activity, whereas astronauts confined to simulated space cabin conditions (see figure 18-4) or in actual orbital flight (see table 18-2) show much lower values.

To illustrate the range of activity, hence the range of energy exchange (i.e., food consumed and heat plus external work output), which adult men exhibit, figure 18-4 shows that a day of "complete rest" involves the use of about 1500 kcal in 24 hours, while a "very active day" calls for about 6500 kcal in 24 hours. The four classifications of work, from light through very heavy,

represent values used in industry for 8 hours a day, year round employment. These figures come from a study by Edholm and Fletcher (1955) of British Army recruits during a very active period of training. Between these two extremes are similar data for many other military and civilian activities. Notice that some of the data are based on counting the calories in the food eaten, and the rest based on estimates of energy exchange from oxygen consumption.

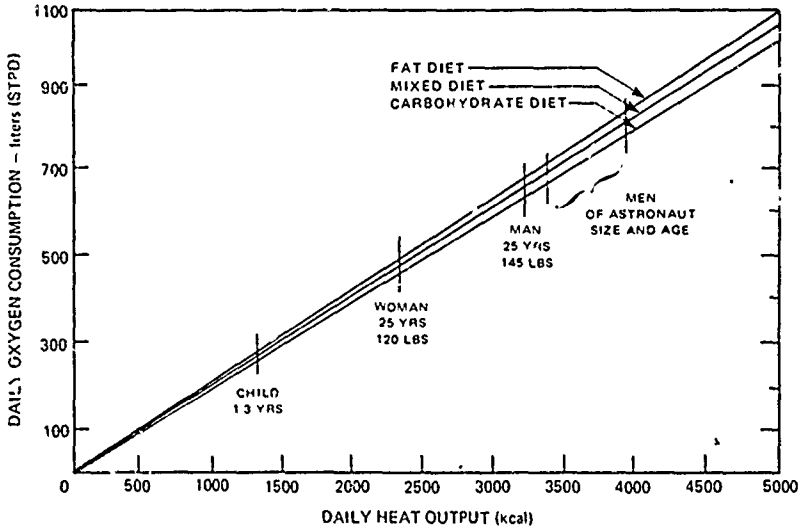


Figure 18–3. Total daily O_2 cost and heat production for normally active people, as affected by body size, calculated by method proposed by UN Food and Agricultural Organization (1957). (Redrawn from Fletcher, 1964)

One quite low level of daily energy exchange in figure 18-4 is that labeled "Space Cabin Simulator" (Welch et al., 1961). The low rate was largely due to the confinement of the subjects. Flight data shown in table 18-2, from the American Gemini and the Russian Vostok orbital space flights (Berry & Catterson, 1967), confirm the low estimates from the simulator. In flight, weightlessness and confinement together can explain the low metabolic rates.

In each of the three preceding figures there were three straight lines showing energy levels versus oxygen cost for three different types of diet. The oxygen used, and the carbon dioxide produced, vary slightly with the fuel oxidized. These dietary effects are relatively small, and it is an unusual diet which is purely one of the three types of food. The mixed diet is common in North America, and for most purposes we do not try to adjust energy estimates for a particular person's diet. There are more important sources of variation, particularly the specific activities one undertakes during the day.

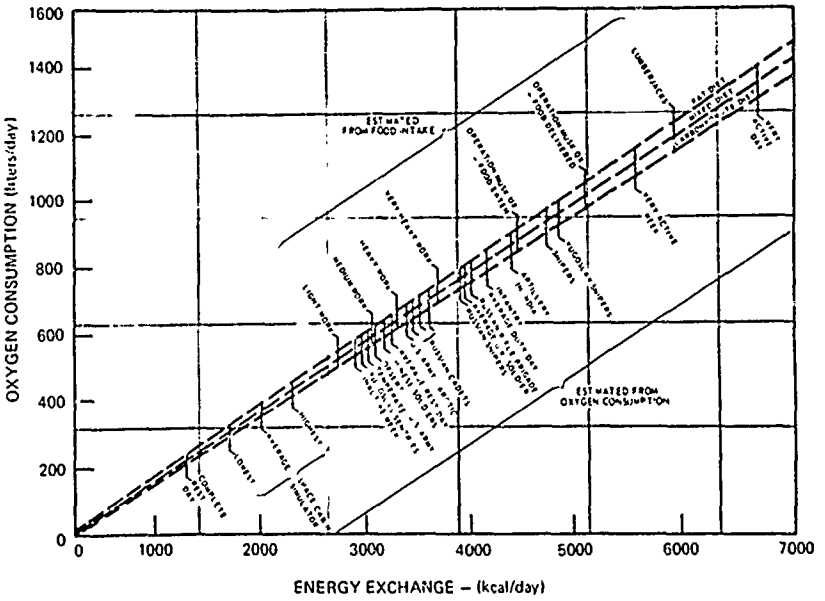


Figure 18–4. O_2 cost and energy exchange levels for daily activities. Values identified below three dietary lines are based on measurements of O_2 consumption; those above are based on careful measurements of daily food consumption and weight change, if any. (Redrawn from Fletcher, 1964; based on data from Buskirk et al., 1956; Buskirk et al., 1957; Consolazio et al., 1956; Edholm & Fletcher, 1955; Fletcher, 1958; Lampietro et al., 1956; Kark et al., 1948; Karvonen & Turpeinen, 1954; Lawton, 1960; Luthman & Lundgren, 1947; Ramzin, 1948; Richardson & Campbell, 1927; Rjabko & Agapov, 1947; Welch et al., 1961)

Table 18--2

Energy Exchange Levels in Space Flight

Flight	Duration (days)	Daily Energy Level* (kcal/24 hr)
Gemini 4	4	2410
5	8	2010
7	14	2219
Vostok	3	2400
	4	2100
	5	2100

*Based on analysis of LiOH canisters for carbon dioxide.

(Data from Berry & Catterson, 1967)

Work and Heat Dissipation

When a man begins muscular work, there is an immediate increase in energy release from the high energy phosphate bonds of adenosine triphosphate, and the breakdown of energy-rich phosphocreatine, followed by renewal from carbohydrate (glucose and glycogen) fuel stores. Some of the muscle energy may be applied to an external load, while the rest is expended in internal work, hence appearing only as heat. When a man walks or runs on a level surface, all the increased energy used appears as heat, that is, all the work is internal. This extra heat is stored, causing a rise in the temperature of the muscle, then is carried off by conduction to the skin and by convective cooling via the increased flow of blood through the muscle. As the work continues, the body begins to dissipate more heat to prevent an uncontrolled rise in general body temperature. This change in the rate of heat dissipation can be measured in a calorimeter, as illustrated in figure 18-5. Total heat loss, indicated in the figure, is the sum of respiratory heat loss, convective heat loss and radiative heat loss from the body surface, and evaporative heat loss from sweating.

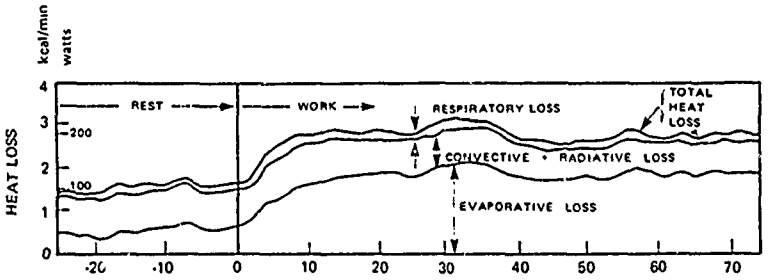


Figure 18–5. Example of direct calorimetric measurement with subject doing mild work. Up to time 0, the subject was resting in the supine position on a net hammock in the calorimeter box; starting at time 0, he worked with a crank ergometer, still lying down, against an external load of .36 kcal/min, or about 25 watts. (Redrawn from Benzinger & Kitzinger, 1963)

It is the skeletal muscles that produce the extra heat during increased physical activity. Some organs, like the heart, become more active; some, like the brain, do not change; and some, like the kidney, decrease their activity. None of these organ is of significant metabolic size compared to skeletal muscle (see table 18-1). As seen in figure 18-5, the increased heat production from muscular work is followed somewhat later by an increase in heat picked up by the calorimeter.

Similar data have been obtained in experiments with men working in water cooled suits. The subjects involved in the study illustrated in figure 18-6 were thermally isolated in insulated, impermeable coveralls, with cooling controlled so that they neither felt cold nor did they sweat (i.e., their weight loss was less than 100 gm/hr). The curves of figures 18-6 and 18-7 show that metabolic heat production (M) calculated from oxygen consumption ($\dot{V}_{O_2}$) increased soon after work began, and that heat loss (H) to the water cooled suit increased somewhat later.

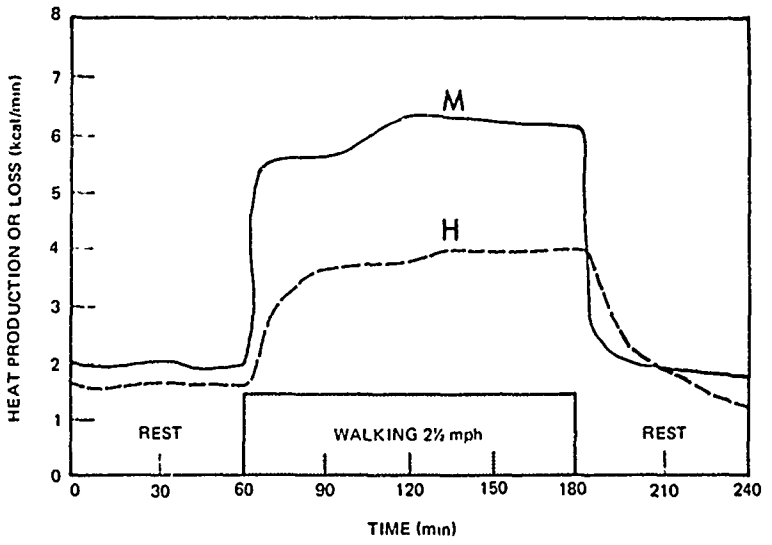


Figure 18–6. Heat production curves (M), calculated from continuous measurement of O_2 consumption and of heat loss (H) to a water cooled suit, including a small increment from evaporative heat loss from the skin and respiratory tract. Averaged data for 6 experiments, 4 subjects. [Discrepancy between M and H, especially in the second hour when there was evidently a physiological steady state, was due in part to the heat storage which occurs naturally in the first part of the day (the first half of the circadian cycle), and in part to measurement error.] (Redrawn from Webb & Annis, 1968)

From the experiments discussed above, it became evident that oxygen consumption and heat dissipation increased exponentially to their final values, and that each function had a characteristic time constant. Webb et al. (1970) gave numerical values to these metabolic time constants, in addition to time constants for some other physiological variables that change with work (table 18-3).

To illustrate the point, the general shapes of the M and H curves, using their characteristic time constants, are given in figure 18-8.

When the initial exponential transient has passed, and heat dissipation has been adjusted to match heat production, a more or less steady state persists throughout the rest of the work, as seen in figure 18-6. When work is over, exponential decays in M and H characterize the return to resting levels.

Figure 18-9 shows heat dissipation during a single experiment lasting 16 hours, during which the subject did muscular work (walked on a treadmill at 4.8 km/hr or 3 mph for two 1-hour periods), and during the rest of the day carried out quiet activities like reading. The kind of near-calorimetric data depicted in the figure verify the general work, heat, and oxygen cost data discussed in this chapter. Calorimetric heat balances accurate to 1 percent have been made since this chapter was written. The technique is described by Webb et al., (1972) and a fundamental circadian rhythm of metabolism reported by Webb (1971).

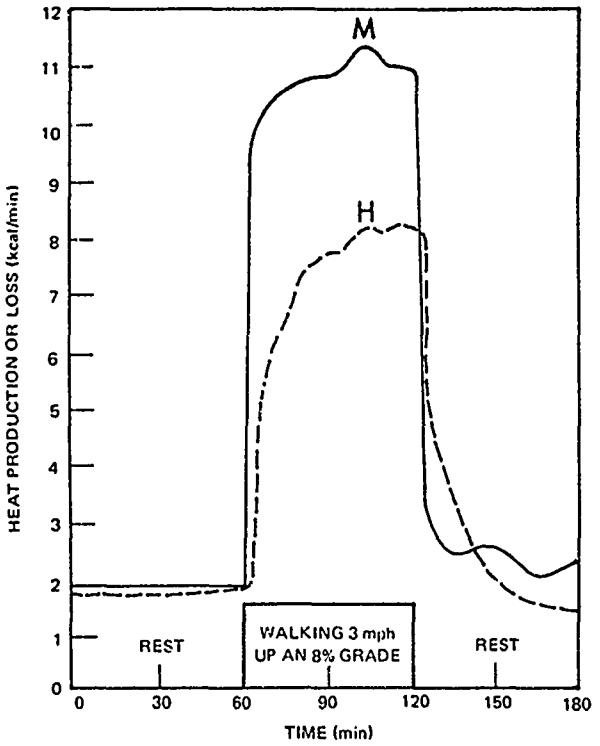


Figure 18–7. Heat production (M) from $\dot{V}O_2$ and heat loss (H) to a water cooled suit, as in figure 18-6 but with double the activity level for half the time. External work of walking uphill for 3 mi. was added to H curve. Averaged data for 6 experiments, 4 subjects. (Redrawn from Webb & Annis, 1968)

Table 18–3

Time Constants for Exponential Changes Following Onset of Work

Physiological Measure	Time Constant (min)
Heart rate	0.4
M (from $\dot{V}O_2$)	0.5
Mean skin temperature	1.0 (Estimated)
Rectal temperature	10.0
Heat loss	10.0

These recent experiments with controlled water cooling in thermally isolated men, along with the comparable measurements in water cooled space suits shown in figures 18-25 and 18-26 at the end of the chapter, are essentially calorimetric. If continued, they should provide excellent design data for human cooling systems, and modernize our information about human energy exchange. Meanwhile, our best source is the extensive

literature on the oxygen costs of specific activities, which translate into heat and work data by the methods already described.

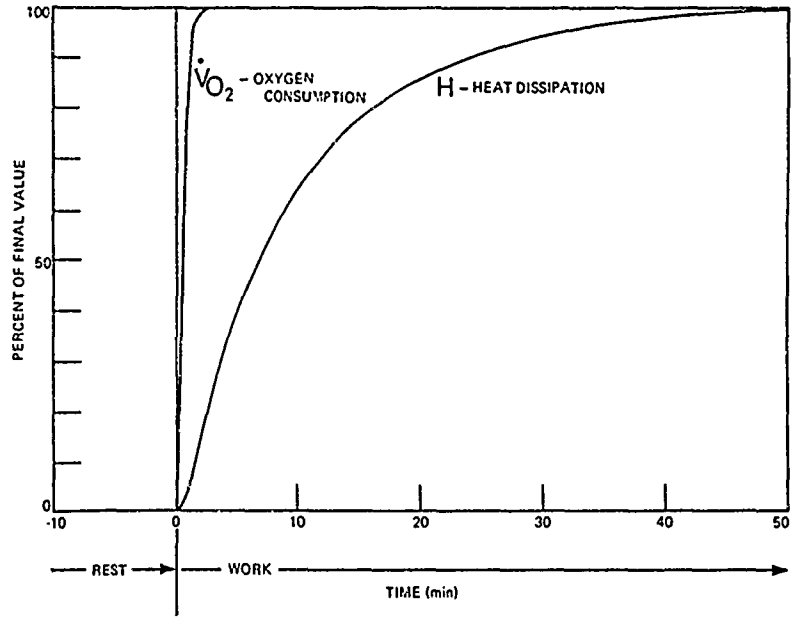


Figure 18--8. Pure shapes of exponential changes of two variables, $\dot{V}O_2$ and H, based on their individual time constants, as given in table 18-3.

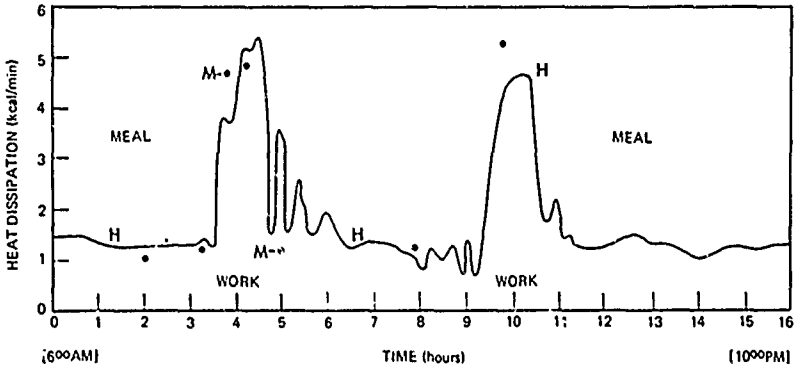


Figure 18–9. Heat dissipation (H) in a water cooled suit, under conditions similar to those for figure 18-6. Data points are for heat production (M) from $\dot{V}O_2$–$\dot{V}CO_2$ measured by collecting expired air and analyzing for O_2 and CO_2. (Redrawn from Webb et al., 1970)

Oxygen Costs of Specific Activities

To design life support equipment it is essential to be able to estimate heat production for the activities involved. There is a sizable body of data available for a large number of specific human activities, all based on oxygen cost, hence heat production. Tables 18-4 and 18-5 give this sort of data. The tabulated values have been adjusted for a man 175 cm (69 inches) tall who weighs 76 kg (167 lb), which are the mean values for the original seven Mercury astronauts. The means for the 43 current astronauts are 177 cm (69-1/2 inches) in height and 74 kg (163-1/2 lb) in weight.

Important subject-to-subject differences exist even in men of the same size. These commonly give rise to variations as high as 60 percent when different men are performing the same task, as high as 30 percent when adjustments for body size are made, and as high as 10 to 15 percent when repeated measurements are taken on the same man.

The efficiency with which external work is accomplished also varies widely. It is lowest in the work of respiration (less than 5 percent), is 10 to 20 percent for common tasks, and highest in bicycling and walking on the inclined treadmill (up to 35 percent and occasionally 40 percent in trained men). Several apparent discrepancies in the tabulated values however, are indicative of the imprecision of such data. This sort of variation is to be expected. For example, "shoveling sand" occurs twice; once under "Moderate activity—standing," and again under "Heavy activity—standing," with an appropriately higher level of energy cost. Both measurements shown have been reported in the literature, and both are probably valid for the subjects and activities measured. These disparities may be due to the wide range of subject-to-subject differences mentioned above, to differences in the rate of work, or to some variation in experimental technique.

The oxygen cost of moving at different speeds over a firm level surface is shown graphically in figure 18-10. If a man walks or runs uphill, and if he is carrying extra weight, oxygen costs increase significantly. Figure 18-11 shows data of this kind for treadmill work. The chart, which permits estimation of oxygen consumption, is based on extensive experiments in few subjects. The upper segment is based on two middle-distance runners, the lower segment, on 10 healthy male volunteer walkers. The hatched area indicates a range of values of the so-called "maximum aerobic capacity," which is approximately equal to the highest oxygen consumption that can be maintained continuously. Its value depends primarily on the body build and degree of training of the subject. Considerable variation must be expected, both between subjects and from experiment to experiment. Since only well-trained men are capable of sustained climbing, few men will be capable of reproducing the most severe combinations depicted.

Certain environmental stresses cause increases in oxygen cost. Three such conditions are vibration (figure 18-12), acceleration (figure 18-13), and heat (figure 18-14).

Table 18–4
Oxygen Cost of Everyday Activities

Activity	Oxygen Consumption (liters/min)	Equivalent Heat Production (kcal/min)
Asleep		
Sleeping, men over 40	0.22	1.1
Sleeping, men aged 30 – 40	0.24	1.2
Sleeping, men aged 20 – 30	0.24	1.2
Sleeping, men aged 15 – 20	0.25	1.3
Resting		
Lying fully relaxed	0.24	1.2
Lying moderately relaxed	0.26	1.3
Lying awake, after meals	0.28	1.4
Sitting at rest	0.34	1.7
Very light activity—seated		
Writing	0.36	1.8
Riding in automobile	0.40	2.0
Typing	0.46	2.3
Polishing	0.48	2.4
Very light activity—standing		
Relaxed	0.36	1.8
Drafting	0.38	1.9
Taking lecture notes	0.40	2.0
Peeling potatoes	0.42	2.1
Light activity—seated		
Playing musical instruments	0.58	2.9
Repairing boots and shoes	0.60	3.0
At lecture	0.60	3.0
Assembling weapons	0.72	3.6
Light activity—standing		
Entering ledgers	0.52	2.6
Washing clothes	0.74	3.7
Ironing	0.88	4.4
Scrubbing	0.94	4.7
Light activity—moving		
Slow movement about room	0.50	2.5
Vehicle repairs	0.68	3.4
Slow walking	0.76	3.8
Washing	0.84	4.2

Table 18 –4 (Continued)
Oxygen Cost of Everyday Activities

Activities	Oxygen Consumption (liters/min)	Equivalent Heat Production (kcal/min)
Moderate activity—lying		
Creeping, crawling, prone resting maneuvers	1.14	5.7
Crawling	1.22	6.1
Swimming breaststroke at 1 mph	1.36	6.8
Swimming crawl at 1 mph	1.40	7.0
Moderate activity—sitting		
Rowing for pleasure	1.00	5.0
Cycling at 8 – 11 mph	1.14	5.7
Cycling rapidly	1.38	6.9
Trotting on horseback	1.42	7.1
Moderate activity—standing		
Gardening	1.16	5.8
Chopping wood	1.24	6.2
Baseball pitching	1.30	6.5
Shoveling sand	1.36	6.8
Moderate activity—moving		
Golf	1.08	5.4
Table tennis	1.16	5.8
Tennis	1.26	6.3
Army drill	1.42	7.1
Heavy activity—lying		
Leg exercises, average	1.50	7.5
Swimming breaststroke at 1.6 mph	1.64	8.2
Swimming backstroke at 1.0 mph	1.66	8.3
Lying on back, head raising	1.76	8.8
Heavy activity—sitting		
Cycling rapidly, own pace	1.66	8.3
Cycling at 10 mph, heavy bicycle	1.78	8.9
Cycling in race (100 mi in 4 hr 22 min)	1.96	9.8
Trotting on horseback	1.96	9.8
Heavy activity—standing		
Chopping wood	1.50	7.5
Shoveling sand	1.54	7.7
Sawing wood by hand	1.60	8.0
Digging	1.78	8.9

Table 18–4 (Continued)
Oxygen Cost of Everyday Activities

Activities	Oxygen Consumption (liters/min)	Equivelent Heat Production (kcal/min)
Heavy activity—moving		
Skating at 9 mph	1.56	7.8
Playing soccer	1.66	8.3
Skiing at 3 mph on level	1.80	9.0
Climbing stairs at 116 steps/min	1.96	9.8
Very heavy activity—sitting		
Cycling at 13.2 mph	2.00	10.0
Rowing with two oars at 3.5 mph	2.20	11.0
Galloping on horseback	2.28	11.4
Sculling (97 strokes/min)	2.52	12.6
Very heavy activity—moving		
Fencing	2.10	10.5
Playing squash	2.10	10.5
Playing basketball	2.28	11.4
Climbing stairs	2.40	12.0
Extreme activity		
Wrestling	2.60	13.0
Marching at double	2.66	13.3
Endurance marching	2.96	14.8
Harvard Step Test	3.22	16.1

Table 18–5
Oxygen Cost of Special Activities

Activities		Oxygen Consumption (liters/min)	Equivalent Heat Production (kcal/min)
Engineering tasks			
Medium assembly work		0.58	2.9
Welding		0.60	3.0
Sheet metal work		0.62	3.1
Machining		0.66	3.3
Punching		0.70	3.5
Machine fitting		0.90	4.5
Heavy assembly work–noncontinuous		1.02	5.1
Driving vehicles and piloting aircraft			
Driving a car in light traffic		0.26	1.3
Night flying–DC-3		0.32	1.6
Piloting DC-3 in level flight		0.34	1.7
Piloting helicopters		0.36	1.8
Instrument landing–DC-4		0.50	2.5
Piloting light aircraft in rough air		0.54	2.7
Taxiing DC-3		0.58	2.9
Piloting bomber aircraft in combat		0.58	2.9
Driving car in heavy traffic		0.64	3.2
Driving truck		0.66	3.3
Driving motorcycle		0.70	3.5
Moving over rough terrain on foot			
Flat, firm road	2.5 mph	0.56 – 0.98	2.8 – 4.9
Grass path	2.5	0.64 – 1.02	3.2 – 5.1
Stubble field	2.5	0.80 – 1.22	4.0 – 6.1
Deeply plowed field	2.0	0.98 – 1.38	4.9 – 6.9
Steep 45° slope	1.5	0.98 – 1.38	4.9 – 6.9
Plowed field	3.3	1.56	7.8
Soft snow, with 44 lb load	2.5	4.2	21.0
Load carrying			
Walking on level with 58 lb load, trained men	2.1 mph	0.38	1.9
	2.7	0.58	2.9
	3.4	0.92	4.6
	4.1	1.66	8.3
Walking on level with 67 lb load, trained men	2.1 mph	0.46	2.3
	2.7	0.58	2.9
	3.4	1.02	5.1
	4.1	1.68	8.4
Walking on level with 75 lb load, trained men	2.1 mph	0.50	2.5
	2.7	0.68	3.4
	3.4	1.04	5.2
	4.1	1.72	8.6
Walking up 36% grade with 43 lb load, sedentary men	0.5 mph	1.34	6.7
	1.0	2.46	12.3
	1.5	3.20	16.0

Table 18–5 (Continued)
Oxygen Cost of Special Activities

Activities		Oxygen Consumption (liters/min)	Equivalent Heat Production (kcal/min)
Swimming on surface			
Breaststroke	1 mph	1.40	7.0
	2	5.80	29.0
	3	19.40	97.0
Crawl	1 mph	1.80	9.0
	2	3.60	18.0
	3	9.60	48.0
Butterfly	1 mph	2.40	12.0
	2	5.80	29.0
	3	15.00	75.0
Walking under water			
Walking in tank	minimal rate	0.58	2.9
Walking on muddy bottom	minimal rate	1.10	5.5
Walking in tank	maximal rate	1.44	7.2
Walking on muddy bottom	maximal rate	1.58	8.4
Movement in snow			
Skiing in loose snow	2.6 mph	1.62	8.1
Sled pulling–hard snow	2.2	1.72	8.6
Snowshoeing (bearpaw)	2.5	1.74	8.7
Skiing on level	3.0	1.80	9.0
Sled pulling–low drag, med. snow	2.0	1.94	9.7
Snowshoeing–trail type	2.5	2.06	10.3
Walking, 12–18 in. snow, breakable crust	2.5	2.54	12.7
Skiing on loose snow	5.2	2.92	14.6
Snowshoeing–trail type	3.5	2.96	14.8
Skiing on loose snow	8.1	4.12	20.6
Measured work at different altitudes			
Bicycle ergometer			
Workload	Altitude		
430 kg-m/min	720 mm Hg	1.02	5.1
430	620	0.98	4.9
430	520	1.08	5.4
Mountain climbing			
880 - 1037 kg-m/min	610 mm Hg	1.84 – 2.20	9.2 – 11.0
566 - 786	425	1.54 – 1.90	7.7 – 9.5
393 - 580	370	1.28 – 2.10	6.4 – 10.5

Data for tables 18–4 and 18–5 were drawn from both published and unpublished sources. The principal references consulted were: Altman et al. (1958), Billings et al. (1962), Buskirk et al. (1956), Cathcart et al. (1923), Christensen (1953), Christensen and Hogberg (1950), Garry et al. (1955), Glasow and Müller (1951), Karpovich (1953), Littell and Joy (1969), Mayor (1959), Morehouse and Cherry (1945), Morehouse and Miller (1959), Passmore et al. (1952), Passmore and Durnin (1955), Pollack et al. (1944), Pugh (1958), Ramzin (1948), Rose (1944), Turner (1955), and U.S. Navy (1956).

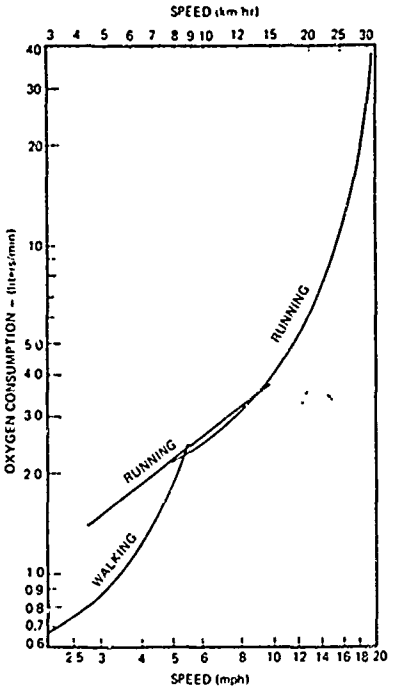


Figure 18–10. Oxygen cost of walking and running at various speeds on level surfaces with no extra load. [Compilation by Altman et al., 1958; straight line for slow running (4–15 km/hr), from Shephard, 1969]

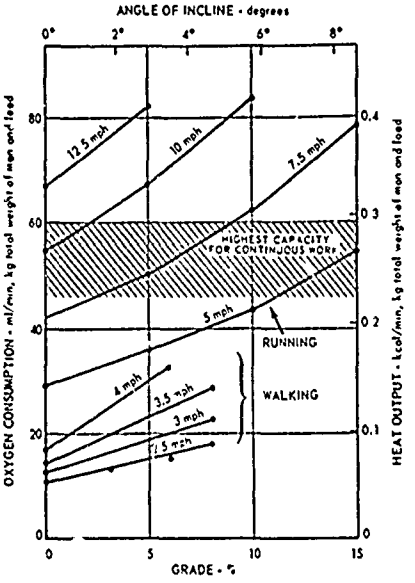


Figure 18–11. Chart for estimating O_2 consumption of men walking or running uphill wearing heavy equipment. To use: estimate percent grade from height of rise in 100 ft., or estimate angle of incline from the tangent, derived from vertical rise and horizontal distance. Note that above hatched area, work is exhausting, and the greater the oxygen consumption, the shorter the running time. (From Åstrand, 1952, with permission of Ejnar Munksgaard, publisher; Goldman & Iampietro, 1962; Margaria et al., 1963)

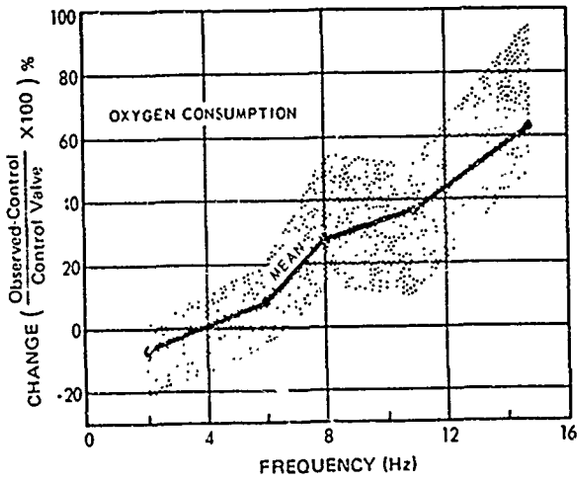


Figure 18–12. Change in O_2 consumption for 4 male subjects during vibration, shown as a percentage change from control value. Subjects were exposed to 20 min. of vibration at an amplitude of 0.132 in. while seated on a chair and entirely unrestrained. (Adapted from Gaeuman et al., 1962)

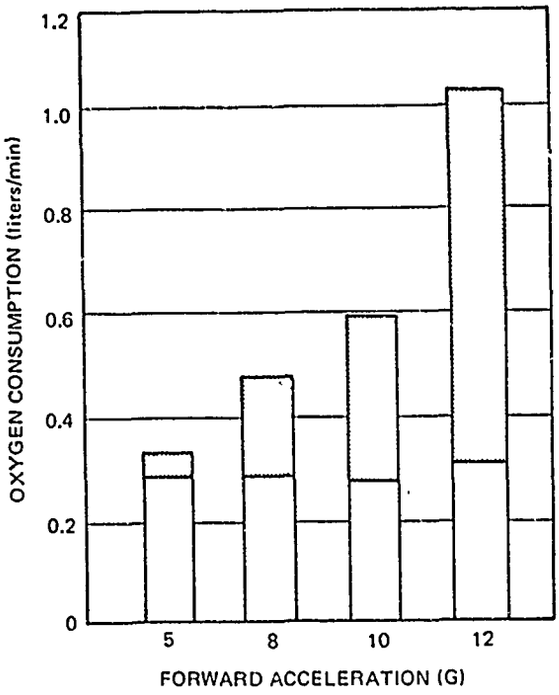
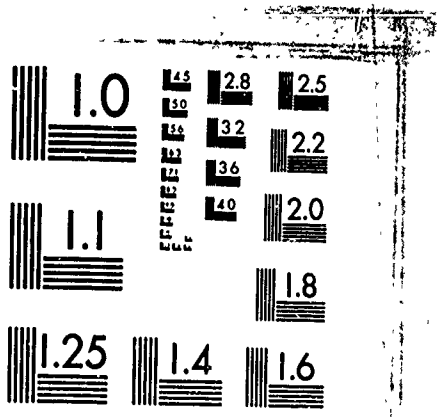


Figure 18–13. Increase in O_2 consumption with increasing levels of acceleration. Subjects were exposed to forward acceleration ($+G_X$) on a centrifuge, with onset time of 1 G/sec. Clear areas show control value of O_2 consumption; hatched areas show additional O_2 consumption for 1 min. of acceleration. (Data from Zechman et al., 1959)



MICROCOPY RESOLUTION TEST CHART
NATIONAL BUREAU OF STANDARDS-1963-A

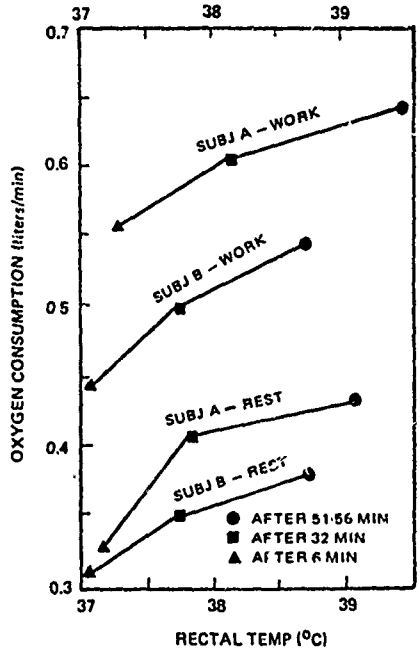


Figure 18–14. Increase in O_2 consumption as body temperature rises during heat exposure, at rest and during the light activity of operating a flight simulator. (Adapted from Jones & Taylor, 1956)

Work Capacity

Although most regular activities are designed to use less than a man's maximum effort, an effort which can be sustained for only a short time, nevertheless in an emergency a man may use his greatest power, and designs of respiratory and cooling equipment must allow for highest peak rates.

Figure 18-15 shows how a man's peak rates depend on the duration of the effort. The harder the effort, the shorter the time for which it can be sustained. For 30 to 60 seconds, men can work against an external load developing a power of around 500 W (about two-thirds of a horsepower), while at the same time, assuming 20 percent efficiency, he will produce excess heat at the rate of 2000 W and burn fuel at the rate of 2500 W (36 kcal/min). Brief periods of maximal exertion, those lasting less than 2 minutes, are done at levels of oxygen demand which cannot be met by the man's capacity to consume oxygen, hence this kind of work is called anaerobic and produces oxygen debt (see figures 18-21 to 18-23). The data shown in figure 18-15 are special in that: (1) the types of work (running, rowing, cycling, and cranking) were chosen to yield highest power, and at efficiencies above 20 percent, and (2) the "healthy men" were young, physically active and fit, and accustomed to doing the work, while the champion athletes were unusual physical specimens highly trained and highly motivated to work at maximum effort.

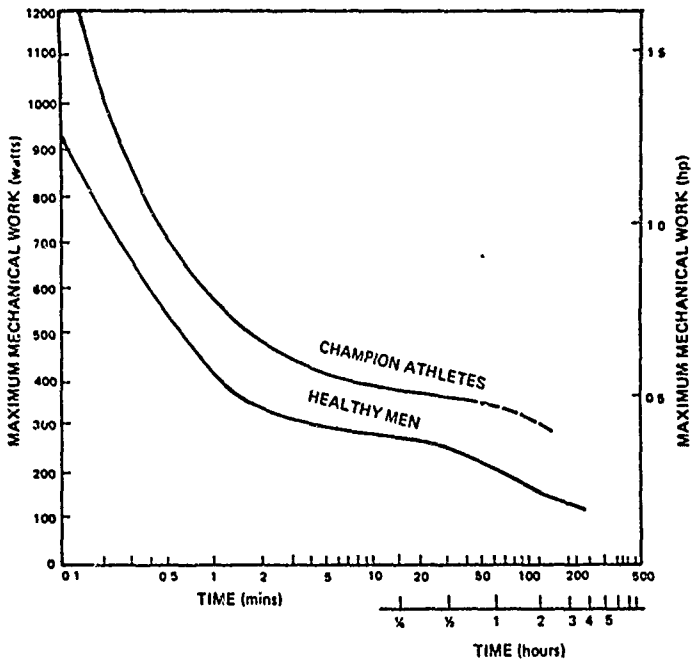


Figure 18–15. Maximum efforts of healthy fit men and champion athletes. (After Fletcher, 1964; from Abbott and Bigland, 1953; Asmussen, 1950; Åstrand, 1952; Bannister & Cunningham, 1954; Benedict & Cathcart, 1913; Benedict & Marschhauser, 1915; Henderson & Haggard, 1925; Nielsen & Hanson, 1937; Robinson, 1938; Wilkie, 1957)

The maximum effort of durations longer than 2 or 3 minutes is limited by a given individual's greatest ability to consume oxygen—his aerobic power. Healthy fit men can consume 50 ml/kg of body weight each minute. Less fit men consume 30 or 40 ml/kg-min. Extremely fit athletes can consume 60 or 70 ml/kg-min, the record figure being 85 ml/kg-min (Saltin & Åstrand, 1967. This maximal oxygen consumption ($\dot{V}_{O_2}$-max) is often used to evaluate the effect of physical conditioning programs.

If one looks at $\dot{V}_{O_2}$-max in men of various ages, it can be seen that this measure reaches its greatest values in the late teens and twenties, then declines slowly as the decades go by. Figures 18-16, 18-17, and 18-18 show mean data of this kind from several studies. These children and men were all healthy, not obese, and reasonably fit. Notice in figure 18-18 that the data are different for different populations. Several comparative studies have been reported, one of which is shown in table 18-6, from Cumming (1967)

Determining a man's $\dot{V}_{O_2}$-max is an important measurement in work physiology. The pure form of the procedure is illustrated in figure 18-19. Note that as work increases, oxygen cost increases until further work loads cause no further increase in $\dot{V}_{O_2}$: 250 W brought the oxygen uptake up to the subject's maximum and 300 W did not further increase the oxygen

uptake. The increased work load was possible thanks to anaerobic processes (maximal aerobic power = 3.5 liters/min).

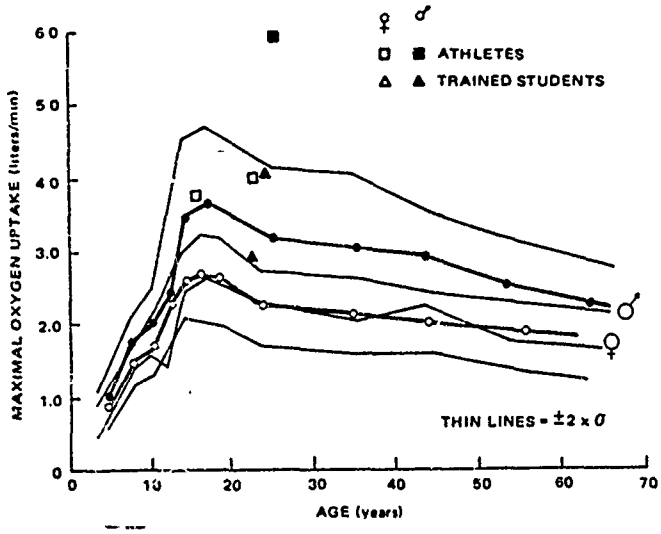


Figure 18–16. Mean values for maximal O_2 uptake during exercise on treadmills or bicycle ergometers in 350 Swedish boys and girls and men and women from 4 to 65 years of age. Included are values for 3 athletes and 86 trained students of physical education. (Redrawn from Åstrand & Rodahl, 1970; used by permission of Pergamon Press, Oxford)

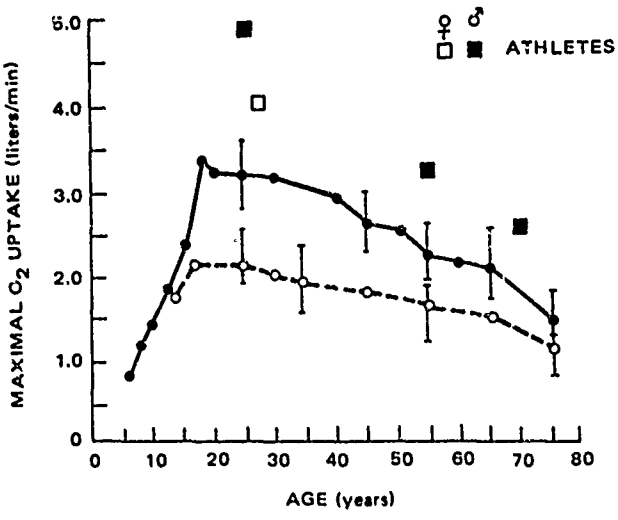


Figure 18–17. Maximal O_2 consumption for German men and women in relation to age, including data from athletes of both sexes. (Redrawn from Astrand & Rodahl, 1970; used by permission of Johann Ambrosius Barth, publisher)

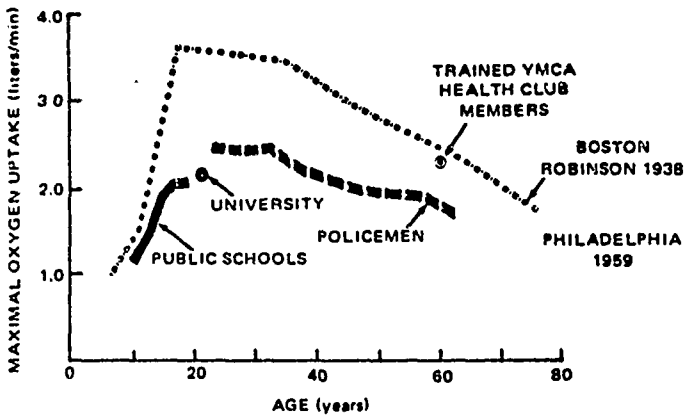


Figure 18–18. Maximal O_2 consumption for American and women in relation to age, from several studies. (Redrawn from Astrand & Rodahl, 1970, by permission of McGraw-Hill Book Company)

Table 18–6

Maximal Oxygen Uptake of Men 20 to 40 Years of Age (Mean Values)

Subjects	Oxygen Uptake (ml/kg – min)
Average Caucasian males	
Stockholm	52
Boston	53
Dallas	45
Norway	44
Winnipeg	44
Army recruits	
U.S.A.	48
South Africa	48
Primitive populations	
Bantu mining recruits	41
Bantu miners	48
Kalahari bushmen	47
U.S.A. Negro sharecroppers	50
Lapps	53
Arctic Indians	49
Eskimos	41
Athletes	
Sweden–physical education students	59
Sweden–athletes	67
Sweden–cross-country skiers	80
Norway–athletes	71
Landy (runner)	77
Winnipeg–water-polo players	53
Winnipeg–track	72

(Cumming, 1970)

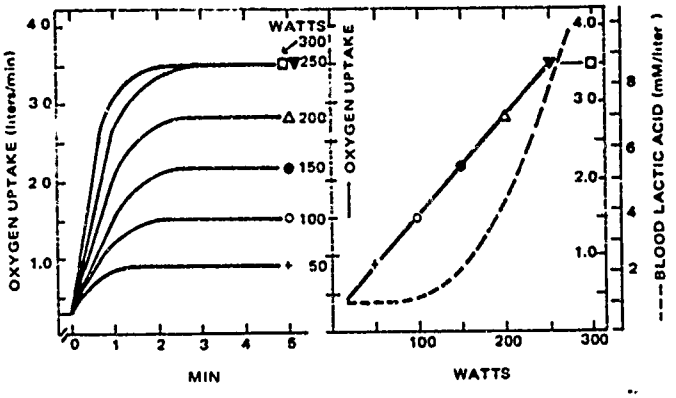


Figure 18–19. Schematic of maximum oxygen uptake ($\dot{V}O_2$ max) determinations. Left: increase in O_2 uptake during exercise on bicycle ergometer with various work loads performed during 5 to 6 min. of work. Right: O_2 uptake after 5 min., plotted in relation to work load. Peak blood lactic acid concentrations for each experiment are included. (Redrawn from Astrand & Rodahl, 1970; used by permission of McGraw-Hill Book Company)

The effect of physical conditioning programs on untrained but otherwise healthy men is to increase their $\dot{V}O_2$-max by 10 to 20 percent, as shown in figure 18-20. Notice also that a trained person can endure a prolonged period of work at a greater proportion of his maximum capacity than can an untrained person.

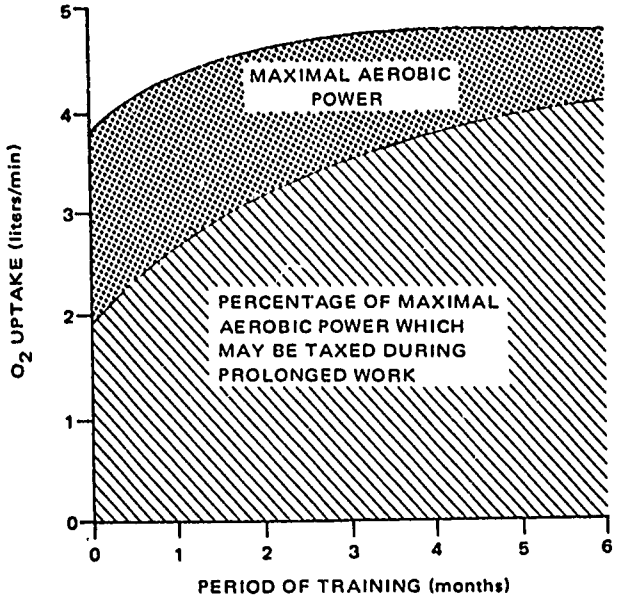


Figure 18–20. Effect of training on maximal O_2 uptake. With training, subject is also able to use a greater percentage of his maximal O_2 uptake during prolonged work. (Redrawn from Astrand & Rodahl, 1970, by permission of McGraw-Hill Book Company)

It seems reasonable to suppose that quite sedentary, hence unfit, people could show greater than 20 percent changes in $\dot{V}O_2$-max following a physical conditioning program. An example is given by Rodahl and Issekutz (1962), who observed a 25 percent change in women who trained by skipping rope daily for 4 weeks. Saltin et al. (1968) reported a 33 percent increase in three sedentary young men who trained vigorously for 55 days, while two other men who were previously active showed little change in $\dot{V}O_2$-max from the same program.

Anaerobic Work

If $\dot{V}O_2$-max data are compared with the maximum power data from figure 18-19, converting watts of external work into $\dot{V}O_2$ (assuming 25 percent efficiency), then the high rates of heat production in efforts lasting less than 1 minute show heat production above 20 kcal/min at an apparent oxygen cost of more than 4 liters per minute. These call for oxygen at rates greater than a healthy man's ability to consume oxygen. He is working anaerobically. For brief maximal efforts lasting only up to 1 or 2 minutes, his muscles get energy by splitting energy rich phosphates and glycogen, as contrasted with the aerobic oxidation of carbohydrates and fat used in the muscle work which can be sustained for 10 minutes or more.

At the beginning of hard work, circulation and oxygen supply increase exponentially, hence some of the work is anaerobic and an oxygen deficit occurs. After the work, oxygen consumption decays exponentially, and the excess oxygen is used to oxidize the end products of anaerobic glycolysis, e.g., lactic acid. Figure 18-21 shows acquisition of oxygen deficit early in hard work and its repayment (oxygen debt) after the work is finished.

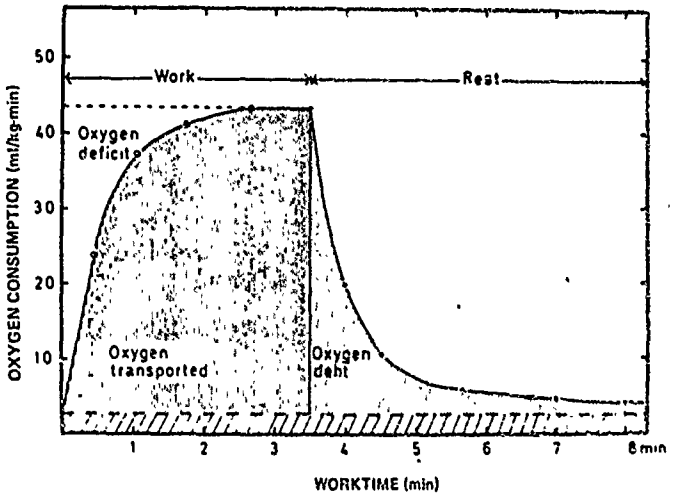


Figure 18-21. Stylized presentation of O_2 uptake during strenuous but submaximal work for 3-1/2 min., followed by the O_2 uptake during recovery. Note that the work has an O_2 cost of 43 ml/kg-min, but that this level of O_2 consumption is reached exponentially (cf. table 18–3 and figure 18–8), so that there is an O_2 deficit before the final value is reached, paid back during recovery period. (Hermansen, 1969; used with permission)

The highest values for oxygen debt are found when a maximum (exhausting) effort is made over a 2 or 3 minute period. Figure 18-22 shows oxygen debt as a function of work load, and figure 18-23 shows the course of oxygen consumption, oxygen debt, and lactic acid accumulation during a maximal effort lasting 3 minutes.

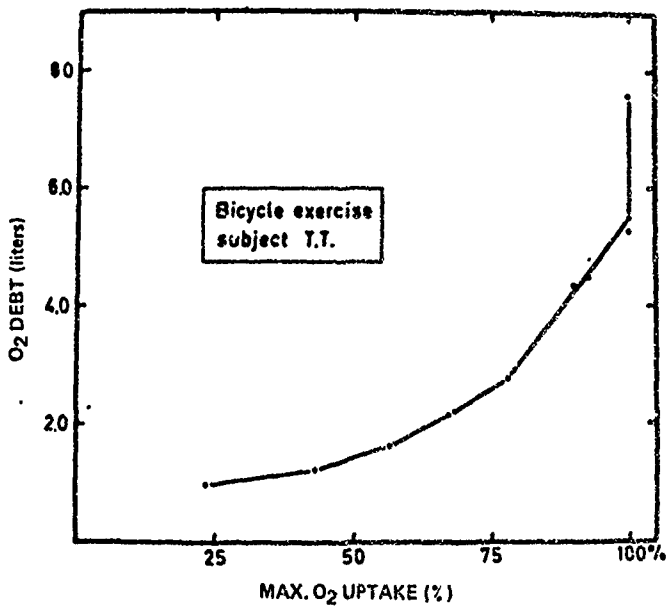


Figure 18–22. O_2 debt increasing as the work becomes more severe, expressed as percentage of subject's maximal O_2 uptake. (Hermansen, 1969; used with permission)

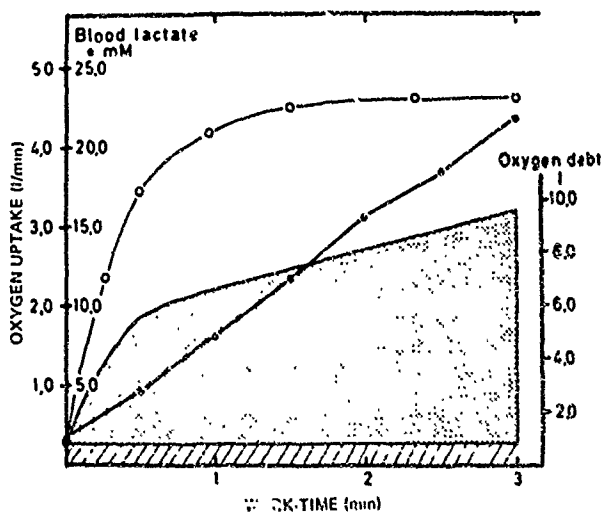


Figure 18–23. Cumulative increases in O_2 debt and lactic acid in the blood, shown during a maximal work effort lasting 3 minutes. (Hermansen, 1969; used with permission)

Working in Space Suits

While ordinary clothing is no great burden, there is sizable extra effort involved in moving about and working in a pressurized space suit. Roth (1966) prepared a thorough analysis of this problem, as well as the mechanics of gait, the effects of variations in terrain, and the probable effect of walking in one-sixth gravity. Table 18-7 gives figures for the primary problem, the added metabolic cost (oxygen cost) of normal activities in space suits.

Table 18–7

Metabolic Cost of Space Suits
(Worn in 1 g in 1 Atm Pressure)

Activity	Heat Production	
	kcal/min	watts
Walking on treadmill at 1.6 km/hr (0.8 mph)		
Light clothing	2.2	152
Space suit unpressurized	3.6	252
Space suit pressurized at 180 mm Hg (3.5 psi)	6.4	445
Space suit pressurized at 258 mm Hg (5.0 psi)	7.7	592
Sitting in spacecraft mockup operating switches every 5 sec		
Space suit unpressurized	1.8	123
Space suit pressurized at 180 mm Hg (3.5 psi)	2.5	173

(Adapted from LaChance, 1964)

Data on the energy cost of moving at various speeds in Earth gravity and a simulated lunar gravity of 1/6 g are summarized in figure 18-24. This figure shows clearly that a pressurized space suit makes walking a strenuous exercise, and that walking speeds above 2 to 3 km/hr (1.2 to 1.9 mph) are probably too difficult to maintain for long. However, by the various techniques used for simulating the 1/6 g lunar gravity, it appears that progression across the moon's surface at 5 km/hr (3 mph) should be possible at reasonable cost. Further details may be found in Wortz et al. (1969) and Robertson and Wortz (1970).

Actual experience with lunar progression in Apollo 11 and 12 confirmed that the astronaut can move about without high metabolic cost. Various hopping and bouncing movements were devised to replace the usual earthly stride. During one 20-minute period late in Apollo 11, Astronaut Neil Armstrong showed a heart rate of 140 to 150 as he hurried to complete a collection of surface samples, but generally the heart rates of the four men who worked on the moon in these missions were 90 to 110 beats/min, which indicates relatively low effort.

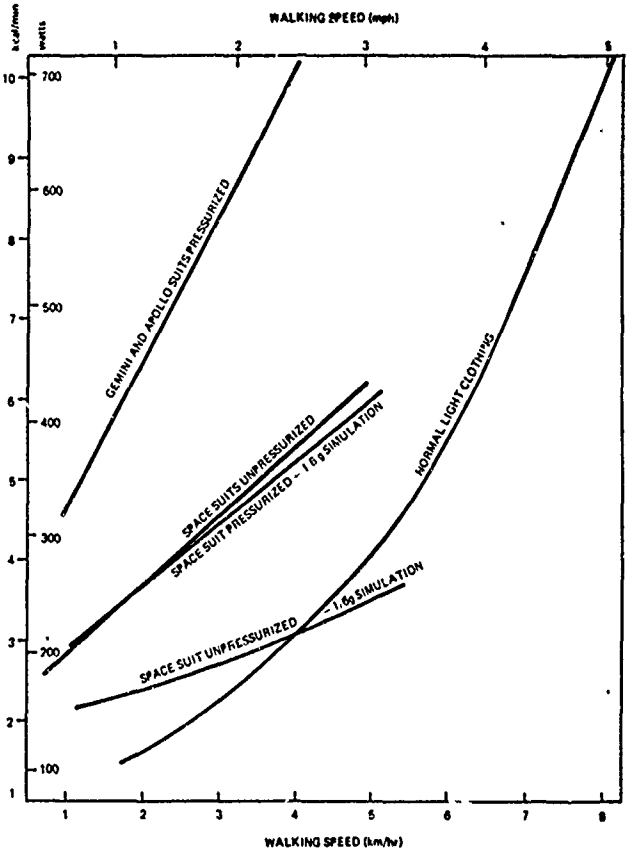


Figure 18–24. Energy expenditure for walking in space suits at various speeds, based on O_2 consumption measurements in laboratory and in simulators which partially produce effects of lunar gravity (1/6 g). (Data from Hewes, 1967; Kincaide, 1966; Robertson & Wortz, 1968)

Energy exchange data are available from the Apollo 11 mission. They are based on three different observations–heart rate, oxygen depletion from a portable reservoir, and temperature data from the water cooled garment worn under the space suit. These data are shown in figures 18-25 and 18-26.

Berry (1970) suggests that the energy data from analysis of the water cooled garment are the most reliable of the three measurements. The technique is close to direct calorimetry, and the data are similar to those shown in figures 18-6, 18-7, and 18-9 earlier in this chapter.

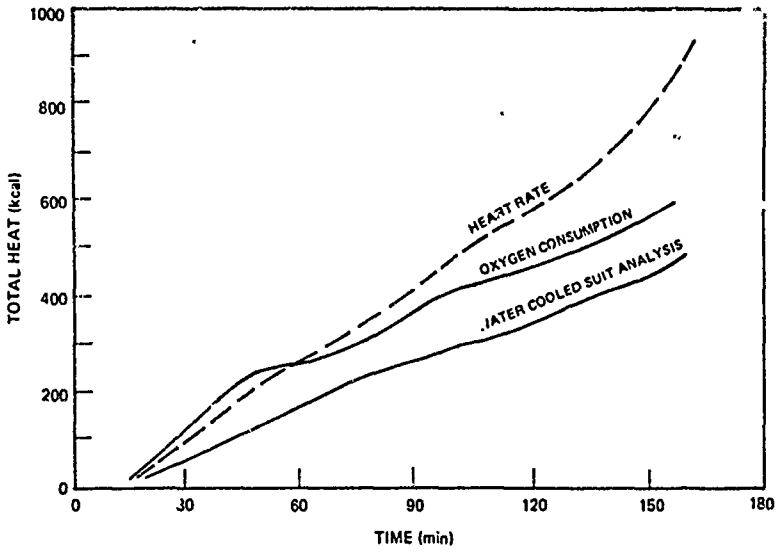


Figure 18–25. Cumulative totals of heat produced in walking and working on the moon for Apollo 11 commander, showing three simultaneous estimates from analyzing temperature data from water cooled suit, from depletion of O_2 from storage cylinder, and from known heart rate response of this man as a function of O_2 consumption. (Redrawn from Berry, 1970)

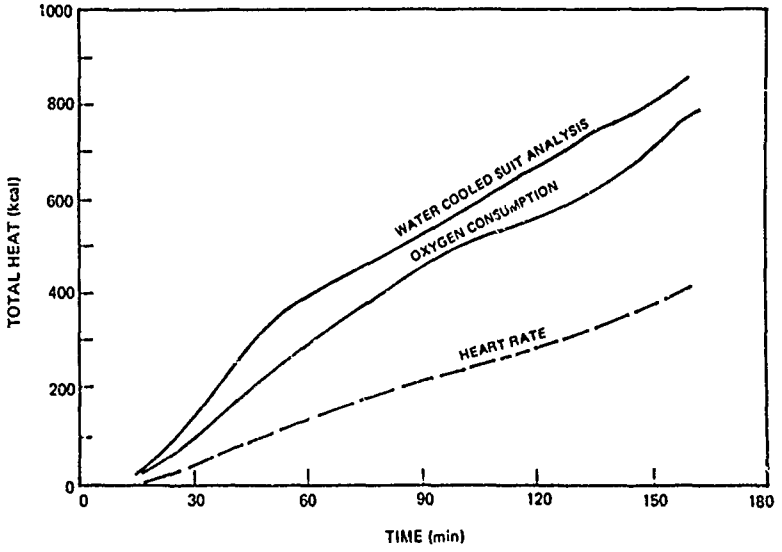


Figure 18–26. Data similar to those in figure 18–25, for the lunar module pilot, during his time on the lunar surface. (Redrawn from Berry, 1970)

References

Abbot, B. C., & Bigland, B. The effects of force and speed changes on the rate of oxygen consumption during negative work. *Journal of Physiology*, 1953, *120*, 319-325.

Altman, P. L., & Dittmer, D. S. (Eds.) *Metabolism*. Bethesda, Maryland: Federation of American Societies for Experimental Biology, 1968.

Altman, P. L., Gibson, J. F., Jr., & Wang, C. C. Handbook of respiration. WADC TR 58-352, Aero Medical Laboratory, Wright Air Development Center, Wright-Patterson AFB, Ohio, August 1958.

Asmussen, E. Blood pyruvate and ventilation in heavy work. *Acta Physiologica Scandinavica*, 1950, *20*, 133-136.

Åstrand, P.-O. *Experimental studies of physical working capacity in relation to sex and age*. Copenhagen: Ejnar Munksgaard, 1952.

Åstrand, P.-O. & Rodahl, K. *Textbook of Work Physiology*. New York: McGraw-Hill, 1970.

Bannister, R. G., & Cunningham, D. J. C. The effects on the respiration and performance during exercise of adding oxygen to the inspired air. *Journal of Physiology*, 1954, *125*, 118-137.

Benedict, F. G., & Cathcart, E. P. Muscular work. A metabolic study with special reference to the study of the human body as a machine, Publication No. 187, Carnegie Institute, Washington, D.C., 1913.

Benedict, F. G., & Murschhauser, H. Energy transformations during horizontal walking. Carnegie Institute, Washington, D.C., 1915.

Benzinger, T. H., & Kitzinger, C. Gradient layer calorimetry and human calorimetry. In J. D. Hardy (Ed.), *Temperature: Its measurement and control in science and industry*. Vol. III, Part 3, Chapter 9, Biology and medicine. New York: Reinhold Publishing Corp., 1963.

Berry, C. A. Summary of medical experience in the Apollo 7 through 11 manned spaceflights. *Aerospace Medicine* 1970, *41*, 500-519.

Berry, C. A., & Catterson, A. D. Pre-Gemini medical predictions versus Gemini flight results. Gemini Summary Conference, NASA SP-138. National Aeronautics and Space Administration, Washington, D.C. 1967, pp. 197-218.

Billings, C. E., Jr., Johnson, P. K., Hoover, G. N., & Mathews, D. K. The effect of moderate altitude on exercise. Report No. 1, Aviation Medicine Research Laboratory, The Ohio State University, Columbus, Ohio, 1962.

Buskirk, E. R., Iampietro, P. F., Welch, B. E., & Marcinek, J. G. Caloric intake and energy expenditure of eight men in a temperate environment. TR EP-52, Hq., Quartermaster Research and Development Command, U.S. Army, Natick, Mass., March 1957.

Buskirk, E. R., Kreider, M., Brebbia, R., Morana, N., Danicis, F., Welch, B. E., Mann, J. B., Insull, W., Jr., & Friedmann, T. E. Caloric intake and energy expenditure in a subarctic environment. TR EP-83, Hq., Quartermaster Research and Development Command, U.S. Army, Natick, Mass., March 1956.

Cathcart, E. P., Richardson, D. T., & Campbell, W. On the maximum load to be carried by the soldier. *Journal of the Royal Army Medical Corps*, 1923, *40*, 443, and *41*, 12-24, 87-98, and 161-178.

Christensen, E. H. *Ergonomics research society symposium on fatigue*. London: H. K. Lewis, Ltd., 1953.

Christensen, E. H., & Hogberg, P. Physiology of skiing. *Arbeitsphysiologie*, 1950, *14*, 292.

Consolazio, C. F., Johnson, R. E., & Pecora, L. J. *Physiological measurements of metabolic functions in man*. New York: McGraw-Hill, 1963.

Consolazio, C. F., Pollack, H., & Crowley, L. V. Studies on nutrition in the Far East. V., Calorie cost of work and energy balance studies. *Metabolism*, 1956, *5*, 259-271.

Cumming, G. R. Current levels of fitness. *Journal of the Canadian Medical Association*, 1967, *96*, 868-877.

Diem, K. (Ed.) *Documenta geigy scientific tables.* (6th ed.) Ardsley, N.Y.: Geigy Pharmaceuticals, 1962.

Edholm, O. G., & Fletcher, J. G. The energy expenditure and food intake of individual men. *British Journal of Nutrition*, 1955, *9*, 286-300.

Fletcher, J. G. Daily energy expenditure in young men. Ph. D. thesis, University of London, January 1958.

Fletcher, J. G. Section 10, Energy costs. In P. Webb (Ed.), *Bioastronautics data book.* NASA SP-3006. Washington, D.C.: National Aeronautics and Space Administration, 1964.

Food and Agriculture Organization of the United Nations. Calorie requirements. Report of the second committee on caloric requirements, FAO nutritional studies No. 15, Rome, 1957.

Gaeuman, J. V., Hoover. G. N., & Ashe, W. F. Oxygen consumption during human vibration exposure. *Aerospace Medicine*, 1962, *33*, 469-474.

Garry, R. C., Passmore, R., Warnock, G. M., & Durnin, J. V. G. A. Studies on expenditure of energy and consumption of food by miners and clerks, Fife, Scotland, 1952. Special report series No. 289, Medical Research Council, Her Majesty's Stationery Office, London, 1955.

Glasow, W., & Müller, E. A. *Arbeitsphysiologie*, 1951, *14*, 319-321.

Goldman, R. F., & Iampietro, P. F. Energy cost of load carriage. *Journal of Applied Physiology*, 1962, *17*, 675-676.

Henderson, Y., & Haggard, H.W. The maximum of human power and its fuel. *American Journal of Physiology*, 1925, *72*, 264-282.

Hermansen, L. Anaerobic energy release. *Medicine and Science in Sports*, 1969, *1*, 32-38.

Hewes, D. E. Analysis of self-locomotive performance of lunar explorers based on experimental reduced-gravity studies. NASA TN-D-3934, National Aeronautics and Space Administration, Washington, D.C., May 1967.

Iampietro, P. F., Vaughan, J. A., MacLeod, A. R., Welch, B. E., Marcinek, J. G., Mann, J. B., Grotheer, M. P., & Friedemann, T. E. Caloric intake and energy expenditure of eleven men in a desert environment. TR EP-40, Hq., Quartermaster Research and Development Command, Natick, Mass., October 1956.

Jones, R., & Taylor, C. L. Metabolic effects of work and heat in a simulated pilot's task. WADC TR 56-2, Aero Medical Laboratory, Wright Air Development Center, Wright-Patterson AFB, Ohio, April 1956.

Kark, R. M., Croome, R. R. M., Cawthorpe, J., Bell, D. M., Bryans, A., MacBeth, R. J., Johnson, R. E., Consolazio, C. F., Poulin, J. L., Taylor, F. H. L., & Cogswell, R. C. Observations on a mobile Arctic force. The health, physical fitness, and nutrition of Exercise "Musk Ox"—February-May, 1945. *Journal of Applied Physiology*, 1948, *1*, 73-92.

Karpovich, P. V. *Physiology of muscular activity.* (4th ed.) Philadelphia: W. B. Saunders, 1953.

Karvonen, M. J., & Turpeinen, O. Consumption and selection of food in competitive lumber work. *Journal of Applied Physiology*, 1954, *6*, 602-612.

Kincaide, W. C. In Apollo Lunar Symposium. NASA Manned Spacecraft Center, Houston, Texas, 1966. Pp. 25-27.

Kleiber, M. *The fire of life: An introduction to animal energetics.* New York: Wiley, 1961.

LaChance, P. A. Nutrition and stresses of short term space flight. In: Conference on Nutrition in Space and Related Waste Problems, NASA SP-70, National Aeronautics and Space Administration, Washington, D.C., 1964. Pp. 71-78.

Lawton, R. W. Food reserves on space trips. Paper 42, Proceedings of XIth International Astronautical Congress, Stockholm 1960.

Lehninger, A. L. *Bioenergetics: The molecular basis of biological energy transformations.* New York: W. A. Benjamin, 1965.

Littell, D. E., & Joy, R. J. T. Energy cost of piloting fixed- and rotary-wing aircraft. *Journal of Applied Physiology*, 1969, *26*, 282-285.

Luthman, G., & Lundgren, N. Studies of working methods in Swedish forestry. In Proceedings of VIIIth International Management Congress, Stockholm, 1947.

Margaria, R., Ceretelli, P., Aghemo, P., & Sassi, G. Energy cost of running. *Journal of Applied Physiology*, 1963, *18*, 367-370.

Maxfield, M. E., & Smith, P. Abbreviated methods for the measurement of oxygen consumption in work physiology. *Human Factors*, 1967, *9*, 587-594.

Mayer, J. Exercise and weight control. In: Exercise and fitness. A collection of papers presented at the Colloquium on Exercise and Fitness, University of Illinois College of Physical Education and The Athletic Institute, Monticello, Illinois, December 1959.

Morehouse, L. E., & Cherry, R. B. Energy cost of progression. Harvard Fatigue Laboratory report to the National Academy of Sciences Committee on Quartermaster Problems, July 1945.

Morehouse, L. E., & Miller, A. T., Jr. *Physiology of exercise*, (3rd ed.) St. Louis: C. V. Mosby Co., 1959.

Nielsen, M., & Hanson, O. Maximale körperliche arbeit bei atmung O_2-reich luft. *Skandinavian Archives of Physiology*, 1937, *76*, 37.

Passmore, R., & Durnin, J.V.G.A. Human energy expenditure. *Physiological Reviews*, 1955, *35*, 801-839.

Passmore, R., Thomson, J. G., & Warnock, G. M. A balance sheet of the estimation of energy intake and energy expenditure as measured by indirect calorimetry, using the Kofranyi-Michaelis calorimeter. *British Journal of Nutrition*, 1952, *6*, 253-264.

Pollack, H., French, C. E., & Berryman, G. H. Calories expended in military activities. *Bulletin of the U.S. Army Medical Department*, 1944, *74*, 110-114.

Pugh, L. G. C. E. Muscular exercise on Mount Everest. *Journal of Physiology*, 1958, *141*, 233-261.

Ramzin, S. Study of the energy balance in soldiers of the Yugoslav Army. *Vojno-Sanit. Pregled.*, 1948, *5*, 131-144.

Richardson, D. T., & Campbell, W. Report on the investigation of the energy expenditure of the British soldier in India. Government of India Press, Calcutta, 1927.

Rjabko, N. A., & Agapov, N. I. Experiences in organizing control of physical condition and feeding in the forces. *Vojenno-medicinskij Zurnal*, 1947, *10*, 3-6.

Robertson, W. G., & Wortz, E. C. Effect of lunar gravity on metabolic rates. *Aerospace Medicine*, 1968, *39*, 799-805.

Robertson, W. G., & Wortz, E. C. Evaluation of the metabolic cost of locomotion in an Apollo space suit. NASA CR-102154, National Aeronautics and Space Administration, Washington, D.C., 1970.

Robinson, S. Experimental studies of physical fitness in relation to age. *Arbeitsphysiologie*, 1938, *10*, 251-323.

Rodahl, K., & Issekutz, B., Jr. Physical performance capacity of the older individual. In K. Rodahl & S. M. Horvath (Eds.) *Muscle as a tissue*. New York: McGraw-Hill Book Co., Inc., 1962.

Rose, M. S. *The foundations of nutrition*. (4th ed.) London: Macmillan, 1944.

Roth, E. M. Bioenergetics of space suits for lunar exploration. NASA SP-84, National Aeronautics and Space Administration, Washington, D.C., 1966.

Saltin, B., & Åstrand, P. O. Maximal oxygen uptake in athletes. *Journal of Applied Physiology*, 1967, *23*, 353-358.

Saltin, B., Blomquist, G., Mitchell, J. H., Johnson, R. L., Jr., Wildenthal, K., and Chapman, C. B. Response to exercise after bedrest and after training. *Circulation*, 1968, *38*, Supplement 7.

Shephard, R. J. A nomogram to calculate the oxygen-cost of running at slow speeds. *Journal of Sports Medicine and Physical Fitness*, 1969, *9*, 10-16.

Turner, D. The energy cost of some industrial operations. *British Journal of Industrial Medicine*, 1955, *12*, 237-239.

U.S. Navy, Bureau of Medicine and Surgery. Submarine medical practice. Washington, D.C., 1956.

Webb, P., Metabolic heat balance data for 24-hour periods. *International Journal of Biometeorology*, 1971, *15*, 151-155.

Webb, P., & Annis, J. F. Cooling required to suppress sweating during work. *Journal of Applied Physiology*, 1968, *25*, 489-493.

Webb, P., Annis, J. F., & Troutman, S. J., Jr. Human calorimetry with a water-cooled garment. *Journal of Applied Physiology*, 1972, *33*, 412-418.

Webb, P., Troutman, S. J., Jr., & Annis, J. F. Automatic cooling in water cooled space suits. *Aerospace Medicine*, 1970, *41*, 269-277.

Weir, J. B. deV. New methods for calculating metabolic rate with special reference to protein metabolism. *Journal of Physiology*, 1949, *109*, 1-9.

Welch, B. E., Morgan, T. E., Jr., & Ulvedal, F. Sealed cabin experimentation. *Journal of Agricultural Research Service*, 1961, *31*, 1541-1544.

Wilkie, D. R. The production of mechanical work by man. MAPAC Communication, (England) 1957.

Wortz, E. C., Robertson, W. G., Browne, L. E., & Sanborn, W. G. Man's capability for self-locomotion on the moon. Vol. I, Detailed report, NASA CR-1402. Vol. II, Summary report, NASA CR-1403, National Aeronautics and Space Administration, Washington, D.C., 1969.

Zechman, F. W., Cherniak, N. S., & Hyde, A. S. Ventilatory response to forward acceleration. WADC TR 59-584, Aerospace Medical Laboratory, Wright Air Development Center, Wright-Patterson AFB, Ohio, September 1959.

CHAPTER 19
COMBINED ENVIRONMENTAL STRESSES

by

Raymond H. Murray, M.D.
Indiana University School of Medicine

and

Michael McCally, M.D., Ph.D.
Aerospace Medical Research Laboratory
Wright-Patterson Air Force Base

Man lives and functions in a physical environment that includes thermal, electromagnetic, and mechanical energies as well as chemical agents which affect the function of his body. In certain life situations and occupations, the physical environment may produce significant subjective responses, or strain. The energies and agents responsible for these effects are referred to as environmental stresses. Many environmental stresses, such as altitude, temperature, acceleration, vibration, noise, hypoxia, and radiation have been well studied in the laboratory and are the classic subject matter of environmental physiology. In most instances, a single environmental stress is studied as a controlled dependent variable in a specialized laboratory facility. Yet in normal circumstances, one rarely experiences exposure to a single environmental stress, but rather to an intricate interplay of several stresses. An astronaut is especially likely to experience complex environmental interactions. During reentry, he may be exposed to vibration which may alter his visual acuity; his visual performance might also be affected by simultaneous exposure to acceleration, noise, heat, and hyperoxic breathing gas mixtures, as well as prior exposure to the deconditioning effects of prolonged confinement, inactivity, and weightlessness.

Relatively few laboratory studies have described the tolerance levels, physiological effects, or performance degradation during simultaneous or sequential exposures to two environmental stresses, and fewer still have involved three or more simultaneous stresses. The available literature on combined environmental stress is summarized and discussed in this chapter. Although a

Reviewed by John P. Meehan, M.D., University of California School of Medicine.

Preceding page blank

moderately large bibliography on combined stress can be accumulated, few studies have actually been addressed to the question of combined stress *interactions* (Broadbent, 1963; Dean & McGlothlen, 1964). Most studies of combined environmental stress are accidents of experimental design or are concerned with ancillary problems.

A number of obvious factors have limited the study of combined environmental stress in spite of the obvious operational importance of such work. First, experimental design is exceedingly complex. The possible number of combinations and permutations of even a small set of environmental stresses is very large. Economy dictates that one select for study in the laboratory only stress combinations of particular scientific interest and relevance to a given mission, occupation, or life style. Second, this type of research requires complex experimental facilities not generally available. Finally, to assure valid conclusions, large numbers of subjects are required.

This chapter is limited to laboratory or exceptionally well-defined field studies. A number of studies of "combined stress" are available that report subject responses in an operational or field situation. The inflight data for astronauts is a case in point. These data describe the physiological responses of men exposed to a combination of weightlessness, confinement, noise, hyperoxia, radiation, and various acceleration forces. Unfortunately, in the operational setting, appropriate experimental design and controls are usually not possible, so that a response (decrease in red cell mass, for example) must be taken as a response to the environment as a whole. It is rarely possible to know which stress, or which combination of stresses, is responsible for the observed response. Operational or field studies may be useful to measure accurately the environment and so define the conditions to be simulated and studied in the laboratory. Such studies may also point up stress combinations of operational concern and thereby complement laboratory work. However, the majority of operational or field studies of environmental stress must be excluded from a consideration of combined stress interactions. Stress interaction, at present, can only be examined in specific laboratory situations where the necessary experimental design can be applied and tight control of conditions assured.

Combined Stress Interactions

The underlying hypothesis of combined stress research is that environmental factors interact in a systematic fashion which can be measured and/or predicted.

Characterization of Interaction

Environmental stress combinations may be characterized by four descriptors: (1) order of occurrence, (2) duration of exposure, (3) severity of exposure, and (4) type of interaction.

Order of Occurrence. Definitions of the pattern or temporal order of exposure to combined stresses are straightforward. Stresses are *simultaneous* when two or more stresses are applied concurrently; they are *sequential* when applied in order, one after another. Note that differing sequences may give

different effects, and that the rate and duration of intermittency will sometimes alter effects. Stresses are *complex* when the pattern of application is not clearly simultaneous or sequential; this includes combinations that are both simultaneous and sequential, time varying, intermittent patterns, and other complex profiles.

Duration of Exposure. Arbitrary definitions and categorizations of combined stress durations cannot be made because of the complexities of the individual stresses as well as their interactions. The following functional definitions are suggested. Stresses may be referred to as *transient* when a steady-state subject response is never achieved or where physiological compensatory mechanisms are inadequate. The term *sustained* applies when a steady state is achieved and compensation is adequate. This refers to exposures of generally less than 24 hours. It must be understood that certain physiological responses to environmental stress, and probably to interactions involving these stresses, may take much longer periods to achieve a steady state; for example, acclimatization to heat and altitude. The term *chronic* denotes exposures lasting longer than 24 hours and includes continuing day-to-day exposures, such as occupational stresses.

Severity of Exposure. The determination of the severity or intensity of combined stress exposure is complicated by differing and often incompatible units of measurement of subject response. Such measurements must begin with the identification of an appropriate index (or indices) of body response, or strain. Subjective assessment can also be used as a quantitative measure of stress response. In this case, the subject is asked to describe how severe the environment was, using descriptors such as noticeable, mild, moderate, severe, very severe, and intolerable. Although simple in concept, such data are often of great utility and considerable validity. Stevens (1951) has shown that reliable and valid scales, particularly ratio scales, can be derived as a result of subjective assessment. The Cooper pilot opinion rating scale of aircraft handling and ride quality is an excellent example of the value of the subjective rating scale (Cooper, 1957). Modifications of this technique may be an important tool with which to rank the relative severity of combined stress environments. The use of criteria based upon diminished ability to perform a particular task which is relevant to the mission under study is also a particularly sensitive and useful index of response.

Type of Interaction. Environmental stresses may, hypothetically, interact in three general ways. When stresses act by *addition*, the physiological effect of a combination of environmental stresses is equal to the linear sum of the single effects of the stresses when presented separately. When *synergism* is involved, the effect of the combination is greater than the simple sum of the effects of each stress alone. *Antagonism* provides a total effect which is less than the linear sum of the single effects. Dean and McGlothlen (1964) describe in detail the complexities of the analysis of such interactions, including the use of analysis of variance models.

The criteria used to define a stress effect or endpoint must always be specified. A combination of stressors that is synergistic by one criterion might be

antagonistic by another. For example, $+G_z$ acceleration and G_y rotation might be synergistic or additive with regard to heart rate but antagonistic with regard to peripheral light loss. Antagonistic interactions should be considered for the development of new protective devices.

The definitions of the words interactive and additive are tied to experimental design and analysis. For example, using three stresses, altitude (A), noise (N), and heat (H), assume the likely use of an experimental design based on Analysis of Variance (ANOVAR).

ADDITION

$$E_A, N, H = E_A + E_N + E_H$$

SYNERGISM

$$E_A, N, H, > E_A + E_N + E_H$$

ANTAGONISM $< E_A, N, H$

E_A, N, H

Where:

E_A, N, H = Total effect of altitude, heat, noise

E_A = effect altitude alone

E_N = effect noise alone

E_H = effect of heat alone

Such a hypothetical ANOVAR model (after Dean & McGlothlen, 1964) implies that a set of scores by a single subject will be made up of the grand mean, the three main effects of the individual stresses, four interaction terms, and an error term. Groups of subjects and time or order are additional sources of variance and add additional terms to the equation. The hypothesis of additivity is checked by testing the interaction terms of the ANOVAR model for statistical significance. ANOVAR assumes additivity, and, if this assumption is met, the interaction effects will be zero, that is, there will be no interaction. Thus, in an ANOVAR model, when addition of effects is present, there is no interaction. Presence of statistically significant interaction terms contradicts the addition of effects hypothesis, and the remaining possibilities of synergism or antagonism are tested by examining the effect of the single stresses not in combination.

Tolerance to Combined Stress

In exposure to most environmental stresses, tolerance is defined by certain unique subjective or objective criteria which determine the endpoint of the

exposure; for example, central light loss during $+G_z$ acceleration or rapidly rising body temperature in heat. In general, a review of the available literature (discussed later) suggests that tolerance to a particular stress combination is determined essentially by that stress which, if taken alone, would be the most severe. Rather than define a new tolerance endpoint, it has usually been found easier to ask, "How does a second stress alter the tolerance to a primary stress?" This approach provides a useful construct for organizing the available literature into sets of combined environmental stresses; primarily acceleration, or primarily heat, etc. It is usually possible to ascertain in a combined stress study which stress was the most severe and which stress was the one of primary interest to the authors. The literature review presented in this chapter is organized in this manner.

Interactions of Environmental Stresses with Host Factors

Environmental physiology describes the interaction of physical environments with the subject or host in terms of the response or modification of the host. It is ordinarily understood that the initial condition of the host is that of complete normality: a healthy young adult (male) with average physical characteristics, unacclimatized and physically fit, rested, relaxed, lightly clothed, unrestrained, without protective equipment, drugs or other countermeasures, and without task assignments. In real life situations, this is rarely the case, and in space missions, few, if any, of these conditions may obtain. However, any deviation from this "normal" state will modify the host and potentially alter, and perhaps determine, the effects of environmental stress. It is important to separate clearly what factors are considered to reside in the host. For example, exercise, though often considered to be an environmental stress, is in fact a subject state or host factor. Exercise is part of a continuum of activity ranging from strict inactivity, as in plaster cast immobilization, to maximal rhythmic exertion. Other factors often considered environmental stresses, but which should be considered host factors, are changes in blood or body fluid volume, change in sleep pattern, and changes in mental set, as in anxiety. The distinction between host and environmental factors are necessary for a correct definition of the subject matter of combined environmental stress.

The subject or host can be represented as the summation of all the physiological and psychological factors which are relevant to the environmental conditions under consideration. The descriptors in figure 19-1 are a set of factors which must be defined to characterize the host. Some of these are relatively fixed, such as height, weight, and age. Others, such as physiological, psychological, and social factors, may vary over wide ranges and profoundly alter the response of the human organism to its environment.

Of special importance for space flight problems is "task loading," which includes all of those demands for sensory, higher mental, and motor performance required for a particular mission. The requirement to perform a complex maneuver in a high performance vehicle while responding to multiple communication channels and simultaneously monitoring several visual displays, for example, may alter the response to environmental stress. Task loading is arbitrarily included for the purposes of this discussion under reciprocative

factors. It represents a segment of the continuous interaction between a subject and his environment.

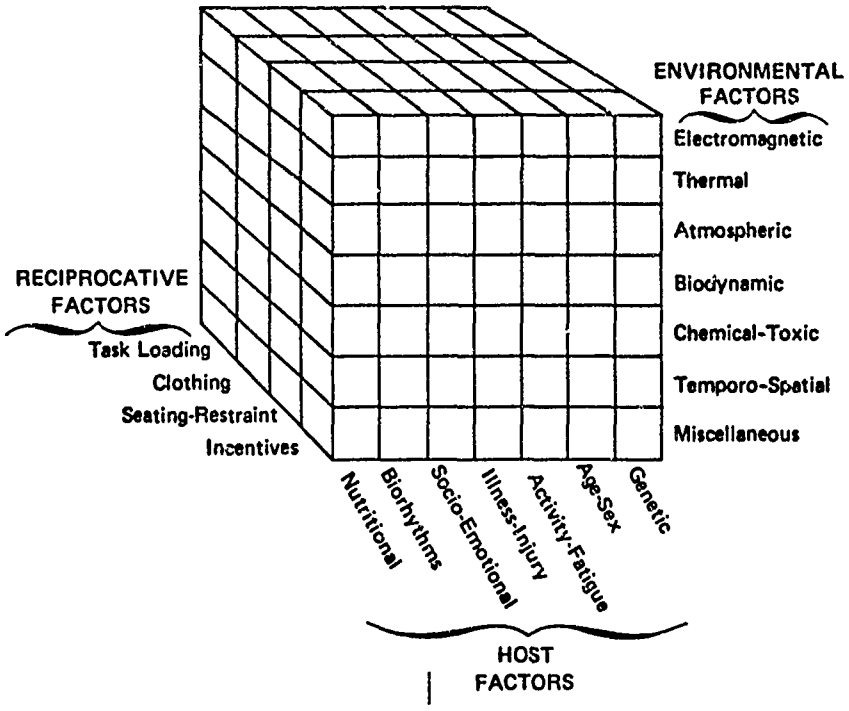


Figure 19–1. Three dimensional representation of the variables which must be controlled or otherwise defined and specified when conducting environmental research. (Modified from Rohles, 1965)

Complexity of the Problem

A study of combined environmental stresses is complex in all its aspects. Definition of each of the environments of concern is sometimes difficult; independent and simultaneous measurements of each environment of the pertinent combination may prove impossible under field conditions. The temperature, humidity, noise, acceleration, and vibration loads to be encountered by the pilot of a particular aircraft on a specific mission are usually not available to either the research scientist or systems designer. The problem of combined environmental stress can only be approached operationally, by studying the specific subsets or combinations which are peculiar to specific mission phases.

A related problem is the limitation of simulator capability. The production of combined stress environments in the laboratory requires the use of complex simulators, available, in general, only in large governmental or industrial facilities. Such facilities are complicated and expensive to operate and limit the scope of potential work in this field. Presently operating combined stress facilities are discussed later.

Another related complexity in the area of combined stress research is the problem of simulation versus representation. For example, a study of heat, noise, and vibration devised to simulate a real vehicle-mission combination would usually generate specific data which are not often representative of the general problem of heat, noise, and vibration. Specificity reduces generalizability. Combined stress studies are generally so large in scope, expensive to conduct, and difficult to replicate that this aspect of the problem becomes very complex. It is obvious that no general body of scientific information about combined stress interactions will develop until relatively nonspecific "representational" simulations are examined.

Another difficult problem in this area is in the selection of measures. A physiological measure appropriate to one environment may be relatively meaningless in another. For example, peripheral light loss, useful in acceleration research, has relatively little meaning in thermal stress. It can be fairly stated that, until a major group of environmental stresses is examined in all possible combinations using the same measures (preferably in the same subjects or comparable populations), no significant progress will be made in combined stress physiology. Only two or three such programs have ever been considered. A closely related problem concerns human performance measures. Do environmental stresses in combination affect the subject's performance more severely than when applied singly? To answer this question, a battery of performance tests is required which is specific, valid, and equally pertinent to a number of stresses. A task which is sensitive and specific for vibration may be insensitive to heat stress. The development of such a performance battery is difficult and apparently has not yet been successfully achieved. Another important problem with the use of performance measures is the variability between and among subjects, which tends to make tests insensitive to small effects. Performance measurements must be developed that relate directly and monotonically to stress intensity, that are generalizable to multiple environments, and that are valid and sensitive measures of operationally relevant tasks. Recent work suggests that certain parameters of a linear human operator model, including the describing function and the remnant term, may represent such measures (Jex & Allen, 1970).

The Use of Models

The use of mathematical and analog models has recently been adapted from engineering practice to the study of physiological systems and offers a number of advantages in handling the complexities involving combined stress studies. Modeling activities allow for the explicit definition of simplifying assumptions of the system in question, incorporate the best available information concerning the system, and, when operated, point out data needed to further refine the model, thereby suggesting new experiments. Good electrical analog models are available for human thermal regulation and for cardiovascular responses to positive acceleration. Attempts to combine such models should allow predictions to be made and hypotheses phrased concerning the interaction of heat and acceleration (particularly on the cardiovascular system). Human psychomotor performance is now being modeled with similar techniques.

Approach to the Study of Combined Environmental Stress

Units

Each environmental stress must be defined and quantified in appropriate measurement units and its pattern and time profile described in detail. A complex environment can sometimes be described by correlating secondary factors with the primary stress, and an integrated unit of stress devised which represents the complete environment. For example, in considering heat stress, temperature can be weighted with humidity and airflow to give an "effective temperature." Unfortunately, practical, comprehensive stress units have not been standardized for most environments.

Simple Relationships

When the effect of an environmental stress is defined in terms of the evoked physiologic response or strain, various degrees of severity of another stress can be evaluated by their effect on the primary stress-strain pattern. These effects can be represented in two general ways.

1. Change in the amplitude of response of the index of strain. For example, an increase in effective temperature of 90°F will be associated with a certain increase of heart rate. Increments of $+G_z$ stress will alter this heart rate response, and the interaction of heat and acceleration can be presented in terms of increments of heart rate above control values. This can also be represented by percent change above control heart rate rise.

2. Alteration of the rate of change of a physiological variable, but not the final amplitude. A temporal relationship can also be shown by demonstrating alteration in time to reach a definitive or arbitrary endpoint; the time-to-peripheral light loss during $+G_z$ stress is shortened as effective temperature increases.

Scaling

Study of the interaction of environments is complicated by the inability to relate the different units and scales used to quantify the various environments. Effects of environmental stress can, however, be added or related to each other quantitatively by appropriate scaling or normalization procedures. Each stress can be represented in terms of the degree of strain or physiologic response it produces in a subject. The scaling of a particular set of environmental stresses is a unique characterization of these individual stresses, and demands the detailed quantification of each environment being considered, and careful definition of the index of strain to be used. Because physiological systems are independent and nonlinear, strain values will hold only for the particular interactions which have been defined.

Choice of Indices of Strain

There are two prime considerations determining the choice of suitable indices of strain for evaluating environmental interactions. First, the

physiological or performance measure to be used must be affected measurably by each of the environments under study. Secondly, the measurement methods must be technically compatible with the constraints imposed by particular conditions in which the study will be carried out. In applied studies, indices would be chosen to provide operationally pertinent information regarding tolerance limits and performance decrements. The indices to be used must be individualized for each environmental interaction and for the test conditions in which the study will be done. Consideration must be given to defining common physiological pathways in the mechanism of action of each stress. This concept is illustrated in figure 19-2. For example, the interaction of heat and vibration can be evaluated by using peripheral vascular responses as well as by changes in respiration, since each environment affects both of these indices. Under space flight conditions, peripheral vascular responses may not be determinable but ventilation changes could be measured accurately. On the other hand, sweat rate would not be a suitable index since it is probably not affected by short-term vibration.

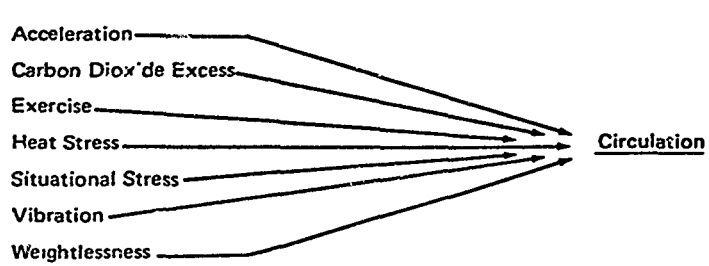
Combined Stress Data

The data on physiological and performance responses of man and animals to combinations of environmental stress which are available in the literature are presented in tables 19-1 through 19-9. In search for an organizing principle, it was felt that in most instances the authors expressed a clear interest in one of the stresses or that one of the stresses was clearly prepotent. For example, Martin and Henry (1951) asked how heat exposure affects $+G_z$ acceleration tolerance, as defined by peripheral light loss. These authors' primary interest in acceleration stress is revealed in their choice of tolerance measures. If interested primarily in heat, they might have used rate of rise of rectal temperature as their criterion; if interested in combined stress effects, they would have chosen both peripheral light loss and rectal temperature responses, and discussed their results with regard to both criteria. For this reason, the tables are organized by reference to the "primary" stress, for example, COMBINED STRESS, PRIMARILY ACCELERATION.

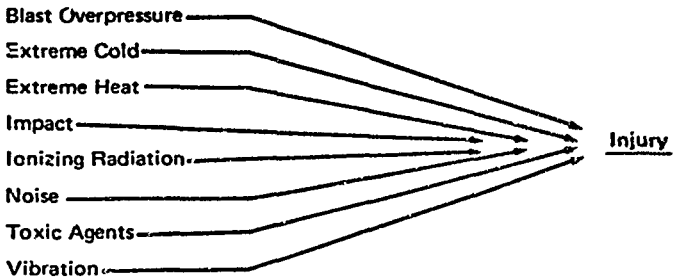
In a subject as complex as this, no literature survey is complete. There is no generally recognized descriptor for combined or multiple environmental stresses. The authors, therefore, urge that, in the future, investigators use the keywords "multiple environmental stresses" or "combined stress" in the title or in the list of index or keywords of any relevant paper. At present, it is impossible to retrieve, by hand or computer, studies dealing with combinations of environmental stresses. For example, heat and acceleration combinations are found by screening references dealing with each stress singly, a large retrieval.

Facilities for Study of Combined Stress

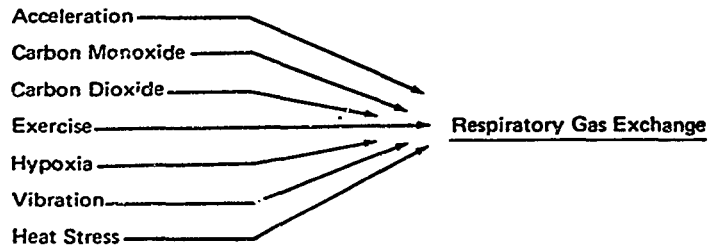
Facilities available in the United States for combined environment simulation have recently been surveyed and reviewed by Tierney (1969). In his article, primary attention is given to engineering tests of systems and hardware. In the last 10 years, Tierney was able to find about 100 papers published on combined



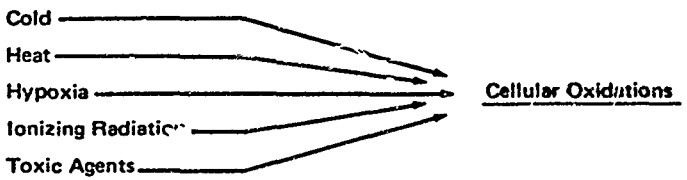
Stresses Which Affect The Circulatory System



Stresses Which Can Produce Injury And Death In Cells And Tissues



Stresses Which Affect The Exchange Of O_2 And CO_2 In The Alveolus



Stresses Which Interfere With Cell Metabolism

Figure 19–2. Common mechanisms of action of selected environmental stress. (Modified from Webb, 1964)

environment testing from numerous facilities throughout the United States. Only a limited number of man-rated or potentially man-rated combined stress facilities are available. All are in government laboratories or in the research divisions of major aircraft companies. A number of single stress human facilities are available to which additional environments have been or could be added. For example, small shakers (vibration devices) have been added to human centrifuges at the National Aeronautics and Space Administration Ames Research Center, the Naval Air Development Center, Johnsville, Pennsylvania, and Deutsches Forschungs und Versuchsanstalt für Luft und Raumfahrt, Bad Godesberg, Federal Republic of West Germany. However, in none of these cases was the original centrifuge arm designed for the added vibration capability, and the shaker forces and displacements on these devices are very limited and well below most human tolerance levels. Many human thermal stress facilities include control of humidity and air motion in addition to temperature and are not included in this enumeration of combined stress facilities. Table 19-10 is a summary of the major combined environmental stress test facilities presently operating in this country.

It must be noted regarding the table that the authors did not conduct a survey, and there may be other facilities with combined stress capabilities unknown to them. To the best of the authors' knowledge, however, only two facilities presently operating were established for the sole purpose of studying combined environmental stress: the Combined Stress Test Facility, Boeing Corporation, Seattle, Washington, and the Dynamic Environment Simulator, Aerospace Medical Research Laboratory, Wright-Patterson Air Force Base, Ohio. These are the only two facilities including moving-base (acceleration and/or vibration) capabilities.

Table 19–1

Combined Stress – Primarily Acceleration

Stresses	Test Animal	Measures	Effect	Interaction	Source
Acceleration and hypoxia	Man	G tolerance (peripheral light loss)	Hypoxia decreases $+G_z$ tolerance	Additive	Burgess (1958), Greeley (1945)
Acceleration (angular) and hypoxia	Man	Nystagmus	Hypoxia causes smaller change in nystagmus than apprehension	None	Newberry et al. (1965)
Acceleration and heat/cold	Man	G tolerance (peripheral light loss)	Heat lowers G tolerance. Cold raises G tolerance	Additive, synergistic	Martin & Henry (1951)
Acceleration and heat	Man	G tolerance (peripheral light loss)	Heat lowers G tolerance	Additive	Burgess (1959)
Acceleration and heat/cold	Mice	Survival rates	High environmental temperature decreases and cold increases the tolerance of mice to positive acceleration	Additive, antagonistic	Chae (1957)
Acceleration (vertical tilt) and heat	Man	Heart rate, forearm blood flow, blood pressure, rectal temperature	Heat lowers tilt table tolerance. Heart rate is higher, blood pressure is lower, and syncope is more common in heat	Additive	Lind, Leithead & McNicol (1968)

Acceleration and cold	Rats	Survival time	Hypothermia (22.5°C) improves tolerance to $+G_z$ at levels of 30 — 40 G	Antagonistic	Stiehm (1963)
Acceleration and heat	Man	Peripheral light loss	Prior heat stress producing minimal dehydration (1 — 3% body weight) decreases acceleration tolerance 15 — 18%	Additive	Taliaferro, Wemper, & White (1965)
Acceleration and dehydration	Man	Peripheral light loss	Prior heat stress producing dehydration decreases acceleration tolerance	Additive	Greenleaf et al. (1966)
Acceleration and hyperoxia	Man	Pulmonary function tests	Breathing 100% O_2 during acceleration does not interact with tolerance but does ameliorate acceleration-induced atelectasis*	Variable	Hendler (1963), Alexander et al. (1966)

*Numerous studies available on this combination. See Gillies et al., (1965)

Table 19–2

Combined Stress – Primarily Vibration

Stresses	Test Animal	Measures	Effect	Interaction	Source
Vibration and acceleration	Man	Whole body mechanical impedance	Vibration (+0.4 G at 2.5 – 20 Hz) combined with linear acceleration (1, 2 1/2, and 4 G) produces increased stiffness, reduces damping, and increases energy transmission to internal organs	Additive	Vykukal (1968)
Vibration and acceleration	Man	Compensatory tracking task	Vibration (0 – +3.0 G at 11 Hz) combined with linear acceleration (1 – 3.5 G) produces performance decrements not significantly different from vibration alone	None	Dolkas & Stewart (1965)
Vibration and heat	Rats	Mortality	Incidence of mortality (62%) is greater after 20 min exposure to heat (46.1°C) and random vibration (5 – 800 Hz 17.5 G RMS) in combination than singly	Additive	Megel et al. (1962)
Vibration and hypoxia	Rats	Mortality	Mortality of restrained rats increases directly with hypoxia (altitude 8 – 18 000 ft) during $+G_x$ vibration (60 Hz 15 G peak acceleration)	Additive	Megel et al. (1963)
Vibration and pressure breathing	Mouse	Mortality, tissue change	Pressure breathing (4 in. H_20) reduces mortality of mice exposed to 10 min of 20 Hz random vibration (7.07 G RMS)	Antagonistic	Brady (1966)
Vibration and acceleration	Man	Visual performance	($+3.85\ G_x$) acceleration improves the visual performance decrement associated with (11 Hz $\pm G_x$) vibration	Antagonistic	Clarke et al. (1965)
Vibration and carbon dioxide	Man	Ventilation	$+G_z$ vibration (40 Hz) and increased inspired CO_2 both increase ventilation but are not additive in combination	None	Young et al. (1965)*

Vibration and noise	Man	Physiological measures, performance	$+G_z$ vibration (semirandom) (.16 — .4 RMSg) and noise (~112 dB) have no significant effect on multiple performance measures or physiological responses in simulated helicopter flight	None	Dean et al. (1964)
Vibration and noise and temperature	Primate, man	Sleep-staged EEG, performance	$+G_z$ vibration (.7 RMS), noise (102 dB), and heat (90°F) in combination produce significant sleep disturbance and performance decrement (shock avoidance)	Not examined	Harris et al. (1971)
Vibration and noise	Man	Performance (compensatory tracking and reaction time)	Noise (100 dB) and vibration (0.25 $+G_z$, 5 Hz) produce additive decrement in vertical component of compensatory tracking task	Additive	Harris & Shoenberger (1970)
Vibration and drugs	Mice	Mortality, tissue damage	Mortality is decreased significantly by CNS depressant and increased by CNS stimulants	Not examined	Ashton & Roberts (1965)

*Selected reference, other studies available on this topic.

Table 19–3

Combined Stress – Primarily Noise

Stresses	Test Animal	Measures	Effect	Interaction	Source
Noise and heat	Man	Performance task battery	Noise (90 dB) and heat (87°ET) produce no significant performance decrement, singly or in combination	None	Viteles et al. (1946)
Noise and heat and sleep deprivation		Performance (tracking and serial reaction)	See table 19–4	Heat and noise – none; noise and sleep deprivation – antagonistic	Broadbent (1963)
Noise and vibration	Man	Performance	See table 19–2		Harris & Shoenberger (1970)
Noise and vibration	Man	Performance, physiological measures	See table 19–2		Dean et al. (1964)
Noise and vibration and heat	Primate	Sleep (EEG), performance	See table 19–2		Harris et al. (1971)
Vibration and noise	Man (adolescent boys)	Sensitivity to vibration	Results vary widely with time of day and work experience with vibration. In general, vibration causes decrease in sensitivity. Exposure to noise and vibration varies but prolonged exposure to both causes a greater decrease in sensitivity	Not examined	Tsyasar (1965)

Table 19–4

Summary of the Effects of Heat, Noise and Sleep Deprivation on Performance (the Serial Reaction Test) Modified From Broadbent (1963)

Stress	Speed	Errors	Place in Work Period Where Effect Appears	Effect of Incentives	Interaction	
					Heat	Noise
Heat	No effect	Increased	Throughout	(No effect)*	——	(None)
Noise	No effect**	Increased**	End**	Impairs performance	(None)	——
Sleep deprivation	Reduced**	No effect**	End**	No effect or improved performance	None	Reduced effect (antagonistic)

*Results in brackets not from the serial reaction test and not strictly comparable.

**Based on the results of more than one study and felt to be more reliable.

Table 19–5

Combined Stress – Primarily Bed Rest or Immersion

Stresses	Subject	Measures	Effect	Interaction	Source
Bed rest and hypoxia	Man	Orthostatic tolerance, blood volume, metabolism	Hypoxia (10 000 ft simulated altitude) prevents changes in red cell mass and calcium metabolism associated with bed rest	Antagonistic	Lamb (1965), Stevens, et al. (1966), Lynch et al. (1967)
Bed rest and heat	Man	Tilt table tolerance	Heat (95°C) and 48 hr of bed rest produced greater orthostatic intolerance in combination than alone	Additive	DiGiovanni & Birkhead (1964)
Bed rest and water immersion (sequential)	Man	Tilt table tolerance	Not defined. Subjects at bed rest at night and immersed by day to simulate deconditioning effects of prolonged weightlessness	Not defined	Graybiel & Clark (1961), Torphy (1966)
Bed rest/immersion and acceleration	Man	Tolerance to $+G_x$, $+G_z$ acceleration	Tolerance to $+G_z$ slow onset acceleration is reduced by prior bed rest or immersion exposure	Not defined	Miller (1965), Benson et al. (1962)
Immersion and acceleration (sequential)	Man	Tolerance to $+G_z$ acceleration	$+G_z$ tolerance reduced in one subject after 5 days of water immersion	Not defined	Graveline & Balke (1961)

Table 19–6
Combined Stress – Primarily Cold

Stresses	Test Animal	Measures	Effect	Interaction	Source
Cold and acceleration			See table 19–1		Stiehm (1963), Martin & Henry (1951), Chae (1957)
Cold and hypoxia			See table 19–8		Luft (1950), Brown (1952), Bullard (1961a)
Cold and radiation	Rats	Survival time	Both neutron (220 rad) and X ray (430 rad) decrease survival time of rates at –20°C	Not defined	Newsome & Kimeldorf (1963)
Cold and radiation	Rats	Survival time, lesions	The reduced longevity, retarded growth, cataracts, and skin ulcers seen after 500 R X irradiation is not altered by 3–hr daily exposure to 32°F (0°C)	None	Gambino et al. (1964), Trujillo (1962)
Cold and alcohol	Man	Skin and rectal temperature, heat production	Alcohol does not significantly alter thermal responses to 8 hr sleep in cold (20°C)	Not examined	Andersen et al. (1963)
Cold and hyperoxia	Mice	Survival time	Survival time in 100% 0_2 normally $>$ 120 hr is reduced to $<$ 72 hr in cold (4°C)	Not examined	Gold & Kolzenitsky (1968)

Table 19–7
Combined Stress – Primarily Heat

Stresses	Test Animal	Measures	Effect	Interaction	Source
Heat and acceleration	Man, mice	Tolerance, survival	See table 19–1		Martin & Henry (1951), Chae (1957), Burgess (1959), Taliaferro et al. (1965)
Heat and hypoxia	Man	—	See table 19–8		Wezler & Frank (1950), Hale (1960)
Heat and vibration	Man, primate	Sleep EEG	Combination of heat (90°F) and sinusoidal vibration reduces amount of REM sleep	Not defined	Harris et al. (1971) (1970)
Heat and vibration			See table 19–2	Additive	Megel et al. (1962)
Heat and noise	Man	Performance (tracking and monitoring), heart and respiration rates, body and skin temperature	Temperatures as high as 110°F (50% RH) and noise (110 dB) produce no significant degradation in performance or physiological thermal equilibrium	None	Deal et al. (1964)
Heat and radiation	Dogs	Rectal temperature thyroid function	X irradiated (270 – 1800 R) dogs are unable to maintain thermal balance during 6 hr exposure to (105°F) heat	Not identified	Thomsen et al. (1969)

Heat and microwave radiation	Dogs	Rectal temperature	Dogs surviving the lethal effects of X irradiation were less able to tolerate the thermal effects of microwaves	Not identified	Michaelson et al. (1967)
Heat and hyperoxia	Mice	Survival time, histopathology	Survival time in 100% O_2 normally $>$ 120 hr was reduced to $<$ 72 hr in heat (34°C)	Not identified	Gold & Kozinitsky (1968), Gold et al. (1964)
Heat and vibration		Rectal temperature	Rectal temperature (T_R), rose in proportion to degree of heat stress. Vibration (up to 15 G) lowered T_R. Combined stress interacted by synergism: T_R rose in proportion to degree of vibration stress	Synergistic	Megel, Keating, & Stern (1961)

Table 19–8

Combined Stress – Primarily Hypoxia

Stresses	Test Animal	Measures	Effect	Interaction	Source
Hypoxia and heat and noise	Man	Performance (compensatory tracking), heart rate, respiration, rectal temperature	Heat (105°F), noise (110 dB white noise), and hypoxia (12 000 ft equiv.) studied in pairs or all three together show additive interactions	Additive	Dean, McGlothlen, & Monroe (1964) a,b
Hypoxia and cold	Man	Tolerance time, peripheral light loss	Rapid collapse and delayed recovery	Additive	Luft (1950), Brown (1952), Bullard (1961b)
Hypoxia and acceleration	Man	Tolerance time, peripheral light loss	Hypoxia decreases $+G_z$ tolerance	Additive	Greeley (1945), Gauer (1950), Burgess (1958)
Hypoxia and heat	Man	Heart rate	Heat (49°C) and hypoxia (PO_2 100 mm Hg) increase heart rate at 15" exposure 10 and 7 bpm respectively and 17 bpm when combined. No significant interaction is seen in other variables (skin and rectal temp., blood pressure, ventilation, and oxygen consumption). Initial synergistic interaction becomes antagonistic after 30 min	Synergistic and antagonistic	Wezler & Frank (1950), Hale (1960)
Hypoxia and radiation	Rats	Tolerance (survival)	Prior whole body X irradiation improves survival rates for acute 25– to 30 00–ft altitude exposure	Antagonistic	Newsom & Kimeldorff (1960)

Hypoxia and cold	Man	Shivering, heart rate, oxygen consumption	Hypoxia (10% inspired O_2) during cold (5°C) inhibits shivering and lowers heat production	Additive	Luft (1950), Brown (1952), Bullard (1961b)
Hypoxia and vibration	Rats	Mortality	Mortality of restrained rats increases directly with hypoxia (8– to 18 000–ft altitude) during $+G_x$ vibration (60 Hz 15 G peak acceleration)	Additive	Megel (1963)
Hypoxia and alcohol	Man	Visual acuity, performance	Combined effect of hypoxia and alcohol greater than simple sum of the (decreased) acuity produced by each	Additive	Bietti & Giardini (1950), Neyman (1949)
Hypoxia and carbon monoxide	Man	Tolerance time	Small amounts of CO reduce tolerance to hypoxia	Additive	Armstrong (1952)
Hypoxia and hypobaria	Rat red cells	Osmotic fragility	Under constant pressure, hypoxia increases RBC osmotic fragility. Under constant PO_2, hypobaria increases osmotic fragility but hypoxia and hypobaria are independent and do not interact	None	Bernardini (1969)
Hypoxia and alcohol	Man	Psychomotor performance	Hypoxia and alcohol combined are additive	Additive	Klein et al. (1966)
Hypoxia and carbon monoxide	Man	—	—	Additive	Gillies (1965)
Hypoxia and alcohol	Man	Flicker fusion frequency	Hypoxia (altitude equivalent 10 000 ft) and the ingestion of alcohol each diminish flicker fusion frequency. The effect of the combined stresses is approximately the sum of the individual effects	Additive	Rosketh & Lorenzen (1954)

Table 19–9

Combined Stress – Primarily Radiation*

Stresses	Test Animal	Measures	Effect**	Interaction	Source
Radiation and acceleration	Rats, Mice	Survival, histopathology	Chronic acceleration improves radiation tolerance, acute acceleration degrades acceleration tolerance	Variable, complex	Casey et al. (1967), Davydov et al. (1965, 1966), Ivanov et al. (1963), Montgomery et al. (1964), Pinchuk et al. (1958), Taylor (1960), Zelmer et al. (1963)
Radiation and decompression	Mice	Survival	No difference in acute survival of radiation when decompressed from air or oxygen environments. 30 d. survival less in oxygen breathing animals	None	Carker et al. (1963), Clemedson et al. (1955), Furry (1964)
Radiation and cold	Rats	Survival, tissue oxygen tension, histopathology	Cold exposure (0°C) has no significant effect on radiation induced histopathology	None	Gambino et al. (1964), Konstantinova (1962), Trujillo et al. (1962)

Radiation and heat	Dogs	Rectal temperature	Both whole body and local thyroid irradiation (7 yr prior to heat) produce measurable changes in thermoregulation response to heat stress	Not specified	Thomsen et al. (1969)
Radiation and hypoxia	Rats	Survival, hematology	Hypoxia, both acute and chronic, is radioprotective	Antagonistic	Devik (1954), Lindop & Rotblat (1965), Newsom & Kimmeldorf (1954), Wright & Shewell (1965)
Radiation and hyperoxia	—	—	A large literature indicates the effects of radiation are enhanced by oxygen-rich atmospheres	Synergistic	Benjamin & Peyser (1964), Livshits (1964)
Radiation (ionizing) and radiation (microwave)	Dogs	Survival, hematology	Mortality is greater after combined X ray and microwave exposure than singly	Additive	Michaelson et al. (1963), Thomsen et al. (1967)
Radiation and vibration	Mice	Histopathology	Damage to all nuclei and chromosomes produced by both radiation and vibration, but interaction of the two stresses is variable	Variable (probably no significant interaction)	Gaydamakin et al. (1966), Ganshina (1961), Demin (1967), Short et al. (1967)

Table 19–9 (Continued)

Combined Stress – Primarily Radiation*

Stresses	Test Animal	Measures	Effect**	Interaction	Source
Radiation and vibration and acceleration	Mice	Histopathology of bone marrow cell nuclei	Damage to cell nuclei and chromosome pattern by radiation is reduced by prior acceleration and vibration singly or in combination	Variable (depending on sequence of treatment)	Arsenova et al. (1965)

*There is an extensive literature on the combined effects of ionizing radiation and other environmental stresses, which has recently been reviewed by Livshits (1964, 1966);

**Little comparison of results across studies is possible due to lack of uniformity of type radiation, dose units, types of response studied, type of animal, etc. No attempt is made in this table to specify the nature of the radiation exposure.

Table 19–10

Major Combined Environmental Stress Test Facilities in the U.S.

Name, Organization, Location	Environments																				
	Microwave	Ionizing	Electric	Magnetic	Light	Heat	Cold	Humidity	Wind Velocity	Lin. Acceleration	Rotation	Vibration	Blast	Noise	Weightlessness	Pressure	Composition	Confinement/Restraint	Work/Rest	Sleep	Chemical/Toxic	Clothing/Equipment	Crew Composition
Dynamic Environment Simulator (DES), USAF Aerospace Medical Research Laboratory, Wright-Patterson AFB, Ohio						X	X	X		X	X	X		X		X	X	X					
Combined Environment Facility (CEF), USAF Aerospace Medical Research Laboratory, Wright-Patterson AFB, Ohio						X	X	X	X							X	X						
Toxic Hazards Research Unit (THRU) USAF Aerospace Medical Research Laboratory, Wright-Patterson AFB, Ohio					X			X								X	X	X	X	X	X	
Combined Stress Test Facility, Boeing Corp., Seattle, Washington						X	X	X				X		X		X	X	X					

References

Alexander, W. C., Sever, R. J., & Hoppin, F. G., Jr. Hypoxemia induced in man by sustained forward acceleration while breathing pure oxygen in a five pounds per square inch absolute environment. *Aerospace Medicine*, 1966, *37*, 372-378.

Andersen, K. L., Hellstrom, B., & Lorentzen, F. V. Combined effect of cold and alcohol on heat balance in man. *Journal of Applied Physiology*, 1963, *18*, 975-982.

Armstrong, H. G. *Principles and practices of aviation medicine.* (3rd ed.) Baltimore: Williams and Wilkins Co., 1952.

Arseneva, M. A., Beliaeva, L. A., & Golobkina, A. V. Effects of combined action of acceleration, vibration and radiation on cell nuclei of the bone marrow in mice. *Problemy Kosinicheskoi Biologii*, 1965, *4*, 373.

Ashton, R., & Roberts, V. L. Effects of drugs on vibration tolerance. *Arch. Int. Pharmacology*, 1965, *155*, 289-299.

Benjamin, F. B., & Peyser, L. Effect of O_2 on radiation resistance in mice. *Aerospace Medicine*, 1964, *35*, 1147.

Benson, V. G., Beckman, E. L., Coburn, K. R., & Chambers, R. M. Effects of weightlessness as simulated by total body immersion upon human response to positive acceleration. *Aerospace Medicine*, 1962, *33*, 198-203.

Bernadini, A. T. Effect of reduced pressure and varied gaseous environment on the osmotic fragility of rat red blood cells. *Federation Proceedings*, 1969, *28*, 1165-1169.

Bietti, G. B., & Giardini, A. The effect of anoxia on eye movements: II. Comparative study of the action of anoxia and alcohol separately and together. *Quarterly Journal of Studies on Alcohol*, 1950, *11*, 492.

Blockley, W. V. Combined physiological stresses. In H. Haber (Ed.), *Proceedings of a symposium on frontiers of man-controlled flight.* Los Angeles: The Institute of Transportation and Traffic Engineering, University of California, 3 April 1953.

Bommarito, C. L., & Ramsey, N. K. Effects of combined environmental stress on humans. *Proceedings of the Institute of Environmental Science*, 1963, 577-585.

Brady, J. F., & Newsom, B. D. Effect of positive pressure breathing on the vibration tolerance of the mouse. *Aerospace Medicine*, 1966, *37*, 40.

Broadbent, D. E. Differences and interactions between stresses. *Quarterly Journal of Experimental Psychology*, 1963, *15*, 205.

Brown, A. L., Vawter, F. G., & Marberger, J. P. Temperature changes in human subjects during exposure to lowered oxygen tension in a cool environment. *Journal of Aviation Medicine*, 1952, *23*, 456.

Bullard, R. W. Effects of hypoxia on shivering in man. *Aerospace Medicine*, 1961, *32*, 1143-1147.

Bullard, R. W., & Crise, J. R. Effects of carbon dioxide on cold-exposed human subjects. *Journal of Applied Physiology*, 1961, *16*, 633-638.

Burgess, B. F. The effect of hypoxia on tolerance to positive acceleration. *Journal of Aviation Medicine*, 1958, *29*, 754-757.

Burgess, B. F. The effect of temperature on tolerance to positive acceleration. *Aerospace Medicine*, 1959, *30*, 567-571.

Carker, M. C., & Close, P. The effect of prior x-irradiation in the survival of mice in explosive decompression. *Aerospace Medicine*, 1963, *24*, 774.

Casey, H. W., Cordy, D., Coleman, M., & Smith, A. H. The influence of chronic acceleration on the effects of whole body irradiation in rats. *Aerospace Medicine*, 1967, *38*, 451.

Chae, E. U. The influence of temperature upon the tolerance of mice to positive radial acceleration, Republic of Korea. *Journal of Aviation Medicine*, 1957, *5*, 51.

Clarke, N. P., Taub, H., Scherer, H. F., & Temple, W. E. Preliminary study of dial reading performance during sustained acceleration and vibration. AMRL-TR-65-110, Wright-Patterson Air Force Base, Ohio, 1965.

Clemedson, C. J., & Nelson, A. Effect of combined whole body roentgen irradiation and high explosive blast injury in mice. *Acta. Radiol.*, 1955, *43*, 161-172.

Cooper, G. E. Understanding and interpreting pilot opinion. *Aeronautical Engineering Review*, 1957, *16*, 47-56.

Davydov, B. I. Endurance of external acceleration increased as a result of exposure to ionizing radiation. NASA-TT-F-10349, National Aeronautics and Space Administration, Washington, D.C., October 1966, Translation of *Doklady Akademii Nauk SSSR*, 1966, *168*(3), 691-693.

Davydov, B. I., Antipov, V. V., & Saksonov, P. P. Reaction of irradiated organism when affected by acceleration of critical magnitude. *Cosmic Research*, 1965, *3*(2), 256-268.

Dean, R. D., McGlothlen, C. L., & Monroe, J. L. Effects of combined heat and noise on human performance, physiology and subjective estimates of comfort and performance. Boeing Company Technical Report D2-90540, Seattle, Washington, 1964. (a)

Dean, R. D., McGlothlen, C. L., & Monroe, J. L. Performance and physiological effects of CH-46A noise and vibration. Boeing Company Technical Report D2-90583, Seattle, Washington, 1964. (b)

Demin, Y. S. The effect of whole body vertical vibration and x-rays on the nucleus of cells of bone marrow cells of mammals. *Effect of ionizing radiation and dynamic factors of the function of the central nervous system; Problems in space physiology*. N68-33288, Foreign Technology Division, Wright-Patterson Air Force Base, Ohio, September 1967, Pp. 13-27.

Devik, F. Protective effects of combined hypoxia and cysteine treatment on whole body irradiation of mice. *British Journal of Radiology*, 1954, *27*, 463-466.

DiGiovanni, G., Jr., & Birkhead, N. C. Effect of minimal dehydration on orthostatic tolerance following short term bed rest. *Aerospace Medicine*, 1964, *35*, 225-228.

Dolkas, C. B., & Stewart, J. D. Effect of combined linear and oscillatory acceleration on pilot attitude-control capabilities. NASA TN-2710, National Aeronautics and Space Administration, Washington, D.C., March 1965.

Furry, D. E. Tolerance of mice x-irradiated in an oxygen rich environment to explosive decompression. *Aerospace Medicine*, 1964, *35*, 459.

Gambino, J. J., Bennett, L. R., Billings, M. S., & Lawson, B. G. Biological effect of stress following ionizing radiation. *Aerospace Medicine*, 1964, *35*, 220.

Ganshina, N. N. Combined effect of radiation and vibration on animals. *Med. Radiologiya*, 1961, *6*, 71-75.

Gauer, O. The physiological effects of prolonged acceleration. In *German aviation medicine in World War II*. Washington, D.C.: U.S. Government Printing Office, 1950.

Gaydamakin, N. A., Petrukhin, V. G., Saksanov, V. V., Saksanov, P. P., & Shashkov, V. C. Pathomorphologic changes in hemopoietic organs of mice exposed to the combined effect of several kinds of ionizing radiation and dynamic space flight factors. *Studies in physiological reactions of humans and animals to space flight*. N66-34322, National Aeronautics and Space Administration, Joint Publications Research Service, Washington, D.C., 29 July 1966, Pp. 22-23.

Gillies, J. A. (Ed.) *A textbook of aviation physiology*. London: Pergamon Press, 1965.

Gold, A. J., & Kosenitzky, I. Effects of cold and heat on survival and pulmonary changes in oxygen-exposed mice. *Aerospace Medicine*, 1968, *39*, 980.

Gold, A. ', Silver, E. C., & Hance, H. E. Influence of environmental temperature on the toxic., of oxygen. *Aerospace Medicine*, 1964, *35*, 563.

Graybiel, A., & Clark, B. Symptoms resulting from prolonged immersion in water: The problem of zero G asthenia. *Aerospace Medicine*, 1961, *32*, 81-96.

Graveline, D. E., et al. Psychobiological effects of water immersion induced hypodynamics. *Aerospace Medicine*, 1961, *32*, 387.

Greeley, P. O., Jorgenson, H., Clark, W. G., et al. Effect of anoxia on G tolerance. NAS-NRC-CAM-480, National Academy of Sciences-National Research Council, Washington, D.C., October 1945.

Greenleaf, J. E., Matter, M., Jr., Bosco, J. S., et al. Effects of hypohydration on work performance and tolerance to $+G_z$ acceleration in man. *Aerospace Medicine*, 1966, *37*, 34-39.

Hale, H. B. Human cardioaccelerative responses to hypoxia in combination with heat. *Aerospace Medicine*, 1960, *31*, 276-287.

Harris, C. S., & Shoenberger, R. W. Combined effects of noise and vibration on psychomotor performance. AMRL-TR-70-14, Wright-Patterson Air Force Base, Ohio, 1970.

Harris, D. A., Pegram, G. V., & Hartman, B. O. Performance and fatigue in experimental double-crew transport missions. *Aerospace Medicine*, 1971, *42*, 980-985.

Hendler, E. Physiological effects of a simulated space flight profile. *Federation Proceedings*, 1963, *22*, 1060-1063.

Ivanov, K. M., Zhukov, M. K., & Melchanova, M. G. Effect of accelerations produced during irradiation of animals on the course of acute radiation sickness. *Patholog. fiziol. i eksper. terap.*, 1962, *5*, 74-75. Abstracted in English in *Soviet literature on life support systems*. Biosciences AID Report P-63-91, Library of Congress, Washington, D.C., 1963.

Jex, H. R., & Allen, R. W. Research on a new human dynamic response test battery. *Proceedings of the Sixth Annual Conference on Manual Control*, Wright-Patterson Air Force Base, Ohio, April 1970, P. 743.

Klein, K. E., Bruner, H., Voigt, E. D., & Wegmann, H. M. Comparative studies on physiological indices of fitness in man under exercise, low pressure and acceleration. In H. Yoshimura, & J. S. Weiner (Eds.), *Human adaptability and its methodology*. Tokyo, 1966, Pp. 234-249.

Konstantinova, M. M. Effect of duration of moderate hypothermia on the oxygen tension in tissues and the radio sensitivity of mice. *Doklady Akademii Nauk SSSR*, 1962, *145*, 436.

Lamb, L. E. Hypoxia – An anti-deconditioning factor for manned space flight. *Aerospace Medicine*, 1965, *36*, 97.

Leblanc, J. Stress and interstress adaptation. *Federation Proceedings*, 1969, *28*, 996-1000.

Lind, A. R., Leithead, G. S., & McNicol, G. W. Cardiovascular changes during syncope induced by tilting men in the heat. *Journal of Applied Physiology*, 1968, *25*, 268-276.

Lindop, P. J., & Rotblat, J. Life-shortening in mice exposed to radiation: Effects of age and hypoxia. *Nature*, 1965, *208*, 1070.

Livshits, N. N. Combined effects of ionizing radiation and other factors. NASA-TT-F-354. Translated from *Effects of Ionizing Radiation and Dynamic Factors on the Functions of the Central Nervous System – Problems of Space Physiology*. Moscow: Science Publishing House, 1964, Pp. 1-23.

Livshits, N. N. The effect of space flight factors on central nervous system functions: Summary of data. DDC AD 642 186, Library of Congress, Washington, D.C., 4 August 1966.

Luft, U. *German aviation medicine.* Washington, D.C.: U.S. Government Printing Office, 1950, Pp. 316-319.

Lynch, T. N., Jensen, R. L., Stevens, P. M., Johnson, R. L., & Lamb, L. E. Metabolic effect of prolonged bed rest: Their modification by simulated altitude. *Aerospace Medicine,* 1967, *38,* 10.

Martin, E. E., & Henry, J. P. The effects of time and temperature upon tolerance to positive acceleration. *Journal of Aviation Medicine,* 1951, *22,* 382.

Megel, H., Keating, F. M., & Stern, J. A. Effects of elevated ambient temperature and vibration on rectal temperature of the restrained rat. *Aerospace Medicine,* 1961, *32,* 1135-1139.

Megel, H., Wozniak, H., Frazier, E., & Mason, H. C. Effect of altitude upon tolerance of rats to vibration stress. *Aerospace Medicine,* 1963, *34,* 319-361.

Megel, H., Wozniak, H., Sun, L., Frazier, E., & Mason, H. C. Effects on rats of exposure to heat and vibration. *Journal of Applied Physiology,* 1962, *17,* 759-762.

Michaelson, S. M., Thomsen, R. A. E., & Howland, J. W. Biologic effects of microwave exposure. RADC-TR-67-461, Rome Air Development Center, Griffiss Air Force Base, New York, September 1967.

Michaelson, S. M., Thomsen, R. A. E., & Odland, O. T. The influence of microwaves on ionizing radiation exposure. *Aerospace Medicine,* 1963, *34,* 111-115.

Miller, P. B., & Leverett, S. D. Tolerance to transverse ($+G_X$) and headward ($+G_Z$) acceleration after prolonged bed rest. *Aerospace Medicine,* 1965, *36,* 13.

Montgomery, P. O. B., Rosenblum, E., & Stapp, B. Gravity radiation and growth. *Aerospace Medicine,* 1964, *35,* 731.

Newberry, P. D., Johnson, W. H., & Smiley, J. R. Effect of hypoxia and nystagmus induced by angular acceleration. *Aerospace Medicine,* 1965, *36,* 1090-1093.

Newman, H. W. Effect of altitude on alcohol tolerance. *Quarterly Journal of Studies on Alcohol,* 1949, *10,* 398.

Newsom, B. D., & Kimeldorf, D. J. Alterations in physiological accommodation to stress induced by irradiation. *Aerospace Medicine,* 1963, *34,* 226-230.

Newsom, B. D., & Kimeldorf, D. J. Increased tolerance to hypoxia in irradiated and in food-deprived rats. *American Journal of Physiology,* 1954, *177,* 390-394.

Newsom, B. D., & Kimeldorf, D. J. Tolerance of irradiated animals to prolonged hypoxia. *American Journal of Physiology,* 1960, *199,* 445-448.

Pinchuk, V. M., & Shcherban', E. I. Effect of moderate physical acceleration, applied just before irradiation, on the course of acute radiation sickness. In *Radiation Sickness and Combined Lesions of the Organism,* Leningrad, Izd-vo Tsentr. Nauchno-Issled. In-ta Rentgenol. i Radiol. Min. Zdrav. USSR, 1958, Pp. 318-325.

Rohles, F. H. Considerations for environmental research in human factors. *Journal of Environmental Sciences,* 1965, *8,* 18-19.

Rosketh, R., & Lorenzen, F. V. Alcohol and altitude. *Journal of Applied Physiology,* 1954, *6,* 559-565.

Short, L. L., Newsom, B. D., & Brady, J. F. X-radiation effects on vibration tolerance of rats. *Aerospace Medicine,* 1967, *38,* 140-144.

Stevens, P. M., Miller, P. B., Lynch, T. N., et al. Effects of lower body negative pressure on physiologic changes due to four weeks of hypoxic bed rest. *Aerospace Medicine,* 1966, *37,* 466-474.

Stevens, S. S. Effects of noise and vibration on psychomotor efficiencies. OSRN #32, National Research Council, Harvard Psycho-Acoustics Laboratory, 1941.

Stevens, S. S. (Ed.) *Handbook of experimental psychology.* New York: John Wiley and Sons, 1951.

Stiehm, E. R. Different effects of hypothermia on two syndromes of positive acceleration. *Journal of Applied Physiology*, 1963, *18*, 387.

Taliaferro, E. H., Wempen, R. R., & White, W. J. The effects of minimal dehydration upon human tolerance to positive acceleration. *Aerospace Medicine*, 1965, *36*, 922-926.

Taylor, J. W. X-irradiation and acceleration stress. NADC MA 6033, Naval Air Development Center, Johnsville, Pennsylvania, 1960.

Thomsen, R. A. E., Michaelson, S. M., & Howland, J. W. Microwave radiation and its effect on response to x-radiation. *Aerospace Medicine*, 1967, *38*, 252.

Thomsen, R. A. E., Michaelson, S. M., & Quinlan, W. J. Thermal regulation in x-irradiated dogs subjected to heat stress. *Aerospace Medicine*, 1969, *40*, 283-286.

Tierney, W. L. Combined environment space simulation in the 1970s. *Environmental Quarterly*, 1969, *15*, 16-18.

Torphy, D. E. Effects of short term bed rest and water immersion on plasma volume and catecholamine response to tilting. *Aerospace Medicine*, 1966, *37*, 383-387.

Trujillo, T. T., Spalding, J. F., & Langham, W. H. A study of radiation induced aging: Response of irradiated and non-irradiated mice to cold stress. *Radiation Research*, 1962, *16*, 144-150.

Tsysar, A. I. The effect of joint action of noise and vibration on the vibration sensitivity of adolescents. *Gig. i. Sanit.*, (USSR), 1965, *6*, 30-36.

Viteles, M. S., & Smith, K. R. An experimental investigation of the effect of change in atmospheric conditions and noise upon performance. *Transactions of the American Society of Heating and Ventilating Engineers*, 1946, *52*, 167-182.

Vykukal, H. C. Dynamic response of the human body to vibration when combined with various magnitudes of linear acceleration. *Aerospace Medicine*, 1968, *39*, 1163-1166.

Webb, P. (Ed.) Bioastronautics data book. NASA SP-3006, National Aeronautics and Space Administration, Washington, D.C., 1964.

Wezler, K., & Frank, E. O_2-Mangel bei wechselnden klimabedingungen. Unpublished report discussed in *German aviation medicine in World War II.* Washington, D.C.: U.S. Government Printing Office, 1950, Pp. 819-821.

Wilkinson, R. T. The interaction of noise with loss of sleep and knowledge of the results. *Journal of Experimental Psychology*, 1963, *66*, 332-337.

Wright, E. A., & Shewell, J. Modification of radiation "cerebral death" by hypoxia. *Nature*, 1965, *208*, 904.

Young, W. A., Shaw, D. B., Navack, J., Shizgal, H., & Kowalsky, N. Effect of CO^2 and whole body vibration on ventilation. *Journal of Applied Physiology*, 1965, *20*, 844-848.

Zellmer, R. W., Granville, J. W., McNee, R. C., & Allen, R. G., Jr. Significance of combined stresses of G forces and irradiation. *Aerospace Medicine*, 1963, *34*, 626-629.

Additional Reading

Adey, W. R., Kado, R. T., & Walter, D. O. Results of electroencephalographic examinations under the influence of vibration and centrifuging in the monkey. In L. Widen (Ed.), *Recent advances in clinical neurophysiology, Electroenceph. Clin. Neurophysiol.* AFOSR-67-1857, Suppl. 25, Amsterdam: Elsevier Publishing Co., 1967, Pp. 227-245.

Altland, P. D., Brubach, H. F., & Parker, M. G. Effects of inert gases on tolerance of rats to hypoxia. *Journal of Applied Physiology*, 1968, *24*, 778-781.

Arkad'yeuskii, A. A. Combined effect of vibration and noise on the human organism. *Gig. i. Sanit.*, 1962, *10*, 25-28.

Berry, C. A., Coons, D. O., Catterson, A. D., et al. Man's response to long-duration flight in the Gemini spacecraft. In Gemini Midprogram Conference, NASA SP-121, Manned Spacecraft Center, Houston, Texas, 23-25 February 1966, Pp. 235-261.

Berry, C. A., & Eastwood, H. K. Helicopter problems: Noise, cockpit contamination and disorientation. *Aerospace Medicine*, 1960, *31*, 170-190.

Bjurstedt, H., Rosenhamer, G., & Wigertz, O. High-G environment and responses to graded exercise. *Journal of Applied Physiology*, 1968, *25*, 713-719.

Cassuto, Y., & Chafee, R. R. J. Cold adaptation and heat. *American Journal of Physiology*, 1966, *210*, 223.

Chetverikov, D. A., Gasteva, S. V., Ivanov, K. P., Vastek, A., & Pospishel, M. Mechanisms of raised resistance of rats to hypoxia in acute radiation injury. *Folic. Biologica*, 1964, *10*, 386.

Corcoran, D. W. Noise and loss of sleep. *Quarterly Journal of Experimental Psychology*, 1962, *14*, 178-182.

Damon, E. G., Gaylord, C. S., Yelverton, J. T., Richmond, D. R., Bowen, I. G., Jones, R. K., & White, C. S. Effects of ambient pressure on tolerance of mammals to air blast. *Aerospace Medicine*, 1968, *39*, 1039.

Damon, E. G., Richmond, D. R., & White, C. S. Effects of ambient pressure on the tolerance of mice to air blast. *Aerospace Medicine*, 1966, *37*, 341.

Davidovid, J., Debijadi, R., Elcic, S., & Davidovic, V. Effects of noise on resistance to acute hypoxia. *Vojnosanitetski Pregled*, 1965, *22*, 625.

Dean, R. Human stress in space. *Science Journal*, 1966, *2*, 70-75.

Dean, R. D. The use of environmental stress in conjunction with simulation testing. *IEEE Transactions, Aerospace and Electronic Systems*, 1967, *3*, 688-696.

Greenleaf, J. E., Greenleaf, C. J., Card, D. H., & Saltin, B. Exercise-temperature regulation in man during acute exposure to simulated altitude. *Journal of Applied Physiology*, 1969, *26*, 290-296.

Gyurdzhian, A. A. The effect of prolonged acceleration on gas exchange and resistance of rats to hypoxia. N67-26573, National Aeronautics and Space Administration, Washington, D.C., November 1966.

Hall, C. E., Schneider, M., & Hall, O. Increased sensitivity to x-irradiation exhibited by stressed rats. *Radiation Research*, 1962, *17*, 118-128.

Ioseliani, K. K. The effect of vibration and noise on the mental faculty of man under time stress. *Kosmicheskaya Biol. & Med.* (USSR), 1967, *1*, 79-82.

Kaehler, R. C. Human pilot performance during boost and atmospheric reentry. *Aerospace Medicine*, 1959, *30*, 481-486.

Kelly, G. F., Coons, D. O., & Carpentier, W. R. Medical aspects of Gemini extravehicular activities. *Aerospace Medicine*, 1968, *39*, 611.

Kotovskaia, A. R., Vartbaronov, R. A., & Simpura, S. F. Human physiological reactions under the action of transverse accelerations after preceding hypodynamia. In *Problems of Space Biology 6*, Moscow, 1967, Pp. 106-117.

Lamb, T. W., et al. Mechanical and chemical ventilatory stimulus interaction. *Journal of Applied Physiology*, 1966, *21*, 399-403.

Loeb, M. Further investigations of the influence of whole body vibration and noise on tremor and visual acuity. AMRL-TR-55-165, Wright-Patterson Air Force Base, Ohio, 1955.

Morrison, P. Responses of mountaineers to multiple stressors. *Archives of Environmental Health*, 1968, *17*, 599-602.

Mukhamedov, T. Effect of combined action of radioiodine-131 and noise on the cardiac activity in dogs. *Biulletin Eksperimental 'noi Biologii i Meditsiny*, 1965, *59*, 43.

Newsom, B. D., & Kimeldorf, D. J. The resistance of animals to acute cold following x-irradiation. *International Journal of Radiation Biology*, 1961, *4*, 143.

Newsom, B. D., & Kimeldorf, D. J. Tolerance of rats to a cold environment during multiple exposures to a low dose of x-rays. *American Journal of Physiology*, 1961, *200*, 1039.

Pepler, R. D. Warmth and lack of sleep: Accuracy or activity reduced. *Journal of Comparative Physiological Psychology*, 1959, *52*, 446-450.

Phillips, R. D., & Kimeldorf, D. J. An immediate irradiation effect on resistances of rats to low temperature. *Journal of Applied Physiology*, 1962, *24*, 768-772.

Pugh, L. G. C. E. Tolerance to extreme cold at altitude in a Nepalese pilgrim, Special communications. *Journal of Applied Physiology*, 1963, *18*, 1234-1238.

Riley, M. B., & Bernardini, A. T. Animal and human studies of the effects of low frequency oscillation combined with transverse acceleration. WADC-TN-59-62, Wright-Patterson Air Force Base, Ohio, 1962.

Sadoff, M., & Dolkas, C. B. Acceleration stress effects on pilot performance. *IEEE Transactions, Human Factors in Electronics*, 1967, *8*, 103-112.

Shebalin, V. A. Change in conditioned reflexes in human beings exposed to carbon monoxide and vibration. *Byull. Eksperim. Biologii i. Meditsiny*, 1962, *53*, 45-48.

Soliday, S. M., & Schohan, B. Performance and physiological responses of pilots in simulated low altitude high speed flight. *Aerospace Medicine*, 1965, *36*, 100-104.

Sorokina, Y. I. The interaction of a series of indices of the oxygen regime of an organism under the influence of reduced barometric pressure and long acting accelerations. In *Problems in Aerospace Medicine*. Joint Publications Research Service, Washington, D.C., 21 October 1966, Pp. 452-453.

Wegmann, H. M., Bruner, H., & Klein, K. E. Enzymatic and hormonal responses to exercise, lowered pressure and acceleration in human plasma and their correlation to individual tolerances. *Federation Proceedings*, 1966, *25*, 1405-1408.

Wunder, C. C., Herrin, W. F., & Crawford, C. R. Combined influence of gravity and temperature upon growth of fruit fly larvae. *Growth*, 1959, *23*, 349-357.

Young, W. A., Shaw, D. B., Buckles, L. J., Outerbridge, J. S., Reeves, C. E., & Truman, J. C. Effect of CO^2 on hyperventilation produced by vibration. *Journal of Applied Physiology*, 1963, *18*, 349.

Zharova, E., Khrustalev, A., Protasova, T. G., Davydov, B. I., Antipov, V. V., Saksonov, P. P., & Raushenbakh, M. O. Remote responses of the hemopoietic tissue to the proton and x-irradiation combined with acceleration. *Izvestiia Akademii Nauk SSSR Seriia Biologicheskaia*, March/April 1967, *2*, 29.

CHAPTER 20

AEROSPACE VEHICLE WATER-WASTE MANAGEMENT

by

Joseph N. Pecoraro
National Aeronautics and Space Administration

The collection and disposal of human wastes, such as urine and feces, in a spacecraft environment, must be performed in an aesthetic and reliable manner to prevent degradation of crew performance. This is a difficult task because the equipment must be designed for use by a human operator in a weightless state, and biological contamination must be prevented. The design of this equipment is further complicated by the usual requirement for minimum size, weight, and power. An artificial force must be created to direct the feces and urine to the appropriate collection receptacles, thus preventing possible spacecraft contamination. One method of providing the force required for waste collection consists of drawing air from the cabin into the collection device so that flatus and fecal odors will not escape into the spacecraft.

The waste management system controls, transfers, and processes materials such as feces, emesis, food residues, used expendables, and other wastes. Control and transfer of urine, condensate, and water from personal hygiene and its reclamation is considered a waste management function.

Aerospace vehicle waste management systems do not exist as separate entities; they are a combination of various techniques designed into hardware for the collection of urine, feces, and waste preservation and disposal and/or recovery of materials such as water, air, etc. For any system, the chosen technique must be physiologically and psychologically acceptable to the crew and provide maximum equipment effectiveness.

Research and development of waste management systems for aerospace vehicles began in 1958 (Ingram, 1958; Des Jardins et al., 1960). This work demonstrated the performance of various techniques for collecting, transporting, storing, and disposal of wastes on missions up to 120 days. The Project Mercury,

---

Reviewed by Robert A. Barnbenck, Amglo Corporation, Chicago, Illinois, and J. D. Zeff, General American Transportation Corporation, Niles, Illinois.

Gemini, and Apollo astronauts were provided with relatively simple equipment, which was adequate for these relatively short missions. Since 1966, emphasis has been placed upon the development of equipment for longer missions, which may require the collection and recovery of usable products from human wastes.

Requirements

Aerospace waste includes all of the items that must be separated from the crew to prevent biological contamination. The items generally classified as wastes are: urine, feces, wipes, wash water, food containers, and debris. The composition and quantity of these wastes are not constant; they are a function of variables such as the individual, his diet, and the mission. Fortunately, the exact composition is less important than the quantity–at least from a design standpoint. The typical composition and nominal quantity of these wastes is presented in table 20-1.

Table 20–1

Nominal Crewman Metabolic Balance[1]
(lb/man-day)

Input			Output		
Solids					
Food		1.36	Urine solids		0.13
Oxygen	0.44		Feces solids		0.07
Hydrogen	0.08		Sweat solids[2]		0.04
Carbon	0.60				
Other	0.24				
Liquids (water)					
Drink[3]		4.09	Urine		3.31
Food preparation		1.58	Content		4.02
Cold[3]	0.79		Sweat	2.02	
Hot[3]	0.79		Insensible[4]	2.00	
Total input		6.77	Total recoverable		7.33
			Feces		0.20
Gases			Total output		7.53
Oxygen	1.84		Carbon dioxide		2.20

[1]Assumes metabolic rate = 11,200 BTU/man-day and RQ = 0.87

[2]1% of sweat (Roth, 1964)

[3]From potable water supply

[4]Composed of lung, latent loss (10% of total metabolic rate) plus skin diffusion.

Wastes must be collected and transported to storage and/or recovery process equipment in such a manner that they do not contaminate the crew and the internal environment of the vehicle. In most cases wastes must also be treated during collection to avoid the production of noxious gases and microorganisms in the collector, transport lines, and storage vessels. If the wastes are to be stored onboard for an extended period of time, they should be sterilized to avoid contamination if the storage vessel fails.

Since at times the aerospace vehicle may be in a weightless state, certain techniques for collection of wastes will have to employed. These include the application of pressure, drag, and/or manual forces. This applies to such waste as urine, feces, vomitus, and debris. Furthermore, for human waste collection, foot restraints and a body restraining belt appear to be needed to enable zero gravity operation.

Collection and Transport

Solid wastes, such as wipes, used food containers and refuse, are easily collected and transported by hand to a storage/disposal unit. The most difficult problem is collecting liquid wastes in a weightless state. This task is especially complicated by the fact that gas is usually collected with the liquids, and it must be separated to avoid gas loss and oversizing liquid storage containers.

Specifically, the collection and transport subsystem must provide the following functions:

1. Collect, treat, and store all solid and liquid wastes and collect and transfer raw urine to the water and waste disposal subsystem.
2. Eliminate odors, aerosols, and existing gases.
3. Sterilize waste matter to:
   a. Inhibit or eliminate microorganism production.
   b. Prevent production of such gases as CO_2, CH_4, H_2, H_2S, in the wastes.
   c. Prevent crew contamination if wastes escape into the living areas.

The variety of wastes and the differences in physical characteristics (volume, density, composition, etc.) and microorganism activity requires that the subsystem be flexible enough to handle wet wastes such as feces, urine, unused food, and wet cloths, as well as food containers, urine sludge (from the water reclamation subsystem), fingernail clippings, hair, vomitus, and miscellaneous debris. The nature of waste products requires that psychological and physiological factors be considered. Urine is rapidly colonized by microorganisms that degrade urea and uric acid components to toxic ammonia gas. Immediate treatment of the urine is required to eliminate the production of ammonia and to insure potability when urine is processed through the water reclamation subsystem. Other waste materials must be collected to reduce particulate matter in the atmosphere. Solid waste matter must be sterilized or treated to inhibit the growth of microorganisms so that health hazards do not

develop and gases are not generated and dispersed into the atmosphere or within storage containers.

Urine and Liquid Waste

The objective of the urine and liquid waste collection and transport subsystem is to provide a means for collecting and transporting these wastes to the water management subsystem where treating and processing are performed. The major liquid waste includes condensate water from equipment and crew and personal hygiene of body wash.

Urine. The urine collection unit must be capable of being operated either by itself or simultaneously with defecation. Acceptable seal-type urinals which provide for dumping overboard have been developed (Des Jardins et al., 1960; Miner et al., 1961). A nonsealing urinal can be used without gas loss overboard by employing a centrifugal fan to draw cabin gas into the urinal. A urine-gas separator is necessary to collect the urine and protect the fan. Tests have demonstrated that the gas flow rate required should be at least 1 cfm and the fan must be capable of developing a minimum pressure differential of 5 inches of water.

The Project Mercury and Gemini astronauts used seal-on urinals and bladder pressure to transfer urine to plastic bags, and saved it for postflight analysis. Since these were relatively short duration missions, there was no major concern about personal or vehicle contamination. The Project Apollo Command Module was provided with a urinal that resembles an aircraft relief tube, with an overboard vacuum used to assist in collection and transfer. Since the gas flow rate required to operate a relief tube is on the order of 1 cfm, the mass of gas lost overboard was substantially less than the mass penalty of a reliable urine-gas separator. Vehicles designed for mission durations longer than several weeks must minimize overboard gas loss, and therefore, can advantageously utilize a pneumatic-type urinal with a urine-gas separator.

Two types of urine-gas separators have been developed, passive separators that utilize surface tension and viscous flow to retain liquids and active separators that utilize centrifugal forces. The passive separator uses a sponge-type hydrophilic material so that the inlet mixture must flow a tortuous path, which causes the urine to collide with the sponge material. After the separation process is complete, the sponge can be (1) squeezed to transfer the urine to a storage vessel or overboard or (2) evacuated to vaporize and/or sublimate water from the urine leaving the residue in the sponge. Typical of the problems associated with passive separators are:

1. Droplets smaller than $50\,\mu$ in diameter will tend to pass through the sponge with the gas. The separator should therefore, be provided with either an agglomerating device at the inlet or a final filter at the outlet.

2. Urine, a source of many gases, requires an odor filter downstream of the separator to remove gases generated by urine on the sponge surfaces.

3. Urine residue will tend to accumulate in the sponge. The sponge must therefore, be oversized or replaceable to compensate for this loss in capacity. Wick-type separators are not recommended for application with mixtures containing heavy solutes that can precipitate and restrict capillary action. The passive or sponge-type separators do not require electric power, but they do lose interstitial gas when urine is transferred to storage or overboard.

The active or centrifugal-type separator can be designed to lose a minimum of gas with separated urine, but they require an electric motor, gas turbine, or manual drive. In these devices, separation is achieved by inducing rotational flow in a urine-gas mixture. Rotating vanes, screens, and sponges can be used for this purpose. Another approach is to impinge the mixture against the inner wall of a rotating bowl so that urine is forced against the wall. Viscous and centrifugal forces will then cause the urine to rotate with the bowl, so that a stationary impact tube can be used to pump urine out of the bowl. The gas is drawn or forced out of the bowl by pressure differences, preferably through a rotating entrainment separator or "final" filter. If the urine outlet is provided with a back pressure regulator, the separator automatically stops "pumping" when the urine-gas interface reaches the tube inlet. The urine remaining in the bowl will stay at the wall when the separator is shut off, if the wall is a hydrophilic material.

Centrifugal separators are most attractive for application where urine must be forced into a pressurized storage vessel. Theoretically, the urine or bowl velocity required is then $\sqrt{2g\Delta p/\rho}$. In practice, however, a higher velocity is required because probe drag creates a velocity profile between the wall and the urine-gas interface. The shaft power required to operate a centrifugal-type urine-gas separator is determined primarily by probe drag. An extremely small diameter probe will minimize peak power demand, but requires long periods of operation to empty the bowl. For minimum expenditure of energy, the probe should be sized to minimize depth of submergence, i.e., pumping rate should equal urination rate. A 0.125 inch diameter probe is sufficient for this purpose when pumping urine into a tank at 5 psig. Provisions should be made for sterilization on a regularly scheduled basis as well as water flushing after each micturition.

Liquid Waste. Liquid-gas separation is required for many different functions within the environmental control subsystem. Condensate collection is required for separation of carbon dioxide concentrator water from the carbon dioxide in the concentrator. A porous plate condenser/separator has been found to fulfill the requirements of the carbon dioxide concentrator. A three-passage configuration (stacked unit) is used, the first and second passages being gas and condensate, respectively (separated by a porous plate). The condensate passage is initially filled with water and maintained at a negative pressure with respect to the gas flow passages. A centrifugal pump is employed to transfer condensate to the water management system. The third passage contains a flowing coolant to maintain the whole unit at a uniform temperature sufficient to condense water vapor on the gas side of the porous plate. The nature of the fluids being processed, the water and carbon dioxide flow rates, and equivalent weight considerations usually dictate the selection of the porous plate condenser/separator.

The use of cabin air/water separators with face wick heat exchangers is one of the more attractive techniques to condense and separate water vapor from the cabin air. These separators are essentially conventional heat exchangers with the addition of face wicking in the air outlet face. Use of a hydrophobic coating on the air side fins minimizes gas pressure drop. Water droplets transported to the heat exchanger outlet face will come into contact with strips of wicking, enter the wick, and be transported to a hydrophilic transfer disk. Capillary forces, in conjunction with a pressure differential across the disk, transfer liquid to the collection system.

Wash Water

In the Gemini and Apollo flights, cleaning of exposed body surfaces was accomplished by use of lintless wet and dry pads dispensed with each meal. The pads were made from rayon, terry-pile cloth, and measured 3.5 x 4.0 x 3/32 inches. The wet pads are treated with 5 ml of cleaning solution composed of one part Hyamine 1620, a quaternary ammonium antiseptic, to 60,000 parts distilled water. Larger pads were provided for body cleaning.

On long duration missions, whole body cleaning will be required, using a shower or bath. Such cleaning must remove the residual materials adhering to the skin from sources external to the body, as well as natural body products. Upon completion, the body must be dried to avoid losing water to the internal environment. Some early tests under weightless conditions (in USAF RC-135 zero "G" aircraft) demonstrated the wetting characteristics of water on skin to be satisfactory: sprayed water wets and adheres to the skin. In fact, water actually builds up on the skin and clings in sheets, if the droplets are not large. The use of airflow for the collection of water in a shower stall does not satisfactorily remove water from the body; only a suction system or sponge can be used for this purpose. It is estimated that a weightless shower would require the collection and processing of 1.5 liters of water.

Feces and Debris

The objective of the feces and debris collection and transport subsystem is to provide a means for collecting and transporting these wastes to the solid waste management subsystem where treating and processing are performed. Collection and transfer must be accomplished under zero gravity conditions, while the escape of solid waste to the cabin is positively prevented. The principal solid wastes include body wastes, unused food, and food containers.

Feces Collection. There are basically two techniques for collecting feces in a weightless state; namely, manual collection with a glove or bag, and pneumatic collection with the use of forced cabin gas for detachment and transfer. The glove method, as developed for Project Gemini, is a simple, low-weight technique but is psychologically objectionable and does not provide a means for preventing flatus from entering the cabin atmosphere. The technique, however, is desirable for use as an emergency fecal collector or where a pneumatic collector cannot be provided. On missions of durations longer than several days, fecal collection

equipment is required to maintain the physiological and psychological well-being of the crew.

Feces can be detached from the anus in a weightless state by gas impingement, and then carried into a collection bag or processing device by the same gas flow (e.g. Des Jardins et al., 1960; Charanian et al., 1965. & Rollo et al., 1967. The gas flow rate required is a function of equipment design; experience has shown that it should be in the range of 2 to 10 cfm. The gas is drawn through the device by a centrifugal blower and passed through a filter with activated carbon before being returned to the cabin. Recent laboratory tests have shown that:

1. Separation of feces from perineal surface was best accomplished by short duration impulse from a 30 to 40 psig air stream aimed at the fecal mass; water or air-water streams are not as effective as air alone.

2. Only small amounts of air are needed to effect separation, e.g. 0.1 to 0.2 std. 3 ft. at 30 to 40 psig, flowing at 6 cfm for 2 seconds.

Many types of fecal collection bags have been devised. None of these bags has all the characteristics desired; namely,

High permeability for gases

Impermeable to liquids

High tear strength

Low weight.

The two materials proven to be most successful so far are porous cellulose and a polyethylene; both are fabricated from 10 mil material and treated to prevent passage of liquids with pressure differentials less than 4 inches of water. Recently, these materials have been laminated with cloth to provide the tear strength desired.

Experiments have demonstrated that man can reliably defecate into a 4 inch diameter opening--provided this opening is indexed with respect to the anal perimeter. This is the minimum size recommended for a fecal collection bag or the opening in a fecal storage container.

Pneumatic collection provides for more natural defecation. In addition, it also entrains any flatus excreted. To minimize odors, the fecal collection gas should be passed through a bed of activated charcoal. If a catalytic oxidation unit is used for contamination control, the fecal collection gas should be directed to this unit for removal of any H_2, CH_4, and H_2S. Also pneumatic collection provides a suitable means for collecting vomitus.

Overboard Dump. Wastes can be disposed of overboard in gaseous or liquid form. Dumping of solids is not permitted to avoid imparting the wastes on the ground and/or the aerospace vehicle. Urine, of course, can be dumped as a liquid directly from a urinal or from a urine-gas separator if it is permissible to contaminate the external environment with microorganisms. Solids, however, should be incinerated or thermally decomposed.

A detailed investigation of waste incineration/decomposition is described in Dodson and Wallman (1964). This study concluded that incineration requires (1) an ignition temperature of 1000°F, (2) an energy input of at least 1 kilowatt-hours per man-day, and (3) an oxygen input of up to 0.2 pounds per man-day. Under these conditions the ash remaining is less than 10 grams per man-day and can be easily blown overboard by venting.

If oxygen is not available for incineration, the wastes can be gasified by thermal decomposition. However, this technique requires approximately 4000 BTU/lb of wastes at a temperature level of 1200°F. In addition, the overboard vent line must be maintained at this temperature to avoid condensation and plugging.

Incineration and thermal decomposition have not appeared to be practical for aerospace vehicles in the absence of a nuclear heat source. However, when these heat sources are available, it will most likely be advantageous to recover usable products from wastes.

Waste Processing

Since any unit capable of handling fecal matter should also dispose of the other wastes, this discussion will be primarily concerned with human waste treatment methods. Currently considered methods are: (1) biodegradation, (2) vacuum/thermal drying, and (3) incineration.

The biological treatment of wastes requires a blending device for feces since bacteria rapidly degrade only soluble and finely dispersed matter. The biological treatment process also requires waste storage facilities so that wastes of reasonably uniform composition and concentration can be treated. Thus, a minimum of two tanks are required for alternate use as storage and feed units. A pump is required to feed the waste to the activated sludge system at some fixed rate. The activated sludge system requires a minimum of one tank with components for gas-liquid contact, gas-liquid separation, and liquid-solid separation. Instrumentation must be provided for control and monitoring of the process. Other components are required for absorbing gases when storage tanks are vented and for heat rejection. This process is being used commercially in sewage treatment plants on a large scale. There has been some minor adaptation of this process for zero-gravity spacecraft use.

The basis for the vacuum drying method is that drying fecal matter to 50 percent of its water content by weight will stop microorganismic activity and allow safe storage. Two methods have been developed for drying waste matter to a bacteriostatic condition. They are:

1. Systems in which the collection and treatment (drying) functions are separated, with manual transfer required from the collection unit to the treatment unit, and thence to storage when drying is complete.

2. Systems in which the collection, treatment, and storage functions are integrated.

In the vacuum drying method, the fecal bags used for collection do not include chemicals for treatment, as is the case for Apollo mission fecal bags. The bags are placed directly into individual vacuum dryers. The number of vacuum drying containers is determined by crew size and waste processing time. If power is available, drying can be reduced by heating the wastes to 240°F and evacuating the evaporated matter to space. Fecal water is lost in this process.

Upon completion of drying, the permeable bags can be removed from the drying chambers, placed in a "Saran" bag with 1 gm of silica gel to maintain dryness, and put into a sealed storage container sized for the number of man-days required. If fecal water is to be saved, drying is accomplished by heating only. The recovered waste water is then sent to the water recovery subsystem.

Several techniques featuring integration of the collection, treatment, and storage processes are available. Two are currently being advanced to the state that will be considered prequalification for system test. A subsystem known as the "Super John" based on an earlier version of the "Dry John" has been designed and fabricated and has been extensively tested. The concepts include (1) fecal collection, and a means of direct sterilization of the seat area; and (2) dynamic phase separation by means of a rotating slinger which shreds and then spreads the feces and toilet tissue in a thin layer over the inner surface of the collection vessel where sterilization then takes place. Initial sterilization takes place at approximately 250°F for 30 minutes; then, processing is accomplished by means of thermal decomposition. Initial test results indicate approximately 3 hours at 800°F plus are required to reduce the original volume by 85 percent. At the end of this time the resultant ash closely resembles charcoal. Tests are being planned to study this ash in order to determine the feasibility of reuse of this material as a back-up regenerative filter source.

Another subsystem referred to as "Hydro John" involves similar hardware except for substitution of calrod heaters with a slurry collection area. In addition to using air, the system uses wash water for cleaning. The water also provides for development of the slurry. The water is collected for thermal decomposition of the solid waste and is returned to the waste management system after its recovery from the waste water reclamation subsystem.

It is recognized that on long-term space missions, there must be systems onboard for disposing of wet waste materials, such as feces. The feasibility of adapting the principle of high pressure wet oxidation to perform these combined operations is under consideration (Jagow & Saunders, undated).

The incineration and/or wet oxidation techniques are operated by adding waste materials, including feces, papers, and plastic food containers, to the incinerator. The waste materials can be dried and sterilized by using electrical resistance heaters and then burned with pure oxygen or oxygen diluted with nitrogen. The residue remaining is a dry, gray powder which could be easily removed.

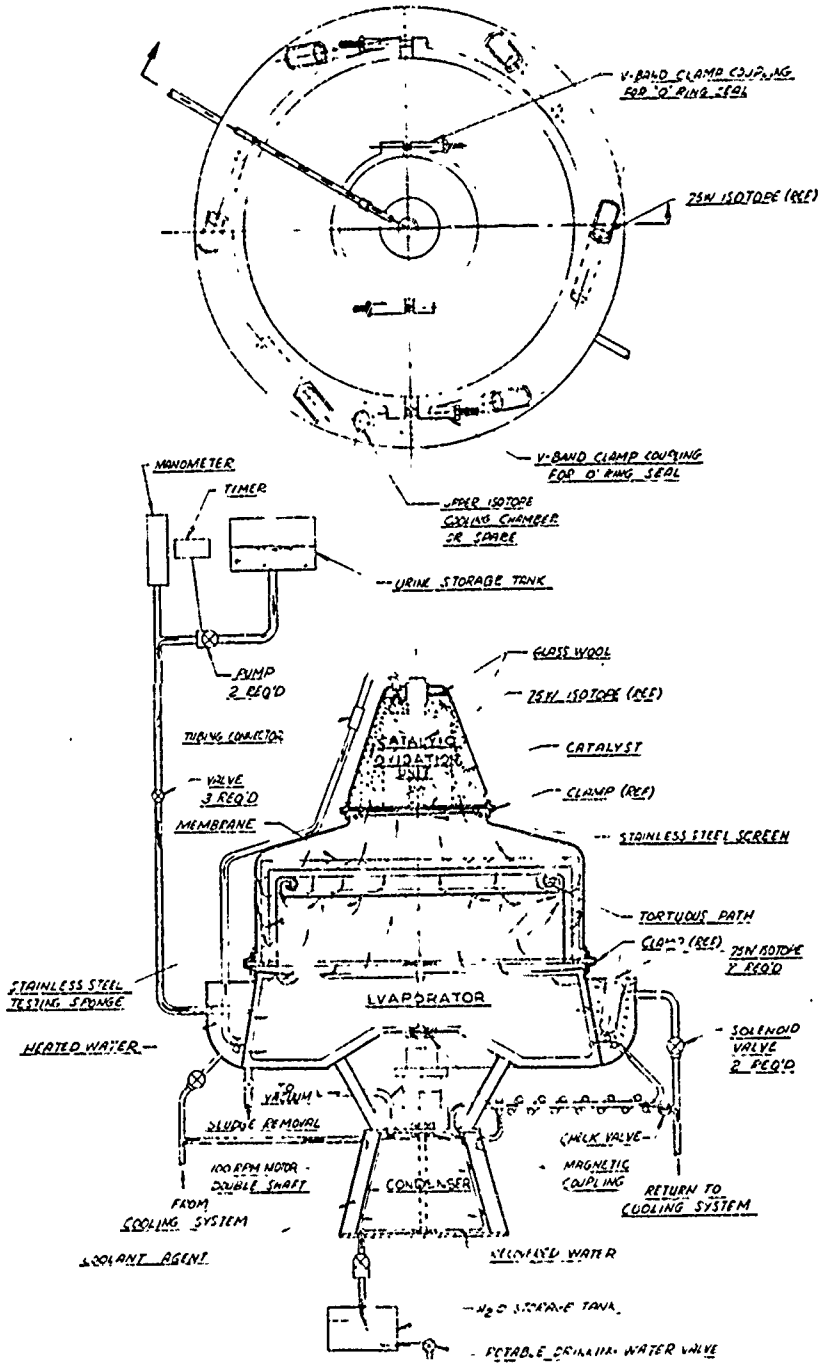


Figure 20–1. Vapor distillation pyrolysis waste water recovery system.

Vapor Compression. Vapor compression, or compression distillation, is a process in which the latent heat of vaporization of the liquid feed is conserved. Heat transfer from the condensing vapor is accomplished by compressing the vapor so that it condenses at a high pressure and thus, a higher temperature. As a result, a temperature difference is created between the evaporator and condenser which makes the process possible. Even though the maximum vapor temperature can be as high as 100°F, the extent of breakdown of urea and other organics is low. Condensate from this process must therefore be further treated to render it potable. Filtration through activated charcoal and ion-exchange resins, and a bacteria filter sufficiently purify the condensate to make it potable.

A schematic diagram of one type of a vapor compression system is shown in figure 20-2. Urine containing a chemical disinfectant is fed to the rotating evaporator where heat from the condenser vaporizes the liquid at about 0.35 psia. The rotating evaporator-condenser is a cylinder: the inside is the evaporating surface and the outside, the condensing surface. The compressor motor, enclosed in the evapor-condenser shell, gives up heat which is utilized as makeup heat for vaporization. This replaces the heat given up by the condensing vapor to the surroundings. Vapor from the evaporating surface is compressed to about 0.70 psia and delivered to the condenser side of the drum. When condensed, a cam-activated pump forces the condensate water back to ambient pressure and out of the condensing chamber. A vacuum pump removes noncondensable gases from the condenser chamber to prevent a buildup in pressure. These gases are passed through an activated charcoal filter to the atmosphere. The urine residue collecting in the evaporator is removed periodically and stored.

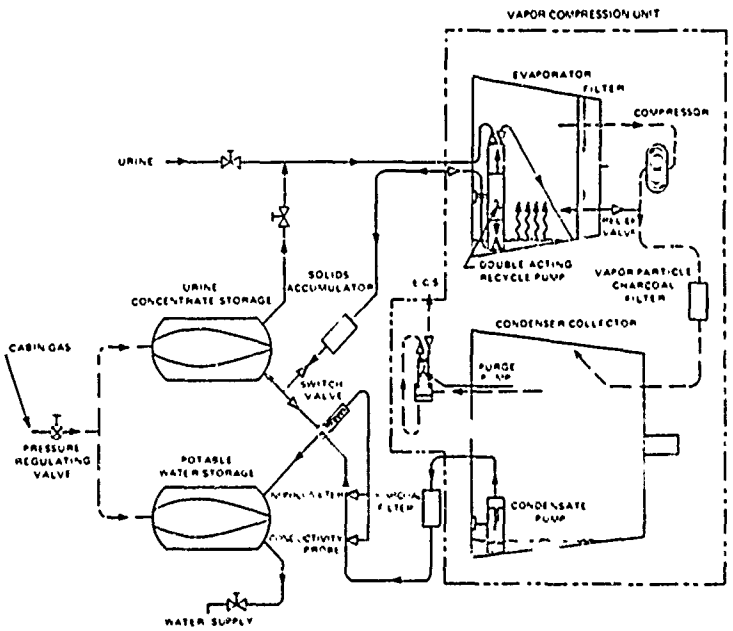


Figure 20–2. Vapor compression system for urine processing.

Waste Recovery Subsystem

One of the first solid waste receivers to be extensively tested was the "Dry John." This device was used by a four-man crew in a sixty day chamber test. Figure 20-3 is a schematic of hardware developed for NASA. The unit consisted of a seat, a mechanical vacuum valve, a receiving chamber, a motorized slinger rotor, exhaust lines, and bacteria and odor control (charcoal) filters.

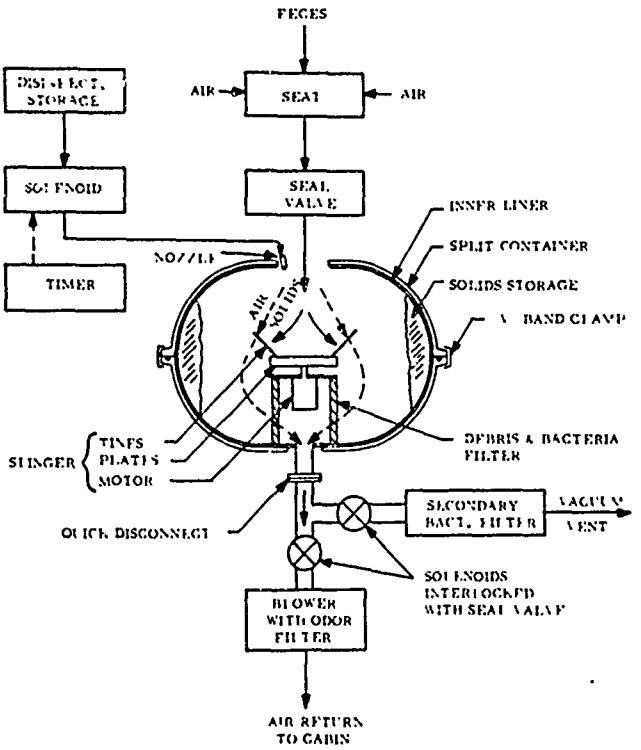


Figure 20–3. "Dry John" solid waste processing unit.

The Dry John test reduced the water content of feces and vomitus to less than 30 percent water. At this point, there appears to be no further bacterial action, no odor, and no danger of infection. No attempt was made to salvage the water removed from the waste matter.

In actual use of the Dry John device, positive control of fecal material was obtained by a control-air flow drawn through the seat by suction created by the control-air fan. The air was directed towards the anal opening, where it turns and sweeps vertically down past the mechanical vacuum valve. In use, the fecal matter was carried down by the airstream to make contact with the spinning slinger. The slinger shredded the fecal matter and centrifuged it, in a thin layer, against the drying chamber's inner surface. The control-air flow passed the slinger, and the slinger motor, into the exhaust line, through the vacuum valve, blower, bacteria filter, charcoal filter, and back to the cabin.

The toilet tissue used by the crew was dropped into the drying chamber. The tissue was centrifuged and mixed with the fecal matter. After use, the mechanical vacuum valve below the seat was closed and the slinger motor turned off, the vacuum valve leading to the cabin air blower closed, the cabin air blower shut off and the vacuum valve leading to the simulated space vacuum source was opened. This caused the pressure in the drying chamber to drop to nearly vacuum and to evaporate the water in the waste matter. Evaporation was relatively fast, because the wet fecal matter had spread in a thin layer over a large area. Heat was drawn into the dryer by conduction through the walls to prevent freezing before all the water was removed. The relatively large drying chamber surface area and the thin waste layer resulted in good heat transfer.

Bacterial and charcoal filters were provided on the vacuum line since the vacuum pump discharged to the atmosphere. Approximately 4 hours were required to dry a man's daily fecal matter. The single unit had the capacity to handle the wastes of the four-man test crew.

When a second crewman used the Dry John, he did not have to wait until the wastes of the previous user had completely dried. He used it immediately by shutting the high vacuum valve, starting the cabin air blower, opening the cabin air vacuum valve, starting the slinger motor and opening the mechanical vacuum valve under the seat.

A vomitus collection adapter was provided for the Dry John. This device inserts into the seat opening so that the control airflow ducts are blocked off. This causes air to be drawn through holes in the adapter for zero-g collection. The vomitus is spread along the drying chamber wall and is dried in the same manner as fecal material.

Debris

The crews of any aerospace vehicle will generate particulate matter from their bodies and their clothing. Equipment also releases particulates. In a weightless state this debris will float in the cabin until it is entrained by the ventilation gas or is separated and captured by a surface (such as a crewman's lungs). Of course, the ventilation gas and filters will remove most of the debris; however, some spaces in the cabin will tend to accumulate floating debris due to a lack of sufficient ventilation. Therefore, on long duration missions (of one or more weeks) a vacuum cleaner should be provided to collect this material--which may include viable microorganisms and the media necessary for growth.

If the vehicle is provided with a pneumatic collection system for urine and/or feces, the fan used for this purpose can also be used to draw gas into a small debris collection bag. This bag can be made from the same material as the fecal collection bag. A gas flow rate of 5 ft^3/min is adequate for this purpose.

A personal grooming device—vacuum cleaner is provided on a branch of the control air circuit of the waste management unit. This collects hair, nail clippings, shaving clippings, etc. Collection bags are provided to dry and store the wastes. There are three key problem areas associated with the Dry John integrated waste management system at the present time. They are:

1. The vacuum seals in the fecal receiver are critical in minimizing the loss of cabin atmosphere.

2. Lubrication of the fecal slinger motor may be required after long exposure to hard vacuum.

3. The adsorbent beds in the fecal collector must be properly sized for odor control.

Disposal and Processing

Collected wastes must be either stored in an aesthetic and sanitary manner or dumped overboard to protect the crew from microorganisms and noxious gases. The best technique for a specific vehicle depends upon the mission duration and the onboard equipment to support a waste disposal subsystem.

Storage Onboard. Wastes can be stored satisfactorily by merely sealing them in a container. However, if the wastes contain microorganisms, water and nutrients, biological activity can occur and produce undesirable gases. The pressure developed is a function of the container ullage, water and nutrient available, types of microorganisms active, gas available, and storage temperature. Under ideal conditions, each gram of waste material could produce 10 ft^3 of gas. For safe storage of wastes such as urine, feces, vomitus, unused food, and debris processing prior to storage is needed to prevent or minimize biological activity. Processing methods include: (1) killing the microorganisms, (2) freezing the wastes, and/or (3) removing the water.

The urine and liquid waste collection subsystem should be disinfected periodically to prevent biological growth and production of noxious gases in this area. Several disinfectants are satisfactory for this purpose; for example, Wescodyne, a mixture containing iodine complexed with surface active agents. In most cases, the quantity of disinfectant required is less than 0.1 percent. If a disinfectant is provided for the urine collection subsystem it will also serve to stabilize the urine for onboard storage or water reclamation.

Disinfectants or germicides have also been used to prepare feces and debris for onboard storage in plastic bags. Tests have been performed to demonstrate that a 15 ml mixture of germicide, water and humectant is capable of inducing virtual sterility in feces; however, only 10 ml of this mixture is required to control gas production. In practice, the germicidal mixture is usually supplied in a small bag within the collection bag; it is then distributed by breaking the small bag and kneading the wastes for ten minutes to uniformly distribute the germicide.

The most positive and reliable method for killing microorganisms is heating the wastes to a temperature above 250°F, and holding at this temperature for at least ten minutes. This technique is attractive when waste heat is available; if electric power must be used, this method usually imposes a higher weight penalty than other storage techniques. Also, heat sterilization has the disadvantages of (1) producing internal pressures higher than 30 psia, and (2) generating obnoxious odors.

Biological activity can be retarded by freezing wastes. For maximum effect, a storage temperature of 0°F is recommended. Conventional refrigeration techniques can be utilized to cool and maintain wastes at this temperature—but at the expense of electric power. Another approach is to freeze-dry the wastes in an insulated storage container, using the latent heat of water sublimation to remove the heat transferred through the insulation (Zeff et al., 1961; Rollo & Popoff 1965). This technique is very attractive for missions without water recovery because the wastes are also dried, which serves to backup the freezing technique. The disadvantages of this technique are that (1) a vacuum storage vessel is required and (2) an appreciable quantity of cabin gas is lost overboard unless a waste loading lock is provided.

The simplest and most versatile method for storing all types of waste is vacuum drying—to remove the water necessary for biological mobility and growth. This technique does not "kill" the microorganisms, but it does inactivate them sufficiently to permit storage in a plastic bag for periods of 120 days or more. The drying pressure recommended is 0.3 psia or less, so that cabin heat can be utilized for vaporization of water and other low molecular weight constituents.

References

Charanian, T. R., Rollo, J., Glueckert, A. J., & Hurley, T. L. Extended mission Apollo study on water reclamation, waste management and personal hygiene. GARD Rept. 1276-6070, November 1965.

Des Jardins, Zeff, J. D., & Bambenek, R. A. Waste collection unit for a space vehicle. WADD, TR-60-290, May 1960.

Dodson, J., & Wallman, H. Research on a waste system for aerospace stations. AMRL-TDR-64-33, May 1964.

Ingram, W. T. The engineering biotechnology of handling wastes resulting from a closed ecological system. AFOSR-TR-58-148, February 1958.

Jagow, R. B., & Saunders, C. G. The processing of human wastes by wet oxidation for manned spacecraft. ASME Rept. 70-AVI SPT-1, undated.

Miner, H. C., Sanford, H. L., Segal, M. R., & Wallman, H. Collection unit for wastes during space travel. ASD TR-61-314, July 1961.

Rollo, E. J., & Popoff, W. A. Waste management system. GARD Rept. 1252-7080, December 1965.

Rollo, E. J., Honegger, R. J., & Candes, R. A. Apollo applications program waste management system. GARD Rept. 1276-9598, March 1967.

Zeff, J. D., Neveril, R. B., et al. Storage unit for waste materials. ASD TR-61-200, June 1961.